Topics in Geobiology 46

Lawrence H. Tanner *Editor*

The Late Triassic World

Earth in a Time of Transition

Springer

Topics in Geobiology

Volume 46

The **Topics in Geobiology** series covers the broad discipline of geobiology that is devoted to documenting life history of the Earth. A critical theme inherent in addressing this issue and one that is at the heart of the series is the interplay between the history of life and the changing environment. The series aims for high quality, scholarly volumes of original research as well as broad reviews.

Geobiology remains a vibrant as well as a rapidly advancing and dynamic field. Given this field's multidiscipline nature, it treats a broad spectrum of geologic, biologic, and geochemical themes all focused on documenting and understanding the fossil record and what it reveals about the evolutionary history of life. The Topics in Geobiology series was initiated to delve into how these numerous facets have influenced and controlled life on Earth.

Recent volumes have showcased specific taxonomic groups, major themes in the discipline, as well as approaches to improving our understanding of how life has evolved.

Taxonomic volumes focus on the biology and paleobiology of organisms – their ecology and mode of life – and, in addition, the fossil record – their phylogeny and evolutionary patterns – as well as their distribution in time and space.

Theme-based volumes, such as predator-prey relationships, biomineralization, paleobiogeography, and approaches to high-resolution stratigraphy, cover specific topics and how important elements are manifested in a wide range of organisms and how those dynamics have changed through the evolutionary history of life.
Comments or suggestions for future volumes are welcomed.

Series Editors
Neil Landman
American Museum of Natural History, New York, NY, USA

Peter J. Harries
Tampa, FL, USA

More information about this series at http://www.springer.com/series/6623

Metabactrites fuchsi De Baets et al. 2013, PWL2010/5251-LSmiddle Kaub Formation, Bundenbach (Hunsrück, Germany). This is one of the most plesiomorphic and oldest ammonoids known. Image by courtesy of Markus Poschmann (Mainz, GDKE).

Lawrence H. Tanner
Editor

The Late Triassic World

Earth in a Time of Transition

Springer

Editor
Lawrence H. Tanner
Department of Biological and Environmental Sciences
Le Moyne College
Syracuse, NY, USA

ISSN 0275-0120
Topics in Geobiology
ISBN 978-3-319-68008-8 ISBN 978-3-319-68009-5 (eBook)
https://doi.org/10.1007/978-3-319-68009-5

Library of Congress Control Number: 2017957651

© Springer International Publishing AG 2018
This work is subject to copyright. All rights are reserved by the Publisher, whether the whole or part of the material is concerned, specifically the rights of translation, reprinting, reuse of illustrations, recitation, broadcasting, reproduction on microfilms or in any other physical way, and transmission or information storage and retrieval, electronic adaptation, computer software, or by similar or dissimilar methodology now known or hereafter developed.
The use of general descriptive names, registered names, trademarks, service marks, etc. in this publication does not imply, even in the absence of a specific statement, that such names are exempt from the relevant protective laws and regulations and therefore free for general use.
The publisher, the authors and the editors are safe to assume that the advice and information in this book are believed to be true and accurate at the date of publication. Neither the publisher nor the authors or the editors give a warranty, express or implied, with respect to the material contained herein or for any errors or omissions that may have been made. The publisher remains neutral with regard to jurisdictional claims in published maps and institutional affiliations.

Printed on acid-free paper

This Springer imprint is published by Springer Nature
The registered company is Springer International Publishing AG
The registered company address is: Gewerbestrasse 11, 6330 Cham, Switzerland

Preface

This volume grew out of a personal interest in the Late Triassic, an interest that was nurtured by the realization early in my career that this roughly 30 million-year interval is unique in Earth's history. The Late Triassic saw the origination of dinosaurs and pterosaurs, but the near simultaneous decline of many other archosaur groups; it witnessed the spread of reptiles in the oceans and on land, the first appearance of mammals. All of this was against a backdrop of climate, tectonics, bolide impacts, and the eruptions of one of the largest of the Large Igneous Provinces, all of which made for an Earth far different from today's world.

This collection of peer-reviewed papers, from researchers distinguished for their work on this time period, presents both reviews and compilations of the latest studies, as well as fresh ideas and new data. Everyone, professionals and students, whose work or interests intersect the Late Triassic will find this collection an essential addition to their library.

The volume begins with an overview of the Earth on which the biologic events played out, starting with a review by Spencer Lucas of the timescale of the Late Triassic, including the certainties and uncertainties of the stage boundaries. Next, Jan Golonka and colleagues provide a global overview of the tectonic activity of the period. The climate of this time, what we know, or suspect, and how we know it, is reviewed by Lawrence Tanner. Andrea Marzoli and colleagues provide a thorough description of the largest volcanic event of the entire early Mesozoic, the eruption of the Central Atlantic magmatic province. More than one bolide impact occurred during the Late Triassic, and the evidence for these, and their consequences, is discussed by Michael Clutson and colleagues.

The next section of the volume is dedicated to the marine environment. Much Triassic biostratigraphy depends on conodonts, and Manuel Rigo and colleagues propose a new Upper Triassic biozonation. Similarly, ammonoids are an essential tool of biostratigraphers, and Spencer Lucas reviews their biostratigraphy and key biotic events. The radiation of the marine reptiles during the Late Triassic is reviewed by Renesto and Dalla Vecchia. Finally, Tintori and Lombardo examine the diversification of actinopterygian fish through the lens of the superbly preserved fossil deposits in the Zorzino Limestone.

The final portion of this collection is centered on the land environment. Spencer Lucas provides a review of terrestrial tetrapods, with attention to their biostratigraphy and key biotic events. The cynodonts and their evolutionary transition to mammals are the focus of the chapter by Abdala and Gaetano. Next, Adrian Hunt and colleagues present a wide-ranging review of the diverse trace of fossils, both vertebrate and invertebrate, found in nonmarine strata of the Upper Triassic. The floral kingdom is not ignored here; Evelyn Kustatscher and colleagues provide a global overview of Upper Triassic floral diversity. Next, Conrad Labandeira and colleagues review the diverse Molteno flora in the course of describing the record of plant-arthropod interactions of this time. To conclude, Lucas and Tanner give a close eye to the biotic decline at the end of the Triassic and the putative mass extinction that marks the end of this period.

In addition to the authors, who rose quite admirably to the challenge of producing these chapters, more or less on deadline, I must thank the numerous individuals who contributed measurably to the success of this project. One of these would have to be Zachary Romano, of Springer US, who invited me to consider the project and encouraged me as I developed the concept. Spencer Lucas, my friend and colleague of many years, was a major factor in bringing this project to completion, through his chapter contributions, chapter reviews, and suggestions regarding authors and reviewers. Finally, there are the many individuals I list here who agreed to lend their time and expertise in reviewing the chapters herein: Gloria Arratia, Sid Ash, Brian Axsmith, Marion Bamford, Paula Dentzian-Dias, Ezat Heydari, Mark Hounslow, Adrian Hunt, Jim Jenks, Julien Kimmig, Tea Kolar-Jurkovšek, Karl Krainer, Evelyn Kustatscher, Spencer Lucas, Michael Orchard, Rose Prevec, John Puffer, Manuel Rigo, Martin Sanders, Martin Schmieder, Hans Sues, Valery Vernikovsky, and Robert Weems.

Syracuse, NY, USA Lawrence H. Tanner

Contents

Contributors

Fernando Abdala Unidad Ejecutora Lillo, CONICET-Fundación Miguel Lillo, Tucumán, Argentina

Evolutionary Studies Institute, University of the Witwatersrand, Johannesburg, South Africa

Heidi M. Anderson Evolutionary Studies Institute, University of the Witwatersrand, Johannesburg, South Africa

John M. Anderson Evolutionary Studies Institute, University of the Witwatersrand, Johannesburg, South Africa

Sidney R. Ash Department of Earth and Planetary Sciences, Northrop Hall, University of New Mexico, Albuquerque, NM, USA

Hervé Bertrand Laboratoire de Géologie de Lyon, Université Lyon 1 and Ecole Normale Supérieure de Lyon, UMR CNRS 5276, Lyon, France

David E. Brown Canada-Nova Scotia Offshore Petroleum Board, Halifax, NS, Canada

Sara Callegaro Centre for Earth Evolution and Dynamics (CEED), University of Oslo, Oslo, Norway

Massimo Chiaradia Sciences de la Terre et de l'Environnement, Université de Genève, Genève, Switzerland

Michael J. Clutson Halifax, NS, Canada

Jacopo Dal Corso Hanse-Wissenschaftskolleg (HWK), Institute for Advanced Study, Delmenhorst, Germany

Joshua H.F.L. Davies Sciences de la Terre et de l'Environnement, Université de Genève, Genève, Switzerland

Ashton Embry Geological Survey of Canada, Calgary, AB, Canada

Leandro C. Gaetano Departamento de Ciencias Geológicas, FCEyN, Instituto de Estudios Andinos "Don Pablo Groeber", IDEAN (Universidad de Buenos Aires-CONICET), Ciudad Autónoma de Buenos Aires, Buenos Aires, Argentina

Evolutionary Studies Institute, University of the Witwatersrand, Johannesburg, South Africa

Jan Golonka Faculty of Geology, Geophysics and Environmental Protection, AGH University of Science and Technology, Kraków, Poland

Adrian P. Hunt Flying Heritage and Combat Armor Museum, Everett, WA, USA

Fred Jourdan Department of Applied Geology, Curtin University, Bentley, WA, Australia

Viktor Karádi Department of Palaeontology, Eötvös Loránd University, Budapest, Hungary

Eugeny Karasev Borissiak Paleontological Institute, Russian Academy of Sciences, Moscow, Russia

Hendrik Klein Saurierwelt Paläontologisches Museum, Neumarkt, Germany

Michał Krobicki Faculty of Geology, Geophysics and Environmental Protection, AGH University of Science and Technology, Kraków, Poland

Carpathian Branch, Polish Geological Institute - National Research Institute, Kraków, Poland

Evelyn Kustatscher Museum of Nature South Tyrol, Bolzano, Italy

Department für Geo– und Umweltwissenschaften, Paläontologie und Geobiologie, Ludwig–Maximilians–Universität, and Bayerische Staatssammlung für Paläontologie und Geologie, Munich, Germany

Conrad C. Labandeira Department of Paleobiology, National Museum of Natural History, Smithsonian Institution, Washington, DC, USA

Department of Entomology and BEES Program, University of Maryland, College Park, MD, USA

College of Life Sciences, Capital Normal University, Beijing, China

Cristina Lombardo Dipartimento di Scienze della Terra Ardito Desio, Universita di Milano, Milan, Italy

Spencer G. Lucas New Mexico Museum of Natural History and Science, Albuquerque, NM, USA

Andrea Marzoli Dipartimento di. Geoscienze, Università di Padova, Padova, Italy

Michele Mazza Department of Earth Sciences “Ardito Desio”, University of Milan, Milan, Italy

Stephen McLoughlin Palaeobiology Department, Swedish Museum of Natural History, Stockholm, Sweden

Renaud Merle Australian National University, Research School of Earth Sciences, Acton, ACT, Australia

Alda Nicora Department of Earth Sciences “Ardito Desio”, University of Milan, Milan, Italy

Christian Pott Palaeobiology Department, Swedish Museum of Natural History, Stockholm, Sweden

LWL-Museum of Natural History, Westphalian State Museum and Planetarium, Münster, Germany

Laurie Reisberg Centre de Recherches Pétrographiques et Géochimiques, UMR 7358 CNRS, Université de Lorraine, Nancy, France

Silvio Renesto DiSTA Dipartimento di Scienze Teoriche ed Applicate, Università degli Studi dell’Insubria, Varese, Italy

Manuel Rigo Department of Geosciences, University of Padova, Padova, Italy

Lawrence H. Tanner Department of Biological and Environmental Sciences, Le Moyne College, Syracuse, NY, USA

Andrea Tintori Dipartimento di Scienze della Terra Ardito Desio, UNIMI, Milan, Italy

Vivi Vajda Palaeobiology Department, Swedish Museum of Natural History, Stockholm, Sweden

Fabio Marco Dalla Vecchia Soprintendenza per i Beni Archeologici del Friuli Venezia Giulia, Nucleo Operativo di Udine, Udine, Italy

Nassrrdine Youbi Department of Geology, Faculty of Sciences-Semlalia, Cadi Ayyad University, Marrakesh, Morocco

Instituto Dom Luiz, Faculdade de Ciências, Universidade de Lisboa, Lisbon, Portugal

Jianxin Yu State Key Laboratory of Biogeology and Environmental Geology, China University of Geosciences, Wuhan, P.R. China

Chapter 1
The Late Triassic Timescale

Spencer G. Lucas

Abstract The Upper Triassic chronostratigraphic scale consists of one Series, the Upper Triassic, divided into three stages (in ascending order)—Carnian, Norian and Rhaetian. Only the base of the Carnian currently has an agreed on GSSP (global boundary stratotype section and point), though agreement on GSSPs for the bases of the Norian and Rhaetian is imminent. Substages of the Carnian and Norian provide more detailed subdivisions of Late Triassic time than do the relatively long Carnian and Norian stages. These substages need boundary definitions and greater use in Late Triassic correlations. Numerical chronology of the Late Triassic is based on very few radioisotopic ages from volcanic ash beds directly related to marine biostratigraphy. The numerical calibration of the Late Triassic favored here is Carnian ~220–237 Ma, Norian ~205–220 Ma and Rhaetian ~201–205 Ma. Late Triassic magnetostratigraphy is fraught with problems because the most complete record from the Newark Supergroup of eastern North America cannot be correlated based on pattern matching to any co-eval magnetostratigraphy from a marine section. The long Norian (beginning at ~228 Ma) was created by magnetostratigraphic correlations that abandoned biostratigraphic constraints and has produced extensive miscorrelation, particularly of nonmarine Carnian strata. A reliable Late Triassic magnetostratigraphy is a succession of multichrons that identifies the Carnian-early Norian and late Norian-Rhaetian as dominantly of normal polarity. Late Triassic cyclostratigraphy of the Newark Supergroup has been advanced as a floating astrochronology of the Late Triassic, but is problematic given evident hiatuses in the Newark record and the presence of non-cyclical lithofacies. Isotope stratigraphy of the Late Triassic, for example the late Rhaetian carbon-isotope excursion, has great potential for use in Late Triassic correlations. The Late Triassic timescale is still very much a work in progress that needs more precise chronostratigraphic definitions, additional numerical ages directly related to marine biostratigraphy, a wholesale rethinking of magnetostratigraphic correlations and additional cyclostratigraphic and isotopic data to achieve greater precision and stability.

S.G. Lucas (✉)
New Mexico Museum of Natural History and Science,
1801 Mountain Road N. W., Albuquerque, NM 87104-1375, USA
e-mail: spencer.lucas@state.nm.us

© Springer International Publishing AG 2018

L.H. Tanner (ed.), *The Late Triassic World*, Topics in Geobiology 46,
https://doi.org/10.1007/978-3-319-68009-5_1

Keywords Late Triassic • Chronostratigraphy • Radioisotopic ages • Magnetostratigraphy • Astrochronology • Isotope stratigraphy

1.1 Introduction

The Late Triassic was a major juncture in Earth history when the vast Pangean supercontinent began its fragmentation, and numerous biotic groups first evolved or suffered extinction on land and in the sea (e.g., Lucas 1999; Lucas and Orchard 2004; Sues and Fraser 2010). The temporal ordering of geological and biotic events during Late Triassic time thus is critical to the interpretation of some unique and pivotal events in Earth history. This temporal ordering is based on the Late Triassic chronostratigraphic scale integrated with numerical ages and other geochronologic tools, notably magnetostratigraphy, cyclostratigraphy and isotope stratigraphy. Here, I review the Late Triassic timescale to highlight ongoing issues and to present its current status.

1.2 Some History

Recognition of a distinctive interval in Earth history (originally identified as a distinct succession of stratified rocks) that corresponds to the current concept of Triassic began in Germany more than 200 years ago. Alberti's (1834) monograph in which he coined the term Trias culminated this early work. The 200-year-long history of the development of a Triassic relative timescale (the standard global chronostratigraphic scale) has been reviewed by Zittel (1901), Silberling and Tozer (1968), Tozer (1984) and Lucas (2010).

Alberti's type Triassic in southwestern Germany (Fig. 1.1) is a sandwich of dominantly nonmarine red beds (Buntsandstein and Keuper) with a restricted marine middle portion (Muschelkalk). Already in the nineteenth century, the recognition of Muschelkalk-equivalent marine strata, based largely on their content of ceratites (ammonoids), became key to recognition of the Trias outside of Germany.

The Alps contain a relatively complete section of Triassic marine strata, so extension of the Triassic into the Alpine marine strata became central to further subdivision and correlation of Triassic time. This subdivision owes more to Austrian geologist Edmund von Mojsisovics (1839–1907) than to any other geologist. Recognition of subdivisions of Triassic time based on ammonoids by Mojsisovics and his collaborators produced most of the stage-level terminology of Triassic time still used today.

This work was culminated by Mojsisovics et al. (1895), the singlemost important article written on the Triassic timescale. It coined the names of most of the marine stages and sub-stages recognized today. This timescale was refined subsequently,

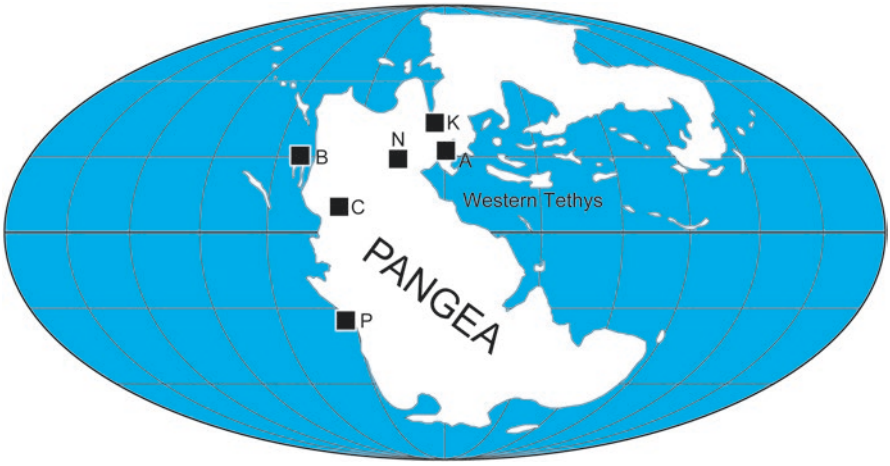

Fig. 1.1 The Triassic world with locations of some key sections and outcrop areas discussed in the text. *A* Southern Alps/central Europe (mainly Austria and northern Italy, see Fig. 1.3), *B* British Columbia, Canada; *C* Chinle basin, western USA, *K* Keuper, Germanic basin, northern Europe (principally Germany), *N* Newark basin, NJ, Pennsylvania, USA; *P* Peru

especially by the addition of Bittner's (1892) Ladinian, but remained the basic Triassic timescale until at least the 1960s.

Beginning in the 1960s, Canadian paleontologist E. Timothy Tozer (1928–2010), in part collaborating with American geologist Norman J. Silberling (1928–2011), assembled a Triassic timescale based on North American ammonoid zones (e.g., Silberling and Tozer 1968; Tozer 1971, 1974, 1984, 1994). Key components of Tozer's Triassic timescale were that it defined Triassic stage boundaries based on North American ammonoid localities and it rejected the Rhaetian as a distinctive stage. During the 1970s and 1980s, Tozer's timescale found wide acceptance in the English language literature on the subdivision of Triassic time, though few abandoned the Rhaetian (e.g., Kummel 1979; Harland et al. 1982, 1990).

Conceived in 1968, and beginning its meetings in the 1970s (Tozer 1985), the Subcommission on Triassic Stratigraphy (STS), as part of the International Commission on Stratigraphy (ICS), was primarily charged to establish a global Triassic timescale based on GSSP (global stratotype section and point) definitions of the bases of the Triassic stages (e.g., Gaetani 1996). The STS began its published discussion (in the STS journal *Albertiana*) with a lively debate over the Tozer timescale—particularly over whether or not to recognize the Rhaetian as a separate stage, which Tozer had regarded as a substage of the Norian. After initial acceptance in 1984 of most aspects of the Tozer timescale, in 1991, the STS agreed on a stage nomenclature of the Triassic that included the Rhaetian as a separate stage (Fig. 1.2). To date, GSSPs in the Upper Triassic have been defined only for the bases of the Carnian (base of Upper Triassic Series) and the Hettangian (base of the Jurassic System) (Fig. 1.2).

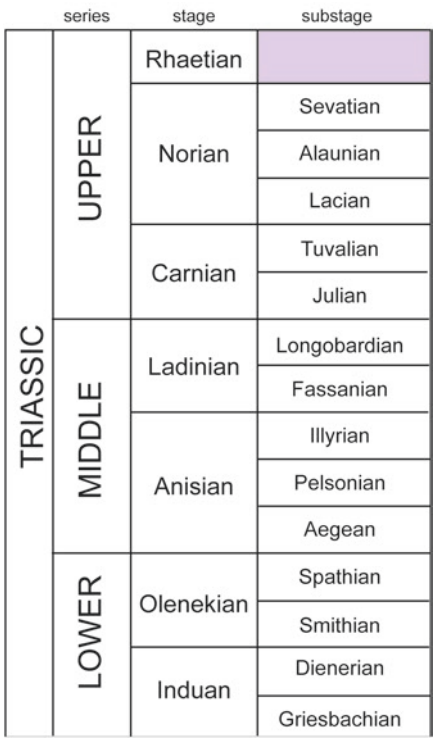

Fig. 1.2 The Triassic chronostratigraphic scale (after Lucas 2010)

1.3 Upper Triassic Chronostratigraphy

1.3.1 Upper Triassic Series

The most significant thing we have learned about the Triassic timescale from numerical chronology is that the three traditional Triassic series are of very uneven duration. The traditional Early Triassic is about 5 million years long, the traditional Middle Triassic is about 10 million years long and the rest of the Triassic (the traditional Late Triassic) is about 36 million years long (Mundil et al. 2010; Ogg 2012; Ogg et al. 2014). Thus, by numerical chronology, the Early and Middle Triassic together make up only about the first third of the period.

Therefore, Lucas (2013) advocated recognizing four Triassic series (epochs) of more even duration. Note that Mojsisovics et al. (1895) also divided the Triassic into four series similar to (but not exactly congruent with) those recognized by Lucas (2013). The four Triassic series that Lucas (2013) proposed are the (ascending order) Scythian, Dinarian, Carnian and Norian. The first two names are from Mojsisovics et al. (1895), and the last two are elevation of the very long Carnian and Norian stages to series rank. However, the traditional and agreed on single Upper Triassic Series and three stages—Carnian, Norian and Rhaetian—are used here (Fig. 1.2).

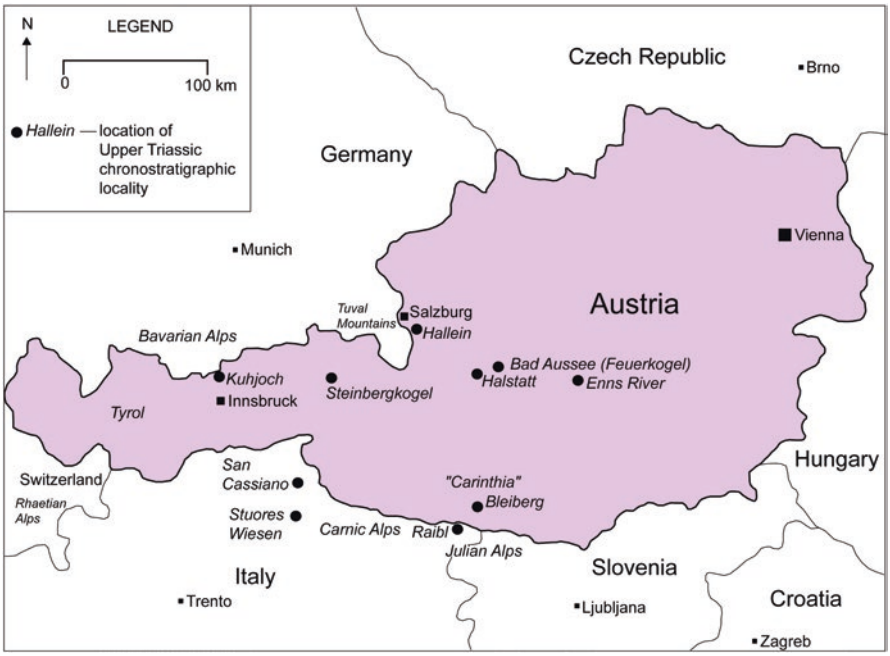

Fig. 1.3 Map of Austria and adjacent areas showing localities important to Upper Triassic chronostratigraphy that are discussed in the text

Marine sections critical to definition of Upper Triassic chronostratigraphic subdivisions are primarily those in the Alps of central and southern Europe (Figs. 1.1 and 1.3).

1.3.2 Carnian Stage

Mojsisovics (1869: 127) introduced the term Carnian Stage for ammonoid-bearing strata in the Austrian state of Kärnten (Carinthia). He initially and erroneously regarded it as younger than the Norian. Mojsisovics (1874) assigned three ammonoid zones to the Carnian (ascending order): *Trachyceras aon, Trachyceras aonoides* and *Tropites subbullatus* zones. Later, Mojsisovics (in Mojsisovics et al. 1895) divided it into three substages (ascending order): Cordevolic (=Aon zone), Julic (=Aonoides Zone) and Tuvalic (= Subbullatus Zone).

Tozer (1984) regarded the type locality of the Carnian as vague, as it was stated to refer to the *Trachyceras* and *Tropites* beds of the Hallstatt Limestone, but also included localities at Raibl, Bleiberg and San Cassiano (Fig. 1.3). Lieberman (1980) proposed the Raibl section as the stratotype of the stage. Tozer (1984) and some others have spelled the name "Karnian," but this spelling has not been widely adopted.

Today, the Carnian Stage is typically divided into two substages named by Mojsisovics (in Mojsisovics et al. 1895)—Julian (lower) and Tuvalian (upper). However, Mojsisovics (in Mojsisovics et al. 1895) also recognized a third (lowermost) Carnian substage, the Cordevolian, still used by some workers. Based on the St. Cassian Beds, Cordevolian derives its name from the Cordevol people who lived in the type area in northern Italy (Mojsisovics et al. 1895: 1298). Krystyn (1978) discussed the original definition of the Cordevolian and argued that it essentially referred to the same time interval as the Julian (also see Tozer 1967, 1974).

The Julian was based on the Raibl Formation in the Julian Alps (southern Alps) by Mojsisovics (in Mojsisovics et al. 1895: 1298), and has come to be viewed by most workers as the lower Carnian (cf. Krystyn 1980; Tozer 1984, 1994; Lucas 2010) (Fig. 1.2). Mojsisovics (in Mojsisovics et al. 1895: 298) took the name Tuvalian from the Tuval Mountains (Bavaria-Austria), which was the Roman name for the area between Hallein and Berchtesgarden in Austria-Germany. He based it on the *Tropites subbullatus* ammonoid zone. Krystyn and Schlager (1971) suggested using the section at Feuerkogel near Aussee, Austria, as the Tuvalian stratotype as well as the place to define the base of the Norian, in large part because the original ammonoids of Mojsisovic's stratotype Tuvalian came from syntectonic fissure fills at Rappolstein. The term Tuvalian has come to be used by most workers to refer to the entire upper Carnian (e.g., Krystyn and Schlager 1971; Tozer 1984, 1994; Lucas 2010) (Fig. 1.2).

A GSSP for the base of the Carnian Stage (= base of the Upper Triassic) has been agreed on (Gaetani 2009). It is the LO (lowest occurrence) of the ammonoid *Daxatina canadensis* (Whiteaves) at the Parti di Stuores/Stuores Wiesen section in northern Italy (Mietto et al. 2007a, b, 2012; Jenks et al. 2015) (Fig. 1.3).

With regard to ammonoid bioevents (Balini et al. 2010; Jenks et al. 2015; Lucas 2017 this volume), the Julian is dominated by Trachyceratinae, in particular *Trachyceras* and *Austrotrachyceras*, and by Sirenitinae. The base of the Tuvalian is marked by one of the major changes in the evolution of Triassic ammonoids, namely the near extinction of the Trachyceratinae, whose only survivor in the late Carnian is *Trachysagenites*, as well as the radiation of Tropitidae (e.g., *Tropites* and closely allied forms) and to a lesser extent Arpaditinae. Among the conodonts, the development of *Metapolygnathus* from *Paragondolella* and the diversification of *Mesogondolella* species marks the base of the Carnian (Orchard 2010).

1.3.3 Norian Stage

Mojsisovics (1869: 127) named the Norian Stage for the Roman province of Noria, which was south of the Danube and included what is now the area of Hallstatt, Austria. He based the stage on the Hallstatt Limestone of the Salzkammergut in Austria, strata containing "*Ammonites" (Pinacoceras) metternichi* Mojsisovics (Tozer 1984). Mojsisovics originally thought the Norian was between the "Alpine Muschelkalk" and the Carnian. When that mistake was discovered, Mojsisovics (1892) moved the

term Norian to refer to pre-Carnian Hallstatt strata and named the Juvavian Stage, which is now regarded as synonymous with the Norian. This caused an acrinomius debate with fellow Austrian geologist Bittner (1892), who argued to retain Norian as originally defined and proposed Ladinian to refer to the time interval before the Carnian (Zittel 1901: 494–497; Tozer 1984). Adding further to the confusion, Mojsisovics also provided no type section for the Juvavian, but instead referred to a succession of ammonoid zones (Mojsisovics 1902), a succession critiqued by Kittl (1903) and Diener (1921, 1926).

The stratotype of the Norian has been considered to be the Bicrenatus Lager at Sommeraukogel, Hallstatt (Zapfe 1971; Krystyn and Schlager 1971; Krystyn et al. 1971) (Fig. 1.3). The Norian is generally divided into three substages: Lacian (early), Alaunian (middle) and Sevatian (upper).

Mojsisovics (in Mojsisovics et al. 1895: 1298) used the term Lacian to refer to the "lower Juvavian." He took the name from the Roman name Lacia, which referred to the Salzkammergut area in Austria, and based it on the *Cladiscites ruber* and *Sagenites giebeli* ammonoid zones of the Hallstatt Limestone. As Tozer (1974) stressed, technically the Lacian was based on upper Norian ammonoids, so it is not a designation for the lower Norian, as it is now recognized. However, this technicality has been largely ignored, and Lacian is frequently used to refer to the lower Norian substage (Fig. 1.2).

Mojsisovics (in Mojsisovics et al. 1895: 1298) named the Alaunian substage for the Alauns, a people who lived around the Hallein, Austria area during Roman times. He based it on what is now the *Cyrtopleurites bicrenatus* ammonoid zone, and it is well accepted as the name of the middle Norian substage.

Mojsisovics (in Mojsisovics et al. 1895: 1298) named the Sevatian substage for a Celtic people who lived between the Inn and Enns Rivers in Austria. It was based on the *Pinacoceras metternichi* and *Sirenites argonautae* ammonoid zones in the Hallstatt area. The term is used by many workers to refer to the upper Norian, though Tozer (1974, 1984), who did not recognize the Rhaetian, did not use it. Problems with the Sevatian have largely been associated with defining a Rhaetian base.

The base of the Norian Stage will likely be defined by a GSSP located either at Black Bear Ridge in British Columbia, Canada or at Pizzo Mondello in Sicily (Fig. 1.1), and it probably will be based on a conodont event close to the base of the *Stikinoceras kerri* ammonoid zone, which has been the traditional Norian base in North American usage (Orchard 2010, 2013, 2014). Both candidate sections have relatively poor ammonoid records but good conodont records. However, the choice of a conodont-based GSSP for the Norian base has been delayed for years by changing stratigraphic ranges and the fluid taxonomy of the relevant conodonts (e.g., Mazza et al. 2010, 2011, 2012; Orchard 2010, 2013, 2014).

The base of the Norian and of the Lacian is characterized by major ammonoid biochronological events (Balini et al. 2010; Jenks et al. 2015; Lucas 2017, this volume): the nearly complete disappearance of Tropitidae and the appearance of new members of Juvavitinae, such as *Guembelites* and *Dimorphites*, and of the Thisbitidae, such as *Stikinoceras*. The base of the Alaunian is marked by the appearance of new genera of Cyrtopleuritidae (*Drepanites* and *Cyrtopleurites*). Members

of this family (including *Himavatites*, *Mesohimavatites*, *Neohimavatites*), together with some Haloritinae, such as *Halorites,* and Thisbitidae, such as *Phormedites*, characterize the Alaunian. The base of the Sevatian is characterized by a decrease in ammonoid diversity and the first heteromorphic ammonoid, *Rhabdoceras*. Common Sevatian ammonoids are Haloritinae (*Gnomohalorites* and *Catenohalorites*) and Sagenitidae (*Sagenites* ex gr. *S. quinquepunctatus* Mojsisovics).

Among conodonts, there is a turnover in *Metapolygnathus* species that has been used to mark the base of the Norian (Orchard 2010).

1.3.4 Rhaetian Stage

Gümbel (1859, 1861: 116) used the term "Rhätische Gebilde" to refer to the uppermost Triassic strata (Kössen beds) in the Bavarian Alps. The name was either for the Roman province of Rhaetium or the rätische Alpen. No type locality was specified, but Gümbel did refer to the "Schichten der *Rhaetavicula contorta*" (beds with the bivalve *R. contorta*). Thus, to Mojsisovics et al. (1895), the Rhaetian was the "Zone der *Avicula contorta*."

Lengthy debate about the Rhaetian (e.g., Pearson 1970; Ager 1987; also see above) has focused on three issues: (1) whether or not the stage should be assigned to the Jurassic; (2) whether or not the stage should be recognized or just subsumed into the Norian; and (3) how to define the Rhaetian base.

The Subcommission on Triassic Stratigraphy now recognizes a distinct Rhaetian, which is the youngest Triassic stage (Fig. 1.2). The currently favored definition of the Rhaetian base is the FAD (first appearance datum) of the conodont *Misikella posthersteini* (Krystyn 2010).

In about 2007, the proposed definition of a GSSP for the base of the Rhaetian was at the classic Steinbergkogel section near Hallstatt in Austria based on the FAD (first appearance datum) of the conodont *Misikella posthernsteini* (Krystyn et al. 2007a, b). The favored definition of the Rhaetian base has as its primary signal the FAD of the conodont *Misikella posthernsteini*. This produces a so-called "long" Rhaetian composed of two or three ammonoid zones. The youngest substage of the Norian, the Sevatian, is thereby reduced to one ammonoid zone. However, after 2007, the formal proposal to ratify the base Rhaetian GSSP at Steinbergkogel never went to the International Commisssion on Stratigraphy.

Some would say that was a fortunate delay, as Giordano et al. (2010) and Rigo et al. (2016) concluded that the LO (lowest occurrence) of *Misikella posthernsteini* is actually younger at Steinbergkogel than it is in the section they studied in the Lagonegro basin in northern Italy, though the taxonomy of *M. posthernsteini* may also be an issue. Thus, the LO of *M. posthernsteini* at Steinbergkogel is not the FAD (first appearance datum) of the species. Currently, the Pignola section in the Lagonegro basin is also proposed as the GSSP location for the base of the Rhaetian (Giordano et al. 2010; Rigo et al. 2016; Bertinelli et al. 2016; Casacci et al. 2016).

The appearance of the heteromorphy ammonoids *Cochloceras* and *Paracochloceras* marks the Rhaetian base among ammonoid bioevents (Balini et al. 2010; Jenks et al. 2015; Lucas 2017 this volume). A substantial drop in diversity of conodonts characterizes the Rhaetian, and the appearances of *Epigondolella mosheri* and *Misikella posthersteini*, though not co-eval, approximately mark its base (Orchard 2010).

The base of the Hettangian Stage (= base of the Jurassic, = base of the Lower Jurassic) is defined by the FAD of the ammonoid *Psiloceras spelae* at the Kuhjoch section in Austria (2013). This, of course, defines the top of the Rhaetian (= top of Triassic, = top of Upper Triassic).

1.3.5 Other Upper Triassic Chronostratigraphic Scales

Current stratigraphic practice seeks to recognize a single global stage for each interval of time, and each series and system base corresponds to the base of a stage. Furthermore, the definition of stages is now based on the GSSP concept and the practice of integrated stratigraphy that applies multiple data sets to the definition of chronostratigraphic units (e.g., Salvador 1994; Remane et al. 1996; Walsh et al. 2004; Smith et al. 2015). However, the provinciality of fossil taxa compounded by limitations of facies distributions (rarely is any taxon or facies global in extent) have often prevented universal recognition and use of a single chronostratigraphic terminology. Indeed, there remains great value in provincial stages, which Cope (1996) has aptly called the "secondary standard" in stratigraphy.

The Triassic has a variety of secondary standards, including that for New Zealand—(ascending) Oretian, Otamitan, Warepan and Otapirian stages encompass the Upper Triassic (e.g., Carter 1974). Here, I do not review these provincial scales, but note that their regional utility will guarantee their continued use.

1.4 Radioisotopic Ages

Ogg (2004, 2012), Mundil et al. (2010) and Ogg et al. (2014) reviewed the Late Triassic numerical timescale (Fig. 1.4). A precise and detailed numerical timescale does not yet exist for the Late Triassic because of the rarity of datable volcanic ash beds that can be correlated unambiguously to marine biostratigraphy.

The few ages that meet those criteria, and that have been published in full, are: (1) various U-Pb ages on ash beds in marine Ladinian strata that indicate the base of the Carnian is no older than 237 Ma (Mundil et al. 2010; Stockar et al. 2012; Ogg et al. 2014); (2) a U-Pb single zircon age of 230.9 ± 0.3 Ma on an ash bed in Italy within the upper Carnian (Tuvalian) *Metapolygnathus nodosus* conodont zone (Furin et al. 2006); (2) U-Pb ages of 205.70 ± 0.15 Ma and 205.30 ± 0.14 Ma on ash beds that bracket the base of the Rhaetian (picked largely on the disappearance of

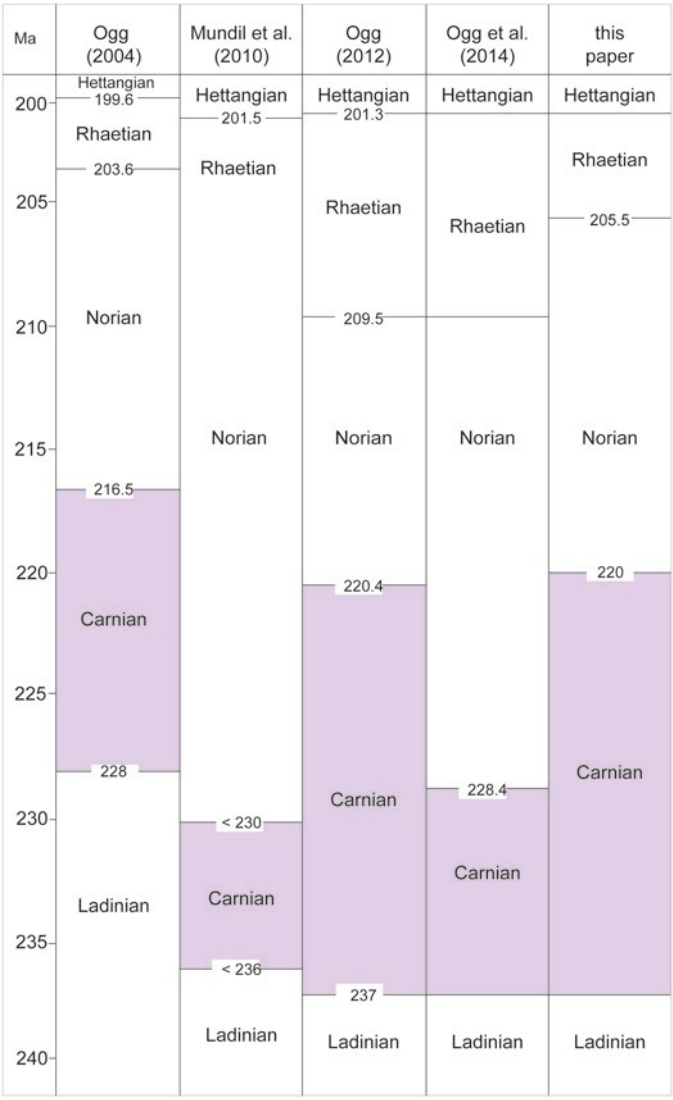

Fig. 1.4 Some Late Triassic numerical timescales of the last 20 years

the bivalve *Monotis*) in Peru (Wotzlaw et al. 2014); and (3) another ash bed in the Peruvian section that yields a U-Pb age of 201.36 ± 0.17 Ma that is just below the LO of *Psiloceras spelae*, and thus just below the base of the Jurassic (Schaltegger et al. 2008; Schoene et al. 2010; also see the detrital zircon ages of Rhaetian strata in western Canada reported by Golding et al. 2016). Most of the other numerical ages being used to calibrate the Late Triassic timescale are detrital zircon ages, which means they are from reworked zircon grains, and thus provide maximum ages of deposition at best.

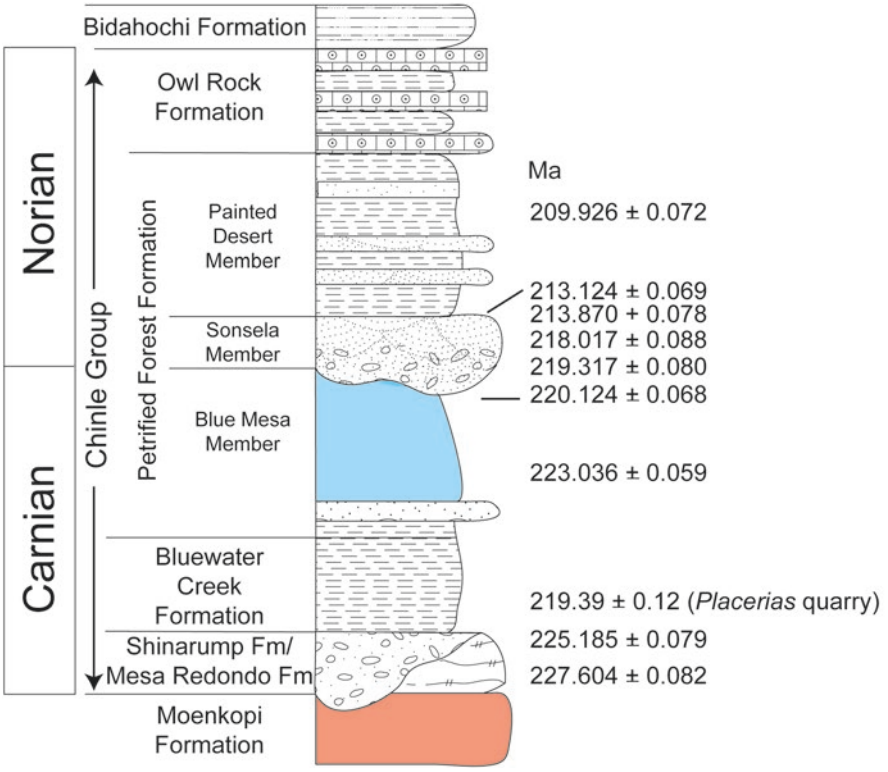

Fig. 1.5 Summary of most of the Chinle Group detrital zircon ages placed on a generalized Chinle lithostratigraphy of the Petrified Forest National Park in Arizona. Sources of numerical ages are primarily Ramezani et al. (2011, 2014). Note that stratigraphic position, supported by biostratigraphy, indicates the age of the *Placerias* quarry reported by Ramezani et al. (2014) is younger than stratigraphically higher ages

Lucas et al. (2012) reviewed these detrital zircon ages, which are mostly from the Upper Triassic Chinle Group, nonmarine fluvial strata in the American Southwest (Fig. 1.5). They also reviewed some other, non-detrital ages, such as those from the Carnian Ischigualasto Formation in Argentina (Rogers et al. 1993; Shipman 2004; Currie et al. 2009; Martínez et al. 2013; Kent et al. 2014). Using the biostratigraphy of palynomorphs, conchostracans and vertebrate fossils advocated by Lucas et al. (2012, and references therein), the lower part of the Chinle Group is Carnian, with the base of the Norian close to the base of the Sonsela Member of the Petrified Forest Formation and its correlatives. The Chinle Group detrital zircon ages (Fig. 1.5) indicate that the inferred base of the Norian (~ base of Sonsela Member) is no older than about 220–222 Ma, and the other ages reviewed by Lucas et al. (2012) are either consistent with that conclusion or are unreliable.

Since the review of Lucas et al. (2012), only a few numerical ages relevant to the age of the Norian base have become available. Thus, in an abstract, Diakow et al. (2011) reported a U-Pb age of 224.52 ± 0.22 Ma from a tuff below early middle

Norian conodonts and 223.81 ± 0.78 Ma from a tuff below early Norian conodonts. These ages suggest a Norian base older than 223 Ma, but remain to be fully documented. Indeed, given that the two ages repoported by Diakow et al. (2011) are out of order (older above younger), the reliability of these ages may be questioned.

Atchley et al. (2013) reported two detrital zircon U-Pb ages from Chinle Group strata in Arizona—227.604 ± 0.082 Ma at about the base of the Chinle Group (Carnian by the Lucas et al. 2012 correlation) and 220.124 ± 0.068 Ma from a stratigraphic level close to the Carnian-Norian boundary using the Lucas et al. (2012) correlation. These ages are concordant and consistent with Chinle Group detrital zircon ages reported by Ramezani et al. (2011) (see Ramezani et al. 2014, Fig. 2) and suggest a Norian base no older than about 220–222 Ma.

However, a U-Pb age recently reported from Chinle Group strata in eastern Arizona by Ramezani et al. (2014) is not consistent with the earlier published ages. This is an age of 219.39 ± 0.16 Ma from near the base of the Chinle Group at the *Placerias* fossil locality in Arizona. Stratigraphic position puts this age well below a series of ages in the 220–227 Ma range reported by Ramezani et al. (2011) and Atchley et al. (2013). To explain this contradiction, Ramezani et al. (2014) claim massive lateral facies changes in the lower Chinle lithosome, and even conclude that "geochronological correlation independent of conventional stratigraphic methods [lithostratigraphy, biostratigraphy] is the only viable means for deciphering the depositional history of rock similar to the Chinle Formation" (p. 995). I prefer instead to rely on a century of geologic mapping, detailed lithostratigraphic analysis and the biostratigraphy of palynomorphs, conchostracans and vertebrates (e.g., Heckert and Lucas 2002 and references cited therein, particularly Darton 1910, 1928; Cooley 1957; Stewart et al. 1972) that demonstrates that the *Placerias* quarry numerical age of Ramezani et al. (2014) is stratigraphically below many older numerical ages. The *Placerias* quarry age is thus anomalously young, possibly due to postcrystallization lead loss.

Very recently, Kohút et al. (2017) published the ages of syn-sedimentary volcanic zircons from the Carnian of Slovakia that have a concordia age of 221.2 ± 1.6 Ma. This also runs contrary to the "long Norian" having a base as old as 227–228 Ma.

In summary, numerical ages can be assigned to the Upper Triassic stage boundaries with varying degrees of precision (Fig. 1.4; also see Mundil et al. 2010; Lucas et al. 2012; Ogg et al. 2014). However, more numbers on primary ash fall deposits that can be correlated unambiguously to marine biostratigraphy are needed to resolve current uncertainties and contradictions among datasets.

1.5 Magnetostratigraphy

There is no agreed GPTS (global polarity timescale) for the Triassic, although a composite GPTS is now becoming available based on successions assembled from marine and nonmarine sections in North America, Europe, and Asia. Hounslow and Muttoni (2010) provided a comprehensive review of Triassic magnetic polarity

history. I rely on this review and some more recent data and reappraisals (e.g., Lucas et al. 2011, 2012) and also emphasize the multichron concept of Lucas (2011), which recognizes intervals of dominant polarity rather than individual polarity chrons. The reason for this is that we are a long way from a well-established succession of Triassic polarity chrons that can receive numbers (or names), like those of the Late Cretaceous-Cenozoic GPTS. We do, however, at least seem to know the polarity of each of the Triassic stage boundaries and the dominant polarity of the stages with some confidence (Hounslow and Muttoni 2010).

One of the largest hindrances to developing a Triassic GPTS is the polarity record of the Newark Supergroup of eastern North America, which has confounded all attempts to correlate it to other Late Triassic magnetostratigraphic records (Fig. 1.6). The Newark Supergroup is the thick (up to 4.5 km) succession of nonmarine sedimentary and intercalated igneous rocks of Triassic and Jurassic age that filled a series of half-graben extensional basins that developed along the eastern seaboard of North America as Pangea began to fragment (e.g., Manspeizer et al. 1978; Froehlich and Olsen 1984; Manspeizer 1988; Olsen 1997; Weems et al. 2016) (Fig. 1.1). A complete Newark magnetostratigraphy, obtained from overlapping drill cores in the Newark basin of New Jersey-Pennsylvania, USA, is arguably the single most complete record of Late Triassic magnetic polarity history available (Fig. 1.6).

Given the great thickness of the Newark section (~ 4 km of section is equivalent to much of the Late Triassic), it likely captures a more complete polarity history than do the much thinner marine sections in Europe for which a magnetic polarity record is available. That, however, is the only thing to recommend the Newark magnetic polarity record, because age control of this record is highly problematic. For decades, the Triassic-Jurassic boundary was located incorrectly in the Newark, below the CAMP basalt sheets; this has only recently been corrected (Kozur and Weems 2005, 2007, 2010; Lucas and Tanner 2007; Cirilli et al. 2009; Lucas et al. 2011).

Biostratigraphic placement of the Carnian-Norian boundary in the Newark (near the base of the Passaic Formation) is one of the few tiepoints to the SGCS and is based on reinforcing correlations from palynomorphs, conchostracans and vertebrate biostratigraphy (Lucas et al. 2012). Abandonment of this boundary was based on an unsupportable correlation of magnetostratigraphy in the marine section at Pizzo Mondello in Italy with the Newark and, coupled with a supposed astronomically-calibrated timescale based on Newark cyclostratigaphy, created the proposal that the Carnian-Norian boundary is at about 228 Ma, the so-called "long Norian" (Muttoni et al. 2004). Correct placement of the Carnian-Norian boundary in the Newark section means it and the beginning of the Jurassic are the only reliable biostratigraphic tiepoints for the Newark magnetic polarity stratigraphy. Placement of any subdivisions of the Carnian and Norian, including identification of the base of the Rhaetian, are currently impossible in the Newark section.

From its initial publication, no convincing correlation of the Newark magnetostratigraphy to broadly correlative magnetostratigraphies could be made, simply because it contains approximately 10 times the number of reversals found in correlative marine sections (Fig. 1.6). Indeed, alternative correlations of the Newark magnetostratigraphy to a GPTS for the Late Triassic based on marine sections are at

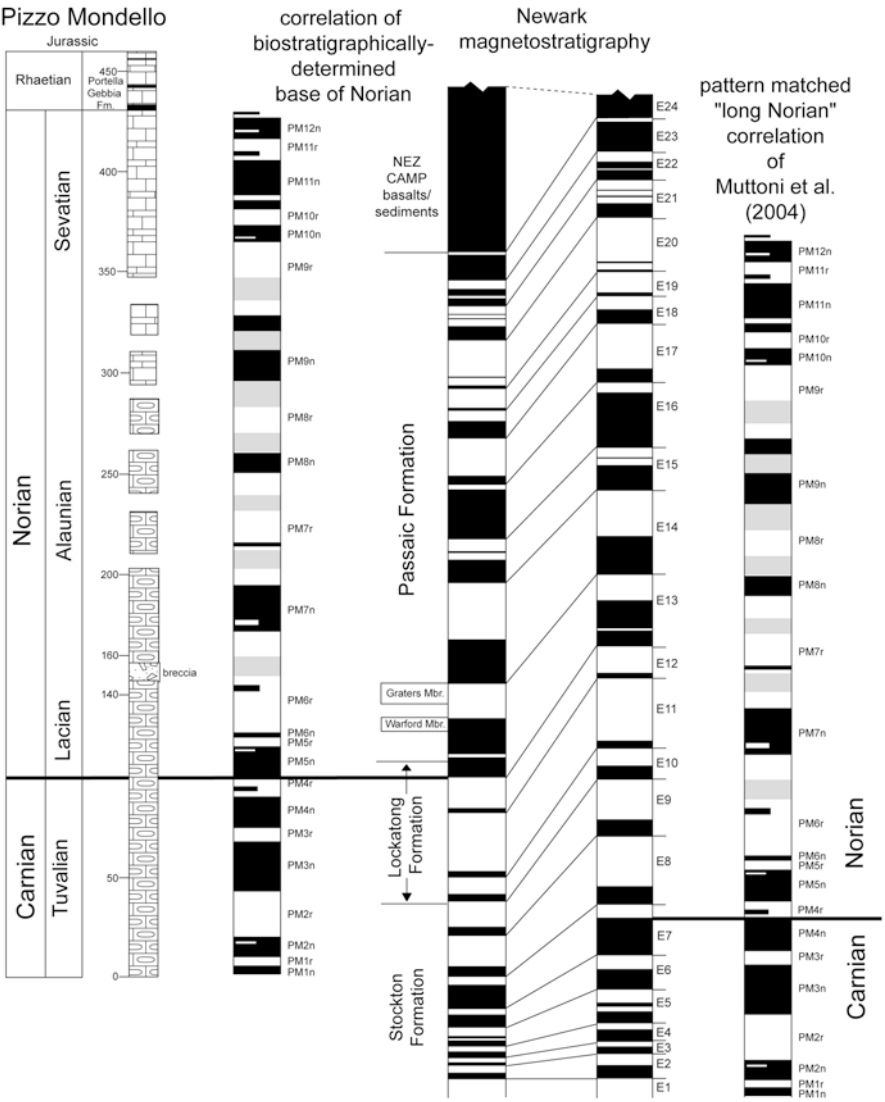

Fig. 1.6 Magnetostratigraphic correlations of the Pizzo Mondello (Sicily) and Newark (USA) sections. On the left, the correlation matches the marine and nonmarine, biostratigraphically-determined Carnian-Norian boundary. On the right is the "pattern matched" correlation of Muttoni et al. (2004), which became the basis of the "long Norian" (after Lucas et al. 2012)

best multichron matches, not detailed correlations of chrons (Hounslow and Muttoni 2010, Fig. 12). Given what I call the rubber ruler effect—sedimentation rate stretches or contracts magnetic polarity chron thicknesses so that matching patterns can be difficult—and the lack of biostratigraphic tiepoints, how could any unambiguous correlation of the Newark magnetostratigraphy be made to other polarity

stratigraphies? And, why use the Newark polarity history as the standard column for the Late Triassic if nothing else can be correlated to it? Indeed, attempts to correlate the Newark polarity record to broadly co-eval records have produced a fractious literature with little agreement on what correlations are reliable. Both Hounslow and Muttoni (2010) and Ogg (2012) have presented the "Solomenesque" solution of advocating at least two correlations ("long Carnian" and "long Norian"), neither of which is defensible (Lucas et al. 2012).

More recent problems with attempting to pattern match the magnetostratigraphy of Rhaetian marine sections to the Newark section are well revealed by Muttoni et al. (2010), Hüsing et al. (2011) and Maron et al. (2015). Thus, Hüsing et al. (2011) present the magnetostratigraphy of the Rhaetian section at Steinbergkogel, Austria (it is mostly of reversed polarity) and match the Rhaetian base to the E16n chron in the Newark magnetostratigraphy. Using the astrochronology of the Newark section of Kent and Olsen (1999), they assign the Rhaetian base an age of ~211 Ma. Muttoni et al. (2010) report the magnetostratigraphy of Rhaetian marine sections in the southern Alps of northern Italy. The polarity patterns (mostly normal polarity) of these sections are very different from that reported by Hüsing et al. (2011). Muttoni et al. (2010) pattern match their results to the Newark magnetostratigraphy to correlate the Rhaetian base to the E17r-E19r interval of the Newark, which is in the range of 207–210 Ma according to the Newark astrochronology. In contrast, Maron et al. (2015) honor a Rhaetian base at ~205 Ma in their attempt to correlate the magnetostratigraphy of Rhaetian strata in the Lagonegro basin of Italy. However, there is no clear pattern match of the Newark magnetostratigraphy to the magnetostratigraphies of the Italian and Austrian sections, as is clear from Maron et al. (2015, Fig. 1.6).

The Late Triassic magnetic polarity timescale I advocate is a set of multichrons (Fig. 1.7). This is a realistic abstraction of what we now know about the Late Triassic GPTS. The obvious way forward in advancing Late Triassic magnetostratigraphy is to ignore the Newark record for the time being and improve the GPTS for the Late Triassic based on marine sections (cf. Hounslow and Muttoni 2010). This still faces the problem that if the Newark polarity record is more complete than the marine records, then the marine sections must contain substantial hiatuses. Much more needs to be understood about Late Triassic magnetic polarity history to make it an important part of Triassic correlation and timescale definition.

1.6 Cyclostratigraphy

At present, a cyclostratigraphy-based numerical timescale, called the astronomical timescale (ATS), is reasonably well-established for much of Cenozoic time. Older parts of the timescale have less complete, disconnected cyclostratigraphies that have been referred to as "floating astrochronologies" (e.g., Hinnov and Ogg 2007). The Newark Supergroup strata in the Newark basin have an inferred cyclostratigraphy that has been proposed as one such floating astrochronology capable of providing a high resolution geochronometry for most of the Late Triassic and the older part of

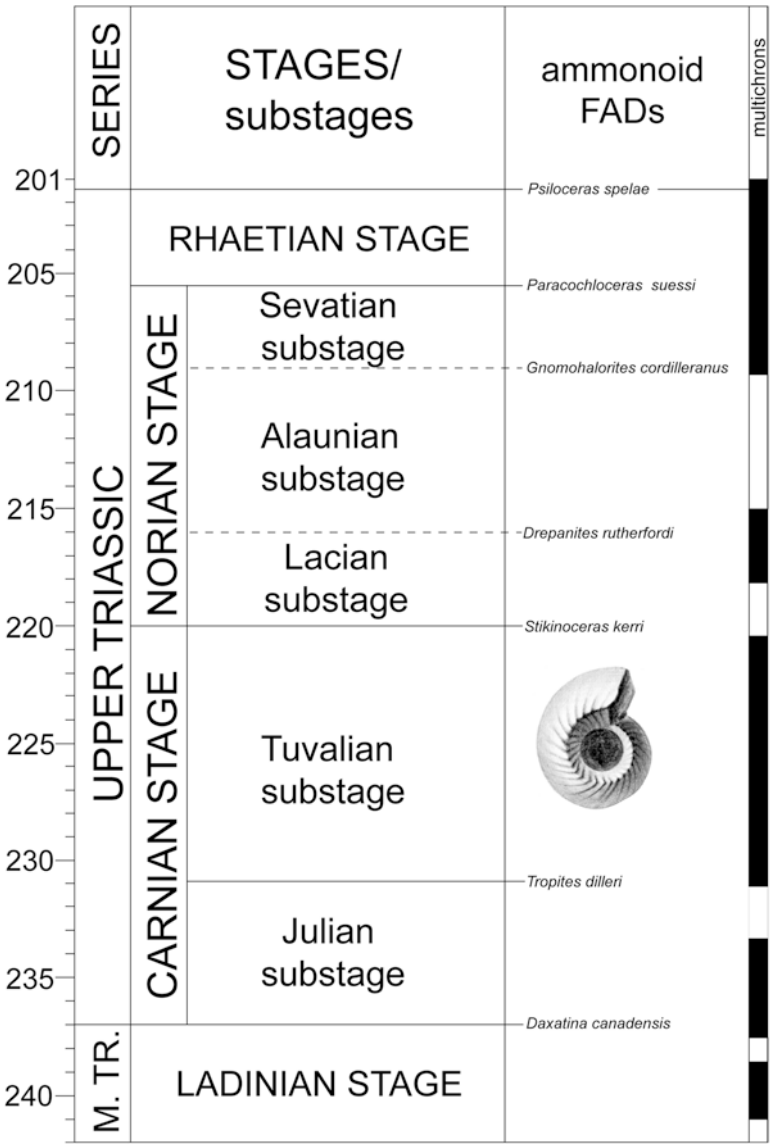

Fig. 1.7 A Late Triassic timescale

the Early Jurassic (Olsen and Kent 1996; Olsen et al. 1996, 2011; Kent and Olsen 1999; Olsen and Whiteside 2008; Ogg 2012; Kent et al. 2017).

Thus, spectral analyses of apparent cyclicity of Triassic-Jurassic strata in the Newark basin have been used to generate peak recurrence intervals within the sequence. When calibrated to sedimentation rates derived from varve counts in lacustrine mudstones, these recurrence intervals yield cycles inferred to correspond

to orbital forcing at basic precession, eccentricity and long eccentricity frequencies. Consequently, the Newark basin cyclostratigraphy has been proposed as a floating astrochronology capable of providing a continuous high resolution geochronometry for most of the Late Triassic and part of the Early Jurassic.

Orbitally-forced cyclicity does appear to be the dominant control of some portions of the Newark basin section. But, the application of the Newark basin cyclostratigraphy as chronostratigraphy requires that the stratigraphic record is complete (no substantial erosional or depositional gaps exist) and cyclical throughout. Several lines of evidence indicate that these requirements are not met (Tanner and Lucas 2015). Outcrop and core data demonstrate that portions of the Newark Basin stratigraphic section are non-cyclic, particularly in the fluvial-dominated strata of the upper Passaic Formation and the Stockton Formation. Correlation of available biostratigraphic data, including both pollen and conchostracan zones between the Newark Supergroup and the Germanic Keuper, indicates that most of Rhaetian and a portion of late Norian time is not represented by sediment in the Newark basin and elsewhere in the Newark Supergroup (Kozur and Bachmann 2005, 2008; Kozur and Weems 2005, 2007, 2010; Weems and Lucas 2015; Weems et al. 2016). This suggests that at least 3 million years of Late Triassic time are not recorded by strata in the Newark Basin.

Indeed, the inability of the Newark cyclostratigraphy to locate and date the base of the Rhaetian or to produce a numerical age for the base of the Norian compatible with independently derived constraints demonstrate that the Newark Basin cyclostratigraphy is not a valid "floating astrochronology." At best, only the middle late Carnian through early late Norian interval, about 10 my in duration, may be sufficiently complete to be useful for astrochronological purposes (Tanner and Lucas 2015).

Ikeda and Tada (2014) have presented another "floating astrochronology" for the Triassic-Early Jurassic based on bedded cherts in Japan that they claim record a range of orbitally-forced cycles. They refer to this as the Inuyama ATS, principally tuned by 405-kyr eccentricity cycles and anchored to the end-Triassic radiolarian extinction to which they assign a numerical age of 201.4 ± 0.2 Ma. However, this astrochronology is questionable. As an example, Ikeda and Tada (2014) claim that their astrochronology establishes a Rhaetian base (identified as close to the LO of the conodont *Epigondolella* and of the radiolarian *Betraccium deweveri*: Carter and Orchard 2007) close to 210 Ma, which conflicts with what appear to be reliable radioistopic ages that make it much younger, close to 205 Ma. Similarly, the Inuyama ATS supposedly supports the long Norian with its base close to 228 Ma. Instead, the presentation of the cyclostratigraphy of the Japanese bedded cherts is very incomplete and not convincingly tied to Milankovitch cycles, which may explain its evident inaccuracy as an ATS.

1.7 Isotope Stratigraphy

Determination of the history of fluctuations in isotopic values in stratigraphic successions—isotope stratigraphy or chemostratigraphy—is increasingly important in the Triassic (Tanner 2010; Ogg 2012; McArthur et al. 2012; Saltzman and Thomas

2012). In order to create a usable isotope stratigraphy the isotopic history of multiple sections with well established ages needs to be obtained so that local effects can be ruled out and a global pattern can be established. At present, such data are being established in parts of the Triassic for carbon and strontium isotopes. In the Late Triassic, only the late Rhaetian negative excursion of carbon has been verified in multiple sections with good age constraints and thus is of value to correlation (Lucas et al. 2007).

The most widely studied isotope has been $\delta^{13}C$, and, indeed, the carbon isotope record for the Triassic System is now known generally, and, in some parts of the Triassic, it has been established in some detail. Relative isotopic stability characterizes much of the Middle and Upper Triassic, with pronounced negative excursions in the early Carnian and late Rhaetian that have been linked to significant biotic turnover (e.g., Korte et al. 2005; Dal Corso et al. 2012). A brief positive excursion of $\delta^{13}C$ at the Norian-Rhaetian boundary coincides with an extinction of deep water invertebrates (Sephton et al. 2002; Rigo et al. 2016). Some workers have considered the late Rhaetian carbon isotope excursion to be at the Triassic-Jurassic boundary (for example, McElwain et al. 2007), but it is actually well constrained in various sections as a late Rhaetian event (Lucas et al. 2007; von Hillebrandt et al. 2013).

General trends in the fluctuation in $^{87}Sr/^{86}Sr$ ratios have also been established for the Late Triassic (e.g., Korte et al. 2003; McArthur et al. 2012; Tackett et al. 2014). The strontium isotope stratigraphy shows an early Carnian minimum, and a peak in the late Norian followed by a fall during the Rhaetian.

The construction of reliable global carbon and strontium isotope curves for the Late Triassic is thus well underway. These curves, with judicious calibration, should become an increasingly important tool for Late Triassic correlation. However, isotope curves, like magnetostratigraphy, are not independent correlation tools and always need to be tied to biostratigraphic or radioisotopic data in order to be of value in correlation.

1.8 Conclusion: A Late Triassic Timescale

The Late Triassic timescale presented here (Fig. 1.7) incorporates the traditional chronostratigraphic subdivisions. Numerical age control of the bases of the Carnian, Rhaetian and Hettangian stages is relatively good, but the numerical age of the base of the Norian remains open to discussion. The magnetostratigraphic record is a series of multichrons that identify the Carnian, early Norian and late Norian-Rhaetian as dominantly of normal polarity. Ammonoid bioevents that could potentially define stage and substage bases are indicated.

This review demonstrates that the Late Triassic timescale is still very much a work in progress. Greater precision and stability needs more precise chronostratigraphic definitions, additional numerical ages directly related to marine biostratigraphy, a wholesale rethinking of magnetostratigraphic correlations and additional cyclostratigraphic and isotopic data.

Acknowledgments I am grateful to numerous colleagues, and particularly members of the STS, for educating me about the Triassic timescale during the last 25 years. Chris McRoberts provided the base map for Figure 1, and Karl Krainer assisted with the preparation of Figure 3. Mark Hounslow and Larry Tanner provided helpful reviews of the manuscript.

References

Ager D (1987) A defense of the Rhaetian Stage. Albertiana 6:4–13

Atchley SC, Nordt LC, Dworkin SJ, Ramezani J, Parker WG, Ash SR, Bowring SA (2013) A linkage among Pangean tectonism, cyclic alluviation, climatic change, and biologic turnover in the Late Triassic: The record from the Chinle Formation, southwestern United States. J Sed Res 83:1147–1161

Balini M, Lucas SG, Jenks JF, Spielmann JA (2010) Triassic ammonoid biostratigraphy: An overview. In: Lucas SG (ed) The Triassic timescale. Geological Society London Special Publications, vol 334, pp 221–262

Bertinelli A, Casacci M, Concheri G, Gattolin G, Godfrey L, Katz ME, Maron M, Mazza M, Mietto P, Muttoni G, Rigo M, Sprovieri M, Stellin F, Zaffani M (2016) The Norian/Rhaetian boundary interval at Pignola-Abriola section (Southern Apennines, Italy) as a GSSP candidate for the Rhaetian Stage: An update. Albertiana 43:5–18

Carter RM (1974) A New Zealand case-study of the need for local time-scales. Lethaia 7:181–202

Carter ES, Orchard MJ (2007) Radiolarian-conodont-ammonoid intercalibration around the Norian-Rhaetian boundary and implications for trans-Panthalassan correlation. Albertiana 36:146–163

Casacci M, Bertinelli A, Algeo TJ, Rigo M (2016) Carbonate-to-biosilica transition at the Norian-Rhaetian boundary controlled by rift-related subsidence in the western Tethyan Lagonegro basin (southern Italy). Palaeogeog, Paleoclimat, Palaeoecol 456:21–36

Cirilli S, Marzoli A, Tanner LH, Bertrand H, Buratti N, Jourdan F, Bellieni G, Kontak D, Renne PR (2009) Late Triassic onset of the Central Atlantic Magmatic Province (CAMP) volcanism in the Fundy Basin (Nova Scotia): New stratigraphic constraints. Earth Planet Sci Lett 286:514–525

Cooley ME (1957) Geology of the Chinle Formation in the upper Little Colorado drainage area, Arizona and New Mexico. MS thesis, University of Arizona, Tucson

Cope JCW (1996) The role of the secondary standard in stratigraphy. Geol Mag 133:107–110

Currie BS, Colombi CE, Tabor NJ, Shipman TC, Montanez IP (2009) Stratigraphy and architecture of the Upper Triassic Ischigualasto Formation, Ischigualasto Provincial Park, San Juan, Argentina. J S Am Earth Sci 27:74–87

Dal Corso J, Mietto P, Newton RJ, Pancost RD, Preto N, Roghi G, Wignall PB (2012) Discovery of a major negative $\delta^{13}C$ spike in the Carnian (Late Triassic) linked to the eruption of Wrangellia flood basalts. Geology 40:79–82

Darton NH (1910) A reconnaissance of parts of northwestern New Mexico and northern Arizona. US Geol Surv Bull 435:1–88

Darton NH (1928) "Red beds" and associated formations in New Mexico with an outline of the geology of the state. US Geol Surv Bull 794:1–356

Diakow L, Orchard MJ, Friedman R (2011) Absolute age for the Norian Stage: A contribution from southern British Columbia, Canada. Canad Paleont Conf Proc 9:27–28

Diener C (1921) Die Faunen der Hallstatter Kalke des Feuerkogels bei Aussee. Akad Wiss Wien, Math-naturwiss Klasse Sitzungsber 130:21–33

Diener C (1926) Die Fossillagerstätten in den Halstätter Kalken des Salzkammergutes. Akad Wissen Wien, Math-naturwiss Klasse Sitzungsber 135:73–101

Froelich AJ, Olsen PE (1984) Newark Supergroup, a revision of the Newark Group in eastern North America. US Geol Surv Bull 1537-A:A55–A58

Furin S, Preto N, Rigo M, Roghi G, Gianolla P, Crowley JL, Bowring SA (2006) High-precision U-Pb zircon age from the Triassic of Italy: Implications for the Triassic time scale and the Carnian origin of calcareous nannoplankton and dinosaurs. Geology 34:1009–1012

Gaetani M (1996) The International Subcommission on Triassic Stratigraphy. Albertiana 18:3–4

Gaetani M (2009) GSSP of the Carnian Stage defined. Albertiana 37:36–38

Giordano N, Rigo M, Ciarapica G, Bertinelli A (2010) New biostratigraphical constraints for the Norian/Rhaetian boundary: Data from Lagonegro basin, Southern Appenines, Italy. Lethaia 43:573–586

Golding ML, Mortensen JK, Zonneveld J-P, Orchard MJ (2016) U-Pb isotopic ages of euhedral zircons in the Rhaetian of British Columbia: Implications for Cordilleran tectonics during the Late Triassic. Geosphere 12:1606–1161

Harland WB, Cox AV, Llewellyn PG, Pickton CAG, Smith AG, Walters R (1982) A geologic time scale. Cambridge University Press, Cambridge

Harland WB, Armstrong RL, Cox AV, Craig LE, Smith AG, Smith DG (1990) A geologic time scale. Cambridge University Press, Cambridge

Heckert AB, Lucas SG (2002) Lower Chinle Group (Upper Triassic: Carnian) stratigraphy in the Zuni Mountains, west-central New Mexico. New Mex Mus Nat Hist Sci Bull 21: 51–72

Hinnov LA, Ogg JG (2007) Cyclostratigraphy and the astronomical timescale. Strat 4:239–251

Hounslow MW, Muttoni G (2010) The geomagnetic polarity timescale for the Triassic: Linkage to stage boundary definitions. In: Lucas SG (ed) The Triassic timescale. Geol Soc London Spec Publ, vol 334, pp 61–102

Hüsing SK, Deenen MHL, Koopmans JG, Krijgsman W (2011) Magnetostratigraphic dating of the proposed Rhaetian GSSP at Steinbergkogel (Upper Triassic, Austria): Implications for the Late Triassic time scale. Earth Planet Sci Lett 302:203–216

Ikeda M, Tada R (2014) A 70 million year astronomical time scale for the deep-sea bedded chert sequence (Inuyama, Japan): Implications for Triassic-Jurassic geochronology. Earth Planet Sci Lett 399:30–43

Jenks JF, Monnet C, Balini M, Brayard A, Meier M (2015) Biostratigraphy of Triassic ammonoids. In: Klug C et al (eds) Ammonoid paleobiology: From macroevolution to paleogeography. Top Geobiol, vol 44. Springer, Dordrecht, pp 329–388

Kent DV, Olsen PE (1999) Astronomically tuned geomagnetic polarity time scale for the Late Triassic. J Geophys Res 104:12831–12841

Kent DV, Malnis PS, Colombi CE, Alcober OA, Martinez RD (2014) Age constraints on the dispersal of dinosaurs in the Late Triassic from magnetochronology of the Los Colorados Formation (Argentina). Proc Nat Acad Sci USA 111:7958–7963

Kent DV, Olsen PE, Muttoni G (2017) Astrochronostratigraphic polarity time scale (ATS) for the Late Triassic and Early Jurassic from continental sediments and correlation with standard marine stages. Earth-Sci Rev 166:153–180

Kittl E (1903) Geologische Exkursionen im Salzkammergut. 9th Internat Geol Congr, Vienna 1903, Führer Exkurs Österr, 4, part 3

Kohút M, Hofmann M, Havrila M, Linnemann U, Havrila J (2017) Tracking an upper limit of the "Carnian crisis" and/or Carnian Stage in the Western Carpathians (Slovakia). Internat J Earth Sci. doi: 10.10007/s00531-017-1491-8

Korte C, Kozur HW, Bruckschen P, Veizer J (2003) Strontium isotope evolution of late Permian and Triassic seawater. Geochim Cosmochim Acta 67:47–62

Korte C, Kozur HW, Veizer J (2005) $\delta^{13}C$ and $\delta^{18}O$ values of Triassic brachiopods and carbonate rocks as proxies for coeval seawater and palaeotemperature. Palaeogeog Palaeoclimat Palaeoecol 226:287–306

Kozur HW, Bachmann GH (2005) Correlation of the Germanic Triassic with the international scale. Albertiana 32:21–35

Kozur HW, Bachmann GH (2008) Updated correlation of the Germanic Triassic with the Tethyan scale and assigned numeric ages. Berich Geol Bundes-Anstalt 76:53–58

Kozur H, Weems RE (2005) Conchostracan evidence for a late Rhaetian to early Hettangian age for the CAMP volcanic event in the Newark Supergroup, and a Sevatian (late Norian) age for the immediately underlying beds. Hall Jahrb Geowisse B27:21–51

Kozur H, Weems RE (2007) Upper Triassic conchostracan biostratigraphy of the continental rift basins of eastern North America: Its importance for correlating Newark Supergroup events with the Germanic basin and the international geologic timescale. New Mex Mus Nat Hist. Sci Bull 41:137–188

Kozur HW, Weems RE (2010) The biostratigraphic importance of conchostracans in the continental Triassic of the northern hemisphere. In: Lucas SG (ed) The Triassic timescale. Geol Soc London Spec Publ 334: 315–417

Krystyn L (1978) Eine neue Zonengliederung im alpin-mediterranean Unterkarn. Schriftenr Erdwissen Kommiss Oster Akad Wissen 4:37–75

Krystyn L (1980) Stratigraphy of the Hallstatt region. Abhand Geol Bundesan Wien 35:69–98

Krystyn L (2010) Decision report on the defining event for the base of the Rhaetian stage. Albertiana 38:11–12

Krystyn L, Schlager W (1971) Der Stratotypus des Tuval. Ann Instit Geol Pub Hungar 54:591–605

Krystyn L, Boquerel H, Kuerschner W, Richoz S, Gallet Y (2007a) Proposal for a candidate GSSP for the base of the Rhaetian Stage. New Mex Mus Nat Hist. Sci Bull 41:189–199

Krystyn L, Richoz S, Gallet Y, Boquerel H, Kurschner W, Spötl C (2007b) Updated bio- and magnetostratigraphy from Steinbergkogel (Austria), candidate GSSP for the base of the Rhaetian Stage. Albertiana 36:164–173

Kummel B (1979) Treatise on Invertebrate Paleontology. Part A. Triassic. Geol Soc Am, Univ Kansas, Boulder and Lawrence, pp 351–389

Lieberman HM (1980) The suitability of the Raibl sequence as a stratotype for the Carnian Stage and the Julian Substage of the Triassic. Newsl Strat 9:35–42

Lucas SG (1999) The epicontinental Triassic, an overview. Zentralbl Geol Paläont Teil I 1998:475–496

Lucas SG (2010) The Triassic chronostratigraphic scale: History and status. In: Lucas SG (ed) The Triassic timescale. Geol Soc London Spec Publ 334: 17–39

Lucas SG (2011) Multichron. Lethaia 43:282

Lucas SG (2013) A new Triassic timescale. New Mex Mus Nat Hist. Sci Bull 61:366–374

Lucas SG (2017) Late Triassic Ammonoids: distribution, biostratigraphy and biotic events. In: Tanner LH (ed) The Late Triassic world: earth in a time of transition. Topics in geobiology, Springer (this volume)

Lucas SG, Orchard MJ (2004) Triassic. In: Selley RC, Cocks LMR, Plimer IR (eds) Encyclopedia of geology. Elsevier, Amsterdam, pp 344–351

Lucas SG, Tanner LH (2007) The nonmarine Triassic-Jurassic boundary in the Newark Supergroup of eastern North America. Earth Sci Rev 84:1–20

Lucas SG, Taylor DG, Guex J, Tanner LH, Krainer K (2007) The proposed global stratotype section and point for the base of the Jurassic System in the New York Canyon area, Nevada, USA: New Mex Mus Nat Hist. Sci Bull 40:139–168

Lucas SG, Tanner LH, Donohoo-Hurley LL, Geissman JW, Kozur HW, Heckert AB, Weems RE (2011) Position of the Triassic-Jurassic boundary and timing of the end- Triassic extinctions on land: Data from the Moenave Formation on the southern Colorado Plateau, USA. Palaeogeog Palaeoecol Palaeoclimatol 302:194–205

Lucas SG, Tanner LH, Kozur HW, Weems RE, Heckert AB (2012) The Late Triassic timescale: Age and correlation of the Carnian-Norian boundary. Earth-Sci Rev 114:1–18

Manspeizer W (1988) Triassic-Jurassic rifting and opening of the Atlantic: an overview. In: Manspeizer W (ed) Triassic-Jurassic rifting, continental breakup, and the formation of the Atlantic Ocean and passive margins. Elsevier, Amsterdam, Developments in Geotectonics, pp 22–41

Manspeizer W, Puffer JH, Cousimer HL (1978) Separation of Morocco and eastern North America: a Triassic-Liassic stratigraphic record. Geol Soc Amer Bull 89:901–920

Maron M, Rigo M, Bertinelli A, Katz ME, Godfrey L, Zaffani M, Muttoni G (2015) Magnetostratigraphy, biostratigraphy, and chemostratigraphy of the Pignola-Abriola section: New constraints for the Norian-Rhaetian boundary. Geol Soc Amer Bull 127:962–974

Martínez RN, Apaldetti C, Alcober OA, Colombi CE, Sereno PC, Fernandez E, Malnis PS, Correa GA, Abelin D (2013) Vertebrate succession in the Ischigualasto Formation. J Vert Paleont Mem 12:10–20

Mazza M, Furin S, Spotl C, Rigo M (2010) Generic turnovers of Carnian/Norian conodonts: Climatic control or competition? Palaeogeogr Palaeoclimat Palaeoecol 290:120–137

Mazza M, Rigo M, Nicora A (2011) A new *Metapolygnathus* platform conodont species and its implications for upper Carnian global correlations. Acta Palaeont Polon 56:121–131

Mazza M, Rigo M, Gullo M (2012) Taxonomy and stratigraphic record of the Upper Triassic conodonts of the Pizzo Mondello section (western Sicily, Italy), GSSP candidate for the base of the Norian. Riv Ital Paleont Strat 118:85–130

McArthur JM, Hawarth RJ, Shields GA (2012) Strontium isotope stratigraphy. In: Gradstein FM, Ogg JG, Schmitz MD, Ogg GM (eds) The geologic time scale 2012. Elsevier, Amsterdam, pp 127–144

McElwain JC, Popa ME, Hesselbo SP, Haworth M, Surlyk F (2007) Macroecological responses of terrestrial vegetation to climatic and atmospheric change across the Triassic/Jurassic boundary in East Greenland. Paleobiology 33:547–573

Mietto P, Andreetta R, Broglio Loriga C, Buratti N, Cirilli S, De Zanche V, Furin S, Gianolla P, Manfrin S, Muttoni G, Neri C, Nicora A, Posenato R, Preto N, Rigo M, Roghi G, Spötl C (2007a) A candidate of the global stratotype section and point for the base of the Carnian Stage (FAD of *Daxatina*) in the Prati di Stuores/Stuores Wiesen section (southern Alps, NE Italy). Albertiana 6:78–97

Mietto P, Buratti N, Cirilli S, De Zanche V, Gianolla P, Manfrin S, Nicora A, Preto N, Rigo M, Roghi G (2007b) New constraints for the Ladinian-Carnian boundary in the southern Alps: Suggestions for global correlation. New Mex Mus Nat Hist. Sci Bull 41:275–281

Mietto P, Manfrin S, Preto N, Rigo M, Roghi G, Furin S, Gianolla P, Posenato R, Muttoni G, Nicora A, Buratti N, Cirilli S, Spitl C, Ramezani J, Bowring SA (2012) The global boundary stratotype section and point (GSSP) of the Carnian Stage (Late Triassic) at Prati di Stuores/Stuores Wiesen section (southern Alps, NE Italy). Episodes 35:414–430

Mundil R, Pálfy J, Renne PR, Brack P (2010) The Triassic time scale: New constraints and a review of geochronological data. In: Lucas SG (ed) The Triassic timescale. Geol Soc London Spec Publ 334: 41–60

Muttoni G, Kent DV, Olsen PE, Di Stefano P, Lowrie W, Bernasconi SM, Hernandez FM (2004) Tethyan magnetostratigraphy from Pizzo Mondello (Sicily) and correlation to the late Triassic Newark astrochronological polarity time scale. Geol Soc Amer Bull 116:1043–1058

Muttoni G, Kent DV, Jadoul F, Olsen PE, Rigo M, Galli MT, Nicora A (2010) Rhaetian magneto-biostratigraphy from the Southern Alps (Italy): Constraints on Triassic chronology. Palaeogeogr Palaeoclimat Palaeoecol 285:1–16

Ogg JG (2004) The Triassic Period. In: Gradstein FM, Ogg J, Smith A (eds) A geologic time scale 2004. Cambridge University Press, Cambridge, pp 271–306

Ogg JG (2012) Triassic. In: Gradstein FM, Ogg JG, Schmitz MD, Ogg GM (eds) The geologic time scale 2012. Elsevier, Amsterdam, pp 681–730

Ogg JG, Huang C, Hinnov L (2014) Triassic timescale status: A brief overview. Albertiana 41:3–30

Olsen PE (1997) Stratigraphic record of the early Mesozoic breakup of Pangea in the Laurasia-Gondwana rift system. Annu Rev Earth Planet Sci 25:337–401

Olsen PE, Kent DV (1996) Milankovitch climate forcing in the tropics of Pangea during the Late Triassic. Palaeogeog Palaeoclimat Palaeoecol 122:1–26

Olsen PE, Whiteside JH (2008) Pre-Quaternary Milankovitch cycles and climate variability. In: Gornitz V (ed) Encyclopedia of paleoclimatology and ancient environments, Earth Science Series. Kluwer Academic Publishers, Dordrecht, The Netherlands, pp 826–835

Olsen PE, Kent DV, Cornet B, Witte WK, Schlische RW (1996) High-resolution stratigraphy of the Newark rift basin (early Mesozoic, eastern North America). Geol Soc Amer Bull 108:40–77

Olsen PE, Kent DV, Whiteside JH (2011) Implications of the Newark Supergroup-based astrochronology and geomagnetic polarity time scale (Newark-APTS) for the tempo and mode of the early diversification of the Dinosauria. Earth Env Sci Trans Royal Soc Edinburgh 101:201–229

Orchard MJ (2010) Triassic conodonts and their role in stage boundary definition. In: Lucas SG (ed) The Triassic timescale. Geol Soc London Spec Publ 334: 139–161

Orchard MJ (2013) Five new genera of conodonts from the Carnian-Norian boundary beds, northeast British Columbia, Canada. New Mex Mus Nat Hist. Sci Bull 61:445–457

Orchard MJ (2014) Conodonts from the Carnian-Norian boundary (Upper Triassic) of Black Bear Ridge, northeastern British Columbia, Canada. New Mex Mus Nat Hist. Sci Bull 64:1–139

Pearson DAB (1970) Problems of Rhaetian stratigraphy with special reference to the lower boundary of the stage. J Geol Soc Lond 146:125–150

Ramezani J, Hoke GD, Fastovsky DE, Bowring SA, Therrien F, Dworkin SI, Atchley SC, Nordt LC (2011) High-precision U-Pb zircon geochronology of the Late Triassic Chinle Formation, Petrified Forest National Park (Arizona, USA): Temporal constraints on the early evolution of dinosaurs. Geol Soc Amer Bull 123:2142–2159

Ramezani J, Fastovsky DE, Bowring SA (2014) Revised chronostratigraphy of the lower Chinle Formation strata in Arizona and New Mexico (USA): High-precision U-Pb geochronological constraints on the Late Triassic evolution of dinosaurs. Amer J Sci 314:981–1008

Remane J, Basset MG, Cowie JW, Gohrandt KH, Lane HR, Michelsen O, Naiwen W (1996) Revised guidelines for the stablishment of global chronostratigraphic standards by the International Commission of Stratigraphy (ICS). Episodes 19:77–81

Rigo M, Bertinelli A, Concheri G, Gattolin G, Godfrey L, Katz ME, Maron M, Mietto P, Muttoni G, Sprovieri M, Stellin F, Zaffani M (2016) The Pignola-Abriola section (southern Appenines, Italy): A new GSSP candidate for the base of the Rhaetian Stage. Lethaia 49:287–306

Rogers RR, Swisher CC III, Sereno PC, Monetta AM, Forster CA, Martinez RC (1993) The Ischigualasto tetrapod assemblage (Late Triassic, Argentina) and $^{40}Ar/^{39}Ar$ dating of dinosaur origins. Science 260:794–797

Saltzman MR, Thomas E (2012) Carbon isotope stratigraphy. In: Gradstein FM, Ogg JG, Schmitz MD, Ogg GM (eds) The geologic time scale 2012. Elsevier, Amsterdam, pp 207–232

Salvador A (1994) International stratigraphic guide, 2nd edn. Geological Society of America, Boulder

Schaltegger U, Guex J, Bartolini A, Schoene B, Ovtcharova M (2008) Precise U-Pb constraints for end-Triassic mass extinction, its correlation to volcanism and Hettangian post-extinction recovery. Earth Planet Sci Lett 267:266–275

Schoene B, Guex J, Bartolini A, Schaltegger U, Blackburn TJ (2010) Correlating the end-Triassic mass extinction and flood basalt volcanism at the 100 ka level. Geology 38:387–390

Sephton MA, Amor K, Franchi IA, Wignall PB, Newton R, Zonneveld J-P (2002) Carbon and nitrogen isotope disturbances and an end-Norian (Late Triassic) extinction event. Geology 30:1119–1122

Shipman TC (2004) Links between sediment accumulation rates and the development of alluvial architecture: Triassic Ischigualasto Formation, northwestern Argentina. PhD dissertation, University of Arizona, Tucson

Silberling NJ, Tozer ET (1968) Biostratigraphic classification of the marine Triassic in North America. Geol Soc Amer Spec Pap 110:1–63

Smith AG, Barry T, Bown P, Cope J, Gale A, Gibbard P, Gregory J, Hounslow M, Kemp D, Knox R, Marshall J, Oates M, Rawson P, Powell J, Waters C (2015) GSSPs, global stratigraphy and correlation. In: Smith DG, Bailey RJ, Burgess PM, Fraser AJ (eds) Strata and time: probing the gaps in our understanding. Geol Soc London Spec Publ 404: 37–67

Stewart JH, Poole FG, Wilson RF (1972) Stratigraphy and origin of the Chinle Formation and related Upper Triassic strata in the Colorado Plateau region. US Geol Surv Prof Pap 690:1–356

Stockar R, Baumgartner PO, Condon D (2012) Integrated Ladinian bio-chronostratigraphy and geochronology of Monte San Giorgio (Southern Alps, Switzerland). Swiss J Geosci 105:85–108
Sues HD, Fraser NC (2010) Triassic life on land: the great transition. Columbia University Press, New York
Tackett LS, Kaufman AJ, Corsetti FA, Bottjer DJ (2014) Strontium isotope stratigraphy of the Gabbs Formation (Nevada): Implications for global Norian-Rhaetian correlations and faunal turnover. Lethaia 47:500–511
Tanner LH (2010) Cyclostratigraphic record of the Triassic: A critical examination. In: Lucas SG (ed) The Triassic timescale. Geol Soc London Spec Publ 334: 119–137
Tanner LH, Lucas SG (2015) The Triassic-Jurassic strata of the Newark basin, USA: A complete and accurate astronomically-tuned timescale? Strat 12:47–65
Tozer ET (1967) A standard for Triassic time. Geol Surv Canada Bull 156:1–103
Tozer ET (1971) Triassic time and ammonoids: Problems and proposals. Canad J Earth Sci 8:989–1031
Tozer ET (1974) Definitions and limits of Triassic stages and substages: Suggestions prompted by comparisons between North America and the Alpine-Mediterranean region. Schrift Erdwissen Kommiss Oster Akad Wiss 2:195–206
Tozer ET (1984) The Trias and its ammonoids: The evolution of a time scale. Geol Surv Canada Misc Rep 35:1–171
Tozer ET (1985) Subcommission on Triassic Stratigraphy (STS): History 1968-1984. Albertiana 3:3–6
Tozer ET (1994) Canadian Triassic ammonoid faunas. Geol Surv Canada Bull 467:1–663
von Alberti F (1834) Beitrag zu einer Monographie des Bunten Sandsteins, Muschelkalks und Keupers, und die Verbindung dieser Gebilde zu einer Formation. Verlag der J. G. Cotta'sschen Buchhandlung, Stuttgart und Tübingen [Facsimile reprinted in 1998 by the Friedrich von Alberti-Stiftung der Hohenloher Muschelkalkwerke, Ingelfingen, Germany]
von Bittner A (1892) Was ist norisch? Geol Reichsanstalt Jahrb 42:387–396
von Gümbel CW (1859) Über die Gleichstellung der Gesteinmasen in den nord-östlichen Alpen mit ausseralpinen Flötzschichten. Verhandn Gesellsch Deutsch Naturforsch Ärtzte Karlsruhe 54:80–88
von Gümbel CW (1861) Geognostische Beschreibung des bayerischen Alpengebirges. J Perthes, Gotha
von Hillebrandt A, Krystyn L, Kürschner WM, Bonis NR, Ruhl M, Richoz S, Schobben MAN, Ulrichs M, Bown PR, Kment K, McRoberts CA, Simms M, Tomãsových A (2013) The global stratotype sections and point (GSSP) for the base of the Jurassic System at Kuhjoch (Karwendel Mountains, Northern Calcareous Alps, Tyrol, Austria). Episodes 36:162–198
von Mojsisovics E (1869) Über die Gliederung der oberen Triasbildungen der östlichen Alpen. Geol Reichsanstalt Jahrb 24:91–150
von Mojsisovics E (1874) Faunengebeite und Faciesgebilde der Trias-Periode in den Ost-Alpen—Eine stratigraphische studie. Geol Reichsanstalt Jahrb 24:81–134
von Mojsisovics E (1892) Die Hallstätter Entwicklunung der Trias. Sitzungsber Akad Wissen Wien 101:769–780
von Mojsisovics E (1902) Die Cephalopoden der Hallstätter Kalke. Geol Reichsanstalt Abhand 6:175–356
von Mojsisovics E, Waagen WH, Diener C (1895) Entwurf einer Gliederung der pelagischen Sediments des Trias-Systems. Akad Wiss Wien. Math-naturwiss Klasse Sitzungsber 104:1279–1302
Walsh SL, Gradstein FM, Ogg JG (2004) History, philosophy, and application of the Global Stratotype Section and Point. Lethaia 37:201–218
Weems RE, Lucas SG (2015) A revision of the Norian conchostracan zonation in North America and its implications for Late Triassic North American tectonic history. New Mex Mus Nat Hist. Sci Bull 67:303–317

Weems RE, Tanner LH, Lucas SG (2016) Synthesis and revision of the lithostratigraphic groups and formations in the upper Permian?-Lower Jurassic Newark Supergroup of eastern North America. Strat 13:111–153

Wotzlaw J-F, Guex J, Bartolini A, Gallet Y, Krystyn L, McRoberts CA, Taylor D, Schoene B, Schaltegger U (2014) Towards accurate numerical calibration of the latest Triassic: High precision U-Pb geochronology constraints on the duration of the Rhaetian. Geology 42:571–574

Zapfe H (1971) Die stratotypen des Anis, Tuval und Nor und ihre Bedeutung für die Biostratigraphie und Biostratinomie der Alpinen Trias. Ann Instit Geol Pub Hungar 54:579–590

Zittel KA (1901) History of geology and palaeontology to the end of the nineteenth century. Walter Scott, London

Chapter 2
Late Triassic Global Plate Tectonics

Jan Golonka, Ashton Embry, and Michał Krobicki

Abstract The Late Triassic was the time of the Early Cimmerian and Indosinian orogenies that closed the Paleotethys Ocean, which occurred earlier in the Alpine-Carpathian-Mediterranean area, later in the Eastern Europe-Central Asia and latest in the South-East Asia. The Indochina Southeastern Asian and Qiangtang plates were sutured to South China. The new, large Chinese-SE Asian plate, including North and South China, Mongolia and eastern Cimmerian plates, was consolidated by the end Triassic, leaving open a large embayment of Panthalassa, known as Mongol-Okhotsk Ocean, between Mongolia and Laurasia,. The Uralian Orogeny, which sutured Siberia and Europe continued during Late Triassic times and was recorded in Novaya Zemlya. The onset of Pangaea break-up constitutes the main Late Triassic extensional event. Continental rifts originating then were filled with clastic deposits comprising mainly red beds. The pulling force of the north-dipping subduction along the northern margin of Neotethys caused drifting of a new set of plates from the passive Gondwana margin, dividing the Neotethys Ocean. Carbonate sedimentation dominated platforms on the Neotethys and Paleotethys margins as well as the Cimmerian microplates. Synorogenic turbidites and postorogenic molasses were associated with the Indosinian orogeny. The late stages of the Uralian orogeny in Timan-Pechora, Novaya Zemlya and eastern Barents regions filled the foreland basin with fine-grained, molasse sediments. Siliciclastics were common in the Siberia and Arctic regions. The widespread, large magnitude, base-level changes of the Late Triassic are interpreted as an expression of relatively rapid and substantial changes in the horizontal and vertical stress fields that affected the Pangaea

J. Golonka (✉)
Faculty of Geology, Geophysics and Environmental Protection, AGH University of Science and Technology, Al. Mickiewicza 30, 30-059 Kraków, Poland
e-mail: jgolonka@agh.edu.pl

A. Embry
Geological Survey of Canada, Calgary, AB, Canada
e-mail: ashton.embry@canada.ca

M. Krobicki
Faculty of Geology, Geophysics and Environmental Protection, AGH University of Science and Technology, Al. Mickiewicza 30, 30-059 Kraków, Poland

Carpathian Branch, Polish Geological Institute – National Research Institute, Kraków, Poland
e-mail: krobicki@geol.agh.edu.pl

© Springer International Publishing AG 2018

L.H. Tanner (ed.), *The Late Triassic World*, Topics in Geobiology 46,
https://doi.org/10.1007/978-3-319-68009-5_2

supercontinent. Such stress changes may be due to abrupt changes in the speed and/or direction of plate movements, which episodically affected Pangaea.

Keywords Paleogeography • Plate tectonics • Paleoenvironment • Paleolithofacies • Paleoclimate • Sea level changes

2.1 Introduction

The Triassic maps used here (Figs. 2.1, 2.2, 2.3, 2.4, 2.5, 2.6, 2.7 and 2.8) were derived from a series of global and regional Phanerozoic paleogeographic and plate tectonic maps which depicted present day coastlines, plate boundaries (sutures), selected transform faults, spreading centers, rifts, normal and thrust faults as well as paleoenvironment and lithofacies (Golonka 2000, 2002, 2007a, b, 2011; Golonka et al. 2003a, 2006a,b). Also included is a corrected and improved version of the Triassic maps previously presented (Golonka 2007a, b). The base maps, (past position of present day coastlines and plate boundaries) were generated by PLATES, PALEOMAP and GPLATES computer software (see Sect. 1.2). The definitions of mapped time slices were presented by Golonka and Kiessling (2002), however, recently the simple stratigraphic "Late Triassic" slice was used (Golonka 2007a, b). The name "Triassic" was derived from the German Trias defined by von Alberti (1834), referring to the division of the period into three stages: the Buntsandstein, Muschelkalk, and Keuper (see Köppen and Carter 2000; Feist-Burkhardt et al. 2008; Scheck-Wenderoth et al. 2008; McKie and Williams 2009 and references therein). This sequence is valid for Central Europe (Germany, Poland), but causes many problems when applied to other regions. The global Late Triassic (Ogg et al. 2016) is now divided into the Carnian, Norian and Rhaetian ages (Fig. 2.9). For the environment and facies assembly we used two units, applying the methods used for the Phanerozoic reefs map (Kiessling and Flügel 1999) and also presented by Golonka (2007a, b). The base maps (Figs. 2.1 and 2.2) depict the configuration of land masses, rifts, spreading centers and subduction and the beginning (Fig. 2.1) and end (Fig. 2.2) of the Late Triassic. The paleoenvironments and lithofacies (Figs. 2.3, 2.4, 2.5, 2.6, 2.7 and 2.8) represent the whole of the Late Triassic Epoch. They are posted on the 224 Ma base maps.

2.2 Methods

The Phanerozoic maps were constructed using a plate tectonic model that describes the relative motions between approximately 300 plates and terranes (Golonka 2000). This model was originally constructed using PLATES and PALEOMAP software, later the GPLATES program was used (see the detailed reconstruction

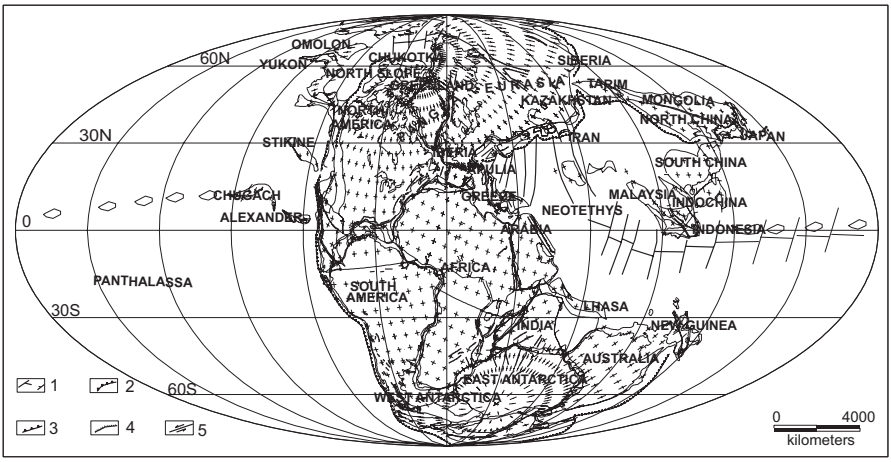

Fig. 2.1 Global plate tectonic map of Late Triassic at 224 Ma ago. Molweide Projection. (1) oceanic spreading center and transform faults, (2) subduction zone, (3) thrust fault, (4) normal fault, (5) transform fault

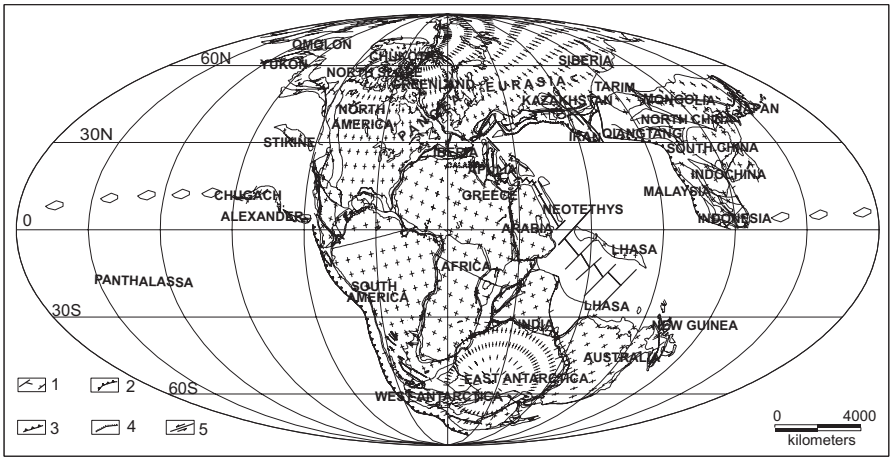

Fig. 2.2 Global plate tectonic map of Late Triassic at 200 Ma ago. Molweide Projection. (1) oceanic spreading center and transform faults, (2) subduction zone, (3) thrust fault, (4) normal fault, (5) transform fault

methodology in Golonka et al. 2003b. The rotation file was presented in Golonka (2007a), and is shown in the appendix of that paper.

We modified this model using new paleomagnetic data, especially in the Tethys and Arctic areas (Kravchinsky et al. 2002; Hounslow and Nawrocki 2008; Kovalenko 2010; Metelkin et al. 2011, 2012; Uno et al. 2011; Domeier et al. 2012; Choulet et al. 2013; Vernikovsky et al. 2013; Wang et al. 2013; Song et al. 2015; Huang and Opdyke 2016; Li et al. 2016a, b; Zhou et al. 2016). We left the position of the major

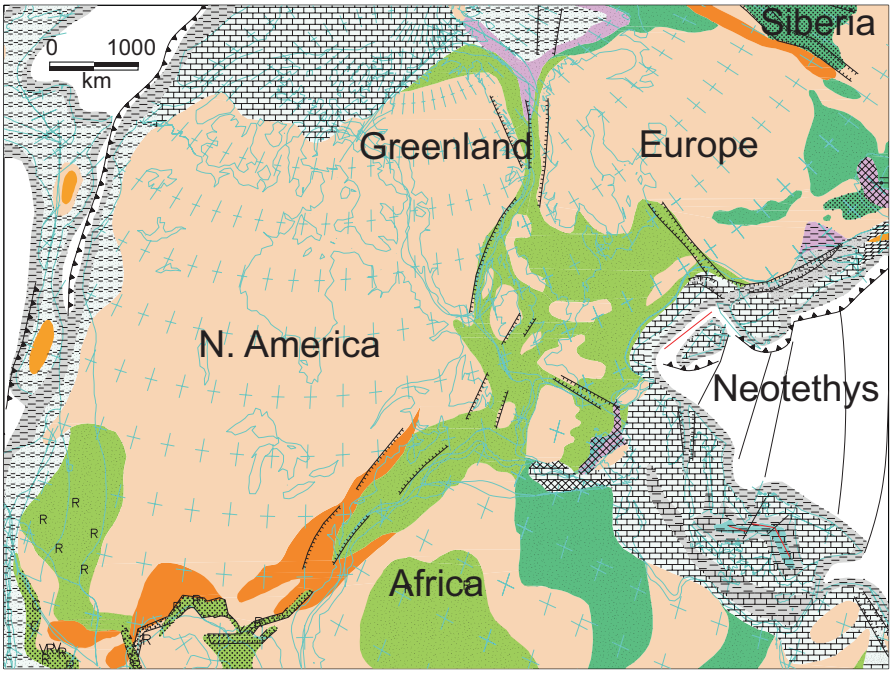

Fig. 2.3 Plate tectonic, paleoenvironment and lithofacies map of the western Tethys, future Central Atlantic and adjacent areas during Late Triassic time. Molweide Projection. Modified from Golonka (2007b)

continent unchanged due to the absence of important new data. For example, according to Metelkin et al. (2011) there is an absence of authentic data for the Middle and Late Triassic from Siberia.

The facies were reconstructed using established sedimentological concepts for reefs and other sedimentary environments (Kiessling and Flügel 1999; Kiessling et al. 2003) and also presented by Golonka et al. (2006b) and Golonka (2007a, b). The calculated paleolatitudes and paleolongitudes were used to generate computer maps in Microstation design (.dgn format) converted later into Corel Draw (.cdr format). Facies and paleoenvironment information were posted after reviewing database files, regional paleogeographic maps and relevant papers. Information from several general and regional paleogeographic papers were filtered and utilized (Vinogradov 1968; Ziegler 1982, 1988; Hongzen 1985; Ronov et al. 1989; Cook 1990; Zonenshain et al. 1990; Doré 1991; Dercourt et al. 1993, 2000; Golonka et al. 1994, 2006a; Metcalfe 1994, 2011, 2013a, b; Veevers 1994, 2006, 2013; Nikishin et al. 1996; Sengör and Natalin 1996; Puchkov 1997; Kiessling and Flügel 1999; Golonka 2000, 2002, 2007a, b, 2011; Golonka and Ford 2000; Ford and Golonka 2003; Scotese 2004; Miller et al. 2006; Robertson 2007; Feist-Burkhardt et al. 2008; Heydari 2008; Maurer et al. 2008; Miall and Blakey 2008; Miall et al. 2008; Pčelina and Korčinskaja 2008; Scheck-Wenderoth et al. 2008; Schmid et al. 2008; Peng et al. 2009; McKie and Williams 2009; Glørstad-Clark et al. 2010; Metelkin et al.

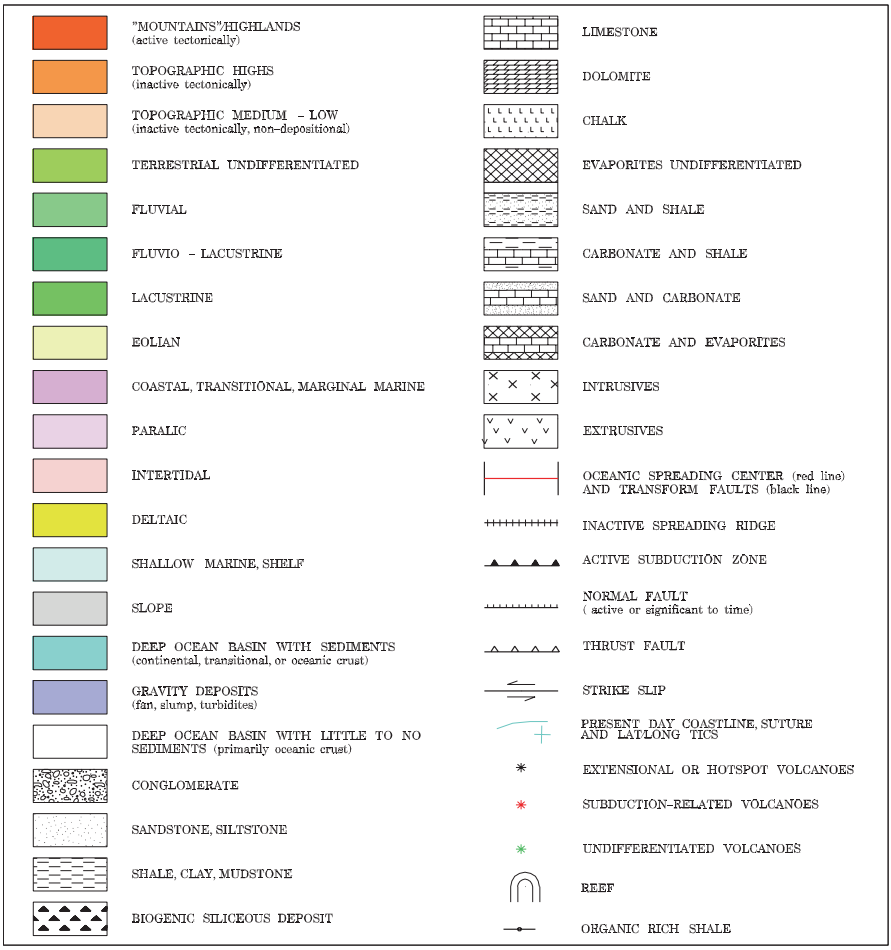

Fig. 2.4 Explanations to Figs, 2.3, 2.4, 2.5, 2.7. Qualifiers: *B* bauxites/laterites, *C* coals, *E* evaporites, *F* flysch, *Fe* Iron, *G* glauconite, *M* marls, *O* oolites, *P* phosphates, *R* red beds, *Si* silica, *T* tillites, *V* volcanics

2011, 2012; Schettino and Turco 2011; Sibuet et al. 2012; Li and Huang 2013; Luo et al. 2014; Ershova et al. 2015a, b; Pease et al. 2015; Lane and Stephenson 2016; Müller et al. 2016; Toro et al. 2016; Cai et al. 2017; Centeno-García 2017).

2.3 Convergent Tectonics

The Late Paleozoic supercontinent Pangaea included North America, South America, Africa, Australia, Europe and Siberia and was surrounded by the Panthalassa Ocean (Figs. 2.1 and 2.2). The collision between Siberia and Europe

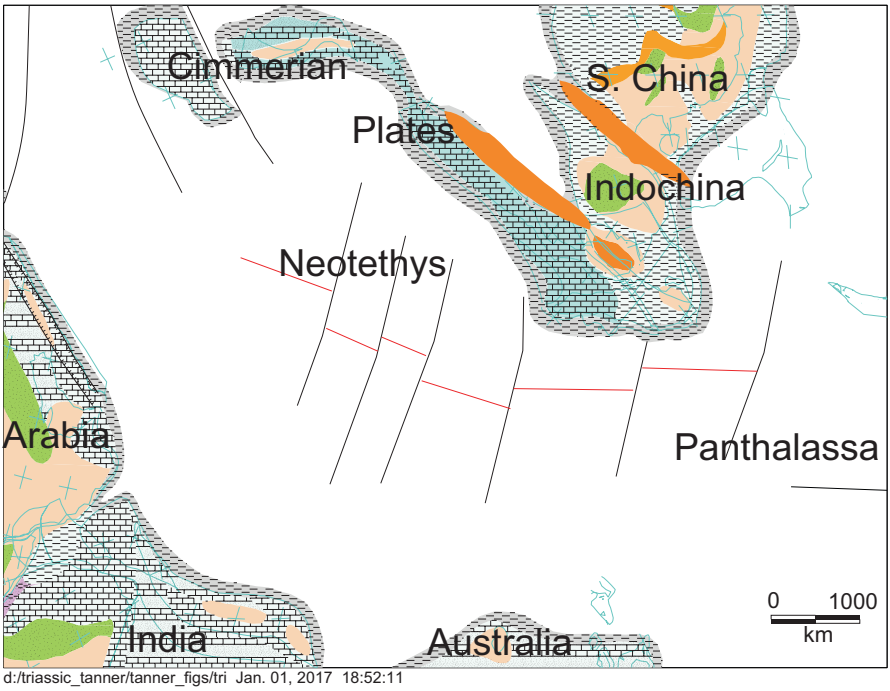

Fig. 2.5 Plate tectonic, paleoenvironment and lithofacies map of eastern Tethys and adjacent areas during Late Triassic time. Molweide Projection

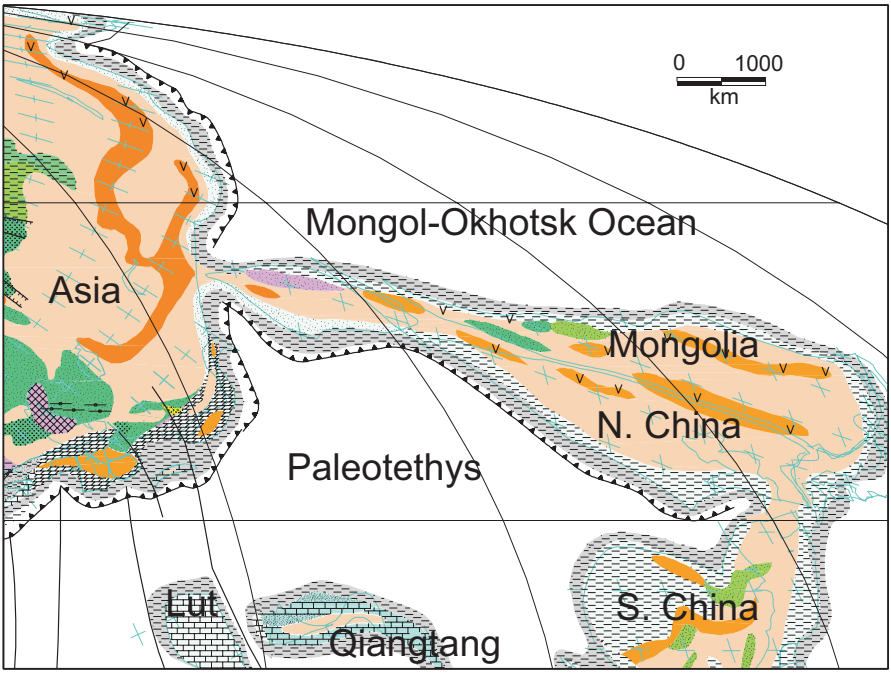

Fig. 2.6 Plate tectonic, paleoenvironment and lithofacies map of the Paleotethys, Chinese plates and adjacent areas during Late Triassic time. Molweide Projection. Modified from Golonka (2007b)

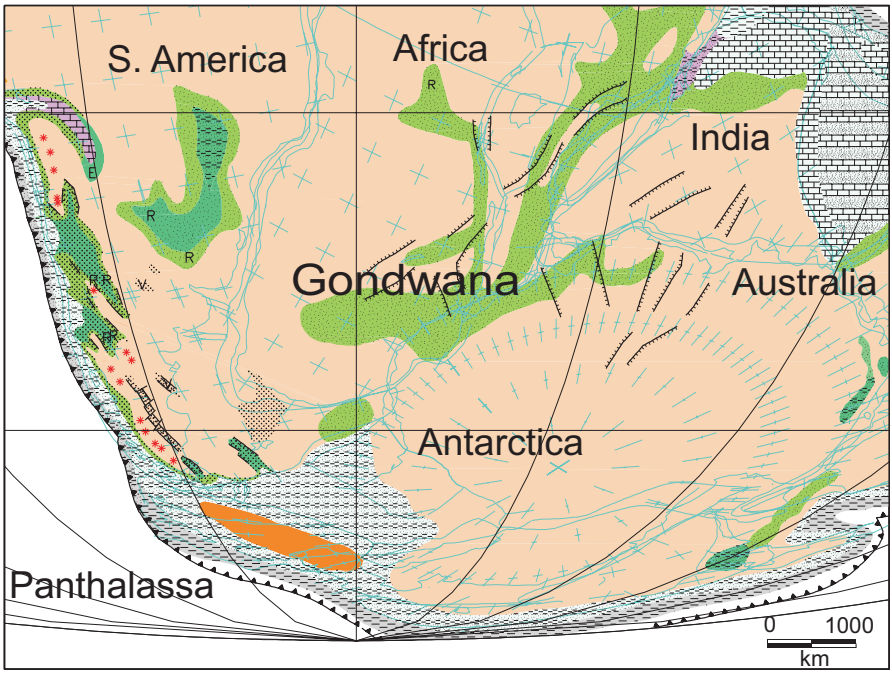

Fig. 2.7 Plate tectonic, paleoenvironment and lithofacies map of the western Gondwana and adjacent areas during Late Triassic time. Molweide Projection. Modified from Golonka (2007b)

formed the Ural Mountains during the Uralian Orogeny (Zonenshain et al. 1990; Nikishin et al. 1996; Puchkov 1997). The last episode of this orogeny occurred at the end of the Triassic in Novaya Zemlya (Toro et al. 2016; Zhang et al. 2017a). Deformation also affected the Taimyr Peninsula (Torsvik and Anderson 2002; Golonka 2007a, b). According to Zhang et al. (2017b) the Taimyr Permo-Triassic magmatic rocks were locally folded and faulted as a result of Late Triassic to Early Jurassic dextral transpression. According to Vernikovsky (1995) and Vernikovsky et al. (2003) the formation of the Taimyr structures is connected with the collision of the Kara microcontinent with Siberia. The uplift of the adjacent areas of Europe and Siberia was related to these orogenic events (Figs. 2.2 and 2.8). The Crockerland uplifted area of the Alaska-Chukotka micro-plate supplied sediments to the adjacent Sverdrup Basin in North America and was linked with Siberia at this time (Fig. 2.8; Anfinson et al. 2016). The subduction zones, known as the Late Paleozoic Pangaean Rim of Fire, were still active during the Triassic (Golonka and Ford 2000; Golonka 2002, 2004, 2007a, b; Matthews et al. 2016). This Rim of Fire was especially active along the western coast of Pangaea (Figs. 2.1 and 2.2). Active volcanism, terrane accretion, and back-arc basin development accompanied the subduction zones (Golonka 2007a, b). The subduction accompanied by magmatism was active in Central and North America (Goodge 1989, 1990; Dorsey and LaMaskin 2007; Centeno-García et al. 2008; Arvizu and Iriondo 2015) as well as

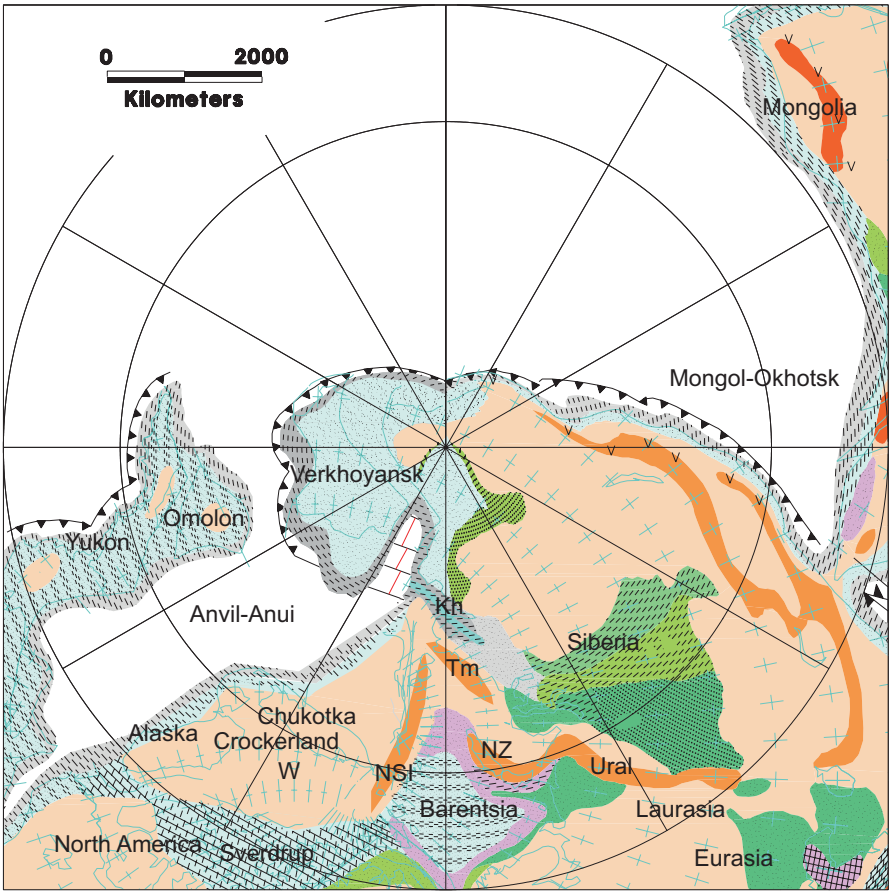

Fig. 2.8 Plate tectonic, paleoenvironment and lithofacies map of the Arctic during Late Triassic time. Stereographic polar. Projection Modified from Golonka (2011)

in South America (Bustamante and Juliani 2011; del Rey et al. 2016). The movement of terranes within Panthalassa was related to the activity of this subduction (Figs. 2.1 and 2.2). According to Dorsey and LaMaskin (2007), the collision of terranes in North America happened during Late Triassic times in the Blue Mountains of Oregon. The position of these terranes is a subject of controversy, however (e.g. Engebretson et al. 1985; Panuska 1985; Debiche et al. 1987; Sengör and Natalin 1996; Keppie and Dostal 2001; Belasky et al. 2002; Trop et al. 2002; Piercey et al. 2006; Golonka 2007a, b; Colpron and Nelson 2011; Roniewicz 2013; Matthews et al. 2016). The relationship between Panthalassa terranes and Cimmerian plates was previously postulated and mapped (Golonka 2007a, b). The Panthalassa terranes bearing reef complexes were also mentioned by Flügel

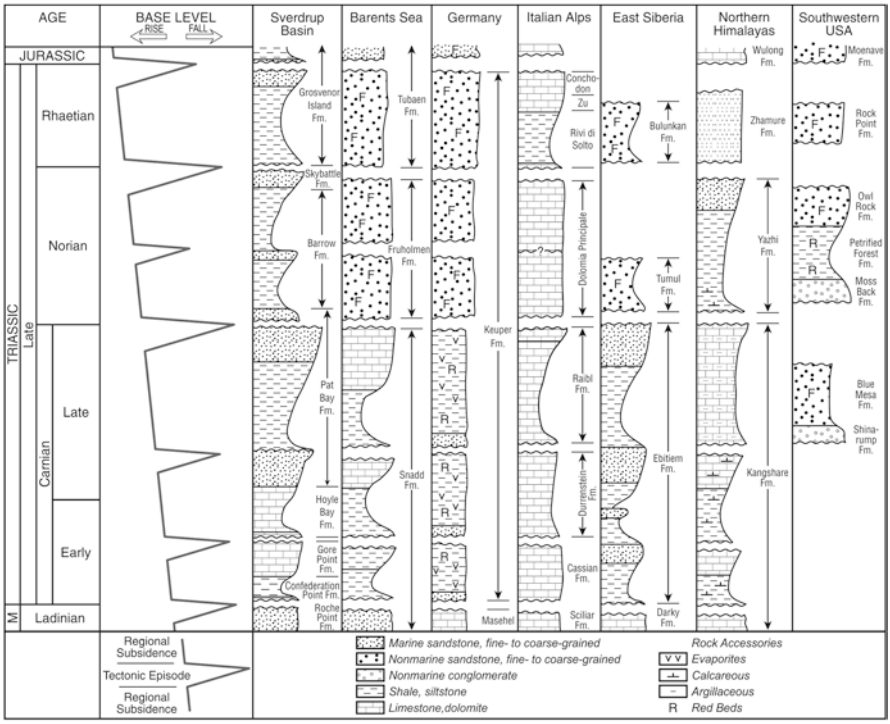

Fig. 2.9 Late Triassic stratigraphy of various basins contains sequence boundaries of basal Carnian, mid-Carnian, basal Norian, mid-Norian, basal Rhaetian, and latest Rhaetian age. The features of these boundaries indicate they represent relatively short-lived, tectonic episodes. Each tectonic episode was characterized by a rapid base level fall followed by rapid rise which punctuated the relatively slow, long term subsidence of the basins

(2002). According to Peyberness et al. (2016, see also Stanley and Onoue 2015) the Western Panthalassa reefs from Japan corresponds with those of the Tethys Ocean during the Late Triassic. The Late Triassic was the time of the collisions now known as the Early Cimmerian and Indosinian orogenies. Blocks of the Cimmerian provenance and Eurasia (Sengör 1984; Sengör et al. 1984; Sengör and Natalin 1996) were involved in these collisions with the southern margin of Eurasia (Golonka 2000, 2002, 2007a, b; Golonka et al. 2003a, 2006a,b; Robertson 2007; Richards 2015). This series of collisions closed the Paleotethys Ocean. The closure happened earlier in the Alpine-Carpathian-Mediterranean area, later in the Eastern Europe-Central Asia and latest in the South-East Asia (Figs. 2.1 and 2.2). Microplates now included in the Alpine-Carpathian systems formed the marginal part of Europe. Subduction developed south of this zone. Late Triassic collisional events occurred also in the Moesia-Rhodopes areas (Tari et al. 1997; Golonka 2004, 2007a, b; Okay and Nikishin 2015; Petrík et al. 2016). The Alborz and the

South Caspian Microcontinent collided with the Scythian platform in Eastern Europe, and the other Iranian plates, including the large Lut block, collided with the Turan platform (Zonenshain et al. 1990; Kazmin 1991; Nikishin et al. 1996, 1998a; Golonka 2004, 2007a, b; Heydari 2008; Wilmsen et al. 2009; Masoodi et al. 2013; Okay and Nikishin 2015; Zanchi et al. 2009, 2016). Compressional deformations were recorded in the Caucasus, and Kopet Dagh areas, accompanied by the general uplift of the Fore-Caucasus, Caucasus and Middle Asia regions (Golonka 2004). According to Okay and Nikishin (2015), the accretion of an oceanic plateau was recorded by Late Triassic eclogites in the Pontides. Collisional events were also noted in Afghanistan and Pamir areas (Sengör 1984; Zonenshain et al. 1990; Golonka 2004, 2007a, b; Montenat 2009; Robinson 2015).

The Paleotethys between Qiangtang and Eurasia was closed during Late Triassic times (Figs. 2.1 and 2.2; Metcalfe 2013a; Zhai et al. 2013; Zhu et al. 2013; Luo et al. 2014; Song et al. 2015; Wu et al. 2016). The eastern Cimmerian plates were involved in the Indosinian orogeny. This name was derived from Indochina, the region where the orogeny was noted over one hundred years ago (Deprat 1913, 1914; Fromaget 1927, 1934, 1941, 1952). A major unconformity was observed in Northwest Vietnam. The deformed Lower – lowermost Upper Triassic (up to Carnian) marine metamorphosed rocks arranged into nappes and thrusts are covered by Upper Triassic continental red conglomerates ("terraines rouges", see Deprat 1913, 1914, also Golonka et al. 2006b). According to Lepvrier et al. (2004 see also Maluski et al. 2001, 2005; Lepvrier and Maluski 2008 and references therein), the main metamorphic event occurred during the Early Triassic, 250–240 Ma. The Late Triassic unconformity and 225–205 Ma postorogenic plutonism was noted by Faure et al. (2014). Hung (2010) describes magmatism in northeastern Vietnam related to Triassic Indosinian orogeny. According to Faure et al. (2014) the Jinshajiang and Ailaoshan belts in China and their geodynamic evolution, with Vietnam orogeny marking the same Indosinian Orogeny. It was related to the closure of Paleotethys Ocean along Raub-Bentong, Sra Kaeo and Nan-Uttaradit suture between Sibumasu and Indochina and Ailaoshan suture between Sibumasu and South China (Metcalfe 1994, 1996, 2000, 2011, 2013a, b; Golonka et al. 2006b and references therein).

One of the best examples of the Late Triassic orogenic event occurs in the Thailand/Myanmar trans-border zone. The Triassic-Jurassic succession in the Mae Sot area (northern Thailand), belongs to the Shan-Thai terrane. This block is subdivided into several zones from the west to east, including the Mae Sariang zone, where the Mae Sot area is located. This zone contains rocks of Triassic cherts (radiolarites), carbonates and flysch (turbiditic) facies, which indicate both pelagic condition and synorogenic deposits. From a paleogeographic point of view, the Shan-Thai block was a remnant of Paleotethys Ocean (Meesook and Sha 2010), which occupied a wide realm between Cimmerian Continent and Eurasian plate during Late Paleozoic-Early Mesozoic times. On the other hand, the Late Triassic Indosinian orogenic event has been associated with the docking and amalgamation of the Indoburma, Shan-Thai (Sibumasu) and Indochina terranes, which recently

constituted the main part of Southeast Asia. Therefore, entire Jurassic units of these regions are represented by post-orogenic continental-shelf deposits, which are underlain discontinuously by older rocks. The oldest Jurassic bed, or the youngest Triassic bed, is the so-called "base-conglomerate", in local nomenclature, and is characterized by limestone and chert pebbles-bearing conglomerate, which is significant for the understanding of the tectonic evolution of the Shanthai terrane (Ishida et al. 2006; Meesook and Sha 2010). The underlying cherts are dated biostratigraphically (based on radiolarians) as Middle-Late Triassic. Limestone and chert pebbles from the "base-conglomerate" are dated as Early-Late Triassic by conodonts and as Middle-Late Triassic by radiolarians, respectively. These microfossils from pebbles constrain the age of the Indosinian (ShanThai = Mae Sariang) orogeny. Additionally, the youngest clasts, both limestones and siliceous rocks, indicate a strictly pelagic character of sedimentation up to Late Triassic time (see Ishida et al. 2006). A full open ocean condition must have existed at least before the end of the Triassic. The "base-conglomerate" is characterized by poorly-sorted, chaotically organized, pebble/fragment-bearing sedimentary breccia with no evidence of bivalve borings on their surfaces. The multicolored clasts are subrounded and subangular, and occur within reddish silt matrix. Chert clasts are red, green and grey and carbonate pebbles are represented both by micritic, pelagic limestones and the entire spectrum of packstones and grainstones, including extremely shallow-water bioclastic limestones (with bivalve fragments, crinoids, fragments of corals, etc.) with ooids and coated grains. The "base-conglomerate" is overlain by limestones and marls with mudstone intercalations of the Khun Huai Formation of the Hua Fai Group, dated by ammonites and bivalves as Early Toarcian. These facts indicate, by superposition, that the "base-conglomerate" is the latest Triassic or earliest Jurassic in age, according to the latest Triassic age of the chert and limestone pebbles within it. Sedimentological features indicate, on the other hand, a very rapid sedimentation event during its origin, such as erosion of steep, submarine "cliffs" that formed proximal aprons of debris flows. Additionally, the composition of this conglomerate, which has both deep-marine clasts and shallow-water ones, without any evidence of their long-distance transport, suggests erosion of different type of source material, which most probably originally took place in a different part of the primary Paleottethys Ocean. Then, they were removed, folded (forming nappes?) and overthrust to another location where they were destroyed and eroded, and produced marine molasse-type deposits unconformably overlying Indosinian deformed rocks. In fact, these data indicate both time and space reorganization of this orogenic system, which took place possibly during latest Triassic to earliest Jurassic time. The examination of the main orogenic events in the Southeast Asia regions indicates diachronous, multi-stages movements of the Indosinian orogeny. These include Early Triassic and Carnian/Norian orogenic pulses in Vietnam (Lepvrier et al. 2004), late Middle Triassic–early Late Triassic activity, the so-called second Indosinian event (Hahn 1984; Lepvrier and Maluski 2008, see also Cai et al. 2017) and close to the Triassic/Jurassic boundary in Thailand, as the Asian plate docked first on the East and later on the West (in modern coordinates).

Additionally, the Late Triassic volcanogenic-sedimentary event in Myanmar correlates presumably with synorogenic processes, which are represented by the Late Triassic flysch deposits with basaltic pillow lavas of the Shweminbon Group (Upper Triassic – Lower Jurassic turbidites), formerly part of Loi-an Group, the Bawgyo Group (Upper Triassic) and their equivalents, and with Upper Triassic turbidites represented by the Thanbaya/Pane Chaung Group/formations (Bannert et al. 2011; Win Swe 2012; Cai et al. 2017).

The collision between the South Chinese plate and the North Chinese block began during the Late Permian and continued during the Triassic (Yin and Nie 1996; Golonka et al. 2006b; Golonka 2007a, b). The Qinling orogenic belt records this collision. According to Dong et al. (2011) the Shangdan zone between the North and South Qinling belts is the suture separating the convergence and collision between North South Chinese plates. The post-suturing plutons were emplaced along the suture zone and on the adjacent plates (Bao et al. 2015; Liang et al. 2015; Lu et al. 2016). Consolidation of North China and Mongolia occurred mainly earlier but continued during the Triassic between North China and Mongolia. The newly formed, larger plate contains volcanics and collisional granites (Fig. 2.6; Chen et al. 2000; Wu et al. 2002; Shi et al. 2016). This consolidation left open a large embayment between Mongolia and Laurasia, the so-called Mongol-Okhotsk Ocean (Zonenshain et al. 1990; Golonka 2000, 2007a; Zeng et al. 2014). Active subduction existed along the margin of this ocean (Figs. 2.6 and 2.8), dipping cratonwards towards East Siberia (Zonenshain et al. 1990; Golonka 2007a, b), and granitic intrusions occurred along the Siberian margin (Zonenshain et al. 1990; Donskaya et al. 2013, 2016). The new, large Chinese-Southeast Asian plate including North and South China, Mongolia and eastern Cimmerian plates was consolidated at the Triassic-Jurassic Boundary (Fig. 2.2).

2.4 Extensional Tectonics

The onset of Pangaean break-up constitutes the main Late Triassic extensional tectonic event (Golonka 2007a, b). The rift basins originated between North America and Africa. The extensional rifting was accompanied by strike-slip faulting and block rotation (Ford and Golonka 2003; Laville et al. 2004; Golonka 2007a, b). Incipient continental rifting occurred also between northern Europe and North America (Fig. 2.2), reactivating the Late Paleozoic fracture system (Ziegler 1982; Doré 1991; Nikishin et al. 2002; Golonka 2011), and activating the North Sea rifts. The Central European Permian rift system known as the Polish/Danish Aulacogene was still active during Late Triassic times. The Upper Permian (Zechstein) salt went into salt tectonic phase with incipient salt diapirism and extrusion (Kutek 2001; Krzywiec 2012). Continental extension also began in isolated areas in South America during the Late Triassic (Macdonald et al. 2003; Ford and Golonka 2003; Golonka 2007a, b). Additionally, rift basins developed behind the subduction zone along the western Pangaean margin (Goodge 1989, 1990; Golonka and Ford 2000; Golonka 2007a, b;

Centeno-García et al. 2008; Dickinson 2009; Bustamante and Juliani 2011; Giambiagi et al. 2011; Baby et al. 2013; Helbig et al. 2013; Spikings et al. 2016; Centeno-García 2017).

The Pangaea rift systems extended also to the Barents shelf, Arctic, and Siberia (Golonka 2011; Golonka et al. 2003a, 2006b). Rifting in Siberia was associated with the subduction zone at the Mongol-Okhotsk Ocean margin (Figs. 2.1, 2.2 and 2.8). Late Triassic sea-floor spreading in Siberia constituted an extension of the Anyui Ocean, which existed between the Alaska-Chukotka and Verkhoyansk terranes (Fig. 2.8; Zonenshain et al. 1990; Sengör and Natalin 1996; Golonka et al. 2003a; Golonka 2011). The opening of the Amerasia Basin appears to have begun near the Norian/Rhaetian boundary resulting in the rotational separation of the Alaska-Chukotka terrane from northern Laurasia (Embry and Anfinson 2014).

The volcanics (flows and intrusions) of the Central Atlantic Magmatic Province (CAMP), were emplaced at the end of Triassic and beginning of the Early Jurassic (e.g., Olsen 1997; Withjack et al. 1998; Marzoli et al. 1999, 2004, 2011; Knight et al. 2004; Golonka 2007a; Cirilli et al. 2009). CAMP constitutes one of the largest known Phanerozoic flood basalt provinces. It triggered climate changes and the end-Triassic extinction event (Wignall 2001; Lucas and Tanner 2008; Preto et al. 2010; Bond and Wignall 2014; Müller et al. 2016). The Late Triassic northward drift of the Cimmerian continent was accompanied by active seafloor spreading within the Neotethys Ocean. The spreading was driven by trench-pulling forces related to the north-dipping subduction, as well as the ridge-pushing forces related to mantle upwelling, expressed by hot spot activity (Golonka and Bocharova 2000; Golonka 2004, 2007a, b). Rifting and the opening of oceanic type basins could have occurred in the Alpine, Carpathian, Balkans and future Mediterranean area (Figs. 2.1, 2.2 and 2.3; Golonka et al. 2006a). The opening of the incipient Pindos–Maliac Ocean was related to the establishment of the Pelagonian, Sakariya and Kirsehir blocks as separate microplates within the Western (Robertson et al. 1991, 1996; Ferriere et al. 2016). The proto-Transylvanian and Vardar oceans originated within Carpathian-Balkan. The Tisa block was perhaps fully separated from the European margin by the Meliata-Halstatt Ocean. The positions of the Vardar, Meliata-Halstatt, Transylvanian, Pindos, Maliac oceans and their embayments within the Western Tethys remain quite speculative and are subjects of the debate (e.g., Kozur and Krahl 1987; Săndulescu 1988; Kozur 1991; Channell and Kozur 1997; Mock et al. 1998; Ivan 2002; Golonka 2004; Haas and Pero 2004; Golonka et al. 2006a; Dallmeyer et al. 2008; Schmid et al. 2008; Hoeck et al. 2009; Gawlick and Missoni 2015; Meinhold and Kostopoulos 2013). The Eurasian platform east of the Carpathians and Meliata Ocean was dissected by rifts that extended from the Dobrogea, through the proto-Black Sea area and along the margins of Scythianturan platform and probably were connected with Polish/Danish Aulacogene (Fig. 2.3; Zonenshain et al. 1990; Kazmin 1990, 1991; Nikishin et al. 1998a, b; Golonka 2004). The Tauric basin, which belonged to this rift system, was located between Pontides and the Dobrogea-Crimea segment of the Scythian platform (Golonka et al. 2006a). The North Dobrogea part of the rift zone separated Moesia and Eastern European platform (Muttoni et al. 2000; Golonka 2004; Golonka et al. 2006a). Several blocks

were located between the rifted zone and the Neotethys (Golonka 2004; Golonka et al. 2006a; Okay and Nikishin 2015). This rifted zone can be interpreted as a back-arc basin resulting from the northward subduction of the Neotethys Ocean (Figs. 2.1, 2.2 and 2.3). The deep-water basin was located between Apulia, the Taurus platform and the African continent (Fig. 2.1; Catalano et al. 1991; Kozur 1991; Marsella et al. 1993; Golonka 2004, Golonka et al. 2006b). It was connected eastwards with an oceanic-type basin recorded by the Mamonia ophiolites complex in Cyprus (Robertson and Woodcock 1979; Morris 1996; Robertson 1998). The rifts cutting Apulia were connected with the western part of Neotethys.

The whole Paleotethys was closed in the western part of the Tethyan realm in the Early Jurassic (Fig. 2.2). The pulling force of the north-dipping subduction along the northern margin of Neotethys caused the drift of a new set of plates from the passive Gondwanian margin. These plates divided the Neotethys Ocean into northern and southern branches (Golonka 2004). Metcalfe (2013a) distinguished Cenotethys as the southern branch. The Lhasa block was the most prominent plate which drifted away from Gondwana (Sengör 1984; Dercourt et al. 1993; Metcalfe 1994, Metcalfe 2013a, b; Sengör and Natalin 1996; Yin and Nie 1996; Golonka 2004; Cai et al. 2016; Li et al. 2016a, b; Lu et al. 2016; Meng et al. 2016; Zhou et al. 2016). According to Li et al. (Li et al. 2016a, b), the Kirsehir, Sakarya (Robertson et al. 1991, 1996), and perhaps the Lesser Caucasus-Sanandaj-Sirjan, Biston-Avoraman plates drifted in the central Neotethys area (Adamia 1991; Robertson et al. 1991, 1996, 2004; Arfania and Shahriari 2009; Mehdipour Ghazi and Moazzen 2015; Nouri et al. 2016). According to Metcalfe (2013a, b) South West Borneo and East Java-West Sulawesi were separated from Northwest Australia in the Late Triassic in the easternmost Tethys area. The consolidation of the Chinese and south-eastern Asian blocks was followed by extensional tectonics caused by the pulling force if the new Neotethys subduction. Consequently, rift basins developed in China and adjacent areas (Golonka et al. 2006b; Luo et al. 2014). This process was enhanced by the Panthalassa (Paleo-Pacific) plate sliding beneath the Eurasian plate (Luo et al. 2014; Li et al. 2016a, b).

2.5 Sedimentation and Paleolithofacies

Continental rifts, which originated during Triassic times, were filled with clastic deposits, particularly abundant red beds consisting of fluvial deposits and accompanied by evaporites (Ziegler 1988; Withjack et al. 1998; Golonka and Ford 2000; Kutek 2001; Feist-Burkhardt et al. 2008). Mixed siliciclastics, carbonates and evaporates were deposited in Central Europe (Figs. 2.3 and 2.9) as to the upper part (Keuper) of the Central European tripartite facies sequence that gave the Triassic its name (Köppen and Carter 2000). The Keuper Formation encompasses the Carnian, Norian and Rhaetian stages (Fig. 2.9). The accumulation of sediments in this area reached up to 4000 m due to significant subsidence (Köppen and Carter 2000; Kutek 2001; Golonka 2007a, b; Feist-Burkhardt et al. 2008). Meanwhile, continental red

beds were deposited in the eastern United States while a marine shelf existed on the western North America margin. Continental rifting occurred between northern Europe and Greenland (Fig. 2.8). The Pangaea rift systems extended from the Newark and Central Europe basins through the North Atlantic, to the Barents shelf and Arctic Alaska (Figs. 2.3, 2.8 and 2.9). These rifts were filled primarily with red continental clastics reflecting arid climate (Ronov et al. 1989; Olsen 1997; Golonka et al. 2003a, 2006a, b; Golonka 2007a, b; Dickinson 2004, 2008, 2009; Miall et al. 2008; Miall and Blakey 2008). Carbonate sedimentation dominated in the Alps and Carpathians (Golonka 2004, 2007a, b; Feist-Burkhardt et al. 2008). This sedimentation was associated with existence of platforms on the Neotethys and Paleotethys margins as well as on Cimmerian microplates. Shallow-water limestones and dolomites with algal/coral-dominated reefs were deposited on these platforms (Golonka 2007a, b). They were accompanied by fine grained clastics (Figs. 2.3 and 2.9). Many of the western Tethyan reefs were located on these platforms. Triassic carbonate platforms and reefs were formed not only in the Tethys, but also in the western and eastern parts of the Panthalassa (Paleo-Pacific) Ocean (Golonka 2007a, b). A large carbonate platform that spread from Apulia to the Taurus zone provides an example (Dercourt et al. 1993, 2000; Golonka 2004, 2007a, b; Feist-Burkhardt et al. 2008) in that it contains significant numbers of reefs (Kiessling and Flügel 1999; Flügel 2002) and was connected with the Alpine-Inner Carpathian carbonate platforms, which also contained abundant reefs (Kiessling and Flügel 1999; Flügel 2002). Dolomitization of the platform limestones was common and dolomites are widespread in Southern Europe and Central Asia. The Dolomia Principale (Fig. 2.9) represents a classic example of the Tethyan dolomites. The Dolomites range in the Italian Southern Alps took their name from the mineral and rock dolomite, which in turn were named after the French geologist Dieudonné Sylvain Guy Tancrède de Gratet de Dolomieu by de Saussure (1792). Dolomites were also widespread on the southern margin of Eurasia in the Caspian area and in Central Asia (Figs. 2.5 and 2.7). Continental and marginal marine sediments with evaporites and volcanics were also deposited in this part of Eurasia (Zonenshain et al. 1990; Dercourt et al. 1993, 2000; Nikishin et al. 1996, 1998a, b; Brunet et al. 2002; Zharkov and Chumakov 2001; Golonka 2004, 2007a, b). The neritic and lagoonal sediments of so-called Carpathian Keuper were deposited in the Northern Carpathians during the latest Triassic, marking the uplift of the Inner Carpathian plate (Kotański 1961; Golonka 2004; Feist-Burkhardt et al. 2008; Rychliński 2008). The Neotethyian margins of Greater India, Arabia and Australia (Figs. 2.5 and 2.7) were occupied by mixed carbonate-clastic facies (Cook 1990; Alsharhan and Magara 1994; Golonka and Ford 2000; Golonka 2007a, b). Basins containing Triassic continental red bed deposits were located in Gondwana (Fig. 2.7), in South America, Africa, Antarctica, Madagascar and India (Golonka 2007a, b). The deposition of synorogenic flysch sequences in South-East Asia was linked to the Indosinian orogenic collisional events (Hahn 1984; Golonka et al. 2006b; Lepvrier and Maluski 2008; Cai et al. 2017). They were accompanied by pelagic cherts, cherty limestones and fine-grained clastics as well as by volcanoclastics and pillow lavas (Ishida et al. 2006; Bannert et al. 2011; Win Swe 2012; Cai et al. 2017) and followed by post-orogenic

molasses. Post-orogenic Upper Triassic continental red conglomerates are known as "terraines rouges" of Deprat (1913, 1914) in Vietnam (Golonka et al. 2006a, b). These red-bed postorogenic facies that follow synorogenic turbidites and pelagic cherts are also known from the Malaysian Peninsula (Oliver and Prave 2013; Ridd 2013). Flysch sequences and volcanoclastic deposits occur on the Lhasa plate, South Tibet (Liu et al. 2012). Shallow marine, carbonate and clastic sedimentation dominated on the Qiantang plate (Zhu et al. 2013; Wu et al. 2016). Various stratigraphic sequences representing different paleogeographic facies existed in South China where paralic clastics, shallow marine clastics, shelf carbonate platform facies and deep water turbidites can be distinguished. Siliciclastic sedimentation prevailed in North China, including shallow marine clastics, marginal marine deposits such as deltas, as well as turbidites accompanied by volcanoclastics (Fig. 2.6; Hongzen 1985; Tong and Yin 2002; Golonka 2007a, b; Cao et al. 2010; Luo et al. 2014; Li et al. 2014). The sediments consisting mainly of fine-grained molasse-type filled the foreland basins following the Uralian orogeny in Timan-Pechora, Novaya Zemlya and eastern Barents regions. Siliciclastics were common in the Siberia and Arctic regions (Figs. 2.8 and 2.9; Embry 1988, 1993, 1997; Nikishin et al. 1996; Golonka and Ford 2000; Golonka et al. 2003a; Golonka 2007a, b, 2011; Toro et al. 2016); the Sverdrup Basin of Arctic Canada was a main depocenter with the Late Triassic succession of fluvial to marine slope deposits being over 2500 m thick (Embry 1997). Triassic, restricted-marine shelf basins contain black shales that have source rock potential (Leith et al. 1993; Golonka et al. 2003a; Golonka 2007b). Upper Triassic source rocks, important for hydrocarbon exploration in the North Atlantic, were identified in the Jameson Land Basin, East Greenland (Andrews et al. 2014).

2.6 Global Base-Level Changes

In this section, we briefly review postulated base-level changes that have been interpreted to affected numerous basins throughout Pangaea during the Late Triassic. We first look at small scale changes with frequencies of less than 500,000 years. Then we address large scale base-level changes with frequencies of greater than 2 million years.

Tanner (2010) comprehensively reviewed the literature for high frequency, small scale cycles for the entire Triassic. Such cycles have been recorded in various Late Triassic successions with the best documentation being from the rift valley deposits of the Newark Group of the northeastern USA (Olsen and Kent 1996) and the carbonate platforms of the Italian Alps (Cozzi et al. 2005; Schwarzacher 2006). The Late Triassic small scale cycles of the Italian Alps are characterized by the presence of exposure surfaces and paleosols. This leaves little doubt as to such cycles being generated by base-level changes caused by either eustasy or tectonics. It must be noted that any high frequency, small scale cycles which do not include exposure surfaces may well have an auto-cyclic explanation for their generation.

Given the occurrence of such high-frequency base level changes in the Late Triassic of the Italian Alps and the apparent coincidence of the calculated frequencies with those of the Milankovitch spectrum (Cozzi et al. 2005; Schwarzacher 2006), it seems reasonable to assume that small-scale, global sea-level changes driven by climate changes characterize the Late Triassic. However, as cautioned by Tanner (2010), this interpretation cannot be considered as unassailable for two main reasons. Given the greenhouse climate of the Late Triassic (Preto et al. 2010) and the consequent unlikelihood that substantial amounts of water could have been stored as ice during cold periods, there are no obvious mechanisms for climate changes to drive eustatic sea level change of the magnitude seemingly recorded by the cycles. The other problem is the general lack of precise radiometric age dates to constrain the interpreted cycle periods.

More studies are needed for Late Triassic, very shallow water carbonate and siliciclastic strata in a number of basins of Pangaea to see if they are characterized by high-frequency cycles that are capped by exposure surfaces. If Milankovitch climate change cycles were operating during the Late Triassic, then such cycles should be present in the successions of most, if not, every basin. In summary, it is quite possible that Milankovitch climate cycles were operating during the Late Triassic but further studies are needed to confirm or deny such a phenomenon.

Large scale, base-level changes are recorded in most Late Triassic successions and are expressed as large-magnitude, sequence boundaries. Such boundaries are characterized by an extensive unconformable portion on the basin margins and are the product of base-level changes that can exceed 100 m. Both eustatic and tectonic explanations have been offered for the generation of these boundaries.

Late Triassic, large-magnitude, sequence boundaries, which have been recorded in different basins throughout Pangaea, have been biostratigraphically dated as near the base Carnian, mid-Carnian, near the base Norian, mid-Norian, near the base Rhaetian and latest Rhaetian. Initially, these boundaries were interpreted to be the product of eustasy, including a significant sea level fall followed by sea level rise (Haq et al. 1987, 1988; Embry 1988; De Zanche et al. 1993; Gianolla and Jacquin 1998). Given a climate change/continental glaciation explanation was not possible, the authors appealed to changes in the volume of the world ocean (tectono-eustasy) as the main driver of such large scale eustatic changes.

Embry (1989, 1997) reversed his earlier interpretation and postulated that the large-magnitude sequence boundaries, which punctuated the entire Mesozoic succession of the Sverdrup Basin of Arctic Canada, were of tectonic origin. This interpretation was based on various characteristics of such boundaries which strongly favor a tectonic origin. Such characteristics included:

- A widespread, often angular, unconformity on the basin margins and positive elements
- A major change in depositional regime
- A notable change in tectonic regime and subsidence pattern
- A change in provenance for siliciclastic sediments
- A widespread transgression with significant deepening directly following the boundary.

Furthermore Embry (1997) demonstrated that the five, Late Triassic large-magnitude sequence boundaries present in the Sverdrup Basin are also present in basins in western Canada, southwestern USA, Barents Sea, Germany, Italian Alps, western Siberia, and northern Himalayas (Fig. 2.9). Notably, the unconformities in all these areas exhibit characteristics which favor a tectonic origin.

To explain the occurrence of simultaneous tectonic episodes in multiple and widely separated basins of Pangaea, Embry (1997) invoked the tectonic model of Cloetingh et al. (1985). The widespread, large magnitude base-level changes of the Late Triassic were interpreted to be an expression of relatively rapid and substantial changes in the horizontal and vertical stress fields that affected the Pangaea supercontinent (Fig. 2.9). Such stress changes would be possibly due to somewhat abrupt changes in the speed and/or direction of the plate movements that episodically affected Pangaea. Notably, it is possible that secondary tectono-eustatic effects were associated with such plate tectonic reorganizations (Embry 1997).

2.7 Climate Change and Episodic Tectonism

The climate of the Triassic has been reviewed by Preto et al. (2010) and they have interpreted that it "was characterized by a non-zonal pattern, dictated by a strong global monsoon system with effects that are most evident in the Tethys realm". For the Late Triassic, Preto et al. (2010) postulated that the monsoonal climate had its maximum expression and that there were three climatic zones which did not have a clear latitudinal distribution. These three zones included a dry climate for the western margin of Tethys and the central part of Pangaea, a wet and dry climate for the coasts of eastern Laurasia and Gondwana and the western coasts of Pangaea, and a wet climate in the high latitudes.

Although, in general, there was not much variability in climate throughout the Late Triassic, significant climate changes seem to be associated with the five tectonic episodes discussed in the last section. The most well-known of these is the "Carnian Pluvial Episode" (Ruffell et al. 2015) which corresponds with the mid-Carnian tectonic episode. This event was marked by warmer, more humid conditions in various parts of Pangaea and a notable increase of siliciclastic supply to numerous basins (Ruffell et al. 2015). Climate changes seem to have occurred associated with the other four tectonic episodes as shown by the marked changes in spore/pollen ratios associated with these boundaries (Hochuli and Vigran 2010). Climate change associated with the latest Rhaetian has been documented by various workers as summarized by Preto et al. (2010). The CAMP flood basalts, which were associated with the extensional phase of the latest Rhaetian tectonic episode, produced enormous amounts of CO_2, triggered global warming, and increased ocean acidification. These factors caused the end of Triassic extinction event (Wignall 2001; Lucas and Tanner 2008; Preto et al. 2010; Bond and Wignall 2014; Müller et al. 2016).

2.8 Concluding Summary

Herein, we present a new set of global and regional paleogeographic maps for the Late Triassic (Carnian-Rhaetian) time interval. The global maps depict the plate tectonic configuration, present day coastlines, subduction zones, selected transform faults, spreading centers and rifts during the beginning (224 Ma) and end (200 Ma) of Late Triassic. The regional maps illustrate the Late Triassic paleoenvironment and paleolithofacies distribution for most important regions. The stratigraphic chart shows Late Triassic stratigraphy of various basins and sequence boundaries of basal Carnian, mid-Carnian, basal Norian, mid-Norian, basal Rhaetian, and latest Rhaetian age.

The Late Triassic was a time of collisional events, now known as Early Cimmerian and Indosinian orogenies. This series of collisions closed the Paleotethys Ocean. The closure happened earlier in the Alpine-Carpathian-Mediterranean area, later in the Eastern Europe-Central Asia and latest in the South-East Asia. The Indochina, Southeastern Asian and Qiangtang plates were sutured to South China. The new, large Chinese-Southeast Asian plate, including the North and South China, Mongolia and eastern Cimmerian plates, was consolidated at the Triassic-Jurassic Boundary. This consolidation left open a large embayment of Panthalassa, between Mongolia and Laurasia, known as Mongol-Okhotsk Ocean. The Uralian Orogeny, which sutured Siberia and Europe continued during Late Triassic times and was recorded in Novaya Zemlya.

The onset of the break-up of Pangaea constitutes the main Late Triassic extensional tectonics event. Continental rifts, which originated during this event, were filled with clastic deposits. Abundant red beds, accompanied by fluvial deposits and evaporites, were deposited in classic sedimentary systems. The pulling force of the north-dipping subduction along the northern margin of Neotethys caused the drift of a new set of plates from the passive Gondwana margin. These plates divided the Neotethys Ocean. Carbonate sedimentation was associated with existence of platforms on the Neotethys and Paleotethys margins as well as on Cimmerian microplates. Synorogenic turbidites and postorogenic molasses were associated with the Indosinian orogeny. The late stages of the Uralian orogeny in Timan-Pechora, Novaya Zemlya and eastern Barents regions included the filling of the foreland basin with fine-grained, molasse sediments. Siliciclastics were common in the Siberia and Arctic regions.

The widespread, large magnitude, base level changes of the Late Triassic are interpreted to be an expression of relatively rapid and substantial changes in the horizontal and vertical stress fields that affected the Pangaea supercontinent. Such stress changes would be possibly due to somewhat abrupt changes in the speed and/or direction of plate movements, which episodically affected Pangaea. The Late Triassic climate changes seem to be associated with the main tectonic episodes. The most well-known of these is the “Carnian Pluvial Episode” which corresponds with the mid-Carnian tectonic episode. The Central Atlantic Magmatic Province flood basalts, which were associated with the extensional phase of the latest Rhaetian

tectonic episode, produced enormous amounts of CO_2, triggering global warming, increasing ocean acidification, and causing the latest Triassic extinction event.

Acknowledgements The research was partially supported by Faculty of Geology, Geophysics and Environmental Protection, AGH University of Science and Technology, Kraków, Poland Statutory grant no. 11.11.140.005. Embry thanks the Geological Survey of Canada for supporting his research on the Triassic of the Canadian Arctic for the past 40 years.

References

Adamia SA (1991) The Caucasus oil and gas province, Occasional Publications. ESRI, New Series No. 7(I-II), Part I: 53–74

Alsharhan AS, Magara K (1994) The Jurassic of the Arabian Gulf Basin: facies, depositional setting and hydrocarbon habitat. In: Embry AF, Beauchamp B, Glass DJ (eds) Pangea; global environments and resources. Can Soc Petr Geolog Mem 17:397–412

Andrews SD, Kelly SRA, Braham W, Kaye M (2014) Climatic and Eustatic controls on the development of a Late Triassic source rock in the Jameson Land Basin, East Greenland. J Geol Soc 171(5):609–619

Anfinson OA, Embry AF, Stockli DF (2016) Geochronologic Constraints on the Permian-Triassic Northern Source Region of the Sverdrup Basin, Canadian Arctic Islands. Tectonophys 691:206–219

Arfania R, Shahriari S (2009) Role of southeastern Sanandaj-Sirjan Zone in the tectonic evolution of Zagros Orogenic Belt, Iran. Island Arc 18(4):555–576

Arvizu HE, Iriondo A (2015) Temporal control and geology of the PermoTriassic magmatism in Sierra Los Tanques, NW Sonora, Mexico: Evidence for the beginning of cordilleran arc magmatism in SW of Laurentia [Control temporal y geología del magmatismo Permo-Triásico en Sierra Los Tanques, NW Sonora, México: Evidencia del inicio del arco magmático cordillerano en el SW de Laurencia]. Boletin de la Sociedad Geologica Mexicana 67(3):545–586

Baby P, Rivadeneira M, Barragàn R, Christophoul F (2013) Thick-skinned tectonics in the Oriente foreland basin of Ecuador. Geol Soc London Spec Publ 377(1):59–76

Bannert D, Sang Lyen A, Htay T (2011) The geology of the Indoburman ranges in Myanmar. Geol Jb B 101:5–101

Belasky P, Stevens CH, Hanger RA (2002) Early Permian location of western North American terranes based on brachiopod, fusulinid, and coral biogeography. Palaeogeogr Palaeoclimatol Palaeoecol 179:245–266

Bao Z, Wang CY, Zeng L, Sun W, Yao J (2015) Slab break-off model for the Triassic syn-collisional granites in the Qinling orogenic belt, Central China: Zircon U-Pb age and Hf isotope constraints. Internat Geol Rev 57(4):492–507

Bond DPG, Wignall PB (2014) Large igneous provinces and mass extinctions: an update. In: Keller G, Kerr AC (eds) Volcanism, impacts, and mass extinctions: causes and effects. Geol Soc Am Spec Pap 505: 29–55

Brunet M-F, Korotaev MV, Ershov AV, Nikishin AM (2002) The South Caspian basin: a review of the evolution with the approach of the subsidence modelling. In: Brunet M-F, Cloetingh S (eds) Integrated PeriTethyan Basins Studies. Sed Geol, vol 156, pp 119–148

Bustamante A, Juliani C (2011) Unraveling an antique subduction process from metamorphic basement around Medellín city, Central Cordillera of Colombian Andes. J S Am Earth Sci 32(3):210–221

Cai F, Ding L, Laskowski AK, Kapp P, Wang H, Xu Q, Zhang L (2016) Late Triassic paleogeographic reconstruction along the Neo-Tethyan Ocean margins, southern Tibet. Earth Planet Sci Lett 435:105–114

Cai F, Ding L, Yao W, Laskowski AK, Xu Q, Zhang J, Sein K (2017) Provenance and tectonic evolution of Lower Paleozoic–Upper Mesozoic strata from Sibumasu terrane, Myanmar. Gond Res 41:325–336

Cao J, Wang X, Wei D, Sun P, Hu W, Jia D, Zha Y (2010) Complex petroleum migration and accumulation in central region of southern Junggar basin, Northwest China. J Earth Sci 21(1):83–93

Catalano R, Di Stefano P, Kozur H (1991) Permian circumpacific deep-water faunas from the western Tethys (Sicily, Italy): new evidence for the position of the Permian Tethys. Palaeogeogr Palaeoclimatol Palaeoecol 87:75–108

Centeno-García E (2017) Mesozoic tectono-magmatic evolution of Mexico: An overview. Ore Geol Rev 81:1035–1052

Centeno-García E, Guerrero-Suastegui M, Talavera-Mendoza O (2008) The Guerrero composite terrane of western Mexico: collision and subsequent rifting in a supra-subduction zone. In: Drau A, Clift PD, Scholl DW (eds) Formation and applications of the sedimentary record in arc collision zones. Geol Soc Am Spec Pap 436: 279–308

Channell JET, Kozur H (1997) How many oceans? Meliata, Vardar, and Pindos oceans in Mesozoic Alpine paleogeography. Geology 25:183–186

Chen B, Jahn B-M, Wilde S, Xu B (2000) Two contrasting paleozoic magmatic belts in northern Inner Mongolia, Chine: petrogenesis and tectonic implications. Tectonophys 328:157–182

Choulet F, Chen Y, Cogné J-P, Rabillard A, Wang B, Lin W, Faure M, Cluzel D (2013) First Triassic palaeomagnetic constraints from Junggar (NW China) and their implications for the Mesozoic tectonics in Central Asia. J Asian Earth Sci 78:371–394

Cirilli S, Marzoli A, Tanner L, Bertrand H, Buratti N, Jourdan F, Bellieni G, Kontak D, Renne PR (2009) Latest Triassic onset of the Central Atlantic Magmatic Province (CAMP) volcanism in the Fundy Basin (Nova Scotia): New stratigraphic constraints. Earth Planet Sci Lett 286(3–4):514–525

Cloetingh S, McQueen H, Lambeck K (1985) On a plate tectonic mechanism for regional sea level variations. Earth Planet Sci Lett 75:157–166

Colpron M, Nelson JL (2011) A Palaeozoic NW passage and the Timanian, Caledonian and Uralian connections of some exotic terranes in the North American Cordillera. In: Spencer AM, Embry AF, Gautier DL, Stoupakova AV, Sørensen K (eds) Arctic petroleum geology. Geol Soc London Mem 35: 463–484

Cook PI (1990) Australia—evolution of a continent. Australian Government Publishing Services, Canberra

Cozzi A, Hinnov LA, Hardie LA (2005) Orbitally forced Lofer cycles in the Dachstein Limestone of the Julian Alps (northeastern Italy). Geol 33:789–792

Dallmeyer RD, Neubauer F, Fritz H (2008) The Meliata suture in the Carpathians: regional significance and implications for the evolution of high-pressure wedges within collisional orogens. Geol Soc London Spec Publ 298:101–115

De Zanche V, Gianolla P, Mietto P, Siorpaes C, Vail PR (1993) Triassic sequence stratigraphy in the Dolomites (Italy). Memorie di Scienze Geologiche 45:1–27

Debiche MG, Cox A, Engebretson D (1987) The motion of allochthonous terranes across the North Pacific basin. Geol Soc Am Spec Pap 207:1–49

del Rey A, Deckart K, Arriagada C, Martínez F (2016) Resolving the paradigm of the late Paleozoic–Triassic Chilean magmatism: Isotopic approach. Gond Res 37:172–181

Deprat J (1913) Les chamages de la région de la Rivière Noire sur les feuilles de Thanh-ba et Van-Yên. Mémoires de Service Géologique d'Indochine 2:47–65

Deprat J (1914) Etude des plissements et des zones d'écrasement de la moyenne et de la basse Rivière Noire. Mémoires de Service Géologique d'Indochine 3:1–59

Dercourt J, Ricou LE, Vrielynck B (eds) (1993) Atlas Tethys Paleoenvironmental maps. Gauthier-Villars, Paris

Dercourt J, Gaetani M, Vrielynck B, Barrier E, Biju-Duval B, Brunet M-F, Cadet JP, Crasquin S, Sandulescu M (eds) (2000) Atlas Peri-Tethys Paleoegeographical maps. CCGM/CGMW, Paris

Dickinson WR (2004) Evolution of the North American Cordillera. Annu Rev Earth Planet Sci 32:13–45

Dickinson WR (2008) Accretionary Mesozoic-Cenozoic expansion of the Cordilleran continental margin in California and adjacent Oregon. Geosphere 4(2):329–353
Dickinson WR (2009) Anatomy and global context of the North American Cordillera. In: Kay SM, Ramos VA, Dickinson WR (eds) Backbone of the Americas: shallow subduction, plateau uplift, and ridge and terrane collision. Geol Soc Am Mem 204: 1–29
Domeier M, Van Der Voo R, Torsvik TH (2012) Paleomagnetism and Pangaea: The road to reconciliation. Tectonophys 514-517:14–43
Dong Y, Zhang G, Neubauer F, Liu X, Genser J, Hauzenberger C (2011) Tectonic evolution of the Qinling orogen, China: Review and synthesis. J Asian Earth Sci 41(3):213–237
Donskaya TV, Gladkochub DP, Mazukabzov AM, Ivanov AV (2013) Late Paleozoic - Mesozoic subduction-related magmatism at the southern margin of the Siberian continent and the 150 million-year history of the Mongol-Okhotsk Ocean. J Asian Earth Sci 62:79–97
Donskaya TV, Gladkochub DP, Mazukabzov AM, Wang T, Guo L, Rodionov NV, Demonterova EI (2016) Mesozoic granitoids in the structure of the Bezymyannyi metamorphic-core complex (western Transbaikalia). Russ Geol Geophys 57(11):1591–1605
Doré AG (1991) The structural foundation and evolution of Mesozoic seaways between Europe and the Arctic. Palaeogeogr Palaeoclimatol Palaeoecol 87:441–492
Dorsey RJ, LaMaskin TA (2007) Stratigraphic record of Triassic-Jurassic collisional tectonics in the Blue Mountains province, northern Oregon. Am J Sci 307(10):1167–1193
Embry AF (1988) Triassic sea-level changes: evidence from the Canadian Arctic Archipelago. In: Wilgus CK, Posamentier H, Ross CA, Kendall, CGStC (eds) Sea-level changes: an integrated approach. Soc Econ Paleontol Mineralog Spec Publ 42: 249–259
Embry A (1989) A tectonic origin for third-order depositional sequences in extensional basins implications for basin modelling. In: Cross T (ed) Quantitative dynamic stratigraphy. Prentice Hall, Upper Saddle River, NJ. p. 491–502
Embry AF, (1993) Crockerland—the northern source area for the Sverdrup Basin, Canadian Arctic Archipelago. In: Vorren T, Bergsager E, Dahl-Stamnes O, Holter E, Johansen B, Lie E, Lund T (eds) Arctic geology and petroleum potential: Norweg Petrol Soc Spec Publ 2: 205–216
Embry AF (1997) Global sequence boundaries of the Triassic and their recognition in the Western Canada Sedimentary Basin. Bull Can Petrol Geol 45:415–433
Embry AF, Anfinson OA (2014) The initiation of the rift phase of the Amerasia Basin (Arctic Ocean). CSPG Geoconvention 2014, Abstr. Calgary, AB, Canada p 1–4
Engebretson DC, Cox A, Gordon RG (1985) Relative motions between oceanic and continental plate in the Pacific basin. Geol Soc Am Spec Pap 206:1–59
Ershova VB, Prokopiev AV, Khudoley AK, Sobolev NN, Petrov EO (2015a) U/Pb dating of detrital zircons from late Palaeozoic deposits of Belkovsky Island (New Siberian Islands): Critical testing of Arctic tectonic models. Internat Geol Rev 57(2):199–210
Ershova VB, Prokopiev AV, Khudoley AK, Sobolev NN, Petrov EO (2015b) Detrital zircon ages and provenance of the Upper Paleozoic successions of Kotel'ny Island (New Siberian Islands archipelago). Lithosph 7(1):40–45
Faure M, Lepvrier C, Nguyen VV, TV V, Lin W, Chen Z (2014) The South China block-Indochina collision: Where, when, and how? J Asian Earth Sci 79:260–274
Feist-Burkhardt S, Götz AE, Szulc J, Borkhataria R, Geluk M, Haas J, Hornung J, Jordan P, Kempf O, Michalík J, Nawrocki J, Reinhardt L, Ricken W, Röhling H-G, Rüffer T, Török Á, Zühlke R (2008). Triassic. In: McCann T (ed) The geology of Central Europe. Volume 2: Mesozoic and Cenozoic, Geol Soc, London, p 749–821
Ferriere J, Baumgartner PO, Chanier F (2016) The Maliac Ocean: the origin of the Tethyan Hellenic ophiolites. Internat J Earth Sci 105(7):1941–1963
Flügel E (2002) Triassic Reef Patterns. In: Kiessling W, Flügel E, Golonka J (eds) Phanerozoic reef patterns. Soc Econ Paleontol Mineral Spec Publ 72: 391–464
Ford D, Golonka J (2003) Phanerozoic paleogeography, paleoenvironment and lithofacies maps of the circum-Atlantic margins. In: Golonka J (ed) Thematic set on paleogeographic reconstruction and hydrocarbon basins: Atlantic, Caribbean, South America, Middle East, Russian Far East, Arctic. Mar Petrol Geol 20: 249–285

Fromaget J (1927) Etudes géologiques sur le Nord de 1'Indochine centrale. Bull Serv Géol Indoch 16(2):1–368
Fromaget J (1934) Observations et reflexions sur la geologic stratigraphique et structurale de l'Indochine. Bull Soc Geol Fr 5(4):101–164
Fromaget J (1941) L'Indochine Française, sa structure geologique, ses roches, ses mines et leurs relations possibles avec la tectonique. Bull Serv Géol Indoch 26(2):1–140
Fromaget J (1952) Etudes geologiques sur le nord-Ouest du Tonkin et le Nord du Haut-Laos. 2ème et 3ème parties. Bull Serv Géol Indoch 29(6):1–198
Gawlick H-J, Missoni S (2015) Middle Triassic radiolarite pebbles in the Middle Jurassic Hallstatt Mélange of the Eastern Alps: implications for Triassic–Jurassic geodynamic and paleogeographic reconstructions of the western Tethyan realm. Facies 61(3):1–19
Giambiagi L, Mescua J, Bechis F, Martínez A, Folguera A (2011) Pre-Andean deformation of the Precordillera southern sector, southern Central Andes. Geosphere 7(1):219–239
Gianolla P, Jacquin T (1998) Triassic sequence stratigraphic framework of Western European basins. In: de Graciansky PC, Hardenbol J, Jacquin T, Vail PR (eds) Mesozoic and Cenozoic sequence stratigraphy of European basins. Soc Econ Paleontol Mineral Spec Publ 60: 643–650
Glørstad-Clark E, Faleide JI, Lundschien BA, Nystuen JP (2010) Triassic seismic sequence stratigraphy and paleogeography of the western Barents Sea area. Marine and Petroleum Geol 27(7):1448–1475
Golonka J (2000) Cambrian-Neogene Plate Tectonic Maps. Wydawnictwa Uniwersytetu Jagiellońskiego, Kraków
Golonka J (2002) Plate-tectonic maps of the Phanerozoic. In: Kiessling W, Flügel E, Golonka J (eds) Phanerozoic reef patterns. Soc Econ Paleontol Mineral Spec Publ 72: 21–75
Golonka J (2004) Plate tectonic evolution of the southern margin of Eurasia in the Mesozoic and Cenozoic. Tectonophys 381:235–273
Golonka J (2007a) Late Triassic and Early Jurassic paleogeography of the world. Palaeogeogr Palaeoclimatol Palaeoecol 244:297–307
Golonka J (2007b) Phanerozoic Paleoenvironment and Paleolithofacies Maps. Mesozoic. Mapy paleośrodowiska i paleolitofacje fanerozoiku. Mezozoik. Kwartalnik AGH. Geologia 33(2):211–264
Golonka J (2011) Phanerozoic palaeoenvironment and palaeolithofacies maps of the Arctic region. In: Spencer, AM, Embry AF, Gautier DL, Stoupakova A, Sørensen K (eds) Arctic petroleum geology. Geol Soc London Mem 35: 79–129
Golonka J, Bocharova NY (2000) Hot spots activity and the break-up of Pangaea. Palaeogeogr Palaeoclimatol Palaeoecol 161:49–69
Golonka J, Ford DW (2000) Pangaean (Late Carboniferous–Middle Jurassic) paleoenvironment and lithofacies. Palaeogeogr Palaeoclimatol Palaeoecol 161:1–34
Golonka J, Kiessling W (2002) Phanerozoic time scale and definition of time slices. In: Kiessling W, Flügel E, Golonka J (eds) Phanerozoic reef patterns. Soc Econ Paleontol Mineral Spec Publ 72:11–20
Golonka J, Ross MI, Scotese C R (1994) Phanerozoic paleogeographic and paleoclimatic modeling maps. In: Embry AF, Beauchamp B, Glass DJ (eds) Pangaea; global environments and resources. Can Soc Petrol Geol Mem 17: 1–47
Golonka J, Bocharova NY, Ford D, Edrich ME, Bednarczyk J, Wildharber J (2003a) Paleogeographic reconstructions and basins development of the Arctic. In: Golonka J (ed) Thematic set on paleogeographic reconstruction and hydrocarbon basins: Atlantic, Caribbean, South America, Middle East, Russian Far East, Arctic. Mar Petrol Geol 20: 211–248
Golonka J, Krobicki M, Oszczypko N, Ślączka A, Słomka T (2003b) Geodynamic evolution and palaeogeography of the Polish Carpathians and adjacent areas during Neo-Cimmerian and preceding events (latest Triassic–earliest Cretaceous). In: McCann T, Saintot A (eds) Tracing tectonic deformation using the sedimentary record. Geol Soc London Spec Publ 208: 138–158
Golonka J, Krobicki M, Pająk J, Van Giang N, Zuchiewicz W (2006a) Global plate tectonics and paleogeography of Southeast Asia. Arkadia, Kraków

Golonka J, Gahagan L, Krobicki M, Marko F, Oszczypko N, Ślączka A (2006b) Plate Tectonic Evolution and Paleogeography of the Circum-Carpathian Region. In: Golonka J. & Picha F (eds) The Carpathians and their foreland: Geology and hydrocarbon resources: Am Assoc Petrol Geol Mem 84: 11–46

Goodge JW (1989) Polyphase metamorphic evolution of a Late Triassic subduction complex, Klamath Mountains, northern California. Am J Sci 289(7):874–943

Goodge JW (1990) Tectonic evolution of a coherent Late Triassic subduction complex, Stuart Fork terrane, Klamath Mountains, northern California. Geol Soc Am Bull 102(1):86–101

Haas J, Pero S (2004) Mesozoic evolution of the Tisza Mega-unit. Internat J Earth Sciences 93:297–313

Hahn L (1984) The Indosinian Orogeny in Thailand and adjacent areas. Mémoires de la Société géologique de France 147:71–82

Haq BU, Hardenbol J, Vail PR (1987) Chronology of fluctuating sea levels since the Triassic. Science 235:1156–1167

Haq BU, Hardenbol J, Vail PR (1988) Mesozoic and Cenozoic chronostratigaphy and cycles of sea-level change In: Wilgus, CK, Posamentier H, Ross CA, Kendall, CGStC (eds) Sea-level Changes: an Integrated Approach. Soc Econ Paleontol Min Spec Publ 42: 71–108

Helbig M, Keppie JD, Murphy JB, Solari LA (2013) Exotic rifted passive margin of a back-arc basin off western Pangaea: Geochemical evidence from the Early Mesozoic Ayú Complex, southern Mexico. Internat Geol Rev 55(7):863–881

Heydari E (2008) Tectonics versus eustatic control on supersequences of the Zagros Mountains of Iran. Tectonophys 451(1–4):56–70

Hochuli PA, Vigran JO (2010) Climate variations in the Boreal Triassic—inferred from palynological records from the Barents Sea. Palaeogeogr Palaeoclimatol Palaeoecol 290:20–42

Hoeck V, Ionescu C, Balintoni I, Koller F (2009) The Eastern Carpathians "ophiolites" (Romania): Remnants of a Triassic ocean. Lithos 108(1–4):151–171

Hongzen W (1985) Atlas of Paleogeography of China. Cartographic Publishing House, Beijing

Hounslow MW, Nawrocki J (2008) Palaeomagnetism and magnetostratigraphy of the Permian and Triassic of Spitsbergen: a review of progress and challenges. Pol Res 27(3):502–522

Huang K, Opdyke ND (2016) Paleomagnetism of the Upper Triassic rocks from south of the Ailaoshan Suture and the timing of the amalgamation between the South China and the Indochina Blocks. J Asian Earth Sci 119:118–127

Hung KT (2010) Overview of magmatism in northwestern Vietnam. Ann Soc Geol Pol 80(2):185–226

Ishida K, Nanba A, Hirsch F, Kozai T, Meesook A (2006) New micropalaeontological evidence for a Late Triassic Shan-Thai orogeny. Geosci J 10(3):181–194

Ivan P (2002) Relics of the Meliata Ocean crust: Geodynamic implications of mineralogical, petrological and geochemical proxies. Geol Carpath 53(4):245–256

Kazmin VG (1990) Early Mesozoic reconstruction of the Black Sea-Caucasus region. Evolution of the northern margin of the Tethys. Mémoires de la Société géologique de France. Nouvelle Series 54:147–158

Kazmin VG (1991) Collision and rifting in the Tethys Ocean: geodynamic implications. Tectonophys 123:371–384

Keppie JD, Dostal J (2001) Evaluation of the Baja controversy using paleomagnetic and faunal data, plume magmatism, and piercing points. Tectonophys 339:427–442

Kiessling W, Flügel E, Golonka J (1999) Paleo Reef Maps: Evaluation of a comprehensive database on Phanerozoic reefs: Am Assoc Petrol Geol Bull 83: 1552–1587

Kiessling W, Flügel E, Golonka J (2003) Patterns of Phanerozoic carbonate platform sedimentation. Lethaia 36:195–226

Knight KB, Nomade S, Renne PR, Marzoli A, Bertrand H, Youbi N (2004) The Central Atlantic magmatic province at the Triassic-Jurassic boundary: paleomagnetic and $^{40}Ar/^{39}Ar$ evidence from Morocco for brief, episodic volcanism. Earth Planet Sci Lett 228:143–160

Köppen A, Carter A (2000) Constraints on provenance of the central European Triassic using detrital zircon fission track data. Palaeogeogr Palaeoclimatol Palaeoecol 161:193–204
Kotański Z (1961) Tectogenesis and paleogeographic reconstruction of the Hig-Tatra chain in Tatra Montains (In Polish, English Summary). Acta Geologica Polonica 11: 401–415
Kovalenko DV (2010) Paleomagnetism of Late Paleozoic, Mesozoic, and Cenozoic rocks in Mongolia. Russ Geol Geophys 51(4):387–403
Kozur H (1991) The evolution of the Meliata-Halstatt ocean and its significance for the early evolution of the Eastern Alps and Western Carpathians. Palaeogeogr Palaeoclimatol Palaeoecol 87:109–130
Kozur H, Krahl W (1987) Erster Nachweis von Radiolarien in tethyalen Perm Europas. N Jahrb Geol Paleontol Abh 174:357–372
Kravchinsky VA, Cogne J-P, Harbert W, Kuzmin MI (2002) Evolution of the Mongol-Okhotsk Ocean as constrained by new paleomagnetic data from the Mongol-Okhotsk suture zone, Siberia. Geophys J Internat 148:34–57
Krzywiec P (2012) Mesozoic and Cenozoic evolution of salt structures within: the Polish Basin: an overview. Geol Soc Spec Publ 363(1):381–394
Kutek J (2001) The Polish Permo-Mesozoic Rift Basin. In: Ziegler PA Cavazza W, Robertson AHF, Crasquin-Soleau S (eds) Peri-Tethys Memoir 6: Peri-Tethyan Rift/Wrench Basins and Passive margins. Mémoires du Muséum national d'Histoire naturelle 186: 213–236
Lane LS, Stephenson RA (2016) Circum-Arctic lithosphere-basin evolution: An overview. Tectonophys 691:1–7
Laville E, Pique A, Amrhar M, Charroud M (2004) A restatement of the Mesozoic Atlantic Rifting (Morocco). J Afric Earth Sci 38:145–153
Leith TL, Weiss HM, Mørk A, Arhus N, Elvebakk N, Embry A F, Brooks P W, Stewart KR, Pchelina TM, Bro EG, Verba M L, Danushevskaya A, Borisov AV (1993) Mesozoic hydrocarbon source rocks of the Arctic region. In: Vorren TO, Bergsear E, Dahl-Stammes OA, Holter E, Johansen B, Lie E, Lund TB (eds) Arctic geology and petroleum potential. Norw Petrol Geol Spec Publ 2: 1–25
Lepvrier C, Maluski H (2008) The Triassic Indosinian orogeny in East Asia. Compt Rendus Geosci 340:75–82
Lepvrier C, Maluski H, Layreloup A, Van Tich V, Thi PT, Vuong NV (2004) The Early Triassic Indosinian orogeny in Vietnam (Truong Son Belt and Kontum Massif): implications for the geodynamic evolution of Indochina. Tectonophys 393:87–118
Li H-Y, Huang X-L (2013) Constraints on the paleogeographic evolution of the North China Craton during the Late Triassic-Jurassic. J Asian Earth Sci 70-71(1):308–320
Li S, Wilde SA, He Z, Jiang X, Liu R, Zhao L (2014) Triassic sedimentation and postaccretionary crustal evolution along the Solonker suture zone in Inner Mongolia, China. Tecton 33(6):960–981
Li X, Zheng J, Li S, Liu B, Xiang L, Wang Y, Liu X (2016a) Late Triassic orogenic collapse and Palaeo-Pacific slab roll-back beneath central South China: constraints from mafic granulite xenoliths and structural features. Geol J 51:123–136
Li Z, Ding L, Lippert PC, Song P, Yue Y, van Hinsbergen DJJ (2016b) Paleomagnetic constraints on the Mesozoic drift of the Lhasa terrane (Tibet) from Gondwana to Eurasia. Geol 44(9):727–730
Liang W, Zhang G, Bai Y, Jin C, Nantasin P (2015) New insights into the emplacement mechanism of the Late Triassic granite plutons in the Qinling orogen: A structural study of the Mishuling pluton. Geol Soc Am Bull 127(11–12):1583–1603
Liu X, Hsu KJ, Ju Y, Li G, Liu X, Wei L, Zhou X, Zhang X (2012) New interpretation of tectonic model in south Tibet. J Asian Earth Sci 56:147–159
Lu YH, Zhao Z-F, Zheng Y-F (2016) Geochemical constraints on the source nature and melting conditions of Triassic granites from South Qinling in central China. Lithos 264:141–157
Lucas SG, Tanner LH (2008) Reexamination of the end-Triassic mass extinction. In: Elewa AMT (ed) Mass Extinction. Springer, p 66–103

Luo M, Lu L, Jia J, Wang S, Xu Y, He W (2014) Evolution of sedimentary basins in China during Mesozoic. Earth Sci J China Univ Geosci 39(8):954–976

Macdonald D, Gomez-Perez I, Francese J, Spalletti L, Lawver L, Gahagan L, Dalziel I, Thomas C, Trewin N, Hole M, Paton D (2003). Mesozoic break-up of SW Gondwana: implications for regional hydrocarbon potential of the southern South Atlantic. In: Golonka J (ed) Thematic set on paleogeographic reconstruction and hydrocarbon basins: Atlantic, Caribbean, South America, Middle East, Russian Far East, Arctic. Mar Petrol Geol 20: 287–308

Maluski H, Lepvrier C, Jolivet L, Carter A, Roques D, Beyssac O, Ta TT, Thang ND, Avigad D (2001) Ar–Ar and fission-track ages in the Song Chay Massif: Early Triassic and Cenozoic tectonics in Northern Vietnam. J Asian Earth Sci 19:233–248

Maluski H, Lepvrier C, Layreloup A, Van Tich V, Thi PT (2005) ^{40}Ar-^{39}Ar geochronology of the charnokites and granulites of the Kan Nack Complex, Kon Tun Massif, Vietnam. J Asian Earth Sci 25:653–677

Marsella E, Kozur H, D'Argenio B (1993) Monte Facito Formation (Scythian - Middle Carnian. A deposit of the ancestral Lagonegro Basin in Southern Apennines. Bolletino de Servisio Geologico Italia 119: 225–248

Marzoli A, Bertrand H, Knight KB, Cirilli S, Buratti N, Verati C, Nomade S, Renne PR, Youbi N, Martini R, Allenbach K, Neuwerth R, Rapaille C, Zaninetti L, Bellieni G (2004) Synchrony of the Central Atlantic magmatic province and the Triassic-Jurassic boundary climatic and biotic crisis. Geol 32:973–976

Marzoli A, Jourdan F, Puffer JH, Cuppone T, Tanner LH, Weems RE, Bertrand H, Cirilli S, Bellieni G, De Min A (2011) Timing and duration of the Central Atlantic magmatic province in the Newark and Culpeper basins, eastern U.S.A. Lithos 122(3–4):175–188

Marzoli A, Renne PR, Piccirillo EM, Ernesto M, Bellieni G, De Min A (1999) Extensive 200-million-year-old continental flood basalts of the Central Atlantic Magmatic Province. Science 284:616–618

Masoodi M, Yassaghi A, Nogole Sadat MAA, Neubauer F, Bernroider M, Friedl G, Genser J, Houshmandzadeh A (2013) Cimmerian evolution of the Central Iranian basement: Evidence from metamorphic units of the Kashmar-Kerman Tectonic Zone. Tectonophysics 588:189–208

Matthews KJ, Maloney KT, Zahirovic S, Williams SE, Seton M, Müller RD (2016) Global plate boundary evolution and kinematics since the late Paleozoic. Glob Planet Ch 46:226–250

McKie T, Williams B (2009) Triassic palaeogeography and fluvial dispersal across the northwest European basins. Geol J 44(6):711–741

Meesook A, Sha J (2010) The Jurassic system of Thailand. Univ Sci Technol China Press, Hefe

Mehdipour Ghazi J, Moazzen M (2015) Geodynamic evolution of the Sanandaj-Sirjan Zone, Zagros Orogen, Iran. Turk J Earth Sci 24(5):513–528

Meinhold G, Kostopoulos DK (2013) The Circum-Rhodope Belt, northern Greece: Age, provenance, and tectonic setting. Tectonophys 595-596:55–68

Meng Y, Xu Z, Santosh M, Ma X, Chen X, Guo G, Liu F (2016) Late Triassic crustal growth in southern Tibet: Evidence from the Gangdese magmatic belt. Gond Res 37:449–464

Metcalfe I (1994) Late Paleozoic and Mesozoic Paleogeography of Eastern Pangaea and Tethys. In: Embry AF, Beauchamp B, Glass DJ (eds) Pangaea; global environments and resources. Can Soc Petrol Geol Mem 17: 97–111

Metcalfe I (1996) Gondwanaland dispersion, Asian accretion and evolution of eastern Tethys, In: Li Z X., Metcalfe I, Powell CM (eds) Breakup of Rodinia and Gondwanaland and assembly of Asia. Austral J Earth Sci 43: 605–623

Metcalfe I (2000) The Bentong-Raub Suture zone. J Asian Earth Sci 18:691–712

Metcalfe I (2011) Palaeozoic-Mesozoic history of SE Asia. In: Hall R, Cottam MA, Wilson MEJ (eds) The SE Asian Gateway: history and tectonics of the Australia–Asia Collision. Geol Soc Spec Publ 355: 7–35

Metcalfe I (2013a) Gondwana dispersion and Asian accretion: Tectonic and palaeogeographic evolution of eastern Tethys. J Asian Earth Sci 66:1–33

Metcalfe I (2013b) Tectonic evolution of the Malay Peninsula. J Asian Earth Sci 76:195–213

Maurer F, Rettori R, Martini R (2008) Triassic stratigraphy, facies and evolution of the Arabian shelf in the northern United Arab Emirates. Internat J Earth Sci 97(4):765–784
Metelkin DV, Kazansky AY, Vernikovsky VA (2011) Paleomagnetic evidence for Siberian plate tectonics from Rodinia through Pangaea to Eurasia. In: Closson D (ed) Tectonics. InTech, Zagreb, pp 159–236
Metelkin DV, Vernikovsky VA, Kazansky AY (2012) Tectonic evolution of the Siberian paleocontinent from the Neoproterozoic to the Late Mesozoic: Paleomagnetic record and reconstructions. Russ Geol Geophys 53(7):675–668
Miall AD, Blakey RC (2008) The Phanerozoic Tectonic and Sedimentary Evolution of North America. Sedimentary Basins of the World 5(C):1–29
Miall AD, Balkwill HR, McCracken J (2008) The Atlantic Margin Basins of North America. Sedimentary Basins of the World 5(C):473–504
Miller EL, Toro J, Gehrels G, Amato JM, Prokopiev A, Tuchkova MI, Akinin VV, Dumitru TA, Moore TE, Cecile MP (2006) New insights into Arctic paleogeography and tectonics from U-Pb detrital zircon geochronology. Tecton 25(3.) TC3013
Mock R, Sýkora M, Aubrecht R, Ožvoldová L, Kronome B, Reichwalder P, Jablonský J (1998) Petrology and stratigraphy of the Meliaticum near the Meliata and Jaklovce Villages, Slovakia. Slovak Geol Mag 4:223–260
Montenat C (2009) The Mesozoic of Afghanistan. GeoArabia 14(1):147–210
Morris A (1996) A review of paleomagnetic research in the Troodos ophiolite, Cyprus. In: Morris A, Tarling DH (eds) Paleomagnetism and Tectonics of the Mediterranean Region. Geol Soc London Spec Publ 105:311–324
Müller RD, Seton M, Zahirovic S, Williams SE, Matthews KJ, Wright NM, Shephard GE, Maloney KT, Barnett-Moore N, Hosseinpour M, Bower DJ, Cannon J (2016) Ocean basin evolution and global-scale plate reorganization events since Pangaea breakup. Annu Rev Earth Planet Sci 44:107–138
Muttoni G, Gaetani M, Budurov K, Zagorchev I, Trifonova E, Ivanova D, Petrounova L, Lowrie W (2000) Middle Triassic paleomagnetic data from northern Bulgaria: constraints on Tethyan magnetostratigraphy and paleogeography. Palaeogeogr Palaeoclimatol Palaeoecol 160:223–237
Nikishin AM, Ziegler PA, Cloething S, Stephenson RA, Furne AV, Fokin PA, Ershov AV, Bolotov SN, Koraev MV, Alekseev AS, Gorbachev I, Shipilov EV, Lankrejer A, Shalimov IV (1996) Late Precambrian to Triassic history of the East European Craton: dynamics of sedimentary basin evolution. Tectonophys 268:23–63
Nikishin AM, Cloetingh S, Bolotov SN, Baraboshkin EY, Kopaevich LF, Nazarevich BP, Panov DI, Brunet M-F, Ershov AV, Il'ina VV, Kosova SS,. Stephenson RA (1998a) Scythian platform: chronostratigraphy and polyphase stages of tectonic history. In: Crasquin-Soleau S, Barrier E (eds) Peri-Tethys Memoir 3: Stratigraphy and Evolution of Peri-Tethyan Platforms. Mémoires du Muséum national d'Histoire naturelle 177: 151–162
Nikishin AM, Cloetingh S, Brunet M-F, Stephenson RA, Bolotov SN, Ershov AV (1998b) Scythian Platform and Black Sea region: Mesozoic-Cenozoic tectonic and dynamics. In: Crasquin-Soleau S, Barrier E (eds) Peri-Tethys Memoir 3: Stratigraphy and Evolution of Peri-Tethyan Platforms. Mémoires du Muséum national d'Histoire naturelle 177: 163–176
Nikishin AM, Ziegler PA, Abbott D, Brunet M-F, Cloetingh S (2002) Permo-Triassic intraplate magmatism and rifting in Eurasia: implications for mantle plumes and mantle dynamics. Tectonophys 351:3–39
Nouri F, Azizi H, Golonka J, Asahara Y, Orihashi Y, Yamamoto K, Tsuboi M, Anma R (2016) Age and petrogenesis of Na-rich felsic rocks in western Iran: evidence for closure of the southern branch of the Neo-Tethys in the Late Cretaceous. Tectonophys 671:151–172
Ogg JG, Ogg GM, Gradstein FM (2016) A concise geologic time scale 2016. Elsevier, Amsterdam
Okay AI, Nikishin AM (2015) Tectonic evolution of the southern margin of Laurasia in the Black Sea region. Internat Geol Rev 57(5–8):1051–1076
Oliver G, Prave A (2013) Palaeogeography of Late Triassic red-beds in Singapore and the Indosinian Orogeny. J Asian Earth Sci 76:214–224

Olsen PE, Kent DV (1996) Milankovitch climate forcing in the tropics of Pangaea during the Late Triassic. Palaeogeogr Palaeoclimatol Palaeoecol 122:1–26
Olsen PE (1997) Stratigraphic record of the early Mesozoic breakup of Pangaea in the Laurasia-Gondwana rift system. Annu Rev Earth Planet Sci 25:337–401
Panuska BC (1985) Paleomagnetic evidence for a post-Cretaceous accretion of Wrangellia. Geol 13:880–883
Pčelina TM, Korčinskaja MV (2008) Palaeogeographic reconstructions of the Russian Boreal areas and Svalbard during the Triassic. Polar Res 27(3):491–494
Pease VL, Kuzmichev AB, Danukalova MK (2015) The new Siberian Islands and evidence for the continuation of the Uralides, Arctic Russia. J Geol Soc 172(1):1–4
Peng Z-M, Peng S-M, Wu Z-P, Li W, Kong X (2009) Basin pattern and evolution of Triassic in North China. J Xi'an Shiyou Univ, Nat Sci Ed 24(2):34–38
Petrík I, Janák M, Froitzheim N, Georgiev N, Yoshida K, Sasinková¡ V, Konečný P, Milovská S (2016) Triassic to Early Jurassic (c. 200 Ma) UHP metamorphism in the Central Rhodopes: Evidence from U-Pb-Th dating of monazite in diamond-bearing gneiss from Chepelare (Bulgaria). J Met Geol 34(3):265–291
Peybernes C, Chablais J, Onoue T, Escarguel G, Martini R (2016) Paleoecology, biogeography, and evolution of reef ecosystems in the Panthalassa Ocean during the Late Triassic: Insights from reef limestone of the Sambosan Accretionary Complex, Shikoku, Japan. Palaeogeogr Palaeoclimatol Palaeoecol 457:31–51
Piercey SJ, Nelson JL, Colpron M, Dusel-Bacon C, Simard R-L, Roots CF (2006) Paleozoic magmatism and crustal recycling along the ancient Pacific margin of North America, northern Cordillera. In: Colpron M, Nelson JL (eds) Paleozoic Evolution and Metallogeny of Pericratonic Terranes at the Ancient Pacific Margin of North America. Canadian and Alaskan Cordillera Geol Ass Can Spec Pap 45: 281–322
Preto N, Kustatscher E, Wignall PB (2010) Triassic climates - State of the art and perspectives. Palaeogeogr Palaeoclimatol Palaeoecol 290(1–4):1–10
Puchkov N (1997) Structure and geodynamics of the Uralian Orogen. In: Burg J-P, Ford M (eds) Orogeny through time. Geol Soc London Spec Publ 121: 201–236
Richards JP (2015) Tectonic, magmatic, and metallogenic evolution of the Tethyan orogen: From subduction to collision. Ore Geol Rev 70:323–345
Ridd MF (2013) A Middle Permian-Middle Triassic accretionary complex and a Late Triassic foredeep basin: Forerunners of an Indosinian (Late Triassic) thrust complex in the Thailand-Malaysia border area. J Asian Earth Sci 76:99–114
Robertson AHF (1998) Mesozoic-tertiary tectonic evolution of the Easternmost Mediterranean area: integration of the Marine and land evidence. In: Robertson AHF, Richter C, Camerlenghi CA (eds) Proceedings of the Ocean Drilling Program Scientific Results 60: 723–782
Robertson AHF (2007) Overview of tectonic settings related to the rifting and opening of Mesozoic ocean basins in the Eastern Tethys: Oman, Himalayas and Eastern Mediterranean regions. Geol Soc Spec Publ 282:325–388
Robertson AHF, Woodcock NH (1979) Mamonia complex, southwest Cyprus: evolution and emplacement of a Mesozoic continental margin. Geol Soc Am Bull 90:651–665
Robertson AHF, Clift PD, Degnan P, Jones G (1991) Paleogeographic and paleotectonic evolution of Eastern Mediterranean Neotethys. Palaeogeogr Palaeoclimatol Palaeoecol 87:289–344
Robertson AHF, Dixon JE, Brown S, Collins A, Morris A, Pickett EA, Sharp I, Ustaomer T (1996) Alternative tectonic models for the Late Palaeozoic-Early Tertiary development of Tethys in the. Eastern Mediterranean region, In: Morris A, Tarling DH, (eds) Palaeomagnetism and tectonics of the Mediterranean region. Geological Society London Special Publication 105: 239–263
Robertson AHF, Ustaömer T, Pickett EA, Collins AS, Andrew T, Dixon JE (2004) Testing models of Late Palaeozoic-Early Mesozoic orogeny in Western Turkey: Support for an evolving open-Tethys model. J Geol Soc 161(3):501–511
Robinson AC (2015) Mesozoic tectonics of the Gondwanan terranes of the Pamir plateau. J Asian Earth Sci 102:170–179

Roniewicz E, Stanley Jr GD (2013) Upper Triassic corals from Nevada, Western North America, and the implications for paleoecology and paleogeography. J Paleontol 87(5): 934–964
Ronov A, Khain V, Balukhovski A (1989) Atlas of Lithological Paleogeographical Maps of the World: Mesozoic and Cenozoic of the Continents. USSR Acad Sci, Leningrad
Ruffell A, Simms M, Wignall P (2015) The Carnian Humid Episode of the late Triassic: a review. Geol Mag 153:271–284
Rychliński T (2008) Facies development and sedimentary environments of the Carpathian Keuper deposits from the Tatra mountains. Poland and Slovakia Annales Societatis Geologorum Poloniae 78(1):1–18
Săndulescu M (1988) Cenozoic tectonic history of the Carpathians, In: Royden L, Horváth F (eds) The Pannonian Basin: a study in basin evolution. Am Assoc Petrol Geol Mem 45: 17–25
de Saussure le fils M (1792) Analyse de la dolomie. J Physique 40:161–173
Scheck-Wenderoth M, Krzywiec P, Zühlke R, Maystrenko Y, Froitzheim N (2008) Permian to Cretaceous tectonics. Geol Centr Eur 6(2):999–1030
Schettino A, Turco E (2011) Tectonic history of the Western Tethys since the Late Triassic. Geol Soc Am Bull 123(1–2):89–105
Schmid SM, Bernoulli D, Fügenschuh B, Matenco L, Schefer S, Schuster R, Tischler M, Ustaszewski K (2008) The Alpine-Carpathian-Dinaridic orogenic system: Correlation and evolution of tectonic units. Swiss J Geosci 101(1):139–183
Schwarzacher W (2006) The stratification and cyclicity of the Dachstein Limestone in Lofer, Leogang and Steinernes Meer (Northern Calcareous Alps, Austria). Sed Geol 181:93–106
Scotese CR (2004) A Continental Drift Flipbook. J Geol 112:729–741
Sengör AMC (1984) The Cimmeride orogenic system and the tectonics of Eurasia. Geol Soc Am Spec Pap 195:1–82
Sengör AMC, Natalin BA (1996) Paleotectonics of Asia: fragment of a synthesis. In: An Y, Harrison TM (eds) The Tectonic Evolution of Asia. Cambridge Univ Press, Cambridge
Sengör AMC, Yilmaz Y, Sungurlu O (1984) Tectonics of the Mediterranean Cimmerides: Nature and evolution of the western termination of Palaeo-Tethys. Geol Soc London Spec Publ 17:77–112
Shi Y, Anderson JL, Li L, Ding J, Liu C, Zhang W, Shen C (2016) Zircon ages and Hf isotopic compositions of Permian and Triassic A-type granites from central Inner Mongolia and their significance for late Palaeozoic and early Mesozoic evolution of the Central Asian Orogenic Belt. Intern Geol Rev 58(8):967–982
Sibuet J-C, Rouzo S, Srivastava S (2012) Plate tectonic reconstructions and paleogeographic maps of the central and North Atlantic oceans. Can J Earth Sci 49(12):1395–1415
Song P, Ding L, Li Z, Lippert PC, Yang T, Zhao X, Fu J, Yue Y (2015) Late Triassic paleolatitude of the Qiangtang block: Implications for the closure of the Paleo-Tethys Ocean. Earth Planet Sci Lett 424:69–83
Spikings R, Reitsma MJ, Boekhout F, Mišković A, Ulianov A, Chiaradia M, Gerdes A, Schaltegger U (2016) Characterisation of Triassic rifting in Peru and implications for the early disassembly of western Pangaea. Gond Res 35:124–143
Stanley GD, Onoue T (2015) Upper Triassic reef corals from the Sambosan Accretionary Complex, Kyushu, Japan. Facies 61(2):1–27
Tanner LH (2010) Cyclostratigraphic record of the Triassic: A critical examination. In: Lucas SG (ed) The Triassic Timescale. Geol Soc London Spec Publ 334: 119–137
Tari G, Dicea O, Faulkerson J, Georgiev G, Popov S, Stefanescu M, Weir G (1997) Cimmerian and Alpine stratigraphy and structural evolution of the Moesian Platform (Romania/Bulgaria). In: Robinson A G (ed) Regional and petroleum geology of the Black Sea and surrounding regions. Am Assoc Petrol Geol Mem 68: 63–90
Tong J, Yin H (2002) The Lower Triassic of South China. J Asian Earth Sci 20:803–815
Toro J, Miller EL, Prokopiev AV, Zhang X, Veselovskiy R (2016) Mesozoic orogens of the Arctic from Novaya Zemlya to Alaska. J Geol Soc 173:989–1006
Torsvik TH, Anderson TB (2002) The Taimyr fold belt, Arctic Siberia: timing of prefold remagnetisation and regional tectonics. Tectonophys 352:335–348

Trop JM, Ridgway KD, Manuszak JD, Layer P (2002) Mesozoic sedimentary-basin development on the allochthonous Wrangellia composite terrane, Wrangell Mountains basin, Alaska: a long-term record of terrane migration and arc construction. Geol Soc Am Bull 114:693–717

Uno K, Furukawa K, Hada S (2011) Margin-parallel translation in the western Pacific: Paleomagnetic evidence from an allochthonous terrane in Japan. Earth Planet Sci Lett 303(1–2):153–165

Veevers JJ (2006) Updated Gondwana (Permian-Cretaceous) earth history of Australia. Gond Res 9(3):231–260

Veevers JJ (2013) Pangaea: Geochronological correlation of successive environmental and strati-tectonic phases in Europe and Australia. Earth-Sci Rev 127:48–95

Veevers JJ (1994) Pangaea: Evolution of a supercontinent and its consequences for Earth's paleo-climate and sedimentary environments. In: Klein GD (ed) Pangaea: Paleoclimate, Tectonics and Sedimentation during Accretion, Zenith and Breakup of a Supercontinent. Geol Soc Am Spec Pap 228: 13–23

Vernikovsky VA (1995) The geodynamic evolution of the Taimyr folded area. In: Simakov KV, Thurston DK (eds) Proceedings of the International Conference on Arctic Margins, Magadan, September, p. 186–193

Vernikovsky VA, Pease VL, Vernikovskaya AE, Romanov AP, Gee DG, Travin AV (2003) First report of early Triassic A-type granite and syenite intrusions from Taimyr: Product of the northern Eurasian superplume. Lithos 66(1–2):23–36

Vernikovsky VA, Metelkin DV, Tolmacheva TY, Malyshev NA, Petrov OV, Sobolev NN, Matushkin NY (2013) Concerning the issue of paleotectonic reconstructions in the Arctic and of the tectonic unity of the New Siberian Islands Terrane: New paleomagnetic and paleontological data. Doklady Earth Sci 451(2):791–797

Vinogradov AP (ed) (1968) Atlas of the Lithological-Paleogeographical Maps of the USSR. Vol. III: Triassic, Jurassic and Cretaceous. Ministr Geol USSR, Acad Sci USSR

von Alberti F (1834) Beitrag zu einer Monographie des bunten Sandsteins, Muschelkalks und Keupers, und die Verbindung dieser Gebilde zu einer Formation. Mit 2 Tafb. lith. Stuttgart & Tübingen

Wang B, Zhang G, Yang Z (2013) New Mesozoic paleomagnetic results from the northeastern Sichuan basin and their implication. Tectonophys 608:418–427

Wignall PB (2001) Large igneous provinces and mass extinctions. Earth Sci Rev 53(1–2):1–33

Wilmsen M, Fürsich FT, Seyed-Emami K, Majidifard MR, Taheri J (2009) The Cimmerian Orogeny in northern Iran: Tectono-stratigraphic evidence from the foreland. Terra Nova 21(3):211–218

Swe W (2012) Outline geology and economic mineral occurrences of the Union of Myanmar. J Myanmar Geosci Soc 1:1–215

Withjack MO, Schlische RW, Olsen PO (1998) Diachronous rifting, drifting, and inversion on the passive margin of central eastern North America: an analog for other passive margins. Am Assoc Petrol Geol Bull 82:817–835

Wu F, Sun D, Li H, Bor M, Wilde S (2002) A-type granites in northeastern China: age and geochemical constraints on their petrogenesis. Chem Geol 187:143–173

Wu H, Li C, Chen J, Xie C (2016) Late Triassic tectonic framework and evolution of Central Qiangtang, Tibet, SW China. Lithosph 8(2):141–149

Yin A, Nie S (1996) A Phanerozoic palinspastic reconstruction of China and its neighboring regions In: Yin AN, Harrison TM (eds) The Tectonic Evolution of Asia. Cambridge Univ Press, Cambridge, p. 442–485

Zanchi A, Zanchetta S, Balini M, Ghassemi MR (2016) Oblique convergence during the Cimmerian collision: Evidence from the Triassic Aghdarband Basin, NE Iran. Gond Res 38:149–170

Zanchi A, Zanchetta S, Berra F, Mattei M, Garzanti E, Molyneux S, Nawab A, Sabouri J (2009) The Eo-Cimmerian (Late? Triassic) orogeny in North Iran. Geol Soc London Spec Publ 312:31–55

Zeng WS, Zhou JB, Dong C, Cao JL, Wang B (2014) Mongolia - Okhotsk oceanic subduction record: Evidence Ergun metamorphic complex area of the mall. Acta Petrol Sin 30(7):1948–1960

Zhai Q-G, Jahn B-M, Su L, Wang J, Mo X-X, Lee H-Y, Wang K-L, Tang S (2013) Triassic arc magmatism in the Qiangtang area, northern Tibet: Zircon U-Pb ages, geochemical and Sr-Nd-Hf isotopic characteristics, and tectonic implications. J Asian Earth Sci 63:162–178

Zhang X, Pease V, Carter A, Scott R (2017b). Reconstructing Palaeozoic and Mesozoic tectonic evolution of Novaya Zemlya: combining geochronology and thermochronology. In: Pease V and Coakley B (eds) Circum-Arctic Lithosphere Evolution. Geol Soc London Spec Publ 460. doi.org/10.1144/SP460.13

Zhang X, Pease V, Carter A, Kostuychenko S, Suleymanov A, Scott R (2017a) Timing of exhumation and deformation across the Taimyr fold–thrust belt: insights from apatite fission track dating and balanced cross-sections In: Pease V, Coakley B (eds) Circum-Arctic Lithosphere Evolution. Geol Soc London Spec Publ 460, doi.org/10.1144/SP460.3

Zharkov MA, Chumakov NM (2001) Paleogeography and sedimentation settings during Permian-Triassic reorganization in biosphere. Stratigr Geol Correl 9:340–363

Zhou Y, Cheng X, Yu L, Yang X, Su H, Peng X, Xue Y, Li Y, Ye Y, Zhang J, Li Y, Wu H (2016) Paleomagnetic study on the Triassic rocks from the Lhasa Terrane, Tibet, and its paleogeographic implications. J Asian Earth Sci 121:108–119

Zhu T, Feng X, Wang X, Zhou M (2013) Reconstruction of the Triassic tectonic lithofacies paleogeography in Qiangtang region, Northern Qinghai-Tibet Plateau, China. Acta Geol Sin 87(2):378–394

Ziegler PA (1982) Geological atlas of western and central Europe. Shell Internationale Petroleum Mij, B.V., The Hague

Ziegler PA (1988) Evolution of the Arctic North Atlantic and the Western Tethys. Am Assoc Petrol Geol Mem 43:1–198

Zonenshain LP, Kuzmin ML, Natapov LN (1990) Geology of the USSR: A Plate-Tectonic Synthesis. Am Geophys Un, Geodynam. Ser 21:1–242

Chapter 3
Climates of the Late Triassic: Perspectives, Proxies and Problems

Lawrence H. Tanner

Abstract The majority of paleoclimate evidence, including climate-sensitive lithofacies, paleobotanical evidence and a lack of evidence of glaciation, indicates a climate that was significantly warmer during the Late Triassic than at present. Multiple proxies demonstrate higher atmospheric pCO_2 during the Late Triassic as the driver for this warmth. Historically, the results of pCO_2 estimates from measurements of stomatal indices and calculations from the isotopic composition of pedogenic carbonate have produced differing results. More recent estimates based on improved methodologies and sampling constraints yield more consistent results, indicating pCO_2 levels well over 1000 ppm, potentially higher, with excursions to even higher levels. Sedimentary evidence, particularly paleosols, indicate a highly seasonal climate for broad areas of Pangaea, suggesting a strongly monsoonal climate controlled by the arrangement of land areas. Most of the seasonal precipitation was limited to coastal regions, while the interior was largely semi-arid to arid at low to mid-latitudes. Humid climates were limited to mid- and higher latitude. The middle Carnian experienced a brief interval of increased warmth and humidity, with high-resolution records indicating that the event occurred as multiple pulses. A trend of aridification from the late Carnian to the Norian is evident across much of Pangaea, generally explained as the result of either weakening monsoonal flow due to the northward shift of Pangaea, or the drifting of regions between latitudinally-controlled climate zones. Biotic events at the end-Triassic have been attributed to CO_2-forced warming caused by outgassing of flood basalts, although initial SO_2-aerosol forced cooling followed by warming is more likely.

Keywords Late Triassic • Megamonsoon • Aridification • Pedogenic carbonate • Stomatal indices • Carnian Pluvial Event • CAMP

L.H. Tanner (✉)
Department of Biological and Environmental Sciences, Le Moyne College,
1419 Salt Springs Road, Syracuse, NY 13214, USA
e-mail: tannerlh@lemoyne.edu

© Springer International Publishing AG 2018

L.H. Tanner (ed.), *The Late Triassic World*, Topics in Geobiology 46,
https://doi.org/10.1007/978-3-319-68009-5_3

3.1 Global Overview

Since the work of pioneers like Edward Suess and Alfred Wegener, a portrait of Late Triassic Earth has emerged of a paleogeography dominated by the supercontinent Pangaea, which enclosed the Tethys Sea and was itself encircled by the ocean Panthalassa. The climate of this continent, straddling as it did the paleoequator, was controlled by the great size of the landmass in each hemisphere, resulting in extreme seasonality, termed by some the "mega-monsoon" (Parrish and Peterson 1988; Kutzbach and Gallimore 1989; Parrish 1993; Yan and Zhao 2002), although the interior of the continental landmass is predicted to have been largely semi-arid to arid. Generally warm and widespread dry conditions during the Late Triassic are evidenced by abundant evaporite and carbonate deposition, the restriction of coal formation mainly to higher latitudes, and a lack of evidence for glaciation (Frakes et al. 1992; Lucas 1999). Overall warmth during the Late Triassic has been further demonstrated by the documented occurrences of warm-climate paleosols and floras to paleolatitudes as high as 85° (Taylor 1989; Retallack 1999; Kidder and Worsley 2004). Taylor et al. (2000) specifically noted (from studies of tree rings in permineralized wood) that light, not temperature, was the limiting factor for the rate of tree growth in polar regions.

Reefs and carbonate platforms, considered to have been confined then as now by the 20 °C ocean isotherm, extended throughout the western Tethyan region and extending eastward, encompassed an area that included Papua (N.G.), Thailand, Timor, northern India, and Malaysia. Along the western coast of Pangaea reefs extended from Oregon (U.S.A.) to Chile by Norian time, encompassing a paleolatitudinal range of ca. 35°N to 35°S (Flügel 2002; Sellwood and Valdes 2006). Kiessling (2010), conversely, has argued that a greater latitudinal range for reefs during the Permian and Jurassic periods indicates a cooler Triassic. Widespread and gradual aridification during the Late Triassic, commencing in the early Norian following a wet Carnian (see Sect. 3.5), is indicated across large areas of tropical to midlatitude Pangaea by abundant sedimentary evidence. These reports are most consistent from formations deposited at low paleolatitudes and in interior regions of Pangaea. Rift basins bordering the future Atlantic rift, such as those of the Newark Supergroup in eastern North America (Fig. 3.1), which occupy a roughly 13° latitudinal transect from the southeastern United States to Atlantic Canada, display a temporal transition of facies that demonstrate progressively decreasing moisture (Whiteside et al. 2011). These are discussed in more detail in Sect. 3.4. Similar to the northern Newark basins is the succession of the Timezgadiwine and Bigoudine formations in the Argana basin, Morocco (Olsen 1997; Hofmann et al. 2000), which would have been near the Newark basins in paleogeographic reconstruction. Another well-known example of aridification in the northern hemisphere for this time is the facies change in the Upper Triassic Mercia Mudstone Group of England (Talbot et al. 1994; Ruffell and Shelton 1999).

Similar climate-related facies trends are reported from southern Pangaea from Madagascar (Wescott and Diggens 1998), and from the Karoo Supergroup of South

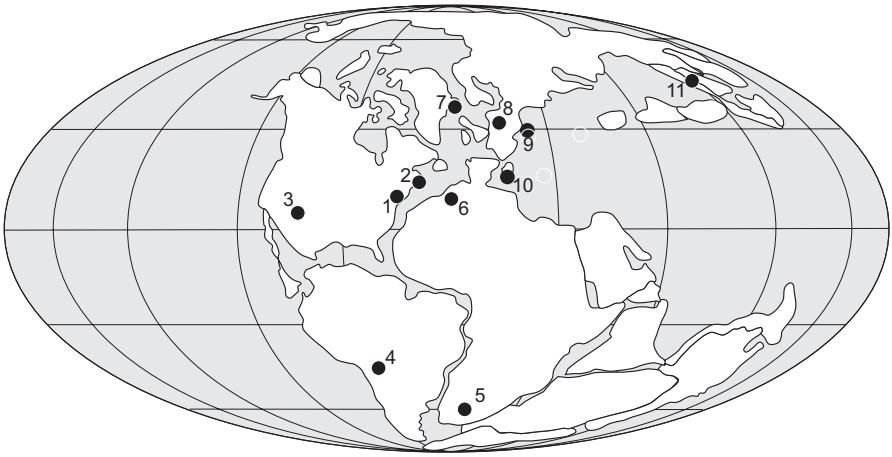

Fig. 3.1 Paleogeographic reconstruction for the Late Triassic illustrating approximate locations of some sedimentary basins/sections described in the text: (1) Newark Basin, USA; (2) Fundy Basin, Canada; (3) Chinle Basin/Colorado Plateau, USA; (4) Ischigualasto Basin, Argentina; (5) Karoo Basin, South Africa; (6) Argana Basin, Morocco; (7) Jameson Land Basin, Greenland; (8) Germanic Basin, Germany; (9) Eiberg Basin, Austria; (10) Dolomites, Italy; (11) Sichuan Basin, China

Africa, as in the transition from the Molteno Formation to the Elliot Formation (Sciscio and Bordy 2016). In the Ischigualasto basin of Argentina (Fig. 3.1), the Carnian-age Ischigualasto Formation is interpreted as recording a climate varying from cool-humid to dry and seasonal and back to humid at the top of the formation (Tabor et al. 2004, 2006; Colombi and Parrish 2008). Overall, however, the Carnian Ischigualasto Formation is generally regarded as having been deposited under significantly more humid conditions than the redbeds of the latest Carnian to Norian Los Colorado Formation (Curtin and Parrish 1999; Currie et al. 2009; Tabor et al. 2004; Colombi and Parrish 2008). The trend of aridification was not uniform across Pangaea, however. Australia became wetter during the Late Triassic, at which time extensive coal deposits formed there (Fawcett et al. 1994), and strata of the Jameson Land Basin of eastern Greenland are interpreted also as exhibiting a trend of increasing humidity (Clemmensen et al. 1998). Similarly, study of the paleosols in the Blue Nile Basin, central Ethiopia, indicate increasing humidity during the Late Triassic (Dawit 2016).

Generally humid climates during the Late Triassic are more evident at middle to higher latitude regions than lower latitude regions. Much of the land area between 30° and 50° in both hemispheres was dominantly warm and temperate (Sellwood and Valdes 2006). This climate was not entirely stable, however. As noted by Ahlberg et al. (2002), the northern parts of the Germanic Basin (or Central European Basin), which was located in the lower midlatitudes, experienced a dramatic change from red-bed deposition during the Norian, to deposition during the Rhaetian in

alluvial and lacustrine environments characterized by gleyed, kaolinitic paleosols and coals.

Elsewhere at midlatitudes, for example in the Junggar Basin of northwestern China, the megaflora from the Huangshanjie Formation indicates a warm, seasonally wet climate during the Norian, while the overlying coal-bearing Haojiagou Formation indicates a warmer, wetter Rhaetian (Ashraf et al. 2010). The latitudinal position of the basin during the Late Triassic has been interpreted variously, however, as at either midlatitudes (Ashraf et al. 2010), or higher paleolatitude (as high as 60° N; Sha et al. 2015). The Sichuan Basin, which was well to the south of the Junggar Basin at a paleolatitude of 35° to 40° N (Fig. 3.1), was characterized by a warm and humid climate through most of the Late Triassic (Li et al. 2016). The palynology of the Xujiahe Formation here demonstrates fluctuations in this climate during the Norian and Rhaetian, with two intervals of increased warmth and humidity, and a cool, dry episode at the very end of the Rhaetian (Li et al. 2016). There is not complete agreement on the paleoclimate of the Sichuan Basin, however, as Tian et al. (2016) interpreted the occurrence of *Xenoxylon* wood from the Xujiahe Formation as an indication of a cool ($\leq$15 °C), wet climate in the basin during the late Norian. The general trends for the Triassic in the Boreal realm are possibly best presented in a study of palynology from boreholes in the Barents Sea by Hochuli and Vigran (2010). In comparing the ratios of hygrophytic elements, such as smooth and ornamented trilete spores, *Cycadopites* and *Araucariocites* Group against xerophytic elements, including bisaccate pollen in particular, the authors demonstrate an increase in humidity in the middle Carnian, following a much drier early Carnian, that persists until the early Rhaetian.

3.2 Global Climate Models

Models of the Pangaean climate for the Late Triassic suggest a largely azonal pattern of climate with mostly dry equatorial and continental interior regions and humid belts at higher latitudes and around the Tethyan margin (Parrish and Peterson 1988; Crowley et al. 1989; Kutzbach and Gallimore 1989; Dubiel et al. 1991; Parrish 1993; Fawcett et al. 1994). Precipitation across Pangaea is generally considered to have been strongly seasonal, produced by a strong monsoonal effect controlled by summer heating of the large land masses (Kutzbach and Gallimore 1989; Parrish 1993; Sellwood and Valdes 2006; Preto et al. 2010; Stefani et al. 2010) that was enhanced during the Late Triassic by the location of the Pangaean supercontinent neatly bisected by the equator (Parrish 1993).

Sellwood and Valdes (2006) modeled the climate of the Late Triassic using an atmosphere-sea ice coupled GCM with 19 atmospheric layers and an atmosphere grid with cells of 2.5° latitude by 3.75° longitude to predict high summer temperatures (in excess of 20 °C) over land at very high latitudes, but similarly extreme winter cold temperatures (−20 °C) at these latitudes. Nevertheless, no permanent snow or ice cover is predicted by this model. Between latitudes 40° N and 40° S,

mean annual temperatures would have exceeded 20 °C, with summer temperatures commonly above 30 °C and even 40 °C. Most precipitation would have fallen over the oceans, but was very unevenly distributed over land. Much of the interior of the continents from 40° N to 40° S received little precipitation, and over a larger area, extending to 50°, evaporation exceeded precipitation, resulting in vast desert interiors. Seasonal, summer precipitation characterized the equatorial region and Tethyan margins. Higher latitudes were characterized by humid, temperate climates to ca. 60°, and winter-wet climates at even higher latitudes. Panthalassa would have been dominated by a strong semi-permanent El Niño. In this model of a largely azonal climate (e.g., Preto et al. 2010), large swaths of Pangaea experienced strongly seasonal precipitation, including the western Tethyan region, central Pangaea, the subtropical latitudes, the eastern coasts of Laurasia and Gondwana, and the western coast of Pangaea (Mutti and Weissert 1995), while the higher latitudes were dominated by a moist climate produced by westerlies and polar easterly winds (Robinson 1973). In this model, the greater aridity of the Norian relative to the Carnian in those regions described above is explained by a weakening of the monsoonal system, potentially a consequence of the shifting position of the land areas as Pangaea drifted northward (Parrish 1993).

In contradiction to the azonal climate model, a zonal model of latitudinal climate gradients is favored by some (Olsen 1997; Kent and Olsen 2000; Olsen and Ken 2000; Ziegler et al. 2003; Kent et al. 2017). The utility of the zonal climate model for Pangaea lies primarily in its explanation of aridification in the basins of the Newark Supergroup basins as a result of a 5–10° northward drift away from a very narrow humid tropical toward more arid climate zones of the subtropics, produced by Hadley circulation, as today. In the latest iteration of this model (Kent et al. 2017), the tropical climate zone produced by the ITCZ is limited to 5° on either side of the paleoequator, and broad arid belts extended to over 30° (Fig. 18, Kent et al. 2017); humid mid- to high latitude belts extended to about 80°.

The apparent increase of humidity in eastern Greenland as it drifted northward, presumably deeper into the humid mid-latitudes (Clemmensen et al. 1998), has been cited in support of the interpretation of zonal climatic gradients (Kent and Olsen 2000; Olsen and Kent 2000). The Jameson Land Basin of eastern Greenland was located at a paleolatitude estimated at near 40° N at the start of the Norian and drifted north by possibly 10° by the end of the Rhaetian (Kent et al. 2017). Deposition of the Fleming Fjord Formation occupied the later part of this time interval (late Norian through Rhaetian) and records a transition from a dry, seasonal climate, during which the ephemeral lake beds of the Malmros Klint and Carlsberg Fjord members were deposited (during the Norian), to the humid climate deposition of perennial lake sediments in the Taitbjerg Beds (during the Rhaetian). Likewise, Dawit (2016) suggested that the trend of increasing humidity evidenced by paleosols in the Blue Nile Basin of Ethiopia described above may have resulted from either orographic effects, due to rift-related doming, or the northward drift of Pangaea, which carried the basin from a paleolatitude of about 20° S to around 10° S by the end of the Triassic, from the drier subtropics toward the ITCZ. Similarly, the zonal climate model also could explain the Norian aridification of the

Ischigualasto Basin in southern Pangaea as the basin moved northward from higher latitude (40º–45° S; Golonka 2007) toward more arid mid-latitudes.

Hence, climatic trends in some regions have been cited as evidence for an azonal model of climate for the Late Triassic, while other regions are presented as exhibiting evidence for a zonal climate for the same time interval. In fact, these disparate views may not be totally incompatible. It is generally conceded that a strong monsoonal system existed from the late Paleozoic through most of the Triassic that created a climate system in which precipitation patterns were determined largely by proximity to Tethys or Panthalassa, not latitude, at low to mid-latitudes. Hence, monsoonal flow, driven by summer heating/winter cooling air pressure contrasts, was more important than Hadley circulation. Potentially, however, weakening of the monsoonal system during the Late Triassic, from repositioning of the northward drifting Pangaea, allowed strengthening of latitudinally controlled atmospheric cells, which permitted the strengthening of zonal climate belts, as suggested by Parrish (1993).

3.3 Estimating Paleo-pCO_2

Decades of investigation into Earth's climate history combined with the use of various proxies for estimating concentrations of CO_2 in the atmosphere from the past have resulted in the firm conclusion that the partial pressure of CO_2 in the atmosphere (pCO_2) is a major controlling factor of climate due to its role in amplifying radiative forcing (reviews in Berner 1998, 2004; Royer et al. 2007). Several techniques have been employed to produce paleo-pCO_2 estimates, including geochemical modelling, isotopic analysis of pedogenic minerals and statistical measurements of stomatal indices from fossil leaf cuticles (reviewed in Ekart et al. 1999; Royer et al. 2001; Tanner et al. 2004). The isotopic composition of fossil plant remains is used to interpret changes in the isotopic composition of atmospheric carbon, rather than paleo-pCO_2, presumably identifying perturbations of the global carbon cycle (e.g., McElwain et al. 1999), not paleo-pCO_2. The study by Fletcher et al. (2008) is notable in that it interpreted changes in paleo-pCO_2 across most of the Mesozoic based on the unique methodology of analyzing the isotopic composition of fossils of nonvascular plants (liverworts). Notably, their work suggested pCO_2 of less than 500 ppm at the end of the Triassic, contrary to most other estimates.

Geochemical modelling, at its simplest, examines the relative sizes of the carbon reservoirs in the atmosphere and geosphere and estimates of the rates of exchange between reservoirs by silicate weathering and carbon burial via mass-balance calculations based on the abundances of different sedimentary rock types. Overall, the Triassic Period, including the Late Triassic, is modeled as a time of much higher pCO_2 than present, in great part due to the presumed decreased rate of carbon burial in sedimentary rocks (coal in particular); Berner and Kothavala (2001) projected pCO_2 of ca. 2000 ppm early in the Triassic, falling to ca. 1500 ppm by the Late Triassic, implying an overall long-term cooling trend. Similarly, Goddéris et al.

(2008) developed a geochemical model based on paleogeographic reconstructions and hydrologic controls on silicate weathering to estimate a dramatic decrease in pCO_2 from a Middle Triassic high of over 3000 ppm to a low of less than 1000 ppm by the end of the Rhaetian.

3.3.1 Isotopic Composition of Pedogenic Carbonate

The use of pedogenic carbonate to estimate the concentration of atmospheric CO_2 in Earth's past was pioneered by Cerling (1991), who developed the methodology based on the carbon isotopic composition, the ratio of ^{13}C to ^{12}C (measured as $\delta^{13}C$), of pedogenic carbonate. The of $\delta^{13}C$ of soil carbonate is controlled by several factors, including: the ratio of C_4 to C_3 vegetation, although C_4 vegetation had not yet appeared in the Mesozoic; the depth of carbonate accumulation below the soil surface, which controls the extent of atmospheric mixing; the temperature of carbonate precipitation, which determines fractionation; the isotopic composition of atmospheric carbon, a value well-constrained by analysis of marine carbonates; and soil productivity ($S(z) = pCO_{2soil} - pCO_{2atmos}$), a factor that is largely dependent on climatic regime (Cerling 1991; Ekart et al. 1999; Tanner 2010a). Values of paleo-pCO_2 derived from $\delta^{13}C$ are broadly consistent with values from other sources, such as geochemical modelling (e.g. Berner 1994; Berner and Kothavala 2001). Ekart et al. (1999), in their invaluable review, cautioned that not all pedogenic carbonate is suitable for this analysis. Specifically, the carbonate must be precipitated 50 cm below the ground surface to avoid direct atmospheric interaction, but also not precipitated under the influence of groundwater; should be from mature Calcisols or calcic Argillisols, but not Protosols; and must be demonstrably free of evidence for recrystallization (Ekart et al. 1999). Ekart et al. (1999) presented tabulated data that included previously published and new measurements from Upper Triassic formations, including the Chinle Group, the Newark Supergroup and the Ischigualasto Formation. The pCO_2 values they calculated ranged from 1650 ppm, from an unspecified formation in the Chinle Group (Colorado Plateau, southwestern U.S.A.) to 3160 ppm in the Sugarloaf Member of the Passaic Formation (formerly New Haven Arkose; Weems et al. 2016), from the Norian of the Hartford Basin, Newark Supergroup (data previously published by Suchecki et al. 1988). Tanner et al. (2001) presented new data from the Newark Supergroup and Chinle Group that suggested fairly stable pCO_2 during the Norian, ca. 2250 ppm (± 900 ppm to account for variance in soil productivity). Tanner (2003) published additional data from the Chinle Group that represented a more complete sampling of the stratigraphic range of the group and found a consistent enrichment (increase in $\delta^{13}C$ of the carbonate) from the stratigraphically lowest formation sampled, the Carnian Blue Mesa Member of the Petrified Forest Formation, to the uppermost formation, the Rhaetian-age Rock Point Formation. The morphology of the paleosols that were sampled varied considerably, suggesting increasing aridity, at least in part. Hence, Tanner (2003) varied the S(z) to account for climatically-controlled variations in soil respiration and

derived pCO_2 values ranging from 2150 to 3300 ppm for the upper Carnian-lower Norian Petrified Forest Formation to 2300 to 3750 ppm for the upper Norian Owl Rock Formation. The paleosol profiles in the Rhaetian Rock Point and equivalent formations were judged too thin to provide reliable measurement of pCO_2 and were discounted for pCO_2 calculation. Prochnow et al. (2006), however, also calculated pCO_2 from pedogenic carbonate in Chinle Group formations from the Colorado Plateau. Their calculations suggested extreme fluctuations in Late Triassic atmospheric composition, with pCO_2 falling to less than 300 ppm during the Carnian, but rising to values of 1390 to 1760 ppm during the Norian. Notably, there is no sedimentary evidence to support the glacial cold that would have accompanied pCO_2 near modern pre-industrial levels during the Carnian, nor is there reason to expect sudden and short-term changes in the carbon cycle that would result in pCO_2 fluctuations of this magnitude. Cleveland et al. (2008a) contributed an additional study of the Chinle, but focused on sampling upper Norian to Rhaetian-age formations from the Chinle Group at just two locations. This study also found evidence of highly variable pCO_2, but characterized by relatively lower levels during the Norian, rising during the Rhaetian, and higher peaks near the end-Rhaetian. Although Cleveland et al. (2008a) attempted well-controlled sampling protocols, they admitted limitations in their data analyses. For instance, rather than analyses of the $\delta^{13}C$ of organic matter from the soils from which they sampled pedogenic carbonate, they relied on the average of two analyses of fossil charcoal from a single horizon for all pCO_2 calculations. While this is not an uncommon practice, due to the typical paucity of organic matter in the strongly oxidized soils in which pedogenic carbonates are usually found, it is a major source of inaccuracy, as the isotopic composition of vegetation can differ significantly within the same plant community, and is also affected by transient climatic factors, such as heat stress or water availability. The other common source of inaccuracy is use of an incorrect value for S(z), which can only be grossly approximated. One or both of these factors could account for systematic differences between the two sections sampled in pCO_2 calculations.

3.3.2 Use of Stomatal Indices

The use of stomatal indices measured from fossil plants to interpret paleoatmospheric composition derives from many laboratory studies that have demonstrated a correlation between atmospheric pCO_2 and stomatal frequency in some, although not all plant genera. Beerling et al. (1998) selected *Gingko biloba* for study because the order to which the species belongs has a fossil record dating back to the Permian. Beerling et al. (1998) showed that specimens grown for three years in growth chambers at elevated (560 ppm) pCO_2 exhibited a demonstrable decrease in both the density (the number of stomata per unit area) and index (the number of stomata relative to the number of epidermal cells) compared to *G. biloba* grown at present CO_2 levels. This effect is generally considered an adaptation that improves water-use efficiency that evolved in plants that grew when CO_2 levels are high. Thus, fossil

leaves on which stomatal counts are possible theoretically can provide a record of paleo-pCO_2. For example, Chen et al. (2001) utilized this apparent correlation to analyze fossils of *Gingko* spp. of various geologic ages and found an approximate (inverse) correlation of stomatal index with the theoretical variation of pCO_2 as calculated by geochemical modeling (Berner and Kothavala 2001). However, this paleofloral evidence is also not without potential sources of error. McElwain et al. (1999) attempted to quantify changes in pCO_2 across the Triassic-Jurassic boundary, but drew their conclusions of a sudden and dramatic increase from measurements of the stomatal indices from different species below and above the boundary interval, rather than comparison within a single taxon on both sides of the boundary.

Retallack (2001a) extended the utilization of the fossil record of stomatal indices to include seed ferns and found evidence of similar transient increases in pCO_2 levels at several important paleontologic boundaries, including the Permian-Triassic, the Triassic-Jurassic, and the Cretaceous-Paleogene. However, the statistical validity of these data has been critiqued by Haworth et al. (2005). Notably, Retallack (2013) used the stomatal indices of the single taxon, *Lepidopteris*, to calculate a history of pCO_2 variation for much of the Permian and all of the Triassic. Although the temporal resolution of the data presented is very coarse, he suggested a series of "greenhouse crises" in which pCO_2 spiked at levels of 1500 to 3000+ ppm, compared to much lower background levels of less than 1000 ppm.

Implicit in the utilization of stomatal indices to calculate paleo-pCO_2 are the assumptions that the physiologic response was quantitatively similar for the fossil plants as in their modern representatives (typically the nearest living relatives), that the stomatal response resulted solely from variation of a single parameter (atmospheric CO_2) and that the physiological response was similar at both low and high atmospheric-CO_2 levels. However, all of these assumptions are debatable (Boucot and Gray 2001; Royer et al. 2001; Tanner 2002a, b; Haworth et al. 2005). In fact, it has been made clear from experimental data that other environmental stresses, such as heat, sun, water deficit and exposure to SO_2 also have the potential to elicit a strong stomatal response (Beerling et al. 1998; Tanner et al. 2007). Most of these factors are not easily evaluated directly from the geologic record. Thus, the application of stomatal indices to quantitative determinations of paleo-pCO_2 should be viewed cautiously (Boucot and Gray 2001; Royer et al. 2001; Tanner 2002a; Tanner et al. 2004; Haworth et al. 2005).

3.4 Regional Trends

3.4.1 Marine Record: Tethyan Realm

Korte et al. (2005) compiled an extensive set of $\delta^{18}O$ analyses comprising 160 articulate brachiopods and a nearly equal number of whole rock analyses from the Middle and Upper Triassic of the Tethyan realm. The Upper Triassic brachiopod $\delta^{18}O$ values range from −0.6 to 3.4‰ (VSMOW) for samples ranging in age from early Carnian (St. Cassian Limestone) to late Rhaetian (Kössen Limestone). Using the equations of O'Neil et al. (1969) and Hays and Grossman (1991), Korte et al. (2005) calculated water temperatures ranging from 18 to 32 °C for brachiopods that coexisted with corals. In comparison to the earlier Muschelkalk sea, for which they calculated water temperatures of 25–37 °C (Korte et al. 2005), $\delta^{18}O$ rose ca. 2‰ in the early Carnian (Cordevollian), which Korte et al. (2005) interpreted as a temperature decrease of ca. 10 °C, but this decline was reversed in the middle Carnian (Julian).

Taken at face value, the data of this study suggest significant temperature variations through the Late Triassic, including episodes of cooling in the early Carnian and Norian, and warming events in the middle Carnian and Rhaetian. However, interpretation of a temperature record from the isotopic signature of marine carbonates (whole rock or brachiopods) is far from straightforward. As Korte et al. (2005) noted, some part of the early Carnian isotopic excursion could be due to increasing salinity, rather than temperature decrease. Furthermore, the rise in $\delta^{18}O$ for the late Carnian through Norian in samples of the Hallstatt Limestone at Silická Brezová (Slovakia) may in fact result from carbonate deposition in deeper waters, close to the thermocline, rather than cooling of surface waters. Moreover, the isotopic depletion exhibited by brachiopods collected from the Rhaetian Kössen Limestone may represent the sheltered water conditions of an intra-basin platform rather than a warming event. Hence, the isotopic signature of marine carbonates must be interpreted carefully to consider water depth and salinity when applied to paleoclimate studies. Stefani et al. (2010) presented a thorough review of the depositional system for the Triassic carbonate platforms exposed in the Dolomites, which during the Late Triassic were situated on the western margin of Tethys at a subtropical paleolatitude of 15–18° N (Muttoni et al. 2010). The Upper Triassic portion, starting with the Wengen and San Cassiano formations, records an initially dry early Carnian, evidenced by the paucity of terrigenous vegetation remains, and arid carbonate paleosols on the platform tops exhibiting pisoids and tepee structures. The carbonate ramps of the middle Carnian Heiligkreuz Formation present evidence for a significant increase in humidity; the mature paleokarst contains caves and dolines, plant remains suggest abundant terrigenous vegetation, the palynomorph assemblage contains many hygrophytic elements and paleosols contain histic and spodic horizons (Stefani et al. 2010). Breda et al. (2009) interpreted this mid-Carnian interval as consisting actually of three distinct humid pulses separated by intervals of dryness. The presence of calcareous paleosols and evaporites in the upper Carnian

to lower Norian Travenanzes Formation demonstrates a return to consistently arid conditions that were maintained through most of the Norian during deposition of the Dolomia Principale (Stefani et al. 2010). Berra et al. (2010) similarly described the evidence for widespread aridity during the Norian in the western Tethyan region, but also noted the cessation of this climate with the onset of humidity at the end of the Norian, coinciding with the sea-level fall that resulted in the emergence of carbonate platforms throughout the region. Interestingly, the authors cite the isotopic data described above (Korte et al. 2005) in support of a cooling climate associated with falling sea level. Trotter et al. (2015) used the oxygen isotope composition from conodonts ($\delta^{18}O_{phos}$) to track ocean temperatures from conodont apatite from the Lagronegro Basin (Italy), an open ocean depositional basin in northwestern Tethys. The use of conodont apatite rather than marine carbonate has the advantage of avoiding the problems of diagenetic alteration of the isotopic signal (e.g., Veizer et al. 1999; Korte et al. 2005). This study differs from most earlier work in that the isotopic composition of individual conodonts was analyzed by secondary mass ion spectrometry (SIMS), allowing species-specific analyses, rather than bulk analyses. The authors acknowledge, however, that calculating seawater temperature requires knowing, or making assumptions about the isotopic composition of the seawater ($\delta^{18}O_{SW}$), which is itself controlled by factors such as precipitation, evaporation and salinity. Nevertheless, Trotter et al. (2015) have reconstructed a $\delta^{18}O_{phos}$ curve for the entire Triassic of the Lagronegro Basin that indicates a cool start to the Carnian encompassing the entire Julian, followed by a negative $\delta^{18}O_{phos}$ excursion of ca. 1.5‰, suggesting a strong warming event starting at the Julian-Tuvalian boundary. The authors calculate warming of 6 °C or more for this event, which continues into the Norian; these data support the interpretation of dramatic warming as the driver of an apparent wide-spread increase in precipitation during the Carnian, the so-called Carnian Pluvial Event (CPE, discussed below). A further excursion, of ca. 1.7‰, suggests additional late Norian (Alaunian) warming that is reversed at the Norian-Rhaetian boundary. Notably, Rigo et al. (2012), also using $\delta^{18}O_{phos}$ of conodont apatite, found that water temperatures were significantly lower in basins marginal to the Tethys Sea. In the Sicani Basin, for example, conodont $\delta^{18}O_{phos}$ indicates water temperatures 8 °C cooler than contemporaneous water temperatures in the nearby open-ocean Lagronegro Basin (Rigo et al. 2012), which they attribute to upwelling currents driven by the predicted monsoonal atmospheric flow.

3.4.2 Continental Record: North America

3.4.2.1 Colorado Plateau

Formations of the Upper Triassic (Carnian through Rhaetian) Chinle Group preserve a semi-continuous record of climate change during the Late Triassic in the Colorado Plateau region of the southwestern United States, and paleosols are prominent features of most formations of the group. The oldest (Carnian-age) formations

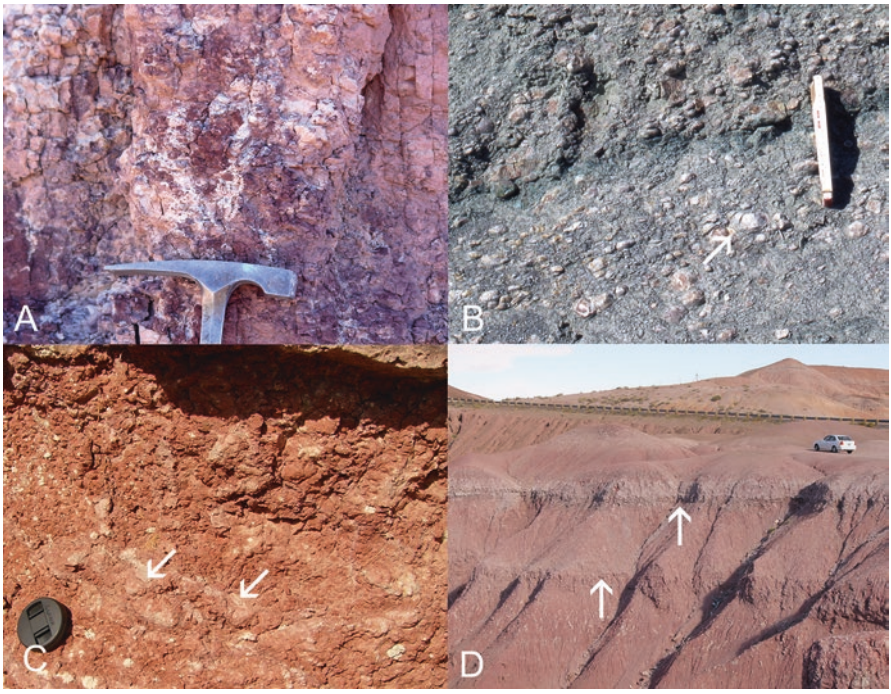

Fig. 3.2 Pedogenic features in a chronological sequence of formations from the Upper Triassic Chinle Group, Colorado Plateau (USA) demonstrating progressive aridification during the Late Triassic. (**a**) Paleosol in the middle Carnian Zuni Mountains Formation (northwestern New Mexico) is heavily gleyed and kaolinitic, indicating high but fluctuating water table during deposition. (**b**) Paleosols in the upper Carnian Blue Mesa Member of the Petrified Forest Formation (photographed in southeastern Utah) are commonly reduced but contain isolated calcrete nodules (*arrow*). (**c**) Paleosols in the lower Norian Painted Desert Member of the Painted Desert Member of the Petrified Forest Formation (northeastern Arizona) are reddened, illitic and typically contain abundant calcrete nodules. (**d**) The upper Norian Owl Rock Formation (northeastern Arizona) is characterized by paleosols containing mature calcrete horizons (*arrows*)

of the Chinle Group (Zuni Mountains and Shinarump formations) contain kaolinitic paleosols that display gley features and spodic horizons, and lack calcretes (Fig. 3.2; Tanner and Lucas 2006). Numerous authors (Hasiotis et al. 1998; Tanner 2003; Prochnow et al. 2006; Tanner and Lucas 2006) have interpreted a humid, but seasonal climate during the Carnian in the Colorado Plateau region on the basis of these gleyed and illuviated paleosols. As reviewed in Lucas et al. (2012), the most likely age assignment of these strata based on biostratigraphy is Julian. Prochnow et al. (2006) described the landscape of the "lower Chinle," referring to all Chinle Group formations stratigraphically below the Petrified Forest Formation, as one with humid open forest communities and estimated mean annual precipitation (MAP) from geochemical indices and depth-to-carbonate paleosol measurements as increasing to levels above 1200 mm a^{-1}.

Subsequent Chinle deposition produced the laterally equivalent Cameron, Monitor Butte and Bluewater Creek formations and the overlying Blue Mesa Member of the Petrified Forest Formation, all of likely Tuvalian age (Lucas 2010; Lucas et al. 2012). Paleosols of these strata are primarily vertic Alfisols that are calcic (stage II to III calcretes) in some locations, gleyed, in others, varying by location on the alluvial plain (Tanner and Lucas 2006). By analogy to modern soils, this classification implies that the soils formed in woodlands and forests in subhumid to semiarid climates (Birkeland 1984; Buol et al. 1997; Retallack 2001b). The abundance of pedogenic slickensides and pseudoanticlines noted at some locations in these paleosols further suggests a seasonal, semi-arid climate (Therrien and Fastovsky 2000). The maturity (i.e., horizonation) of the Blue Mesa floodplain paleosols is notable, attesting to a low rate of sediment accumulation. The general absence of spodic and histic horizons in these strata, and the lack of kaolinite demonstrate a decrease in precipitation near the end of the Carnian stage. The overlying Sonsela Member, specifically the Jim Camp Wash Bed, and the Painted Desert Member of the Petrified Forest Formation, lower to middle Norian (Lacian to Alaunian), host mature paleosols with abundant stage II to stage IV calcretes (Tanner and Lucas 2006). Calcrete horizons in these members are generally more mature than in the underlying Blue Mesa Member, and gleying less common, as noted by Therrien and Fastovsky (2000), and thus likely reflect more arid conditions. Paleosols of the overlying (late Norian, likely Sevatian) Owl Rock Formation increase in maturity, with stage II to stage III calcretes characterizing the lower part of the formation transitioning to stage III to IV calcretes higher (Tanner 2000a; Tanner and Lucas 2006). Nordt et al. (2015) noted the occurrence of relatively mature calcretes in the Sonsela Member and interpreted this as evidence of "sudden" collapse of the monsoonal system during the Norian. This ignores the pedogenic evidence of gradual aridification present in the strata underlying the Sonsela. In fairness, however, Sonsela paleosols do appear significantly more arid than those in the underlying Blue Mesa Member, which are separated by an unconformity. The upper Norian-Rhaetian Rock Point Formation generally lacks pedogenic features in many areas, but the uppermost strata in some locations host multiple pedogenic horizons that display drab root traces, desiccation cracks, and stage II to III calcretes. Prochnow et al. (2006) described the "upper Chinle," in reference to the Petrified Forest, Owl Rock and Rock Point formations, as a semiarid desert-shrub landscape with MAP of 400–600 mm a^{-1}. In general, the sedimentary evidence from the Colorado Plateau, in particular from the pedogenic features of the Chinle Group, indicates that climate was drier during the Norian-Rhaetian than during the Carnian, confirming the interpretation of Blakey and Gubitosa (1984) and Tanner (2000a, 2003). Cleveland et al. (2008b) also used the pedogenic features of the Chinle Group formations, specifically the Petrified Forest and Rock Point formations, to interpret an overall semi-arid to arid climate, corroborating the earlier studies. Additionally, they estimated mean annual precipitation from measurement of the depth to carbonate in individual profiles to suggest 200–500 mm MAP during the Norian through Rhaetian. Conversely, Dubiel et al. (1991) and Parrish (1993) interpreted the same evidence as indicating a relatively moist climate at least until

the end of the Norian. As noted above, Parrish (1993) modeled a strong monsoonal effect during the Triassic, and predicted abundant moisture in the western equatorial region, which included the Colorado Plateau. Potentially, weakening of the monsoon could have resulted in insufficient strength to draw moisture from the west and aridification of the western equatorial region. Nordt et al. (2015) attribute the weakening of the monsoon on the Colorado Plateau to the orographic effects from the rise of a magmatic arc in the Western Cordillera at this time, rather than to the repositioning of the Pangaean continent. Alternatively, if the Pangaean climate was in fact zonal, as has been proposed by some (Kent and Olsen 2000; Olsen and Ken 2000; Kent et al. 2017), northward drift of the continent over the course of ca. 20 Ma carried the Colorado Plateau region by 5–7° away from the humid tropical belt (Kent et al. 2017). As suggested earlier, the zonal and azonal models are not necessarily mutually exclusive, as weakening of the monsoonal system from continental drift may have allowed strengthening of a latitudinally controlled zonal climate.

3.4.2.2 Newark Supergroup Basins

Vertical changes in sedimentary facies, localized occurrences of evaporites, and paleosol morphology all have been cited in support of a general trend of increasing aridity during deposition of the Upper Triassic to Lower Jurassic formations of the Newark Supergroup, spanning 13° paleolatitude (Olsen 1997; Kent and Olsen 2000). Coals occur in the lower to middle Carnian formations of the southern basins (Olsen 1997), e.g., the lower Chatham Group (formerly the Cumnock, Leaksville and Tuckahoe formations of the Deep River, Danville and Richmond basins, respectively; Weems et al. 2016). Deep-water, perennial lacustrine deposits are interpreted from the middle to late Carnian strata of many of the basins, including the Lockatong Formation of the Danville (former Leaksville Formation), Richmond (former Turkey Branch Formation) and Newark basin. In the southern basins (the Deep River and Taylorsville basins), an increase in the maturity of calcrete paleosols with stratigraphic height (decreasing geological age) is noted in the Norian-age formations (Coffey and Textoris 1996; LeTourneau 2000; Driese and Mora 2003). In the more northerly Newark basin, the thick succession of the Lockatong and Passaic formations is locally evaporite-bearing and interbedded with minor eolian sandstones close to the Rhaetian-age top of the sequence (Olsen 1997). In the Fundy basin, the northernmost of the Newark basins, calcrete-bearing alluvial deposits of the mostly Carnian-age lower Passaic Formation (former Wolfville Formation; Weems et al. 2016) are succeeded by eolian sandstones and evaporite-bearing sheetwash deposits of the Norian to Rhaetian-age upper Passaic Formation (former Blomidon Formation) (Olsen et al. 1989; Olsen 1997; Tanner 2000a, b). As described above, this climate trend in the Newark Supergroup strata has been interpreted in support of the zonal climate model as a consequence of the latitudinal drift of eastern North America by 5–10°, which carried the basins from a moist subtropical to a more northerly arid climate zone (Olsen 1997; Kent and Olsen 2000; Whiteside et al. 2011). Parrish (1993), in contrast, postulated that aridification on the Colorado

Plateau occurred due to the weakening of monsoonal circulation. The weakening monsoon, potentially controlled by the northerly drift of Pangaea, as described above, resulted in strengthening of zonal circulation and allowed the latitudinal drift of the Newark basins, as well as the Colorado Plateau, between climate zones (Parrish 1993). But according to this interpretation, the drying trend occurred during the Early Jurassic, whereas the evidence from the Newark basins suggests that this aridification took place much earlier, during the Norian. Some formations of the Newark Supergroup have long been noted for the cyclical bedding of the lithofacies. Van Houten (1962, 1964) recognized an apparent fine-scale periodicity in the lacustrine cycles of the Lockatong Formation in which he described coarsening-upward cycles of shale, calcareous mudstone and siltstone to sandstone, some of which contained dolomite and zeolites in the mudstones. Van Houten proposed that these sedimentary cycles resulted from the expansion and contraction of shallow, thermally stratified lakes in an alluvial-lacustrine basin. By assuming that thin carbonate-clastic couplets within the dark mudstones recorded the net annual deposition of varves, Van Houten estimated an average sedimentation rate for the cycles, and from this calculated an average depositional duration of approximately 21 kyr per cycle. From this, Van Houten hypothesized that the Milankovitch precessional orbital frequencies controlled the cycles. Van Houten further recognized groupings of the cycles in compound cycles of five and 20 individual cycles, corresponding to the frequency of eccentricity cycles, and suggested that these cycles resulted from longer-term variations in climate that modified the basin hydrology from closed to open, or through-flowing (Van Houten 1964). The original work of Van Houten was expanded upon by Olsen et al. (1989), mainly through the application of spectral analysis to time series of the facies in stratigraphic successions. This allowed identification of a period of 18 kyr to 25 kyr for the basic Van Houten cycle, 95 kyr and 125 kyr for the eccentricity cycle and 400 kyr for the long eccentricity cycle. Although the applicability of the cyclicity of the strata as a complete and accurate astrochronology has been argued (cf. Tanner 2010b; Tanner and Lucas 2015), it is generally acknowledged that the cyclicity stems from climatic variations. Specifically, the Newark cycles are attributed to variations in the strength of the monsoon controlled by variations in solar insolation (Olsen 1986). During the Late Triassic, the Newark Basin would have been located in a near-equatorial position, for which modeling suggests the dominant orbital cycle of insolation variation would have been precession, modulated by eccentricity (Laskar et al. 2004). Computer models have suggested that precipitation in low-latitude regions could have varied by as much 25% due to precession-forced changes in insolation (Kutzbach 1994). Milankovitch-frequency climate variations have been interpreted in other Upper Triassic terrestrial sequences, but definitive evidence of the periodicity of the cycles is lacking for the most part (see review in Tanner 2010b).

3.5 Major Climate Events

3.5.1 The Mid-Carnian Event

3.5.1.1 Evidence for Mid-Carnian humidity

As described elsewhere in this volume (Lucas and Tanner 2017), climate change has been suggested as a contributing factor in biotic turnover during the Late Triassic, specifically in regard to nonmarine tetrapods (Tucker and Benton 1982; Simms and Ruffell 1990). Tucker and Benton (1982), in particular, believed that a major biotic turnover occurred at the Carnian-Norian boundary, which they attributed to the cessation of humid climate conditions at the end of the Carnian. The development of the concept of a widespread climatic event in the mid-Carnian, termed the Carnian Pluvial Event (CPE) was largely advanced by Simms and Ruffell (Simms and Ruffell 1989, 1990) for the western Tethys and Germanic Basin. The general climate of the Carnian has been projected as strongly monsoonal, powered in part by the equatorial position of Tethys (Hay et al. 1982; Hallam 1985; Simms and Ruffell 1990). Mean annual precipitation in the tropics and subtropics, extending to as far as 40° paleolatitude, has been estimated as increasing to over 400 mm. Plant communities during the middle Carnian show more humid affinities, consisting of filocopsids, lycopods, equisetopsids and cycadaleans, followed by a return to xerophytic communities in the lower Tuvalian (Roghi 2004; Roghi et al. 2010; Dal Corso et al. 2015). Visscher et al. (1994), however, disputed that the hygrophytic flora associated with the mid-Carnian in the Germanic Basin were the consequence of a change in climate, but were instead the record of the riparian vegetation of a fluvial system in an otherwise arid setting. Kozur and Bachmann (2010), in contrast to Visscher et al. (1994), described a wet late Julian in the Germanic Basin and northwestern Tethys, which they termed the Middle Carnian Wet Intermezzo (MCWI), with a duration of just 0.7 to 0.8 Ma. Although precipitation exceeded evaporation across this region, they contended that is was not a true pluvial event except between 30° and 50° N paleolatitude. Kozur and Bachmann (2010) attributed their MCWI to Julian strengthening of the megamonsoon, noting the apparent freshening of the Germanic Basin during deposition of the Stuttgart Formation, evidenced by lacustrine, fluvial and brackish facies that contrast with the underlying evaporate-rich Lower Keuper. In their interpretation, monsoonal air flow from northwest Tethys through the Germanic Basin was intercepted by an uplifted rift shoulder in the Caledonides between Scandinavia and Greenland, resulting in an influx of freshwater into the Germanic Basin. On the Iberian Peninsula, the CPE is expressed by the occurrence of continental siliciclastic sediments of Julian age sandwiched between marine evaporites (Arche and López-Gómez 2014). Correlative expressions of a mid-Carnian increase in moisture cited by Arche and López-Gómez (2014) include the Argana basin of Morocco (the Bigoudine Formation), the Fundy Basin of the Canadian Maritimes (the lower Passaic Formation) and the Newark Basin of New Jersey, U.S.A. (the Stockton Formation). Each of these examples presents a similar

stratigraphic case of an upward transition from alluvial fan deposition to a fluvial system that is overlain in turn by eolian and/or playa sediments. We note, however, that although these stratigraphic sequences present evidence for aridification in the upper portion, the superposition of the fluvial systems on basal alluvial fan deposits demonstrates a decrease in the initial high depositional relief on the margin of a rift basin, and does not by itself demonstrate an arid paleoclimate prior to the onset of mid-Carnian humidity.

The CPE has been particularly well studied in the Tethyan realm. Hornung et al. (2007a) examined the $\delta^{18}O$ record of conodont apatite from northwestern Tethys and documented a negative shift at the Julian 1-Julian 2 boundary of 2‰. They interpreted an ocean temperature from 12 to 16 °C in the early Carnian rising to 19 °C during Julian 2, and continuing to rise to as high as 22–25 °C in the Tuvalian. The CPE appears to have been synchronous with a late-early Carnian fall in sea level (Arche and López-Gómez 2014). In much of the western Tethyan realm, the middle Julian (start of Julian 2) through early Tuvalian was marked by the widespread collapse of carbonate platforms, which were exposed during regression, and multiple incursions of siliciclastic sediments, as in the Dolomites, the Northern Calcareous Alps and the Southern Calcareous Alps (Roghi et al. 2010; Stefani et al. 2010; Arche and López-Gómez 2014). Admittedly, there are difficulties in some of these examples in disentangling the effects of the proposed climate shift from eustatic changes and the consequent facies changes (Arche and López-Gómez 2014). In the Lagronegro Basin in the southern Apennines, the event is marked by the incursion of a six-meter thick green clay and radiolarite in the otherwise carbonate-dominated sequence (Rigo et al. 2007). The CPE has also been recognized at Spiti in the Himalayas (Hornung et al. 2007b), which had an estimated palaeolatitude of 28° S (Golonka 2007), thus demonstrating the extent of this perturbation extending to the southern hemisphere, reaching to the southern margin of Neotethys.

Evidence that the CPE extended to eastern Tethys is provided by the Long Chang section at the edge of the Nanpanjiang Basin in southern China at a paleolatitutde of 15° N (Sun et al. 2016). Evidence suggests that the effects of the CPE extended even to the Boreal region. Sedimentary facies in the Barents Sea indicate a dry start to the Carnian, but humidity increased sufficiently to allow coal formation (Hochuli and Vigran 2010). On Spitsbergen, a transition to humid sporophytes from Julian 1 to Julian 2 coincides with the xerophytic to hygrophytic transition observed in the Tethyan (Mueller et al. 2015). The CPE apparently is recorded in Panthalassa as well. Nakada et al. (2014) presented analyses of the clay mineralogy in cherts from Japan that demonstrate a change in the clays consistent with increased weathering in continental environments that sourced pelagic sediment during the late Julian. Notably, the paleoclimatic record of the Ischigualasto Basin from southern Pangaea suggests variable humidity during the Carnian, with the greatest moisture during the middle Carnian (Colombi and Parrish 2008), implying that the CPE may have been global in extent.

3.5.1.2 Isotopic Record of the CPE

Dal Corso et al. (2015) presented carbon isotope data from the Dolomites (Southern Calcareous Alps) that display a negative excursion of 4‰ in terrestrial biomarkers (n-alkanes) and of 2‰ in bulk organic matter approximately at the Julian1—Julian 2 boundary. They correlate this excursion to similar excursions of 2–4‰ in bulk organic matter from the Northern Calcareous Alps (Austria) and the Transdanubian Range (Hungary). Dal Corso et al. (2015) noted a lack of a carbon isotope excursion in the $\delta^{13}C_{carb}$ record from the Dolomites, but considered the excursion in the higher land-plant biomarkers as more compelling evidence for a perturbation of the global carbon cycle. In the Long Chang section (Sun et al. 2016), $\delta^{13}C_{carb}$, $\delta^{13}C_{org}$, $\delta^{18}O$ and U/Th all deviate strongly in Julian 2, with the excursions terminating abruptly at the base of the Tuvalian 1. Although the $\delta^{13}C_{org}$ record exhibits just a single excursion lasting through all of Julian 2, the $\delta^{13}C_{carb}$ record exhibits multiple shifts. Sun et al. (2016) interpreted a warming trend consisting of two separate pulses from the geochemical data and calculated an increase in SST of 4 °C from the initial excursion, followed by a 7 °C increase.

3.5.1.3 Causal Mechanism

Significant to discussions of the age of the Carnian-Norian boundary (see Lucas et al. 2012), Kohút et al. (2017) determined an isotopic age of 221.2 ± 1.6 Ma for zircons from the Lunz Formation, which represents the siliciclastic expression of the CPE in the Carpathians (Slovakia); this finding thereby places the age of the Carnian-Norian boundary as younger than 221 Ma. In the estimation of Kozur and Bachmann (2010), the CPE was a rather brief event of 0.7–0.8 Ma duration; this is reinforced by the interpretation of Arche and López-Gómez (2014) of a duration of less than 1 Ma. In contrast, Miller et al. (2017) recently applied astrochronology to the multiple isotope excursions associated with the CPE in a core from southwestern England to interpret a duration of 1.09 Ma for the CPE. Regardless, the relatively short duration and apparent pulsed nature of the CPE raises questions about the forcing mechanism. Kozur and Bachmann (2010) attributed the influx of freshwater into the Germanic Basin primarily to tectonic factors, as discussed above. Arche and López-Gómez (2014), in reviewing potential causes, considered tectonic uplift and potential reorganization of atmospheric flow as responsible for the temporary increase in precipitation, citing the suggestion of Hornung and Brandner (2005) that uplift of Fennoscandia could have been responsible. Additionally, they note the suggestion that the Late Triassic was a time of peak land area and that increased land-ocean temperature contrast could have heightened the strength of monsoonal flow. However, Arche and López-Gómez (2014) also noted the suggestions that the trigger for the CPE was related to volcanism, either the basaltic eruptions of the Wrangellia province (Furin et al. 2006), or alkaline volcanism in the eastern Mediterranean (Hornung et al. 2007a, b), but conceded that proving cause and effect is difficult. Indeed, the voluminous basalt eruptions that produced the

Wrangellia Large Igneous Province have been suggested by numerous authors as the ultimate cause of the CPE (Furin et al. 2006). In particular, the outgassing of ^{13}C-depleted CO_2 during the extrusion of perhaps 10^6 km^3 of basalt lava is suggested as the proximal cause of the negative carbon isotope excursion (Dal Corso et al. 2012, 2015; Xu et al. 2014). Miller et al. (2017) insist that a highly depleted source of carbon is required to explain the isotope excursions and therefore invoke a combination of volcanic activity and dissociation of marine methane clathrate. We note, however, that attribution of the CPE to Wrangellian activity is somewhat problematic. Although the age of the LIP does overlap the timing of the CPE, it is biostratigraphically constrained only broadly as initiating in the late Ladinian and potentially continuing to the early Tuvalian (Dal Corso et al. 2015). Similarly, $^{187}Os/^{188}Os$ data suggest initiation in the late Ladinian (Xu et al. 2014), 3 Ma prior to the onset of the CPE. Without more definitive evidence that peak eruptive activity occurred during Julian 2, the interpretation of a volcanic trigger for the CPE remains speculative.

3.5.2 End-Triassic Event

As described elsewhere in this volume (Lucas and Tanner 2017), the latest Triassic was a time of biotic crisis, marked by a significant decline in diversity resulting from the combination of low origination rates and several pulses of extinction, the last and largest of which, during the late Rhaetian, reduced or eliminated some characteristic Triassic taxa (Hallam 1990; Sepkoski 2002; Tanner et al. 2004; Kiessling et al. 2007; McElwain et al. 2007; Götz et al. 2009; Guex et al. 2012; McRoberts et al. 2012; Lucas and Tanner 2017). Various forcing mechanisms have been proposed to explain the final extinction pulse, including sea-level change, widespread marine anoxia, climate change, bolide impact, catastrophic release of methane and flood basalt volcanism (reviewed in Tanner et al. 2004; Hesselbo et al. 2007, van de Schootbrugge et al. 2013; Lucas and Tanner 2017). There now exists ample evidence to support the hypothesis that the final biotic decline of the Triassic was largely a consequence of the environmental effects of the eruptions of the flood basalt of the Central Atlantic Magmatic Province (CAMP), the outgassing of which may have sufficiently affected atmospheric properties to impact climate on multiple time scales. Investigation continues on identifying the precise mechanisms by which biota were impacted by the CAMP eruptions; these may have included some combination of intense warming forced by outgassed CO_2, alternating with episodes of SO_2 aerosol-induced cooling and ocean acidification (Hautmann 2004; Marzoli et al. 2004, 2017; Tanner et al. 2004, 2007; Nomade et al. 2007; van de Schootbrugge et al. 2007, 2008, 2009, 2013; Hautmann et al. 2008; Schaltegger et al. 2008; Whiteside et al. 2010; Ruhl et al. 2011; Schaller et al. 2011; Steinthorsdottir et al. 2011; Pálfy and Zajzon 2012; Pieńkowski et al. 2012, 2014; Richoz et al. 2012; Blackburn et al. 2013; Lucas and Tanner 2017).

The association of the CAMP eruptions with the late Rhaetian extinctions was driven in part by the recognition of a negative carbon isotope excursion (CIE) in the

$\delta^{13}C$ record (typically ca. −3.5 °/$_{oo}$) in both marine carbonate and organic carbon in multiple Rhaetian-Hettangian boundary sections, including St Audrie's Bay, southwest England (Hesselbo et al. 2002, 2004), Csövár, Hungary (Pálfy et al. 2001), and several sections in the Northern Calcareous Alps of Austria (Kuerschner et al. 2007; Ruhl et al. 2009). For the greater part, the excursions begin below the highest occurrence of conodonts and Triassic ammonites (e.g. choristocerids), supporting their correlatability, and also consistently below the lowest occurrence of the oldest Jurassic ammonites (i.e. (psilocerids). A similar negative CIE, purportedly correlative with that in the marine realm, has been interpreted for terrestrial plant $\delta^{13}C_{org}$ (McElwain et al. 1999, 2009; Hesselbo et al. 2002; McElwain and Punyasena 2007), although the terrestrial records are much less robust than those of the marine, and their correlation much less certain. The general assumption by the authors of most studies has been that the negative CIEs in both marine and terrestrial environments resulted from the catastrophically large injection of isotopically light carbon into the atmosphere, presumably from outgassing during the CAMP eruptions, potentially accompanied by the release of frozen methane hydrate from the ocean floor.

Review of the calculations of the volumes and composition of the CO_2 involved in producing this perturbation have found errors and flaws in the assumptions, most typically in the form of unrealistic estimates of the volume of gas released (cf. Tanner et al. 2004; Lucas and Tanner 2008, 2017). Nevertheless, the association of CAMP activity with the (marine) negative CIE, and by extension with the late-Rhaetian extinctions, is strongly indicated by Pálfy and Zajzon (2012) and Zajzon et al. (2012), who described pseudomorphs of mafic mineral grains, clay spherules and HREE enrichment in REE profiles, all indicative of mafic volcanism, at the top of the Kössen Formation at Kendlbachgraben, Eiberg Basin, Austria, coincident with the initiation of the CIE. CAMP outgassing of CO_2, and resultant greenhouse warming, was long cited as the primary driver of late Rhaetian extinction, as noted elsewhere in this volume (Lucas and Tanner 2017). Increased pCO_2 during the late Rhaetian has been interpreted from the isotopic composition of soil carbonates, although the published results have been inconsistent. Yapp and Poths (1996) analyzed pedogenic goethite to interpret a catastrophic pCO_2 increase at the end of the Triassic, by a factor of 16, but this conclusion has been reviewed unfavorably (Tanner et al. 2001, 2004). The research of Tanner et al. (2001) directly contradicted this earlier work, finding only a modest pCO_2 increase of several hundred ppm, although neither work used samples tightly constrained to the latest Rhaetian-earliest Hettangian time interval. Schaller et al. (2011, 2012) presented samples with appropriate temporal constraint and interpreted multiple pulsed increases in pCO_2 from 2000 to 4400 ppm, but as critiqued by Lucas and Tanner (2017), these calculations also are compromised by significant methodological flaws. Evidence for an increase in atmospheric CO_2 at this time primarily has been derived from analyses of fossil leaf stomatal indices, a potentially useful proxy for paleo-pCO_2, as described above. McElwain et al. (1999) and Retallack (2001a) presented stomatal evidence for a very large increase of paleo-pCO_2 at the system boundary. The study by McElwain et al. (1999) interpreted a near four-fold pCO_2 increase, from

600 to 2100–2400 ppm. As critiqued by Tanner et al. (2004), however, this conclusion is methodologically flawed by the use of different species from below and above the interpreted system boundary, rather than the same species. Nonetheless, McElwain et al. (1999) interpreted 3° to 4 °C warming as a consequence of the increased pCO_2 and cited decreased leaf size and increased leaf dissection as supporting evidence. Bonis et al. (2010), in contrast to McElwain et al. (1999), used stomatal indices data collected from *Gingko* and *Lepidopteris* samples that continued across the boundary and estimated an increase in pCO_2 of 67%, from 1650 to 2750 ppm, although they acknowledged that their conclusion could overestimate the increase due the effects on stomata of atmospheric SO_2 also produced by CAMP outgassing as predicted by Tanner et al. (Tanner et al. 2007; reviewed in Lucas and Tanner 2017). Similar to Bonis et al. (2010), Steinthorsdottir et al. (2011) utilized taxon-specific stomatal data from fossil gingkos and bennetitaleans at the presumed system boundary in East Greenland to interpret a pCO_2 rise from 1000 ppm to 2000–2500 ppm, following which pCO_2 declined to pre-boundary levels during the Hettangian.

In contrast to the interpretation of significant CO_2-induced warming at the end-Rhaetian based on stomatal data, palynological data from northern European boundary sections have been interpreted as indicating the onset of an abrupt and widespread cooling event (Hubbard and Boulter 1997, 2000). This interpretation is based on analyses of stratigraphic sections spanning the Rhaetian-Hettangian boundary in Great Britain, East Greenland, southern Sweden, and Austria, and posits that *Heliosporites* and *Concavisporites* pollen assemblages are cold-tolerant and hydrophilic, although this interpretation has been disputed by others (cf. McElwain et al. 2007; Steinthorsdottir et al. 2011). The climatic consequences of large sulfur emissions during prolonged flood basalt eruptions are not particularly clear, primarily for lack of modern analogs of large igneous provinces. Explosive volcanism, associated with volcanic arcs, is well-known to be capable of rapidly injecting large volumes of SO_2 into the atmosphere, where it can form H_2SO_4 aerosols, which, in addition to causing acidic precipitation, are known to increase atmospheric opacity and result in reduced short-wave radiant heating, causing global cooling (Sigurdsson 1990; Robock 2000). Unfortunately, the behavior of volcanic sulfur produced by long-term mafic eruptions, and the consequent formation of aerosols, is less predictable than that of CO_2, so the effects are even more difficult to quantify. Sulfur emitted as SO_2 by the CAMP eruptions may have been driven upward convectively by the heat of the eruptions to the stratosphere where it was converted to H_2SO_4 aerosols (Woods 1993; Parfitt and Wilson 2000). This is considered an important mechanism of global cooling because of the increased atmospheric opacity from the aerosol droplets and the resultant decrease in radiative forcing (Sigurdsson 1990; Robock 2000). In the troposphere, these aerosols may have residence times of only several weeks because they are washed out quickly. In the stratosphere, however, aerosols may reside for periods of several years, and the effects of continuing eruptions may be cumulative. Schmidt et al. (2016) recently modeled that LIP eruptions at the scale of CAMP and Deccan may release 2.4 Gt SO_2 a^{-1} for decades at a time, and the formation of aerosols could force a net radiative decrease of -16.2 W m^{-2},

potentially causing 4.5° cooling over decadal intervals. Importantly, the conversion of SO_2 to H_2SO_4 is limited by the availability of atmospheric oxidants in the stratosphere, so the climatic response to a large supply of SO_2 is expected to be nonlinear at the size and time scales of CAMP or Deccan-sized igneous provinces. A very likely scenario is that during the Rhaetian and earliest Hettangian, climate cycled between short, potentially very intense cooling episodes, forced by sulfur emissions, alternating with longer term CO_2-forced warming, throughout the duration of CAMP activity. Schaller et al. (2011, 2012) presented such an interpretation, although as described elsewhere (Lucas and Tanner 2017), their assumptions on the volume of CO_2 emissions appear unrealistic. The relative durations of these climate swings would have been greatly unequal, given the very short residence time of the sulfate aerosols and the much longer residence time of CO_2 in the atmosphere, lasting until equilibration with the mixing layer of the ocean and silicate weathering reduced pCO_2 to near pre-eruption levels.

Hence, the cold episodes lasted only as long as the actual eruptive events, possibly tens to hundreds of years, while warming occupied the extended intervals between major eruptive episodes, lasting tens of thousands to hundreds of thousands of years. Other than the aforementioned and disputed interpretation of cooling from the palynological record (Hubbard and Boulter 1997, 2000), there is little direct evidence of such short but intense cold episodes. Importantly, however, the changes in leaf morphology during the latest Rhaetian are not incompatible with episodes of strong cooling. Studies of modern leaves indicate that increased leaf dissection is produced by the decreased precipitation (Royer et al. 2005; Peppe et al. 2011; Royer 2012) that would accompany sudden cooling; increased precipitation, as might be expected during warming episodes, produces less dissected leaf shapes. These studies were conducted on modern tree species, however, and the response of species more similar to those of the Late Triassic has not been studied.

Perhaps the most unequivocal evidence for warming is found in the clay mineralogy of sedimentary sections from the latest Triassic-earliest Jurassic (van de Schootbrugge et al. 2009; Pieńkowski et al. 2012; Pálfy and Zajzon 2012). Zajzon et al. (2012), for example, found that the kaolinite-dominated assemblage at the base of the Tiefengraben Member of the Kendlbach Formation transitioned upsection to an illite/muscovite dominated assemblage, suggesting more intense weathering conditions during initial Tiefengraben deposition driven by greenhouse warming. This interpretation is consistent with changes in the Al_2O_3/TiO_2 ratio in equivalent strata from the section at Kuhjoch (Tanner et al. 2016). Pálfy and Kocsis (2014), however, noted that increased weathering could also result from acidification of the environment by SO_2 released by the CAMP eruptions. In summary, despite the numerous estimates of CO_2-induced warming and/or SO_2-forced cooling, there is as yet no conclusive geologic evidence that allows direct calculation of the magnitude and duration of the climate changes that occurred during the CAMP eruptions.

3.6 Conclusions

Although there remain many questions regarding the climate of the Late Triassic to be answered, some aspects are now well understood.

1. The Late Triassic was an interval of relatively warm climate, as indicated by lithofacies, the distribution of warm climate flora and coral reefs and the lack of evidence for glaciation, although temperature variations occurred. In particular, episodes of warming occurred during the middle Carnian and end-Rhaetian.
2. This overall warmth was a consequence of high atmospheric pCO_2, as indicated by estimates based on geochemical modeling, the isotopic composition of pedogenic carbonate and stomatal indices measured from fossil leaves, all of which suggest paleo-pCO_2 greater than 1000 ppm, possibly over 2000 ppm, for most of the Late Triassic. Some, but not all, of these proxies suggest declining pCO_2 through the Late Triassic, and consequent overall cooling. The evidence for such a trend is equivocal, however.
3. The sedimentary evidence for highly seasonal precipitation patterns for much of Pangaea is consistent with a highly monsoonal climate, as predicted for the arrangement of large land areas on either side of the equator. Thus, the global climate system at the start of the Late Triassic was primarily azonal.
4. Many regions show evidence of aridification during the Norian, which may have been a consequence of weakening of the monsoonal system and allowed the strengthening of latitudinally-controlled climate belts. Hence, specific regions experienced climate shifts as they drifted from humid climate belts to arid climate belts during the northward drift of Pangaea.
5. The middle Carnian experienced an interval of increased humidity, the CPE, that more precisely seems to have consisted of multiple warm and humid pulses that appear to have been global in extent. Although strengthening of the monsoonal system has been suggested as the cause of the increased humidity, the pulsed and sudden nature of the humidity is consistent with volcanic outgassing as a forcing mechanism. The Wrangellia Igneous Province has been suggested as the eruptive source of the greenhouse gases responsible for the increased warmth and consequent humidity, but the age of the Wrangellian basalts cannot be shown conclusively to match the timing of the humid events.
6. The Rhaetian concluded with an episode of environmental disruption and biotic extinction that can be linked to the eruption of the CAMP basalts. Outgassing of the CAMP caused climate disruption through short episodes of intense cooling forced by H_2SO_4 aerosols (from outgassed SO_2), followed by longer-lasting intervals of warming produced by CO_2-triggered radiative forcing.

Acknowledgments The initial manuscript version of this chapter was improved greatly by the insights and helpful suggestions of Evelyn Kustatscher and Spencer Lucas.

References

Ahlberg A, Arndorff L, Guy-Ohlson D (2002) Onshore climate change during the Late Triassic marine inundation on the Central European Basin. Terra Nova 14:241–248

Arche A, López-Gómez JL (2014) The Carnian Pluvial Event in Western Europe: new data from Iberia and correlation with the Western Neotethys and Eastern North America–NW Africa regions. Earth-Sci Rev 128:196–231

Ashraf AR, Sun Y, Sun G, Uhl D, Mosbrugger V, Li J, Herrman M (2010) Triassic and Jurassic palaeoclimate development in the Junggar Basin, Xinjiang, Northwest China—a review and additional lithological data. Palaeobio Palaeoenv 90:187–201

Beerling DJ, McElwain JC, Osborne CP (1998) Stomatal responses of the "living fossil" *Gingko biloba* L. to changes in atmospheric CO_2 concentrations. J Experiment Bot 49:1603–1607

Berner RA (1994) GEOCARB II: a revised model of atmospheric CO2 levels over Phanerozoic time. Science 249:1382–1386

Berner RA (1998) The carbon cycle and CO_2 over Phanerozoic time: The role of land plants. Philos Trans R Soc London, Ser B 353:75–82

Berner RA (2004) The Phanerozoic Carbon Cycle: CO_2 and O_2. Oxford University Press, Oxford

Berner RA, Kothavala Z (2001) GEOCARB III: a revised model of atmospheric CO_2 over Phanerozoic time. Am J Sci 301:182–204

Berra F, Jadoul F, Anelli A (2010) Environmental control on the end of the Dolomia Principale/Hauptdolomit depositional system in the central Alps: Coupling sea-level and climate changes. Palaeogeogr Palaeoclimatol Palaeoecol 290:138–150

Birkeland PW (1984) Soils and geomorphology. New York, Oxford

Blackburn TJ, Olsen PE, Bowring SA et al (2013) Zircon U-Pb geochronology links the end-Triassic extinction with the Central Atlantic Magmatic Province. Science 340:941–945

Blakey RC, Gubitosa R (1984) Controls of sandstone body geometry and architecture in the Chinle Formarion (Upper Triassic), Colorado Plateau. Sed Geol 38:51–86

Bonis NR, van Konijnenburg-van Cliffert JHA, Kürschner WM (2010) Changing CO_2 conditions during the end-Triassic inferred from stomatal frequency analysis on *Lepidopteris ottonis* (Goeppert) Schimper and *Ginkgoites taeniatus* (Braun) Harris. Palaeogeogr Palaeoclimatol Palaeoecol 295:146–161

Boucot AJ, Gray J (2001) A critique of Phanerozoic climatic models involving changes in the CO_2 content of the atmosphere. Ear Sci Rev 56:1–159

Breda A, Preto N, Roghi G, Furin S, Meneguolo R, Ragazzi E, Fedele P, Gianolla P (2009) The Carnian Pluvial Event in the Tofane area (Cortina d'Ampezzo, Dolomites, Italy). Geo Alp 6:80–115

Buol SW, Hole FD, McCracken RJ, Southard RJ (1997) Soil genesis and classification. Iowa State University, Ames

Cerling TE (1991) Carbon dioxide in the atmosphere: evidence from Cenozoic and Mesozoic paleosols. Am J Sci 291:377–400

Chen L-Q, Cheng-Sen L, Chaloner WG, Beerling DJ, Sun Q-G, Collinson ME, Mitchell PL (2001) Assessing the potential for the stomatal characters of extant and fossil Ginkgo leaves to signal atmospheric CO2 change. Am J Bot 88:1309–1315

Clemmensen LB, Kent DV, Jenkins FA Jr (1998) A Late Triassic lake system in East Greenland: facies, depositional cycles and palaeoclimate. Palaeogeogr Palaeoclimatol Palaeoecol 140:135–159

Cleveland DM, Nordt LC, Atchley SC (2008a) Paleosols, trace fossils, and precipitation estimates of the uppermost Triassic strata in northern New Mexico. Palaeogeogr Palaeoclimatol Palaeoecol 257:421–444

Cleveland DM, Nordt LC, Dworkin SI, Atchley SC (2008b) Pedogenic carbonate isotopes as evidence for extreme climatic events preceding the Triassic-Jurassic boundary: Implications for the biotic crisis? Geol Soc Am Bull 120:1408–1415

Coffey BP, Textoris DA (1996) Paleosols and paleoclimatic evolution, Durham sub-basin, North Carolina. In: LeTourneau PM, Olsen PE (eds) Aspects of Triassic-Jurassic rift basin geoscience. State Geol Nat Hist Surv Connecticut Misc Rep 1

Colombi CE, Parrish JT (2008) Late Triassic environmental evolution in southwestern Pangea; plant taphonomy of the Ischigualasto Formation. Palaios 23:778–795

Crowley TJ, Hyde WT, Short DA (1989) Seasonal cycle variations on the supercontinent of Pangaea. Geol 17:457–460

Currie BS, Colombi CE, Tabor NA, Shipman TC, Montañez IP (2009) Stratigraphy and architecture of the Upper Triassic Ischigualasto Formation, Ischigualasto Provincial Park, San Juan, Argentina. J S Am Earth Sci 27:74–87

Curtin TM, Parrish JT (1999) The Pangean megamonsoon in SW Pangea; preliminary results from Middle Triassic lacustrine rocks and Paleosols, NW Argentina. Geol Soc Am Abs Prog 31:417–418

Dal Corso J, Mietto P, Newton RJ, Pancost RD, Preto N, Roghi G, Wignall P (2012) Discovery of a major 13C spike in the Carnian (Late Triassic) linked to the eruption of Wrangellia flood basalts. Geol 40:79–82

Dal Corso J, Gianolla P, Newton RJ, Franceschi M, Roghi G, Caggiati M, Raucsik B, Budai T, Haas J, Preto N (2015) Carbon isotope records reveal synchronicity between carbon cycle perturbation and the "Carnian Pluvial Event" in the Tethys realm (Late Triassic). Glob Planet Change 127:79–90

Dawit EL (2016) Paleoclimatic records of Late Triassic paleosols from Central Ethiopia. Palaeogeogr Palaeoclimatol Palaeoecol 449:127–140

Driese SG, Mora CI (2003) Paleopedology and stable-isotope geochemistry of Late Triassic (Carnian-Norian) paleosols, Durham sub-basin, North Carolina, U.S.A.; implications for paleoclimate and paleoatmospheric pCO_2. In: Renault RW, Ashley GM (eds) Sedimentation in continental rifts. SEPM Spec Publ 73:207–218

Dubiel RF, Parrish JT, Parrish JM, Good SC (1991) The Pangaean megamonsoon—evidence from the Upper Triassic Chinle Formation, Colorado Plateau. Palaios 6:347–370

Ekart DD, Cerling TE, Montañez IP, Tabor NJ (1999) A 400 million year carbon isotope record of pedogenic carbonate: implications for paleoatmospheric carbon dioxide. Am J Sci 299:805–827

Fawcett PJ, Barron EJ, Robinson VD, Katz BJ (1994) The climatic evolution of India and Australia from the Late Permian to Mid-Jurassic: a comparison of climate model results with the geologic record. In: Klein GD (ed) Pangea: paleoclimate, tectonics and sedimentation during accretion, zenith and break-up of a supercontinent. Geol Soc Am Spec Pap 288:139–157

Fletcher BJ, Brentnall SJ, Anderson CW, Berner RA, Beerling DJ (2008) Atmospheric carbon dioxide linked with Mesozoic and early Cenozoic climate change. Nat Geosci 1:43–48. https://doi.org/10.1038/ngeo.2007.29

Flügel E (2002) Triassic reef patterns. In: Kiessling W, Flügel E, Golonka J (eds) Phanerozoic reef patterns. SEPM Spec Pub 72: 91–463

Frakes LA, Francis JE, Syktus JI (1992) Climate modes of the Phanerozoic: the history of the Earth's climate over the past 600 million years. Cambridge University Press, Cambridge

Furin S, Preto N, Rigo M, Roghi G, Gianolla P, Crowley JL, Bowring SA (2006) High-precision U–Pb zircon age from the Triassic of Italy: implications for the Triassic time scale and the Carnian origin of nannoplankton and dinosaurs. Geology 34:1009–1012

Goddéris Y, Donnadieu Y, de Vargas C, Pierrehumbert RT, Dromart G, van de Schootbrugge B (2008) Causal or casual link between the rise of nanoplankton calcification and a tectonically-driven massive decrease in Late Triassic atmospheric CO_2? Earth Planet Sci Lett 267:247–255

Golonka J (2007) Phanerozoic paleoenvironment and paleolithofacies maps: Mesozoic. Geologia 33:211–264

Götz AE, Ruckwied H, Pálfy J, Haas J (2009) Palynological evidence of synchronous changes within the terrestrial and marine realm at the Triassic/Jurassic boundary (Csövár section, Hungary). Rev Palaeobot Palynol 126:401–409

Guex J, Schoene B, Bartolini A, Spangenberg JE, Schaltegger U, O'Dougherty L, Taylor D, Bucher H, Atudorei V (2012) Geochronological constraints on post-extinction recovery of the ammonoids and carbon cycle perturbations during the Early Jurassic. Palaeogeogr Palaeoclimatol Palaeoecol 346-347:1–11

Hallam A (1985) A review of Mesozoic climates. J Geol Soc Lond 142:433–445

Hallam A (1990) The end-Triassic mass extinction event. In: Sharpton VL, Ward PD (eds) Global catastrophes in Earth history: an interdisciplinary conference on impacts, volcanism, and mass mortality. Geol Soc Am Spec Pap 247:577–583

Hasiotis ST, Dubiel RF, Demko TM (1998) A holistic approach to reconstructing Triassic paleoecosystems: using ichnofossil and paleosols as a basic framework. Nat Park Serv Paleontol Res Tech Rep NPS/NRGRDTR-98/01

Hautmann M (2004) Effect of end-Triassic CO_2 maximum on carbonate sedimentation and marine mass-extinction. Facies 50:257–261

Hautmann M, Benton MJ, Tomasových A (2008) Catastrophic ocean acidification at the Triassic-Jurassic boundary. N Jb Geol Paläont Abh 249:119–127

Haworth M, Hesselbo SP, McElwain JC, Robinson SA, Brunt JW (2005) Mid-Cretaceous pCO_2 based on stomata of the extinct conifer *Pseudofrenelopsis* (Cheirolepidiaceae). Geol 33:749–752

Hay WH, Behensky JF, Barron EJ (1982) Late Triassic–Jurassic paleoclimatolgy of the proto-Central North Atlantic rift system. Palaeogeogr Palaeoclimatol Palaeoecol 40:13–30

Hays PD, Grossman EL (1991) Oxygen isotopes in meteoric calcite cements as indicators of continental paleoclimate. Geol 19:441–444

Hesselbo SP, Robinson SA, Surlyk F, Piasecki S (2002) Terrestrial and marine extinction at the Triassic-Jurassic boundary synchronized with major carbon-cycle perturbation: a link to initiation of massive volcanism? Geol 30:251–254

Hesselbo SP, Robinson SA, Surlyk F (2004) Sea-level change and facies development across potential Triassic–Jurassic boundary hosizons, SW Britain. J Geol Soc Lond 161:365–379

Hesselbo SP, McRoberts CA, Pàlfy J (2007) Triassic–Jurassic boundary events: problems, progress, possibilities. Palaeogeogr Palaeoclimatol Palaeoecol 244:1–10

Hochuli PA, Vigran JO (2010) Climate variations in the Boreal Triassic—inferred from palynological records from the Barents Sea. Palaeogeogr Palaeoclimatol Palaeoecol 290:20–42

Hofmann A, Tourani A, Gaupp R (2000) Cyclicity of Triassic to Lower Jurassic continental red beds of the Argana Valley, Morocco: implications for palaeoclimate and basin evolution. Palaeogeogr Palaeoclimatol Palaeoecol 161:229–266

Hornung T, Brandner R (2005) Biochronostratigraphy of the Rheingraben Turnover (Hallstatt Facies Belt): local black shale events controlled by regional tectonics, climatic change and plate tectonics. Facies 51:460–479

Hornung T, Brandner R, Krystyn L, Joachimsky MM, Keim L (2007a) Multistratigraphic constrains on the NW Tethyan "Carnian Crisis". New Mex Mus Nat Hist Sci Bull 41:59–67

Hornung T, Krystyn L, Brandner R (2007b) A Tethys-wide mid-Carnian (Upper Triassic) carbonate productivity crisis: evidence for the Alpine Rheingraben Event from Spiti (Indian Himalaya)? J Asian Earth Sci 30:285–302

Hubbard RNL, Boulter MC (1997) Mid Mesozoic floras and faunas. Palaeontology 40:43–70

Hubbard RNL, Boulter MC (2000) Phytogeography and paleoecology in Western Europe and Eastern Greenland near the Triassic-Jurassic boundary. PALAIOS 15:120–131

Kent DV, Olsen PE (2000) Magnetic polarity stratigraphy and paleolatitude of the Triassic-Jurassic Blomidon Formation in the Fundy basin (Canada): implications for early Mesozoic tropical climate gradients. Earth Planet Sci Lett 179:311–324

Kent DV, Olsen PE, Muttoni G (2017) Astrochronostratigraphic polarity time scale (APTS) for the Late Triassic and Early Jurassic from continental sediments and correlation with standard marine stages. Earth-Sci Rev 166:153–180

Kidder DL, Worsley TR (2004) Causes and consequences of extreme Permo–Triassic warming to globally equable climate and relation to Permo–Triassic extinction and recovery. Palaeogeogr Palaeoclimatol Palaeoecol 203:207–237

Kiessling W (2010) Reef expansion during the Triassic: Spread of photosymbiosis balancing climatic cooling. Palaeogeogr Palaeoclimatol Palaeoecol 290:11–19

Kiessling W, Aberhan M, Brenneis B, Wagner PJ (2007) Extinction trajectories of benthic organisms across the Triassic-Jurassic boundary. Palaeogeogr Palaeoclimatol Palaeoecol 244:201–222

Kohút M, Hofmann M, Havrila M, Linnemann U, Havrila J (2017) Tracking an upper limit of the "Carnian Crisis" and/or Carnian stage in the Western Carpathians (Slovakia). Int J Earth Sci (Geol Rundsch). https://doi.org/10.1007/s00531-017-1491-8

Korte C, Kozur HW, Veizer J (2005) $*^{13}C$ and $*^{18}O$ values of Triassic brachiopods and carbonate rocks as proxies for coeval seawater and palaeo-temperature. Palaeogeogr Palaeoclimatol Palaeoecol 226:287–306

Kozur H, Bachmann GH (2010) Correlation of the predominantly continental Upper Triassic of the Germanic Basin with the Tethyan scale. In: Di Stefano P, Balini M (eds) New developments on Triassic integrated stratigraphy, workshop Palermo, September 12–16, 2010, 25–27

Kuerschner WM, Bonis NR, Krystyn L (2007) Carbon-isotope stratigraphy and palynostratigraphy of the Triassic-Jurassic transition in the Tiefengraben section—Northern Calcareous Alps (Austria). Palaeogeogr Palaeoclimatol Palaeoecol 244:257–280

Kutzbach JE (1994) Idealized Pangean climates: Sensitivity to orbital change. In: Klein GD (ed) Pangea: Paleoclimate, tectonics, and sedimentation during accretion, zenith, and breakup of a supercontinent. Geol Soc Am Spec Pap 288:41–55

Kutzbach JE, Gallimore RG (1989) Pangaean climates: megamonsoons of the Megacontinent. J Geophys Res 94:3341–3357

Laskar J, Robutel P, Joutel F, Gastineau M, Correia ACM, Levrard B (2004) A long term numerical solution for the insolation quantities of the Earth. Astron Astrophys 428:261–285

LeTourneau PM (2000) From coal to caliche: the sedimentary record of Late Triassic paleoclimate from the Taylorsville rift basin, Virginia. Geol Soc Am Abstr Prog 32(1): 1–30

Li L, Wang Y, Liu Z, Zhou N, Wang Y (2016) Late Triassic palaeoclimate and palaeoecosystem variations inferred by palynological record in the northeastern Sichuan Basin. China Paläontol Zeitschr. https://doi.org/10.1007/s12542-016-0309-5

Lucas SG (1999) The epicontinental Triassic, an overview. Zentralbl Geolog Paläontol Teil 1(1998):475–496

Lucas SG (2010) The Triassic timescale based on nonmarine tetrapod biostratigraphy and biochronology. In: Lucas SG (ed) The Triassic timescale. Geol Soc London Spec Pub 334:447–500

Lucas SG, Tanner LH (2008) Reexamination of the end-Triassic mass extinction. In: Elewa AMT (ed) Mass extinction. Springer, pp 66–103

Lucas SG, Tanner LH (2017) Timing and mechanisms of extinctions during the Late Triassic. In: Tanner LH (ed) The Late Triassic world: Earth in a time of transition. Topics in geobiology, Springer (this volume)

Lucas SG, Tanner LH, Kozur HW, Weems RE, Heckert AB (2012) The Late Triassic Timescale: Age and correlation of the Carnian–Norian boundary. Earth-Sci Rev 114:1–18

Marzoli A, Bertrand H, Knight KB, Cirilli S, Buratti N, Vérati C, Nomade S, Renne PR, Youbi N, Martini R, Allenbach J, Neuwerth R, Rapaille C, Zaninetti L, Bellieni G (2004) Synchrony of the Central Atlantic magmatic province and the Triassic-Jurassic boundary climatic and biotic crisis. Geology 32:973–976

Marzoli A, Callagaro S, Dal Corso J, Youbi N, Bertrand H, Reisberg L, Chiaradia M, Merle R, Jourdan F (2017) The Central Atlantic magmatic province: a review. In: Tanner LF (ed) The Late Triassic world: Earth in a time of transition. Topics in geobiology, Springer (this volume)

McElwain JC, Punyasena SW (2007) Mass extinction events and the plant fossil record. Trends Ecol Evol 22:548–557

McElwain JC, Beerling DJ, Woodward FI (1999) Fossil plants and global warming at the Triassic-Jurassic boundary. Science 285:1386–1390

McElwain JC, Popa ME, Hesselbo SP, Haworth M, Surlyk F (2007) Macroecological responses of terrestrial vegetation to climatic and atmospheric change across the Triassic/Jurassic boundary in East Greenland. Paleobiol 33:547–573

McElwain JC, Wagner PJ, Hesselbo SP (2009) Fossil plant relative abundances indicate sudden loss of late Triassic biodiversity in East Greenland. Science 324:1554–1556

McRoberts CA, Krystyn L, Hautmann M (2012) Macrofaunal response to the end-Triassic mass extinction in the west-Tethyan Kossen Basin, Austria. Palaios 27:607–616

Miller CS, Peterse F, da Silva A-C, Branyi V, Reichart, GJ, Kürschner WM (2017) Astronomical age constraints and extinction mechanisms of the Late Triassic Carnian crisis. Sci Rep 7: 2557 | doi: 10.1038/s41598-017-02817-7

Mueller S, Hounslow MW, Kürschner WM (2015) Integrated stratigraphy and palaeoclimate history of the Carnian Pluvial Event in the Boreal realm; new data from the Upper Triassic Kapp Toscana Group in central Spitsbergen (Norway). J Geol Soc 173:186–202

Mutti M, Weissert H (1995) Triassic monsoonal climate and its signature in Ladinian–Carnian carbonate platforms (Southern Alps, Italy). J Sed Res 65:357–367

Muttoni G, Kent DV, Jadoul F, Olsen PE, Rigo M, Galli MT, Nicora A (2010) Rhaetian magnetostratigraphy from the Southern Alps (Italy): constraints on Triassic chronology. Palaeogeogr Palaeoclimatol Palaeoecol 285:1–16

Nakada R, Ogawa K, Suzuki N, Takahashi S, Takahashi Y (2014) Late Triassic compositional changes of aeolian dusts in the pelagic Panthalassa: response to the continental climatic change. Palaeogeogr Palaeoclimatol Palaeoecol 393:61–75

Nomade S, Knight KB, Beutel E, Renne PR, Verati C, Feraud G, Marzoli A, Youbi N, Bertrand H (2007) Chronology of the Central Atlantic Magmatic Province: implications for the Central Atlantic rifting processes and the Triassic–Jurassic biotic crisis. Palaeogeogr Palaeoclimatol Palaeoecol 244:326–344

Nordt L, Atchley S, Dworkin S (2015) Collapse of the Late Triassic megamonsoon in western equatorial Pangea, present-day American Southwest. Geol Soc Am Bull 127:1798–1815

O'Neil JR, Clayton RN, Mayeda TK (1969) Oxygen isotope fractionation in divalent metal carbonates. J Chem Phys 51:5547–5558

Olsen PE (1986) A 40-million year lake record of Early Mesozoic orbital climate forcing. Science 234:842–848

Olsen PE (1997) Stratigraphic record of the early Mesozoic breakup of Pangea in the Laurasia-Gondwana rift system. Annu Rev Earth Planet Sci 25:337–401

Olsen PE. Ken, DV (2000) High resolution early Mesozoic Pangaean climatic transect in lacustrine environments. In: Bachman G, Lerche I (eds) Epicontinental Triassic, Volume 3. Zentralblatt für Geologie and Paläontologie, Teil I, Heft 11/12:1475–1496

Olsen PE, Schlische RW, Gore PJW (1989) Tectonic, depositional and paleoecological history of early Mesozoic rift basins, eastern North America. Int Geol Cong Field Trip Guidebook T351. Am Geophys Union, Washington, DC

Pálfy J, Kocsis TÁ (2014) Volcanism of the Central Atlantic Magmatic Province as the trigger of environmental and biotic changes around the Triassic-Jurassic boundary. In: Keller G, Kerr AC (eds) Volcanism, impacts and mass extinctions: causes and effects. Geol Soc Am Spec Pap 505:245–261

Pálfy J, Zajzon N (2012) Environmental changes across the Triassic-Jurassic boundary and coeval volcanism inferred from elemental geochemistry and mineralogy in the Kendlbachgraben section (northern Calcareous Alps, Austria). Earth Planet Sci Lett 335-336:121–134

Pálfy J, Demeny A, Haas J, Htenyi M, Orchard MJ, Veto I (2001) Carbon isotope anomaly at the Triassic-Jurassic boundary from a marine section in Hungary. Geology 29:1047–1050

Parfitt EA, Wilson L (2000) Impact of basaltic eruptions on climate. Geol Soc Am Abs Prog 32(7):501

Parrish JT (1993) Climate of the supercontinent Pangea. J Geol 101:215–233

Parrish JT, Peterson F (1988) Wind direction predicted from global circulation models, and wind direction directions determined from eolian sandstones of the Western United States—a comparison. Sed Geol 56:261–282
Peppe DJ, Royer DL, Cariglino B, Oliver SY, Newman S et al (2011) Sensitivity of leaf size and shape to climate: global patterns and paleoclimatic applications. New Phytol 190:724–739
Pieńkowski G, Niedźwiedzki G, Waksmundzka M (2012) Sedimentological, palynological and geochemical studies of the terrestrial Triassic-Jurassic boundary in northwestern Poland. Geo Mag 149:308–332
Pieńkowski G, Niedźwiedzki G, Branski P (2014) Climatic reversals related to the Central Atlantic magmatic province caused the end-Triassic biotic crisis—evidence from continental strata in Poland. Geol Soc Am Spec Pap 505:263–286
Preto N, Kustatscher E, Wignall PB (2010) Triassic climates—state of the art and perspectives. Palaeogeogr Palaeoclimatol Palaeoecol 290:1–10
Prochnow SJ, Nordt LC, Atchley SC, Hudec MR (2006) Multiproxy paleosol evidence for Middle and Late Triassic climate trends in eastern Utah. Palaeogeogr Palaeoclimatol Palaeoecol 232:53–72
Retallack GJ (1999) Post-apocalyptic greenhouse paleoclimate revealed by earliest Triassic paleosols in the Sydney Basin, Australia. Geol Soc Am Bull 111:52–70
Retallack GJ (2001a) A 300-million-year record of atmospheric carbon dioxide from fossil plant cuticles. Nature 411:287–290
Retallack GJ (2001b) Soils of the past: an introduction to paleopedology. Blackwell, London
Retallack GJ (2013) Permian and Triassic greenhouse crises. Gondwana Res 24:90–103
Richoz S, van de Schootbrugge B, Pross J, Püttmann W, Quan TM, Lindström S, Heunisch C, Fiebig J, Maquil R, Schouten S, Hauzenberger CA, Wignall PB (2012) Hydrogen sulphide poisoning of shallow seas following the end-Triassic extinction. Nat Geosci 5:662–667
Rigo M, Preto N, Roghi G, Tateo F, Mietto P (2007) A rise in the carbonate compensation depth of western Tethys in the Carnian (Late Triassic): Deep-water evidence for the Carnian pluvial event. Palaeogeogr Palaeoclimatol Palaeoecol 246:188–205
Rigo M, Trotter JA, Preto N, Williams IS (2012) Oxygen isotopic evidence for Late Triassic monsoonal upwelling in the northwestern Tethys. Geol 40:515–518
Robinson PL (1973) Palaeoclimatology and continental drift. In: Tarling DH, Runcorn SK (eds) Implications of continental drift to the Earth sciences, vol. 1. Academic Press, London, 449–476
Robock A (2000) Volcanic eruptions and climate. Rev Geophys 38:191–219
Roghi G (2004) Palynological investigations in the Carnian of Cave del Predil area (once Raibl, Julian Alps). Rev Paleobot Palynol 132:1–35
Roghi G, Gianolla P, Minarelli C, Pilati C, Preto N (2010) Palynological correlation of Carnian humid pulses throughout the western Tethys. Palaeogeogr Palaeoclimatol Palaeoecol 290:89–106
Royer DL (2012) Leaf shape responds to temperature but not CO_2 in Acer rubrum. PLoS One 7(11):e49559. https://doi.org/10.1371/journal.pone.0049559
Royer DL, Berner RA, Beerling DJ (2001) Phanerozoic atmospheric CO_2 change: evaluating geochemical and paleobiological approaches. Earth-Sci Rev 54:349–392
Royer DL, Wilf P, Janesko DA, Kowalski EA, Dilcher DL (2005) Correlations of climate and plant ecology to leaf size and shape: potential proxies for the fossil record. Am J Bot 92:1141–1151
Royer DL, Berner RA, Park J (2007) Climate sensitivity constrained by CO_2 concentrations over the past 420 million years. Nature 446:530–532
Ruffell A, Shelton R (1999) The control of sedimentary facies by climate during phases of crustal extension. Examples from the Triassic of onshore and offshore England and Northern Ireland. J Geol Soc Lond 156:779–789
Ruhl M, Kuerschner WM, Krystyn L (2009) Triassic-Jurassic organic carbon isotope stratigraphy of key sections in the western Tethys realm (Austria). Earth Planet Sci Lett 281:169–187
Ruhl M, Bonis NR, Reichart G-J, Sinninghe D, Jaap S, Kuerschner WF (2011) Atmospheric carbon injection linked to end-Triassic mass extinction. Science 333:430–434

Schaller MF, Wright JD, Kent DV (2011) Atmospheric pCO_2 perturbations associated with the Central Atlantic magmatic province. Science 331:1404–1409

Schaller MF, Wright JD, Kent DV, Olsen PE (2012) Rapid emplacement of the Central Atlantic Magmatic Province as net sink for CO_2. Earth Planet Sci Lett 323-324:27–39

Schaltegger U, Guex J, Bartolini A, Schoene B, Ovtcharov M (2008) Precise U-Pb age constraints for end-Triassic mass extinction, its correlation to volcanism and Hettangian post-extinction recovery. Earth Planet Sci Lett 267:266–275

Schmidt A, Skeffington RA, Thordarson T, Self S, Forster PM et al (2016) Selective environmental stress from sulphur emitted by continental flood basalt eruptions. Nat Geosci 9:77–82

Sciscio L, Bordy E (2016) Palaeoclimatic conditions in the Late Triassic-Early Jurassic of southern Africa: a geochemical assessment of the Elliot Formation. J African Earth Sci 119:102–119

Sellwood BW, Valdes PJ (2006) Mesozoic climates, general circulation models and the rock record. Sed Geol 190:269–287

Sepkoski JJ (2002) A compendium of fossil marine animal genera. Bull Am Paleonto 363:1–560

Sha J, Olsen PE, Xu D, Yao X, Pan Y, Wang Y, Zhang X, Vajda V (2015) Early Mesozoic, high-latitude continental Triassic–Jurassic climate in high-latitude Asia was dominated by obliquity-paced variations (Junggar Basin, Urumqi, China). Proc Natl Acad Sci U S A 112:3624–3629

Sigurdsson H (1990) Assessment of atmospheric impact of volcanic eruptions. In: Sharpton VL, Ward PD (eds) Global catastrophes in Earth history. Geol Soc Am Spec Pap 247:99–110

Simms MJ, Ruffell AH (1989) Synchroneity of climatic change and extinctions in the Late Triassic. Geology 17:265–268

Simms MJ, Ruffell AH (1990) Climatic and biotic change in the Late Triassic. J Geol Soc Lond 147:321–327

Stefani M, Furin S, Gianolla P (2010) The changing climate framework and depositional dynamics of the Triassic carbonate platforms from the Dolomites. Palaeogeogr Palaeoclimatol Palaeoecol 290:43–57

Steinthorsdottir M, Jeram AJ, McElwain JC (2011) Extremely elevated CO_2 concentrations at the Triassic/Jurassic boundary. Palaeogeogr Palaeoclimatol Palaeoecol 308:418–432

Suchecki RK, Hubert JF, Birney de Wet CC (1988) Isotopic imprint of climate and hydrogeochemistry on terrestrial strata of the Triassic-Jurassic Hartford and Fundy rift basins. J Sed Res 58:801–811

Sun YD, Wignall PB, Joachimski MM, Bond DPG, Grasby SE, Lai XL, Wang LN, Zhang ZT, Sun S (2016) Climate warming, euxinia and carbon isotope perturbations during the Carnian (Triassic) Crisis in South China. Earth Planet Sci Lett 444:88–100

Tabor NJ, Yapp CJ, Montañez IP (2004) Goethite, calcite and organic matter from Permian and Triassic soils; carbon isotopes and CO_2 concentrations. Geochim Cosmochim Acta 68:1503–1517

Tabor NJ, Montañez IP, Kelso KA, Currie BS, Shipman TA, Colombi, CE (2006) Late Triassic soil catena: Landscape and climate controls on paleosol morphology and chemistry across the Carnian-age Ischigualasto-Villa Union basin, northwestern Argentina. In: Alonso-Zarza AM, Tanner LH (eds) Paleoenvironmental record and applications of calcretes and palustrine carbonates. Geol Soc Am Spec Pap 416:17–42

Talbot MR, Holm K, Williams MAJ (1994) Sedimentation in low-gradient desert margin systems: a comparison of the Late Triassic of northwest Somerset (England) and the late Quaternary of east-central Australia. In: Rosen MR (ed) Paleoclimate and basin evolution of playa systems. Geol Soc Am Spec Pap 289:97–117

Tanner LH (2000a) Palustrine-lacustrine and alluvial facies of the (Norian) Owl Rock Formation (Chinle Group), Four Corners Region, southwestern U.S.A.: implications for Late Triassic paleoclimate. Jour Sed Res 70:1280–1289

Tanner LH (2000b) Triassic-Jurassic lacustrine deposition in the Fundy rift basin, eastern Canada. In: Gierlowski-Kordesch E, Kelts K (eds) Lake basins through space and time. Am Assoc Petr Geol Stud Geol 46:159–166

Tanner LH (2002a) Mesozoic atmospheric CO_2 spike: Comment and Reply. Nature 415:388

Tanner LH (2002b) Pedogenic record of paleoclimate and basin evolution in the Triassic-Jurassic Fundy rift basin, eastern Canada. In: LeTourneau P, Olsen PE (eds) Aspects of Triassic-Jurassic rift basin geoscience. Columbia University Press, New York

Tanner LH (2003) Pedogenic features of the Chinle Group, Four Corners region; Evidence of Late Triassic aridification. New Mex Geol Soc Guidebook 54th Field Conf

Tanner LH (2010a) Terrestrial carbonates as indicators of palaeoclimate. In: Alonsa-Zarza AM, Tanner LH (eds) Carbonates in continental settings: geochemistry, diagenesis and applications. Elsevier, Devel Sedimentol 62:179–214

Tanner LH (2010b) Cyclostratigraphic record of the Triassic: A critical examination. In: Lucas SG (ed) The Triassic timescale. Geol Soc London Spec Publ 334:119–137

Tanner LH Lucas SG (2006) Calcretes of the Upper Triassic Chinle Group, Four Corners region, southwestern U.S.A.: climatic implications. In: Alonso-Zarza AM, Tanner LH (eds) Paleoenvironmental record and applications of calcretes and palustrine Carbonates. Geol Soc Am Spec Pap 416:53–74

Tanner LH, Lucas SG (2015) The Triassic-Jurassic strata of the Newark Basin, USA: A complete and accurate astronomically-tuned timescale? Stratigraphy 12:47–65

Tanner LH, Hubert JF, Coffey BP, McInerney DP (2001) Stability of atmospheric CO_2 levels across the Triassic/Jurassic boundary. Nature 411:675–677

Tanner LH, Lucas SG, Chapman MG (2004) Assessing the record and causes of Late Triassic extinctions. Earth-Sci Rev 65:103–139

Tanner LH, Smith DL, Allan A (2007) Stomatal response of swordfern to volcanogenic CO and SO from Kilauea volcano, Hawaii. Geophys Res Lett 34:L15807. https://doi.org/10.1029/2007GL030320

Tanner LH, Kyte FT, Richoz S, Krystyn L (2016) Distribution of iridium and associated geochemistry across the Triassic-Jurassic boundary in sections at Kuhjoch and Kendlbach, Northern Calcareous Alps, Austria. Palaeogeogr Palaeoclimatol Palaecol 449:13–26, https://doi.org/10.1016/j.palaeo.2016.01.011

Taylor EL (1989) Tree-ring structure in woody axes from the central Transantarctic Mountains, Antarctica. Proc Internat Sympos Antarctic Res, Hangzhou, China, May, 1989, China Ocean Press, Tianjin, pp. 109–113

Taylor EL, Taylor TN, Cuneo RN (2000) Permian and Triassic high latitude and paleoclimates; evidence from fossil biotas. In: Huber BT, MacLeod KG, Wing SL (eds) Warm climates in Earth history. Cambridge University Press, Cambridge, pp 321–350

Therrien F, Fastovsky DE (2000) Paleoenvironments of early theropods, Chinle Formation (Late Triassic), Petrified Forest National Park, Arizona. Palaios 15:194–211

Tian N, Wang Y, Philippe M, Li L, Xie X, Jiang Z (2016) New record of fossil wood *Xenoxylon* from the Late Triassic in the Sichuan Basin, southern China and its paleoclimatic implications. Palaeogeogr Palaeoclimatol Palaeoecol 464:65–75

Trotter JA, Williams IS, Nicora A, Mazza M, Rigo M (2015) Long-term cycles of Triassic climate change: a new $\delta^{18}O$ record from conodont apatite. Earth Planet Sci Lett 415:165–174

Tucker ME, Benton MJ (1982) Triassic environments, climates, and reptile evolution. Palaeogeogr Palaeoclimatol Palaeoecol 40:361–379

Van de Schootbrugge B, Tremolada F, Rosenthal Y, Bailey TR, Feist-Burkhardt S, Brinkhuis H, Pross J, Kent DV, Falkowski PG (2007) End-Triassic calcification crisis and blooms of organic-walled 'disaster species. Palaeogeogr Palaeoclim Palaeoecol 244:126–141

Van de Schootbrugge B, Payne JL, Tomasovych A, Pross J, Fiebig J, Benbrahim M, Föllmi KB, Quan TM (2008) Carbon cycle perturbation and stabilization in the wake of the Triassic-Jurassic boundary mass-extinction event. Geochem Geophys Geosys 9. https://doi.org/10.1029/2007GC001914

Van de Schootbrugge B, Quan T, Lindström S, Püttmann W, Heunisch C, Pross J, Fiebig J, Petschick R, Röhling H-G, Richoz S, Rosenthal Y, Falkowski PG (2009) Floral changes across the Triassic/Jurassic boundary linked to flood basalt volcanism. Nat Geosci 2:589–594

Van de Schootbrugge B, Bachan A, Suan G, Richoz S, Payne JL (2013) Microbes, mud and methane: cause and consequence of recurrent Early Jurassic anoxia following the end-Triassic mass-extinction. Palaeontology 56(4):685–709

Van Houten FB (1962) Cyclic sedimentation and the origin of analcime-rich Upper Triassic Lockatong Formation, west-central New Jersey and adjacent Pennsylvania. Am J Sci 260:561–576

Van Houten FB (1964) Cyclic lacustrine sedimentation, Upper Triassic Lockatong Formation, central New Jersey and adjacent Pennsylvania. Kansas Geol Surv Bull 169:497–532

Veizer J, Ala D, Azmy K, Bruckschen P, Buhl D, Bruhn F, Carden GAF, Diener A, Ebneth S, Godde'ris Y, Jasper T, Korte C, Pawellek F, Podlaha OG, Strauss H (1999) $^{87}Sr/^{86}Sr$, $\delta^{13}C$ and $\delta^{18}O$ evolution of Phanerozoic seawater. Chem Geol 161:59–88

Visscher H, Van Houte M, Brugman WA, Poort RJ (1994) Rejection of a Carnian (Late Triassic) "pluvial event" in Europe. Rev Palaeobot Palynol 83:217–226

Weems RJ, Tanner LH, Lucas SG (2016) Synthesis and revision of the lithostratigraphic groups and formations in the Upper Permian?–Lower Jurassic Newark Supergroup of eastern North America. Stratigraphy 13:111–153

Wescott WA, Diggens JN (1998) Depositional history and stratigraphical evolution of the Sakamena Group (middle Karoo Supergroup) in the southern Morondava Basin, Madagascar. J African Earth Sci 27:461–479

Whiteside JH, Olsen PE, Eglinton T, Brookfield ME, Sambrotto RN (2010) Compound-specific carbon isotopes from Earth's largest flood basalt eruptions directly linked to the end-Triassic mass extinction. Proc Nat Acad Sci USA 107:6721–6725

Whiteside JH, Grogan DS, Olsen PE, Kent DV (2011) Climatically driven biogeographic provinces of Late Triassic tropical Pangea. Proc Natl Acad Sci U S A 108:8972–8977

Woods AW (1993) A model of the plumes above basaltic fissure eruptions. Geophys Res Lett 20:1115–1118

Xu G, Hannah JL, Stein HJ, Mørk A, Vigran JO, Bingen B, schutt DL, Lundschien BA (2014) Cause of Upper Triassic climate crisis revealed by Re–Os geochemistry of Boreal black shales. Palaeogeogr Palaeoclim Palaeoecol 395:222–232

Yan JX, Zhao K (2002) Permian–Triassic paleogeography of the East Tethyan region-the ancient climate and the evolution of ancient oceans and the Earths' surface-coupled multilayer case. Sci China Ser D 32:751–759

Yapp CJ, Poths H (1996) Carbon isotopes in continental weathering environments and variations in ancient atmospheric CO_2 pressure. Earth Planet Sci Lett 137:71–82

Zajzon N, Kristaly F, Nemeth T (2012) Detailed clay mineralogy of the Triassic-Jurassic boundary section at Kendlbachgraben (northern Calcareous Alps, Austria). Clay Min 47:177–189

Ziegler AM, Eshet G, McAllister Rees P, Rothfus TA, Rowley DB, Sunderlin D (2003) Tracing the tropics across land and sea: Permian to present. Lethaia 36:227–254

Chapter 4
The Central Atlantic Magmatic Province (CAMP): A Review

Andrea Marzoli, Sara Callegaro, Jacopo Dal Corso, Joshua H.F.L. Davies, Massimo Chiaradia, Nassrrdine Youbi, Hervé Bertrand, Laurie Reisberg, Renaud Merle, and Fred Jourdan

Abstract The Central Atlantic magmatic province (CAMP) consists of basic rocks emplaced as shallow intrusions and erupted in large lava flow fields over a land surface area in excess of 10 million km^2 on the supercontinent Pangaea at about 201 Ma.

A. Marzoli (✉)
Dipartimento di. Geoscienze, Università di Padova, 35137 Padova, Italy

Department of Applied Geology, Curtin University, Bentley, WA 6102, Australia
e-mail: andrea.marzoli@unipd.it

S. Callegaro
Centre for Earth Evolution and Dynamics (CEED), University of Oslo,
PO Box 1028, Blindern, 0316 Oslo, Norway

J. Dal Corso
Hanse-Wissenschaftskolleg (HWK), Institute for Advanced Study,
Lehmkuhlenbusch 4, 27753 Delmenhorst, Germany

J.H.F.L. Davies • M. Chiaradia
Sciences de la Terre et de l'Environnement, Université de Genève, Genève, Switzerland

N. Youbi
Department of Geology, Faculty of Sciences-Semlalia, Cadi Ayyad University,
Marrakesh 40000, Morocco

Instituto Dom Luiz, Faculdade de Ciências, Universidade de Lisboa,
1749-016 Lisbon, Portugal

H. Bertrand
Laboratoire de Géologie de Lyon, Université Lyon 1 and Ecole Normale Supérieure de Lyon,
UMR CNRS 5276, 46 Allée d'Italie, 69364 Lyon, Cedex 7, France

L. Reisberg
Centre de Recherches Pétrographiques et Géochimiques, UMR 7358 CNRS, Université de
Lorraine, BP 20, 54501 Vandoeuvre-les-, Nancy, Cedex, France

R. Merle
Australian National University, Research School of Earth Sciences,
142 Mills Rd, Acton, ACT 0200, Australia

F. Jourdan
Department of Applied Geology, Curtin University, Bentley, WA 6102, Australia

© Springer International Publishing AG 2018

L.H. Tanner (ed.), *The Late Triassic World*, Topics in Geobiology 46,
https://doi.org/10.1007/978-3-319-68009-5_4

The peak activity of the CAMP straddled the Triassic-Jurassic boundary and probably lasted less than 1 million years, while late activity went on for several Ma more into the Sinemurian. Emission of carbon and sulfur from the CAMP magmas and from intruded sediments probably caused extinctions at the end-Triassic. Intrusive rocks are represented by isolated dykes up to 800 km-long, by dense dyke swarms and by extremely voluminous sills and a few layered intrusions. Lava fields were erupted as short-lived pulses and can be traced over distances of several hundred km within sedimentary basins. They consist of either compound or simple pahoehoe flows. Globally, the intrusive and effusive rocks are estimated to represent an original magmatic volume of at least 3 million km^3. Herein we subdivide the CAMP basalts for the first time into six main geochemical groups, five represented by low-Ti and one by high-Ti rocks. Except for one low-Ti group, which is ubiquitous throughout the entire province, all other groups occur in relatively restricted areas and their compositions probably reflect contamination from the local continental lithosphere. Major and trace elements and Sr-Nd-Pb-Os isotopic compositions indicate that the basaltic magmas had an enriched composition compared to Mid-Ocean Ridge basalts and different from Atlantic Ocean Island basalts. The enriched composition of CAMP basalts is only in part attributable to crustal contamination. It also probably requires subducted upper and lower continental crust material that enriched the shallow upper mantle from which CAMP basalts were generated. A contribution from a deep mantle-plume is not required by geochemical and thermometric data, but it remains unclear what other possible heat source caused mantle melting on the scale required to form CAMP.

Keywords Large igneous province • End-Triassic • Radioisotopic ages • Mantle melting • Volcanic • Thermogenic gases

4.1 Introduction

The Central Atlantic magmatic province (CAMP; Marzoli et al. 1999) is a large igneous province (LIP) formed by basaltic magmas emplaced on Pangaea shortly before its break-up (Fig. 4.1). The peak CAMP magmatic activity occurred at ca. 201 Ma and lasted for less than 1 Ma (Marzoli et al. 2011; Blackburn et al. 2013; Davies et al. 2017). CAMP shares some features with other well-known LIPs, such as the Deccan Traps, the Karoo and the Paranà-Etendeka (Melluso et al. 2006; Jourdan et al. 2007; Peate 1997). All these LIPs are associated with continental break-up events and are composed of widespread, mainly basaltic magmas emplaced within a short time span. On the other hand, CAMP is peculiar because of its enormous aerial extent and volume of intruded mafic magmas, coupled with only thin and relatively rare preserved lava piles. Unlike many other LIPs, CAMP lacks alkaline magmatism and acid rocks are also very rare. The atypical traits of the CAMP indicate that its formation cannot easily be attributed to the same processes invoked

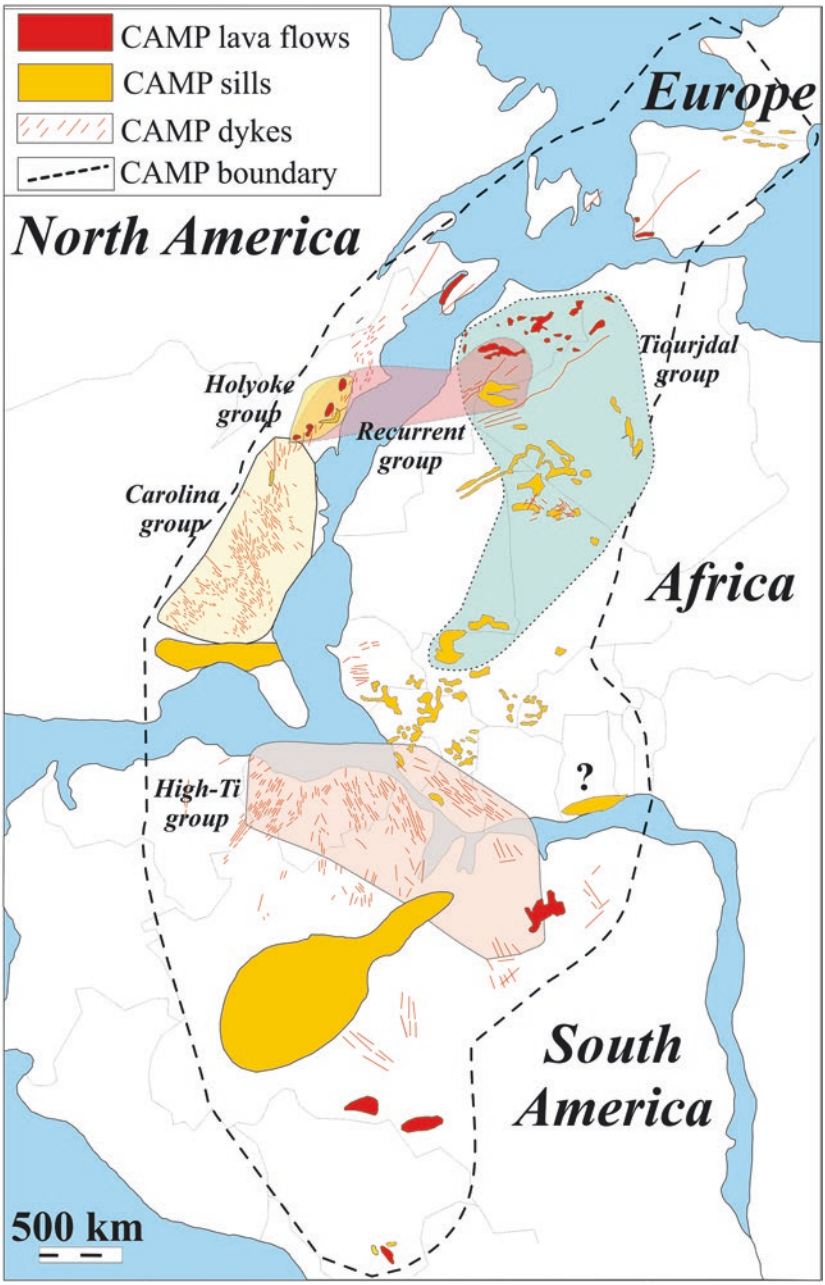

Fig. 4.1 Schematic map of the Central Atlantic magmatic province (CAMP), on the Pangaean continent. Modified from Marzoli et al. (2011). The *dashed line* indicates the approximate surface wherein CAMP remnants have been sampled. The colored fields with *dotted outlines* indicate the area of occurrence of the Tiourjdal (NW-Africa), Holyoke, Recurrent, and High-Ti groups, all other CAMP rocks belong to the Prevalent-CAMP group

for other LIPs. In particular, classical mantle-plume models seem not to be consistent with its large area and relative sparseness of erupted basalts. Therefore, while mantle-plume models have been previously proposed for the CAMP, especially, but not exclusively during the later twentieth century (e.g., May 1971; Morgan 1983; Hill 1991), more recently alternative scenarios of mantle melting have emerged (McHone 2000; Coltice et al. 2007; Ruiz-Martínez et al. 2012). In this review, we briefly describe the main aspects of the CAMP, including its age, surface area and volume, its volcanologic and geochemical characteristics, and its origin and links with the end-Triassic mass extinction. We also propose a new subdivision of CAMP basalts into six main geochemical groups.

4.2 Defining the Central Atlantic Magmatic Province

The CAMP is a newcomer among the recognized LIPs. Although portions of it, notably in Morocco and in the USA, have been recognized as belonging to the same event since the work of May (1971), until the end of the twentieth century (e.g., Coffin and Eldholm 1994) and even later the CAMP was not considered among the main Phanerozoic LIPs.

May (1971) recognized that dyke swarms were radially emplaced around a center located between the southeastern USA (Florida) and northwestern Africa (Senegal) and interpreted them as resulting from an uprising mantle plume. The first geochemical-petrologic studies were subsequently conducted on basaltic lava flows and dykes from eastern North America (e.g., Weigand and Ragland 1970; Dostal and Dupuy 1984) and North-West Africa (Bertrand et al. 1982; Bertrand 1991). These studies showed that the compositions of basaltic dykes and flows on both sides of the Atlantic (Bertrand and Coffrant 1977) were largely identical, even though subtle time-related changes were recognized in lava piles from the USA (Puffer et al. 1982; Puffer 1992; Tollo and Gottfried 1992) and from Morocco (Bertrand et al. 1982; Youbi et al. 2003). In the northeastern USA in particular, geochemical data combined with field evidence allowed recognition of the association between flow units and feeder dykes (e.g., McHone 1996; Philpotts and Reichenbach 1985; Philpotts and Asher 1993). The first geochemical-petrologic studies on the South American CAMP were published in the 1990s (Bellieni et al. 1990; Fodor et al. 1990; Montes-Lauar et al. 1994) and early studies of the European basalts date back to the works of Alibert (1985), Azambre et al. (1981, 1987), Bertrand (1987), and Caroff et al. (1995). The first Sr-Nd-Pb isotopic data for CAMP basalts were published by Alibert (1985), Dupuy et al. (1988), Pegram (1990), and Puffer (1992), but it is only since the beginning of the twenty-first century that numerous geochemical studies reporting large sets of Sr-Nd-Pb-Os isotopic data have been made available on CAMP basalts from Europe (Cebriá et al. 2003; Jourdan et al. 2003; Martins et al. 2008; Marzoli et al. 2014; Callegaro et al. 2014a), Africa (Verati et al. 2005; Deckart et al. 2005; Chabou et al. 2010), North America (Callegaro et al. 2013; Merle et al. 2014; Whalen et al. 2015), and South America (Nomade et al.

2002; De Min et al. 2003; Merle et al. 2011; Klein et al. 2013; Bertrand et al. 2014). These works confirm the global similarity of basalts all over the province, with all samples showing an incompatible element enriched character compared to Mid-Ocean Ridge basalts (MORB). Even so, a quite large spread of Sr-Nd-Pb isotopic compositions highlights regional differences which represent contributions from distinct (mantle) source components and shallow contamination by the diverse components of the continental crust and lithosphere (e.g., Alibert 1985; Pegram 1990; Callegaro et al. 2013; Merle et al. 2014).

The first geochronological data were whole-rock K-Ar analyses (e.g., Hailwood and Mitchell 1971; Dalrymple et al. 1975) that resulted in a large spread of ages. However, the implementation of the more modern $^{40}Ar/^{39}Ar$ technique to date mineral separates (plagioclase, mostly) has produced a much refined constraint on the emplacement age of the CAMP. Starting from the first studies on African basalts (Sebai et al. 1991; Deckart et al. 1997) and then on the South American CAMP (Baksi and Archibald 1997; Marzoli et al. 1999), it became clear that basaltic magmas were emplaced at ca. 200 Ma over a total surface area of several millions of km^2. Successive $^{40}Ar/^{39}Ar$ geochronological studies (Jourdan et al. 2003, 2009; Marzoli et al. 2004, 2011; Knight et al. 2004; Verati et al. 2007; Nomade et al. 2007; Merle et al. 2011; Bertrand et al. 2014), combined with a revised value for the ^{40}Ar decay constant (Renne et al. 2010, 2011) further refined this age, and indicated that peak magmatic activity occurred synchronously throughout the province at ca. 201 Ma. More recently, Schoene et al. (2010), Blackburn et al. (2013) and Davies et al. (2017) obtained $^{206}Pb/^{238}U$ ages on zircon from two flows and 14 intrusive units, which confirm the ca. 201 Ma peak activity. Globally, high quality $^{40}Ar/^{39}Ar$ ages (as screened following the criteria presented in Nomade et al. 2007, and in Marzoli et al. 2011) range from about 202 to 192 Ma, demonstrating an early peak of magmatism followed by late protracted low-volume magmatism.

4.3 Outcrops and Estimates of Surface Area and Volume

Remnants of basaltic lava flows and basic intrusions (sills and dykes, mostly) presently crop out over a North-South (France to Bolivia) distance of more than 10,000 km in the four continents rimming the Atlantic Ocean. Sample coverage in several remote areas of Africa (e.g., Ivory Coast, Burkina Faso, Ghana and Mauritania) and South America (e.g., Guyana, Venezuela, or Peru) is still sparse, making the definition of the surface area covered by the LIP partially incomplete. Several intrusive CAMP rocks, sills mainly, are known from core data only (e.g., in Senegal; Ndiaye et al. 2016). Lava flows are preserved in sedimentary basins only and are relatively rare. The thickness of the preserved lava piles is much less than in most other LIPs (e.g., Deccan Traps, Paranà-Etendeka, Karoo) and does not exceed 500 m. In contrast, the CAMP intrusions show quite impressive dimensions; dyke swarms (e.g., in southeastern USA, Mali, Liberia, Guyana, Brazil) are formed by hundreds of dykes intruded over areas of thousands of km^2, while single dykes (e.g.,

in Spain-Portugal, Morocco, Algeria, USA, Canada, Brazil) reach lengths of several hundred km (up to ca. 800 km) and widths of up to 300 m. Sill swarms are known from France and Spain, USA, Morocco, Algeria, Mali, Guinea, and are formed by tens of shallow level intrusions, covering hundreds to thousands of km^2. The sills intruding the Paleozoic Amazonian (s.l.) basins of northern Brazil are particularly impressive. These sills reach a global volume of nearly 1 million km^3, although they crop out only locally in NE-Brazil (De Min et al. 2003; Milani and Zalàn 1999).

It is very difficult to estimate the total original volume of erupted CAMP basalts. A large part of the CAMP was quickly eroded away shortly after its emplacement, as suggested by Sr and Os isotopic variations in sea sediments and fossils (Cohen and Coe 2002; Callegaro et al. 2012) and also by mineralogical composition and C stable isotope variations in sediments at the base of the oldest preserved Moroccan CAMP flows (Dal Corso et al. 2014).

A total pre-erosional CAMP volume of 2×10^6 km^3 generally has been used since the data presented by Marzoli et al. (1999). However, other estimations of the original CAMP volumes have since been attempted by McHone (2003) and Svensen et al. (2004). Some of the more recently recognized CAMP occurrences were not taken into account in McHone (2003), e.g. the layered intrusions from Guinea and Sierra Leone, and intrusive and extrusive rocks from Bolivia, Morocco, Algeria, and Europe. However, the basalts and intrusive rocks forming East Coast Magnetic Anomaly (ECMA; Oh et al. 1995) were considered part of the CAMP. This massive coastal wedge has a volume of ~2.75×10^6 km^3 according to McHone's (2003) estimation. Furthermore, along the northwestern African coast, a similar structure (the West African Coast Magnetic Anomaly) has been identified (Sahabi et al. 2004; Labails et al. 2010). Due to lack of conclusive data (age data, in particular) concerning the link of the North American East Coast and African West Coast oceanic margin volcanics to the CAMP, we do not include them here.

A minimum estimate of the pristine CAMP volume can be given based on assessments of the surface of Paleozoic and Mesozoic basins intruded by CAMP sills or flooded by CAMP lavas. Besides the sedimentary basins, CAMP basalts also occur as dykes in Proterozoic areas. CAMP sills and flows often can be tracked for the entire extension of the basin that hosts them, thus the surface of the basin multiplied by the cumulative thickness of the CAMP products can give their total volume. With this approach, we estimate a volume of about 1.5 million km^3 for the CAMP sills. Due to the lack of published data, this appraisal does not include large sill bodies probably occurring in the sub-surface of the southern USA and in the forested areas of South America (Brazil, Venezuela, Bolivia) and western Africa (Ivory Coast, Ghana, Sierra Leone). The preserved lava flows make up about 0.1 million km^3 within the Triassic-Jurassic basins. The layered intrusions (Kakoulima laccolith in Guinea and the Freetown Layered Complex in Sierra Leone) sum up to ca. 0.03 million km^3. Estimating the total dyke volume is even more difficult, due to the lack of constraints concerning the depth to which these bodies extend. McHone (2003) assumed 50 km depth for dykes with widths ranging between 0.01 and 0.05 km. We were able to sum up a length of 52,300 km of CAMP dykes. Notably, CAMP dykes

can be subdivided into two main types, i.e. isolated extremely long (up to 500 km) and wide (about 200–300 m) dykes or thinner and shorter ones occurring within swarms of tens of dykes.

Considering that the vast majority of CAMP rocks are found as sills and flows with slightly evolved basaltic compositions, requiring some 30–50% fractionation from the parental mantle-derived magma (see below), a volume equivalent to that intruded as sills and erupted as flows must have intruded also into the deep continental crust, possibly at the MOHO (cf., Black and Manga 2017). It is therefore possible to estimate a total volume of CAMP magmas in the neighborhood of 3 million km^3, including those intruded at various levels of the crust and those erupted to the surface.

4.4 Volcanologic Aspects

The physical volcanology of the extrusive products of the CAMP has been investigated in Portugal, Canada, USA, and Morocco (e.g., Puffer and Student 1992; Puffer and Volkert 2001; Martins et al. 2008; Kontak 2008; El Hachimi et al. 2011). These studies focused on the morphology and internal structures of lava flows and their emplacement mechanisms. For the description of the morphology and internal structures of the CAMP lava flows, we followed the terminology and methodology proposed by Self et al. (1997).

The thickest, best preserved and most complete lava flow sequences of the Moroccan CAMP are exposed in the Central High Atlas (Fig. 4.2a, c). Four lava flow fields, emplaced in a subaerial environment, are recognized: the Lower, Intermediate, Upper and Recurrent basalts. The Lower unit is a 55–173 m-thick succession of 2–9 individual flows. The Intermediate basalt (up to 130 m) is also composed of 2–9 individual flows. The Upper basalt (15–76 m-thick) is formed of one or two lava flow units. The Recurrent basalt is formed by one single flow, 5–50 m thick (Fig. 4.2c). These basaltic lava flow fields are separated by thin sedimentary units (siltstones, sandstones, stromatolitic limestones) and paleosols that represent short periods of volcanic quiescence (Marzoli et al. 2017). Compound pahoehoe flows are almost exclusively present in the Lower and Intermediate basalts (Fig. 4.2b), while simple flows dominate the Upper and Recurrent basalts. The larger lobes forming the compound pahoehoe flows display a characteristic three-tiered structure with a thin "basal lava crust", a dense "lava core", and an "upper lava crust". The latter may present "tumuli", "squeeze up" and horizontal "squeeze" structures, whereas the lava core displays segregation structures such as vesicle cylinders, spherical vesicles and vesicle sheets. The simple flows are simple cooling units and can be traced over large distances. They also display a three-tiered structure with a thin basal zone, a dense central zone, and a thick vesicular crust. Segregation structures are rare in the central zone of simple flows. Pillow lavas, displaying radial jointing and glassy rinds, are occasionally found at the base of the Intermediate basalt (Fig. 4.2d) or in the Upper one. The pillows represent subaerial flows that entered small lakes occupying depressions on the volcanic topography.

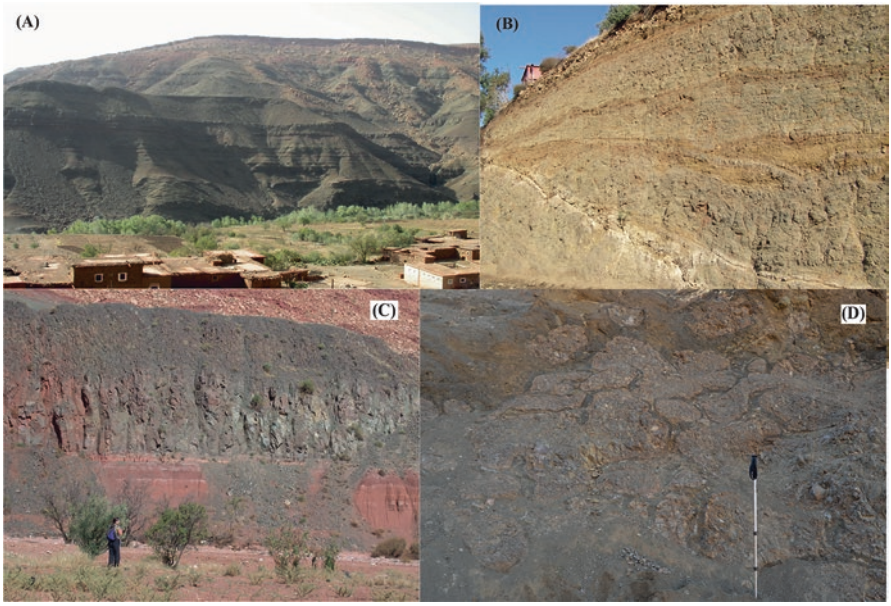

Fig. 4.2 Pictures of CAMP lava flows from Morocco. (**a**) (*top left*) The lava sequence at Tiourjdal (central High Atlas). (**b**) (*top right*) Lava lobes of a compound pahoehoe flow, Intermediate Unit, Middle Atlas. (**c**) (*bottom left*) Simple flow, Recurrent Unit at Agouim, Central High Atlas. (**d**) (*bottom right*) Pillow lava structures, Intermediate Unit, Ait Ourir, Central High Atlas

The CAMP basalt flows of Morocco show clear evidence of internal growth or inflation (e.g. Self et al. 1997). They are similar to the inflated pahoehoe flows in Hawaii (Hon et al. 1994), the Columbia River Basalt Province (e.g. Self et al. 1997), and the Deccan Traps (Bondre et al. 2004). The features indicating endogenous growth are: (a) the three-tiered structural division of the flows; (b) the presence of break-outs, tumuli, and associated structures (squeeze-ups and horizontal squeezes); (c) a vertical distribution of vesicles with the presence of segregation structures.

CAMP basalt flows are preserved in the Saharan Atlas (Algeria), cropping out as three (Lower, Intermediate, Upper) units separated by sedimentary levels. Compared to Morocco, their thickness is considerably reduced (down to 5 m, 2–3 m and 5 m, respectively; Meddah et al. 2007, 2017).

The CAMP volcanic products of the Algarve (southern Portugal) include subaerial lava flows, pyroclastic deposits and peperites, and their contemporaneous sedimentation is dominated by mudstones and conglomerates, often containing volcanic fragments (Martins et al. 2008). The thickness of the preserved volcanosedimentary pile is 30–50 m. Five to eight pahoehoe lava flows are present in the most complete sections. The CAMP lava flows of the Algarve basin are simple flows.

In Nova Scotia, Canada, three lava members were defined for the North Mountain Basalt flows (Kontak 2008): (i) East Ferry; (ii) Margaretsville; and (iii) Brier Island.

The lower and upper members are massive flows with pervasive joint development on varying scales; the most notable difference between the two is the presence of pegmatite layering in the oldest East Ferry member, whereas segregation pipes are locally present in the youngest Brier Island member. Although neither of these flows contains internal features like the sheet lobe flows of the Margaretsville member, they are nevertheless considered to reflect products of inflation (Kontak 2008). These large flows are the products of single sustained effusive events, while numerous, shorter duration effusive events are reflected in the thinner sheet lobe flows of the Margaretsville member. Thus, the East Ferry and Brier Island members are simple flows, whereas the Margaretsville member is a compound flow.

Studies on the physical volcanology of different Continental Flood Basalt (CFB) provinces indicate that they do not have a simple "layer-cake stratigraphy", but rather that they display complex internal and external architectures governed by the volume of individual eruptions, the location and abundance of volcanic centres, and the evolution of the centres through time (e.g., Jerram and Widdowson 2005). In the Moroccan CAMP, "compound pahoehoe flows" are found almost exclusively at the bottom of the volcanic pile, while "simple flows" dominate the Upper and Recurrent basalts. In contrast, the Nova Scotia basaltic flows show alternating simple, compound, and again simple flows. In Portugal and the USA, all subaerial lava flows are simple pahoehoe flows (the Orange Mt. and Talcott flows are mostly sub-aqueous pillow lava flows). Compound flows are characteristic of near-vent settings in active basaltic systems and, by analogy, are likely to represent vent proximity when found in a prehistoric succession. In contrast, simple flows, where each individual thick a'a or pahoehoe flow represents an eruptive event, are commonly found at distal locations (Lesher et al. 1999). In general, the architecture of most, if not all, of the CFB provinces reveals that, like for the Moroccan CAMP, compound pahoehoe flows were followed in time by flows with a simple sheet-like geometry, indicating a fundamental temporal change in the emplacement of flows (e.g., Jerram and Widdowson 2005). It appears that flood basalt volcanism initially starts out at relatively low effusion rate, with low-volume eruptions that gradually accelerate to high effusion rate, with high volume eruptions. This must reflect a common gradual increase of magma production rates pointing to similar magma generation processes associated with the origin of other CFBs throughout the world.

4.5 Age of CAMP Basalts

The age of the CAMP has been investigated since the early 1970s, when the first K-Ar measurements from dykes and intrusions in Morocco (Hailwood and Mitchell 1971) and Liberia (Dalrymple et al. 1975) suggested that widespread magmatic activity was associated with the breakup of Pangaea and the opening of the Atlantic Ocean at ca. 190 Ma. Since then, the advent of the $^{40}Ar/^{39}Ar$ technique on carefully picked plagioclase feldspars using single collector machines enabled a significant improvement in the accuracy and precision of the dated CAMP samples, with

uncertainties in the range of ±1–2 Ma (2σ) attainable for a given sample (e.g. Jourdan et al. 2009; Marzoli et al. 2011). Furthermore, the $^{40}Ar/^{39}Ar$ technique includes a quality assessment of an age date with its age spectrum and inverse isochron allowing screening of accurate emplacement ages from apparent error-ages perturbed by geological events (e.g., alteration; Verati and Jourdan 2014). Thanks to those features, the number and reliability of CAMP $^{40}Ar/^{39}Ar$ ages increased dramatically though the 1990s to the present day (e.g. Sebai et al. 1991; Baksi and Archibald 1997; Deckart et al. 1997; Marzoli et al. 1999, 2004, 2011; Hames et al. 2000; Knight et al. 2004; Verati et al. 2005, 2007; Beutel et al. 2005; Nomade et al. 2007; Jourdan et al. 2009; Merle et al. 2011).

In concert with the increase in accuracy and precision of the CAMP ages, the estimated duration of the CAMP event decreased to around 10 Ma. Most of the ages fall between 200 and 202 Ma, suggesting that most of the volume of the province was emplaced at ~201 Ma (Fig. 4.3). However, the accuracy of these $^{40}Ar/^{39}Ar$ ages still suffers from the small concentrations of potassium in the Ca-rich plagioclase derived from basaltic rocks, and the propensity of basalts for weathering and alteration with the consequence that (1) the eruptions of some completely altered formations are impossible to date with this technique and (2) due to the relatively low age precision, the effect of alteration on a given age may remain undetected. The most up-to-date compilations of $^{40}Ar/^{39}Ar$ data which are filtered for suspect analyses include >80 ages (Marzoli et al. 2011 and the dataset therein). Using only the most robust data, various geochronological trends have been postulated, such as a north to south age progression (Jourdan et al. 2009) and early onset of magmatism in Africa relative to the rest of the province (Nomade et al. 2007). Although the north-south age progression remains speculative without more precise data, the early onset of magmatism in North Africa is supported both by geochemical and paleomagnetic records (Bertrand et al. 1982; Deenen et al. 2010; Marzoli et al. 2004; Knight et al. 2004; Dal Corso et al. 2014). $^{40}Ar/^{39}Ar$ ages highlight that prolonged, though volumetrically minor activity continued until about 192 Ma, i.e. through the Hettangian stage into the Sinemurian stage. Such prolonged activity has been recognized also in other LIPs, such as the Karoo (Jourdan et al. 2008).

More recently, the U-Pb technique on zircon and baddeleyite has been applied to some of the sills, dykes, intrusives and lava flows of the CAMP (Schoene et al. 2010; Blackburn et al. 2013; Davies et al. 2017). Two sills and a basalt flow from the eastern USA and Canada were dated using this technique in the 1990s with a precision similar to the $^{40}Ar/^{39}Ar$ ages (Dunning and Hodych 1990; Hodych and Dunning 1992). With the development of single-zircon analysis, the chemical abrasion technique, and finally the EARTHTIME initiative which created and calibrated a double U-double Pb spike solution for interlaboratory use (Condon et al. 2015), the reproducibility and accuracy of U-Pb ages has improved to the level that weighted mean ages with uncertainties of <0.05% of the actual age now are routinely possible throughout geologic time (e.g., Wotzlaw et al. 2014). A compilation of the recent U-Pb ages from the CAMP is shown in Fig. 4.3 and is compared to the filtered $^{40}Ar/^{39}Ar$ dataset. It is immediately apparent that the U-Pb ages form a much

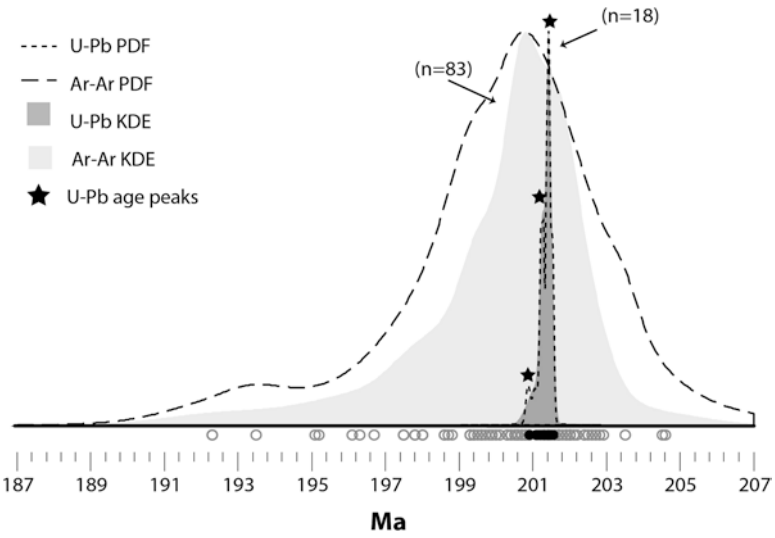

Fig. 4.3 Probability density functions (PDFs) and Kernel density estimates (KDEs) of the $^{40}Ar/^{39}Ar$ and U-Pb ages from the CAMP. The $^{40}Ar/^{39}Ar$ plateau ages are from the compilation of Marzoli et al. (2011). The U-Pb zircon ages are from Blackburn et al. (2013) and Davies et al. (2017), and the North Mountain Basalt age from Schoene et al. (2010), which has been updated with the new spike calibration by Wotzlaw et al. (2014). The black stars mark the pulses of magmatism suggested by the PDF and KDE (Vermeesch 2012) of the U-Pb data

tighter cluster in time than the $^{40}Ar/^{39}Ar$ ages. The U-Pb ages cover most of the geographic extent of the CAMP however there are four times less U-Pb ages than $^{40}Ar/^{39}Ar$ ages and therefore the U-Pb ages may be biased. Nonetheless, the short duration of CAMP magmatism suggested by the U-Pb data is likely to be real, and is consistent with the durations of other LIP's also dated to high precision (Burgess et al. 2015; Schoene et al. 2015; Renne et al. 2015; Parisio et al. 2016) indicating that peak activity of LIP events typically lasts ~1 Ma. Nevertheless, the selection of the rocks used for U-Pb dating is restricted to rocks that contain zircon (usually found in Si-rich late crystallized pockets in intrusive and much more rarely volcanic rocks) and this introduces a sample bias in the age coverage achievable for a given province.

As far as geochronology is concerned, the next challenge is to obtain precise yet widespread age coverage of CAMP. Precisely dating plagioclase at the ±0.1–0.2% level using the $^{40}Ar/^{39}Ar$ technique is now possible using the latest generation of multicollection noble gas mass spectrometers, so it will be interesting to test the distribution of ages on a province scale using this new approach.

In summary, modern geochronological studies of the CAMP indicate that this province likely formed relatively rapidly (ca. 1 Ma for the peak activity), even if the total global activity persisted much longer, probably from the Rhaetian to the Sinemurian, i.e. for some 10 Ma. The CAMP may have been emplaced as distinct pulses (see Fig. 4.3). Of great relevance for the global effect of the CAMP is its

relation to the end-Triassic mass extinction. While both of these events yield indistinguishable radio-isotopic ages, the exact relationship is stratigraphically rather complex and is discussed in detail in Sect. 4.8.

4.6 Rock Compositions

4.6.1 Major and Trace Element Composition and Volcano-Stratigraphic Correlations

Almost all CAMP rocks can be classified as basalts or as basaltic andesites (SiO_2 in the range 48–55 wt.%) in the TAS diagram (Fig. 4.4). A few of the over 500 analyzed samples are relatively enriched in $Na_2O + K_2O$ and can be described as moderately alkaline basic rocks, however all these apparently alkaline samples are altered and display a LOI (loss on ignition) higher than 2 wt.%. The few samples that are relatively enriched in SiO_2 (55–60 wt.%) are altered and are classified as andesites, while rocks with high SiO_2 (>60 wt.%) are found only as segregation sheets within thick flows, sills, and dykes (e.g., Shirley 1987; Puffer et al. 2009; Block et al. 2015). It thus can be concluded that the CAMP is entirely characterized by basaltic and basaltic andesite magmas, while high-Si and alkaline rocks are essentially absent.

Basaltic CAMP rocks are also generally evolved (not primitive) in composition, i.e. their MgO (general range 12–2 wt.%, with most samples yielding between 10 and 4 wt.% MgO), Ni and Cr concentrations are lower than in primitive basaltic melts. Mg-rich intrusive rocks from Kakoulima and Freetown are in fact cumulates of mafic minerals (olivine mainly) and thus cannot be considered as representative of a primitive magmatic liquid. In contrast, some porphyritic dykes from the south-eastern USA and lava flows from Morocco, which have high Mg# up to 70 ($Mg\# = 100 \times Mg/(Mg + F^{e2+})$, where Fe^{2+} is 87% of total Fe), as well as high Cr and Ni (up to 1400 ppm), may be considered to be near-primitive. These primitive compositions only represent 2–3% of the several hundreds of analyzed rocks.

As has been observed in other LIPs such as the Paranà-Etendeka or the Karoo (De Min et al. 2003; Jourdan et al. 2007), CAMP rocks include both low- and high-Ti varieties (Fig. 4.5). However, CAMP rocks with $TiO_2 < 2.0$ wt.% represent the vast majority of the lithologies in the province (more than 90% of the analyzed rocks). Phosphorous (P_2O_5) contents are positively correlated with TiO_2, while incompatible trace elements such as La, Nb, Zr or incompatible element ratios such as La/Yb reach similar values in both low- and high-Ti basalts. In general, incompatible trace element contents of CAMP basalts are similar to those found in some other CFB provinces. Typically, they show depletion in high field strength elements (HFSE), such as Nb or Ta, and enrichment in large ion lithophile elements (LILE). Such geochemical features are frequently encountered in within-plate continental basalts that interacted with the continental lithosphere (crust or mantle), e.g., those

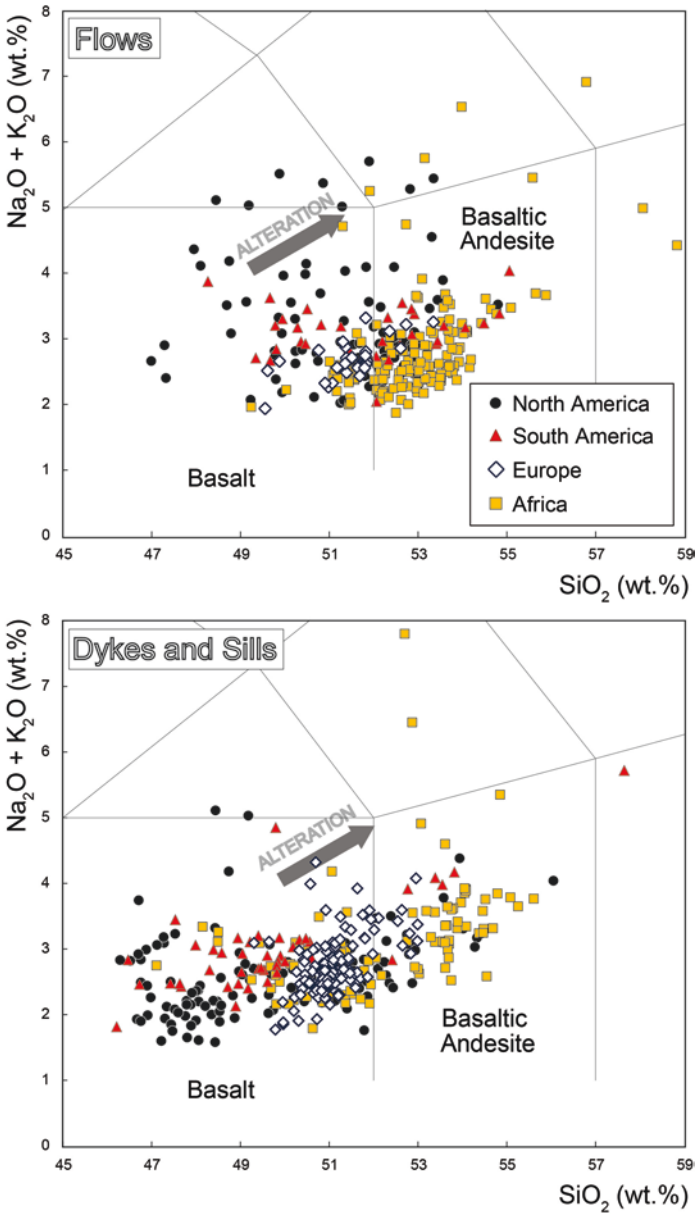

Fig. 4.4 Total-Alkali-Silica classification diagram (after Le Bas et al. 1986) for CAMP intrusive (dykes and sills) and effusive rocks. Data are taken from: Alibert (1985), Azambre et al. (1981, 1987), Bellieni et al. (1990), Bertrand (1987, 1991), Bertrand et al. (1982, 2014), Block et al. (2015), Callegaro et al. (2013, 2014a), Caroff et al. (1995), Cebriá et al. (2003), Chabou et al. (2010), Deckart et al. (2005), De Min et al. (2003), Dostal and Dupuy (1984), Dupuy et al. (1988), Fodor et al. (1990), Grossman et al. (1991), Jourdan et al. (2003), Klein et al. (2013), Kontak (2008), Martins et al. (2008), Marzoli et al. (2004), 458, 130–140 (2017), Merle et al. (2011, 2014), Nomade et al. (2002), Philpotts and Reichenbach (1985), Philpotts and Asher (1993), Philpotts (1998), Puffer et al. (1982, 2009), Puffer (1992), Shirley (1987), Tollo and Gottfried (1992), Verati et al. (2005), Whalen et al. (2015), Weigand and Ragland (1970)

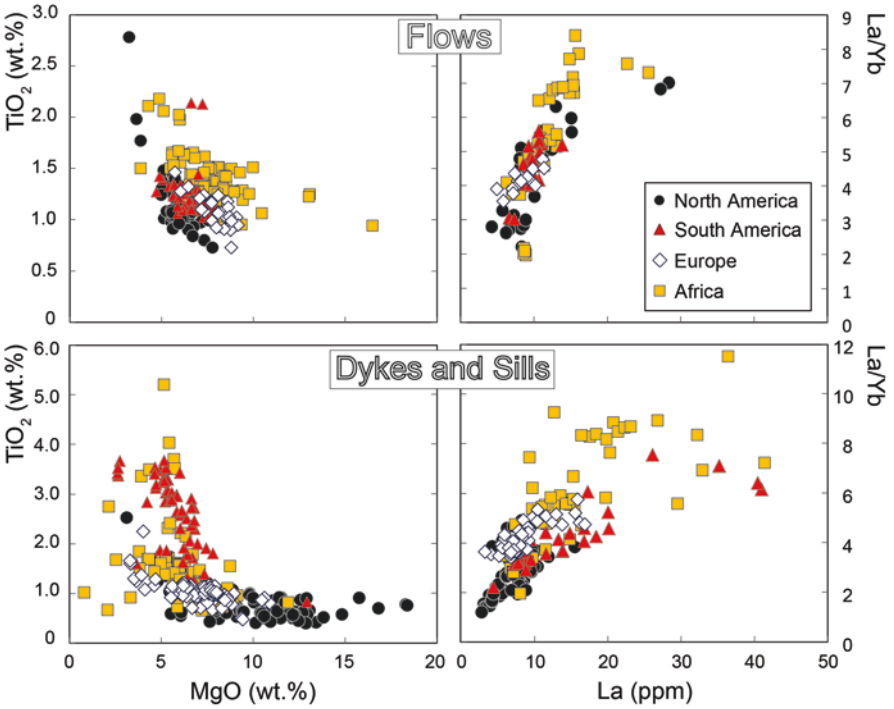

Fig. 4.5 Major (wt.%) and trace element (ppm) compositions of CAMP intrusive and effusive rocks. Same data sources as for Fig. 4.4

of the Paranà-Etendeka, Karoo or Siberian Traps CFB provinces (Jourdan et al. 2007; Peate 1997; Puffer 2001), but are not typical of Mid Ocean Ridge basalts (MORB) or Ocean Island basalts (OIB).

In general whole-rock compositions are rather uniform across the entire CAMP region even though moderate space- and time-related variations can be recognized. In particular, high-Ti rocks are known from a restricted area of the CAMP, i.e., northeastern South America (Amapà and Tocantins states of Brazil; Surinam and French Guiana) as well as Liberia and Sierra Leone in western Africa (Dupuy et al. 1988; Bertrand 1991; Chalokwu 2001; Nomade et al. 2002; De Min et al. 2003; Deckart et al. 2005; Merle et al. 2011). Interestingly, the areas where high-Ti basalts occur are all close to cratonic regions, i.e. the Man shield in Africa and the Amazonian craton in South America.

In volcanic sequences from Morocco and eastern North America, TiO_2, P_2O_5, and other incompatible elements such as Nb, Zr, La or trace element ratios such as La/Yb show clear up-section trends. This allows definition of geochemical groups (or Units) for CAMP lava-piles hosted in Moroccan and North American sedimentary basins (e.g., Weigand and Ragland 1970; Bertrand et al. 1982; Weems et al. 2016). In general, incompatible elements show a progressive decrease in the first part of the sequence (e.g. from Lower to Upper basalts in Morocco and from Talcott or Orange

Mt. to Holyoke or Preakness) basalt in the Newark Supergroup basins), while the youngest flows in these basins (Recurrent basalt in Morocco and Hampden or Hook Mt. basalt in the Newark Supergroup basins) are further enriched in Ti and Zr but display low La and the lowest La/Yb ratio.

It is intriguing that lava flows with nearly identical composition can be traced in the northeastern USA (from Virginia to Connecticut), in central-northern Morocco (from the High Atlas to the Mediterranean coast), and also from western Morocco to the Saharan Atlas in Algeria, respectively, for distances of hundreds of km. Likewise, in these areas the time-related evolution of magma compositions seems identical. Based on these observations, attempts have been made to correlate CAMP lava flows within and among continents (Bertrand and Coffrant 1977; Manspeizer et al. 1978; Marzoli et al. 2004). When Moroccan and North American flows are compared, close similarity is observed between the Intermediate and Upper Units in Morocco and the Talcott (or Orange Mt.) basalts in Newark Supergroup basins, as well as between the Moroccan Recurrent Unit and the Newark Supergroup Hampden (or Hook Mt.) basalts. Notably, flows of the Moroccan Lower Unit are unique because they yield relatively high TiO_2 (ca. 1.4 wt.%) and La/Yb unlike any lava flow from the USA Newark Supergroup basins. On the other hand, the Newark Supergroup Holyoke (or Preakness) -type basalt also displays its own peculiar composition, for example in terms of quite low TiO_2 (<1.0 wt.%) and relatively low La/Yb. In Algeria, lava flows from the Saharan Atlas display a close similarity in composition with those from Moroccan Lower, Intermediate and Upper units, while those from the Bechar basin are similar to the Lower unit. Lava flows from Portugal are almost identical in composition to the Moroccan Intermediate-Upper and the Newark Supergroup Talcott (or Orange Mt.) basalts. The North Mt. basalts from Nova Scotia in Canada have compositions mostly resembling the Moroccan Intermediate-type while only a few Canadian samples overlap the composition of the Moroccan Lower Unit basalts. Most lava flows from South America (Brazil and Bolivia) are geochemically similar to the Moroccan Intermediate basalts, with only two flows from Tocantins State in Brazil being high in TiO_2 (ca. 2.1 wt.%).

Dykes and sills show a significantly larger geochemical variability than the flows, at least in terms of major element contents (Figs. 4.4 and 4.5). For example, many dykes from the southeastern USA have high MgO contents (10–13 wt.%) and low TiO_2 (about 0.5 wt.%). There are also several dyke samples from Europe and Africa that yielded low MgO (2–5 wt.%). Most notably, high TiO_2 contents (> 2.1 wt.%) are found in dykes and sills from Africa and South America only. Despite this local geochemical variability, most dykes and sills from throughout the CAMP show compositions comparable to the Moroccan-Intermediate-Upper lava flows. This is the case for the dykes and sills from Europe, most dykes and sills in northeastern North America, in northwestern Africa (e.g., Mali, Morocco, Algeria), and in South America. Some intrusive rocks also have compositions similar to the Moroccan-Lower group, e.g. dykes and sills from Mali. Finally, a few dykes and sills from Morocco, Algeria (Tindouf basin), and the northeastern USA resemble the Recurrent-Hampden flows.

Direct comparison between volcanic and intrusive rocks can be tricky, since the latter may not represent original magmatic liquid compositions. An example of an incorrect correlation between sills and lava flows was reported in Blackburn et al. (2013). There, the Butner (or Durham) sill from North Carolina was considered as geochemically equivalent to the Hampden and Hook Mt. flow of the Newark Supergroup. While samples from the two sites overlap for some geochemical parameters (e.g., the Y/Nb ratio cited by those authors), they differ for others, for example in terms of MgO (9 vs. 5 wt.% in the Butner sill vs. the Hampden and Hook Mt. flows, respectively) or TiO_2 (0.5 vs. 1.5 wt.%; Tollo and Gottfried 1992; Callegaro et al. 2013; Merle et al. 2014). Moreover, the Butner sill and the Hampden (or Hook Mt.) flows display markedly different Sr-Nd-Pb isotopic compositions (see below) that exclude derivation from the same magma.

4.6.2 Sr-Nd-Pb-Os Isotopic Compositions of CAMP Rocks

Sr-Nd-Pb-Os isotopic compositions of CAMP rocks (back-calculated to the emplacement age of ca. 201 Ma) show a wide range of values (Fig. 4.6). However, most low-Ti basalts (flows and intrusions) display high $^{87}Sr/^{86}Sr_i$ (0.705–0.707), low $^{143}Nd/^{144}Nd_i$ (0.5125–0.5122, epsilon-Nd +1 to −4), and high radiogenic Pb isotopic compositions ($^{206}Pb/^{204}Pb_i$ = 18.2–18.7; $^{207}Pb/^{204}Pb_i$ = 15.59–15-67; $^{208}Pb/^{204}Pb_i$ = 38.00–38.50). They yield slightly less radiogenic Sr-Pb isotopic compositions than the EM-2 mantle end-member of Zindler and Hart (1986). Such compositions are typical, for example, for all African, European, and North American CAMP lava flows, as well as for all low-Ti lava flows from South America. An exception is represented by the dykes from southeastern USA (Pegram 1990; Callegaro et al. 2013; Whalen et al. 2015), whose Sr-Nd-Pb isotopic compositions plot between the DMM, EM-1 and EM-2 mantle end-members. High-Ti flows from South America and high-Ti intrusive rocks from South America and Africa display the most depleted Sr-Nd isotopic compositions as well as relatively low Pb isotopic ratios (De Min et al. 2003; Deckart et al. 2005; Merle et al. 2011; Klein et al. 2013), reaching compositions comparable to those of Mesozoic Atlantic Mid-Ocean-Ridge-basalts (Janney and Castillo 2001). Notably, high-Ti CAMP basalts do not overlap in their Sr-Nd-Pb isotopic compositions with the low-Ti ones.

$^{187}Os/^{188}Os_i$ compositions of most analyzed CAMP rocks (from Europe, North America, and South America), including both high- and low-Ti groups, range from 0.125 to 0.145 (Merle et al. 2011, 2014; Callegaro et al. 2013, 2014a). Such range of values is common for mantle-derived magmas that are not significantly contaminated by old continental crust. Only a few samples show $^{187}Os/^{188}Os_i$ considerably higher than 0.150, and these are all evolved rocks with low MgO, Ni, and Os and thus prone to modification of their initial magmatic isotopic signature by crustal assimilation. If samples with less than 0.03 ppb of Os are excluded, more than two-thirds of these rocks have initial $^{187}Os/^{188}Os$ ratios in the range of 0.126–0.136, which are compositions similar to or slightly more radiogenic than the Primitive

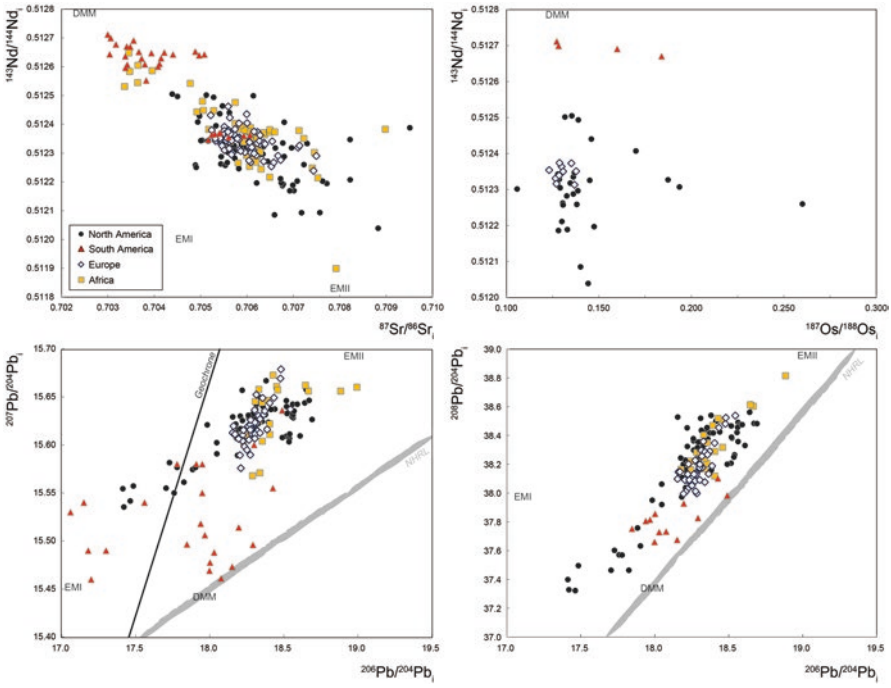

Fig. 4.6 $^{87}Sr/^{86}Sr_i$, $^{143}Nd/^{144}Nd_i$, $^{206}Pb/^{204}Pb_i$, $^{207}Pb/^{204}Pb_i$ and $^{187}Os/^{188}Os_i$ compositions of CAMP rocks. NHRL is the northern hemisphere reference line (Hart 1984). Data sources: Alibert (1985), Bertrand et al. (2014), Block et al. (2015), Callegaro et al. (2013, 2014a), Cebriá et al. (2003), Deckart et al. (2005), De Min et al. (2003), Dupuy et al. (1988), Jourdan et al. (2003), Klein et al. (2013), Merle et al. (2011, 2014), Verati et al. (2005), Whalen et al. (2015)

Upper Mantle (Meisel et al. 2001) or asthenospheric melts (Gannoun et al. 2007; Dale et al. 2009). CAMP samples with $^{187}Os/^{188}Os_i$ ratios less than 0.125, which are typical of ancient sub-continental mantle lithosphere, are extremely rare.

4.6.3 Main Magma Types and Intra- and Inter-Continental Correlations

Combined major and trace element and Sr-Nd-Pb isotopic compositions suggest that CAMP basaltic lava flows, dykes and sills can be subdivided into six main groups (Fig. 4.7):

1. The Tiourjdal group (named for the locality in Morocco where these flows are thickest) includes the Lower Unit flows from Morocco and Algeria, a few lava flows from Canada (from the East Ferry member) and some dykes and sills from northern Africa (e.g., Mali, Taoudenni basin). This group has TiO_2 in the range 1.3–1.5 wt.% for 6–8 wt.% MgO and La/Yb 6–8.

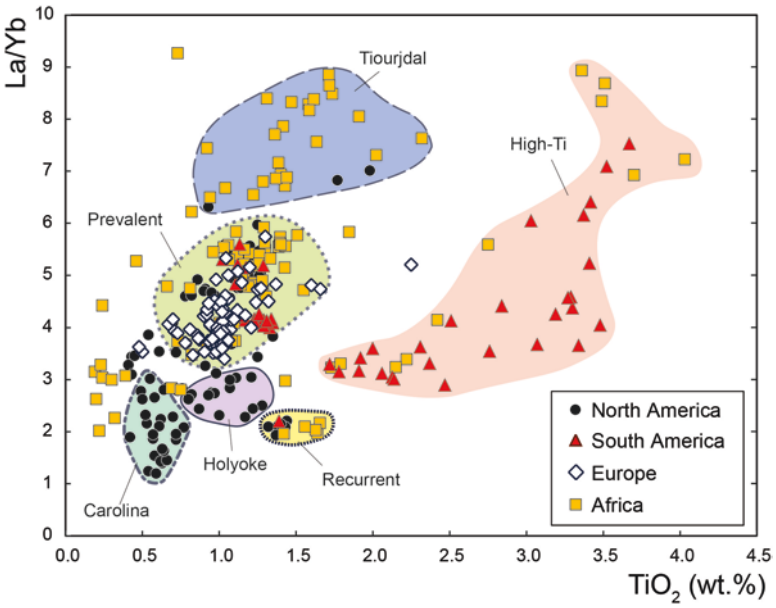

Fig. 4.7 TiO_2 (wt.%) vs. La/Yb of CAMP samples (data sources as for Fig. 4.4). The six geochemical groups described in the text are outlined. Most of the outliers are coarse-grained intrusive rocks, for example samples from the Kakoulima layered intrusion

2. The Prevalent-CAMP group (TiO_2 about 1.0–1.3 wt.% for MgO 6–8 wt.%; La/Yb = 3.5–5.5), which includes the Moroccan Intermediate and Upper Unit flows, all flows from Portugal, the Talcott (or Orange Mt.) basalts from the Newark Supergroup from Virginia to Connecticut (cf. Weems et al. 2016), most of the Canadian flows, and nearly all South American flows. Most dykes and sills from Africa and some from northeastern North America (New England to Canada) also belong to this group.
3. The Holyoke group (TiO_2 0.8–1.0 wt.%, for MgO 6–8 wt.%; La/Yb = 2.5–3.5), which includes the Holyoke flows and the stratigraphically equivalent flows from Massachusetts to Virginia in the USA and their feeder dykes and sills.
4. The Recurrent group (TiO_2 1.4–1.6 wt.%, for MgO about 4–6 wt.%; La/Yb about 2.0), which is composed of the Moroccan Recurrent lava flows and the Hook Mt. and Hampden basaltic flows from the northeastern USA and their feeder dykes. Also some dykes and sills from Algeria (Tindouf basin) belong to this group.
5. The Carolina group formed by dykes from the southeastern USA (Georgia to Virginia), which are generally rich in MgO (up to 13 wt.%) and low in TiO_2 (about 0.5 wt.%) and La/Yb (1–3).
6. The high-Ti group ($TiO_2 > 2.1$ wt.%, 3–8 wt.% MgO, La/Yb 2–8), which includes high-Ti flows from the Parnaiba basin (Brazil) and the high-Ti dykes from Liberia, French Guiana, Suriname, and north-eastern Brazil, as well as the Freetown Layered Intrusion in Sierra Leone (Callegaro et al. 2017).

The Tiourjdal, Prevalent-CAMP, and Holyoke groups have almost identical Sr-Nd-Pb-Os isotopic compositions. The Recurrent group has slightly lower $^{87}Sr/^{86}Sr$ and slightly higher $^{143}Nd/^{144}Nd$ and $^{206}Pb/^{204}Pb$, compared to the previously cited groups. The Carolina group has more depleted Sr-Nd isotopic compositions than the previous groups, and also displays a large scatter of Pb isotopic compositions ranging from compositions similar to those of the other low-Ti basalts to substantially lower $^{206}Pb/^{204}Pb$. The High-Ti group shows variable Sr-Nd-Pb isotopic ratios, which are in general closer to typical depleted mantle values compared to all of the low-Ti groups and broadly similar to the isotopic compositions of Jurassic Atlantic Mid-Ocean Ridge basalts (Janney and Castillo 2001).

Given the above definitions of the main geochemical groups of CAMP basalts, one main observation is that the Prevalent-CAMP group is nearly ubiquitous in the entire LIP, from France to Bolivia. All other geochemical groups are geographically limited. The Tiourjdal group occurs in a rather restricted area of northwestern Africa, from Mali to Algeria and Morocco at the northern margin of the West African Craton (Fig. 4.1). The Carolina group has an even more limited area and is found only in the southeastern USA occurring as dykes only. The Holyoke group is limited to the Newark Supergroup from Massachusetts to Virginia. The Recurrent group is represented by volumetrically very scarce flows in the northeastern USA and northwestern Africa (Morocco and Algeria). The High-Ti group occurs only in the areas surrounding the southeastern margin of the West African Craton (Liberia and Sierra Leone) and the northeastern margin of the Amazonian craton in northeastern South America.

4.7 Origin of CAMP Magmas

4.7.1 Fractional Crystallization

A large majority of the analyzed CAMP basalts have MgO ranging between 14 and 3 wt.%. This range is even more restricted when only the lava flows are considered (MgO generally 9–5 wt.%). Therefore, very few, if any, of these rocks may be considered as representing a primary mantle-derived melt composition. The lack or scarcity of high-Mg (i.e. primary) magmas is common also to some other LIPs, such as the Paranà-Etendeka LIP (Peate 1997). In contrast, in other LIPs such as the Deccan Traps, high-Mg picritic compositions are rather common (Melluso et al. 2006). Notably, the presence of high-Mg picritic magmas are considered to be one of the signatures for the involvement of an anomalously hot mantle source, i.e. a mantle-plume in the genesis of LIPs (Campbell and Griffiths 1990).

The majority of CAMP rocks are quite evolved, reflecting some 10–50 wt.% fractional crystallization of primary mantle melts. This can be estimated for example by considering experimentally derived mantle melts as primary magmas and modelling the formation of CAMP basaltic composition with the MELTS code

(Ghiorso and Sack 1995; cf. Callegaro et al. 2013). Even so, evolved rocks such as andesites or dacites are virtually absent. All acid rocks are limited to thin granophyre levels within some sills, dykes, or thick flows, resulting from in-situ differentiation processes within the sill and intrusions (e.g., Philpotts and Reichenbach 1985). In general, the range of differentiation of CAMP magmas is roughly similar to that of MORBs, which suggests that they erupted in a similar extensional tectonic regime (Jennings et al. 2017).

4.7.2 Crustal Assimilation

The enriched Sr-Nd-Pb isotopic composition of most CAMP basalts and of the low-Ti groups, in particular, coupled with depleted Nb and relatively high LILE (such as Rb, Ba) and light REE (such as La) may suggest that CAMP magmas were contaminated by the continental crust assimilated within crustal magma chambers or en-route to the surface. However, the relatively low $^{187}Os/^{188}Os$ ratios of the vast majority of analyzed CAMP basalts argue against any substantial contamination by continental crustal rocks. Modeling of the crustal assimilation process, based either on whole-rock or on mineral compositions, has been attempted by several authors (Dorais and Tubrett 2008; Callegaro et al. 2013, 2014a; Merle et al. 2011, 2014; Marzoli et al. 2014). These results suggest that the maximum amount of assimilated crustal rocks generally does not exceed about 10 wt.% of the primary magma mass. Such relatively low degrees of crustal contamination may shift the pristine isotopic compositions to slightly more enriched compositions, but cannot explain the geochemical difference observed between almost all CAMP samples and basaltic rocks from Atlantic ocean islands (i.e., deep mantle plume products) or present-day Atlantic MORBs (i.e., shallow upper mantle products).

4.7.3 Mantle Source of CAMP Basalts

Given that the enriched Sr-Nd-Pb isotopic ratios and the only mildly radiogenic $^{187}Os/^{188}Os$ of CAMP basalts can only partially be explained by crustal contamination, an enriched mantle component has to be envisaged for the source of CAMP magmas. According to most authors the enriched signature of the CAMP mantle source is provided by recycled continental crustal material (e.g., Pegram 1990; Puffer 2001; Dorais and Tubrett 2008; Callegaro et al. 2013, 2014a; Merle et al. 2011, 2014; Whalen et al. 2015). This material may have been introduced into the shallow mantle during Paleozoic or Proterozoic subduction events. In particular, most low-Ti basalts (except the Carolina group) plot quite close to the EM-II mantle pole. For these basalts, the above cited authors suggested an origin from a mantle that was enriched by subducted continental sediments. Small amounts of this enriched material within the mantle source would explain the enriched Sr-Nd-Pb

isotopic compositions of CAMP basalts, leaving their Os isotopic ratios largely unchanged due to the much higher Os content in the ambient peridotitic mantle compared to the recycled sediments. In order to explain the low-radiogenic Pb isotopic composition observed for some CAMP dykes of the Carolina group, Callegaro et al. (2013) and Whalen et al. (2015) have suggested the involvement of subducted lower continental crust material in their mantle source.

The peculiar isotopic composition of the High-Ti group basalts requires a distinct mantle source component. According to Deckart et al. (2005), Merle et al. (2011) and Callegaro et al. (2017), the composition of high-Ti CAMP basalts from northeastern South America trending towards the EM-I mantle pole would require contributions from enriched portions of the sub-continental lithospheric mantle, possibly metasomatic veins. Given the paleo-proximity of the cratonic areas of the West African and Amazonian shields, it may be envisaged that enriched veins may occur in the continental lithospheric mantle, in particular within the deep cratonic keels (Callegaro et al. 2017).

In general, what emerges from the geochemical studies of CAMP basalts is the involvement of enriched components of variable nature, i.e. recycled upper or lower crustal materials or lithospheric mantle veins that are significant at a local scale. However, for all CAMP basalts the volumetrically dominant component seems to be the depleted upper mantle or DMM. CAMP basalts appear to derive from such depleted mantle that was variously enriched by 2–5% subducted material (Callegaro et al. 2013, 2014a; Merle et al. 2014). In this sense, it is interesting to note the similarity of some CAMP basalts, in particular the high-Ti group, with Mesozoic mid-ocean-ridge basalts from the Central Atlantic Ocean (Janney and Castillo 2001). Therefore, the geochemical signatures of CAMP basalts, which are characterized by a dominant depleted component with subordinate enrichments of variable origins, point to a shallow mantle source. If this interpretation of the geochemical data for the CAMP is correct, deep mantle (i.e. mantle-plume) involvement seems unnecessary or at least is undetectable within the available geochemical data.

The geochemical and isotopic data do not explain, however, why the shallow mantle should melt. CAMP basalts are tholeiitic magmas and require melting degrees of about 5–10% of a peridotitic mantle probably located at the base of the continental lithosphere, i.e. at about 60–100 km depth. For such conditions, an excess mantle temperature of about 50–100 °C is required compared to the "normal" ambient mantle temperature, i.e. that necessary to produce normal MORB (Herzberg et al. 2007). This excess temperature may have been slightly lower in the presence of enriched components, such as those described above, which would lower the melting temperature (solidus) of the peridotites. According to Herzberg and Gazel (2009), Callegaro et al. (2013), and Whalen et al. (2015) the mantle potential temperature for the CAMP source, calculated from its olivine compositions, would have been about 1430–1480 °C. Such a temperature value is slightly higher than that of the ambient upper mantle (about 1300–1400 °C), but significantly lower than temperatures obtained with the same method for plume-related LIPs (> 1500 °C and up to 1600 °C; Herzberg and Gazel 2009).

Such moderately hot mantle temperatures may be the expression of a weak mantle plume or may be explained by alternative models such as edge-driven convection (McHone et al. 2005) or heat incubation underneath the Pangaea super-continent (Coltice et al. 2007; Hole 2015). Torsvik et al. (2010) suggested that the origin of CAMP and other LIPs is linked to mantle structures rooted at the core-mantle boundary called Large Low Shear Velocity Provinces (LLSVPs). One LLSVP is apparently located under the African plate and the other one under the Pacific plate (Burke et al. 2008). In this scenario, the steep sides of the LLSVPs generate plumes, channeling hot lower mantle portions that find their surface expression in LIP and kimberlitic volcanism. Plate reconstructions show that at 200 Ma (Ruiz-Martínez et al. 2012) part of the CAMP coincided spatially with the margin of the African LLSVP. This LLSVP margin, from which the main flux of deep-mantle magma would be expected (Torsvik et al. 2010), was probably located under a belt going from NE-Brazil to NW-Africa and NE North America. While we cannot exclude a thermal role played by the African LLSVP, we do not see any clear evidence of a geochemical lower mantle component in CAMP basalts, whose geochemical compositions seem more consistent with derivation from the depleted upper mantle overprinted by variously enriched lithospheric signatures.

Globally, we conclude that none of these models fully explains the peculiar features of the CAMP, in particular its enormous surface area extent, coupled with its relatively low volume of basalts erupted near-synchronously over about 10 million km^2. The mantle plume model is not compatible with the relatively low temperatures calculated from olivine compositions, and geochemical data similarly do not require a deep mantle contribution. At the same time however, the shallow mantle melting models (such as edge-driven convection or thermal incubation) do not justify a sudden onset of voluminous melt production over distances of thousands of kilometers. Therefore, the origin of the CAMP is certainly not fully explained at present.

4.8 CAMP and the End-Triassic Extinction

As previously mentioned, the emplacement of CAMP basalts has an age that is very similar to that of the end-Triassic mass extinction (ETE), suggesting a cause-and-effect relationship between the two phenomena. The ETE is one of the "big five" biological crises that occurred during the Phanerozoic (e.g., Raup and Sepkoski 1982; Tanner et al. 2004). The environmental and biological crisis at the end of the Triassic is synchronous with a major disturbance of the global carbon cycle, a characteristic that is also observed during other LIP-related events (Wignall 2001). This carbon cycle perturbation is recorded in the geological record as multiple sharp negative carbon isotope excursions (CIEs). These excursions suggest sudden inputs of huge quantities of ^{13}C-depleted CO_2 into the ocean–atmosphere system. The exact origin of this CO_2, either from dissociation of ocean floor clathrates, thermogenic production of methane from the sediments, or volcanic CO_2, is still debated (e.g. Hesselbo et al. 2002; Ruhl et al. 2011; Paris et al. 2016; Bachan and Payne 2016).

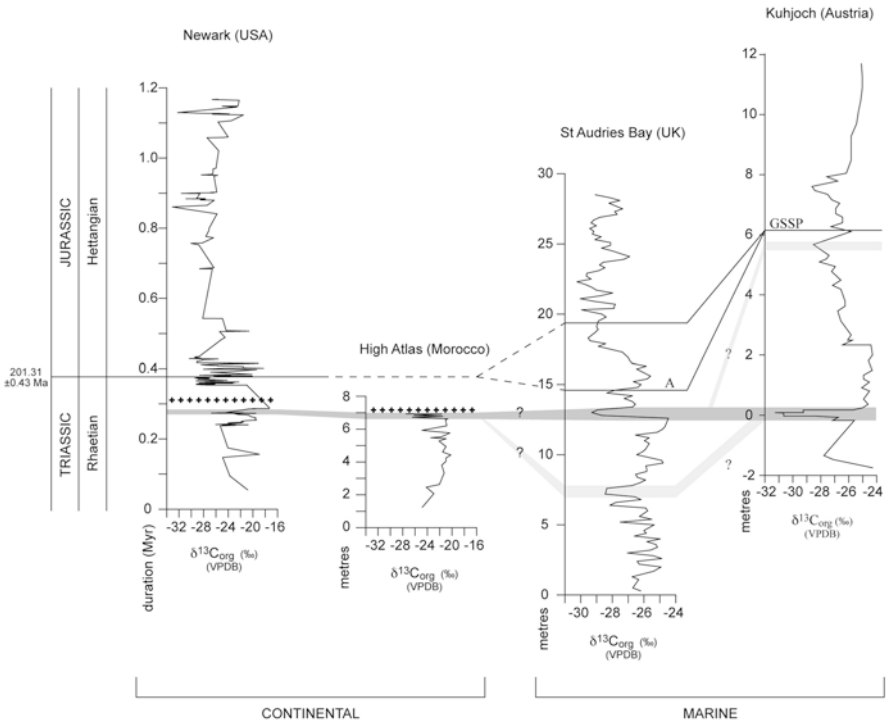

Fig. 4.8 Carbon-isotope stratigraphy across the Triassic-Jurassic boundary (modified after Dal Corso et al. 2014). The correlation between the sections is based on biostratigraphy, magneto-stratigraohy and chemostratigraohy (e.g. Hesselbo et al. 2002; Ruhl et al. 2009; Deenen et al. 2010; Whiteside et al. 2011; Dal Corso et al. 2014). Three major negative carbon-isotope excursions (CIEs) record major disruptions of the carbon cycle associated to the end-Triassic mass extinction (ETME) and the CAMP volcanism. The Global Boundary Stratotype Section and Point (GSSP) of the base of the Hettangian (Jurassic) is placed at Kuhjoch at the level of the first occurrence of the ammonite *Psiloceras spelae* Guex, within the "main" CIE (von Hillebrandt et al. 2007). Based on the ammonoid biostratigraphy and $\delta^{13}C$ data from the New York Canyon section (Nevada, USA), other authors put the Triassic–Jurassic boundary between the "initial" and the "main" CIEs ('A' in St. Audries Bay curve; Guex et al. 2004; Bartolini et al. 2012). In the continental stratigraphic successions of the Newark Basin (USA) and the High Atlas (Morocco) the "initial" negative CIE and associated ETE occur below the first outcropping CAMP basalt. However, mineralogical and geochemical analysis of the sediments underlying the first basalt in Morocco show CAMP volcanism was already active at least from the positive rebound of the "precursor" CIE (Dal Corso et al. 2014). The alternative correlation proposed by Lindstrom et al. (2017) for the end-Triassic events is shown in pale-gray. The little crosses indicate the stratigraphic position of the first CAMP lava flow in the Newark Supergroup (USA) and High Atlas basins (Morocco)

To date, three consecutive negative CIEs (named "precursor", "initial", and "main") have been detected in different end-Triassic stratigraphic successions (Fig. 4.8). The "main" CIE corresponds to the Triassic-Jurassic boundary as it is defined in the Global Boundary Stratotype Section and Point (GSSP) at Kuhjoch, Austria (von Hillebrandt et al. 2007), which is dated at 201.36 ± 0.17 Ma (U-Pb

zircon age; Schoene et al. 2010; Wotzlaw et al. 2014). However, the peak extinction event (ETE) should correspond to the "initial" CIE, estimated at 201.564 ± 0.015 Ma in the Newark basin by Blackburn et al. (2013) and dated at 201.51 ± 0.15 Ma in marine strata from Peru and Nevada (Schoene et al. 2010; Wotzlaw et al. 2014). More recently, Lindström et al. (2017) proposed a new model for the negative CIE succession during the latest Triassic. Consistent with this interpretation, the "precursor" CIE may be correlated with the CIE observed in the sediments at the base of the CAMP lava piles in Morocco and Canada (Deenen et al. 2010, 2011; Dal Corso et al. 2014), while the "initial" CIE may postdate the onset of CAMP volcanism (Lindström et al. 2017).

Radioisotopic ages show that the end-Triassic CAMP volcanism, carbon cycle disruption and mass extinction are geologically synchronous (Schoene et al. 2010; Marzoli et al. 2011; Blackburn et al. 2013; Davies et al. 2017). For example, the U–Pb ages for the Messejana dyke (Spain), Tarabuco sill (Bolivia) and an Amazonas sill (Brazil) (201.585 ± 0.034 Ma, 201.612 ± 0.046 Ma, 201.525 ± 0.065 Ma, respectively) are equal to the age (201.564 ± 0.015 Ma) of the ETE in the Newark Basin (Davies et al. 2017). Moreover, Dal Corso et al. (2014) demonstrated that CAMP volcanism was active when the first two negative CIEs occurred. Therefore, after years of debate (cf. Marzoli et al. 2004, 2008; Whiteside et al. 2007, 2008), there now is general consensus in the scientific community that volcanic gases released by CAMP likely were the trigger mechanisms of the end-Triassic mass extinction and accompanying carbon cycle disruption (e.g., Hesselbo et al. 2002; Marzoli et al. 2004; Guex et al. 2004; Pálfy et al. 2007; Deenen et al. 2010; Whiteside et al. 2011; Ruhl et al. 2011; Schaller et al. 2011; Lindström et al. 2012, 2017; Dal Corso et al. 2014; Callegaro et al. 2014b).

4.8.1 Volcanogenic Gases from the CAMP

Transfer of CAMP volcanogenic gases (chiefly water vapor, carbon and sulfur dioxide and halogens) into the ocean and the atmosphere has been invoked as the mechanism responsible for the end-Triassic climate change and mass extinction (Wignall 2001; Ernst and Youbi 2017). A causal relationship is substantiated by the temporal overlap between these events (e.g. Marzoli et al. 2011; Blackburn et al. 2013; Davies et al. 2017), as well as by the existence of modern examples of volcanically forced climate changes following big eruptions (Robock 2000).

High quality data for S, H, C, F and Cl are difficult to obtain for old, largely degassed, and slightly altered basaltic rocks such as those of the CAMP. Based on whole-rock data reported in Grossman et al. (1991), McHone (2003) estimated a total degassed volume of 5.19×10^{12} tons CO_2, 2.31×10^{12} tons S and 1.11×10^{12} tons F from the CAMP. However, it should be considered that volatile elements are controlled also by secondary processes. Moreover, initial degassing of volatiles may commence within crustal magma chambers and in particular within shallow intrusions such as those analyzed by Grossman et al. (1991).

Callegaro et al. (2014b) calculated that CAMP basalts were able to release up to 8 Mt. per km^3 of volcanogenic SO_2 by analyzing sulfur concentration in clinopyroxenes and combining it with a cpx/melt sulfur partition coefficient. These data show that CAMP melts are close to sulfide saturation, i.e., ca. 2000 ppm for near-anhydrous basaltic melts at an oxygen fugacity around the FMQ buffer. Sulfur content in CAMP magmas is similar to that found by Self et al. (2008) for Deccan Traps magmatism. Schmidt et al. (2015) modeled the atmospheric response to volcanogenic injections of sulfur and demonstrated that sulfur loads compatible with Deccan estimations would only cause environmental stress if eruption rates were sustained and long-lived.

Reliable carbon data are lacking for the CAMP and, to our knowledge, for all basaltic LIPs. Indirect evidence for the amount and isotopic composition of carbon emitted during the latest Triassic emplacement of the CAMP comes from the previously described CIEs and from proxy data. Stomatal index data and carbon-isotope analysis of pedogenic carbonates show doubling of pCO_2 levels at the Triassic–Jurassic boundary (McElwain et al. 1999; Schaller et al. 2011). What appears from interpretation of the CIEs, however, is that the source of volatiles degassed during the CAMP event was not merely "juvenile". Indeed, in paleoclimatic reconstructions volcanic CO_2 is considered to be insufficiently depleted to cause a negative CIE given that its carbon-isotope signature ($\delta^{13}C$) is generally fixed at $-6 \pm 2‰$ on the basis of present-time observations on asthenosphere-derived basalts from, for example, Hawaii, Iceland and Ethiopia (Gerlach and Taylor 1990; Barry et al. 2014). Therefore, the need for additional depleted carbon to be introduced into the system forced paleoclimatologists to invoke alternative reservoirs with strongly negative $\delta^{13}C$ signatures, i.e., ocean floor methane hydrates ($\delta^{13}C$ ca. -60‰; Dickens et al. 1995) and methane thermally released by organic-rich sediments ($\delta^{13}C$ ca. -35 to $-50‰$; Svensen et al. 2004). Clathrate destabilization is hard to prove with independent proxies in the geological record. Release of thermogenic methane might instead have been initiated by intrusion of voluminous CAMP sills into the organic-rich sediments of the Amazon and Solimoes basins in Brazil (De Min et al. 2003).

4.9 Conclusions

The Central Atlantic magmatic province (CAMP) was emplaced over an area of more than 10 million km^2 at ca. 201 Ma and its peak magmatic activity had a short duration of about 1 Ma or less. Magmas were erupted as short-lived pulses and formed lava fields flowing over distances of hundreds of km. Lava flows are either of compound or of simple pahoehoe type, the latter perhaps reflecting a higher magma eruption rate. The total volume of intruded and erupted magmas can be conservatively estimated at 3 million km^3, the vast majority being represented by intrusive rocks, e.g. dykes, sills and layered intrusions. Deep crustal intrusions should correspond in volume to about 50–100% of the volume of the shallow intrusions and the erupted products.

Nearly all CAMP rocks are basalts or basaltic andesites, while acid rocks are limited to small layers or pockets within the larger flows and shallow intrusions. Primitive magmatic rocks are absent and MgO contents ranging between about 10 and 5 wt.% for the vast majority of analyzed basalts indicate that CAMP rocks are the result of about 30–50% fractionation from parental mantle-derived melts. The rock geochemical compositions and, in particular, their relatively low radiogenic Os isotopic compositions allow for a maximum of 10% crustal assimilation. Together these characteristics indicate that the enriched trace element and Sr-Nd-Pb isotopic compositions demand some contribution from enriched mantle components, superimposed on a dominantly depleted mantle source. It is proposed here that the mantle source enrichment happened either through shallow recycling of subducted continental sediments or lower crust or through assimilation of enriched material hosted within the sub-continental lithospheric mantle.

Six main groups of rock compositions can be defined based on trace element and isotopic compositions. Of these, five are low-Ti basalts. One of these groups (the Prevalent CAMP) is found nearly everywhere within the CAMP. The other four low-Ti and the only high-Ti group are geographically limited to restricted areas of the LIP, arguing in favor of a strong regional control on magma composition, possibly related to the age, thickness, and composition of the local lithospheric mantle.

CAMP magmatism straddled the Triassic-Jurassic boundary and most likely triggered the end-Triassic mass extinction and global climate changes. This is supported by high pre-eruptive sulfur contents inferred for CAMP magmas based on their clinopyroxene S contents. A simple magmatic origin of the increased end-Triassic CO_2 is not easy to constrain but seems inconsistent with the carbon isotopic composition of CAMP basalts, assuming that these were similar to present-day basalts.

Overall, the state of the art of CAMP-related literature reveals that some aspects of this LIP are well studied and understood, whereas other aspects still need to be investigated. Sampling in remote areas of South America and Africa is still limited, as are borehole data from intrusive CAMP rocks from the southern USA and the Brazilian basins. Available high quality $^{40}Ar/^{39}Ar$ geochronological data are sufficiently numerous to allow statistical definition of the main peak of magmatism; U-Pb ages are mostly limited to intrusive rocks. The geochemical dataset is abundant for low-Ti rocks, but very limited for the High-Ti group, over represented for the USA and European CAMP and scarce for the African and South American CAMP. CAMP magmatism straddled the Triassic-Jurassic boundary and quite possibly triggered the end-Triassic mass extinction and global climate changes.

Acknowledgements This work is a contribution to the following collaborative research projects: (i) PICS, CNRS (France)-CNRST (Morocco) to HB and NY, (ii) CNRi (Italy)-CNRST (Morocco) to AM and NY and (iii) FCT (Portugal)-CNRST (Morocco) to NY, (iv) PRIN (20158A9CBM) CARIPARO (Eccellenza 2008) and Progetto di Ateneo 2013 (Università di Padova, CPDA132295/13; all to AM). JDC acknowledges the Hanse-Wissenschaftskolleg Institute for Advanced Study (Delmenhorst, Germany) for financial support. We acknowledge also the precious help from numerous colleagues all around the world, including: P.R. Renne, E.M. Piccirillo,

M. Ernesto, A. De Min, G. Bellieni, S. Cirilli, E. Vasconcellos, T. Sempere, R. Weems, L. Tanner, J. Puffer, G. McHone, D. Kontak, M. Bensalah, F. Medina, A. Mahmoudi, C. Chabou, A. Meddah, L. Martins, J. Madeira, J. Mata, and C.M. Meyzen. R. Weems and J. Puffer provided very detailed and helpful reviews, which substantially improved the original text. This work would not have been possible without the careful editorial work of L. Tanner.

References

Alibert C (1985) A Sr-Nd isotope and REE study of Late Triassic dolerites from the Pyrenees (France) and the Messejana Dyke (Spain and Portugal). Ear Planet Sci Lett 73:81–90

Azambre B, Rossy M, Elloy R (1981) Les dolérites triasiques (ophites) des Pyrénées: données nouvelles fournies par les sondages pétroliers en Aquitaine. Bull Societè Géol France 23:263–269

Azambre B, Rossy M, Lago M (1987) Caractéristiques pétrologiques des dolérites tholéiitiques d'âge triasique (ophites) du domaine pyrénéen. Bull Minéralog 110:379–396

Bachan A, Payne C (2016) Modelling the impact of pulsed CAMP volcanism on pCO_2 and $\delta^{13}C$ across the Triassic–Jurassic transition. Geol Mag 153:252–270

Baksi AK, Archibald DA (1997) Mesozoic igneous activity in the Maranhão province, northern Brazil, $^{40}Ar/^{39}Ar$ evidence for separate episodes of basaltic magmatism. Ear Planet Sci Lett 151:139–153

Barry PH, Hilton DR, Füri E, Halldórsson SA, Grönvold K (2014) Carbon isotope and abundance systematics of Icelandic geothermal gases, fluids and subglacial basalts with implications for mantle plume-related CO_2 fluxes. Geochim Cosmochim Acta 134:74–99

Bartolini A, Guex J, Spangenberg J, Taylor D, Schoene B, Schaltegger U, Atudorei V (2012) Disentangling the Hettangian carbon isotope record: implications for the aftermath of the end-Triassic mass extinction. Geochem Geophys Geosyst 13:1–11

Bellieni G, Piccirillo EM, Cavazzini G, Petrini R, Comin-Chiaramonti P, Nardy AJR, Civetta L, Melfi AJ, Zantedeschi P (1990) Low- and High-TiO_2 Mesozoic tholeiitic magmatism of the Maranhao basin (NE-Brazil): K/Ar age, geochemistry, petrology, isotope characteristics and relationships with Mesozoic low- and high-TiO_2 flood basalts of the Paraná basin (SE-Brazil). N Jb Mineralog Abh 162:1–33

Bertrand H (1987) Le magmatisme tholéiitique continental de la marge ibérique, précurseur de l'ouverture de l'Atlantique central: les dolérites du dyke de Messejana-Plasencia (Portugal-Espagne). C R Acad Sci 304:215–220

Bertrand H (1991) The Mesozoic tholeiitic province of Northwest Africa: A volcanotectonic record of the early opening of Central Atlantic. In: Kampuzu AB, Lulaba RT (eds) Magmatism in extensional settings: The Phanerozoic African Plate, Springer, pp. 147–188

Bertrand H, Coffrant D (1977) Geochemistry of tholeiites from eastern North American margin; correlation with Morocco. Contr Min Petrol 63:65–74

Bertrand H, Dostal J, Dupuy C (1982) Geochemistry of early Mesozoic tholeiites from Morocco. Ear Planet Sci Lett 58:225–239

Bertrand H, Fornari M, Marzoli A, García-Duarte R, Sempere T (2014) The Central Atlantic Magmatic Province extends into Bolivia. Lithos 188:33–43

Beutel EK, Nomade S, Fronabarger AK, Renne PR (2005) Pangaea's complex breakup: A new rapidly changing stress field model. Ear Planet Sci Lett 236:471–485

Black BA, Manga M (2017) Volatiles and the tempo of flood basalt magmatism. Ear Planet Sci Lett 458:130–140

Blackburn TJ, Olsen PE, Bowring SA, Mclean NM, Kent DV, Puffer J, McHone G, Rasbury ET, Et-Touhami M (2013) Zircon U-Pb geochronology links the end-Triassic extinction with the Central Atlantic Magmatic Province. Science 340:941–945

Block KA, Steiner JC, Puffer JH, Jones KM, Goldstein SL (2015) Evolution of late stage differentiates in the Palisades Sill, New York and New Jersey. Lithos 230:121–132

Bondre NR, Duraiswami RA, Dole G (2004) Morphology and emplacement of flows from the Deccan volcanic province, India. Bull Volcanol 66:29–45

Burgess SD, Bowring SA, Fleming TH, Elliot DH (2015) High-precision geochronology links the Ferrar large igneous province with early-Jurassic ocean anoxia and biotic crisis. Ear Planet Sci Lett 415:90–99

Burke K, Steinberger B, Torsvik TH, Smethurst MA (2008) Plume generation zones at the margins of large low shear velocity provinces on the core-mantle boundary. Ear Planet Sci Lett 265:49–60

Callegaro S, Rigo M, Chiaradia M, Marzoli A (2012) Latest Triassic marine Sr isotopic variations, possible causes and implications. Terra Nova 24:130–135

Callegaro S, Marzoli A, Bertrand H, Chiaradia M, Reisberg L, Meyzen C, Bellieni G, Weems RE, Merl R (2013) Upper and lower crust recycling in the source of CAMP basaltic dykes from southeastern North America. Ear Planet Sci Lett 376:186–199

Callegaro S, Rapaille C, Marzoli A, Bertrand H, Chiaradia M, Reisberg L, Bellieni G, Martin L, Madeira J, Mata J, Youbi N, De Min A, Azevedo MR, Bensalah MK (2014a) Enriched mantle source for the Central Atlantic magmatic province: new supporting evidence from Southwestern Europe. Lithos 188:15–32

Callegaro S, Baker DF, DeMin A, Marzoli A, Geraki K, Nestola F, Viti C (2014b) Microanalyses link sulfur from large igneous provinces and Mesozoic mass extinctions. Geol 42:895–898

Callegaro S, Marzoli A, Bertrand H, Blichert-Toft J, Reisberg L, Cavazzini G, Jourdan F, Davies J, Parisio L, Bouchet RAP, Schaltegger U, Chiaradia M (2017) Geochemical constraints provided by the Freetown Layered Complex (Sierra Leone) on the origin of high-Ti tholeiitic CAMP magmas. J Petrol (in press)

Campbell IH, Griffiths RW (1990) Implications of mantle plume structure for the evolution of flood basalts. Ear Planet Sci Lett 99:79–93

Caroff M, Bellon H, Chauris L, Carro J-P, Chevrier S, Gardinier A, Cotton J, Le Moan Y, Neidhart Y (1995) Magmatisme fissural triasico-liasique dans l'ouest du Masif armoricain (France): pétrologie, géochimie, age et modalités de la mise en place. Can J Ear Sci 32:1921–1936

Cebriá JM, López-Ruiz J, Doblas M, Martíns LT, Munha J (2003) Geochemistry of the Early Jurassic Messejana-Plasencia dyke (Portugal-Spain); Implications on the origin of the Central Atlantic Magmatic Province. J Petrol 44:547–568

Chabou MC, Bertrand H, Sebaï A (2010) Geochemistry of the Central Atlantic Magmatic Province (CAMP) in south-western Algeria. J Afr Ear Sci 58:211–219

Chalokwu CI (2001) Petrology of the Freetown layered complex, Sierra Leone: part II. Magma evolution and crystallization conditions. J Afr Ear Sci 32:519–554

Coffin MF, Eldholm O (1994) Large Igneous Provinces: crustal structure, dimensions and external consequences. Rev Geophys 32:1–36

Cohen AS, Coe AL (2002) New geochemical evidence for the onset of volcanism in the Central Atlantic magmatic province and environmental change at the Triassic-Jurassic boundary. Geol 30:267–270

Coltice N, Phillips BR, Bertrand H, Ricard Y, Rey P (2007) Global warming of the mantle at the origin of flood basalts over supercontinents. Geol 35:391–394

Condon DJ, Schoene B, McLean NM, Bowring SA, Parrish RR (2015) Metrology and traceability of U–Pb isotope dilution geochronology (EARTHTIME Tracer Calibration Part I). Geochim Cosmochim Acta 164:464–480

Dal Corso J, Marzoli A, Tateo F, Jenkyns HC, Bertrand H, Youbi N, Mahmoudi A, Font E, Buratti N, Cirilli S (2014) The dawn of CAMP volcanism and its bearing on the end-Triassic carbon cycle disruption. J Geol Soc Lond 171:153–164

Dale CW, Pearson DG, Starkey NA, Stuart FM, Ellam RM, Larsen LM, Fitton JG, Macpherson CG (2009) Osmium isotopes in Baffin Island and West Greenland picrites: Implications for the $^{187}Os/^{188}Os$ composition of the convecting mantle and the nature of high 3He/4He mantle. Ear Planet Sci Lett 278:267–277

Dalrymple GB, Grommé CS, White RW (1975) Potassium-Argon Age and Paleomagnetism of Diabase Dikes in Liberia: Initiation of Central Atlantic Rifting. Geol Soc Am Bull 86:399–411

Davies JHFL, Marzoli A, Bertrand H, Youbi N, Ernesto M, Schaltegger U (2017) End-Triassic mass extinction started by intrusive CAMP activity. Nat Commun. https://doi.org/10.1038/NCOMMS15596

Deckart K, Féraud G, Bertrand H (1997) Age of Jurassic continental tholeiites of French Guyana, Surinam and Guinea: Implications for the initial opening of the Central Atlantic Ocean. Ear Planet Sci Lett 150:205–220

Deckart K, Bertrand H, Liégeois J-P (2005) Geochemistry and Sr, Nd, Pb isotopic composition of the Central Atlantic magmatic Province (CAMP) in Guyana and Guinea. Lithos 82:289–314

Deenen MHL, Ruhl M, Bonis NR, Krijgsman W, Kuerschner WN, Reitsma M, van Bergen MJ (2010) A new chronology for the end-Triassic mass extinction. Ear Planet Sci Lett 291:113–125

Deenen MHL, Krijgsman W, Ruhl M (2011) The quest for chron E23r at Partridge Island, Bay of Fundy, Canada: CAMP emplacement postdates the end-Triassic extinction event at the North American craton. Can J Ear Sci 48:1282–1291

De Min A, Piccirillo EM, Marzoli A, Bellieni G, Renne PR, Ernesto M, Marques LS (2003) The Central Atlantic Magmatic Province (CAMP) in Brazil: Petrology, geochemistry, 40Ar/39Ar ages, paleomagnetism and geodynamic implications. In: Hames W, McHone G, Renne PR, Ruppel C (eds), The Central Atlantic magmatic province: Insights from fragments of Pangaea. Am Geophys Un Geophys Monogr 136:91–128

Dickens GR, O'Neill JR, Rea DK, Owen RM (1995) Dissociation of oceanic methane hydrate as a cause of the carbon isotope excursion at the end of the Paleocene. Paleoceanogr 10:965–971

Dorais MJ, Tubrett M (2008) Identification of a subduction zone component in the Higganum dike, Central Atlantic Magmatic Province: A LA-ICPMS study of clinopyroxene with implications for flood basalt petrogenesis. Geochem Geophys Geosyst 9:Q10005. https://doi.org/10.1029/2008GC002079

Dostal J, Dupuy C (1984) Geochemistry of the North Mountain Basalts (Nova Scotia, Canada). Chem Geol 45:245–261

Dunning GR, Hodych JP (1990) U-Pb zircon and baddeleyite ages for the Palisades and Gettysburg sills of the northeastern United States: Implications for the age of the Triassic-Jurassic boundary. Geol 18:795–798

Dupuy C, Marsh J, Dostal J, Michard A, Testa S (1988) Asthenospheric sources for Mesozoic dolerites from Liberia (Africa): Trace element and isotopic evidence. Ear Planet Sci Lett 87:100–110

El Hachimi H, Youbi N, Madeira J, Bensalah MK, Martins L, Mata J, Bertrand H, Marzoli A, Medina F, Munhá J, Bellieni J, Mahmoudi A, Ben Abbou M, Assafar H (2011) Morphology, internal architecture, and emplacement mechanisms of lava flows from the Central Atlantic Magmatic Province (CAMP) of Argana basin (Morocco). In: Van Hinsbergen DJJ, Buiter S, Torsvik TH, Gaina C, Webb S (eds), Out of Africa—a synopsis of 3.8 Ga of Earth history. Geol Soc Lond Spec Publ 357:167–193

Ernst RE, Youbi N (2017) How Large Igneous Provinces affect global climate, sometimes cause mass extinctions, and represent natural markers in the geological record. Palaeogeogr Palaeoclimatol Palaeoecol 478:30–52

Fodor RV, Sial AN, Mukasa SB, Mckee EH (1990) Petrology. isotope characteristics and K-Ar ages of the Maranhão, northern Brazil, Mesozoic basalt province. Contrib Mineral Petrol 104:555–567

Gannoun A, Burton KW, Parkinson IJ, Alard O, Schiano P, Thomas LE (2007) The scale and origin of the osmium isotope variations in mid-ocean ridge basalts. Ear Planet Sci Lett 259:541–556

Gerlach TM, Taylor BE (1990) Carbon isotope constraints on degassing of carbon dioxide from Kilauea Volcano. Geochim Cosmochim Acta 54:2051–2058

Ghiorso MS, Sack RO (1995) Chemical transfer in magmatic processes IV. A revised and internally consistent thermodynamic model for the interpolation and extrapolation of liquid-solid equilibria in magmatic systems at elevated temperatures and pressures. Contrib Mineral Petrol 119:197–212

Grossman JN, Gottfried D, Froelich J (1991) Geochemical data for Jurassic diabase associated with early Mesozoic rift basins in the eastern United States. US Geol Surv Open File Rep 91–322

Guex J, Bartolini A, Atudorei V, Taylor D (2004) High-resolution ammonite and carbon isotope stratigraphy across the Triassic–Jurassic boundary at New York Canyon (Nevada). Ear Planet Sci Lett 225:29–41

Hailwood EA, Mitchell JG (1971) Palaeomagnetism and radiometric dating results from Jurassic intrusions in South Morocco. Geophys J Roy Astronom Soc 24:351–364

Hames WE, Renne PR, Ruppel C (2000) New evidence for geologically instantaneous emplacement of earliest Jurassic Central Atlantic magmatic province basalts on the North American margin. Geol 28:859–862

Hart SR (1984) A large-scale isotope anomaly in the Southern Hemisphere mantle. Nat 309:753–757

Herzberg C, Gazel E (2009) Petrological evidence for secular cooling in mantle plumes. Nat 458:619–622

Herzberg C, Asimow PD, Arndt N, Niu Y, Lesher CM, Fitton JG, Cheadle MJ, Saunders AD (2007) Temperatures in ambient mantle and plumes: Constraints from basalts, picrites, and komatiites. Geochem Geophys Geosyst 8:Q02006. https://doi.org/10.1029/2006GC001390

Hesselbo SP, Robinson SA, Surlyk F, Piasecki S (2002) Terrestrial and marine mass extinction at the Triassic-Jurassic boundary synchronized with initiation of massive volcanism. Geol 30:251–254

Hill RI (1991) Starting plumes and continental break-up. Ear Planet Sci Lett 104:398–416

Hodych JP, Dunning GR (1992) Did the Manicouagan impact trigger end-of-Triassic mass extinction? Geol 20:51–54

Hole MJ (2015) The generation of continental flood basalts by decompression melting of internally heated mantle. Geol 43:311–314

Hon K, Kauahikaua J, Denlinger R, Mackay K (1994) Emplacement and inflation of pahoehoe sheet flows: observations and measurements of active lava flows on Kilauea Volcano, Hawaii. Geol Soc Am Bull 106:351–370

Janney PE, Castillo PR (2001) Geochemistry of the oldest Atlantic oceanic crust suggests mantle plume involvement in the early history of the Central Atlantic Ocean. Ear Planet Sci Lett 192:291–302

Jennings ES, Gibson SA, Maclennan J, Heinonen IS (2017) Deep mixing of mantle melts beneath continental flood basalt provinces: Constraints from olivine-hosted melt inclusions in primitive magmas. Geochim Cosmochim Acta 196:36–57

Jerram DA, Widdowson M (2005) The anatomy of Continental Flood Basalt Provinces: geological constraints on the processes and products of flood volcanism. Lithos 79:385–405

Jourdan F, Marzoli A, Bertrand H, Cosca M, Fontignie D (2003) The northernmost CAMP: 40Ar/39Ar Age, Petrology and Sr-Nd-Pb Isotope Geochemistry of the Kerforne Dike, Brittany, France. In: Hames WE, McHone JG, Renne, PR, Ruppel C (eds), The Central Atlantic magmatic province: Insights from fragments of Pangaea. Am Geophys Un Geophys Monogr 136: 209–226

Jourdan F, Bertrand H, Schärer U, Blichert-Toft J, Féraud G, Kampunzu AB (2007) Major and Trace element and Sr, Nd, Hf and Pb isotope compositions of the Karoo Large Igneous Province, Botswana-Zimbabwe: lithosphere vs. mantle plume contribution. J Petrol 48:1043–1077

Jourdan F, Féraud G, Bertrand H, Watkeys MK, Renne PR (2008) The $^{40}Ar/^{39}Ar$ ages of the sill complex of the Karoo large igneous province: Implications for the Pliensbachian-Toarcian climate change. Geochem Geophys Geosyst 9:Q06009

Jourdan F, Marzoli A, Bertrand H, Cirilli S, Tanner LH, Kontak DJ, McHone G, Renne PR, Bellieni G (2009) $^{40}Ar/^{39}Ar$ ages of CAMP in North America: implications for the Triassic-Jurassic boundary and the ^{40}K decay constant bias. Lithos 110:167–180

Klein EL, Angélica RS, Harris C, Jourdan F, Babinski M (2013) Mafic dykes intrusive into Pre-Cambrian rocks of the São Luís cratonic fragment and Gurupi Belt (Parnaíba Province), north–

northeastern Brazil: Geochemistry, Sr–Nd–Pb–O isotopes, $^{40}Ar/^{39}Ar$ geochronology, and relationships to CAMP magmatism. Lithos 172–173:222–242

Knight KB, Nomade S, Renne PR, Marzoli A, Bertrand H, Youbi H (2004) The Central Atlantic Magmatic Province at the Triassic-Jurassic boundary: paleomagnetic and $^{40}Ar/^{39}Ar$ evidence from Morocco for brief, episodic volcanism. Ear Planet Sci Lett 228:143–160

Kontak DJ (2008) On the edge of CAMP: Geology and volcanology of the Jurassic North Mountain Basalt, Nova Scotia. In: Dostal J, Greenough JD, Kontak DJ (eds) Rift-related magmatism. Lithos 101:74–101

Labails C, Olivet JL, Aslanian D, Roest WR (2010) An alternative early opening scenario for the Central Atlantic Ocean. Ear Planet Sci Lett 297:355–368

Le Bas MJ, Le Maitre RW, Streckeisen A, Zanettin B (1986) A chemical classification of volcanic rocks based on the total alkali-silica diagram. J Petrol 27:745–750

Lesher CE, Cashman KV, Mayfield JD (1999) Kinetic controls on crystallization of Tertiary North Atlantic basalt and implications for the emplacement and cooling history of lava at site 989, southeast Greenland rifted margin. In: Larsen HC, Duncan RA, Allan JF, Brooks K (eds). Proc Ocean Drill Program Sci Results 163:135–148

Lindström S, van de Schootbrugge B, Dybkjær K, Pedersen GK, Fiebig J, Nielsen LH, Richoz S (2012) No causal link between terrestrial ecosystem change and methane release during the end-Triassic mass-extinction. Geol 40:531–534

Lindström S, van de Schootbrugge B, Hansen KH, Pedersen GK, Alsen P, Thibault N, Dybkjær K, Bierrum CJ, Nielsen LH (2017) A new correlation of Triassic–Jurassic boundary successions in NW Europe, Nevada and Peru, and the Central Atlantic Magmatic Province: A time-line for the end-Triassic mass extinction. Palaeogeogr Palaeoclimatol Palaeoecol 478:80–102

Manspeizer W, Puffer JH, Cousminer HL (1978) Separation of Morocco and eastern North America: a Triassic-Liassic stratigraphic record. Geol Soc Am Bull 89:901–920

Martins LT, Madeira J, Youbi N, Munhá J, Mata J, Kerrich R (2008) Rift-related magmatism of the Central Atlantic magmatic province in Algarve, Southern Portugal. Lithos 101:102–124

Marzoli A, Renne PR, Piccirillo EM, Ernesto M, Bellieni G, DeMin A (1999) Extensive 200 million years old continental flood basalts from the Central Atlantic Magmatic Province. Sci 248:616–618

Marzoli A, Bertrand H, Knight KB, Cirilli S, Buratti N, Vérati C, Nomade S, Renne PR, Youbi N, Martini R, Allenbach K, Neuwerth R, Rapaille C, Zaninetti L, Bellieni G (2004) Synchrony of the Central Atlantic magmatic province and the Triassic-Jurassic boundary climatic and biotic crisis. Geol 32:973–976

Marzoli A, Bertrand H, Knight K, Cirilli S, Nomade S, Renne P, Vérati C, Youbi N, Martini R, Bellieni G (2008) Comments on "Synchrony between the Central Atlantic magmatic province and the Triassic–Jurassic mass-extinction event?" by Whiteside et al. (2007). Palaeogeogr Palaeoclimatol Palaeoecol 262:189–193

Marzoli A, Jourdan F, Puffer JH, Cuppone T, Tanner LH, Weems RE, Bertrand H, Cirilli S, Bellieni G, De Min A (2011) Timing and duration of the Central Atlantic magmatic province in the Newark and Culpeper basins, eastern USA. Lithos 122:175–188

Marzoli A, Jourdan F, Bussy F, Chiaradia M, Costa F (2014) Petrogenesis of tholeiitic basalts from the Central Atlantic magmatic province as revealed by mineral major and trace elements and Sr isotopes. Lithos 188:44–59

Marzoli A, Davies JHFL, Youbi N, Merle R, Dal Corso J, Dunkley DJ, Fioretti AM, Bellieni G, Medina F, Wotzlaw J-F, McHone G, Font E, Bensalah MK (2017) Proterozoic to Mesozoic evolution of North-West Africa and Peri-Gondwana microplates: Detrital zircon ages from Morocco and Canada. Lithos 278-281:229–239

May PR (1971) Pattern of Triassic-Jurassic diabase dikes around the North Atlantic in the context of pre-drift position of the continents. Geol Soc Am Bull 82:1285–1291

McElwain JC, Beerling DJ, Woodward FI (1999) Fossil plants and global warming at the Triassic–Jurassic boundary. Sci 285:1386–1390

McHone JG (1996) Broad-terrane Jurassic flood basalts across northeastern North America. Geol 24:319–322
McHone JG (2000) Non-plume magmatism and rifting during the opening of the central Atlantic Ocean. Tectonophys 316:287–296
McHone JG (2003) Volatile emissions from Central Atlantic Magmatic Province basalts: mass assumptions and environmental consequences. In: Hames WE, McHone JG, Renne PR, Ruppel C (eds) The Central Atlantic magmatic province: insights from fragments of Pangaea. Am Geophys Un Geophys Monogr 136:241–254
McHone JG, Anderson DL, Beutel EK, Fialko YA (2005) Giant dikes, rifts, flood basalts and plate tectonics: a contention of mantle models. In: Foulger GR, Natland JH, Presnall DC, Anderson DL (eds) Plates, plumes and paradigms. Geol Soc Am Spec Vol 388:401–420
Meddah A, Bertrand H, Elmi S (2007) La province magmatique de l'Atlantique central dans le bassin des Ksour (Atlas saharien, Algérie). Compt Rend Geosci 339:24–30
Meddah A, Bertrand H, Seddiki A, Tabeliouna M (2017) The Triassic-Liassic volcanic sequence and rift evolution in the Saharan Atlas basins (Algeria). Eastward vanishing of the Central Atlantic magmatic province. Geol Acta 15:11–23
Meisel T, Walker RJ, Irving AJ, Lorand J-P (2001) Osmium isotopic compositions of mantle xenoliths: A global perspective. Geochim Cosmochim Acta 65:1311–1323
Melluso L, Mahoney JJ, Dallai L (2006) Mantle sources and crustal input as recorded in high-Mg Deccan Traps basalts of Gujarat (India). Lithos 89:259–274
Merle R, Marzoli A, Bertrand H, Reisberg L, Verati C, Zimmermann C, Chiaradia M, Bellieni G, Ernesto M (2011) $^{40}Ar/^{39}Ar$ ages and Sr-Nd-Pb-Os geochemistry of CAMP tholeiites from Western Maranhão basin (NE Brazil). Lithos 122:137–151
Merle R, Marzoli A, Reisberg L, Bertrand H, Nemchin A, Chiaradia M, Callegaro S, Jourdan F, Bellieni G, Kontak D, Puffer J, McHone JG (2014) Sr, Nd, Pb and Os isotope systematics of CAMP tholeiites from Eastern North America (ENA): Evidence of a subduction-enriched mantle source. J Petrol 55:133–180
Milani EJ, Zalàn PV (1999) An outline of the geology and petroleum systems of the Paleozoic interior basins of South America. Episodes 22:199–205
Montes-Lauar CR, Pacca IG, Melfi AJ, Piccirillo EM, Bellieni G, Petrini R, Rizzieri R (1994) The Anarí and Tapirapuá Jurassic formations, western Brazil; paleomagnetism, geochemistry and geochronology. Ear Planet Sci Lett 128:357–371
Morgan WJ (1983) Hotspot tracks and the early rifting of the Atlantic. Tectonophys 94:123–139
Ndiaye M, Ngom PM, Gorin G, Villeneuve M, Sartori M, Medou J (2016) A new interpretation of the deep-part of Senegal-Mauritanian Basin in the Diourbel-Thies area by integrating seismic, magnetic, gravimetric and borehole data: Implication for petroleum exploration. J Afr Ear Sci 121:330–341
Nomade S, Pouclet A, Chen Y (2002) The French Guyana doleritic dykes: Geochemical evidence of three populations and new data for the Jurassic Central Atlantic magmatic province. J Geodynam 34:595–614
Nomade S, Knight K, Beutel E, Renne PR, Verati C, Feraud G, Marzoli A, Youbi N, Bertrand H (2007) The chronology of CAMP: relevance for the central Atlantic rifting processes and the Triassic-Jurassic biotic crisis. Palaeogeogr Palaeoclimatol Palaeoecol 244:326–344
Oh J, Austin JA Jr, Phillips JD, Coffin MF, Stoffa PL (1995) Seaward-dipping reflectors offshore the southeastern United States: Seismic evidence for extensive volcanism accompanying sequential formation of the Carolina through and Blake Plateau basin. Geol 23:9–12
Pálfy J, Demény A, Haas J, Carter ES, Görög Á, Halász D, Oravecz-Scheffer A, Hetényi M, Márton E, Orchard MJ, Ozsvárt P, Vető I, Zajzon N (2007) Triassic–Jurassic boundary events inferred from integrated stratigraphy of the Csovár section, Hungary. Palaeogeogr Palaeoclimatol Palaeoecol 244:11–33
Paris G, Donnadieu Y, Beaumont V, Fluteau F, Goddéris Y (2016) Geochemical consequences of intense pulse-like degassing during the onset of the Central Atlantic Magmatic Province. Palaeogeogr Palaeoclimatol Palaeoecol 441:74–82

Parisio L, Jourdan F, Marzoli A, Melluso L, Sethna S, Bellieni G (2016) $^{40}Ar/^{39}Ar$ ages of alkaline and tholeiitic rocks from the northern deccan traps: Implications for magmatic processes and the K–Pg boundary. J Geol Soc Lond 173:679–688

Peate DW (1997) The Paraná-Etendeka province. In: Mahoney JJ, Coffin MF (eds) Large igneous provinces: Continental, oceanic, and planetary flood volcanism. Am Geophys Un Geophys Monogr 100:217–246

Pegram WJ (1990) Development of continental lithospheric mantle as reflected in the chemistry of the Mesozoic Appalachian tholeiites, USA. Ear Planet Sci Lett 97:316–331

Philpotts AR (1998) Nature of a flood-basalt-magma reservoir based on the compositional variation in a single flood basalt flow and its feeder dike in the Mesozoic Hartford Basin, Connecticut. Contrib Mineral Petrol 133:69–82

Philpotts AR, Asher PM (1993) Wallrock melting and reaction effects along the Higganum diabase dyke in Connecticut: Contamination of a continental flood basalt feeder. J Petrol 34:1029–1058

Philpotts AR, Reichenbach I (1985) Differentiation of Mesozoic basalts of the Hartford basin, Connecticut. Geol Soc Am Bull 96:1131–1139

Puffer JH (1992) Eastern North American flood basalts in the context of the incipient breakup of Pangaea. In: Puffer JH, Ragland PC (eds) Eastern North American Mesozoic magmatism. Geol Soc Am Spec Pap 268:95–119

Puffer JH (2001) Contrasting high field strength element contents of continental flood basalts from plume versus reactivated-arc sources. Geol 29:675–678

Puffer JH, Student JJ (1992) The volcanic structure and eruptive style of the Watchung Basalts, New Jersey. In: Puffer JH, Ragland PC (eds) Eastern North American Mesozoic magmatism. Geol Soc Am Spec Pap 268:261–279

Puffer JH, Volkert RA (2001) Pegmatoid and gabbroid layers in Jurassic Preakness and Hook Mountain basalts. J Geol 109:585–601

Puffer JH, Geiger FJ, Caamano EJ (1982) The geochemistry of the Mesozoic igneous rocks of Rockland County, New York. Northeast Geol 4:121–130

Puffer JH, Block KA, Steiner JC (2009) Transmission of flood basalts through a shallow crustal sill and the correlations of the sill layers with extrusive flows: the Palisades intrusive system and the basalts of the Newark Basin, New Jersey, USA. J Geol 117:139–155

Raup DM, Sepkoski JJ (1982) Mass Extinctions in the Marine Fossil Record. Sci 215:1501–1503

Renne PR, Mundil R, Balco G, Min K, Ludwig KR (2010) Joint determination of ^{40}K decay constants and $^{40}Ar^*/^{40}K$ for the Fish Canyon sanidine standard, and improved accuracy for $^{40}Ar/^{39}Ar$ geochronology. Geochim Cosmochim Acta 74:5349–5367

Renne PR, Balco G, Ludwig KR, Mundil R, Min K (2011) Response to the comment by W.H. Schwarz et al. on "Joint determination of ^{40}K decay constants and $^{40}Ar^*/^{40}K$ for the Fish Canyon sanidine standard, and improved accuracy for $^{40}Ar/^{39}Ar$ geochronology" by P.R. Renne et al. (2010). Geochim Cosmochim Acta 75:5097–5100

Renne PR, Sprain CJ, Richards MA, Self S, Vanderkluysen L, Pande K (2015) State shift in Deccan volcanism at the Cretaceous-Paleogene boundary, possibly induced by impact. Sci 350:76–78

Robock A (2000) Volcanic eruptions and climate. Rev Geophys 38:191–219

Ruhl M, Kürschner WM, Krystyn L (2009) Triassic–Jurassic organic carbon isotope stratigraphy of key sections in the western Tethys realm (Austria). Ear Planet Sci Lett 281:169–187

Ruhl M, Bonis NR, Reichard GL, Sinninghe Danste JS, Kurschner WM (2011) Atmospheric carbon injection linked to end-Triassic mass extinction. Sci 333:430–434

Ruiz-Martínez VC, Torsvik TH, van Hinsbergen DJJ, Gaina C (2012) Earth at 200 Ma: Global palaeogeography refined from CAMP palaeomagnetic data. Ear Planet Sci Lett 331–332:67–79

Sahabi M, Aslanian D, Olivet JL (2004) A new starting point for the history of the central Atlantic. Compt Rend Geosci 336:1041–1052

Schaller MF, Wright JD, Kent DV (2011) Atmospheric pCO_2 perturbations associated with the Central Atlantic magmatic province. Sci 331:1404–1409

Schmidt A, Skeffington RA, Thordarson T, Self S, Forster PM, Rap A, Ridgwell A, Fowler D, Wilson M, Mann GW (2015) Selective environmental stress from sulphur emitted by continental flood basalt eruptions. Nat Geosci 9:77–82

Schoene B, Guex J, Bartolini A, Schaltegger U, Blackburn TJ (2010) Correlating the end-Triassic mass extinction and flood basalt volcanism at the 100 ka level. Geol 38:387–390

Schoene B, Samperton KM, Eddy MP, Keller G, Adatte T, Bowring SA, Khadri SFR, Gertsch B (2015) U-Pb geochronology of the Deccan Traps and relation to the end-Cretaceous mass extinction. Sci 347:9–12

Sebai A, Féraud G, Bertrand H, Hanes J (1991) $^{40}Ar/^{39}Ar$ dating and geochemistry of tholeiitic magmatism related to the early opening of the Central Atlantic rift. Ear Planet Sci Lett 104:455–472

Self S, Thordarson TH, Keszthelyi L (1997) Emplacement of continental flood basalt lava flows. In: Mahoney JJ, Coffin MF (eds) Large igneous provinces: Continental, oceanic, and planetary flood volcanism. Am Geophys Uni Geophys Monogr Ser 100:381–410

Self S, Blake S, Sharma K, Widdowson M, Sephton S (2008) Sulfur and chlorine in Late Cretaceous Deccan magmas and eruptive gas release. Sci 319:1654–1657

Shirley DN (1987) Differentiation and compaction in the Palisades sill, New Jersey. J Petrol 28:835–865

Svensen H, Planke S, Malthe-Sorenssen A, Jamtveit B, Myklebust R, Rasmussen-Eidem T, Rey SS (2004) Release of methane from a volcanic basin as a mechanism for initial Eocene global warming. Nat 429:542–545

Tanner LH, Lucas SG, Chapman MG (2004) Assessing the record and causes of Late Triassic extinctions. Ear Sci Rev 65:103–139

Tollo RP, Gottfried D (1992) Petrochemistry of Jurassic basalt from eight cores, Newark basin, New Jersey: Implications for the volcanic petrogenesis of the Newark supergroup. In: Puffer JH, Ragland PC (eds) Eastern North American Mesozoic magmatism. Geol Soc Am Spec Pap, vol 268, pp 233–259

Torsvik TH, Burke K, Steinberger B, Webb SJ, Ashwal LD (2010) Diamonds sampled by plumes from the core – mantle boundary. Nat 466:352–355

Verati C, Jourdan F (2014) Modelling effect of sericitization of plagioclase on the K/Ar and Ar/Ar chronometers: implication for dating basaltic rocks and mineral deposits. Geol Soc Lond Spec Publ 378(1):155–174

Verati C, Bertrand H, Féraud G (2005) The farthest record of the Central Atlantic magmatic province into the West Africa craton: Precise $^{40}Ar/^{39}Ar$ dating and geochemistry of Taoudenni basin intrusives (northern Mali). Ear Planet Sci Lett 235:391–407

Verati C, Rapaille C, Féraud G, Marzoli A, Bertrand H, Youbi N (2007) $^{40}Ar/^{39}Ar$ ages and duration of the Central Atlantic Magmatic Province volcanism in Morocco and Portugal and its relation to the Triassic-Jurassic boundary. Palaeogeogr Palaeoclimatol Palaeoecol 244:308–325

Vermeesch P (2012) On the visualization of detrital age distributions. Chem Geol 312–313:190–194

Von Hillebrandt A, Krystin L, Kurschner WM (2007) A candidate GSSP for the base of the Jurassic in the Northern Calcareous Alps (Kuhjoch section, Karwendel Mountains, Tyrol, Austria). ISJS Newslett 34:2–20

Weems RE, Tanner LH, Lucas SG (2016) Synthesis and revision of the lithostratigraphic groups and formations in the Upper Permian?–Lower Jurassic Newark Supergroup of eastern North America. Stratigraphy 13(2):111–153

Weigand PW, Ragland PC (1970) Geochemistry of Mesozoic dolerite dikes from eastern North America. Contrib Mineral Petrol 29:195–214

Whalen L, Gazel E, Vidito C, Puffer J, Bizimis M, Henika W, Caddick MJ (2015) Supercontinental inheritance and its influence on supercontinental breakup: The Central Atlantic magmatic province and the breakup of Pangaea. Geochem Geophys Geosyst 16:3532–3355

Whiteside JH, Olsen PE, Kent DV, Fowell SJ, Et-Touhami M (2007) Synchrony between the Central Atlantic magmatic province and the Triassic–Jurassic mass-extinction event? Palaeogeogr Palaeoclimatol Palaeoecol 244:345–367

Whiteside JH, Olsen PE, Kent DV, Fowell SJ, Et-Touhami M (2008) Synchrony between the Central Atlantic magmatic province and the Triassic–Jurassic mass-extinction event? Reply to comment of Marzoli et al., 2008. Palaeogeogr Palaeoclimatol Palaeoecol 262:194–198

Whiteside JH, Olsen PE, Eglinton T, Brookfield ME, Sambrotto RN (2011) Compound-specific carbon isotopes from Earth's largest flood basalt eruptions directly linked to the end-Triassic mass extinction. Proc Nat Acad Sci 107:6721–6725

Wignall PB (2001) Large igneous provinces and mass extinctions. Ear Sci Rev 53:1–33

Wotzlaw JF, Guex J, Bartolini A, Gallet Y, Krystyn L, McRoberts CA, Taylor D, Schoene B, Schaltegger U (2014) Towards accurate numerical calibration of the Late Triassic: high-precision U–Pb geochronology constraints on the duration of the Rhaetian. Geol 42:571–574

Youbi N, Martíns LT, Munha JM, Ibouh H, Madeira J, Chayeb A, El Boukhari A (2003) The Late Triassic–Early Jurassic volcanism of Morocco and Portugal in the geodynamic framework of the opening of the Central Atlantic ocean. In: Hames WE, McHone JG, Renne PR, Ruppel C (eds), The Central Atlantic magmatic province: Insights from fragments of Pangaea. Am Geophys Un Geophys Monogr 136:179–207

Zindler A, Hart SR (1986) Chemical geodynamics. Ann Rev Ear Planet Sci 14:493–571

Chapter 5
Distal Processes and Effects of Multiple Late Triassic Terrestrial Bolide Impacts: Insights from the Norian Manicouagan Event, Northeastern Quebec, Canada

Michael J. Clutson, David E. Brown, and Lawrence H. Tanner

Abstract The Late Triassic (Carnian to Rhaetian Stages: ca. 237–201 Ma) has a long history of geological research, although controversy remains over the precise definition of key sub-unit boundaries, including those defining the three constituent stages. Within this context, at least five terrestrial bolide impact structures ranging from 9 to 85 km in diameter have been identified at present-day northern latitudes, the proximal remnant crater aspects of which have been studied in increasing detail over the last few decades. The more elusive distal sedimentary expressions of these multi-sized hypervelocity events remain largely unknown, although if preserved, identified and interpreted correctly, may (as precisely dateable event horizons) help to address certain existing stratigraphic uncertainties, particularly pertaining to the (longest) Norian Stage. Detailed absolute age-dating using a range of radioisotopic methods (e.g. U-Pb and $^{40}Ar/^{39}Ar$) currently indicates that at least three of the confirmed Late Triassic impact craters formed prior to commencement of the major Rhaetian Central Atlantic Magmatic Province (CAMP) volcanic episode by several million years. Impact research efforts to date have focused mainly on describing and process modeling the relatively well-preserved largest impact structure, Manicouagan (215.5 Ma; 85 km diameter) located in northeastern Quebec, Canada and, to a lesser extent, the Saint Martin (227.8 Ma; 40 km) and Rochechouart (ca. 207–201 Ma; ca. 23–50 km) structures in central Manitoba, Canada and west-central France respectively. The smaller, subsurface Red Wing structure (ca. 200 Ma; 9 km diameter, ca. 2.5 km burial depth) located in South Dakota, USA, also has attracted significant

M.J. Clutson (✉)
1411 Edward Street, Halifax, NS B3H 3H5, Canada
e-mail: mjclutson3@gmail.com

D.E. Brown
Canada-Nova Scotia Offshore Petroleum Board,
800 TD Centre, 1791 Barrington Street, Halifax, NS B3J 3K9, Canada

L.H. Tanner
Department of Biological and Environmental Sciences, Le Moyne College, 1419 Salt Springs Road, Syracuse, NY 13214, USA

© Springer International Publishing AG 2018

L.H. Tanner (ed.), *The Late Triassic World*, Topics in Geobiology 46,
https://doi.org/10.1007/978-3-319-68009-5_5

economic interest. Unlike the well-documented End Cretaceous Chicxulub impact (66 Ma; ca. 180 Km), attempts to establish a globally significant causal extinction connection between the larger impacts (e.g. Manicouagan and Rochechouart) and Late Triassic marine and terrestrial bioevents, culminating with the 'End Triassic Extinction' (ETE), have essentially proved unsuccessful.

Keywords Bolide • Impact structure • Microtektite • Spherule • Ejecta • Paleoseismology • Paleoearthquake • Synsedimentary deformation • Microfracture • Biotic extinction

5.1 Introduction

5.1.1 Previous Work

The identification, description and interpretation of bolide (asteroid, meteoroid or comet) impact-cratering events on Earth's crust have focused largely on continental intracratonic occurrences, where impact structural preservation potential and recognition are generally considered to be highest (Grieve 2017, Fig. 6). Impact research to date has mostly entailed a series of integrated studies relating to a particular impactor type, size, velocity, target response and timing. As stated by the latter author, impacts typically represent hypervelocity high-energy collisional events resulting in the redistribution, disruption and reprocessing of multiple target lithologies. The constituent factors are generally described as interrelated suites of shock-metamorphic and thermally modified petrofacies, contained within variably preserved surface and subsurface crater configurations (morphometries), ranging from simple to highly complex. Detailed descriptions of impact cratering processes and products, and the diverse traces they have left in the mainly terrestrial geologic record, are provided in French (1998) and Osinski and Pierazzo (2013) respectively. Recently Grieve (2017) presented a comprehensive summary of large-scale impact contributions to Earth history, expressed in geological, environmental and socio-economic terms. On comparatively rare occasions, impact investigations (Glass and Simonson 2013) have extended to characterize the contents and inferred depositional histories of often thin, correlative units ('event horizons') containing first-order distal ejecta, especially sand-grade spherules (Glass and Simonson 2012) and/or detrital shocked quartz and other minerals. This has allowed tentative assessments of potentially global catastrophic paleoenvironmental effects, including associated biotic responses, as discussed in Koeberl and MacLeod (2002), Kring (2007), Racki (2012) and Schedl (2015).

The global locations of 190 confirmed impact structures illustrated in the Earth Impact Database (EID June 2017: www.passc.net/EarthImpactDatabase/Worldmap.html) collectively display a non-random spatial distribution that partly reflects a recognition bias towards Northwest Europe, North America and Australia—as

opposed to an "original random bombardment flux" throughout the geologic timescale (French 1998). Meier and Holm-Alwmark (2017) have further suggested that there is also no current evidence for any periodicity in the ('robustly-dated') impact record. Approximately 50% of the total structures shown are considered understudied based on current research standards (Osinski 2013), with an even higher percentage still requiring reliable age control (Schmieder et al. 2014). Interest in Earth impacts historically has been driven by a combination of crater/impact size and complexity, geologic/economic importance, degree/style of preservation, geographic accessibility and various environmental factors. In addition to the EID mapped occurrences, numerous other (300+), mostly smaller (<6 km diameter) impact structures are estimated probabilistically to exist (Hergarten and Kenkmann 2015). These may also include glacially-constrained target imprints relating, for example, to possibly the last (Wisconsinan) Ice Age (cf. Spooner et al. 2009, 2015) and/or geophysically-defined (inferred) impact structures located within continental polar regions such as present-day Antarctica (von Frese et al. 2009). Also omitted on the EID map are larger-scale cataclastic lithofacies assemblages. These are exemplified by the well-studied, although controversial Azura/Rubielos de la Cérida structures in northeast Spain (Ernstson et al. 1985, 2001; Diaz-Martinez et al. 2002), and large subsurface complexes such as that in South Australia described by Glikson et al. (2013) to contain multiple quartz microdeformation styles of currently uncertain origin. The global locations and general details of suspected impact sites (including possible and probable among other technical confidence categories) was provided by Rajmon (2010).

A confirmed (≫95% probability) impact structure status requires established technical recognition criteria in support of any proposed model that satisfactorily preclude alternative causal explanations, e.g. tectono-metamorphic, diapiric and/or cryptoexplosive volcanic processes. French and Koeberl (2010) stated that only the presence of diagnostic shock-metamorphosed (planar deformation in quartz, and melt) rocks or breccias, and/or the discovery of actual meteorites (either whole or most likely in part), constitute unambiguous evidence of an impact origin for interpreted 'crater-like' (typically circular) structures. More precise definitions of these terms are discussed in Reimold et al. (2014, and references therein). Confirmation of any associated distal impact ejecta (identifiable beyond ca. 2.5–5 times crater radii from impact loci (Glass and Simonson 2012; Osinski et al. 2013) also requires a carefully considered geochronological approach, in the absence of more geospatially and temporally constrained proximal crater evidence. Ejecta deposits may consist of various mixtures of impact-generated air-fall material including transport-abraded and/or diagenetically-modified microtektitic melt/vapor products (e.g. spherule pseudomorphs), shocked clasts/grains (e.g. quartz, feldspar, mica and heavy minerals), as described in Glass and Simonson (2012, 2013 and references therein). Depending on original projectile composition, certain layers also may be characterized by extraterrestrially-sourced geochemical signatures related to original bolide composition. These often comprise anomalous concentrations, relative to normal crustal abundances, of platinum group elements (PGEs) such as iridium (Ir) (Alvarez et al. 1980; Orth 1989; Orth et al. 1990; Rampino and Haggerty 1996;

Pearson 1999; Smit 1999; Kyte 2002) or unusual isotopic ratios of these elements, in particular osmium (Os) (Sato et al. 2016).

As mentioned above, almost all the currently identified Proterozoic (2000 Ma+) through Recent-aged impact structures occur in present-day continental areas, which infers that both the number and environmental consequences of historical impacts, especially within the geologically ephemeral oceanic plate domain, are likely to be significantly underestimated (Hergarten and Kenkmann 2015). In this context, Racki (2012) has noted that the apparent paucity of unequivocal impact evidence (confirmed craters ± diagnostic ejecta) found to be synchronous with stratigraphically-dateable mass extinction events, for example, could be misleading. Currently only the well-studied terminal Cretaceous Chicxulub impact (66 Ma; ca. 180 Km diameter) is unequivocally associated with a major global extinction event (Alvarez et al. 1980; Renne et al. 2013; Bond and Grasby 2017). This attribution reflects the fact that many components of the benchmarked Cretaceous-Palaeogene (K-Pg) stratigraphic boundary bed(s) had already been identified, described and modeled in significant detail in *crater absentia* (Izett 1990 and references therein), prior to discovery of the parent impact structure buried beneath the Yucatán Peninsula of southern Mexico (Hildebrand et al. 1991). Racki (2012) has provided a detailed discussion on the practicalities of (ongoing) attempts to apply similar 'Alvarez-type' extraterrestrial causal models to other Phanerozoic mass extinction events, including that marking the end-Triassic. In a similar vein, Reimold et al. (2014) and others, continued to caution extinction researchers against rushing too quickly to join the "impact bandwagon" without an appropriate technical boarding pass.

5.1.2 Impact Research Databases

The most significant (centralized) repository of published impact research information and supporting data is the on-line Earth Impact Database (EID) comprising part of the Planetary and Space Science Center at the University of New Brunswick, eastern Canada under the management of Dr. John Spray. PASSC also hosts the Manicouagan Impact Research Program (MIRP), a 10-year multidisciplinary project designed in part to investigate potential terrestrial impact cratering analogues for planetary applications. The searchable EID website contains general details and publication listings pertaining to all 190 confirmed impacts, plus other impact-related subjects with links to multiple on-line sources (Related Sites) sharing additional information, including country-specific and planetary data. Impact specialists such as Reimold et al. (2014), however, have queried the EID 'confirmation' status of certain listed structures that "did not seem to be justified on the basis of geological contexts and/or lack of bona fide impact evidence." The latter comment serves to illustrate the often controversial nature of qualitative impact geology research, in the disputable absence of, for example, confirmed planar deformation features and shatter cones (high magnitude shock indicators) and/or quantifiably significant PGE anomalies (extraterrestrial connectivity), in both proximal and distal geologic settings.

5.2 Late Triassic Terrestrial Impact Structures

The globally mappable impact crater total includes only five (northern hemisphere) Late Triassic (Carnian, Norian and Rhaetian) impact structures. These range in interpreted size (collapsed transient diameter—*sensu* EID) from 9 to 85 km (Fig. 5.1), with general details presented in Tables 5.1 and 5.2. Scientific interest in these features commenced mostly during the late 1970s and has increased significantly in the twenty-first century (Schmieder 2010; Schmieder et al. 2010a, b; Schmieder et al. 2014; and references therein). Their current research status—pertaining to impact cratering processes/products, timing and possible paleoenvironmental consequences—is described and discussed at length by Spray et al. (2010), Schmieder et al. (2014), and Sapers et al. (2014) among others. Ranked according to decreasing size, the structures are: Manicouagan (215.5 Ma, 85 km diameter) located in northeastern Quebec, Canada; Lake Saint Martin (227.8 Ma; 40 km) in central Manitoba; Rochechouart (206.9 Ma; ca. 23–50 km) in west-central France; and the smallest (buried) structure, Red Wing (ca. 200 Ma; 9 km; ca 2500 m TVD) located in South Dakota, USA. A fifth, relatively new addition is Paasselkä (228.7–231 Ma; 10 km), located in Finland (Schmieder et al. 2010b; Schwarz et al. (2015). This replaces the former 18–20 km Obolon (subsurface marine) impact structure in Ukraine, the radioisotopic age of which is reassigned from 215 ± 25 Ma (Masaitis et al. 1980) to 169 Ma (Mid-Jurassic) based on K-Ar dating by Gurov et al. (2009). Similarly, it should be noted that Racki (2012) references the poorly dated, although large (80 km diameter) Puchezh-Katunki structure in Russia (Pálfy 2004; Schmieder and Buchner 2008) as being Late Triassic. However, the EID currently lists this as a

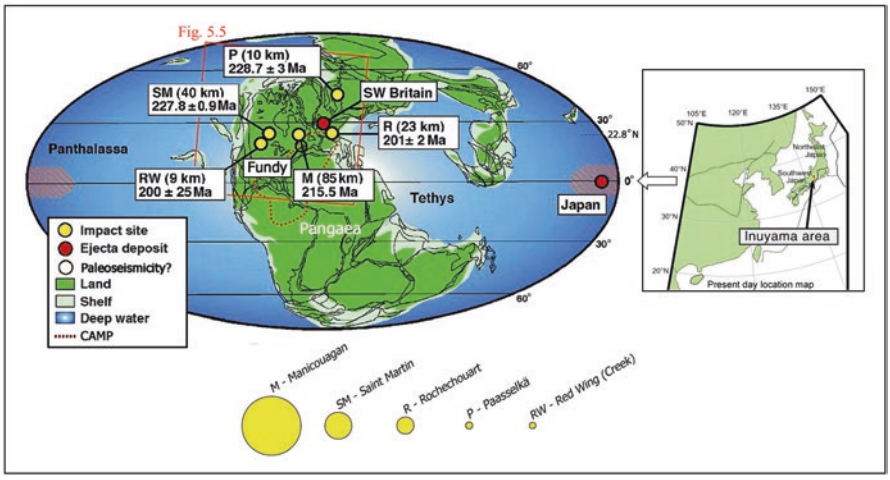

Fig. 5.1 Late Triassic global paleogeographic map showing the locations of confirmed terrestrial Carnian-Rhaetian impact structures (craters) and locally preserved interpreted distal ejecta deposits in southwestern Britain and central/southwestern Japan (Sakahogi, Inuyama-Kamiaso), assignable to the mid-Norian Manicouagan impact event. (Modified from Onoue et al. 2012, Suppl. I)

Table 5.1 General details of the five confirmed (EID 2017) Late Triassic terrestrial impact structures

	Manicouagan	Saint Martin	Rochechouart	Paasselkä	Red Wing (Creek)
Country	Canada	Canada	France	Finland	United States
Region	Northeastern Quebec	Central Manitoba	West of Massif Central area	Southern Savonia (SE Finland)	North Dakota (Williston Basin)
Latitude	N 51° 23'	N 51° 47'	N 45° 50'	N 62° 02'	N 47° 36'
Longitude	W 68° 42'	W 98° 32'	E 00° 56'	E 29° 05'	W 103° 33'
Drilled	Yes	Yes	No (Planned 2017)	Yes	Yes (producing HC field)
Field Setting	Surface with annular lake	Surface—partially flooded to south.	Surface	Surface lake	Buried at ~2000–2500 m TVD
Preservation Status	Relatively well-preserved with undeformed impact melt sheet exposed and accessible	Moderately preserved complex crater	Deeply eroded down to crater floor with no primary crater morphology preserved	Deeply eroded (esp. glacial)	Subsurface structure identifiable by seismic and gravity surveys plus drilling
Diameter (Km; EID)	85	40	23	10	9
Bolide Type (Est.)	?Chondrite[a]	N/D	Non-magmatic iron meteorite[b]	N/D	N/D
Target Rock 1	Crystalline basement	Crystalline/ sedimentary layers	Crystalline basement	Crystalline basement	Sedimentary (mixed)
Target Rock 2	Surficial carbonates & shales			Sedimentary (sandstones)	
Ejecta 'blanket'	Present and discontinuous	N/D	N/D	N/D	N/D
Distal Ejecta?	Spherule beds ± shocked quartz (SW England) and PGE anomalies (SW & C Japan)	N/D	N/D	N/D	N/D
Distal Seismicity?	?M-L Norian (Eastern Canada)	N/D	?Late Rhaetian (NW Europe)	N/D	N/D
Biotic Effects?	?Late Norian marine (Japan)	N/D	N/D	N/D	N/D

[a]Sato et al. (2016)
[b]Tagle et al. (2009)

Table 5.2 Summary of Carnian-Norian impact structure radioisotopic and stratigraphic (Red Wing only) age-dating results (1982–2017)

	Crater Age *(Ma)*	Dating Method (*Radioisotopic/ Other*)	Reference *(Date)*	StageOgg et al. (2016)	GPTS Chron *(Newark)*[a]
Manicouagan (85 km)	214 ± 1	U-Pb (melt rock zircon)	Hodych and Dunning (1992)	Mid-Late Norian	E14r
	215.5 ± 1	U-Pb (melt rock zircon)	Ramezani et al. (2005)	Mid-Late Norian	E14n
	213.2 ± 5.4	U-Th (melt rock zircon)	van Soest et al. (2011)	Mid-Late Norian	E15n
	208.9 ± 5.1	U-Th/He (central uplift titanite)	Biren et al. (2014)	Late Norian–Early Rhaetian	E17r
Saint Martin (40 km)	220.0 ± 32	Rb-Sr (impact melt rock)	Reimold et al. (2014)	Mid-Norian	E11r
	235.2 ± 6.2	U-Th/He (melt rock zircon)	Wartho et al. (2009)	Mid-Carnian	Pre-E1
	231.5 ± 7.2	U-Th/He (melt rock apatite)	Wartho et al. (2010)	Late Carnian	E2r
	227.8 ± 0.9	$^{40}Ar/^{39}Ar$ (melt rock K-feldspar)	Schmieder et al. (2014)	Latest Carnian	E7n
Rochechouart (23 km)	186 ± 5	Rb-Sr (impact melt rock)	Reimold and Oskierski (1987)	Pliensbachian	Post-E24
	214 ± 8	$^{40}Ar/^{39}Ar$ (pseudotachylites)	Kelley and Spray (1997)	Mid-Late Norian	E14r
	201 ± 2	$^{40}Ar/^{39}Ar$ (impact melt K-feldspar)	Schmieder et al. (2010a)	End Rhaetian–Earliest Hettangian	E24/H24
	202.7 ± 2.2	Re-calculated (K-fspr + adularia).	Jourdan et al. (2012)	Late Rhaetian	E23r base
	206.92 ± 0.20/0.32	$^{40}Ar/^{39}Ar$ (impact melt K-feldspar) ARGUS -V mass spectrometry	Cohen et al. (2017)	Late Norian–Mid-Rhaetian	E19r
Paasselkä (10 km)	228.7 ± 3.4	$^{40}Ar/^{39}Ar$ (melt rock recrystallized feldspar glass)	Schmieder et al. (2010b)	Latest Carnian	E6r
	231 ± 1.8		Schwarz et al. (2015)	Late Carnian	E4n
Red Wing (9 km)	200 ± 25	Lithostratigraphic estimate	Gerhard et al. (1982)	Norian-Toarcian	E24/H24u

[a]Kent et al. (2017, Fig. 1)

smaller (40 km) Mid-Jurassic (167 ± 3 Ma) impact feature (also dated as Early Jurassic: 192 ± 0.8 Ma by Holm-Alwmark et al. 2016).

For several of the above Late Triassic impact structures, the estimated absolute ages have significant uncertainty ranges (Table 5.2), resulting in temporal overlap with the Triassic-Jurassic boundary. This allowed early speculation concerning their potential effects on extinction patterns, including whether the largest impact, Manicouagan, could have 'triggered' the major 'end-of-Triassic' mass extinction (ETE; Olsen et al. 1987, 2002a, b). The latter hypothesis was refuted by subsequent Manicouagan absolute age-dating (Hodych and Dunning 1992), although the compounded impact effects on various interpreted earlier, lower magnitude Late Triassic biotic crises cannot yet be ruled out (Tanner et al. 2004; Lucas and Tanner 2008, 2017). A key impact research imperative has therefore been to refine further the respective cratering age estimates to establish/confirm relationships between proximal impact datasets and their more loosely constrained stratigraphic distal signatures. Currently, the latter are evidenced (only for the Manicouagan event) in southwestern Britain (Walkden et al. 2002; Kirkham 2003), central and southwestern Japan (Onoue et al. 2012, 2016; Sato et al. 2013, 2016) and, based on mostly associative interpreted paleoseismic evidence, eastern Canada (Tanner 2006, 2013).

The five structures listed above vary significantly in current morphological expression, reflecting different combinations of original (simple and complex) cratering style and subsequent tectonostratigraphic (burial, uplift, and unroofing) plus regional glacial modifications. Characteristic present-day features include flooded 'negative' topographic expressions (e.g. Manicouagan, Saint Martin and Paasselkä) which have affected outcrop accessibility in the field. The majority of existing Late Triassic impact research efforts have focused on Manicouagan, as the largest, most complex and best-preserved structure (Grieve and Head 1983; Spray et al. 2010; see also Schmieder 2010), further aspects of which are discussed below as a potential distal impact signature case study.

Detailed radioisotopic absolute age-dating (summarized in Schmieder et al. 2014; see also Cohen et al. 2017) currently indicates that as many as four of the above impacts occurred within a ca. 229–207 Ma time window preceding commencement of the major Late Triassic-Early Jurassic Central Atlantic Magmatic Province (CAMP) volcanic episode by several million years. This igneous activity was associated with early passive margin rifting of the northern Pangaea supercontinent, prior to initiation of Atlantic seafloor spreading (Cirilli et al. 2009; Withjack et al. 2012). It is now widely considered a significant contributor to the late Rhaetian extinctions, primarily from the environmental effects owing to outgassing (Hautmann 2004; Marzoli et al. 2004, 2017; Tanner et al. 2004, 2007; Nomade et al. 2007; van de Schootbrugge et al. 2007, 2008, 2009, 2013; Hautmann et al. 2008; Schaltegger et al. 2008; Whiteside et al. 2010; Ruhl et al. 2011; Schaller et al. 2011; Steinthorsdottir et al. 2011; Pálfy and Zajzon 2012; Pieńkowski et al. 2012, 2014; Richoz et al. 2012; Blackburn et al. 2013; Lucas and Tanner 2017). Beyond the uncertainties of age, any assessment of impact paleoenvironmental contributions is constrained because of the complete destruction of many original crater expressions by erosion and/or tectonic processes, especially subductive plate margin activity.

Grieve (2017), for example has recently stated that most of the 30 impact events currently recorded in the stratigraphic column (as confirmed ejecta deposits) do not have an associated impact structure. Given the paleogeographic plate configuration at the time (Fig. 5.1), the long-ranging Late Triassic impact record is therefore very likely incomplete. Consequently, several workers (Olsen et al. 1987, 2002a, b) have postulated that certain terrestrial (and marine) impact events causally relatable to observed Late Triassic biotic turnovers (e.g. Tanner et al. 2004) may now only be represented by more subtle evidence preserved distally (Glass and Simonson 2013). However, unlike that for the Late Cretaceous Chicxulub impact, all previous impact-related attempts to establish similar causal connections with both regional and/or global Late Triassic extinction phenomena (including the ETE) have essentially proved unsuccessful (Pálfy et al. 2000; Tanner et al. 2004; Lucas and Tanner 2008, 2015, 2017; Racki 2012). The question therefore remains as to why, in spite of historical research efforts, more distal impact sedimentological evidence has not proved identifiable, at least regionally and possibly globally, especially ejecta associated with the Manicouagan event, which offers the capacity to provide insights for developing an 'Alvarez-lite' Late Triassic impact biospheric crisis analytical tool, as discussed in Racki (2012). Presumably, this absence relates to: a) Late Triassic geochronologic inconsistencies (where to look geospatially and temporally), b) lack of preservation (nothing left to identify), c) poor and/or subtle diagnostic feature recognition (uncertainty in exactly what to look for), or, d) any combination of these factors. Concerning where stratigraphically-constrained distal impact evidence potentially exists, Schedl (2015) has suggested preservation potential may have been greater in epeiric/epicontinental marine (and by extension possibly long-lived lacustrine) successions, namely, those areas where sedimentation/accommodation rates exceeded continental erosion run-off and/or extensive sedimentary reworking at the time of impact and during subsequent, paleoclimatically-influenced strewn field development.

5.2.1 Paleogeographic Setting

The timing and paleomagnetically-constrained intra-Pangaean impact distributions during the Late Triassic provoked Spray et al. (1998) to investigate the three largest structures (Manicouagan, Rochechouart and Saint Martin) interpreted to occur co-latitudinally at an estimated 22.8° N (Fig. 5.1). What was striking is that the two smaller craters at the time, Red Wing and Obolon (the latter now re-assigned to the Mid-Jurassic) plotted on great circles with the other impact locations. This observation led these authors to propose that the five structures represented a long crater chain formed by multiple impacts—possibly within a period of hours—similar in pattern to the Comet Shoemaker-Levy 9 multiple impact events witnessed on the planet Jupiter in 1994 (Noll et al. 1996). However, Kent (1998) quickly rejected this hypothesis because of opposing paleomagnetic polarities identified in the respective Manicouagan and Rochechouart melt rocks. In addition, subsequent and more

accurate $^{40}Ar/^{39}Ar$ dating of the latter two impacts (Schmieder et al. 2010a; Schmieder et al. 2014; Cohen et al. 2017) have confirmed the respective events were not synchronous. This refutation, however, does not necessarily preclude the near terminal Triassic synchroneity apparent between the Red Wing and (possibly) Rochechouart structures dated at ca. 200 Ma and 201–206.9 Ma respectively, pending any geochronologic confirmation of the former crater age that is only broadly constrained stratigraphically. The approximate paleogeographic location of the Manicouagan impact structure in relation to interpreted coeval ejecta deposits in southwestern Britain (Walkden et al. 2002; Kirkham 2003; Thackrey et al. 2008, 2009), eastern Canada (Tanner 2006) and central Japan (Onoue et al. 2012) is shown in Fig. 5.1.

5.2.2 Stratigraphic Distribution

Schmieder (2010, Fig. 9.5) has provided a detailed summary of Triassic-aged impact structures categorizable as 'proven, probable and possible' (see also general terminology in Rajmon 2010). The general temporal distributions of Late Triassic impacts are also shown plotted on various composite stratigraphic charts in Walkden et al. (2002, Fig. 1), Tanner et al. (2004, Fig. 4), Onoue et al. (2012, Fig. 1) and Schmieder et al. (2014, Fig. 7), illustrating mostly radioisotopic absolute ages and their associated uncertainty ranges. Differences in the stage boundaries indicated reflect the stratigraphic dating controversy that currently exists, particularly concerning duration of the Norian and Rhaetian units (Lucas 2010, 2013; Lucas et al. 2012; Wotzlaw et al. 2014; Tanner and Lucas 2015; Ogg et al. 2016; Kent et al. 2017; and multiple references therein). Fig. 5.2 shows the Manicougan event timing in relation to Norian-Rhaetian biostratigraphic chart nomenclature used by Weems et al. (2016), Lucas et al. (2012) and Onoue et al. (2016). This enables a tentative (visual) comparison of the non-marine Newark Basin palynoflora, conchostracan and vertebrate faunachronology to the marine American Cordilleran/European Tethyan (ammonoid) and Japanese east Panthalassan (radiolarian and conodont) zonal schemes. Olsen et al. (2010) and others have, however, discussed the limitations imposed on marine versus non-marine biostratigraphic correlation attempts, specifying the general absence of scientifically reliable temporal control at both stage and substage levels within what Racki (2012) has termed a "flawed" epoch. For example, Lucas et al. (2012) drew attention to what they considered the questionable paleomagnetostratigraphic basis for the 'long Norian' that resulted in the abandonment of the previous palynologically-determined Carnian-Norian boundary in the Newark Basin. Indeed, these "short Norian" advocates have received recent support from new radioisotopic data published by Kohút et al. (2017). Other recent examples of current attempts to address this issue by using a combination of bio-, cyclo- and chemostratigraphic (elemental isotope) criteria as a high-resolution correlation tool are presented in Kent et al. (2017, and references therein). In addition, recently revised dating of the Rochechouart impact from 201 Ma to 206.9 Ma

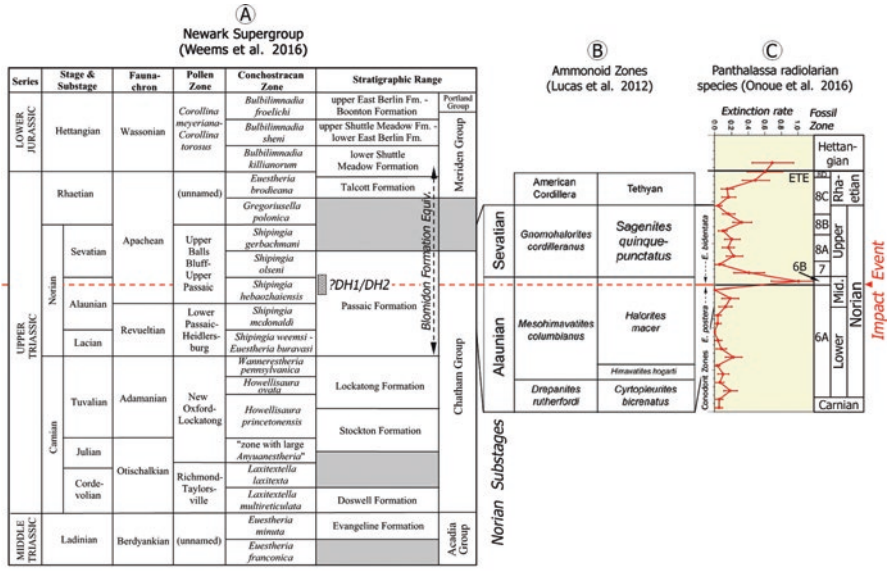

Fig. 5.2 Norian-Rhaetian biostratigraphic nomenclature. (**a**) The non-marine Newark Basin: palynology, conchostracans and vertebrate faunachronology. (**b**) The marine American Cordilleran/European Tethyan ammonoid zonation. (**c**) Japanese east Panthalassan radiolarian zonal assemblages. The label 'DH1/DH2?' indicates the approximate stratigraphic position of the Blomidon Formation deformation units (interpreted evaporite dissolution products and/or Manicouagan-related 'seismites') in the eastern Fundy Basin. (After Weems et al. 2016; Lucas et al. 2012 and Onoue et al. 2016)

by Cohen et al. (2017) would suggest both this, and the earlier Manicouagan event (215.5 Ma) may have played a significant role in shaping Late Norian through Rhaetian biotic evolutionary trends.

5.2.3 Geochronologic Control

Kelley and Sherlock (2013) provide a general overview of the geochronological methodologies applied to impact craters (see also Cohen et al. 2017 and references therein, for latest updates). The multiple interpretational challenges imposed by ambiguous impact-based geologic datasets, particularly when constrained by poor extra-crater chronostratigraphic control, has been reviewed and discussed by Racki (2012) using various examples of unsuccessful attempts to apply Alvarez-type extinction models to potential other Phanerozoic impact scenarios. With the exception of the (subsurface) Red Wing, all confirmed Late Triassic impact structures have proved dateable using a variety of radioisotopic techniques (according to sample type/availability) resulting in (often overlapping) ranges of acceptable (median) absolute ages and their respective uncertainty ranges (Table 5.2).

5.2.3.1 Radioisotopic Age-dating

Differences in projectile size/type, target lithologies, 'impactofacies' and preservation status of Late Triassic impact structures has necessitated the application of several radioisotopic dating techniques to determine their absolute ages. Reviews of the various chronometric methods used for dating the Late Triassic impacts are given in Schmieder (2010; see also Jourdan et al. 2012; Wartho et al. 2012). In a more recent paper explaining their rational behind 'unchaining' of the Late Triassic terrestrial impact crater model originally proposed by Spray et al. (1998), Schmieder et al. (2014) noted that the majority of confirmed impact structures still require further method refinements, the accuracy of which is likely to be constrained by melt rock type, timing of deformation, degree of hydrothermal diagenetic overprinting and stratigraphic context, in addition to confidence in the respective methods available ($^{40}Ar/^{39}Ar$, U-Pb, K/Ar or Rb/Sr etc.). The same publication (pp. 45–46) also offered a short discussion highlighting the accuracy and pitfalls of the differing isotopic dating techniques historically applied to Late Triassic impact structure melt products (Schmieder 2010; Schmieder et al. 2010a, b), as reflected in the absolute age ranges presented (Table 5.2). Schmieder et al. (2014) concluded by stating a preference for high-temperature isotopic chronometers as the most accurate method for dating impact events. They referenced (p. 47) the 40 km Lake Saint Martin (227.8 ± 0.9 Ma) structure in central Manitoba as one of the "most precisely dated larger impact structures on Earth", given the relatively small error bar of ±0.4% using the $^{40}Ar/^{39}Ar$ chronometer. This was applied to both impact-melted potassium feldspars and impact melt rock with an accuracy considered to compare favourably to the widely accepted U-Pb method used for dating the Manicouagan structure (214–215.5 Ma) by Hodych and Dunning (1992), and Ramezani et al. (2005) respectively, based on zircons from the impact melt sheet (Biren et al. 2014). In conclusion, Cohen et al. (2017) have also emphasized that (e.g. Rochechouart) chronometric sample location (as well as type)—ideally analyzed by a single laboratory—offers the potential for higher-precision $^{40}Ar/^{39}Ar$ dating, especially the latest generation of noble gas mass spectrometers (e.g. ARGUS VI), potentially applicable to selective ('cleaner') subsurface sample material acquired as part of the ongoing Rochechouart 2017 drill core program (Lambert et al. 2016).

5.2.3.2 Biostratigraphic Dating/Correlation

Of the five currently confirmed Late Triassic impact structures only the small (9 km) Red Wing structure, buried up to 2500 m beneath a Jurassic and younger sedimentary succession, is completely lacking suitable melt samples for isotopic measurements (Schmieder 2010), and thus only datable stratigraphically (Butcher et al. 2012). Although this hydrocarbon-bearing (and -producing) structure has been drilled extensively and defineable geophysically, its age can only be estimated as widely bracketing the Triassic-Jurassic boundary (TJB) viz.: ca. 220–200 Ma (Koeberl et al. 1996); 200 ± 25 Ma (Gerhard et al. 1982) and 200 ± 5 Ma (Grieve 1991).

Whilst timing of the remaining four impact collisions is constrained radioisotopically, only one, Manicouagan, has a confirmed distal ejecta record (in Britain, Japan and tentatively eastern Canada). However, this factor does not necessarily preclude causal associations of the identified (Norian-aged) ejecta layers with possibly other synchronous impact events, the crater evidence for which is either currently unrecognized or has been removed by erosion and/or, in the case of potential Panthalassan-Tethyan marine impacts, oceanic plate subduction processes. While the linkage between the British continental red bed occurrence is supported by authigenic potassium feldspar absolute age-dating (214 ± 2.5 Ma) and (Grenvillian) mineral provenance studies (Thackrey et al. 2008, 2009), its precise chronostratigraphic position within an unconformable and unfossiliferous Norian (basal Mercia Mudsone Group) host section still remains uncertain. In contrast, the more distal Japanese pelagic marine claystone ejecta horizon is biostratigraphically well constrained, but displays differing, impact-diagnostic (PGE/other) geochemical anomalies. This suggests the latter relates potentially to a different extraterrestrial event, pending demonstration within time-equivalent beds at other localities of a common impact signature(s), in addition to the ubiquitous 'shocked quartz' tag. This presents an interpretational need for additional supporting associative evidence (*sensu* Racki 2012), preferably within more proximal, seismically sensitive areas, including northern Atlantic conjugate margin rift domains such as the early Mesozoic Fundy Basin in eastern Canada.

5.3 Types of Evidence (Proximal vs. Distal)

5.3.1 Impact Geoscience Terminology

The descriptive terminology and classification schemes applicable to the impact cratering process, the products ('impactites' *sensu lato*) and subsequent geologic history (impact structuration and preservation) are presented in a systematic manner in several key publications. Among these are French (1998, 2004), Stöffler and Grieve (2007), Glass and Simonson (2013), Osinski and Pierazzo (2013) and Reimold et al. (2014), with Grieve (2017) having recently provided a detailed contextual summary of Earth processes and effects pertaining to large impacts. Listed impactite categories include both proximal (shocked/brecciated/melted target rocks) and distal (glass melt, tektites/microtektites, air-fall beds). The processes discussed in Osinski and Pierazzo (2013) include hypervelocity contact and compression, ejecta mobilization, crater formation/collapse kinematics and impact-induced hydrothermal activity. In addition, French and Koeberl (2010) have discussed the potentially deceptive nature of various types of deformation features (e.g. tectonometamorphic quartz planar lineaments) that are commonly misinterpreted as 'convincing' impact shock-diagnostic planar deformation features (PDFs) in both proximal and distal settings. Racki (2012) also provided a critical review of the applicability of mass extinction theories based on cataclysmic impact scenarios expressed at variable scales using the terms 'conclusive' and 'incredible' applicable

to (mostly distal) tracer elements. General descriptive aspects of potential impact evidence pertinent to specific biostratigraphic intervals are summarized also in Tanner et al. (2004), as part of their review of the record and interpreted causes of Late Triassic extinctions.

The complex inter-relationships of both diagnostic and supplementary proximal impact signature data noted above are shown in Fig. 5.3a, modified from an original process chart by Stöffler and Grieve (2007) to include interpreted 'associative' distal expressions (Fig. 5.3b, *sensu* Racki 2012), candidate examples of which are briefly described in Sect. 5.4. Reference is also made to comments by Walkden and Parker (2008) on comparative Chicxulub versus Manicouagan impact effect modeling results, plus the use of multivariate analysis to model-match outcrop and drill core records of the K-Pg (Chicxulub) event horizon (Artemieva and Morgan 2009).

5.3.2 Shock Metamorphism

The visual identification of shock-metamorphosed detrital mineral grains, particularly a certain type of quartz crystallographic microdeformation, is uniquely diagnostic (and durable) evidence of hypervelocity impact pressure signatures in the 10–35 GPa range (Osinski and Pierazzo (2013). Similar features may also be present in (less mineralogically-stable) feldspar grains, particularly plagioclase the impact shock metamorphic effects on which have been described by Pickersgill (2014), Pickersgill et al. (2015) and Thompson (2015), as well as accessory minerals e.g. zircon. The latter publication includes analyses of samples from the Manicouagan structure central uplift gneisses, which display multiple orientated sets of planar features within twins, in association with typical shocked quartz and isotropic glasses. Several other petrographic studies, however, have indicated that shock metamorphism, as typically evidenced (in quartz) by one or more sets of PDFs, may also appear stylistically similar to other, singular lamellar features. The latter resulting from either tectono-metamorphic (Alexopoulos et al. 1988; French and Koeberl 2010; Hamers and Drury 2011; Glikson et al. 2013) and/or cryptoexplosive volcanic mechanisms (Carter et al. 1986; Sharpton and Schuraytz 1989a, b; Chesner 2011; Osinski et al. 2011, 2013).

Formally defined, PDFs are linear crystallographic microstructures typically less than a micron wide and arranged as crosscutting sets in which individual parallel discontinuities are spaced several microns apart (Grieve et al. 1996; Ferrière et al. 2009). The latter filled initially with amorphous glass, although annealing over time may form 'decorative' sets of distinctive linear inclusions, locally resulting in a cloudy appearance observable in thin section (Grieve 1998). As stated above, tectono-metamorphic processes are also capable of forming superficially similar features (e.g. Böhm lamellae and Brazil twins) visually resembling PDFs (Grieve and Pesonen 1996; Reimold et al. 2014). Consequently, the employment of optical microscopy methods using a universal stage mount (USM or U-Stage) has now largely become mandatory for diagnosis of impact shock signature. This four-axis

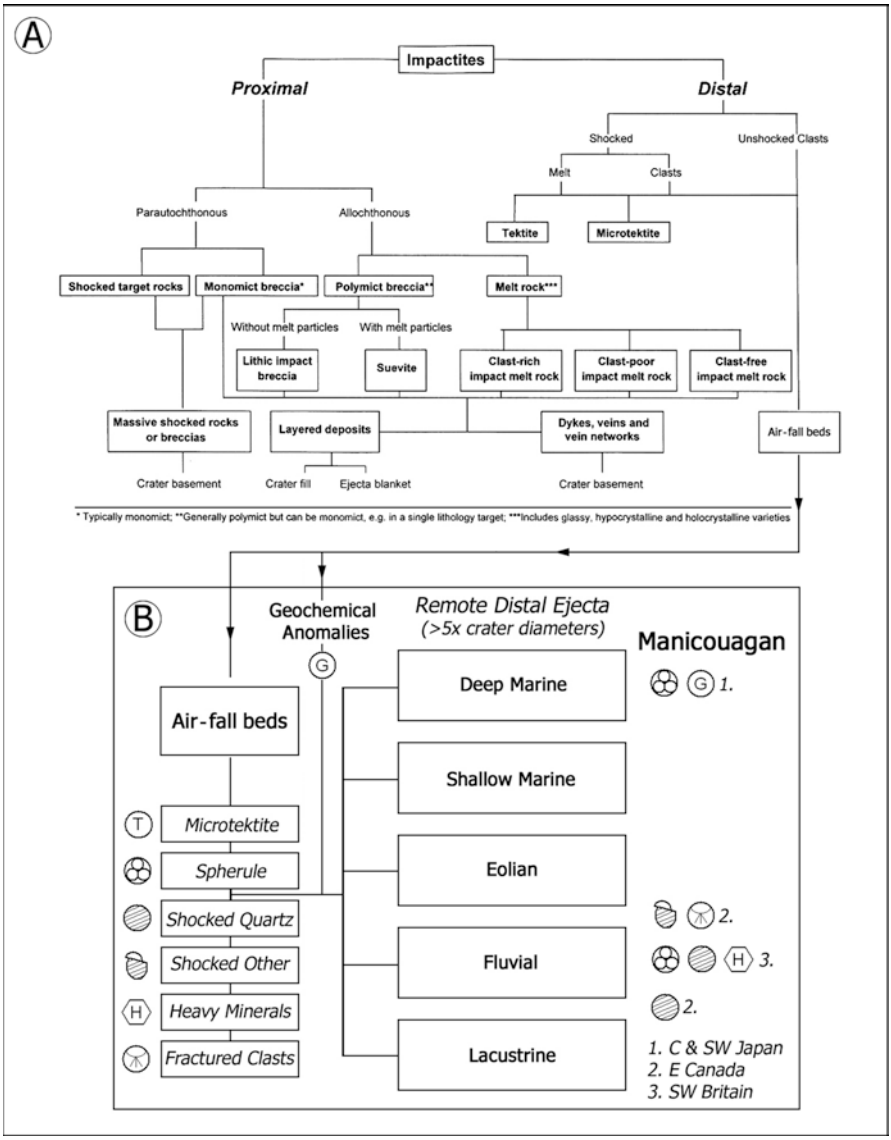

Fig. 5.3 Chart illustrating the relationships of proximal and distal impact signatures with application to Manicouagan. (**a**) Geologically identifiable key diagnostic and supplementary proximal/distal impact signatures. (**b**) Currently interpreted Manicouagan-related distal features. (Modified from Stöffler and Grieve 2007)

method enables confirmation of the orientation of PDF planes of low Miller indices at separate angles to the granular crystallographic c-axis, which serves to differentiate shock metamorphism from other microdeformation mechanisms. It also enables estimations of shock magnitudes in (preferably) multiple grain samples, based on the frequency and orientation of individual PDF sets.

Mossman et al. (1998; after Goltrant et al. 1991) have further demonstrated that transmission electron microscopy (TEM) also offers a high-resolution capability of discriminating between 'true' shock-metamorphosed and 'apparent' PDFs (i.e. planar features/fractures, or = 'PF's) identifiable optically using a standard petrographic microscope only. TEM specifically permits recognition of those features indicative of a tectonic origin such as a) non-parallel sub-grain boundaries, b) fringe patterns at the boundaries and c) the presence of perfect dislocations. Cavosie et al. (2015) have also applied both TEM and cathodoluminescence (CL) to interpret mechanical Brazil twin sets as a secondary record of shock metamorphism preserved in detrital quartz grains sourced from the Meso-Proterozoic (2.02 Ga) Vredefort Dome impact structure in South Africa. Hamers and Drury (2011) have additionally documented how scanning electron microscopy (SEM) combined with cathodoluminescence (SEM-CL) can be used (relatively reliably) to distinguish shock features from tectonic deformation lamellae in quartz. In addition to the above methods, SEM of whole siliciclastic (notably quartz) grains partially etched by exposure to (undiluted) hydrofluoric acid (HF) is considered a reliable (destructive) secondary technique for identification of shock-metamorphosed minerals (Gratz et al. 1996). Recent applications of both TEM and SEM methodologies for differentiating multiple quartz planar microstructure styles are discussed in detail by Glikson et al. (2013), as related to granite-hosted occurrences in a large, deeply buried potential impact structure located in the eastern Warburton Basin of South Australia.

5.3.3 Distal Impact Signatures

5.3.3.1 Ejecta Layer Characteristics

Hypervelocity impact crater excavation generates high initial volumes of ballistic ejecta of variable particle size (blocks, clasts, grains, melt, dust, vapor condensates) sourced from a combination of highly shocked target lithofacies and disintegrated/vaporized projectile material (Glass and Simonson 2013; Grieve 2017). The latter also commonly, though not exclusively, occur in association with impact diagnostic (extraterrestrial/melt) geochemical signatures e.g. anomalously concentrated PGE (e.g. Ir) levels. Osinski et al. (2013) have defined impact ejecta deposits as "any target materials, regardless of their physical state, that are transported beyond the rim of the transient cavity formed directly by the cratering flow-field." According to them, the term 'distal ejecta' is applied correctly to deposits that occur at distances ≥5 times crater radii from the impact center (see also Glass and Simonson 2012).

Melosh (1989) noted that relatively-recent age impact craters on terrestrial planets are surrounded typically by a "continuous ejecta blanket". This extends approximately 1–2 times crater radii beyond the rim perimeter, the constituents of which then generally thin out distally. Wrobel and Schultz (2003) also have discussed the potential effect of Earth's rotation on impact trajectories and the resultant global distribution of ejecta, using the Chesapeake Bay, Popigai and Manicouagan events as examples. A key ejecta modeling case study by Artemieva and Morgan (2009) utilized a multivariate numerical approach to determine the global effects of the Chicxulub impact and resultant strewn field characteristics. The range of Chicxulub models presented was designed specifically to match the ejecta material currently evidenced within the 'benchmark' K-Pg boundary layer/event horizon. Input variables included impactor mass, velocity, impact angle, target lithology (generic) and target status (wet vs. dry) among other factors. In addition, Schedl (2015) has discussed in detail the significance of post-impact atmospheric conditions and distance controls on ejecta timing, flow and emplacement, presumably modifiable by paleoclimatic wind patterns and extant paleotopography. Laboratory mesoscale modeling, based on high velocity impacts into both wet and dry porous sandstone targets using a range of projectiles at variably high velocities also has been conducted by Güldemeister et al. (2013), Kowitz et al. (2013) and Wünnemann et al. (2016). This provides a basis for understanding Late Triassic siliciclastic microdeformation styles potentially resulting from proximal coseismicity (Thompson and Spray 2014), and possibly (lower magnitude) seismically-induced distal sedimentary fabrics (Tanner 2006, 2013). Recent work by Fazio et al. (2014, Fig. 5) describes rare natural field evidence from the 45 m Kamil crater located in an arid desert area of southern Egypt, which provides additional insights into the shorter-term effects of a small, hypervelocity (iron) meteorite impact on a naturally layered sandstone target (cf. Kieffer 1971). Kamil displays a wide range of largely undegraded ('fresh') shock metamorphic features (shatter cones, coesite, stishovite, diamond, and melt products) offering the potential to be an important small impact case study, including investigations of the early (first order) depositional history of associated distal ejecta.

As noted above, the physical character of primary distal impact ejecta layers relates to paleodistance from the crater site, climate-influenced depositional setting (dry/wet/frozen), thickness, composition (host section and allochthons) and respective lithofacies. Physical features include depositional style and energy, contact relationships, bed thickness, accretionary lapilli diameter, grain-size range and the respective degrees of subsequent transportational, diagenetic and compactional alterations. Schedl (2015) has discussed how this information may be used to establish workable causal linkages between interpreted ejecta layers and source craters (impact structures), which may offer constraints on where to look for either component in the absence of the other. For the Chicxulub impact, Artemieva and Morgan (2009) used modeling results to explain the presence and size distribution of shocked quartz in distal ejecta up to distances of 15,000 km, in addition to clarifying controls on timing, thickness trends (down to millimeter-scale) and specific, diagnostic compositional elements including Ir-enriched spinel-bearing microspherules. This

ground-truthing approach enabled these authors to establish a working range of impact scenarios to determine which models best reproduce the observable field data, the paleogeographic expressions of which are considered to have varied considerably.

With respect to the lower magnitude Late Triassic impact signatures, Schedl (2015) has repeated the widely held mantra that distal ejecta layers are "rare and hard to spot in the field because of their thinness", contingent on the causal factors noted above plus final depositional setting and subsequent burial history. The same author referred to earlier observations by Melosh (1989) in stating that only ca. 10% of ejecta material is likely classifiable as distal, significantly reducing its subsequent detectability in geologically overprinted stratigraphic successions (see also Glass and Simonson 2013; Grieve 2017). Consequently, the suggestion of an 'identification by association' approach, based on iterative impact-modeled relationships with larger-scale sedimentary features would appear practical for primary level research. The latter for example, include assessment of terrestrial soft/synsedimentary deformation structures (SSDS *sensu lato*) plus or minus competing causal deformation models (cf. Ackermann et al. 1995; Tanner 2006). Other scenarios might include geophysically-identifiable marine slope failure packages (e.g. Deptuck and Campbell 2012) plus high energy tsunami deposits ('tsunamites') (Plado 2012; Brookfield et al. 2013) in former shallow marine (and possibly permanent lake) settings. As earlier noted by Tanner (2006) reference is also made to vertical stratigraphic relationships, suggesting that distal ejecta (candidates) may directly overlie (post-date) SSDS units resulting from initial seismic shock (and weaker aftershock) waves. The latter having traveled faster within the upper crustal subsurface than any associated clastic air-fall (Fig. 5.3b). However, Shanmugam (2016, 2017) has stressed that a significant majority of SSDS do not require a seismic triggering mechanism, thus introducing the interpretational dangers of impact force-fitting as discussed in Racki (2012). A preliminary decision tree process chart for determining distal impact data (singular diagnostic and associative) assemblages potentially resulting from the five confirmed, terrestrial Late Triassic impact events, based on the current Manicouagan example is presented in Fig. 5.4.

5.3.3.2 Late Triassic Shocked Quartz Occurrences

Detrital quartz grains displaying 'shock-like' characteristics have been reported from a number of Late Triassic sections in both Europe and North America. Because of causal implications relating to the ETE, initial search emphasis was focused mainly on the uppermost Rhaetian Stage, either approximating, or at the Triassic-Jurassic system boundary (TJB). Badjukov et al. (1987, 1988) published abstracts that reported finding quartz grains with 'PDF's in the Kendlbach Formation at Kendlbachgraben in the Northern Calcareous Alps of Austria, although these occurrences do not appear to have been verified by any published follow-up research (Tanner et al. 2016). Bice et al. (1992) similarly reported quartz with multiple 'PDF' sets from a section of the Calcare á Rhaetivicula near Corfino in Tuscany, Italy at

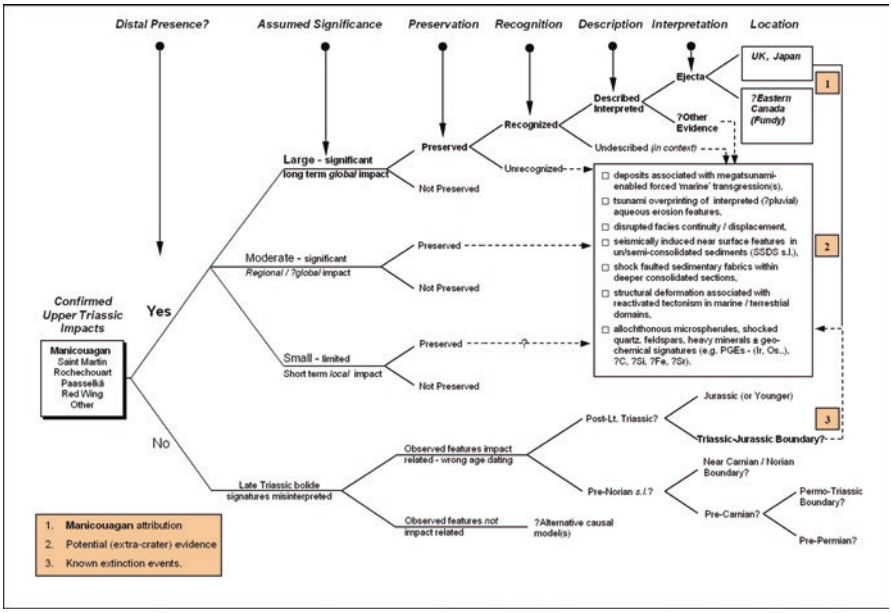

Fig. 5.4 Preliminary decision-tree process chart for determining possible distal evidence (*sensu* Schedl 2015) sourced from confirmed (and potentially unconfirmed/undiscovered) Late Triassic impact events, using the Manicouagan example

several horizons that occur several meters below a marl bed traditionally interpreted as the TJB. However, most grains described from within the Tuscan section contained only a single set of lamellae, some of which appear sinuous in nature, unlike verifiable PDFs as defined above. Nonetheless, the tentative identification of these putative shocked grains in several beds both near, and at the Italian system boundary led Bice et al. (1992) to postulate by causative association, that multiple bolide impact events had occurred towards the end of the Triassic (latest Rhaetian). Consequently, Hallam and Wignall (1997) and Hallam (1998) specifically labeled all reports of shock-metamorphosed quartz occurrences approximating the TJB as "dubious", citing questions concerning both the technical validity of the identifications and the petrographic techniques employed (e.g. Grieve and Pesonen 1996). Research efforts undertaken to identify shocked quartz in Rhaetian-aged (Newark Supergroup) rift-related continental sediments within the Fundy Basin (Olsen et al. 1990; Mossman et al. 1998) and the Jacksonville syncline (Upper Passaic Formation) of the Newark Basin (Mossman et al. 1998; Olsen et al. 2002a) similarly proved unsuccessful. The latter authors, for example, found quartz grains with Böhm-style lamellae and other PFs in the uppermost (Late? Norian-Rhaetian Partridge Island Member) strata of the Blomidon Formation (recently reassigned to the overlying Talcott Formation in Weems et al. 2016) of the eastern Fundy Basin. However, they were unable to confirm these unequivocally as the product of impact shock, as opposed to progressive regional metamorphism.

Verifiable shocked quartz in older (mid-Norian) sediments, however, has been identified and described in Western Europe (Walkden et al. 2002; Kirkham 2003)) and to a lesser degree, from the Canadian Atlantic rift margin (Tanner 2006) east of the Mossman et al. (1998) Fundy Rhaetian sample localities. All occurrences have been interpreted to represent distal effects of the Manicouagan impact, based on (heavy) mineral provenance/age analysis (Thackrey et al. 2008, 2009) and tectonostratigraphic setting ca. 750 km southeast of the Quebec crater site (Tanner 2006, 2013) respectively. Walkden et al. (2002, Figs. 4 and 5) used both USM-based analysis and SEM/HF acid etching to confirm an agreed impact origin for fine-grained detrital quartz found in association with spherulized microtektite pseudomorphs in a thinly developed calcarenite quarry section in southwest Britain (see also descriptions in Kirkham (2003, 2006) based on earlier unpublished work from the 1970s). Tanner (2006) applied similar techniques to verify shock characteristics of rare sandstone grains present near the top of a stacked synsedimentary deformation zone of comparable age in the lower Blomidon Formation of the north shore of the Minas Subbasin. The latter unit, a possible impact-induced 'seismite', is also reported to contain other quartz grains with a 'toasted' appearance (*sensu* Whitehead et al. 2002), that occur locally in association with sub-spherical sericitized feldspars of uncertain diagenetic origin, though described as having a 'chondulitic' appearance in thin section, as discussed in Sect. 5.4. However, unlike the British shocked quartz occurrence, there is no report of diagnostic distal impact spherules (or microtektites) from the Blomidon Formation, or any other North American Norian successions referenced in Sues and Olsen (2015) and Weems et al. (2016)—despite locally extensive core-based and other stratigraphic evaluations.

5.3.3.3 Impact Spherule Evidence

As noted above, diagenetically-altered microtektites (microspherules) are identified only in southwestern Britain and Japan from widely differing fluvial continental and deep marine sections respectively, though possibly sharing a common impact origin. Various details of these Norian-aged spherules—interpreted as probable Manicouagan ejecta (Walkden et al. 2002; Kirkham 2003; Onoue et al. 2012, 2016)—are presented in Sect. 5.4. The collective descriptions provided by these authors invoked direct comparisons to the globally-distributed Chicxulub impact ejecta 'splash form' spherule beds as described in Kring and Boynton (1991) and Bohor and Glass (1995) (see also Izett 1990, Figs. 15–16; Kring 2007 and Glass and Simonson 2012, 2013).

5.3.3.4 Geochemical Anomalies

The initial hypothesis by Alvarez et al. (1980) postulating a bolide impact concurrent with the Cretaceous-Paleogene boundary (K-Pg) was inspired by the measurement of anomalous Ir concentrations of up to 30 parts per billion (ppb), in the

marine boundary clay beds of Italy, Denmark and New Zealand. It is widely known that Ir occurs at very low concentrations in the Earth's crust; Fenner and Presley (1984) suggested that the typical crustal concentration is 40 parts per trillion (or picograms per gram, pg/g), an estimate based on the concentration in the suspended sediment load of the Mississippi River. McLennan (2001) was more specific, estimating that the concentration ranges from 20 pg/g in the upper continental crust to 130 pg/g in the lower crust, for an average concentration of 100 pg/g for bulk continental crust. By comparison, the mean Ir concentration in CI chondrites is ca. 465 ppb (Osawa et al. 2009). Hence, the discovery of the anomaly at the K-Pg boundary led to a search for similar Ir anomalies coincident with other extinction horizons. There are, of course, terrestrial Ir sources e.g. mantle-sourced volcanism, and depositional or diagenetic processes that can result in selective enrichment at certain stratigraphic horizons. Therefore, elevated levels of Ir are not considered indicative of solely extraterrestrial impact contributions. Sato et al. (2016), commenting on a recently recognized middle Norian Ir occurrence in central Japan, have also highlighted the possibility of significant contamination in PGE assessments based on sources extracted from dominantly sedimentary ejecta. Commonly, PGEs, including Ir and Os, are analyzed and their ratios compared to those of ordinary chondrite (Orth et al. 1990). Also, potential mafic sources may be identified by their geochemical signatures such as rare earth element (REE) profiles (Pearson 1999). Consequently, terrestrial (i.e. non-impact) sources are considered a feasible alternative for many of the Ir anomalies that have historically been reported at other paleontologically-defined boundaries (Orth et al. 1990; Hallam 1998).

Olsen et al. (1987, 2002a, b) hypothesized a connection between the end-Rhaetian extinctions and one or more bolide impact events, specifically the Manicouagan structure in northeastern Quebec, Canada, discussed in the next section. The initial proposal (Olsen et al. 1987) predated establishment of the now generally accepted mid-Norian radioisotopic age determination for this largest Late Triassic impact structure (Hodych and Dunning 1992; Ramezani et al. 2005) and more recently, a supportive biostratigraphic age (Onoue et al. 2012, 2016). However, subsequent $^{40}Ar/^{39}Ar$ age dating (e.g. Schmieder et al. 2010a; Jourdan et al. 2012; Sapers et al. 2014) for the significantly smaller (23 km diameter) Rochechouart structure in west-central France overlapped the late-Rhaetian extinction horizon (see also subsequent Ar-Ar dating at 206.9 Ma (Late Norian–Early Rhaetian) by Cohen et al. 2017). This raises the possibility of a preserved sedimentary record of the impact associated with these, or possibly other more regional extinctions, as noted in Schmieder et al. (2010a, pp. 1235–1236). Investigating the potential connection of the extinctions to impact, Orth et al. (1990) analyzed Ir levels in the boundary marl beds ("Grenzmergel") at Kendlbach, Austria where they observed a maximum level of 51 pg/g. These authors noted that Ir concentration in the section correlated strongly with aluminum content, and concluded that enrichment resulted from decreased sediment accumulation. Recent work by Tanner et al. (2016) on the Kendlbach section and the GSSP section at Kuhjoch, Austria, has largely supported this conclusion, although the more recent study also found peak concentrations up to 145 pg/g above the extinction horizon, which the authors link to the CAMP flood

basalt eruptions. At the boundary section in St. Audrie's Bay, on the north Somerset coast of southwestern England, McLaren and Goodfellow (1990) measured Ir as high as 400 pg/g, but this enrichment occurred in phosphatic nodules and consequently attributed to diagenesis. Hori et al. (2007) analyzed a deep-sea section of bedded cherts spanning the system boundary in Japan and noted PGE enrichment, including a maximum Ir concentration of 70 pg/g, at a stratigraphic level corresponding to a radiolarian extinction that precedes the end-Triassic extinction by less than 500 kyr. The authors discounted a volcanic origin for the PGEs based on the REE profile, which resembled that for continental shale, plus the lack of volcanic debris, but unequivocally did not declare an impact origin.

The end-Triassic record in continental sediments is well represented in the various synrift basins of the Newark Supergroup (Newark and Fundy Groups) of eastern North America, including the Blomidon Formation within the northernmost inshore Fundy Basin. Orth et al. (1990) reported Ir concentrations up to 150 pg/g from mid-Norian to latest Rhaetian in the Blomidon. Mossman et al. (1998) also later reported a maximum Ir level of approximately 200 pg/g in its uppermost 2 m, directly beneath the terminal Triassic North Mountain Formation (CAMP basalt), although using less precise techniques than those employed by Orth et al. (1990). Tanner and Kyte (2005) and Tanner et al. (2008) subsequently re-examined these strata in detail using neutron activation analysis (NAA) and found that Ir occurred at concentrations up to 450 pg/g in multiple horizons in which the organic carbon content was also elevated. Their interpretation was that the Ir had a volcanic igneous (i.e. CAMP) source, potentially via extrusive fallout and/or outgassing, leading to localized Ir concentrations within the sedimentary section at redox boundaries. In the Newark Basin, Olsen et al. (2002a, b) reported a "modest Ir anomaly" maximizing at 285 pg/g, which correlates with the 'fern spike' (peak abundance of trilete spores) at the horizon of maximum palynological turnover in the upper Passaic Formation. Olsen et al. (2002b) interpreted this floral anomaly as analogous to that noted at certain K-Pg boundary sections considered to represent the aftermath of an ecological catastrophe (Tschudy et al. 1984). Olsen et al. (op cit.) discounted a volcanic source for the anomaly based on a lack of correlation between the Ir concentrations and other trace elements that might indicate mafic volcanism, or with other siderophile elements, such as cobalt, nickel, or chromium. To date, there are no confirmed reports of impact debris (shock-metamorphosed grains, tektites, microtektites, microspherules or microdiamonds) in the horizons containing the end-Rhaetian Ir anomalies. Thus, an extraterrestrial source for reported latest Triassic Ir occurrences still remains unlikely.

Elsewhere, Onoue et al. (2012) originally reported 'Manicouagan impact-aged' geochemical and microtektite evidence, including PGE anomalies, nickel-rich magnetite and microspherule pseudomorphs, from a thinly developed mid-Norian (late Alaunian) pelagic marine claystone bed near Sakahogi in the Mino Belt of central Japan. A high degree of chronostratigraphic control is provided in the section by detailed radiolarian and conodont zonal analyses. Sato et al. (2016) subsequently demonstrated that the high abundances of Ir, up to 41.5 ppb (comparable to the K-Pg levels), plus other concentrated PGEs such as Os, Ru and Pt occur within the

same ejecta deposit at several offset localities, and consequently might provide a chemostratigraphic basis for determining similar ejecta layers on a wider, possibly global scale. A paleomagnetic analysis of Late Triassic ferruginous-bedded chert samples from the Sakahogi sample locality (Uno et al. 2015) suggested that ejecta dispersal most likely sourced directly from the Manicouagan impact (at 22.8° N; Spray et al. 1998) had extended to near-equatorial eastern Panthalassan latitudes (Fig. 5.1).

5.3.3.5 Associated (syn- to post-) Sedimentary Deformation

The occurrence of distal ejecta deposits has occasionally been associated with often complexly deformed brittle and/or ductile sedimentary units (observable at both macro- and microscale) collectively referred to as 'seismites' (cf. Tanner 2006). This naming convention, however, presumes one specific (coseismic) primary causal mechanism out of a potentially wide range of feasible alternatives e.g. gravity overloading or evaporitic dissolution contingent on regional geologic setting. Definition of the genetic term 'seismite' (comparable to that of 'tsunamite') has thus been the subject of much discussion in the literature, most recently by Shanmugam (2016, 2017 and references therein; see also Montenat et al. 2007) who cited multiple examples of inappropriate usage "without a rigorous scientific analysis". The same author noted that paleoearthquake displacement(s) comprise a dynamic triggering mechanism only (rather than a specific depositional process) which in the context of both terrestrial and marine impacts requires a demonstrable structural connectivity at upper crustal level, synchronously between source crater and distal signature location. Key interpretative issues pertaining to this matter relate largely to confidence in the timing of the respective events, distal bedding relationships and the diagnostic quality of ejecta components (unequivocal mineralogic shock evidence, microtektites, spherules, etc.) required in support of any remote tectono-sedimentological impact connection.

Further to the above, Schedl (2015) has discussed the timing relationship between ejecta arrival and liquefaction associated with transmissible seismic 'wave' generation and concomitant ground shaking, raising the issue of what best constitutes evidence for an "impact-induced seismite", and (associatively) suggesting this comprises identifiable ejecta either overlying, or entrained within SSDS. This author also distinguished between impact- and earthquake-induced SSDS (e.g. the Recent Dead Sea—Lake Lisan area examples in Alsop and Marco 2011; see also lacustrine discussion in Doughty et al. 2014) that share similar deformation signatures—notably concerning bedding-style repeatability. The latter relating to the fact that impact-induced sedimentological responses are generally considered to represent 'one-off' catastrophic geologic signatures, the distal expressions of which are typically thinly constrained between undeformed, more cyclically bedded units contingent on depositional setting, physical stability, etc.

Well-developed Late Triassic (Rhaetian) 'seismites', are known to occur widely throughout parts of northwest Europe as described in detail by Simms (2003, 2007)

who postulated a then undetermined impact-triggered origin, subsequently associated with the French Rochechouart impact (then dated at 201 Ma, although recently revised to ca. 207 Ma in Cohen et al. 2017; see Table 5.2). However, Lindström et al. (2015) have since postulated an alternative causal mechanism for the Cotham Member seismites of repeated shallow crustal disturbances induced by (CAMP) volcanic activity, which, presumably may also be represented within various Newark Supergroup successions associated with similarly active igneous areas. Tanner (2013) tentatively proposed a potential Manicouagan impact-induced seismic origin for brittle deformation (interpreted concussion fracturing) observed in the conglomeratic clasts of the coarsely fluvial Fundy Group Quaco Formation (Ladinian in Weems et al. 2016) of coastal New Brunswick, eastern Canada (discussed below). The latter author drew comparisons to the currently unconfirmed (EID) northeast Spanish Azura and Rubielos de la Cérida impact structures (Palaeogene). These are characterized by a similar, though more intense variety of (Early Triassic Bundsandstein) cobble deformation fracture styles (clast spallation, radial fracturing, quartz planar features/PDFs) considered to be indicative of Hertzian-style dynamic shock mechanisms at impact magnitudes (Ernstson et al. 2001; Ernstson and Hiltl 2002; see also www.impact-structures.com).

The previously mentioned occurrence of rare shocked quartz at the top of a 'seismically-deformed' mid-Norian Blomidon Formation coastal section at Red Head 120 km east of the Quaco section (Tanner 2006) does not necessarily indicate synchronicity of (possibly uniquely styled) Late Triassic deformation processes within the western North Atlantic rift-margin. However, the above author has presented evidence to suggest the two Fundy Group examples (Blomidon and Quaco Formations), by association, collectively demonstrate the possibility of impact-triggered structural reactivation, namely a singular, major Norian paleoearthquake event. As suggested by this author, a primary candidate mechanism is transcratonic margin linkage via the east-west trending terrane-bounding Minas Fault Zone. This microplate boundary was active in an extensional sense regionally during Late Triassic-Early Jurassic rifting of the Fundy Basin region (Wade et al. 1996; Withjack et al. 2009), as well as precursory Late Palaeozoic basin development (Eisbacher 1969; Murphy et al. 2011; Waldron et al. 2015). When originally proposing this model, Tanner (2002, 2003) referred to preliminary numerical Manicouagan impact modeling results. These suggested a potential energy release of 10^8 megatons resulting in earthquake(s) within the Richter-scale Magnitude 10 range, and estimated vertical ground displacements of up to 5 m at 700 km distance from the crater site to the northwest (see also Walkden and Parker 2008; Collins et al. 2005). However, as in the case of many impact-related geologic models, technical acceptance of this 'cause and effect' association presumably will require more detailed, data-constrained intra-Norian tectonostratigraphic modeling. Schedl (2015) for example, has discussed various Recent age earthquake magnitudes and effects in a marine impact-related context, highlighting the physical constraints on fault-slip trigger mechanisms imposed by tectonic setting and the style of plate margin activity.

5.3.3.6 Additional Tectono-sedimentological Evidence

None of the confirmed terrestrial Late Triassic impacts currently has a direct marine connection, other than the interpreted Manicouagan-associated pelagic ejecta deposits identified in central and southwestern Japan. However, as noted in Schedl (2015), relatively thin distal ejecta units potentially may also be found to directly overlie marine 'seismites', i.e., slope-failure features such as slumps and possibly displaced Norian olistostrome shelfal units as described in Fink (1975, p. 33; see also Orchard et al. 2007, Fig. 4), if remotely triggered by larger terrestrial (as well as marine) impacts. The former author has also discussed the potential nature and stratigraphic implications of impact-related tsunami deposits in epeiric marine (and presumably larger lacustrine) domains (see also Dypvik and Jansa 2003), subject to the interpretational constraints/approaches discussed in Shanmugam (2016, 2017). Of particular note is the competing diversity of alternative wave-generating mechanisms, especially paleoearthquake triggers in response to both plate margin tectonism and dynamic (back arc) volcanic activity. With regard to the Manicouagan event, this may be addressed in part by employment, where possible, of refined marine chronostratigraphic calibration techniques potentially incorporating the distal chemo- and biostratigraphic signatures recently described from Japan (Onoue et al. 2012, Supplement 1; Onoue et al. 2016; Sato et al. 2016).

5.4 The Norian Manicouagan Impact

General geological summaries of the Manicouagan impact structure (N 51° 23°, W 68° 42°) are presented in Spray et al. (2010), Thompson and Spray (2013) and Brown et al. (2016) together with supporting technical references. Approximately 130 pertinent publications are listed on the EID (MIRP) website, with initial research commencing in the early 1960s. Further details including field images (as well as complementary information on other Late Triassic impacts) are presented at www.craterexplorer.ca/manicouagan-impact-structure/. Being large, complex, relatively well preserved, and accessible, Manicouagan has become one of the most extensively studied impact structures on Earth. The impact crater site is considered "unique amongst the large terrestrial impact craters (D ≥ 90 km) in that its impact melt sheet is exposed, accessible, and undeformed…" (O'Connell-Cooper and Spray 2010). Research is continuing currently through MIRP (Thompson and Spray 2013). Recent work (e.g. Thompson and Spray 2017) has focused on increasing the already significant understanding of complex crater tectonic processes, the formation and evolution of impact melt and subjacent breccias plus associated hydrothermal circulation systems, in addition to controls on assorted shock phenomena. Interpretations have been based on multiple datasets acquired through extensive fieldwork, supported by extensive drill cores (38 holes, ~18 km total

footage) plus subsurface remote sensing, including both 2D seismic and vintage gravity surveys (Brown and Spray 2015). Results of these integrated analyses have also allowed terrestrial analogue comparisons with various planetary and lunar crater configurations, including those visible on Earth's moon and Mars (Spray et al. 2010).

5.4.1 General Description (Crater Area and Vicinity)

The Manicouagan impact structure (ca. 215.5 Ma, U-Pb melt rock zircon; Ramezani et al. 2005) is located within the Precambrian Grenville geologic province of northeastern Quebec, Canada. This circular remnant crater feature (markedly visible from space) comprises several topographic components, the most pronounced is a flooded, 70 km diameter annular moat (dammed reservoir) surrounding a central, dissected plateau capped by melt rocks (O'Connell-Cooper and Spray 2010). With an estimated crater diameter of ca. 85–100 km (collapsed transient to full) this complex structure is the third largest of the Phanerozoic, after Chicxulub (ca. 150–180 Km) and Popigai (90 km). The Manicouagan target rocks originally formed part of an intracratonic semi-arid area of the northern Pangaea supercontinent (Figs. 5.1 and 5.5) at an approximate paleolatitude of 23° N (Spray et al. 1998), comparable to the present-day mid-Sahara desert. Target lithologies at the time of impact (mid-Norian) consisted of variably thin (<200 m) Ordovician carbonate and shale sedimentary cover resting on Late Proterozoic (ca. 1 Ga) metamorphic basement dominantly comprising quartz-feldspar gneisses and local anorthosites. Thackrey et al. (2008) noted these crystalline target rocks are "exceptionally rich in heavy minerals, typically garnet, zircon, biotite, olivine and rutile.", and used the respective garnet suites to provenance-match those found within interpreted Manicouagan clastic ejecta deposits preserved locally in southwestern Britain, some 2000 km to the east at the time (Thackrey et al. 2009).

Sato et al. (2016) analyzed the elemental ratio of the concentrated PGE (Ir, Ru, Rh) anomalies within the Sakahogi pelagic claystone ejecta layer, and several other chemostratigraphically correlatable sections in central Japan. They suggest that the Manicouagan (or possibly another, similar-aged) bolide may have been a large (ca. 3–8 km diameter), non-specific chondritic impactor (i.e. current data resolution precluded an "unequivocal assignment to specific chondrite groups e.g. carbonaceous, ordinary and enstatite."). These authors did not fully discount the possibility of an iron meteoritic component, concluding (pp. 44–45) that the impact most likely resulted in substantial volumes of clastic debris, potentially accompanied by the injection of substantial (chondrite) meteoritic sulphates into the stratosphere. Here, they would be converted to H_2SO_4 aerosols, which block incoming solar radiation and can cause sudden cooling, as documented for large volcanic eruptions (Sigurdsson 1990; Robock 2000). This interpretation suggests the Manicouagan

event may have had significant, probably global, paleoenvironmental and associated biotic consequences during the mid- to late Norian (Alaunian-Sevatian; Chron E15r equivalent in Kent et al. 2017) substage transition, contingent on stage length definition (Lucas 2013).

From a broader perspective, several Manicouagan researchers (including Walkden et al. 2002) have highlighted the apparent global paucity of distal ejecta predicted from modeling (Walkden and Parker 2008; Sato et al. 2016; after Collins et al. 2005). This reasonably might be expected to have occurred, either as a discrete post-impact Chicxulub-style (K-Pg) layer (cf. Artemieva and Morgan 2009), and/or more locally disseminated via syndepositional reworking throughout a broader stratigraphic section (Schedl 2015). As noted above, attempts to identify a similar globally significant PGE-enriched spherule-bearing event horizon within the Norian and uppermost Rhaetian stages *sensu lato* have essentially proved unsuccessful (Tanner et al. 2004; Racki 2012). However, based on preliminary trajectory modeling, Wrobel and Schultz (2003) suggested that Manicouagan would make a "unique crater" for distal ejecta studies. The model presented by these authors (based on 45° and 70° ejection angles) predicted ejecta thicknesses of 5 cm or greater in mid-Norian depositional catchment areas located within ~30° of the impact, i.e. including all of North America, parts of northwest Africa and Western Europe (Figs. 5.1 and 5.5).

In spite of the above model predictions, with the possible exception of the rare "shocked" quartz described by Tanner (2006), no diagnostic Manicouagan (or any other Late Triassic impact) ejecta material have yet been identified within the immediately adjacent (pre-drift) Atlantic conjugate margin synrift successions (Fig. 5.5). This is particularly notable considering that the Passaic and Blomidon Formations of the upper Newark Supergroup (*sensu* Leleu and Hartley 2010, Fig. 1; Sues and Olsen 2015), in addition to their northwest African Moroccan equivalents, are the most accessible and best-studied Norian-aged host sections present within the near-distal strewn field areas.

In comparing potential biotic effects of large Phanerozoic bolide impacts such as Chicxulub and Manicouagan, Walkden and Parker (2008, Fig. 3) modeled a ca. 14 mm-thick ejecta layer for the latter event at a Norian section in southwestern Britain 2000 km (pre-drift configuration) from the crater site in eastern Canada. However, the layer thickness observable at this (former quarry) outcrop locality was described as being locally variable in distribution and thickness, probably a result of high energy reworking (Kirkham 2003, 2006). In contrast, the significantly more distal Japanese Sakahogi ejecta layer of Onoue et al. (2012) is separated from Manicouagan by nearly 180° longitude and comprises a compacted, but otherwise undeformed and continuous, 8 mm-thick, PGE-rich pelagic claystone layer. This implies significantly greater ejecta layer thicknesses were likely deposited across proximal strewn fields, particularly within North America, the Boreal Arctic region, Northwest Africa and Europe (northern Pangaea, Fig. 5.5).

Fig. 5.5 Late Triassic (210 Ma) paleogeographic map showing the Manicouagan impact crater location in relation to key North American sedimentary basins, containing the (cored) Newark Supergroup and Chinle Group lithofacies units among other successions. The general locations of the eastern Canadian (Fundy Group) and southwestern British (Mercia Mudstone Group) sections discussed in Sect. 5.4 are highlighted. (Modified from Blakey 2014)

5.4.2 Distal Evidence: Continental Sections

5.4.2.1 Europe: Wickwar, Southwestern Britain

Mercia Mudstone Group. Localized occurrences of non-marine 'glauconitic' spherule (microtektite) pseudomorphs and secondary shocked quartz from southwestern Britain (Fig. 5.6a) have been described in situ by both Walkden et al. (2002) and Kirkham (2002, 2003, 2006, based on earlier 1970s work) as diagnostic evidence of a Late Triassic Norian (probably Manicouagan) impact. The latter author (Kirkham 2003, Figs. 4–10) described these as being "emerald green" in appearance, up to 1.0 mm in diameter and present within "erosional troughs" unconformably resting

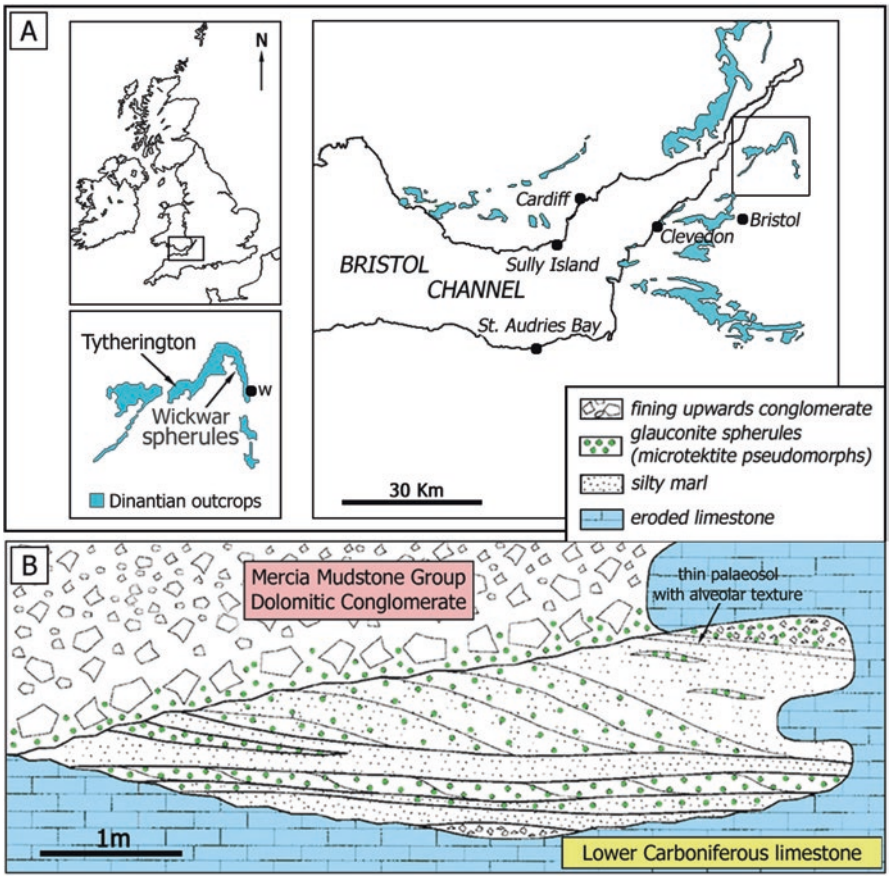

Fig. 5.6 Location and outcrop features of Mercia Mudstone spherule deposit. (**a**) Outline map of the eastern Bristol Channel area, southwestern Britain indicating the location of the (former) microspherule localities at Churchwood Quarry, near Wickwar, north of Bristol. (**b**) Sketch detail of the "largest and most accessible spherule-bearing lens" within the Norian-aged basal Mercia Mudstone Group resting unconformably on Lower Carboniferous (?karst) limestone. (Modified from BGS Geology of Britain Map [Accessed 2017] and Kirkham 2003, Figs. 2 and 3)

on Lower Carboniferous (Arundian-Holkerian) Clifton Down Limestone Formation basement at Churchwood Quarry, Wickwar, north of Bristol. The basal Mercia Mudstone Group (Carnian-Rhaetian) host section comprises a "partly cross-bedded deposit, approximately 6 m across and 1 m thick dominated by hard and soft silty marls." (as illustrated in Kirkham's Fig. 3; see also Fig. 5.6b). In contrast, Walkden et al. (2002) described a different spherule bed in the same quarry as ranging "in thickness from 0 to 150 mm (average of 25 mm from eight points that were sampled within a 200 m-wide region) and shows evidence of turbulent reworking in water such as grading, convolution, rippling, and mixing with local mud and lithoclasts".

Both authors described in contrasting detail, the morphological, geometric and geochemical characteristics of the respective spherule datasets, concluding, via comparisons with Chicxulub impact spherule ejecta, that the Late Triassic spherules represented 'splash form' microtektite pseudomorphs resulting from extensive diagenetic clay alterations of original unstable (impact melt/vaporization) glass products. The role in this process of glauconite *sensu lato* (Jeans 2006) and its implications for an aqueous marine contribution was subsequently discussed in Huggett (2004). The feasibility of the proposed spherule model was also reviewed by Glass et al. (2003), who accepted the interpreted impact melt origin subject to further geochronological constraints with respect to a source crater, and demonstration of spherule-bearing beds at other localities. In a follow-up study, Thackrey et al. (2008, 2009) later confirmed a 'Manicouagan-aged' (i.e. ca. 214 Ma) microtektite source via authigenic K-feldspar radioisotopic dating and discrete geochemical fingerprinting of associated allochthonous heavy mineral suites. The latter included detrital garnets that display geochemical characteristics comparable to those analysed from the Manicouagan Grenvillian target rocks, impact melt and central uplift. Use of both techniques suggesting that similar clastic ejecta may be identifiable in other parts of the Manicouagan strewn field in the absence of spherulitic-microtektites and the more traditionally diagnostic shocked quartz evidence, within age-correlative stratigraphic units if preserved.

Confirmed (USM/HF-etch method) shocked quartz (Walkden et al. 2002, Figs. 4 and 5) associated with the spherules strongly support an impact source, although the precise 'fluvial' depositional origin of the variably thick host beds (since removed by quarrying operations) remains uncertain. Particularly concerning is the apparent mineralogic uniqueness of this deposit within the well-studied Mercia Mudstone Group (Leslie et al. 1993; Milroy 1998; Jeans 2006). Kirkham (2003) provided a detailed discussion of the spherule component and its potential origins, with comparisons to widely distributed Chicxulub ejecta that show similar grain morphologies, intragranular geometries and clay mineralogy indicative of diagenetically-altered glassy microtektites, possibly within a saline-influenced environment. This allows speculation on the relative contributions of climatically-driven eolian and aqueous depositional influences on dynamic catastrophic events (Ruffell 1991; Milroy 1998).

5.4.2.2 North America: Bay of Fundy, Eastern Canada

Blomidon Formation. The Late Triassic outcrop maps of key Fundy Group coastal localities interpreted to contain potential distal Manicouagan impact evidence (Tanner 2006, 2013) include the Blomidon Peninsula and Five Islands-Red Head coastal sections, respectively located on the southern and northern margins of the Minas Subbasin of western Nova Scotia (Figs. 5.7 and 5.8). A major structural element in this region comprises the east-west trending Minas Fault Zone (MFZ, including the Cobequid-Chedabucto master fault), an historically active, microplate transform-oblique slip tectonic boundary that separates the northern Precambrian

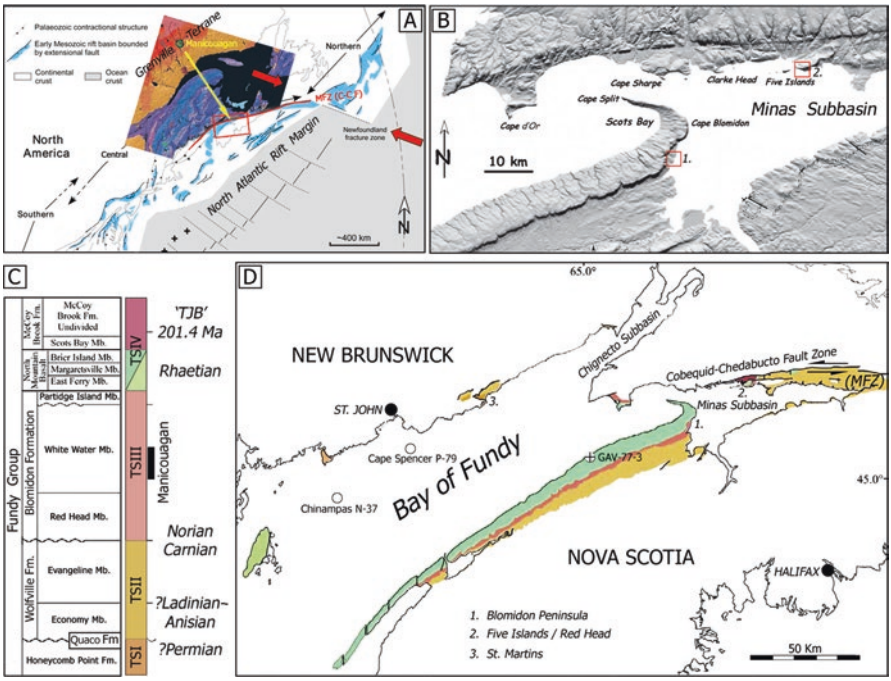

Fig. 5.7 Late Triassic outcrop maps of key Fundy Group coastal localities interpreted to contain potential distal Manicouagan impact evidence. (**a**) Regional setting showing the present-day location of the Manicouagan impact structure. (**b**) Shaded-relief map of the Minas Subbasin, highlighting major structural elements including the Cobequid-Chedabucto (C-CF) master fault (part of the 'Minas Fault Zone' = MFZ), an historically active continent-microplate boundary that separates the northern Avalon terrane from the Meguma terrane to the south. (**c**) Late Triassic Fundy Group stratigraphic column. (**d**) Regional geology map showing key coastal outcrops and locations of pertinent onshore/offshore subsurface and industry well control (i.e. N-37 and P-79). (Modified from USGS I-2781, Thomas 2006, Withjack et al. 2009, 2012, and Sues and Olsen 2015)

Avalon terrane from the Early Palaeozoic Meguma terrane to the south. The southern Minas Subbasin coastal cliff sections described in Ackermann et al. (1995; after Olsen et al. 1989), Gould (2001) and Tanner (2006) are shown in Fig. 5.9. These are assignable to the Norian White Water Member of the Blomidon Formation (Sues and Olsen 2015; also named the Blomidon Member of the Passaic Formation in Weems et al. 2016). Ackermann et al. (1995) attributed the variably-developed 'soft-sediment deformation structures' (SSDS *sensu lato,* Fig. 5.10) to subsidence and gravity collapse in response to intra-Norian meter-scale evaporite dissolution processes in the subjacent section(s). The timing of dissolution is considered to have begun "following the partial lithification of the [upper] fish bed" unit (also containing conchostracans; Ackermann et al. 1995, Fig. 2). However, there is no evidence elsewhere within the Fundy Group successions of comparable evaporite (halite and gypsum) units and/or their derivatives. Whilst the trigger for this (potentially unique)

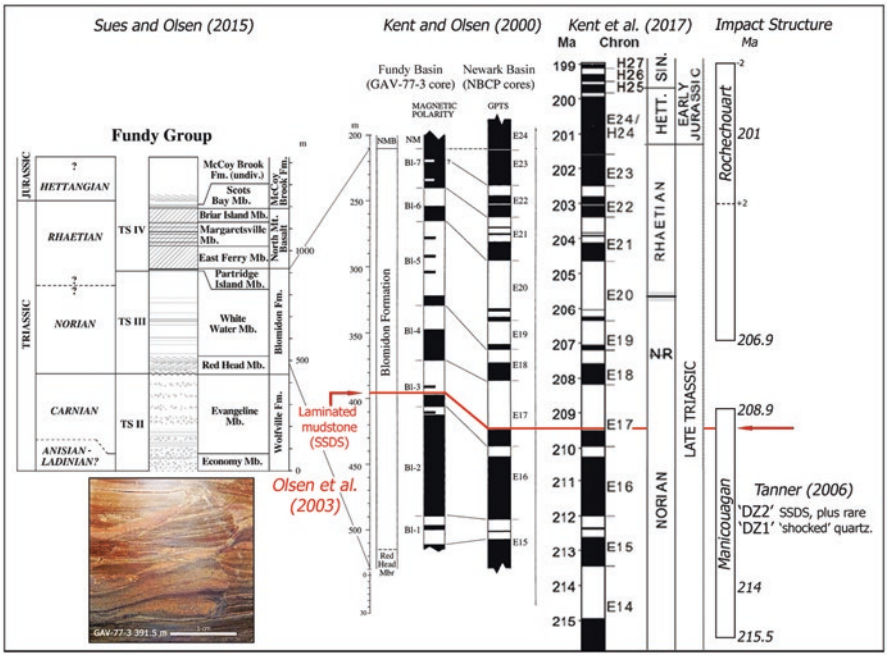

Fig. 5.8 Generalized stratigraphy and age relationships of Fundy Group (Blomidon and Wolfville) formations described within the Minas Subbasin (Sues and Olsen 2015). The magnetostratigraphy of the Blomidon Formation (BF) for the GAV-77-3 drill core and interpreted correlative magnetochrons from the Newark Basin (Kent and Olsen 2000; Kent et al. 2017), are indicated. The approximate stratigraphic positions of the various 'soft-sediment deformation structures' (SSDS *sensu* Shanmugam 2016, 2017), plus the radioisotopic age bars for the Manicouagan and Rochechouart impact structures are also shown. Minor scale(?) salt dissolution-related features evident at ca. 390 m and 397 m in the GAV-77-3 industry drill core were interpreted by Olsen et al. (2003) as potentially correlative with the 'DH1-DH2' deformation zones at Delhaven/Red Head described by Ackermann et al. (1995). Tanner (2006, 2013) subsequently suggested these deformed units may represent seismicity triggered by the Manicouagan bolide impact (ca. 214–215.5 Ma)

basin-wide sedimentary deformation event remains disputed, fault-related seismicity is considered to be one of several potential causal mechanisms (cf. Lake Lisan examples in Alsop and Marco 2011). Given this possibility, Tanner (2003, 2006, 2013) subsequently suggested such movement(s) may have been related to the Manicouagan bolide impact located in northeastern Quebec, Canada approximately 750 km to the northwest. Supporting evidence presented by the latter author included "potential impact-generated" shocked quartz and chondrulitic-style feldspar sandstone grains from the top of Unit 'DZ1' exposed in the northern Minas Subbasin Red Head section located ca. 35 km northeast of the Blomidon Peninsula (Figs. 5.11 and 5.12). More recently Thompson and Spray (2014) have described proximal impact-related arenaceous 'seismites' from within the Manicouagan crater vicinity, containing both fine angular (?fluvial) and larger rounded (?eolian) quartz grains,

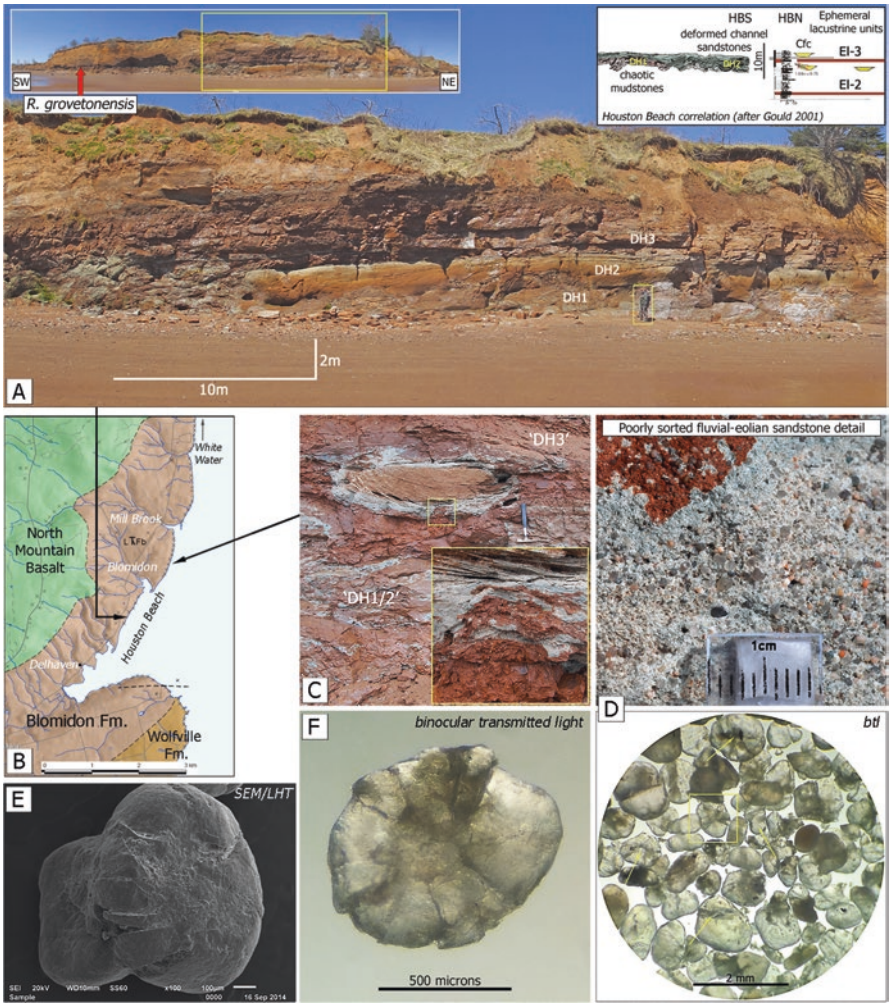

Fig. 5.9 Features of the Blomidon Formation deformation zones. (**a**) Panorama of the southern Minas Subbasin coastal cliff section at Houston Beach 'South' (HBS/Delhaven) described in Ackermann et al. (1995), Gould (2001), and Tanner (2006). The arrow shows the approximate location of the Aluanian (mid-Norian) conchostracan identified as *Redondestheria grovetonensis* (Weems et al. 2016, pers. comm.). (**b**) Location in the southern Minas Subbasin of Blomidon Formation (Norian White Water Member) coastal outcrops ca. 5 km SSW of the stratigraphic type section defined in Sues and Olsen (2015). (**c**) Detail of a Houston Beach 'North' (HBN) confined fluvial channel ('Cfc') subfacies (Gould 2001). (**d**) Basal channel sandstone containing locally-developed brittle microdeformation features including quartz grain spallation (**d**, **e**, & **f**) suggestive of contact concussion (Solid geology map modified from Moore et al. 2009)

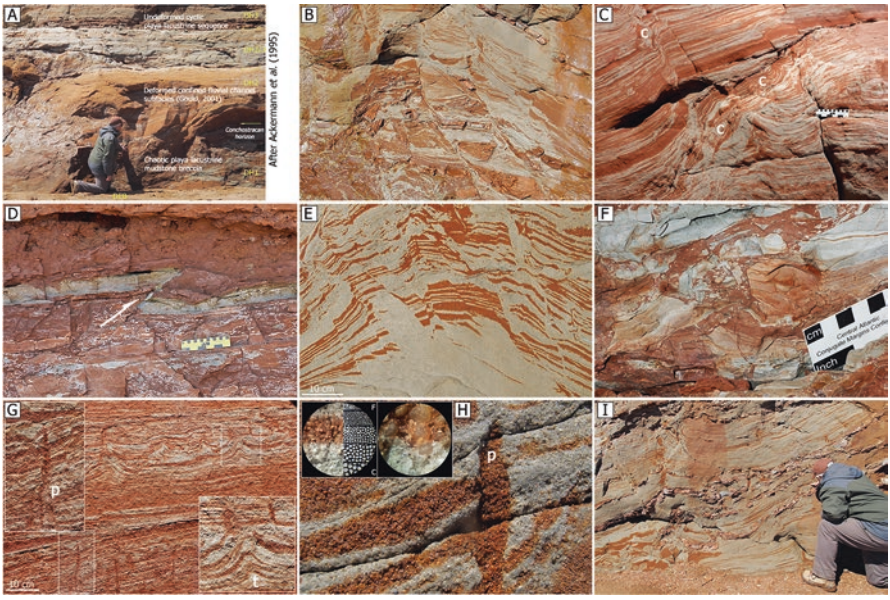

Fig. 5.10 Examples of macroscale sedimentary deformation (SSDS *sensu lato*) observed within the Blomidon Formation (White Water Member) at Houston Beach. (**a**) Deformation unit terminology (DH) after Ackermann et al. (1995). (**b**) Complexly-faulted sandstone/mudstone brittle deformation and brecciation. (**c**) Convoluted (c) fluvio-eolian sandstones. (**d**) Low-angled intramudstone minor reverse fault (arrowed) with uppermost bed undisturbed. (**e**) Variable synsedimentary fault styles in color-banded DH2 fluvial channel sandstones, (**f**) Chaotic sandy mudstone collapse breccia (DH1). (**g**) Vertical flame (*p* pipe) and other fluid escape structures (t)—detail in (**h**), showing typically coarse-grained eolian sand component. (**i**) Disorganized brittle and ductile 'chaotic' bedding

considered by these authors to be of possible early post-impact mid-Norian age. This description suggests a proximal impact signature may exist for siliciclastic comparisons, specifically relating to potential seismites and/or early post-impact transportation of unconsolidated sand-grade material. An impact-triggered paleoearthquake origin for similar 'seismite-style' sedimentary expressions within the younger Rhaetian (Lilstock Formation, Cotham Member) exposed throughout western Britain was also suggested by Simms (2003, 2007), although this model was subsequently disputed by Lindström et al. (2015) in favor of synchronous CAMP-related volcanic activity (Blackburn et al. 2013).

Cashman et al. (2007) have evaluated sedimentary microstructures in unlithified, near-surface siliciclastics in an attempt to differentiate between earthquake rupture-related (seismic) and creep-related (aseismic) deformation mechanisms within the San Andreas Fault region of western California. These authors concluded that certain grain microdeformation styles (among other factors) might be indicative of coseismicity in variably saturated unlithified sediments, potentially comparable to the weak (Barringer Class 1b) impact shock concussion fractures reported by

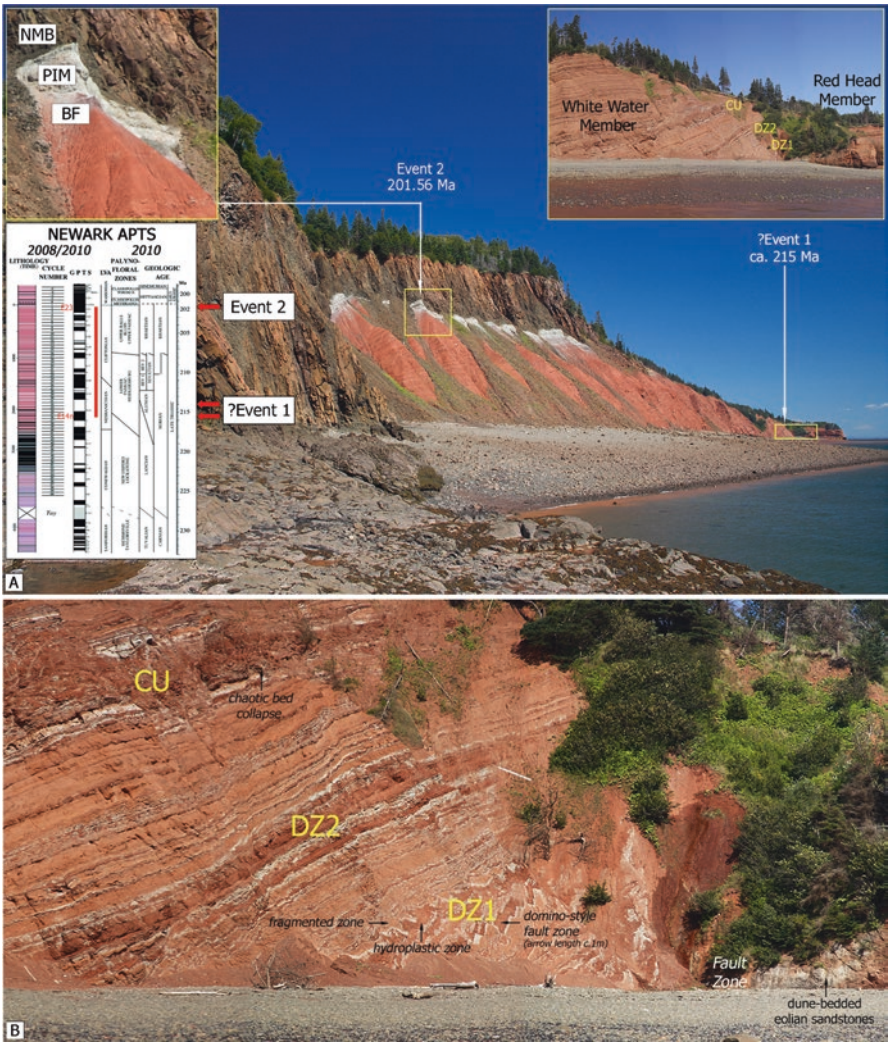

Fig. 5.11 Event horizons within or bounding the Blomidon Formation exposed on the northern shore of the Minas Subbasin near Five Islands. (**a**) Coastal section of the Blomidon Formation (Norian-Rhaetian?) below the North Mountain Basalt (NMB) looking east. Constituent units are, from top to base, the Partridge Island (PIM), White Water and Red Head Members (Fig. 5.8). (**b**) Detail of the 'seismite' zones DZ1 and DZ2 described by Tanner (2006) at Red Head, beneath the uppermost 'collapsed unit' (CU) interpreted by Ackermann et al. (1995) as potentially correlative with the southern Minas 'DH2' deformed sandstone unit (Figs. 5.9 and 5.10). The radioisotopically-dated 'event horizons' indicated refer to the interpreted Manicouagan impact (1) and onset of northern Minas CAMP volcanism (2 = basal NMB; Blackburn et al. 2013), representing a time interval of approximately 14 Myr

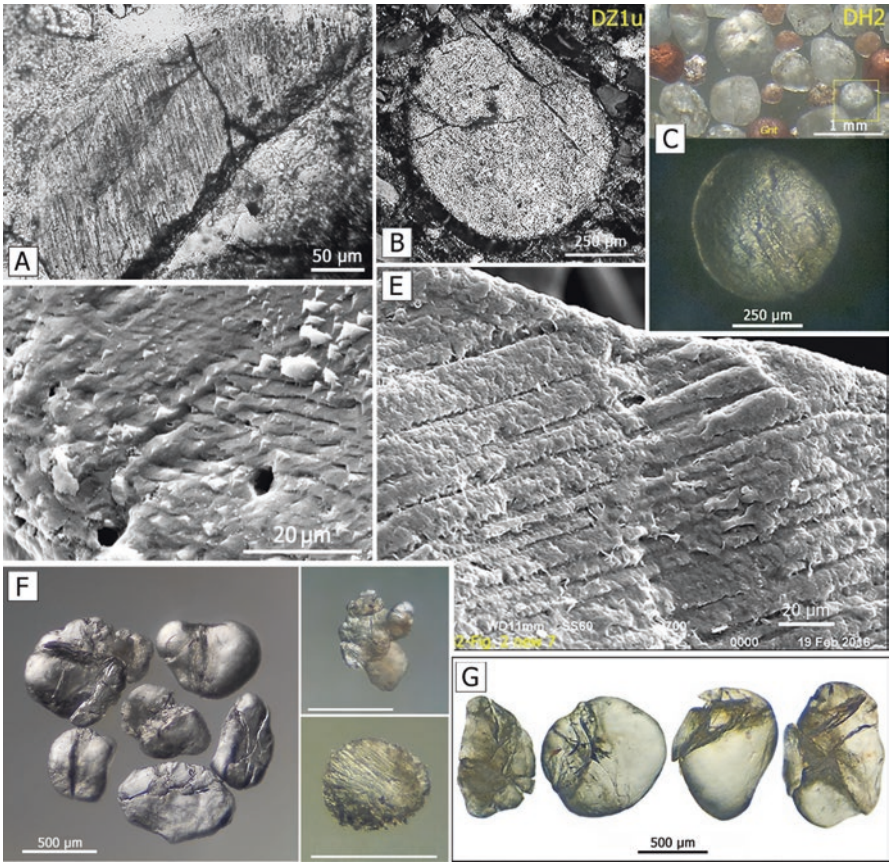

Fig. 5.12 Photomicrographs of fluvio-eolian siliciclastic grains from the lower Blomidon Formation Red Head section (Fig. 5.11b) potentially indicative of (?impact-related) seismic shock. (**a**) Toasted quartz grain showing a single set of planar lamellae (PPL). (**b**) Subspherical grain of partially sericitized albite (XPL) described in Tanner (2006). (**c**) For comparison to (**b**), Houston Beach DH2 channel sandstone feldspar diagenetic alteration and associated heavy minerals (garnets). (**d**) SEM view of an HF acid-etched DZ1 quartz grain displaying intersecting planar features (Tanner 2006). (**e**) For comparison to (**d**), an example from the upper Wolfville Formation (Carnian -?Ladinian Evangeline Member) coastal section in the southern Minas Subbasin (Tanner et al. 2016, pers. comm.). (**f**) Examples of eolian quartz grain alterations from near base collapsed unit 'CU' (Ackermann et al. 1995), including brittle microfracturing similar to that observed in: (**g**) Tectonized grain samples collected from the Lower? Norian eolian sandstone Red Head Member fault-juxtaposed to the east

Kieffer (1971) from the Coconino Sandstone at the 1.2 km-diameter Meteor (Barringer) Crater, Arizona. Preliminary petrographic work (binocular microscope and SEM) conducted by the current authors on sandstone samples from several Fundy Basin localities in both the southern and northern Minas Subbasin has revealed relatively rare examples of quartz grain concussion signatures (Figs. 5.9 and 5.12). Samples of particular interest include fluvio-eolian sandstones collected

from the DH1 and DH2 deformation zones described by Ackermann et al. (1995) at Houston Beach. Here are found grains displaying open fracture ('spallation') features (Figs. 5.9d–f) similar to those considered by Ernstson et al. (2001) to represent dynamic contact concussion. However, controls and timing of the observed granular microdeformation features, as well the potential co-occurrence of diagnostic distal ejecta material (shocked quartz, spherules and/or heavy minerals) remain uncertain.

Quaco Formation. Highly fractured, dominantly quartzite cobbles characterize the (Carnian-Ladinian) fluvial conglomeratic Quaco Formation (Nadon and Middleton 1985; Leleu and Hartley 2016; see also Weems et al. 2016) at St. Martins on the western Bay of Fundy coast (Fig. 5.7). They have also tentatively been interpreted by Tanner (2013) as evidence of a major regional paleoseismic event, possibly synchronous with that discussed above for the lower Blomidon Formation. As noted by the latter author, the observed brittle deformation styles (Fig. 5.13) share similar characteristics with early Triassic Buntsandstein intensely fractured conglomerate cobbles interpreted by Ernstson et al. (2001), and Ernstson and Hiltl (2002) as (proximal) shock signatures of an undetermined Palaeogene

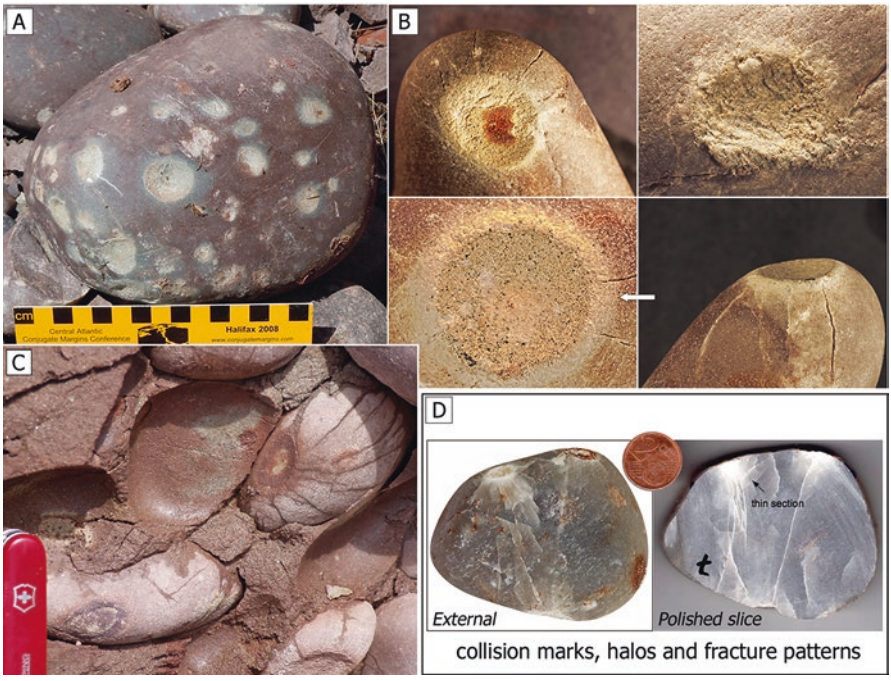

Fig. 5.13 Summary of the Quaco Formation cobble deformation features described and discussed in Tanner (2013). (**a**) Circular to elliptical surface markings and indentations. (**b**) Halo and radial fracture details. (**c**) Outcrop detail showing *in situ* cobble deformation features within a fluvial sandstone matrix. (**d**) Illustration of external versus internal collision marks, contact halo and associated fracture expressions (polished slice courtesy of Kord Ernstson)

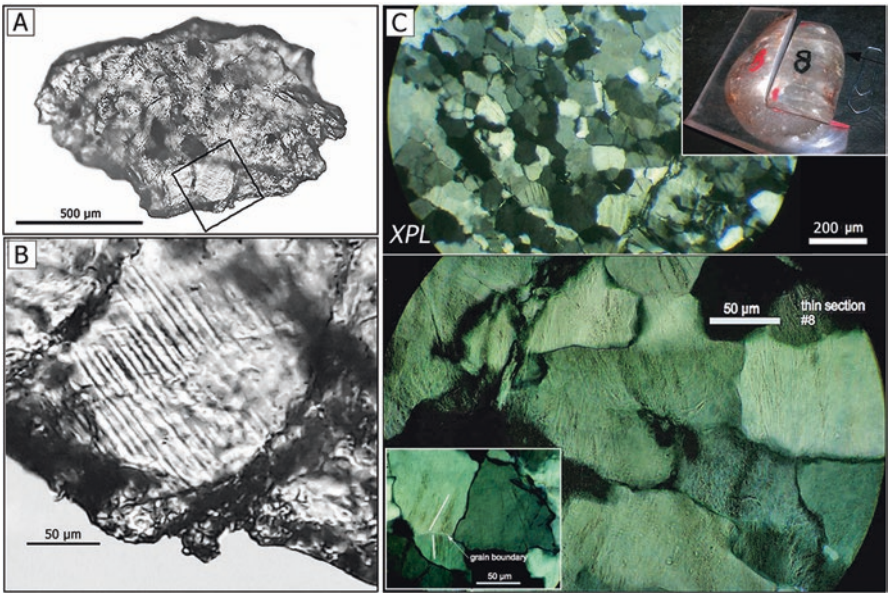

Fig. 5.14 Photomicrograph images of internal Quaco Formation quartzite clast microdeformation features. (**a**) Parallel planar sets observed locally on a thin quartzite chip using a variably-angled transmitted light source. (**b**) Binocular enlargement of a single quartz grain lamellae applying the same technique. (**c**) Traditional petrographic thin section (XPL) views of multiple quartz intragranular planar lamellae sets (PF and/or ?PDFs) interpreted, among other factors, to be indicative of dynamic clast-on-clast (seismic) shock collision (prepared by Kord Ernstson)

terrestrial impact. General similarities, notably in both external and internal microfracture patterns (Fig. 5.13) plus intragranular planar features observable in thin-section (Fig. 5.14c) would appear to support a common, dynamic clast concussion causal mechanism. However, consistent with the general interpretative impact-connection constraints discussed by Racki (2012), past workers (deVries Klein 1963; Chapman et al. 2004) have suggested a variety of alternative, causal explanations, including transport percussion, overburden compaction/contact pressure-solution and local/regional tectonism. While a precise origin of the multiple Quaco cobble fracture styles still remains uncertain, the Tanner (2013) model considers that, contingent on post-Carnian burial history, they more likely reflect major (fault-assisted) regional seismicity potentially triggered by the Manicouagan impact. As acknowledged by this author (pp. 579–581) any original impact-related effects are also very likely to have been overprinted (diluted) by a combination of subsequent terminal Triassic and younger CAMP activity, regional plate margin extensional rifting, basin inversion and possibly glacial isostasy.

Paleoearthquake analogues for the Quaco clast deformation styles possibly comprise similarly fractured Late Carboniferous and Late Cretaceous (Oakland) conglomeratic lithofacies described by Eisbacher (1969, Fig. 7) and Strayer and Allen

(2008) from geologically active strike-slip fault zones in central Nova Scotia (CC-F/MFZ) and northern California (Hayward Fault) respectively. More locally, Latjai and Stringer (1981) described preferentially orientated (orthogonal joint system 'A') fracture sets within the Quaco unit, which extend throughout parts of eastern New Brunswick and are possibly tectonically inherited from older, more regionally extensive Palaeozoic stress fabrics discussed in the same paper. In this context Plint (1985) subsequently described a Late Carboniferous (Pennsylvanian) "earthquake bed" (SSDS) potentially reflective of shallow upper crustal, plate suture weakness trends in the greater Fundy region (Thomas 2006; Withjack et al. 2009, 2012).

5.4.3 Distal Evidence: Marine Sections

Sakahogi, central Japan. As referred to above, clear evidence of impact ejecta (spherules and PGE anomalies) preserved in a distal marine setting occurs within Upper Triassic successions of the subduction-generated accretionary complexes of central and southwestern Japan (Onoue et al. 2012; Sato et al. 2013, 2016). Specifically, Onoue et al. (2012, Fig. 4) and Sato et al. (2013, 2016) described late mid-Norian (latest Alaunian) clinochlore-rich chlorite microspherules and Ni-rich magnetite-spinel grains from thin pelagic marine claystones in various bedded chert-dominated sections. These were first observed at Sakahogi in the Inuyama-Kamiaso area of the Mino Belt of central Japan (Fig. 5.1), where they are confined to the lower part of a single 4–5 cm-thick claystone bed (Sato and Onoue 2010; Sato et al. 2013, Fig. 2). Subsequently, they were identified at other Mino Belt locations as well as in the Chichubi Belt to the southwest (Sato et al. 2016, Fig. 2). The age of the claystone layer is tightly constrained by radiolarian and conodont biostratigraphy and potentially contemporaneous with the southwestern Britain spherule layer(s). An impact origin for the deposit components is supported by detailed PGE (including Ir) and Os isotopic analyses. In addition to elevated levels of PGEs in the microspherule-bearing claystone, Sato et al. (2013, 2016) document peak PGE/Al_2O_3 and siderophile element/Al_2O_3 ratios, demonstrating that these concentrations were not a consequence of simple changes in sedimentation rate. Specific details of the supporting biostratigraphic datasets are provided in Supplement 1 of Onoue et al. (2012). Additional information on these occurrences also appears in Onoue et al. (2016) and Sato et al. (2016).

5.4.4 Stratigraphic Implications

Significant uncertainty still exists concerning the timing of the Manicouagan event based on the nature of presented (extra-crater) stratigraphic evidence alone. The radioisotopic crater ages shown in Table 5.2 range from 208.9 Ma ± 5.1 Ma by (U-Th)/He measurement of titanite grains from the central uplift (Biren et al. 2014)

to 215.5 ± 1 Ma using the U-Pb method on meltrock zircons (Ramezani et al. 2005). As the latter accords well with the earlier U-Pb measurement of 214 ± 1 Ma (Hodych and Dunning 1992), and is much more tightly constrained, it is now widely cited as the agreed impact age. This timing overlaps with a wide selection of candidate sections representing the thickly developed mid-Norian (Aluanian) Substage (*sensu* Ogg et al. 2014, 2016) in eastern North American (Figs. 5.2 and 5.8). However, in spite of extensive research, supported by highly calibrated core control through key sections, unequivocal Manicouagan distal ejecta is not reported from any of the Late Triassic Newark Supergroup basins, or in similar-aged units in the southwestern United States. The latter include the continental Chinle and equivalent groups in the Colorado Plateau area, shallow marine equivalents represented by the Luning/Gabbs and San Hipolito Formations in western Nevada and southern California respectively, in addition to the western Canadian and Arctic basins to the north (Fig. 5.5). The reasons for this apparent absence are uncertain, but possibly related to poor ejecta preservation potential in sedimentologically-active, semi-arid to arid continental environments and/or depositional hiatii in the Norian sections of interest examined to date.

Microspherules/tektites and shocked detrital quartz were originally described from localized fluvial deposits of the (undifferentiated) Norian Mercia Mudstone Group in southwestern England (Walkden et al. 2002; Kirkham 2002, 2003). ^{40}Ar-^{39}Ar dating of authigenic K-feldspar from this layer in the former publication yielded an age of 214 ± 2.5 Ma, consistent with the then widely-supported U-Pb zircon value obtained by Hodych and Dunning (1992) for the Manicouagan crater. Referring to glassy (splash form) microtektite preservation at the British ejecta site, Walkden et al. (2002) suggested that preservation potential may have been enhanced by the presence of standing water, which is essential for the hydration and palagonitization processes evident in the highly altered spherulized microtektite pseudomorphs ('spherules'). On the same subject Tanner (2006) also referenced the potentially preventative "dynamics of eolian and sheetwash sediment movement" in an environment of "exceedingly slow" sediment accumulation, although deformation of the sediment surface by gravity collapse (Ackermann et al. 1995) potentially may have allowed localized 'nesting' of ejecta material within paleotopographic lows. Kirkham (2003, 2006) commenting on the uncertain stratigraphic nature of the spherule deposits in southwestern Britain, concluded they were most likely fluvially-reworked, although this author's figured spherule images do not show signs of extensive transport abrasion.

Subsequent work on marine pelagic deposits of onshore central and southwestern Japan (Onoue et al. 2012, Fig. S7; Sato et al. 2013, 2016, Fig. 1) identified a microspherule (tektite) layer also potentially attributable to the Manicouagan impact, with a suggested age of late Alaunian (or possibly earliest Sevatian; *Epigondolella postera* to *E. bidentata* zonal transition) based on a detailed radiolarian and conodont biostratigraphy (Fig. 5.2).

5.5 Late Triassic Impact Effects

5.5.1 Paleoenvironmental Changes

As described above, early searches for Late Triassic distal impact signatures, namely shocked quartz and/or associated PGE (Ir) geochemical anomalies, in familiar stratigraphic sections of North America and Europe have largely proved disappointing. The extinction-related multiple impact hypothesis (Spray et al. 1998) tentatively suggested that widely distributed distal ejecta were likely to occur in vicinity of the then accepted terminal Triassic extinction event, and by extension, earlier horizons would likely record similar biotic crises, albeit of lower magnitude. Walkden and Parker (2008) presented generalized Chicxulub (150 km) vs. Manicouagan (85 km) comparative models based on relative size, hypervelocity speed, approach angle and other trigger factors, to determine potential global environmental effects of two of the largest Phanerozic terrestrial impacts. These authors concluded (Fig. 2) that impact location (target geology and paleogeographic position) and timing (biological/geological evolutionary status) were most likely major contributory factors to any associated extinction severity. Schedl (2015) provided a comprehensive account of potential marine impact effects including seismically induced shelf-slope failure, submarine landslides, slump sheets and offshore tsunamis (cf. Bralower et al. 1998; Deptuck and Campbell 2012, after Jansa and Pe-Piper 1987). Tackett et al. (2009) have also remarked that the apparent disparity between the Chicxulub and Manicouagan events with respect to biotic effects possibly reflects differences in paleoecological resilience and/or resistance to rapidly induced change. Alternatively, perhaps insufficient biostratigraphic control currently exists to determine accurately the appropriate biotic group responses within multiple affected marine and terrestrial habitats (see also discussion in Schmieder et al. 2010a).

Racki (2012) has similarly reviewed the general manner in which mass extinctions causally reflect interaction(s) of both longer-term biospheric stress processes and comparatively rapid (punctuated/catastrophic) events *sensu* Ager (1995). Consequently, a satisfactory understanding of major (potentially unique) biotic crises requires an integrated, case-by-case approach that also considers alternative contributory causal mechanisms, the geological expressions of which may further be complicated by temporal and/or geospatial overlap. White and Saunders (2005) for example, have discussed the coincidental significances of volcanism, impact and mass extinction phenomena (see also Ernst and Youbi 2017). A number of mechanisms are invoked to explain the Late Triassic extinctions, such as paleoclimatic changes (long-term aridification and/or pluvial episodes; Simms and Ruffell 1990), eustatic sea-level fluctuations, changes in ocean salinity or oxygenation, and, atmospheric perturbations caused by severe CAMP volcanic outgassing and/or dissociation of sea-floor methane hydrates (Hautmann 2004; Marzoli et al. 2004,

2017; Tanner et al. 2004, 2007; Golonka 2007; Nomade et al. 2007; van de Schootbrugge et al. 2007, 2008, 2009, 2013; Hautmann et al. 2008; Schaltegger et al. 2008; Whiteside et al. 2010; Ruhl et al. 2011; Schaller et al. 2011; Pálfy and Zajzon 2012; Pieńkowski et al. 2012, 2014; Richoz et al. 2012; Blackburn et al. 2013; Lindström et al. 2017; Lucas and Tanner 2017). Thus, the environmental significance of bolide impact events would seem to depend on the context and timing of extant terrestrial and marine biospheric processes, in addition to bolide size and location.

Tanner et al. (2004) discussed the nature of several interpreted extinction scenarios in a comprehensive review of potential causes of multiple Late Triassic biotic turnovers. The authors concluded that the common misconception of a single catastrophic end-Triassic extinction (cf. Chicxulub) is unsupported by the paleontological record, but instead results from location/sample bias and stratigraphic correlation uncertainties. Instead, they suggested a significant number of major marine and terrestrial biotic groups experienced step-wise pulses of decline in diversity throughout the entire epoch, combined with low origination rates. These crises are evidenced at: (i) the Carnian-Norian boundary, (ii) within the Early Norian, (iii) the Norian–Rhaetian boundary, (iv) within the Rhaetian, and (v) at/near the TJB (see also Lindström et al. 2017 and references therein). In the case of impact-induced environmental traumas, the same authors stated that their clarification has traditionally remained largely contingent on the dual confirmation of crater age and unambiguously identifiable (i.e. correlative) distal evidence upon which to base detailed paleoecological assessments. These constraints are further complicated by the wide diversity of declining marine faunal groups such as ammonoids, bivalves and conodonts during the Norian-Rhaetian (Silberling 1985; Tanner et al. 2004; Tackett and Bottjer 2012, 2016; Onoue et al. 2012, 2016) and various terrestrial vertebrate assemblages, notably tetrapods (Olsen et al. 2010). The latter authors noted that direct evidence for an impact precisely at the TJB (201.4 Ma; Ogg et al. 2016) is lacking, although currently bracketed by the radioisotopic age uncertainty ranges of both Rochechouart (ca. 207–201 Ma; see Cohen et al. 2017) and Red Wing (200 ± 25 Ma) noted in Schmieder (2010). However, the smaller sizes of these two particular impacts dictates their limited role as significant drivers of extinction.

5.5.2 Biotic Response

Attempts to apply a catastrophic impact theory (Alvarez et al. 1980) to other Phanerozoic mass extinction boundaries, including (unsuccessfully) the ammonoid-defined Triassic-Jurassic transition (Olsen et al. 1987; Tanner et al. 2004; Onoue et al. 2012) are summarized and discussed at length by Racki (2012). The latter author expressed concern regarding data-constrained interpretational ‘force-fitting’ to preconceived biotic crisis models, which he termed the “great expectations

syndrome." Based on this critical review, he assigned research categories leading to potential misunderstandings into three successional model 'test' levels respectively relating to (a) factual misidentification (ambiguous datasets), (b) correlative misinterpretation (geochronologic uncertainty), and (c) causal overestimation (signature and scale of contemporaneous catastrophe). Until recently (cf. Onoue et al. 2016) most, if not all previously proposed Late Triassic impact-related extinction 'scenarios' failed to progress beyond the first level, reflecting "an erroneous or indefinite recognition of the extraterrestrial record in sedimentological, physical and geochemical contexts." This terminology is equally applicable to both the marine and continental terminal Triassic candidate extinction horizons across multiple regions. They all failed to confirm an unequivocally unique impact origin for either 'PDF-style' detrital quartz lamellae (Badjukov et al. 1987); Bice et al. 1992; Mossman et al. 1998) and/or anomalously elevated (terrestrial) Ir levels (Olsen et al. 2002a, b; Tanner and Kyte 2005; Tanner et al. 2008, 2016), as discussed above.

Recognition that mass extinction causes represent a complex interaction of long-term ecosystem stress processes and geologically rapid, catastrophic disturbances (including bolide impacts; cf. Chicxulub discussion in Renne et al. 2013) led Racki (2012) to recommend a "holistic event-stratigraphic approach" to multicausal environmental traumas, refinable on a case-by-case basis. Preliminary modeling of the Manicouagan impact (Walkden and Parker 2008; Wrobel and Schultz 2003) suggests that this major mid-Norian event could have had a measurable global impact on both marine and continental biospheres. The potential (biochemical, climatic) effects of the impact significantly predate (ca. 215.5 vs. 201.5 Ma), and are thus not causally competitive with, the late Rhaetian CAMP emissions, associated seismicity and other chemical imbalancing described by Lindström et al. (2015, 2017) and others. Consequently, a conclusive Manicouagan signature may yet prove to be determinable for certain biotic groups, especially those in the marine realm.

The taxonomic and paleoecological aspects of Late Triassic benthic, nektonic and pelagic marine faunal assemblages within the Tethyan, Panthalassan and Boreal Ocean domains have been studied extensively, in variable detail and collectively provide a practical basis for correlatable Carnian, Norian and Rhaetian biostratigraphic reference. Onoue et al. (2012, 2016) have recently demonstrated that a stepwise radiolarian and conodont extinction event occurred during the last 15 Myr of the Triassic (late Norian-Rhaetian), reflecting a catastrophic collapse of the pelagic ecosystem, initially associated with a decline in pelagic faunal diversity which commenced towards the end of the mid-Norian (Alaunian). These authors tentatively regard this biocrisis as the first documentation of a paleoecological response (decreased biogenic radiolarian silica flux) to the Manicouagan impact event (ca. 214–215.5 Ma). Subject to results of ongoing chemostratigraphic correlative work, the Sakahogi spherulitic claystone section of interest would now appear to provide critical biostratigraphic control for determining whether similar biospheric responses occurred in other marine provinces. Locations to investigate

initially may include paleogeographically discrete Panthalassan and northern Tethyan Norian benthic assemblages in west-central Nevada, USA (Tackett et al. 2009; Tackett et al. 2014; Tackett and Bottjer 2016) and northern Italy (Tackett and Bottjer 2012).

Based on their current accepted ages, the terrestrial effects of confirmed Late Triassic impacts may potentially be reflected within the Adamanian (?Saint Martin), Revueltian (Saint Martin and Manicouagan) and Apachean (Rochechouart, ?Red Wing) land-vertebrate faunachrons (LVFs) proposed by Lucas (2010). Identification of precisely dateable and correlatable 'event horizons' within, or at the boundaries of any of these units would allow a 'before and after' approach to investigating both catastrophic and transitional biotic responses, as discussed in Tanner et al. (2004). More specifically, from a paleogeographic perspective, ejecta distribution modeling of the Manicouagan impact may enable high-grading (via estimated thickness mapping) of those regional biospheres likely to have been most affected. In this respect areas for consideration include selective Norian successions in the Colorado Plateau, USA, such as the Chinle Group, various parts of Europe e.g. the Germanic Basin or the Northern Calcareous Alps region, the Argana Basin of northwestern Africa and the East Greenland Jameson Land Basin.

Impact response investigations within the continental invertebrate community are likely to be more challenging, given the biostratigraphically barren nature of much of the representative Late Triassic continental fluvio-eolian and playa-lacustrine facies associations. However, the presence and biozonal significance of, for example, conchostracans found to occur throughout the generally poorly fossiliferous Newark Supergroup red beds (Kozur and Weems 2010; Weems and Lucas 2015) suggests this faunal group may have been affected, though possibly only within 'local biospheres' (*sensu* Grieve 2017; see also Weems and Lucas 2015, Fig. 16). In this regard, Cameron and Jones (1987) and Olsen and Et-Touhami (2008) have both noted "abundant clam shrimp" (i.e. conchostracans) plus other more discrete occurrences at various Minas Subbasin coastal localities containing the Blomidon Formation deformation zones shown in Figs. 5.9 and 5.10. The Late Triassic Fleming Fjord Formation of the Jameson Land Basin (Clemmensen et al. 1998) has also recently been reported to contain (?Norian-aged) conchostracans locally in association with diverse terrestrial vertebrate assemblages (Sulej et al. 2014). However, if an interpreted distal impact signature in the Bay of Fundy area proves correct, this may have had only a limited, possibly short term 'catastrophic' effect on the respective faunal communities.

5.6 Directions and Recommendations

As recommended by Racki (2012) and others, future attempts to clarify potential impact-related geologic contributions may benefit from applying an integrated research approach that (ideally) is able to:

1. Constrain erroneous/indefinite impact-diagnostic sedimentological, physical and geochemical data, notably petrographic/mineralogical shock and/or melt feature identifications, potentially supported by accepted associative signatures.
2. Minimize impact structure absolute age-dating uncertainty concurrent with proximal to distal correlation errors through (where practical) the integration of high-resolution lithostratigraphic, biostratigraphic, petrographic, radioisotopic, and geochemical data to determine/promote a respective 'event horizon' and reference locality.
3. Avoid causal overestimation of stratigraphic relationships concerning confirmed impact signatures that appear to be only temporally coincident with a given biodiversity decline (turnover/extinction) and other ecosystem collapse attributes, as evidenced within marine, terrestrial and atmospheric domains.

The two widely separated occurrences of interpreted Manicouagan microtektite spherule pseudomorphs, plus associated shocked mineral grains within late mid-Norian (Alaunian) pelagic marine and continental facies of central Japan and southwestern Britain respectively, is significant. Subject to geochronologic confirmation (initially biostratigraphic, mineralogic and geochemical), these deposits strongly suggest that similar stratigraphically-discrete ejecta units are likely to be preserved, and are thus identifiable in other basins possibly in association with impact-induced sedimentary units including 'seismites' *sensu stricto*, tsunami deposits and/or larger chaotic lithofacies groups such as olistostromes. With the dual benefit of PGE-enrichment (e.g. Ir, Os) plus detailed (radiolarian and conodont) biostratigraphic control, global exportation of the Japanese (late Alaunian Substage) event horizon, particularly, would now appear feasible assuming any future impact-diagnostic ejecta datasets have not been subject to extensive sedimentary reworking. Recognition of potentially synchronous, locally fossiliferous fluvio-playa-lacustrine 'seismite' deposits in eastern Canada, located <750 km (ca. 9 crater diameters) southeast of the Manicouagan impact site may provide additional insights concerning the nature and controls on distal ejecta distribution patterns. The respective Bay of Fundy coastal sections thus merit further investigation as a potential paleoearthquake response to the Manicouagan impact event (*sensu* Tanner 2003, 2006), via dynamic regional tectonism, possibly expressed uniquely within a near-distal strewn field capture area. Directly comparable microspherule deposits have yet to be reported anywhere on the North American host continent. However, the demonstrated presence of rare quartz grains displaying possible shock features in similar-aged (mid-Norian) seismically-affected zones suggest critical technical comparisons (*sensu* Reimold et al. 2014) of the reported PDFs. Other granular microdeformation style(s) will be required to determine any common ?Grenvillian provenance, in support of a Manicouagan impact causal origin.

In conclusion, while the evidence relating to virtually all Late Triassic terrestrial bolide impact effects significantly beyond crater signature appears to be severely limited and/or controversial, important clues now exist as to where it might be found stratigraphically, and possibly expressed discretely within the geologic record. As

the third largest impact in the Phanerozoic (after Chicxulub and Popagai), the currently evolving Manicouagan 'global' scenario, if supportable by additional and correlatable diagnostic impact datasets, will enable the development of a working multi-regional (initially North America, Western Europe and Eastern Asia) geologic model with the capacity to be expanded globally. Such an integrated approach offers the potential to:

1. Clarify why researchers have consistently been unable to identify remote impact diagnostic evidence throughout most of the international Carnian, Norian and Rhaetian sections—is it really an ejecta preservation issue?
2. Determine—through selectively focused research—the types of diagnostic impact evidence (physical, geochemical/isotopic and biological) that have remained preserved within the distal stratigraphic record—and the factors controlling these occurrences.
3. Facilitate the applicability of Manicouagan project methods and results to investigating other Triassic impact scenarios, e.g. Saint Martin and Rochechouart, including any direct or indirect contributions to the end-Triassic mass extinction plus multiple earlier, potentially hereditary terrestrial and marine biotic crises events.

5.7 Conclusions

The globally distributed Late Triassic stratigraphic succession represents a combination of variably thick continental and marine tectonostratigraphic units reflecting a complex geologic history of Pangaean supercontinent break-up, CAMP flood basalt volcanism, and initiation of passive conjugate plate margin formation. At least five variably-sized (9–85 km diameter) terrestrial bolide impacts are currently interpreted to have occurred during this paleoenvironmentally sensitive time-frame, three of which (Saint Martin, ca. 228 Ma; Manicouagan, ca. 215.5 Ma; Rochechouart, 201–206.9 Ma) are considered sufficiently large to have left significant traces within the geologic record at local, multi-regional, and possibly global scale. Until recently, research on these (and impacts in general) has traditionally focused on impact structure morphometry, impactite distribution/composition and hypervelocity process modeling, including post-impact metasomatism. An ongoing investigation of longer range distal impact effects, including potential contributions to multiple biotic crises recognized throughout the Late Triassic, has proved to be less successful, especially relating to the latest Rhaetian ETE. Recent confirmation of spherule (microtektite) deposits and associated PGE anomalies in mid-Norian deep sea sediments of central and southwestern Japan supports a need for further investigation of the Manicouagan distal impact signature.

Acknowledgements The authors especially wish to thank Martin Schmieder for his comprehensive review of the current manuscript and impactful comments. Rob Weems, Kord Ernstson, Fernando Claudin and Luther Strayer are acknowledged for their technical contributions, knowledge sharing and informative discussions. Thanks are also extended to Grant D. Wach, Yawooz Kettanah, Ricardo L. Silva, Gordon Brown, Ian Spooner, Rob Raeside, Lucy Thompson, Mike Simms among others, and especially to Bill Richards for his assistance in the field and practical research advice.

References

Ackermann RV, Schlische RW, Olsen PE (1995) Synsedimentary collapse of portions of the lower Blomidon Formation (Late Triassic), Fundy Rift Basin, Nova Scotia. Can J Earth Sci 32(11):1965–1976. https://doi.org/10.1139/e95-150

Ager D (1995) The new catastrophism: the importance of the rare event in geological history. Cambridge University Press, Cambridge

Alexopoulos JS, Grieve RAF, Robertson PB (1988) Microscopic lamellar deformation features in quartz: discriminative characteristics of shock-generated varieties. Geology 16(9):796–799. https://doi.org/10.1130/0091-7613(1988)

Alsop GI, Marco S (2011) Soft-sediment deformation within seismogenic slumps of the Dead Sea Basin. J Struct Geol 33(4):433–457. https://doi.org/10.1016/j.jsg.2011.02.003

Alvarez LW, Alvarez W, Asaro F, Michel HV (1980) Extraterrestrial cause for the Cretaceous-Tertiary extinction. Science 208(4448):1095–1108. https://doi.org/10.1126/science.208.4448.1095

Artemieva N, Morgan J (2009) Modeling the formation of the K-Pg boundary layer. Icarus 201:768–780. https://doi.org/10.1016/j.icarus.2009.01.021

Badjukov DD, Lobitzer H, Nazarov MA (1987) Quartz grains with planar features in the Triassic-Jurassic Boundary sediments from northern Limestone Alps, Austria. Proceedings of the 18th Lunar and Planetary Science Conference, 16–20 March 1987, Houston, TX:38–39

Badjukov DD, Barsukova LD, Kolesov GM, Nizhegorodova LV, Nazarov MA, Lobitzer H (1988) Element concentrations at the Triassic-Jurassic boundary in the Kendlbachgraben section (Austria). In: Stradner H, Faupl P, Grass F, Mautitsch HJ, Preisinger A, Schwarz C, Zobets E (eds) IGCP Project 199, Rare Events in Geology, Vienna, 12–17 September 1988. Abstracts of Lectures and Excursion Guide, Ber Geol Bundesanst 15:1–2

Bice D, Newton CR, McCauley SE, Reiners PW, McRoberts CA (1992) Shocked quartz at the Triassic/Jurassic boundary in Italy. Science 255(5043):443–446. https://doi.org/10.1126/science.255.5043.443

Biren MB, van Soest M, Wartho J-A, Spray JG (2014) Dating the cooling of exhumed central uplifts of impact structures by the (U-Th)/He method: a case study at Manicouagan. Chem Geol 377:56–71. https://doi.org/10.1016/j.chemgeo.2014.03.013

Blackburn TJ, Paul E, Olsen PE, Bowring SA, McLean NM, Kent DV, Puffer J, McHone G, Rasbury T, Et-Touhami M (2013) Zircon U-Pb geochronology links the End-Triassic extinction with the Central Atlantic Magmatic Province. Science 330:941–945. https://doi.org/10.1126/science.1234204

Blakey RC (2014) Deep Time Maps. http://www2.nau.edu/rcb7/namTr210.jpg. Accessed 2014

Bohor BF, Glass BB (1995) Origin and diagenesis of K/T impact spherules—from Haiti to Wyoming and beyond. Meteorit 30:182–198. https://doi.org/10.1111/j.1945-5100.1995.tb01113

Bond DPG, Grasby ES (2017) On the causes of mass extinctions. Paleogeogr Palaeoclimat Palaeoecol 478:3–29. https://doi.org/10.1016/j.palaeo.2016.11.005

Bralower TJ, Paull CK, Leckie RM (1998) The Cretaceous-Tertiary boundary cocktail: Chicxulub impact triggers margin collapse and extensive sediment gravity flows. Geology 26(4):331–334. https://doi.org/10.1130/0091-7613(1999)

Brookfield ME, Algeo TJ, Hannigan R, William J, Bhat GM (2013) Shaken and stirred: Seismites and tsunamites at the Permian-Triassic boundary, Guryul Ravine, Kashmir, India. PALAIOS 28(8):568–582. https://doi.org/10.2110/palo.2012.p12-070r

Brown JJ, Spray JG (2015) Constraining the dimensions of the Manicouagan impact structure: analysis of the gravity anomaly. 46th Lunar and Planetary Science Conference, The Woodlands, TX, 16–20 March 2015, Abst:1482

Brown JJ, Spray JG, Thompson LM (2016) Shock Attenuation within the Manicouagan Impact Structure. 47th Lunar and Planetary Science Conference, The Woodlands, TX, 21–25 March 2016, Abst:1996

Butcher GS, Kendall AC, Boyce AJ, Millar IL, Andrews JE, Dennis PF, Steve Grasby S (2012) Age determination of the Lower Watrous red-beds of the Williston Basin, Saskatchewan, Canada. Bull Can Pet Geo 60(4):227–238. https://doi.org/10.2113/gscpgbull.60.4.227

Cameron B, Jones JR (1987) Discovery of fossils and meandering stream deposits in the Late Triassic Blomidon Formation of Nova Scotia. In: Bates JL, MacDonald DR (eds) Mines Min Br Rep Activ 1987, Part A. Nova Scotia Dep Mines En Rep 87-5:179–181

Carter NL, Officer CB, Chesner CA, Rose WI (1986) Dynamic deformation of volcanic ejecta from the Toba caldera; Possible relevance to Cretaceous/Tertiary boundary phenomena. Geology 14(5):380–383. https://doi.org/10.1130/0091-7613(1986)

Cashman SM, Baldwin JN, Cashman KV, Swanson K, Crawford R (2007) Microstructures developed by coseismic and aseismic faulting in near-surface sediments, San Andreas fault, California. Geology 35(7):611–614. https://doi.org/10.1130/G23545A.1

Cavosie AJ, Quintero RR, Radovan HA, Moser DE (2015) A record of ancient cataclysm in modern sand: shock microstructures in detrital minerals from the Vaal River, Vredefort Dome, South Africa. Geol Soc Am Bull 122(11/12):1968–1980. https://doi.org/10.1130/B30187.1

Chapman MG, Evans MA, McHone JF (2004) Triassic cratered cobbles: shock effects or tectonic pressure? Proceedings of the 25th Lunar and Planetary Science Conference, League City, TX, 15–19 March 2004, Abst 35:1424

Chesner CA (2011) The Toba Caldera Caldera complex. Quat Int 258:5–18. https://doi.org/10.1016/j.quaint.2011.09.025

Cirilli S, Marzoli A, Tanner LH, Bertrand H, Buratti N, Jourdan F, Bellieni G, Kontak D, Renne RP (2009) The onset of CAMP eruptive activity and the Tr-J boundary: stratigraphic constraints from the Fundy Basin, Nova Scotia. Earth Planet Sci Lett 286(3–4):514–525. https://doi.org/10.1016/j.epsl.2009.07.021

Clemmensen L, Kent DV, Jenkins FA (1998) A late Triassic lake system in East-Greenland: facies, depositional cycles and paleoclimate. Paleogeogr Paleoclimat Paleoecol 140(1–4):135–159. https://doi.org/10.1016/S0031-0182(98)00043-1

Cohen BE, Mark DF, Lee MR, Simpson SL (2017) A new high-precision 40Ar-39Ar age for the Rochechouart impact structure-At least 5 Ma older than the Triassic-Jurassic boundary. Meteorit Planet Sci 52:1600–1611. https://doi.org/10.1111/maps.12880

Collins GS, Melosh HJ, Marcus RA (2005) Earth impact effects program: a Web-based computer program for calculating the regional environmental consequences of a meteoroid impact on Earth. Meteorit Planet Sci 40(6):818–840. https://doi.org/10.1111/j.1945-5100.2005.tb00156

Deptuck M, Campbell C (2012) Widespread erosion and mass failure from the ~51 Ma Montagnais marine bolide impact off southwestern Nova Scotia, Canada. Can J Earth Sci 49(12):1567–1594. https://doi.org/10.1139/e2012-075

Diaz-Martinez E, Sanz-Rubio E, Martınez-Frias J (2002) Sedimentary record of impact events in Spain. In: Koeberl C, MacLeod KG (eds) Catastrophic events and mass extinctions: impacts and beyond. Geological Society of America Special Paper 356:551–562

Doughty M, Eyles N, Eyles CH, Wallace K, Boyce JI (2014) Lake sediments as natural seismographs: earthquake-related deformations (seismites) in central Canadian lakes. Sed Geol 313:45–67. https://doi.org/10.1016/j.sedgeo.2014.09.001

Dypvik H, Jansa LF (2003) Sedimentary signatures and processes during marine bolide impacts: a review. Sed Geol 161(3–4):309–337. https://doi.org/10.1016/S0037-0738(03)00135-0

Earth Impact Database (2017) Planetary and Space Science Centre (PASSC), University of New Brunswick. http://www.passc.net/EarthImpactDatabase/

Eisbacher GH (1969) Displacement and stress field along part of the Cobequid Fault, Nova Scotia. Can J Earth Sci 6(5):1095–1104. https://doi.org/10.1139/e69-111

Ernst RE, Youbi N (2017) How Large Igneous Provinces affect global climate, sometimes cause mass extinctions, and represent natural markers in the geological record. Paleogeogr Palaeoclimat Palaeoecol 478:30–52. https://doi.org/10.1016/j.palaeo.2017.03.014

Ernstson K, Hiltl M (2002) Cratered cobbles in Triassic Buntsandstein conglomerates in northeastern Spain: an indicator of shock deformation in the vicinity of large impacts: comment and reply. Geology 30(11):1051–1052. https://doi.org/10.1130/0091-7613(2002)

Ernstson K, Hammann W, Fiebag J, Graup G (1985) Evidence of an impact origin for the Azuara structure (Spain). Earth Planet Sci Lett 74(4):361–370. https://doi.org/10.1016/S0012-821X(85)80008-X

Ernstson K, Rampino MR, Hiltl M (2001) Cratered cobbles in Triassic Buntsandstein conglomerates in northeastern Spain: an indicator of shock deformation in the vicinity of large impacts. Geology 29(1):11–14. https://doi.org/10.1130/0091-7613(2001)

Fazio A, Folco L, D'Orazio M, Frezzotti ML, Cordier C (2014) Shock metamorphism and impact melting in small impact craters on Earth: evidence from Kamil Crater, Egypt. Meteorit Planet Sci 49(12):2175–2200. https://doi.org/10.1111/maps.12385

Fenner FD, Presley BJ (1984) Iridium in Mississippi river suspended matter and Gulf of Mexico sediment. Nature 312(5991):260–262. https://doi.org/10.1038/312260a0

Ferrière L, Morrow JR, Amgaa T, Koeberl C (2009) Systematic study of universal-stage measurements of planar deformation features in shocked quartz: implications for statistical significance and representation of results. Meteorit Planet Sci 44(6):925–940. https://doi.org/10.1111/j.1945-5100.2009.tb00778.x/full

Fink JW (1975) Petrology of the Triassic San Hipolito Formation, Vizcaino Peninsula, Baja California Sur, Mexico. Dissertation, San Diego State University

French BM (1998) Traces of Catastrophe: a handbook of shock-metamorphic effects in Terrestrial Meteorite impact structures. Lunar and Planetary Institute Contribution 954, Lunar and Planetary Institute, Houston

French BM (2004) Impact cratering; bridging the gap between modeling and observations. Meteorit Planet Sci 39(2):169–197. https://doi.org/10.1111/j.1945-5100.2002.tb00884

French BM, Koeberl C (2010) The convincing identification of terrestrial meteorite impact structures: what works, what doesn't, and why. Earth Sci Rev 98(1–2):123–170. https://doi.org/10.1016/j.earscirev.2009.10.009

von Frese R, Potts L, Wells S, Leftwich T, Kim H et al (2009) GRACE gravity evidence for an impact basin in Wilkes Land, Antarctica. Geochem Geophys Geosyst 10(2):1–14. https://doi.org/10.1029/2008GC002149

Gerhard LC, Anderson SB, Le Fever JA, Carlson CG (1982) Geological development, origin and energy mineral resources of Williston Basin, North Dakota. Am Assoc Pet Geo Bull 66(8):989–1020

Glass BP, Simonson BM (2012) Distal impact ejecta layers: spherules and more. Elements 8:43–48. https://doi.org/10.2113/gselements.8.1.43

Glass BP, Simonson BM (2013) Distal impact ejecta layers: a record of large impacts in sedimentary deposits. Springer, Berlin

Glass BP, Koeberl C, Kirkham A (2003) Glauconitic spherules from the Triassic of the Bristol area, SW England: probably microtektite pseudomorphs: discussion and reply. Proc Geol Assoc 114(2):175–179. https://doi.org/10.1016/S0016-7878(03)80011-1

Glikson AY, Tonguç Uysal I, FitzGerald JD, Saygin E (2013) Geophysical anomalies and quartz microstructures, Eastern Warburton Basin, North-east South Australia: tectonic or impact shock metamorphic origin? Tectonophys 589:57–76. https://doi.org/10.1016/j.tecto.2012.12.036

Golonka J (2007) Late Triassic and Early Jurassic palaeogeography of the world. Palaeogeogr Palaeoclimat Palaeoecol 244(1–4):297–307. https://doi.org/10.1016/j.palaeo.2006.06.041

Goltrant O, Cordier P, Doukhan J-C (1991) Planar deformation features in shocked quartz; a transmission electron microscopy investigation. Earth Planet Sci Lett 106(1–4):103–115. https://doi.org/10.1016/0012-821X(91)90066-Q

Gould SR (2001) Integrated sedimentological and whole-rock trace element geochemical correlation of alluvial red-bed sequences at outcrop and in the subsurface. Dissertation, University of Aberdeen

Gratz AJ, Fisher DK, Bohor BH (1996) Distinguishing shocked from tectonically deformed quartz by the use of SEM and chemical etching. Ear Plan Sci Lett 142(3–4):513–521. https://doi.org/10.1016/0012-821X(96)00099-4

Grieve RAF (1991) Terrestrial impact: the record in the rocks. Meteoritics 26(3):175–194. https://doi.org/10.1111/j.1945-5100.1991.tb01038

Grieve RAF (1998) Extraterrestrial impacts on earth: the evidence and the consequences. In: Grady MM, Hutchison R, McCall GJH, Rothery DA (eds) Meteorites: flux with time and impact effects. Geological Society of London Special Publication 140:105–131

Grieve RAF (2017) Logan medallist 4: large-scale impact on earth history. Geosci Can 44:1–26. 10.12789/geocanj.2017.44.113

Grieve RAF, Head JW (1983) The Manicouagan impact structure: an analysis of its original dimensions and form. Proceedings of the 13th Lunar Science Conference Part 2, Houston, TX, 15–19 March 1983. J Geophys Res 88:807–818. https://doi.org/10.1029/JB088iS02p0A807/full

Grieve RAF, Pesonen LJ (1996) Terrestrial impact craters: their spatial and temporal distribution and impacting bodies. Earth, Moon, Planets 72(1–3):357–376. https://doi.org/10.1007/BF00117541

Grieve RAF, Langenhorst F, Stöffler D (1996) Shock metamorphism of quartz in nature and experiment: II. Significance in geoscience. Meteorit Planet Sci 31(1):6–35. https://doi.org/10.1111/j.1945-5100.1996.tb02049

Güldemeister N, Wünneman K, Durr N, Hiermaier S (2013) Propagation of impact-induced shock waves in porous sandstone using mesoscale modeling. Meteorit Planet Sci 48(1):115–133. https://doi.org/10.1111/j.1945-5100.2012.01430

Gurov E, Gurova E, Cernenko Y, Yamnichenko A (2009) The Obolon impact structure, Ukraine, and its ejecta deposits. Meteorit Planet Sci 44(3):389–404. https://doi.org/10.1111/j.1945-5100.2009.tb00740

Hallam A (1998) Mass extinctions in Phanerozoic time. In: Grady MM, Hutchison R, McCall GJH, Rothery DA (eds) Meteorites: flux with time and impact effects. Geological Society of London Special Publication 140:259–274

Hallam A, Wignall PB (1997) Mass extinctions and their aftermath. Oxford University Press, Oxford

Hamers MF, Drury MR (2011) Scanning electron microscope-cathodoluminescence (SEM-CL) imaging of planar deformation features and deformation lamellae in quartz. Meteorit Planet Sci 46(12):1814–1831. https://doi.org/10.1111/j.1945-5100.2011.01295.

Hautmann M (2004) Effect of end-Triassic CO_2 maximum on carbonate sedimentation and marine mass extinction. Facies 50(2):257–261. https://doi.org/10.1007/s10347-004-0020-y

Hautmann M, Benton MJ, Tomasovych A (2008) Catastrophic ocean acidification at the Triassic-Jurassic boundary. N Jb Geol Pal Abhand 249(1):119–127. https://doi.org/10.1127/0077-7749/2008/0249-0119

Hergarten S, Kenkmann T (2015) The number of impact craters on Earth: any room for further discoveries? Earth Planet Sci Lett 425:187–192. https://doi.org/10.1016/j.epsl.2015.06.009

Hildebrand AR, Penfield GT, Kring DA, Pilkington M, Camargo ZA, Jacobsen S, Boynton WV (1991) Chicxulub crater: a possible Cretaceous-Tertiary boundary impact crater on the Yucatán Peninsula, Mexico. Geology 19(9):867–871. https://doi.org/10.1130/0091-7613(1991)

Hodych JP, Dunning GR (1992) Did the Manicouagan impact trigger end-of-Triassic mass extinction? Geology 20(1):51–54. https://doi.org/10.1130/0091-7613(1992)

Holm-Alwmark S, Alwmark C, Lindström S, Ferrière L, Scherstén A, Masaitis VL, Mashchak MS, Naumov MV (2016) An Early Jurassic $^{40}Ar^{39}Ar$ Age for the Puchezh-Katunki Impact Structure (Russia)—No Causal Link to an Extinction Event. 79th Annual Meeting of the Meteoritical Society, 7–12 August, 2016, Berlin, Germany, Abst. 6171. https://www.hou.usra.edu/meetings/metsoc2016/pdf/6171.pdf

Hori RS, Fujiki T, Inoue E, Kimura J-I (2007) Platinum group element anomalies and bioevents in the Triassic–Jurassic deep-sea sediments of Panthalassa. Palaeogeog Palaeoclim Palaeoecol 224(1-4): 391-406. https://doi.org/10.1016/j.palaeo.2006.06.038

Huggett J (2004) Comments on Kirkham's glauconitic spherules from the Triassic of the Bristol area, SW England: probable microtektite pseudomorphs, with reply by A. Kirkham. Proc Geol Assoc 115(2):189–192. https://doi.org/10.1016/S0016-7878(04)80028-2

Izett GA (1990) The Cretaceous/Tertiary boundary interval, Raton Basin, Colorado and New Mexico, and its content of shock-metamorphosed minerals; evidence relevant to the K-T boundary impact-extinction theory. Special Paper 249. Boulder: Geological Society of America. https://doi.org/10.1130/SPE249

Jansa LF, Pe-Piper G (1987) Identification of an underwater extraterrestrial impact structure. Nature 327(6123):612–614. https://doi.org/10.1038/327612a0

Jeans CV (2006) Clay mineralogy of the Permo-Triassic strata of the British Isles: onshore and offshore. Clay Miner 41(1):309–354. https://doi.org/10.1180/0009855064110199

Jourdan F, Reimold WU, Deutsch A (2012) Dating terrestrial impact structures. Elements 8:49–53. https://doi.org/10.2113/gselements.8.1.49

Kelley SP, Sherlock SC (2013) The geochronology of impact craters. Impact cratering: processes and products. In: Osinski GR, Pierazzo E (eds) Impact cratering. Wiley-Blackwell, Chichester, pp 240–253

Kelley SP, Spray JG (1997) A late Triassic age for the Rochechouart impact structure, France. Meteorit Planet Sci 32:629–636

Kent DV (1998) Impacts on Earth in the Late Triassic: discussion. Nature 395(6698):126. https://doi.org/10.1038/25874

Kent DV, Olsen PE (2000) Magnetic polarity stratigraphy and paleolatitude of the Triassic–Jurassic Blomidon Formation in the Fundy basin (Canada): implications for Early Mesozoic tropical climate gradients. Earth Planet Sci Lett 179(2):311–324. https://doi.org/10.1016/S0012-821X(00)00117-5

Kent DV, Olsen PE, Muttoni G (2017) Astrochronostratigraphy polarity time scale (APTS) for the Late Triassic and Early Jurassic from continental sediments and correlation with standard marine stages. Earth Sci Rev 166:153–180. https://doi.org/10.1016/j.earscirev.2016.12.014

Kieffer SW (1971) Shock metamorphism of the Coconino Sandstone at Meteor Crater, Arizona. J Geophy Res 76(23):5449–5473. https://doi.org/10.1029/JB076i023p05449

Kirkham A (2002) Triassic microtektite pseudomorphs of the Bristol area. Geoscient 12(7): 17–18

Kirkham A (2003) Glauconitic spherules from the Triassic of the Bristol area, S.W. England: probable microtektite pseudomorphs. Proc Geol Assoc 114(1):11–21. https://doi.org/10.1016/S0016-7878(03)80025-1

Kirkham A (2006) Triassic Meteorite Impact? Mag Geol Assoc 5(4):21

Koeberl C, MacLeod KG (eds) 2002. Catastrophic events and mass extinctions: impacts and beyond. Geological Society of America Special Paper 356, Geological Society of America, Boulder

Koeberl C, Reimold WU, Brandt D (1996) Red Wing creek structure, North Dakota: petrographical and geochemical studies, and confirmation of impact origin. Meteorit Planet Sci 31:335–342. https://doi.org/10.1111/j.1945-5100.1996.tb02070

Kohút M, Hofmann M, Havrila M, Linnemann U, Havrila J (2017) Tracking an upper limit of the "Carnian crisis" and/or Carnian Stage in the Western Carpathians (Slovakia). Internat J Earth Sci. https://doi.org/10.10007/s00531-017-1491-8

Kowitz A, Güldemeister N, Reimold WU, Schmitt RT, Wünnemann K (2013) Diaplectic quartz glass and SiO_2 melt experimentally generated at only 5 GPa shock pressure in porous sandstone: laboratory observations and meso-scale numerical modeling. Earth Planet Sci Lett 384:17–26. https://doi.org/10.1016/j.epsl.2013.09.021

Kozur HW, Weems RE (2010) The biostratigraphic importance of conchostracans in the continental Triassic of the northern hemisphere. In: Lucas SG (ed) The Triassic Timescale. Geological Society of London Special Publication 334:315–417

Kring DA (2007) The Chicxulub impact event and its environmental consequences at the Cretaceous-Tertiary boundary. Palaeogeogr Palaeoclimat Palaeoecol 255(1–2):4–21. https://doi.org/10.1016/j.palaeo.2007.02.037

Kring DA, Boynton WV (1991) Altered spherules of impact melt and associated relic glass from the KIT boundary sediments in Haiti. Geochim Cosmochim Act 55(6):1737–1742. https://doi.org/10.1016/0016-7037(91)90143-S

Kyte FT (2002) Tracers of the extraterrestrial component in sediments and inferences for Earth's accretion history. In: Koeberl C, MacLeod K (eds) Catastrophic events and mass extinctions: impacts and beyond. Geological Society of America Special Paper 356:21–28

Lambert P, Goderis S, Hodges KV, Kelley S, Lee MR, Jourdan F, Osinski GR, Sapers HM, Schmieder M, Schwenzer S, Trumel H, Wittmann A (2016) Preparing the 2017 drilling campaign at Rochechouart impact structure. 79th Annual Meeting of the Meteoritical Society, 7-12 August 2016, Berlin, Germany. Abst: Meteorit Planet Sci 51 (Suppl.): A6471. https://www.hou.usra.edu/meetings/metsoc2016/pdf/6471.pdf; https://www.hou.usra.edu/meetings/metsoc2016/eposter/6471.pdf

Latjai EZ, Stringer P (1981) Joints, tensile strength and preferred fracture orientation in sandstones, New Brunswick and Prince Edward Island, Canada. Mar Sed Atl Geol 17(2):70–87. https://doi.org/10.4138/1377

Leleu S, Hartley AJ (2010) Controls on the stratigraphic development of the Triassic Fundy Basin, Nova Scotia: implications for the tectonostratigraphic evolution of Triassic Atlantic rift basins. J Geol Soc Lond 167(3):437–454. https://doi.org/10.1144/0016-76492009-092

Leleu S, Hartley AJ (2016) Constraints on synrift intrabasinal horst development from alluvial fan and eolian deposits (Triassic, Fundy Basin, Nova Scotia. In: Ventra D, Clarke LE (eds) Geology and geomorphology of alluvial and fluvial fans: terrestrial and planetary perspectives. Geological Society of London Special Publication 440. https://doi.org/10.1144/SP440.8

Leslie AB, Spiro B, Tucker ME (1993) Geochemical and mineralogical variations in the upper Mercia Mudstone Group (Late Triassic), Southwest Britain; correlation of outcrop sequences with borehole geophysical logs. J Geol Soc Lond 150(1):67–75. https://doi.org/10.1144/gsjgs.150.1.0067

Lindström S, Pedersen GK, van de Schootbrugge B, Hovedskov K, Hansen K, Kuhlmann N, Thein J, Johansson L, Petersen HI, Alwmark C, Dybkjær K, Weibel R, Erlström M, Nielsen LH, Wolfgang N, Oschmann W, Tegner C (2015) Intense and widespread seismicity during the end-Triassic mass extinction due to emplacement of a large igneous province. Geology 43(5):387–390. https://doi.org/10.1130/G36444.1

Lindström S, van de Schootbrugge B, Hansen KH, Pedersen GK, Alsen P, Thibault N, Dybkjær K, Bjerrum CJ, Nielsen LH (2017) A new correlation of Triassic-Jurassic boundary successions in NW Europe, Nevada and Peru, and the Central Atlantic Magmatic Province: a time-line for the end-Triassic mass extinction. Paleogeogr Palaeoclimat Palaeoecol 478:80–102. https://doi.org/10.1016/j.palaeo.2016.12.025

Lucas SG (2010) The Triassic timescale based on nonmarine tetrapod biostratigraphy and biochronology. In: Lucas SG (ed) The Triassic Timescale. Geological Society of London Special Publication 334:447–500

Lucas SG (2013) A new Triassic timescale. In: Tanner LH, Spielmann JA, Lucas SG (eds) The Triassic System New Mex Mus Nat Hist Sci Bull 61:366–374

Lucas SG, Tanner LH (2008) Reexamination of the end-Triassic mass extinction. In: Elewa AMT (ed) Mass extinction. Springer Verlag, New York, pp 66–103. https://doi.org/10.1007/978-3-540-75916-4_8

Lucas SG, Tanner LH (2015) End-Triassic nonmarine biotic events. J Palaeogeogr 4(4):331–348. https://doi.org/10.1016/j.jop.2015.08.010

Lucas SG, Tanner LH (2017) Timing and mechanisms of extinctions during the Late Triassic. In: Tanner LH (ed) The Late Triassic world: earth in a time of transition. Topics in Geobiology, Springer (this volume)

Lucas SG, Tanner LH, Kozur HW, Weems RE, Heckert AB (2012) The Late Triassic timescale: age and correlation of the Carnian–Norian boundary. Earth-Sci Rev 114(1–2):1–18. https://doi.org/10.1016/j.earscirev.2012.04.002

Marzoli A, Bertrand H, Knight KB, Cirilli S, Buratti N, Vérati C, Nomade S, Renne PR, Youbi N, Martini R, Allenbach J, Neuwerth R, Rapaille C, Zaninetti L, Bellieni G (2004) Synchrony of the Central Atlantic magmatic province and the Triassic-Jurassic boundary climatic and biotic crisis. Geology 32(11):973–976. https://doi.org/10.1130/G20652.1

Marzoli A, Callagaro S, Dal Corso J, Youbi N, Bertrand H, Reisberg L, Chiaradia M, Merle R, Jourdan F (2017) The Central Atlantic magmatic province: a review. In: Tanner LH (ed) The Late Triassic world: earth in a time of transition. Topics in Geobiology, Springer (this volume)

Masaitis VL, Danilin AN, Mashchak MS, Raikhlin AI, Selivanovskaya TV, Shadenkov EM (1980) The geology of astroblemes. Nedra, Leningrad

McLaren DL, Goodfellow WD (1990) Geological and biological consequences of giant impacts. Ann Rev Ear Plan Sci 18:123–171. https://doi.org/10.1146/annurev.ea.18.050190.001011

McLennan SM (2001) Relationships between the trace element composition of sedimentary rocks and upper continental crust. Geochem Geophys Geosyst 2(4):1–10. https://doi.org/10.1029/2000GC000109

Meier MM, Holm-Alwmark S (2017) A tale of clusters: no resolvable periodicity in the terrestrial impact cratering record. Mon Not R Astron Soc 467(3):2545–2551. https://doi.org/10.1093/mnras/stx211

Melosh HJ (1989) Impact cratering: a geologic process. Oxford University Press, New York

Milroy P (1998) Palaeoenvironmental Analysis of the Upper Triassic Mercia Mudstone Group Southwest Britain. Dissertation, University Bristol. https://www.researchgate.net/publication/35719076

Montenat C, Barrier P, Ott d'Estevou P, Hibsch C (2007) Seismites: an attempt at critical analysis and classification. Sed Geol 196(1–4):5–30. https://doi.org/10.1016/j.sedgeo.2006.08.004

Moore RG, Ferguson SA, Boehner RC, Kennedy CM (2009) Bedrock geology map of the Wolfville-Windsor Area, NTS sheet 21H/01 and part of 21A/16, Hants and Kings Counties, Nova Scotia. Nova Scotia Depart Nat Res Min Res Branch, Open File Map ME 2000–3, version 2, 1:50,000

Mossman DJ, Grantham RG, Lagenhorst F (1998) A search for shocked quartz at the Triassic-Jurassic boundary in the Fundy and Newark basins of the Newark Supergroup. Can J Earth Sci 35(2):101–109. https://doi.org/10.1139/e97-101

Murphy B, Waldron JWF, Kontak DJ, Pe-Piper G, Piper DJW (2011) Minas fault zone: Late Paleozoic history of an intra-continental orogenic transform fault in the Canadian Appalachians. Jour Struct Geol 33(3):312–328. https://doi.org/10.1016/j.jsg.2010.11.012

Nadon GC, Middleton GV (1985) The stratigraphy and sedimentology of the Fundy Group (Triassic) of the St. Martins area, New Brunswick. Can J Earth Sci 22(8):1183–1203. https://doi.org/10.1139/e85-121

Noll KS, Feldman PD, Weaver HA (eds) (1996) The collision of Comet Shoemaker–Levy 9 and Jupiter. Cambridge University Press, Cambridge

Nomade S, Knight KB, Beutel E, Renne PR, Verati C, Feraud G, Marzoli A, Youbi N, Bertrand H (2007) Chronology of the Central Atlantic Magmatic Province: implications for the Central Atlantic rifting processes and the Triassic–Jurassic biotic crisis. Palaeogeogr Palaeoclimat Palaeoecol 244(1–4):326–344. https://doi.org/10.1016/j.palaeo.2006.06.034

O'Connell-Cooper CD, Spray JG (2010) Geochemistry of the Manicouagan Impact melt sheet. Proceedings of the 41st Lunar and Planetary Science Conference, The Woodlands, TX, 1–5 March 2010, Abst: 1755

Ogg JG, Huang C, Hinnov L (2014) Triassic timescale status: a brief overview. Albertiana 41:3–30

Ogg JG, Ogg G, Gradstein FM (2016) A concise geologic time scale. Elsevier. store.elsevier.com/9780444637710

Olsen PE, Et-Touhami M (2008) Field Trip #1: tropical to subtropical syntectonic sedimentation in the Permian to Jurassic Fundy Rift Basin, Atlantic Canada, in relation to the Moroccan Conjugate Margin. Central Atlantic Conjugate Margins Conference, Halifax, Canada, 13–15 August 2008

Olsen PE, Shubin NH, Anders MH (1987) New Early Jurassic tetrapod assemblages constrain Triassic-Jurassic tetrapod extinction event. Science 237(4818):1025–1029. https://doi.org/10.1126/science.3616622

Olsen PE, Schlische RW, Gore PJW et al (1989) Field Guide to the Tectonics, stratigraphy, sedimentology, and paleontology of the Newark Supergroup, eastern North America. 28th International Geological Congress, Washington DC, 9–19 August 1989, Field Trip Guidebook T351

Olsen PE, Fowell SJ, Cornet B (1990) The Triassic/Jurassic boundary in continental rocks of eastern North America; a progress report. In: Sharpton VL, Ward PD (eds) Global catastrophes in Earth history: an interdisciplinary conference on impacts, volcanism, and mass mortality. Geological Society of America Special Paper 247:585–593

Olsen PE, Kent DV, Sues HD, Koeberl C, Huber H, Montanari A, Rainforth EC, Fowell SJ, Szajna MJ, Hartline BW (2002a) Ascent of dinosaurs linked to an iridium anomaly at the Triassic-Jurassic boundary. Science 296(5571):1305–1307. https://doi.org/10.1126/science.1065522

Olsen PE, Koeberl C, Huber H, Montanari A, Fowell S, Et-Touhami M, Kent DV (2002b) The continental Triassic–Jurassic boundary in central Pangea: recent progress and preliminary report of an Ir anomaly. In: Koeberl C, MacLeod KG (eds) Catastrophic events and mass extinctions: impacts and beyond. Geological Society of America Special Paper 356:505–522

Olsen P, Kent DV, Et-Touhami M (2003) Chronology and stratigraphy of the Fundy and related Nova Scotia offshore basins and Morocco based on core and outcrop. Conventional Core Workshop. Joint Annual Conference of the Geological Society of America (NE Section) and Atlantic Geoscience Society, Halifax, Nova Scotia, Canada, 27–29 March 2003, 51–63

Olsen PE, Kent DV, Whiteside JH (2010) Implications of the Newark Supergroup-based astrochronology and geomagnetic polarity time scale (Newark-APTS) for the tempo and mode of the early diversification of the Dinosauria. Earth Env Sci Trans Roy Soc Edinburgh 101(3–4):201–229. https://doi.org/10.1017/S1755691011020032

Onoue T, Sato H, Nakamura T, Noguchi T, Hidaka Y, Shiraid N, Ebihara M, Osawa T, Hatsukawa Y, Toh Y, Koizumi M, Harada H, Orchard MJ, Nedachig M (2012) Deepsea record of impact apparently unrelated to mass extinction in the Late Triassic. Proc Nat Acad Sci USA 109(47):19134–19139. https://doi.org/10.1073/pnas.1209486109

Onoue T, Sato H, Yamashita D, Ikehara M, Yasukawa K, Fujinaga K, Kato Y, Matsuoka A (2016) Bolide impact triggered the Late Triassic extinction event in equatorial Panthalassa. Sci Rep 6:29609. https://doi.org/10.1038/srep29609

Orchard MJ, Whalen A, Carter E, Taylor H (2007) Latest Triassic Conodonts and Radiolarian-bearing Successions in Baja California Sur. In: Lucas SG, Spielmann JA (eds) The Global Triassic. New Mex Mus Nat Hist Sci Bull 41:355–365

Orth CJ (1989) Geochemistry of the bio-event horizons. In: Donovan SK (ed) Mass extinctions: processes and evidence. Columbia University Press, New York, pp 37–72

Orth CJ, Attrepe M Jr, Quintana LR (1990) Iridium abundance patterns across bio-event horizons in the fossil record. In: Sharpton VL, Ward PD (eds) Global catastrophes in Earth history: an interdisciplinary conference on impacts, volcanism, and mass mortality. Geological Society of America Special Paper 247:45–59

Osawa T, Hatsukawa Y, Nagao K, Koizumi M, Oshima M, Toh Y, Kimura A, Furutaka K (2009) Iridium concentration and noble gas composition of Cretaceous-Tertiary boundary clay from Stevns Klint, Denmark. Geochem J 43(6):415–422

Osinski GR (2013) Processes and products of impact cratering; glossary and definitions. In: Osinski GR, Pierazzo E (eds) Impact cratering: processes and products. Blackwell, Oxford, pp 306–309

Osinski GR, Pierazzo E (2013) Impact cratering: processes and products. In: Osinski GR, Pierazzo E (eds) Impact cratering: processes and products. Wiley-Blackwell, Chichester, pp 125–145

Osinski GR, Tornabene LL, Grieve RAF (2011) Impact ejecta emplacement on terrestrial planets. Earth Planet Sci Lett 310(3–4):167–181. https://doi.org/10.1016/j.epsl.2011.08.012

Osinski GR, Grieve RAF, Tornabene LL (2013) Excavation and impact ejecta emplacement. Impact cratering: processes and products. In: Osinski GR, Pierazzo E (eds) Impact cratering. Wiley-Blackwell, Chichester, pp 43–59

Pálfy J (2004) Did the Puchezh-Katunki impact trigger an extinction? In: Dypvik H, Burchel MJ, Claeys P (eds) Cratering in marine environments and on Ice. Submarine craters and ejecta-crater correlation. Impact studies series. Springer, Berlin, pp 135–148

Pálfy J, Zajzon N (2012) Environmental changes across the Triassic-Jurassic boundary and coeval volcanism inferred from elemental geochemistry and mineralogy in the Kendlbachgraben section (northern Calcareous Alps, Austria). Earth Planet Sci Lett 335–336:121–134. https://doi.org/10.1016/j.epsl.2012.01.039

Pálfy J, Mortensen JK, Carter ES, Smith PL, Friedman RM, Tipper HW (2000) Timing the end-Triassic mass extinction: first on land, then in the sea? Geology 28(1):39–42. https://doi.org/10.1130/0091-7613(2000)

Pearson DG (1999) The age of continental roots. Lithos 48(1–4):171–194. https://doi.org/10.1016/S0024-4937(99)00026-2

Pickersgill AE (2014) Shock metamorphic effects in lunar and terrestrial plagioclase feldspar investigated by optical petrography and micro-X-ray diffraction. Dissertation, University of Western Ontario

Pickersgill AE, Lee MR, Mark DF, Osinski GR (2015) Shock metamorphism in impact melt rocks from the Gow Lake impact structure, Saskatchewan, Canada. 46th Lunar and Planetary Science Conference, The Woodlands, TX, 16–20 March 2015, Abst 46:2181

Pieńkowski G, Niedźwiedzki G, Waksmundzka M (2012) Sedimentological, palynological and geochemical studies of the terrestrial Triassic-Jurassic boundary in northwestern Poland. Geo Mag 149(2):308–332. https://doi.org/10.1017/S0016756811000914

Pieńkowski G, Niedźwiedzki G, Branski P (2014) Climatic reversals related to the Central Atlantic magmatic province caused the end-Triassic biotic crisis—evidence from continental strata in Poland. Geological Society of America Special Paper 505:263–286

Plado J (2012) Meteorite impact craters and possibly impact-related structures in Estonia. Meteorit Planet Sci 47(10):1590–1605. https://doi.org/10.1111/j.1945-5100.2012.01422

Plint AG (1985) Possible earthquake-induced soft-sediment faulting and remobilization in Pennsylvanian alluvial strata, southern New Brunswick, Canada. Can J Earth Sci 22(6):907–912. https://doi.org/10.1139/e85-094

Racki G (2012) The Alvarez impact theory of mass extinction; limits to its applicability and the "great expectations syndrome". Act Palaeontol Pol 57(4):681–702. https://doi.org/10.4202/app.2011.0058

Rajmon D (2010) Impact Database. http://impacts.rajmon.cz/index.html

Ramezani J, Bowring SA, Pringle MS, Winslow FD III, Rasbury ET (2005) The Manicouagan impact melt rock: a proposed standard for the intercalibration of U-Pb and $^{40}Ar/^{39}Ar$ isotopic systems. Geochim Cosmochim Act 69(10) Suppl: Goldschmidt Conference Abstracts 2005:301–350, Abst:A321.

Rampino MR, Haggerty BM (1996) Impact crises and mass extinctions: a working hypothesis. In: Ryder G, Fastovsky D, Gartner S (eds) The Cretaceous Tertiary event and other catastrophes in Earth history. Geological Society of America Special Paper 307:11–30

Reimold WU, Oskierski W (1987) The Rb-Sr-age of the Rochechouart impact structure, France, and geochemical constraints on impact melt-target rock-meteorite compositions. In: Pohl J (ed) Research in terrestrial impact structures. Vieweg, Braunschweig; Wiesbaden, pp 94–114. https://doi.org/10.1002/gj.3350240211

Reimold WU, Ferrière L, Deutsch A, Koeberl C (2014) Impact controversies: impact recognition criteria and related issues. Meteorit Planet Sci 49(5):723–731. https://doi.org/10.1111/maps.12284

Renne PR, Deino AL, Hilgen FJ, Kuiper KF, Mark DF, Mitchell WS, Morgan LE, Mundil R, Smit J (2013) Time scales of critical events around the cretaceous-paleogene boundary. Science 39(6120):684–687. https://doi.org/10.1126/science.1230492

Richoz S, van de Schootbrugge B, Pross J, Püttmann W, Quan TM, Lindström S, Heunisch C, Fiebig J, Maquil R, Schouten S, Hauzenberger CA, Wignall PB (2012) Hydrogen sulphide poisoning of shallow seas following the end-Triassic extinction. Nat Geosci 5(9):662–667. https://doi.org/10.1038/ngeo1539

Robock A (2000) Volcanic eruptions and climate. Rev Geophys 38(2):191–219. https://doi.org/10.1029/1998RG000054

Ruffell A (1991) Palaeoenvironmental analysis of the late Triassic succession in the Wessex Basin and correlation with surrounding areas. Proc Ussher Soc 7(4):402–407

Ruhl M, Bonis NR, Reichart G-J, Sinninghe D, Jaap S, Kuerschner WF (2011) Atmospheric carbon injection linked to end-Triassic mass extinction. Science 333(6041):430–434. https://doi.org/10.1126/science.1204255

Sapers HM, Osinski GR, Banerjee NR, Ferrière L, Lambert P, Izawa RM (2014) Revisiting the Rochechouart impact structure, France. Meteorit Planet Sci 49(12):2152–2168. https://doi.org/10.1111/maps.12381

Sato H, Onoue T (2010) Discovery of Ni-rich spinels in Upper Triassic chert of the Mino Terrane, central Japan. J Geol Soc Jpn 116:575–578. https://doi.org/10.5575/geosoc.116.575

Sato H, Onoue T, Nozaki T, Suzuki K (2013) Osmium isotope evidence for a large Late Triassic impact event. Nat Commun 4:2455. https://doi.org/10.1038/ncomms3455

Sato H, Shirai N, Ebihara M, Onoue T, Kiyokawa S (2016) Sedimentary PGE signatures in the Late Triassic ejecta deposits from Japan: implications for the identification of impactor. Paleogeogr Palaeoclimat Palaeoecol 442:36–47. https://doi.org/10.1016/j.palaeo.2015.11.015

Schaller MF, Wright JD, Kent DV (2011) Atmospheric pCO_2 perturbations associated with the Central Atlantic magmatic province. Science 331(6023):1404–1409. https://doi.org/10.1126/science.1199011

Schaltegger U, Guex J, Bartolini A, Schoene B, Ovtcharov M (2008) Precise U-Pb age constraints for end-Triassic mass extinction, its correlation to volcanism and Hettangian post-extinction recovery. Earth Planet Sci Lett 267(1–2):266–275. https://doi.org/10.1016/j.epsl.2007.11.031

Schedl A (2015) Searching for distal ejecta on the craton: the sedimentary effects of meteorite impact. J Geol 123(3):201–203. https://doi.org/10.1086/681624

Schmieder M (2010) New aspects of the Middle-Late Triassic terrestrial impact cratering record. Dissertation, University of Stuttgart

Schmieder M, Buchner E (2008) Dating impact craters: palaeogeographic versus isotopic and stratigraphic methods—a brief case study. Camb Univ Geol Mag 145(4):586–590. https://doi.org/10.1017/s0016756808005049

Schmieder M, Buchner E, Schwarz WH, Trieloff M, Lambert P (2010a) A Rhaetian $^{40}Ar/^{39}Ar$ age for the Rochechouart impact structure (France) and implications for the latest Triassic sedimentary record. Meteorit Planet Sci 45(8):1225–1242. https://doi.org/10.1111/j.1945-5100.2010.01070.x/

Schmieder M, Schwarz WH, Buchner E, Trieloff M, Moilanen J, Öhman T (2010b) A Middle Late Triassic $^{40}Ar/^{39}Ar$ age for the Paasselkä impact structure (SE Finland). Meteorit Planet Sci 45(4):572–582. https://doi.org/10.1111/j.1945-5100.2010.01041.x/full

Schmieder M, Jourdan F, Tohver E, Cloutis E (2014) $^{40}Ar/^{39}Ar$ age of the Lake Saint Martin impact structure (Canada)—Unchaining the Late Triassic terrestrial impact craters. Lunar Plan Sci Lett 406:37–48. https://doi.org/10.1016/j.epsl.2014.08.037

van de Schootbrugge B, Tremolada F, Rosenthal Y, Bailey TR, Feist-Burkhardt S, Brinkhuis H, Pross J, Kent DV, Falkowski PG (2007) End-Triassic calcification crisis and blooms of organic-walled 'disaster species'. Palaeogeogr Palaeoclim Palaeoecol 244(1–4):126–141. https://doi.org/10.1016/j.palaeo.2006.06.026

van de Schootbrugge B, Payne JL, Tomasovych A, Pross J, Fiebig J, Benbrahim M, Föllmi KB, Quan TM (2008) Carbon cycle perturbation and stabilization in the wake of theTriassic-Jurassic boundary mass-extinction event. Geochem Geophys Geosys 9(4):Q04028. https://doi.org/10.1029/2007GC001914

van de Schootbrugge B, Quan T, Lindström S, Püttmann W, Heunisch C, Pross J, Fiebig J, Petschick R, Röhling H-G, Richoz S, Rosenthal Y, Falkowski PG (2009) Floral changes across the Triassic/Jurassic boundary linked to flood basalt volcanism. Nat Geosci 2(8):589–594. https://doi.org/10.1038/ngeo577

van de Schootbrugge B, Bachan A, Suan G, Richoz S, Payne JL (2013) Microbes, mud and methane: cause and consequence of recurrent Early Jurassic anoxia following the end-Triassic mass-extinction. Palaeontology 56(4):685–709. https://doi.org/10.1111/pala.12034

Schwarz WH, Schmieder M, Buchner E, Trieloff M, Moilanen J, Öhman T (2015) A Carnian 40Ar/39Ar age for the Paasselkä impact structure (SE Finland)—an update. Meteorit Planet Sci 50(1):135–140. https://doi.org/10.1111/maps.12407/full

Shanmugam G (2016) The seismite problem. J Palaeogeogr 5(4):318–362. https://doi.org/10.1016/j.jop.2016.06.002

Shanmugam G (2017) The fallacy of interpreting SSDS with different types of breccias as seismites amid the multifarious origins of earthquakes: implications. J Palaeogeogr 6(1):12–44. https://doi.org/10.1016/j.jop.2016.09.001

Sharpton VL, Schuraytz BC (1989a) On reported occurrences of shock-deformed clasts in the volcanic ejecta from Toba Caldera, Sumatra. Proceedings of the 20th Lunar and Planetary Science Conference, Houston, TX, 13–17 March 1989, Abst 20:992

Sharpton VL, Schuraytz BC (1989b) On reported shock deformation in Toba volcanic deposits. Proceedings of the 20th Lunar and Planetary Science Conference, Houston, TX, 13–17 March 1989, Abst 20:993

Sigurdsson H (1990) Assessment of atmospheric impact of volcanic eruptions. In: Sharpton VL, Ward PD (eds) Global catastrophes in Earth history. Geological Society of America of Special Paper 247:99–110

Silberling NJ (1985) Biogeographic significance of the Upper Triassic Bivalve Monotis in Circum-Pacific Accreted Terranes. In: Howell DG (ed) Tectonostratigraphic terranes of the Circum-Pacific Region. Circum-Pacific Council on Energy and Mineral Resources, Earth Science Series 1:63–70

Simms MJ (2003) Uniquely extensive seismite from the latest Triassic of the United Kingdom: evidence for bolide impact? Geology 31(6):557–560. https://doi.org/10.1130/0091-7613(2003)

Simms MJ (2007) Uniquely extensive soft-sediment deformation in the Rhaetian of the UK: evidence for earthquake or impact? Palaeogeogr Palaeoclimat Palaeoecol 244(1–4):407–423. https://doi.org/10.1016/j.palaeo.2006.06.037

Simms MJ, Ruffell AH (1990) Climatic and biotic change in the late Triassic. J Geol Soc Lond 147(2):321–327. https://doi.org/10.1144/gsjgs.147.2.0321

Smit J (1999) The global stratigraphy of the Cretaceous-Tertiary boundary impact ejecta. Annu Rev Earth Planet Sci 27:75–113. https://doi.org/10.1146/annurev.earth.27.1.75

van Soest MC, Hodges KV, Wartho JA, Biren MB, Monteleone BD, Ramezani J, Spray JG, Thompson LM (2011) (U–Th)/He dating of terrestrial impact structures: The Manicouagan example. Geochem Geophys Geosyst 12(5):Q0AA16, 1–8. https://doi.org/10.1029/2010GC003465

Spooner I, Stevens G, Morrow J, Pufahl P, Grieve R, Raeside R, Pilon J, Stanley C, Barr S, McMullin D (2009) Identification of the Bloody Creek structure, a possible bolide impact crater in southwestern Nova Scotia, Canada. Meteorit Planet Sci 44(8):1193–1202. https://doi.org/10.1111/j.1945-5100.2009.tb01217

Spooner I, Pufahl P, Brisco T, Morrow J, Nalepa M, Williams P, Stevens G (2015) The North structure: evidence for a possible second impact near the Bloody Creek site, Nova Scotia, Canada. Atlant Geol 51:44–50. https://doi.org/10.4138/atlgeol.2015.002

Spray JG, Kelley SP, Rowley DB (1998) Evidence for a Late Triassic multiple impact event on Earth. Nature 392(6672):171–173. https://doi.org/10.1038/32397

Spray JG, Thompson LM, Biren MB, O'Connell-Cooper CD (2010) The Manicouagan impact structure as a terrestrial analogue site for lunar and Martian planetary science. Planet Space Sci 58(4):538–551. https://doi.org/10.1016/j.pss.2009.09.010

Steinthorsdottir M, Jeram AJ, McElwain JC (2011) Extremely elevated CO_2 concentrations at the Triassic/Jurassic boundary. Palaeogeogr Palaeoclimat Palaeoecol 308(3–4):418–432. https://doi.org/10.1016/j.palaeo.2011.05.050

Stöffler D, Grieve RAF (2007) Impactites, Chapter 2.11. In: Fettes D, Desmons J (eds) Metamorphic rocks: a classification and glossary of terms. Cambridge University Press, Cambridge UK, 82–91, 111–125, 126–242

Strayer LM, Allen JR (2008) The Oakland Conglomerate: a Hayward Fault Tectonite? American Geophysical Union Fall Meeting, San Francisco, CA, 15–19 December 2008, Abst: T51A-1862

Sues HD, Olsen PE (2015) Stratigraphic and temporal context and faunal diversity of Permian-Jurassic continental tetrapod assemblages from the Fundy rift basin, eastern Canada. Atlan Geol 51:139–205. https://doi.org/10.4138/atlgeol.2015.006

Sulej T, Wolniewicz A, Bonde N, Błażejowski B, Niedźwiedzki G, Tałanda M (2014) New perspectives on the Late Triassic vertebrates of East Greenland: preliminary results of a Polish-Danish palaeontological expedition. Pol Pol Res 35(4):541–552. https://doi.org/10.2478/popore-2014-0030

Tackett LS, Bottjer DJ (2012) Faunal succession of Norian (Late Triassic) level bottom benthos in the Lombardian Basin: implications for the timing, rate, and nature of the early Mesozoic marine revolution. PALAIOS 27(8):585–593. https://doi.org/10.2110/palo.2012.p12-028r

Tackett LS, Bottjer DJ (2016) Paleoecological succession of Norian (Late Triassic) benthic fauna in eastern Panthalassa (Luning and Gabbs Formations, west-central Nevada). PALAIOS 31(4):190–202. https://doi.org/10.2110/palo.2015.070

Tackett LS, Bottjer DJ, Sheehan PM, Fastovsky D (2009) Comparative effects of two large bolide impact events: Chicxulub and Manicouagan. Geological Society of America Annual Meeting, Portland, OR, 18–21 October 2009, Abstracts & Program 41(7), Abst: 240

Tackett LS, Kaufman AJ, Corsetti FA, Bottjer DJ (2014) Strontium isotope stratigraphy of the Gabbs Formation (Nevada): implications for global Norian–Rhaetian correlations and faunal turnover. Lethaia 47(4):1–11. https://doi.org/10.1111/let.12075

Tagle R, Schmitt RT, Erzinger J (2009) Identification of the projectile component in the impact structures Rochechouart, France and Sääksjärvi, Finland: implications for the impactor population for the earth. Geochim Cosmochim Act 73(16):4891–4906. https://doi.org/10.1016/j.gca.2009.05.044

Tanner LH (2002) Stratigraphic record in the Fundy rift basin of the Manicouagan impact: Bolide with a bang or a whimper? Geological Society of America, Northeast Section—37th Annual Meeting, Springfield MA, 25–27 March 2002, Abst: 31805

Tanner LH (2003) Far-reaching seismic effects of the Manicouagan impact: evidence from the Fundy basin. Geological Society of America Annual Meeting, Seattle, WA, 2–5 November 2003, Abstracts and Program, 35(6), Abst:167

Tanner LH (2006) Synsedimentary seismic deformation in the Blomidon Formation (Norian-Hettangian), Fundy basin, Canada. New Mex Mus Nat Hist Sci Bull 37:35–42

Tanner LH (2013) The enigmatic Quaco cobbles, Upper Triassic, Canadian Maritimes: deformation by tectonics or seismic shock? The Triassic System. New Mex Mus Natural Hist Sci Bull 61:577–581

Tanner LH, Kyte FT (2005) Anomalous iridium enrichment at the Triassic–Jurassic boundary, Blomidon Formation, Fundy basin, Canada. Earth Planet Sci Lett 240(3–4):634–641. https://doi.org/10.1016/j.epsl.2005.09.050

Tanner LH, Lucas SG (2015) The Triassic-Jurassic strata of the Newark Basin, USA: a complete and accurate astronomically-tuned timescale? Stratigraphy 12:47–65

Tanner LH, Lucas SG, Chapman MG (2004) Assessing the record and causes of Late Triassic extinctions. Earth-Sci Rev 65(1–2):103–139. https://doi.org/10.1016/S0012-8252(03)00082-5

Tanner LH, Smith DL, Allan A (2007) Stomatal response of swordfern to volcanogenic CO_2 and SO_2 from Kilauea volcano, Hawaii. Geophys Res Lett 34:L15807. https://doi.org/10.1029/2007GL030320

Tanner LH, Kyte FT, Walker AE (2008) Multiple Ir anomalies in uppermost Triassic to Jurassic-age strata of the Blomidon Formation, Fundy basin, eastern Canada. Earth Planet Sci Lett 274(1–2):103–111. https://doi.org/10.1016/j.epsl.2008.07.013

Tanner LH, Kyte FT, Richoz S, Krystyn L (2016) Distribution of iridium and associated geochemistry across the Triassic-Jurassic boundary in sections at Kuhjoch and Kendlbach, Northern Calcareous Alps, Austria. Palaeogeogr Palaeoclimat Palaecol 449:13–26. https://doi.org/10.1016/j.palaeo.2016.01.011

Thackrey S, Walkden G, Kelley S, Parrish R, Horstwood M, Indares A, Stills J, Spray J (2008) Determining source of ejecta using heavy mineral provenance techniques; A Manicouagan distal ejecta case study. Proceedings of the 39th Lunar and Planetary Science Conference, 10–14 March 2008, League City, TX, Abst:1254.

Thackrey S, Walkden G, Indares A, Horstwood A, Kelley S, Parrish R (2009) The use of heavy mineral correlation for determining the source of impact ejecta: a Manicouagan distal ejecta case study. Earth Planet Sci Lett 285(1–2):163–172. https://doi.org/10.1016/j.epsl.2009.06.010

Thomas WA (2006) Tectonic inheritance at a continental margin. GSA Today 16(2):4–11

Thompson LM (2015) Shock attenuation constraints at Manicouagan: evidence from plagioclase and quartz in proximity to shatter cones. Bridging the Gap III: impact Cratering in Nature, Experiments and Modeling Conference, University of Freiburg, Germany, Abst: 1111

Thompson LM, Spray JG (2013) The Manicouagan impact research program, and other Canadian impact crater studies. 76th Annual Meeting of the Meteoritical Society, 29 July–2 August 2013, Edmonton, AB, Abst: 5289

Thompson LM, Spray JG (2014) Impact-related seismites at Manicouagan. Geological Association of Canada-Mineralogical Association of Canada Joint Annual Meeting, 21–23 May 2014, Fredericton, NB, Abst 37:268

Thompson LM, Spray JG (2017) Dynamic interaction between impact melt and fragmented basement at Manicouagan: the suevite connection. Meteorit Planet Sci 52(7):1300–1329. https://doi.org/10.1111/maps.12889

Tschudy RH, Pilmore CL, Orth CJ, Gilmore JS, Knight JD (1984) Disruption of the terrestrial plant ecosystem at the Cretaceous-Tertiary boundary, western interior. Science 225(4666):130–1032. https://doi.org/10.1126/science.225.4666.1030

Uno K, Yamashita D, Onoue T, Uehara D (2015) Paleomagnetism of Triassic bedded chert from Japan for determining the age of an impact ejecta layer deposited on peri-equatorial latitudes of the paleo-Pacific Ocean: a preliminary analysis. Phys Earth Planet Inter 249:59–67. https://doi.org/10.1016/j.pepi.2015.10.004

deVries Klein G (1963) Boulder surface markings in Quaco Formation (Upper Triassic), St. Martin's, New Brunswick, Canada. J Sediment Petrol 33(1):49–52. https://doi.org/10.1306/74D70DC1-2B21-11D7-8648000102C1865D

Wade JA, Brown DE, Fensome RA, Traverse A (1996) The Triassic-Jurassic Fundy Basin, Eastern Canada: regional setting, stratigraphy and hydrocarbon potential. Atl Geol 32(3):189–231. https://doi.org/10.4138/2088

Waldron JWF, Barr SM, Park AF, White CE, Hibbard J (2015) Late Paleozoic strike-slip faults in Maritime Canada and their role in the reconfiguration of the northern Appalachian orogeny. Tectonics 34(8):1661–1684. https://doi.org/10.1002/2015TC003882

Walkden G, Parker J (2008) The biotic effects of large bolide impacts: size vs time and place. Int Jour Astrobiol 7(3–4):209–215. https://doi.org/10.1017/S1473550408004266

Walkden G, Parker J, Kelley S (2002) A Late Triassic impact ejecta layer in southwestern Britain. Science 298(5601):2185–2188. https://doi.org/10.1126/science.1076249

Wartho, J-A, Schmieder M, van Soest MC, Buchner E, Hodges KV, Bezys RK, Reimold WU (2009). New (U–Th)/He zircon and apatite ages for the Lake Saint Martin impact structure (Manitoba, Canada) and implications for the Late Triassic multiple impact theory. Proceedings of the 40th Lunar and Planetary Science Conference, Woodlands, TX, 23–27 March 2009, Abst:2004.

Wartho J-A, van Soest MC, Cooper FJ, Hodges, KV, Spray JG, Schmieder, M, Buchner E, Bezys RK, Reimold WU (2010) Updated (U-Th)/He Zircon Ages for the Lake Saint Martin impact structure (Manitoba, Canada) and implications for the Late Triassic multiple impact theory. Proceedings of the 41st Lunar and Planetary Science Conference, Woodlands, TX, 1–5 March 2010, Abst: 1930.

Wartho J-A, van Soest MC, Cooper FJ, Spray JG, Schmieder M, Buchner E, King DT, Ukstins Peate I, Koeberl C, Reimold WU, Biren MB, Petruny LW, Hodges KV (2012) (U–Th)/He dating of impact structures—the big, the small, and the potential limitations. Meteorit Planet Sci 75(S1):A401

Weems RE, Lucas SG (2015) A revision of the Norian conchostracan zonation in North America and its implications for Late Triassic North American tectonic history. In: Sullivan RM, Lucas SG (eds) Fossil Record 4. New Mex Mus Nat Hist Sci Bull 67:303–317

Weems RJ, Tanner LH, Lucas SG (2016) Synthesis and revision of the lithostratigraphic groups and formations in the Upper Permian?–Lower Jurassic Newark Supergroup of eastern North America. Stratigraphy 13(2):111–153

White RV, Saunders AD (2005) Volcanism, impact and mass extinctions: incredible or credible coincidences? Lithos 79(3–4):299–316. https://doi.org/10.1016/j.lithos.2004.09.016

Whitehead J, Spray JG, Grieve RAF (2002) Origin of "toasted" quartz in terrestrial impact structures. Geology 30(5):431–434. https://doi.org/10.1130/0091-7613(2002)

Whiteside JH, Olsen PE, Eglinton T, Brookfield ME, Sambrotto RN (2010) Compound-specific carbon isotopes from Earth's largest flood basalt eruptions directly linked to the end-Triassic mass extinction. Proc Nat Acad Sci U S A 107(15): 6721–6725. https://doi.org/10.1073/pnas.1001706107

Withjack MO, Schlische RW, Baum MS (2009) Extensional development of the Fundy rift basin, southeastern Canada. Geol J 44(6):631–651. https://doi.org/10.1002/gj.1186

Withjack MO, Schlische RW, Olsen PE (2012) Development of the passive margin of eastern North America: Mesozoic rifting, igneous activity, and breakup. In: Bally AW, Roberts DG (eds) Principles of Phanerozoic Regional Geology, vol 1. Elsevier, Amsterdam, pp 301–335

Wotzlaw J-F, Guex J, Bartolini A, Gallet Y, Krystyn L, McRoberts CA, Taylor D, Schoene B, Schaltegger U (2014) Towards accurate numerical calibration of the Late Triassic: high-precision U-Pb geochronology constraints on the duration of the Rhaetian. Geology 42(7):571–574. https://doi.org/10.1130/G35612.1

Wrobel KE, Schultz PH (2003) The effect of rotation on the deposition of terrestrial impact ejecta. Proceedings of the 34th Lunar and Planetary Science Conference, League City, TX, 17–21 March 2003, Abst:1190

Wünnemann K, Zhu M-H, Stöffler D (2016) Impacts into quartz sand: crater formation, shock metamorphism, and ejecta distribution in laboratory experiments and numerical models. Meteorit Planet Sci 51(10):1762–1794. https://doi.org/10.1111/maps.12710

Chapter 6
New Upper Triassic Conodont Biozonation of the Tethyan Realm

Manuel Rigo, Michele Mazza, Viktor Karádi, and Alda Nicora

Abstract Conodonts are biostratigraphically very important microfossils in the Upper Triassic, occurring in different marine habitats, from deep-ocean to shallow-shelf waters. Because of their great abundance, worldwide distribution, strong resistance to rock metamorphism, and mineralogical composition that makes them reliable tools for biostratigraphic and geochemical studies, conodonts have proven to be important tools in defining the Geological Time Scale (GTS) and Global Stratotype Section and Points (GSSPs). We present here an original Upper Triassic conodont biozonation for the Tethyan Realm integrated, where possible, with ammonoid and radiolarian zones, providing also numerical ages for stages and substages. Based on the most recent conodont biostratigraphic and systematic studies, we propose a subdivision of the Upper Triassic interval into 22 conodont zones (nine for the Carnian, ten for the Norian, and three for the Rhaetian), correlated, where possible, with the most recent North American conodont zonations. Discussions on the most biostratigraphically important conodont taxa are also provided, in particular for the stratigraphic intervals around the base of the Norian and Rhaetian stages, the GSSPs of which have yet to be defined. In this view, we provide data supporting the validity of conodonts as reliable tools for global correlations, recommending two conodont biovents as possible primary biomarkers: the FAD (First Appearance Datum) of *Metapolygnathus parvus* for the base of the Norian and the FAD of *Misikella posthernsteini* for the base of the Rhaetian. The conodont species *Norigondolella carlae* n. sp. from the upper Tuvalian (Carnian) is also defined.

Keywords Upper Triassic • Conodont • Biozonation • Tethyan • Correlation

M. Rigo (✉)
Department of Geosciences, University of Padova, Via G. Gradenigo 6, 35131 Padova, Italy
e-mail: manuel.rigo@unipd.it

M. Mazza • A. Nicora
Department of Earth Sciences "Ardito Desio", University of Milan,
Via Mangiagalli 34, 20133 Milan, Italy

V. Karádi
Department of Palaeontology, Eötvös Loránd University,
1/c Pázmány Péter sétány, Budapest H-1117, Hungary

© Springer International Publishing AG 2018

L.H. Tanner (ed.), *The Late Triassic World*, Topics in Geobiology 46,
https://doi.org/10.1007/978-3-319-68009-5_6

6.1 Introduction

The Upper Triassic was first divided by Mojsisovics von Mojsvár (1869) into three stages, the Carnian, Norian and Rhaetian. Originally, these stage definitions were based on ammonoids (Carnian and Norian) and bivalves (Rhaetian) and described in different localities in the northern Alps (Austria) with uncertain stratigraphic relationships between Carnian and Norian (Tozer 1984; Ogg 2012). Only after the discovery of conodonts in unequivocally Triassic strata in Sinai (Egypt) by Eicher (1946) was the presence of conodonts in Triassic sediments considered suitable for a reliable biostratigraphy for the early Mesozoic. Since then, and following the pioneering papers by Youngquist (1952), Tatge (1956) and Müller (1956), Triassic conodonts have become one of the most important biostratigraphic tools for dating and regional to global correlations. In the last few decades, Triassic conodonts have been the subject of intensive investigation and an extensive literature is now available. In fact, in recent years the number of species of Upper Triassic conodonts known has increased quickly as a result of detailed researches conducted in multiple sections worldwide, mostly in order to define the Upper Triassic GSSPs. Unfortunately, the taxonomic position of many conodont species is not firmly defined, mostly because of personal approaches to their taxonomy. Furthermore, the true distribution of most conodont species is represented only by scattered and sporadic occurrences in several stratigraphic sections, hampering the recognition of phylogenetic relationships. However, a constantly increasing amount of available data—conodont distributions on long and continuous sections, sometimes tied to ammonoid and radiolarian occurrences or chemo- and magnetostratigraphy—is improving the situation.

Unfortunately, few authors have presented images and/or range distributions of the species collected during their studies, preferring more often to use open nomenclature to gather conodont elements with presumably similar features. Furthermore, some proposed conodont biozonations are affected by stratigraphic condensation, which at the extreme may result in fossil associations consisting of species of differing age or in the loss or misinterpretation of important bioevents horizons (Salvador 1994). Similarly, an inappropriate and confused classification and nomenclature, mostly due to a general lack of consensus, has failed to provide an "unambiguous species concept", as stated also by Orchard (1991a). This has had a severely negative impact on conodont biostratigraphy. Moreover, the misinterpretation of the originally-described features of species can also have a negative effect on chronostratigraphy, with repercussions in all the other fields for which time is the key point (e.g. palaeoclimate reconstructions, geodymanics), for instance, the inclusion of an older chronostratigraphic unit (Sevatian 2) into a younger one (Rhaetian) (Krystyn et al. 2007a, b).

In this paper we propose a conodont biozonation based mainly on very detailed and tightly spaced samplings of continuous sections, rather than on isolated occurrences, following the recommendations of Tanner et al. (2004) among others. Where possible, our biozonation is built on phylogenetic reconstructions in order to provide a framework in which taxonomical attributions and biostratigraphic studies could be less aleatory. There are several reasons why phylogenetic reconstructions are necessary. First, within a phylogenetic framework, the distribution of conodont species

would be constrained by their phylogenetic relationships. Second, open taxonomic issues, including disputed synonymies and the position of transitional forms, may be best untangled on the basis of phylogeny. Third, the recognition of transitional forms and morphoclines in the biostratigraphic practice would greatly improve the chances of identifying true FADs (First Appearance Datum). The phylogenetic approach to biostratigraphy is, in fact, an ultimate achievement of well-established scales, and this approach is recommended by Remane (2003). Fourth, provincialism and migrations can be fully understood only within an established phylogeny. Finally, the reconstruction of Upper Triassic conodont phylogeny unveils the evolutionary trends of the class Conodonta during its last 40 Myrs.

The biozonation presented herein, based on 20 Interval Zones and 2 Taxon-Range Zones, is meant to facilitate the discussion of the three stages, despite the fact that only the base of the Carnian stage is formally defined and ratified by the International Commission on Stratigraphy (Mietto et al. 2012). When possible, the proposed conodont biozonation are compared with ammonoid, radiolarian or bivalve biozones or numerical ages. We consider this proposed biozonation as a starting point for future Upper Triassic investigations, hoping for a constructive integration in order to delineate a reference conodont biozonation commonly applied to Tethyan and global correlations.

6.2 Upper Triassic Conodonts: Overview

The pectiniform conodont record of the Upper Triassic documents pulses of severe extinctions followed by recovery events, testifying that the evolutionary history of the class Conodonta in its last 38 Myrs is characterised by a continuous decline of the conodonts specific diversity (see e.g. Martínez-Pérez et al. 2014 and references therein). The same decline was noticed earlier by De Renzi et al. (1996), who identified an irregular decrease from a climax of lineage during the Middle Triassic (late Anisian) until the final extinction of conodonts at the end of the Triassic.

In the Late Triassic, conodonts suffer four main extinction events before the end of the Rhaetian: the first, a weak one, in the early Julian; the second, more significant, at the Julian/Tuvalian boundary (mid-Carnian); the third one, which is more similar to a faunal turnover rather than to a proper extinction, occurred at the Tuvalian/Lacian boundary (Carnian/Norian boundary); the fourth, across the Norian/Rhaetian boundary, testifies to a morphological change towards simple cavitated species. From the point of view of conodont morphology, each extinction was followed by a new speciation and by evident changes in the morphological diversity of the platform elements. These morphological trends were observed also by Mosher (1968), although he did not connect them with extinctions. Notably, all of these faunal turnovers seem to be related to climatic changes (Trotter et al. 2015).

The Julian (Lower Carnian) pectiniform species that survive the first extinction in the early Julian might be considered as the relict forms inherited from the richness climax of lineages achieved during the Ladinian (De Renzi et al. 1996). The most complex and advanced species disappear (i.e. budurovignathids), while the survivors are morphologically simple, characterised by elongated platforms without ornamen-

tation and a posterior pit (i.e. paragondolellids). After the first extinction pulse, within the Julian substage, some small conodonts with tiny nodes on the platform occur (genera *Mazzaella* and *Hayashiella*). The second extinction, at the Julian/Tuvalian boundary (Lower/Upper Carnian), is more intense and related to the well know humid pulse called the Carnian Pluvial Event (Rigo et al. 2007, 2012b; Rigo and Joachimski 2010; Kolar-Jurkovšek and Jurkovšek 2010; Trotter et al. 2015). The following recovery is slow, but it brings conodont specific diversity to a new peak in the middle-late Tuvalian (i.e. the rise of genera *Carnepigondolella*, *Metapolygnathus*, and *Epigondolella*). All the Tuvalian substage is thus characterised by conodonts with node or denticle ornamented platforms, independently of which lineage they arose from, and by a gradual reduction of the platform length and the forward shifting of the pit, except for rare paragondolellids in the lowermost Tuvalian.

Late Triassic conodonts experienced another extinction event around the Carnian/Norian boundary, when almost all Tuvalian carnepigondolellids became extinct. Conodonts exhibit two different evolutionary trends. The first trend is characterised by the returning to ancestral features, by the extension of the platform with loss of the lateral margin nodes and of the free blade (i.e. genus *Norigondolella*). The second trend, instead, consists of species (i.e. *Epigondolella* and *Mockina*) that bear high denticles, distributed on the platform margins, which make the pectiniform elements compact and robust. After this last pulse, the evolutionary history of conodonts until the end of the Triassic is characterised by a constant morphological and diversity decline. At the end of the Norian, the tendency to a general simplification of the morphological features may be observed, following a progenetic process started in the Early Norian (Mazza and Martínez-Pérez 2015). Even if two different branches evolved from the same species *Mockina bidentata*, all the uppermost Triassic pectiniform conodonts loose the platform and decrease in dimension (genera *Parvigondolella* and *Misikella*). This evolutionary decline is similar to that observed at the Permian/Triassic boundary for genus *Hindeodus*, which brings analogous characters to genus *Misikella* (stressful environmental conditions). But, in contrast to the Early Triassic, this morphological simplification represented by *Misikella* is no longer successful, and after the disappearance of the last platform-bearing conodonts (such as *Norigondolella*), also platformless genus *Misikella* disappears at the end of Rhaetian.

6.3 The New Conodont Zonation

Conodonts are a leading fossil group for the definition of the biostratigraphic scale of Palaeozoic and Triassic, as demonstrated by the GSSP database of the International Commission on Stratigraphy (Gradstein et al. 2012). For instance, the stratigraphic importance of conodonts is testified by the FAD of *Hindeodus parvus* to define the Induan Stage (=base of the Mesozoic Era), after the end-Permian extinction (Yin et al. 2001). During Triassic, however, conodonts are less favoured from the stratigraphic point of view than other fossil groups such as ammonoids. In the Upper Triassic, in particular, the uncertain age attribution and the ambiguous systematic of some taxa have created confusion during the time, leading some Lower Mesozoic specialists of other disciplines to state that Upper Triassic conodonts are almost

stratigraphically useless (e.g. Lucas 2016). But incredible improvements achieved in conodont research in the last years have disentangled many of these issues, proving the reliability of conodonts as a valid and sound biostratigraphic tool for the Lower Mesozoic as for the Palaeozoic Era, making conodont a leading fossil group also for the Upper Triassic (e.g. Orchard 2016).

The dawn of the modern Upper Triassic conodont taxonomy and systematics began in the late 1950s and continued through the 1960s and 1970s, when most of the conodont genera and species representing the key taxa for modern Upper Triassic conodont biostratigraphy were established and described. The research include forms described by Huckriede (1958) (for genus *Epigondolella*), Budurov and Stefanov (1965) (*Paragondolella polygnathiformis*), Mostler (1967) (*Misikella hernsteini*), Mosher (1968) (genus *Paragondolella*, *Mockina bidentata*), Hayashi (1968) (genus *Metapolygnathus*, *Metapolygnathus communisti*), Budurov (1972) (*Epigondolella triangularis*), Kozur (1972) (genus *Mockina*, *Metapolygnathus parvus*), and Kozur and Mock (1974) (*Misikella posthernsteini*). A selection of conodont biozonations is here presented. Mosher (1968) subdivided the Carnian and the Norian into two zones. Subsequently, Sweet et al. (1971) subdivided the Carnian in two and the Norian in three zones. In both the papers the Rhaetian presented no zones (Fig. 6.1). In 1972, Kozur proposed the first detailed Upper Triassic conodont biozonation for both Tethys and North America, suggesting a total of nine zones. However, this biozonation was affected by some biases due to conodont taxonomic misinterpretations by the author, as noted by Krystyn (1980). The same biases were also reported in the successive conodont biozonation by Kovács and Kozur (1980), with ten zones (Fig. 6.1). Successively, Krystyn (1980) proposed a new conodont/ammonoid integrated biozonation (Fig. 6.1) of 4 zones and 14 subzones, which differed from that proposed by Kozur (1972) in both the taxonomic concepts and ammonoid correlations (as stated in Orchard 1991b). In North America, the first accurate conodont biozonations were by Orchard (1983, 1991a, b), followed by some successive refinements during the years (Orchard et al. 2000, 2001, 2007b; Orchard 2007), which remain valid at present (Fig. 6.2). The most detailed and recent zonation for the Carnian-Norian interval is by Orchard (2014), being the result of intense studies on the conodonts of the Norian GSSP candidate section of Black Bear Ridge (British Columbia, Canada) (Fig. 6.2), in which he described numerous new taxa, consisting of 80 new species and 47 morphotypes, and presenting a new conodont biozonation, making also important calibrations with ammonoids and halobiids (bivalves) in the perspective of correlations with the Tethys. The most recent Tethyan conodont biozonation of the Upper Triassic is by Kozur, in Moix et al. (2007) modified after Kozur (2003), in which the author proposed a total of 17 conodont zones (Fig. 6.3).

The conodont biozonation presented in this work (Figs 6.4, 6.5, 6.9, 6.14) is completely original and it is based on personal studies on Tethyan successions and comparisons with data from literature on conodonts from the Tethys and North America Provinces. All the conodonts present in the biozones are indicated, but in Fig. 6.4 only the index species and biostratigraphically most important species are reported. For the lower Carnian (Julian) most of the data are from the literature whilst for the Tuvalian (upper Carnian) to the Rhaetian we followed the same methodology applied in Orchard (2014). In fact, the biozones proposed are based on

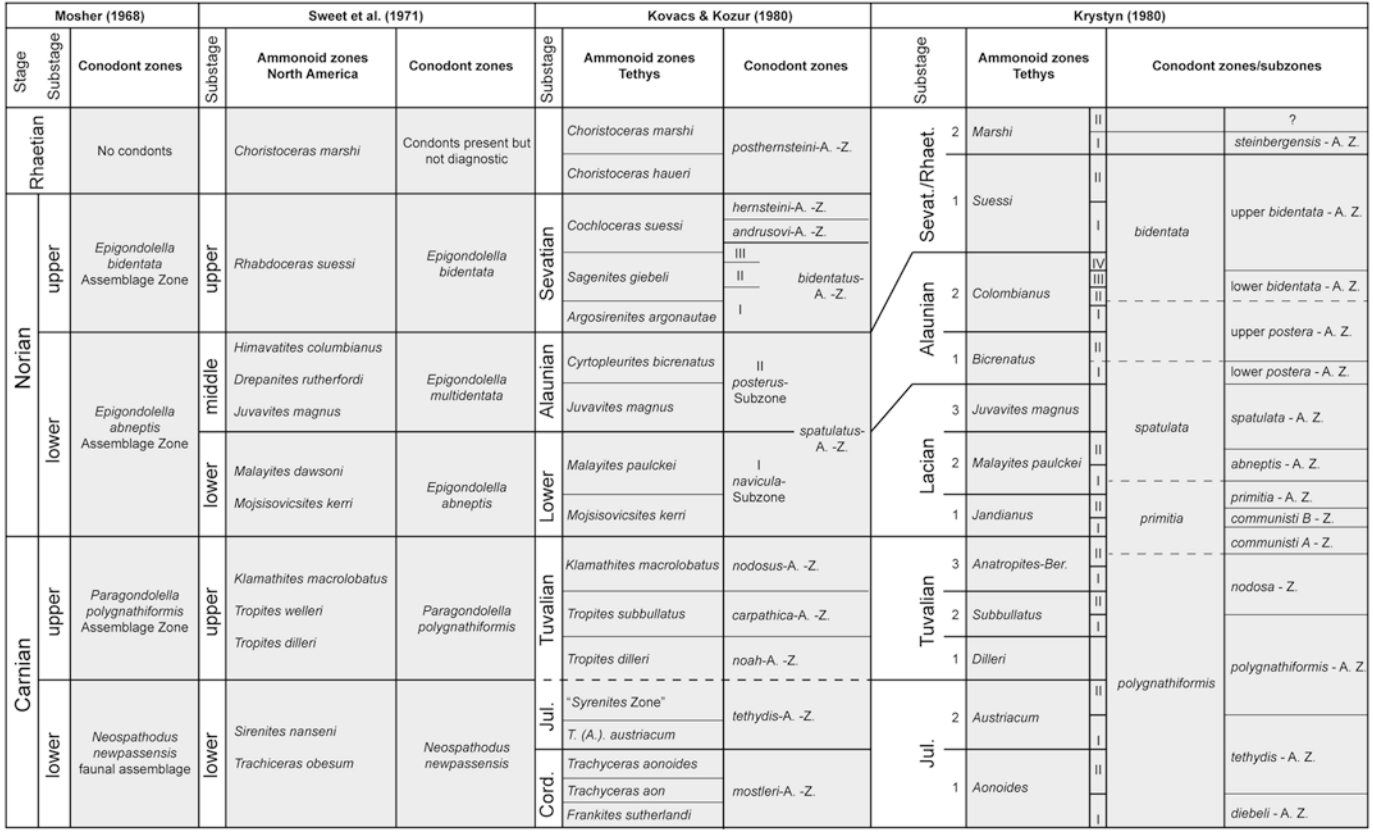

Fig. 6.1 Selected integrated Upper Triassic conodont/ammonoid biozonations, showing their evolution from the 1960s to the 1980s

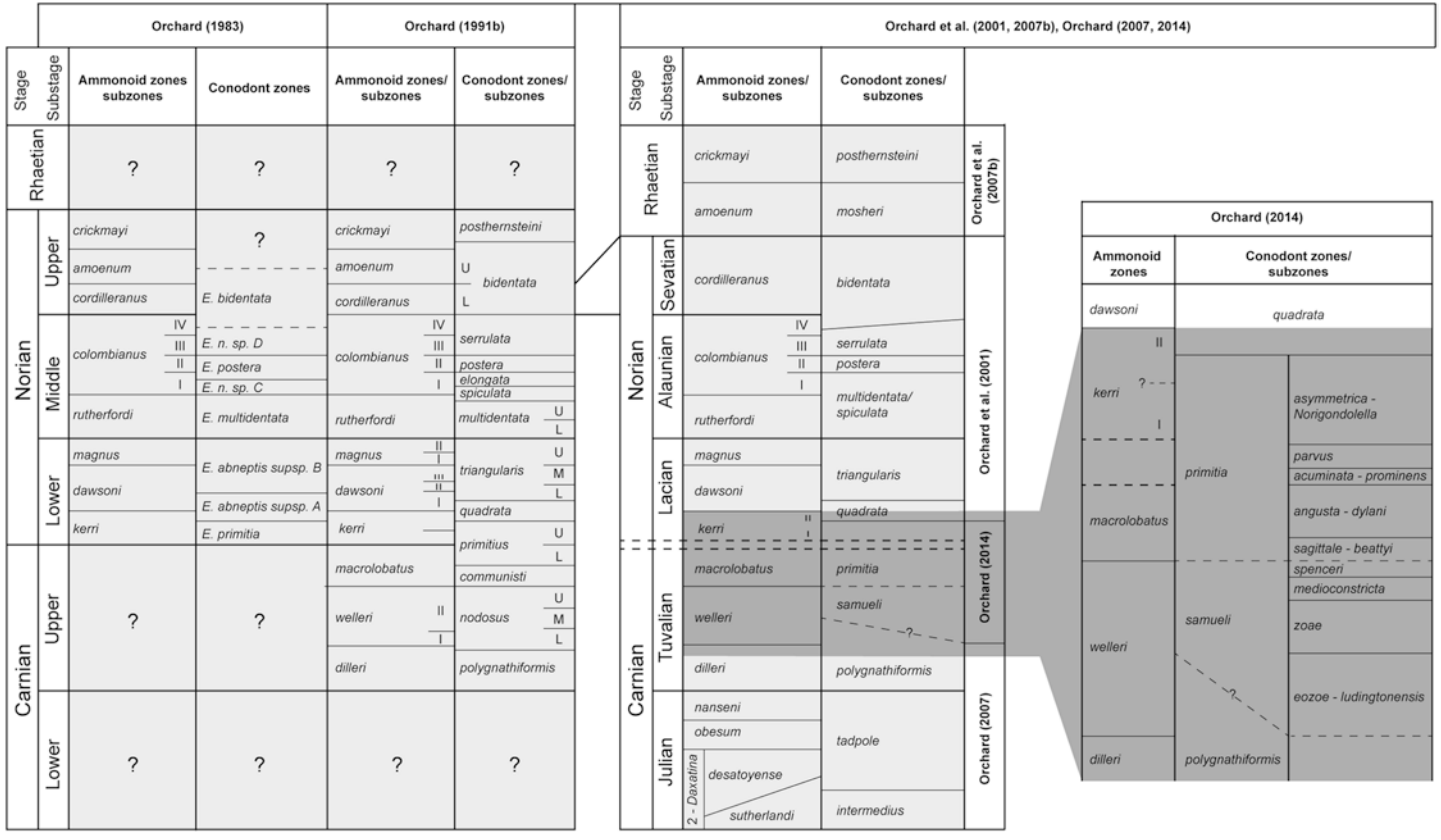

Fig. 6.2 Evolution of the integrated ammonoid/conodont biozonations of the North American province, from 1983 to 2014

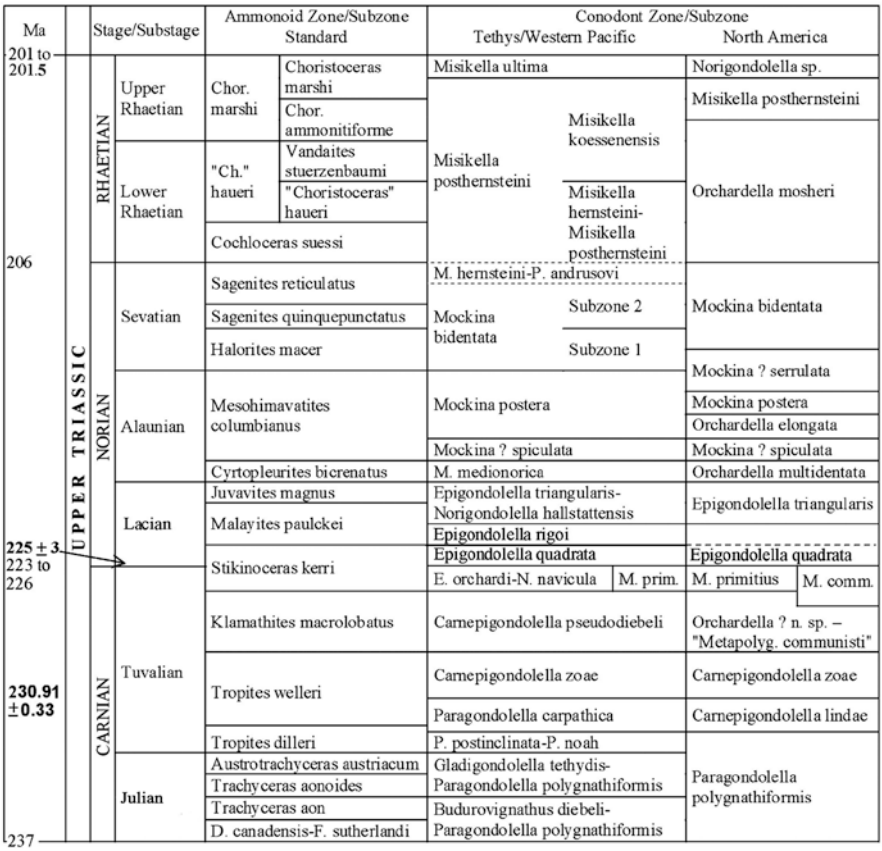

Fig. 6.3 Most recent Upper Triassic conodont/ammonoid biozonations, integrated also with radiometric ages (modified after Moix et al. 2007)

phyletic lineages and conodont ranges from continuous pelagic successions with highly detailed and tightly spaced sampling. The main sources of data are the GSSP Tethyan candidate sections for the base of the Norian (Pizzo Mondello, western Sicily, Italy) and the base of the Rhaetian (Pignola-Abriola, southern Appennins, Italy), integrated with the conodont distributions from other localites in all the Tethyan provinces, taken from the literature.

6.4 The Ladinian/Carnian Boundary and the Carnian Stage

The Carnian was named after the Austrian localities in the Carinthia region (Kärnten) and applied for all those strata yielding the ammonoids belonging to genera *Trachyceras* and *Tropites* (Mojsisovics von Mojsvár 1869). Originally, the base of the Carnian stage was placed at the base of the ammonoid *Trachyceras aon* or

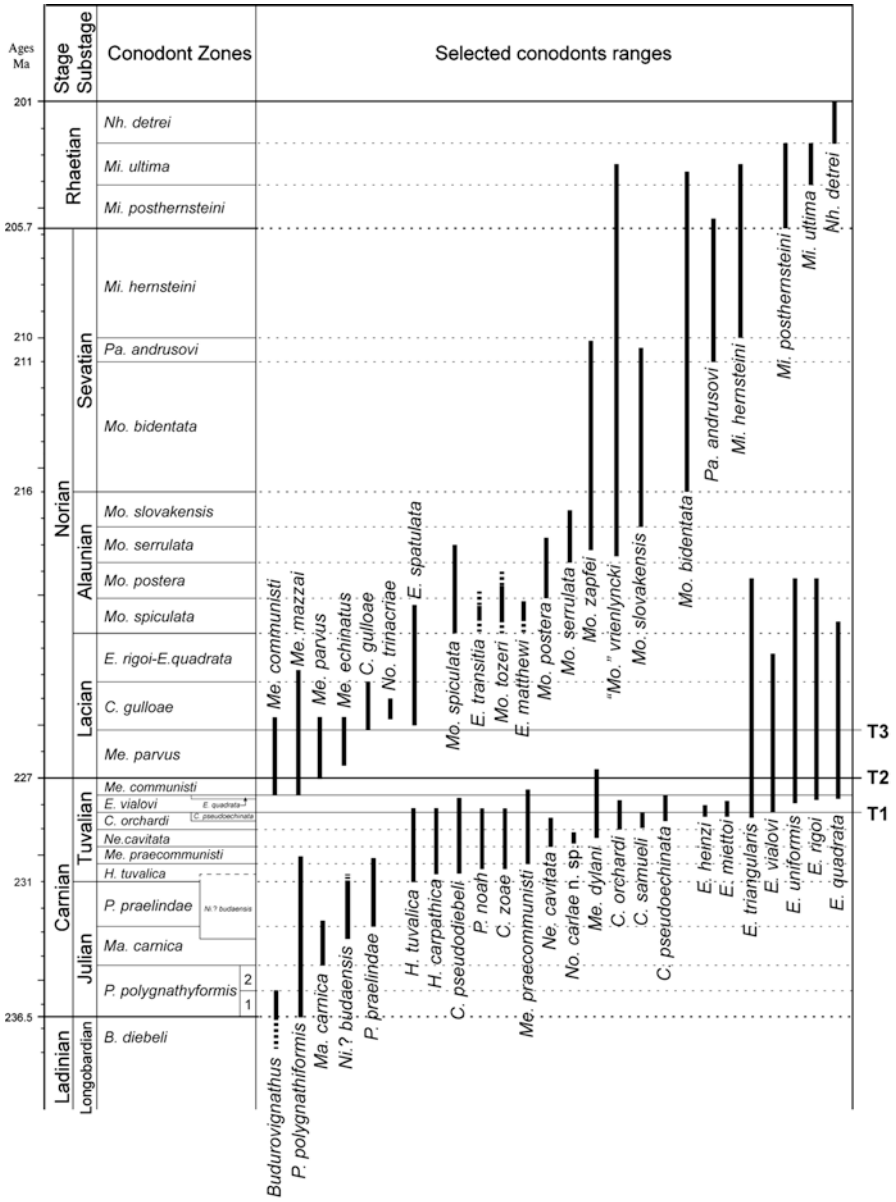

Fig. 6.4 The new Upper Triassic conodont biozonation proposed in this work and ranges of the index species and the most important conodonts for global correlations. The zonation is constrained, where possible, with radiometric ages. *B.* = *Budurovignathus*, *C.* = *Carnepigondolella*, *E.* = *Epigondolella*, *H.* = *Hayashiella*, *Me.* = *Metapolygnathus*, *Ma.* = *Mazzaella*, *Mi.* = *Misikella*, *Mo.* = *Mockina*, *Ne.* = *Neocavitella*, *Nh.* = *Neohindeodella*, *Ni.*? = *Nicoraella*, *No.* = *Norigondolella*, *P.* = *Paragondolella*, *Pa.* = *Parvigondolella*. *T1* = Turnover 1, *T2* = Turnover 2, *T3* = Turnover 3 sensu Mazza et al. (2010)

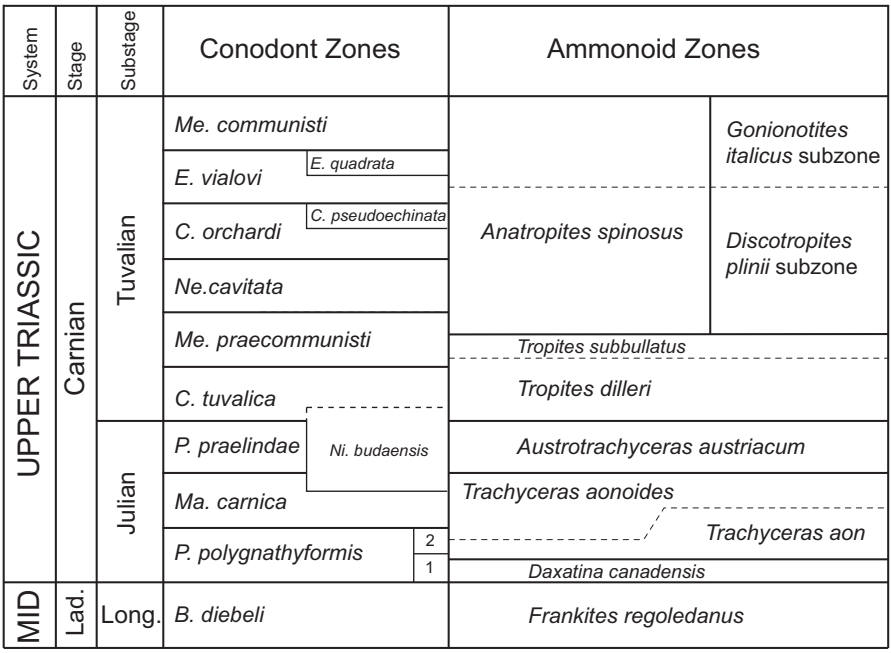

Fig. 6.5 New conodont/ammonoid integrated biozonation of the latest Ladinian and Carnian stages. See caption of Fig. 6.4 for genera abbreviations

Trachyceras desatoyense zones in Tethys and Canada respectively, but the occurrence of genus *Trachyceras* appeared to be asynchronous (e.g. Mietto and Manfrin 1999). Thus, the FAD of *Daxatina canadensis* was proposed (Broglio Loriga et al. 1999) and accepted to define the base of the Carnian Stage, the GSSP of which is placed at the Prati di Stuores type locality in the Dolomites (Northern Italy) (Mietto et al. 2012). The Carnian is subdivided into two substages, Julian and Tuvalian. The Cordevolian was originally the first substage of the Carnian Stage proposed by Mojsisovics von Mojsvár et al. (1895). Kozur (2003) suggested that Cordevolian was characterised by a mixture of Ladinian fossils (i.e. conodonts, ammonoids, bivalves) that ranged up into the earliest Carnian. Later, the Cordevolian substage was included in the Julian by Krystyn (1980), even if Cordevolian is still occasionally used by some authors in their biostratigraphic scales (e.g. Kozur 2003; Moix et al. 2007). It is noteworthy that the radiation of the Julian species is not comparable with the large variety of species occurring during the Tuvalian radiation. We consider the Julian, defined by the FAD of ammonoid *Daxatina canadensis* (Mietto et al. 2012), as the base of the Carnian stage and of the Upper Triassic (Fig. 6.5). The appearance of *D. canadensis* is very close to the FO of the conodont *Paragondolella polygnathiformis,* suggested as a secondary marker to recognize the base of the Carnian (Mietto et al. 2012).

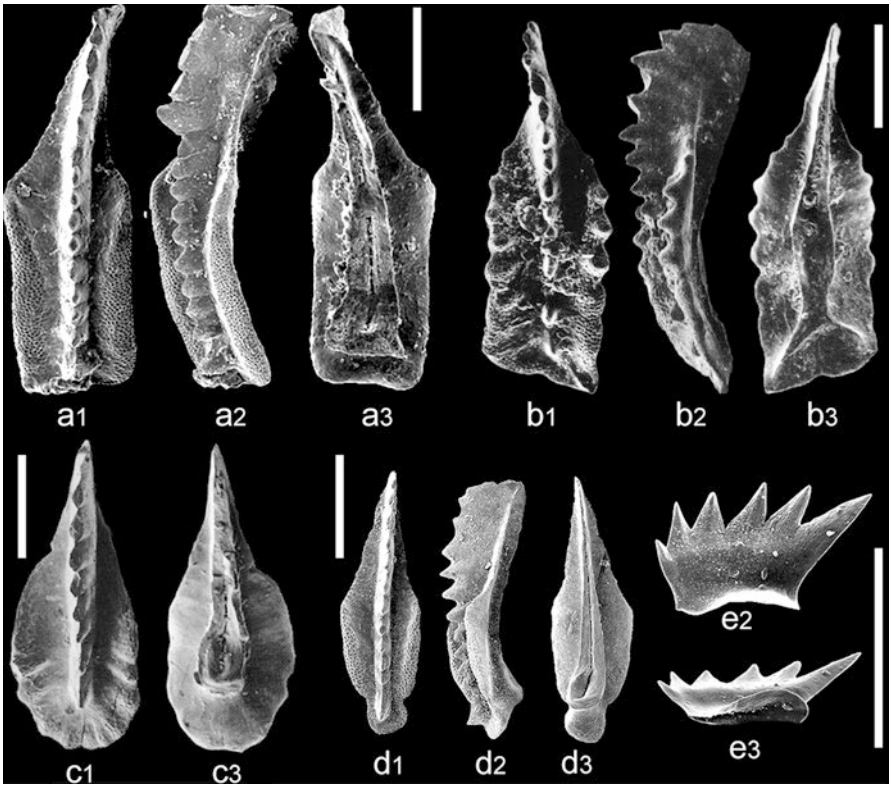

Fig. 6.6 Index conodont species for the Julian (Lower Carnian) zones. Where possible, all the three views are provided: (1) upper view, (2) lateral view, (3) lower view. Scale bars are 200 μm. (**a**) *Paragondolella polygnathiformis* (Budurov and Stefanov) (from Gaetani et al. 2013). (**b**) *Budurovignathus diebeli* (Kozur and Mostler) (from Mastrandrea et al. 1998). (**c**) *Mazzaella carnica* (Kristan-Tollmann and Krystyn) (from Krystyn 1983). (**d**) *Paragondolella praelindae* Kozur (from Mazza et al. 2012a) (**e**) *Nicorella* ? *budaensis* Kozur and Mock (from Kolar-Jurkovšek and Jurkovšek 2010)

6.4.1 Julian Conodont Biozonation

6.4.1.1 *Paragondolella polygnathiformis* Interval Zone

Definition: the lower boundary is marked by the FO of the index species *Paragondolella polygnathiformis* (Budurov and Stefanov 1965); the upper boundary by the FO of *Mazzaella carnica* (Kristan-Tollmann and Krystyn 1975).

Paragondolella polygnathiformis (Fig. 6.6a) descends from *P. inclinata* (Kovács 1983; Kozur 1989; Mazza et al. 2010, 2011), by developing an abrupt step at the geniculation point, on the anterior platform margins. The transitional forms between *Paragondolella inclinata/polygnathiformis* are documented in the latest Ladinian, during a period characterised by a monotonous conodont association persisting also in the early Carnian (e.g. Gallet et al. 1998; Broglio Loriga et al. 1999; Balini et al.

2000; Rigo et al. 2007; Mietto et al. 2012). This conodont assemblage characterises the upper portion of the Ladinian Stage (i.e. Longobardian) and is represented mainly by species belonging to genera *Budurovignathus* [e.g. *B. deibeli* (Fig. 6.6b), *B. mostleri, B. mungoensis, B. longobardicus*], *Paragondolella* (e.g. *P. foliata; P. inclinata*), *Pseudofurnishius* (*P. murcianus murcianus; P. murcianus preacursor*), and *Gladigondolella* (e.g. *G. malayensis malayensis, G. tethydis, G. arcuata*). *Paragondolella polygnathiformis* is a long-ranged species, present until the mid Tuvalian (Upper Carnian) and, more important, it is the ancestor of most of the Tuvalian conodonts (e.g. Rigo et al. 2007; Mazza et al. 2010, 2011, 2012a, b). We thus suggest *P. polygnathiformis* Zone as the first conodont Interval Zone for the base of the Carnian stage, defined by the first occurrence of the index species.

We subdivided this Zone into two Subzones, which we informally named *Paragondolella polygnathiformis* 1 and 2 Subzones (Fig. 6.5), basing on the disappearance of the Ladinian conodont *Budurovignathus* relict species at the end of Subzone 1.

Age: The *P. polygnathiformis* Zone corresponds to the ammonoid Zone *Daxatina candensis* and the lower portion of the *Trachyceras aon* Zone, at the base of which the Ladinian relict species disappear definitely (e.g. Broglio Loriga et al. 1999; Mietto et al. 2012) (Fig. 6.5).

6.4.1.2 *Mazzaella carnica* Interval Zone

Definition: the lower boundary is marked by the FO of the index species *Mazzaella carnica* (Kristan-Tollmann and Krystyn 1975); the upper boundary by the FO of *Paragondolella praelindae* Kozur (2003).

After the disappearance of the surviving Ladinian conodonts (i.e. *Budurovignathus*) in the Lower Carnian, new species as *Mazzaella carnica* (Fig. 6.6c) and *Paragondolella auriformis*, along with *Ma. baloghi*, appear in the upper part of the lower Julian. A correlation with ammonoid zonation is not well defined, in fact the occurrence of *Paragondolella auriformis* might fall in both the *Trachyceras aon* and *T. aonoides* Zones (Krystyn 1983), followed by the occurrence of the conodont *Ma. carnica*.

Age: The disappearance of the conodont *Ma. carnica* corresponds to the occurrence of *Austrotrachyceras triadicum*, which is a species characterising the base of the ammonoid *Austrotrachyceras austriacum* Zone (Krystyn 1983) (Fig. 6.5). We thus suggest that the *Ma. carnica* Interval Zone corresponds to the upper portion of the ammonoid *Trachyceras aonoides* Zone (Krystyn 1983; Mastandrea 1995), taking into account that the first occurrence of the *P. aurifomis* should be better constrained within the *Trachyceras aon* or *T. aonoides* Zones. Locally, in particular in the Buda Mountains, Slovenian and Julian Alps, *Nicoraella*? *budaensis* (Fig. 6.6e) occurs along with ammonoids of the *T. aonoides* Zone up to the Julian/Tuvalian boundary (e.g. Kozur and Mock 1991; Kolar-Jurkovšek et al. 2005; Kolar-Jurkovšek and Jurkovšek 2010).

6.4.1.3 *Paragondolella praelindae* Interval Zone

Definition: the lower boundary is marked by the FO of the index species *Paragondolella praelindae* Kozur (2003); the upper boundary by the FO of *Hayashiella tuvalica* Mazza and Rigo, 2012 (in Mazza et al. 2012a).

After the disappearance of *Mazzaella carnica*, the conodont species *Paragondolella praelindae* (Fig. 6.6d) occurs in the uppermost Julian commonly. *Paragondolella praelindae* occurs with indisputable Julian species, such as *Gladigondolella* spp., *Paragondolella inclinata, P. foliata, P. tadpole, Nicoraella postkockeli* (Rigo et al. 2007, 2012a).

Age: The *P. praelindae* conodont zone corresponds to the ammonoid *Austrotrachyceras austriacum* Zone (Rigo et al. 2007, 2012a) (Fig. 6.5).

6.4.2 *The Julian/Tuvalian Boundary and the Tuvalian Substage*

The Julian/Tuvalian boundary is traditionally placed with the first occurrence of the ammonoid *Tropites dilleri* (Krystyn 1978; Kovács and Kozur 1980; Tozer 1994; Kozur 2003; Lucas 2010). At the Julian/Tuvalian boundary a significant faunal and floral turnover occurs (Simms and Ruffell 1989, 1990; Simms et al. 1995), and it coincides with important ecological events linked to the so called Carnian Pluvial Event (CPE): a warming cycle (Rigo and Joachimski 2010; Rigo et al. 2012b; Trotter et al. 2015), an enhanced siliciclastic input in the basins (e.g. Simms and Ruffell 1989; Rigo et al. 2007), a rise in carbonate compensation depth (CCD) (Rigo et al. 2007), and a $\delta^{13}C$ perturbation (Dal Corso et al. 2012). All these events were probably linked to the onset of the Wrangellia magmatic province (Furin et al. 2006).

At the base of the Tuvalian substage (Upper Carnian) only few conodont taxa survive the extinction caused by the CPE (*Paragondella praelindae, P. polygnathiformis, Hayashiella nodosa, Neocavitella* spp., *Cornudina*/"*Misikella*" spp.) (Rigo et al. 2007; Mazza et al. 2012b; Chen et al. 2015), and a new radiation arose from *P. polygnathiformis* (Rigo et al. 2007; Mazza et al. 2012a, b). In the early Tuvalian the specific diversity is still low and populations are quite poor, because conodonts are still recovering from the environmental crisis affecting their ecosystem. The faunas are mainly represented by *P. polygnathiformis, P. noah, Hayashiella tuvalica, H. carpathica, Carnepigondolella zoae* and the first primitive representatives of *C. pseudodiebeli*. The true evolutionary radiation occurs in the late Tuvalian, when genus *Carnepigondolella* dominates the conodont faunas, originating a great variety of species and intraspecific morphologies (see Orchard 1991a, b, 2014; Channell et al. 2003; Mazza et al. 2012b; Martínez-Pérez et al. 2014). The peak of the late Carnian radiation is reached in the latest Tuvalian, when species belonging to genera *Epigondolella* and *Metapolygnathus* occur together with genus *Carnepigondolella*, while genus *Paragondolella* became only a relict Middle Triassic taxon with few representatives (*P. noah* and *P. oertlii*) (Kozur 2003; Mazza et al. 2012a, b).

6.4.2.1 *Hayashiella tuvalica* Interval Zone

Definition: the lower boundary is marked by the FO of the index species *Hayashiella tuvalica* Mazza and Rigo 2012 (in Mazza et al. 2012a); the upper boundary by the FO of *Metapolygnathus praecommunisti* Mazza, Rigo and Nicora (2011).

Hayashiella tuvalica (Fig. 6.7e) is a long ranging species that encompasses all the Tuvalian and replaces the old late Carnian range of *Hayashiella nodosa*, which is now morphologically better defined with a range restricted to the Tuvalian (for discussion see Moix et al. 2007; Noyan and Kozur 2007; Mazza et al. 2012a; Kiliç et al. 2015). *Hayashiella nodosa* still occurs sporadically in the *H. tuvalica* Zone, together with the Julian species *Paragondolella polygnathiformis* and *P. praelindae* (Moix et al. 2007; Mazza et al. 2012a; Rigo et al. 2012a). Characteristic of this zone is also the Tuvalian conodont association of *H. tuvalica* with *P. noah*, *H. carpathica*, *C. zoae* and the first primitive representatives of *C. pseudodiebeli* (Channell et al. 2003; Mazza et al. 2012a).

Age: The *Hayashiella tuvalica* Zone corresponds to the lower part of the ammonoid *Tropites dilleri* Zone (Fig. 6.5).

6.4.2.2 *Metapolygnathus praecommunisti* Interval Zone

Definition: the lower boundary is marked by the FO of the index species *Metapolygnathus praecommunisti* Mazza, Rigo and Nicora (2011); the upper boundary by the FO of *Neocavitella cavitata* Sudar and Budurov (1979).

The index species of this zone, *Metapolygnathus praecommunisti* (Fig. 6.7b), is an important Tuvalian conodont because it is the first representative of genus *Metapolygnathus*, sensu Mazza et al. (2011). Furthermore, the lineage *Paragondolella noah-Metapolygnathus praecommunisti-Metapolygnathus communisti* permits documenting the transitional forms (morphoclines) between the ancestor *P. noah* and *Me. praecommunisti*, and thus recognising the first appearance datum (FAD) of the descendent species *Me. praecommunisti* (Mazza et al. 2011), according to Remane (2003). The *Me. praecommunisti* Zone is also characterised by the occurrence of *P. oertlii* and by rich populations of *C. zoae*, which develops into two very distinctive morphotypes (morphotype A and B; Mazza et al. 2012a). Furthermore, in this zone the last occurrence of *P. polygnathiformis, P. praelindae*, and *Hayashiella nodosa* is documented.

Age: *Metapolygnathus praecommunisti* has been collected in the Santa Croce/Heiligkreuz Formation (Dolomites—Maron et al. 2017), along with the ammonoid *Shastites* cf. *pilari* that is typical of the *Tropites dilleri* Zone (Gianolla et al. 1998; De Zanche et al. 2000; Breda et al. 2009; Gattolin et al. 2015; Maron et al. 2017). Thus, the base of the *Me. praecommunisti* Zone falls into the ammonoid *Tropites dilleri* Zone and spans into the ammonoid *Anatropites spinosus* Zone (Balini et al. 2010b) (Fig. 6.5). In particular, the occurrence of *Me. praecommunisti* seems to be global, since this species has been collected in the Neotethys, in northern Tethys and in North America (Mazza et al. 2011; Orchard 2014).

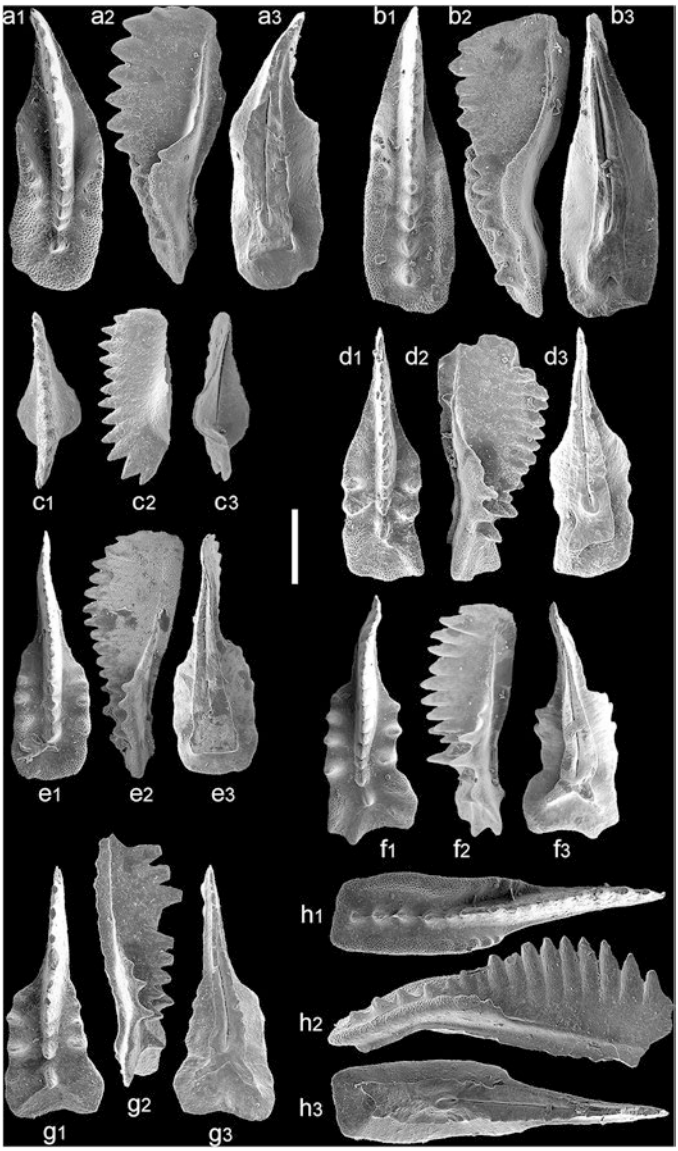

Fig. 6.7 Index conodont species for the Tuvalian (Lower Carnian) zones. For each specimen all the three views are provided: (1) upper view, (2) lateral view, (3) lower view. Scale bar is 200 μm, all the specimens are at the same scale. (**a**) *Carnepigondolella tuvalica* Mazza and Rigo (from Mazza et al. 2012a, b). (**b**) *Metapolygnathus praecommunisti* Mazza, Rigo and Nicora (from Mazza et al. 2011). (**c**) *Neocavitella cavitata* (Sudar and Budurov) (from Mazza et al. 2012a). (**d**) *Carnepigondolella orchardi* (Kozur) (from Mazza et al. 2012a). (**e**) *Carnepigondolella pseudoechinata* (Kozur) (from Mazza et al. 2012a). (**f**) *Epigondolella vialovi* (Burij) (from Mazza et al. 2010). (**g**) *Epigondolella quadrata* Orchard (sample FNP112, from the Pizzo Mondello section, Italy; see Mazza et al. 2012a). (**h**) *Metapolygnathus communisti* Hayashi (sample FNP125 from the Pizzo Mondello section, Italy; see Mazza et al. 2012a)

6.4.2.3 *Neocavitella cavitata* Interval Zone

Definition: the lower boundary is marked by the FO of the index species *Neocavitella cavitata* Sudar and Budurov (1979); the upper boundary by the FO of *Carnepigondolella orchardi* (Kozur 2003).

Neocavitella cavitata (Fig. 6.7c) is a platformless P_1 conodont, characterised by a densely denticulated and arched blade, with a subterminal cusp, and a large and deep basal cavity. Even though the ancestry of this species is doubtful (probably *Ne. tatrica*), we establish a *Ne. cavitata* Zone as this species is easily recognizable, very common and spread in the middle Tuvalian in all the Tethyan province (e.g. Sudar and Budurov 1979; Krystyn and Gallet 2002; Channell et al. 2003; Mazza et al. 2012a). Within this biozone in the Sicani Basin (Pizzo Mondello section), the acme and the intraspecific diversification of *Hayashiella tuvalica* and *Metapolygnathus praecommunisti* is documented. It is notable that *Norigondolella carlae* n. sp. (Fig. 6.8) has its entire range in this Zone (see Systematics chapter below). *Norigondolella carlae* was illustrated for the first time (but not described) as *Gondolella* cf. *navicula* by Krystyn in 1980, from Tuvalian II strata at Feuerkogel (Austria). It was also reported as *Norigondolella* cf. *navicula* in Balini et al. (2010b), and Mazza et al. (2012a, b) or in open nomenclature in Nicora et al. (2007) and Rigo et al. (2007). Furthermore, *Metapolygnathus dylani* has its FAD in the middle part of this Zone, lower than documented in Black Bear Ridge. The appearance of *Me. dylani* occurs along the phylogenetic lineage of *Me. praecommunisti-Me. communisti,* being *Me. dylani* evolved from a morphotype of *Me. praecommunisti*. Thus, in the Tethys *Me. dylani* appears earlier than in North America.

Age: The *Neocavitella cavitata* Zone falls in the lower part of the ammonoid *Anatropites spinosus* Zone, in particular in the mid *Discotropites plinii* subzone (sensu Balini et al. 2012) (Fig. 6.5).

6.4.2.4 *Carnepigondolella orchardi* Interval Zone

Definition: the lower boundary is marked by the FO of the index species *Carnepigondolella orchardi* (Kozur 2003); the upper boundary by the FO of *Epigondolella vialovi* (Buryi 1989).

Carnepigondolella orchardi (Fig. 6.7d) is the direct descendant of *C. pseudodiebeli* (Kozur 2003; Mazza et al. 2012b), the morphocline of which allows to define the first appearance datum of *C. orchardi.* At the base of the *C. orchardi* Zone, the conodonts *C. angulata*, *C. samueli* and *Metapolygnathus mersinensis* occur together, and they represent an important evolutionary step of the Carnian carnepigondolellids, which is characterised by the development of sharp denticles on the platform lateral margins. These become thinner and sub-parallel, while the posterior platform margin turns out to be more squared. Furthermore, typical *C. pseudodiebeli* reaches its acme, and it is characterised by sharp nodes in the number of four-five, growing all along the lateral platform margins (Plate 2, Figs. 8–10 in Mazza et al. 2012a). Instead, in the upper part of the *C. orchardi* Zone, species with very reduced platform length, covering half or less than half of the entire element, such in *C. pseudoechinata*, *C. spenceri*, and *Epigondolella heinzi*, first occur (Mazza

Fig. 6.8 *Norigondolella carlae* n. sp. Both the specimens are from the Pizzo Mondello section. All the three views are provided: (1) upper view, (2) lateral view, (3) lower view. (**a**) Holotype (rep. Micro-Unimi no. 2019), sample NA16 (from Nicora et al. 2007). (**b**) specimen from the LO level, sample NA18 (see Nicora et al. 2007). Scale bar is 200 μm

et al. 2012a; Orchard 2014). These species represent the beginning of another important evolutionary trend of the Upper Triassic conodonts, which is the shortening of the platform and the forward shifting of the pit (Mazza et al. 2012a). The appearance of morphologies with a reduced platform is a global event, because it is documented in the upper Tuvalian both in the Tethys and in North America (Mazza et al. 2012a; Orchard 2014). Particularly significant species are *C. pseudoechinata* (Fig. 6.7e) and *C. spenceri*, since their occurrence is reported in Black Bear Ridge (BBR) section (British Columbia, Canada) in the *C. spenceri* Subzone (Orchard 2014) and in the tethyan Pizzo Mondello (PM) section (Sicily, Italy). The occurrences of *E. heinzi*, together with *E. miettoi* and primitive *E. triangularis* at the top of the zone, mark the beginning of the *Epigondolella* genus, even if the representatives of this genus are still scarce.

Age: The *C. orchardi* Zone represents the upper part of the ammonoid *Discotropites plinii* subzone (lower *Anatropites spinosus* Zone sensu Balini et al. 2012).

6.4.2.5 *Epigondolella vialovi* Interval Zone

Definition: the lower boundary is marked by the FO of the index species *Epigondolella vialovi* (Buryi 1989); the upper boundary by the FAD of *Metapolygnathus communisti* Hayashi (1968).

The more common conodont of this zone is *Epigondolella vialovi* (Fig. 6.7f), established as *Metapolygnathus vialovi* by Buryi in 1989, but never really considered by other specialists, who assigned *E. vialovi* to other species such as *E. abneptis*, *E. triangularis* or *E. quadrata* (e.g. De Capoa-Bonardi 1984; Channell et al. 2003; Celarc and Kolar-Jurkovšek 2008; Mazza et al. 2010). Only recently, this species has been revaluated and its occurrence documented both in the Tethys and in North America (Mazza et al. 2010, 2012a; Karádi et al. 2013; Orchard 2014). In this zone *Epigondolella heinzi*, *E. miettoi*, and *Carnepigondolella pseudoechinata* are very abundant (at least in the Sicani Basin). The upper part of the *E. vialovi* Zone is characterised by the occurrences of *E. quadrata* (Fig. 6.7g), *E. rigoi*, and *E. uniformis* (Mazza et al. 2012a, b; Mazza and Martínez-Pérez 2015) (Figs. 6.4 and 6.5). This zone represents thus an important faunal turnover in all the Tethys, described as T1 (=Turnover 1) in Mazza et al. (2010). In T1, the carnepigondolellids become scarcer until they completely disappear towards the upper boundary of the zone, except for *C. pseudoechinata*. Contemporaneously, rich populations of the genus *Epigondolella* replace the carnepigondolellids (Mazza et al. 2010).

Age: The *E. vialovi* Zone represents the lower part of the ammonoid *Gonionotites italicus* subzone, which is the upper *Anatropites spinosus* Zone sensu Balini et al. (2012).

6.4.2.6 *Metapolygnathus communisti* Interval Zone

Definition: the lower boundary is marked by the FO of the index species *Metapolygnathus communisti* Hayashi (1968); the upper boundary by the FO of *Metapolygnathus parvus* Kozur (1972).

This is the last conodont zone of the Carnian and it marks the beginning of the rise of the *Metapolygnathus* genus over the other genera (*Carnepigondolella* and *Epigondolella*), reaching its acme at the base of the following *Me. parvus* Zone. The documentation of the transitional species between *Me. praecommunisti* and *Me. communisti* identified the FAD of *Me. communisti* (Fig. 6.7h) during the mass proliferation of the metapolignathids. In his Fig. 46, Orchard (2014) described seven morphotypes belonging to *Metapolygnathus* ex gr. *communisti* of the Black Bear Ridge section that can be referred to the Tethyan species *Me. praecommunisti* and *Me. communsti* of Mazza et al. (2011, 2012a). In particular, morphotypes 1–3 (Fig. 46, 1–9) are referable to *Me. praecommunisti*; morphotypes 4–5 (Fig. 46, 10–18) to transitional forms between *Me. praecommunisti* and *Me. communisti*; and morphotypes 6–7 (Fig. 46, 19–32) to true *Me. communisti*. Since the phylogenetic lineage between *Me. precommunisti-communisti* is documented in both the Tethys and North America, the FAD of *Me. communisti* can be considered a synchronous event and the *Me. communisti* Zone, which corresponds to the upper part of the North American *Acuminatella angusta—Metapolygnathus dylani* Zone (Orchard 2014), can be useful for global correlation.

The *Me. communisti* Zone is almost a monogeneric interval, being composed mainly by species belonging to the *Metapolygnathus* genus that are *Me. mersinensis*, *Me. communisti*, *Me. mazzai* (= *Metapolygnathus* cf. *primitius* in Mazza et al. 2012a, b), *Me. dylani*, and *Me. praecommunisti* that disappears in the lower part of this zone. Occurrences of *Epigondolella vialovi*, *E. quadrata*, *E. rigoi* and *E. triangularis* are sporadic.

Age: The range of the *Me. communisti* Zone is restricted to the upper part of the ammonoid *Gonionotites italicus* subzone, corresponding to the upper *Anatropites spinosus* Zone sensu Balini et al. (2012) (Fig. 6.5).

6.5 The Carnian/Norian Boundary and the Norian Stage

The Norian Stage (Fig. 6.9) is named after the Roman province of Noria in Austria (Mojsisovics von Mojsvár 1869) and reviewed by Tozer in 1984, who assigned its base to the first occurrence of ammonoid *Stikinoceras kerri* in Canada, overlying the *Klamathites macrolobatus* Zone (Silberling and Tozer 1968). The *S. kerri* Zone is considered approximately coeval with the Tethyan ammonoid *Guembelites jandianus* ammonoid zone (Krystyn 1980; Orchard et al. 2000). The Norian Stage is subdivided in three substages by Mojsisovics von Mojsvár et al. (1895) that are in stratigraphic order: (1) Lacian that was the name of the Salzkammergut region (northern Austrian Alps) during Roman time; (2) Alaunian after Alaun tribe from the Hallein region (Austria), the base of which is defined by the Tethyan ammonoid *Cyrtopleurites bicrenatus*; and (3) Sevatian, after the name of the Celtic tribe, the base of which is marked by the occurrences of the ammonoids *Sagenites quinquepunctatus* or *Gnomohalorites cordilleranus* in the Tethys and North America respectively. Informally, Lacian and Alaunian are subdivided into 1, 2 and 3, while Sevatian is split into 1 and 2.

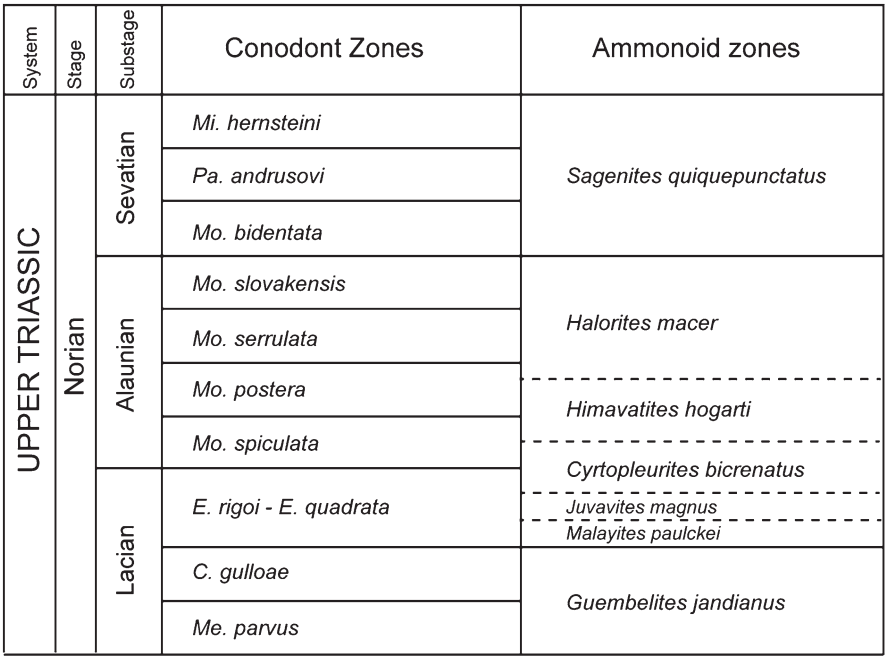

Fig. 6.9 New conodont/ammonoid integrated biozonation of the Norian stage. See caption of Fig. 6.4 for genera abbreviations

6.5.1 Lacian Conodont Biozonation

6.5.1.1 *Metapolygnathus parvus* Interval Zone

Definition: the lower boundary is marked by the FO of the index species *Metapolygnathus parvus* Kozur (1972); the upper boundary by the FO of *Carnepigondolella gulloae* Mazza and Rigo, 2012 (in Mazza et al. 2012a).

This is the first zone of the Norian and its base approximates the second important conodont faunal turnover of the Late Triassic, named as T2 (=Turnover 2) by Mazza et al. (2010), characterised by a great abundance of genus *Metapolygnathus* species over the epigondolellids and carnepigondolellids (Mazza et al. 2010), and well documented in all the Tethys (Krystyn and Gallet 2002; Mazza et al. 2012a, b; Mazza and Krystyn 2013, 2015; Karádi and Mazza 2015). *Metapolygnathus parvus* (Fig. 6.10a) is the last representative of the lineage *Paragondolella noah -Me. praecommunisti-Me. dylani-Me. parvus* and it is thus easily possible to recognise the FAD of *Me. parvus* documenting the transitional forms of the *Me. dylani/parvus* morphocline. The conodont species *Me. parvus* was first defined by Kozur in 1972, and successively amended by Noyan and Kozur in 2007 as those forms similar to *Me. communisti*, but characterised by a shorter platform, the absence of nodes on the anterior platform margins and with a more forwarded pit (Fig. 6.11), indicating thus the strict phylogenetic relationship with *Me. dylani* (see also Mazza et al. 2012b). Orchard (2014) identified and included the species described and illustrated as "advanced forms of *Me.*

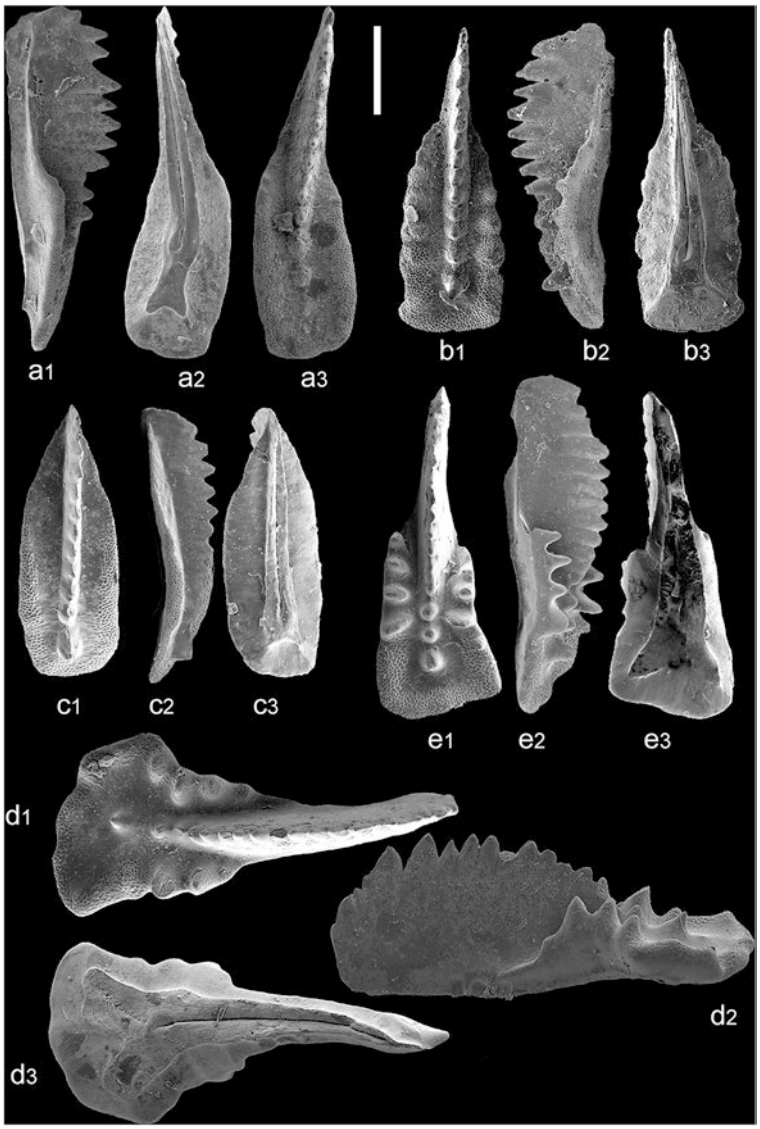

Fig. 6.10 Index conodont species for the Lacian (Lower Norian) zones. For each specimen all the three views are provided: (1) upper view, (2) lateral view, (3) lower view. Scale bar is 200 μm, all the specimens are at the same scale. (**a**) *Metapolygnathus parvus* Kozur (sample NA40a of the Pizzo Mondello section, Italy; see Mazza et al. 2012a). (**b**) *Carnepigondolella gulloae* Mazza and Rigo (from Mazza et al. 2012a). (**c**) *Norigondolella trinacriae* Mazza, Cau and Rigo (from Mazza et al. 2012b). (**d**) *Epigondolella rigoi* Noyan and Kozur (from Mazza and Martínez-Pérez 2015). (**e**) *Epigondolella quadrata* Orchard (from sample NA60 of the Pizzo Mondello section, Italy; see Mazza et al. 2012a)

praecommunisti" by Mazza et al. (2011) as typical *Me. dylani*, recognizing thus the presence of *Me. dylani* at Pizzo Mondello section. This important occurrence of *Me. dylani* permits to document also in the Tethys the phylogenetic lineage between the

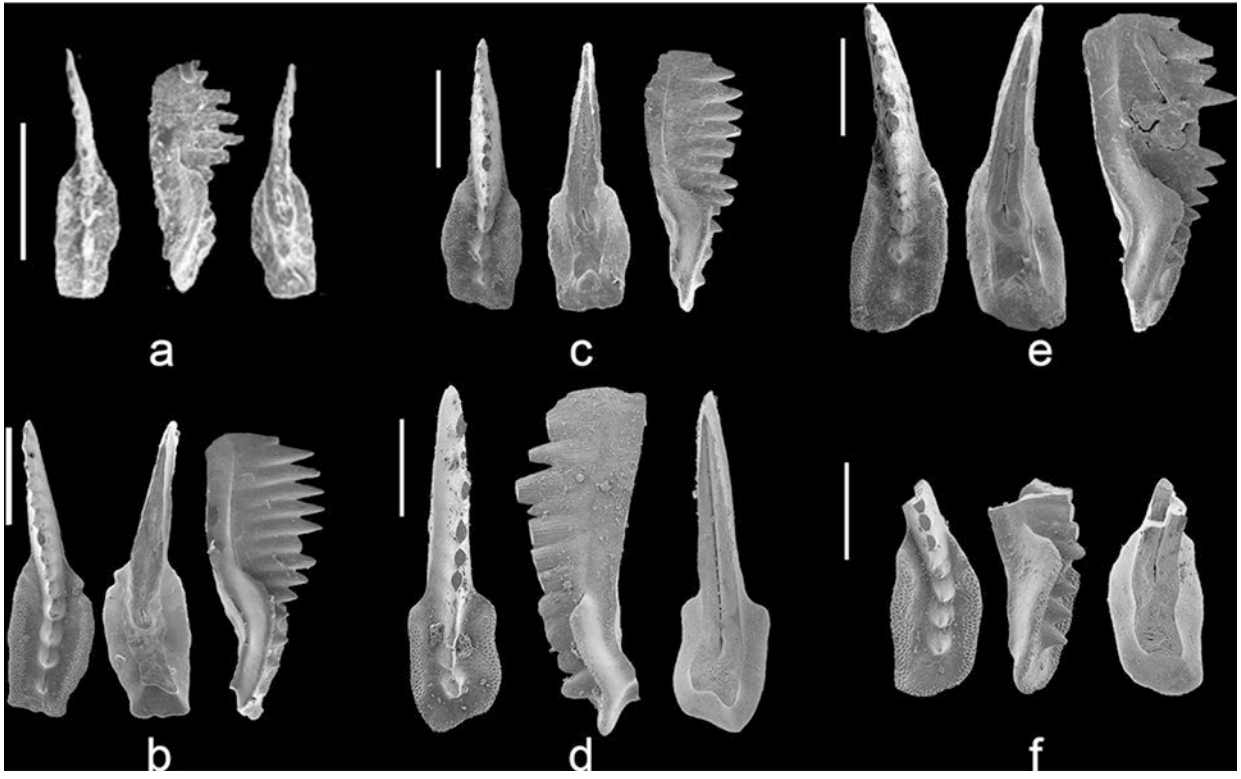

Fig. 6.11 Comparison between six specimens of *Metapolygnathus parvus* Kozur from three different areas: Northern Tethys, Neotethys and North America. Morphologically similar specimens are aligned vertically to facilitate comparisons (**a**–**b**, **c**–**d**, **e**–**f**). The specimens from Neotethys are from Mazza and Martínez-Pérez 2015 and were classified as "*M. communisti* morphotype without nodes" that, according to the description emended in Noyan and Kozur 2007, corresponds to true *M. parvus*. (**a**) Northern Tethys (from Noyan and Kozur 2007, fig. 7.1). (**b**) Neotethys (from Mazza and Martínez-Pérez 2015, Pl. 6, fig. 24). (**c**) Neotethys (from Mazza and Martínez-Pérez 2015, Pl. 6, fig. 23). (**d**) North America, from Orchard 2014, fig. 48, 14–16; (**e**) Neotethys (from Mazza and Martínez-Pérez 2015, Pl. 6, fig. 25). (**f**) North America (from Orchard 2014, fig. 48, 17–19). Scale bars are 200 μm

ancestor *Me. dylani* and descendant *Me. parvus* (Mazza et al. 2011; Mazza et al. 2012b), allowing thus to recognize the FAD of *Me. parvus*. In North America, Orchard (2014) described three different morphotypes of *Me. parvus,* named alpha, beta and gamma from the *Metapolygnathus* ex gr. *parvus* population. The morphotype alpha of *Metapolygnathus parvus* by Orchard (2014, Fig. 48, 1–25) corresponds to the Tethyan *Me. parvus* (Fig. 6.11), which first occurs above the FAD of its precursor *Me. dylani*, both in PM and BBR sections. The appearance of *Me. parvus* is thus a synchronous bioevent in both Tethyan and North America realms and it can be thus considered as a real First Appearance Datum. In fact, in the two condidate sections Pizzo Mondello and Black Bear Ridge, the FAD of *Me. parvus* occurs not only along its phylogenetic lineage but also homotaxially between the last occurrence (LO) of the last Carnian ammonoid genus *Anatropites* and the first occurrence (FO) of the first Norian ammonoid genus *Dimorphites* or *Geumbelites* in Tethys or North America respectively (Balini et al. 2010b; Orchard 2014). Recently, the STS (Subcommission on Triassic Stratigraphy) has also recognised the occurrence of the bivalve *Halobia austriaca* as another possible primary marker event to define the base of the Norian Stage (Balini et al. 2010a, 2012; McRoberts and Krystyn 2011; Levera 2012). At both the GSSP candidate sections PM and BBR, the bivalve *Halobia austriaca* occurs just above the occurrence of *Me. parvus* (Balini et al. 2010b; Levera 2012; Orchard 2014). However, the occurrence of *H. austriaca* is also documented below the FAD of *Me. parvus* and from Carnian strata (e.g. Levera 2012 and references herein), and from the Carnian ammonoid *macrolobatus* Zone as reported by Orchard (2014). Furthermore, the FAD of *Metapolygnathus parvus* is documented close to the positive $\delta^{13}C_{carb}$ trend recognized in both PM and the BBR sections (Muttoni et al. 2004, 2014; Mazza et al. 2010; Onoue et al. 2015). It should be also noted that independent of the possible primary bioevents suggested to define the GSSP, which are the FAD of *Me. parvus* or the occurrence of the bivalve *H. austriaca*, the typically Carnian ammonoid genus *Anatropites* would range up into the Norian.

Thus, we propose the *Me. parvus* Interval Zone as the first conodont biozone for the Lacian and the FAD of *Metapolygnathus parvus* as the primary marker bioevent to define the base of the Norian (Figs. 6.4 and 6.9), as previously suggested by Nicora et al. (2007) and Orchard (2013). *Metapolygnathus parvus* is easily recognizable in lineage from its ancestor *Me. dylani* (another global species easy to identify), and its occurrence is homotaxial between indisputably Carnian (below) and Norian (above) ammonoids in both the two GSSP candidate sections PM and BBR.

In the *Me. parvus* Interval Zone, the conodont species *Me. communisti, Me. multinodosus, Me. parvus, Me. echinatus, Me. mazzai*, and *M. linguiformis* reach their acme. *Epigondolella quadrata*, *E. rigoi*, *E. triangularis*, *E. uniformis*, and *E. vialovi* also occur. At the very base of the *Me. parvus* Interval Zone, the species *Me. dylani* has its last occurrence.

6.5.1.2 *Carnepigondolella gulloae* Taxon-range Zone

Definition: taxon range distribution of the index species *Carnepigondolella gulloae* Mazza and Rigo, 2012 (in Mazza et al. 2012a).

Close to the first occurrence of *Carnepigondolella gulloae* (Fig. 6.10b), the disappearance of the metapolignathids is documented in the Tethyan Realm. In fact, the base of this zone approximates the third important conodont faunistic turnover of the Tethys, defined as T3 (=Turnover 3) by Mazza et al. (2010), in which almost all the metapolygnathids disappear just above the base of the zone, except for *Metapolygnathus mazzai*, which ranges up higher into the *C. gullaoe* Zone (Fig. 6.4). Metapolygnathids are replaced by a new rich conodont population, probably belonging to a new genus, which shows intermediate morphologies between the Tuvalian carnepigondolellids and paragondolellids. These characters are a more forward position of the pit and a more posteriorly oriented platform development, often associated with the occurrence of nodes behind the cusp, as stated in Mazza et al. (2012b). The forms belonging to this population were assigned in the past to *Metapolygnathus communisti* B by Krystyn (1980), but this species was never formally established nor described. Thus, Mazza et al. (2012a, b) redescribed partially the old *Me. communisti* B population, splitting *Me. communisti* B into two new species, *Carnepigondolella gulloae* and *Norigondolella trinacriae* (Fig. 6.10c). The occurrence of *No. trinacriae* is very close to the base of the *C. gulloae* Zone (Fig. 6.4). The described turnover and the occurrence of this population can be easily recognized in all the Tethys synchronously (Karádi et al. 2013; Mazza and Krystyn 2013, 2015; Muttoni et al. 2014). Genus *Norigondolella* is instead facies controlled (Trotter et al. 2015) and not all the species belonging to this genus are globally documented. Furthermore, *E. triangularis* has been proved to occur below the *C. gullaoe* Zone, even if as primitive forms (Mazza and Martínez-Pérez 2016). Orchard (2014) referred the forms belonging to the *C. gullaoe-No. trinacriae* population to genus *Primitella*, a generic name not adopted here due to unclear diagnostic features. Contemporaneous with the occurrence of *Primitella* species (sensu Orchard 2014), the metapolygnathids slowly disappear, recording a similar conodont turnover T3 documented in the Tethys (Mazza et al. 2010). The stratigraphic range of *Primitella* units has been documented in the uppermost Tuvalian but they became predominant in the first Norian conodont biozone *Pr. asymmetrica—Norigondolella* sp. of Orchard (2014) at Black Bear Ridge, easily correlatable to the Tethyan *C. gulloae* Zone. In the *C. gulloae* Zone, the metapolygnathids disappear but the epigondolellids proliferate: for instance, *E. spatulata* has its first occurrence while *E. uniformis* and *E. triangularis* become very abundant.

Age: The *C. gulloae* Zone corresponds to the ammonoid the *Dimorphites selectus* subzone, which is the first subzone of the *Guembelites jandianus* Zone sensu Balini et al. (2012) (Fig. 6.9).

6.5.1.3 *Epigondolella rigoi-Epigondolella quadrata* Interval Zone

Definition: the lower boundary is the LO of *Carnepigondolella gulloae,* the upper boundary is the FO of *Mockina spiculata*. The zone is characterised by the predominant association of the species *Epigondolella rigoi* Noyan and Kozur (2007) and *Epigondolella quadrata* (Orchard 1991b).

Both in the Tethys and in North America, the mid and upper part of the Lacian corresponds to a stratigraphic interval characterised by an intense proliferation of evolved epigondolellids with advanced morphological characters (Mazza et al. 2012a, b; Orchard 2014; Mazza and Martínez-Pérez 2015). The diagnostic features of these species are a centrally or anteriorly located pit, a long free blade, a carinal node growing behind the cusp, and the occurrence of large and high denticles on the platform lateral platform margins and sometimes on the posterior one. In North America these kinds of epigondolellids are considered by Orchard (2014) as epigondolellids sensu stricto where they seem to first occur above the occurrence of *Metapolygnathus* ex gr. *parvus*. In the Tethys the first representatives of *Epigondolella* occur already in the upper Tuvalian (i.e. below the FAD of *Me. parvus*) and no first occurrences of epigondolellids are documented in the upper part of the *Carnepigondolella gulloae* Zone. At Pizzo Mondello section it is possible to identify a conodont association given by massive presence of *E. quadrata, E. rigoi, E. uniformis*, and *E. triangularis*. *Epigondolella spatulata* also occurs, along with the last representatives of *E. viavoli* (Mazza et al. 2012a). This corresponds to the profileration documented by Orchard (2014) at BBR. In particularly, data from the Pizzo Mondello section, indicate that *E. rigoi* (the more numerous) (Fig. 6.10d) and *E. quadrata* (Fig. 6.10e) are the most abundant species, thus giving the name to the *E. rigoi-E. quadrata* biozone. When the conditions are favorable (Trotter et al. 2015), in the *E. rigoi-E. quadrata* Zone representatives of the genus *Norigondolella*, like *N. navicula* and *N. halstattensis*, also occur in the Tethys realm (Krystyn and Gallet 2002; Channell et al. 2003; Kozur 2003).

Age: This zone resembles the ammonoid *Malayites paulckei* Zone (sensu Balini et al. 2012), the *Juvavites magnus* Zone (sensu Balini et al. 2012), and the *Cyrtopleurites bicrenatus* Zone (sensu Krystyn in Zapfe 1983) (Donofrio et al. 2003) (Fig. 6.9). Similarly, in North America, these species occur in the ammonoid *Malayites dawsoni, Juvavites magnus* and *Drepanites rutherfordi* zones (e.g. Orchard 1991a; Orchard and Tozer 1997).

6.5.2 *The Lacian/Alaunian Boundary and the Alaunian Substage*

The base of the Alaunian substage is traditionally marked by the first occurrence of the ammonoid *Cyrtopleurites bicrenatus* (Krystyn 1973; Kozur 2003; Lucas 2010). The usage of open nomenclature and oversimplified concept of conodont species together with the lack of proper illustration of the lower and mid Alaunian specimens affected the definition and subdivision of the Alaunian substage in conodont biozones. This issue is in part attributable to the studies of Alaunian successions that are condensed (e.g. Gallet et al. 1992, 2000); brecciated (Channell et al. 2003); disturbed with allodapic blocks (Gallet et al. 1992); not well exposed (Mazza et al. 2012a; Karádi 2017) or where the Alaunian interval is incomplete (Gallet et al. 2000; Moix et al. 2007; Bertinelli et al. 2005; Rigo et al. 2012a). In most of the studies, Alaunian conodonts of the Tethyan Realm were assigned only to three species,

Epigondolella abneptis, "*Epigondolella*" *postera* and "*Epigondolella*" *multidentata* (e.g. Krystyn 1973; Cafiero and De Capoa-Bonardi 1981; Wang and Dong 1985; Mao and Tian 1987; Wang and Wang 1990; Gallet et al. 1992, 1993, 1996). Orchard (1991a, b) established several new species from middle Norian strata of the Canadian Cordillera (e.g. *Epigondolella carinata*, *E. elongata*, *E. matthewi*, *E. serrulata*, *E. spiculata*, *E. tozeri*), all of which are also present in the Tethys (Channell et al. 2003; Donofrio et al. 2003; Kozur 2003; Rigo et al. 2005, 2012a, b; Karádi et al. 2016, Karádi 2017). *"Epigondolella" multidentata* is restricted to North America (Kozur 2003), while *Epigondolella abneptis* is an ambiguous species in which the lower Alaunian epigondolellids *E. rigoi*, *E. uniformis*, *E. triangularis* and *E. spatulata* are gathered. Furthermore, due to the small size and neotenic features of *Mockina postera*, many juveniles or subadults of other mockinae were determined as "*Epigondolella*" *postera*. Recent studies revealed that the diversity of middle Norian conodont species in the Tethyan Realm is much higher (Ji et al. 2003; Karádi et al. 2016, Karádi 2017) and a palaeontological revision needs to be carried out along with clear conodont illustrations and detailed range charts.

6.5.2.1 *Mockina spiculata* Interval Zone

Definition: the lower boundary is marked by the FO of the index species *Mockina spiculata* (Orchard 1991b); the upper boundary by the FO of *Mockina postera* (Kozur and Mostler 1971).

In North America the *Mockina spiculata* Zone characterises the lower Alaunian following the *Orchardella multidentata* Zone (e.g. Orchard 1991a, b, 2010). However, *Orchardella multidentata* is absent in the Tethys and the FO of *Mockina spiculata* is not yet well calibrated with other biostratigraphically important fossil groups. In 2003, Kozur established the condont species *Mockina medionorica*, index species of the homonymous biozone, which should correspond to the North American *Orchardella multidentata* Zone. *Mockina medionorica* was described from the uppermost Lacian to middle Alaunian brecciated interval of the Silická Brezová section (Channell et al. 2003; Kozur 2003). However, *Mo. medionorica* is not easy to recognize because it is very similar to the juvenile specimens of other middle Norian mockinae and its occurrence is rather sporadic (Kovács and Kozur 1980; Moix et al. 2007). We thus prefer to avoid using *Mo. medionorica* as zonal marker and we suggest *Mo. spiculata* (Fig. 6.12a) as index species for the lower Alaunian, because it is easily recognizable, and it commonly appears in the entire Tethys (Ji et al. 2003; Rigo et al. 2005, 2012a; Karádi 2017) and North America (Orchard 1991a, b). In the *Mockina spiculata* Zone, *Epigondolella rigoi*, *E. spatulata*, *E. transitia*, *E. triangularis,* and *E. uniformis* are common, while *Mockina matthewi* and *Mo. tozeri* are scarce (Ji et al. 2003; Rigo et al. 2005, 2012a, b; Karádi 2017). In the lower part of this zone *Epigondolella quadrata* disappears.

Age: In the Tethys, the *Mockina spiculata* Zone corresponds to the ammonoid *Himavavites watsonii* subzone, which is the lower part of the ammonoid *Himavavites hogarti* Zone (sensu Krystyn in Zapfe 1983; Donofrio et al. 2003; Rigo et al. 2005)

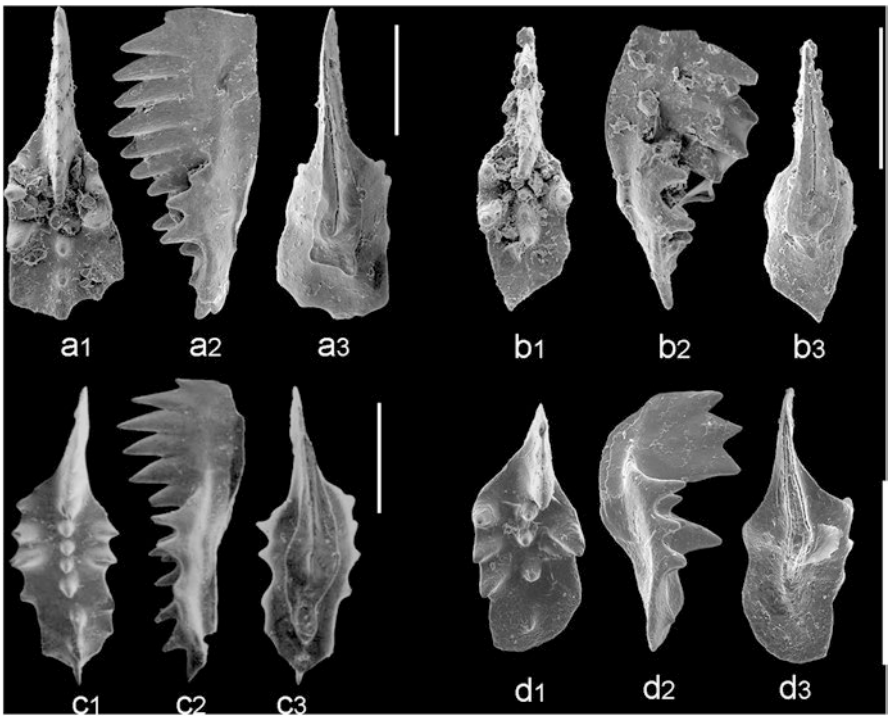

Fig. 6.12 Index conodont species for the Alaunian (Middle Norian) zones. For each specimen all the three views are provided: (1) upper view, (2) lateral view, (3) lower view. Scale bar is 200 μm. (**a**) *Mockina spiculata* Orchard (from Karádi 2017). (**b**) *Mockina postera* (Kozur and Mostler) (from Karádi 2017). (**c**) *Mockina serrulata* Orchard (from Orchard 1991b); (**d**) *Mockina slovakensis* (Kozur) (from Belvedere et al. 2008)

(Fig. 6.9), and to the lower *Himavavites columbianus* Zone in North America (Orchard et al. 1991a, b; Donofrio et al. 2003).

6.5.2.2 *Mockina postera* Interval Zone

Definition: the lower boundary is marked by the FO of the index species *Mockina postera* (Kozur and Mostler 1971); the upper boundary by the FO of *Mockina serrulata* (Orchard 1991b).

The *Mockina postera* Zone is the second conodont zone of the Alaunian. *Mockina postera* (Fig. 6.12b) is abundant all over the Tethys and easily to identify. However, its small size caused incorrect determinations in many cases. To avoid misinterpretations, it is very important to assign to *Mo. postera* only the original characters that are an asymmetric platform with a pointed posterior end, a prolonged keel with a pointed end, two denticles on one anterior platform margin and one denticle on the other and a short posterior carina that never reaches the end of the platform. The last

occurrences of *Epigondolella rigoi*, *E. triangularis*, *E. uniformis* are in the *Mockina postera* Zone. *Mockina spiculata* and *Mo. tozeri* are still present.

Age: In Tethys, the *Mockina postera* Zone corresponds to the upper part of the ammonoid *Himavavites hogarti* Zone (sensu Krystyn in Zapfe 1983; Donofrio et al. 2003; Rigo et al. 2005), and to the mid *Himavavites columbianus* Zone in North America (Fig. 6.9) (Orchard 1991a, b; Donofrio et al. 2003).

6.5.2.3 *Mockina serrulata* Interval Zone

Definition: the lower boundary is marked by the FO of the index species *Mockina serrulata* (Orchard 1991b); the upper boundary by the FO of *Mockina slovakensis* (Kozur 1972).

The *Mockina serrulata* Zone represents the third conodont zone of the Alaunian and its index species is documented throughout the Tethys (e.g. Pl. 1, Fig. 10 in Wang and Wang 1990; Ishida and Hirsch 2001; Rigo et al. 2005, 2012a). Characteristic of this zone is the presence of *E. spiculata* (the range of which ends in the middle part of the zone), *Mo. postera* (which ranges until the upper part of the zone), and *Mo. elongata* (the distribution of the latter is not well defined) and the FAD of *Mo. zapfei*. In the upper part of the *Mo. serrulata* Zone, *"Mockina" vrienlyncki* is common. This species is characterised by the absence of a platform around a long blade but this is probably derived from *Mo. serrulata* (Fig. 6.12c), which shares the same blade and carina profile by losing entirely the platform.

Age: In the Tethys, the *Mockina serrulata* Zone corresponds to the lower part of the ammonoid *Halorites macer* Zone (Fig. 6.9) (sensu Krystyn in Zapfe 1983; Donofrio et al. 2003; Rigo et al. 2005), and to the upper *Himavavites columbianus* Zone in North America (Orchard 1991a, b; Donofrio et al. 2003).

6.5.2.4 *Mockina slovakensis* Interval Zone

Definition: the lower boundary is marked by the FO of the index species *Mockina slovakensis* (Kozur 1972); the upper boundary by the FO of *Mockina bidentata* (Mosher 1968).

In the Tethys, *Mockina slovakensis* (Fig. 6.12d) directly descends from *E. praeslovakensis* Kozur, Masset and Moix (in Moix et al. 2007) and it is very common in the uppermost part of the Alaunian and documented in open sea environments (Martini et al. 2000; Moix et al. 2007; Rigo et al. 2012a; Mazza et al. 2012a), restricted basins (e.g. Budai and Kovács 1986; Kovács and Nagy 1989; Roghi et al. 1995; Donofrio et al. 2003) and even in carbonate platform sediments (Belvedere et al. 2008). Even though in the northern Tethys, *Mockina slovakensis* seems to be rather rare in pelagic facies (Channell et al. 2003), we describe the *Mockina slovakensis* Zone because its index species is easy to identify and almost occurred in lineage with its predecessor and mostly because it is an opportunist species thriving in

all marine environments, making this species a good biostratigraphic tool for also spatial correlation.

The zone is characterised by the presence of *Mo. serrulata* (which ends in the middle part) *Mo. zapfei, "Mockina" vrienlyncki* and *Epigondolella praeslovakensis*.

Age: In the Tethys, the *Mockina slovakensis* Zone corresponds to the upper part of the ammonoid *Halorites macer* Zone (Fig. 6.9) (sensu Krystyn in Zapfe 1983; Donofrio et al. 2003).

6.5.3 *The Alaunian/Sevatian Boundary and the Sevatian Substage*

For the uppermost Triassic, conodonts and radiolarians are the main biostratigraphic tools for regional and global correlations (e.g. Carter and Orchard 2007; Giordano et al. 2010, 2011; Rigo et al. 2012a, 2016; Bertinelli et al. 2016).

During this time interval, the overall trend recorded by conodonts is characterised by general size decrease and retention of juvenile conditions (progenesis). The trend is well illustrated by the *Mockina* (=*Epigondolella*) *bidentata* population (Orchard 1983, pp. 189–190), which preserves only a single pair of sharp denticles, sometimes with tiny accessory nodes. Adult specimens of *Mo. bidentata* look similar to the small growth stages of the lower/middle Norian *Epigondolella quadrata* and *E. triangularis* (Orchard 1983, 1991a; Mazza and Martínez-Pérez 2016), which do not reach the same size, however, but still present juvenile features (i.e. poorly-fused carina denticles).

6.5.3.1 *Mockina bidentata* Interval Zone

Definition: the lower boundary is marked by the FO of the index species *Mockina bidentata* (Mosher 1968); the upper boundary by the FO of *Parvigondolella andrusovi* Kozur and Mock, 1972.

Mockina bidentata (Fig. 6.13a) is the index species of the homonymous zone, the occurrence of which marks the base of the zone, in accordance with Kozur and Mock (1991) and Orchard (1991a). Even if *Mockina bidentata* is the typical Sevatian conodont, some specimens have been collected associated with undoubtedly Rhaetian conodonts (i.e. *Misikella posthernsteini*) (e.g. Kozur and Mock 1991; Orchard 1991a; Rigo et al. 2005, 2012a, 2016). Noteworthy, *Mo. bidentata* is the common ancestor of most of the latest Triassic conodont taxa, such as genera *Parvigondolella* (Kozur and Mostler 1971; Kozur 1989; Moix et al. 2007) and *Misikella* (Figs. 5-1a,b in Rigo et al. 2005). The zone is characteriszed by the occurrence of *Mockina slovakensis*, *Mo. zapfei*, *"Mockina" vrienlyncki* and *Mo. bidentata*.

Age: The *Mo. bidentata* Zone commonly defines the substage Sevatian 1 (lower Sevatian) and it is correlated to the lower portion of the Tethyan ammonoid *Sagenites quinquepunctatus* Zone (Fig. 6.9) (e.g. McRoberts et al. 2008; Rigo et al. 2016) and the lowermost part of the *Gnomohalorites cordilleranus* Zone from North America (Orchard 1991a). *Mockina bidentata* Zone corresponds also to the lower part of the radiolarian *Betraccium deweveri* Zone (Giordano et al. 2010), applicable both for Tethyan and North America domains (Carter 1993).

6.5.3.2 *Parvigondolella andrusovi* Interval Zone

Definition: the lower boundary is marked by the FO of the index species *Parvigondolella andrusovi* Kozur and Mock, 1972; the upper boundary by the FO of *Misikella hernsteini* (Mostler 1967).

The top of the *Mo. bidentata* Zone is commonly placed with the first occurrence of *Misikella hernsteini* (e.g. Kozur and Mock 1991), a descendant of *Mockina bidentata* (transitional form illustrated in Rigo et al. 2005), which names the overlying biozone (i.e. *Misikella hernsteini* Zone). However, between these *Mo. bidentata* and *Mi. hernsteini* biozones there is another important bioevent, which corresponds to the occurrence of the conodont genus *Parvigondolella* with the species *Pa. andrusovi* (Fig. 6.13b). *Parvigondolella andrusovi* consists of a single blade without a vestigial platform, which instead charaterizes the transitional forms between *Mo. bidentata* (mother) and *Pa. andrusovi* (daughter), and it occurred in the uppermost portion of the *Mo. bidentata* Zone. However, this genus did not find a broad consensus as an independent genus (e.g. Krystyn et al. 2007a; Pálfy et al. 2007), being considered by some as a morphological variation or ecostratigraphic morphotype of *Mockina bidentata* in unfavourable conditions/environments (Krystyn et al. 2007a). Genus *Parvigondolella* was instead collected from different settings both in the Tethys and North America (e.g. Kozur and Mock 1991; Orchard et al. 2007a; Rigo et al. 2016) and it originates during a warm period (W3) (Trotter et al. 2015). Since its stratigraphical distribution spans between upper Sevatian 1 to mid-upper Rhaetian, *Pa. andrusovi* also crosses a drastic climate change of ca. 6 °C corresponding to ~1.7‰ of $\delta^{18}O_{phos}$, at least in the Tethys where this genus is common (Trotter et al. 2015), testifying that *Pa. andrusovi* is not a ecostratigraphic morphotype of *Mo. bidentata,* but instead an independent species.

We consider this bioevent as an important biomarker, and thus we prefer distinguishing an independent biozone as first suggested by Kozur (2003) and Channell et al. (2003), and used by Korte et al. (2005), since a clear stratigraphic range of this biozones is easily recognisable. The zone is characterised by the occurrence of *Mo. slovakensis* (which last occurs in the middle part), *Mo. bidentata*, *Mo. zapfei*, *"Mockina" vrienlyncki* and *Parvigondolella andrusovi*.

Age: The *Pa. andrusovi* Zone corresponds to the upper portion of the *Mockina bidentata* Zone sensu Kozur and Mock (1991), and thus represents the uppermost Sevatian 1. It is thus correlated to the mid portion of the Tethyan ammonoid

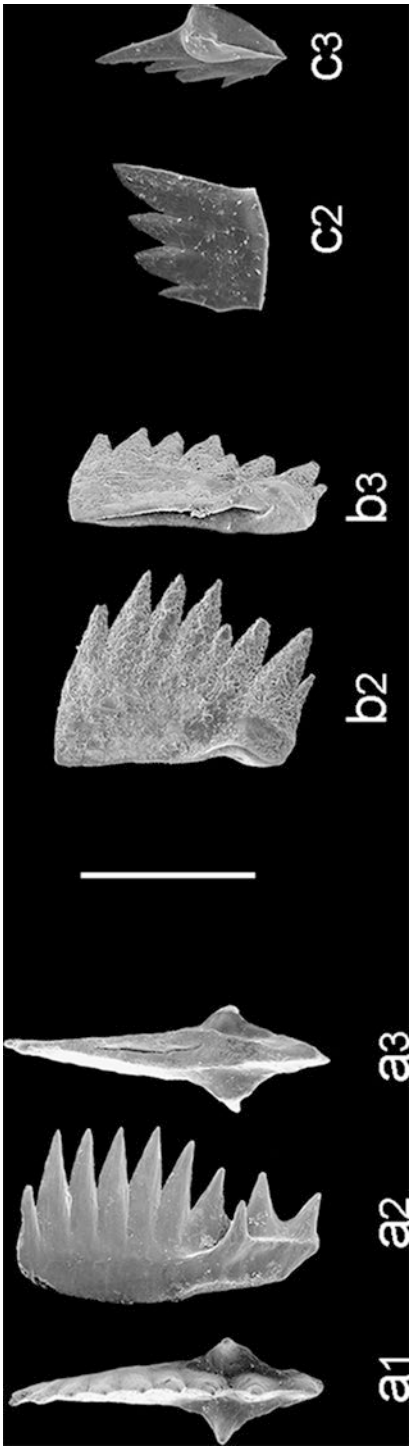

Fig. 6.13 Index conodont species for the Sevatian (Upper Norian) zones. Where possible, all the three views are provided: (1) upper view, (2) lateral view, (3) lower view. Scale bars are 200 µm. (**a**) *Mockina bidentata* (Mosher) (from Mazza et al. 2012a). (**b**) *Parvigondolella andrusovi* Kozur and Mock (from Mazza et al. 2012a). (**c**) *Misikella hernsteini* (Mostler) (from Mazza et al. 2012a)

Sagenites quinquepunctatus Zone (Fig. 6.9) and the mid portion of the radiolarian *Betraccium deweveri* Zone (sensu Carter 1993).

6.5.3.3 *Misikella hernsteini* Interval Zone

Definition: the lower boundary is marked by the FO of the index species *Misikella hernsteini* (Mostler 1967); the upper boundary by the FO of *Misikella posthernsteini* Kozur and Mock (1974).

Misikella hernsteini is the first species that belongs to the genus *Misikella*. *Misikella hernsteini* is characterised by 4–6 denticles decreasing forwardly, with posterior cusp and a teardrop-shaped basal cavity (Fig. 6.13c). It occurs in the upper Sevatian and is a useful species to characterise the Sevatian 2 (Kozur and Mock 1991). Within this biozone it is possible to collect those specimens belonging to the *Misikella hernsteini/posthernsteini* morphocline (Giordano et al. 2010; Bertinelli et al. 2016; Rigo et al. 2016), allowing the definition of the FAD of *Mi. posthernsteini* undoubtedly since it occurs along its phylogenetic lineage. The misinterpretation of some specimens belonging to the *Misikella hernsteini/posthernsteini* morphocline led to the inclusion of an entire Norian chronostratigraphic unit, such as substage Sevatian 2, into a different and younger Stage (i.e. Rhaetian) (Krystyn et al. 2007a, b). The zone is characterised by the occurrence of *Mockina zapfei* (which last occurs in the first half of the zone), *Mo. bidentata*, *Parvigondolella andrusovi*, and *Misikella hernsteini*.

Age: The *Mi. hernsteini* Zone represents the upper Sevatian, that is Sevatian 2, and it corresponds to the upper ammonoid *Gnomohalorites cordilleranus* and *Sagenites quiquepunctatus* Zones of the North American and Tethyan Realms respectively (Fig. 6.9) (Dagys and Dagys 1994; McRoberts et al. 2008; Rigo et al. 2016). It also corresponds to the upper portion of the radiolarian *Betraccium deweveri* Zone (Bazzucchi et al. 2005; Giordano et al. 2010; Rigo et al. 2016).

6.6 The Norian/Rhaetian Boundary and the Rhaetian Stage

The Rhaetian stage (Fig. 6.14) was named after the Roman Province of *Raetia* by von Gümbel in 1861, applying to the strata containing the bivalve *(Rhaet)Avicula contorta*. After more than one century of debate, the Rhaetian became an independent Stage in 1991 (e.g. Ogg 2012; Rigo et al. 2016). A formal definition for its GSSP is still pending, although the FAD of conodont *Misikella posthernsteini* has been identified as primary event to define the Rhaetian base by the Norian/Rhaetian Working Group (e.g. Krystyn 2010; Ogg 2012; Rigo et al. 2016). Recently, a physical marker corresponding of a negative shift of the $\delta^{13}C_{org}$ has been also proposed to define the NRB (Maron et al. 2015; Rigo et al. 2016), which has been documented worldwide (Bertinelli et al. 2016; Rigo et al. 2016; Zaffani et al. 2017).

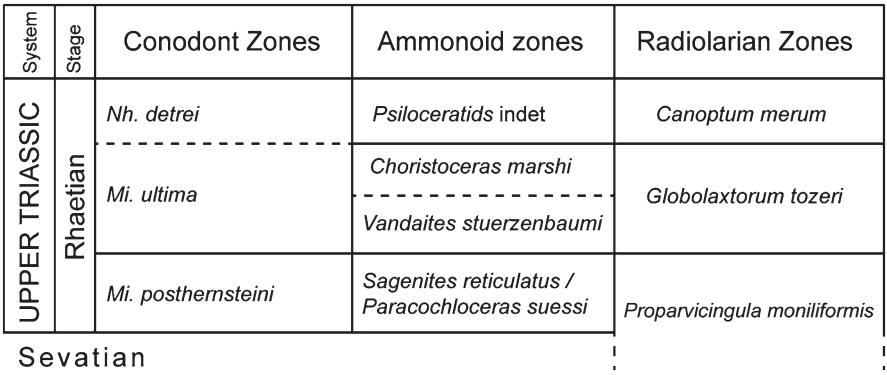

Fig. 6.14 New conodont/ammonoid integrated biozonation of the Rhaetian stage. See caption of Fig. 6.4 for genera abbreviations

Across the Norian/Rhaetian boundary specific conodont bioevents occurred homotaxially within at least the Tethyan basins. These events were first recognized and described by Kozur and Mock (1991) and they correspond to the first occurrence of *Mockina bidentata, Parvigondolella andrusovi, Misikella hernsteini, Misikella posthernsteini* and *Misikella ultima*. All these bioevents define the Tethyan conodont biozonation here proposed for the uppermost Norian and Rhaetian stages, the biozones of which are defined by the first occurrence of the homonymous conodont species. In particular, the FAD of *Misikella posthernsteini* is conventionally adopted to place the Norian/Rhaetian boundary (Krystyn 2010; Gale et al. 2012; Bertinelli et al. 2016; Rigo et al. 2016). To minimize the error for the definition of the first occurrence, and thus place a GSSP independently from the common taxonomic issues, Remane (2003) suggested considering those descendent species where the transitional forms from the ancestral (morphocline) are well documented along the stratigraphic succession. In this way, the consistency of the appearance of the descendent species is thus greatly improved. According to Remane (2003), the definition of descendent species, including its morphology and phylogenesis, should be thus clear and well defined to avoid misunderstandings and confusion that can have repercussions on the chronostratigraphy, and thus on the Geological Time Scale (GTS).

Biostratigraphically, the most important Rhaetian conodont genus for the Tethyan is *Misikella*, which is very common and frequent in both fully pelagic and shallow-marine sediments (e.g. Kozur and Mock 1991; Krystyn et al. 2007a, b; Muttoni et al. 2010). Other genera represented by *Mockina*, *Parvigondolella* and *Zieglericonus* are often present throughout the Rhaetian. Also, genus *Norigondolella* can be present in Rhaetian sediments (e.g. Pálfy et al., 2007; Kolar-Jurkovšek 2011; Rigo et al., 2016), but it seems to be restricted to cool water conditions (Trotter et al. 2015). In the uppermost Triassic, ramiform elements are very often collected with few other pectiniform conodonts or even without any in the uppermost Rhaetian (e.g. Kozur and Mock 1991; Kozur 1993; Pálfy et al. 2007). This issue is probably due to a

conodont loss during extraction, commonly using 0.1 mm sieves (Kozur and Mock 1991). In fact, the youngest conodont zone consists of *Neohindeodella detrei* (Kozur and Mock 1991), a ramiform index species occurring above the LOs of *Misikella* and all the other Rhaetian genera, at the "Initial" CIE and below the Triassic/Jurassic boundary (e.g. Hesselbo et al. 2002; Pálfy et al. 2007).

6.6.1 Rhaetian Conodont Biozonation

6.6.1.1 *Misikella posthernsteini* Interval Zone

Definition: the lower boundary is marked by the FO of the index species *Misikella posthernsteini* Kozur and Mock (1974); the upper boundary by the FO of *Misikella ultima* Kozur and Mock (1991).

The occurrence of *Misikella posthernsteini* (Fig. 6.15a) defines the base of its homonymous biozone and most important the base of the Rhaetian after being voted by the Norian/Rhaetian Boundary Task Force (Krystyn 2010), and conventionally adopted as the primary marked for the NRB. The definition of *Misikella posthernsteini* was given by Kozur and Mock (1974) and largely argued in Giordano et al. (2010) and more recently in Rigo et al. (2016) and Bertinelli et al. (2016), and here is accepted and used. The zone is characterised by *Parvigondolella andrusovi* (which last occurs at the base), *Mockina bidentata* (rare), *Misikella koessenensis*, *"Mockina" vrienlyncki* and *Mi. hernsteini*.

Age: *Misikella posthernsteini* with features corresponding to the original description by Kozur and Mock (1974) has been documented occurring within the radiolarian *Proparvicingula moniliformis* Zone (sensu Carter 1993; Giordano et al. 2010), and mostly coincident with a marked negative $\delta^{13}C_{org}$ excursion (Maron et al. 2015; Bertinelli et al. 2016; Rigo et al. 2016; Zaffani et al. 2017). Similarly, in North America (Nevada and British Columbia), *Mockina* (=*Epigondollela*) *mosheri* A occurred at the *P. moniliformis* Zone (Orchard et al. 2007a; Tackett et al. 2014), which is biochronologically equivalent to the North American ammonoid *Paracochloceras amoenum* Zone (e.g. Carter 1993; Orchard and Tozer 1997; Orchard et al. 2007a). The *P. moniliformis* Zone occurs after the radiolarian *Betraccium deweveri* Zone (i.e. Carter 1993), at the end of which the standard-size *Monotis* bivalves disappear (Ward et al. 2001), and coinciding with a negative shift of $\delta^{13}C_{org}$ (Ward et al. 2004; Whiteside and Ward 2011; Rigo et al. 2016; Zaffani et al. 2017) and $^{87}Sr/^{86}Sr$ ratio (e.g. Callegaro et al. 2012). The close correlation of the end-Norian extinction of *Monotis* and the negative $\delta^{13}C_{org}$ shift is further recorded in Canada (British Columbia) at Williston Lake, during background anoxic conditions punctuated by transient oxygenation events (Wignall et al. 2007). These environmental conditions have been documented also in the western Tethys (Casacci et al. 2016; Rigo et al. 2016; Zaffani et al. 2017). The negative shift of $\delta^{13}C_{org}$ at the NRB is thus documented on both sides of the Panthalassa Ocean, representing an important physical tool for global correlations (Rigo et al. 2016; Zaffani et al. 2017).

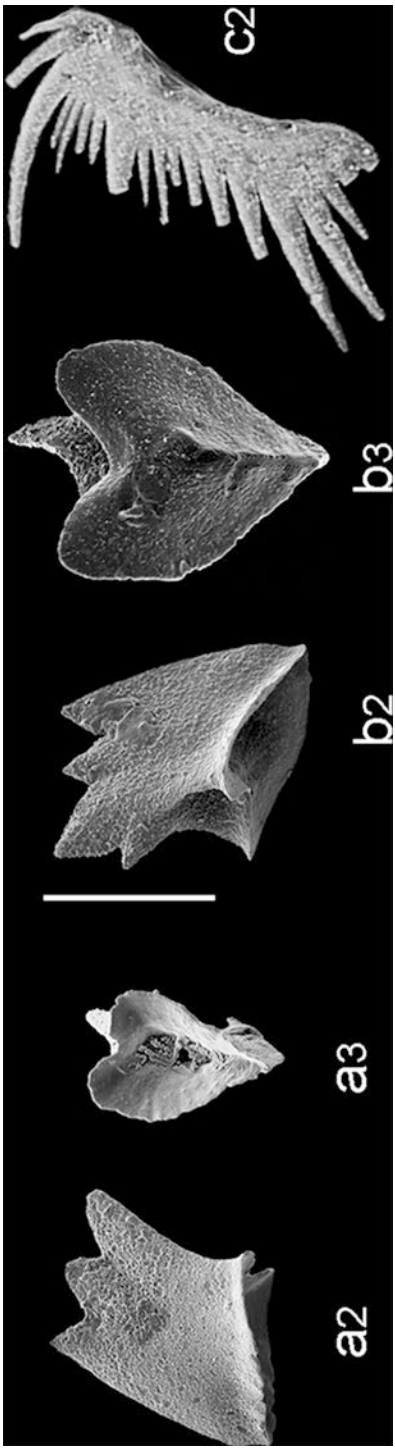

Fig. 6.15 Index conodont species for the Rhaetian zones. Where possible, all the three views are provided: (1) upper view, (2) lateral view, (3) lower view. Scale bars are 200 μm. (**a**) *Misikella posthernsteini* Kozur and Mock (from Mazza et al. 2012a). (**b**) *Misikella ultima* Kozur and Mock (from Mazza et al. 2012a). (**c**) *Neohindeodella detrei* Kozur and Mock (from Kozur and Mock 1991)

All these events are well correlated and occurred around the age of 205.7 Ma, as further confirmed by the high-precision U-Pb geochronology age of 205.70 ± 0.15 Ma (Wotzlaw et al. 2014; Golding et al. 2016) for the NRB (LO of bivalve *Monotis*) and the statistical correlation with the Newark APTS of the NRB (FAD of *Mi. posthernsteini* and negative $\delta^{13}C_{org}$) at 205.7 Ma by Maron et al. (2015).

6.6.1.2 *Misikella ultima* Interval Zone

Definition: the lower boundary is marked by the FO of the index species *Misikella ultima* Kozur and Mock (1991); the upper boundary by the FO of the of *Neohindeodella detrei* Kozur and Mock (1991).

Misikella ultima was first illustrated by Kozur and Mock (1991) who described its evolution directly from *Misikella posthernsteini,* developing 1–3 denticles in a secondary posterior blade (Fig. 6.15b). This secondary blade grows up within the deep groove along the backside of the cusp, which is the last denticle posteriorly reclined of *Mi. posthernsteini*. In this zone, *Mockina bidentata* last occurs at its base while *Misikella hernsteini* in the middle; *Mi. posthernsteini* and *Mi. ultima* are common, along with *Mi. kovacsi*.

Age: *Misikella ultima* is constrained with the base of the radiolarian *Globolaxtorum tozeri* Zone (Pálfy et al. 2007). In North America, the base of *G. tozeri* Zone is considered coeval to the base of the ammonoid *Choristoceras crickmayi* Zone (Carter 1993), which in turn corresponds to the base of the Tethyan ammonoid *Vandaites stuerzenbaumi* Zone (Dagys and Dagys 1994; Whiteside and Ward 2011). The ammonoid *V. stuerzenbaumi* Zone is subdivided by Maslo (2008) into two ammonoid subzones that are *Vandaites saximontanus* (=ex-*"Choristoceras" haueri* Subzone) and *Vandaites stuerzenbaumi* s.s. Subzone.

6.6.1.3 *Neohindeodella detrei* Taxon-range Zone

Definition: presence of *Neohindeodella detrei* Kozur and Mock (1991) and disappearance of other conodont index fossils; the upper boundary is represented by the extinction of the class Conodonta.

Conodont *Neohindeodella detrei* is a ramiform conodont first described by Kozur and Mock (1991) (Fig. 6.15c), occurring above the last observed occurrence of ammonoid *Choristoceras* along with no other conodont index elements. For this reason, Kozur and Mock (1991) established the *Nh. detrei* Zone as the last conodont biozone, uppermost Rhaetian in age. *Neohindeodella detrei* was found above the last occurrence of *Misikella ultima* and other conodonts, and it was described along with *Neohindeodella* sp. A, supporting the suggestion that conodonts survived to the End-Triassic mass exctinction (ETE) within the latemost Rhaetian (Kozur 1993; Pálfy et al. 2007).

6.7 Systematic Palaeontology

Phylum CHORDATA (Bateson 1886).
Subphylum VERTEBRATA (Linnaeus 1758).
Class CONODONTA (Eichenberg 1930).
Order OZARKODINIDA (Dzik 1976).
Superfamily GONDOLELLACEA (Lindström 1970).
Family GONDOLELLIDEA (Lindström 1970).
Genus *Norigondolella* (Kozur 1989).
Norigondolella carlae n. sp.

1980 *Gondolella* cf. *navicula*—Krystyn, pl.11, figs 8, 9
2007 *Norigondolella* sp.—Nicora et al. pl.3, fig.1
2007 *Norigondolella* sp.—Rigo et al. fig. 5/9
2010 *Norigondolella* cf. *navicula*—Balini et al. pl.2, fig.11
2012b *Norigondolella* cf. *navicula*—Mazza et al. fig. 3B

Origin of the name—In honor of Mrs. Carla Galli Nicora, mother of Alda Nicora.

Holotype—The specimen illustrated in Fig. 6.8a.

Type horizon—Bed NA16 (Upper Carnian) of the Pizzo Mondello section, a white micritic calcilutite with black-brown cherty nodules, belonging to the Scillato Fm.

Type locality—Pizzo Mondello section (Monti Sicani, Western Sicily, Italy), the abandoned quarry ("la Cava" locality) on the south-western slope of Pizzo Mondello Mountain.

Repository—The holotype is stored at the Dipartimento di Scienze della Terra "A. Desio", Università degli Studi di Milano (Italy). Repository number: Micro-Unimi no. 2019.

Diagnosis—Small conodont with a long and broad platform extending for the entire length of the element. The platform margins are flat and they have no ornamentation on the margins, except for a coarse microcrenulation. The cusp is always the last denticle of the carina, it is big in size and posteriorly inclined, and it is located just in front of the posterior platform margin. The keel is prominent and the pit is terminal both to the platform and to the keel end. The blade is high anteriorly but it gradually descends into a low carina posteriorly. The carinal nodes are fused at their base but the tips are widely spaced.

Description—This species has a low intraspeciefic variability, with very few recogniziable characters. The element has a small size (about 500 μm length), characterised by a wide platform with sub-parallel margins that never bear any ornamentation, except for the typical conodont microcrenulation. The platform is tapered at the anterior and posterior ends and it covers the entire length of the element, leaving no free blade. The lateral margins are low, giving a flat profile to the lateral platform. The posterior end of the platform is always rounded. Cusp and carina are distinctive elements of this species. The cusp is always the last denticle, it is located just in front to the posterior margin of the platform, it is bigger in size with respect to the preceding carinal nodes and it is posteriorly reclined. The carina

is low, composed by nodes that are fused at their base but characterised by widely spaced tips. The pit is very narrow, surrounded by a prominent loop and it is terminal with respect both to the platform and to the keel end. The keel termination is rounded and it is never prolonged. Laterally the element is usually arched in its middle part and the keel is prominent. The blade is high in correspondence to the anterior third of the element but it descends gradually into the low carina.

Remarks—Norigondolella carlae was mentioned for the first time (but not described) as *Gondolella* cf. *navicula* by Krystyn in 1980, from Tuvalian II strata at Feuerkogel (Austria). Successively it was reported as *Norigondolella* sp. in Nicora et al. (2007) and Rigo et al. (2007), and as *Norigondolella* cf. *navicula* in Balini et al. (2010a, b), and Mazza et al. (2012a, b). This species is now formally described and established here. *No. carlae* is a primitive and less evolved *Norigondolella* species, with a smaller size than typical norigondolellids and with more spaced carinal nodes, thus seemingly representing a forerunner of genus *Norigondolella*.

Stratigraphical and geographical distribution—Norigondolella carlae has a short stratigraphic range that is limited to the *Neocavitella cavitata* Zone. This species is never present in rich populations, but its short range and very distinctive morphological characters makes *No. carlae* a very useful guide form for the Upper Tuvalian.

No. carlae is spread in all the Tethys: Austria (Feuerkoegel section, Krystyn 1980), southern Apennines (Pignola 2 section, Rigo et al. 2007), Sicily (Pizzo Mondello section, Mazza et al. 2012a), and Turkey (Buleketasi Tepe and Erenkolu Mezarlik sections, unpublished data).

6.8 Conclusion

Conodonts have proven to be important tools for detailed biostratigraphic investigations for the Upper Triassic, because of their great abundance and worldwide distribution. We present here an original Upper Triassic conodont biozonation for the Tethyan Realm, consisting of 22 conodont zones (nine for the Carnian, ten for the Norian, and three for the Rhaetian), integrated with ammonoid and radiolarian zones. We also provide data supporting the validity of conodonts as reliable tools for global correlations, recommending two conodont biovents as possible GSSP primary biomarkers that are the FAD (First Appearance Datum) of *Metapolygnathus parvus* for the base of the Norian and the FAD of *Misikella posthernsteini* for the base of the Rhaetian.

Acknowledgements Funding for this research was provided through EX60% 60A05-7013/15 and PRAT CPDA152211/15 to Manuel Rigo by the University of Padova, and through MIUR PRIN (2008BEF5Z7_001; PI M. Balini, Università degli Studi di Milano). MM is grateful to Leopold Krystyn (University of Wien) for giving access to his conodont collections from the Buleketasi Tepe and Erenkolu Mezarlik (Turkey) sections. The manuscript was improved by reviews from M.J. Orchard and T. Kolar-Jurkovšek who are sincerely thanked. We warmly thank Larry Tanner, the Editor of this volume, for the invitation to contribute with this chapter.

References

Balini M, Bertinelli A, Di Stefano P, Guaiumi C, Levera M, Mazza M, Muttoni G, Nicora A, Preto N, Rigo M (2010a) The late Carnian succession at Pizzo Mondello (Sicani Mountains). Albertiana 39:36–57

Balini M, Germani D, Nicora A, Rizzi E (2000) Ladinian/Carnian ammonoids and conodonts from the classic Schilpario-Pizzo Camino area (Lombardy): revaluation of the biostratigraphic support to chronostratigraphy and paleogeography. Riv Ital Paleontol Stratigr 106(1):19–58

Balini M, Krystyn L, Levera M, Tripodo A (2012) Late Carnian-early Norian ammonoids from the GSSP candidate section Pizzo Mondello (Sicani Mountains, Sicily). Riv Ital Paleontol Stratigr 118:47–84

Balini M, Lucas SG, Jenks JF, Spielmann JA (2010b) Triassic ammonoid biostratigraphy: an overview. In: Lucas SG (ed) The Triassic timescale. Geol Soc Spec Publ 334:221–262

Bateson W (1886) The ancestry of the Chordata. The Quart J Microscop Sci 26:535–571

Bazzucchi P, Bertinelli A, Ciarapica G, Marcucci M, Passeri L, Rigo M, Roghi G (2005) The Late Triassic–Jurassic stratigraphic succession of Pignola (Lagonegro-Molise Basin, Southern Apennines, Italy). Bollett Soc Geolog Ital 124:143–153

Belvedere M, Avanzini M, Mietto P, Rigo M (2008) Norian dinosaur footprints from the "Strada delle Gallerie" (Monte Pasubio, NE Italy). Stud Trent Scienze Natur Acta Geolog 83:267–275

Bertinelli A, Casacci M, Concheri G, Gattolin G, Godfrey L, Katz ME, Maron M, Mazza M, Mietto P, Muttoni G, Rigo M, Sprovieri M, Stellin F, Zaffani M (2016) The Norian/Rhaetian Boundary interval at Pignola-Abriola section (southern Apennines, Italy) as a GSSP candidate for the Rhaetian stage: an update. Albertiana 43:5–18

Bertinelli A, Ciarapica G, De Zanche V, Marcucci M, Passeri L, Rigo M, Roghi G (2005) Stratigraphic evolution of the Triassic-Jurassic Sasso di Castalda succession (Lagonegro basin, Southern Apennines, Italy). Bollett Soc Geolog Ital 124:161–175

Breda A, Preto N, Roghi G, Furin S, Meneguolo R, Ragazzi E, Fedele P, Gianolla P (2009) The Carnian Pluvial event in the Tofane Area (Cortina d'Ampezzo, Dolomites, Italy). Geo Alp 6:80–115

Broglio Loriga C, Cirilli S, De Zanche V, Di Bari D, Gianolla P, Laghi MF, Lowrie W, Manfrin S, Mastandrea A, Mietto P, Muttoni G, Neri C, Posenato C, Rechichi MC, Rettori R, Roghi G (1999) The Prati di Stuores/Stuores Wiesen Section (Dolomites, Italy): a candidate Global Stratotype section and point for the base of the Carnian stage. Riv Ital Paleont Strat 105(1):37–78

Budai T, Kovács S (1986) Contributions to the stratigraphy of the Rezi Dolomite Formation [Metapolygnathus slovakensis (Conodonta, Upper Triassic) from the Keszthely Mts (W Hungary)]. M. Áll. Földtani Intézet jelentése az 1984. évről:175–191

Budurov K (1972) Ancyrogondolella triangularis gen. et sp. n. (Conodonta). Mitt Ges Geol Bergbaustud 21:853–860

Budurov K, Stefanov S (1965) Gattung *Gondolella* aus der Trias Bulgariens. Travaux sur la Géologie de Bulgarie—Série Paléontol 7:115–127

Buryi GI (1989) Morfologija verchnetriasovych platformennych konodontov *Epigondolella* i *Metapolygnathus*. In: Paleontologo-stratigraficheskie issledovanija fanerozoja dalnego vostoka.—AN SSSR, dalnevostochnoe otdelenie 45–48

Cafiero B, De Capoa-Bonardi P (1981) I conodonti dei calcari ad Halobia del Trias superiore del Montenegro (CRNA-GORA, JUGOSLAVIA). Riv Ital Paleont 86:563–576

Callegaro S, Rigo M, Chiaradia M, Marzoli A (2012) Latest Triassic marine Sr isotopic variations, possible causes and implications. Terra Nova 24:130–135

Carter ES (1993) Biochronology and Paleontology of uppermost Triassic (Rhaetian) radiolarians, Queen Charlotte Islands, British Columbia, Canada. Mém Géolog (Lausanne) 11:1–176

Carter ES, Orchard MJ (2007) Radiolarian—conodont—ammonoid intercalibration around the Norian-Rhaetian Boundary and implications for trans-Panthalassan correlation. Albertiana 36:149–163

Casacci M, Bertinelli A, Algeo TJ, Rigo M (2016) Carbonate-to-biosilica transition at the Norian–Rhaetian boundary controlled by rift-related subsidence in the western Tethyan Lagonegro Basin (southern Italy). Palaeogeogr Palaeoclimatol Palaeoecol 456:21–36

Celarc B, Kolar-Jurkovšek T (2008) The Carnian-Norian basin-platform system of the Martuljek Mountain group (Julian Alps, Slovenia): progradation of the Dachstein carbonate platform. Geolog Carpath 59:211–224

Channell JET, Kozur HW, Sievers T, Mock R, Aubrecht R, Sykora M (2003) Carnian-Norian biomagnetostratigraphy at Silickà Brezovà (Slovakia): correlation to other Tethyan sections and to the Newark Basin. Palaeogeogr Palaeoclimatol Palaeoecol 191:65–109

Chen Y, Krystyn L, Orchard MJ, Lai X-L, Richoz S (2015) A review of the evolution, biostratigraphy, provincialism and diversity of Middle and early Late Triassic conodonts. Palaeontology 2:235–263

Dagys AS, Dagys AA (1994) Global correlation of the terminal Triassic. In: Guex J, Baud A (eds) Recent developments on Triassic stratigraphy. Mém Géol Lausanne 22:25–34

Dal Corso J, Mietto P, Newton RJ, Pancost RD, Preto N, Roghi G, Wignall PB (2012) Discovery of a major negative δ13C spike in the Carnian (Late Triassic) linked to the eruption of Wrangellia flood basalts. Geol 40:79–82

De Capoa-Bonardi P (1984) *Halobia* zones in the pelagic Late Triassic sequences of the central Mediterranean area (Greece, Yugoslavia, Southern Apennines, Sicily). Boll Soc Paleontol It 23(1):91–102

De Renzi M, Budurov K, Sudar M (1996) The extinction of conodonts—in terms of discrete elements—at the Triassic-Jurassic boundary. Cuader Geolog Ibèrica 20:347–364

De Zanche V, Gianolla P, Roghi G (2000) Carnian stratigraphy in the Raibl/Cave del Predil area (Julian Alps, Italy). Eclog Geolog Helvet 93:331–347

Donofrio DA, Brandner R, Poleschinski W (2003) Conodonten der Seefeld—Formation: ein Beitrag zur Bio- und Lithostratigraphie der Hauptdolomit-Plattform (Obertrias, Westliche Nördliche Kalkalpern, Tirol). Geol Paläont Mitt Innsbruck 26:91–107

Dzik J (1976) Remarks on the evolution of Ordovician conodonts. Acta Palaeont Pol 21:395–455

Eichenberg W (1930) Conodonten aus dem Culm des Harzes. Paläontol Z 12:177–182

Eicher DB (1946) Conodonts from the Triassic of Sinai (Egypt). Am Assoc Petrol Geol Bull 30:613–616

Furin S, Preto N, Rigo M, Roghi G, Gianolla P, Crowley JL, Bowring SA (2006) High-precision U-Pb zircon age from the Triassic of Italy: Implications for the Triassic time scale and the Carnian origin of calcareous nannoplankton and dinosaurs. Geol 34:1009–1012

Gaetani M, Nicora A, Henderson C, Cirilli S, Gale L, Rettori R, Vuolo I, Atudorei V (2013) Refinements in the Upper Permian to Lower Jurassic stratigraphy of Karakorum, Pakistan. Facies 59:915–948

Gale, L, Kolar-Jurkovšek, T, Šmuc, A, Rožič (2012) Integrated Rhaetian foraminiferal and conodont biostratigraphy from the Slovenian Basin, eastern Southern Alps. Swiss J Geosci 105:435–462

Gallet Y, Besse J, Krystyn L, Marcoux J (1996) Norian magnetostratigraphy from the Scheiblkogel section, Austria: constraint on the origin of the Antalya Nappes, Turkey. Earth Planet Sci Lett 140:113–122

Gallet Y, Besse J, Krystyn L, Marcoux J, Guex J, Théveniaut H (2000) Magnetostratigraphy of the Kavaalani section (southwestern Turkey): Consequence for the origin of the Antalya Calcareous Nappes (Turkey) and for the Norian (Late Triassic) magnetic polarity timescale. Geophys Res Lett 27:2033–2036

Gallet Y, Besse J, Krystyn L, Marcoux J, Théveniaut H (1992) Magnetostratigraphy of the late Triassic Bolücektasi Tepe section (southwestern Turkey): implications for changes in magnetic reversal frequency. Phys Earth Planet Inter 93:273–282

Gallet Y, Besse J, Krystyn L, Théveniaut H, Marcoux J (1993) Magnetostratigraphy of the Kavur Tepe section (southwestern Turkey): a magnetic polarity time scale for the Norian. Earth Planet Sci Lett 117:443–456

Gallet Y, Krystyn L, Besse J (1998) Upper Anisian to Lower Carnian magnetostratigraphy from the Northern Calcareous Alps (Austria). J Geophys Res 103:605–621
Gattolin G, Preto N, Breda A, Franceschi M, Isotton M, Gianolla P (2015) Sequence Stratigraphy after the demise of a high-relief carbonate platform (Carnian of the Dolomites): sea-level and climate disentangled. Palaeogeogr Palaeoclimatol Palaeoecol 423:1–17
Gianolla P, Ragazzi E, Roghi G (1998) Upper Triassic amber from the Dolomites (Northern Italy). A paleoclimatic indicator? Riv Ital Paleontol Stratigr 104:381–390
Giordano N, Ciarapica G, Bertinelli A, Rigo M (2011) The Norian-Rhaetian interval in two sections of the Lagonegro area: the transition from carbonate to siliceous deposition. Ital J Geosci 130:380–393
Giordano N, Rigo M, Ciarapica G, Bertinelli A (2010) New biostratigraphical constraints for the Norian/Rhaetian boundary: data from Lagonegro Basin, Southern Apennines, Italy. Lethaia 43:573–586
Golding ML, Mortensen ZJ-P, Orchard MJ (2016) U-Pb isotopic ages for euhedral zircon in the Rhaetian of British Columbia: implications for Cordilleran tectonics during the Late Triassic. Geosphere 12(5):1–11
Gradstein FM, Ogg JG, Schmitz M, Ogg G (2012) The Geologic Time Scale 2012. Elsevier, Amsterdam, pp 1–1142
von Gümbel CW (1861) Geognostische Beschreibung des bayerischen Alpengebirges und seine Vorlandes 1-950. Perthes, Gotha
Hayashi S (1968) The Permian Conodonts in Chert of the Adoyama Formation, Ashio Mountains, Central Japan. Earth Sci 22:63–77
Hesselbo SP, Robinson SA, Surlyk F, Piasecki S (2002) Terrestrial and marine extinction at the Triassic-Jurassic boundary synchronized with major carbon- cycle perturbation: a link to initiation of massive volcanism? Geol 30:251–254
Huckriede R (1958) Die Conodonten der mediterranen Trias und ihr stratigraphischer Wert. Paläont Z 32(3):141–175
Ishida K, Hirsch F (2001) Taxonomy and faunal affinity of Late Carnian-Rhaetian conodonts in the Southern Chichibu Belt, Shikoku, SW Japan. Riv It Paleont Strat 107(2):227–250
Ji Z-S, Yao J-X, Yang X-D, Zang W-S, Wu G-C (2003) Conodont zonations of Norian in Lhasa area, Xizang (Tibet) and their global correlation. Acta Palaeontol Sin 42(3):382–392. (in Chinese with English abstract)
Karádi V (2017) Middle Norian conodonts from the Buda Hills, Hungary: an exceptional record from the western Tethys. J Iber Geol. https://doi.org/10.1007/s41513-017-0009-3
Karádi V, Kozur HW, Görög Á (2013) Stratigraphically important Lower Norian conodonts from the Csővár borehole (CSV-1), Hungary—comparison with the conodont succession of the Norian GSSP candidate Pizzo Mondello (Sicily, Italy). In Tanner LH, Spielmann JA, Lucas SG (eds), The Triassic System. New Mex Mus Nat Hist Sci Bull 61:284–295
Karádi V, Mazza M (2015) New advances in the conodont biostratigraphy of the Upper Triassic successions in Csővár and the Buda Mts., Transdanubian Range, Hungary. Ber Inst Erdwiss K-F-Univ, Graz 21:192
Karádi V, Pelikán P, Haas J (2016) Conodont biostratigraphy of Upper Triassic dolomites of the Buda Hills (Transdanubian Range, Hungary). Földtani Közlöny 146(4):371–386. (in Hungarian with English abstract)
Kiliç AM, Plasencia P, Ishida K, Hirsch F (2015) The Case of the Carnian (Triassic) Conodont Genus *Metapolygnathus* Hayashi. J Earth Sci 26:219–223
Kolar-Jurkovšek T (2011) Latest Triassic conodonts of the Slovenian Basin and some remarks on their evolution. Geologija 54(1):81–90
Kolar-Jurkovšek T, Gazdzicki A, Jurkovšek B (2005) Conodonts and foraminifera from the "Raibl Beds" (Carnian) of the Karavanke Mountains, Slovenia: stratigraphical and paleobiological implications. Geol Quart 49(4):429–438

Kolar-Jurkovšek T, Jurkovšek B (2010) New paleontological evidence of the Carnian strata in the Mežica area (Karavanke Mountains, Slovenia): conodont data for the Carnian Pluvial Event. Palaeogeogr Palaeoclimatol Palaeoecol 290:81–88

Korte C, Kozur H, Veizer J (2005) δ13C and δ18O values of Triassic brachiopods and carbonate rocks as proxies for coeval seawater and paleotemperature. Paleogeogr Paleoclimatol Palaeoecol 226:287–306

Kovács S (1983) On the evolution of excelsa-stock in the Upper Ladinian-Carnian (Conodonta, genus *Gondolella*, Triassic). Osterr Akad Wiss Schriften Erdwiss Komm 5:107–120

Kovács S, Kozur H (1980) Stratigraphische Reichweite der wichtigsten Conodonten (ohne Zahnreihenconodonten) der Mittel- und Obertrias. Geol Paläont Mitt Innsbruck 10(2):47–78

Kovács S, Nagy G (1989) Contributions to the age of the Avicula- and Halobia-limestones (Feketehegy Limestone Formation) in Pilis Mts (NE Transdanubian Central Range, Hungary). M. Áll. Földtani Intézet jelentése az 1987. évről:95–129 (in Hungarian with English abstract)

Kozur H (1972) Die Conodontengattung Metapolygnathus HAYASHI 1968 und ihr stratigraphischer Wert. Geol Paläont Mitt Innsbruck 2(11):1–37

Kozur H (1989) Significance of events in conodont evolution for the Permian and Triassic stratigraphy. Courier Forsch Inst Senckenberg 117:385–408

Kozur H (1993) First evidence of Liassic in the vicinity of Csővár (Hungary), and its palaeogeographic and palaeotectonic significance. Jahrb Geol Bundesanst 136:89–98

Kozur H (2003) Integrated Permian ammonoid, conodont and radiolarian zonation of the Triassic. Hallesch Jahrb Geowissensch 25:49–79

Kozur H, Mock R (1974) *Misikella posthernsteini* n. sp., die jündste Conodontenart der tethyalen Trias. Ćas Mineral Geol 19:245–250

Kozur H, Mock R (1991) New Middle Carnian and Rhaetian conodonts from Hungary and the Alps, stratigraphic importance and tectonic implications for the Buda Mountains and adjacent areas. Jahrb Geol Bundesanst 134:271–297

Kozur H, Mostler H (1971) Probleme der Conodontenforschung in der Trias. Geol Paläont Mitt Ibk 1(4):1–19

Kristan-Tollmann E, Krystyn L (1975) Die Mikrofauna der ladinisch-karnischen Hallstätter Kalke von Saklibeli (Taurus-Gebirge, Türkei). Sitz ber Österr Akad Wiss Math-naturw Kl Abt I 184(8–10):259–340

Krystyn L (1973) Zur Ammoniten- und Conodonten-Stratigraphie der Hallstätter Obertrias (Salzkammergut, Österreich). Verh Geol B-A 1973(1):113–153

Krystyn L (1978) Eine neue Zonengliederung im alpin-mediterranen Unterkarn. Schr Erdwiss Komm Öster Akad Wiss 4:37–75

Krystyn L (1980) Triassic conodont localities of the Salzkammergut region (northern Calcareous Alps). In: Schonlaub HP (ed) Second European Conodont Symposium ECOS II: Guidebook and Abstracts. Abh- lung Geologisch Bundes 35:61–98

Krystyn L (1983) Das Epidaurus-Profil (Griechenland)—ein Beitrag zur Conodonten-Standardzonierung des tethyalen Ladin und Unter- karn. Schrift Erdwiss Komm Öster Akad Wiss 5:231–258

Krystyn L (2010) Decision report on the defining event for the base of the Rhaetian stage. Albertiana 38:11–12

Krystyn L, Bouquerel H, Kuerschner W, Richoz S, Gallet Y (2007a) Proposal for a candidate GSSP for the base of the Rhaetian stage. In: Lucas SG, Spielman JA (eds) The global Triassic. New Mex Mus Nat Hist Sci Bull 41:189–199

Krystyn L, Gallet Y (2002) Towards a Tethyan Carnian-Norian boundary GSSP. Albertiana 27:12–19

Krystyn L, Richoz S, Gallet Y, Bouquerel H, Kürschner WM, Spötl C (2007b) Updated bio- and magnetostratigraphy from Steinbergkogel (Austria), candidate GSSP for the base of the Rhaetian stage. Albertiana 36:164–173

Levera M (2012) The Halobiids from the Norian GSSP candidate section of Pizzo Mondello (Western Sicily, Italy): systematics and correlations. Riv Ital Paleontol Stratigr 118:3–45

Lindström M (1970) A suprageneric taxonomy of the conodonts. Lethaia 3:427–445
Linnaeus C (1758) Systema naturae per regna tria nturae, 10th edn. Laurenti Salvi, Stockholm
Lucas SG (2010) The Triassic timescale: an introduction. In: Lucas SG (ed) The Triassic Timescale. Geol Soc Spec Publ 334:1–16
Lucas SG (2016) Base of the Rhaetian and a critique of Triassic conodont-based chronostratigraphy. Albertiana 43:24–27
Mao L, Tian C (1987) Late Triassic conodonts from the uppermost Mailonggang Formation in Mailonggang village of Lhünzhub County, Xizang (Tibet), China. Bull Chinese Acad Geol Sci 17:159–168. (in Chinese with English abstract)
Maron M, Muttoni G, Dekkers MJ, Mazza M, Roghi G, Breda A, Krijgsman W, Rigo M (2017) Improving the magnetostratigraphy of the Carnian: new magneto-biostratigraphic constraints from Pignola-2 and Dibona marine sections, Italy. Newslett Strat 50(2):187–203
Maron M, Rigo M, Bertinelli A, Katz ME, Godfrey L, Zaffani M, Muttoni G (2015) Magnetostratigraphy, biostratigraphy, and chemostratigraphy of the Pignola-Abriola section: new constraints for the Norian-Rhaetian boundary. Geol Soc Am Bull 127:962–974
Martínez-Pérez C, Plasencia P, Cascales-Miñana B, Mazza M, Botella H (2014) New insights into the diversity dynamics of Triassic conodonts. Hist Biol 26:591–602
Martini R, Zaninetti L, Villeneuve M, Cornée JJ, Krystyn L, Cirilli S, De Wever P, Dumitrica P, Harsolumakso A (2000) Triassic pelagic deposits of Timor: palaeogeographic and sea-level implications. Palaeogeogr Palaeoclimatol Palaeoecol 60:123–151
Maslo M (2008) Taxonomy and stratigraphy of the Upper Triassic heteromorphic ammonoids: preliminary results from Austria. Berich Geolog Bundes-A 76:15–16
Mastandrea A (1995) Carnian conodonts from upper Triassic strata of the Tamarin section (San Cassiano FM., Dolomites, Italy). Riv It Paleont Strat 100(4):493–506
Mastrandrea A, Neri C, Russo F (1998) Stop 4.1- Gardena Pass Section; Stop 4.2 - Sella Pass Section. - Giorn. Geol., ser. 3°, 60, Spec. Issue, ECOS VII - Southern Alps Field Trip Guidebook, 278–291
Mazza M, Cau A, Rigo M (2012a) Application of numerical cladistic analyses to the Carnian–Norian conodonts: a new approach for phylogenetic interpretations. Journ System Palaeont 10(3):401–422
Mazza M, Furin S, Spötl C, Rigo M (2010) Generic turnovers of Carnian/Norian conodonts: climatic control or competition? Palaeogeogr Palaeoclimatol Palaeoecol 290:120–137
Mazza M, Krystyn L (2013) Revision of the conodonts of key Upper Triassic Tethyan sections: a step forward in definition of the Carnian/Norian boundary and new correlation oprtions. In: Albanesi GL, Ortega G (eds) Conodonts from the Andes—Proceedings of the 3rd International Conodont Symposium & Regional Field Meeting of the IGCP project 591. Asociación Paleontológica Argentina—Publicación Especial, 13:146
Mazza M, Krystyn L (2015) The revised Upper Triassic conodont record of the Tethys: a new step towards a better definition of the conodont bioevents around the base of the Norian stage. Ber Inst Erdwiss K-F-Univ Graz 21:243
Mazza M, Martínez-Pérez C (2015) Unravelling conodont (Conodonta) ontogenetic processes in the Late Triassic through growth series reconstructions and X-ray microtomography. Boll Soc Paleontol Ital 54(3):161–186
Mazza M, Martínez-Pérez C (2016) Evolutionary convergence in conodonts revealed by Synchrotron-based Tomographic Microscopy. Palaeontol Electron 19(3):52A. http://palaeo-electronica.org/content/2016/1710-conodont-x-ray-tomographies
Mazza M, Rigo M, Gullo M (2012b) Taxonomy and stratigraphic record of the Upper Triassic conodonts of the Pizzo Mondello section (Western Sicily, Italy), GSSP candidate for the base of the Norian. Riv Ital Paleontol Stratigr 118:85–130
Mazza M, Rigo M, Nicora A (2011) A new *Metapolygnathus* platform conodont species and its implications for Upper Carnian global correlations. Acta Palaentol Pol 56(1):121–131

McRoberts CA, Krystyn, L (2011) The FOD of Halobia austraica at the Black Bear Ridge (northeastern British Columbia) as the potential base-Norian GSSP. In Haggart JW, Smith PL (eds) Canadian Paleontology Conference, Proceedings 9:38–39

McRoberts CA, Krystyn L, Shea A (2008) Rhaetian (Late Triassic) *Monotis* (Bivalvia: Pectinoida) from the eastern Northern Calcareous Alps (Austria) and the end-Norian crisis in pelagic faunas. Palaeontology 51:571–535

Mietto P, Manfrin S (1999) A debate on the Ladinian-Carnian boundary. Albertiana 22:23–27

Mietto M, Manfrin S, Preto P, Rigo M, Roghi G, Furin S, Gianolla P, Posenato R, Muttoni G, Nicora A, Buratti N, Cirilli S, Spötl C, Ramezani J, Bowring SA (2012) The Global Boundary Stratotype Section and Point (GSSP) of the Carnian Stage (Late Triassic) at Prati di Stuores/Stuores Wiesen Section (Southern Alps, NE Italy). Episodes 35:414–430

Moix P, Kozur HW, Stampfli GM, Mostler H (2007) New paleontological, biostratigraphic and paleogeographic results from the Triassic of the Mersin Mélange, SE Turkey. In: Lucas SG, Spielmann JA, (eds.) The Global Triassic. New Mex Mus Nat Hist Sci Bull 41:282–311

Mojsisovics von Mojsvár, E (1869) Ueber die Gliederung der oberen Triasbildungen der östlichen Alpen. Jahrb Geolog Reichsan 19:91–150

Mojsisovics von Mojsvár E, Waagen WH, Diener C (1895) Entwurf einer Gliederung der pelagischen Sediments des Trias-Systems. Akad Wissensch Wien Mathemat -naturwiss Klasse Sitzungsber 104:1279–1302

Mosher LC (1968) Triassic conodonts from western North America and Europe and their correlation. J Paleontol 42(4):895–946

Mostler H (1967) Conodonten und Holoturiensklerite aus den norischen Hallstätter-Kalken von Hernstein (Niederösterreich). Verh Geol B –A ½:177–188

Müller KJ (1956) Triassic conodonts from Nevada. J Paleontol 30:818–830

Muttoni G, Kent DV, Jadoul F, Olsen PE, Rigo M, Galli MT, Nicora A (2010) Rhaetian magnetobiostratigraphy from the Southern Alps (Italy): constraints on Triassic chronology. Palaeogeogr Palaeoclimatol Palaeoecol 285:1–16

Muttoni G, Kent DV, Olsen PE, Di Stefano P, Lowrie W, Bernasconi SM, Hernández FM (2004) Tethyan magnetostratigraphy from Pizzo Mondello (Sicily) and correlation to the Late Triassic Newark astrochronological polarity time scale. Geol Soc Am Bull 116:1043–1058

Muttoni G, Mazza M, Mosher D, Katz ME, Kent DV, Balini M (2014) A Middle–Late Triassic (Ladinian–Rhaetian) carbon and oxygen isotope record from the Tethyan Ocean. Palaeogeogr Palaeoclimatol Palaeoecol 399:246–259

Nicora A, Balini M, Bellanca A, Bertinelli A, Bowring SA, Di Stefano P, Dumitrica P, Guaiumi C, Gullo M, Hungerbuehler A, Levera M, Mazza M, McRoberts CA, Muttoni G, Preto N, Rigo M (2007) The Carnian/Norian boundary interval at Pizzo Mondello (Sicani Mountains, Sicily) and its bearing for the definition of the GSSP of the Norian Stage. Albertiana 36:102–129

Noyan O, Kozur H (2007) Revision of the late Carnian-early Norian conodonts from the Stefanion section (Argolis, Greece) and their paleobiogeographic implications. N Jb Geol Paläont Abh 245(2):159–178

Ogg JG (2012) Triassic. In: Gradstein FM, Ogg JG, Schmitz M, Ogg G (eds) The Geologic Time Scale 2012, vol 2. Elsevier, Amsterdam, pp 681–730

Onoue T, Zonneveld J-P, Orchard MJ, Yamashita M, Yamashita K, Sato H, Kusaka S (2015) Paleoenvironmental changes across the Carnian/Norian boundary in the Black Bear Ridge section, British Columbia, Canada. Palaeogeogr Palaeoclimatol Palaeoecol 441:721–733

Orchard MJ (1983) *Epigondolella* populations and their phylogeny and zonation in the Upper Triassic. Fossils Strata 15:177–192

Orchard MJ (1991a) Late Triassic conodont biochronology and biostratigraphy of the Kunga Group, Queen Charlotte Islands, British Columbia. In: Woodsworth GW (ed) Evolution and hydrocarbon potential of the Queen Charlotte Basin, British Columbia. Geol Surv Can 90(10):173–193

Orchard MJ (1991b) Upper Triassic conodont biochronology and new index species from the Canadian Cordillera. In: Orchard MJ, McCracken AD (eds) Ordovician to Triassic conodont paleontology of the Canadian Cordillera. Geol Surv Can 417:299–335
Orchard MJ (2007) New conodonts and zonation, Ladinian-Carnian boundary beds, British Columbia, Canada. In: Lucas SG, Spielman JA (eds) The Global Triassic. New Mex Mus Nat Hist Sci Bull 41:321–330
Orchard MJ (2010) Triassic conodonts and their role in stage boundary definitions. In: Lucas SG (eds) The Triassic Timescale. Geological Society, Special Publication 334:139–161
Orchard MJ (2013) Five new genera of conodonts from the Carnian-Norian Boundary beds, northeast British Columbia, Canada. In Tanner LH, Spielman JA, Lucas SG (eds) The Triassic System. New Mex Mus Nat Hist Sci Bull 61:445–457
Orchard MJ (2014) Conodonts from the Carnian-Norian Boundary (Upper Triassic) of Black Bear Ridge, Northeastern British Columbia, Canada. New Mex Mus Nat Hist Sci Bull 64:1–139
Orchard MJ (2016) Base of the Rhaetian and a critique of Triassic conodont-based chronostratigraphy: comment. Albertiana 43:28–32
Orchard MJ, Carter ES, Lucas SG, Taylor DG (2007a) Rhaetian (Upper Triassic) conodonts and radiolarians from New York Canyon, Nevada, USA. Albertiana 35:59–65
Orchard MJ, Carter ES, Tozer ET (2000) Fossil data and their bearing on defining a Carnian-Norian (upper Triassic) boundary in western Canada. Albertiana 24:43–50
Orchard MJ, Tozer ET (1997) Triassic conodont biochronology, its calibration with the ammonoid standard, and a biostratigraphic summary for the Western Canada Sedimentary Basin. Bull Can Petrol Geol 45:675–692
Orchard MJ, Whalen PA, Carter ES, Taylor HJ (2007b) Latest Triassic conodonts and radiolarian-bearing successions in Baja California Sur. In: Lucas SG, Spielman JA (eds) The Global Triassic. New Mex Mus Nat Hist Sci Bull 41:355–365
Orchard MJ, Zonneveld JP, Johns MJ, McRoberts CA, Sandy MR, Tozer ET, Carrelli GG (2001) Fossil succession and sequence stratigraphy of the Upper Triassic of Black Bear Ridge, Northeast British Columbia, a GSSP prospect for the Carnian-Norian boundary. Albertiana 25:10–22
Pálfy J, Demény A, Haas J, Carter ES, Görög Á, Halász D, Oravecz-Scheffer A, Hetényi M, Márton E, Orchard MJ, Ozsvárt P, Vető I, Zaizon N (2007) Triassic-Jurassic boundary events inferred from integrated stratigraphy of the Csővár section, Hungary. Palaeogr Palaeoclimatol Palaeoecol 224:11–33
Remane J (2003) Chronostratigraphic correlations: their importance for the definition of geochronologic units. Palaeogeogr Palaeoclimatol Palaeoecol 196:7–18
Rigo M, Bertinelli A, Concheri G, Gattolin G, Godfrey L, Katz M, Maron M, Mietto P, Muttoni G, Sprovieri M, Stellin F, Zaffani M (2016) The Pignola-Abriola section (southern Apennines, Italy): a new GSSP candidate for the base of the Rhaetian Stage. Lethaia 49:287–306
Rigo M, De Zanche V, Mietto P, Preto N, Roghi G (2005) Biostratigraphy of the Calcari con Selce formation. Boll Soc Geol Ital 124:293–300
Rigo M, Joachimski MM (2010) Palaeoecology of Late Triassic conodonts: Constraints from oxygen isotopes in biogenic apatite. Acta Palaeontol Pol 55:471–478
Rigo M, Preto N, Franceschi M, Guaiumi C (2012a) Stratigraphy of the Carnian-Norian Calcari con Selce Formation in the Lagonegro Basin, Southern Apennines. Riv Ital Paleontol Stratigr 118:143–154
Rigo M, Preto N, Roghi G, Tateo F, Mietto P (2007) A rise in the carbonate compensation depth of western Tethys in the Carnian (Late Triassic): deep-water evidence for the Carnian Pluvial event. Palaeogeogr Palaeoclimatol Palaeoecol 246:188–205
Rigo M, Trotter J, Preto N, Williams I (2012b) Oxygen isotopic evidence for Late Triassic monsoonal upwelling in the northwestern Tethys. Geol 40:515–518

Roghi G, Mietto P, Dalla Vecchia FM (1995) Contribution to the Conodont Biostratigraphy of the Dolomia di Forni (Upper Triassic, Carnia, NE Italy). Mem Sci Geol 47:125–133
Salvador A (1994) International stratigraphic guide: a guide to stratigraphic classification, terminology, and procedure: International Union of Geological Sciences, and Geological Society of America, pp 1–214
Silberling NJ, Tozer ET (1968) Biostratigraphic classification of the marine Triassic in North America. Geol Soc Am Spec Pap 10:1–63
Simms MJ, Ruffell AH (1989) Synchroneity of climatic change and extinctions in the Late Triassic. Geol 17:265–268
Simms MJ, Ruffell AH (1990) Climatic and biotic change in the late Triassic. J Geol Soc Lond 147:321–327
Simms MJ, Ruffell AH, Johnson ALA (1995) Biotic and climatic changes in the Carnian (Triassic) of Europe and adjacent areas. In: Fraser NC, Sues HD (eds) In the Shadow of the Dinosaurs. Early Mesozoic Tetrapods. Cambridge University Press, Cambridge, pp 352–365
Sudar MN, Budurov KJ (1979) New Conodonts from the Triassic in Yugoslavia and Bulgaria. Geol Balcan 9:47–52
Sweet WC, Mosher LC, Clark DL, Collinson JW, Hasenmueller WA (1971) Conodont biostratigraphy of the Triassic. In: Sweet WC, Bergström SM (eds) Symposium on Conodont Biostratigraphy. Geol Soc Am Mem 127:441–465
Tackett LS, Kaufman AJ, Corsetti FA, Bottjer DJ (2014) Strontium isotope stratigraphy of the Gabbs Formation (Nevada): implications for global Norian-Rhaetian correlations and faunal turnover. Lethaia 47:500–511
Tanner LH, Lucas SG, Chapman MG (2004) Assessing the record and causes of Late Triassic extinctions. Earth Sci Rev 65:103–139
Tatge U (1956) Conodonten aus dem Germanischen Muschelkalk. I. Teil. Paläontol Z 30:108–127
Tozer ET (1984) The Trias and its Ammonites: The evolution of a time scale. Geol Surv Can Misc Rep 35:1–171
Tozer ET (1994) Canadian Triassic ammonoid faunas. Geol Surv Can Misc Rep 467:1–663
Trotter JA, Williams IS, Nicora A, Mazza M, Rigo M (2015) Long-term cycles of Triassic climate change: a new δ18O record from conodont apatite. Earth Planet Sci Lett 415:165–174
Wang Z, Dong Z (1985) Discovery of conodont *Epigondolella* fauna from Late Triassic in Baoshan area, western Yunnan. Acta Micropalaeontol Sin 2(2):125–132. (in Chinese with English abstract)
Wang Z, Wang, L (1990) Several species of the Middle and Late Triassic conodonts from Yushu, Qinghai. In: Devonian-Triassic Stratigraphy and Palaeontology from Yushu Region of Qinghai, China, Part I, Nanjing Univ Press:123–134 (in Chinese with English abstract)
Ward PD, Garrison GH, Haggart JW, Kring DA, Beattie MJ (2004) Isotopic evidence bearing on Late Triassic extinction events, Queen Charlotte Islands, British Columbia, and implications for the duration and cause of the Triassic/Jurassic mass extinction. Earth Planet Science Lett 224:589–600
Ward PD, Haggart JW, Carter ES, Wilbur D, Tipper HW, Evans T (2001) Sudden productivity collapse associated with the Triassic-Jurassic boundary mass extinction. Science 292:1148–1151
Whiteside JH, Ward PD (2011) Ammonoid diversity and disparity track episodes of chaotic carbon cycling during the early Mesozoic. Geol 39:99–102
Wignall PB, Zonneveld JP, Newton RJ, Amor K, Sephton MA, Hartley S (2007) The end Triassic mass extinction record of Williston Lake, British Columbia. Palaeogeogr Palaeoclimatol Paleoecol 253:385–406
Wotzlaw JF, Guex J, Bartolini A, Gallet Y, Krystyn L, McRoberts CA, Taylor D, Schoene B, Schaltegger U (2014) Towards accurate numerical calibration of the Late Triassic: High-precision U-Pb geochronology constraints on the duration of the Rhaetian. Geol 42:571–574
Yin H, Zhang K, Tong J, Yang Z, Wu S (2001) The Global Stratotype Section and Point (GSSP) of the Permian-Triassic boundary. Episodes 24:102–114
Youngquist WL (1952) Triassic conodonts from southeastern Idaho. J Paleontol 26:650–655

Zaffani M, Agnini C, Concheri C, Godfrey L, Katz M, Maron M, Rigo M (2017) The Norian "chaotic carbon interval": new clues from the δ13Corg record of the Lagonegro Basin (southern Italy). Geosphere 13(4):1–16

Zapfe E (1983) Das Forschungsprojekt "Triassic of the Tethys Realm" (IGCP Proj 4). Abschlußbericht Schriftenr Erdwiss Komm Österr Akad Wiss 5:7–16

Chapter 7
Late Triassic Ammonoids: Distribution, Biostratigraphy and Biotic Events

Spencer G. Lucas

Abstract Late Triassic ammonoids have been studied for nearly 200 years. Their most extensive fossil records come from Canada (British Columbia), the USA (Nevada), Mexico (Sonora), the Alpine regions of southern Europe (especially Austria and northern Italy), the Himalayas and Russia (Siberia). At least two provinces (Tethyan and Boreal) can be identified using Late Triassic ammonoids, but the cosmopolitanism of selected genera allows Late Triassic ammonoid correlations between provinces. The official definition of the base of the Carnian stage is based on a GSSP (global stratotype section and point) in northern Italy with its primary signal the lowest occurrence of the ammonoid *Daxatina canadensis* (Whiteaves). Ammonoids are also used (less formally) to define the bases of the Carnian and Norian substages, the (ascending order) Julian, Tuvalian, Lacian, Alaunian and Sevatian. The LO of the ammonoid *Psiloceras spelae* Guex is the primary signal for the GSSP of the base of the Hettangian (base of Jurassic = top of Triassic) in Austria. The Late Triassic evolutionary history of the Ammonoidea was punctuated by a series of events: (1) the near extinction of the trachyceratids at the beginning of the Tuvalian, followed by the diversification of the Tropitidae; (2) the extinction of the Tropitidae at the beginning of the Norian followed by the diversification of the Thisbitidae and Juvavitinae; (3) a drop in diversity and the appearance of heteromorphs during the Sevatian; (4) a substantial extinction across the Norian-Rhaetian boundary; (5) a final extinction of most of the remaining Rhaetian ammonoids followed by their Early Jurassic recovery. The Late Triassic ammonoid extinction thus was stepwise, with the most substantial drop in diversity at the end of the Norian, not at the end of the Triassic.

Keywords Late Triassic Ammonoidea • Carnian • Norian • Rhaetian • Biotic Events • Extinctions

S.G. Lucas (✉)
New Mexico Museum of Natural History and Science,
1801 Mountain Road N. W., Albuquerque, NM 87104-1375, USA
e-mail: spencer.lucas@state.nm.us

© Springer International Publishing AG 2018

L.H. Tanner (ed.), *The Late Triassic World*, Topics in Geobiology 46,
https://doi.org/10.1007/978-3-319-68009-5_7

7.1 Introduction

The Triassic Period was an important time interval in the history of the subclass Ammonoidea. The group almost disappeared during the Permian-Triassic extinctions, and suffered a major extinction later in the Early Triassic (late Smithian) only to again suffer near extinction across the Triassic-Jurassic boundary. The intervening 51 million years of the Triassic saw an impressive succession of evolutionary radiations and crises, including the first experiment in heteromorphic coiling by the Ammonoidea. The Triassic ammonoid record encompasses three orders, and about 80 families, 700 valid genera and 5000 valid species (e.g., Tozer 1981a, b).

Late Triassic ammonoids were among the first ammonoids described scientifically during the early 1800s. By the end of the 1800s, ammonoid biostratigraphy became the basis of the Triassic chronostratigraphic scale. Indeed, the Standard Global Chronostratigraphic Scale of the Triassic (Fig. 7.1) was, until the 1990s, totally based on ammonoid biostratigraphy. Today, ammonoids still provide a strong basis for Late Triassic marine correlations and are used to define two of the Triassic stage boundaries and, less formally, all of the substage boundaries (e.g., Lucas 2010; Balini et al. 2010; Jenks et al. 2015).

My goal here is first to discuss briefly the history of study of Late Triassic ammonoids. I then present a short overview of the geographic and stratigraphic distribution of the Late Triassic ammonoids (Fig. 7.2). A review follows of the ammonoid biostratigraphy and biochronology of the Upper Triassic. I conclude by discussing major biotic events in the Late Triassic history of the Ammonoidea.

7.2 Some History

Tozer (1984) provided a detailed history of the use of ammonoids in the development of the Triassic chronostratigraphic scale. Additional discussion of aspects of this history can be found in Zittel (1901), Silberling and Tozer (1968), Tozer (1984), Lucas (2010), Balini et al. (2010) and Jenks et al. (2015). Here, I provide a brief historical review of the discovery and development of our knowledge of Late Triassic ammonoids.

After the first description of a Triassic ammonoid ("*Ammonites nodosa*") in 1789 (cf. Rieber and Tozer 1986), the first 60 years of the 1800s saw numerous descriptions of Triassic ammonoids from the Alpine regions of western Europe (Tozer 1984). This work was part of the effort to extend the "Trias formation" of von Alberti (1834) from its largely nonmarine "type section" in southwestern Germany into the marine strata of the Alps (e.g., von Hauer 1850). As part of this work, one of the first formally named Upper Triassic ammonoids was *Ammonites subbullatus* of von Hauer (1849; now *Tropites subbullatus*).

The paleontologist central to the subsequent development of Alpine Triassic ammonoid biostratigraphy was Edmund Mojsisovics von Mojsvár (1839–1907),

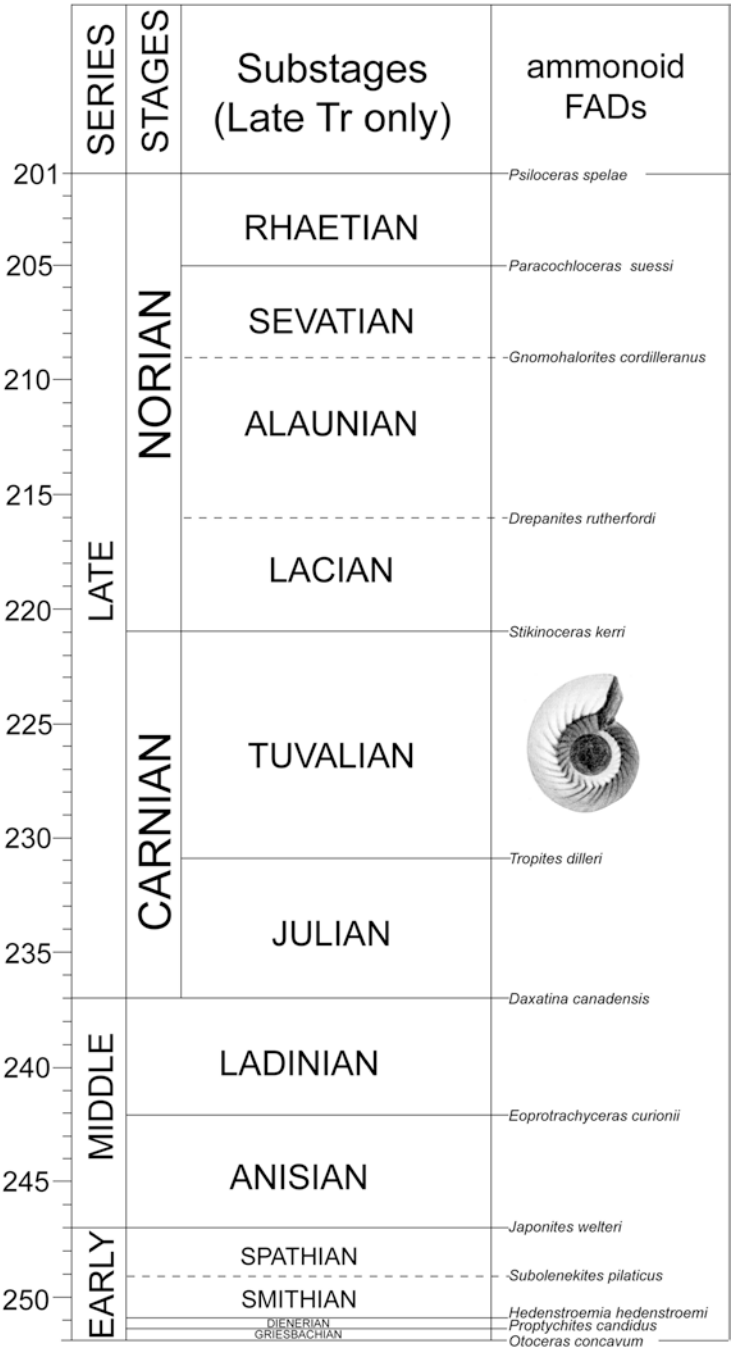

Fig. 7.1 Triassic timescale showing ammonoid-based definitions of stage and substage boundaries (after Lucas 2013)

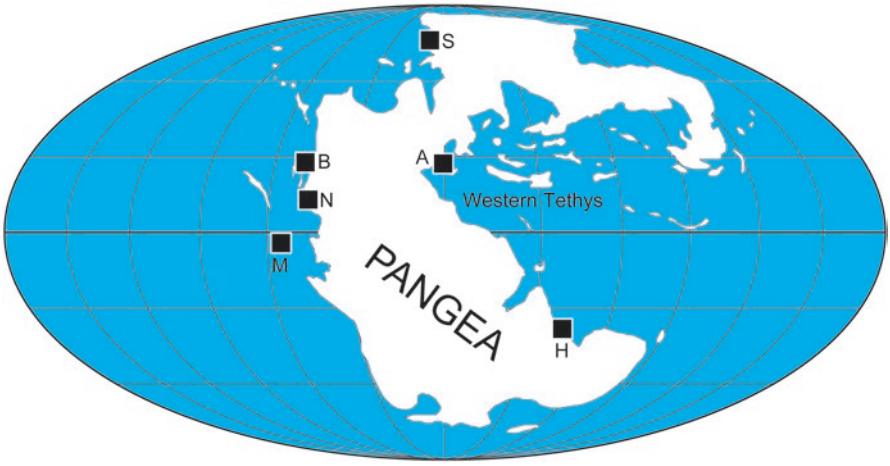

Fig. 7.2 Map of Late Triassic Pangea showing the most significant locations for Upper Triassic ammonoids. Locations are: *A* Alps (Austria and Italy), *B* British Columbia, Canada, *H* Himalayas (India, Tibet), *M* Sonora, Mexico, *N* Nevada, USA, and *S* Siberia (Russia)

whose 40-year career began in the 1860s (Rosenberg 1958; Tozer 1984). Mojsisovics worked as a paleontologist at the Geological Survey of Austria (Geologische Reichsanstalt) where he became the world authority on Triassic ammonoids. He collected many ammonoids, with an emphasis on the Late Triassic ammonoids of the Alps (e.g., Mojsisovics 1869, 1873, 1874, 1875, 1882a, b, 1893, 1902). Mojsisovics published detailed and lavishly illustrated monographs describing more than 1000 new species (about 20% of the Triassic ammonoid species so far described) and 111 new genera (Fig. 7.3).

The extensive work by Mojsisovics was culminated by an 1895 article co-authored with Carl Diener (1862–1928) and Wilhelm Heinrich Waagen (1841–1900) (Mojsisovics et al. 1895). This paper integrated the results of research carried out by Mojsisovics and Diener, mostly on the Middle and Upper Triassic ammonoid zones of the Alps (primarily Austria, Italy and Bosnia) with Waagen and Diener's work on the Lower Triassic of the Salt Range (Pakistan) and the Lower and Middle Triassic of the Himalayas (India). This integrated succession of ammonoid zones was used to define substages, stages and series for the first complete chronostratigraphic scale of the Triassic System (Fig. 7.4). Many of the Triassic substages and stages Mojsisovics et al. (1895) introduced are still used in the present version of the Standard Global Chronostratigraphic Scale for the Triassic (Fig. 7.1; cf. Lucas 2010; Ogg 2012; Ogg et al. 2014).

A different subdivision of the Triassic was provided by British Museum paleontologist Leonard Frank Spath (1888–1957), who emphasized the usefulness of ammonoids by subdividing the entire Triassic into ages, named for the most important ammonoid families (e.g., Trachyceratan, Carnitan and Tropitan for the Carnian) (Spath 1934, 1951). Spath's "ages" were not conceived as hierarchically equivalent

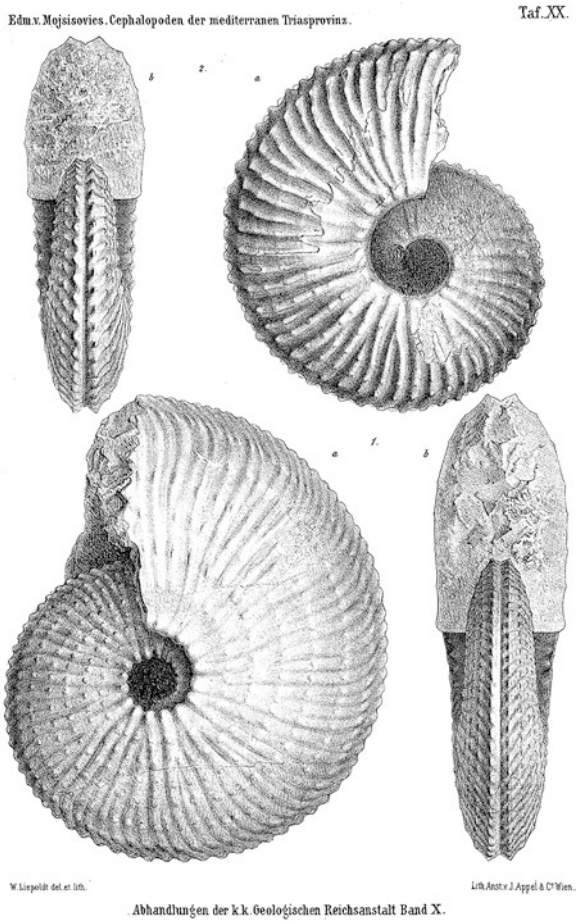

Fig. 7.3 Plate 20 of Mojsisovics (1893) monograph on the ammonoids of the Triassic "Mediterraneanprovinz" is typical of the lavish illustrations he published of Triassic ammonoids. Figure 1 is "*Trachyceras longobardicus*," and Figure 2 is "*Trachyceras pseudo-Archelaus*". Each "a" and "b" refers to two views of the same fossil

to stages, but rather as equivalent to substages (Spath 1934, tables IV–V), and were further divided into zones. Spath's approach was the first application of a biochronologic scheme to the Triassic by means of ammonoids, but it did not find general use by other workers.

At the beginning of the 1960s, the North American paleontologists E. Timothy Tozer (1928–2010) and Norman J. Silberling (1928–2011) advocated the North American ammonoid succession as the best and the most complete in the world. They built on the pioneering work of Alpheus Hyatt (1838–1902) and James Perrin Smith (1864–1931) (Hyatt and Smith 1905; Smith 1914, 1927, 1932), as well as on the work of Frank H. McLearn (1885–1964) in Canada and Siemon W. Muller (1900–1970, a student of Smith) in the western USA.

Tozer (1967) first described a biostratigraphic scale for the Canadian Triassic, consisting of 31 zones. Silberling and Tozer (1968) presented a biostratigraphic correlation chart of the most important marine successions of Nevada, Idaho, California,

Serien	Stufen	Unterstufen	Mediterrane Triasprovinz: Zone (der pelagischen Facies)	Mediterrane Triasprovinz: Schichtbezeichnung (verschiedenartiger örtlicher Entwicklung)		Indische Triasprovinz: Zone (der pelagischen Facies)	Indische Triasprovinz: Schichtbezeichnung (verschiedenartiger örtlicher Entwicklung)	
Bajuvarisch	Rhaetisch		22. Z. der *Avicula contorta*	Koessener Sch.	Dachsteinkalk			
	Juvavisch	oberjuvavisch (Sevatisch)	21. Z. des *Sirenites Argonautae*	Juvavische Hallstätter Kalke		Juvavische Cephalopodenfaunen des Himalaya		
			20. Z. des *Pinacoceras Metternichi*					
		mitteljuvavisch (Alaunisch)	19. Z. des *Cyrtopleurites bicrenatus*					
		unterjuvavisch (Lacisch)	18. Z. des *Cladiscites ruber*					
			17. Z. des *Sagenites Giebeli*					
Tirolisch	Karnisch	oberkarnisch (Tuvalisch)	16. Z. des *Tropites subbullatus*	Sandling Sch.		Karnische Cephalopodenfaunen des Himalaya		
		mittelkarnisch (Julisch)	15. Z. des *Trachyceras Aonoides*	Raibler Sch.				
		unterkarnisch (Cordevolisch)	14. Z. des *Trachyceras Aon.*	Cassianer Sch.				
	Norisch	obernorisch (Longobardisch)	13. Z. des *Protrachyceras Archelaus*	Wengener Sch.				
		unternorisch (Fassanisch)	12. Z. des *Dinarites avisianus*	Marmolatakalk				
			11. Z. des *Protrachyceras Curionis*	Buchensteiner Sch.				
Dinarisch	Anisisch	Bosnisch	10. Z. des *Ceratites trinodosus*	Oberer Muschelkalk		Z. des *Ptychites rugifer*	Muschelkalk des Himalaya	
		Balatonisch	9. Z. des *Ceratites binodosus*	Unterer Muschelkalk		Z. des *Sibirites Prahlada*	Brachiopoden-Schichten mit *Rhynchonella Griesbachi* (Himalaya)	
	Hydaspisch					8. Z. des *Stephanites superbus*	Obere Ceratiten-Kalke der Salt Range	
Skythisch	Jakutisch		Z. des *Tirolites Cassianus*	Werfner Schichten		7. Z. des *Flemingites Flemingianus*	Ceratiten-Sandstein der Salt Range	Subrobustus Beds des Himalaya
						6. Z. des *Flemingites radialus*		
						5. Z. des *Ceratites normalis*		
	Brahmanisch	Gandarisch		der Ostalpen		4. Z. des *Proptychites trilobatus*	Ceratite Marls der Salt Range	
						3. Z. des *Proptychites Lawrencianus*		
						2. Z. des *Gyronites frequens*	Untere Ceratiten-Kalke der Salt Range	
		Gangetisch				1. Z. des *Otoceras Woodwardi*	Otoceras Beds des Himalaya	

Fig. 7.4 The ammonoid-based Triassic chronostratigraphic timescale of Mojsisovics et al. (1895)

Oregon, British Columbia, Alaska and Arctic Canada. Further refinements of this scale (Tozer 1971, 1974, 1978, 1981b, 1984) produced the final version (Tozer 1994) consisting of 37 zones (11 for the Lower, 12 for the Middle and 14 for the Upper Triassic), with 11 of them divided into a total number of 28 subzones.

During the 1970s, a new wave of research on Upper Triassic ammonoids from Europe was catalyzed by IGCP (International Geological Correlation Programme) 4, "Triassic of the Tethys Realm" and by the beginning of the activities of the Subcommission on Triassic Stratigraphy (Tozer 1983; Zapfe 1983). In particular, the Austrian paleontologist Leo Krystyn restarted investigations of the Upper Triassic condensed facies of the Northern Alps originally studied by Mojsisovics (Krystyn and Schlager 1971; Krystyn et al. 1971; Krystyn 1973, 1978, 1980). Krystyn's revision of Late Triassic biostratigraphy also integrated the use of conodonts and ammonoids (e.g., Krystyn 1983). This type of integrated approach was later applied in North America (e.g., Orchard and Tozer 1997a, b).

The Lithuanian paleontologist A. S. Dagys (1933–2000) worked extensively on the ammonoids of Siberia. His collaboration with E. T. Tozer and W. Weitschat pro-

duced very precise correlation charts of the ammonoid assemblages from Siberia, Arctic Canada and Svalbard (Dagys and Tozer 1989; Weitschat and Dagys 1989; Dagys and Weitschat 1993).

Recent work has described ammonoid faunas from the Anisian to the lower Carnian of the Southern Alps (e.g., Balini 1992a, b, 1997; Balini et al. 2000; Mietto et al. 2008). Relatively new publications on Upper Triassic ammonoids from Turkey (Lukeneder and Lukeneder 2014) and Sonora, Mexico (Lucas et al. 2015) have improved knowledge of Carnian ammonoid assemblages.

7.3 Geographic Distribution

Discoveries of Triassic ammonoids in the early 1800s revealed an essentially global record early during their history of study (Tozer 1984). The most important records of Upper Triassic ammonoids have been those in: (1) British Columbia, Canada; (2) Nevada, USA; (3) Sonora, Mexico; (4) the western Tethys (from the Alps to Turkey); (5) the Himalayas (India and Tibet); and (6) Siberia (Fig. 7.2).

1. In British Columbia, in the western Canadian Cordillera, important successions of Upper Triassic ammonoid assemblages are known from the Canadian Rocky Mountains and adjacent foothills, particularly from the Ludington and Pardonet formations (Tozer 1994). In some mid-paleolatitude northeastern British Columbia localities, many boreal and paleoequatorial Tethyan ammonoids occur together, thus facilitating correlation between the Arctic and the Tethys (Tozer 1994). The well-preserved Upper Triassic ammonoid fauna of the Pardonet Formation contributed immensely to deciphering the correct sequence of upper Carnian/lower and middle Norian ammonoid zones (Tozer 1994). Indeed, the section of the Pardonet Formation at Black Bear Ridge is one of the GSSP candidates for the Carnian/Norian boundary (e.g., Orchard 2007, 2014). On the British Columbia coast, important assemblages of uppermost Triassic and lowermost Jurassic ammonoids are present on Vancouver Island and in the Queen Charlotte Islands (e.g., Tozer 1994; Tipper et al. 1994; Longridge et al. 2007).
2. In the western USA in Nevada, significant Upper Triassic ammonoid assemblages are known from diverse localities (e.g., Smith 1927; Silberling 1956, 1959; Silberling and Tozer 1968; Jenks et al. 2007; Balini 2008), including an important record of uppermost Triassic and lowermost Jurassic ammonoids in the New York Canyon area in west-central Nevada (e.g., Taylor et al. 1983, 2000; Guex et al. 2004; Lucas et al. 2007). Other well-known Upper Triassic ammonoid assemblages from Nevada include the lower Carnian "*Trachyceras*" *desatoyense* succession from the New Pass Range (Johnston 1941; Balini et al. 2007, 2012; Balini and Jenks 2007) and the upper Carnian-lower Norian *Klamathites-Guembelites* successions from West Union Canyon in the Shoshone Range (Silberling 1959; Balini et al. 2014). Also, in Shasta County, California, important upper Carnian ammonoid assemblages are known (Smith 1927; Silberling and Tozer 1968).

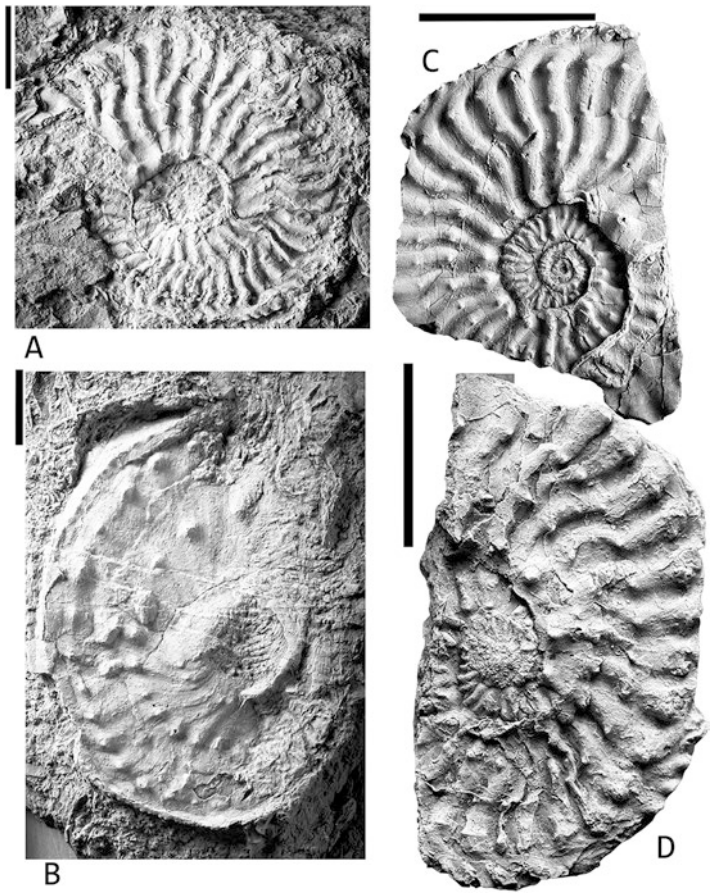

Fig. 7.5 *Sirenites* from Sonora, Mexico, helps to confirm the stratigraphic succession of ammonoid biozones across the Julian-Tuvalian boundary developed in British Columbia, Canada. (**a**–**d**) *Sirenites nanseni* Tozer, all specimens in *lateral* view. Scale bars = 1 cm. After Lucas et al. (2015)

3. In Sonora, northwestern Mexico, Keller (1928) first reported on the Carnian ammonoid assemblages near El Antimonio. Detailed studies of these assemblages (Lucas and Estep 1999; Lucas et al. 2015) documented the succession of ammonoid zones across the Julian-Tuvalian boundary, thus confirming the succession established in British Columbia (Fig. 7.5).
4. In what was Western Tethys (Fig. 7.2), the extensive ammonoid assemblages from the Alpine regions of Austria and Italy provided the basis for definition of most of the Middle and Upper Triassic stages and substages (see above). In the Alpine region, carbonate facies (both limestone and dolomite) with extensive reef development yield most of the Upper Triassic ammonoid assemblages, including the Hallstatt facies, which contains exquisitely preserved ammonoids but suffers from problems of condensed fossil assemblages. Particularly

significant ammonoid successions include those from basinal facies of Lombardy, the Dolomites and the Julian Alps in northern Italy (e.g., Mietto and Manfrin 1995; Mietto et al. 2007), and the Northern Calcareous Alps of Austria (e.g., Krystyn 1973, 1978, 2008).

In Italy, the GSSPs of the Ladinian and Carnian stages are defined at Bagolino (Lombardy) and Prati di Stuores/Stuores Wiesen (Dolomites), respectively, with ammonoid biochronological datums (FADs = first appearance datums) as their primary signals. Other important GSSP candidate sections are Pizzo Mondello (Sicily, Italy) and Steinbergkogel in the Northern Alps (Austria). Pizzo Mondello is located in western Sicily, famous for the upper Carnian-lower Norian ammonoid faunas illustrated by Gemmellaro (1904), and is one of two candidate sections for the definition of the GSSP of the base of the Norian (Nicora et al. 2007; Balini et al. 2008). Steinbergkogel, located in the world famous Hallstatt region (Northern Alps, Austria), until recently, is one of the two GSSP candidate sections for the base of the Rhaetian (Krystyn et al. 2007, b). From what was much farther east in Tethys, assemblages of Carnian ammonoids from Turkey have also been described recently (Lukeneder and Lukeneder 2014).

5. Triassic ammonoid assemblages are present in the Himalayas from Kashmir to Spiti and were first published by Oppel (1865). Most extensive are Lower and Middle Triassic ammonoid assemblages, but Upper Triassic ammonoids are also present (Diener 1906, 1908, 1912). In India, sections in the Mud (Muth) Valley of Spiti have been studied for their rich upper Ladinian to lowermost Carnian ammonoid-bivalve-conodont record (Krystyn 1982; Balini et al. 1998, 2001). In Tibet, there is also an important succession of Carnian-Norian ammonoid assemblages (Wang and He 1976).
6. Important Carnian, Norian and Rhaetian ammonoid successions have been documented from Siberia, from the Olenek River east to the shoreline of the Sea of Okhotsk (e.g., Zakharov 1997; Konstantinov and Klets 2009; Konstantinov 2012, 2014).

7.4 Paleobiogeography

The general outline of ammonoid paleobiogeographic distribution, consisting of at least three paleoprovinces, has been well established for decades (e.g., Tozer 1981b; Dagys 1988). The main paleoprovinces are Tethyan, Boreal (Arctic Canada, Svalbard, Siberia) and Notal (southern hemisphere), though much of the ammonoid record around the Pacific margins comes from terranes that were part of Panthalassa, and thus may identify another paleoprovince.

Notal asssemblages of Late Triassic ammonoids are unknown. The Late Triassic ammonoid record is dominated by diverse Tethyan assemblages that are readily distinguished from much less diverse and somewhat endemic Boreal ammonoid assemblages. Thus, the faunal diversity ratio between low and high paleolatitudes is about 10:1 during both the Carnian and the Norian (Dagys 1988).

The Boreal ammonoid assemblages from the Carnian to the middle Norian are mostly composed of Sirenitinae and rarer Ussuritidae, Arcestidae (*Arcestes*) and Gymnitidae (*Placites*). The Boreal late Norian record consists of very few *Arcestes*, *Placites* and *Rhacophyllites* (Dagys 1988; Konstantinov et al. 2003). Fortunately, throughout the Late Triassic there were some cosmopolitan genera, and this allows correlation of ammonoid assemblages between the different paleoprovinces. Thus, the cosmopolitan genera *Sirenites* and *Jovites* allow Carnian correlations, whereas the cosmopolitan genera *Halorites*, *Himavatites* and *Rhabdoceras* allow correlation during the Norian. More genera are shared between the Tethys and Pacific margins than with the Boreal realm. However, there are a few genera, such as Carnian *Arctosirenites* and Norian *Neohimavatites,* shared between the Boreal and Tethys, but not known in the Pacific.

The provincial differences between the Late Triassic ammonoid assemblages are seen as related to water temperatures. Warm Tethyan (up to 30 degrees paleolatitude) water temperatures are indicated by extensive biogenic carbonate accumulations, whereas many fewer carbonate accumulations are taken to indicate cooler Boreal and Notal water temperatures (Tozer 1981b).

7.5 Biostratigraphy

7.5.1 Base Carnian GSSP

Ammonoid datums have been used to define two Triassic stage bases. The FAD (first appearance datum) of *Eoprotrachyceras curionii* (Mojsisovics) is the marker event for the base of the Ladinian (Brack et al. 2005), and the FAD of *Daxatina canadensis* (Whiteaves) is the marker event for the base of the Carnian (Mietto et al. 2007, b, 2012; Gaetani 2009).

The Upper Triassic encompasses at least 17 ammonoid zones (Figs. 7.6 and 7.8). However, given the provincialism of Late Triassic ammonoids (see above), there is no single global biozonation. Instead, there are two important biozonations, from western North America and from the Tethys (Figs. 7.6 and 7.8).

7.5.2 Carnian Ammonoid Biostratigraphy

The Carnian is the oldest Upper Triassic stage. Most workers divide the Carnian into two substages, which in the Tethyan realm are referred to as Julian and Tuvalian (Fig. 7.6), and these should be the global substage terms (Lucas 2010, 2013). Lucas (2013) defined the base of the Tuvalian by the FAD of *Tropites dilleri* Smith (Fig. 1). The most high resolution Carnian ammonoid biozonations are in Canada and in Tethys (Fig. 7.6).

Most workers in southern Europe use the Carnian ammonoid zonation of Krystyn (1978, 1983, 2008) that recognizes seven zones (Fig. 7.6). The other well-established Carnian ammonoid biozonation is from British Columbia. It was most recently

Stage/ Substages		Siberia (Arctica Russia)	Canada (British Columbia and Arctic)	Nevada, USA and Sonora, Mexico	Tethys Northern Alps, Himalayas, Timor	Italy (Southern Alps)	China Southern Tibet)
Carnian	Tuvalian	"Striatosirenites" kedonensis	Klamathites macrolobatus	Klamathites macrolobatus	Anatropites spinosus		Parahauerites acutus
		Sirenites yakutensis					Hoplotropites
		Yakutosirenites pentastichus	Tropites welleri	Klamathites schucherti	Tropites subbullatus		
			Tropites dilleri	"Tropites dilleri"	Tropites dilleri	Tropites dilleri	Indonesites dieneri
	Julian	N. armiger-Y. ochotensis	Sirenites nanseni	Sirenites nanseni			
		Okhotrach. seimkanense	Austrotrachyceras obesum		Austrotracyceras austriacum	Austrotracyceras austriacum	
		Yanosirenites buralkitensis			Trachyceras aonoides	Trachyceras aonoides	
		Seimkanites aculeatus	Trachyceras desatoyense				
		Boreotrach. ornkutchanicum		Trachyceras silberlingi	Trachyceras aon	Trachyceras aon	
		Stolleyites tenuis					
		Nathorsites liendstroemi	Frankites sutherlandi				Protrachyceras-Joannites
		Nathorsites macconnelli		Daxatine canadensis	Daxatine canadensis	Daxatina canadensis	

Fig. 7.6 Carnian ammonoid biostratigraphy (after Jenks et al. 2015)

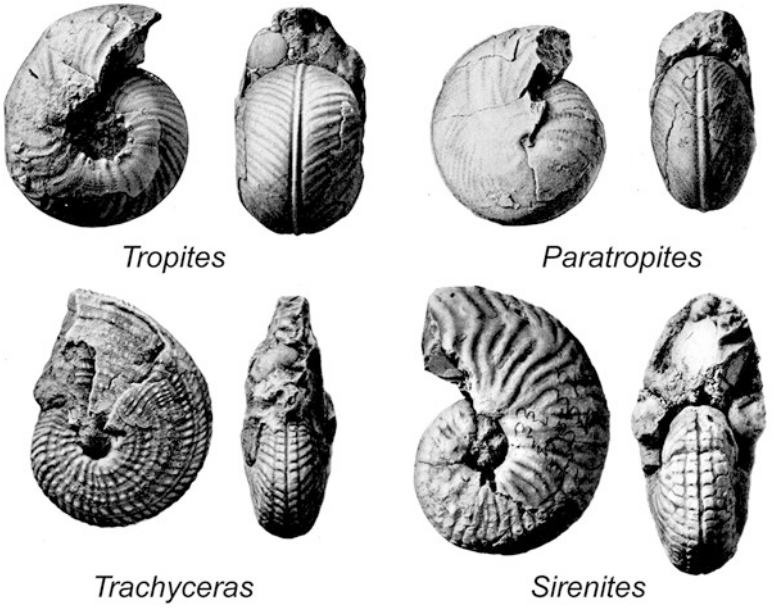

Fig. 7.7 Some characteristic Carnian ammonoids (images after Smith 1927)

reviewed by Tozer (1994) as consisting of seven zones that are readily correlated to the European zonation (Fig. 7.6). The cosmopolitanism of *Tropites dilleri* at the base of the Tuvalian is a key element in this correlation.

On the whole, the Julian is dominated by the Trachyceratinae, in particular *Trachyceras* and *Austrotrachyceras*, and by the Sirenitinae (Fig. 7.7). The base of the Tuvalian is marked by one of the major changes in the evolution of Triassic ammonoids, namely the near extinction of the Trachyceratinae, whose only survivor in the Upper Carnian is *Trachysagenites*, as well as the radiation of Tropitidae (e.g., *Tropites* and closely allied forms: Fig. 7.7) and to a lesser extent Arpaditinae (see below). Although much progress

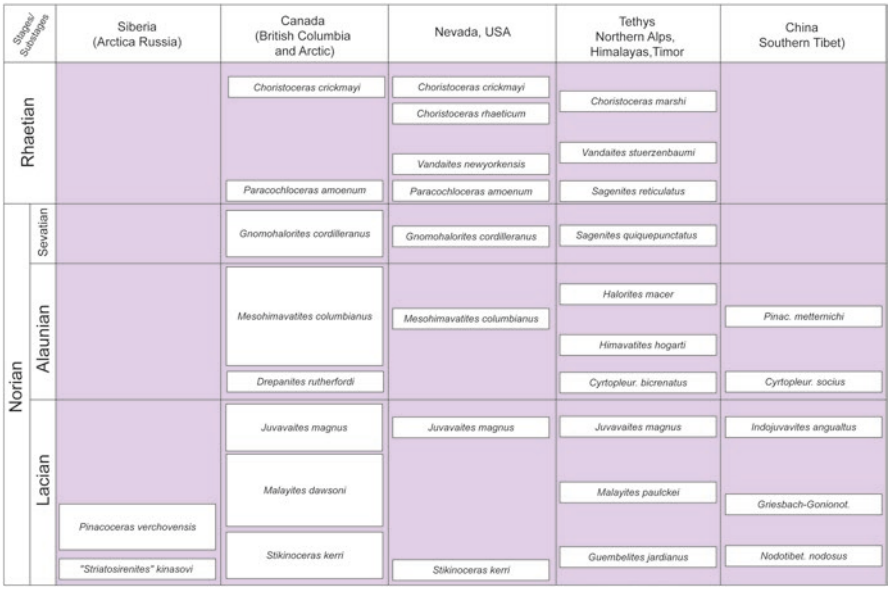

Fig. 7.8 Norian-Rhaetian ammonoid biostratigraphy (after Jenks et al. 2015)

has been made in Carnian ammonoid biostratigraphy during the last 20 years, existing schemes (Fig. 7.6) merit more study and refinement (Jenks et al. 2015).

7.5.3 Norian Ammonoid Biostratigraphy

The Norian Stage is divided into three substages, which are simply distinguished as lower, middle and upper in North America, whereas in the Tethys they are named Lacian, Alaunian and Sevatian (Fig. 7.8). These names should be used as formal terms. Tozer (1994), with some modification by Lucas (2013), defined the base of the Lacian by the FAD of *Stikinoceras kerri* McLearn, the beginning of the Alaunian by the FAD of *Drepanites rutherfordi* McLearn and the base of the Sevatian by the FAD of *Gnomohalorites cordilleranus* Tozer (Fig. 7.1).

As with the Carnian, the most detailed Norian ammonoid biozonations are in Canada and the former Tethys (Fig. 7.8). Given the great length of the Norian Stage (at least 16 million years: Lucas et al. 2012), Lucas (2013) argued that the Norian substages should be elevated to stage status, but this suggested radical change to the Late Triassic chronostratigraphic scale has not been adopted yet.

The base of the Norian and of the Lacian is characterized by the nearly complete disappearance of Tropitidae and the appearance of new members of Juvavitinae, such as *Guembelites* and *Dimorphites*, and of the Thisbitidae, such as *Stikinoceras* (Fig. 7.9).

The base of the Alaunian is marked by the appearance of new genera of Cyrtopleuritidae (*Drepanites* and *Cyrtopleurites*). Members of this family (e.g.,

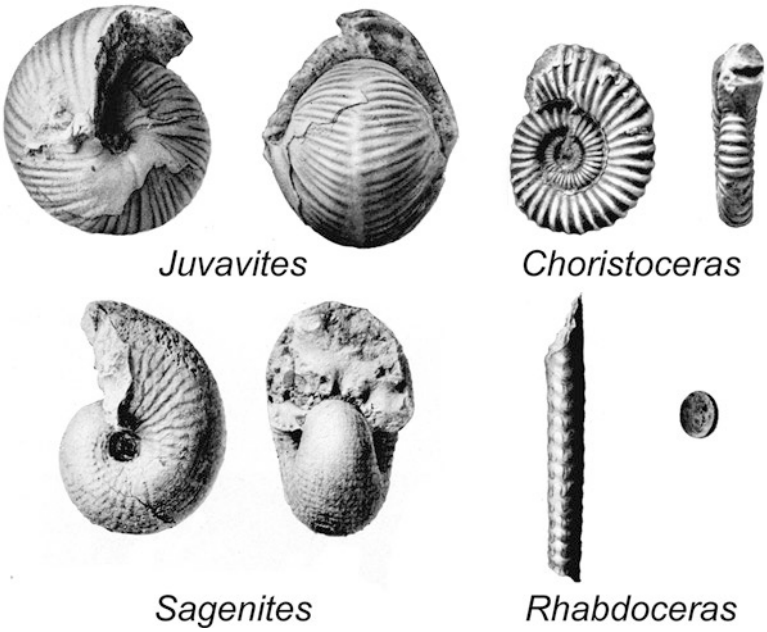

Fig. 7.9 Some characteristic Norian-Rhaetian ammonoids (images after Smith 1927)

Himavatites, *Mesohimavatites*, *Neohimavatites*) characterize the substage together with certain Haloritinae such as *Halorites* and Thisbitidae (e.g., *Phormedites*).

The base of the Sevatian is characterized by a decrease in ammonoid diversity and the first occurrence of *Rhabdoceras*, the oldest heteromorphic ammonoid (Fig. 7.9). Common forms are Haloritinae (*Gnomohalorites* and *Catenohalorites*) and Sagenitidae (Fig. 7.9).

Although much progress has been made in Norian ammonoid biostratigraphy during the last 20 years, existing schemes (Fig. 7.8) merit more study and refinement (Jenks et al. 2015).

7.5.4 Rhaetian Ammonoid Biostratigraphy

The STS recognizes the Rhaetian as the youngest Triassic stage. The generally agreed-on definition of the Rhaetian (based on a conodont datum: Krystyn et al. 2007; Krystyn 2010) essentially equates the base of the stage with the *Paracochloceras amoenum* zone (Fig. 7.8). This produces a so-called "long" Rhaetian generally comprised of two or three ammonoid zones. The youngest substage of the Norian, the Sevatian, is thereby reduced to one ammonoid zone (Fig. 7.8).

Lucas (2013) defined the base of the Rhaetian by the FAD of *Paracochloceras suessi* Mojsisovics (Fig. 7.1). However, the favored definition of the Rhaetian base is the FAD of the conodont *Misikella posthersteini* (Krystyn et al. 2007, b; Krystyn

2010; Rigo et al. 2016). In terms of ammonoids, the Norian/Rhaetian boundary is characterized by the disappearance of *Metasibirites*, the appearance of *Sagenites reticulatus* Mojsisovics and of the heteromorphs *Cochloceras* and *Paracochloceras* (Krystyn et al. 2007; Krystyn 2008). Low ammonoid diversity characterizes the Rhaetian (Tozer 1980).

The Subcommission on Jurassic Stratigraphy has chosen the LO of the ammonoid *Psiloceras spelae* Guex as the base of the Hettangian stage (= base of the Jurassic) (cf. Lucas et al. 2007; von Hillebrandt et al. 2007, 2013; von Hillebrandt and Krystyn 2009). This formally defines the top of the Triassic System.

7.6 Biotic Events

7.6.1 Major Features of Late Triassic Ammonoid Evolution

Most of the Triassic ammonoids are ceratitids with quadrilobate ceratitic suture lines. A few Triassic ammonoid families consist of smooth, relatively long-ranging forms that are informally referred to as the "leiostraca," whereas the majority belong to the group "trachyostraca," which encompasses the ornamented, fast-evolving and short-ranging forms. In general, the Triassic was characterized by the evolution and diversification of ammonoids with complex shells: involute or evolute, ribbed, tuberculate and/or carinate. As is clear from earlier text, the major subdivisions of the Late Triassic chronostratigraphic scale directly reflect the appearance and diversification of several important ammonoid genera and families, as well as extinctions.

An important point that merits further investigation is the rates of evolution of Late Triassic ammonoids. If we use the duration of biozones as a proxy of rates of evolution (they certainly are a proxy to some degree of rates of evolutionary turnover), we find that biozone durations are very short during the Early Triassic, for example, on the order of 60 kyr per zone during the Smithian. By Middle Triassic time, the rates decrease nearly tenfold; for example, 0.43 Ma per ammonoid biozone during the Anisian. However, during the Late Triassic, ammonoid biozone durations are between 2 and 3 Ma per zone. Jenks et al. (2015) suggest that this in part reflects relatively less study of late Triassic ammonoids than of Early and Middle Triassic ammonoids. However, the Canadian Late Triassic records have been studied relatively intensively (Tozer 1994 and literature cited therein) and, here, there are 7 biozones in the 16 Ma of the Carnian and 6 biozones in the 16 Ma of the Norian. This raises the real possibility that ammonoid evolutionary turnover rates slowed considerably from the Early-Middle Triassic into the Late Triassic. More research is needed here.

7.6.2 Late Carnian Events

The Carnian was ushered in by the late Ladinian extinction of various ammonoid families, the Ceratitidae, Danubitidae, Nathorsitidae, Rimkinitidae, Stuviidae and Thanamiidae. However, these were families of relatively low generic diversity, so their extinction only encompassed the loss of about 10 genera.

In general, the Julian is dominated by Trachyceratinae, in particular *Trachyceras* and *Austrotrachyceras*, and by Sirenitinae. Trachyceratids were generally involute, highly ornamented forms with a venter that had a median furrow bordered by rows of tubercles or continuous keels (Fig. 7.7). The end of the Julian encompassed the extinction of the Badiotiidae, Lobritidae, Joannitidae, Noritidae and the Sphingitidae.

The base of the Tuvalian is marked by the near extinction of the Trachyceratinae, whose only survivor in the Tuvalian is *Trachysagenites*. The diversification of the Tropitidae (e.g., *Tropites* and closely allied forms) and, to a lesser extent, Arpaditinae, also characterizes the Tuvalian. Arpaditines are evolute, compressed forms with sigmoidal ribs and tubercles and median ventral furrows. Tropitids are mainly involute, subspherical forms with ventral keels bordered by furrows (Fig. 7.7).

7.6.3 Early-Middle Norian Events

The base of the Norian (and of the Lacian) is characterized by major ammonoid biotic events: the complete disappearance of Tropitidae and the appearance of new members of Juvavitinae, such as *Guembelites* and *Dimorphites*, and of the Thisbitidae, such as *Stikinoceras* (Fig. 7.9). The thisbitids are involute, compressed forms with falcoid ribs on the flanks and a continuous keel on the venter. Juvavitines, a subfamily of haloritids, are involute, subglobose, lack keels or ventral furrows and thus have flank ribs that cross the venter (Fig. 7.9).

The base of the Alaunian is marked by the appearance of new genera of Cyrtopleuritidae (*Drepanites* and *Cyrtopleurites*). Cyrtopleuritids are involute, compressed with flanks that have flexuous ribs and spiral rows of tubercles and have a narrow, furrowed venter bordered by tubercles or keels. Members of this family (including *Himavatites*, *Mesohimavatites*, *Neohimavatites*), together with some Haloritinae, such as *Halorites* and Thisbitidae, such as *Phormedites*, characterize the Alaunian. Indeed, Late Triassic ammonoid diversity peaked during the Alaunian.

7.6.4 Late Norian Events

The base of the Sevatian is characterized by a decrease in ammonoid diversity, with the loss of about 14 genera. Indeed, several families became extinct at the base of the Sevatian: Clionitidae, Clydonitidae, Distichitidae, Episculitidae, Heraclitidae, Noridiscitidae and Thetiditidae. The first heteromorphic ammonoid, *Rhabdoceras*,

appeared during the Sevatian. Common Sevatian ammonoids are Haloritinae (*Gnomohalorites* and *Catenohalorites*) and Sagenitidae (*Sagenites* ex gr. *S. quinquepunctatus)* (Fig. 7.9). Sagenitids are similar to haloritids but have prominent spiral ornamentation and a more complex suture. The Sevatian ended with the most substantial extinction of Late Triassic ammonoids, discussed below.

7.6.5 Rhaetian Events

Heteromorph ammonoids are those that are uncoiled or that have helicoidal coiling. The oldest heteromorphs, the first experiment in ammonoid hetermorphy, are of late Norian age, marked by the first appearance of *Rhabdoceras* (Wiedmann 1973; Gradinaru and Sobolev 2010). The heteromorphs then underwent a modest evolutionary diversification during the Rhaetian of four genera: *Choristoceras*, *Cochloceras*, *Hannaoceras* and *Rhabdoceras*. They became extinct during the late Rhaetian.

The Late Triassic heteromorphs have generally been seen as a single clade (here the Choristoceratidae) united by their shared, simple suture pattern (Wiedmann 1973). The origin of the clade has been unclear to some (Tozer 1981a) or suggested to have been from the Thisbitidae (Kummel 1957) or from *Cycloceltites* (Guex 2001). The choristoceratids are evolute, becoming uncoiled or straight in the outer whorls with radial ribs on the whorl flanks and a very simple suture (Fig. 7.9).

The heteromorphs were broadly distributed across Late Triassic Tethys and along the Panthalassan margin (Wiedmann 1973; Gradinaru and Sobolev 2010). Some regard them as having been vagile epibenthos, evolving from planktonic to epibenthic scavengers and micropredators driven by the overall Rhaetian regression (Wiedmann 1973; Lehmann 1975; Laws 1978, 1982). This is best exemplified by what Laws termed the *Cochloceras* association in the Nun Mine Member of the Gabbs Formation in Nevada. Here, very small *Cochloceras* and *Rhabdoceras* are 87% of the invertebrate fossil assemblage and are readily seen as predators or scavengers in the benthic community.

The Rhaetian witnessed the extinction of the heteromorphs and of the other ceratitid ammonoids, as is discussed below.

7.7 Conclusion: Late Triassic Extinctions

Biostratigraphic recognition (and definition) of the Triassic-Jurassic boundary has long been based on a clear change in the ammonoid fauna from the diverse and ornamented ceratites and their peculiar heteromorphs of the Late Triassic to the less diverse and smooth psiloceratids of the Early Jurassic. In other words, this is the extinction of the Ceratitida followed by the diversification of the Ammonitida (e.g., House 1989). All workers agree that all but one lineage of ammonites (the Phylloceratina) became extinct by the end of the Triassic, and the subsequent Jurassic diversification of ammonites evolved primarily from that lineage (Guex

1982, 1987, 2001, 2006; Rakús 1993). The Early Jurassic encompasses a complex and rapid re-diversification of the ammonoids (e.g., Rakús 1993; Dommergues et al. 2001, 2002; Sandoval et al. 2001; Guex 2001, 2006).

As early as the work of Kummel (1957), House (1963) and Newell (1967), it was clear that the main extinction of Late Triassic ammonoids took place at the end of the Norian, not at the end of the Triassic. After that extinction, only a few ammonoid taxa remained--the heteromorphs, and some of the Arcestaceae and the Clydonictacea (Wiedmann 1973).

The Triassic ammonoid extinctions are the complete extinction of the Ceratitina before the end of the Rhaetian followed by the sudden appearance of the Ammonitina and Lytioceratina at the base of the Hettangian. However, the origin of these new groups had a long history. The Phylloceratida first appeared during the Early Triassic as generally discoidal, involute forms with gently inflated flanks and rounded venters that gave rise to all post-Rhaetian ammonoids. The details of the Late Triassic origin of the Ammonitina and Lytoceratina are presented by Wiedmann (1973, fig. 6) and Wiedmann and Kullman (1996).

House (1989: 78) considered the end-Triassic ammonoid extinction "the greatest in the history of the Ammonoidea." However, it has been clear for at least 40 years that the Late Triassic extinction of the ammonoids was a succession of diversity drops, with the last, most substantial drop at the end of the Norian, not at the end of the Triassic (Fig. 7.10) (e.g. Tanner et al. 2004). In other words, ammonoid extinction across the Triassic-Jurassic is best described as stepwise (Wiedmann and Kullman 1996).

Here, I use Tozer's (1981a, b) compilation to plot the diversity of Late Triassic ammonoid families and genera (Fig. 7.10). At the family level, his diversity data can be plotted at the Late Triassic substage level, but not all the generic data are reported at the substage level, so they are simply plotted here at the stage level. Tozer's (1981a, b) compilation is nearly 40 years old, but it is the most recent compilation of all Triassic ammonoid families and genera. Much work has been done on Early and Middle Triassic ammonoids since 1981, but much less study of Late Triassic ammonoids since then, and, in particular, the few new Late Triassic ammonoid taxa recognized since 1981, indicate that Tozer's compilation remains useful for examining compiled Late Triassic ammonoid diversity. The fact remains that Tozer's compiled data only permit stage-level resolution for generic diversity, and thus suffer from the compiled correlation effect (Lucas 1994) by indicating that the Late Triassic ammonoid extinctions are concentrated at stage boundaries (Fig. 7.10). Nevertheless, the earlier discussion and a consideration of the best sections for documenting end-Triassic ammonoid extinctions allow a more detailed understanding of the Late Triassic ammonoid extinctions than one based solely on the compiled diversity.

The compiled diversity numbers (Fig. 7.10) indicate that, after a Norian (moistly Alaunian) peak in diversity, the most substantial extinction of ammonoid families and genera took place across the Norian-Rhaetian boundary. The numbers based on Tozer (1981a, b) differ somewhat from some other compilations in the literature, but all show the same pattern. For example, Teichert (1988) listed more than 150 ammonite genera and subgenera during the Carnian, which was reduced to 90 in the Norian, and reduced again to 6 or 7 during the Rhaetian. Similarly, Kennedy (1977) stated there are 150 or so Carnian genera, less than 100 during the Norian, and the number of Rhaetian genera is in single figures.

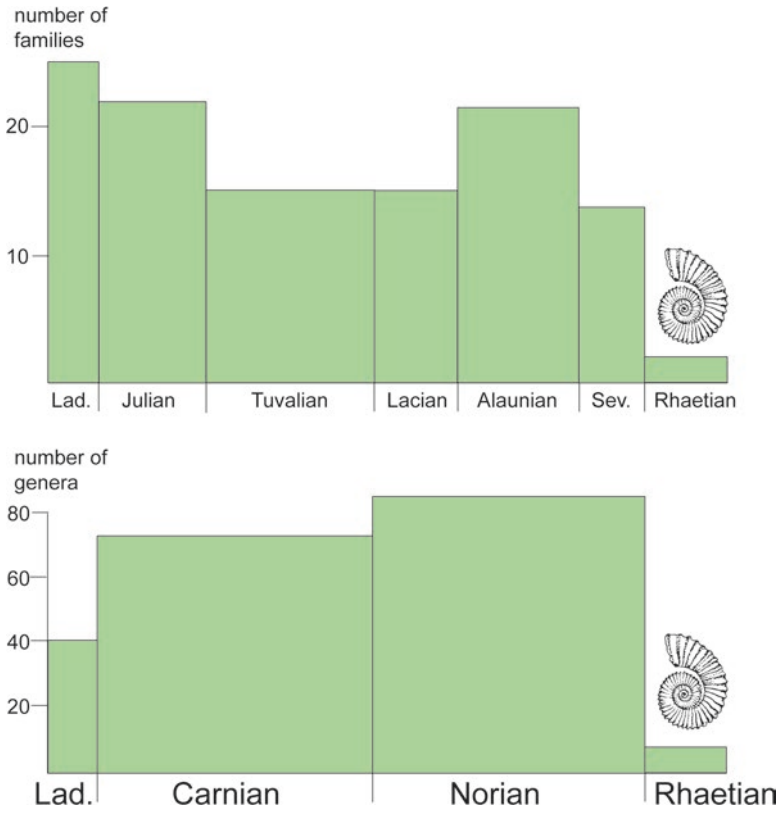

Fig. 7.10 Compiled family-level and genus-level diversity of Late Triassic ammonoids. Based on data in Tozer (1981a, b)

The most completely studied and ammonoid-rich section in the world that crosses the TJB is in the New York Canyon area of Nevada, USA (Fig. 7.11). Taylor et al. (2000, 2001), Guex et al. (2002, 2003) and Lucas et al. (2007) plotted ammonoid distribution in this section based on decades of collecting and study; of 11 Rhaetian species, seven extend to the upper Rhaetian, and only one is present at the stratigraphically highest Rhaetian ammonite level (Fig. 7.11). Taylor et al. (2000) presented a compelling conclusion from these data: a two-phase latest Triassic ammonoid extinction, one in the late Norian followed by a low diversity Rhaetian ammonoid fauna that became extinct by the end of the Triassic (also see Lucas and Tanner 2008).

Another detailed study of latest Triassic ammonoid distribution in a best section is in the Austrian Kössen Beds (Urlichs 1972; Mostler et al. 1978). The youngest Triassic zone here, the *marshi* zone, has three ammonoid species, two with single level records low in the zone, and only *Choristoceras marshi* is found throughout the zone. This, too, does not indicate a sudden end-Triassic mass extinction of ammonoids. However, note that Whiteside and Ward's (2011) compiled ammonoid

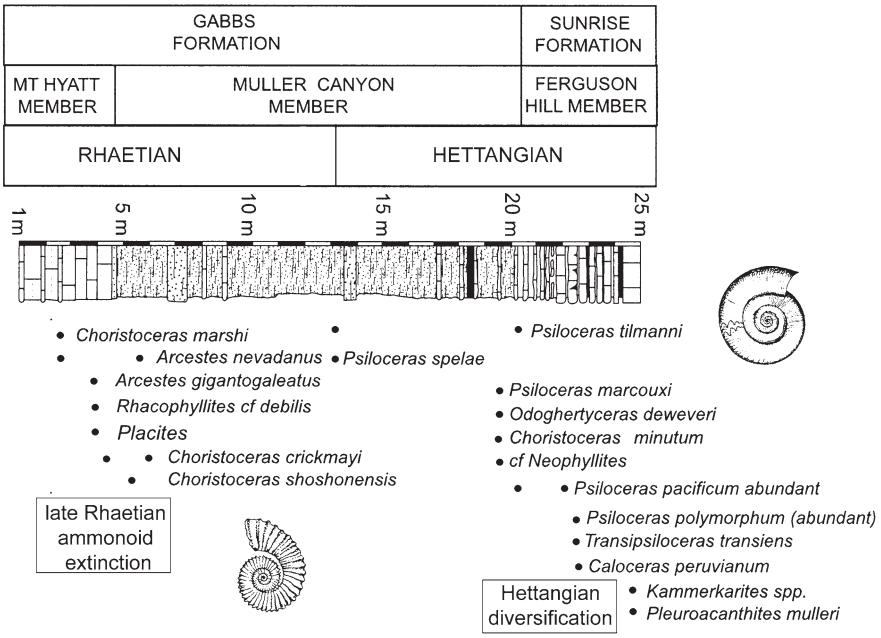

Fig. 7.11 Stratigraphic ranges of ammonoids across the Triassic-Jurassic boundary in the New York Canyon area of Nevada, USA (after Guex et al. 2004). Note the extinction of the low diversity Rhaetian ammonoid assemblage well before the end of the Rhaetian. The only Rhaetian ammonoid taxon to reach the base of the Jurassic is *Choristoceras marshi*

range data across the TJB look very different from these ammonoid ranges from best sections in Nevada and Austria, which suggests that the compiled data are not accurate.

Thus, the change in ammonoids across the Triassic-Jurassic boundary is profound, but both compiled data and actual stratigraphic ranges in best sections indicate it took place as a series of extinction events spread across Norian and Rhaetian time, not as a single mass extinction at the end of the Triassic.

The evolutionary turnover of ammonoids across the Triassic-Jurassic boundary is an important change from diverse and morphologically complex forms (including various heteromorphs) to less diverse and morphologically simple forms (the psiloceratids). Guex (2001, 2006) argued that this kind of morphological change occurred in response to environmental stress, as had occurred at several other crisis points in the history of the Ammonoidea. The Triassic-Jurassic transition was such a crisis in ammonoid history, but not a single mass extinction.

Acknowledgments Jim Jenks and an anonymous reviewer provided comments that improved the content and clarity of this article. Larry Tanner provided needed editorial oversight. I dedicate this paper to the memory of the late Norman Silberling, a good friend, a fine gentleman and one of the great students of the Triassic Ammonoidea.

References

von Alberti, F (1834) Beitrag zu einer Monographie des Bunten Sandsteins, Muschelkalks und Keupers, und die Verbindung dieser Gebilde zu einer Formation. Verlag der J. G. Cotta'sschen Buchhandlung, Stuttgart und Tübingen. [Facsimile reprinted in 1998 by the Friedrich von Alberti-Stiftung der Hohenloher Muschelkalkwerke, Ingelfingen, Germany]

Balini M (1992a) *Lardaroceras* gen. n., a new Late Anisian ammonoid genus from the Prezzo Limestone (Southern Alps). Riv Ital Paleontol Stratigr 98:3–27

Balini M (1992b) New genera of Anisian ammonoids from the Prezzo Limestone (Southern Alps). Atti Tic Scienze Terra 35:179–198

Balini M (1997) Taxonomy, stratigraphy and phylogeny of the new genus *Lanceoptychites* (Ammonoidea, Anisian). Riv Ital Paleontol Stratigr 104:143–166

Balini M (2008) Discovery of Upper Ladinian ammonoids at the type locality of the Lower Carnian Desatoyense Zone (South Canyon, New Pass Range, Nevada). J Paleontol 82:162–168

Balini M, Bertinelli A, Di Stefano P, Dumitrica P, Furin S, Gullo M, Guaiumi C, Hungerbuehler A, Levera M, Mazza M, McRoberts CA, Muttoni G, Nicora A, Preto N, Rigo M (2008) Integrated stratigraphy of the Norian GSSP candidate Pizzo Mondello section (Sicani Mountains, Sicily). Ber Geol Bundesanstalt 76:23–25

Balini M, Germani D, Nicora A, Rizzi E (2000) Ladinian/Carnian ammonoids and conodonts from the classic Schilpario-Pizzo Camino area (Lombardy): revaluation of the biostratigraphic support to chronostratigraphy and paleogeography. Riv Ital Paleontol Stratigr 106:19–58

Balini M, Jenks JF (2007) The Trachyeratidae from South Canyon (central Nevada): record, taxonomic problems and stratigraphic significance. N M Mus Nat Hist Sci Bull 41:14–23

Balini M, Jenks J, Martin R (2012) Taxonomy and stratigraphic significance of *Trachyceras silberlingi* n. sp., from the lower Carnian of South Canyon (New Pass Range, central Nevada, USA). Boll Soc Paleontol Ital 51:127–136

Balini M, Jenks JF, Martin R, McRoberts CA, Orchard MJ, Silberling NJ (2014) The Carnian/Norian boundary succession at Berlin-Ichthyosaur State Park (Upper Triassic, central Nevada, USA). Paläont Zeitschr 89:399–433

Balini M, Jenks JF, McRoberts CA, Orchard MJ (2007) The Ladinian-Carnian boundary succession at South Canyon (New Pass Range), central Nevada. N M Mus Nat Hist Sci Bull 40:127–138

Balini M, Krystyn L, Nicora A, Torti V (2001) The Ladinian/Carnian boundary succession in Spiti (Tethys Himalaya) and its bearing to the definition of the GSSP for the Carnian stage (Upper Triassic). J Asian Earth Sci 19:3–4

Balini M, Krystyn L, Torti V (1998) The Ladinian-Carnian boundary interval of Spiti (Tethys Himalaya). Albertiana 21:26–32

Balini M, Lucas SG, Jenks JF, Spielmann JA (2010) Triassic ammonoid biostratigraphy: an overview. In: Lucas SG (ed) The Triassic timescale. Geol Soc Lond Spec Publ 334:221–262

Brack P, Rieber H, Nicora A, Mundil R (2005) The global boundary stratotype section and point (GSSP) of the Ladinian Stage (Middle Triassic) at Bagolino (southern Alps, northern Italy) and its implications for the Triassic time scale. Episodes 28:233–244

Dagys AS (1988) Major features of the geographic differentiation of Triassic ammonoids. In: Wiedmann J, Kullmann J (eds) Cephalopods present and past. E. Schweizerbart'sche Verlagsbuchhandlung, Stuttgart, pp 341–349

Dagys A, Tozer ET (1989) Correlation of Triassic of northern Canada and Siberia. USSR Acad Sci Siber Br Inst Geol Geophys 1989(6):3–9

Dagys A, Weitschat W (1993) Correlation of the Boreal Triassic. Mitteil Paläont Inst Univ Hamburg 75:249–256

Diener C (1906) Fauna of the *Tropites*-Limestone of Byans. Mem Geol Surv India Palaeont Indica 15(5/1):1–201

Diener C (1908) Ladinic, Carnic, and Noric faunae of Spiti. Mem Geolog Surv India Palaeontol Indica 15(5/3):1–157

Diener C (1912) The Trias of the Himalayas. Mem Geol Surv India Palaeont Indica 36:1–176
Dommergues J-L, Laurin B, Meister C (2001) The recovery and radiation of Early Jurassic ammonoids: morphologic versus palaeobiogeographical patterns. Palaeogeogr Palaeoclimatol Palaeoecol 165:195–213
Dommergues J-L, Montuire S, Neige P (2002) Size patterns through time: the case of the Early Jurassic ammonite radiation. Paleobiology 28:423–434
Gaetani M (2009) GSSP of the Carnian Stage defined. Albertiana 37:36–38
Gemmellaro GG (1904) I Cefalopodi del Trias Superiore della Regione Occidentale della Sicilia. Gior Sci Natural Econom Palermo 24:319
Gradinaru E, Sobolev ES (2010) First record of *Rhabodoceras suessi* (Ammonoidea, Late Triassic) from the Transylvanian Triassic Series of the Eastern Carpathians (Romania) and a review of its biochronology, paleobiogeography and paleoecology. Cent Europ Geol 53:261–309
Guex J (1982) Relations entre le genre *Psiloceras* et les Phylloceratida au voisinage de la limite Trias-Jurassique. Bull Géol Lausanne 260:47–51
Guex J (1987) Sur la phylogenèse des ammonites du Lias inférieur. Bull Géol Lausanne 305:455–469
Guex J (2001) Environmental stress and atavism in ammonoid evolution. Eclog Geol Helvet 94:321–328
Guex J (2006) Reinitialization of evolutionary clocks during sublethal environmental stress in some invertebrates. Earth Planet Sci Lett 242:240–253
Guex J, Bartolini A, Atudorei V, Taylor D (2003) Two negative $\delta^{13}C_{org}$ excursions near the Triassic-Jurassic boundary in the New York Canyon area (Gabbs Valley Range, Nevada). Bull Géo Lausanne 360:1–4
Guex J, Bartolini A, Atudorei V, Taylor D (2004) High-resolution ammonite and carbon isotope stratigraphy across the Triassic-Jurassic boundary at New York Canyon (Nevada). Earth Planet Sci Lett 225:29–41
Guex J, Bartolini A, Taylor D (2002) Discovery of *Neophyllites* (Ammonita, Cephalopoda, early Hettangian) in the New York Canyon sections (Gabbs Valley Range, Nevada) and discussion of the $\delta^{13}C$ negative anomalies located around the Triassic-Jurassic boundary. Bull Soc Vaud Sci Natur 88(2):247–255
von Hauer FR (1849) Über neue Cephalopoden aus den Marmorschichten von Halstatt und Aussee. Haid Naturwiss Abhand 3:1–26
von Hauer FR (1850) Uber die Gliederung des Alpen-Kalks in den Ost-Alpen. Neues Jahrb 850:584
von Hillebrandt A, Krystyn L (2009) On the oldest Jurassic ammonites of Europe (Northern Calcareous Alps, Austria) and their global significance. Neues Jahrb Geol Paläont Abhand 253:163–195
von Hillebrandt A, Krystyn L, Kuerschner WM et al (2007) A candidate GSSP for the base of the Jurassic in the Northern Calcareous Alps (Kuhjoch section, Karwendel Mountains, Tyrol, Austria). Internat Subcomm Jurassic Strat Newsl 34:2–20
von Hillebrandt A, Krystyn L, Kürschner WM, Bonis NR, Ruhl M, Richoz S, Schobben MAN, Ulrichs M, Bown PR, Lment K, McRoberts CA, Simms M, Tomãsovýc A (2013) The global stratotype sections and point (GSSP) for the base of the Jurassic System at Kuhjoch (Karwendel Mountains, Northern Calcareous Alps, Tyrol, Austria). Episodes 36:162–198
House MR (1963) Burst in evolution. Adv Sci 19:499–507
House MR (1989) Ammonoid extinction events. Philos Trans R Soc Lond B 325:307–326
Hyatt A, Smith JP (1905) The Triassic cephalopod genera of America. US Geol Surv Prof Pap 40:1–394
Jenks JF, Monnet C, Balini M, Brayard A, Meier M (2015) Biostratigraphy of Triassic ammonoids. In Klug C et al (eds) Ammonoid paleobiology: from macroevolution to paleogeography. Top Geobiol 44:329–388
Jenks JF, Spielmann JA, Lucas SG (2007) Triassic ammonoids: a photographic journey. N M Mus Nat Hist Sci Bull 40:33–80

Johnston FN (1941) Trias at New Pass, Nevada (New Lower Karnic Ammonoids). J Paleontol 50:447–491
Keller WT (1928) Stratigraphische Beobachtungen in Sonora (Nordwest Mexico). Eclog Geol Helvet 21:327–335
Kennedy WJ (1977) Ammonite evolution. In: Hallam A (ed) Patterns of evolution as illustrated in the fossil record. Elsevier, Amsterdam, pp 251–304
Konstantinov AG (2012) A revision of the early Carnian Trachyceratidae (Ammonoidea) of northeastern Asia. Paleontol J 46:453–460
Konstantinov AG (2014) Zonal correlation and boundaries of the lower Carnian substage in northeastern Asia. Stratigr Geol Correl 22:190–201
Konstantinov AG, Klets TV (2009) Stage boundaries of the Triassic in northeast Asia. Stratigr Geol Correl 17:173–191
Konstantinov AG, Sobolev ES, Klets TV (2003) New data on fauna and biostratigraphy of Norian deposits in the Kotel'nyi Island (Bew Siberian Islands). Stratigr Geol Correl 11:231–243
Krystyn L (1973) Zur Ammoniten- und Conodonten-Stratigraphie der Hallstätter Obertrias (Salzkammergut, Österreich). Verh Geol Bundesanst 1:113–153
Krystyn L (1978) Eine neue Zonengliederung im alpin-mediterranean Unterkarn. In: Zapfe H (ed) Beiträge zur Biostratigraphie der Tethys-Trias. Schriften Erdwissen Kommiss Osterr Akad der Wissen 4:37–75
Krystyn L (1980) Stratigraphy of the Hallstatt region. Abhand Geol Bundesanstalt 35:69–98
Krystyn L (1982) Obertriassische Ammonoideen aus dem zentralnepalesischen Himalaya (Gebiet vom Jomsom). Abhand Geol Bundesanstalt 36:1–63
Krystyn L (1983) Das Epidauros-Profil (Griechenland)—ein Beitrag zur Conodonten-Standardzonierung des tethyalen Ladin und Unterkarn. In: Zapfe H (ed) Das Forschungsproject "Triassic on Tethys Realm" (IGCP Project 4). Schriften Erdwissen Kommiss Osterr Akad Wissen 5:231–258
Krystyn L (2008) The Hallstatt pelagics—Norian and Rhaetian Fossillagerstaetten of Hallstatt. Berichte Geol Bundesanstalt 76:81–98
Krystyn L (2010) Decision report on the defining event for the base of the Rhaetian stage. Albertiana 38:11–12
Krystyn L, Boquerel H, Kuerschner W, Richoz S, Gallet Y (2007) Proposal for a candidate GSSP for the base of the Rhaetian Stage. N M Mus Nat Hist Sci Bull 41:189–199
Krystyn L, Richoz S, Gallet Y, Bouquerel H, Kürschner WM, Spötl C (2007) Updated bio- and magnetostratigraphy from the Steinbergkogel (Austria), candidate GSSP for the base of the Rhaetian stage. Albertiana 36:164–173
Krystyn L, Schaffer G, Schlager W (1971) Der stratotypus des Nor. Ann Instit Geologici Publ Hungar 54:591–605
Krystyn L, Schlager W (1971) Der Stratotypus des Tuval. Ann Instit Geol Publ Hungar 54:591–605
Kummel B (1957) Triassic Ammonoidea. In: Arkell WJ, Furnish WM, Kummel B, Miller AK, Moore RC, Schindewolf O, Sylvester-Bradley PC, Wright CW (eds) Treatise on invertebrate paleontology, Part L, Mollusca 4, Cephalopoda. Geol Soc Amer. University of Kansas Press, Denver, University of Kansas
Laws RA (1978) Paleoecology of Late Triassic faunas from Mineral County, Nevada and Shasta County, California. MS thesis, University of California, Berkeley
Laws RA (1982) Late Triassic depositional environments and molluscan associatiosn from west-central Nevada. Palaeogeogr Palaeoclimatol Palaeoecol 37:131–148
Lehmann U (1975) Uber Nahrung und Ernahrungsweise von Ammoniten. Paläont Zeitsch 49:187–195
Longridge LM, Carter ES, Smith PL, Tipper HW (2007) Early Hettangian (Early Jurassic) ammonites and radiolarians from the Queen Charlotte Islands, British Columbia and their bearing on the definition of the Triassic-Jurassic boundary. Palaeogeogr Palaeoclimatol Palaeoecol 244:142–169
Lucas SG (1994) Triassic tetrapod extinctions and the compiled correlation effect. Can Soc Petrol Geol Mem 17:869–875
Lucas SG (2010) The Triassic chronostratigraphic scale: history and status. In: Lucas SG (ed) The Triassic timescale. Geol Soc Lond Spec Publ 334:17–39

Lucas SG (2013) A new Triassic timescale. N M Mus Nat Hist Sci Bull 61:366–374
Lucas SG, Cantrell AK, Suazo TL, Estep JW (2015) Carnian (Late Triassic) ammonoids from El Antimonio, Sonora, Mexico. N M Mus Nat Hist Sci Bull 67:189–203
Lucas SG, Estep JW (1999) Permian, Triassic, and Jurassic stratigraphy, biostratigraphy, and sequence stratigraphy in the Sierra del Alamo Muerto, Sonora, Mexico. Geol Soc Am Spec Pap 340:271–286
Lucas SG, Tanner LH (2008) Reexamination of the end-Triassic mass extinction. In: Elewa AMT (ed) Mass extinction. Springer Verlag, New York, pp 66–103
Lucas SG, Tanner LH, Kozur HW, Weems RE, Heckert AB (2012) The Late Triassic timescale: age and correlation of the Carnian-Norian boundary. Earth-Sci Rev 114:1–18
Lucas SG, Taylor DG, Guex J, Tanner LH, Krainer K (2007) The proposed global stratotype section and point for the base of the Jurassic System in the New York Canyon area, Nevada, USA. N M Mus Nat Hist Sci Bull 40:139–167
Lukeneder S, Lukeneder A (2014) A new ammonoid fauna from the Carnian (Upper Triassic) Kasimlar Formation of the Taurus Mountains (Anatolia, Turkey). Palaeontology 57:357–396
Mietto P, Andreetta R, Broglio Loriga C, Buratti N, Cirilli S, De Zanche V, Furin S, Gianolla P, Manfrin S, Muttoni G, Neri C, Nicora A, Posenato R, Preto N, Rigo M, Roghi G, Spötl C (2007) A candidate of the global stratotype section and point for the base of the Carnian Stage (FAD of *Daxatina*) in the Prati di Stuores/Stuores Wiesen section (southern Alps, NE Italy). Albertiana 16:78–97
Mietto P, Buratti N, Cirilli S, De Zanche V, Gianolla P, Manfrin S, Nicora A, Preto N, Rigo M, Roghi G (2007) New constraints for the Ladinian-Carnian boundary in the southern Alps: suggestions for global correlation. N M Mus Nat Hist Sci Bull 41:275–281
Mietto P, Manfrin S (1995) La successione delle faune ad ammonoidi al limite Ladinico-Carnico (Sudalpino, Italia). Ann Univer Ferr Sci Terra 5(supplement):13–35
Mietto P, Manfrin S, Preto N, Gianolla P (2008) Selected ammonoid fauna from Prati di Stuores/Stuores Wiesen and related sections across the Ladinian/Carnian boundary (Southern Alps, Italy). Riv Ital Paleontol Stratigr 114:377–429
Mietto P, Manfrin S, Preto N, Rigo M, Roghi G, Furin S, Gianolla P, Posenato R, Muttoni G, Nicora A, Buratti N, Cirilli S, Spitl C, Ramezani J, Bowring SA (2012) The global boundary stratotype section and point (GSSP) of the Carnian Stage (Late Triassic) at Prati di Stuores/Stuores Wiesen section (southern Alps, NE Italy). Episodes 35:414–430
Mojsisovics E (1869) Über die Gliederung der oberen Triasbildungen der östlichen Alpen. Jahrb Geol Reichsanstalt 24:91–150
Mojsisovics E (1873) Das Gebirge um Hallstatt. Th. 1. Die Mollusken-Faunen der Zlambach- und Hallstätter Schichten. Abhand Geol Reichsanstalt 6:1–82
Mojsisovics E (1874) Faunengebeite und Faciesgebilde der Trias-Periode in den Ost-Alpen—Eine stratigraphische studie. Jahrb Geol Reichsanstalt 24:81–134
Mojsisovics E (1875) Das Gebirge um Hallstatt, Theil I, Die Mollusken-Faunen der Zlambach- und Halstätter Schichten. Abhand Geol Reichsanstalt Wien 6:83–174
Mojsisovics E (1882a) Die Hallstätter Entwicklung der Trias. Sitzungsberi Akad Wissenschaft Wien, Mathem-naturwissen Klasse 101:769–780
Mojsisovics E (1882b) Die Cephalopoden der medterranean Triasprovinz. Abhand Geol Reichsanstalt 10:1–322
Mojsisovics E (1893) Die Cephalopoden der Halstätter Kalke. Abhand Geol Reichsanstalt 6:1–835
Mojsisovics E (1902) Die Cephalopoden der Hallstätter Kalke. Abhand Geol Reichsanstalt 6:175–356
Mojsisovics E, Waagen WH, Diener C (1895) Entwurf einer Gliederung der pelagischen sediments des Trias-systems. Sitzungsber Akad Wissen Wien Mathemat-naturwissen Klasse 104:1279–1302
Mostler H, Scheuring R, Urlichs M (1978) Zur Mega-, Mikrofauna und Mikroflora der Kossenen Schichten (alpine Obertrias) von Weissloferbach in Tirol unter besonderer Berucksichtigung der in der suessi- und marshi- Zone auftreitenden Conodonten. Osterr Akad Wissen Erdwissenschaft Komm Schriftenreihe 4:141–174
Newell ND (1967) Revolutions in the history of life. Geol Soc Am Spec Pap 89:63–92

Nicora A, Balini M, Bellanca A, Bertinelli A, Bowring SA, Di Stefano P, Dumitrica P, Guaiumi C, Gullo M, Hungerbuehler A, Levera M, Mazza M, McRoberts CA, Muttoni G, Preto N, Rigo M (2007) The Carnian/Norian boundary interval at Pizzo Mondello (Sicani Mountains, Sicily) and its bearing for the definition of the GSSP of the Norian Stage. Albertiana 36:102–115

Ogg JG (2012) Triassic. In: Gradstein FM, Ogg JG, Schmitz MD, Ogg GM (eds) The geologic time scale 2012. Elsevier, Amsterdam, pp 681–730

Ogg JG, Huang C, Hinnov L (2014) Triassic timescale status: a brief overview. Albertiana 41:3–30

Oppel A (1865) Über ostindische Fossilreste aus den sekundären Ablagerungen von Spiti und Gnari Khorsum in Tibet. Palaeont Mitteil Mus konig bayer Staat 1(4):267–304

Orchard MJ (2007) A proposed Carnian-Norian Boundary GSSP at Black Bear Ridge, northeast British Columbia, and a new conodont framework for the boundary interval. Albertiana 36:130–141

Orchard MJ (2014) Conodonts from the Carnian-Norian boundary (Upper Triassic) of Black Bear Ridge, northeastern British Columbia, Canada. N M Mus Nat Hist Sci Bull 64:1–139

Orchard MJ, Tozer ET (1997a) Triassic conodont biochronology and intercalibration with the Canadian ammonoid sequence. Albertiana 20:33–44

Orchard MJ, Tozer ET (1997b) Triassic conodont biochronology, its intercalibration with the ammonoid standard, and a biostratigraphic summary for the western Canada sedimentary basin. Canad Soc Petrol Geol Bull 45:675–692

Rakús M (1993) Late Triassic and Early Jurassic phylloceratids from the Salzkammergut (Northern Calcareous Alps). Jahrb Geol Bundes-Anstalt 136:933–963

Rieber H, Tozer ET (1986) Discovery of the original specimen of *Ammonites nodosa* Bruguière 1789, type species of *Ceratites* de Haan 1825 (Ammonoidea, Triassic). Eclog Geol Helvet 79:827–834

Rigo M, Bertinelli A, Concheri G, Gattolin G, Godfrey L, Katz ME, Maron M, Mietto P, Muttoni G, Sprovieri M, Stellin F, Zaffani M (2016) The Pignola-Abriola section (southern Appenines, Italy): a new GSSP candidate for the base of the Rhaetian Stage. Lethaia 49:287–306

Rosenberg G (1958) 50 Jahre nach Mojsisovics. Mitteil Geol Gesell Wien 50:293–314

Sandoval J, O'Dogherty L, Guex J (2001) Evolutionary rates of Jurassic ammonites in relation to sea-level fluctuations. PALAIOS 16:311–335

Silberling NJ (1956) "Trachyceras Zone" in the Upper Triassic of the western United States. J Paleontol 30:147–153

Silberling NJ (1959) Pre-Tertiary stratigraphy and Upper Triassic paleontology of the Union District Shoshone Mountains, Nevada. US Geol Surv Prof Pap 322:1–67

Silberling NJ, Tozer ET (1968) Biostratigraphic classification of the marine Triassic in North America. Geol Soc Am Spec Pap 110:1–63

Smith JP (1914) The Middle Triassic marine invertebrate faunas of North America. US Geol Surv Prof Pap 83:1–254

Smith JP (1927) Upper Triassic marine invertebrate faunas of North America. US Geol Surv Prof Pap 141:1–262

Smith JP (1932) Lower Triassic ammonoids of North America. US Geol Surv Prof Pap 167:1–199

Spath LF (1934) Catalogue of the fossil Cephalopoda in the British Museum (Natural History). Part IV The Ammonoidea of the Trias. The Trustees of the British Museum, London

Spath LF (1951) The Ammonoidea of the Trias (II). Catalogue of the fossil Cephalopoda in the British Museum (Natural History), Part V. The Trustees of the British Museum, London

Tanner LH, Lucas SG, Chapman MG (2004) Assessing the record and causes of Late Triassic extinctions. Earth Sci Rev 65:103–139

Taylor DG, Boelling K, Guex J (2000) The Triassic/Jurassic System boundary in the Gabbs Formation, Nevada. In: Hall RL, Smith PL (eds) Advances in Jurassic research 2000. Trans Tech Publications Ltd, Zurich, pp 225–236

Taylor DG, Guex J, Rakus M (2001) Hettangian and Sinemurian ammonoid zonation for the western Cordillera of North America. Bull Géol Univers Lausanne 350:381–421

Taylor DG, Smith PL, Laws RA, Guex J (1983) The stratigraphy and biofacies trends of the Lower Mesozoic Gabbs and Sunrise formations, west-central Nevada. Can J Earth Sci 20:1598–1608
Teichert C (1988) Crises in cephalopod evolution. In: Marois M (ed) L'évolution dans sa Réalité et ses Diverses Modalités. Fondation Singer-Polignac, Paris, pp 7–64
Tipper HW, Carter ES, Orchard MJ, Tozer ET (1994) The Triassic-Jurassic boundary in Queen Charlotte Islands, British Columbia. Geobios Mémo Spec 17:485–492
Tozer ET (1967) A standard for Triassic time. Geol Surv Canada Bull 156:1–103
Tozer ET (1971) Triassic time and ammonoids: problems and proposals. Can J Earth Sci 8:989–1031
Tozer ET (1974) Definitions and limits of Triassic stages and substages: suggestions prompted by comparisons between North America and the Alpine-Mediterranean region. Schriftenr Erdwissen Kommiss Osterr Akad Wissen 2:195–206
Tozer ET (1978) Review of the Lower Triassic ammonoid succession and its bearing on chronostratigraphic nomenclature. Schriftenr Erdwissen Kommiss Osterr Akad Wissen 4:21–36
Tozer ET (1980) Latest Triassic (upper Norian) ammonoid and *Monotis* faunas and correlations. Riv Ital Paleontol Stratigr 85:843–876
Tozer ET (1981a) Triassic Ammonoidea: classification, evolution and relationship with Permian and Jurassic forms. In: House MR, Senior JR (eds) The Ammonoidea. Systemat Assoc Spec Vol 18:69–100
Tozer ET (1981b) Triassic Ammonoidea: geographic and stratigraphic distribution. In: House MR, Senior JR (eds) The Ammonoidea. Systemat Assoc Spec 18: 397–431
Tozer ET (1983) Subcommission on Triassic Stratigraphy (STS) history 1968-1984. Albertiana 3:3–6
Tozer ET (1984) The Trias and its ammonoids: the evolution of a time scale. Geol Surv Canada Misc Report 35:1–171
Tozer ET (1994) Canadian Triassic ammonoid faunas. Geol Surv Canada Bull 467:1–663
Urlichs M (1972) Ostracoden aus den Kössener Schichten und ihre Abhängigkeit von der Ökologie. Mitteil Gesell Geol Bergbaustudent Österr 21:661–710
Wang YG, He GX (1976) Triassic ammonoids from the Mount Jolmo Lungma region. In: Xizang scientific expedition team of Chinese Academy of Sciences (ed) A report of the Scientific expedition in the Mount Jolmo Lungma region (1966–1968) Paleontology, vol 3 Science Press, Beijing
Weitschat W, Dagys AS (1989) Triassic biostratigraphy of Svalbard and a comparison with NE-Siberia. Mitteil Geol-Paläont Instit Univers Hamburg 68:179–213
Whiteside JH, Ward PD (2011) Ammonoid diversity and disparity track episodes of chaotic carbon cycling during the early Mesozoic. Geology 39:99–102
Wiedmann J (1973) Upper Triassic heteromorph ammonites. In: Hallam A (ed) Atlas of paleobiogeography. Elsevier, Amsterdam, pp 235–249
Wiedmann J. Kullman J (1996) Crises in ammonoid evolution. In: Landman N et al (eds) Ammonoid paleobiology. Topics in Geobiol 13:795–813
Zakharov YD (1997) Carnian and Norian sirenitid ammonoids of the north-western circum-Pacific and their role in the Late Triassic faunal succession. In: Baud A, Popova I, Dickins JM, Lucas S, Zakharov Y (eds) Late Paleozoic and early Mesozoic circum-Pacific events: biostratigraphy, tectonic and ore deposits of Primoryie (Far East Russia). Memior Geol Lausanne 30:137–144
Zapfe H (ed) (1983) Neue beiträge zur Biostratigraphie der Tethys-Trias. Schriftenr Erdwissenschaft Kommiss Osterreich Akad der Wissen 5:1–383
Zittel KA (1901) History of geology and palaeontology to the end of the nineteenth century. Walter Scott, London

Chapter 8
Late Triassic Marine Reptiles

Silvio Renesto and Fabio Marco Dalla Vecchia

Abstract During faunal recovery after the Permo-Triassic mass extinction (PTME), several tetrapod lineages independently evolved adaptations to marine life. Thus reptiles became significant elements of marine environments already at the beginning of the Mesozoic Era. The emergence of a diverse assemblage of marine reptiles in the Triassic marked the development of ecosystem complexity comparable with that of modern oceans. Different lineages (ichthyopterygians, sauropterygians and thalattosaurs) diversified quickly throughout the Middle Triassic and their disparity peaked during the late Anisian-early Carnian interval. Subsequently, both diversity and disparity underwent a substantial decrease during the Late Triassic. The last 'pachypleurosaur' and nothosauroid record is early Carnian in age; non-cyamodontoid placodonts were already extinct before the Carnian. Ichthyosaur diversity decreases from the Carnian to the Norian and reaches its minimum in the Rhaetian. Cyamodontoid placodonts are practically missing in the upper Carnian-middle Norian, to appear again in the upper Norian-Rhaetian with the single genus *Psephoderma*. The last record of the tanystropheid *Tanystropheus* is late Norian in age, and the range of the enigmatic *Pachystropheus* is possibly late Norian to early Rhaetian. Non-plesiosaurian sauropterygians, thalattosaurs, and non-parvipelvian ichthyosaurs were already extinct before the Triassic-Jurassic boundary. Pelagic forms, i.e. parvipelvian ichthyosaurs among ichthyosaurs and plesiosaurs among sauropterygians, which had appeared during the Late Triassic, crossed the Triassic-Jurassic boundary, giving rise to subsequent radiations in the Jurassic. Also, chelonians obviously crossed the boundary, while the earliest Jurassic reported record of phytosaurs needs to be confirmed.

Keywords Late Triassic • Marine reptiles • Diversity • Phylogeny • Evolution • Extinction

S. Renesto (✉)
DiSTA Dipartimento di Scienze Teoriche ed Applicate, Università degli Studi dell'Insubria, Via Dunant 3, I-21100 Varese, Italy
e-mail: silvio.renesto@uninsubria.it

F.M. Dalla Vecchia
Soprintendenza per i Beni Archeologici del Friuli Venezia Giulia, Nucleo Operativo di Udine, Via Zanon 22, I-33100 Udine, Italy

© Springer International Publishing AG 2018

L.H. Tanner (ed.), *The Late Triassic World*, Topics in Geobiology 46,
https://doi.org/10.1007/978-3-319-68009-5_8

8.1 Introduction

Reptiles did not play a major role in marine ecosystems until the Triassic Period of the Mesozoic Era. They began to colonize the seas during the faunal recovery subsequent to the Permo-Triassic mass extinction (PTME), when some diapsid lineages independently evolved adaptation to marine life (Benson et al. 2012). During the Triassic, marine reptiles reached a great taxonomic diversity (e.g. Rieppel 2000; McGowan and Motani 2003; Motani 2009), and often became the top predators in marine environments (Kelley and Pyenson 2015).

The radiation of Triassic marine reptiles filled trophic niches that had been left empty after the PTME or did not exist during the Paleozoic, thus producing a massive increase of ecomorphological diversity (Benton et al. 2013; Stubbs and Benton 2016). The first sauropterygians and ichthyopterygians are documented from the Lower Triassic (Maxwell and Kear 2013; Motani et al. 2015; Jiang et al. 2016); subsequently, both sauropterygians and ichthyopterygians, along with thalattosaurs, diversified in the early Middle Triassic (Anisian) and both their diversity and disparity increased rapidly during the Anisian–Ladinian interval. However, sauropterygians were fundamentally restricted to the Tethyan coastal areas, from the Western Europe and Northern Africa to China. Highly specialized taxa, like basal plesiosaurs, gigantic edentulous ichthyosaurs, cyamodontoid placodonts with a few very large crushing teeth or toothless, semi-durophagous thalattosaurs with a peculiar heterodont dentition, and turtles appeared in the early Carnian (although there is possible ichnological evidence of older turtles; von Lilienstern 1939; Lovelace and Lovelace 2012); while many ichthyosaur taxa, nothosaurs and pachypleurosaurs were apparently extinct. During the Carnian, both diversity and disparity of marine reptiles went through a substantial decrease with the extinction of the last non-plesiosaurian eosauropterygians. During the late Norian-Rhaetian interval, there were the last placodonts, thalattosaurs, tanystropheids, and non-parvipelvian ichthyosaurs. The disappearance of those taxa from the fossil record was apparently not linked to a mass extinction event at the Triassic-Jurassic boundary, as those last occurrences are apparently diluted in an interval spanning over 5 million years. Some authors hypothesized that the extinctions may have been related to sea level fluctuations causing widespread marine regressions during the Late Triassic (Kelley et al. 2014; Benson and Butler 2011 and references therein). However, this is not supported by the geology of the Alpine realm, for instance, where shallow water environments were widespread during the Norian-Rhaetian interval (e.g., Brandner and Poleschinski 1986; Furrer 1993; Jadoul et al. 1994). The pelagic ichthyosaurs independent from shallow marine habitats and plesiosaurs, crossed the Triassic-Jurassic boundary and appear to be rather differentiated already at the base of the Jurassic, to radiate later in the Jurassic and finally become extinct during the Late Cretaceous.

8.2 Ichthyopterygia

The Ichthyopterygia were the Mesozoic marine reptiles with the highest adaptation to an aquatic lifestyle. The oldest ichthyosaurs come from the Lower Triassic (Olenekian) of Svalbard, China, Thailand, Japan and Canada (Maxwell and Kear 2013). They are already taxonomically diversified and show a set of unique characters (e.g., very large eyes, elongate snout, "ash-tray" deeply amphicoelous vertebral centra, and limbs modified into flippers) that are correlated with a fully aquatic lifestyle. The evidence of viviparity is first reported for ichthyopterygians from the uppermost Anisian. With the possible exception of *Cartorhynhchus* (see Motani et al. 2015), which however is outside the Ichthyopterygia, being a basal ichthyosauriform, ichthyosaurs were in fact unable to move on land, even for reproduction, like cetaceans.

Major evolutionary trends in the evolution of the locomotor apparatus of the ichthyopterygians concern the limbs and the vertebral column (Motani 2005). The 'fin' skeleton increasingly modified into a mosaic of relatively short bones, with the shortening of the stylopodium, carpal and tarsal bones that are virtually undistinguishable from proximal phalanges, polyphalangy and polydactyly. The shortening and stiffening of the body and the appearance of a distinct tail bend in the vertebral column to support the ventral lobe of a semilunate tail fin probably marked the transition from an anguilliform (in the earliest forms) or sub-carangiform swimming mode to a thunniform swimming mode, which probably occurred during the Late Triassic.

The successful adaptation of the ichthyosaurs to the marine environment is testified by their cosmopolitan distribution in open marine deposits since the Middle Triassic.

Ichthyopterygian diversity peaked in the Middle Triassic, with piscivorous and durophagous forms with heterodont dentition. Another peak of diversity was reached in the Liassic, and then ichthyosaurs declined. Only the genus *Platypterygius* reached the Cenomanian (Late Cretaceous); ichthyosaurs become extinct before the end of the Cenomanian, about 93–94 million years ago.

Many phylogenetic hypotheses on ichthyopterygians have been proposed in the last two decades. The first were by Motani (1999), Sander (2000) and Maisch and Matzke (2000), followed by Maisch (2010); the most recent ones are by Motani et al. (2015) and Ji et al. (2016). The latter has been taken as reference for the present work (Fig. 8.1). According to the cladistic analyses by Sander (2000) and Ji et al. (2016), the Hupesuchia are the sister group of the Ichthyopterygia. According to Ji et al. (2016), the Ichthyopterygia comprise the basal *Chaohusaurus* followed along the spine by the Grippioidea and the more derived Ichthyosauria.

Among the Ichthyosauria, the Shastasauridae represent the sister group of all of the other ichthyosaurs, the Euichthyosauria. The Shastasauridae were a cosmopolitan group of medium-sized to very large long-snouted ichthyosaurs that probably fed on fishes, cephalopods and possibly also smaller marine reptiles. They range from the Anisian or possibly the uppermost Lower Triassic (Massare and Callaway

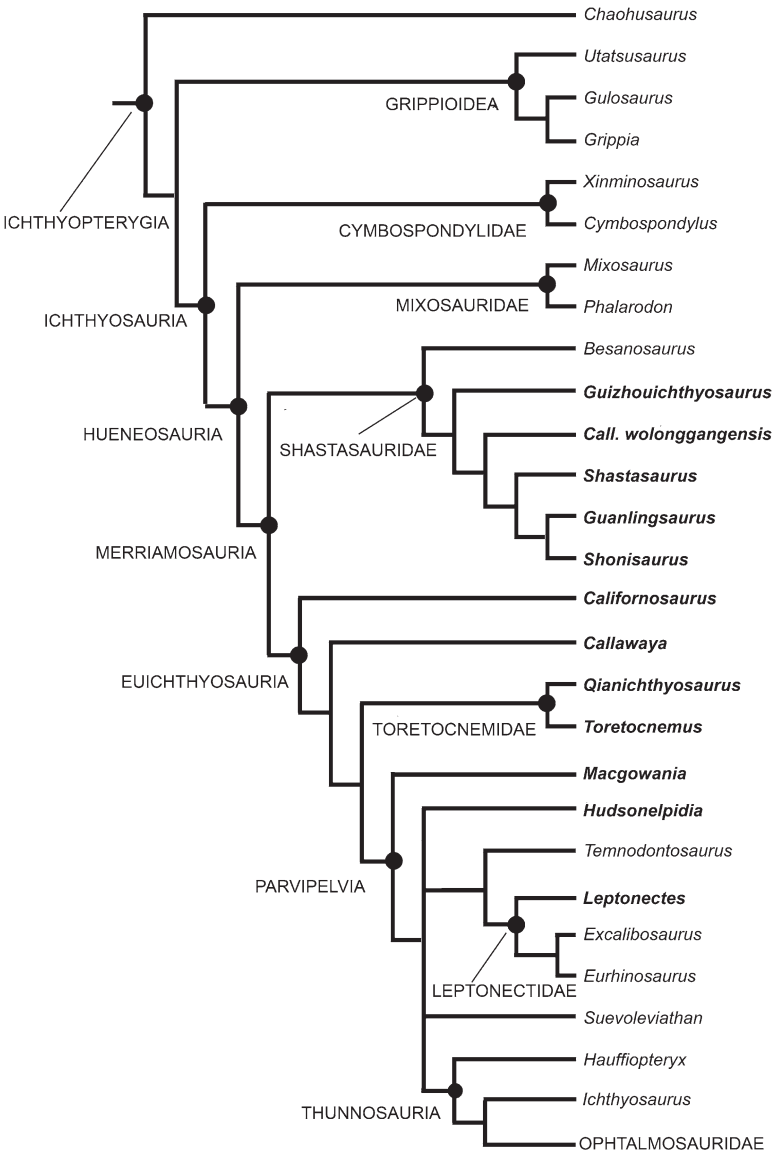

Fig. 8.1 Phylogenetic relationships among ichthyopterygian genera (strict consensus tree) from Ji et al. (2016), redrawn. Late Triassic genera are shown in *bold*

1990) to the lower Rhaetian, but they are basically a Late Triassic clade. Also, the basal euichthyosaurians *Californosaurus*, *Callawayia*, the Torectonemidae and the basal Parvipelvia *Macgowania* were Late Triassic in age, as well as *Hudsonelpidia* Finally, the more derived Triassic ichthyosaur appears to be the parvipelvian

Leptonectes, which is reported from the upper Norian or Rhaetian of England and Austria.

8.2.1 Late Triassic Shastasauridae

The Shastasauridae are represented by the genera *Besanosaurus*, *Guizhouichthyosaurus*, '*Callawayia*' *wolonggannggensis, Guanlingsaurus*, *Shastasaurus*, *Shonisaurus* and *Himalayasaurus*. Only *Besanosaurus* is an exclusively Middle Triassic taxon.

Guizhouichthyosaurus tangae Cao and Luo in Yin et al. (2000) from the lower Carnian Wayao Member of the Falang Formation of Guizhou, China (Zhou et al. 2015) is a fairly large ichthyosaur over 5 m long, with a robust and long rostrum (Fig. 8.2a).

Guanlingsaurus liangae Yin in Yin et al. (2000) is also from the Wayao Member of Guizhou Formation; it is a very large shastasaurid, reaching 11 m in length (Fig. 8.3). It has an extremely short and edentulous snout and narrow forelimbs with no more than three digits. Sander et al. (2011) suggested that *Guanlingsaurus* may be a junior synonym of *Shastasaurus*, but the genus is considered valid by Chen et al. (2013) and Ji et al. (2016).

'*Callawayia*' *wolonggangensis* Chen et al. 2007 (Fig. 8.2b), from the Carnian Xiaowa Formation of Guizhou, was originally referred to *Callawayia* because it was supposed to have a parietal shelf and a straight anterior margin of the scapula, which occur also in *Callawayia neoscapularis*. More recently, Ji et al. (2016) noticed that the anterior portion of the scapula of '*C.' wolonggangensis* is not complete, and the anterior striations of the same bone are radial instead of parallel to the margin, which is the condition observed in *Guizhouichthyosaurus* and *Shastasaurus*. In addition, Ji et al. (2016) stated that '*C.' wolonggangensis* actually lacks the diagnostic features of *C. neoscapularis* listed by Chen et al. (2007), such as the parietal shelf and the absence of a dorsal lamina in the maxilla. Finally, the topology of the cladogram by Ji et al. (2016) does not support the monophyly of *Callawayia*, '*C.*' *wolonggangensis* falling within the Shastasauridae.

The genus *Shastasaurus* was erected by Merriam, 1895 based upon a series of articulated vertebrae and associated ribs of a large-sized ichthyosaur from the Carnian of Shasta County, California. Merriam (1895, 1902) described a total of five *Shastasaurus* species from Shasta County: *S pacificus S. alexandrae S. altispinus*, *S. careyi* and *S. osmonti*. von Huene (1925) added a sixth species, *S. carinthiacus* based on some vertebrae and ribs from the Carnian of the Austrian Alps (see also Callaway and Massare 1989). However, the conclusions of McGowan's (1994) revision of *Shastasaurus* species was that most of the referred material was not diagnostic at the species level, only *S. pacificus* being valid among the Shasta County named species. *S. carinthiacus* was considered of dubious validity. McGowan (1994) erected also a new species, *S. neoscapularis,* based on a partial skeleton from the Norian of Williston Lake, British Columbia (Canada). This latter

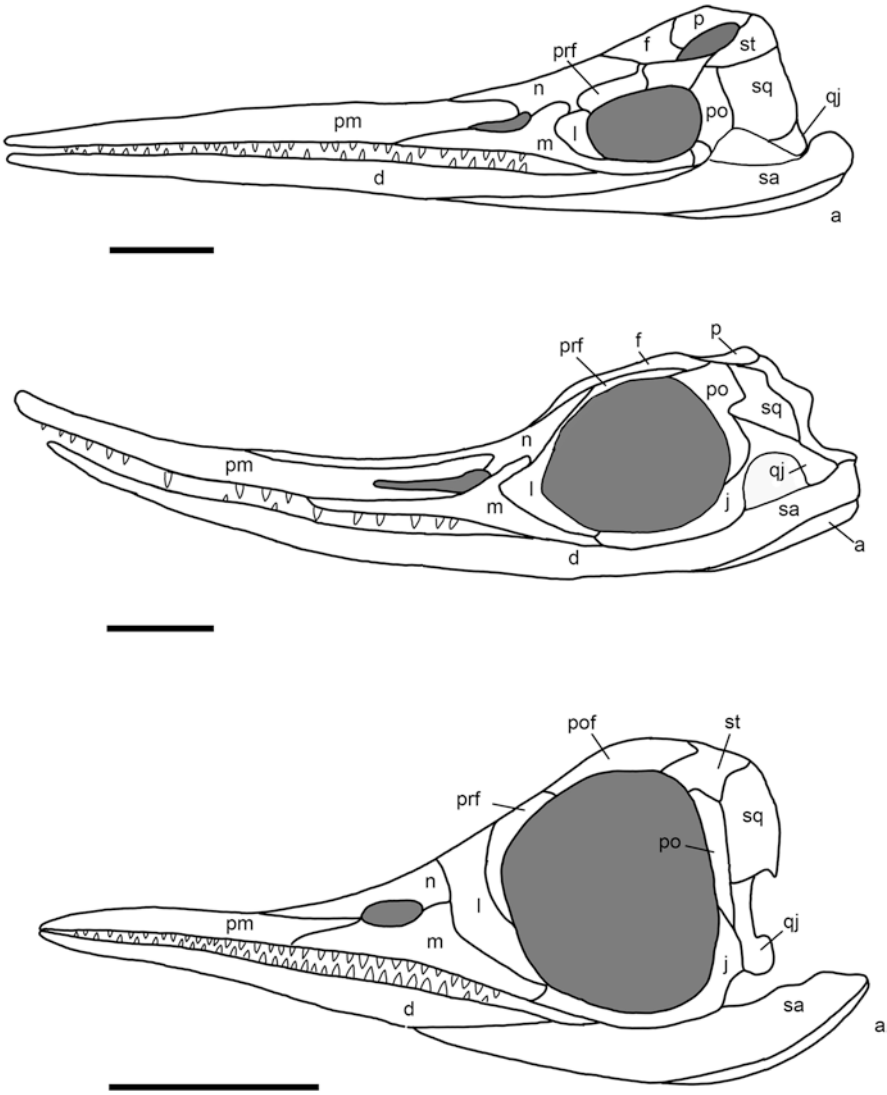

Fig. 8.2 Skulls of ichthyopterygians from the Carnian of Guizhou Province, China, in *lateral* view. (**a**) *Guizhouichthyosaurus tangae* (after Maisch et al. 2008, redrawn). (**b**) *Callawayia' wolonggangensis* (after Ji et al. 2016, redrawn). (**c**) *Qianichthyosaurus zhoui* (after Nicholls et al. 2003, redrawn) Abbreviations: *a* angular, *d* dentary, *f* frontal, *j* jugal, *l* lacrimal, *m* maxilla, *n* nasal, *p* parietal, *prf* prefrontal, *pm* premaxilla, *po* postorbital, *pof* postfrontal, *q* quadrate, *qj* quadratojugal, *sq* squamosal, *sa* surangular, *sp* splenial, *st* supratemporal. Scale bars equal 10 cm

Fig. 8.3 The ichthyosaur *Guanlingasurus liangae* from the Carnian of China. Scale bar equals 50 cm. From Sander et al. (2011), under CCBY2.5 http://www.plosone.org/article/info%3Adoi%2F10.1371%2Fjournal.pone.0019480

species was later assigned to the new genus *Callawayia* by Maisch and Matzke (2000), becoming *C. neoscapularis.* In conclusion, the genus *Shastasaurus* is unquestionably represented only by *S. pacificus* and is diagnosed by a narrow contact between the nasal and the postfrontal; an anteroposteriorly elongated orbit; narrow cheek; and presence of an anterior notch in the radiale.

Two species were named of the genus *Shonisaurus*: *S. popularis* Camp, 1976 and *S. sikanniensis* Nicholls and Manabe, 2004. *Shonisaurus* is known from the Carnian of Nevada (Camp 1980; McGowan and Motani 1999), New Caledonia (Mazin and Sander 1993) and possibly Mexico (Motani 1999); from the base of the upper Carnian of the Dolomites, Italy (Dalla Vecchia and Avanzini 2002); and from the Norian of British Columbia (McGowan 1997), Switzerland (Callaway and Massare 1989) and Germany (Karl et al. 2014).

Shonisaurus popularis reached a length of 15 m. The skull may have been up to 2 m long, with a very long rostrum and relatively large eyes. The postorbital region is dominated by a tall sagittal crest separating large temporal openings. Apparently, only juveniles bear teeth, which are low in number, large and conical and set in individual sockets. The rib articular facets on the dorsal vertebrae are similar to those of the large Jurassic *Temnodontosaurus* and *Leptonectes*. Some features of the appendicular skeleton such as the elongate and waisted scapula, the small T-shaped interclavicle, the very elongate fore- and hind fins resulting from strong hyperphalangy and the isometric and flattened proximal phalanges are also shared with some Jurassic taxa.

Shonisaurus sikanniensis from the Norian Pardonet Formation of northeastern British Columbia (Canada) is the largest ichthyopterygian species, possibly reaching 21 m in length (Nicholls and Manabe 2004). Sander et al. (2011) referred it to *Shastasaurus*, but recent works (e. g., Ji et al. 2016) kept the species in the genus *Shonisaurus*.

Shonisaurus (Fig. 8.4) was probably not as deep-bodied as previously reconstructed (Kosch 1990), and teeth were present only in small (supposedly juvenile) individuals, while larger (supposedly adult) specimens were probably edentulous like *Guanlingsaurus* (Sander et al. 2011). Some of the centra, at about the level of the 97th vertebra, are wedge-shaped, indicating a very slight tail bend.

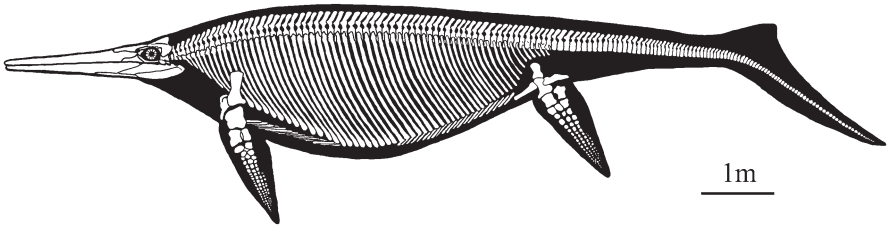

Fig. 8.4 Recostruction of *Shonisaurus popularis*. From Sanders (2000), redrawn

Himalayasaurus tibetensis Young and Dong (1972) was erected on the basis of jaw fragments from the Upper Triassic of Tibet and some probably associated postcranial material belonging to a very large ichthyosaur possibly exceeding 15 m in length. It was subsequently redescribed by Motani et al. (1999), who confirmed the shastasaurid affinity of the genus. Ji et al. (2016) do not include the genus in their phylogenetic analysis, although they apparently seem to consider it as a valid taxon (Ji et al. 2016, p.16). According to Motani et al. (1999), *H. tibetensis* is diagnosed by the presence of labiolingually flattened tooth crowns with distinct cutting-edges on the mesial and distal margins, a character indicating adaptation to feed on large preys that is shared only with the Anisian genus *Thalattoarchon* among Triassic ichthyosaurs.

8.2.2 Feeding Adaptations in the Shastasauridae

Nicholls and Manabe (2004) investigated the possible strategies of such a large and edentulous animal like *Shonisaurus.* They proposed that it may have been the ecological equivalent to the extant suction-feeding odontocetes, like the beaked whales. After the discovery of *Guanlingsaurus* from China and the reexamination of shastasaurid material from the western USA, Sander et al. (2011) suggested that a high diversity of large suction-feeding ichthyosaurs existed during the Late Triassic. However, Motani et al. (2013) questioned this hypothesis, stating that it had not been tested quantitatively. Motani et al. (2013) searched for evidence of four osteological features that are strictly related to suction feeding (hyoid corpus ossification/calcification, hyobranchial apparatus robustness, mandibular bluntness and mandibular pressure concentration index) in 18 species of Triassic and Early Jurassic ichthyosaurs, including the presumed suction feeders. The results of statistical comparisons between ichthyosaurs and extant sharks and marine mammals of known diets suggest that ichthyosaurs are not suction feeders because they lack features that occur in suction-feeders of both groups. For example, they lack an integration of the ossified corpus and cornua of the hyobranchial apparatus, their hyobranchial bones are significantly more slender than in suction feeders and the mandibles do not narrow rapidly to allow high suction pressure. In all these features, ichthyosaurs are instead comparable with ram-feeding sharks.

8.2.3 Late Triassic Euichthyosauria

As anticipated above, some Euichthyosauria lived during the Late Triassic together with the Shastasauridae: the basal genera *Californosaurus* and *Callawaya*, the Torectonemidae (*Toretocnemus* and *Qianichtyosaurus*), the basal parvipelvian *Macgowania*, the more derived *Hudsonelpidia* and possibly also *Leptonectes*.

Californosaurus perrini (Merriam 1902) from the Lower Hosselkus Limestone (Carnian) of California, reached 2–3 m in length, was the first ichthyosaur to develop a distinct downward bend in the tail; the phalanges were distinctly rounded and widely spaced, giving a more rounded shape to the flipper. The number of presacral vertebrae is fairly low (45–50) but vertebral centra are more elongate than in shastasaurids. *Californosaurus* is considered the basal most euichthyosaur in Ji et al. (2016) analysis.

Callawayia neoscapularis (McGowan 1994) from the Upper Triassic (Norian), Pardonet Formation, British Columbia, Canada is a small ichthyosaur, reaching about 2 m, in total length, the scapula has an elongated dorsomedial blade while anterior and posterior extensions are reduced, coracoids that met at a definite medial symphysis, clavicle very slender, humerus short, forefin is tridactyl.

Callawayia was once considered as belonging to the genus *Shastasaurus (S. neoscapularis* McGowan 1994). It was subsequently assigned to a new genus, *Callawayia,* by Maisch and Matzke (2000). It was considered as closely related with the Shastasauridae (e.g. Nicholls and Manabe 2001). Indeed, *Callawayia* shares a high presacral count of over 60 vertebrae with the shastasaurids and shows a similar forefin pattern. However, Ji et al. (2016) noticed that *Callawayia* has more derived cranial features than the Shastasauridae and its femur is more similar to that of *Toretocnemus*. In the phylogenetic analysis by Ji et al. (2016), *Callawaya* falls within the basal Euichthyosauria, between *Californosaurus* and the Torectonemidae (Fig. 8.1); this is also in accordance with its stratigraphic occurrence.

The poorly known genus *Toretocnemus* Merriam, 1902 is represented by a single species, *Toretocnemus californicus* Merriam, 1902 from the Carnian-Norian of the U.S.A and Mexico (Lucas 2002). It has tridactyl forefins and hind fins, and its pubis and ischium meet medially at a well-defined symphysis. *Qianichthyosaurus* Li 1999 is (Fig. 8.2c) is represented by two species, *Q. zhoui* Li 1999 and *Q. xingyiensis* Ji et al. (in Yang et al. 2013), from the Carnian Wayao Member of the Falang Formation of Guizhou, China. *Qianichthyosaurus* has a femur with a greatly expanded distal end, tridactyl forefins with one accessory digit, tetradactyl hind fins, and notching on both leading and trailing edges of the flippers (Nicholls et al. 2002).

Macgowania janiceps (McGowan 1996) from the Norian of British Columbia is the basalmost Parvipelvia (Fig. 8.1). It was initially described as a species of *Ichthyosaurus (I. janiceps*; McGowan 1996) and the oldest record of this genus, which is common in the Lower Jurassic of England. However, Motani (1999) noticed that although the constriction of its humerus is unremarkable as in *Ichthyosaurus*, the manus lacks digital bifurcations or accessory digits. Motani (1999) transferred *I. janiceps* to the new genus *Macgowania* because it shares no

apomorphies with *Ichthyosaurus* and it does not fall in the same clade as the other *Ichthyosaurus* species in his phylogenetic hypothesis, making *Ichthyosaurus* paraphyletic.

Another non-thunnosaurian parvipelvian is *Hudsonelpidia brevirostris* McGowan 1995, which has phylogenetic relationships with the other parvipelvians that are not resolved in Ji et al. (2016) analysis (Fig. 8.1). It is a small ichthyosaur from the Norian of British Columbia, with a short rostrum, high and narrow dorsal neural spines and several peculiar features in the pelvic elements and limb bone proportions.

The genus *Leptonectes* is a temnodontosauroid parvipelvian that ranges from the upper Rhaetian to the Pliensbachian of England, France, and Switzerland, according to Ji et al. (2016). It is represented by three species: the 'Rhaetian'-Sinemurian *L. tenuirostris* (Conybeare 1822), the Sinemurian *L. solei* (McGowan 1993) and the Pliensbachian *L. moorei* (McGowan and Milner 1999). The inclusion of *L. tenuirostris* in the Triassic is just a matter of establishing whether the Pre-*planonbis* beds of the Blue Lias of Street and nearby localities (Somerset, UK) are latest Triassic or earliest Jurassic in age. According to Benson et al. (2012), they are earliest Jurassic, while Ji et al. (2016) apparently consider them to be latest Triassic in age. Those beds contain derived ichthyosaurs of 'Jurassic-type' as well as plesiosaurs of 'Jurassic-type', but unfortunately they do not contain ammonoids. The Tr-J boundary is formally marked by the first appearance of the ammonite *Psiloceras spelae tirolicum* in the Kuhjoch Pass section of Austria (Hillebrandt et al. 2013); *Psiloceras spelae tirolicum* is supposed to appear before *P. planorbis* (Hillebrandt et al. 2013), so the Pre-*planorbis* beds of England could formally be Jurassic in age. An earliest Jurassic age of the Pre-*planorbis* beds is supported also by carbon and oxygen isotope stratigraphy (Korte et al. 2009; Lucas et al. 2011). However, a single *Leptonectes* humerus from the 'Rhaetian' (more probably Norian) Westbury Formation of Chipping Sodbury, Gloucestershire, England, was reported by Storrs (1999). Furthermore, a vertebral centrum from the upper Norian portion of the Kössen Beds near Vienna (Austria) was referred as *Leptopterygius* (= *Leptonectes*) sp. by Zapfe (1976), and two centra from the same formation of the Achental, Austria were described as similar to those of *Ichthyosaurus tenuirostris* (= *Leptonectes tenurostris*) by von Meyer (1856). If these referrals are correct, the genus occurs anyway in the Upper Triassic.

According to Ji et al. (2016), the basal thunnosaurian *Ichthyosaurus* also has an Upper Triassic record. However, the 'Triassic' specimens are also from the Blue Lias of Street and are most probably earliest Jurassic in age.

McGowan (1991) reported an isolated forelimb from the middle Norian of Williston Lake (British Columbia), that shows a typical 'Jurassic' structure in having a relatively elongate and wedged humerus, metacarpals and phalanges that are polygonal instead of discoidal and four main digits. On the basis of these features, McGowan (1991, p. 1559) concluded that the Williston Lake "forefin" was more similar to those of the Jurassic *Ichthyosaurus communis*, *Leptonectes tenuirostris* and *Stenopterygius quadriscissus* than to those of any Triassic taxa. This supports the hypothesis that the forelimbs had evolved to a more advanced structure, typical

of Jurassic taxa, already in the middle Norian, so the transition toward the 'Jurassic bauplan' may have occurred well before the end of the Triassic.

8.2.4 *Problematical or Invalid Ichthyosaurian Taxa from the Upper Triassic*

Yin et al. (2000), Li and You (2002) and Chen and Cheng (2003) erected several ichthyosaur genera and species based on specimens from the upper Carnian Wayao Member of the Falang Formation, Guanling, China, whose validity has subsequently been questioned. Some of these taxa were considered as junior synonyms of already named taxa. Li and You (2002) described two isolated skulls as a new species of *Cymbospondylus*, *C. asiaticus,* which would be the only Late Triassic species of *Cymbospondylus*, a genus that is otherwise known only from the Middle Triassic of Europe and North America (Merriam 1908; Sander 1989; Maisch and Matzke 2004, see also Balini and Renesto 2012). Yu (in Yin et al. 2000) erected *Typicusichthyosaurus tsaihuae* on the basis of a rather complete, but not very well-preserved, skeleton. Chen and Cheng (2003) described *Panjiangsaurus epicharis* based on a complete skeleton and a skull with an associated forefin.

However, Ji et al. (2016) stated that the skull material attributed to *Cymbospondylus asiaticus* shows none of the diagnostic characters of the genus *Cymbospondylus,* while it closely resembles *Guizhouichthyosaurus tangae*. They also noticed that the shape of the flippers of *Typicusichthyosaurus*, which supposedly distinguishes this genus from *Guizhouichthyosaurus* and *Guanlingsaurus*, is affected by preparation, thus it is not a valid diagnostic feature. In addition, the small head and the very high presacral vertebral count suggest that the specimen on which *Typicusichthyosaurus* is based actually belongs to *Guanlingsaurus* or to a closely related taxon. Ji et al. (2016) also suggested that *Pangjiangsaurus epicharis* is a junior synonym of *Guizhouichthyosaurus tangae*.

8.3 Sauropterygia

Sauropterygia is the most diverse clade of Mesozoic marine reptiles. Sauropterygians appeared during the Early Triassic and became extinct at the end of the Late Cretaceous. The Sauropterygia were divided into the Placodontia and the Eosauropterygia by Rieppel (1994, 2000). Eosauropterygia included the Pachypleurosauria and the Eusauropterygia, which in turn were divided into the Nothosauroidea and the Pistosauroidea (these latter including the Plesiosauria) (Rieppel 1994, 2000; Liu et al. 2011). However, some recent phylogenetic analyses (e.g. Wu et al. 2011; Ma et al. 2015), did not find support for the clade Pachypleurosauria. The inclusion of several new taxa from the Triassic of China

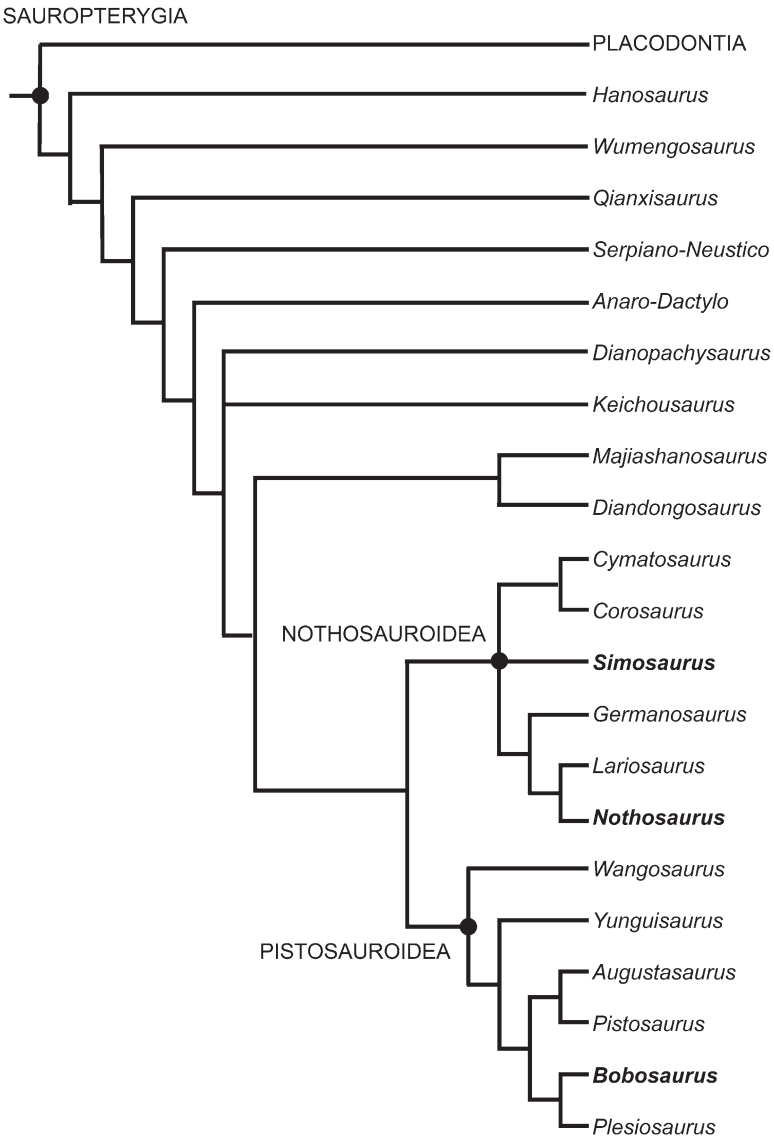

Fig. 8.5 Phylogenetic relationships among Sauropterygians (strict consensus tree), from Ma et al. (2015), redrawn. Late Triassic genera are shown in *bold*

caused the collapse of this clade, and the taxa previously included in the Pachypleurosauria were found to be scattered in the pectinate basal part of the eosauropterygian tree (Fig. 8.5). According to Wu et al. (2011) and Ma et al. (2015), Sauropterygia includes the Placodontia and the Eosauropterygia, the latter containing the "pachypleurosaur-grade" taxa, the Nothosauroidea and the Pistosauroidea.

Other recent phylogenetic hypotheses including partly or all of the sauropterygian taxa and obtaining discordant results have been published by Lee (2013), and Neenan et al. (2013). In this chapter, we follow the phylogenetic hypothesis by Ma et al. (2015), where Sauropterygia is retained (unlike Lee 2013), but "Pachypleurosauria" is considered to be a grade rather than a clade (Fig. 8.5).

Many different ecomorphological adaptations evolved within the Sauropterygia. "Placodonts were durophagous reptiles, with a stout skull and large, plate-like teeth (Fig. 8.6). The paraphyletic 'placodontoids' had a superficial similarity with the living marine iguana, while the armoured cyamodontoids were turtle-like and not adapted to efficient rapid swimming in open waters".

The 'Pachypleurosauria' were characterized by a lizard-like appearance (Fig. 8.7), with a moderately elongate neck, a relatively reduced size (maximum length was about 1.5 m) and a proportionally smaller skull with respect to the eusauropterygians (Rieppel 2000). They mainly employed lateral undulation for propulsion, were confined to coastal environments and probably fed upon small prey, possibly performing suction feeding (Rieppel 2002a). They are mainly known from the Middle Triassic intraplatform basins and shallow epicontinental seas of Europe and China. The oldest basal eosauropterygians come from the Lower Triassic of China (Jiang et al. 2014).

The nothosauroids have a dorsally flattened skull with a postorbital region that is longer than the preorbital one, anteroposteriorly elongate temporal fenestrae and, in most cases, also strongly procumbent premaxillary and dentary teeth suggesting a mainly piscivorous diet. The robust forelimbs (with enlarged and flattened ulna, at least in *Lariosaurus*) suggest that they may have played a major propulsive role replacing lateral undulation in larger taxa. However, their manus and pes do not show any particular adaptation to swimming. In some nothosauroid taxa, neural spines were very high, and additional articulations (zygosphene-zyganthrum) were present, stiffening the trunk. The lifestyle of those sauropterygians may have been similar to that of extant seals or sea lions. Some reached very large sizes (*Nothosaurus giganteus* and *Nothosaurus zhangi* reached over 4.5 m in length). The nothosauroids are mostly known from the Middle Triassic of Europe, North Africa, Israel, Saudi Arabia and China; *Corosaurus* comes from the Lower Triassic (Olenekian) of Wyoming, USA and *Simosaurus* and *Nothosaurus* are reported from the lower Carnian.

During the Middle to Late Triassic, the morphological features that allowed paraxial locomotion, a pelagic life style and a cosmopolitan distribution of the plesiosaurs later in the Jurassic, evolved within the pistosauroids. In the Plesiosauria, the trunk was stiffened, the tail was reduced, the fore and hind-flippers were robust and morphologically nearly identical, and the girdles were broad and plate-like. These improvements allowed a more efficient and continuous paraxial swimming. Together with a possibly higher metabolic rate (Lécuyer et al. 2010; Krahl et al. 2013), these features allowed them to colonize the open sea.

Late Triassic sauropterygians are known from several localities in Europe (e.g., Benton and Spencer 1995; Rieppel 2000; Albers and Rieppel 2003), a few in the

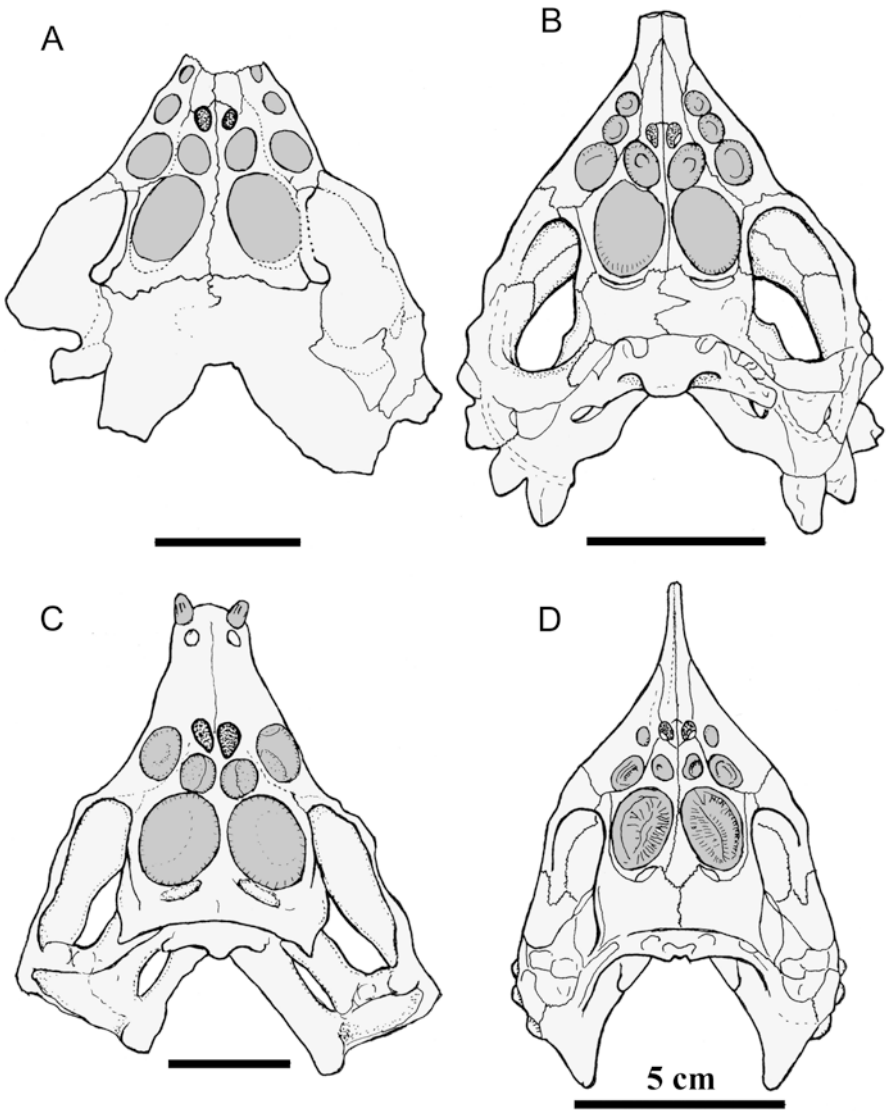

Fig. 8.6 Placodont skulls in palatal view. (**a**) ?*Cyamodus* from Fusea (MFSN 26830). (**b**) *Placochelys placodonta.* (**c**) *Protenodontosaurus italicus*; holotype (MFSN 1819). (**d**) *Psephoderma*. From Dalla Vecchia (1994), modified

Middle East and North Africa (Rieppel 1997; Rieppel et al. 1997), China (e.g., Holmes et al. 2008; Liu et al. 2011), and a couple in the USA (Storrs 1991; Sander et al. 1997). Early Carnian sauropterygians are represented by cyamodontoid placodonts, the last 'pachypleurosaurs', the last nothosauroids and the first plesiosaurs, which are the most derived Pistosauroidea. *Bobosaurus forojuliensis* from the lower

Fig. 8.7 The 'pachypleurosaur' *Keichousaurus*, from the Anisian of China. Length about 20 cm

Carnian of Italy is the oldest and most primitive plesiosaur, according to Fabbri et al. (2014), Liu et al. (2015) and Ma et al. (2015), while it is the sister taxon of the Plesiosauria for Benson et al. (2012). A wide gap exists in the eosauropterygian fossil record, spanning the upper Carnian and most of the Norian (an interval of over 20 million years). The only exception is the purported elasmosaurid plesiosaur *Alexeyisaurus karnoushenkoi* from the lower-middle Norian of Russia (Sennikov and Arkhangelsky 2010). Placodonts appear again in the uppermost middle Norian-Rhaetian of the Alpine Region and Western Europe. Scattered remains from the 'Rhaetian' of England, France and Germany are referred to plesiosaurs. Plesiosaur are well-preserved, relatively abundant and diversified in the Pre-*planorbis* beds of Street and nearby localities of England, which, however, are most probably of earliest Jurassic age (as reported above in the section about the ichthyosaurs). They radiated rapidly during the Early Jurassic and became cosmopolitan later in the Jurassic and Cretaceous, with a great diversity.

8.3.1 Placodontia

The oldest placodonts are reported from the lower Anisian (Middle Triassic; about 245 million years ago). The group diversified significantly during the Middle Triassic (Peyer 1931; Pinna 1990a; Pinna and Mazin 1993; Rieppel 2000). The last record is represented by isolated remains of *Psephoderma alpinum* from the Fissure Infillings at the Holwell locality near Bristol, UK, which Whiteside et al. (2016) tentatively dated to the Rhaetian (however, the traditional 'Rhaetian' of UK workers probably does not correspond exactly with the Alpine Rhaetian and the formal definition of this Stage).

The main feature of the placodonts, from which the clade got its name, is the highly specialised crushing dentition, which is composed of broad, plate-like teeth located on the jaw margins and on the enlarged palatine bones as well (Mazin and

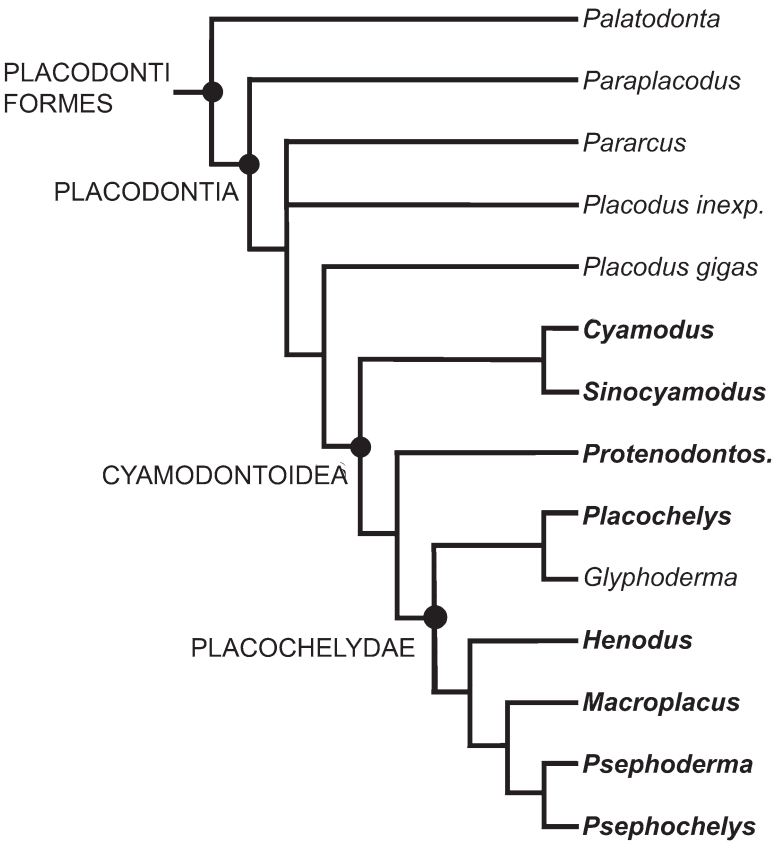

Fig. 8.8 Phylogenetic relationships among Placodonts (strict consensus tree), from Neenan et al. (2015), redrawn. Late Triassic genera are shown in *bold*

Pinna 1993; Rieppel 2001; Fig. 8.6). Placodont skull morphologies range from box-shaped and stout, bearing anterior chisel-like grasping teeth to wide and flattened with elongate narrow rostra (Mazin and Pinna 1993; Rieppel and Zanon 1997; Rieppel 2000). Most placodonts had a durophagous diet, a singular exception being the highly derived *Henodus*, which may have been either a filter feeder (sieving food with baleen-like structures) and/or a grazer (Rieppel 2002a).

Following the recent phylogenetic analysis by Neenan et al. (2015; Fig. 8.8), the Placodontia include *Paraplacodus* and *Placodus* (the armourless taxa, which were grouped in the Suborder Placodontoidea by Rieppel 2000) and the more derived Cyamodontoidea. The latter include the Cyamodontidae (*Cyamodus* + *Sinocyamodus*) as the basal clade, followed along the spine by *Protenodontosaurus* and the Placochelyidae, the latter comprising *Placochelys, Glyphoderma, Henodus, Macroplacus, Psephoderma* and *Psephochelys*. However, that analysis does not include all the Chinese taxa.

'Placodontoids' were rather slow, tail-propelled and undulatory swimmers. The Cyamodontoidea is a monophyletic group (but not in Ma et al. 2015 analysis) that is characterized by the possession of a dorsal armour protecting the trunk, which was formed by the fusion of small osteoderms during growth (Westphal 1975, 1976; Rieppel 2002b; Scheyer 2007). The dorsal armour usually consists of a dorsal thoracal shield; some taxa also have a smaller shield covering the base of the tail (Pinna 1980; Pinna and Nosotti 1989) or, according to Scheyer (2010), the pelvic area. Cyamodontoideans are also characterized by a dorsoventrally flattened skull with a premaxillary rostrum. The latter bears a few blunt teeth in basal taxa, while it is narrower, more elongate and edentulous in more derived taxa (with the exception of *Henodus*, which has a short and widely squared snout). The number of maxillary and palatine teeth for each side vary from five to one and from three to two, respectively. The upper temporal fenestrae are large to house the powerful jaw adductor muscles. The lower jaw shows a very high coronoid process, providing an extensive area for jaw adductor muscles; the mandibular symphysis is elongate, matching the premaxillary rostrum. Despite the superficial similarity with that of turtles, the placodont carapace is structurally different and it is not fused to the endoskeleton (Gregory 1946), just leaning on the vertebrae that have long transverse processes.

Placodonts were believed to have been restricted to the coasts of the western Paleotethys, i. e. to the epicontinental seas of Central Europe and Alpine domains (Brotzen 1956; Haas 1969; Pinna 1990a; Rieppel and Hagdorn 1997). In the last two decades, discoveries of placodonts from China extended their distribution to the eastern Tethyan faunal province, with four new species: *Sinocyamodus xinpuensis* (see Li 2000); *Psephochelys polyosteoderma* (see Li and Rieppel 2002); *Placodus inexpectatus* (see Jiang et al. 2008), and *Glyphoderma kangi* (see Zhao et al. 2008).

It has been suggested that placodonts initially evolved in the eastern Paleotethys and then moved westwards (Rieppel and Hagdorn 1997; Rieppel 1999a); however, Neenan et al. (2013) have recently proposed a western (European) origin.

8.3.1.1 Late Triassic Placodonts

All Late Triassic placodonts belong to the Cyamodontoidea. Rieppel and Nosotti (2002) ascribed to *Cyamodus* (a genus otherwise reported from the Middle Triassic) a skull (Fig. 8.6a) from the uppermost Ladinian or basal Carnian (Dalla Vecchia and Carnevale 2011) of Fusea (Friuli, northeastern Italy) that had previously been assigned to *Placochelys placodonta* (see Pinna and Zucchi Stolfa 1979). The poor preservation, however, prevented the erection of a new species. Abundant armour remains and a few postcranial elements from the same site and horizon and plausibly from the same species, have been reported by Rieppel and Dalla Vecchia (2001) and Dalla Vecchia (2008a).

Sinocyamodus xinpuensis Li 2000 is the first placodont discovered in China (Fig. 8.9). It was collected in the lower Carnian Wayao Member of the Falang Formation of Xinpu, Guizhou Province. It is a relatively small placodont, with elongate orbits, a short rostrum and the premaxilla bearing three bulbous teeth. The

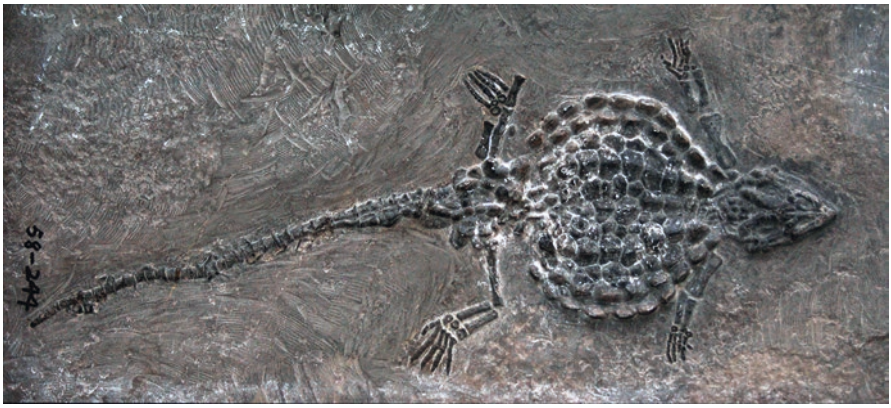

Fig. 8.9 The placodont *Sinocyamodus xinpuensis* from the lower Carnian of China. Total length is about 50 cm. Author: Bruce McAdam; CCBY-SA2.0 https://en.wikipedia.org/wiki/Sinocyamodus#/media/File:Armoured_reptile.jpg

dorsal armour has a subcircular outline and is made of quite large osteoderms. According to Li (2000), pectoral and pelvic girdles are not covered by the armour; isolated osteoderms occur on the limbs, and there is also a dorsal row of osteoderms along most of the tail.

Protenodontosaurus italicus Pinna 1990a, b is known by two skulls from the lower Carnian of Dogna, Friuli, northeastern Italy (Fig. 8.6c). Also, armour fragments and isolated teeth from the same horizon (Rio del Lago Formation) and area probably belong to this taxon (Pinna 1990b; Dalla Vecchia 2008a). This taxon is characterized by the possession of a single posterior maxillary tooth, which is separated by a wide diastema from the premaxillary tooth; maxilla as high as it is long due to the presence of a wide ascending process; prefrontal not extending far down along the anterior margin of the orbit; orbital margin of frontal rather straight; postorbital not extending beyond the midpoint of the upper temporal fenestra along its lateral margins; and vomers much enlarged and reaching far anteriorly into the rostrum (Rieppel 2000).

Placochelys placodonta Jaekel 1902 is known from two skulls, one associated with remains of the postcranial skeleton, from the Carnian (probably lower Carnian) of the Bakony Hills, Hungary (Jaekel 1907; Rieppel 2001). Part of the postcranial remains was lost during World War II (Westphal 1975; Rieppel 2001). *Placochelys* has a flattened skull (Fig. 10.6b) with a triangular outline in dorsoventral view and a short, narrow snout with edentulous premaxillae. It shows diagnostic features in the skull bones, but some are shared with other cyamodontoids (Rieppel 2001). The upper dentition consists of three maxillary teeth and two teeth of different size on the palatine. The carapace is incompletely known; it was made of small, scale-like osteoderms with longitudinal rows of much larger, conical and low osteoderms.

Macroplacus rhaeticus Schubert-Klempnauer 1975 is represented by a nearly complete skull from an unknown level within the Kössen Formation (upper

Norian-Rhaetian p.p.) of the Bavarian Alps (Germany). It is diagnosed by the presence of hypertrophied posterior palatine teeth, posterior processes of the premaxillae that are enlarged and extend backwards reaching the frontals, thus separating the nasals from each other (convergent in *Psephoderma*) and greatly reduced posttemporal fossae. Pinna (1990a) considered *Macroplacus* as a junior synonym of *Psephoderma* and proposed to rename it as *Psephoderma rhaeticus.* However, Rieppel (2000) supported the validity of the genus on the basis of the presence of diagnostic characters and the results of his cladistic analysis; the topology of the tree by Neenan et al. (2015; Fig. 8.8) also supports this result.

Psephoderma alpinum von Meyer 1858 (Fig. 8.6d) has a flattened skull with a triangular outline in dorsoventral view and a very narrow, elongate and edentulous rostrum, presumably used for probing soft sediments for shelled mollusks and other prey items (Mazin and Pinna 1993; Rieppel 2002a). It is mostly reported from the uppermost middle Norian-lower Rhaetian of the Alpine region (e.g., Rieppel 2000, 2001; Neenan and Scheyer 2014); fragments of placodont armour and isolated teeth from the 'Rhaetian' Fissure infillings of United Kingdom have been referred to *Psephoderma* (*Psephoderma anglicum*; von Meyer 1867; Whiteside et al. 2016). It is diagnosed by squamosals projecting far posteriorly; upper temporal fenestra relatively narrow; nasal process of the premaxilla reaching the frontals; frontal reaching the anterior margin of the pineal foramen; and palatine tooth plates that are elongate in adults. Thanks to the finding of complete and articulated specimens from the middle-upper Norian of northern Italy, *Psephoderma* is one of the best known placodonts. Its osteology has been described in detail by Pinna (1976, 1978) and Pinna and Nosotti (1989). Studies on its armour were published by Westphal (1976), and its palaeoecology has been discussed by Mazin and Pinna (1993). *Psephoderma alpinum* is a fairly large placodont, the longest complete specimen being 1.8 m in total length (Renesto and Tintori 1995), but isolated teeth suggest that it may have reached even larger sizes. The rostrum is more elongate than in *Placochelys* and the maxillae are well-developed, forming part of the anterior margin of the nasal openings. Two flat crushing teeth are present on both maxilla and palatine; the posterior palatine teeth are enormously developed. The postcranial skeleton consists of 5 cervical, 15 dorsal, 3 sacral and up to 30 caudal vertebrae. The hind limb is oar-shaped, with rounded terminal phalanges that were presumably clawless. The dorsal armor consists of a flattened, rounded carapace and of a smaller posterior plate, both bearing three longitudinal ridges formed by keeled osteoderms; the tail also bears a median row of osteoderms. *Psephoderma* is usually reconstructed with a rather dorsoventrally flattened body, giving it a ray-like appearance. Renesto and Tintori (1995) noticed a strong positive allometry in the hind limbs during growth (Fig. 8.10), suggesting that they may have played a major role in aquatic locomotion.

The study of the complete specimens of *Psephoderma* allowed also recognition that several placodont species erected on the basis of isolated skulls or other fragmentary remains from the upper Norian-Rhaetian (*Placochelyanus stoppanii*, *Placochelys malanchinii*, *Placochelys stoppanii*, *Placodus zittelii*, *Placochelys*

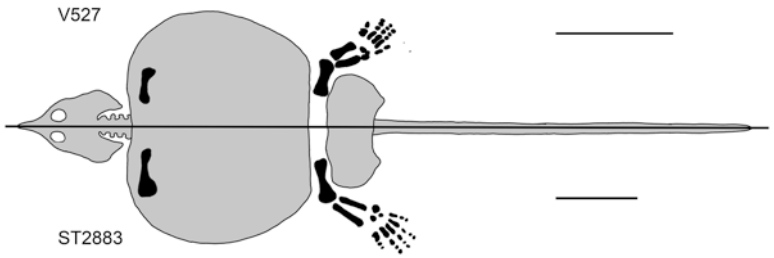

Fig. 8.10 The placodont *Psephoderma alpinum* specimen V527 and ST2883 from the Norian of Italy drawn at the same size to show differences in limb proportions, from Renesto and Tintori (1995), modified. Scale bars equal 20 cm

alpis-sordidae and *Psephoderma anglicum)* represent junior synonyms of *Psephoderma alpinum* (Pinna 1976, 1978; Rieppel 2000).

Psephochelys (with the only species *P. polyosteoderma* Li and Rieppel 2002) is the sister taxon of *Psephoderma* in the phylogenetic hypothesis by Neenan et al. (2015; Fig. 8.8). It occurs in the lower Carnian Wayao Member of the Falang Formation, of Guizhou, like *Sinocyamodus xinpuensis*. It is unique among cyamodontoid placodonts by the apparent entry of the postfrontal into the anteromedial margin of the upper temporal fossa. It shares with *Placochelys* and *Psephoderma* the spatulate and edentulous premaxillary rostrum. It shares with *Psephoderma* the presence of two maxillary teeth; upper temporal fenestrae relatively long and narrow; squamosals projecting far posteriorly; and tubercle-like osteoderms fused to the squamosals at their posterior extremity only.

Henodus chelyops von Huene 1936 is represented by only one complete and articulated specimen from the uppermost Gipskeuper (Estherienschichten, lower Carnian) of Lustnau, near Tübingen, southern Germany (Fig. 8.11). *Henodus* falls within the Placochelyidae in Neenan et al.'s (2015) phylogenetic analysis, but they (Neenan et al. 2015, p. 426) consider this to be "an artifact of a convergent morphology with some members of the Placochelyidae". *Henodus* shows many peculiarities. Its skull is completely different from that of other placodonts, being anteriorly truncated and with laterally wide premaxillae. Nostrils and orbits are located very close to the tip of the snout, and the latter is curved ventrally, so that the nostrils and orbits are cranially facing. Furthermore, the upper temporal fenestrae are secondarily closed. The dentition is strongly reduced: the margins of the premaxillae form a cutting edge bearing just a single row of tiny teeth. The maxillae are toothless, bearing a deep groove that may have housed baleen-like structures. The palatines have a single tooth plate each. Dentaries also bear a longitudinal groove and a single small flattened tooth at their posterior end. The coronoid is small, forming a small coronoid process. The posterior border of the skull bears some sub-pyramidal tubercles. The carapace is proportionally wider than that of other cyamodontoid placodonts. Its borders are bent downward, forming a lateral wall linking the carapace to the plastron, fully enclosing the body within the shell. Reconstruction of jaw musculature (Rieppel 2002a) suggests that *Henodus* may have been able to perform

Fig. 8.11 The placodont *Henodus chelyops* from the lower Carnian of Germany. The specimen is 1 m long. Author: Ghedoghedo; CC BY-SA 3.0. https://en.wikipedia.org/wiki/Henodus#/media/File:Henodus_chelyops_1.JPG

rapid jaw opening; the presence of large and ossified hyoid elements indicates that it could expand the throat for suction feeding, perhaps filtering small organisms with baleen-like structures. Also, it may have used the premaxillary flange and denticles for grazing rocks, feeding on algae or other kinds of aquatic vegetation.

8.3.1.2 Palaeoecology of Late Triassic Placodonts

Placodonts, with the exception of the highly derived *Henodus*, had a durophagous diet. The claim that *Placodus* and *Cyamodus* were macroalgae feeders (Diedrich 2010, 2011a, b) was refuted on the basis of osteological, biomechanical and taphonomic evidence (Scheyer et al. 2012) and it is no longer tenable. The feeding behaviour of Late Triassic cyamodontoids like *Psephoderma alpinum* was parallel to that of the durophagous batoids (Rajiformes and Myliobatiformes; Mazin and Pinna 1993; Pinna and Nosotti 1989). Like these fishes, cyamodontoid placodonts have a rather dorsoventrally flattened body and may have been bottom walkers that probed the sediments with their rostra, searching for food. They do not have adaptations for efficient locomotion in water, so they may have been relatively slow swimmers, propelled by alternate strokes of the robust hind limbs (Renesto and Tintori 1995).

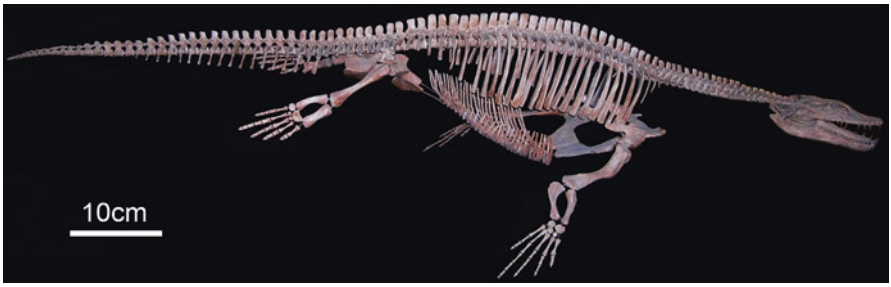

Fig. 8.12 Reconstruction of the skeleton of the nothosauroid *Simosaurus gaillardoti*. (Photo FM Dalla Vecchia)

8.3.2 'Pachypleurosauria'

Fragmentary remains referred to 'pachypleurosaurians' are reported in the lower Carnian of Germany (*Anatina*-Bank, Upper Gipskeuper; Hagdorn and Rieppel 1999) and northeastern Italy (Rio del Lago Formation; Dalla Vecchia 2008a). As they are identified only on the basis of their small size, the possibility exists that they are juvenile individuals of other eosauropterygians (Dalla Vecchia 2008a).

8.3.3 Nothosauroidea

According to Rieppel (2000), Nothosauroidea is a clade composed of *Simosaurus* and the Nothosauria. The latter is formed by *Germanosaurus* and the Nothosauridae (*Nothosaurus* + *Lariosaurus*). According to Ma et al. (2015; Fig. 8.5), it is composed by the Cymatosauridae (*Cymatosaurus* + *Corosaurus*), which were basal Pistosauroidea in Rieppel (2000), *Simosaurus* and the Nothosauria (as defined by Rieppel 2000). Nothosauroidea is not found by Neenan et al. (2015), whose strict consensus tree shows a large politomy involving the Nothosauroidea and the Pistosauroidea taxa of Ma et al. (2015); this is probably a consequence of the fact that their analysis was focused on the placodonts. Nothosauroidea is a prevailing Middle Triassic group. Middle Triassic remains are reported from localities in Europe, Tunisia, Israel, Saudi Arabia and China. *Corosaurus* comes from the Lower Triassic of the USA (Lin and Rieppel 1998; Rich et al. 1999; Rieppel 1999a, b, 2000; Rieppel et al. 1997). Only a few remains of *Nothosaurus* and *Simosaurus* (Fig. 8.12) are reported from the lower Carnian. Nothosauroids are characterized by great size variability, with very large taxa, like *Nothosaurus giganteus* (Rieppel and Wild 1996; Rieppel 2000 and references therein) and *N. zhangi* (see Liu et al. 2014), which reached up to 4.5 m in length.

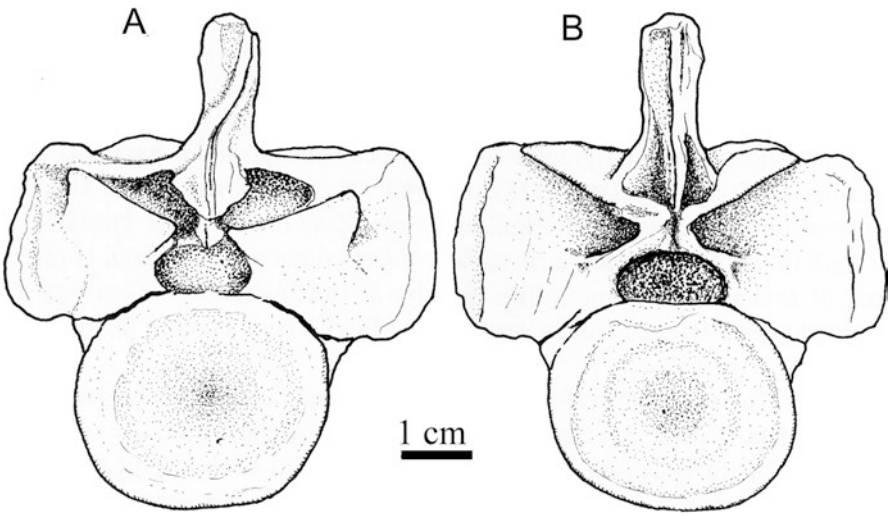

Fig. 8.13 Dorsal vertebra of the nothosauroid *Nothosaurus* cf. *giganteus* (MFSN 16851) from the basal Carnian or top Ladinian of Fusea, Italy. (**a**) *anterior*; (**b**) *posterior* view. From Rieppel and Dalla Vecchia (2001) redrawn

8.3.3.1 Late Triassic Nothosauroidea

Nothosaurus edingerae comes from the Upper Gipskeuper (*Acrodus*-bank and *Anatina*-Bank; basal lower Carnian) of southern Germany (Rieppel and Wild 1996; Rieppel 2000). The *Anatina*-Bank yielded also the pachyostotic ribs of a mid to large-sized eusauropterygian (Hagdorn and Rieppel 1999) that could be *Simosaurus* or *Bobosaurus*.

Skull and lower jaw bones, teeth and postcranial elements of a large nothosaur (Fig. 8.13) were reported from Fusea, Friuli, northeastern Italy (Dalla Vecchia 1994, 2008a; Rieppel and Dalla Vecchia 2001), which is latest Ladinian or earliest Carnian in age (Dalla Vecchia and Carnevale 2011). They were referred to *Nothosaurus* cf. *giganteus* by Rieppel and Dalla Vecchia (2001) because of their large size and the low neural spine of the vertebrae.

Dalla Vecchia (2008b) described postcranial remains of *Simosaurus* from the lower Carnian Rio del Lago Formation near Dogna, Friuli, northeastern Italy, confirming the presence of the genus in the Carnian. The taxon is reported also from the lowermost Gipskeuper of Germany (Rieppel 1994) that is latest Ladinian in age according to Hagdorn and Rieppel (1999). Dorsal vertebrae of *Simosaurus* (Fig. 8.14) are characterized by 'infraprezygapophyses' and 'infrapostzygapophyses' in addition to the 'normal' zygapophyseal articular facets (i.e., wedge-shaped prezygapophyses with both dorsal and ventral articular surfaces) in the neural arches (see Dalla Vecchia 2008b). Rieppel and Dalla Vecchia (2001) refer to *Nothosaurus* sp. a neural arch with a low neural spine from the same area and horizon.

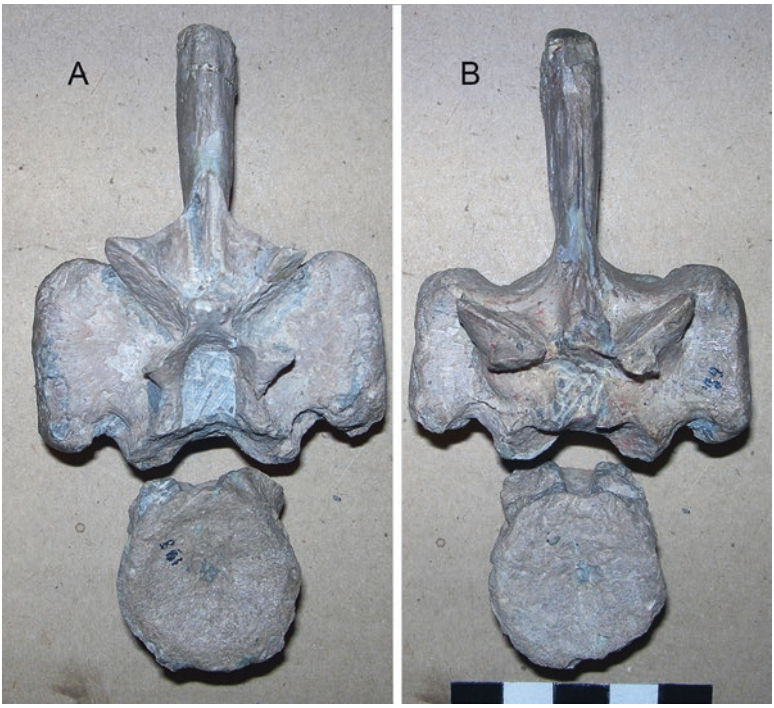

Fig. 8.14 Dorsal vertebra of the nothosauroid *Simosaurus gaillardoti* (SMNS 14733). (Photo FM Dalla Vecchia): (a) anterior(cranial) view; (b) posterior (caudal) view

Associated postcranial remains of a relatively large eusauropterygian are reported also from the upper part of the lower Carnian (San Cassiano Formation) of Stuores Wald in the Dolomites, northern Italy (Bizarrini et al. 2003). It could be a nothosauroid, but also a pistosauroid cannot be excluded as the specimen was never described in detail. It appears to be the youngest eusauropterygian before the 'Rhaetian' plesiosaurs from Western Europe.

8.3.4 Pistosauroidea

According to Ma et al. (2015), Pistosauroidea is a clade composed of the basal *Wangosaurus,* followed along the pectinate tree by *Yunguisaurus*, the Pistosauridae (sensu Rieppel 2000) and the Plesiosauria (see Fig. 8.5). Two purported pistosauroids from China are *Chinchenia* and *Kwangsisaurus* (Rieppel 1999b). They are all Middle Triassic in age, excluded the Plesiosauria that are all Late Triassic and post-Triassic in age. Pistosauroids are fairly rare in the Triassic, named taxa being represented by only a few specimens from Europe, China and USA (see Ma et al. 2015

and references therein). Derived pistosauroids, the plesiosaurs, had a great evolutionary success and spread worldwide in the Jurassic and Cretaceous.

8.3.4.1 Late Triassic Pistosauroids

As anticipated above, *Bobosaurus forojuliensis* Dalla Vecchia 2006 from the lower Carnian Rio del Lago Formation of Dogna, Italy, is the oldest and most basal plesiosaur according to Fabbri et al. (2014), Liu et al. (2015) and Ma et al. (2015), while it is the sister group of Plesiosauria for Benson et al. (2012). It represents an early diverging branch in the evolution of the plesiosaurian body plan from the ancestral pistosaurian grade (Fabbri et al. 2014). The holotype (Fig. 8.15) is a partial but mostly articulated skeleton consisting of the tip of the rostrum with some teeth, part of the cervical vertebral column, the dorsal and sacral segments of the vertebral column, most of the caudal segment, some gastralia, a humerus, the pelvic girdle and some elements of the hind limbs; an isolated neural arch from the same locality, was also referred to this species (Dalla Vecchia 2006). *Bobosaurus* was a relatively large eusauropterygian reaching a length of over 3 m. It has at least five autapomorphies in the vertebral column, including a vertebral zygapophyseal articulation that is the opposite with respect to that of *Simosaurus* (Dalla Vecchia 2006). Teeth, vertebrae and the pubis of *Bobosaurus* show affinities with plesiosaurian grade sauropterygians in their morphology, while other skeletal features are shared with less derived eusauropterygians or were previously considered apomorphic of distinct taxa (i.e., very tall neural spines and uncinate processes of the dorsal ribs). Dalla Vecchia (2006) considered *Bobosaurus* as a pistosaurid or, alternatively, a member of a clade closer to Liassic plesiosaurians than to pistosaurids. The cladistic analysis performed by Fabbri et al. (2014), found *Bobosaurus* to be closer to plesiosaurians than to the paraphyletic "pistosaurids" *Pistosaurus* and *Augustasaurus*. Fabbri et al. (2014) underlined that this result is congruent with the chronostratigraphic positions of these taxa (*Pistosaurus* and *Augustasaurus* are from the upper Anisian, and *Yunguisaurus* from the upper Ladinian, while *Bobosaurus* is from the lower Carnian). Its position as the oldest and basal plesiosaurian is in agreement with the hypothesis by Benson et al. (2012) that the earliest plesiosaurian diversification already occurred in the Late Triassic (see below). *Bobosaurus* lived 30 millon years y before the Rhaetic specimen that Wintrich (2015) considers as the most basal plesiosaur (as detailed further), therefore it is supposed to be more primitive. As Fabbri et al. (2014) pointed out, the inclusion or not of *Bobosaurus* in the Plesiosauria depends upon the way Plesiosauria is formally defined. *Bobosaurus* was possibly a surface swimmer with a stiff trunk that mainly used its forelimbs, and perhaps hind limbs, in swimming.

Alexeyisaurus karnoushenkoi Sennikov and Arkhangelsky 2010 from the lower-middle Norian Wilczek Formation, Wilczek Land of Franz-Josef Land, Russia is represented by an incomplete skeleton consisting of portions of the dorsal and caudal regions of the vertebral column, some ribs, and a few incomplete girdles and limbs bones. It has been considered as a peculiar plesiosaur belonging to the

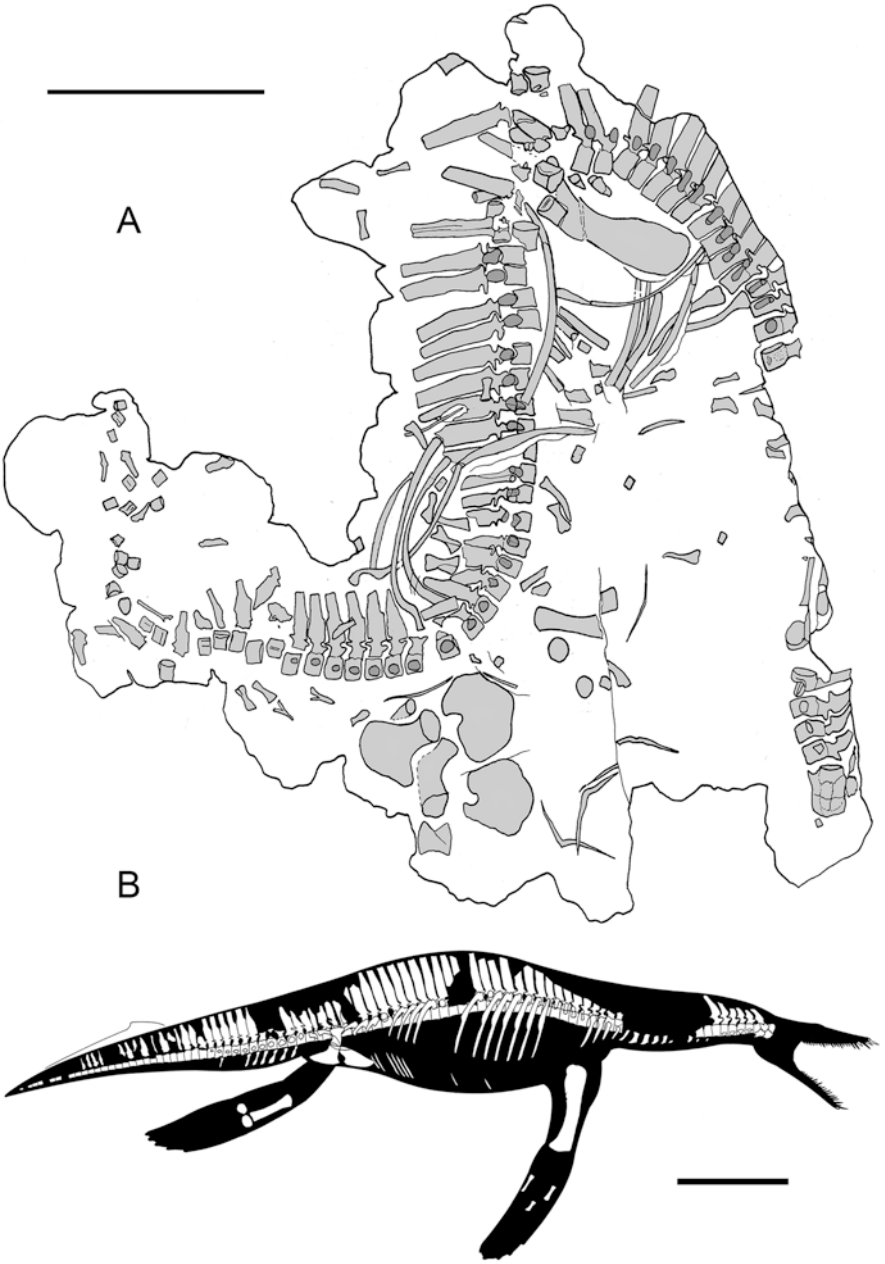

Fig. 8.15 (**a**) drawing of the holotype of the basal plesiosaur *Bobosaurus forojuliensis* (MFSN 27285) redrawn from Dalla Vecchia (2006). (**b**) silhouette with the preserved parts of the skeleton; drawing by Marco Auditore. Scale bars equal 50 cm

Elasmosauridae (Sennikov and Arkhangelsky 2010), an advanced clade otherwise exclusively Cretaceous in age (Ketchum and Benson 2010; Druckenmiller et al. 2008; Otero et al. 2014; Sato et al. 2006). However, this taxon does not show any unambiguous synapomorphies of the Elasmosauridae. Only the outline of the coracoid has some resemblance with that of the elasmosaurids, which could be a case of morphological convergence. In addition, the humerus and femur differ from those of all other sauropterygians. Finally, its phylogenetic affinity was not tested by a cladistic analysis. For these reasons, we consider as dubious its attribution to the Elasmosauridae, while it may well represent a peculiar sauropterygian of uncertain affinity. Wintrich (2015) reports the discovery of a nearly complete and largely articulated skeleton of a subadult (1.6 m long) plesiosaur from the Rhaetian of Westphalia (Germany). This specimen would have V-shaped neurocentral suture of the cervical vertebrae, humerus with a straight shaft and femur and zeugopodials that are only slightly longer than wide, which are considered plesiosaur features. However, to date (may 2017) the description of this specimen has not been published yet.

Fragmentary plesiosaur remains (mainly vertebrae, teeth, partial humeri and phalanges) are reported from the 'Rhaetian' Westbury Formation of England (Storrs 1994, 1999; Mears et al. 2016). Owen (1840) described many isolated plesiosaur vertebrae from the 'Rhaetian' of SW England, erecting several taxa that are *nomina dubia* today. Possible plesiosaur material (vertebrae and teeth) is reported from the 'Rhaetian' of Provenchères-sur-Meuse, Haute Marne, France (Cuny 1995) and possibly Germany (Wintrich 2015). We report 'Rhaetian' within brackets because it is unclear whether the Rhaetian of western Europe corresponds totally or just partly with the Alpine Rhaetian, which is the world reference for this Stage; probably it includes also part of the upper Norian, i.e., the Sevatian.

Taylor and Cruickshank (1993) report a plesiosaurian vertebral string and a tooth from an erratic block at Linksfield, Scotland, which could be late Rhaetian or early Jurassic in age.

The oldest good plesiosaur record comes from the Pre-*planorbis* beds of the Blue Lias cropping out near Street and nearby localities (Somerset, UK) (Storrs and Taylor 1996; Benson et al. 2012). We have already discussed the problem of the age of those beds in the ichthyosaur section. They contain several plesiosaur species based on wonderful material: *Thalassiodracon hawkinsii* (Owen 1840) (see Storrs and Taylor 1996 and Benson et al. 2011); *Eurycleidus arcuatus* (Owen 1840) (see Cruickshank 1994); *Atychodracon (Rhomaleosaurus) megacephalus* (Stutchbury 1846) (see Smith 2015)*;* '*Plesiosaurus*' *cliduchus* (Seeley 1865)*; Stratesaurus taylori* Benson, Evans and Druckenmiller 2012; *Avalonnectes arturi* Benson, Evans and Druckenmiller 2012; and *Eoplesiosaurus antiquior* Benson, Evans and Druckenmiller 2012.

As suggested by Benson et al. (2012) on the basis of their stratigraphically calibrated cladogram, at least a dozen distinct plesiosaurian lineages are represented in the Pre-*planorbis* beds of England, implying that plesiosaurs diversified during the Late Triassic despite the rarity of their Triassic remains.

8.4 Thalattosauria

The Thalattosauria are a monophyletic clade of marine reptiles from the Middle to Upper Triassic of North America, Europe and China (Merriam 1905; Peyer 1936a, b; Kuhn-Schnyder 1952; Renesto 1992; Nicholls and Brinkman 1993; Nicholls 1999, Rieppel et al. 2000; Liu et al. 2013 and references therein). They were fairly large aquatic reptiles, ranging from 1 m up to 4 m in length. Thalattosaurs are characterized by a skull with an elongated and tapering premaxillary rostrum; retracted nares; contact of the premaxilla with the frontal; reduced and slit-like upper temporal fossa; deeply concave occiput with the occipital condyle located well in front of the mandibular articulations; and an incomplete lower temporal arch (Rieppel 1987; Nicholls 1999). The trunk is elongate, and the tail is very long and laterally compressed and deep, due to the presence of relatively high neural spines and long chevrons. In most taxa the limbs are very short relative to the body. These animals swum by lateral undulations of the tail and body axis. Thalattosauria are divided into two major groups, the Askeptosauroidea and the Thalattosauroidea by most authors (see Liu and Rieppel 2005; Cheng et al. 2011; Liu et al. 2013). The Askeptosauroidea differ from the Thalattosauroidea in the presence of a longer, pointed rostrum and a longer neck (more than 10 cervical vertebrae). Also, the Thalattosauroidea have a downturned tip of the premaxillae. However, Nicholls (1999) excluded *Endennasaurus* and *Askeptosaurus* from the Thalattosauria and proposed the clade Thalattosauriformes to comprise these two taxa, restricting the use of Thalattosauria to the other known thalattosaurs. The Thalattosauriformes were retained by Müller (2004, 2005), but recent phylogenetic analyses, such as those by Wu et al. (2009), Cheng et al. (2011) and Liu et al. (2013), maintained the subdivision of the Thalattosauria into Askeptosauroidea and Thalattosauroidea, the first including *Endennasaurus* and *Askeptosaurus*. In this chapter, we follow the phylogenetic hypothesis by Liu et al. (2013) (Fig. 8.16).

Until the last decade, Late Triassic thalattosaurians were represented by a few genera, namely *Nectosaurus* and *Thalattosaurus* from the Carnian of California, and *Endennasaurus* form the Norian of Lombardy, northwestern Italy (Rieppel et al. 2000; Liu and Rieppel 2001; Liu et al. 2013). Subsequent discoveries of excellently preserved specimens from the lower Carnian of Guanling in China have added substantial knowledge of thalattosaur diversity and witnessed their cosmopolitan distribution, raising an increased interest in their palaeobiogeography. As Liu et al. (2013) pointed out, the thalattosaur fauna from the Xiaowa Formation is the best preserved and most diverse known so far. Four further genera have been erected: *Anshunsaurus* Liu 1999; *Xinpusaurus* Yin 2000 (in Yin et al. 2000); *Miodentosaurus* Cheng Wu and Sato 2007b; and *Concavispina* Zhao, Liu, Li and He 2013.

The affinities of the thalattosaurs have been discussed by different authors, but are still debated. According to Müller (2004, 2005), they may be either the sister group of Sauria or of the Ichthyosauria. In the analysis by Motani et al. (2015), they are the sister group of Ichthyopterygia +Sauropterygia, while they are the sister

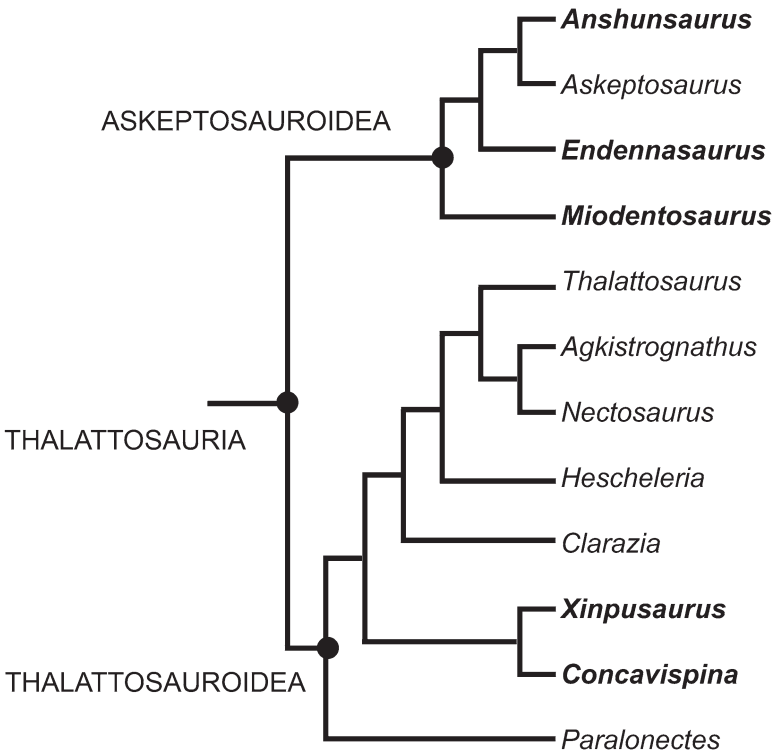

Fig. 8.16 Phylogenetic relationships among the thalattosaurs (strict consensus tree), from Liu et al. (2013), redrawn. Late Triassic genera are shown in *bold*

group of a clade including *Eusarosphargis*, *Helveticosaurus*, Ichthyopterygia, *Sinosarosphargis* and Sauropterygia in the analysis by Neenan et al. (2015).

Thalattosaurs reveal a great morphological diversity mostly linked to different feeding adaptations, from toothless forms with elongate beak-like rostra, such as *Endennasaurus* (see Müller et al. 2005), to taxa with a well-developed semi-durophagous or durophagous dentition and a downturned or shortened rostrum (Rieppel et al. 2005), such as *Anshunsaurus* and *Miodentosaurus*.

8.4.1 Late Triassic Thalattosaurs

Thalattosaurus alexandrae Merriam 1904 from the Carnian Hosselkus Limestone of California, USA is a large thalattosaur that reached 2–3 m in length. It was characterized by an edentulous premaxilla bearing a "pseudodont" dentition made by bony projections. Small teeth with button-like crowns occur on the maxilla, vomer

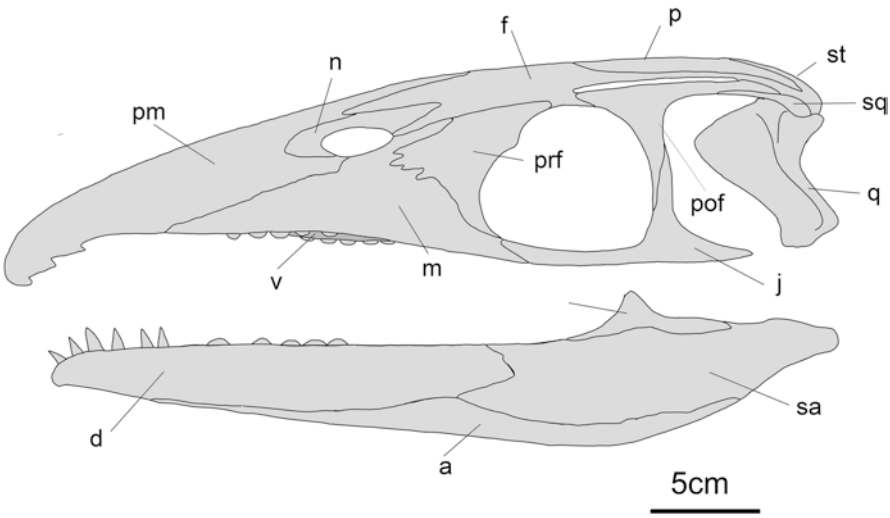

Fig. 8.17 Drawing of the skull of *Thalattosaurus alexandrae* based on the reconstruction by Nicholls (1999). Abbreviations: *a* angular, *d* dentary, *f* frontal, *j* jugal, *m* maxilla, *n* nasal, *p* parietal, *prf* prefrontal, *pm* premaxilla, *pof* postfrontal, *q* quadrate, *sq* squamosal, *sa* surangular, *st* supratemporal, *v* vomer

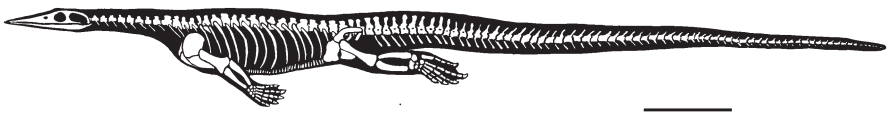

Fig. 8.18 Reconstruction of the thalattosaur *Endennasaurus acutirostris.* Scale bar equals 10 cm

and posterior portion of the dentary, whereas the anterior portion of the dentary bears procumbent conical teeth (Fig. 8.17).

Nectosaurus halius Merriam 1905, also from the Carnian Hosselkus Limestone of California, is a relatively small thalattosaur known mostly from fragmentary skull and vertebral material (Nicholls 1999). It was characterized by teeth with a thecodont implantation and conical, pointed and heavily striated crowns. *N. halius* may have reached 1 m in length, but other *Nectosaurus* material suggests the presence of much larger individuals. Consequently, either the specimens ascribed to *N. halius* were juveniles or the larger specimens belong to another species; Nicholls (1999) tentatively supported the second hypothesis and referred the larger specimen to *Nectosaurus* sp.

Endennasaurus acutirostris Renesto 1984 (Fig. 8.18) is from the Norian Calcare di Zorzino of Lombardy, northwestern Italy. It is 1 m in length and has the following features: a long, sharp and straight rostrum; edentulous jaws and palate; relatively massive shoulder girdle; strong basket of gastralia with overlapping articulations between consecutive rows of elements; limbs that are comparatively long with respect to those of other thalattosaurs; and well-ossified manus and pes (Renesto

1992). Müller et al. (2005) revised the anatomy and relationships of *Endennasaurus*, placing it within the Askeptosauridae, possibly as a most basal member of the group. According to Liu and Rieppel (2005), *Endennasaurus* is instead the sister taxon of the Askeptosauridae (comprising *Askeptosaurus* + *Anshunsaurus*), with the Askeptosauridae + *Endennasaurus* forming the Askeptosauroidea. The long and toothless rostrum suggests that *Endennasaurus* occupied a specialized niche, feeding upon soft-shelled invertebrates, small fishes and/or crustaceans that did not require teeth for either capture, holding or crushing. The long and relatively deep tail, together with the rigid basket of gastralia, suggest that it was primarily adapted to an aquatic lifestyle, swimming mainly by lateral undulation of the tail. However, the presence of robust limbs that are proportionally larger than in other known thalattosaurs, indicates that it could also move on land (possibly for reproduction).

Anshunsaurus huangguoshuensis Liu 1999 from the lower Carnian Wayao Member of the Falang Formation of Guizhou, China was originally described by Liu (1999) as a sauropterygian on the basis of a skull that is exposed in dorsal view. The specimen was later correctly referred to the Thalattosauria by Rieppel et al. (2000). The skull and the postcranial skeleton were subsequently studied by Liu and Rieppel (2005), while Maisch (2015) described an excellently preserved juvenile individual. A second and a third species of *Anshunsaurus*, *A. wushaensis* Rieppel and Liu 2006 (see also Liu 2007) and *A. huangnihensis* Cheng, Chen and Wang 2007a, were described. In the phylogenetic analysis by Cheng et al. (2011), this genus belongs to the Askeptosauridae as the sister taxon of *Askeptosaurus*. *Anshunsaurus* was a fairly large marine reptile very similar to *Askeptosaurus*, with an elongate and pointed skull, a long neck, trunk and a very long and laterally compressed tail. The limbs were proportionally very small. *Anshunsaurus* is characterized by the maxilla forming part of the anteroventral orbital margin; fusion of the postorbital and postfrontal; the posterolateral process of the frontal extending posteriorly far beyond the anterior margin of lower temporal fossa; a long and slender ventral process of the squamosal extending to the lower margin of the cheek; a jugal with an elongate posterior process; a well developed deltopectoral crest on the humerus, and a large fibula.

Xinpusaurus is represented by at least three species: *X. suni* Yin et al. 2000, *X. bamaolinensis* Cheng 2003 and *X. kohi* (Jiang et al., 2004), which are all from the Wayao Member of the Falang Formation of Guizhou. It is characterized by a highly derived rostral structure: the premaxilla is downturned and nearly vertically placed; the maxilla is short with an anteriorly truncated (vertical) margin; the ascending process of maxilla is narrow but high; and the medial flange of maxilla is dorsally curved and articulated with the ventrally deflected vomer (Liu and Rieppel 2001; Luo and Yu 2002).

Miodentosaurus is represented by only one species, *M. brevis* Cheng et al. 2007a, b, which is also from the Wayao Member of the Falang Formation. It differs from *Askeptosaurus* and *Endennasaurus* in having a much shorter rostrum and fewer teeth.

Concavispina is also represented by a single species, *C. biseridens* Zhao, Liu, Li and He 2013, that is characterized by a long skull (measuring approximately half the length of presacral portion of the vertebral column); two rows of blunt teeth on the anterior part of the maxilla; neural spines with convex anterior or posterior mar-

gins; and V-shaped notches in the dorsal margin of the neural spines. *Concavispina* differs from all other thalattosaurs, except *Xinpusaurus*, in having a dorsally curved anterior end of the maxilla. There are less than five cervical vertebrae, and the proximal end of the humerus is wider than the distal end. Like ichthyosaurs, and different from most thalattosaurus, *Concavispina* has a very short neck. The tail is very deep laterally due to the presence of relatively high neural spines and long chevrons. Its limbs are short respect to the body size, with short and wide epipodials and a poorly ossified carpus and tarsus. *Concavispina* probably relied on lateral undulations of the body axis for propulsion.

A partial thalattosaur skeleton belonging to an indeterminate taxon close to *Nectosaurus* or *Xinpusaurus* was reported by Müller (2007) from the upper Norian-lower Rhaetian Kössen Formation near Salzburg, Austria. A tail fragment from the lower Carnian (Calcare del Predil) Riofreddo locality near Tarvisio, northeastern Italy has been tentatively referred to a thalattosaur by Dalla Vecchia (1994) because of the tall neural spines and long chevrons. More recently a partial skeleton of a large thalattosaur has been reported from the Norian Hound Islands Volcanics of Alaska (Druckenmiller 2015).

8.5 Chelonia

Li et al. (2008) described the turtle *Odontochelys semitestace*a (Fig. 8.19) from the lower Carnian and marine Wayao Member of the Falang Formation of Guanling, China. Apart for the possible older ichnological evidence already mentioned (von

Fig. 8.19 The basal turtle *Odontochelys semitestacea* (IVPP V 13240, paratype) from the ower Carnian of China. Author: Ghedoghedo; CC BY-SA 4.0. https://it.wikipedia.org/wiki/Odontochelys_semitestacea#/media/File:Odontochelys_semitestacea_433.jpg

Lilienstern 1939; Lovelace and Lovelace 2012) *Odontochleys* is the oldest turtle so far known with a well developed plastron. It is over 15 million years older than the Norian terrestrial/freshwater genera *Proganochelys* Baur 1887 from Germany (Gaffney 1990) and Thailand (de Broin 1984) *Proterochersis* Fraas 1913 again from the Norian of Germany, and *Chinlechelys* Joyce et al. 2009, from the Norian of the USA. The Middle Triassic stem turtle Pappochelys (Schoch and Sues 2015) lacks in fact a true plastron showing only a peculiar arrangement of gastralia and *Eunothosaurus*-like expansion of the ribs. *Odontochelys* represents an intermediate step in the evolution of the turtle shell and associated structures Li et al (2008), while *Proganochelys* already had complete armour offering no clue to its origin. The ventral plastron of *Odontochelys* is fully developed, while the dorsal carapace consists of neural plates only. The dorsal ribs are expanded and osteoderms are absent. The new species shows that the plastron evolved before the carapace and that the first step of carapace formation is the ossification of the neural plates coupled with a broadening of the dorsal ribs. This corresponds to the early embryonic stages of carapace formation in extant turtles and shows that the turtle shell did not originate from the fusion of osteoderms. According to the phylogenetic analysis by Li et al. (2008), the new species is the basalmost turtle. The completeness and perfect articulation of specimens and depositionary environment of the Wayao Member indicates that *Odontochelys* lived in shallow waters in a coastal setting (Li et al. 2008), Joyce (2015) on anatomical basis, suggested instead that it may have lived in freshwater ponds.

8.6 Phytosauria

Phytosaurs are crocodile-like Triassic archosauriforms (outside the Archosauria according to Nesbitt 2011, inside according to Ezcurra 2016) that are represented by numerous finds from Europe, the southwestern and eastern USA, Greenland, Madagascar, North Africa, Turkey, Thailand, India and Brazil (Stocker and Butler 2013). Phytosaurs mainly lived in fluvio-lacustrine environments, but they are reported also from Upper Triassic marine deposits of the Alpine Region (Austria and Italy).

Austrian finds comprise relatively abundant remains from the Rhaetian Dachsteinkalk of the Totes Gebirge in Styria (Buffetaut 1993); they had been referred to *Mystriosuchus planirostris* (a species that was found also in continental settings, Fig. 8.20), but they were never described in detail. Italian specimen include a 4.5 m long, almost complete and articulated skeleton, a complete skull and some articulated vertebrae from the uppermost part of the Norian Calcare di Zorzino and lowermost part of the Argillite di Riva di Solto of Lombardy, Italy (Renesto and Paganoni 1998; Renesto and Lombardo 1999; Gozzi and Renesto 2003; Renesto 2008). They are all referred to *Mystriosuchus planirostris*.

Maisch and Kapitzke (2010) also reported a fragment of a phytosaur lower jaw from the Pre-*planorbis* beds of the Blue Lias of Somerset, England, which are most probably earliest Jurassic in age, as we have already seen; Lucas and Tanner (2015)

Fig. 8.20 Skull of the phytosaur *Mystriosuchus planirostris* from the continental Norian of Germany. Author: Ghedoghedo; CCBY-SA3.0. https://en.wikipedia.org/wiki/Mystriosuchus#/media/File:Mystriosuchus_planirostris_skull.JPG, modified

also consider this as a Jurassic phytosaur record. However, according to Stocker and Butler (2013), the hypothesis that phytosaurs passed through the Tr-J boundary requires to be supported by further findings.

It is worth noting that the postcranium of the complete *Mystriosuchus* specimen from the Zorzino Limestone shows adaptations to an aquatic lifestyle that are more marked than in other phytosaurs. Its overall body proportions, with reduced limbs and long tail, are more reminiscent of the thalattosuchian crocodyliforms, than to other phytosaurs. In addition, some features of the caudal vertebrae, such as the inverted T-shaped haemal spines of the terminal portion of the tail (Renesto and Lombardo 1999) and the reduction of dermal covering are also reminiscent of that of the thalattosuchians. *M. planirostris*, which undoubtedly lived also in continental settings of Central Europe, could have colonized shallow marine habitats thanks to its adaptations to swimming (Gozzi and Renesto 2003).

8.7 Tanystropheidae

The Tanystropheidae are a clade of bizarre archosauromorph diapsids that are characterized mainly by a long and rather stiff neck made up by 8–13 elongate cervical vertebrae (depending on the taxon), with low neural spines and long filiform ribs that run parallel to the ventral margin of the neck. Tanystropheids were firstly included in the Prolacertiformes, then in the Protorosauria, but these clades are both paraphyletic according to recent phylogenetic hypotheses (Pritchard et al. 2015; Ezcurra 2016). According to Pritchard et al. (2015), the Tanystropheidae comprise *Macrocnemus*, *Tanystropheus, Amotosaurus*, *Langobardisaurus* and *Tanytrachelos*. The tanystropheids that are supposed to be terrestrial dwellers were of rather small size. The Middle Triassic *Macrocnemus* may have been up to 1 m long (Rieppel 1989), and the Norian *Langobardisaurus* was less than half a meter in length; both were probably facultative bipedal runners (Rieppel 1989; Renesto et al. 2002). Supposedly semi-aquatic or fully aquatic Tanystropheidae ranged in size from the very small freshwater *Tanytrachelos ahyni*s Olsen 1979 (about 20 cm long) to the very large coastal/littoral dweller *Tanystropheus longobardicus* (Bassani 1886) that may have reached 5 m in length (Wild 1973).

8.7.1 Late Triassic Tanystropheids

Tanystropheus remains have been mostly found in marine deposits and these animals probably lived on the sea shore or in shallow waters, preying on fishes and invertebrates with the aid of the extremely long and rather stiff neck. *Tanystropheus* is mostly known from the Middle Triassic of northern Italy, southern Switzerland and Central Europe (Wild 1973; Nosotti 2007), but also from China (Li 2007; Rieppel et al. 2010) and North America (Sues and Olsen 2015) as well. Along with *Macrocnemus* (reported from China by Jiang et al. 2011), it testifies to the success and widespread distribution of these archosauromorphs, suggesting that there was a common vertebrate fauna along the northern coastline of the Paleotethys since the Middle Triassic.

A nearly complete skeleton without skull, which was referred to *Tanystropheus* cf. *T. longobardicus*, has been found in the Xingy *Lagerstätte* in the Zhuangpo Member of the Falang Formation of Guizhou, China. It was originally considered as possibly early Carnian in age; however, recent revision of the stratigraphy of the locality demonstrated that it's age is late Ladinian (Zhou et al. 2015). Anyway, a few finds testify that the genus occurs also in the Upper Triassic. A typical cervical vertebra of *Tanystropheus* (Fig. 8.21) from the basal Carnian or latest Ladinian of Fusea, Friuli, northeastern Italy was reported by Dalla Vecchia (2000) associated with placodont, nothosauroid and fish remains (Dalla Vecchia and Carnevale 2011). A series of articulated cervical vertebrae with associated ribs from the upper Norian and marine Argillite di Riva di Solto Formation of Lombardy, northwestern Italy has been assigned to a new small species of *Tanystropheus*, *T. fossai* Wild 1980. If actually a *Tanystropheus* specimen and not a distinct tanystropheid genus, it would be the youngest evidence of this genus.

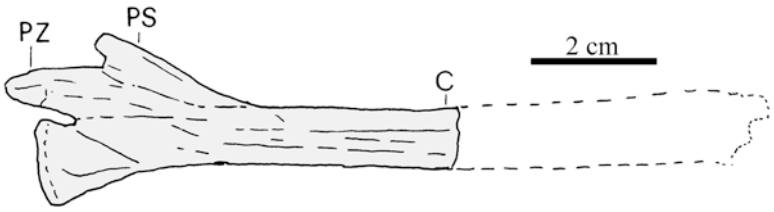

Fig. 8.21 Cervical vertebra of the tanystropheid *Tanystropheus* (MFSN 25760) from the basal Carnian or top Ladinian of Fusea, Italy. From Dalla Vecchia (2000). Abbreviations: *PS* processus spinosus, *PZ* potzygapophysis

8.8 Choristodera

Choristodera is a clade of aquatic or semi-aquatic diapsid reptiles of uncertain affinities. Choristoderans are characterized by a dorsoventrally flattened skull with elongate rostrum and wide temporal fenestrae. Their temporal range spans from the Middle Jurassic to the early Miocene, their best record being from the Cretaceous and the Palaeogene (Evans and Hecht 1993; Matsumoto and Evans 2010). However, one putative choristodere—*Pachystropheus*—has been reported also from the Upper Triassic.

Pachystropheus rhaeticus von Huene 1935 is represented by abundant disarticulated and scattered bones from the 'Rhaetian' (i.e., the Westbury Formation) of England and Wales (Storrs and Gower 1993; Storrs 1994; Allard et al. 2015) and also from the 'Rhaetian' of Germany (Storrs and Gower 1993). *Pachystropheus* was ascribed to the Choristodera both by von Huene (1935) and in the revision by Storrs and Gower (1993). If *Pachystropheus* is a choristodere, it would extend back by 45 million years the fossil record of the group. However, its attribution to the Choristodera is debated, being based on vertebral and girdle characters that could be more indicative of adaptation to an aquatic lifestyle than of phylogenetic relationships. In fact, most diagnostic features of choristoderes are in the skull, which is practically unknown in *Pachystropheus*. Renesto (2005) found similarities between the postcranial skeleton of *Pachystropheus* and the thalattosaur *Endennasaurus*, suggesting that *Pachystropheus* may rather have been a thalattosaur; however, convergence in the postcranial skeleton due to adaptation to an aquatic lifestyle, again hinders any firm attribution. *Pachystropheus* specimens are from shallow marine deposits (Storrs and Taylor 1996), while younger choristoderans come from freshwater, often fluvial, deposits.

8.9 Is a Triassic-Jurassic Boundary Extinction of Marine Reptile Clades Supported?

Many groups of marine reptiles that were abundant and diverse in the Triassic did not reach the Jurassic: non-parvipelvian ichthyosaurs, placodonts, all non-plesiosaurian eosauropterygians, thalattosaurs and tanystropheids disappeared before the Jurassic. Only dubious evidence exists of the survival of phytosaurs into the earliest Jurassic.

According to Bardet (1994), major extinctions among Triassic marine reptiles occurred at the Middle-Late Triassic transition (Ladinian-Carnian boundary), rather than during the Late Triassic, in coincidence with an important regressive phase, and affected essentially coastal taxa. However, the Italian sites of Fusea, Dogna and Raibl/Cave del Predil, which yielded placodonts and eosauropterygians (nothosauroids and possibly 'pachypleurosaurs') are above the evidence of the emersion event

related to the regression that occurred close to the Ladinan-Carnian boundary (Dalla Vecchia 2008a). Placodonts were still relatively diverse during the early Carnian (*Protenodontosaurus*, *Placochelys*, *Henodus*, *Sinocyamodus* and possibly *Cyamodus*) and *Simosaurus* and *Nothosaurus* occur in the lower Carnian of north-eastern Italy in levels corresponding to the *aonoides* Subzone of ammonoid biostratigraphy (Preto et al. 2005) that is the third of the five subzones of the Julian (De Zanche et al. 1993).

Other authors (e. g. Benson et al. 2010; Benson and Butler 2011; Thorne et al. 2011) observed that there was a great reduction of species diversity during the Late Triassic, with the disappearance of entire clades and several morphotypes, thus marine reptile extinctions may have occurred throughout the Late Triassic rather than at the Triassic-Jurassic boundary.

According to Kelley et al. (2014), shallow-marine reptiles, especially durophagous taxa, were most affected by marine regressions, while pelagic forms were less sensible to sea level fluctuations. According to Hallam and Wignall (1997 and references therein), most of the significant extinction events in the marine biota seem to coincide with marked sea level falls, strengthening Newell's (1952) hypothesis that marine extinctions are related to the loss of shelf habitat during severe regressions. According to Kelley et al. (2014), the relationship between loss of diversity and sea level fluctuations may explain the evolutionary trend observed in different marine reptiles groups (Thorne et al. 2011), highlighting how sea-level changes influenced the ecological structure of marine ecosystems during the early Mesozoic. However, there is no evidence of a dramatic reduction of shallow seas in the Alpine realm during the Rhaetian, as can be easily verified by looking at the local geology (e.g., Plöchinger 1980; Brandner and Poleschinski 1986; Kovacs et al. 1989; Furrer 1993; Jadoul et al. 1994; Carulli et al. 2000).

What is reported in this paper shows clearly that extinctions of marine reptile taxa occurred throughout the Late Triassic rather than being concentrated at the Triassic=Jurassic boundary. The whole record of marine reptiles is quite rare in the Rhaetian (spanning from 205.7 to 201.3 million years ago; Maron et al. 2015), more so if the fossil-bearing 'Rhaetian' of western Europe is actually to refer partially or totally to the upper Norian (Sevatian) of modern global chronostratigraphy. The position of the Norian-Rhaetian boundary and Rhaetian extent have been long debated (see Muttoni et al. 2010; Maron et al. 2015 and references therein) and correlations between the Tethyan and western European Upper Triassic are difficult. Authors have never accurately correlated the traditional English 'Rhaetian' with the Tethyan Rhaetian, which is the standard for the boundaries, chronostratigraphy and biostratigraphy of this Stage (e.g., Krystyn et al. 2007a, b; Krystyn 2010; Maron et al. 2015), they just accepted the English traditional 'Rhaetian' as an equivalent of the Rhaetian Stage of chronostratigraphy (see, for example, Mears et al. 2016; Slater et al. 2016).

8.10 Conclusion

Ichthyosaurs diversified in the Carnian (eight genera) and also in the Norian (five genera), but are dramatically rare in the Rhaetian and with apparently no diversity (no genus reported in Ji et al. 2016, fig. 6; actually, it is possible that at least *Leptonectes* is represented in this Stage, as said above), to appear again at the base of the Jurassic with a relatively good record and three genera (Fig. 8.22). The evolutionary bottleneck seems to have occurred at the Norian-Rhaetian rather than at the Tr-J boundary. Placodonts apparently disappeared between the early and late

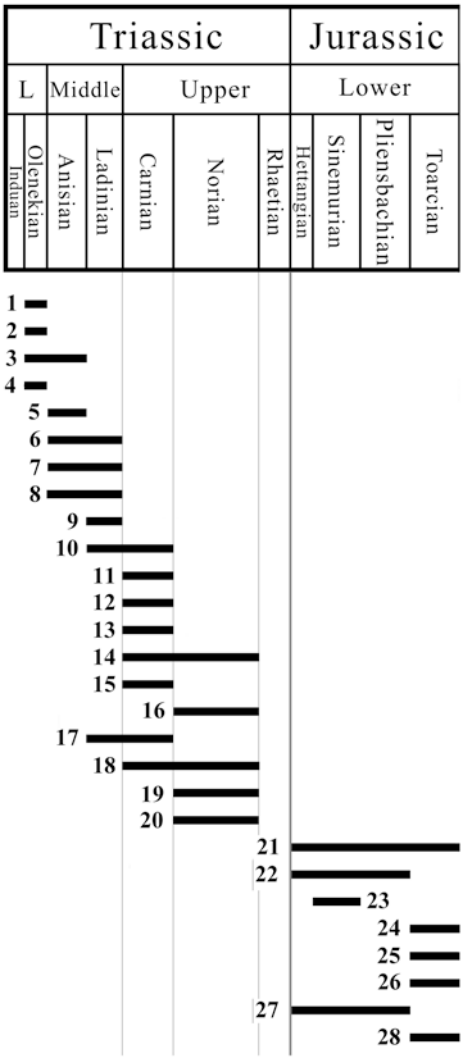

Fig. 8.22 Stratigraphic distribution of the ichthyosaurian genera in the Triassic and Jurassic, after Ji et al. (2016), modified and redrawn

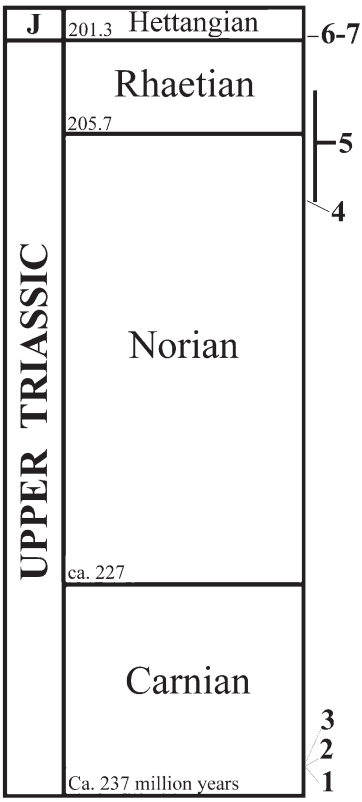

Fig. 8.23 Last and first appearances of some clades of marine reptiles in the Upper Triassic. Legend: *1* first plesiosaur (*Bobosaurus*), *2* last 'pachypleurosaurs', *3* last nothosauroids, *4* last *Tanystropheus, 5* *Pachystropheus* range, first UK plesiosaurs and last placodonts (UK Fissure Fillings and bone beds), *6* Pre-*planorbis* beds, and *7* possibly last phytosaur record

Carnian to reappear at the end of the middle Norian after a gap of at least 20 million years. They possibly occur in the lower Rhaetian, although they are undoubtedly much rarer than in the Middle Triassic or lower Carnian, but their presence in the upper Rhaetian (*Choristoceras marshi* Zone of ammonoid biostratigraphy) must be demonstrated. 'Pachypleurosaurians' probably disappeared at the end of the Middle Triassic and surely they do not occur in the upper Carnian (Tuvalian), as it is also the case of the nothosauroids (Fig. 8.23). As far as we know, the only pistosaurians documented in the upper Norian-lower Rhaetian interval are the plesiosaurs (Fig. 8.23); their presence in the upper Rhaetian is to be demonstrated, but they surely existed during the late Rhaetian given their diversification at the very beginning of the Jurassic. The record of other marine reptiles is quite scanty in the Upper Triassic. Thalattosaurs are relatively common in the Carnian and Norian, but apparently they are not recorded from the Rhaetian (Fig. 8.23). Turtles obviously crossed the Tr-J boundary, although we have no record of them from the Rhaetian. Phytosaurs possibly crossed the Tr-J boundary, but even if they did it, they did not go further than the base of the Jurassic. The last tanystropheids are late Norian in age (Fig. 8.23). The presence of *Pachystropheus*—essentially a late Norian or early

Rhaetian taxon—from the upper Rhaetian is unclear. It is instead clear that there is a strong taphonomic bias regarding marine reptiles in the Rhaetian, preventing understanding of whether significant extinctions of marine reptiles at the Tr-J boundary actually occurred or not. While a gradualistic, or stepwise pattern of extinction is exhibited by well-sampled marine invertebrate clades, including bivalves, and ammonoids, which show intervals of concentrated extinction prior to the end of the Triassic, most notably at the end of the Norian and throughout the Rhaetian (see, Hallam and Wignall 1997; Tanner et al. 2004; McRoberts et al. 1995; Tackett and Bottjer 2012). The marine vertebrates apparently do not show a peak of extinctions at the end of the Triassic. On the other hand, the absence of Rhaetian vertebrate-bearing *Konservat Lagerstätten* and the rarity of the Norian ones render the fossil record too scanty, thus it is difficult to make a reliable picture of the real pattern of marine reptile extinctions at the end of the Triassic.

References

Albers PCH, Rieppel O (2003) A new species of the sauropterygian genus *Nothosaurus* from the Lower Muschelkalk of Winterswijk, the Netherlands. J Paleontol 77:738–744

Allard H, Carpenter SC, Duffin CG, Benton MJ (2015) Microvertebrates from the classic Rhaetian bone beds of Manor Farm Quarry, near Aust (Bristol, UK). Proc Geol Assoc 126(6):762–776

Balini M, Renesto S (2012) *Cymbospondylus* vertebrae (Ichthyosauria, Shastasauridae) from the Late Anisian Prezzo Limestone (Middle Triassic, Southern Alps) with an overview of the chronostratigraphic distribution of the group. Riv Ital Paleontol Stratigr 118(1):155–172

Bardet N (1994) Extinction events among Mesozoic marine reptiles. Hist Biol 7:313–324

Bassani F (1886) Sui Fossili e sull' età degli schisti bituminosi triasici di Besano in Lombardia. Atti Soc Ital Sci Nat 19:15–72

Baur G (1887) On the phylogenetic arrangement of the Sauropsida. J Morphol 1:93–104

Benson RBJ, Bates KT, Johnson MR, Withers PJ (2011) Cranial anatomy of *Thalassiodracon hawkinsii* (Reptilia, Plesiosauria) from the Early Jurassic of Somerset, United Kingdom. J Vertebr Paleontol 31(3):562–574

Benson RBJ, Butler RJ (2011) Uncovering the diversification history of marine tetrapods: ecology influences the effect of geological sampling biases. Spec Publ Geol Soc London 358:191–208

Benson RBJ, Butler RJ, Lindgren J, Smith AS (2010) Mesozoic marine tetrapod diversity: mass extinctions and temporal heterogeneity in geological megabiases affecting vertebrates. Proc R Soc Lond B 277:829–834

Benson RBJ, Evans M, Druckenmiller PS (2012) High diversity, low disparity and small body size in plesiosaurs (Reptilia, Sauropterygia) from the Triassic-Jurassic boundary. PLoS One 7:1–15

Benton MJ, Spencer PS (1995) Fossil reptiles of Great Britain. In: Geological conservation review series, vol 10. Chapman and Hall, London, pp 1–386

Benton MJ, Zhang Q, Hu S, Chen ZQ, Wen W, Liu J, Huang J, Zhou C, Xie T, Tong J, Choo B (2013) Exceptional vertebrate biotas from the Triassic of China, and the expansion of marine ecosystems after the Permo–Triassic mass extinction. Earth-Sci Rev 137:85–128

Bizarrini F, Prosser G, Prosser FI, Prosser I (2003) Osservazioni preliminari sui resti di vertebrati della Formazione di S. Cassiano del Bosco di Stuores (Dolomiti nord-orientali). Ann Mus Civ Rovereto 17:137–148

Brandner R, Poleschinski W (1986) Stratigraphie und Tektonik am Kalkalpensüdrand zwischen Zirl und Seefeld in Tirol (Excursion D am 3. April 1986). Jb Mitteil ob geol Verein 68:67–92
de Broin F (1984) *Proganochelys ruchae* n. sp., chélonien du Trias supérieur de Thaïlande. St Geol Salmanticensia (Stvdia Palaeochelonіologica 1) 1:87–97
Brotzen F (1956) Stratigraphical studies on the Triassic vertebrate fossils from Wadi Raman, Israel. Arkiv for Mineralogi Geologi 2:191–217
Buffetaut E (1993) Phytosaurs in time and space. Paleontologia Lombarda 2:39–44
Callaway JM, Massare JA (1989) *Shastasaurus altispinus* (Ichthyosauria, Shastasauridae) from the Upper Triassic of the El Antimonio District, Northwestern Sonora, Mexico. J Paleontol 63:930–939
Camp CL (1976) Vorläufige Mitteilungüber grosse Ichthyosaurier aus der oberen Trias von Nevada. Österreich Akad Wissenschaf, Mathematisch-Naturwissenschaftliche Klasse, Sitzungsberichte. Abt I 185:125–134
Camp CL (1980) Large ichthyosaurs from the Upper Triassic of Nevada. Palaeontographica A 170:139–200
Carulli GB, Cozzi A, Longo Salvador G, Pernancic E, Podda F, Ponton M (2000) Geologia delle Prealpi Carniche. Note illustrative alla carta geologica delle Prealpi Carniche, vol 44 (e carta geologica alla scala 1:50.000). Pubbl Mus Friul St Nat, Udine, p 47
Chen X, Cheng L (2003) A new species of large-sized and long-body ichthyosaur from the Late Triassic Guanling biota, Guizhou, China. Geol Bull China 22:228–235
Chen X, Cheng L, Sander PM (2007) A new species of *Callawayia* (Reptilia: Ichthyosauria) from the Late Triassic in Guanling, Guizhou. Geol China 34:974–982
Chen X, Sander PM, Cheng L, Wang X (2013) A New Triassic Primitive Ichthyosaur from Yunnan, South China. Acta Geol Sin 87(3):672–677
Cheng L (2003) A new species of Triassic Thalattosauria from Guanling, Guizhou. Geol Bull China 22:274–277
Cheng L, Chen X, Wang C (2007a) A new species of Late Triassic *Anshunsaurus* (Reptilia: Thalattosauria) from Guizhou Province. Acta Geol Sin 81(10):1345–1351
Cheng L, Chen X, Zhang B, Cai Y (2011) New Study of *Anshunsaurus huangnihensis* Cheng, 2007 (Reptilia: Thalattosauria): Revealing its Transitional Position in Askeptosauridae. Acta Geol Sin 85(6):1231–1237
Cheng YN, Wu XC, Li C, Sato T (2007b) A new thalattosaurian (Reptilia: Diapsida) from the Upper Triassic of Guizhou, China. Vertebrata PalAsiatica 45:246–260
Conybeare WD (1822) Additional notices on the fossil genera *Ichthyosaurus* and *Plesiosaurus*. Trans Geol Soc London 2(1):103–123
Cruickshank ARI (1994) A juvenile plesiosaur (Plesiosauria: Reptilia) from the Lower Lias (Hettangian: Lower Jurassic) of Lyme Regis, England: a Pliosauroid-plesiosaurid intermediate?. Zool J Linnean Soc 112:151–78
Cuny G (1995) French vertebrate faunas and the Triassic- Jurassic boundary. Palaeogeogr Palaeoclimatol Palaeoecol 119:343–358
Dalla Vecchia FM (1994) Reptile remains from the Middle-Upper Triassic of Carnic and Julian Alps (Friuli-Venezia Giulia, Northeastern Italy). Gortania—Atti Mus Friul St Nat 15(1993):49–66
Dalla Vecchia FM (2000) *Tanystropheus* (Archosauromorpha, Prolacertiformes) remains from the Triassic of the Northern Friuli (NE Italy). Riv Ital Paleontol Stratigr 106(2):135–140
Dalla Vecchia FM (2006) A new sauropterygian reptile with plesiosaurian affinity from the Late Triassic of Italy. Riv Ital Paleontol Stratigr 112(2):207–225
Dalla Vecchia FM (2008a) Vertebrati fossili del Friuli—450 milioni di anni di evoluzione. Mem Mus Friulano St Nat 50, Museo Friulano di Storia Naturale, Udine, 304 pp, 279 figs (In Italian)
Dalla Vecchia FM (2008b) First Record of *Simosaurus* (Sauropterygia Nothosauroidea) from the Carnian (Late Triassic) of Italy. Riv Ital Paleontol Stratigr 114(2):273–285
Dalla Vecchia FM, Avanzini M (2002) New findings of isolated remains of Triassic reptiles from Northeastern Italy. Boll Soc Paleontol Ital 41(2–3):215–235

Dalla Vecchia FM, Carnevale G (2011) Ceradontoid (Dipnoi) calvarial bones from the Triassic of Fusea, Carnic Alps: the first Italian lungfish. It J Geosci 130(1):128–135
De Zanche V, Gianolla P, Mietto P, Siorpaes C, Vail PR (1993) Triassic sequence stratigraphy in the Dolomites (Italy). Mem Sci Geol 45:1–23
Diedrich CG (2010) Palaeoecology of *Placodus gigas* (Reptilia) and other placodontids—evidence for convergent evolution with Sirenia. Palaeogeog Palaeoclim Paleoecol 285:287–306
Diedrich CG (2011a) The shallow marine placodont *Cyamodus* of the central European Germanic Basin: its evolution, paleobiogeography and paleoecology. Hist Biol 23:391–409
Diedrich CG (2011b) Fossil middle triassic "sea cows"—placodont reptiles as macroalgae feeders along the north-western Tethys coastline with pangaea and in the Germanic basin. Nat Sci 3:9–27
Druckenmiller P (2015) An exceptional new thalattosaur (Reptilia) from the Late Triassic (Norian) Hound Island Volcanics of Southeastern Alaska. Geological Society of America 111th Annual Meeting (11–13 May 2015) Abstracts with Programs. 47(4):54
Druckenmiller PS, Patrick S, Russell AP (2008) Skeletal anatomy of an exceptionally complete specimen of a new genus of plesiosaur from the Early Cretaceous (Early Albian) of northeastern Alberta, Canada. Palaeontographica Abt A 283:1–3
Evans SE, Hecht MK (1993) A history of an extinct reptilian clade, the Choristodera: longevity, Lazarus taxa, and the fossil record. Evol Biol 27:323–338
Ezcurra MD (2016) The phylogenetic relationships of basal archosauromorphs, with an emphasis on the systematics of proterosuchian archosauriforms. PeerJ 4:e1778. https://doi.org/10.7717/peerj.1778
Fabbri M, Dalla Vecchia FM, Cau A (2014) New information on *Bobosaurus forojuliensis* (Reptilia: Sauropterygia): implications for plesiosaurian evolution. Hist Biol 26(5):661−669
Fraas E (1913) *Proterochersis*, eine pleurodire Schildkröte aus dem Keuper. Jahreshefte Vereins vaterländische Naturkunde in Württemberg 80:13–30
Furrer H (1993) Stratigraphie un facies der Trias/Jura Grenzschichten in den oberostalpinen Decken Graubündens. Unpublished Ph.D. Thesis, University of Zurich, 99 pp
Gaffney ES (1990) The comparative osteology of the Triassic turtle *Proganochelys*. Bull Am Mus Nat Hist 194:1–263
Gozzi E, Renesto S (2003) A complete specimen of *Mystriosuchus* (Reptilia, Phytosauria) from the Norian (Late Triassic) of Lombardy (Northern Italy). Riv Ital Paleontol Stratigr 109(3):475–498
Gregory WK (1946) Pareiasaurs versus placodonts as near ancestors to the turtles. Bull Am Mus Nat Hist 86:275–326
Haas G (1969) The armour of placodonts from the Muschelkalk of Wadi Ramon (Israel). Israel J Zool 18(2–3):135–147
Hagdorn H, Rieppel O (1999) Stratigraphy of Marine reptiles in the Triassic of Central Europe. Zentbl Geol Palaeont 1(7–8):651−−678
Hallam A, Wignall PB (1997) Mass extinctions and sea level changes. Earth Sci Rev 48(4):217–250
Hillebrandt A, Krystyn L, Kürschner WM, Bonis NR, Ruhl M, Richoz S, Schobben MAN, Urlichs M, Bown PR, Kment K, McRoberts CA, Simms M, Tomãsových A (2013) The Global Stratotype Sections and Point (GSSP) for the base of the Jurassic System at Kuhjoch (Karwendel Mountains, Northern Calcareous Alps, Tyrol, Austria). Episodes 36(3):162–198
Holmes R, Cheng Y-N, Wu XC (2008) New information on the skull of *Keichosaurus hui* (Reptilia: Sauropterygia) with comments on sauropterygian interrelationships. J Vertebr Paleontol 28(1):76–84
von Huene F (1925) *Shastasaurus*-Reste in der alpinen Trias. Zentbl Mineral Geol Paläont B 1925:412–417

von Huene F (1935) Ein Rhynchocephale aus dem Rhät *(Pachystropheus* n. g.) Neu Jahrbuch Mineral Geolog Paläontol 74:441–447
von Huene F (1936) *Henodus chelyops*, ein neuer Placodontier. Palaeontographica A 84:99–147
Jadoul F, Masetti D, Cirilli S, Berra F, Claps S, Frisia S (1994) Norian-Rhaetian stratigraphy and paleogeographic evolution of the Lombardy Basin (Bergamasc Alps). In: 15th IAS Regional Meeting, April 1994, Ischia, Italy, Field Excursions, Excursion B1:5–38
Jaekel O (1902) Wirbelthierreste aus der Trias des Bakonyerwaldes. Result Wissenschaft Erforsch Balatonsees 1. Teil Paläontolo Anh III(7):1–22
Jaekel O (1907) *Placochelys placodonta* aus der Obertrias des Bakony. Resultate der Wissenschaftlichen Erforschung des Balatonsees 8:3–90
Ji C, Jiang DY, Motani R, Rieppel O, Hao WC, Sun ZY (2016) Phylogeny of the Ichthyopterygia incorporating recent discoveries from South China. J Vertebr Paleontol 36(1):e1025956
Jiang DA, Maisch MW, Sun SL, Matzke AT, Hao WC (2004) A new species of *Xinpusaurus* (Thalattosauria) from the Upper Triassic of China. Jf Vertebr Paleontol 24(1):80–88
Jiang DY, Motani R, Huang JD, Tintori A, Hu YC, Rieppel O, Fraser NC, Ji C, Kelley NP, Fu WL, Zhang R (2016) A large aberrant stem ichthyosauriform indicating early rise and demise of ichthyosauromorphs in the wake of the end-Permian extinction. Nature Scientific Reports 6:1–9. https://doi.org/10.1038/srep26232
Jiang DY, Motani R, Tintori A, Rieppel O, Chen GB, Huang JD, Sun ZY, Ji C (2014) The Early Triassic eosauropterygian *Majiashanosaurus discocoracoidis*, gen. et sp. nov. (Reptilia, Sauropterygia), from Chaohu, Anhui Province, People's Republic of China. J Vertebr Paleontol 34(5):1044–1052
Jiang DY, Rieppel O, Fraser NC, Motani R, Hao WC, Tintori A, Sun YL, Sun ZY (2011) New information on the protorosaurian reptile *Macrocnemus fuyuanensis* Li et al., 2007, from the Middle/Upper Triassic of Yunnan, China. J Vertebr Paleontol 31(6):1230–1237
Jiang DY, Rieppel O, Motani R, Hao WC, Sun YL, Schmitz L, Sun ZY (2008) A new Middle Triassic Eosauropterygian (Reptilia, Sauropterygia) from Southwestern China. J Vertebr Paleontol 28(4):1055–1062
Joyce W (2015) The origin of turtles: a paleontological perspective. J Experimental Zoology Part B Molecular and Developmental Evolution 00B:1–13
Joyce WG, Lucas SG, Scheyer TM, Heckert AB, Hunt AP (2009) A thin-shelled reptile from the Late Triassic of North America and the origin of the turtle shell. Proc R Soc B 276(1656):507–513
Karl HV, Arp G, Siedersbeck E, Reitner J (2014) A large ichthyosaur vertebra from the lower Kössen Formation (Upper Norian) of the Lahnewiesgraben near Garmisch- Partenkirchen, Germany. Göttingen Contr Geosci 77:191–197
Kelley NP, Motani R, Jiang DY, Rieppel O, Schmiz L (2014) Selective extinction of Triassic marine reptiles during long-term sea-level changes illuminated by seawater strontium isotopes. Palaeogeogr Palaeoclimatol Palaeoecol 400:9–16
Kelley NP, Pyenson ND (2015) Evolutionary innovation and ecology in marine tetrapods from the Triassic to the Anthropocene. Science 348(6232):301
Ketchum HF, Benson RBJ (2010) Global interrelationships of Plesiosauria (Reptilia, Sauropterygia) and the pivotal role of taxon sampling in determining the outcome of phylogenetic analyses. Biol Rev Camb Philos Soc 85(2):361–392
Korte C, Hesselbo SP, Jenkyns HC, Rickaby REM Spötl C (2009) Palaeoenvironmental significance of carbon- and oxygen-isotope stratigraphy of marine Triassic–Jurassic boundary sections in SW Britain. J Geol Soc Lond 166:431–445
Kosch BF (1990) A revision of the skeletal reconstruction of *Shonisaurus popularis* (Reptilia: Ichthyosauria). J Vertebr Paleontol 10(4):512–514
Kovacs S, Less G, Piros D, Réti Z, Ròth L (1989) Triassic Formations of the Aggtelek-Rudabanya Mountains, Northeastern Hungary. Acta Geol Ungarica 32:31–63
Krahl A, Klein N, Sander PM (2013) Evolutionary implications of the divergent long bone histologies of *Nothosaurus* and *Pistosaurus* (Sauropterygia, Triassic). Evol Biol 13:123

Krystyn L (2010) Decision report of the defining event for the base of the Rhaetian Stage. Albertiana 38:11–12
Krystyn L, Bouquerel H, Kuerschner W, Richoz S, Gallet Y (2007a) Proposal for a candidate GSSP for the base of the Rhaetian Stage. In: Lucas SG, and Spielman JA (eds) The Global Triassic: New Mexico Mus Nat Hist Sci Bull 41:189–199
Krystyn L, Richoz S, Gallet Y, Bouquerel H, Kürschner WM, Spötl C (2007b) Updated bio- and magnetostratigraphy from Steinbergkogel (Austria), candidate GSSP for the base of the Rhaetian Stage. Albertiana 36:164–173
Kuhn-Schnyder E (1952) Die Triasfauna der Tessiner Kalkalpen. XVII. *Askeptosaurus italicus* Nopcsa. Schweiz Palaontol Abhandl 69:1–73
Lécuyer BA, Amiot VP, Bardet N, Buffetaut E, Cuny G, Fourel F, Martineau F, Mazin JM, Prieur A (2010) Regulation of body temperature by some Mesozoic marine reptiles. Science 328(5984):1379–1382
Lee MSY (2013) Turtle origins: Insights from phylogenetic retrofitting and molecular scaffolds. J Evol Biol 26(12):2729
Li C (1999) Ichthyosaur from Guizhou, China. Chin Sci Bull 44:1318–1321
Li C (2000) Placodont (Reptilia: Placodontia) from Upper Triassic of Guizhou, Southwest China. Vertebr Palasiatica 38:314–317
Li C (2007) A juvenile *Tanystropheus* sp. (Protorosauria, Tanystropheidae) from the Middle Triassic of Guizhou, China. Vertebr Palasiatica 45:37–427
Li C, Rieppel O (2002) A new cyamodontoid placodont from Triassic of Guizhou, China. Chin Sci Bull 47:156–159
Li C, Wu XC, Rieppel O, Wang LT, Zhao LJ (2008) An ancestral turtle from the Late Triassic of southwestern China. Nature 456:497–501
Li C, You HL (2002) *Cymbospondylus* from the Upper Triassic of China. Vertebr Palasiatica 40:9–16
von Lilienstern HR (1939) Fährten und Spuren im Chirotheriumsandstein von Südthüringen. Fortschr Geolog und Paläontol 12(40):293–389
Lin K, Rieppel O (1998) Functional morphology and ontogeny of *Keichousaurus hui* (Reptilia, Sauropterygia). Fieldiana Geol (NS) 39:1–35
Liu J (1999) Sauropterygian from Triassic of Guizhou, China. Chin Sci Bull 44(4):1312–1315
Liu J (2007) A juvenile specimen of *Anshunsaurus* (Reptilia: Thalattosauria). Am Mus Novit 3582:1–9. https://doi.org/10.1206/0003-
Liu J, Hu SX, Rieppel O, Jiang DY, Benton MJ, Kelley NP, Zhou CY, Wen W, Huang JY Xie T, Lu T (2014) A gigantic nothosaur (Reptilia: Sauropterygia) from the Middle Triassic of SW China and its implication for the Triassic biotic recovery. Nature Sci Rep 4:7142. https://doi.org/10.1038/srep07142
Liu J, Lin WB, Rieppel O, Sun ZY, Li ZG, Lu H, Jiand DY (2015) A new specimen of *Diandongosaurus acutidentatus* (Sauropterygia) from the Middle Triassic of Yunnan, China. Vertebr Palasiatica 10:281–290
Liu J, Rieppel O (2001) A second thalattosaur from the Triassic of Guizhou, China. Vert Palasiatica 39:77–87
Liu J, Rieppel O (2005) Restudy of *Anshunsaurus huangguoshuensis* (Reptilia: Thalattosauria) from the Middle Triassic of Guizhou, China (PDF). Am Mus Novit 3488:1–34. https://doi.org/10.1206/0003-0082(2005)488
Liu J, Rieppel O, Jiang DY, Aitchison JC, Motani R, Zhang QY, Zhou CY, Sun YY (2011) A new pachypleurosaur (Reptilia: Sauropterygia) from the lower Middle Triassic of southwestern China and the phylogenetic relationships of Chinese pachypleurosaurs. J Vertebr Paleontol 31(2):292–302
Liu J, Zhao LJ, Li C, He T (2013) Osteology of *Concavispina biseridens* (Rptilia: Thalattosauria) from the Xiaowa Formation (Crnian), Guanling, Guizhou, China. J Paleontol 87:341–350
Lovelace D, Lovelace S (2012) Paleoenvironments and paleoecology of a Lower Triassic invertebrate and vertebrate ichnoassemblage from the Red Peak Formation (Chugwater Group), central Wyoming. PALAIOS 27(9):637–658

Lucas SG (2002) *Toretocnemus*, a Late Triassic ichthyosaur from California, U.S.A. and Sonora, Mexico in Heckert AB, Lucas SG (eds) Upper Triassic Stratigraphy and Paleontology. N M Mus Nat Hist Sci Bull 21:275–278

Lucas SG, Tanner LH (2015) End-Triassic nonmarine biotic events. Journ Paleogeogr 4:331–348

Lucas SG, Tanner LH, Donohoo-Hurley LL, Geissman JW, Kozur HW, Heckert AB, Weems RE (2011) Position of the Triassic–Jurassic boundary and timing of the end-Triassic extinctions on land: data from the Moenave Formation on the southern Colorado Plateau, USA. Palaeogeogr Palaeoclimatol Palaeoecol 302(2011):194–205

Luo Y, Yu Y (2002) The restudy on the skull and mandible of *Xinpusaurus suni*. Guizhou Geol 19:71–75

Ma LT, Jiang DY, Rieppel O, Motani R, Tintori A (2015) A new pistosauroid (Reptilia, Sauropterygia) from the late Ladinian Xingyi marine reptile level, southwestern China. J Vertebr Paleontol 35(1):e881832

Maisch MW (2010) Phylogeny, systematics, and origin of the Ichthyosauria—the state of the art. Palaeodiversity 3:151–214

Maisch MW (2015) A juvenile specimen of *Anshunsaurus huangguoshuensis* Liu, 1999 (Diapsida: Thalattosauria) from the Upper Triassic of China. Palaeodiversity 8:71–87

Maisch MW, Kapitzke M (2010) A presumably marine phytosaur (Reptilia: Archosauria) from the pre-planorbis beds (Hettangian) of England. Neues Jahrb Geol Paläont Abhandl 257(3):373–379

Maisch MW, Matzke AT (2000) The Ichthyosauria. Stuttgarter Beitr B 298:1–159

Maisch MW, Matzke AT (2004) Observations on Triassic ichthyosaurs. Part XIII: New data on the cranial osteology of *Cymbospondylus petrinus* (Leidy, 1868) from the Middle Triassic Prida Formation of Nevada. Neu Jahrb Geol Paläont Monat 2004(6):370–384

Maron M, Rigo M, Bertinelli A, Katz ME, Godfrey L, Zaffani M, Muttoni G (2015) Magnetostratigraphy, biostratigraphy, and chemostratigraphy of the Pignola-Abriola section: new constraints for the Norian-Rhaetian boundary. Geol Soc Am Bull 127(7):962–974

Massare JM, Callaway JA (1990) The affinities and ecology of Triassic ichthyosaurs. Bull Geol Soc Am 102:409–416

Matsumoto R, Evans SE (2010) Choristoderes and the freshwater assemblages of Laurasia. J Iber Geol 36:253–274

Maxwell EE, Kear BP (2013) Triassic ichthyopterygian assemblages of the Svalbard archipelago: a reassessment of taxonomy and distribution. GFF J Geol Soc Sweden 135(1):85–94

Mazin JM, Pinna G (1993) Palaeoecology of the armoured placodonts. Paleontol Lombarda NS 2:83–91

Mazin JM, Sander PM (1993) Palaeobiogeography of the Early and Late Triassic Ichthyopterygia. Paleontol Lombarda NS 2:93–107

McGowan C (1991) An ichthyosaur forefin from the Triassic of British Columbia exemplifying Jurassic features. Can J Earth Sci 28(10):1553–1560

McGowan C (1993) A new species of large, long-snouted ichthyosaur from the English lower Lias. Can J Earth Sci 30(6):1197–1204

McGowan C (1994) A new species of *Shastasaurus* (Reptilia:Ichthyosauria) from the Triassic of British Columbia. The most complete exemplar of the genus. J Vertebr Paleontol 14(2):168–179

McGowan C (1995) A remarkable small ichthyosaur from the Upper Triassic of British Columbia, representing a new genus and species. Can J Earth Sci 32:292–303

McGowan C (1996) A new and typically Jurassic ichthyosaur from the Upper Triassic of British Columbia. Can J Earth Sci 33:24–32

McGowan C (1997) A transitional ichthyosaur fauna. In: Callaway JM, Nicholls EL (eds) Ancient marine reptiles. Academic Press, San Diego, CA, pp 61–80

McGowan C, Milner AC (1999) A new Pliensbachian ichthyosaur from Dorset, England. Palaeontology 42:761–768

McGowan C, Motani R (1999) A reinterpretation of the Upper Triassic ichthyosaur *Shonisaurus*. J Vertebr Paleontol 19(1):42–49

McGowan C, Motani R (2003) Handbook of Paleoherpetology, Part 8. Ichthyopterygia. Verlag Dr. Friedrich Pfeil, Munich. 175 pp
McRoberts CA, Newton CR, Allasinaz A (1995) End-Triassic bivalve extinction: Lombardian Alps, Italy. Hist Biol 9:297–317
Mears EM, Rossi V, MacDonald E, Coleman G, Davies TG, Arias-Riesgo V, Hildebrandt C, Thiel H, Duffin CJ, Whiteside DI, Benton MJ (2016) The Rhaetian (Late Triassic) vertebrates of Hampstead Farm Quarry, Gloucestershire, UK. Proc Geol Assoc 127:478–505
Merriam JC (1895) On some reptilian remains from the Triassic of northern California. Am J Sci 50:55–57
Merriam JC (1902) Triassic Ichthyopterygia from California and Nevada. Bull Dep Geol Univ Calif 3:63–108
Merriam JC (1904) A new marine reptile from the Triassic of California. Univ Calif Publ Bull Dep Geol 3:419–421
Merriam JC (1905) The Thalattosauria, a group of marine reptiles from the Triassic of California. Mem Calif Acad Sci 5:1–38
Merriam JC (1908) Notes on the osteology of the thalattosaurian genus *Nectosaurus*. Univ Calif Publ Bull Dep Geol 5:217–223
von Meyer H (1856) Mittheilungen an Professor Bronn gerichtet. Neues Jahrb Miner 1856:824–825
von Meyer H (1858) *Psephoderma Alpinum* aus dem Dachstein-Kalke der Alpen. Neues Jahrb Miner Neues Jahrb Miner 858:646–650
von Meyer H (1867) *Psephoderma Anglicum* aus dem Bone Bed in England. Palaeontographica 15:261–263
Motani R (1999) Phylogeny of the Ichthyopterygia. J Vertebr Paleontol 19(3):472–495
Motani R (2005) Evolution of fish-shaped reptiles (Reptilia:Ichthyopterygia) in their physical environments and constraints. Annu Rev Earth Planet Sci 33:395–420
Motani R (2009) The evolution of marine reptiles. Evolution: Education and Outreach 2:224–235
Motani R, Ji C, Tomita T, Kelley N, Maxwell E, Jiang DY (2013) Absence of suction feeding ichthyosaurs and its implications for Triassic Mesopelagic paleoecology. PLoS One 8(12):e66075
Motani R, Jiang DY, Chen GB, Tintori A, Rieppel O, Ji C, Huang JD (2015) A basal ichthyosauriform with a short snout from the Lower Triassic of China. Nature 517:485–488
Motani R, Manabe M, Dong ZM (1999) The status of *Himalayasaurus tibetensis* (Ichthyopterygia). Paludicola 2:174–181
Müller J (2004) The relationships among diapsid reptiles and the influence of taxon selection. In: Arratia G, Wilson MVH, Cloutier R (eds) Recent advances in the origin and early radiation of vertebrates. Verlag Dr. Friedrich Pfeil, München, pp 379–408
Müller J (2005) The anatomy of *Askeptosaurus italicus* from the Middle Triassic of Monte San Giorgio and the interrelationships of thalattosaurs (Reptilia, Diapsida). Can J Earth Sci 42(7):1347–1367
Müller J (2007) First record of a thalattosaur from the Upper Triassic of Austria. J Vertebr Paleontol 27(1):236–240
Müller J, Renesto S, Evans SE (2005) The marine diapsid reptile *Endennasaurus* from the Upper Triassic of Italy. Palaeontology 48(1):15–30
Muttoni G, Kent DV, Jadoul F, Olsen PE, Rigo M, Galli MT, Nicora A (2010) Rhaetian magnetobiostratigraphy from the southern Alps (Italy): constraints on Triassic chronology. Palaeogeogr Palaeoclimatol Palaeoecol 285:1–16. https://doi.org/10.1016/j.palaeo.2009.10.014
Neenan JM, Klein N, Scheyer TM (2013) European origin for sauropterygian marine reptiles and the evolution of placodont crushing dentition. Nature Comm 4:1621. https://doi.org/10.1038/ncomms2633
Neenan JM, Li C, Rieppel O, Scheyer TM (2015) The cranial anatomy of Chinese placodonts and the phylogeny of Placodontia (Diapsida: Sauropterygia). Zool J Linnean Soc 175(2):415–428

Neenan JM, Scheyer TM (2014) New specimen of *Psephoderma alpinum* (Sauropterygia, Placodontia) from the Late Triassic of Schesaplana Mountain, Graubünden, Switzerland. Swiss J Geosci 107(2):349–357
Nesbitt SJ (2011) The early evolution of archosaurs: relationships and the origin of major clades. Bull Am Mus Nat Hist 352:1–292
Newell ND (1952) Periodicity in invertebrate evolution. J Paleontol 26:371–385
Nicholls EL (1999) A reexamination of *Thalattosaurus* and *Nectosaurus* and the relationships of the Thalattosauria (Reptilia, Diapsida). PaleoBios 19:1–29
Nicholls EL, Brinkman DB (1993) New thalattosaurs (Reptilia: Diapsida) from the Triassic Sulphur Mountain Formation of Wapiti Lake, British Columbia. J Paleontol 67:263–278
Nicholls EL, Chen W, Manabe M (2003) New material of Qianichtyosaurus Li, 1999 (Reptilia, Ichthyosauria) from the late Triassic of southern China, and Implications for the Distribution of Triassic Ichthyosaurs. J Vertebr Paleontol 22(4):759–765
Nicholls EL, Manabe M (2001) A new genus of ichthyosaur from the Late Triassic Pardonet Formation of British Colombia: bridging the Triassic Jurassic gap. Can J Earth Sci 38:983–1002
Nicholls EL, Manabe M (2004) Giant ichthyosaurs of the Triassic–a new species of *Shonisaurus* from the Pardonet Formation (Norian: Late Triassic) of British Columbia. J Vertebr Paleontol 24(3):838–849
Nosotti S (2007) *Tanystropheus longobardicus* (Reptilia, Protorosauria): re-interpretations of the anatomy based on new specimens from the Middle Triassic of Besano (Lombardy, northern Italy). Mem Soc Ital Sci Nat Mus Civ St Nat Milano 35:1–88
Olsen PE (1979) A new aquatic eosuchian from the Newark Supergroup (Late Triassic–Early Jurassic) of North Carolina and Virginia. Postilla 176:1–14
Otero RA, Soto-Acuña S, Vargas AO, Rubilar-Rogers D, Yury-Yáñez RE, Gutstein CS (2014) Additions to the diversity of elasmosaurid plesiosaurs from the Upper Cretaceous of Antarctica. Gondwana Res 26(2):772–784
Owen R (1840) Report on British fossil reptiles. Report of the Ninth Meeting of the British Association for the Advancement of Science, Reports on the State of Science:43–126
Peyer B (1931) Die Triasfauna der Tessiner Kalkalpen III. Placodontia. Abhandl Schweiz Paläontol Gesells 51:1–25
Peyer B (1936a) Die Triasfauna der Tessiner Kalkalpen. X. *Clarazia schinzi* nov. gen. nov. sp. Schweiz palaeontol Abhandl 57:1–61
Peyer B (1936b) Die Triasfauna der Tessiner Kalkalpen. XI. *Hescheleria ruebeli* nov. gen. nov. sp. Schweiz Palaontol Abhandl 58:1–48
Pinna G (1976) Osteologia del cranio del rettile placodonte *Placochelyanus stoppanii* (Osswald 1930) basata su un nuovo esemplare del Retico Lombardo. Atti Soc Ital Sci Nat Mus Civ St Nat Milano 117:3–45
Pinna G (1978) Descrizione di un nuovo esemplare di Placochelydae del Retico Lombardo (*Psephoderma alpinum* Meyer, 1858) e discussione sulla sinonimia *Psephoderma-Placochelyanus*. Atti Soc It Sci Nat Mus Civ St Nat Milano 119:341–352
Pinna G (1980) Lo scheletro postcraniale di *Cyamodus hildegardis* Peyer, 1931 descritto su un esemplare del Triassico Medio Lombardo (Reptilia Placodontia). Atti Soc Ital Sci Nat Mus Civ St Nat Milano 121:275–306
Pinna G (1990a) Notes on stratigraphy and geographical distribution of placodonts. Atti Soc Ital Sci Nat Mus Civ St Nat Milano 131:145–156
Pinna G (1990b) *Protenodontosaurus italicus* n.g., n.sp., un nuovo placodonte del Carnico italiano. Atti Soc Ital Sci Nat Mus Civ St Nat Milano 131:5–12
Pinna G, Mazin JM (1993) Stratigraphy and paleobiogeography of the Placodontia. Paleontol Lombarda NS 2:125–130
Pinna G, Nosotti S (1989) Anatomia, morfologia funzionale e paleoecologia del rettile placodonte *Psephoderma alpinum* Meyer, 1858. Mem Soc Ital Sci Nat Mus Civ St Nat Milano 25:17–50
Pinna G, Zucchi Stolfa ML (1979) Il cranio di *Placochelys placodonta* Jaekel, 1902, del Raibliano di Fusea (Udine). Atti Soc It Sci Nat Mus Civ St Nat Milano 120:307–313

Plöchinger B (1980) The Salzkammergut and its geological setting within the Northern Calcareous Alps. 2nd European Conodont Symposium, ECOS 2, Guidebook, Abstracts, p 62–65
Preto N, Spötl C, Mietto P, Gianolla P, Riva A, Manfrin S (2005) Aragonite dissolution, sedimentation rates and carbon isotopes in deepwater hemipelagites (Livinallongo Formation, Middle Triassic, northern Italy). Sediment Geol 181:173–194
Pritchard AC, Turner AH, Nesbitt SJ, Irmis RB, Smith ND (2015). Late Triassic tanystropheids (Reptilia, Archosauromorpha) from northern New Mexico (Petrified Forest Member, Chinle Formation) and the biogeography, functional morphology, and evolution of Tanystropheidae. J Vertebr Paleontol 35 (2): e911186–2
Renesto S (1984) A new Lepidosaur (Reptilia) from the Norian beds of the Bergamo Prealps. Riv Ital Paleontol Stratigr 90(2):156–167
Renesto S (1992) The anatomy and relationships of *Endennasaurus acutirostris* (Reptilia: Neodiapsida) from the Norian (Late Triassic) of Lombardy. Riv Ital Paleontol Stratigr 97(3–4):409–430
Renesto S (2005) A possible find of *Endennasaurus* (Reptilia, Thalattosauria) with a comparison between *Endennasaurus* and *Pachystropheus*. Neu Jahrb Geol Paläontol Monatsh 2005(2):118–128
Renesto S (2008) Remains of a juvenile phytosaur from the Late Triassic of Northern Italy. Riv Ital Paleontol Stratigr 114(1):155–160
Renesto S, Dalla Vecchia FM, Peters D (2002) Morphological evidence for bipedalism in the Late Triassic Prolacertiform reptile *Langobardisaurus*. Senckemberg Leth 82(1):95–106
Renesto S, Lombardo C (1999) Structure of the tail of a phytosaur (Reptilia, Archosauria) from the Norian (Late Triassic) of Lombardy (Northern Italy). Riv Ital Paleontol Stratigr 105(1):135–144
Renesto S, Paganoni A (1998) A phytosaur skull from the Norian (Late Triassic) of Lombardy (Northern Italy). Riv Ital Paleontol Stratigr 104(1):115–122
Renesto S, Tintori A (1995) Functional morphology and mode of life of the Late Triassic placodont *Psephoderma alpinum*, Meyer from the Calcare di Zorzino (Lombardy, N. Italy). Riv Ital Paleontol Stratigr 101(1):37–48
Rich VP, Rich T, Rieppel O, McClure HA (1999) A Middle Triassic Vertebrate Fauna from the Jilh Formation, Saudi Arabia. Neu Jahrb Geol Paläontol Abhandl 213(2):201–232
Rieppel O (1987) *Clarazia* and *Hescheleria*, a re-investigation of two problematic reptiles from the Middle Triassic of Monte San Giorgio, Switzerland. Palaeontograph A 195:101–129
Rieppel O (1989) The hind limb of *Macrocnemus bassanii* (Nopcsa) (Reptilia, Diapsida): development and functional anatomy. J Vertebr Paleontol 9(4):373–387
Rieppel O (1994) Osteology of *Simosaurus gaillardoti* and the relationships of stem-group Sauropterygia. Fieldiana Geol 28:1−−112
Rieppel O (1997) Sauropterygia from the Muschelkalk of Djebel Rehach, southern Tunisia. N Jb Geol Paläont 9:517–530
Rieppel O (1999a) Phylogeny and paleobiogeography of Triassic Sauropterygia: problems solved and unresolved. Palaeogeogr Palaeoclimatol Palaeoecol 153:1–15
Rieppel O (1999b) The sauropterygian genera *Chinchenia*, *Kwangsisaurus*, and *Sanchiaosaurus* from the Lower and Middle Triassic of China. J Vertebr Paleontol 19(2):321–337
Rieppel O (2000) Sauropterygia I—Placodontia, Pachypleurosauria, Nothosauroidea, Pistosauroidea. In: Wellnhofer P (ed) Encyclopedia of paleoherpetology. Verlag Dr. Friedrich Pfeil, Munich, p 134
Rieppel O (2001) The cranial anatomy of *Placochelys placodonta* Jaekel, 1902, and a review of the Cyamodontoidea (Reptilia, Placodonta). Fieldiana Geol 45:1–101
Rieppel O (2002a) Feeding mechanics in Triassic stem-group sauropterygians: the anatomy of a successful invasion of Mesozoic seas. Zool J Linnean Soc 135:33–63
Rieppel O (2002b) The dermal armor of the cyamodontoid placodonts (Reptilia, Sauropterygia): morphology and systematic value: Fieldiana. Geology 46:1–41
Rieppel O, Dalla Vecchia FM (2001) Marine Reptiles from the Triassic of the Tre Venezie, northeastern Italy. Fieldiana Geol 44:1–25

Rieppel O, Hagdorn H (1997) Paleobiogeography of Middle Triassic Sauropterygia in Central and Western Europe. In: Callaway JM, Nicholls EL (eds) Ancient marine reptiles. Academic Press, San Diego, CA, pp 121–144

Rieppel O, Liu J, Bucher H (2000) The first record of a thalattosaur reptile from the Late Triassic of Southern China (Guizhou Province, PR China). J Vertebr Paleontol 20(3):507–514

Rieppel O, Mazin JM, Tchernov E (1997) Speciation along rifting continental margins: a new nothosaur from the Negev (Israel). C R Acad Sci 325:991–997

Rieppel O, Müller J, Liu J (2005) Rostral structure in Thalattosauria (Reptilia, Diapsida). Can J Earth Sci 42:2081–2086

Rieppel O, Nosotti S (2002) A skull of *Cyamodus* (Sauropterygia, Placodontia) from the Triassic of Fusea, Province of Udine, Northeastern Italy. Atti Soc It Sci Nat Mus Civ St Nat Milano 142:173–183

Rieppel O, Wild R (1996) revision of the genus *Nothosaurus* (Reptilia. Sauropterygia) from the Germanic Triassic with comments on the status of *Conchiosaurus clavatus*. Fieldiana 1(34):1–82

Rieppel O, Yang DY, Fraser NC, Hao WC, Motani R, Sun YL, Sun ZY (2010) *Tanystropheus* cf. *T. longobardicus* from the Early Late Triassic of Guizhou Province, Southwestern China. J Vertebr Paleontol 30(4):1082–1089

Rieppel O, Zanon RT (1997) The interrelationships of Placodontia. Hist Biol 12:211−227

Sander PM (1989) The large ichthyosaur *Cymbospondylus buchseri*, sp. nov., from the Middle Triassic of Monte Giorgio (Switzerland), with a survey of the genus in Europe. J Vertebr Paleontol 9(2):163–173

Sander PM (2000) Ichthyosauria: their diversity, distribution, and phylogeny. Paläontol Z 74:1–35

Sander PM, Chen X, Cheng L, Wang X (2011) Short-snouted toothless ichthyosaur from China suggests Late Triassic diversification of suction feeding ichthyosaurs. PLoS One 6:e19480

Sander PM, Rieppel O, Bucher H (1997) A new pistosaurid (Reptilia: Sauropterygia) from the Middle Triassic of Nevada and its implications for the origin of the plesiosaurs. J Vertebr Paleontol 17(3):526–533

Sato T, Hasegawa Y, Manabe M (2006) A new Elasmosaurid plesiosaur from the Upper Cretaceous of Fukushima, Japan. Palaeontology 49(3):467–484

Scheyer TM (2007) Skeletal histology of the dermal armor of Placodontia: the occurrence of "postcranial fibro-cartilaginous bone" and its developmental implications. J Anat 211:737–753

Scheyer TM (2010) New interpretation of the postcranial skeleton and overall body shape of the placodont *Cyamodus hildegardis* Peyer, 1931 (Reptilia, Sauropterygia). Palaeontol Electron 13(2):15A–15p

Scheyer TM, Neenan JM, Renesto S, Saller F, Hagdorn H, Furrer H, Rieppel O, Tintori A (2012) Revised paleoecology of placodonts—with a comment on "The shallow marine placodont *Cyamodus* of the central European Germanic Basin: its evolution, paleobiogeography and paleoecology" by C.G. Diedrich (Historical Biology, iFirst article, 2011, 1–19). Hist Biol 24:257–267

Schoch RR, Sues HD (2015) A Middle Triassic stem-turtle and the evolution of the turtle body plan. Nature 523(7562):584–587

Schubert-Klempnauer H (1975) *Macroplacus raeticus* n. g. n. sp.-ein neuer Placodontier aus dem Rät der Bayerischen Alpen: Mitteil Bayerischen Staatssam. Palaontol Hist Geol 15:33–55

Sennikov AG, Arkhangelsky MS (2010) On a Typical Jurassic Sauropterygian from the Upper Triassic of Wilczek Land (Franz Josef Land, Arctic Russia). Paleontol J 44(5):567–572

Slater TS, Duffin C, Hildebrandt C, Davies TG, Benton MJ (2016) Microvertebrates from multiple bone beds in the Rhaetian of the M4–M5 motorway junction, South Gloucestershire, UK. Proc Geol Assoc 57(1):53–77. https://doi.org/10.1016/j.pgeola.2016.07.001

Smith AS (2015) Reassessment of '*Plesiosaurus' megacephalus* (Sauropterygia: Plesiosauria) from the Triassic-Jurassic boundary, UK. Palaeontol Electron 18(1):1–20

Stocker MR, Butler RJ (2013). Phytosauria. In: Nesbitt SJ, Desojo JB, Irmis RB (eds) Anatomy, phylogeny and palaeobiology of early archosaurs and their kin. Geological Society, London, Spec Publ, 379:91–117

Storrs GW (1991) Anatomy and relationships of *Corosaurus alcovensis* (Diapsida: Sauropterygia) and the Triassic Alcova Limestone of Wyoming. Bull Peabody Mus Nat Hist 44:1–151

Storrs GW (1994) Fossil vertebrate faunas of the British Rhaetian (latest Triassic). Zool J Linnean Soc 112:217–259

Storrs GW (1999). Tetrapods. In: Swift A, Martill DM (eds) Fossils of the Rhaetian Penarth Group. The palaeontological Association. Field Guide to Fossils 9:223–238

Storrs GW, Gower DJ (1993) The earliest possible choristodere (Diapsida) and gaps in the fossil record of semi-aquatic reptiles. J Geol Soc 150(6):1103–1107

Storrs GW, Taylor MA (1996) Cranial anatomy of a new plesiosaur genus from the lowermost Lias (Rhaetian/Hettangian) of Street, Somerset, England. J Vertebr Paleontol 16(3):403–420

Stubbs TL, Benton MJJ (2016) Ecomorphological diversifications of Mesozoic marine reptiles: the roles of ecological opportunity and extinction. Paleobiology 42:547–573. https://doi.org/10.1017/pab.2016.15

Stutchbury S (1846) Description of a New Species of *Plesiosaurus*, in the Museum of the Bristol Institution: Quart. J Geol Soc Lond 1846:411–417

Sues HD, Olsen PE (2015) Stratigraphic and temporal context and faunal diversity of Permian-Jurassic continental tetrapod assemblages from the Fundy rift basin, eastern Canada. Atl Geol 51:139–205

Tackett LS, Bottjer D (2012) Faunal succession of Norian (Late Triassic) level-bottom benthos in the Lombardian basin: Implications for the timing, rate, and nature of the early Mesozoic Marine Revolution. PALAIOS 27(7):585–593

Tanner LH, Lucas SG, Chapman MG (2004) Assessing the record and causesof Late Triassic extinctions. Earth Sci Rev 65:103–139

Taylor MA, Cruickshank ARI (1993) A plesiosaur from the Linksfield Erratic (Rhaetian, Upper Triassic) near Elgin, Morayshire. Scott J Geol 29:191–196

Thorne PM, Ruta M, Benton MJ (2011) Resetting the evolution of marine reptiles at theTriassic-Jurassic boundary. Proc Natl Acad Sci 108(20):8339–8344

Westphal F (1975) Bauprinzipien im Panzer der Placodonten (Reptilia triadica)- Principles of structure and growth in the dermal armor of placodonts (Reptilia triadica). Paläontol Z 49(1/2):97–125

Westphal F (1976) The dermal armour of some Triassic placodont reptiles. In: Bellairs ADA, Cox CB (eds) Morphology and Biology of Reptiles. Academic Press, London, pp 31–41

Whiteside DI, Duffin C, Gill PG (2016) The late Triassic and early Jurassic fissure faunas from Bristol and South Wales: Stratigraphy and setting. Palaeontol Pol 67:257–287

Wild R (1973) Tanystropheus longobardicus (Bassani) (Neue Ergenbnisse); Die Triasfauna der Tessiner Kalkalpen XXIV. Abh Schweiz Palaeont Ges 95:1–162

Wild R (1980) Die Triasfauna der Tessiner Kalkalpen. XXIV. Neue Funde von *Tanystropheus* (Reptilia, Squamata). Abh Schweiz Paläont Ges 102:1–31

Wintrich T (2015) The first Triassic plesiosaur: a skeleton from the Raetian of Germany and its implications for the evolution of plesiosaur locomotion. SVP meeting Dallas 2015 abstract volume:55

Wu XC, Cheng YN, Li C, Zhao LJ, Sato T (2011) New information on *Wumengosaurus delicato-mandibularis* Jiang et al., 2008 (Diapsida: Sauropterygia), with revision of the osteology and phylogeny of the taxon. J Vertebr Paleontol 31(1):70–83

Wu XC, Cheng YN, Sato T, Shan HY (2009) *Miodentosaurus brevis* Cheng et al., 2007 (Diapsida: Thalattosauria): its postcranial skeleton and phylogenetic relationships. Vertebr PalAs 47(1):1–20

Yang P, Ji C, Jiang DY, Motani R, Tintori A, Sun Y, Sun Z (2013) A new species of *Qianichthyosaurus* (Reptilia: Ichthyosauria) fromXingyi Fauna (Ladinian, Middle Triassic) of Guizhou. Acta Sci Nat Univ Pekin 49:1002–1008

Yin GZ, Zhuo XG, Cao ZT, Yu YY, Luo YM (2000) A preliminary study on the early Late Triassic marine reptiles from Gunanling, Guizhou, China. Geol Geochem 28(3):1–22

Young CC, Dong Z (1972) On the Triassic aquatic reptiles of China. Mem Nanjing Inst Geol Paleontol 9:1–34

Zapfe H (1976) Ein großer Ichthyosaurier aus den Kössener Schichten der Nordalpen. Ann Naturhist Mus Wien 80:239–250

Zhao LJ, Li C, Liu J, He T (2008) A new armored placodont from the Middle Triassic of Yunnan Province, southwestern China. Vertebr PalAsiatica 46:171–177

Zhao LJ, Liu J, Li C, He T (2013) A new thalattosaur, *Concavispina biseridens* gen. et sp. nov. from Guanling, Guizhou, China. Vertebr PalAs 51:24–28

Zhou X, Balini M, Jia D, Tintori A, Sun Z, Sun Y (2015) Ammonoids from the Zhuangpo Member of the Falang Formation at Nimaigu and their relevance for dating the Xingyi fossil Lagerstaette (late Ladinian Guizhou, China). Riv Ital Paleontol Stratigr 121(2):133–161

Chapter 9
The Zorzino Limestone Actinopterygian Fauna from the Late Triassic (Norian) of the Southern Alps

Andrea Tintori and Cristina Lombardo

Abstract The ichthyofauna of the Zorzino Limestone represents an important step in the biodiversity of the bony fishes. With its richness and variety at the highest point of the Triassic, this fauna also testifies to the beginning of the faunal transition that will be realized during the Jurassic. Thousands of specimens and extraordinary preservation of the fossils yielded by these levels have allowed the monitoring of such a crucial moment in the evolution of vertebrates. These favourable conditions allowed also the reconstruction of the mode of life and the trophic adaptations performed by the different fish groups that dwelled in those depositional basins surrounded by the largest carbonate platform ever, now known as the Dolomia Principale (or Haupt Dolomite of German-speaking geologists). As further proof of this peculiar evolutionary period, the large predators occupying the highest trophic levels were still represented by 'primitive' basal actinopterygians; on the contrary, the most derived neopterygians developed a specialization in durophagy, a trophic niche formerly unexploited by actinopterygians. Within the main trophic categories, we can find different morphological specializations, which probably allowed the fishes to exploit most of the available trophic resources. The blooming of the stem-group Teleostei, the Pholidophoriformes, is also recorded, with several genera occurring together in the best represented localities.

Keywords Late Triassic • Norian • Actinopterygii • Trophic web • Predation • Northern Italy

A. Tintori (✉)
Dipartimento di Scienze della Terra Ardito Desio, UNIMI,
Via Mangiagalli 34, 20133 Milan, Italy
e-mail: paleo.tintori@outlook.it

C. Lombardo
Dipartimento di Scienze della Terra Ardito Desio, Universita di Milano, Milan, Italy
e-mail: cristina.lombardo@unimi.it

© Springer International Publishing AG 2018

L.H. Tanner (ed.), *The Late Triassic World*, Topics in Geobiology 46,
https://doi.org/10.1007/978-3-319-68009-5_9

9.1 Introduction: Historical Background

The studies of fossil fishes from the Upper Triassic in the Alps have a long history. Agassiz (1833–1843) had already described a few taxa from organic–rich Norian shales around Seefeld, near Innsbruck (Austria). The specimens were rather fragmentary and unfortunately nobody has ever carried out detailed field research in the area. In the following decades, a few taxa from the Early Carnian of Raibl (now Cave del Predil, Italy, see Tintori et al. 1985) and from Seefeld, were added by Bronn (1858, 1859) and Kner (1866a, b, 1867, 1868a, b). Later on, Bassani (1892, 1895) resumed and amended the work formerly made by Costa (1862) on the Norian fishes from Giffoni (Salerno, southern Italy), proving their similarity with those from Seefeld.

Except for the monograph that Gorjanovic-Kramberger (1905) wrote on the Norian fishes from Hallein (Salzburg, Austria), these assemblages were then almost totally neglected until the end of the last Century, when new Norian localities were discovered in northern Italy, mainly in the surroundings of Bergamo and Udine (Fig. 9.1). Unfortunately, we have very few marine vertebrate faunas during the Late Triassic, while in the Early–Middle Triassic many assemblages characterize the sequence. In fact, the stratigraphic distribution of the marine vertebrate Fossil Lagerstätten is certainly sparser in the Late Triassic (35 Ma in total) than in the Early–Middle Triassic (15 Ma in total) (Tintori et al. 2014a). The Zorzino Limestone is inferred to have been deposited in marine basins associated with early Mesozoic rifting (Jadoul et al. 1994), like the coeval lithostratigraphic units yielding these fish assemblages in Friuli, Campania, Sicily and Austria. These basins opened within an extremely wide and stable carbonate platform, that extended over all the western margin of Tethys; the result is the Dolomia Principale Formation, the thickness of which is usually around 1000 m. Today, after the tectonic movements occurred during the Alpine orogenesis, several similar basins are present for 350 km from the Lugano Lake to the West, up to the Tolmezzo area (Udine) to the East, and for 1200 km from Salzburg (Austria) southwards to the Egadi Islands in Sicily. These deeper basinal paleoenvironments are missing in the Dolomia Principale of the Dolomites.

The connections of these wide basins with the open sea were probably scarce and represented only by very long tidal channels (Renesto and Tintori 1995). On the other hand, this relative isolation promoted the differentiation of a largely endemic vertebrate fauna, composed by marine taxa as well as by terrestrial reptiles; these latter lived on small, temporary islands across the carbonate platform. This could explain the predominance of terrestrial reptile taxa, with very few marine ones and none strictly acquatic, such as ichthyosaurs, in the Zorzino Fauna. Shallow waters were well oxygenated, allowing nekton to thrive, and bottom conditions were favourable to life also at the margins of the basin (Blake et al. 2000; Tintori 1995).

After years of scattered finds, following the construction of several mountain roads in the 1960s, a few crustaceans and fishes were recorded from the uppermost part of the Zorzino Limestone in Valvestino, a remote valley NE of Brescia (Zambelli

Fig. 9.1 Map indicating (*red dots/light gray dots*) the position of the Norian Localities yielding the Zorzino Fauna composed of complete and well preserved specimens. The 'Rhaetian' Bone Beds, yielding only very fragmentary elements or just isolated teeth, are shown in *brown/dark gray dots*

1980a). At that time the find was not given the proper importance and since then no more collecting has been done, although the fossiliferous outcrops are easy to reach and to exploit (A.T. pers. obs. 2015).

It was only at the beginning of the 1970s, when an overnight landslide in a quarry near Cene (Bergamo, Italy) cleared a large bed surface in the upper part of the Zorzino Limestone that the 'fossil hunt' started (Fig. 9.2a). The level exposed by the landslide consisted of a thin (6–7 cm thick) layer. It yielded large amounts of beautifully preserved fishes, crustaceans and also a few reptiles. From a seemingly single lucky find, the quarry actually proved to be the first of many Triassic sites that were discovered in Lombardy and in Friuli during the following years, although in somewhat different lithologies (limestone, marly–limestone, dolostone) and preservation conditions. Another major fossil–bearing horizon has been excavated in a few sites

Fig. 9.2 The first Zorzino Limestone sites that have been exploited for fossils were both related to landslides. (**a**) The Cene quarry in 1976: the bed surface is the thin fossiliferous level uncovered by the landslide that removed the corresponding layers seen on the left. (**b**) The Endenna-Zogno (Bergamo) site in 1980. A superficial landslide removed the tree along the slope and uncovered the fossiliferous level (about 1.5 m thick) at the boundary between Zorzino Limestone and Riva di Solto Shale allowing a large-scale excavation

in Lombardy by the authors. This level represents the transition from the Zorzino Limestone to the overlying Riva di Solto Shale (Figs. 9.2b and 9.3): it was considered the base of the latter formation by Casati (1964). The fossil assemblage is called the 'Zorzino Fauna', even when it has been found in a unit bearing a different name. One of these cases is the Forni Dolostone, in Friuli, northeastern Italy. Here specimens are never found in great concentrations: paleontological collections were almost totally assembled from scattered blocks on the mountain slopes (Dalla Vecchia, pers. comm.). Given that the Forni Dolostone is usually several hundred meters thick (Dalla Vecchia 2008; Jadoul 1986; Jadoul et al. 1992), like the Zorzino Limestone, its fossil fauna (mostly stored in the Museo Friulano di Storia Naturale in Udine) could represent a fairly wide time interval. On the other hand, the 'Zorzino' fishes generally lie at the boundary between the Zorzino Limestone and the Riva di Solto Shales (Zogno–Endenna and Zogno2 sites) in the Lombardian Prealps, but they are also certainly present a few dozen meters below (Cene quarry) or above (Ponte Giurino site) this boundary. Actually, given the very high sedimentary rate, the difference in age should not exceed a few tens of thousands of years (Rigo et al. 2009). Following Tintori et al. (2014a), this Norian Fauna best represents the Triassic Late Fish Fauna (TLFF), although it is not clear where the boundary between the Triassic Middle Fish Fauna (TMFF) and the TLFF should be set. For instance, groups believed to be typical of the TLFF were very recently recorded in the Late Ladinian (Tintori et al. 2012, 2015) of southern China. Still, as far as we know, the general composition of the Norian fish fauna is definitely different from that of late Ladinian or early Carnian, at least in the ratio between neopterygians and basal actinopterygians. The Norian assemblages are absolutely dominated by neopterygians, both in taxa and specimen numbers.

We should know what happened in the previous few million years to better comprehend the evolutionary meaning of the Zorzino ichthyofauna and how fast was the Norian fish radiation. We know that not far north of Brescia a fish assemblage is probably of Early Norian age (Tintori et al. 2014a), but unfortunately it has never been studied by the local Museum, which is in charge of the research; the next younger one known approximately dates back to the base of the Carnian, thus about 15–20 My earlier.

Regarding the Early Carnian Raibl faunas, after the mid-nineteenth century fieldwork, largely related to the presence of rich ore deposits, only sporadic exploitations have been carried out in the last 30 years, yielding small collections. Luckily, the bulk of the nineteenth century unpublished collection, believed lost during World War II, came recently back to light and it is now stored in the Natural History Museum in Vienna (Raibl was part of the Austrian Empire in the nineteenth century). Most specimens have not been yet described or prepared, but at least they are now easily accessible. At a first survey (A.T. pers. obs.) it appears that this collection comprises a lower number of species, if compared to the younger faunas. Actually, it is possible that researchers in the nineteenth century focused their studies on the levels around the mines, thus on just one fossiliferous horizon. More recent surveys have expanded to the whole lower Carnian series around Raibl. We guess possibly more than one fish assemblage is present in those sites, but scientific

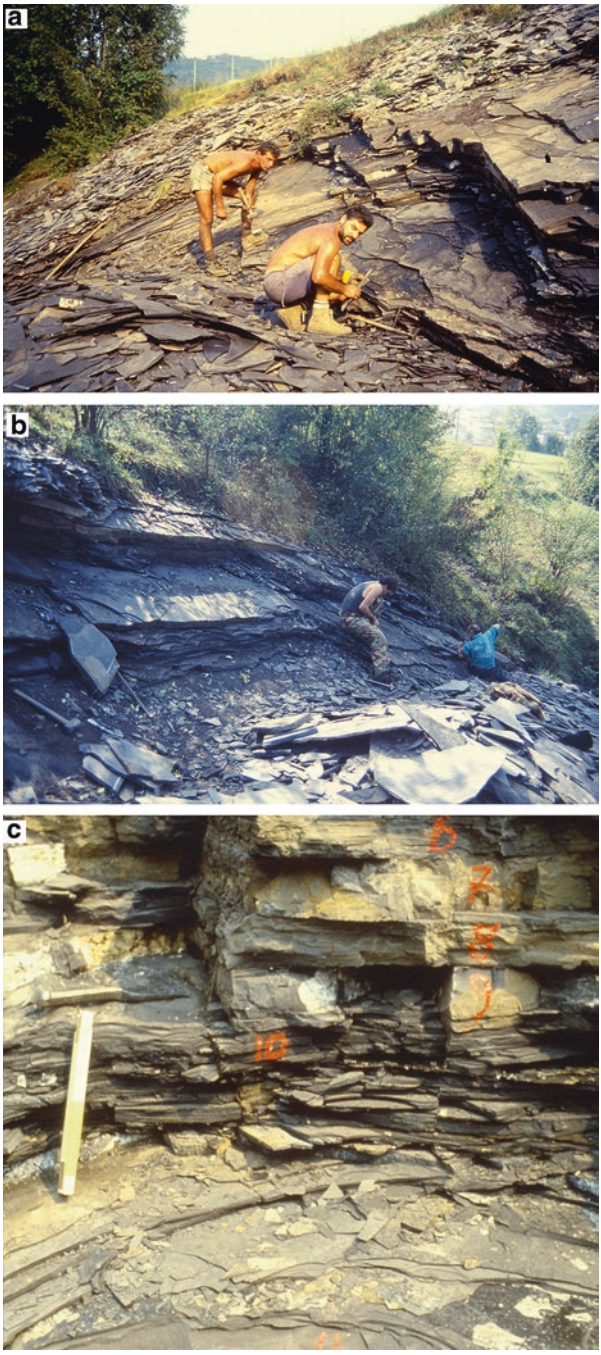

Fig. 9.3 The Zogno2 site (Poscante, Zogno, Bergamo). (**a**) A.Tintori and GF Pesenti in 1982 at the beginning of the excavation. (**b**) The site in 1990. (**c**) detail of the fossiliferous level

fieldwork is difficult due to the very rough mountain topography. The finds from the Lower Carnian of the Predil Limestone (Raibler Schichten Authorum) enable us to draw a picture of the fish assemblage at the end of a period, the Middle Triassic, that saw an intense radiation in both neopterygians and subholosteans (Tintori et al. 2014a). A similar assemblage was described from Polzberg, near Lunz (Austria), by Griffith (1977). Its precise stratigraphic position is not clear at present, although an Upper Julian (Early Carnian) age is generally assumed (Griffith 1977; Forchielli and Perveler 2013). We suspect that the Polzberg fish fauna comes from more than a single horizon, as previously stated, because the holotype of *Saurichthys calcaratus* Griffith 1977 is preserved with fresh–water dwellers such as conchostracan crustaceans (I. Kogan, pers. comm.), while the other taxa often lie with ammonoids (A.T. pers. obs.).

At the other end of the Tethys, now southern China, there is another marine vertebrate assemblage dated to earliest Carnian, the Guanling Fauna; the fish components are scarce and largely consist of genera known also from the Alps (Tintori et al. 2014a).

Finally, the time gap between the Carnian fauna and the Norian Zorzino Fauna is as long as the whole Early/Middle Triassic, a time interval which yields a considerable series of Fossil Lagerstätten. Today we usually deal with precisely dated fish assemblages, so a better time resolution is certainly needed for the early Carnian fauna, as well as the discovery of new assemblages to bridge the gap with the Zorzino Fauna.

9.2 The Zorzino Fish Fauna

In the last 45 years the Zorzino Limestone has yielded an extraordinarily rich ichthyofauna: at least 25 genera have been already described or are under study, but probably more than 50 are represented (Tintori 1981, 1983, 1990, 1996; Tintori and Renesto 1983; Tintori and Sassi 1987, 1992; Tintori and Lombardo 1996; Lombardo and Brambillasca 2005; Lombardo and Tintori 2008; Zambelli 1975, 1978, 1980a, b, c, 1986, 1990; Arratia 2013). A few species, belonging to pholidophorids, count hundreds or even thousands of specimens; other genera, like *Saurichthys* or *Paralepidotus*, are represented only by the dozen; most taxa are just known by a few or even a single specimen.

This fauna is fundamental in order to understand and monitor the extraordinary diversification that the bony fishes achieved during the Late Triassic, after the first radiation of the Middle Triassic, a few millions years after the largest ever biological crisis: the P/Tr mass mortality event (Tintori et al. 2014a). Actually, this first post-Palaeozoic radiation occurred in subholosteans and basal neopterygians, while in the Norian we record the passage from still ‘primitive’ assemblages (i.e. dominated by paleopterygians) to a more advanced one, thus dominated by neopterygians. We can see a preview of the Jurassic/Cretaceous faunas: after a new, major radiation the

Fig. 9.4 *Saurichthys* spp. From Endenna-Zogno in the exhibit of the Museo della Valle in Zogno

Fig. 9.5 *Birgeria acuminata* from Cene (Bergamo). The specimen has been recovered by an amateur and it is unfortunately fragmentary

neopterygians overtook the paleopterygians in number of species and specimens (Tintori 1998; Lombardo and Tintori 2005).

Thus, the importance of this fauna lies in the radiation of specialized neopterygians (among them pycnodonts, semionotids, macrosemiids) and in the blooming of pholidophorids (stem group Teleostei) when paleopterygians were still at the top of the trophic hierarchy, with *Saurichthys, Birgeria* and *Gabanellia* (Tintori 1990, 1998; Tintori and Lombardo 1996). At the same time, we record the comparison of a very specialized way of life in the 'flying' fish *Thoracopterus* (Tintori and Sassi 1987, 1992).

The largest predator fishes, *Saurichthys* and *Birgeria* (Figs. 9.4 and 9.5), could both exceed 1.5 m in length and are considered to have occupied the highest trophic levels. So far, only the phytosaur *Mystriosuchus* (Gozzi and Renesto 2003) seems to have the characteristics of a top–predator, being more than 3 m long. Both genera are found almost everywhere throughout the Triassic, evidencing an extremely suc-

cessful adaptation which had begun just after the P/Tr event (Kogan and Romano 2016). Starting from the Middle Triassic, these fish genera are usually overtaken only by some marine reptiles (Tintori 2013). Despite the fact that *Saurichthys* and *Birgeria* share the reduction in scale covering, aimed at a body lightening, they are very different in morphology. *Saurichthys* is long and narrow, with an elongated snout (pike–like predator in Kogan et al. 2015), while *Birgeria* is more massive, with a stout but strongly kinetic skull. Accordingly, their mode of preying on the other fishes was very different, making them able to share the same paleonvironment. Most species of *Saurichthys* used to catch prey with quick and sudden darts (Kogan et al. 2015), taking advantage of the strong forward push provided by their median fins. On the contrary, *Birgeria* was probably a slow swimmer; its large mouth and very mobile skull (Fig. 9.5) allowed this fish to quickly expand the oral cavity, sucking prey into it, just as many extant groupers do. The dentition of both taxa consists of large, striated, conical teeth alternating with medium and small ones, typically adapted to hold prey. Similar teeth are very commonly found isolated in the sediments, especially in the so called 'Rhaetian Bone Beds' of England and central Europe. They have been usually referred to as '*Saurichthys*–type' and '*Birgeria*–type'. Actually, a comparative study by Gozzi (2006) shows it is impossible to distinguish between them when found isolated. On the other hand, *Saurichthys* is always much more common than *Birgeria* in all the well known Triassic fossil fish assemblages (Stensio 1921 and pers. obs.). Indeed, the present Barracudas, whose way of life is perfectly comparable to that of several *Saurichthys* species, mostly live in very large schools, whereas groupers prefer to gather in much smaller ones.

Saurichthys is represented by three/four species in the Zorzino Fauna (Tintori 1990), but only *S. deperditus* (Costa 1862) = *S. krambergeri* Schlosser 1918 = *S*. sp. A in Tintori (1990) and *S. seefeldensis* Strand 1928 have been described (Gozzi 2006; Tintori 2013). The latter species could be somewhat older than the typical Zorzino Fauna, while the other three are coeval: *S. deperditus* and *S*. sp. B are found in the same layers in Lombardy, and *S*. sp. C comes from the Forni Dolostone. Every Triassic site ordinarily yields more than one *Saurichthys* species (Rieppel 1985, 1992; Mutter et al. 2008; Wu et al. 2009, 2011; Maxwell et al. 2015; Tintori 2013). *Birgeria* was a much more stable taxon: always a single species, in fact, is found in each fossiliferous horizon (Nielsen 1949; Gozzi 2006; Romano and Brinkmann 2009). As far as we know, the Zorzino Fauna is the youngest Triassic fish assemblage and still *Saurichthys* has higly differentiated species. Romano et al. (2012) supposed a strong decrease in the diversity of this fish in the Late Triassic, disregarding the rarity of fish assemblages in those last 35 My we discussed above. On the contrary, we believe *Saurichthys* maintained a high intrageneric diversity up to the end of the Triassic: in Late Carnian, Norian and Rhaetian probably only preservational bias prevented this genus from having a good paleontological record, although usually at least two species are present in the same bed as in the case of the Zorzino Limestone in Lombardy.

The most remarkable differences among the Norian species are found in the postcranial skeleton, especially in the stucture of the dorsal (neural) elements of the

vertebral column (Tintori 1990), in the scale rows arrangement and in the segmentation of the rays of the median fins (Tintori 2013). The peculiar neural elements in *S. deperditus* and *S.* sp. B, form a 'grid structure' with the praezygapophyses, which are as long as the neural spines, spanning up to six neural arches. When described for the first time (Tintori 1990), the grid structure was interpreted as a kind of a response to a change in presumed prey: pholidophorids become very common replacing the small subholosteans, as well as other less advanced neopterygians that had thrived during the Middle Triassic and Early Carnian. A similar vertebral column was recently described in the lower Ladinian *S. grignae* Tintori 2013 (more than 20 My younger than *S. deperditus*), belonging to a typical TMFF with plenty of miniature peltopleuriforms and neopterygians (Tintori 2013). This is clear evidence of the inconsistence of the above cited theory proposed by Tintori (1990). Since *S. deperditus* and *S. grignae* are very large species (both well over 130 m in total length), this peculiar structure of the vertebrate column is thought to be instead related to the adult size. *S.* sp. B is somewhat smaller and its neural spines and praezygapophyses are much thinner, though as long as in *S. deperditus* (Tintori 1990). Other postcranial differences distinguish the two species of the Zorzino Limestone, suggesting that pointing out any morphologic trend of *Saurichthys* throughout the Triassic, as tentatively postulated by Rieppel (1992), is a hopeless challenge. In both species the number of scale rows is much reduced: they just show the mid dorsal and the mid ventral rows, even though a single specimen of *S. deperditus* bears traces of a lateral line row (Gozzi 2006). Although the general trend points to a reduction in scale covering, nonetheless two median scale rows have been described in the Spathian (Early Triassic) *S. majiashanensis* (Tintori et al. 2014b) and in *S. grignae* (Tintori 2013). Regarding the segmentation of the median fin rays, in *S. deperditus* they are all clearly segmented, while in *S.* sp. B. they are almost unsegmented: though living together, the two taxa express opposite characters for this feature, once more denying the supposed trend from highly segmented to unsegmented rays (Rieppel 1992). *S. deperditus* shows an interesting wide geographical distribution compared to that of other species, which are mostly restricted to small areas, endemic and/or lasted for a very short time. *S. deperditus* ranges from Hallein, near Salzburg, Austria (I. Kogan, pers. comm. Kogan and Romano 2016), to Giffoni (Salerno, southern Italy), today about 800 km distant, spread in several sites representing basins with different paleoenvironmental conditions. Is this related to its large size? As far as we know, only *S. (Costasaurichthys) costasquamosus* has been described from different basins (Tintori 2013) in the early Ladinian, even if the total distance between the single basins is much less than for *S. deperditus*, just about 50 km: however, this species is also very large, some specimens measuring over 130 cm in extimated total length (Tintori 2013).

Only one species of *Birgeria* has been recognized in the Norian–Rhaetian, but recently Storrs (1994) questioned the generic attribution on the grounds of isolated teeth and very fragmentary remains found in the English Rhaetian Bone Beds. The few complete specimens found in the Zorzino Fauna show all the main generic

characters that Nielsen (1949) also indicated: naked body, except for a scaly field on the body lobe of the tail, extremely kinetic skull owing to multiple suborbitals and to a subopercular organized like fans, and vertebral column with median neural spines immediately behind the dorsal fin. For this reason, we have no doubts about the attribution to *Birgeria*. Already Boni (1937, unfortunately the paper was written in Italian) ascribed the specimens of this Fauna to *B. acuminata* and established a neotype on Italian material. As mentioned above, the English fossils consist of isolated teeth and jaw fragments. Therefore, we cannot accept the erection of a new genus (*Severnichthys*) by Storrs (1994), never considering the Alpine specimens. The age of the two sites can be surely discussed: the Alpine one is around the Norian Middle/Upper boundary, the English level is 'Rhaetian'. But a Bone Bed is defined as a secondary sedimentay deposit, consisting of reworked specimens that have possibly undergone deposition, erosion, transport, selection, to an extent impossible to determine in terms of time and space. If thence the comparison between the two associations cannot rely on their biodiversity, it certainly can be based on the presence of common significant and hardly misdiagnosed species like *Sargodon tomicus* Plieninger 1847 and *Pseudodalatias barnstonensis* (Sykes 1974). They both have been re–described on specimens belonging to the Zorzino Fauna (Tintori 1980, 1983) and their teeth are also frequently found in the Rhaetian Bone Beds.

It must be pointed out that large *Saurichthys* also usually preyed on small fishes, as can be seen in some Norian specimens where pholidophorids and juveniles of *Paralepidotus* are preserved inside *Saurichthys* (A.T. pers. obs.). Nothing is known about the size of the prey of *B. acuminata*, even if the the large mouth and the possibility of sucking prey (Gozzi 2006) could make it able to engulf at least medium size prey, compared to the predator size. So far, only a specimen from the Lower Triassic of Madagascar has been described with prey content, even if the two prey, belonging to two different genera, were interpreted as *Birgeria* embryos by Beltan (1980). *Birgeria* is much less common than *Saurichthys*: only a few specimens of *B. acuminata* have been found and described (Gozzi 2006): another aspect apparently unvaried throughout the Triassic! Even if we must remember that articulaled Rhaetian specimens are not known, it is really peculiar to these genera that they maintained a fairly stable maximum size throughout the Triassic and just as constant is the ratio between the number of *Saurichthys* and *Birgeria* specimens in almost each Triassic fish assemblage. But, in the meantime *Saurichthys* went through multiple variations of the same general morphology (Bauplan), wheareas *Birgeria* shows few and small modifications in the same period of time (about 10 species, 5 of which are controversial as mainly based on scanty material).

Conical teeth, arranged in several rows, are also visible in an underscribed neopterygian genus from the Bergamo area, belonging to a halecomorph. This fish represents quite an exception, among the Norian advanced actinopterygians, as it shows three series of conical and striated marginal teeth, regularly arranged on both upper and lower jaws, and minute palatal ones, surely not suited for crushing hard exoskeletons. However, the real shape of these teeth is quite different from that of those of the cited paleopterygians, being more blunt, so probably less efficient in piercing the body of the prey. Actually, these teeth could well belong to some generalized

subholostean perleidiform (i.e. *Colobodus*, *Perleidus*, etc.), thus, in some way, an 'advanced' neopterygian simply was 'copying' more primitive (phylogenetically) subholosteans, probably without reaching their high degree of specialization. If compared with the other piscivorous predators previously seen, it's worth stressing how this neopterygian actually appears less specialized, not only in the teeth shape: teeth borne by maxillary and dentary are not much differentiated in size; the massive body, covered with heavy ganoid scales and the hemiheterocercal caudal fin, owing to its asymmetry, were not particularly efficient for fast swimming or quick movements. Therefore, we can consider this fish as a small generalist predator, which could use its teeth to catch prey such as small, slow swimming fishes or crustaceans.

9.2.1 Subholosteans

By the Late Triassic, the Palaeonisciforms were very rare. They are represented by only a few undescribed, small specimens and by even less common *Gyrolepis alberti* Agassiz, 1835. Indeed, this species needs a re–description because the original material consists only of isolated scales from the Rhaetian Bone Beds: significant or complete specimens have never been published. The same species has also been recorded in the German Muschelkalk, 20 My older than the Zorzino Limestone; scale ornamentation is the unique distinguishing character, but, unfortunately, this kind is fairly common among the paleonisciforms, potentially leading to mistakes. At any rate, because the Zorzino Fauna and the Rhaetian Bone Beds have a comparable age and there is a correspondence in the scales of some specimens, we are quite certain about the attribution to *Gyrolepis alberti* for our rare specimens.

The most varied and numerous group inside the non–neopterygian actinopterygians is that of 'subholosteans', characterized by an almost vertical preopercle, still fixed to the maxilla, and by a peculiar caudal fin, called hemiheterocercal, which has epaxial rays that are inserted dorsal to the vertebral column, making the tail externally almost symmetrical. The subholosteans appear in the earliest Triassic with *Australosomus* (Piveteau 1930); their most common and diverse representatives are Perleidiformes and Peltopleuriformes, appearing between the Spathian (Early Triassic) and the Anisian (Middle Triassic). The Pholidopleuriformes, comprising *Australosomus*, are generally represented by just one single species in each marine fish assemblage. *Pholidopleurus* has been described from the Alpine Middle Triassic as well from the Alpine and Chinese Lower Carnian (Bronn 1858; Bürgin 1992; Liu et al. 2006). In a few sites of Lombardy (Cene, Zogno–Endenna), the Zorzino Limestone yielded many specimens of *Pholidopleurus* representing a new species. *Pholidopleurus* sp. n. is characterized by an almost symmetrical tail showing a huge number of rays (70 at least) equally subdivided between ventral and dorsal lobes, and the vertebral column ending straight. Complete chordacentra surround the unconstricted notochord all along the vertebral column. The squamation is limited to the abdominal region, where scales are very thin and much deeper than long, as

in most subholosteans. Noteworthily, the Early Carnian type species, *Pholidopleurus typus* Bronn 1858, has a complete scale covering; the scale pattern of the possibly coeval *P. xiaowaensis* Liu et al. 2006, belonging to the Guanling Fauna, closely resembles that of the Norian species despite a remarkable difference in the dimension: up to 25 cm instead of the 6–7 cm of the Norian fishes.

Among Perleidiformes, apparently only *Gabanellia agilis* Tintori and Lombardo 1996 and *Endennia licia* Lombardo and Brambillasca 2005 lived during the Norian. This group, in fact, had the highest diversity in the Middle Triassic, when they gave rise to specializations both in body shape and trophism. Among the Ladinian actinopterygians of the western Tethys, only *Felberia* and *Stoppania* are deep–bodied. As often happens, this shape is associated with a high specialization in the dentition and hence in trophism (Lombardo and Tintori 2005; Lombardo et al. 2008). Actually, many Middle Triassic perleidiforms show more or less specialized dentitions: some species of *Perleidus* have stout, peg–like teeth (Lombardo 2001; Lombardo et al. 2011) while *Ctenognatichthys* (Bürgin 1992) has thin, anterior rake–like teeth. The Upper Triassic genus *Endennia* probably evolved this trend of catching prey provided with shells, but possibly a thin or non–calcareous exoskeleton. The dentition of *Endennia* consists of long, cylindrical marginal teeth with a flattened apex and differentiated, palatal crushing teeth. This morphology could have allowed the fish to be almost entirely durophagous, but with some differences with respect to the neopterygians (see below). Given the limited possibility of the ethmoidal region to be protruded, the projecting marginal teeth, together with the inner crushing set, could have improved the feeding skills of *Endennia*, both in catching and processing prey. Its fusiform body was completely covered with thick, ganoid scales that have joints that were probably loose enough to provide this fish a sufficient mobility to pursue just slow swimming prey. Hence, we hypothesize that *Endennia* was able to seize small swimming organisms such as crustaceans with its anterior teeth and to crush them using the grinding teeth. On the other hand, we cannot rule out the possibility of this fish feeding upon other invertebrates with harder mineralized parts, for example molluscs or echinoderms, commonly found in the Zorzino Limestone.

Many taxa of the Zorzino Fauna are considered demersal, living near the bottom of the basins, where they most likely fed on crustaceans and/or small fish or on encrusting and hard shelled organisms. The majority of marine Triassic fishes were covered with ganoid scales, which are thicker than those borne by teleosts, and certainly not easy to be pierced by medium–sized predators. *Gabanellia* seems to be the opposite of this model: it was a fast swimmer, and its dentition was perfect for biting fishes. Its markedly fusiform body, 20–30 cm long, covered with thin scales and ending in a large, forked tail, suggest *Gabanellia* was able to pursue its prey over long distances, occupying a completely different ecologic niche with respect to the large predators like *Saurichthys* and *Birgeria*. *Gabanellia* is up until now the only medium–sized perleidid fish specialized as an active predator on nektonic organisms. This evolution testifies to a fair vitality of perleidids, also in the last period of their stratigraphic distribution. Actually, we ignore the precise time of the

Late Triassic when they became extinct, but certainly nobody has ever recorded any perleidid in the Jurassic units.

Among the most interesting peltopleuriforms, are *Thoracopterus* (Tintori and Sassi 1992), with the species *T. magnificus* Tintori and Sassi 1987 from Lombardy (Zorzino Limestone and Riva di Solto Shale) and Campania (Giffoni, Salerno) and *T. martinisi* Tintori and Sassi 1992, found in Friuli (Forni Dolostone). Both species have a totally naked body, but they differ in the ratio of paired fin length to standard length. *Thoracopterus* shows specialized features in body and fin morphology that are fully comparable to those of the extant Exocoetidae flying fish. Like in *Thoracopterus,* representatives of Exocoetidae have long pectoral and pelvic fins, and the ventral lobe of the caudal fin is longer than the dorsal one. Other similarities are in the caudal region of the vertebral column, where neural spines are modified for the attachment of the muscles moving the tail during taxi (Tintori and Sassi 1992). Actually, Triassic flying fishes were gliders due to the opening of their 'wings' (the paired fins) without flapping. The tooth–row pattern on both jaws of *Thoracopterus* suggests this fish used to catch its prey while swimming upward, allowing the maximum possible gape (Tintori and Sassi 1992). Hence this fish most likely preyed on small fishes swimming at high speed, also necessary to take flight. Three other species of *Thoracopterus* are known, two from the Lower Carnian of Raibl and Lunz (Tintori and Sassi 1992) and one from from the Upper Ladinian Upper Vertebrate assemblage of the Xingyi Fauna, southern China (Tintori et al. 2012). Like most peltopleurids and some perleidids, *Thoracopterus* shows a marked sexual dimorphism (Bürgin 1992; Tintori and Lombardo 1996; Lombardo 2001; Tintori et al. 2012), especially in the modification of the anal fin in specimens interpreted as males. This modification appears unfit for an internal fertilization: the anal fins are too much expanded to make a true gonopodium, which usually is a narrow, elongate structure. Some modern teleosts, in fact, perform an internal fertilization by means of narrow fins bearing very long rays (Rosen and Gordon 1953).

Some other peltopleuriforms are very rarely found in the Zorzino Fauna. Among these few specimens only *Peltopleurus humilis* Kner 1867 from Seefeld (Austria), has been described. Despite the thousands of fossil fishes collected, this taxon is still missing in Lombardy Norian sites. On the whole, the share of the subholosteans during the Norian (and therefore the TLFF) is lower than earlier in the Triassic (TMFF). Nonethess, some of these taxa are highly specialized such as the flying fish *Thoracopterus* and the fast predator *Gabanellia* among the subholosteans.

9.2.2 The Durophagous

The appearance of several taxa highly specialized in durophagy is probably the most relevant aspect of the Zorzino fish fauna outside of phylogenesis. For the first time actinopterygians were able to catch calcareous hard–shelled prey, crushing them with tooth batteries borne on their lower jaw and vomers and/or parasphenoid. Among actinopterygians, only *Bobasatrania* had formerly developed a

durophagous behaviour; its pharyngeal tooth plates performed a grinding action on the prey, which was sucked into the mouth, with no other teeth present (Tintori et al. 2014a).

The term 'durophagy' has never been formally defined. With this term we generally mean the strategy of feeding on hard–shelled prey: too hard to be pierced, these are crushed or ground, and the soft tissues inside are swallowed, often together with shell fragments (Cate and Evans 1994; Tintori 1995). Mollusks with carbonate shells are largely the most preyed upon. The majority of the modern durophagous teleosts, like the sparids, feed on mollusks besides crustaceans, sea urchins and other organisms. A mandatory requirement for a durophagous fish is obviously to bear proper crushing teeth supported by robust bone elements. Omitting the pharyngeal tooth plates—borne by several modern teleosts such as the Scaridae (Grassé 1958) and by the Permo/Triassic *Bobasatrania* (Tintori et al. 2014a) among the basal actinopterygians—a true crushing dentition certainly characterizes several actinopterigyan groups since the Triassic. During the Paleozoic this trophic niche was occupied only by chondrichthyans, presently still counting some durophagous groups such as the Myliobatidae rays. Their totally different body morphology suggests chondrichthyans are not in competition with actinopterygians: rays are dorso–ventrally flattened and they show a wide ventral mouth, whereas durophagous actinopterigyans are generally laterally compressed and deep–bodied, with a terminal mouth.

Nonetheless, a field of stout, low–crowned teeth more or less regularly arranged is not enough to determine a durophagous behaviour of actinopterygians. Teeth must be properly large and stout. Opposite to the pharyngeal tooth plates, the teeth of these batteries are rarely replaced and also rarely worn, because they never get in touch with each other, just like the levers of a nutcraker. Another characteristic feature of a durophagous fish is a small mouth gape, because prey either are fixed or move very slowly. The need of catching, ripping and scraping prey before processing them is met by anteriorly amassed prehensile teeth. The most representative modern group of grazing durophagous fishes are the sea breams (Sparidae), thriving in most tropical and temperate seas with more than 150 species (Bray and Gomon 2017; http://www.fishbase.org/summary/FamilySummary.php?ID=330. Almost all these fishes live in shallow waters, feeding mainly on mollusks, sea urchins and crustaceans. Despite a highly specialized dentition, they also eat a variety of other organisms such as small fish and algae (A.T. pers. obs. on *Diplodus sargus* kept in a fish tank and on gut contents of commercial specimens).

During the Norian, for the first time in actinopterygian history, taxa bearing all the features that characterize modern durophagous fishes appear in different groups: small mouth, anterior prehensile teeth, molariform tooth batteries, more or less deep and laterally compressed body. As pointed out by Tintori (1998) and by Lombardo and Tintori (2005), the Norian was a crucial period for the origin and stabilization of the important durophagy trophic niche. Actually, already in the Middle Triassic a few taxa among suboholosteans (among them *Colobodus* and *Perleidus*), as well as the halecomorph *Asialepidotus* (A.T. pers. obs.), had showed adaptations concerning the treatment of prey with hard exoskeleton: for example, palatal bones com-

pletely covered with small, low–crowned teeth. These fishes should not be considered strictly durophagous, because their gape is very wide, and the marginal teeth, not yet modified, are arranged all along the oral margin. In addition, teeth borne by the palatal bones are small to very small, and the bones themselves (pterygoids), are thin and were probably flexible. Both *Felberia* and *Stoppania* (Lombardo and Tintori 2004; Lombardo et al. 2008) were better adapted: small mouth, large anterior prehensile teeth, stout inner teeth and very deep body. Their size could reach 30–40 cm. Large dimensions are decisive to produce the power required to effectively crush shells or scrape corals (Tintori 1996; Lokrantz et al. 2008). However, these two genera are rarely found in the Alpine Middle—early Late Triassic sites, in many cases only one or just a few specimens. On the contrary, during the Norian true durophagous fishes can be relatively common (pycnodonts or *Sargodon tomicus*) or even very common (*Paralepidotus*), making up a significant share of the Zorzino assemblage both in specimens and in taxa.

The first blooming of pycnodonts (Gorjanovic-Kramberger 1905; Tintori 1981) is one of the most relevant events witnessed by the Zorzino Fauna. This important group will be almost cosmopolitan later on, and the fossil fish fauna from Bolca (Italy) testifies that the extinction occured only as recently as the Eocene. Actually, the first appearance of pycnodonts is a little older than the Zorzino Fauna s.s.. Rare specimens in fact have been recorded in lower/middle Norian levels north of Brescia (northern Italy) but they are unfortunately not yet available because they have been under study for the last 15 years by the local natural history museum. The Zorzino Fauna contains three pycnodont species: *Eomesodon hoeferi* Gorjanovic-Kramberger 1905 (this species is also present in the northernmost site, Hallein near Salzburg), *Brembodus ridens* Tintori 1981 from the Bergamo area (Fig. 9.6) and *Gibbodon cenensis* Tintori 1981 from the Bergamo and Friuli areas. The latter two species are apparently endemic to the southern Alps.

While later in the Mesozoic the size of pycnodonts is large (up to over one meter), in the Norian it is medium (like in *Brembodus*, 10–20 cm) to very small, just around 5 cm (*E. hoeferi* and *Gibbodon*). The recently renewed interest in this extremely specialized group (see Poyato-Ariza 2015 for an updated bibliography) reveals its great importance. The phylogenetic relationships with the other advanced actinopterygians have been debated, as well as the ingroup relationships, but the results are so far highly controversial (Nursall 1996a, 2010; Poyato-Ariza 2015). Pycnodonts have certainly been a very successful group for as long as 170 My: their appearance in the Norian is one of the bases on which the TLFF has been defined by Tintori et al. (2014a). To the above mentioned three genera of the Zorzino Fauna, one/two will be likely added when specimens stored in the Brescia Museum are described. Such numbers suggest how this group rapidly occupied a formerly uncrowded trophic niche. Pycnodonts are considered ‘grazing’ durophages, adapted to the rich communities evolving in the vicinity of shallow, tropical reefs of algal, sponge, rudist and scleractinian origin’ (Nursall 1996b). However, Nursall (1996b: 121) reports a few medium–sized specimens with gut that contained shell and echinoderm fragments, implying that rather than grazing, these fishes actually grabbed and crushed their prey (mollusks, echinoderms, corals?) just as modern sparids do.

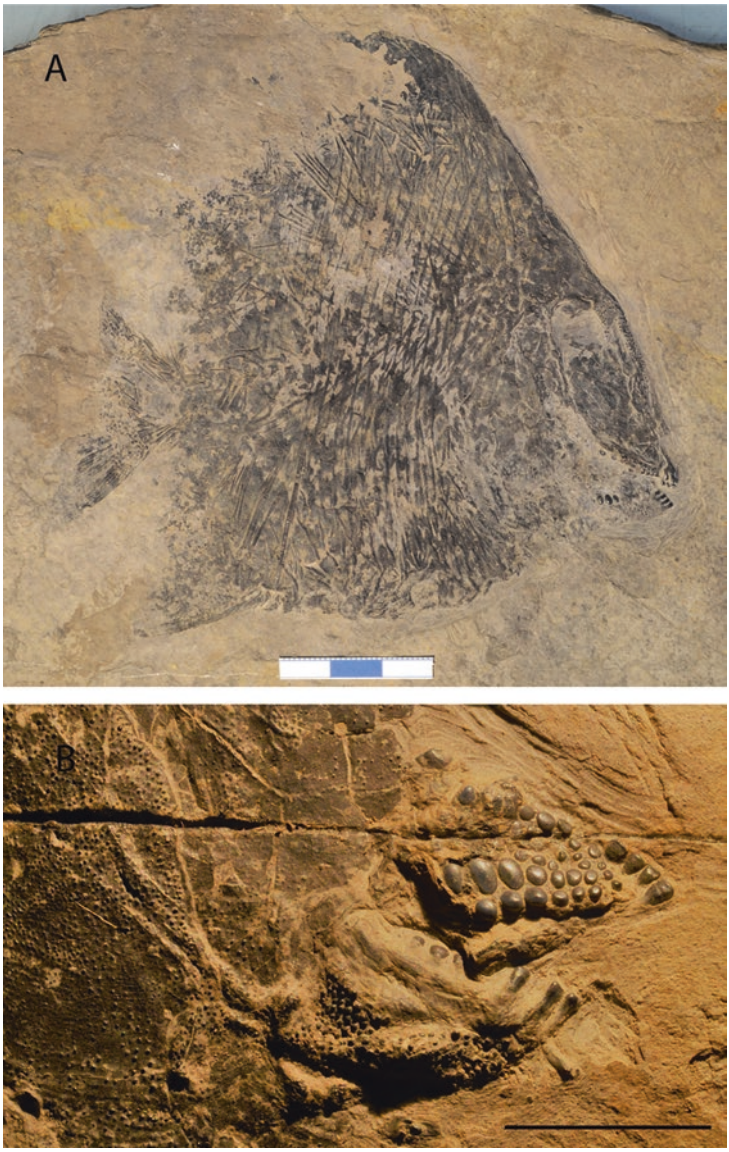

Fig. 9.6 *Brembodus ridens* from Endenna-Zogno site. Specimens from the Museo Brembano in S. Pellegrino (Bergamo). (**a**) A complete adult specimen. (**b**) Detail of the lower jaw dentition, left jaw in medial view, right one in lateral view

Well developed in the Late Paleozoic, the tropical reefs were dramatically affected by the huge P/T crisis. Their subsequent recovery was so slow that only in the lowermost Carnian relatively complex reef environments are found again in the San Cassiano Formation in the Dolomites area (Fürsich and Wendt 1977). The San Cassiano fauna is famous for the spongal/coral reefs but also for an incredibly rich and well preserved assemblage of mollusks, echinoids and brachiopods, suggesting a shallow water environment where benthic life flourished. Durophagous fishes are, however, still missing; only scattered remains of *Felberia* (Lombardo and Tintori 2004) and *Paleobates*, a hybodont shark (A.T. pers. obs.), have been collected. The Norian Zorzino Limestone was deposited at the margin of the Dolomia Principale carbonate platform, where life was far poorer than on the San Cassiano platform. Mostly serpulids and microbials (stromatolites) and rare corals (Berra and Jadoul 1996) made up the bioconstruction while other invertebrates are represented by almost mono–specific bivalve associations (Tintori 1995; Tackett and Bottjer 2012). Surprisingly, pycnodonts and the other deep body taxa appear in this poor environment and perform a fairly quick development. Only their dimensions were rather smaller than in the Jurassic and Cretaceous (except *Sargodon*, see below). As Nursall (1996b) pointed out, the ability of pycnodonts to thrive in basins surrounded by different kinds of bioconstruction throughout a time span of 175 million years is evidence of the sensational success of this group. The reef was prevalently built by sponges in the Jurassic, by rudists in the Cretaceous, and by scleractinians in the Cenozoic. Pycnodonts are replaced by teleosts, probably sparids, only starting from the Eocene. The appearance of the first durophagous teleosts in fact is recorded in the Bolca fish fauna, although forms bearing chisel–like prehensile teeth like those of pycnodonts (and *Sargodon*) are not known until the Oligocene (A.T. pers. obs. on Castelgomberto Calcarenite, near Vicenza).

The miniature fishes *Gibbodon* and *Eomesodon* are really rarely found: only two/three specimens per taxon, considering all the sites. If this rarity in some localities could be explained by the lack of systematic excavations (for example at Giffoni and Seefeld), in other sites it certainly could not. In the sites around Bergamo tens of thousands of specimens have been collected, mostly representing small–sized taxa, with a large predominance of Pholidphoridae, suggesting that these two genera were already uncommon in the original assemblage. The small size could represent a primitive character of the group because all specimens coming from lower–middle Norian sites are likewise small (A.T. pers. obs.).

Gibbodon has been differently interpreted by Nursall (1996a) and Poyato-Ariza (2015): the former believes it is the most basal form, while the latter confirms it is inside the more advanced Brembodontidae together with *Brembodus*, according to the original description by Tintori (1981). A heavy scale covering on the whole body characterizes this fish; the scales and dermal bones of the skull are very strongly ornamented. Its anterior teeth are tiny and elongate, with a spatulate and bifurcate crown, a peculiarity of *Gibbodon* among all the other pycnodonts. Due to the very small size and the tiny dentition, it was likely able to graze on only soft organisms, but the coexistence of a crushing dentition necessarily implies that also some hard parts were processed.

Eomesodon hoeferi shows more advanced characters; in particular, the caudal region lacks scales, the loricate type according to Nursall (1996b). It also bears anterior chisel–like teeth, that are considered by Nursall (1996a) more advanced than styliform prehensile teeth. Actually, these latter are present on the marginal jaw bones of a few specimens found in the surroundings of Brescia (A.T. pers. obs.), which are older than *Gibbodon* and *Eomesodon*. Thus, being the oldest known pycnodonts, these undescribed specimens take on even greater importance.

Though not a pycnodont, the quite rare, small and deep–bodied *Dandya ovalis* (Gorjanovic-Kramberger 1905), seems to have a similar behaviour but it deserves a redescription based on better specimens, after Tintori (1983) described those coming from the mountains surrounding Bergamo. This taxon was originally described from Hallein, signifying that its geographic distribution is wide, spreading from the Northern Calcareous Alps to the Southern Calcareous Alps. Both anterior and inner teeth are pencil–like. Small size combined with anterior specialized teeth suggest this fish possibly grazed on soft material from a hard substrate, like *Eomesodon hoeferi* and *Gibbodon*.

This kind of small, deep–bodied grazing fish has never been found in the Jurassic and Cretaceous reef–related assemblages, where pycnodonts were at least the size of *Brembodus*, and is apparently also missing from the modern ones (Konow et al. 2008). On the other hand the cranial anatomy of *Dandya* and pycnodonts is fairly different from that of the modern teleost ecomorphological equivalent. This could also account for the remarkable difference in biodiversity between the modern teleosts and the Norian fish fauna (Konow et al. 2008): at that time only a few species shared the same substrate grazing/scraping trophic niche. Nonetheless, some of their distinctive features have disappeared in the meantime, for example the small size.

Brembodus is the most common genus among the Norian pycnodonts. Its size, 12–15 cm in standard length, is comparable to that of the widespread Jurassic and Cretaceous species. It has anterior chisel–like teeth and well-developed crushing batteries, as did most of the younger pycnodonts. The fragments contained in the gut of several Jurassic and Cretaceous specimens (Nursall 1996b) suggest that *Brembodus* not only grazed on hard substrates, but it also was able to crush shells. Scales, entirely covering its body, grow thinner in the posterior part, giving rise to the trend which later on will lead to the progressive demise of scales in the caudal region (loricate, peltate and clathrate pattern in Nursall 1996b). Another feature that appeared for the first time in *Brembodus* is an anterior bar (Nursall 1996b) on almost all scales, including those of the caudal anterior region. In the forms with highest specialization, this will be the only remaining part of the scales, even in the caudal anterior region. Interestingly, the imbricate (*Gibbodon*) and loricate (*Eomesodon*) patterns coexist with an intermediate form (*Brembodus*). This evolution of the scale covering in the caudal region is not exclusive to pycnodonts: several of the deep–bodied fishes show it as well, for example the Norian *Sargodon* (Tintori 1983) and *Hemicalypetrus* (Schaeffer 1967), appearing in the new, hyper–specialized Norian neopterygians. The deep–bodied middle Triassic neopterygians—such as *Luoxiongichthys* and *Kyphosichthys* from southern China (Wen et al. 2012; Xu and

Wu 2012)—and subholosteans—such as *Felberia* and *Stoppania* (Lombardo and Tintori 2004; Lombardo et al. 2008)—show no traces of this evolutionary trend. Their scale ornamentation can be different in the anterior and caudal regions, but they never show a thinning in the posterior region (Garbelli and Tintori 2015).

Some Norian deep–bodied fishes kept a homogeneous covering of ganoid scales. One of these is *Dapedium*; after the first occurrence with the species *D. noricum* Tintori 1983, the genus greatly expands during the Early Jurassic (Thies and Waschkewitz 2016). Despite its robust dentition (Thies and Hauff 2011) *Dapedium* is not as specialized as *Sargodon* or pycnodonts; the anterior prehensile teeth are missing, so it probably was not a demersal fish. Like pycnodonts and the more advanced semionotiforms, this genus will survive the new dramatic biological crisis of the T/J boundary (Van De Schootbrugge and Wignall 2016).

A behavior comparable to that of pycnodonts can be found in *Sargodon tomicus* (Fig. 9.7). Compared to the Triassic pycnodonts, however, with its maximum size over one meter, it was much larger and nearer to the largest Jurassic (up to 1.5 m—F. Poyato-Ariza, pers. com. Poyato-Ariza 2015) and Cretaceous pycnodonts. *Sargodon* was described in the middle nineteenth century on the basis of anterior chisel teeth. The first complete specimens were found in the Zorzino Fauna (Tintori 1983; Muscio 1988). Besides a peculiar histology that makes the identification easy and reliable (Orvig 1978), teeth of *Sargodon* have large size and a peculiar chisel–like to swallow–tailed morphology (Fig. 9.7). Concerning general morphology, the rhomboidal body is extremely laterally compressed, enabling good maneuverability in the fairly simple reefal habitat surrounding the Norian basins. *Sargodon*'s teeth are also frequently found in the Rhaetian Bone Beds, confirming the very wide geographic distribution of this genus, from southern Italy to Hallein (Austria) up to England. The stratigraphic distribution ranges at least from middle/upper Norian to Rhaetian: some isolated teeth have been found also in the Rhaetian Zu Limestone in Lombardy (A.T. pers. obs.). In general, we can define *Sargodon* as a greatly successful genus, even though no descendants took its place when it became extinct at the end of the Triassic. Furthermore, the only ecological equivalents are the uppermost Jurassic large pycnodonts *Gyrodus* and *Arduafrons*.

While in the TMFF deep–bodied demersal fishes are present only one genus at a time, in the Norian there are three very small taxa (two pycnodonts plus *Dandya*), one middle–sized pycnodont and the large *Sargodon*. This expresses a first step on the way of diversification, obviously not comparable to the diversity observed in Late Jurassic assemblages, where several more, middle to large species of pycnodonts are known.

One more similar taxon has been detected in the Forni Dolostone in Friuli, but so far only two specimens have been collected and are at present under study by the authors (Fig. 9.8). The new taxon, not a pycnodont, has a size close to *Brembodus*, the body outline being somewhat more elongate. The scale covering follows the general deep-bodied pattern (reduction or vanishing in the caudal region), but the scales are only in the abdominal region, thus being more specialized than *Brembodus* itself. Prehensile teeth are bifurcate and at least six on each premaxilla and five on each dentary.

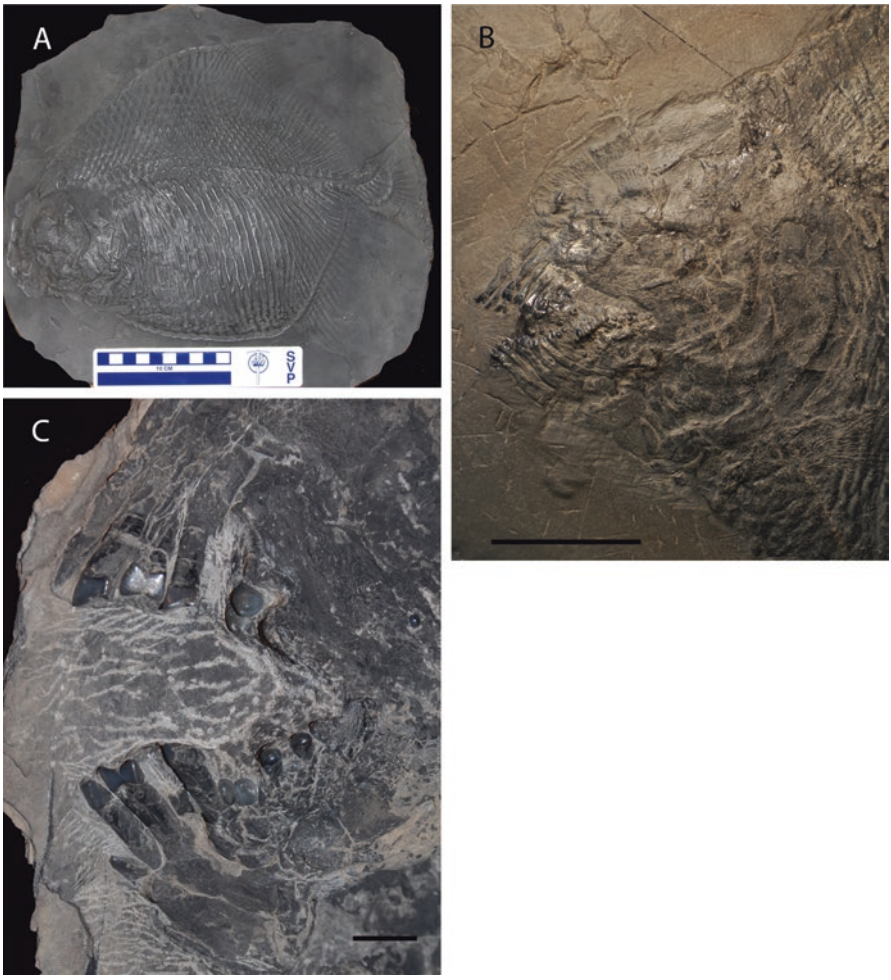

Fig. 9.7 *Sargodon tomicus*. (**a**) Cast of the specimen from Riva di Solto Shale around Berbenno (Bergamo): the specimen is only the imprint of the actual specimen that has not been recovered. Original in Museo di Scienze Naturali 'E.Caffi', Bergamo. (**b**) Skull of a juvenile from Zogno2 site. Paleontological Collection UNIMI. (**c**) Prehensil dentition of a fully adult specimen from Zogno-Endenna at Museo Brembano (S. Pellegrino, Bergamo)

Another group of demersal durophagous fishes is represented by semionotids like *Paralepidotus* (Fig. 9.9a, b). This fish is commonly found in most Norian sites, from Hallein to Giffoni. As an adult, *Paralepidotus* had a deep fusiform body (Tintori and Olivetti 1988; Tintori 1996), provided with a powerful crushing dentition made up of hemispheric teeth. As a juvenile, its body was much more slender and its teeth were higher and somewhat pointed (Tintori 1996), implying that in this period of life it was less strictly tied to the bottom environment and its diet was different. A small *Paralepidotus* in fact has been preyed by a *Saurichthys* (A.T. pers. obs.):

Fig. 9.8 Gen. n sp. n. (under description by the authors) from the Forni Dolostone in the Tolmezzo (Udine) area. Museo Friulano di Storia Naturale in Udine. (**a**) Complete specimen. (**b**) Detail of the dentition. Scale bar equals 5 mm

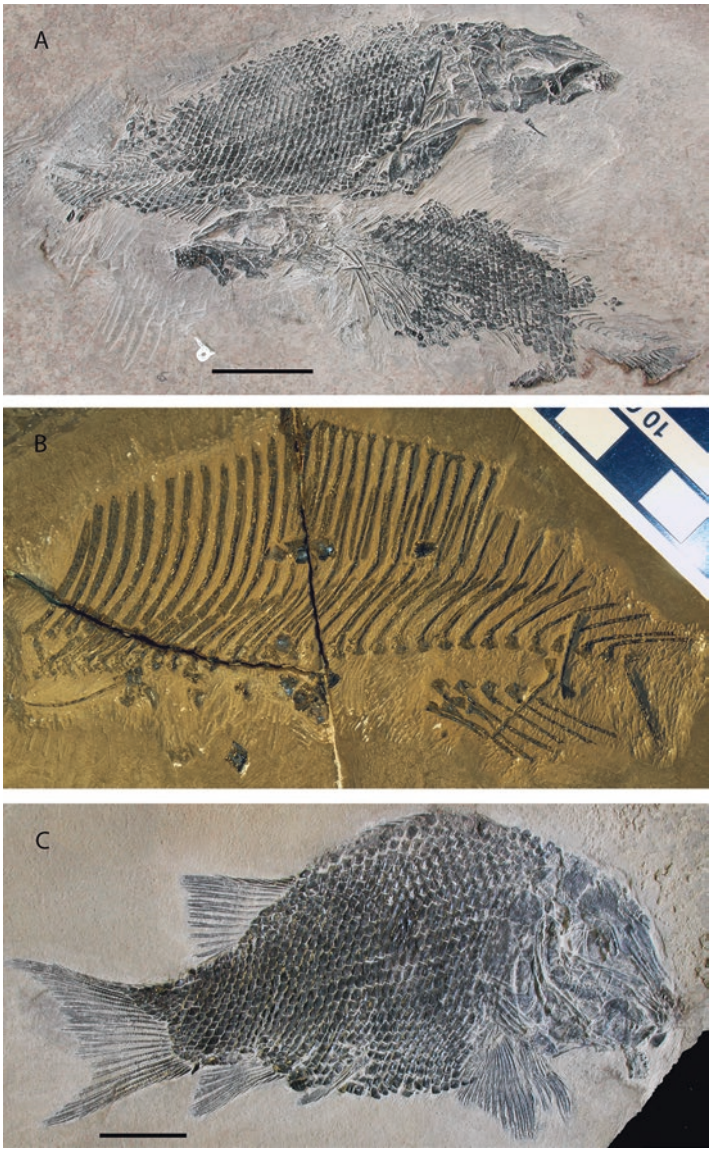

Fig. 9.9 (**a**, **b**) *Paralepidotus ornatus* from Bed 11 in Zogno2 site. (**a**) Young adults. Most skull dermal bones and fin rays as well as scales are missing possibly due to after death floating. This kind of preservation is recorded only in specimens of such a size. (**b**) partial axial skeleton of a larger specimen. (**c**) *Semiolepis brembanus*, the holotype from Bed 6 in Zogno2 site. Paleontological collection UNIMI. Scale bars equal 10 mm

it likely lived in the water column, feeding on the small crustaceans, which are commonly found in the same fossil–bearing levels. When it grew over 20 cm, the body of *Paralepidotus* increased in depth and teeth became lower and more domed. At this ontogenetic phase it probably approached the sea bottom and started to feed on bivalves, as is demonstrated by very abundant coprolites made up of bivalve shell fragments (Tintori 1995). These mollusks were epibenthic, presumably fixed into the mud by bissum filaments, like the modern *Modiolus*. The somewhat elongate prehensile anterior teeth of *Paralepidotus* are clearly less specialized than those borne by *Sargodon* and pycnodonts. The kind of prey and the body shape of *Paralepidotus* suggest it lived near the uppermost slope connecting the deepest, anoxic part of the lagoon to the carbonate platform. Such an oxic soft sandy/muddy bottom allowed a rather poor diversity of a thriving benthic fauna consisting of echinoderms, corals, crustaceans and, most of all, mollusks (Pinna 1974; Basso and Tintori 1994). These latter likely lived in huge banks, given the resedimented shell beds occasionally interbedded in the anoxic sediments of the Calcare di Zorzino and overlying units (Tintori 1995; Tackett and Bottjer 2012). *Paralepidotus* introduces something new in the relationships with bottom sediments and with benthic organisms, being the first very common durophagous fish. With its large size (easily over 50 cm) and great abundance, often present in mass mortality surfaces (like beds 11–12 at Zogno2, or at Hallein), in fact it contributes to sediment accumulation: nowadays, up to 50 g per month of broken *Mytilus* shells have been recorded from a small *Diplodus* in a lab tank (A.T. pers. obs.). This relationship between fishes and benthic fauna will have an extraordinary development with teleosts, especially sparids, during the Cenozoic (Cadée 1968, A.T. pers. obs. from *Diplodus* in lab tank).

For a final comment on the comparison between Mesozoic and Cenozoic durophagous fishes, it is worth pointing out the remarkable differences in the jaw mechanics. Pycnodonts and semionotiforms in fact bear a single tooth battery on the superior jaw. This battery is immobile, being supported by vomers, which are securely fixed to the ethmoidal region and to the parasphenoid (Nursall 1996a). Teleosts, on the contrary, bear batteries of crushing teeth on the mobile premaxillaries. Consequently, during the processing of prey (crushing), pycnodonts and semionotiforms move only the lower jaw, whereas in the sparids the movement involves two pairs of tooth batteries, each element being mobile.

Other neopterygian taxa in the Zorzino Fauna, although specialized, are not strictly durophagous: in particular *Semiolepis brembanus* Lombardo and Tintori 2008 and *Legnonotus krambergeri* Bartram 1977. *Semiolepis* (Fig. 9.9c) is related to semionotids and close to *Paralepidotus* (Lòpez-Arbarello 2012; Gibson 2013). It was included in the Callipurbeckiidae family (Lòpez-Arbarello 2012), despite a wide time gap separating *Paralepidotus* and *Semiolepis* from the other genera, Late Jurassic in age. Compared to *Paralepidotus*, *Semiolepis* is smaller (within 25 cm in total length), and its dentition is less adapted to crushing hard exoskeletons; its body has a shape comparable to that of adult *Paralepidotus*, suggesting its habitat, though not inside the actual reef, was close to the bottom. *Legnonotus krambergeri* (Fig. 9.10), slenderer and even smaller (less than 10 cm), may have

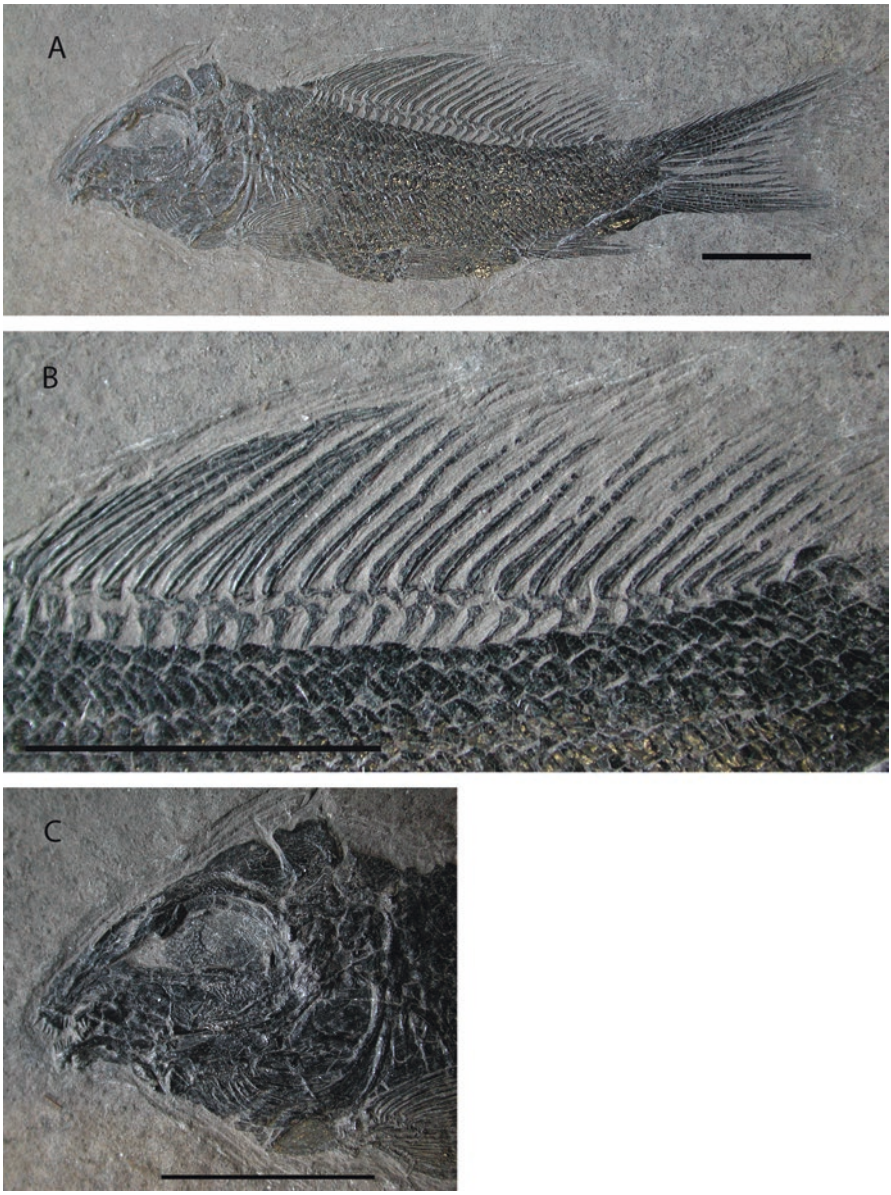

Fig. 9.10 *Legnonotus krambergeri* from Zogno-Endenna, with details of the dorsal fin area and the skull. Paleontological collection UNIMI

shared the same environment with *Semiolepis:* a smooth, sandy/muddy bottom, rich in invertebrates endowed with rather soft endoskeletons. Some other undescribed specimens of the Zorzino Fauna show other specialized dentitions, with elongate anterior teeth developed as prehensile teeth (see for instance Lombardo and Tintori 2005, pl. 2 Fig. B). The new taxa further increase the variety of trophic specializations developed by this fauna, corroborating the idea that Norian neopterygians represent an important radiation event, reaching a biodiversity level never achieved again throughout most of the Mesozoic Era.

9.2.3 The Stem Teleostei, The Pholidophoriformes

Systematic fieldwork on the Zorzino Fauna in Lombardy has yielded huge amounts of specimens, mainly represented by small–sized (less than 10 cm) pholidophorids. On the contrary, at Hallein, a private excavation (I. Kogan, pers. comm.) apparently shows a preponderance of *Paralepidotus*, due to almost monospecific mass mortality surfaces; complete scientific results are not yet available. Regarding other localities, pholidophorid findings are common but not as overwhelmingly as in Lombardy. We must keep in mind that random fossil collections mostly consist of large specimens (or fragments): small fishes, in fact, are easily overlooked, and also rapidly destroyed once exposed to weathering. Therefore, the hundreds of well–preserved specimens found in the 1970s in the new sites of Lombardy have aroused new interest in small fishes. Zambelli—at the time director of the Museo di Storia Naturale 'Caffi' di Bergamo—published a first sequence of descriptive papers (Zambelli 1975, 1978, 1980a, b, c, 1986, 1990): he described *Parapholidophorus, Pholidorhynchodon, Pholidoctenus, Eopholidophorus*, and ascribed a new species to the type genus *Pholidophorus*. Unfortunately, being written in Italian, these works never reached the international scientific community.

The genus *Pholidophorus* was erected by Agassiz (1832) to include *Pholidophorus latiusculus* (the type species) and *P. pusillus*, from the Norian of Seefeld (Austria). Since then, many other species have been ascribed to this taxon, soon becoming a 'basket genus', as it gathered diverse Triassic and Jurassic small fishes with a fusiform body covered with ganoid scales.

Woodward (1890) erected the family Pholidophoridae and Berg (1937) the order Pholidophoriformes (see Arratia 2013 for a detailed history of the group). Only in 1966, Nybelin resumed the studies on this group; following the modern guidelines, he gave a more limited interpretation to the order. Only recently, Arratia (2013) almost completely revised the Late Triassic (mostly Norian) taxa, previously generally neglected to the advantage of the Jurassic taxa. In this monograph, Arratia (2013) gives a comprehensive redescription of all the Late Triassic Pholidophoridae, adding a couple of new genera from the Zorzino Fauna: *Annaichthys* and *Zambellichthys*. At present, the total number of genera coming from the various

Norian localities is seven: most are found only in the Italian sites. Actually, the hundreds of specimens considered by Arratia (2013) were ultimately found in just two sites in the surroundings of Bergamo: Cene (upper Zorzino Limestone) and Ponte Giurino (lower Riva di Solto Shale). A huge amount of other fossils (hundreds of specimens) yielded by other sites still have to be studied. Most of them mainly belong to known taxa, but every site shows a slightly different assemblage, from both the quantitative and qualitative point of view (A. T. pers. obs.), so that in the future it will likely be necessary to erect new taxa. Actually, Arratia (2017) erected a new *Pholidoctenus* species on specimens from a small Riva di Solto Shale outcrop in the vicinity of San Pellegrino (Bergamo) and also ascribed the species *Ph. gervasuttii* Zambelli, 1980 to the new genus *Lombardichthys*. Recently Taverne and Capasso (2015) erected a new genus on a single, poorly preserved specimen purchased in the last century and said to have been found at Cene. We believe this taxon is not valid for two reasons: very bad preservation prevents the observation of most fundamental features and the only specimen (thus the holotype) is stored in a private collection, which is not at present available to other researchers (Arratia 2017). In our opinion, it is probably a *Pholidorhynchon* specimen, quite common in the Cene assemblage.

We underline once more the impressive diversification of several fish groups in this otherwise scarcely varied marine paleoenvironment. In a blooming group such as that of Norian pholidophorids (Fig. 9.11), even a short time gap or a slight difference in the habitat could have greatly affected the diversification. The first appearance of the group occurred in the late Ladinian of southwestern China (Tintori et al. 2015) where *Malingichthys* is quite common, to proceed then in the Carnian, with certainly less rich and well preserved fossil material (Arratia 2013). In the middle–late Norian Pholidoriphormes (*sensu* Arratia 2013) had their maximum diversification. Eventually, given the huge number of well–preserved specimens, the pholidophorid fauna of the Zorzino Limestone represents a favorable opportunity to study the intraspecific variability, as well as the reasons of such a high diversification in a habitat where life in general was not thriving nor greatly varied (isolated, relatively small lagoons). While several studies on both the mutual relationships and on the origin of teleosts often produce divergent results (Arratia 1999, 2000, 2013, 2017; Taverne 2011), it is unquestionable that in the Zorzino Fauna pholidiphorids replace subholosteans at the base of the vertebrate trophic chain, deeply contributing to an almost totally new fish assemblage. *Peltopleurus* and *Pholidopleurus* in fact made up the basal bulk still in the early Carnian (Griffith 1977), even though some pholidophorids, *Knerichthys* and *Pholidophoretes,* were already present (Arratia 2013). As discussed above, though still ecologically important, subholosteans in the Norian numerically represented only a small part of the total fauna. This is the major difference from the TLFF, but we cannot precisely determine when this substitution occurred (Tintori et al. 2014a).

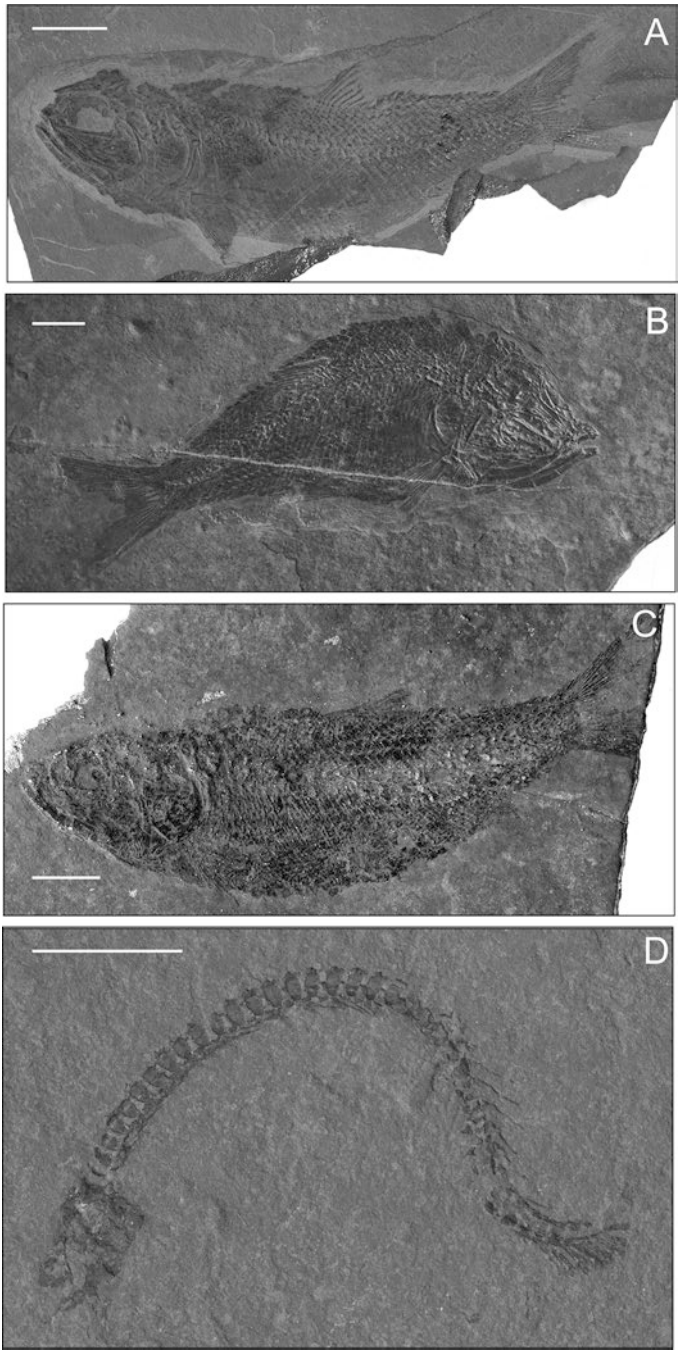

Fig. 9.11 Pholidophoridae specimens from Zogno-Endenna site. (**a–c**) complete, totally articulated, specimens. (**d**) endocranium plus a complete vertebral column. Paleontological collection UNIMI. Scale bars equal 10 mm

9.3 Conclusions

The discovery of the Zorzino Fauna in the early 1970s, with the resulting early studies, represent one of the crucial events in the paleontological landscape of the twentieth century. The most important one is probably the description of the oldest flying reptiles (Wild 1978), that has allowed to date the appearance of pterosaurs to 30 Ma earlier than previously stated. This fauna had been neglected for a long time after Agassiz had described some specimens from Seefeld, in the first half of the nineteenth century: the reason could be that neither the Zorzino Limestone nor the other coeval rocks—spread from northern Austria to southern Italy—were exploited for economical purposes. On the contrary, large quarries and mines were opened in the Besano Formation on Monte San Giorgio (Middle Triassic), in the Toarcian rocks at Holzmaden and in the upper Jurassic units at Solnhofen/Eichstätt; in all these sites fossils were abundantly found by quarrymen, seeking extra–salary earnings. Only about 50 years ago the landslide in the Cene quarry (Bergamo) allowed the discovery of a fossil–bearing level, rich enough to deserve systematic field work. In several localities of northern Italy, during the following 20 years, excavations and fieldwork have concerned various fossiliferous horizons, stratigraphically situated around the Middle–Upper Norian boundary. Thousands of fish remains have been collected, beside reptiles and invertebrates such as arthropods, echinoderms, mollusks, corals and a few insects. Many fishes are still awaiting preparation.

In the light of the foregoing, the difference in biodiversity among sites of northern Italy, Austria and southern Italy could be deceptive: some localities (northern Italy, Hallein) yielded hundreds of fossils, while others (Seefeld, Giffoni) just a few scattered specimens. This applies mainly to pholidophorids, but also to the different faunas in their entirety. Nonetheless, the general structure of each faunal assemblage is always similar: top predator paleopterigyans + small pholidophorids + durophagous neopterygians. A comparison of the different assemblages would be important also because the present latitudinal distance among the sedimentary basins (spread from Sicily to northern Austria) could correspond to a climatic differentiation during the Triassic. Unfortunately, only Hallein seems to be useful for this at the moment, owing to number of species recorded, even if large amounts of specimens come mainly from almost monospecific mass mortality surfaces (Hornung, T., Salzburg, written comm. 2016).

Just as in the TEFF and TMFF, *Saurichthys* and *Birgeria* shared the top position in the trophic web of the Zorzino Fauna, at least throughout the whole Triassic, being the only two genera among actinopterygians to have such a long range; the first record of *Saurichthys* dates back to Late Permian (Tintori 2013). The general morphology of their body—shape and size, especially those of *Birgeria*—remained almost unvaried for about 50 My. Nonetheless, in *Saurichthys* other features change after the oldest species. Tintori (1990) proposed that the Zorzino species show the most advanced characters in the structure of the vertebral column. On the contrary, Rieppel (1992) hypothesized a variety of evolutionary trends, especially in body scale covering and median fin patterns. More recently, Tintori (2013) and Tintori

et al. (2014b) proved that specializations in *Saurichthys* do not follow a regular trend: the two most common Norian species (*S. deperditus* and *S.* sp. b.) show the coexistence of 'primitive' and 'specialized' characters. Furthermore, the most 'specialized' characters had been already achieved by species of the TMFF and remained unchanged in the Norian, even if most part of the ichthyofauna became totally different.

For the first time teleosts—with the most primitive taxa, such as pholidophorids—play a strategically important role in the marine ecosystem: a preview of the radiation that will begin during the Late Jurassic, without reaching immediately a high diversification. Primitive teleosts, in fact, become the base of the vertebrate trophic chain, replacing both the subholostean and basal neopterigyan miniature taxa that had occupied the same position in the TMFF. Following recent studies, there is evidence that even if the Pholidophoridae had a rather long history before the Norian, their blooming probably occurred around the Middle/Late Norian boundary in areas now corresponding to the Southern Calcareous Alps. Early Jurassic marine fish assemblages are rather different from those of the Zorzino Fauna, the former seemingly containing less abundant primitive teleosts (leptolepids) and non–teleostean neopterygians—such as pycnodonts and semionotiforms. Actually, this difference could also be attributable to the respective preservation environments. In the Jurassic basins of Lyme Regis or Holzmaden—commonly yielding ichthyosaurs, plesiosaurs and pseudo–planktonic crinoids—the paleoenvironment was much more pelagic than in the Middle–Late Triassic intra–platform lagoons. Due to the scantiness of preservation windows, the following Jurassic marine Fossil–Lagerstätten are too sporadic to obtain a sequence of evolutionary events for fishes, as accurate as the one of Early–Middle Triassic. Only in the Late Jurassic Kimmeridgian/Tithonian time the 'Solnhofen Archipelago' will provide a series of Fossil–Lagerstätten whose frequency and biodiversity are comparable to—or even higher than– those of the Late Triassic. Nonetheless, the number of durophagous taxa is low and limited to pycnodonts (Bellwood and Hoey 2004), a few semionotiforms and macrosemiids (Lòpez-Arbarello and Sferco 2011; Lòpez-Arbarello 2012), without significant changes. The paleoenvironment in the topmost Jurassic consisted, as in the Triassic, of lagoons surrounded by carbonate platforms with marginal reefs basically built by sponges; on the bottom of these basins conditions were finally favorable again to preservation (Arratia et al. 2015).

The appearance or radiation of groups with durophagy–specialized trophism (pycnodonts and Semionotiformes s.l.) is seemingly not related to reef differentiation: in the southern alpine Middle Norian, in fact, where the variety of specialized fishes is at a maximum, bioconstructions are very poor (Berra and Jadoul 1996) and benthic organisms (mostly bivalves) are often oligo– or even mono–specific (Tintori 1995). Later on, during the Late Norian/Rhaetian, while benthic invertebrates become more varied (Tackett and Bottjer 2012), fish taxa remain pretty stable despite conditions for preservation that are no longer optimal (A.T. pers. obs., mainly on scattered remains from shell beds in Riva di Solto Shale and Zu Limestone Authorum). Therefore, what triggered the differentiation is still unknown.

On the basis of the above considerations, Norian ichthyofaunas (TLFF) represent the apex of the Triassic recovery/revolution that has seen completely different assemblages following one another (TEFF and TMFF) for 30 My since the P/T, up to the advent of the TLFF. The latter contains elements inherited from the TMFF (e.g. subholosteans and *Saurichthys*), as well as new groups such as the Pycnodontiformes and the more advanced Semionotiformes (Macrosemiidae and Callipurbeckiidae), and also the blooming primitive teleosteans. Thus, rather than a substitution by more specialized forms, we hypothesize the actual appearance of new trophic and ecologic niches.

Finally, we underline the still remarkable presence of some highly specialized subholosteans: the gliding fish *Thoracopterus*, for example, spans for at least 30 My, starting from Late Ladinian (Tintori and Sassi 1992; Tintori et al. 2012). Due to the scarcity of Fossil–Lagerstaetten recorded in the Late Norian/Rhaetian, it is impossible to say whether the disappearance of both subholosteans and many other non–neopterigyan actinopterygians coincides with the T/J crisis. Certainly, the Sinemurian ichthyofauna of Lyme Regis, the first in the Jurassic, as well as the somewhat younger Holzmaden one, prove to be ultimately different from that of the Zorzino Fauna in both systematics and trophic/swimming structure. However, we must point out that these two fish assemblages reflect also a different paleoenvironment, a more open sea, instead of the coastal lagoons mostly surrounded by carbonate platform. Similarities to the Late Triassic fish assemblage paleoenvironment is seen again in the Late Jurassic, with what it is now called 'Solnhofen archipelago' faunas. Small basins surrounded by shallow water carbonatic banks and reef yield rich ichthyofaunas made mainly by the neoptergian groups that have originated in the Late Triassic, as subholosteans and most other paleopterygians are missing.

References

Agassiz L (1832) Untersuchungen über die fossilen Fische der Lias–Formation. Jahr Mineral Geogn Geol Petrefakt 3:139–149

Agassiz L (1833–1844) Recherches sur les Poissons Fossiles, vol 5 volumes. Neuchâtel and Soleure, Petit Pierre, p 1798

Arratia G (1999) The monophyly of Teleostei and stem–group teleosts: consensus and disagreements. In: Arratia G, Schultze HP (eds) Mesozoic Fishes 2—systematics and fossil record. Verlag Dr. F. Pfeil, Munich, pp 265–334

Arratia G (2000) New teleostean fishes from the Jurassic of southern Germany and the systematic problems concerning the 'pholidophoriforms'. Paläont Zeit 74:113–143

Arratia G (2013) Morphology, taxonomy, and phylogeny of Triassic Pholidophorid fishes (Actinopterygii, Teleostei). J Vert Paleontol 33(Suppl):1–138

Arratia G (2017) New Triassic teleosts (Actinopterygii: Teleosteomorpha) and the phylogenetic relationships of most basal teleosts and their classification. J Vert Paleontol. https://doi.org/10.1080/02724634.2017.1312690

Arratia G, Schultze HP, Tischlinger H, Viohl G (2015) Solnhofen—Ein Fenster in die Jurazeit. Verlag Dr. F. Pfeil, Munich, p 616

Bartram AWH (1977) The Macrosemiidae, a Mesozoic family of Holostean fishes. Bull Br Mus Nat Hist (Geol) 29:137–234

Bassani F (1892) Sui fossili e sull'età degli scisti bituminosi di Monte Pettine presso Giffoni Valle Piana in Provincia di Salerno (Dolomia Principale). Mem Soc It Sc dei XL, serie 3(9):1–27
Bassani F (1895) La ittiofauna della Dolomia Principale di Giffoni (prov. di Salerno). Paleontol It 1:169–210
Basso D, Tintori A (1994) New Triassic isopod crustaceans from Northern Italy. Paléo 37:801–810
Bellwood D, Hoey A (2004) Feeding in Mesozoic fishes: a functional perspective. In: Arratia G, Tintori A (eds) Mesozoic Fishes 3–Systematics. Palaeoenvironment and Biodiversity. Verlag Dr. Pfeil, Munich, pp 639–649
Beltan L (1980) Eotrias du nord–ouest de Madagascar: Etude de quelques poissons, dont un est en parturition. Ann Soc Géol Nord 99:453–464
Berg LS (1937) Classification of fishes, both Recent and fossil. Doklady Zoological Institute 5:85–517 (English translation by JW Edwards, Ann Arbor, Michigan, 1940)
Berra F, Jadoul F (1996) Norian Serpulid and Microbial bioconstructions: implications for the platform evolution in the Lombardy Basin (Southern Alps, Italy). Facies 35:43–162
Blake DB, Tintori A, Hangdorn H (2000) A new, early crown–group asteroid (Echinodermata) from the Norian (Triassic) of Northern Italy. Riv It Paleont Strat 106:141–156
Boni A (1937) Vertebrati retici italiani. Reale Accademia Nazionale dei Lincei VI 6(0):521–719
Bray DJ, Gomon MF (2017) Breams, Sparidae in: Fishes of Australia. http://fishesofaustralia.net.au/home/family/129. Accessed 14 Jan 2017
Bronn HG (1858) Beitrage zur triasischen Fauna und Flora der bituminosen Schiefer von Raibl. N Jahr Min Geogn Geol Petrefakt 1858(1–32):129–142
Bronn HG (1859) Nachtrag über die Trias–Fauna von Raibl. N Jahr Min Geogn Geol Petrefakt 1858:39–45
Bürgin T (1992) Basal Ray–finned Fishes (Osteichthyes; Actinopterygii) from the Middle Triassic of Monte San Giorgio (Canton Tessin, Switzerland). Schweiz Paläontol Abh 114:1–164
Cadée GC (1968) Molluscan biocoenoses and thanatocoenoses in the Ria de Arosa, Galicia, Spain. Zool Werhandel 95:1–121
Casati P (1964) Il Trias in Lombardia (Studi geologici e paleontologici). VI. Osservazioni stratigrafiche sull'"Infraretico" delle Prealpi bergamasche. Riv It Paleont Strat 70:447–465
Cate AS, Evans I (1994) Taphonomic Significance of the Biomechanical Fragmentation of Live Molluscan Shell Material by a Bottom–feeding Fish (*Pogonias cromis*) in Texas Coastal Bays. PALAIOS 9:254–274
Costa OG (1862) Studii sopra i terreni ad ittiolitti del Regno di Napoli diretti a stabilire l'età geologica dei medesimi. Parte I: Scisti bituminiferi di Giffoni. Appendice agli atti della Real Accademia delle Scienze, Napoli 1862:1–44
Dalla Vecchia FM (2008) Vertebrati Fossili del Friuli—450 milioni di anni di evoluzione. Ed Museo Friulano di Storia Naturale, Udine. 303 pp
Forchielli A, Perveler P (2013) Phosphatic cuticle in thylacocephalans: a taphonomic case study of (Arthropoda, Thylacocephala) from the Fossil–Lagerstätte Polzberg (Reingraben shales, Carnian, Upper Triassic, Lower Austria). Austr J Earth Sci 106:46–61
Fürsich FT, Wendt J (1977) Biostratinomy and palaeoecology of the Cassian Formation (Triassic) of the Southern Alps. Palaeogeogr Palaeoclimatol Palaeoecol 22:257–323
Garbelli C, Tintori A (2015) A preliminary study of the ornamentation pattern of ganoid scales in some Mesozoic actinopterygian fishes. Boll Soc Paleont It 54:219–228. https://doi.org/10.4435/BSPI.2015.14
Gibson SZ (2013) Biodiversity and Evolutionary History of †*Lophionotus* (Neopterygii: †Semionotiformes) from the Western United States. Copeia 2013(4):582–603
Gorjanovic-Kramberger D (1905) Die Obertriadische Fischfauna von Hallein in Salzburg. Beítr Palaeont Geol Oest–Ung Or 18:193–224
Gozzi E (2006) Analisi tassonomica e morfo–funzionale di Saurichthys e Birgeria (Osteichthyes, Actinopterygii). Unpublished PhD Thesis, Università degli Studi di Milano
Gozzi E, Renesto S (2003) A complete specimen of *Mystriosuchus* (Reptilia, Phytosauria) from the Norian (Late Triassic) of Lombardy (Northern Italy). Riv It Paleont Strat 109:475–498

Grassé PP (1958) Traité de zoologie. 13: Agnathes et poissons. Anatomie, éthologie, systématique. Masson Ed

Griffith J (1977) The Upper Triassic Fishes from Polzberg bei Lunz, Austria. Zool J Linnean Soc 60:1–93

Jadoul F (1986) Stratigrafia e paleogeografia del Norico nelle Prealpi Bergamasche occidentali. Riv It Paleont Strat 91:479–512

Jadoul F, Berra F, Frisia S (1992) Stratigraphic and paleogeographic evolution of a carbonate platform in an extensional tectonic regime: The example of the Dolomia Principale in Lombardy (Italy). Riv It Paleont Strat 98:29–44

Jadoul F, Masetti F, Cirilli S, Berra F, Claps M, Frisia S. (1994) Norian–Rhaetian stratigraphy and paleogeographic evolution of the Lombardy Basin (Bergamasc Alps). In Carannante G, Tonielli R (eds) 15th Reg Meet, April 1994, Ischia, Italy, post–meeting fieldtrip guidebook, Excursion B1, 5–38

Kner R (1866a) Die fossilen Fische der Asphaltschiefer von Seefeld in Tirol. Sitz Ak Wiss Wien 54:303–334

Kner R (1866b) Die Fische der bituminösen Schiefer von Raibl in Kärnthen. Sitz Ak Wiss Wien 53:152–197

Kner R (1867) Nachtrag zu den fossilen Fischen von Raibl. Sitz Ak Wiss Wien 55(1):718–722

Kner R (1868a) Nachtrag zur Fossilen Fauna der Asphaltschiefer von Seefeld in Tirol. Sitz Ak Wiss Wien 56/1:898–909, 911–913

Kner R (1868b) Noch ein Nachtrag zur Kenntniss der fossilen Fische von Raibl in Kärnthen. Sitz Ak Wiss Wien 56(1):909–910

Kogan I, Romano C (2016) Redescription of *Saurichthys madagascariensis* Piveteau, 1945 (Actinopterygii, Early Triassic), with implications for the early saurichthyid morphotype. J Vert Paleontol DOI. https://doi.org/10.1080/02724634.2016.1151886

Kogan I, Pacholak S, Licht M, Schneider JW, Brücker C, Brandt S (2015) The invisible fish: hydrodynamic constraints for predator–prey interaction in fossil fish *Saurichthys* compared to recent actinopterygians. Biol Open 4:1715–1726

Konow N, Bellwood DR, Wainwright PC, Kerr AM (2008) Evolution of novel jaw joints promote trophic diversity in coral reef fishes. Biol J Linnean Soc 93:545–555

Liu GB, Yin GZ, Luo YM, Wang XH, Wang SY (2006) Preliminary examination of fish fossils from Upper Triassic Wayao Member of Falang Formation in Guanling of Guizhou. Acta Paleontol Sin 45:1–20. (In Chinese with English abstract)

Lokrantz J, Nyström M, Thyresson M, Johansson C (2008) The non–linear relationship between body size and function in parrotfishes. Coral Reefs 27:967–974. https://doi.org/10.1007/s00338–008–0394–3

Lombardo C (2001) Actinopterygians from the Middle Triassic of northern Italy and Canton Ticino (Switzerland): anatomical descriptions and nomenclatural problems. Riv It Paleont Strat 107:345–369

Lombardo C, Brambillasca F (2005) A new perleidiform (Actinopterygii, Osteichthyes) from the Late Triassic of Northern Italy. Boll Soc Paleont It 44:25–34

Lombardo C, Tintori A (2004). New perleidiforms from the Triassic of the Southern Alps and the revision of Serrolepis from the Triassic of Würtemberg (Germany). In: Arratia G, Tintori A, (eds) Mesozoic Fishes 3–Systematics, palaeoenvironment and biodiversity. Verlag Dr. Pfeil, Munich pp 179–196

Lombardo C, Tintori A (2005) Feeding specializations in Late Triassic fishes. Annali Università Ferrara, Museologia Scientifica e Naturalistica, special volume 2005:25–31

Lombardo C, Tintori A (2008) A new Semionotid fish (Actinopterygii) from the Upper Triassic of northern Italy. Mesozoic Fishes 4—Homology and Phylogeny. Arratia G, Schultze HP, Wilson MVH. (eds) Verlag Dr. Friedrich Pfeil, München pp 129–142

Lombardo C, Rusconi M, Tintori A (2008) New perleidiform from the Lower Ladinian (Middle Triassic) of the Northern Grigna (LC). Riv It Paleont Strat 114:263–272

Lombardo C, Sun ZY, Tintori A, Jiang DY, Hao WC (2011) A new species of the genus *Perleidus* (Actinopterygii: Perleidiformes) from the Middle Triassic of southern China. Boll Soc Pal It 50:75–83

Lòpez-Arbarello A (2012) Phylogenetic interrelationships of Ginglymodian Fishes (Actinopterygii: Neopterygii). PLoS One 7:e39370

Lòpez-Arbarello A, Sferco E (2011) New semionotiform (Actinopterygii: Neopterygii) from the Late Jurassic of southern Germany. J Syst Palaeontol 9:197–215

Maxwell EE, Romano C, Wu FX, Furrer H (2015) Two new species of *Saurichthys* (Actinopterygii: Saurichthyidae) from the Middle Triassic of Monte San Giorgio, Switzerland, with implications for character evolution in the genus. Zool J Linnean Soc 173:887–912

Muscio G (1988) Sargodon tomicus, Plieninger, 1847, from the Norian of Val Preone (Udine, Italy). Gortania 9:57–66

Mutter RJ, Cartanya J, Basaraba SAU (2008) New evidence of Saurichthys from the Lower Triassic with an evaluation of early saurichthyid diversity. In: Arratia G, Schultze HP, Wilson MVH (eds) Mesozoic Fishes 4—Homology and Phylogeny. Verlag Dr. Friedrich Pfeil, Munich pp 103–127

Nielsen E (1949) Studies on Triassic fishes from East Greenland. II. *Australosomus* and *Birgeria*. Palaeozoologica Groenlandica 3:1–309

Nursall JR (1996a) The phylogeny of pycnodont fishes. In Arratia G, Viohl G. (eds) Mesozoic fishes—systematics and paleoecology. Verlag Dr. Friedrich Pfeil, München pp 125–152

Nursall JR (1996b) Distribution and ecology of pycnodont fishes. In Arratia G, Viohl G (eds) Mesozoic fishes: systematics and paleoecology. Verlag Dr. Friedrich Pfeil, München pp 115–124

Nursall JR (2010) The case of pycnodont fishes as the fossil sister–group of teleosts. In: Nelson JS, Schultze HP, MVH W (eds) Origin and phylogenetic interrelationships of teleosts. Verlag Dr. Friedrich Pfeil, München, pp 37–60

Nybelin O (1966) On certain Triassic and Liassic representatives of the family Pholidophoridae s. str. Bull Br Museum (NH). Geology 11:351–432

Orvig T (1978) Microstructure and growth of the dermal skeleton in fossil Actinopterygian fishes: *Nephrotus* and *Colobodus*, with remarks on the dentition in other forms. Zool Scripta 7:297–326

Pinna G (1974) I Crostacei della fauna Triassica di Cene in Val Seriana (Bergamo). Atti Soc It Sc Nat 21:7–33

Piveteau J (1930) Particularités structurales d'un type nouveau de poisson fossile des formations prmotriasiques du nord de Madagascar. Acad Sc C R Paris 191(11):456–458

Plieninger T (1847) Abbildungen von Zahnen aus der oheren Grenzbreccie des Keupers bei Degerloch und Steinenbronn. Jahr Ver Vaterl Naturk Wurttemb 3:164–167

Poyato-Ariza FJ (2015) Studies on pycnodont fishes (I): Evaluation of their phylogenetic position among Actinopterygians. Riv It Paleont Strat 121:329–343

Renesto S, Tintori A (1995) Functional morphology and mode of life of the Late Triassic placodont *Psephoderma alpinum* Meyer from the Calcare di Zorzino (Lombardy, N. Italy). Riv It Paleont Strat 101:37–48

Rieppel O (1985) Die Triasfauna der Tessiner Kalkalpen. XXV. Die Gattung *Saurichthys* (Pisces, Actinopterygii) aus der mittleren Trias des Monte San Giorgio. Schweiz Palaontol Abh 108:1–103

Rieppel O (1992) A new species of the genus *Saurichthys* (Pisces: Actinopterygii) from the Middle Triassic of the Monte San Giorgio (Switzerland), with comments on the phylogenetic interrelationships of the genus. Palaeontogr Abt A 221:63–94

Rigo M, Galli MT, Jadoul F (2009) Late Triassic biostratigraphic constraintsin the Imagna Valley (western Bergamasc Alps, Italy). Albertiana 37:39–42

Romano C, Brinkmann W (2009) Reappraisal of the lower actinopterygian *Birgeria stensioei* Aldinger, 1931 (Osteichthyes; Birgeriidae) from the Middle Triassic of Monte San Giorgio (Switzerland) and Besano (Italy). N Jahr Geol Paläontol 252:17–31

Romano C, Kogan I, Jenks J, Jerjen I, Brinkmann W (2012) *Saurichthys* and other fossil fishes from the late Smithian (Early Triassic) of Bear Lake County (Idaho, USA), with a discussion of saurichthyid palaeogeography and evolution. Bull Geosci 87:543–570

Rosen DE, Gordon M (1953) Functional anatomy and evolution of male genitalia in poeciliid fishes. Zoologica 38:1–47

Schaeffer B (1967) Late Triasic fishes fron the Westem United States. Bull Am Mus NH 135:285–342

Schlosser M (1918) Pisces. in K. A. Zittel (ed.) Grundzuge der Palaeontologie, Abt. II, Vertebrata, 3. SR Oldenbourg, Munchen and Berlin

Stensio E (1921) Triassic Fishes from Spitzbergen. Part I. Vienna 307 pp

Storrs GW (1994) Fossil vertebrate faunas of the British Rhaetian (latest Triassic). Zool J Linnean Soc 112:217–259

Strand E (1928) Miscellanea nomenclatorial zoological et palaeontologica. Arch Naturgesch 29A:30–75

Sykes JH (1974) Teeth of *Dalatias barnstonensis* in the British Rhaetic. Mercian Geol 5:39–48

Tackett LS, Bottjer DJ (2012) Faunal succession of Norian (Late Triassic) level–bottom benthos in the Lombardian Basin: implications for the timing, rate, and nature of the early Mesozoic marine revolution. PALAIOS 27:585–593. https://doi.org/10.2110/palo.2012.p12–028r

Taverne L (2011) Ostéologie et relations de *Catervariolus* (Teleostei, "Pholidophoriformes") du Jurassique moyen de Kisangani (Formation de Stanleyville) en République Démocratique du Congo. Bull Inst R S N Belg, Sc Terre 81:175–212

Taverne L, Capasso L (2015) Osteology and relationships of *Ceneichthys zambellii* gen. and sp. nov. (Teleostei, Pholidophoridae) from the Late Triassic of northern Italy. Boll Mus Civ SN Verona. Geol Paleont Preist 39:13–26

Thies D, Hauff RB (2011) A new species of *Dapedium* Leach, 1822 (Actinopterygii, Neopterygii, Semionotiformes) from the Early Jurassic of South Germany. Palaeodiv 4:185–221

Thies D, Waschkewitz J (2016) Redescription of *Dapedium pholidotum* (Agassiz, 1832) (Actinopterygii, Neopterygii) from the Lower Jurassic Posidonia Shale, with comments on the phylogenetic position of Dapedium Leach, 1822. J Syst Palaeontol 14:339–364. https://doi.org/10.1080/14772019.2015.1043361

Tintori A (1980) Teeth of the selachian genus *Pseudodalatias* Sykes, 1971, from the Norian (Upper Triassic) of Lombardy. Riv It Paleont Strat 86:19–30

Tintori A (1981) Two new Pycnodonts (Pisces, Actinopterygii) from the Upper Triassic of Lombardy (N. Italy). Riv It Paleont Strat 86:795–824

Tintori A (1983) Hypsisomatic Semionotidae (Pisces, Actinopterygii) from the Upper Triassic of Lombardy (N. Italy). Riv It Paleont Strat 88:417–442

Tintori A (1990) The vertebral column of the Triassic fish *Saurichthys* and its stratigraphical significance. Riv It Paleont Strat 96:93–102

Tintori A (1995) Biomechanical fragmentation in shell–beds from the Late Triassic of the Lombardian Basin (Northern Italy). Preliminary report. Riv It. Paleont Strat 101:371–380

Tintori A (1996) *Paralepidotus ornatus* (Agassiz 1833–43): a semionotid from the Norian (Late Triassic) of Europe. In Arratia G, Viohl G (eds) Proceedings of the Symposium "Mesozoic fishes: systematics and paleoecology", Eichstät, 1993. Verlag F. Pfeil, Munchen pp 167–179

Tintori A (1998) Fish biodiversity in the marine Norian (Late Triassic) of northern Italy: the first Neopterygian radiation. Ital J Zool 65(Suppl):193–198

Tintori A (2013) A new species of *Saurichthys* (Actinopterygii) from the Middle Triassic (Early Ladinian) of the Northern Grigna Mountain (Lombardy, Italy). Riv It Paleont Strat 119:287–302

Tintori A, Lombardo C (1996) Gabanellia agilis gen. n. sp. n. (Actinopterygii, Perleidiformes) from the Calcare di Zorzino of Lombardy (N.Italy). Riv It Paleont Strat 102:227–236

Tintori A, Olivetti L (1988) Paralepidotus ornatus nel Norico della Val Vestino (Magasa, Brescia). Natura bresciana 24:37–45

Tintori A, Renesto S (1983) The Macrosemiidae (Pisces Actinopterygii) from the Upper Triassic of Lombardy (N. Italy). Riv It Paleont Strat 89:209–222

Tintori A, Sassi D (1987) Pesci volanti del genere *Thoracopterus* nel Norico Lombardo. Nota preliminare. Riv It Paleont Strat 93:337–346
Tintori A, Sassi D (1992) *Thoracopterus* Bronn (Osteichthyes: Actinopterygii): a gliding fish from the Upper Triassic of Europe. J Vert Paleontol 12:265–283
Tintori A, Muscio G, Nardon S (1985) The Triassic fossil Fishes localities in Italy. Riv It Paleont Strat 91:197–210
Tintori A, Sun ZY, Lombardo C, Jiang DY, Ji C, Motani R (2012) A new "Flying" fish from the Late Ladinian (Middle Triassic) of Wusha (Guizhou Province, southern China). Gortania 33:39–50
Tintori A, Hitij T, Jiang DY, Lombardo C, Sun ZY (2014a) Triassic actinopterygian fishes: the recovery after the end–Permian crisis. Integr Zool 9: 394–411. First available on–line 10/2013, DOI: https://doi.org/10.1111/1749–4877.12077
Tintori A, Huang JD, Jiang D, Sun ZY, Motani R, Chen G (2014b) A new *Saurichthys* (Actinopterygii) from the Spathian (Early Triassic) of Chaohu (Anhui Province, China). Riv It Paleont Strat 120:157–164
Tintori A, Sun ZY, Ni PG, Lombardo C, Jiang DY, Motani R (2015) Oldest stem Teleostei from the Late Ladinian (Middle Triassic) of southern China. Riv It Paleont Strat 121:285–296
Van De Schootbrugge B, Wignall PB (2016) A tale of two extinctions: converging end–Permian and end–Triassic scenarios. Geol Mag 153:332–354
Wen W, Zhang QY, Hu SX et al (2012) A new basal actinopterygian fish from the Anisian (Middle Triassic) of Luoping, Yunnan Province, southwest China. Acta Palaeontol Pol 57:149–160
Wild R (1978) Die Flugsaurier (Reptilia, Pterosauria) aus der Oberen Trias von Cene bei Bergamo, Italien. Boll Soc Paleont It 17:176–256
Woodward AS (1890) The fossil fishes of the Hawkesbury Series at Gosford. Mem Geol Surv New South Wales (Palaeontogr Ser) 4:1–56
Wu FX, Sun YL, Hao WC, Jiang DY, Xu G, Sun ZY, Tintori A (2009) New species of *Saurichthys* (Actinopterygii: Saurichthydae) from Middle Triassic (Anisian) of Yunnan Province, China. Acta Geol Sin 83:440–450
Wu FX, Sun YL, Xu GH, Hao WC, Jiang DY, Sun ZY (2011) New saurichthyid actinopterygian fishes from the Anisian (Middle Triassic) of southwestern China. Acta Palaeontol Pol 56:581–614
Xu GH, Wu FX (2012) A deep–bodied ginglymodian fish from the Middle Triassic of eastern Yunnan Province, China, and the phylogeny of lower neopterygians. Chinese Sci Bull 57:111–118
Zambelli R (1975) Note sui Pholidophoriformes. I. *Parapholidophorus nybelini* gen. n. sp. n. Rendiconti Istituto Lombardo, Accademia di Scienze e Lettere 109:3–49
Zambelli R (1978) Note sui Pholidophoriformes. II. Pholidoctenus serianus gen. n. sp. n. Rendiconti della Accademia Nazionale dei Lincei, Serie 5 3:101–123
Zambelli R (1980a) Note sui Pholidophoriformes. V contributo: Pholidophoridae dell'Alta Valvestino (Brescia, Italia). Natura Bresciana 17:77–88
Zambelli R (1980b) Note sui Pholidophoriformes. III contributo: *Pholidophorus gervasuttii* sp. n. Rivista del Museo Civico di Science Naturali "E. Caffi," Ther Ber 1:5–44
Zambelli R (1980c) Note sui Pholidophoriformes. IV contributo: *Pholidorynchodon malzannii* gen. n. sp. n. Rivista del Museo Civico di Scienze Naturali "E. Caffi," Ther Ber 2:129–168
Zambelli R (1986) Note sui Pholidophoriformes. VI—Pholidophorinae subfamiglia nuova del Triassico superiore. Rivista del Museo Civico di Scienze Naturali "E. Caffi," Ther Ber 10: 1–32
Zambelli R (1990) Note sui Pholidophoriformes. VII—*Eopholidophorus forojuliensis* n. g., n. s. Gortania 11:63–76

Chapter 10
Late Triassic Terrestrial Tetrapods: Biostratigraphy, Biochronology and Biotic Events

Spencer G. Lucas

Abstract The fossil record of Late Triassic tetrapods can be organized biostratigraphically and biochronologically into five, temporally successive land-vertebrate faunachrons (LVFs) that encompass Late Triassic time (in ascending order): Berdyankian, Otischalkian, Adamanian, Revueltian and Apachean. An up-to-date review of the age constraints on Late Triassic tetrapod fossil assemblages and correlation within the framework of the LVFs is presented. This makes possible a much more accurate evaluation of the timing of biotic events of Late Triassic tetrapod evolution, including: (1) Otischalkian, HO (highest occurrence) of almasaurids and chroniosuchians?, LOs (lowest occurrences) of crocodylomorphs and dinosaurs; (2) Adamanian, HO of mastodonsaurids and trematosaurids, LO of mammals; (3) Revueltian, HOs of capitosaurids, rhynchosaurs and dicynodonts; and (4) Apachean, HOs of metoposaurids, plagiosaurids and aetosaurs. The LO of turtles is Early Triassic or older, and the HO of phytosaurs is an Early Jurassic record. There is no compelling evidence of tetrapod mass extinctions at either the Carnian-Norian or the Triassic-Jurassic boundaries.

Keywords Late Triassic • Tetrapods • Berdyankian • Otischalkian • Adamanian • Revueltian • Apachean • Dinosaurs • Extinctions

10.1 Introduction

The Late Triassic was a major juncture in the evolution of terrestrial tetrapods (amphibians and reptiles) marked by many evolutionary events, including the oldest records of crocodylomorphs, pterosaurs, dinosaurs and mammals. It was also an interval of extinctions of some important tetrapod taxa, notably most of the

S.G. Lucas (✉)
New Mexico Museum of Natural History and Science,
1801 Mountain Road N. W., Albuquerque, NM 87104-1375, USA
e-mail: spencer.lucas@state.nm.us

© Springer International Publishing AG 2018

L.H. Tanner (ed.), *The Late Triassic World*, Topics in Geobiology 46,
https://doi.org/10.1007/978-3-319-68009-5_10

temnospondyl amphibians and all of the crurotarsan archosaurs ("thecodonts" of older terminology). Much of the recent literature on Late Triassic terrestrial tetrapods takes a phylogenetic and taxonomic approach, which means it focuses on the origin, phylogenetic relationships and evolution of a particular taxon or taxa. Such an approach takes place within the context of phylogenetic (cladistic) analysis that dominates the discussion of the evolution of Late Triassic terrestrial tetrapods.

My approach here focuses on establishing the timing of biotic events in the evolution of Late Triassic terrestrial tetrapods. First, I review the temporal succession of Late Triassic terrestrial tetrapod assemblages to provide the most precise global correlation and temporal ordering possible. Within that framework, I then discuss key biotic (origination and extinction) events in the Late Triassic history of terrestrial tetrapods.

10.2 Temporal Framework

I organize the Late Triassic fossil record of terrestrial tetrapods within the temporal framework of land-vertebrate faunachrons (LVFs) developed by Lucas and Hunt (1993a), Lucas (1998, 2010) and Lucas et al. (2007a). This framework identifies five LVFs that encompass Late Triassic time (ascending order): Berdyankian, Otischalkian, Adamanian, Revueltian and Apachean (Fig. 10.1). All Late Triassic terrestrial tetrapod assemblages can be assigned to a LVF based on the genus-level taxa present in each assemblage, so the LVFs provided a means of ordering and correlating Late Triassic tetrapod assemblages that is independent of the standard global chronostratigraphic scale (SGCS, also sometimes called the "marine timescale"). Nevertheless, the cross correlation of the LVFs to the SGCS is important because it allows the tetrapod record to be correlated to physical events well constrained by marine biostratigraphy. However, that cross correlation is complicated, in places debatable, and at several points imprecise (Lucas and Heckert 2000; Lucas 2010).

The base of the Upper Triassic Series (base of the Carnian Stage) is defined by its GSSP (global stratotype section and point) at Prati di Stuori/Stuores Wiesen in northern Italy, with the primary signal the FAD (first appearance datum) of the ammonoid *Daxatina canadensis* (Mietto et al. 2012). Radioisotopic ages from Ladinian-age rocks indicate that the base of the Carnian is ~237 Ma (Mundil et al. 2010; Ogg 2012; Ogg et al. 2014; Lucas 2017b). However, direct correlation of the base of the Carnian to the LVFs is only possible in the Germanic basin, where the Carnian base is located in the middle Keuper (Gipskeuper) at about the base of the upper Grabfeld Formation (Bachmann and Kozur 2004; Kozur and Bachmann 2005, 2008). The Berdyankian tetrapod assemblage from the lower Keuper (Lettenkohle = Erfurt Formation) and the oldest Otischalkian tetrapod assemblage in the Schilfsandstein (Stuttgart Formation), which is "middle" Carnian in age, indicate the base of the Carnian correlates to a point in Berdyankian time. However, no tetrapod assemblage is known from the upper part of the Gipskeuper, so the tetrapod succession across the Ladinian-Carnian boundary is not clear in the Germanic basin.

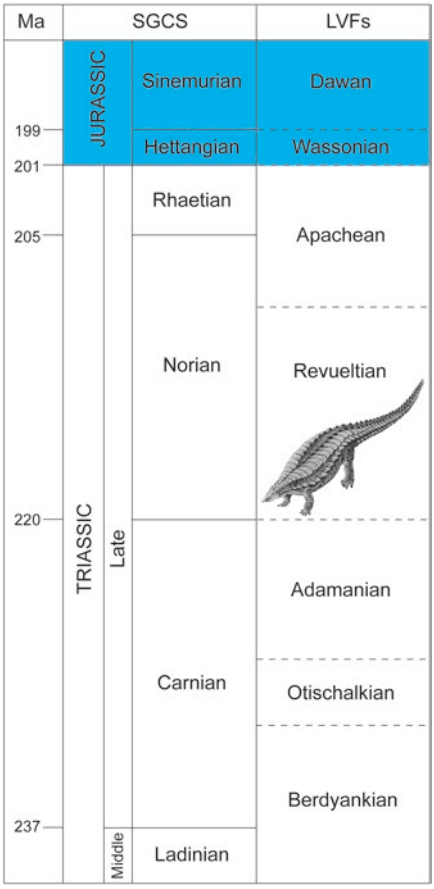

Fig. 10.1 Late Triassic land-vertebrate faunachrons (LVFs) and their correlation to the Standard Global Chronostratigraphic Scale (SGCS). After Lucas and Tanner (2015). See Lucas (2017b) for further details, especially of the numerical calibration shown here

The age of the base of the Otischalkian is well constrained as being during Carnian time, co-eval with the mid-Carnian wet episode, which is late Julian, and close in age to 231 Ma (e.g., Ruffell et al. 2016). Thus, the base of the Otischalkian in the Germanic basin is in the mid-Carnian Schilfsandstein, and that is the oldest possible age of the Otischalkian type assemblage from the basal Chinle Group in the western USA.

There is no agreed on GSSP for the base of the Norian, but that base will likely be defined using conodont biostratigraphy in western Canada or Sicily. The expectation is that the definition will be close to the longstanding working definition, which equates the base of the Norian to the base of the North American *Stikinoceras kerri* ammonoid zone (Orchard 2010, 2014). I have long advocated the equivalence or near equivalence of the base of the Norian and the beginning of the Revueltian LVF (Lucas 1998, 2010, 2015; Lucas et al. 2012). However, the "long Norian" of Muttoni et al. (2004, 2010), based on a magnetostratigraphic correlation, makes the base of the Norian much older (about 227–228 Ma) and places it within the Adamanian LVF. Lucas et al. (2012) provided a lengthy refutation of the "long Norian," placing

the base of the Norian close to 220 Ma, and that correlation is followed here (Fig. 10.1). However, numerical ages that constrain the age of the base of the Norian are mostly from detrital zircons and are fraught with inconsistencies and contradictions discussed at length by Lucas et al. (2012) and Lucas (2017b). Recent work by Kohút et al. (2017) provides detrital zircon ages from Central Europe that indicate the base of the Norian is close to 221 Ma, but more data are needed to resolve fully the numerical age of the Carnian-Norian boundary.

Like the Norian, the Rhaetian base has no agreed on GSSP, though it will be defined based on the FAD (first appearance datum) of the conodont *Misikella posthernsteini*. Currently, there are two candidate GSSP sections, at Steinbergkogel in Austria, and in the Lagonegro basin of southern Italy (Krystyn et al. 2007a, b; Rigo et al. 2016; Bertinelli et al. 2016). The Apachean LVF encompasses the Norian-Rhaetian boundary, based on conchostracan biostratigraphy, magnetostratigraphic correlations and the presence of the aetosaur *Aetosaurus* in Apachean strata (Lucas 2010; Weems and Lucas 2015). Thus, Lucas (2010) regarded the Apachean as late Norian-Rhaetian.

Magnetostratigraphy, palynostratigraphy, conchostracan biostratigraphy and vertebrate biostratigraphy indicate the beginning of the Wassonian LVF is very close to the base of the Hettangian (Kozur and Weems 2005, 2007, 2010; Lucas and Tanner 2007b; Cirilli et al. 2009). Thus, I regard the Apachean-Wassonian boundary as a good approximation of the Triassic-Jurassic boundary (Fig. 10.1).

10.3 Biofacies and Biases

During the Early and Middle Triassic, terrestrial tetrapod assemblages can be divided into amphibian dominated and dicynodont dominated (Lucas and Hunt 1993b). These two kinds of assemblages likely are biofacies that represent aquatic (including shallow marine), amphibian-dominated communities and terrestrial, dicynodont-dominated communities. This dichotomy mostly ends in Berdyankian time, when the dicynodont dominated assemblages largely disappear, though they do persist into the Adamanian in South America (see below). The different composition of the tetrapod assemblages of each biofacies makes difficult direct comparisons and correlation of assemblages of the two different biofacies.

Late Triassic terrestrial tetrapod assemblages have been collected and studied for nearly 200 years, going back to the earliest studies in the Germanic basin during the early 1800s. Nevertheless, it is clear that the temporal coverage of Late Triassic time provided by terrestrial tetrapod assemblages is patchy at best. Lucas (1997) advocated using the Chinle Group tetrapod assemblages from the western USA as the standard succession of Late Triassic tetrapod assemblages. Indeed, the Otischalkian, Adamanian, Revueltian and Apachean LVFs are based primarily on Chinle Group assemblages (Lucas and Hunt 1993a; Lucas 1998, 2010; Lucas et al. 2007a). But, the Chinle Group is a succession of fluvial strata no more than 600 m thick that encompasses most of Late Triassic time, 30 million years or more. Therefore, a

priori, the Chinle succession must be riddled with hiatuses ranging from paraconformities to substantial unconformities (Lucas 1993; Lucas and Spielmann 2013). This means the succession of Chinle Group tetrapod assemblages provides "snapshots" of the Late Triassic record, not a continuous and complete succession of assemblages.

Indeed, numerical calibration of the Late Triassic LVFs indicates that they are about 2–10 million years long (Fig. 10.1). Thus, at the level of LVF, the temporal resolution is poor. Subdivision of the Adamanian and Revueltian LVFs has been proposed in the Chinle Group section (Hunt 1991; Hunt et al. 2005), but these subdivisions cannot readily be correlated to other non-Chinle assemblages. This means that plotting vectors of tetrapod evolution within each LVF is difficult to impossible, so the comparisons are between LVFs, not within them.

10.4 Late Triassic Terrestrial Tetrapod Record

Terrestrial tetrapod fossil assemblages have a broad paleogeographic distribution over what was Late Triassic Pangea (Fig. 10.2). Here, I review the composition and correlation (Figs. 10.3 and 10.4) of these assemblages.

10.4.1 Berdyankian Tetrapod Assemblages

Berdyankian-age tetrapod assemblages are known from Russia (the assemblage characteristic of the LVF), Germany, Argentina, Brazil and Namibia (Figs. 10.2 and 10.3). The characteristic assemblage from the Bukobay Formation in the Russian Ural foreland basin includes an anthracosaur, the amphibians *Mastodonsaurus*, *Bukobaja*, *Cyclotosaurus*?, *Plagioscutum* and *Plagiosternum,* an erythrosuchid, a rauisuchid, and the dicynodonts "*Elephantosaurus jachimovitschi*" Vyushkov (a *Stahleckeria*-like form) and a generically indeterminate kannemeyeriid (e.g., Shishkin et al. 1995, 2000a, b; Ivakhhnenko et al. 1997; Gower and Sennikov 2000).

The Lettenkohle (Lettenkeuper, Lower Keuper, Erfurt Formation) in Germany and the Chanarian LVF localities in Argentina and Brazil are the principal correlatives of the Berdyankian type assemblage. The Lettenkohle record is important because it establishes the Ladinian age of at least part of the Berdyankian (see above). The Lettenkohle fossils are from the Grenze bonebed, the laterally equivalent/overlying Vitriolschiefer and the Kupferzell locality, so they are above the unconformity that separates the Keuper from the underlying Muschelkalk. Lettenkohle tetrapods include a chroniosuchian, the amphibians *Mastodonsaurus giganteus*, *Callistomordax*, *Plagiosternum, Plagiosuchus* and *Kupferzella*, the rauisuchian *Batrachotomus*, the prolacertiform *Tanystropheus* and small cynodonts (e.g., Wild 1978, 1980; Schoch 1997, 2000; Lucas 1999; Schoch and Werneburg 1999; Damiani et al. 2009; Gower and Schoch 2009).

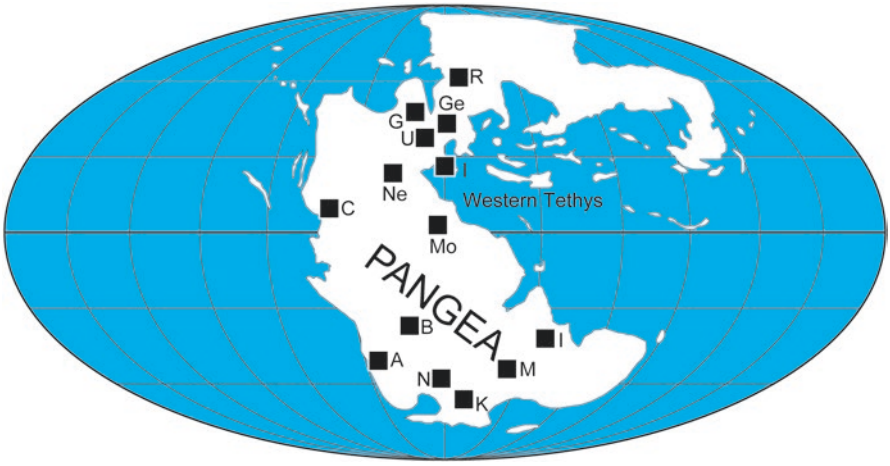

Fig. 10.2 Map of Late Triassic Pangea showing locations of principal tetrapod assemblages discussed in the text. Localities are: A = Argentina, B = Brazil, C = Chinle basin, western USA, G = Greenland, Ge = Germanic basin, I = Northern Italy, In = India, K = Karoo basin, South Africa, M = Madagascar, N = Namibia, Ne = Newark Supergroup, eastern North America, R = Russian Urals, U = United Kingdom

The Chañares local fauna from the Ischichuca (formerly Chañares) Formation of the Ischigualasto-Villa Unión basin of northwestern Argentina includes various archosaurs such as *Lagerpeton, Marasuchus* and *Chanaresuchus*, the dicynodont *Dinodontosaurus*, the traversodontid *Massetognathus*, the chiniquodontid *Chiniquodon* and the probainognathid *Probainognathus* (Bonaparte 1970, 1997; Romer 1973; Sereno and Arcucci 1993, 1994; Lucas and Harris 1996; Arcucci and Marsicano 1998; Hsiou et al. 2002; Mancuso et al. 2014). Bonaparte (1966, 1967, 1982) based the Chanarian "provincial age" on this assemblage.

Marsicano et al. (2016) reported U-Pb ages on detrital zircons of ~236–234 Ma for the Chanarian tetrapod assemblage, which, on face value indicate that they are early Carnian. However, as they noted, the "samples contain complex age inventories" (Marsicano et al. 2016: 511), so the reliability of the reported ages are open to question. However, if accurate, these ages indicate that the Chanarian tetrapod assemblage is likely of early Carnian age.

The lower part of the Santa Maria Formation in the Paraná basin of Rio Grande do Sul, Brazil, yields vertebrate fossil assemblages from Candelaria and Chiniquá considered by Barberena (1977) and Barberena et al. (1985) to be two different local faunas of different ages. Lucas (2002, 2010) regarded them as a single biostratigraphic assemblage that includes a procolophonid, archosaurs, including *Tarjadia* (=*Archaeopelta* Desojo et al. 2011; Lucas et al. 2013), the dicynodonts *Dinodontosaurus* and *Stahleckeria*, chiniquodontids, and the traversodontids *Massetognathus, Belesodon, Traversodon*, *Exaeretodon, Santacruzodo, Protuberum* and *Probelesodon* (e.g., Abdala and Ribeiro 2003; Cisneros et al. 2004; Langer et al. 2007; Reichel et al. 2009). This assemblage and the Chanarian type assemblage in

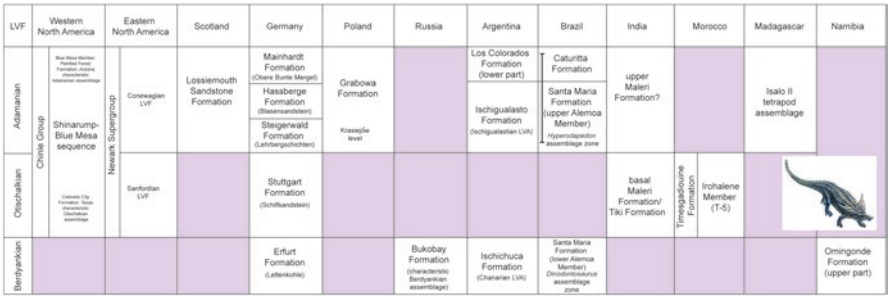

Fig. 10.3 Correlation chart of Berdyankian-Adamanian tetrapod assemblages

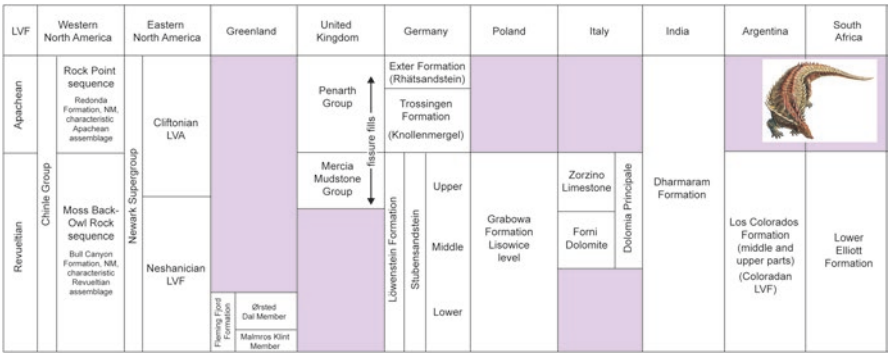

Fig. 10.4 Correlation chart of Revueltian-Apachean tetrapod assemblages

Argentina are assigned a Berdyankian age based largely on their dicynodonts and traversodontids and their stratigraphic position, which places them between tetrapod assemblages of Nonesian and Adamanian age.

The upper part of the Omingonde Formation in Namibia produces a tetrapod assemblage that includes an eryopoid temnospondyl, the dicynodonts *Kannemeyeria, Dolichuranus,* and *Rhopalorhinus*, a bauriamorph, and cynodonts (Keyser 1973a, b, 1978; Pickford 1995; Smith and Swartt 2002) that was long considered Perovkan in age (e.g., Lucas 2010). However, recent work has identified the cynodont *Chiniquodon* and the dicynodont *Stahleckeria* in the upper part of the Omingonde Formation (e.g., Abdala and Smith 2009; Abdala et al. 2013). This supports correlation to Berdyankian assemblages in South America, as detailed by Abdala et al. (2013).

Global correlation of tetrapod assemblages within the Berdyankian (Fig. 10.3) is problematic in part because of the biofacies problems outlined above. Thus, the Argentinian and Brazilian tetrapod assemblages are dicynodont-cynodont dominated and readily correlated to each other. The German and Russian assemblages are amphibian dominated and also readily correlated to each other. But, correlation of the tetrapod assemblages from the two biofacies to each other is less certain, though all of these assemblage do fall into a time interval between Perovkan and Otischalkian.

10.4.2 Otischalkian Tetrapod Assemblages

Otischalkian tetrapod assemblages are broadly distributed: in western and eastern North America, Germany, India, Morocco and possibly Kyrgyzstan (Figs. 10.2 and 10.3). The characteristic tetrapod assemblage of the Otischalkian is the assemblage of vertebrate fossils from just north of the defunct town of Otis Chalk in Howard County, Texas (Fig. 10.3). Lucas et al. (1993) and Long and Murry (1995) reviewed the fauna, which is from the Colorado City Formation of the Chinle Group. The following taxa are present: the amphibians *Latiscopus, Buettneria* and *Apachesaurus*, a procolophonid, the rhynchosaur *Otischalkia*, the archosaurs *Doswellia, Trilophosaurus* (=*Malerisaurus*) and *Poposaurus*, the aetosaurs *Longosuchus* (=*Lucasuchus*) and *Coahomasuchus*, the phytosaurs *Parasuchus* and *Angistorhinus* and the dinosaur *Lepidus* (Lucas et al. 1993; Long and Murry 1995; Heckert and Lucas 1999; Spielmann et al. 2006c; Nesbitt and Ezcurra 2015).

Otischalkian tetrapod assemblages are found across a broad geographic range of Chinle Group outcrops in Wyoming, New Mexico and Texas. The most well-known principal correlative of the type Otischalkian fauna in the Chinle Group is the vertebrate-fossil assemblage from the Popo Agie Formation of Wyoming (Branson and Mehl 1928; Mehl 1928; Colbert 1957; Lucas 1994; Lucas et al. 2002) that includes the metoposaurid *Koskinonodon*, the phytosaurs *Parasuchus* and *Angistorhinus*, the aetosaur *Desmatosuchus,* the archosaurs *Poposaurus* and *Heptasuchus*, the rhynchosaur *Hyperodapedon*, and the dicynodont *Placerias*. A less well-known principal correlative is the small assemblage from the Salitral Formation in Rio Arriba County, New Mexico, that consists of a metoposaur, *Longosuchus*, a phytosaur, and an indeterminate dinosaur (Lucas and Hunt 1992). Heckert (2004) provided some microvertebrate basis for recognition of the Otischalkian in Chinle Group strata, such as the LO of the "dinosaur" *Protecovasaurus* and the archosaur *Trilophosaurus buettneri* (also see Spielmann et al. 2008). Outside of the Chinle Group, Otischalkian assemblages are also known from the Newark Supergroup in eastern North America, the Germanic basin, Morocco, India and, possibly, Kyrgyzstan.

In the Newark Supergroup of eastern North America, the stratigraphically lower formations of the Deep River, Gettysburg, Newark and Fundy basins contain two distinct vertebrate fossil assemblages. The older of these was used by Huber et al. (1993b) as the basis of the Sanfordian LVF, after the characteristic assemblage from the Passaic ("Sanford") Formation in the Sanford sub-basin of the Deep River basin complex (see Weems et al. 2016 for a revised lithostratigraphy of the Newark Supergroup used throughout this article). An age-equivalent assemblage from the Passaic Formation (Fundy basin) is also assigned to this LVF. The collective Newark tetrapod fauna of the Sanfordian LVF includes a metoposaurid, the trematosauroid *Calamops,* procolophonids, the traversodontids *Arctotraversodon* and *Plinthogomphodon*, the dicynodont *Placerias*, the rhynchosaur *Hyperodapedon*, the archosaur *Doswellia*, the aetosaurs *Desmatosuchus* and *Longosuchus*, indeterminate rauisuchians ("*Zamotus*"), the rauisuchian *Postosuchus*, the "sphenosuchian"

Dromicosuchus, indeterminate phytosaur fragments and fragmentary dinosaur remains (e.g., Cope 1871; Olsen et al. 1989; Hunt and Lucas 1990; Huber et al. 1993a; Hunt 1993; Sues et al. 1994, 1999, 2003; Langer et al. 2000; Lucas et al. 2002; Peyer et al. 2008; Dilkes and Sues 2009; Sues and Schoch 2013). The Sanfordian correlates with the Chinle Group Otischalkian LVF based on the shared presence of *Koskinonodon*, *Hyperodapedon*, *Desmatosuchus*, *Longosuchus*, *Doswellia*, and *Placerias*.

In Germany, the Schilfsandstein (Stuttgart Formation) produces *Metoposaurus* and *Parasuchus* but lacks *Stagonolepis*, so it can be assigned an Otischalkian age (Hunt and Lucas 1991; Lucas 1999; Schoch and Werneburg 1999; Hungerbühler 2001; Kimmig and Arp 2010). Note that the Schilfsandstein is the age of the Carnian wet episode, which is "middle" Carnian (late Julian) in age (e. g., Hornung et al. 2007; Ruffell et al. 2016).

The 500-m-thick Irohalene Member of the Timesgadiouine Formation (interval T-5 of Dutuit 1966; Tixeront 1971) has produced most of the Late Triassic vertebrate fauna from Morocco. It contains the majority of vertebrate fossil localities described by Dutuit (1972, 1976, 1977, 1988, 1989a, b). Most of these occur in the lower part of the member, and they have produced a moderately diverse assemblage that includes the amphibians *Almasaurus* and *Dutuitosaurus*, the phytosaur *Parasuchus*, the aetosaur *Longosuchus*, the dicynodont *Placerias* (=*Moghreberia*, =*Azarifeneria*: Cox 1991; Lucas and Wild 1995) and the archosauromorph *Azendohsaurus* (Gauffre 1993; Lucas 1998; Jalil 1999; Flynn et al. 2010). Several of Dutuit's (1976) localities are in the upper part of the Irohalene Member, which is a distinct faunal horizon that includes the amphibian *Arganasaurus*, the phytosaur *Angistorhinus*, and the dicynodont *Placerias*. The presence of *Parasuchus*, *Angistorhinus, Longosuchus* and *Placerias* supports assigning the Irohalene Member tetrapod assemblage(s) an Otischalkian age.

In the Pranhita-Godavari Valley of India, the basal Maleri Formation produces a tetrapod assemblage that includes the amphibian *Metoposaurus*, the rhynchosaur *Paradapedon*, the phytosaur *Parasuchus*, the archosaur "*Malerisaurus*," an aetosaur, the theropod dinosaur *Alwalkeria*, a prosauropod ("cf. *Massospondylus*" of Kutty and Sengupta 1989), a large dicynodont, and the cynodont *Exeraetodon* (e.g., von Huene 1940; Jain et al. 1964; Roychowdhury 1965; Chatterjee 1967, 1974, 1978, 1980, 1982, 1987; Chatterjee and Roychowdhury 1974; Jain and Roychowdhury 1987; Bandyopadyhay and Sengupta 2006; Spielmann et al. 2006c; Kammerer et al. 2016). This is the only well-described Upper Triassic tetrapod assemblage from the Pranhita-Godavari Valley. It includes *Parasuchus* and *Metoposaurus*, taxa indicative of an Otischalkian age.

Northeast of the Pranhita-Godavari valley, in the Rewa basin of India, the Tiki Formation yields an Otischalkian tetrapod assemblage. This includes *Metoposaurus*, *Parasuchus*, the rhynchosaur *Hyperodapedon*, the supposed agamid lizard *Tikiguana*, the cynodont *Rewacodon* and the supposed mammals *Tikitherium* and *Gondwanodon* (e.g., Datta and Das 1996; Datta 2005; Mukherjee et al. 2012).

In the Fergana basin of Kyrgyzstan, the upper part of the Madygen Formation yields a tetrapod assemblage usually assigned a Ladinian-Carnian age based on the

associated paleoflora (e.g., Dobruskina 1995a). Voigt et al. (2017) recently reported a U-Pb age of 237 ± 2 Ma on six concordant zircons from a pyroclastic bed stratigraphically below the tetrapod assemblage, which suggests the tetrapods may be of Carnian age. However, the entire tetrapod assemblage from the Madygen Formation is endemic and of no value to biostratigraphy. It consists of the amphibian *Triassurus*, the reptiliomorph *Madygenerpeton*, the unusual diapsids *Sharovipteryx, Kyrgyzsaurus* and *Longisquama* and the cynodont *Madygenia* (Sharov 1970, 1971; Ivakhnenko 1978; Tatarinov 2005; Unwin et al. 2000; Schoch et al. 2010; Alifanov and Kurochkin 2011). The assemblage may be of Otischalkian age, but more precise data are needed to confirm this.

10.4.3 Adamanian Tetrapod Assemblages

The characteristic tetrapod assemblage of the Adamanian is the assemblage of vertebrate fossils found in the Blue Mesa Member of the Petrified Forest Formation in the Petrified Forest National Park, near the defunct railroad siding of Adamana, Arizona (Fig. 10.3). Recent faunal lists have been provided by Murry and Long (1989), Long and Murry (1995), Heckert et al. (2005) and Parker et al. (2006). The fauna includes the following tetrapods: the amphibians *Apachesaurus* and *Koskinonodon*, the aetosaurs *Desmatosuchus* (=*Acaenasuchus*), *Stagonolepis*, *Adamanasuchus* and *Paratypothorax*, *Rutiodon*-grade phytosaurs (including *Leptosuchus* and *Smilosuchus*), the rauisuchian *Postosuchus*, the archosaurs *Hesperosuchus, Acallosuchus*, *Parrishea* and *Vancleavea*, and the dicynodont *Placerias*, as well as many microvertebrate taxa.

Besides the Chinle Group correlatives, major Adamanian faunas are those of the Conewagian interval of the Newark Supergroup basins of eastern North America; Lossiemouth Sandstone Formation, Scotland; Lehrberg Schichten-Obere Bunte Mergel interval of the German Keuper; the Krasiejów locality in Poland; Ischigualasto Formation, Argentina; and upper Santa Maria Formation and Caturitta Formation, Brazil (Fig. 10.3).

In the Chinle Group, Adamanian vertebrates are widespread and include the vertebrate fossil assemblages of the *Placerias* and Downs' quarries, Bluewater Creek Formation, Arizona (Camp and Welles 1956; Kaye and Padian 1994; Long and Murry 1995; Lucas et al. 1997; Heckert 2004; Heckert et al. 2005); the Bluewater Creek Formation and Blue Mesa Member of the Petrified Forest Formation in the Blue Hills, Arizona; the Bluewater Creek Formation and Blue Mesa Member of the Petrified Forest Formation, McKinley and Cibola counties, New Mexico (Heckert 1997); the Los Esteros and Tres Lagunas members, Santa Rosa Formation, and the Garita Creek Formation in the vicinity of Lamy, Santa Fe County, New Mexico (Hunt et al. 2005; Lucas et al. 2010); Garita Creek Formation, Santa Rosa and vicinity, Guadalupe County, New Mexico (Hunt and Lucas 1993a); and Tecovas Formation, West Texas (Murry 1986, 1989; Long and Murry 1995; Lucas et al. 2016).

The fauna at the *Placerias* and Downs' quarries has been discussed by Kaye and Padian (1994), Long and Murry (1995), Lucas et al. (1997) and Heckert (2004). It includes the amphibians *Koskinonodon* and *Apachesaurus*, the prolacertiform *Gwyneddosaurus* (=*Tanytrachelos*), the phytosaurs *Parasuchus* and *Rutiodon*/*Leptosuchus*, the aetosaurs *Stagonolepis* and *Desmatosuchus* (=*Acaenasuchus*), the rauisuchid *Postosuchus*, the archosaurs *Trilophosaurus, Acallosaurus, Poposaurus, Chatterjeea, Hesperosuchus, Tecovasaurus* and cf. *Uatchitodon*, an indeterminate ceratosaur and the dicynodont *Placerias*.

A U-Pb age recently reported from Chinle Group strata at the *Placerias*/Downs' quarries by Ramezani et al. (2014) is not consistent with earlier published ages. This is an age of 219.39 ± 0.16 Ma from near the base of the Chinle Group at the *Placerias* fossil locality in Arizona. Stratigraphic position puts this age well below a series of ages in the 220–227 Ma range reported by Ramezani et al. (2011) and Atchley et al. (2013). To explain this contradiction, Ramezani et al. (2014) claim massive lateral facies changes in the lower Chinle lithosome, and even conclude that "geochronological correlation independent of conventional stratigraphic methods [lithostratigraphy, biostratigraphy] is the only viable means for deciphering the depositional history of rock similar to the Chinle Formation" (p. 995). I prefer instead to rely on a century of geologic mapping, detailed lithostratigraphic analysis and the biostratigraphy of palynomorphs, conchostracans and vertebrates (e.g., Heckert and Lucas 2002 and references cited therein) that demonstrates that the *Placerias* quarry numerical age of Ramezani et al. (2014) is stratigraphically below many older numerical ages. Thus, the *Placerias* quarry age published by Ramezani et al. (2014) is anomalously young, likely due to postcrystallization lead loss, and should be ignored.

The following tetrapod taxa are known from the Los Esteros Member, Santa Rosa Formation, near Lamy, New Mexico: the amphibian *Apachesaurus*, the phytosaurs *Rutiodon* and *Angistorhinus*, the aetosaurs *Desmatosuchus, Tecovasuchus* and *Stagonolepis* and the dicynodont cf. *Ischigualastia* (Hunt and Lucas 1993a, 1994; Hunt et al. 2005; Heckert et al. 2007). The overlying Garita Creek Formation contains the following taxa: the amphibian *Koskinonodon*, phytosaurs, rauisuchians, and the aetosaurs *Desmatosuchus, Stagonolepis* and *Paratypothorax* (Hunt et al. 2005; Lucas et al. 2010).

The Tecovas Formation of West Texas yields the following tetrapod taxa: the amphibians *Koskinonodon* and *Apachesaurus*, the probable tetrapod *Colognathus*, the archosauromorphs *Trilophosaurus*, *Spinosuchus, Parrishea, Tecovasaurus*, and *Crosbysaurus*, the phytosaurs *Rutiodon, Leptosuchus* and *Smilosuchus,* the aetosaurs *Desmatosuchus* and *Stagonolepis*, the rauisuchian *Postosuchus*, and the oldest known mammal, *Adelobasileus* (Lucas and Luo 1993; Lucas et al. 1994, 2016; Long and Murry 1995; Spielmann et al. 2008, 2013).

In the Deep River basin of North Carolina, an assemblage of the Conewagian LVF from the Cumnock Member of the Lockatong Formation (cf. Weems et al., 2016) is superposed on the characteristic Sanfordian assemblage. Conewagian assemblages are characterized by the tetrapod assemblage in the basal Lockatong (="Gettysburg") Formation (Kozur and Weems 2010) along Little Conewago Creek

in south-central Pennsylvania (Gettysburg basin: Huber et al. 1993b; Sullivan et al. 1995; Lucas and Sullivan 1997) and also are known from the Lockatong (="Cow Branch") Formation (Dan River basin), and upper Stockton and Lockatong formations (Newark basin). The most widespread and characteristic Conewagian tetrapod is the phytosaur *Rutiodon*, which co-occurs with the amphibian *Koskinonodon*, archosaurs of uncertain affinity, the problematic reptile *Colognathus*, an aetosaur (*Desmatosuchus*), one or more "ornithischian dinosaurs" (e.g., *Pekinosaurus, Crosbysaurus, Revueltosaurus* and *Galtonia*), the archosaurs *Uatchitodon* and *Gwyneddosaurus* (=*Tanytrachelos*), lepidosaurs, including the single record of the gliding lepidosauromorph *Icarosaurus* and cynodonts, including aff. *Boreogomphodon* and *Microconodon* (e.g., Emmons 1856; Olsen 1980, 1988; Olsen et al. 1989; Sues 1992; Huber et al. 1993a; Hunt 1993; Hunt and Lucas 1994; Doyle and Sues 1995; Lucas and Huber 2003; Heckert et al. 2012). Conewagian assemblages correlate with the Adamanian LVF of the Chinle Group, based on the shared presence of *Koskinonodon*, *Colognathus*, *Uatchitodon*, *Rutiodon* and other *Rutiodon*-grade phytosaurs (*Smilosuchus* of Long and Murry 1995), *Desmatosuchus* and broadly similar "ornithischian dinosaurs" (e.g., Murry and Long 1989; Lucas et al. 1992, 1997, 2016; Huber et al. 1993b; Hunt 1993; Hunt and Lucas 1994; Heckert 2004; Heckert et al. 2012).

The tetrapod assemblage of the Lossiemouth Sandstone Formation of Grampian (Elgin) Scotland comes from small quarries and the coastal section at Lossiemouth. Benton and Spencer (1995; also see Fraser 2006) provided a detailed summary that indicates that all sites come from a narrow stratigraphic interval, so they are a single biostratigraphic assemblage. It includes the procolophonid *Leptopleuron*, the sphenodontid *Brachyrhinodon*, the rhynchosaur *Hyperodapedon*, the aetosaur *Stagonolepis*, the ornithosuchid *Ornithosuchus*, the crocodylomorph *Erpetosuchus*, the probable ornithodiran *Scleromochlus* and the "dinosaur" *Saltopus*. The presence of *Hyperodapedon* and *Stagonolepis* supports assigning this assemblage an Adamanian age.

In Germany, strata in the interval between the Schilfsandstein and the Stubensandstein (Lehrberg Schichten, Blasensandstein and Kieselsandandstein) produce *Stagonolepis*, *Parasuchus* and *Metoposaurus* (e.g., Lucas 1999), and are assigned an Adamanian age (Kozur and Weems 2005).

Kear et al. (2016) recently identified a temnospondyl skull fragment as *Cyclotosaurus* from the DeGeerdalen Formation in Svalbard. These are marine strata assigned a middle-late Carnian age based on ammonoids. Thus, if correctly identified, this would be the oldest record of *Cyclotosaurus*, which is otherwise known from Revueltian (Norian) strata.

The Polish fossil record of Late Triassic tetrapods advanced greatly during the 1990s, when scientific study of the extensive bonebed in the Krasiejów clay pity near Ople began, and much has been published since (see especially the reviews by Dzik and Sulej 2007; Szulc et al. 2015). The Krasiejów tetrapod assemblage includes the amphibians *Cyclotosaurus* and *Metoposaurus*, the phytosaur *Parasuchus*, the aetosaur *Stagonolepis*, the rauisuchian *Teratosaurus* and the dinosauriform *Silesaurus* (Dzik 2001, 2003; Sulej 2002, 2005, 2007, 2010; Sulej and

Majer 2005; Dzik and Sulej 2007; Lucas et al. 2007b; Szulc et al. 2015; Lucas 2015). This assemblage is from strata ~80 m above the Reed Sandstone (a Schilfsandstein equivalent) that are homotaxial to the German Lehrberg Schichten and is of Adamanian age (Lucas 2015).

In Argentina, the Ischigualasto Formation is 500–900 m thick and consists of drab mudstones, tuffs and sandstones that produce an extensive tetrapod assemblage, including: the amphibian *Promastodonsaurus*, the archosaurs *Saurosuchus, Sillosuchus*, and *Proterochampsa*, the ornithosuchid *Venaticosuchus*, the aetosaur *Stagonolepis* (=*Aetosauroides*), the rhynchosaur *Hyperodapedon*, the dinosaurs *Herrerasaurus* (=*Ischisaurus*? =*Frenguellisaurus*), *Eoraptor* and *Pisanosaurus,* the chiniquodontid cynodont *Chiniquodon*, the gomphodont cynodonts *Exeraetodon*, *Proexaraetodon*, and *Ischignathus* and the dicynodont *Ischigualastia* (e.g., Cabrera 1944; Reig 1959, 1961, 1963; Casamiquela 1960, 1962; Cox 1965; Bonaparte 1976, 1997; Rogers et al. 1993; Sereno et al. 1993; Alcober and Parrish 1997; Heckert and Lucas 2002; Baczko and Ezcurra 2013). This assemblage was the basis of the Ischigualastian land-vertebrate "age" of Bonaparte (1966, 1967, 1982).

Martínez et al. (2013) reviewed the stratigraphic distribution of the tetrapod fossils in the Ischigualasto Formation to show that most are from the lower 300 m of the formation. They also reviewed the radioisotopic ages associated with the Ischigualasto Formation tetrapods (e. g., Valencio et al. 1975; Rogers et al. 1993; Currie et al. 2009) to assign them an age range of ~226–231 Ma. This suggests a late Carnian (Tuvalian) age, which fits well with the conclusion that the Ischigualasto tetrapods are of Adamanian age (Lucas 2010; Lucas et al. 2012).

In northwestern Argentina, the Puesto Viejo Group contains a tetrapod assemblage that includes *Kannemeyeria* and *Cynognathus* and has long been considered to be of Nonesian (late Olenekian) age (e. g., Lucas 2010). However, Ottone et al. (2014) reported a SHRIMP 238 U/206Pb age of 235.8 ± 2.0 Ma from a rhyolitic tuff in the approximate middle of the Puesto Viejo succession. They accepted this numerical age as evidence of the Carnian age of the Puesto Viejo tetrapod assemblage. Instead, it is much more likely that the age reported by Ottone et al. (2014) is simply incorrect (too young) and does not indicate that Nonesian tetrapods (including the classic *Cynognathus* Assemblage Zone of the South African Karoo) are of Late Triassic age.

In Brazil, the principal Upper Triassic vertebrate assemblage from the Santa Maria Formation is from the vicinity of Santa Maria City. This is the Rhynchocephalia assemblage zone of Barberena (1977) or the *Scaphonyx* assemblage of Barberena et al. (1985), from the upper part of the Santa Maria Formation. The assemblage consists of abundant fossils of the rhynchosaur *Hyperodapedon* and the aetosaur *Stagonolepis* (=*Aetosauroides*); traversodontids, proterochampsids; the archetypal rauisuchian *Rauisuchus* and the primitive dinosaur *Staurikosaurus* (Barberena et al. 1985; Lucas 2002; Lucas and Heckert 2001; Abdala et al. 2001; Langer et al. 2007; Raugust et al. 2013; Melo et al. 2015). Clearly, the presence of *Scaphonyx* and *Stagonolepis* supports correlation with the vertebrates of the Ischigualasto Formation in Argentina, and therefore an Adamanian (=Ischigualastian) age (Lucas and Heckert 2001; Heckert and Lucas 2002; Lucas 2002, 2010).

Abdala et al. (2001) identified a "traversodontid biozone" (later termed the *Santacruzodon* Assemblage Zone) intermediate between the *Dinodontosaurus* and *Hyperodapedon* assemblages of the Santa Maria Formation. This biozone yielded the cynodont *Menadon*, also found in the Isalo II strata of Madagascar (Melo et al. 2015). Abdala et al. (2001) and Melo et al. (2015) consider the *Santacruzodon* Assemblage Zone to be of Ladinian or early Carnian age. However, correlation to Isalo II suggests an age of Adamanian, which is late Carnian. Furthermore, there is no lithostratigraphic basis for placing the so-called *Santacruzodo*n Assemblage Zone between the *Dinodontosaurus* and *Hyperodapedon* assemblages (cf. Langer et al. 2007). In effect, the *Santacruzodon* Assemblage Zone is a hypothetical biostratigraphic construct based on a single locality that is the same age as the *Hyperodapedon* assemblage of the Santa Maria Formation. The *Santacruzodon* Assemblage Zone should be abandoned.

The tetrapod assemblage of the Caturrita Formation, which overlies the Santa Maria Formation, includes a mastodonsauroid amphibian, the procolophonid *Soturnia*, the sphenodont *Clevosaurus*, the lepidosaur *Cargninia*, the rhynchosaur *Hyperodapedon*, the proterochampsid *Proterochampsa*, the supposed pterosaur *Faxinalipterus* (but see Dalla Vecchia 2013), the dinosaurs *Unaysaurus* and *Guaibisaurus*, the dinosauriform *Saccasaurus*, a phytosaur, the cynodonts *Exaeretodon* and *Riograndia*, the dicynodont *Ischigualastia* (=*Jachaleria*) and diverse cynodonts (Araújo and Gonzaga 1980; Barberena et al. 1985; Dornelles 1990; Bonaparte et al. 1999, 2001, 2007, 2010a, b; Cisneros and Schultz 2003; Kischlat and Lucas 2003; Leal et al. 2003; Ferigolo and Langer 2006; Bonaparte and Sues 2006; Langer et al. 2007; Dias-da-Silva et al. 2009; Soares et al. 2011).

Philipp et al. (2013), in an extended abstract, reported U-Pb ages on 13 zircons from an ash bed (though Schultz et al. 2016 referred to these as "detrital zircons") that form an isochron of 236 ± 3.5 Ma. This ash bed is approximately at the stratigraphic level of the "*Santacruzodon* assemblage," so it suggests an age close to the Ladinian-Carnian boundary between the Berdyankian and Adamanian tetrapod assemblages of the Santa Maria Formation. Further publication of the analytical data associated with these ages is needed to assess their accuracy.

Most South American workers (e.g., Bonaparte 1982; Barberena et al. 1985; Langer 2005a, b; Rubert and Schultz 2004; Dias-da-Silva et al. 2007; Langer et al. 2007; Soares et al. 2011) advocate dividing the Brazilian Upper Triassic tetrapod succession into two biostratigraphically distinct assemblages largely based on their judgment that the dicynodonts *Jachaleria* and *Ischigualastia* are not the same taxon. They, therefore, correlate the Brazilian Caturrita Formation to the Argentinian Los Colorados Formation. Langer (2005b) also claimed that the Ischigualastian = Otischalkian + Adamanian, largely based on not recognizing the temporal range of *Hyperodapedon* as longer than the temporal range of the Ischigualastian. I do not accept either evaluation of the Brazilian Upper Triassic tetrapod biostratigraphy (Lucas 2002, 2010). Thus, I regard the Caturitta Formation as a correlative of the Ischigualasto Formation, so it is Adamanian, of late Carnian age.

In the Pranhita-Godavari Valley of India, the upper vertebrate fossil assemblage from the Maleri Formation is stratigraphically above the lower assemblage, but its stratigraphic range is not clear. This upper assemblage includes an aetosaur, prosauropods and a large dicynodont. Chigutisaurid amphibians (*Compsocerops* and *Kuttycephalus*: Sengupta 1995) and a "*Rutiodon*-like" phytosaur are also present (Bandyopadyhay and Sengupta 2006). Therefore, this assemblage may be Adamanian, but needs further documentation.

In western Madagascar, the Isalo group ("Groupe d l'Isalo" of Besarie 1930; also see Besarie and Collignon 1960, 1971) has long been divided into Isalo I, Isalo II and Isalo III based on perceived geologic age. The Isalo II strata yield Late Triassic tetrapods, including metoposaurs, sphenodontids, phytosaurs, dinosaurs, the rhynchosaur *Hyperodapedon*, the aetosaur *Desmatosuchus*, the archosaur *Azendohsaurus*, various cynodonts (including the traversodontids *Dadadon* and *Menadon*) and a dicynodont (Guth 1963; Westphal 1970; Dutuit 1978; Buffetaut 1983; Flynn et al. 1999, 2000, 2008; Lucas et al. 2002; Flynn and Wyss 2003; Burmeister et al. 2006; Kammerer et al. 2010; Ranovharimanana et al. 2011). The stratigraphic range of the Isalo II tetrapods is about 1200 m, but the rhynchosaur *Hyperodapedon* is one of the stratigraphically lowest taxa in the assemblage. This means the Isalo II assemblage is no older than Otischalkian and, based on the *Desmatosuchus* record, likely to be Adamanian. Flynn and collaborators (e.g., Flynn and Wyss 2003) advocate an older age, perhaps as old as Ladinian, for the Isalo II assemblage, but no data support that conclusion.

10.4.4 Revueltian Tetrapod Assemblages

The characteristic tetrapod assemblage of the Revueltian is that of the Bull Canyon Formation in east-central New Mexico (Fig. 10.4), and the following taxa are present: the amphibian *Apachesaurus*, the turtle *Chinlechely*s, the phytosaur *Pseudopalatus* and other *Pseudopalatus*-grade phytosaurs, the aetosaurs *Rioarribasuchus*, *Paratypothorax*, *Typothorax coccinarum* and *Aetosaurus*, the suchian *Revueltosaurus*, the "dinosaur" *Lucianosaurus*, the rauisuchian *Postosuchus*, the chatterjeeids *Shuvosaurus* (=*Effigia*) and *Chatterjeea*, the sphenosuchian *Hesperosuchus* and the cynodont *Pseudotriconodon* (e.g., Hunt 1994, 2001; Lucas et al. 2001; Joyce et al. 2009).

In the Chama basin of north-central New Mexico, the Petrified Forest Formation of the Chinle Group also yields Revueltian tetrapods, especially from the Snyder, Hayden and Canjilon phytosaur-dominated bonebeds (Sullivan and Lucas 1999; Zeigler et al. 2003; Heckert et al. 2005; Ezcurra 2006; Nesbitt and Stocker 2008). In northern Arizona, two Chinle Group units, the Painted Desert Member of the Petrified Forest Formation and the overlying Owl Rock Formation, have produced numerous Revueltian fossils, especially from the Petrified Forest National Park and from localities on Ward's Terrace north of Flagstaff (e.g., Kirby 1989, 1991, 1993; Heckert et al. 2005; Spielmann et al. 2007).

Outside of the Chinle Group, Revueltian tetrapod assemblages are known from the Newark Supergroup in eastern North America, Greenland, the Germanic basin, (including eastern Poland), northern Italy, India, Argentina and South Africa (Fig. 10.4). In eastern North America, the provincial Neshanician LVF is based on a limited fossil assemblage typified by the aetosaur *Aetosaurus arcuatus* (Lucas et al. 1998; Lucas and Huber 2003). This taxon is present in the Passaic Formation in the Durham sub-basin of the Deep River basin, the Newark Basin (range zone: Warford through Neshanic members of the lower Passaic Formation), and the middle Sugarlof Member of the Passaic Formation of central Connecticut. Other vertebrates from the Neshanician LVF include indeterminate metoposaurid and phytosaur teeth, skull and scute fragments (e.g. "*Belodon validus*"), a rauisuchian, a crocodylomorph, a traversodontid and a sphenodontid. The dominance of the primitive neopterygian *Semionotus* sp. over other fish taxa is a trend also apparent in age-equivalent strata of the Chinle Group and German Keuper (Huber et al. 1993c; Lucas and Huber 2003).

The Cliftonian LVF is based on a low-diversity assemblage defined by the distribution of the procolophonid *Hypsognathus fenneri*. This taxon is common in the type area, from the middle (?Mettlars Member) to the upper (?Member TT) Passaic Formation of the northern Newark basin (e.g., Baird 1986). It is also known from the upper Passaic Formation of the Hartford basin, central Connecticut, and the basal Blomidon Formation in the Fundy basin, Nova Scotia (Sues et al. 1997). The Fundy basin specimen of *Hypsognathus* was obtained from pebble conglomerate at the base of the Blomidon Formation, which unconformably overlies the Wolfville Formation. The only other vertebrates that occur in the interval of Cliftonian age are indeterminate phytosaur remains (including the holotype of "*Clepsysaurus pennsylvanicus*" Lea 1851) from the Ukrainian Member of the Passaic Formation in the Newark basin, moderately diverse tetrapod footprint assemblages at many horizons in the Passaic Formation (e.g., Szajna and Silvestri 1996; Lucas and Sullivan 2006), and an indeterminate sphenodontid from the upper Passaic Formation (Olsen 1980; Sues and Baird 1993; Lucas and Huber 2003).

The Malmros Klint and overlying Ørsted Dal members of the Fleming Fjord Formation in eastern Greenland yield tetrapod fossils of Revueltian age (Jenkins et al. 1994, 1997, 2001, 2008; Clemmensen et al. 2016). The Malmros Klint Member has produced fragmentary fossils of plagiosaurid amphibians, the amphibian *Cyclotosaurus*, phytosaur bones and the prosauropod dinosaur *Plateosaurus*. The Ørsted Dal Member assemblage is much more diverse: the amphibians *Gerrothorax* and *Cyclotosaurus*, the turtle cf. *Proganochelys*, unidentified sphenodontians, the aetosaurs *Aetosaurus* and *Paratypothorax*, the pterosaur *Eudimorphodon*, the prosauropod dinosaur "*Plateosaurus*," a theropod dinosaur, theropod dinosaur footprints (*Grallator*), and the mammals *Kuehneotherium*, cf. *Brachyzostrodon*? and *Haramiyavia*. As Jenkins et al. (1994) argued, this assemblage shares many taxa with the German Stubensandstein. More specifically, other than *Plateosaurus*, most taxa from the Ørsted Dal Member are known in the Lower Stubensandstein, to which I correlate the Greenland assemblage (Fig. 10.4).

In Germany, the best known and most diverse Keuper tetrapod assemblage is that of the Lower Stubensandstein (Löwenstein Formation). This assemblage includes the amphibians *Cyclotosaurus* and *Gerrothorax*, the turtles *Proganochelys* and *Proterochersis*, *Pseudopalatus*-grade phytosaurs (*Nicrosaurus*), the aetosaurs *Aetosaurus* and *Paratypothorax*, rauisuchians (*Teratosaurus*), theropod dinosaurs, and the prosauropod dinosaurs *Sellosaurus* and *Thecodontosaurus* (e.g., Benton 1993; Hungerbühler 1998; Lucas 1999; Schoch and Werneburg 1999; Schoch 2007; Kimmig and Arp 2010). The phytosaurs, aetosaurs, and rauisuchians provide a strong basis for assigning a Revueltian age to the Lower Stubensandstein (Lucas and Hunt 1993a; Hunt 1994; Lucas 1999). The younger, Middle and Upper Stubensandstein, produce a similar, but less diverse assemblage, so I also assign them a Revueltian age (Lucas 1999). Whether or not the lowest occurrence of *Mystriosuchus* in the Middle Stubensandstein is of biochronologic significance is not clear.

The tetrapod assemblages of the Upper Stubensandstein and Knollenmergel (Trossingen Formation) are almost entirely dinosaurian—95% or more of the fossils are of dinosaurs (Benton 1986, 1991). This contrasts sharply with the Lower and Middle Stubensandstein assemblages, in which dinosaurs are a much smaller percentage of the fossils collected. However, I regard this change to dinosaur domination as largely a local facies/taphonomic effect, not a biochronologically significant event (Hunt 1991). It seems likely but not certain that the Knollenmergel assemblage is of Apachean age (see below).

In eastern Poland, Dzik et al. (2008) announced the discovery of an Upper Triassic bonebed at the Lipie Slaski clay pit near Lubliniec. This bonebed yields an assemblage dominated by dicynodonts and archosaurs. There are three other correlative fossil vertebrate localities in Silesia. Another bonebed in the Woźniki clay pit yield vertebrates similar to those from Lipie (Sulej et al. 2011). Sulej et al. (2011) correlated the Woźniki assemblage with the Krasiejów locality, but Szulc et al. (2015) argue convincingly that the Woźniki assemblage and the Lipie assemblage are stratigraphically equivalent and subsume it under what they call the Lisowice level. Bones from Poręba were discovered in 2008 and include amphibians, turtles, and aetosaurs, among others, and have in part been described (Sulej et al. 2012; Niedźwiedzki et al. 2014). This locality, and very recently discovered bones from another locality at Zawiercie, are stratigraphically equated to Lipie (Szulc et al. 2015). Thus, the Lisowice level comprises the fossil vertebrate localities at Lipie, Woźniki, Poręba and Zawiercie.

Biochronologically significant tetrapod taxa reported and/or documented from the Lisowice level include the amphibians *Cyclotosaurus* and *Gerrothorax*, the turtle cf. *Proterochersis*, an aetosaur I judge to be *Paratypothorax* (Lucas 2015) and a large dicynodont (Dzik et al. 2008; Sulej et al. 2012; Niedźwiedzki et al. 2012, 2014; Świło et al. 2014). Szulc et al. (2015) represents the first explicit correlation of the Lipie bonebed to the Triassic LVFs, assigning it a Revueltian age.

In the Lombardian Alps of northern Italy, after the regional progradation of platform carbonates during the early-middle Norian (Dolomia Principale), extensional tectonism produced intraplatform depressions occupied by patch reefs, turbiditic

debris flows and lagoonal to freshwater facies (Jadoul 1985; Jadoul et al. 1994). Tetrapods from these intraplatform strata, the Zorzino Limestone at the Cene and Endenna quarries in Lombardy, are the diapsids *Endennasaurus* and *Vallesaurus,* the prolacertiform *Longobardisaurus*, the rhynchocephalian *Diphydontosaurus*, the drepanosaurids *Drepanosaurus* and *Megalancosaurus*, the phytosaur *Mystriosuchus*, the aetosaur *Aetosaurus,* the pterosaurs *Eudimorphodon* and *Peteinosaurus* and the placodont *Psephoderma* (e.g., Wild 1989; Pinna 1993; Renesto 2006; Renesto et al. 2010). In Germany, *Mystriosuchus* is well known from the Middle Stubensandstein (Hungerbühler 2002) and *Aetosaurus* from the Lower-Middle Stubensandstein, so a Revueltian age of the Zorzino Limestone is certain. The Calcare di Zorzino also crops out in Austria, where it yields specimens of *Langobardisaurus* and the pterosaur *Austriadactylus* (Dalla Vecchia 2009, 2013). Also, in Austria, unpublished specimens of *Mystriosuchus* are known from Totes Gebirge (possibly Dachstein) (Buffetaut 1993).

The other Italian Late Triassic tetrapod sites are in the Forni Dolomite (Dolomia di Forni) in the Veneto Prealps of northeastern Italy. They yield the drepanosaurids *Drepanosaurus* and *Megalancosaurus,* the pterosaurs *Eudimorphodon* and *Preondactylus* (Dalla Vecchia 1995, 2003, 2006) and a specimen of *Langobardisaurus*. The presence of *Eudimorphodon* supports a Revueltian age assignment.

Upper Triassic tetrapod assemblages from the Indian Subcontinent come from the Pranhita-Godavari Valley of south-central India. Several summaries (Jain et al. 1964; Kutty 1969; Kutty and Roychowdhury 1970; Sengupta 1970; Jain and Roychowdhury 1987; Yadagiri and Rao 1987; Kutty et al. 1988; Kutty and Sengupta 1989; Bandyopadhyay and Roychowdhury 1996; Bandyopadyhay and Sengupta 2006; Kammerer et al. 2016) have been published, but other than the lower Maleri assemblage (see above), relatively few of the fossils have been adequately documented in print, forcing me to rely largely on unsubstantiated genus-level identifications to evaluate the ages of the tetrapod assemblages. A case in point is the Dharmaram Formation, which yields two stratigraphically discrete vertebrate fossil assemblages (lower and upper). The stratigraphic range of the lower assemblage has not been published, and it includes a phytosaur that Kutty and Sengupta (1989: table 2) list as *Nicrosaurus*, aetosaurs, including a so-called "*Paratypothorax*-like" form, and prosauropod dinosaurs. Based primarily on the supposed *Nicrosaurus* record, I consider the lower assemblage of the Dharmaram Formation a possible Revueltian correlative.

I formerly and tentatively regarded the Coloradan LVF of Argentina and the tetrapod assemblage of the Lower Elliot Formation in South Africa as of Apachean age. In Argentina, the Los Colorados Formation consists of siliciclastic red beds approximately 800 m thick. Near its base, a single tetrapod fossil—a dicynodont skull, the holotype of "*Jachaleria" colorata* Bonaparte 1970—was collected. I regard *Jachaleria* as a synonym of *Ischigualastia*, so it is likely the lower part of the Los Colorados Formation is of Adamanian age.

The remainder of the tetrapod fossils from the Los Colorados Formation are from its middle and upper parts but have not been stratigraphically organized. The assemblage includes the turtle *Palaeochersis*, the ornithosuchid *Riojasuchus,*

the aetosaur "*Neoaetosauroides*" (see below), the rauisuchid *Fasolasuchus*, the crocodylomorphs *Hemiprotosuchus* and *Pseudhesperosuchus*, the prosauropod dinosaurs *Riojasaurus* and *Coloradisaurus*, the theropod dinosaur *Zupaysaurus* and the tritheledontid cynodont *Chaliminia* (e.g., Bonaparte 1970, 1971, 1978, 1980, 1997; Lucas and Hunt 1994; Rougier et al. 1995; Arcucci et al. 2004). The correlative Quebrada del Barro and El Tranquilo formations also produce prosauropods (e.g., *Riojasaurus*, "*Mussaurus*") (Bonaparte and Vince 1979; Casamiquela 1980; Bonaparte and Pumares 1995). The Los Colorados assemblage clearly is of Late Triassic age (Arcucci et al. 2004) and must be post-Ischigualastian. However, its endemism makes it difficult to correlate precisely. I tentatively considered it an Apachean correlative based primarily on its abundant prosauropods. However, the possibility that it is Revueltian needs to be considered, especially given the similarity of *Neoaetosauroides* to *Aetosaurus*.

Indeed, having now had the opportunity to study the type material of *Neoaetosauroides engaeus* firsthand, it is abundantly clear that *Neoaetosauroides* is a junior synonym of *Aetosaurus*. Thus, the armor plates of *Neoaetosauroides* (Fig. 10.5) display all of the diagnostic features of the armor of *Aetosaurus* (cf. Fraas 1877; Heckert and Lucas 2000; Schoch 2007). To wit, the dorsal paramedian plates are moderately wide (width/length = 2.4–3.1) and possess a radial pattern of elongate ridges and pits and a low dorsal boss near the posterior margin of the plate (Fig. 10.5). The work of Desojo and Baéz (2007: text-fig. 5) makes it clear that the skulls of *Neoaetosauroides* and *Aetosaurus* have virtually identical suture patterns and proportions. This synonymy will be documented in greater detail elsewhere. But, I draw attention to it here because *Aetosaurus* is an index taxon of the Revuletian LVF. Thus, its presence in the middle-upper Los Colorados Formation indicates a Revueltian age.

Kent et al. (2014) presented a magnetostratigraphy of the Los Colorados Formation based on limited sampling of only 52 geomagnetic sites with a stratigraphic spacing of 10 m or more. The 15 polarity intervals identified were pattern matched to the E8-E15 interval of the Newark section, which, if correctly correlated, means the Los Colorados Formation crosses the Carnian-Norian boundary (is of Adamanian-Revueltian age). This is consistent with my interpretation that the Los Colorados is of Adamanian-Revueltian age. Nevertheless, I have little confidence in the pattern matching to the Newark magnetostratigraphy of so few and such widely spaced samples from the Los Colorados Formation.

The age of the tetrapod assemblage from the Lower Elliott Formation in South Africa has long been considered Late Triassic. Lucas and Hancox (2001) reviewed the age of this assemblage, which is dominated by sauropodomorph dinosaurs, but also has rare amphibians (a large chigutisaurid), a possible rauisuchian (*Basutodon*), the ornithischian dinosaur *Eocursor*, a traversodontid (*Scalenodontoides*) and the characteristic Late Triassic footprint ichnogenus *Brachychirotherium* (Kitching and Raath 1984; Lucas and Hancox 2001; Butler et al. 2007). This is the "*Euskelosaurus* range zone" of Kitching and Raath (1984), the youngest Triassic tetrapod assemblage in the Karoo basin. Yates (2003) re-evaluated the prosauropods of the Lower Elliott Formation and concluded that most are indeterminate sauropodomorphs or

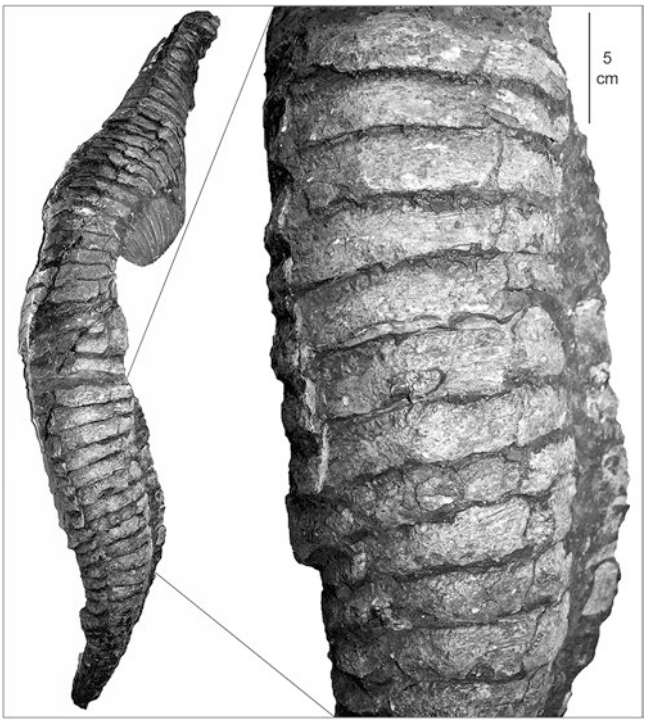

Fig. 10.5 Part of the holotype of *Aetosaurus* ("*Neoaetosauroides*") *engaeus*, Instituto Miguel Lillo, Tucuman, Argentina, PVL 3525. On *left* is a dorsal view of the dorsal armor, and on the *right* is a detail of part of the armor showing paramedian and lateral plates of the posterior dorsal to sacral region

basal sauropods. He noted similarities of indeterminate prosauropods from the Lower Elliott Formation to *Riojasaurus* from the Los Colorados Formation of Argentina, and similarities between the basal sauropod *Antetonitrus* from South Africa and *Lessemsaurus* from Argentina (Yates and Kitching 2003). These conclusions suggest a Lower Elliott-Los Colorados correlation, and thus a tentative Revueltian age assignment.

10.4.5 Apachean Tetrapod Assemblages

The characteristic tetrapod assemblage of the Apachean LVF is from the Redonda Formation of the Chinle Group in Guadalupe and Quay Counties, New Mexico, USA. The following taxa are present: the amphibian *Apachesaurus*, a sphenodontid, a procolophonid, the phytosaur *Redondasaurus*, the aetosaurs *Redondasuchus* and *Apachesuchus*, the rauisuchian *Redondavenator*, the archosauriform *Vancleavea*, theropod dinosaurs and the cynodont *Redondagnathus* (e.g., Hunt 1994; Hunt and

Lucas 1993b, 1997; Heckert et al. 2001; Hunt et al. 2005; Spielmann et al. 2006a, b; Spielmann and Lucas 2012).

Principal correlatives of the type Apachean assemblage are the Whitaker quarry in the Rock Point Formation of the Chinle Group at Ghost Ranch, New Mexico, the Cliftonian LVF assemblages (in part) of the Newark Supergroup, the Knollenmergel (Trossingen Formation), time-equivalent upper Arnstadt Formation and the "Rhaetian Bonebed" (Exter Formation) of the Germanic Basin (Fig. 10.4). Some of the fissure-fill assemblages in the uppermost Mercia Mudstone Group and/or lowermost Penarth Group of the United Kingdom (Fraser 1994; Benton and Spencer 1995; Whiteside and Marshall 2008) may be Apachean correlatives. Some of the so-called Rhaetian vertebrate sites in France, such as Saint-Nicolas-de-Port, may be Apachean correlatives as well (Lucas and Huber 2003).

At Ghost Ranch in New Mexico, the Whitaker quarry bone bed is dominated by skeletons of the theropod dinosaur *Coelophysis bauri* (Colbert 1989; Rinehart et al. 2009). Nevertheless, it also includes the sphenodont *Whitakersaurus*, at least one drepanosaur, a rauisuchian skeleton (cf. *Postosuchus*), the sphenosuchians *Hesperosuchus* and *Vancleavea*, the chatterjeeid *Shuvosaurus* (=*Effigia*), the phytosaur *Redondasaurus* and the theropod dinosaur *Daemonosaurus* (e.g., Hunt and Lucas 1993b; Clark et al. 2000; Harris and Downs 2002; Hungerbühler 2002; Hunt et al. 2002; Lucas et al. 2003; Nesbitt 2007; Lucas et al. 2005; Heckert et al. 2008; Renesto et al. 2009; Rinehart et al. 2009; Sues et al. 2011).

A recently discovered bonebed (the "Saints and Sinners Lagerstätte") in the Wingate Sandstone (which is the lower part of the "Nugget Sandstone" of Sprinkle et al., 2011) of northeastern Utah includes fossils of sphenodonts, sphenosuchians, drepanosaurs, theropod dinosaurs and a pterosaur, yet to be described (Britt et al. 2016: table 1). Given its stratigraphic position, this bonebed is likely of Apachean age.

The uppermost Triassic strata of the Newark Supergroup in eastern North America yield a low diversity tetrapod assemblage of mostly fragmentary material that defies precise identification. The tetrapods present include the procolophonid *Hypsognathus*, sphenodontids, indeterminate phytosaurs and the synapsid *Oligokyphus* (e.g., Gilmore 1928; Baird 1986; Huber et al. 1993b; Fedak et al. 2015). These are the tetrapods of the Cliftonian LVF of Huber et al. (1993b) and at least some are of likely Apachean age.

In the United Kingdom, fissure fills such as Durdham Down in Clifton yield fossils that include phytosaurs, aetosaurs, dinosauriforms and dinosaurs (e.g., Fraser 1994, 2006; Fraser et al. 2002; Galton 2005, 2007a, b; Whiteside and Marshall 2008). Unfortunately, other than a tentative record of *Aetosaurus* based on a single osteoderm (Lucas et al. 1999), the fissure fill tetrapods are mostly endemic taxa of no biochronological significance or cosmopolitan taxa with long age ranges, such as the sphenodontian *Clevosaurus*.

Whiteside and Marshall (2008), based primarily on the palynoflora, assigned the Tytherington fissure fill a Rhaetian age, and extrapolated this age to the other fissures. If this Rhaetian age is correct, then the fissure fill tetrapods are of Apachean age. However, as Lucas and Hunt (1994: 340) noted, "a single age should not necessarily

be assigned to the fossils from one fissure and…individual fossils from the fissures may range in age from middle Carnian to Sinemurian." Therefore, I continue to regard as problematic the precise age of the Triassic tetrapod assemblages from the British fissure fills.

10.4.6 Wassonian LVF

Lucas and Huber (2003) introduced the Wassonian LVF, and Lucas and Tanner (2007a) defined is as the time interval between the FAD of the crocodylomorph *Protosuchus*, and the beginning of the Dawan LVF, which is defined by the FAD of the theropod dinosaur *Megapnosaurus* (Lucas 2008). The FAD of *Protosuchus* in Arizona, Nova Scotia and South Africa appears to be lowermost Jurassic, so I take the beginning of the Wassonian LVF to approximate the Triassic-Jurassic boundary (Fig. 10.1). Most Early Jurassic tetrapod assemblages, however, are younger, of Dawan (~Sinemurian) age (Lucas 2008).

10.5 Late Triassic Tetrapod Footprints and Bromalites

The Upper Triassic record of tetrapod footprints was reviewed by Klein and Lucas (2010a) and is also reviewed by Hunt et al. (2017), so I do not review it here. It only resolves into one or two biochronological units, and is thus of much less significance to Late Triassic tetrapod biochronology than is the body-fossil record (e.g., Lucas 2007; Hunt and Lucas 2007; Klein and Lucas 2010a). Similarly, the Late Triassic bromalite (principally coprolite) record has some biochronological utility, but, like the footprint record, it resolves Late Triassic time rather poorly (see Hunt et al. 2017).

Brachychirotherium (*sensu stricto*), the footprint of aetosaurs (Fig. 10.6; Lucas and Heckert 2011), appears at the beginning of the Otischalkian. It is a characteristic ichnotaxon of the Late Triassic, together with *Atreipus-Grallator* (quadrupedal to bipedal trackways), *Grallator* and *Eubrontes* (bipedal trackways), the latter all attributed to theropods, except for *Atreipus*, which may also have had an ornithischian trackmaker. The stratigraphic upper limit of *Brachychirotherium* is the Triassic-Jurassic boundary (end of the Apachean); there is no evidence of *Brachychirotherium* in post-Triassic strata (Rainforth 2003; Lucas and Tanner 2007a, b, 2015).

Late Triassic tetrapod footprint assemblages are characteristically archosaur-dominated, particularly by chirothere and theropod tracks, but also feature the oldest records of sauropodomorph tracks. They thus mirror the overall pattern of the body fossil record but provide much less detailed insight into Late Triassic tetrapod distribution and evolution.

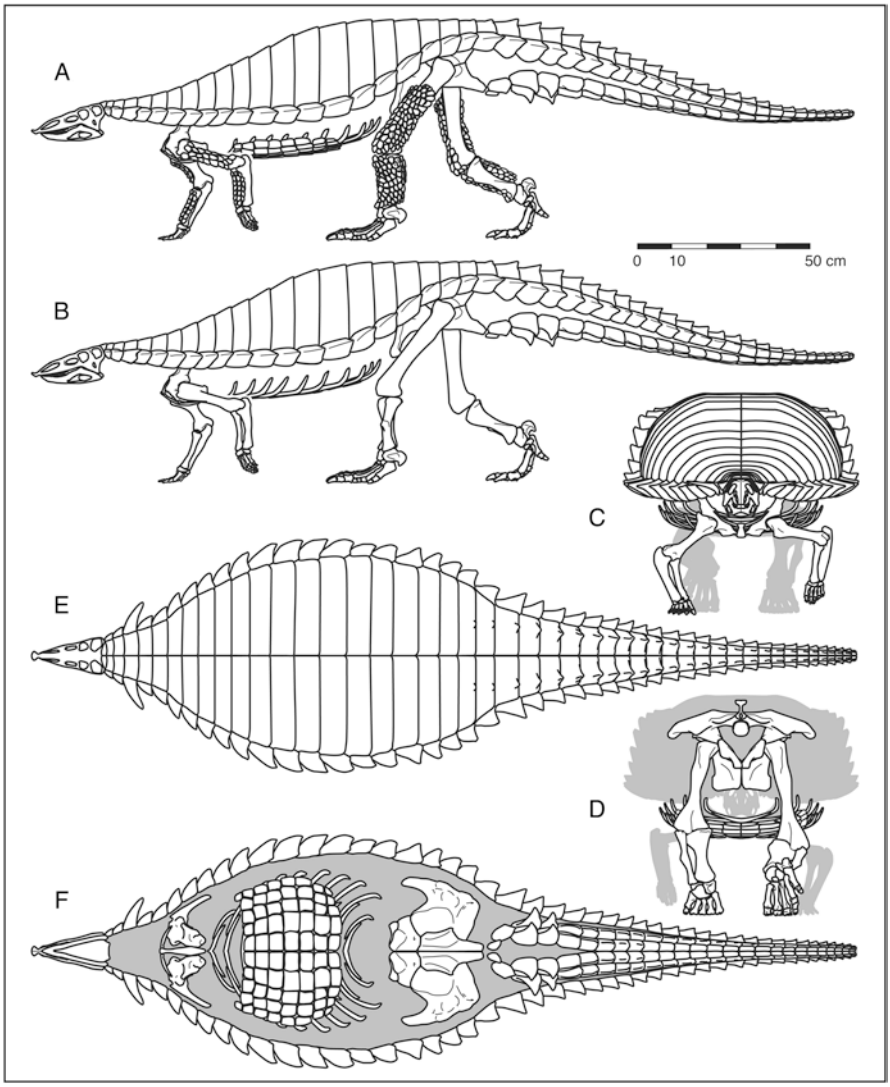

Fig. 10.6 The skeleton of the aetosaur *Typothorax coccinarum* as the trackmaker of *Brachychirotherium*, in lateral (**a**, **b**), anterior (**c**), posterior (**d**), dorsal (**e**) and ventral (**f**) views. After Lucas and Heckert (2011)

10.6 Biotic Events

10.6.1 Introduction

The Late Triassic has long been recognized as a critical juncture in the evolution of terrestrial tetrapods because it was an interval of both important originations

and extinctions (e.g., Fraser 2006; Sues and Fraser 2010). Here, I discuss the nature and timing of some of these events (Figs. 10.7, 10.8, 10.9, 10.10, 10.11, 10.12, and 10.13).

10.6.2 Archosaurs Rise to Dominance

The Berdyankian is the time of most of the youngest, dicynodont-dominated tetrapod assemblages. These assemblages are primarily from Argentina and Brazil and are dominated by fossils of dicynodonts (mostly the genus *Dinodontosaurus*), rhynchosaurs and traversodontid cynodonts. Fossils of amphibians and archosaurs are much less common constituents of these assemblages.

In contrast, the amphibian biofacies of Berdyankian time is dominated by mastodonsaurids and plagiosaurs, with much lesser numbers of prolacertiforms, archosaurs and small cynodonts. These assemblages are best known from the Germanic basin and from Russia. An acme in plagiosaur diversity and abundance in these assemblages characterizes Berdyankian time. No procolophonids are known from Berdyankian strata, but this must be due to a lack of discovery, not a real absence, as both pre- and post-Berdyankian procolophonids are known.

Otischalkian tetrapod assemblages are different from Berdyankian assemblages in being dominated by archosaur fossils, particularly of phytosaurs and aetosaurs. Indeed, it is during Otischalkian time, about 15 million years after the end-Permian extinctions that archosaur-dominated tetrapod fossil assemblages first appear. Thus, the old idea (e.g., Benton 1991; McGhee et al. 2004) that the Permo-Triassic extinctions were characterized by the takeover of many terrestrial tetrapod niches by archosauromorphs is erroneous (also see Lucas 2017a).

A new group of temnospondyls, the metoposaurs, is also abundant during Otischalkian time. It is striking how uniform in overall composition the Otischalkian tetrapod assemblages are, from North America, Western Europe, Morocco and India. This implies a degree of cosmopolitanism and no major biofacies differences.

The beginning of the Otischalkian essentially corresponds or overlaps the onset of the Carnian humid episode (e. g., Ruffell et al. 2016). Two groups of dominantly amphibious/aquatic tetrapods are abundant at this time, the metoposaurs and the phytosaurs. This may be a real acme as a response to wetter climates, but that conclusion may be confounded by taphonomy—preferential preservation of aquatic tetrapods by widespread river systems of the Carnian "pluvial." That caveat aside, metoposaurs and phytosaurs are the dominant components of almost all Otischalkian and younger Late Triassic tetrapod assemblages.

The overall character of many Adamanian tetrapod assemblages is very similar to Otischalkian assemblages—domination by fossils of metoposaurs, phytosaurs and aetosaurs. However, Adamanian tetrapod assemblages from Argentina and Brazil are dominated by dicynodonts, cynodonts and rhynchosaurs, with few to no phytosaurs and metoposaurs. Nevertheless, aetosaurs are common in these assemblages.

Fig. 10.7 Restoration of the Late Triassic metoposaurid amphibian *Koskinonodon* (artwork by Matt Celeskey)

Fig. 10.8 Restorations of the female (above) and male (below) heads of the phytosaur *Pseudopalatus*, showing the cranial sexual dimorphism evident in population samples of this phytosaur (artwork by Matt Celeskey)

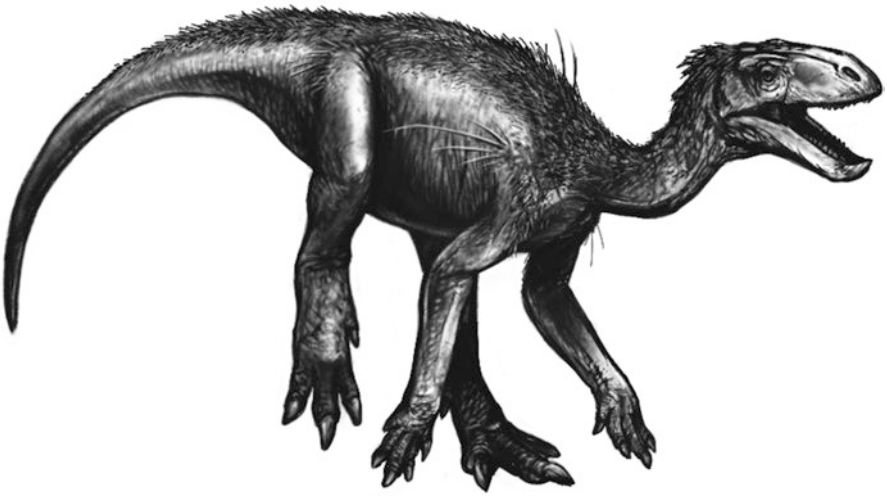

Fig. 10.9 The Late Triassic dinosauromorph *Silesaurus* has a foot structure that would make tracks like those of early theropod dinosaurs (artwork by Matt Celeskey)

Revueltian and Apachean tetrapod assemblages are also dominated mostly by archosaurs and metoposaurs. In some assemblages, dinosaurs are very abundant, and it is clear that the diversification of the dinosaurs had already begun by Revueltian time (Hunt 1991).

10.6.3 Temnospondyl Diminishment and Extinctions

The Late Triassic was the last interval of any substantial temnospondyl diversity (Milner 1990, 1993; Schoch and Milner 2000; Schoch 2008, 2014) (Fig. 10.7). It is also clear that this diversity collapsed stepwise throughout the Late Triassic, so that by Jurassic time few temnospondyl clades remained (Fig. 10.13). The lissamphibian radiation had begun in the Early Triassic (e.g., Rage and Roček 1989), though no definite lissamphibian fossils are known from the Upper Triassic, with the possible exception of *Triassurus* from Madygen (Ivakhnenko 1978).

The Late Triassic temnospondyl families are the Brachyopidae, Capitosauridae, Chigutisauridae, Almasauridae, Mastodonsauridae, Metoposauridae, Plagiosauridae and Trematosauridae. All are families of low diversity following much greater temnospondyl diversity earlier in the Permian and Triassic (Milner 1990; Ruta and Benton 2008). The record of almasaurids ends in the Otischalkian, and that of mastodonsaurids and trematosaurids ends in the Adamanian. Capitosaurid records are no younger than Revueltian, and metoposaurids and plagiosaurids have records that end in the Apachean. Brachyopids continued into the Jurassic, whereas chigutisaurids continued to the Cretaceous. Chroniosuchians have their last record at Madygen

Fig. 10.10 One of the last dicynodonts, Adamanian *Placerias*, attacked by a phytosaur (artwork by Matt Celeskey)

during the Otischalkian(?). Clearly, old ideas of a major extinction of temnospondyls at the end of the Triassic can be abandoned (Lucas and Tanner 2015).

10.6.4 Turtle Origins

The oldest turtles were long considered to be Revueltian in age. Best known is *Proganochelys* from Germany (Gaffney 1990), and Revueltian or younger turtle records are also known from Poland, Thailand, Greenland, the USA and South America (e.g., Lucas et al. 2000; Joyce et al. 2009; Joyce 2017). Recently added to this record is *Odontochelys* from marine lower Carnian strata in China (Li et al. 2008) and a supposed Ladinian turtle, *Pappochelys* from Germany (Schoch and

Fig. 10.11 Restoration of the oldest mammal, *Adelobasileus* (artwork by Matt Celeskey)

Fig. 10.12 The drepanosaur *Hypuronector* (artwork by Matt Celeskey)

Sues 2015). Furthermore, the middle Permian *Eunotosaurus*, with expanded ribs, originally proposed as a close turtle relative by Watson (1914), is now being placed back into that position (Lyson et al. 2010, 2012, 2013, 2016).

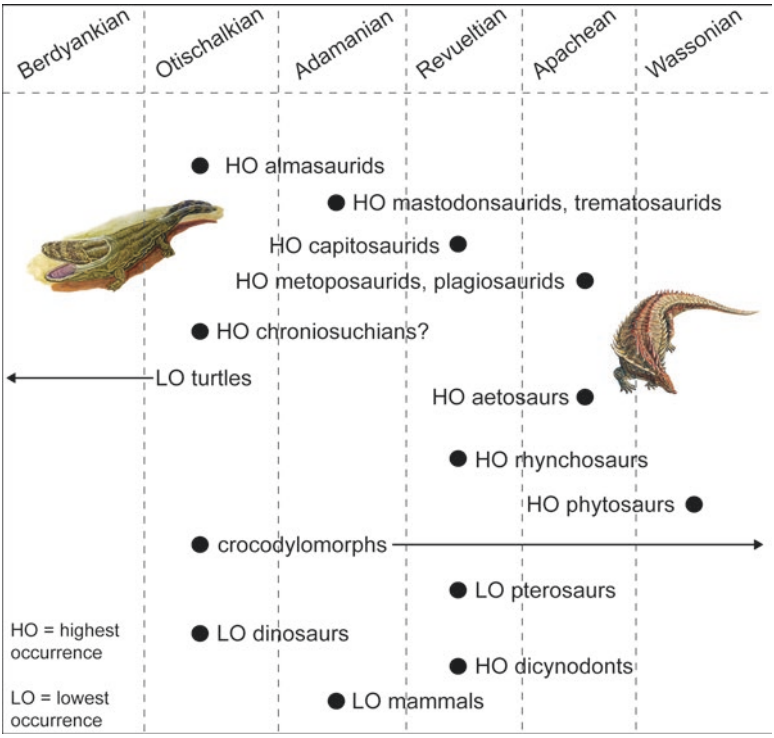

Fig. 10.13 Timing of the records of some important biotic events in the Late Triassic evolution of terrestrial tetrapods

.

Much overlooked in the discussion of turtle origins is their footprint record, which begins in the late Early Triassic (Spathian) (Rühle v. Lilienstern 1939; Haubold 1971; Lovelace and Lovelace 2012; Thomson and Lovelace 2014; Lichtig et al. 2017). Thus, recent claims that *Odontochelys* or *Pappochelys* are the oldest turtles are incorrect—the oldest turtle fossils (footprints) are of Early Triassic (Nonesian) age. They thus predate the oldest body fossils of turtles (and I do not consider *Pappochelys* to be a turtle; it is a placodont) by at least 10 million years. The origin of turtles thus is not, as long thought, a Late Triassic event, but took place much earlier (Fig. 10.13).

10.6.5 Rhynchosaurs

Rhynchosaurs are a Triassic group of herbivorous archosauromorphs that were most diverse during the Middle Triassic. Indeed, Romer (1966) long argued that together with gomphodont cynodonts they were dominant elements of Middle Triassic

tetrapod assemblages. However, rhynchosaurs were of low diversity during the Late Triassic, known from only a few genera. Most interesting is the very cosmopolitan *Hyperodapedon* found in Otischalkian-Adamanian assemblages in North America, western Europe, India, South America, Africa and Madagascar (Lucas et al. 2002).

The rhynchosaur genus *Otischalkia* is known from Otischalkian-Revueltian strata of the Chinle Group in the western USA (Hunt and Lucas 1991; Long and Murry 1995; Spielmann et al. 2013; Lucas et al. 2016). The Revueltian record of *Otischalkia* is the only bona fide Norian record of a rhynchosaur, and demonstrates that they did not go extinct at the Carnian-Norian boundary, as long thought (e.g., Benton 1991).

Schultz et al. (2016: fig. 10) recently presented what I regard as an erroneous time calibration of Late Triassic rhynchosaurs. Thus, they show "*Isalorhynchus*" (a synonym of *Hyperodapedon*) predating *Hyperodapedon* during the Carnian. They show *Teyumbatia* (a cladotaxon named and described by Montefeltro et al. 2010, 2013, likely synonymous with *Hyperodapedon;* cf. Azevedo and Schultz 1987) as Norian, though the fossil is from the Adamanian Caturitta Formation and therefore of Carnian age (see above). Schultz et al. (2016) also uniquely claim that *Otischalkia* is not diagnostically a rhynchosaur. Clearly, my view of Late Triassic rhynchosaur distribution differs markedly from that of Schultz et al. (2016), though all agree that rhynchosaur diversity was low during the Late Triassic.

10.6.6 Phytosaurs and Aetosaurs

Recent analysis identifies Middle Triassic *Diandongosuchus* as the oldest phytosaur and cladotaxonomically splits many long-recognized phytosaur genera into multiple genera (e. g., Stocker 2012; Stocker and Butler 2013; Butler et al. 2014; Stocker et al. 2017). This work ignores important factors of biological variation in phytosaurs (e.g., Fig. 10.8; Kimmig and Spielmann 2011) and will need substantial revision. The peak of phytosaur diversity was during the Adamanian-Revueltian, with perhaps no more than one genus surviving into Apachean time. A phytosaur snout fragment from the Lower Jurassic of the UK is the stratigraphically highest phytosaur fossil not clearly reworked, so it suggests phytosaur survival across the Triassic-Jurassic boundary (Maisch and Kapitzke 2010) (Fig. 10.13).

Aetosaur taxonomy is similarly being overspilt by cladotaxonomy (Desojo et al. 2013) and will need revision. The oldest aetosaur records are Otischalkian, with an acme during the Adamanian-Revueltian. Most of the evidence of Apachean aetosaurs is based on the footprint ichnogenus *Brachychirotherium* (see above).

Assemblages dominated by metoposaurs, phytosaurs and/or aetosaurs characterize much of the Late Triassic tetrapod record. Clearly, a taphonomic overprint is at least in part responsible for this. Metoposaurs and phytosaurs were amphibious tetrapods that would have been preferentially preserved/fossilized in the fluvial sediments from which comes most of the Late Triassic tetrapod fossil record. Nevertheless, before the Otischalkian no such metoposaur/phytosaur/aetosaur

assemblages are known, though these groups likely had a Middle Triassic ancestry. The abundance and ubiquity of metoposaurs and phytosaurs is a Late Triassic phenomenon across Pangea, with the exception of South America.

10.6.7 Crocodylomorphs

The oldest crocodylomorphs are sphenosuchans, with a record that begins in the Otischalkian (Lucas et al. 1998). Among them are taxa well-known from comprehensive cranial and postcranial material such as *Hesperosuchus*, *Sphenosuchus*, *Saltoposuchus, Dibothrosuchus* and *Protosuchus* (e. g., Colbert and Mook 1951; Colbert 1952; Crush 1984; Parrish 1991; Sereno and Wild 1992; Wu and Chatterjee 1993; Lucas et al. 1998; Clark et al. 2004). These early crocodiles have long been interpreted as lightly built cursorial and fully terrestrial forms.

No substantial change takes place in the Sphenosuchia across the Triassic-Jurassic boundary (Klein and Lucas 2015). What does occur much later, definitely in the Late Jurassic, perhaps as early as the Middle Jurassic, is the appearance of aquatic/amphibious crocodylians. The body fossil and footprint records document this (e.g., Lockley et al. 2010; Klein and Lucas 2010b, 2015). Clearly, the aquatic predator niches now associated with crocodylians were not occupied by crocodylomorphs during the Late Triassic-Early Jurassic. Phytosaurs occupied at least some of those niches during the Late Triassic (Hunt 1989).

10.6.8 Pterosaur Origins

Pterosaurs appear suddenly and completely adapted to flight during the Late Triassic. The lack of antecedents has made the origin and precise phylogenetic placement of pterosaurs somewhat unclear. Certainly pterosaurs are archosaurs, and most (but not all) analyses place them close to dinosaurs (see Hone and Benton 2008; Dalla Vecchia 2013 for reviews). *Scleromochlus* from the Adamanian of Scotland has been considered to be related to the ancestry of pterosaurs by some (e.g., Padian 1984), but others have dismissed that idea (e.g., Sereno 1991).

The oldest complete and reliable skeletal records of pterosaurs are Revueltian, from Italy, but isolated teeth and bones of Adamanian age have also been identified (with less certainty) as pterosaur (see Barrett et al. 2008; Dalla Vecchia 2013). *Faxinalipterus* from the Adamanian of Brazil, a supposed pterosaur (Bonaparte et al. 2010b), is not demonstrably a pterosaur according to Dalla Vecchia (2013). Given the phylogenetic analysis and their temporal distribution it seems that, as with dinosaur origins (see below), pterosaur origins was likely a Middle Triassic event for which we need a fossil record. However, on face value, the pterosaur first appearance is a sudden one during the Revuletian of forms very similar to the long-tailed, non-pterodactyloid pterosaurs of the Jurassic.

10.6.9 Dinosaur Origins

Understanding dinosaur origins has been beset by three problems: (1) semantic, namely what is and what is not a dinosaur; (2) cladistic—disagreements over the phylogeny of dinosaur origins, confounded by an inability to sort out convergence; and (3) biochronologic—disagreements over the actual age of the "oldest dinosaur." Despite these problems, all agree that the oldest dinosaur body fossils are Carnian (e.g. Langer et al. 2009; Lucas 2010; Benton 2012; Nesbitt and Ezcurra 2015). More precisely, they are Otischalkian, from the Chinle Group in the western USA (*Lepidus*) and the Maleri Formation of India (*Alwalkeria*). Otischalkian or Adamanian records of "dinosaurs" (*Azendohsaurus*) from Morocco and Madagascar have been discounted as not being based on dinosaurs (see Langer 2014 for discussion). Records from South America are Adamanian, so they are not the oldest records of dinosaur body fossils (contra Langer et al. 2009; Langer 2014).

The footprint record of the earliest dinosaurs also does not demonstrate dinosaurs older than Carnian. This, despite diverse claims (one of the most recent being by Marsicano et al. 2007) that tridactyl, apparently mesaxonic footprints from Middle Triassic strata are dinosaurian. Most of these are tridactyl remnants of chirothere tracks (see review by Klein and Lucas 2010a). Also, some could be the tracks of dinosauromorphs (Fig. 10.9) or of ornithodirans close to dinosaur origins, as discussed by Marsicano et al. (2007).

Particularly misleading, however, was the claim of dinosauromorph tracks in the Lower Triassic of Poland (Brusatte et al. 2011). This claim was based on the ichnogenus *Protorodactylus*, which is barely, if at all distinguishable from *Rhynchosauroides* (Klein and Niedzwiedźki 2012). The so-called "dinosauromorph" tracks of Brusatte et al. (2011) thus are most likely the tracks of lepidosauromorphs.

To conclude, the oldest dinosaur fossils are Carnian, more specifically of Otischalkian age. Importantly, they are not from South America, as many have erroneously claimed, though, clearly, much more remains to be discovered of dinosaur origins.

10.6.10 Dicynodont Diminishment and Extinction

The dinocephalian extinction event near the end of the middle Permian opened up the tetrapod herbivore niches to dicynodonts (Lucas 2017a). During the late Permian and Early Triassic, successive tetrapod assemblages were dominated by a single dicynodont genus, most famously *Lystrosaurus* of the earliest Triassic. However, other than in South America, by Berdyankian time dicynodont domination of the tetrapod herbivore niches had diminished (Fig. 10.10). Dicynodont diversity was low in the Late Triassic, with only one-two genera per LVF, and dicynodonts are only abundant in some South American assemblages. Late Triassic dicynodonts are also known from mass death assemblages in Arizona, Morocco and Poland.

The tetrapod herbivore niches occupied by dicynodonts may have been taken over by herbivorous aetosaurs, rhynchosaurs, prosauropod dinosaurs and cynodonts. However, the feeding mechanism of these herbivores are very different than those of dicynodonts, so replacement seems unlikely.

The HO (highest occurrence) of dicynodonts was long thought to be Adamanian. However, there is a putative Cretaceous record from Australia (Thulborn and Turner 2003), though it seems extremely doubtful. Dzik et al. (2008) recently reported a Triassic dicynodont from Poland in strata they deemed Rhaetian based on paleobotany, but that are Revueltian (Lucas 2015). These are the youngest known dicynodonts (Fig. 10.13).

10.6.11 Cynodont Evolution and Mammal Origins

The first cynodonts appear at about the end of the middle Permian and gradually increased in generic diversity through the Permo-Triassic boundary, the prelude to a much greater diversification during the Middle-Late Triassic (e. g., Abdala and Ribeiro 2010; Smith et al. 2012; Ruta et al. 2013; Abdala and Gaetano 2017). Late Triassic cynodont families are primarily the Traversodontidae, Trithelodontidae and Tritylodontidae. Traversodontids were most diverse (~ 17 genera), mostly of Adamanian age and mostly known from Gondwana (Liu and Abdala 2014). The only well-documented, post-Adamanian traversodontid is *Scalenodontoides* from the Revueltian Lower Elliott Formation of South Africa.

Tritylodontids were very mammal-like, especially in their postcranial anatomy. Their first appearance is during the Revueltian. However, most of their diversity is Early Jurassic. Trithelodontids (including the "dromatheres") were also not very diverse during the Late Triassic, but they most likely include the ancestors of mammals.

For decades, the oldest mammals were considered to be of Late Triassic age, notably *Morganucodon* from the British fissure fills. Cladistic analysis of the earliest mammals by Rowe (1988), however, changed that by redefining Mammalia as a crown clade consisting of the common ancestor of living monotremes and therians.

Cladistic analysis also "made" mammals monophyletic, even though such authorities as Olson and Simpson had entertained the possibility of a polyphyletic Mammalia. Questions of mammal origins had long been deeply emeshed in functional-adaptive analyses of the biology of the transition, particularly changes in the auditory and masticatory apparatuses. In the abiological world of numerical cladistics, these questions were trivialized as "essentialist" and not of scientific interest (Rowe and Gauthier, 1992; DeQuieroz 1994).

Miao (1991) provided a pointed discussion of these issues, rejecting cladistic redefinition of the Mammalia (also see Lucas 1992). Following Lucas and Luo (1993), I define Mammalia as the monophyletic group that includes *Adelobasileus* (Fig. 10.11), *Sinoconodon* and *Morganucodon* in the Mammalia.

Thus, I recognize a monophyletic Mammalia defined primarily by the biologically significant novelty of a petrosal promontorium, likely with a coiled cochlea. The oldest mammal thus is *Adelobasileus* from the Adamanian of Texas, USA (Lucas and Luo 1993). Potentially older mammals may be known from teeth from the Tiki Formation of India (Datta and Das 1996; Datta 2005). Mammal origins from a trithelodontid cynodont seem likely, and this was a Late Triassic event.

During the Revueltian-Apachean there was a diversification of morganucodontids, haramiyids and "symmetrodonts," particularly in Europe (Kielan-Jaworowska et al. 2004; Luo 2011; Debuysschere et al. 2015). Moganucodonts achieved a Pangean distribution and were small (less than 100 g estimated body weight) insectivores represented by 16 genera. All of the well known morganucodontid genera cross the Triassic-Jurassic boundary.

10.6.12 Oddities

There are a variety of highly specialized, ergo bizarre, Late Triassic diapsids. These include drepanosaurs (Fig. 10.12), trilophosaurs and the possible gliders *Icarosaurus*, *Sharovipteryx* and *Longisquama*. Most or all of these taxa defy precise classification and lack antecedents that would connect them morphologically to more generalized ancestors. They demonstrate just how incomplete our knowledge is of the Late Triassic tetrapod record. In effect, they are end members of clades that have been little sampled.

10.6.13 Provinciality

There have been at least two views of tetrapod paleobiogeography across Late Triassic Pangea. The traditional view is one of cosmopolitanism, and whatever provinciality existed was the difference between Laurussian archosaur-dominated assemblages and Gondwanan therapsid-dominated assemblages (e. g., Romer 1966; Cox 1973). More recent studies argue for a distinction between Laurussian and Gondwanan tetrapod assemblages largely predicated on floral differences or for provinciality driven by paleoatitude (zonal climate belts) (Ezcurra 2010; Whiteside et al. 2011).

Shubin and Sues (1991) inferred tetrapod cosmopolitanism during the Middle Triassic followed by latitudinal variation that correlated to long-recognized paleofloral differences (e.g., Dobruskina 1995b; Artabe et al. 2003). However, their correlation of tetrapod assemblages (see especially Shubin and Sues 1991: fig. 3) is fraught with inaccuracies. Furthermore, their analysis identifies India and Madagascar as having affinities with the tetrapod assemblages of Europe and North America, even though the floras of India and Madagascar are Gondwanan (*Dicroidium* dominated).

Whiteside et al. (2011) claimed latitudinal differences between tetrapod faunas as due to the differences between areas in which sedimentation was driven by ~10 kyr cycles (cynodont-dominated) and those driven by ~20 kyr cycles (procolophonid-dominated). Their analysis was based on the tetrapod record of the Newark Supergroup in which there is essentially no temporal overlap between older, cynodont-dominated assemblages and younger procolophonid-dominated assemblages. Clearly, the differences between these assemblages could be due to their different geological ages, not to paleolatituidinal differences.

Ezcurra (2010) analyzed the paleobiogeography of Triassic tetrapods for three time slices: Middle Triassic, "Ischigualastian" and "Coloradan." Like Shubin and Sues (1991), his analysis identified Middle Triassic cosmopolitanism. Interestingly, his analysis of the "Ischigualastian" linked India and Europe but not North America, despite the great similarity between North American and European tetrapod assemblages. In general, his analysis employs too coarse of temporal resolution to identify meaningful paleobiogeographic differences.

The correlations advocated here indicate that the strikingly distinct Late Triassic tetrapod assemblages are those from the Berdyankian-Adamanian of South America. Whether or not these assemblages, dominated by dicynodonts, represent a distinct province or a distinct facies, however, is difficult to determine. Given the inland nature of deposition in the South American basins that produce these assemblages, the possibility that they are just representatives of the dicynodont-dominated biofacies seen earlier in the Triassic (see discussion above) needs to be entertained. Otherwise, the Late Triassic tetrapod record seems to demonstrate much cosmopolitanism.

10.7 Conclusion: Late Triassic Extinctions

Colbert (1958) long ago drew attention to the striking differences between Late Triassic and Early Jurassic tetrapod faunas. Late Triassic tetrapod faunas are populated by many "thecodonts," notably phytosaurs, aetosaurs and rauisuchians. Dinosaurs were not major components of most Late Triassic tetrapod faunas, and metoposaurs dominated the amphibians. In strong contrast, Early Jurassic tetrapod faunas are dinosaur dominated, with various crocodylomorphs, and totally lack "thecodonts" and metoposaurs, taxa that suffered extinction across the Triassic-Jurassic boundary. The question has been when and how did these extinctions take place.

Lucas and Tanner (2015) recently analyzed the Late Triassic tetrapod extinctions to conclude that they were not a single extinction at the Triassic-Jurassic boundary. There is also no evidence of a tetrapod extinction across the Carnian-Norian boundary (e.g. Lucas 1994; Sues and Fraser 2010).

Using the best temporal resolution, the Late Triassic looks like a prolonged interval of stepwise tetrapod extinctions and low origination rates. However, none of these is a mass extinction, and no reliable data support continued claims

of a tetrapod extinction just before or at the end of the Triassic (contra Kent et al. 2017). With new and more detailed stratigraphic data, the perceived Triassic-Jurassic boundary tetrapod extinction is mostly an artifact of coarse temporal resolution, the compiled correlation effect. The amphibian, archosaur and synapsid extinctions of the Late Triassic were not concentrated at the Triassic-Jurassic boundary, but instead occurred stepwise, beginning in the Norian and extending into the Hettangian (Fig. 10.13; Lucas and Tanner 2015).

Acknowledgments I thank many colleagues for access to specimens in museum collections and/or for assistance in the field. I am particularly grateful to Jaime Powell for access to the *Neoatosauroides* fossils in Tucuman, Argentina. Andy Heckert, Adrian Hunt and Larry Tanner have collaborated extensively with me in the field studying Late Triassic rocks and fossils, and they have taught me much. Adrian Hunt and Julien Kimmig provided helpful reviews of the manuscript.

References

Abdala F, Gaetano LC (2017) Late Triassic cynodont life: time of innovations in the mammal lineage. In: Tanner LH (ed) The Late Triassic world: earth in a time of transition. Topics in geobiology. Springer, New York (this volume)

Abdala F, Ribeiro AM (2003) A new traversodontid cynodont from the Santa Maria Formation (Ladinian-Carnian) of southern Brazil, with a phylogenetic analysis of Gondwanan traversodontids. Zool J Linnean Soc 139:529–545

Abdala F, Ribeiro AM (2010) Distribution and diversity patterns of Triassic cynodonts (Therapsida, Cynodontia) in Gondwana. Palaeogeogr Palaeoclimatol Palaeoecol 286:202–217

Abdala F, Smith RMH (2009) A Middle Triassic cynodont fauna from Namibia and its implications for the biogeography of Gondwana. J Vert Paleont 29:837–851

Abdala F, Ribeiro AM, Schultz CL (2001) A rich cynodont fauna of Santa Cruz do Sul, Santa Maria Formation (Middle-Upper Triassic), in southern Brazil. Neues Jahrb Geol Paläont Monat 2001:669–687

Abdala F, Marsicano CA, Smith RHM, Swart R (2013) Strengthening western Gondwanan correlations: a Brazilian dicynodont (Synapsida, Anomodontia) in the Middle Triassic of Namibia. Gondwana Res 23:1151–1162

Alcober O, Parrish JM (1997) A new poposaurid from the Upper Triassic of Argentina. J Vert Paleont 17:548–556

Alifanov VR, Kurochkin EN (2011) *Kyrgyzsaurus bukhanchenkoi* gen. et. sp. nov., a new reptile from the Triassic of southwestern Kyrgyzstan. Paleont J 45:639–647

Araújo DC, Gonzaga TD (1980) Uma nova especie de *Jachaleria* (Therapsida, Dicynodonta) do Triassico de Brasil. Actas II Congr Paleontol Bioestrat I Congr Latinoamer Paleont Buenos Aires 1:159–174

Arcucci AB, Marsicano CA (1998) A distinctive new archosaur from the Middle Triassic (Los Chañares Formation) of Argentina. J Vert Paleont 18:222–232

Arcucci AB, Marsicano CA, Caselli AT (2004) Tetrapod association and palaeoenvironment of the Los Colorados Formation (Argentina): a significant sample from western Gondwana at the end of the Triassic. Geobios 37:557–568

Artabe AE, Morel EM, Spalletti LA (2003) Caracterización de las provincias fitogeográficas triásicas del Gondwana extratropical. Ameghin 40:387–405

Atchley SC, Nordt LC, Dworkin SJ, Ramezani J, Parker WG, Ash SR, Bowring SA (2013) A linkage among Pangean tectonism, cyclic alluviation, climatic change, and biologic turnover

in the Late Triassic: the record from the Chinle Formation, southwestern United States. J Sed Res 83:1147–1161
Azevedo SAK, Schultz CL (1987) *Scaphonyx sulcognathus* sp. nov., um novo rincossaurídeo Neotriássico do Rio Grande do Sul, Brasil. Anais do X Congr Brasil Paleont, Rio de Janeiro 1987:99–113
Bachmann GH, Kozur HW (2004) The Germanic Triassic: correlations with the international scale, numerical ages and Milankovitch cyclicity. Hall Jahrb Geowissen B26:17–62
Baczko MB, Ezcurra MD (2013) Ornithosuchidae: a group of Triassic archosaurs with a unique ankle joint. In: Nesbitt SJ, Desojo JB, Irmis RB (eds) Anatomy, phylogeny and paleobiology of early archosaurs and their kin. Geol Soc London Spec Publ 379: 187–202
Baird D (1986) Some Upper Triassic reptiles, footprints, and an amphibian from New Jersey. Mosasaur 3:125–153
Bandyopadhyay S, Roychowdhury TK (1996) Beginning of the continental Jurassic in India: a paleontological approach. Mus North Ariz Bull 60:371–378
Bandyopadyhay S, Sengupta DP (2006) Vertebrate faunal turnover during the Triassic-Jurassic transition: an Indian scenario. New Mex Mus Nat Hist Sci Bull 37:77–85
Barberena MC (1977) Bioestratigrafia preliminar da Formacâo Santa Maria. Pesquisas Porto Alegre 7:111–129
Barberena MC, Araújo DC, Lavina EL (1985) Late Permian and Triassic tetrapods of southern Brazil. Nat Geog Res 1:5–20
Barrett PM, Butler RJ, Edwards NP, Milner AR (2008) Pterosaur distribution in time and space. Zitteliana B28:35–60
Benton MJ (1986) The Late Triassic tetrapod extinction events. In: Padian K (ed) The beginning of the age of dinosaurs. Cambridge University Press, New York, pp 303–320
Benton MJ (1991) What really happened in the Late Triassic? Hist Biol 5:263–278
Benton MJ (1993) Late Triassic terrestrial vertebrate extinctions: stratigraphic aspects and the record of the Germanic basin. Paleont Lomb Nu Ser 2:19–38
Benton MJ (2012) Origin and early evolution of dinosaurs. In: Brett-Surman MK, Holtz TR Jr, Darlow J (eds) The complete dinosaur. Indiana University Press, Bloomington, pp 331–345
Benton MJ, Spencer PS (1995) Fossil reptiles of Great Britain. Chapman and Hall, London
Bertinelli A, Casacci M, Concheri G, Gattolin G, Godfrey L, Katz ME, Maron M, Mazza M, Mietto P, Muttoni G, Rigo M, Sprovieri M, Stellin F, Zaffani M (2016) The Norian/Rhaetian boundary interval at Pignola-Abriola section (Southern Apennines, Italy) as a GSSP candidate for the Rhaetian stage: an update. Albertiana 43:5–18
Besarie H (1930) Recherches géologiques à Madagascar. Contribution à l'étude des resources minérales. Bull Soc Hist Nat Toul 59:345–616
Besarie H, Collignon M (1960) Madagascar (Supplément). Lex Strat Internat Paris 4(2):1–190
Besarie H, Collignon M (1971) Géologie de Madagascar I. Les Terrains Sedimentaires. Ann Geol Madagascar 35:1–461
Bonaparte JF (1966) Chronological survey of the tetrapod-bearing Triassic of Argentina. Breviora 251:1–13
Bonaparte JF (1967) Cronología de algunas formaciones Triásicas de Argentina: Basada en restos de tetrápodos. Assoc Geol Argent Rev 21:20–38
Bonaparte JF (1970) Annotated list of the South American Triassic tetrapods. In: Second Gondw Symp Proc Pap, pp 665–682
Bonaparte JF (1971) Los tetrapodos del sector superior de la formacion Los Colorados, La Rioja, Argentina (Triásico Superior). I Parte. Op Lillo 22:1–183
Bonaparte JF (1976) *Pisanosaurus mertii* Casamiquela and the origin of the Ornithischia. J Paleontol 50:808–820
Bonaparte JF (1978) El Mesozoico de América del Sur y sus tetrápodos. Op Lillo 26:1–596
Bonaparte JF (1980) El primer ictidosaurio (Reptilia-Therapsida) de America del Sur, *Chaliminia musteloides*, del Triásico Superior de La Rioja, República Argentina. Actas II Congr Argent Paleontol Bioestrat Buenos Aires 1978(1):123–133

Bonaparte JF (1982) Faunal replacement in the Triassic of South America. J Vert Paleont 2:362–371
Bonaparte JF (1997) El Triasico de San Juan-La Rioja Argentina y sus dinosaurios. Museo Argentino de Ciencias Naturales, Buenos Aires
Bonaparte JF, Pumares JA (1995) Notas sobre el primer craneo de *Riojasaurus incertus* (Dinosauria, Prosauropoda, Melanorosauridae) del Triasico Superior de La Rioja, Argentina. Ameghin 32:341–349
Bonaparte JF, Sues HD (2006) A new species of *Clevosaurus* (Lepidosauria: Rhynchocephalia) from the Upper Triassic of Rio Grande do Sul, Brazil. Palaeont 49:917–923
Bonaparte JF, Vince M (1979) El hallazgo del primer nido de dinosaurios Triásicos (Saurischia, Prosauropoda), Triásico superior de Patagonia, Argentina. Ameghin 16:173–182
Bonaparte JF, Ferigolo J, Ribeiro AM (1999) A new early Late Triassic saurischian dinosaur from Rio Grande do Sul State, Brazil. Nat Sci Mus Monog 15:89–109
Bonaparte JF, Ferigolo J, Ribeiro AM (2001) A primitive Late Triassic 'ictidosaur' from Rio Grande do Sul, Brazil. Palaeontology 44:623–635
Bonaparte JF, Brea G, Schultz CL, Martinelli AG (2007) A new specimen of *Guaibasaurus candelareiensis* (basal Saurischia) from the Late Triassic Caturrita Formation of southern Brazil. Hist Biol 19:73–82
Bonaparte JF, Schultz CL, Soares MB (2010a) Pterosauria from the Late Triassic of southern Brazil. In: New aspects of Mesozoic biodiversity. Springer, Berlin, pp 63–71
Bonaparte JF, Schultz CL, Soares MB, Martinelli A (2010b) La fauna local de Faxinal do Soturno, Triássico Tardío de Rio Grande do Sul, Brazil. Rev Brasil Paleont 13:1–14
Branson EB, Mehl MG (1928) Triassic vertebrate fossils from Wyoming. Science 67:325–326
Britt BB, Chure DJ, Engelmann GF, Shumway JD (2016) Rise of the erg—paleontology and paleoenvironments of the Triassic-Jurassic transition in northeastern Utah. Geol Intermount West 3:1–30
Brusatte SL, Niedźwiedzki G, Butler RJ (2011) Footprints pull origin and diversification of dinosaur stem lineage deep into Early Triassic. Proc R Soc B 278:1107–1113
Buffetaut E (1983) *Isalorhynchus genovefae*, n. g. n. sp. (Reptilia, Rhynchocephalia), un noveau rhynchosaure du Trias de Madagascar. Neues Jahrb Geol Paläont Monats 1983:465–480
Buffetaut E (1993) Phytosaurs in time and space. Paleontol Lomb Nuo Serie 2:39–44
Burmeister KC, Flynn JJ, Parrish JM, Wyss AR (2006) Paleogeographic and biostratigraphic implications of new early Mesozoic vertebrates from Poamay, central Morondova basin, Madagascar. New Mex Mus Nat Hist Sci Bull 37:457–475
Butler RJ, Smith RMH, Norman DB (2007) A primitive ornithischian dinosaur from the Late Triassic of South America, and the early diversification of Ornithischia. Proc R Soc B 274:2041–2046
Butler RJ, Rauhut OWM, Stocker MR, Bronowicz R (2014) Redescription of the phytosaurs *Paleorhinus* (*Francosuchus*) *angustifrons* and *Ebrachosuchus neukami* from Germany, with implications for Late Triassic biochronology. Zool J Linnean Soc 170:155–208
Cabrera A (1944) Sobre un estegocéfalo de la Provincia de Mendoza. Not Mus La Plata 9:421–429
Camp CL, Welles SP (1956) Triassic dicynodont reptiles. Mem Univ Cal 13:255–348
Casamiquela RM (1960) Noticia preliminar sobre dos nuevos estagonolepoideos Argentinos. Ameghin 2:3–9
Casamiquela RM (1962) Dos nuevos estagonolepoideos Argentinos. Rev Assoc Geol Argent 16:143–203
Casamiquela RM (1980) La presencia del genero *Plateosaurus* (Prosauropoda) en el Triásico Superior de la Formación El Tranquilo, Patagonia. Actas II Congr Argent Paleontol Bioestratig, I Congr Latinoamer Paleont 1:143–158
Chatterjee S (1967) New discoveries contributing to the stratigraphy of the continental Triassic sediments of the Pranhita Godavari Valley. Bull Geol Soc India 4:37–41
Chatterjee S (1974) A rhynchosaur from the Upper Triassic Maleri Formation of India. Phil Trans R Soc Lond B267:209–261

Chatterjee S (1978) A primitive parasuchid (phytosaur) reptile from the Upper Triassic Maleri Formation of India. Palaeontology 21:83–127
Chatterjee S (1980) *Malerisaurus*, a new eosuchian reptile from the Late Triassic of India. Phil Trans R Soc Lond B291:163–200
Chatterjee S (1982) A new cynodont reptile from the Triassic of India. J Paleontol 56:203–214
Chatterjee S (1987) A new theropod dinosaur from India with remarks on the Gondwana-Laurasia connection in the Late Triassic. In: McKenzie GD (ed) Gondwana six: stratigraphy, sedimentology and paleontology. Amer Geophys Un Monog 41: 183–189
Chatterjee S, Roychowdhury T (1974) Triassic Gondwana vertebrates from India. Ind J Earth Sci 12:96–112
Cirilli S, Marzoli A, Tanner LH, Bertrand H, Buratti N, Jourdan F, Bellieni G, Kontak D, Renne PR (2009) Late Triassic onset of the Central Atlantic Magmatic Province (CAMP) volcanism in the Fundy Basin (Nova Scotia): new stratigraphic constraints. Earth Planet Sci Lett 286:514–525
Cisneros JC, Schultz CL (2003) *Soturnia caliodon* n. g. n. sp., a procolophonid reptile from the Upper Triassic of southern Brazil. Neues Jahrb Geol Paläont Monats 227:365–380
Cisneros JC, Damiani R, Schultz C, de Rosa A, Schwanke C, Neto LW, Aurélio PLP (2004) A procolophonoid reptile with temporal fenestration from the Middle Triassic of Brazil. Proc R Soc Lond B271:1541–1546
Clark JM, Sues HD, Berman DS (2000) A new specimen of *Hesperosuchus agilis* from the Upper Triassic of New Mexico and the interrelationships of basal crocodylomorph archosaurs. J Vert Paleont 20:683–704
Clark JM, Xu X, Forster CA, Wang Y (2004) A Middle Jurassic 'sphenosuchian' from China and the origin of the crocodilian skull. Nature 430:1021–1024
Clemmensen LB, Milàn J, Adolfssen JS, Estrup EJ, Frobose N, Klein N, Mateus O, Wings O (2016) The vertebrate-bearing Late Triassic Fleming Fjord Formation of central Greenland revisited: stratigraphy, palaeoclimate and new palaeontological data. In: Kear PB, Lindgren J, Hurm JH, Milàn J, Vajda V (eds) Mesozoic biotas of Scandinavia and its Arctic territories. Geol Soc London Spec Publ 434: 31–47
Colbert EH (1952) A pseudosuchian reptile from Arizona. Bull Am Mus Nat Hist 99:561–592
Colbert EH (1957) Triassic vertebrates of the Wind River basin. Wyo Geol Assoc Guidebk 12:89–93
Colbert EH (1958) Triassic tetrapod extinction at the end of the Triassic Period. Proc Natl Acad Sci U S A 44:973–977
Colbert EH (1989) The Triassic dinosaur *Coelophysis*. Bull Mus North Ariz 57:1–174
Colbert EH, Mook CC (1951) The ancestral crocodilian *Protosuchus*. Bull Am Mus Nat Hist 97:143–182
Cope ED (1871) Observations on the distribution of certain extinct vertebrates in North Carolina. Proc Am Philos Soc 12:210–216
Cox CB (1965) New Triassic dicynodonts from South America, their origins and relationships. Phil Trans R Soc Lond B248:457–516
Cox CB (1973) Triassic tetrapods. In: Hallam A (ed) Atlas of palaeobiogeography. Elsevier, Amsterdam, pp 213–223
Cox CB (1991) The Pangea dicynodont *Rechnisaurus* and the comparative biostratigraphy of Triassic dicynodont faunas. Palaeontology 34:767–784
Crush PJ (1984) A late Upper Triassic sphenosuchid crocodilian from Wales. Palaeontology 27:131–157
Currie BS, Colombi CE, Tabor NJ, Shipman TC, Montanez IP (2009) Stratigraphy and architecture of the Upper Triassic Ischigualasto Formation, Ischigualasto Provincial Park, San Juan, Argentina. J S Am Earth Sci 27:74–87
Dalla Vecchia FM (1995) A new pterosaur (Reptilia, Pterosauria) from the Norian (Late Triassic) of Friuli (northeastern Italy). Preliminary note. Gortania 16:59–66
Dalla Vecchia FM (2003) A review of the Triassic pterosaur record. Riv Mus Civ Sci Natural "E. Caffi" 22:13–29

Dalla Vecchia FM (2006) The tetrapod fossil record from the Norian-Rhaetian of Friuli (northeastern Italy). New Mex Mus Nat Hist Sci Bull 37:432–444
Dalla Vecchia FM (2009) Anatomy and systematics of the pterosaur *Carniadactylus* gen. n. *rosenfeldi* (Dalla Vecchia, 1995). Riv Ital Paleont Stratig 115:159–198
Dalla Vecchia FM (2013) Triassic pterosaurs. In: Nesbitt SJ, Desojo JB, Irmis RB (eds) Anatomy, phylogeny and paleobiology of early archosaurs and their kin. Geol Soc London Spec Publ 379: 119–155
Damiani R, Schoch RR, Hellrung H, Werneburg R, Gastou S (2009) The plagiosaurid temnospondyl *Plagiosuchus pustuliferus* (Amphibia: Temnospondyli) from the Middle Triassic of Germany: anatomy and functional morphology of the skull. Zool J Linnean Soc 155:348–373
Datta PM (2005) Earliest mammal with transversely expanded upper molar from the Late Triassic (Carnian) Tiki Formation, South Rewa Gondwana basin, India. J Vert Paleont 25:200–207
Datta PM, Das DP (1996) Discovery of the oldest fossil mammal from India. India Min 50:217–222
Debuysschere M, Gheerbrant E, Ailian R (2015) Earliest known European mammals. A review of *Morganucodon* from Saint-Nicolas-de-Port (Upper Triassic, France). J Syst Palaeont 13:825–855
DeQuieroz K (1994) Replacement of an essentialist perspective on taxonomic definition as exemplified by the definition of “Mammalia”. Syst Biol 43:497–510
Desojo JB, Baéz AM (2007) Cranial morphology of the Late Triassic South American archosaur *Neoaetosauroides engaeus*: evidence for aetosaurian diversity. Palaeontology 50:267–276
Desojo JB, Ezcurra MD, Schultz CL (2011) An unusual new archosauriform from the Middle-Late Triassic of southern Brazil and the monophyly of Doswelliidae. Zool J Linnean Soc 161:839–871
Desojo JB, Heckert AB, Martz JW, Parker WG, Schoch RR, Small BJ, Sulej T (2013) Aetosauria: a clade of armoured pseudosuchians from the Upper Triassic continental beds. In: Nesbitt SJ, Desojo JB, Irmis RB (eds) Anatomy, phylogeny and palaeobiology of early archosaurs and their kin. Geol Soc London Spec Publ 379: 203–240
Dias-da-Silva S, Carvalho IC, Schwanke C (2007) Vertebrate dinoturbation from the Caturrita Formation (Late Triassic, Parana basin), Rio Grande do Sul State, Brazil. Gondwana Res 11:303–310
Dias-da-Silva S, Dias EV, Schultz CL (2009) First record of stereospondyls (Tetrapoda, Temnospondyli) in the Upper Triassic of southern Brazil. Gondwana Res 15:131–136
Dilkes D, Sues H-D (2009) Redescription and phylogenetic relationships of *Doswellia kaltenbachi* (Diapsida: Archosauriformes) from the Upper Triassic of Virginia. J Vert Paleont 29:58–79
Dobruskina IA (1995a) Keuper (Triassic) flora from Middle Asia (Madygen, southern Fergana). New Mex Mus Nat Hist Sci Bull 5:1–49
Dobruskina IA (1995b) Triassic plants and Pangea. Palaeobotanist 44:116–127
Dornelles JEF (1990) Registro sobre a ocorrencia de dentes de um arccossaurio para a Formacao Caturrita, Triassico Superior do Rio Grande do Sul, Brasil. Cie Natur Santa Maria 12:99–101
Doyle KD, Sues HD (1995) Phytosaurs (Reptilia: Archosauria) from the Upper Triassic New Oxford Formation of York County, Pennsylvania. J Vert Paleont 15:545–553
Dutuit JM (1966) Apport des déscovertes de vertébrès à la stratigraphie du Trias continental du coloir d’Argana (Haut-Atlas occidental, Maroc). Maroc Serv Géol Notes 26:29–31
Dutuit JM (1972) Découverte d’un dinosaure ornithischien dans le Trias Supérieur de l’Atlas occidental marocain. Compt Rend Acad Sci D 275:2841–2844
Dutuit JM (1976) Introduction à l’etude paléontologique du Trias continental marocain. Description des premiers stégocéphales recuellis dans le couloir d’Argana. Mém Mus Nat Hist Nat C 36:1–253
Dutuit JM (1977) Paleorhinus magnoculus. Phytosaure du Trias Supérieur de l’Atlas Marocain Anns de Univers Provence 4:255–268
Dutuit JM (1978) Description de quelques fragments osseux provenant de la région de Folakara (Trias supérieur Malgache). Bull Mus Hist Natur 69:79–89

Dutuit JM (1988) Ostéologie crânienne et ses enseignements apports géologique et paléoécologique de *Moghreberia nmachouensis*, dicynodonte (Reptilia, Therapsida) du Trias Supérieur Marocain. Bull Mus Nat Hist Nat 10:227–285

Dutuit JM (1989a) *Azarifeneria barrati*, un deuxième genre de dicynodonte du Trias Supérieur Marocain. Compt Rend Acad Sci 309:303–306

Dutuit JM (1989b) Confirmation des affinités entre Trias Supérieurs Marocain et Sud-Americain: Découverte d'un troisième dicynodonte (Reptilia, Therapsida), *Azarifeneria robustus*, n. sp., de la formation d'Argana (Atlas occidental). Compt Rend Acad Sci 309:1267–1270

Dzik J (2001) A new *Paleorhinus* fauna in the early Late Triassic of Poland. J Vert Paleont 21:625–627

Dzik J (2003) A beaked herbivorous archosaur with dinosaur affinities from the early Late Triassic of Poland. J Vert Paleont 23:556–574

Dzik J, Sulej T (2007) A review of the Late Triassic Krasiejów biota from Silesia, Poland. Palaeont Polon 64:1–27

Dzik J, Sulej T, Niedźwiedzki G (2008) A dicynodont-theropod association in the latest Triassic of Poland. Acta Palaeont Polon 53:733–738

Emmons E (1856) Geologic report of the midland counties of North Carolina. George P. Putnam and Co., New York

Ezcurra MD (2006) A review of the systematic position of the dinosauriform archosaur *Eucoelophysis baldwini* Sullivan and Lucas, 1999 from the Upper Triassic of New Mexico, USA. Geodiversitas 28:649–684

Ezcurra MD (2010) Biogeography of Triassic tetrapods: evidence for provincialism and driven sympatric cladogenesis in the early evolution of modern tetrapod lineages. Proc R Soc B 277:2547–2552

Fedak TJ, Sues H-D, Olsen PE (2015) First record of the tritylodontid cynodont *Oligokyphus* and cynodont postcranial bones from the McCoy Brook Formation of Nova Scotia, Canada. Can J Earth Sci 52:244–249

Ferigolo J, Langer MC (2006) A Late Triassic dinosauriform from south Brazil and the origin of the ornithischian predentary bone. Hist Biol 18:1–11

Flynn JJ, Wyss AR (2003) Mesozoic terrestrial vertebrate faunas: the early history of Madagascar's vertebrate diversity. In: Goodman SM, Benstead JP (eds) The natural history of Madagascar. University of Chicago Press, Chicago, pp 34–40

Flynn JJ, Parrish JM, Rakotosamimanana B, Simpson WF, Whatley RL, Wyss AR (1999) A Triassic fauna from Madagascar, including early dinosaurs. Science 286:763–765

Flynn JJ, Parrish JM, Rakotosamimanana B, Ranivoharimanana L, Simpson WF, Wyss AR (2000) New traversodontids (Synapsida: Eucynodontia) from the Triassic of Madagascar. J Vert Paleont 20:422–427

Flynn J, Nesbitt S, Parrish M, Ranivoharimanana L, Wyss A (2008) A new species of basal archosauromorph from the Late Triassic of Madagascar. J Vert Paleont 28(3):78A

Flynn JJ, Nesbitt SJ, Parrish JM, Ranivoharimanana L, Wyss AR (2010) A new species of *Azendohsaurus* (Diapsida: Archosauromorpha) from the Triassic Isalo Group of southwestern Madagascar: cranium and mandible. Palaeontology 53:669–688

Fraas O (1877) *Aetosaurus ferratus* Fr. Die gepanzerte Vogel-Echse aus dem Stubensandstein bei Stuttgart. Festschr Feier s vierhundertjähr Jubiläums Eberhard-Karls-Univers Tübingen, Wurttemberg naturwissene Jahresh 33:1–22

Fraser NC (1994) Assemblages of small tetrapods from British Late Triassic fissure deposits. In: Fraser NC, Sues H-D (eds) In the shadow of the dinosaurs. Cambridge University Press, Cambridge, pp 214–226

Fraser N (2006) Dawn of the dinosaurs: life in the Triassic. Indiana University Press, Bloomington

Fraser NC, Padian K, Walkden GM, Davis ALM (2002) Basal dinosauriform remains from Britain and the diagnosis of the Dinosauria. Palaeontology 45:79–95

Gaffney ES (1990) The comparative osteology of the Triassic turtle *Proganochelys*. Bull Am Mus Nat Hist 194:1–263

Galton PM (2005) Bones of large dinosaurs (Prosauropoda and Stegosauria) from the Rhaetic bone bed (Upper Triassic) of Aust Cliff, southwest England. Rev Paléobiol Genève 24:51–74

Galton PM (2007a) Notes on the remains of archosaurian reptiles, mostly basal sauropodomorph dinosaurs, from the 1834 fissure fill (Rhaetian, Upper Triassic) at Clifton in Bristol, southwest England. Rev Paléobiol Genève 26:505–591

Galton PM (2007b) *Pantydraco* n. gen. for *Thecodontosaurus cauducus* Yates, 2003, a basal sauropodomorph dinosaur from the Upper Triassic or Lower Jurassic of South Wales, UK. Neues Jahrb Geol Paläont Abhand 243:119–125

Gauffre F (1993) The prosauropod dinosaur *Azendohsaurus laaroussii* from the Upper Triassic of Morocco. Palaeontology 36:897–908

Gilmore CW (1928) A new fossil reptile from New Jersey. Proc US Nat Mus 73:1–8

Gower DJ, Schoch RR (2009) Postcranial anatomy of the rauisuchian archosaur *Batrachotomus kupferzellensis*. J Vert Paleont 29:103–122

Gower DJ, Sennikov AG (2000) Early archosaurs from Russia. In: Benton MJ, Shishkin MA, Unwin DM, Kurochkin EN (eds) The age of dinosaurs in Russia and Mongolia. Cambridge University Press, Cambridge, pp 140–159

Guth C (1963) Au sujets de restes de reptiles de Madagascar. Compt Rend Acad Sci 25:2661–2663

Harris JD, Downs A (2002) A drepanosaurid pectoral girdle from the Ghost Ranch (Whitaker) *Coelophysis* quarry (Chinle Group, Rock Point Formation, Rhaetian), New Mexico. J Vert Paleont 22:70–75

Haubold H (1971) Ichnia Amphibiorum et Reptiliorum fossilium. Encyc Paleoherp 18:1–124

Heckert AB (1997) The tetrapod fauna of the Upper Triassic lower Chinle Group (Adamanian: latest Carnian) of the Zuni Mountains, west-central New Mexico. New Mex Mus Nat Hist Sci Bull 11:29–40

Heckert AB (2004) Late Triassic microvertebrates from the lower Chinle Group (Otischalkian-Adamanian: Carnian). New Mex Mus Nat Hist Sci Bull 27:1–170

Heckert AB, Lucas SG (1999) A new aetosaur (Reptilia: Archosauria) from the Upper Triassic of Texas and the phylogeny of aetosaurs. J Vert Paleont 19:50–68

Heckert AB, Lucas SG (2000) Taxonomy, phylogeny, biostratigraphy, biochronology, paleobiogeography, and evolution of the Late Triassic Aetosauria (Archosauria:Crurotarsi). Zentralbl Geol Paläont I 1(11–12):1539–1587

Heckert AB, Lucas SG (2002) Lower Chinle Group (Upper Triassic: Carnian) stratigraphy in the Zuni Mountains, west-central New Mexico. New Mex Mus Nat Hist Sci Bull 21:51–72

Heckert AB, Lucas SG, Hunt AP, Harris JD (2001) A giant phytosaur (Reptilia: Archosauria) skull from the Redonda Formation (Upper Triassic: Apachean) of east-central New Mexico. New Mex Geol Soc Guideb 52:171–178

Heckert AB, Lucas SG, Hunt AP (2005) Triassic vertebrate fossils in Arizona. New Mex Mus Nat Hist Sci Bull 29:16–44

Heckert AB, Spielmann JA, Lucas SG, Hunt AP (2007) Biostratigraphic utility of the Upper Triassic aetosaur *Tecovasuchus* (Archosauria: Stagonolepididae), an index taxon of St. Johnsian (Adamanian:Late Carnian) time. New Mex Mus Nat Hist Sci Bull 41:51–57

Heckert AB, Lucas SG, Rinehart LF, Hunt AP (2008) A new genus and species of sphenodontian from the Ghost Ranch *Coelophysis* quarry (Upper Triassic: Apachean), Rock Point Formation, New Mexico, USA. Palaeontology 51:827–845

Heckert AB, Mitchell JS, Schneider VP, Olsen PE (2012) Diverse new microvertebrate assemblage from the Upper Triassic Cumnock Formation, Sanford subbasin, North Carolian, USA. J Paleontol 86:368–390

Hone DWE, Benton MJ (2008) Contrasting supertree and total-evidence methods: the origin of pterosaurs. Zitteliana B28:35–60

Hornung T, Brandner R, Krystyn L, Joachimski MM, Keim L (2007) Multistratigraphic constraints on the NW Tethyan "Carnian crisis". New Mex Mus Nat Hist Sci Bull 41:59–67

Hsiou A, Abdala F, Arcucci A (2002) Novo registro de proterocampsideo (Reptilia, Archosauriformes) do Triasico medio-superior do Brasil. Revista Brasil Paleontol 5:48–55

Huber P, Lucas SG, Hunt AP (1993a) Revised age and correlation of the Upper Triassic Chatham Group (Deep River basin, Newark Supergroup), North Carolina. Southeast Geol 33:171–193

Huber P, Lucas SG, Hunt AP (1993b) Vertebrate biochronology of the Newark Supergroup Triassic, eastern North America. New Mex Mus Nat Hist Sci Bull 3:179–186
Huber P, Lucas SG, Hunt AP (1993c) Late Triassic fish assemblages of the North American Western Interior and their biochronologic significance. Mus North Ariz Bull 59:51–66
Hungerbühler A (1998) Taphonomy of the prosauropod dinosaur *Sellosaurus*, and its implications for carnivore faunas and feeding habits in the Late Triassic. Palaeogeogr Palaeoclimatol Palaeoecol 143:1–29
Hungerbühler A (2001) The status and phylogenetic relationships of "*Zanclodon*" *arenaceus*: the earliest known phytosaur? Paläont Zeitschr 75:97–112
Hungerbühler A (2002) The Late Triassic phytosaur *Mystriosuchus westphali*, with a revision of the genus. Palaeontology 45:377–418
Hunt AP (1989) Cranial morphology and ecology among phytosaurs. In: Lucas SG, Hunt AP (eds) Dawn of the age of dinosaurs in the American Southwest. New Mexico Museum of Natural History, Albuquerque, pp 349–354
Hunt AP (1991) The early diversification of dinosaurs in the Late Triassic. Mod Geol 16:43–60
Hunt AP (1993) Revision of the Metoposauridae (Amphibia: Temnospondyli) and description of a new genus from western North America. Mus North Ariz Bull 59:67–97
Hunt AP (1994) Vertebrate paleontology and biostratigraphy of the Bull Canyon Formation (Chinle Group: Norian), east-central New Mexico with revisions of the families Metoposauridae (Amphibia: Temnospondyli) and Parasuchidae (Reptilia: Archosauria). PhD dissertation, University of New Mexico, Albuquerque
Hunt AP (2001) The vertebrate fauna, biostratigraphy and biochronology of the type Revueltian land-vertebrate faunachron, Bull Canyon Formation (Upper Triassic), east-central New Mexico. New Mex Geol Soc Guideb 52:123–151
Hunt AP, Lucas SG (1990) Re-evaluation of "Typothorax" meadei, a Late Triassic aetosaur from the United States. Paläont Zeitschr 64:317–328
Hunt AP, Lucas SG (1991) A new rhynchosaur from the Upper Triassic of West Texas, and the biochronology of Late Triassic rhynchosaurs. Palaeontology 34:927–938
Hunt AP, Lucas SG (1993a) Triassic vertebrate paleontology and biochronology of New Mexico. New Mex Mus Nat Hist Sci Bull 2:49–60
Hunt AP, Lucas SG (1993b) A new phytosaur (Reptilia: Archosauria) genus from the uppermost Triassic of the western United States and its biochronologic significance. New Mex Mus Nat Hist Sci Bull 3:193–196
Hunt AP, Lucas SG (1994) Ornithischian dinosaurs from the Upper Triassic of the United States. In: Fraser NC, Sues HD (eds) In the shadow of the dinosaurs. Cambridge University Press, New York, pp 227–241
Hunt AP, Lucas SG (1997) Stratigraphy, paleontology and biochronology of the Upper Triassic Chinle Group in east-central New Mexico. Southwest Paleont Symp Proc 1:25–40
Hunt AP, Lucas SG (2007) The Triassic tetrapod track record: ichnofaunas, ichnofacies and biochronology. New Mex Mus Nat Hist Sci Bull 41:78–78
Hunt AP, Lucas SG, Heckert AB (2002) A Revueltian (Norian) phytosaur from the Sonsela Member of the Petrified Forest Formation (Chinle Group: Upper Triassic), Petrified Forest National Park, Arizona. New Mex Mus Nat Hist Sci Bull 21:165–169
Hunt AP, Lucas SG, Heckert AB (2005) Definition and correlation of the Lamyan: a new biochronological unit for the nonmarine late Carnian (Late Triassic). New Mex Geol Soc Guideb 56:357–366
Hunt AP, Lucas SG, Klein H (2017) Late Triassic nonmarine vertebrate and invertebrate trace fossils and the pattern of the Phanerozoic record of vertebrate trace fossils. In: Tanner LH (ed) The Late Triassic world: earth in a time of transition. Topics in geobiology. Springer, New York (this volume)
Ivakhhnenko MF, Golubev VK, Gubin YM, Kalandadze NN, Novikov IV, Sennikov AG, Rautian AS (1997) Permskiye i Triasoviye tetrapodi Vostochnoi Evropi [Permian and Triassic tetrapods of Eastern Europe]. GEOS, Moscow

Ivakhnenko MF (1978) Urodelans from the Triassic and Jurassic of Soviet Central Asia. Paleont J 1978(3):84–89. [in Russian]
Jadoul F (1985) Stratigrafia e paleogeografia del Norico nelle Prealpi Bergamasche occidentali. Riv Ital Paleont Stratig 91:479–512
Jadoul F, Masetti D, Cirilli S, Berra S, Claps N, Frisia S (1994) Norian-Rhaetian stratigraphy and paleogeographic evolution of the Lombardy basin (Bergamasc Alps). In: 15th Internat Assoc Sedimentol Reg Meet, April 1994, Ischia, Italy, Field Excurs B1, Salermo, Italy, pp 5–38
Jain SL, Roychowdhury T (1987) Fossil vertebrates from the Godavari Valley (India) and their stratigraphic correlation. In: McKenzie GD (ed) Gondwana Six: stratigraphy, sedimentology and paleontology. Am Geophys Un Monogr 41: 219–228
Jain SL, Robinson PL, Roychowdhury TK (1964) A new vertebrate fauna from the Triassic of Deccan, India. J Geol Soc Lond 120:115–124
Jalil N (1999) Continental Permian and Triassic vertebrate localities from Algeria and Morocco and their stratigraphical correlations. J Afr Earth Sci 29:219–226
Jenkins FA, Shubin NH, Amaral WW, Gatesy SM, Schaff CR, Clemmensen LB, Downs WR, Davidson AR, Bonde N, Osbaeck F (1994) Late Triassic vertebrates and depositional environments of the Fleming Fjord Formation, Jameson Land, east Greenland. Meddel Grønl 32:1–25
Jenkins FA Jr, Gatesy SM, Shubin NH, Amaral WW (1997) Haramiyids and Triassic mammalian evolution. Nature 385:715–718
Jenkins FA Jr, Shubin NH, Gatesy SM, Padian K (2001) A diminutive pterosaur (Pterosauria: Eudimorphodontidae) from the Greenland Triassic. Bull Mus Comp Zool 156:151–170
Jenkins FA Jr, Shubin NH, Gatesy SM, Warren A (2008) *Gerrothorax pulcherrimus* from the Upper Triassic Fleming Fjord Formation of east Greenland and a reassessment of head lifting in temnospondyl feeding. J Vert Paleont 28:935–950
Joyce WG (2017) A review of the fossil record of basal Mesozoic turtles. Bull Peab Mus Nat Hist 58:65–113
Joyce WG, Lucas SG, Scheyer TM, Heckert AB, Hunt AP (2009) A thin-shelled reptile from the Late Triassic of North America and the origin of the turtle shell. Proc R Soc B276:507–513
Kammerer CF, Flynn JJ, Ranovharimanana L, Wyss AR (2010) The first record of a probainognathian (Cynodontia: Chiniquodontidae) from the Triassic of Madagascar. J Vert Paleont 30:1889–1894
Kammerer CF, Butler RJ, Bandyopadhyay S, Stocker MR (2016) Relationships of the Indian phytosaur *Parasuchus hislopi* Lydekker, 1885. Papers Palaeontol 2:1–23
Kaye FT, Padian K (1994) Microvertebrates from the *Placerias* quarry: a window on Late Triassic vertebrate diversity in the American Southwest. In: Fraser NC, Sues HD (eds) The shadow of the dinosaurs. Cambridge University Press, New York, pp 171–196
Kear BP, Poropat SF, Bazzi M (2016) Late Triassic capitosaurian remains from Svalbard and the palaeobiogeographical context of Scandinavian Arctic temnospondyls. In: Kear PB, Lindgren J, Hurm JH, Milàn J, Vajda V (eds) Mesozoic biotas of Scandinavia and its Arctic territories. Geol Soc Lond Spec Publ 434: 113–126
Kent DV, Malnis PS, Colombi CE, Alcober SA, Martinez RN (2014) Age constraints on the dispersal of dinosaurs in the Late Triassic from magnetochronology of the Los Colorados Formation (Argentina). Proc Natl Acad Sci U S A 11:7958–7963
Kent DV, Olsen PE, Muttoni G (2017) Astrochronostratigraphic polarity time scale (ATS) for the Late Triassic and Early Jurassic from continental sediments and correlation with standard marine stages. Earth-Sci Rev 166:153–180
Keyser AW (1973a) A new Triassic vertebrate fauna from South West Africa. South Afr J Sci 69:113–115
Keyser AW (1973b) A new Triassic vertebrate fauna from South West Africa. Palaeont Afr 16:1–15
Keyser AW (1978) A new bauriamorph from the Omongonde Formation (Middle Triassic) of South West Africa. Palaeont Afr 21:177
Kielan-Jaworowska Z, Cifelli RL, Luo Z (2004) Mammals from the age of dinosaurs. Columbia University Press, New York

Kimmig J, Arp G (2010) Phytosaur remains from the Norian Arnstadt Formation (Leine Valley, Germany), with reference to European phytosaur habitats. Palaeodiversity 3:215–224
Kimmig J, Spielmann JA (2011) Biologic factors influencing phytosaur (Archosauria: Phytosauridae) taxonomy. New Mex Mus Nat Hist Sci Bull 53:289–294
Kirby RE (1989) Late Triassic vertebrate localities of the Owl Rock Member (Chinle Formation) in the Ward Terrace area of northern Arizona. In: Lucas SG, Hunt AP (eds) Dawn of the age of dinosaurs in the American Southwest. New Mex Mus Nat Hist, Albuquerque, pp 12–28
Kirby RE (1991) A vertebrate fauna from the Upper Triassic Owl Rock Member of the Chinle Formation in northern Arizona. MS thesis, Northern Arizona University, Flagstaff
Kirby RE (1993) Relationships of Late Triassic basin evolution and faunal replacement events in the southwestern United States: Perspectives from the upper part of the Chinle Formation in northern Arizona. New Mex Mus Nat Hist Sci Bull 3:233–242
Kischlat E, Lucas SG (2003) A phytosaur from the Upper Triassic of Brazil. J Vert Paleont 23:464–467
Kitching JW, Raath MA (1984) Fossils from the Elliot and Clarens Formations (Karoo sequence) of the northern Cape, Orange Free State, and Lesotho, and a suggested biozonation based on tetrapods. Palaeont Afr 25:111–125
Klein H, Lucas SG (2010a) Tetrapod footprints—their use in biostratigraphy and biochronology of the Triassic. In: Lucas SG (ed) The Triassic timescale. Geol Soc Lond Spec Publ 334: 219–446
Klein H, Lucas SG (2010b) The Triassic footprint record of crocodylomorphs—a critical re-evaluation. New Mex Mus Nat Hist Sci Bull 51:55–60
Klein H, Lucas SG (2015) Evolution of the semi-aquatic lifestyle in archosaurs—evidence from the tetrapod footprint record. Geol Assoc Canada Misc Pub 9:105–111
Klein H, Niedzwiedźki G (2012) Revision of the Lower Triassic tetrapod ichnofauna from Wióry, Holy Cross Mountains, Poland. New Mex Mus Nat Hist Sci Bull 56:1–62
Kohút M, Hofmann M, Havrila M, Linnemann U, Havrila J (2017) Tracking an upper limit of the "Carnian crisis" and/or Carnian Stage in the Western Carpathians (Slovakia). Int J Earth Sci. doi: 10.10007/s00531-017-1491-8
Kozur HW, Bachmann GH (2005) Correlation of the Germanic Triassic with the international scale. Albertiana 32:21–35
Kozur HW, Bachmann GH (2008) Updated correlation of the Germanic Triassic with the Tethyan scale and assigned numeric ages. Berichte GeolBundesanstalt 76:53–58
Kozur HW, Weems RE (2005) Conchostracan evidence for a late Rhaetian to early Hettangian age for the CAMP volcanic event in the Newark Supergroup, and a Sevatian (late Norian) age for the immediately underlying beds. Hall Jahrb Geowissen B27:21–51
Kozur HW, Weems RE (2007) Upper Triassic conchostracan biostratigraphy of the continental rift basins of eastern North America: its importance for correlating Newark Supergroup events with the Germanic basin and the international geologic timescale. New Mex Mus Nat Hist Sci Bull 41:137–188
Kozur HW, Weems RE (2010) The biostratigraphic importance of conchostracans in the continental Triassic of the northern hemisphere. In: Lucas SG (ed) The Triassic timescale. Geol Soc Lond Spec Publ 334: 315–417
Krystyn L, Boquerel H, Kuerschner W, Richoz S, Gallet Y (2007a) Proposal for a candidate GSSP for the base of the Rhaetian stage. New Mex Mus Nat Hist Sci Bull 41:189–199
Krystyn L, Richoz S, Gallet Y, Boquerel H, Kurschner W, Spötl C (2007b) Updated bio- and magnetostratigraphy from Steinbergkogel (Austria), candidate GSSP for the base of the Rhaetian stage. Albertiana 36:164–173
Kutty TS (1969) Some contributions to the stratigraphy of the upper Gondwana formations of the Pranhita-Godavari Valley, central India. J Geol Soc India 10:33–48
Kutty TS, Roychowdhury T (1970) The Gondwana sequence of Pranhita-Godavari Valley, India, and its vertebrate faunas. In: Second Gond Symp Proc Pap, pp 303–308
Kutty TS, Sengupta DP (1989) The Late Triassic formations of the Pranhita-Godavari Valley and their vertebrate faunal succession—a reappraisal. Indian J Earth Sci 16:189–206

Kutty TS, Jain SL, Roychowdhury T (1988) Gondwana sequence of the northern Pranhita-Godavari Valley: its stratigraphy and vertebrate faunas. Palaeobotanist 36:263–282
Langer MC (2005a) Studies on continental late Triassic tetrapod biochronology. I. The type locality of *Saturnalia tupiniquim* and the faunal succession in South Brazil. J S Am Earth Sci 19:205–218
Langer MC (2005b) Studies on continental late Triassic tetrapod biochronology. II. The Ischigualastian and a Carnian global correlation. J S Am Earth Sci 19:219–239
Langer MC (2014) The origins of Dinosauria: much ado about nothing. Palaeontology 2014:1–10
Langer MC, Ferigolo J, Schultz CL (2000) Heterochrony and tooth evolution in hyperodapedontine rhynchosaurs (Reptila, Diapsida). Lethaia 33:119–128
Langer MC, Ribeiro AM, Schultz CL, Ferigolo J (2007) The continental tetrapod-bearing Triassic of southern Brazil. New Mex Mus Nat Hist Sci Bull 41:201–218
Langer MC, Ezcurra M, Bittencourt JS, Novas F (2009) The origin and early evolution of dinosaurs. Biol Rev 85:55–110
Lea I (1851) Remarks on the bones of a fossil reptilian quadruped. Proc Acad Nat Sci Phil 5:171–172
Leal LA, Azevedo SK, Kellner AW, Da Rosa AS (2003) A new early dinosaur (Sauropodomorpha) from the Caturrita Formation (Late Triassic), Paraná basin, Brazil. Zootaxa 690:1–24
Li C, Wu X, Rieppel O, Wang L, Zhao L (2008) An ancestral turtle from the Late Triassic of southwestern China. Nature 456:491–501
Lichtig AJ, Lucas SG, Klein H, Lovelace DM (2017) Triassic turtle tracks and the origin of turtles. Hist Biol. https://doi.org/10.1080/08912963.2017.1339037
Liu J, Abdala FA (2014) Phylogeny and taxonomy of the Traversodontidae. In: Kammerer CF, Angielczyk KD, Fröbisch J (eds) Early evolutionary history of the Synapsida. Springer, Dordrecht, pp 255–279
Lockley MG, Lucas SG, Milan J, Harris JD, Avanzini M, Foster JR, Spielmann JA (2010) The fossil record of crocodilian tracks and traces: an overview. New Mex Mus Nat Hist Sci Bull 51:1–13
Long RA, Murry PA (1995) Late Triassic (Carnian and Norian) tetrapods from the southwestern United States. New Mex Mus Nat Hist Sci Bull 4:1–254
Lovelace DM, Lovelace SD (2012) Paleoenvironments and paleoecology of a Lower Triassic invertebrate and vertebrate ichnoassemblage from the Red Peak Formation (Chugwater Group), central Wyoming. PALAIOS 27:636–657
Lucas SG (1992) Extinction and the definition of the Class Mammalia. Syst Biol 41:370–371
Lucas SG (1993) The Chinle Group: revised stratigraphy and chronology of Upper Triassic nonmarine strata in the western United States. Mus North Ariz Bull 59:27–50
Lucas SG (1994) Triassic tetrapod extinctions and the compiled correlation effect. Can Soc Petrol Geol Mem 17:869–875
Lucas SG (1997) Upper Triassic Chinle Group, western United States: a nonmarine standard for Late Triassic time. In: Dickins JM et al (eds) Late Paleozoic and early Mesozoic Circum-Pacific events and their global correlation. Cambridge University Press, Cambridge, pp 209–228
Lucas SG (1998) Global Triassic tetrapod biostratigraphy and biochronology. Palaeogeogr Palaeoclimatol Palaeoecol 143:347–384
Lucas SG (1999) Tetrapod-based correlation of the nonmarine Triassic. Zentralbl r Geol Paläont Teil I 7-8:497–521
Lucas SG (2002) A new dicynodont from the Triassic of Brazil and the tetrapod biochronology of the Brazilian Triassic. New Mex Mus Nat Hist Sci Bull 21:131–141
Lucas SG (2007) Tetrapod footprint biostratigraphy and biochronology. Ichnos 14:5–38
Lucas SG (2008) Global Jurassic tetrapod biochronology. Volum Jura 6:99–108
Lucas SG (2010) The Triassic timescale based on nonmarine tetrapod biostratigraphy and biochronology. In: Lucas SG (ed) The Triassic timescale. Geol Soc Lond Spec Publ 334: 447–500
Lucas SG (2015) Age and correlation of Late Triassic tetrapods from southern Poland. Ann Soc Geol Polon 85:627–635

Lucas SG (2017a) Permian tetrapod extinction events. Earth-Sci Rev 170:31–60
Lucas SG (2017b) The Late Triassic timescale. In: Tanner LH (ed) The Late Triassic world: earth in a time of transition. Topics in geobiology. Springer, New York (this volume)
Lucas SG, Hancox J (2001) Tetrapod-based correlation of the nonmarine Upper Triassic of Southern Africa. Albertiana 25:5–9
Lucas SG, Harris SK (1996) Taxonomic and biochronological significance of specimens of the Triassic dicynodont *Dinodontosaurus* Romer, 1943 in the Tübingen collection. Paläont Zeitschr 70:603–622
Lucas SG, Heckert AB (2000) Biochronological significance of Triassic nonmarine tetrapod records from marine strata. Albertiana 24:27–32
Lucas SG, Heckert AB (2001) The aetosaur *Stagonolepis* from the Upper Triassic of Brazil and its biochronological significance. Neues Jahrb Geol Paläont Monatsh 2001:719–732
Lucas SG, Heckert AB (2011) Late Triassic aetosaurs as the trackmaker of the tetrapod footprint ichnotaxon *Brachychirotherium*. Ichnos 18:197–208
Lucas SG, Huber P (2003) Vertebrate biostratigraphy and biochronology of the nonmarine Triassic. In: LeTourneau PM, Olsen PE (eds) The great rift valleys of Pangea in eastern North America, vol 2. Sedimentology and paleontology. Columbia University Press, New York, pp 143–191
Lucas SG, Hunt AP (1992) Triassic stratigraphy and paleontology, Chama basin and adjacent areas, north-central New Mexico. New Mex Geol Soc Guideb 43:151–172
Lucas SG, Hunt AP (1993a) Tetrapod biochronology of the Chinle Group (Upper Triassic), western United States. New Mex Mus Nat Hist Sci Bull 3:327–329
Lucas SG, Hunt AP (1993b) A review of Triassic labyrinthodont amphibians from China. Geobios 26:121–128
Lucas SG, Hunt AP (1994) The chronology and paleobiogeography of mammalian origins. In: Fraser NC, Sues HD (eds) The shadow of the dinosaurs. Cambridge University Press, New York, pp 335–351
Lucas SG, Luo Z (1993) *Adelobasileus* from the Upper Triassic of West Texas: the oldest mammal. J Vert Paleont 13:309–334
Lucas SG, Spielmann JA (2013) Magnetostratigraphy of the Upper Triassic Chinle Group in New Mexico: an appraisal of 40 years of analysis. New Mex Mus Nat Hist Sci Bull 61:375–381
Lucas SG, Sullivan RM (1997) Fossils provide a Pennsylvania standard for part of Late Triassic time. Penn Geol 27(4):8–14
Lucas SG, Sullivan RM (2006) Tetrapod footprints from the Upper Triassic Passaic Formation near Graterford, Montgomery County, Pennsylvania. New Mex Mus Nat Hist Sci Bull 37:251–256
Lucas SG, Tanner LH (2007a) Tetrapod biostratigraphy and biochronology of the Triassic-Jurassic transition on the southern Colorado Plateau, USA. Palaeogeogr Palaeoclimatol Palaeoecol 244:242–256
Lucas SG, Tanner LH (2007b) The nonmarine Triassic-Jurassic boundary in the Newark Supergroup of eastern North America. Earth-Sci Rev 84:1–20
Lucas SG, Tanner LH (2015) End-Triassic nonmarine biotic events. J Palaeogeogr 4:331–348
Lucas SG, Wild R (1995) A Middle Triassic dicynodont from Germany and the biochronology of Triassic dicynodonts. Stuttgart Beitr Naturk 220:1–16
Lucas SG, Hunt AP, Long RA (1992) The oldest dinosaurs. Naturwiss 79:171–172
Lucas SG, Hunt AP, Kahle RW (1993) Late Triassic vertebrates from the Dockum Formation near Otis Chalk, Howard County, Texas. New Mex Geol Soc Guideb 44:237–244
Lucas SG, Anderson OJ, Hunt AP (1994) Triassic stratigraphy and correlations, southern High Plains of New Mexico-Texas. New Mex Bur Mines Min Res Bull 150:105–126
Lucas SG, Heckert AB, Hunt AP (1997) Stratigraphy and biochronology of the Late Triassic *Placerias* quarry, eastern Arizona (U.S.A.) Neues Jahrb Geol Paläont Abhand 203:23–46
Lucas SG, Wild R, Hunt AP (1998) *Dyoplax* O. FRAAS, a Triassic sphenosuchian from Germany. Stuttg Beitr Naturk B263:1–13
Lucas SG, Heckert B, Fraser NC, Huber P (1999) *Aetosaurus* from the Upper Triassic of Great Britain and its biochronological significance. Neues Jahrb Geol Paläont Monats 1999:568–576

Lucas SG, Heckert AB, Hunt AP (2000) Probable turtle from the Upper Triassic of east-central New Mexico. Neues Jahrb Geol Palaeont Monats 5:287–300
Lucas SG, Heckert AB, Hunt AP (2001) Triassic stratigraphy, biostratigraphy and correlation in east-central New Mexico. New Mex Geol Soc Guideb 52:85–101
Lucas SG, Heckert AB, Hotton N III (2002) The rhynchosaur *Hyperodapedon* from the Upper Triassic of Wyoming and its global biochronological significance. New Mex Mus Nat Hist Sci Bull 21:149–156
Lucas SG, Zeigler KE, Heckert AB, Hunt AP (2003) Upper Triassic stratigraphy and biostratigraphy, Chama basin, north-central New Mexico. New Mex Mus Nat Hist Sci Bull 24:15–39
Lucas SG, Tanner LH, Heckert AB (2005) Tetrapod biostratigraphy and biochronology across the Triassic-Jurassic boundary in northeastern Arizona. New Mex Mus Nat Hist Sci 29:84–94
Lucas SG, Hunt AP, Heckert AB, Spielmann JA (2007a) Global Triassic tetrapod biostratigraphy and biochronology: 2007 status. New Mex Mus Nat Hist Sci Bull 41:229–240
Lucas SG, Spielmann JA, Hunt AP (2007b) Biochronological significance of Late Triassic tetrapods from Krasiejów, Poland. New Mex Mus Nat Hist Sci Bull 41:248–258
Lucas SG, Rinehart LF, Krainer K, Spielmann JA, Heckert AB (2010) Taphonomy of the Lamy amphibian quarry: a Late Triassic bonebed in New Mexico, USA. Palaeogeogr Palaeoclimatol Palaeoecol 298:388–398
Lucas SG, Tanner LH, Kozur HW, Weems RE, Heckert AB (2012) The Late Triassic timescale: age and correlation of the Carnian-Norian boundary. Earth-Sci Rev 114:1–18
Lucas SG, Spielmann JA, Hunt AP (2013) A new doswelliid archosauromorph from the Upper Triassic of West Texas. New Mex Mus Nat Hist Sci Bull 61:382–388
Lucas SG, Rinehart LF, Heckert AB, Hunt AP, Spielmann JA (2016) Rotten Hill: a Late Triassic bonebed in the Texas Panhandle, USA. New Mex Mus Nat Hist Sci Bull 72:1–97
Luo Z (2011) Transformation and diversification in early mammal evolution. Nature 450:1011–1019
Lyson TR, Bever GS, Bhullar BS, Joyce WG, Gauthier JA (2010) Transitional fossils and the origin of turtles. Biol Lett. rsbl.20100371
Lyson TR, Sperling EA, Heimberg AM, Gauthier JA, King BL, Peterson KJ (2012) MicroRNAs support a turtle+lizard clade. Biol Lett 8:104–107
Lyson TR, Bever GS, Scheyer TM, Hsiang AY, Gauthier JA (2013) Evolutionary origin of the turtle shell. Curr Biol 23:1113–1119
Lyson TR, Rubidge BS, Scheyer TM, de Queiroz K, Schachner ER, Smith RM, Bever GS (2016) Fossorial origin of the turtle shell. Curr Biol 26:1887–1894
Maisch MW, Kapitzke M (2010) A presumably marine phytosaur (Reptilia: Archosauria) from the pre-planorbis beds (Hettangian) of England. Neues Jahrb Geol Paläont Abhand 257:373–379
Mancuso AC, Gaetano LC, Leardi JM, Abdala F, Arcucci AB (2014) The Chañares Formation: a window to a Middle Triassic tetrapod community. Lethaia 47:242–265
Marsicano CA, Domnanovich NS, Mancuso AC (2007) Dinosaur origins: evidence from the footprint record. Hist Biol 19:83–91
Marsicano CA, Irmis RB, Mancuso AC, Mundil R, Chemale F (2016) The precise temporal calibration of dinosaur origins. Proc Natl Acad Sci U S A 113:509–513
Martínez RN, Apaldetti C, Alcober OA, Colombi CE, Sereno PC, Fernandez E, Malnis PS, Correa GA, Abelin D (2013) Vertebrate succession in the Ischigualasto Formation. J Vert Paleont Mem 12:10–20
McGhee GR Jr, Sheehan PM, Bottjer DJ, Droser ML (2004) Ecological ranking of Phanerozoic biodiversity crises: ecological and taxonomic severities are decoupled. Palaeogeogr Palaeoclimatol Palaeoecol 211:289–297
Mehl MG (1928) The Phytosauria of the Wyoming Triassic. Denison Univ Bull J Sci Lab 23:141–172
Melo TP, Abadala F, Soares MB (2015) The Malagasy cynodont *Menadon besairei* (Cynodontia: Traversodontidae) in the Middle-Upper Triassic of Brazil. J Vert Paleont. https://doi.org/10.1080/027724634.2014.1002562

Miao D (1991) On the origins of mammals. In: Schultze H-P, Trueb L (eds) Origins of the higher groups of tetrapods: controversy and consensus. Comstock Publishing Associates, London, pp 579–597

Mietto P, Manfrin S, Preto N, Rigo M, Roghi G, Furin S, Gianolla P, Posenato R, Muttoni G, Nicora A, Buratti N, Cirilli S, Spitl C, Ramezani J, Bowring SA (2012) The global boundary stratotype section and point (GSSP) of the Carnian stage (Late Triassic) at Prati di Stuores/Stuores Wiesen section (southern Alps, NE Italy). Episodes 35:414–430

Milner AR (1990) The radiations of temnospondyl amphibians. In: Taylor PD, Larwood GP (eds) Major evolutionary radiations. System Assoc Spec Vol 42: 321–349

Milner AR (1993) Amphibian-grade Tetrapoda. In: Benton MJ (ed) The fossil record. Chapman and Hall, London, pp 665–679

Montefeltro FC, Langer MC, Schultz CL (2010) Cranial anatomy of a new genus of hyperodapedontine rhynchosaur (Diapsida, Archosauromorpha) from the Upper Triassic of southern Brazil. Earth Environ Sci Trans Royal Soc Edinb 101:27–52

Montefeltro FC, Bittencourt JS, Langer MC, Schultz CL (2013) Postcranial anatomy of the hyperodapedontine rhynchosaur *Teyumbatia sulcognathus* (Azevedo and Schultz, 1987) from the Late Triassic of southern Brazil. J Vert Paleont 33:67–84

Mukherjee D, Ray S, Chandra S, Pal S, Bandyopadhyay S (2012) Upper Gondwana succession of the Rewa basin, India: understanding the interrelationship of lithologic and stratigraphic variables. J Geol Soc India 79:563–575

Mundil R, Pálfy J, Renne PR, Brack P (2010) The Triassic timescale: a review of geochronological constraints. In: Lucas, SG (ed) The Triassic timescale. Geol Soc Lond Spec Publ 334: 41–60

Murry PA (1986) Vertebrate paleontology of the Dockum Group, western Texas and eastern New Mexico. In: Padian K (ed) The beginning of the age of dinosaurs. Cambridge University Press, Cambridge, pp 109–137

Murry PA (1989) Geology and paleontology of the Dockum Formation (Upper Triassic), West Texas and eastern New Mexico. In: Lucas SG, Hunt AP (eds) Dawn of the age of dinosaurs in the American Southwest. New Mex Mus Nat Hist, Albuquerque, pp 102–144

Murry PA, Long RA (1989) Geology and paleontology of the Chinle Formation, Petrified Forest National Park and vicinity, Arizona and a discussion of vertebrate fossils of the southwestern Upper Triassic. In: Lucas SG, Hunt AP (eds) Dawn of the age of dinosaurs in the American Southwest. New Mex Mus Nat Hist, Albuquerque, pp 29–64

Muttoni G, Kent DV, Olsen PE, DiStefano P, Lowrie W, Bernasconi SM, Hernández FM (2004) Tethyan magnetostratigraphy from Pizza Mondelo (Sicily) and correlation to the Late Triassic Newark astrochronological polarity time scale. Geol Soc Am Bull 116:1043–1058

Muttoni G, Kent DV, Jadoul F, Olsen PE, Rigo M, Galli MT, Nicora A (2010) Rhaetian magnetobiostratigraphy from the Southern Alps (Italy). Constraints on Triassic chronology. Palaeogeogr Palaeoclimatol Palaeoecol 285:1–16

Nesbitt SJ (2007) The anatomy of *Effigia okeeffeae* (Archosauria, Suchia), theropod-like convergence, and the distribution of related taxa. Bull Am Mus Nat Hist 302:1–84

Nesbitt SJ, Ezcurra MD (2015) The early fossil record of dinosaurs in North America: a new neotheropod from the base of the Upper Triassic Dockum Group of Texas. Acta Palaeont Polon 60:513–526

Nesbitt SJ, Stocker MR (2008) The vertebrate assemblage of the Late Triassic Canjilon quarry (northern New Mexico, USA), and the importance of apomorphy-based assemblage comparisons. J Vert Paleont 28:1063–1072

Niedźwiedzki G, Sulej T, Dzik J (2012) A large predatory archosaur from the Late Triassic of Poland. Acta Palaeont Polon 57:267–276

Niedźwiedzki G, Brusatte SL, Sulej T, Butler RJ (2014) Basal dinosauriform and theropod dinosaurs from the mid–late Norian (Late Triassic) of Poland: implications for Triassic dinosaur evolution and distribution. Palaeontology 57:1121–1142

Ogg JG (2012) Triassic. In: Gradstein FM, Ogg JG, Schmitz MD, Ogg GM (eds) The geologic time scale 2012. Elsevier, Amsterdam, pp 681–730

Ogg JG, Huang C, Hinnov L (2014) Triassic timescale status: a brief overview. Albertiana 41:3–30
Olsen PE (1980) A comparison of vertebrate assemblages from the Newark and Hartford basins (early Mesozoic, Newark Supergroup) of eastern North America. In: Jacobs LL (ed) Aspects of vertebrate history: essays in honor of Edwin Harris Colbert. Museum of Northern Arizona Press, Flagstaff, pp 35–53
Olsen PE (1988) Paleontology and paleoecology of the Newark Supergroup (early Mesozoic, eastern North America). In: Manspeizer W (ed) Triassic-Jurassic rifting: continental breakup and the origin of the Atlantic Ocean and passive margins, Part A. Elsevier, Amsterdam, pp 185–230
Olsen PE, Schlische RW, Gore PJW (1989) Tectonic, depositional and paleoecological history of early Mesozoic rift basins, eastern North America. In: American Geophysical Union Guidebook T351, International Geological Congress, Washington, DC
Orchard MJ (2010) Triassic conodonts and their role in stage boundary definition. In: Lucas SG (ed) The Triassic timescale. Geol Soc Lond Spec Publ 334: 139–161
Orchard MJ (2014) Conodonts from the Carnian-Norian boundary (Upper Triassic) of Black Bear Ridge, northeastern British Columbia, Canada. New Mex Mus Nat Hist Sci Bull 64:1–139
Ottone EG, Monti M, Marsicano CA, de la Fuente M, Naipauer M, Armstrong R, Mancuso AC (2014) A new Late Triassic age for the Puesto Viejo Group (San Rafael depocenter, Argentina): SHRIMP U-Pb zircon dating and biostratigraphic correlation across southern Gondwana. J S Am Earth Sci 56:186–199
Padian K (1984) The origin of the pterosaurs. In: Reif WE, Westphal F (eds) Third symposium on mesozoic terrestrial ecosystems, short papers. Attempto Verlag, Tübingen, pp 163–168
Parker WG, Ash SR, Irmis RB (2006) A century of research at Petrified Forest National Park 1906-2006. Mus North Ariz Bull 62
Parrish MJ (1991) A new specimen of an early crocodylomorph (cf. *Sphenosuchus* sp.) from the Upper Triassic Chinle Formation of Petrified Forest National Park. J Vert Paleont 11:198–212
Peyer K, Carter JG, Sues H-D, Novak SE, Olsen PE (2008) A new suchian archosaur from the Upper Triassic of North Carolina. J Vert Paleont 28:363–381
Philipp RP, Kloss HP, Schultz CL, Basei MAS, Horn BLD, Soares MB (2013) Provenência por U-Pb LA-ICP-MS em zircão detrítico e ipade de deposição da Formacão Santa Maria, Triassico da bacia do Paraná, RS: Evidências de estructuração do arco do Rio Grande. Anais do VIII Symp Internat Tectonics and XIV Simp Na Estud Tectón, Cuiabá, pp 154–157
Pickford M (1995) Karoo Supergroup palaeontology of Namibia and brief description of a thecodont from Omingonde. Palaeont Afr 32:51–66
Pinna G (1993) The Norian reptiles of northern Italy. Paleont Lombard Nuova Serie 2:115–124
Rage J-C, Roček Z (1989) Redescription of *Triadobatrachus massinoti* (Piveteau, 1936) an anuran amphibian from the Early Triassic. Palaeontograph Abt A 206:1–16
Rainforth EC (2003) Revision and re-evaluation of the Early Jurassic dinosaurian ichnogenus *Otozoum*. Palaeontology 46:803–838
Ramezani J, Hoke GD, Fastovsky DE, Bowring SA, Therrien F, Dworkin SI, Atchley SC, Nordt LC (2011) High-precision U-Pb zircon geochronology of the Late Triassic Chinle Formation, Petrified Forest National Park (Arizona, USA): temporal constraints on the early evolution of dinosaurs. Geol Soc Amer Bull 123:2142–2159
Ramezani J, Fastovsky DE, Bowring SA (2014) Revised chronostratigraphy of the lower Chinle Formation strata in Arizona and New Mexico (USA): high-precision U-Pb geochronological constraints on the Late Triassic evolution of dinosaurs. Am J Sci 314:981–1008
Ranovharimanana L, Kammerer CF, Flynn JJ, Wyss AR (2011) New material of *Dadadon isaloi* (Cynodontia, Traversodontidae) from the Triassic of Madagascar. J Vert Paleont 31:1292–1302
Raugust T, Lacerda M, Schultz CL (2013) The first occurrence of *Chanaresuchus bonapartei* Romer 1971 (Archosauriformes, Proterochampsia) of the Middle Triassic of Brazil from the *Santacruzodon* Assemblage Zone, Santa Maria Formation (Paraná basin). In: Nesbitt SJ, Desojo JB, Irmis RB (eds) Anatomy, phylogeny and paleobiology of early archosaurs and their kin. Geol Soc Lond Spec Publ 379: 303–318

Reichel M, Schultz CL, Soares MB (2009) A new traversodontid cynodont (Therapsida, Eucynodontia) from the Middle Triassic Santa Maria Formation of Rio Grande do Sul, Brazil. Palaeontology 52:229–250

Reig OA (1959) Primeros datos descríptivos sobre nuevos reptiles arcosaurios del Triásico de Ischigualasto (San Juan, Argentina). Rev Assoc Geol Argent 13:257–270

Reig OA (1961) Acerca de la posición sistemática de la familia Rauisuchidae y del género *Saurosuchus* (Reptilia, Thecodontia). Public Mus Cienc Natur Mar del Plata 1:73–114

Reig OA (1963) La presencia de dinosaurios saurisquios en los "Estratos de Ischigualasto" (Mesotriásico superior) de las provincias de San Juan y La Rioja (República Argentina). Ameghin 3:3–20

Renesto S (2006) A reappraisal of the diversity and biogeographic significance of the Norian (Late Triassic) reptiles from the Calcare di Zorzino. New Mex Mus Nat Hist Sci Bull 37:445–456

Renesto S, Spielmann JA, Lucas SG (2009) The oldest record of drepanosaurids (Reptilia, Diapsida) from the Late Triassic (Adamanian *Placerias* quarry, Arizona, USA) and the stratigraphic range of the Drepanosauridae. Neues Jahrb Geol Paläont Abhand 252:315–325

Renesto S, Spielmann JA, Lucas SG, Spagnoli G (2010) The taxonomy and paleobiology of the late Triassic (Carnian-Norian: Adamanian-Apachean) drepanosaurs (Diapsida: Archosauromorpha: Drepanosauromorpha). New Mex Mus Nat Hist Sci Bull 46:1–81

Rigo M, Bertinelli A, Concheri G, Gattolin G, Godfrey L, Katz ME, Maron M, Mietto P, Muttoni G, Sprovieri M, Stellin F, Zaffani M (2016) The Pignola-Abriola section (southern Apennines, Italy): a new GSSP candidate for the base of the Rhaetian stage. Lethaia 49:287–306

Rinehart LF, Lucas SG, Heckert AB, Spielmann JA, Celeskey MD (2009) The paleobiology of *Coelophysis bauri* (Cope) from the Upper Triassic (Apachean) Whitaker quarry, New Mexico, with detailed analysis of a single quarry block. New Mex Mus Nat Hist Sci Bull 45:1–260

Rogers RR, Swisher CC III, Sereno PC, Monett AM, Forster CA, Martinez RC (1993) The Ischigualasto tetrapod assemblage (Late Triassic, Argentina) and $^{40}Ar/^{39}Ar$ dating of dinosaur origins. Science 260:794–797

Romer AS (1966) Vertebrate paleontology, 3rd edn. Univ Chicago Press, Chicago

Romer AS (1973) The Chanares (Argentina) Triassic reptile fauna. XX. Summary. Breviora 413:1–20

Rougier GW, de la Fuente MS, Arcucci AB (1995) Late Triassic turtles from South America. Science 268:855–858

Rowe T (1988) Definition, diagnosis and origin of Mammalia. J Vert Paleont 8:241–264

Rowe T, Gauthier J (1992) Ancestry, paleontology, and definition of the name Mammalia. Syst Biol 41:372–378

Roychowdhury T (1965) A new metoposaurid amphibian from the Triassic Maleri Formation, central India. Phil Trans R Soc Lond B250:1–52

Rubert RR, Schultz CL (2004) Um novo horizonte de correlação para o Triássico superior do Rio Grande do Sul. Pesquisas 31:71–88

Ruffell A, Simms MJ, Wignall PB (2016) The Carnian humid episode of the Late Triassic: a review. Geol Mag 153(2):271–284

Rühle v. Lilienstern H (1939) Fährten und Spüren im Chirotheriem−Sandstein von Südthüringen. Fortschr Geol Paläont 12:293–387

Ruta M, Benton MJ (2008) Calibrated diversity, tree topology and the mother of mass extinctions: the lesson of temnospondyls. Palaeontology 51:1261–1288

Ruta M, Botha-Brink J, Mitchell SA, Benton MJ (2013) The radiation of cynodonts and the ground plan of mammalian morphological diversity. Proc R Soc B280:20131865

Schoch RR (1997) A new capitosaur amphibian from the Upper Lettenkeuper (Triassic: Ladinian) of Kupferzell (southern Germany). Neues Jahrb Geol Paläont Abhand 203:239–272

Schoch RR (2000) Biogeography and dispersal of stereospondyl amphibians. Neues Jahrb Geol Paläont Abhand 215:201–231

Schoch RR (2007) Osteology of the small archosaur *Aetosaurus* from the Upper Triassic of Germany. Neues Jahrb Geologie Paläont Abhand 246:1–35

Schoch RR (2008) The Capitosauria (Amphibia): characters, phylogeny, and stratigraphy. Palaeodiversity 1:189–226
Schoch RR (2014) Amphibian evolution: the life of early land vertebrates. Wiley Blackwell, Chichester
Schoch RR, Milner AR (2000) Stereospondyli. Encycl Paleoherp 3B:1–203
Schoch RR, Sues H-D (2015) A Middle Triassic stem-turtle and the evolution of the turtle body plan. Nature 523(7562):584–587. https://doi.org/10.1038/nature14472
Schoch RR, Werneburg R (1999) The Triassic labyrinthodonts from Germany. Zentralbl Geol Paläont Teil I 1998:629–650
Schoch R, Voigt S, Buchwitz M (2010) A chroniosuchid from the Triassic of Kyrgyzstan and analysis of chroniosuchian relationships. Zool J Linnean Soc 160:515–530
Schultz CL, Langer MC, Montefeltro FC (2016) A new rhynchosaur from south Brazil (Santa Maria Formation) and rhynchosaur diversity patterns across the Middle-Late Triassic boundary. Paläont Zeitschr 90(3):593–609. https://doi.org/10.1007/s12542-016-0307-7
Sengupta S (1970) Gondwana sedimentation around Bheemaram (Bhimaram), Pranhita-Godavari Valley, India. J Sediment Petrol 40:140–170
Sengupta DP (1995) Chigutisaurid temnospondyls from the Late Triassic of India and a review of the Family Chigutisauridae. Palaeontology 38:313–339
Sereno PC (1991) Basal archosaurs: phylogenetic relationships and functional implications. J Vert Paleont Mem 2:1–53
Sereno PC, Arcucci AB (1993) Dinosaurian precursors from the Middle Triassic of Argentina: *Lagerpeton chanarensis*. J Vert Paleont 13:385–399
Sereno PC, Arcucci AB (1994) Dinosaurian precursors from the Middle Triassic of Argentina: *Marasuchus lilloensis,* gen. nov. J Vert Paleont 14:53–73
Sereno PC, Wild R (1992) *Procompsognathus*: Theropod, "thecodont" or both ? J Vert Paleont 12:435–458
Sereno PC, Forster CA, Rogers RR, Monette AM (1993) Primitive dinosaur skeleton from Argentina and the early evolution of Dinosauria. Nature 361:64–66
Sharov AG (1970) A peculiar reptile from the Lower Triassic of Fergana. Paleont J 1970(1):127–130. [in Russian]
Sharov AG (1971) New flying reptiles from the Mesozoic of Kazakhstan and Kyrgyzstan. Dokl Akad Nauk SSSR 130:104–113. [in Russian]
Shishkin MA, Ochev VG, Tverdokhlebov VP (eds) (1995) Biostratigrafiya kontinentalnovo Triasa yuzhovo Priuralya [Biostratigraphy of the continental Triassic of the southern pre-Urals]. Nauka, Moscow. [in Russian]
Shishkin MA, Novikov IV, Gubin YM (2000a) Permian and Triassic temnospondyls from Russia. In: Benton MJ, Shishkin MA, Unwin DM, Kurochkin EN (eds) The age of dinosaurs in Russia and Mongolia. Cambridge University Press, Cambridge, pp 35–59
Shishkin MA, Ochev VG, Lozovskii VR, Novikov IV (2000b) Tetrapod biostratigraphy of the Triassic of eastern Europe. In: Benton MJ, Shishkin MA, Unwin DM, Kurochkin EN (eds) The age of dinosaurs in Russia and Mongolia. Cambridge University Press, Cambridge, pp 120–139
Shubin N, Sues H-D (1991) Biogeography of early Mesozoic continental tetrapods: patterns and implications. Paleobiology 17:214–230
Smith RMH, Swartt R (2002) Changing fluvial environments and vertebrate taphonomy in response to climatic drying in a mid-Triassic rift valley fill: the Omingonde Formation (Karoo Supergroup) of central Namibia. PALAIOS 17:249–267
Smith RMH, Rubidge B, van der Walt M (2012) Therapsid biodiversity patterns and paleoenvironments of the Karoo basin, South Africa. In: Chinsamy-Turan A (ed) Forerunners of mammals. Radiation. Histology. Biology. Indiana Univ Press, Bloomington, pp 31–62
Soares MB, Schultz CL, Horn BLD (2011) New information on *Riograndia guaibensis* Bonaparte, Ferigolo & Ribeiro, 2011 (Eucynodontia, Trithelodontidae) from the Late Triassic of southern Brazil: anatomical and biostratigraphic implications. Anais Acada Brasil Ciênc 83:329–354

Spielmann JA, Lucas SG (2012) Tetrapod fauna of the Upper Triassic Redonda Formation, east-central New Mexico: the characteristic assemblage of the Apachean land-vertebrate faunachron. New Mex Mus Nat Hist Sci Bull 55:1–119

Spielmann JA, Hunt AP, Lucas SG, Heckert AB (2006a) Revision of *Redondasuchus* (Archosauria: Aetosauria) from the Upper Triassic Redonda Formation, New Mexico, with description of a new species. New Mex Mus Nat Hist Sci Bull 37:583–587

Spielmann JA, Lucas SG, Hunt AP (2006b) The vertebrate macrofauna of the Upper Triassic (Apachean) Redonda Formation, east-central New Mexico. New Mex Mus Nat Hist Sci Bull 37:502–509

Spielmann JA, Lucas SG, Hunt AP, Heckert AB (2006c) Reinterpretation of the holotype of *Malerisaurus langstoni*, a diapsid reptile from the Upper Triassic Chinle Group of West Texas. New Mex Mus Nat Hist Sci Bull 37:543–547

Spielmann JA, Lucas SG, Heckert AB (2007) Tetrapod fauna of the Upper Triassic (Revueltian) Owl Rock Formation, Chinle Group, Arizona. New Mex Mus Nat Hist Sci Bull 41:371–383

Spielmann JA, Lucas SG, Rinehart LF, Heckert AB (2008) The Late Triassic archosauromorph *Trilophosaurus*. New Mex Mus Nat Hist Sci Bull 43:1–177

Spielmann JA, Lucas SG, Hunt AP (2013) The first Norian (Revueltian) rhynchosaur: Bull Canyon Formation, New Mexico, U.S.A. New Mex Mus Nat Hist Sci Bull 61:562–565

Sprinkle DA, Kowallis BJ, Jensen PH (2011) Correlation and age of the Nugget Sandstone and Glen Canyon Group, Utah. Utah Geol Assoc Publ 40:131–149

Stocker MR (2012) A new taxonomic arrangement for *Paleorhinus scurriensis*. Earth Environ Trans R Soc Edinb 103:251–263

Stocker MR, Butler RJ (2013) Phytosauria. In: Nesbitt SJ, Desojo JB, Irmis RB (eds) Anatomy, phylogeny and palaeobiology of early archosaurs and their kin. Geol Soc Lond Spec Publ 379: 91–117

Stocker MR, Zhao L, Nesbitt SJ, Wu X, Li C (2017) A short-snouted, Middle Triassic phytosaur and its implications for the morphological evolution and biogeography of Phytosauria. Nat Sci Rep 7:46028. https://doi.org/10.1038/srep46028

Sues H-D (1992) A remarkable new armored archosaur from the Upper Triassic of Virginia. J Vert Paleont 12:142–149

Sues H-D, Baird D (1993) A skull of a sphenodontian lepidosaur from the New Haven Arkose (Upper Triassic: Norian) of Connecticut. J Vert Paleont 13:370–372

Sues H-D, Fraser NC (2010) Triassic life on land: the great transition. Columbia University Press, New York

Sues H-D, Schoch RR (2013) Anatomy and phylogenetic relationships of *Calamops paludosus* (Temnospondyli, Stereospondyli) from the Triassic of the Newark basin, Pennsylvania. J Vert Paleont 35:1061–1070

Sues H-D, Olsen PE, Kroehler PA (1994) Small tetrapods from the Upper Triassic of the Richmond basin (Newark Supergroup), Virginia. In: Fraser NC, Sues H-D (eds) In the shadow of the dinosaurs. Cambridge University Press, New York, pp 161–170

Sues H-D, Baird D, Olsen PE (1997) Procolophonidae (Amniota: Parareptilia) from the Upper Triassic of Nova Scotia, Canada. J Vert Paleont 17(3):79A

Sues H-D, Olsen PE, Carter JG (1999) A Late Triassic traversodont cynodont from the Newark Supergroup of North Carolina. J Vert Paleont 19:351–354

Sues HD, Olsen PE, Carter JG, Scott DM (2003) A new crocodylomorph archosaur from the Upper Triassic of North Carolina. J Vert Paleont 23:329–343

Sues HD, Nesbitt SJ, Berman DS, Henrici AC (2011) A late-surviving basal theropod dinosaur from the latest Triassic of North America. Proc Biol Sci 278(1723):3459–3464

Sulej T (2002) Species discrimination of the Late Triassic temnospondyl amphibian *Metoposaurus diagnosticus*. Acta Palaeont Polon 47:535–546

Sulej T (2005) A new rauisuchian reptile (Diapsida: Archosauria) from the Late Triassic of Poland. J Vert Paleont 225:78–86

Sulej T (2007) Osteology, variability and evolution of *Metoposaurus*, a temnospondyl from the Late Triassic of Poland. Palaeont Polon 64:29–139
Sulej T (2010) The skull of an Early Late Triassic aetosaur and the evolution of the stagonolepidid archosaurian reptiles. Zool J Linnean Soc 158:860–881
Sulej T, Majer D (2005) The temnospondyl amphibian *Cyclotosaurus* from the Upper Triassic of Poland. Palaeontology 48:157–170
Sulej T, Bronowicz R, Tałanda M, Niedźwiedzki G (2011) A new dicynodont-archosaur assemblage from the Late Triassic (Carnian) of Poland. Earth Environ Sci Trans R Soc Edinb 101:261–269
Sulej T, Niedźwiedzki G, Bronowicz R (2012) A new Late Triassic vertebrate fauna from Poland with turtles, aetosaurs, and coelophysoid dinosaurs. J Vert Paleont 32:1033–1041
Sullivan RM, Lucas SG (1999) *Eucoelophysis baldwini*, a new theropod dinosaur from the Upper Triassic of New Mexico, and the status of the original types of *Coelophysis*. J Vert Paleont 19:81–90
Sullivan RM, Lucas SG, Randall KA (1995) Late Triassic vertebrate fauna from the Zions View locality (Little Conewago Creek), York County, Pennsylvania. J Vert Paleont 15(3):55A
Świło M, Niedźwiedzki G, Sulej T (2014) Mammal-like tooth from the Upper Triassic of Poland. Acta Palaeont Polon 59:815–820
Szajna MJ, Silvestri SM (1996) A new occurrence of the ichnogenus *Brachychirotherium*: implications for the Triassic-Jurassic mass extinction event. In: Morales M (ed) The continental Jurassic. Mus N Arizona Bull 60: 275–283
Szulc J, Racki G, Jewuła K, Środoń J (2015) How many Upper Triassic bone-bearing levels in the Upper Silesia (southern Poland)? Ann Soc Geol Polon 85:587–626
Tatarinov LP (2005) A new cynodont (Reptilia, Theriodonta) from the Madygen Formation (Triassic) of Fergana, Kyrgyztan. Paleont J 39:192–198
Thomson TJ, Lovelace DM (2014) Swim track morphotypes and new track localities from the Moenkopi and Red Peak formations (Lower-Middle Triassic) with preliminary interpretations of aquatic behaviors. New Mex Mus Nat Hist Sci Bull 62:103–128
Thulborn T, Turner S (2003) The last dicynodont: an Australian Cretaceous relict. Proc R Soc Lond B 270:985–993
Tixeront M (1971) Lithostratigraphie et minéralisations cuprifères et uranifères stratiformes syngenetiques et familières des formations detritiques Permo-Triasiques du couloir d'Argana (Haut-Atlas occidental, Maroc) et possibilitiés de recherches. Maroc Dir Mines Géol Div Géol Rep Serv Études Gîtes Min 921:1–37
Unwin DM, Alifanov VR, Benton MJ (2000) Enigmatic small reptiles from the Midde-Late Triassic of Kyrgyzstan. In: Benton MJ, Shishkin DM, Kurochkin EN (eds) The age of dinosaurs in Russia and Mongolia. Cambridge University Press, Cambridge, pp 177–186
Valencio DA, Mendía JE, Vilas JF (1975) Palaeomagnetism and K-Ar ages of Triassic igneous rocks from the Ischigualasto-Ischichuca basin and Puesto Viejo Formation, Argentina. Earth Planet Sci Lett 26:319–330
Voigt S, Buchwitz M, Fischer J, Kogan I, Moisan P, Schneider JW, Spindler F, Brosig A, Preusse M, Scholze F, Linnemann U (2017) Triassic life in an inland lake basin of the warm-temperate biome—the Madygen Lagerstätte (southwest Kyrgyzstan, Central Asia). In: Fraser NC, Sues H-D (eds) Terrestrial conservation Lagerstätten: windows into the evolution of life on land. Dunedin Academic Press, Edinburgh. in press
von Huene F (1940) The tetrapod fauna of the Upper Triassic Maleri beds. Palaeont Indica New Ser 32(1):1–42
Watson DMS (1914) *Eunotosaurus africanus* Seeley, and the ancestry of the Chelonia. Proc Zool Soc Lond 11:1011–1020
Weems RE, Lucas SG (2015) A revision of the Norian conchostracan zonation in North America and its implications for Late Triassic North American tectonic history. New Mex Mus Nat Hist Sci Bull 67:303–317

Weems RE, Tanner LH, Lucas SG (2016) Synthesis and revision of the lithostratigraphic groups and formations in the upper Permian?-Lower Jurassic Newark Supergroup of eastern North America. Stratigraphy 13:111–153

Westphal F (1970) Phytosaurier-Hautplatten aus der Trias von Madagaskar-ein Beitrag zur Gondwana-Paläogeographie. Neues Jahrb Geol Paläont Monats 1970:632–638

Whiteside DI, Marshall JEA (2008) The age, fauna and palaeoenvironment of the Late Triassic fissure deposits of Tytherington, South Gloucestershire, UK. Geol Mag 145:105–147

Whiteside JH, Grogan DS, Olsen PE, Kent DV (2011) Climatically driven biogeographic provinces of Late Triassic tropical Pangea. Proc Natl Acad Sci U S A 108:8972–8977

Wild R (1978) Die Saurier von Kupferzell-Bauersbach. Württemb Franken Jahrb 62:1–16

Wild R (1980) The fossil deposits of Kupferzell, southwest Germany. Mes Vert Life 1:15–18

Wild R (1989) *Aetosaurus* (Reptilia: Thecodontia) from the Upper Triassic (Norian) of Cene near Bergamo, Italy, with a revision of the genus. Riv Mus Civ Sci Nat 14:1–24

Wu X, Chatterjee S (1993) *Dibothrosuchus elaphros*, a crocodylomorph from the Lower Jurassic of China and the phylogeny of the Sphenosuchia. J Vert Paleont 13:58–89

Yadagiri P, Rao BRJ (1987) Contribution to the stratigraphy and vertebrate fauna of the Lower Jurassic Kota Formation, Pranhita-Godavari Valley, India. Palaeobotanist 36:230–244

Yates AM (2003) A definite prosauropod dinosaur from the Lower Eliot Formation (Norian: Upper Triassic) of South Africa. Palaeont Afr 39:63–68

Yates AM, Kitching JW (2003) The earliest known sauropod dinosaur and the first steps toward sauropod locomotion. Proc R Soc Lond B270:1753–1758

Zeigler KE, Heckert AB, Lucas SG eds (2003) Paleontology and geology of the Upper Triassic (Revueltian) Snyder quarry, New Mexico. New Mex Mus Nat Hist Sci Bull 24: 1–132

Chapter 11
The Late Triassic Record of Cynodonts: Time of Innovations in the Mammalian Lineage

Fernando Abdala and Leandro C. Gaetano

Abstract The Triassic period witnessed a great diversification of lineages, recovering from one of the worst extinction events known in Earth's history. Therapsids, the lineage that includes mammals as the only living members, enjoyed remarkable success during the Triassic. This clade includes the Late Permian to Early Cretaceous non-mammaliaform cynodonts, represented by a paraphyletic array of taxa successively more closely related to mammaliaforms (considered as basal mammals by several palaeontologists). In the Middle Triassic, cynodonts are represented by numerous taxa that thrived mostly in Gondwana, whereas only one taxon, *Nanogomphodon,* has been registered in Laurasia. Cynodont diversity during this time interval is mainly composed of gomphodonts, featuring bucco-lingually expanded postcanines, whereas the members of their sister-group, the mostly sectorial-toothed probainognathians, are very scarce. On the contrary, Early Jurassic non-mammaliaform cynodonts are most abundant in Laurasia (although also present in Gondwana) and only represented by probainognathians, particularly the sectorial-toothed tritheledontids and the ubiquitous herbivorous tritylodontids. The Late Triassic thus constitutes a pivotal time lapse, marked by an expansion of the geographical distribution and diversification of cynodonts. During this time, cynodont assemblages include representatives of old and new lineages and the first mammaliaforms are documented. This contribution presents a review of the diversity and geographic distribution of Late Triassic to Early Jurassic cynodonts, and summarizes the main morphologies represented in the lineage, including Mammaliaformes, a key group in our understanding of the early evolution of mammals.

F. Abdala (✉)
Unidad Ejecutora Lillo, CONICET-Fundación Miguel Lillo, Tucumán, Argentina

Evolutionary Studies Institute, University of the Witwatersrand, Johannesburg, South Africa
e-mail: 1viutiabdala2@gmail.com

L.C. Gaetano
Departamento de Ciencias Geológicas, FCEyN, Instituto de Estudios Andinos "Don Pablo Groeber", IDEAN (Universidad de Buenos Aires-CONICET), Ciudad Autónoma de Buenos Aires, Buenos Aires, Argentina

Evolutionary Studies Institute, University of the Witwatersrand, Johannesburg, South Africa
e-mail: lcgaetano@gl.fcen.uba.ar

© Springer International Publishing AG 2018

L.H. Tanner (ed.), *The Late Triassic World*, Topics in Geobiology 46,
https://doi.org/10.1007/978-3-319-68009-5_11

Keywords Cynodontia • Mammaliaformes • Late Triassic • Traversodontidae • Probainognathia • Tritylodontidae • Tritheledontidae • Diversity

11.1 Introduction

Several changes took place in the ancient world of the early Mesozoic, transforming the climate and, with that, the faunal composition of the ecosystems. The Triassic for a start was a time of key changes in faunas (Sues and Fraser 2010) after the colossal extinction event at the end of the Permian that wiped out a massive proportion of the life forms from the Earth (Erwin 1994; Joachimski et al. 2012). For the tetrapod communities, the end of the Permian represented the demise of two main therapsid lineages, biarmosuchians and gorgonopsians, and the extreme decline of therocephalians and dicynodonts, the latter being indeed one of the most diverse and abundant Permian lineages (Rubidge and Sidor 2001; Kemp 2005; Fröbisch 2008). The extinction process also affected the large herbivorous pareiasaurian parareptiles that were key components of Middle and Late Permian faunas. The Triassic witnessed the diversification of cynodonts, a second pulse of diversification of dicynodonts, the continuity and last days of therocephalians, and the diversification of the small procolophonian parareptiles (Kemp 2005; Fröbisch 2008; Abdala and Ribeiro 2010; Huttenlocker and Sidor 2016; Cisneros 2008). Indeed, the Triassic was an important time for amniote evolution, as exemplified by the origin of dinosaurs and of turtles (Rougier et al. 1995; Li et al. 2008; Barrett et al. 2009; Langer et al. 2010; Schoch and Sues 2015; Marsicano et al. 2016).

The Triassic is also the major period during which the evolutionary development of essential mammalian features in the non-mammalian cynodonts, extinct predecessors of living mammals, took place. These characters include differentiation of postcanine morphology, two occipital condyles for articulation with the vertebral column, development of an osseous secondary palate, mandibular masseteric fossa, and basicranial promontorium, among others (Kielan-Jaworowska et al. 2004; Kemp 2005). Here we present an account of cynodont diversification at the end of the Triassic and the last pulse of the non-mammaliaform cynodonts, which produced important morphological novelties. This diversification is represented by the radiation of the herbivorous traversodontid cynodonts, the origin of small-sized insectivorous-carnivorous forms with sectorial postcanines, and the evolution of one of the first rodent-like experiments in the synapsid lineage.

Institutional abbreviations: BP, Evolutionary Studies Institute (formerly Bernard Price Institute for Palaeontological Research), University of the Witwatersrand, Johannesburg, South Africa; MCZ, Museum of Comparative Zoology, Harvard University, Cambridge, United States; NHMUK, The Natural History Museum, London, United Kingdom; PVL, Colección Paleontología de Vertebrados Lillo, Universidad Nacional de Tucumán, Argentina; USNM, National Museum of Natural History, Smithsonian Institution,Washington DC, United States.

11.2 Cynodont Diversity

Cynodontia is the last therapsid lineage to appear in the fossil record. Two species are known from the early Late Permian *Tropidostoma* Assemblage Zone (AZ) and at least five species are represented in faunal associations closer to the end of the Permian in South Africa (Botha et al. 2007; Botha-Brink and Abdala 2008; Kammerer 2016). By the beginning of the Triassic the number of species remained nearly the same, however, there are no common species between the Permian and Triassic (Abdala and Ribeiro 2010). The Middle Triassic records perhaps the highest peak in diversity in the history of Triassic cynodonts. This epoch, represented in South Africa by the *Cynognathus* AZ (here we consider this AZ as Middle Triassic, but see Ottone et al. 2014 who supports a Carnian age for *Cynognathus* AZ correlated faunas from Argentina), is when Triassic cynodonts reached their largest body sizes and experimented with profound transformations in their dentition, with forms bearing occluding bucco-lingually expanded (gomphodont) postcanines (Abdala and Ribeiro 2010). These two novelties among basal cynodonts (large size and expanded occluding postcanines) are suggestive of a change in the food resources represented in the Middle Triassic terrestrial ecosystems.

Presently, there are ~150 cynodont genera recognized in the fossil record from the Late Permian to the Early Jurassic, 75 of which (50% of the total) are represented in the 36 million year (Ma) extent of the Late Triassic and 42 (28%) in the 27.2 Ma span of the Early Jurassic (Table 11.1). In the Late Triassic-Early Jurassic transition, eucynodonts are represented by traversodontids, members of the monophyletic Cynognathia, and by several taxa of the clade Probainognathia, including prozostrodontids, tritheledontids, tritylodontids, and mammaliaforms (Fig. 11.1).

11.2.1 Traversodontid Supremacy

It is mainly among gomphodonts that non-mammaliaform cynodonts explored the development of bucco-lingually expanded postcanine crowns, which allowed for an elementary dental occlusion. The first record of gomphodonts is from the end of the Olenekian. Basal gomphodonts, represented by diademodontids and trirachodontids, had expanded postcanines lacking an occlusal basin. Diademodontids, in particular, presented an extremely heterogeneous postcanine series with simple anteriormost teeth, expanded mid-row elements, and sectorial posterior teeth (Hopson 1971; Grine 1977). These two families are mostly represented at the end of the Early Triassic and in the Middle Triassic, although there is an unusually late record of a form tentatively identified as a diademodontid and originally attributed to levels of the Late Triassic Lower Elliot Formation (Abdala et al. 2007). The horizon of this record was recently reassigned to the Lower Jurassic Upper Elliot Formation (Bordy et al. 2017). Besides diademodontids and trirachodontids, a derived gomphodont clade named Traversodontidae (*sensu* Liu and Abdala 2014) was well represented in

Table 11.1 Late Triassic-Early Jurassic cynodont taxa

	Genus	Lineage	Country
Carnian (9 Ma) 237–228 My			
1	*Titanogomphodon*	Diademodontidae	Namibia
2	*Aleodon cromptoni*	Probainognathia	Namibia, Brazil
3	*Massetognathus pascuali*	Traversodontidae	Argentina
4	*Chiniquodon theotonicus*	Probainognathia	Argentina, Brazil
5	*Chiniquodon kalanoro*	Probainognathia	Madagascar
6	*Chiniquodon sp.*	Probainognathia	Namibia
7	*Probainognathus*	Probainognathia	Argentina
8	*Exaeretodon argentinus*	Traversodontidae	Argentina
9	*Ischignathus*	Traversodontidae	Argentina
10	*Ecteninion*	Probainognathia	Argentina
11	*Diegocanis*	Probainognathia	Argentina
12	*Exaeretodon riograndensis*	Traversodontidae	Brazil
13	*Luangwa sudamericana*	Traversodontidae	Brazil
14	*Luangwa sp.*	Traversodontidae	Namibia
15	*Traversodon*	Traversodontidae	Brazil
16	*Protuberum*	Traversodontidae	Brazil
17	*Scalenodon ribeiroae*	Traversodontidae	Brazil
18	*Bonacynodon*	Probainognathia	Brazil
19	*Protheriodon*	Probainognathia	Brazil
20	*Charruodon*	Probainognathia	Brazil
21	*Prozostrodon*	Probainognathia	Brazil
22	*Therioherpeton*	Probainognathia	Brazil
23	*Gomphodontosuchus*	Traversodontidae	Brazil
24	*Santacruzodon*	Traversodontidae	Brazil
25	*Candelariodon*	Probainognathia	Brazil
26	*Santacruzgnathus*	Probainognathia	Brazil
27	*Alemoatherium*	Probainognathia	Brazil
28	*Massetognathus ochagaviae*	Traversodontidae	Brazil
29	*Deccanodon*	?	India
30	*Ruberodon*	Traversodontidae	India
31	*Rewaconodon*	Dromatheridae	India, United States
32	*Dadadon*	Traversodontidae	Madagascar
33	*Menadon*	Traversodontidae	Madagascar, Brazil
34	*Boreogomphodon*	Traversodontidae	United States
35	*Gondwanadon*	Morganucodontidae	India
36	*Tikitherium*	Docodonta	India
37	*Adelobasileus*	Stem Mammaliaformes	United States
Norian (14 Ma) 227–213			
38	*Chaliminia*	Tritheledontidae	Argentina
39	*Riograndia*	Tritheledontidae	Brazil
40	*Brasilodon*	Prozostrodontia	Brazil
41	*Irajatherium*	Tritheledontidae	Brazil

(continued)

Table 11.1 (continued)

	Genus	Lineage	Country
42	*Minicynodon*	Prozostrodontia	Brazil
43	*Botucaraitherium*	Prozostrodontia	Brazil
44	*Arctotraversodon*	Traversodontidae	Canada
45	*Scalenodontoides*	Traversodontidae	South Africa, Lesotho
46	*Elliotherium*	Tritheledontidae	South Africa
47	*Microconodon*	Dromatheridae	United States
48	*Dromatherium*	Dromatheridae	United States
49	*Thomasia hahni*	Haramiyidae	Germany
Late Norian-Rhaetian (19 Ma) 201–220			
50	*Microscalenodon*	?Traversodontidae	Belgium
51	*Meurthodon*	Dromatheridae	France
52	*Hahnia*	Probainognathia	Belgium
53	*Gaumia*	Probainognathia	Belgium, Luxemburg
54	*Lepagia*	Probainognathia	Belgium
55	*Maubeugia*	?Traversodontidae	France
56	*Rosieria*	?Traversodontidae	France
57	*Oligokyphus triserialis*	Tritylodontidae	Germany
58	*Oligokyphus* sp.	Tritylodontidae	Canada
59	*Tricuspes*	Dromatheridae	Germany, Luxembourg, France and Belgium
60	*Mitredon*	?	Greenland
61	*Pseudotriconodon*	Dromatheridae	Luxemburg, Belgium, France, United States
62	*Mojo*	Multituberculata	Belgium
63	*Theroteinus*	Haramiyidae	France
64	*Brachyzostrodon*	Morganucodontidae	France
65	*Woutersia*	Docodonta	France
66	*Delsatia*	Docodonta	France
67	*Megazostrodon chenali*	Morganucodontidae	France
68	*Paceyodon*	Morganucodontidae	France
69	*Paikasigudodon* cf. *yadagirii*	Morganucodontidae	France
70	*Rosierodon*	Morganucodontidae	France
71	*Kuehneotherium*	Symmetrodonta	France; Luxemburg; United Kingdom; Greenland
72	*Fluctuodon*	Symmetrodonta	France
73	*Thomasia*	Haramiyidae	Germany; France; Belgium; Luxemburg; Switzerland; United Kingdom
74	*Haramiyavia*	Haramiyidae	Greenland
75	*Helvetiodon*	Morganucodontidae	Switzerland

(continued)

Table 11.1 (continued)

	Genus	Lineage	Country
76	*Morganucodon peyeri*	Morganucodontidae	Switzerland, France
77	*Hallautherium schalchi*	Morganucodontidae	Switzerland; Poland
78	*Eozostrodon*	Morganucodontidae	United Kingdom
Hettangian-Toarcian (27 Ma) 201–174			
79	*Bienotherium magnum*	Tritylodontidae	China
80	*Bienotherium yunnanense*	Tritylodontidae	China
81	*Lufengia*	Tritylodontidae	China
82	*Dianzhongia*	Tritylodontidae	China
83	*Yunnanodon*	Tritylodontidae	China
84	*Oligokyphus lufengensis*	Tritylodontidae	China
85	*Kunminia*	?	China
86	*Bocatherium*	Tritylodontidae	Mexico
87	*Tritheledon*	Tritheledontidae	South Africa
88	*Diarthrognathus*	Tritheledontidae	South Africa
89	*Tritylodontoideus*	Tritylodontidae	South Africa
90	*Pachygenelus*	Tritheledontidae	South Africa, Canada
91	*Tritylodon*	Tritylodontidae	South Africa, Lesotho
92	*Oligokyphus major*	Tritylodontidae	United Kingdom; United States
93	*Dinnebitodon*	Tritylodontidae	United States
94	*Kayentatherium*	Tritylodontidae	United States
95	*Argentoconodon*	Triconodontidae	Argentina
96	*Condorodon*	Triconodontidae	Argentina
97	*Asfaltomylos*	Australosphenida	Argentina
98	*Henosferus*	Australosphenida	Argentina
99	*Sinoconodon*	Stem Mammaliaformes	China
100	*Hadrocodium*	basal mammaliaform (more derived than Docodonta but less than Triconodontidae)	China
101	*Erythrotherium*	Morganucodontidae	Lesotho
102	*Bocaconodon*	Morganucodontidae	Mexico
103	*Victoriaconodon*	Triconodontidae	Mexico
104	*Huasteconodon*	Triconodontidae	Mexico
105	*Megazostrodon*	Morganucodontidae	South Africa; Lesotho
106	*Kuehneotherium*	Symmetrodonta	United Kingdom
107	Pantotherid indet	Symmetrodonta	United Kingdom
108	*Bridetherium*	Morganucodontidae	United Kingdom
109	*Paceyodon*	Morganucodontidae	United Kingdom
110	*Thomasia* cf. *moorei*	Haramiyidae	United Kingdom
111	*Dinnetherium*	Morganucodontidae	United States
112	*Morganucodon*	Morganucodontidae	United States, United Kingdom, China

(continued)

Table 11.1 (continued)

	Genus	Lineage	Country
113	*Indozostrodon* (Kota Fm.)	Morganucodontidae	India
114	Indotherium (Kota Fm.)	Morganucodontidae	India
115	*Dyskritodon*	?Triconodontidae	India
116	*Paikasigudodon* (Kota Fm.)	Morganucodontidae	India
117	*Trishulotherium* (Kota Fm.)	Symmetrodonta	India
118	*Nakunodon* (Kota Fm.)	Symmetrodonta	India
119	*Kotatherium* (Kota Fm.)	Symmetrodonta	India
120	*Indobaatar* (Kota Fm.)	Multituberculata	India

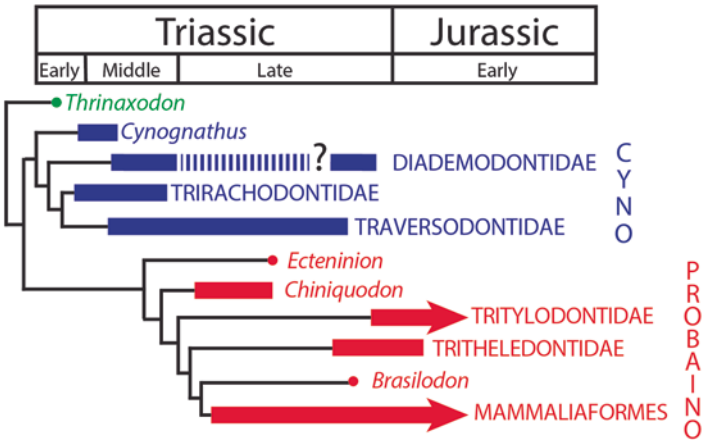

Fig. 11.1 Phylogenetic relationships of eucynodonts, plotted against the time scale. Abbreviations: *CYNO* Cynognathia, *PROBAINO* Probainognathia. Phylogeny after Liu and Olsen (2010)

the Middle and Upper Triassic (Fig. 11.2). Twenty-three of the 96 cynodont genera (24%) from the Middle–Late Triassic are traversodontids. This group was already widely distributed through East Africa, South America, and Europe by the Anisian-Ladinian (Kemp 1980; Hopson and Sues 2006; Abdala et al. 2009). Traversodontids are predominantly from Gondwana and a major component of the Late Triassic cynodont faunas from South America (Fig. 11.3). They are dominant in the Carnian fauna of the Chañares Formation in Argentina, represented by *Massetognathus* (Abdala and Giannini 2000; Mancuso et al. 2014). The *Dinodontosaurus* AZ (Santa Maria Formation) in southern Brazil shows a strong faunal correlation with the Chañares Formation. Traversodontids in this Brazilian association are represented by *Massetognathus*, *Traversodon*, *Protuberum*, and the recently discovered *Scalenodon* (Melo et al. 2017), but none of them dominate the faunal assemblage. The Santa Cruz do Sul AZ of the Santa Maria Formation is the only Brazilian fauna in which traversodontids are diverse (including *Santacruzodon*, *Menadon,* and a third as-yet unnamed taxon) and also dominant (Abdala et al. 2001; Melo et al. 2015). The Santa Cruz do Sul fauna correlates biostratigraphically with the fossil

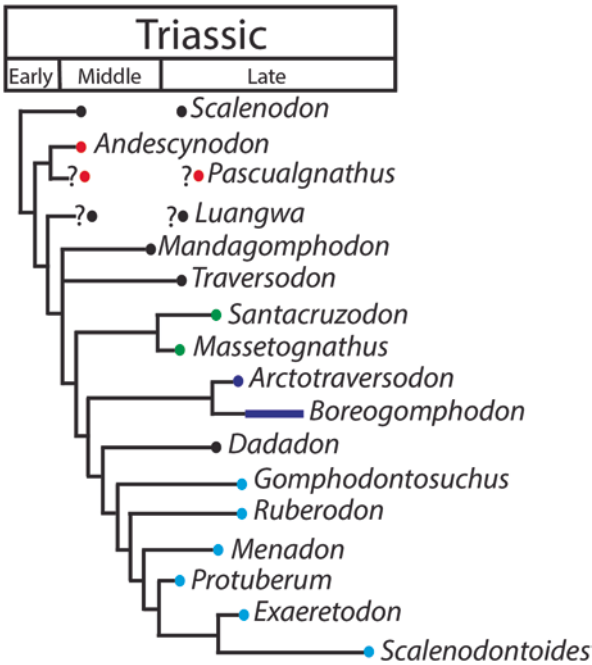

Fig. 11.2 Phylogenetic relationships of traversodontids plotted against the time scale. Phylogeny after Liu and Abdala (2014) and Ray (2015). *Colours* indicate monophyletic groups: *light blue*, Gomphodontosuchinae

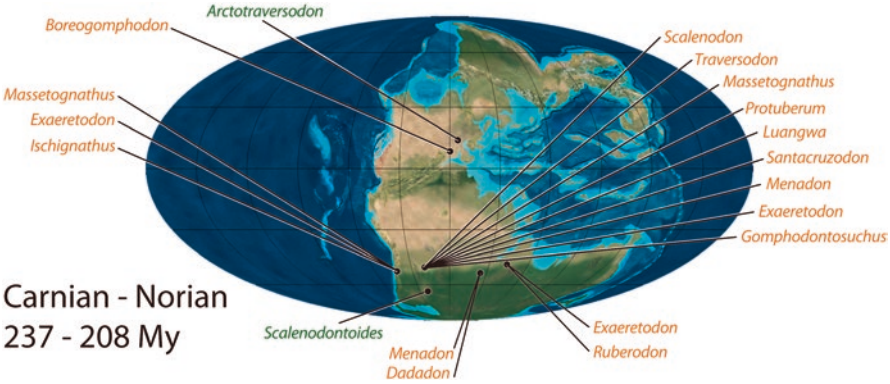

Fig. 11.3 Paleogeographic reconstruction depicting traversodontid distribution during the Carnian (taxa in *red*) and Norian (taxa in *green*). Map modified from Ron Blakey

assemblage of the Makay Formation of Madagascar through the shared occurrence of the traversodontid *Menadon* (Melo et al. 2015). In this latter formation, traversodontids are represented by *Menadon*, only known by a couple of specimens, and *Dadadon*, documented by several specimens representing different ontogenetic stages (Flynn et al. 2000; Kammerer et al. 2012). At the end of the Carnian and the beginning of the Norian, traversodontids are known from the Ischigualasto

Formation through *Exaeretodon* and *Ischignathus* (Bonaparte 1962, 1963). The first is represented by several skeletons whereas only one specimen of the latter has been found. *Exaeretodon* is also well represented in the *Hyperodapedon* AZ from southern Brazil (Abdala et al. 2002; Liparini et al. 2013), along with *Gomphodontosuchus*, which is known only from one specimen (von Huene 1928; Hopson 1985). Detailed prospection in the Ischigualasto Formation makes clear that *Exaeretodon* is outnumbered by rhynchosaurs at the base of this unit and becomes a dominant taxon towards the upper levels (Martinez et al. 2011). A similar condition has been suggested for the distribution and abundance of *Exaeretodon* in different levels of the *Hyperodapedon* AZ in the Santa Maria Formation (Liparini et al. 2013). Traversodontids have also been recorded in Carnian formations in India. Fragments of two *Exaeretodon* specimens of estimated skull length of 200 mm were found in the Maleri Formation (Chatterjee 1982) and, more recently, at least seven lower jaws of the traversodontid *Ruberodon* were described from the Tiki Formation (Ray 2015). The youngest record of traversodontid from Gondwana is represented by the large and bizarre *Scalenodontoides* (Fig. 11.4a) from the Norian Lower Elliot Formation of South Africa (Crompton and Ellenberger 1957; Gow and Hancox 1993; Battail 2005) and by a small fragmentary specimen only preliminary reported (Ribeiro et al. 2011; Martinelli and Soares 2016) from the ?late Norian- ?Early Jurassic *Riograndia* AZ of Brazil (Abdala and Ribeiro 2010; Barboni and Dutra 2013; Rohn et al. 2014).

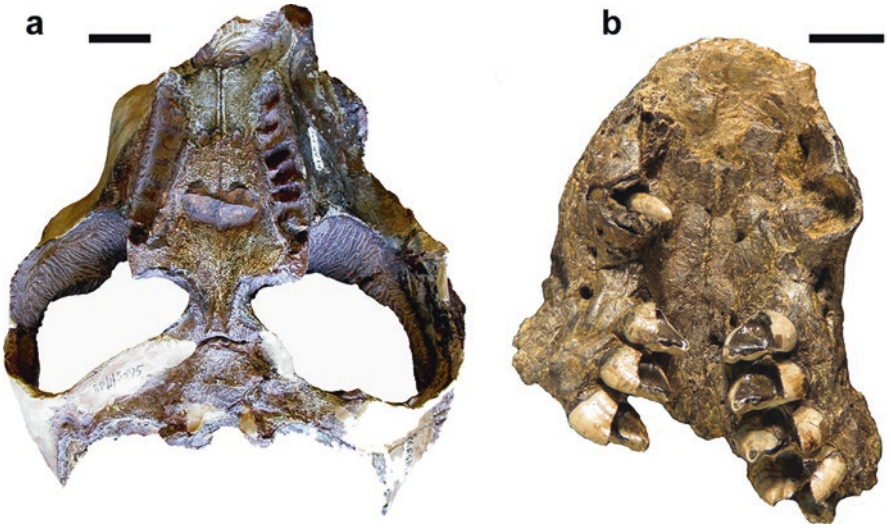

Fig. 11.4 Traversodontidae. (**a**) *Scalenodontoides macrodontes* (BP/1/5395), Lower Elliot Formation, Karoo Basin, South Africa, palatal view of the skull. Scale bar = 40 mm. (**b**) *Boreogomphodon jeffersoni* (USNM 437636), Vinita Formation, Virginia, United States, palatal view of the snout. Scale bar = 5 mm. These species nearly represent the total range of size in traversodontid cynodonts. Photography of *Boreogomphodon* by Christophe Hendrickx, copyright Smithsonian Institution

The known history of traversodontids is less extensive in Laurasia. They are restricted to the east side of North America and to only one undisputed record in Europe. Of the four species registered in Laurasia, only the small-sized *Boreogomphodon* from the Carnian Vinita Formation in Virginia, United States, is represented by numerous specimens (Sues and Hopson 2010; Fig. 11.4b). Specimens recovered from the Carnian Pekin Formation and the type and only specimen of *Plinthogomphodon* from the Norian (Sues et al. 1999), both from North Carolina, United States, were also tentatively assigned to *Boreogomphodon* by Liu and Sues (2010). In Europe there is one confirmed record of *Nanogomphodon* represented by an isolated lower tooth from the Ladinian of Germany (Hopson and Sues 2006). Four species from the Norian and Rhaetian of France and Belgium represented by tiny expanded isolated crowns have been assigned to traversodontids (Hahn et al. 1988; Godefroit and Battail 1997; Godefroit 1999); however, their attribution to this group has been questioned and needs stronger validating evidence (Hopson and Sues 2006; Liu and Abdala 2014).

In summary, the traversodontid history is mostly a Gondwanan one (17 taxa versus three from Laurasia) and covers approximately 30 Ma, with the peak of representation clearly in the Late Triassic. There is a trend toward increased morphological complexity of the postcanines (Martinelli and Soares 2016) in the younger representatives of the family as well as to increase the body size. The larger traversodontids are represented in the Carnian-Norian of Argentina (i.e., *Exaeretodon*, *Ischignathus*; Bonaparte 1962, 1963; Abdala et al. 2002), South Africa (i.e., *Scalenodontoides*; Crompton and Ellenberger 1957; Hopson 1984; Gow and Hancox 1993; Battail 2005), and Canada (i.e., *Arctotraversodon*; Hopson 1984; Sues et al. 1992; Sues and Olsen 2015).

11.2.2 Proliferation of the Small Probainognathians

Probainognathians are well represented in the Upper Triassic (Fig. 11.5), although less diverse and clearly not as abundant as traversodontids. The oldest representatives of this group are *Aleodon* and *Cromptodon* from the Middle Triassic of Africa and South America, respectively (Crompton 1955; Bonaparte 1972a), which also have expanded postcanine crowns, although to a lesser degree than gomphodont cynodonts. *Aleodon* was also recently reported from the Carnian *Dinodontosaurus* AZ of southern Brazil (Martinelli et al. 2017b). Other basal probainognathians presented typical sectorial postcanines with different degrees of complexity. *Chiniquodon*, a medium-to-large-sized probainognathian is characterized by the presence of a long osseous secondary palate and posterior sectorial postcanines featuring the main cusp strongly curved backwards (Fig. 11.6a). This genus is represented in faunas ranging from the Carnian to the Norian in South America and Africa (Martinez and Forster 1996; Abdala and Giannini 2002; Abdala and Smith 2009; Kammerer et al. 2010). The uppermost faunal assemblage from the upper Omingonde Formation in Namibia has been considered of possible Ladinian age

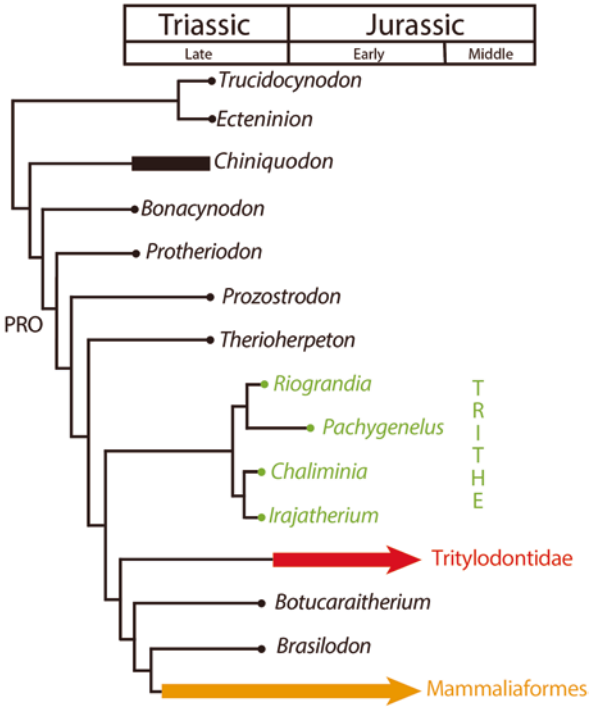

Fig. 11.5 Phylogenetic relationships of probainognathians plotted against the time scale. Abbreviations: *PRO* Prozostrodontia, *TRITHE* Tritheledontidae. Phylogeny after Martinelli et al. (2016)

(Abdala and Smith 2009; Abdala et al. 2013), however, the early Carnian geochronologic age recently presented for the Chañares Formation from Argentina (Marsicano et al. 2016) points to the possibility that this Namibian association, correlated with the Chañares and *Dinodontosaurus* AZ faunas from South America, could be of the same age. Other basal probainognathians are represented by the medium-sized *Trucidocynodon* and the tiny *Alemoatherium* from the Carnian *Hyperodapedon* AZ of Brazil (Oliveira et al. 2010; Martinelli et al. 2017a) and the closely related small sized *Ecteninion* (Fig. 11.6b) and *Diegocanis* from the coeval Ischigualastian fauna (Martinez et al. 1996, 2013). Younger records of probainognathians are globally represented by tiny to small animals that are particularly diverse (Bonaparte and Barberena 2001; Bonaparte et al. 2006; Martinelli et al. 2016), and abundant (for example *Riograndia*) in the ?late Norian - ?early Jurassic *Riograndia* AZ (Bonaparte et al. 2003, 2005; Soares et al. 2011). Probainognathians are represented in this Brazilian assemblage zone by five named taxa (following Liu and Olsen 2010 in that *Brasilodon* and *Brasilitherium* likely represent the same taxon), representing the most diverse putative Late Triassic faunal assemblage with prozostrodontians (Fig. 11.7) (Bonaparte et al. 2001, 2003, 2005; Martinelli et al. 2016, 2017a; Pacheco et al. 2017). The record of small probainognathians is also diverse in South Africa where *Elliotherium* is represented in the Norian Lower Elliot Formation (Sidor and Hancox 2006), and three species, the rare *Tritheledon*

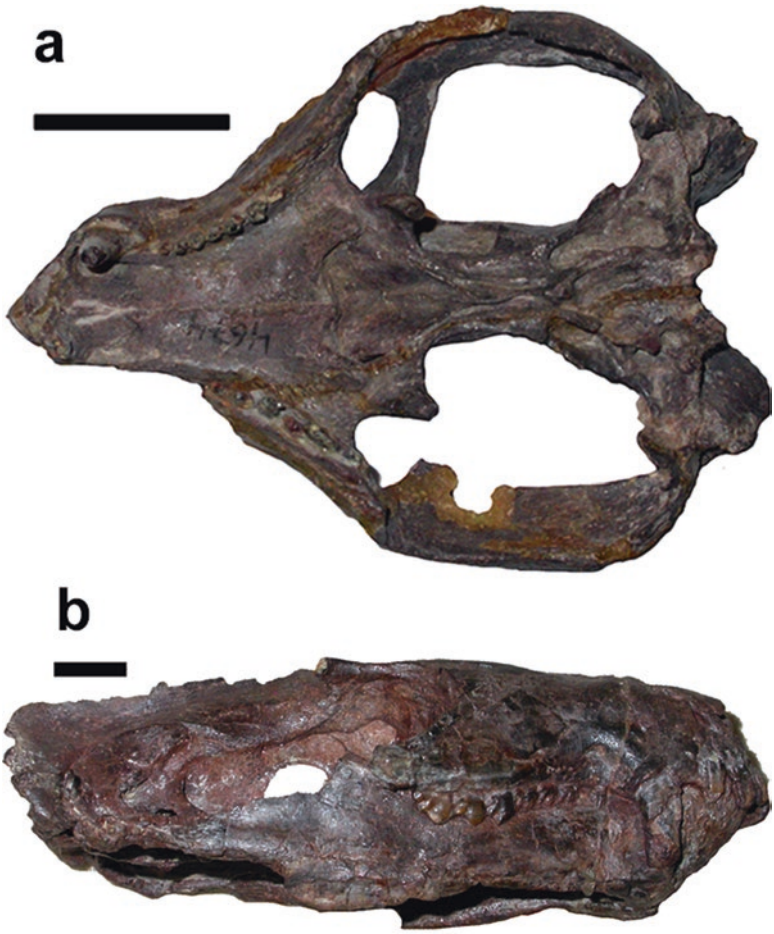

Fig. 11.6 Basal probainognathian (**a**) *Chiniquodon theotonicus* (PVL 4674), Chañares Formation, Ischigualasto-Villa Union Basin, Argentina, palatal view of the skull. Scale bar = 30 mm; (**b**) *Ecteninion lunensis* (PVSJ 422) lateral view of the skull. Scale bar = 10 mm

and *Diarthrognathus* from the Lower Jurassic Upper Elliot and the more common *Pachygenelus* from the same unit and also from the Clarens Formation (Gow 1980; Bordy et al. 2017). Dromatheriids also encompass small cynodonts with sectorial postcanines represented by fragmentary specimens (Sues 2001). They are documented mostly in Laurasia, although they were recently described in the Late Triassic of India (Datta et al. 2004). Their phylogenetic placement among non-mammaliaform cynodonts has never been properly tested. Some scholars consider that the morphological evidence only indicates that dromatheriids are eucynodonts (Sues 2001). Other researchers suggest they are the sister taxon to the Brazilian *Therioherpeton*, forming a group that is closely related to tritheledontids (Battail 1991) and finally Hahn et al. (1994) considered dromatheriids to be the sister group

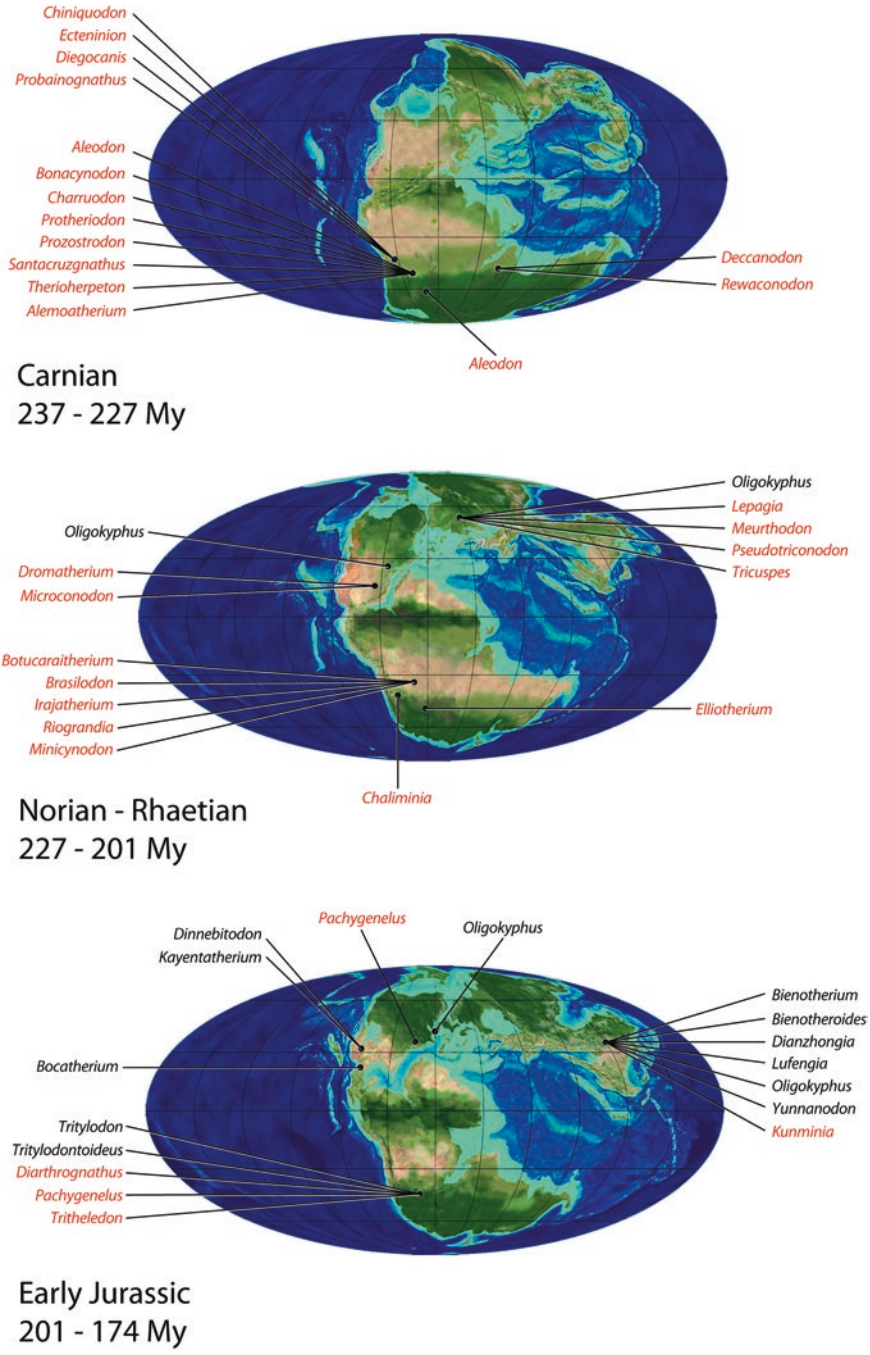

Fig. 11.7 Paleogeographic reconstructions depicting probainognathian distribution, including tritylodontids (in *black*) during the Carnian, Norian-Rhaetian and Early Jurassic. Maps modified from Blakey

of mammaliaforms. By the Late Triassic and Early Jurassic, mammaliaform and tritylodontid probainognathians develop complex expanded postcanines capable of dental occlusion (Kielan-Jaworowska et al. 2004).

11.2.3 Twilight of the Non-mammaliaform Cynodonts: The Tritylodontids

The last vestige of non-mammaliaform cynodonts is characterized by the appearance, diversification, and extinction of tritylodontids, a lineage that features prominently in discussions on mammaliaform ancestry. Most of the scholars consider this group in the probainognathian lineage, representing the sister-taxon of Mammaliaformes or of Tritheledontidae + Mammaliaformes (Kemp 1983; Rowe 1988, 1993; Wible 1991; Luo 1994; Abdala 2007; Liu and Olsen 2010; Ruta et al. 2013; Martinelli et al. 2016) (Fig. 11.1), whereas others interpret tritylodontids as member of the cynognathian lineage (Sues 1985a, b; Sues and Jenkins 2006), closely related to a paraphyletic Traversodontidae (Hopson and Kitching 2001; Sidor and Hopson in press), removing them from the ancestry of mammals.

Tritylodontids have a marked size variation with larger forms such as *Kayentatherium* reaching skull total length of 260 mm and *Oligokyphus* being ~90 mm (Gaetano et al. 2017; Fig. 11.8a, b). They have a feeding system with strong propalinal jaw movements, mimicked by that of rodents (Crompton 1972). The dental pattern is quite conservative in the group: at least one large incisor, no canines, and labiolingually expanded molariforms with longitudinal cusp rows separated by furrows into which opposing cusps occlude (Clark and Hopson 1985; Sues 1985b) (Fig. 11.8a, c). The dental conservatism (Hu et al. 2009) contrasts with a disparate variation in skull morphology (see, for example, variation of the snout and palate in Clark and Hopson 1985: figure 3). At the end of the Triassic and beginning of the Jurassic, tritylodontids and haramiyid mammaliaforms shared the presence of expanded postcanines with occluding longitudinal cusp rows for the second time in the cynodont lineage. This pattern was achieved before in non-mammaliaform cynodonts from the Lower Triassic of South Africa, currently only known by isolated teeth (Gaetano et al. 2012).

Tritylodontids are basically a Jurassic group with isolated older records in the Rhaetian of Germany and Canada (Fedak et al. 2015; Fig. 11.9), and the last representatives known from the Early Cretaceous of Russia and Japan (Tatarinov and Matchenko 1999; Matsuoka et al. 2016). The group is almost exclusively Laurasian, with the only Gondwanan record restricted to the Lower Jurassic of South Africa (Fig. 11.7). A putative record from the Norian of Argentina (Bonaparte 1972b) was recently dismissed by Gaetano et al. (2017). Tritylodontids are represented by approximately 23 taxa, including several species from the Lower Jurassic of the United States and China. This group can be envisaged as an Early Jurassic ecological replacement of the traversodontids, a lineage that was particularly prolific in the

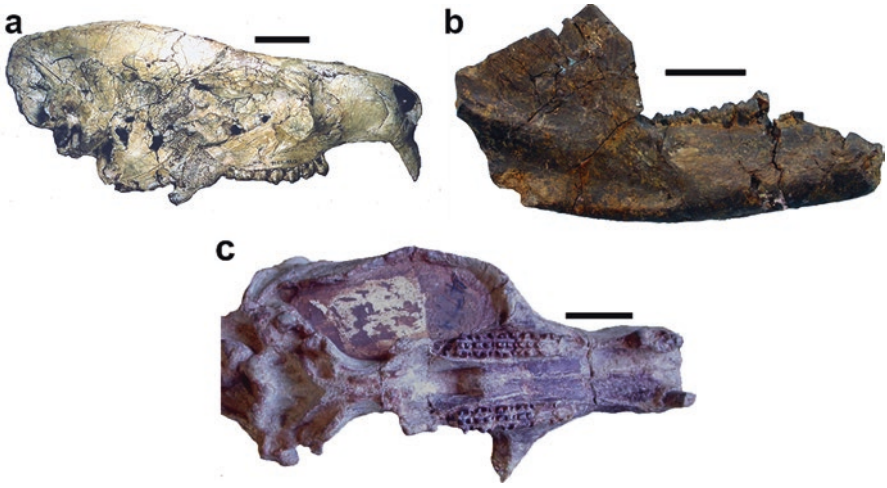

Fig. 11.8 Tritylodontidae (**a**) *Kayentatherium wellesi* (MCZ 8812), Kayenta Formation, Glen Canyon Group, United States, lateral view of the skull. Scale bar = 40 mm. (**b**) *Oligokyphus major* (NHMUK R7119), fissure fill limestone "Mendip 14", Windsor Hill Quarry, United Kingdom, lateral view of the partial right lower jaw. Scale bar = 10 mm. (**c**) *Tritylodon longaevus* (BP/1/4778), upper Elliot Formation, Karoo Basin, South Africa, upper palatal view of the skull. Scale bar = 20 mm

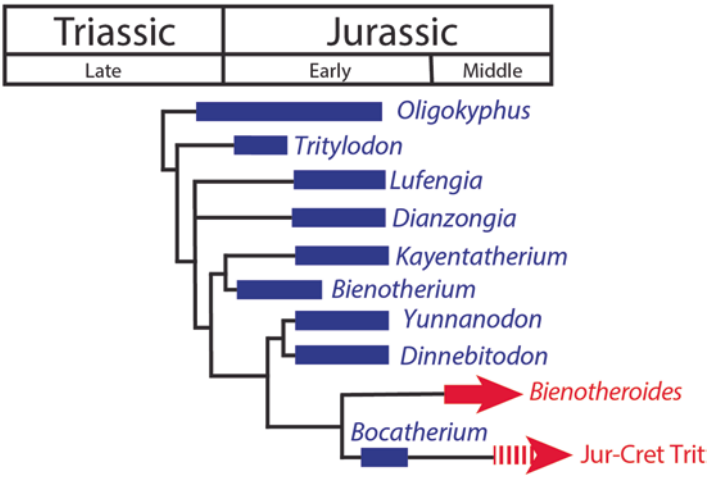

Fig. 11.9 Phylogenetic relationships of tritylodontids plotted against the time scale. Abbreviations: *JUR-CRET Trit* tritylodontids from the Middle Jurassic of the United Kingdom and from the Early Cretaceous of Russia and Japan

Middle and Late Triassic. During the Late Triassic, 18 taxa of traversodontids thrived during an interval of 35.7 million years, whereas 14 species of tritylodontids are known from the Lower Jurassic, spanning a period of 27.2 Ma. In both groups there are several species that are abundant and sometimes even dominant in their respective faunal assemblages (Luo and Wu 1994; Smith and Kitching 1997; Sues and Hopson 2010; Mancuso et al. 2014). Tritylodontids are in need of an extensive phylogenetic analysis. The most recent and one of the few cladistic analyses published is that by Watabe et al. (2007), who considered only five cranial and six dental features. Following the hypotheses presented by Watabe et al. (2007), the basal-most tritylodontids are represented by the Rhaetian to Sinemurian *Oligokyphus* from Laurasia (Fig. 11.9), and the Hettangian-Sinemurian *Tritylodon* from southern Africa, two taxa with a prominent long snout (Clark and Hopson 1985). These basal forms are followed in a pectinate fashion by Hettangian to Sinemurian species from China and North America (Fig. 11.9). The final diversification of this group comprises several species of *Bienotheroides* from the Middle and Late Jurassic of China and the Early Cretaceous of Mongolia, *Bocatherium* from the Pliensbachian of Mexico, *Stereognathus* from the Middle Jurassic of the United Kingdom, and the geologically youngest representatives from the Early Cretaceous of Russia and Japan. The most profuse record of this group is indeed in China, where it is represented by 10 named taxa (nearly half of the named tritylodontid species) in a temporal sequence that starts in the Hettangian with *Bienotherium* and ends in the Late Jurassic with *Bienotheroides*.

11.2.4 Enter Mammaliaforms

It is among basal mammaliaforms that cynodonts progressively become morphologically closer to what we imagine as the first representatives of living mammals. The evolution of this clade during the Mesozoic has been envisaged as successive diversification events of relatively short-lived clades (Luo 2007).

Known from the Carnian Tecovas Formation of Texas (Lucas and Hunt 1990), *Adelobasileus* is only represented by the posterior portion of a skull that shares several features with mammaliaforms, but also retains a set of primitive characters. Phylogenetic studies argued that *Adelobasileus* is a basal mammaliaform (see Kielan-Jaworowska et al. 2004), but it has been suggested that it may well be a dromatheriid (Lucas and Luo 1993; Kielan-Jaworowska et al. 2004).

Mammaliaforms (in the sense of Kielan-Jaworowska et al. 2004) make their appearance in the fossil record with only two records from a single Late Triassic (Carnian) formation (Fig. 11.10). *Gondwanadon* and *Tikitherium*, each of them represented by a single isolated tooth (Fig. 11.11), are known from the Tiki Formation, Madhya Pradesh, India (Datta and Das 1996; Datta 2005). These early representatives already conspicuously differ in their dental anatomy (Kielan-Jaworowska et al. 2004; Kermack et al. 1973; Gill et al. 2014; Luo et al. 2015). *Gondwanadon* (Fig. 11.11a) has been tentatively included in Morganucodonta (Kielan-Jaworowska et al. 2004; Debuysschere

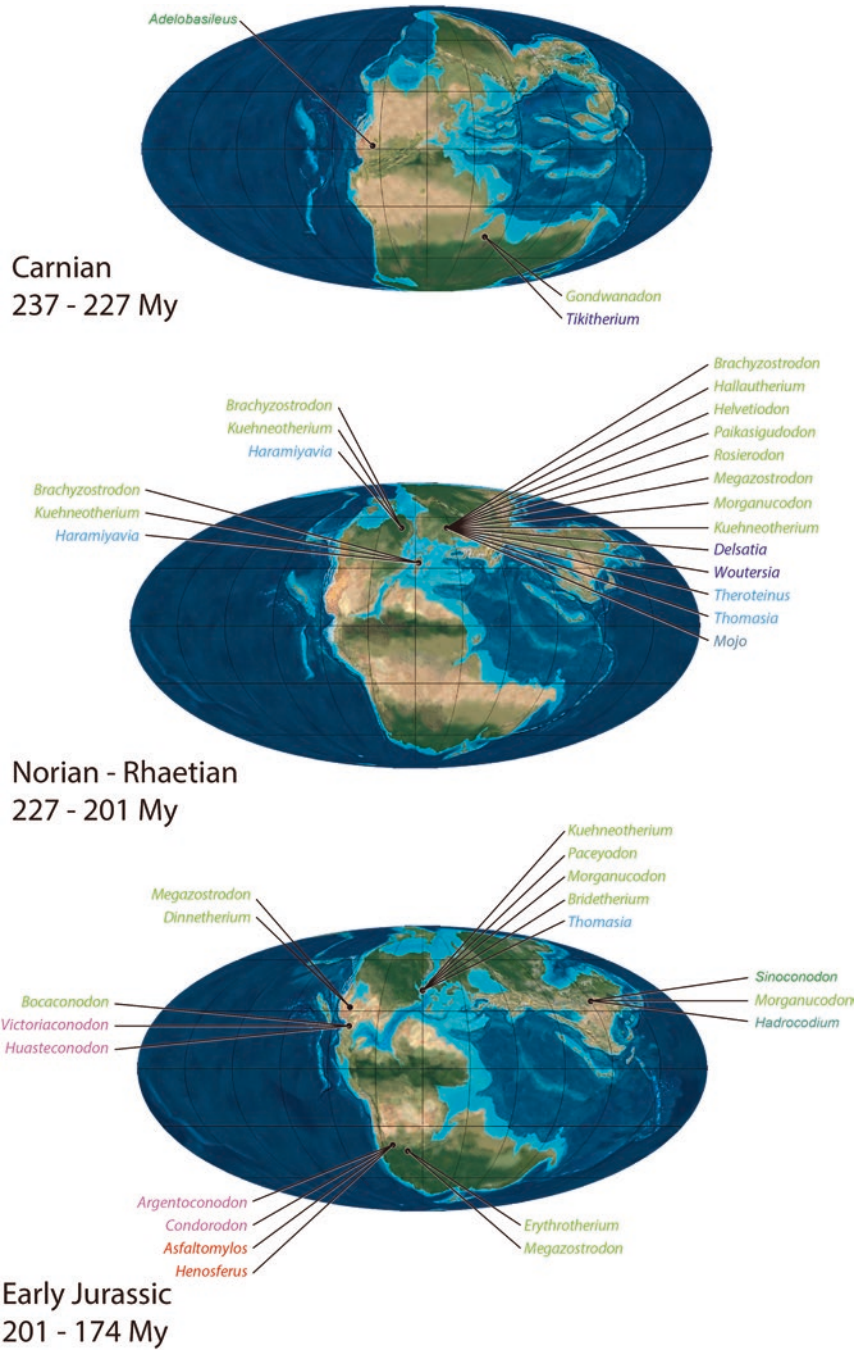

Fig. 11.10 Paleogeographic reconstructions depicting mammaliaform distribution during the Carnian, Norian–Rhaetian, and Early Jurassic. Maps modified from Ron Blakey. Taxon colors represent the purported phylogenetic placement after the hypothesis presented in Fig. 11.12

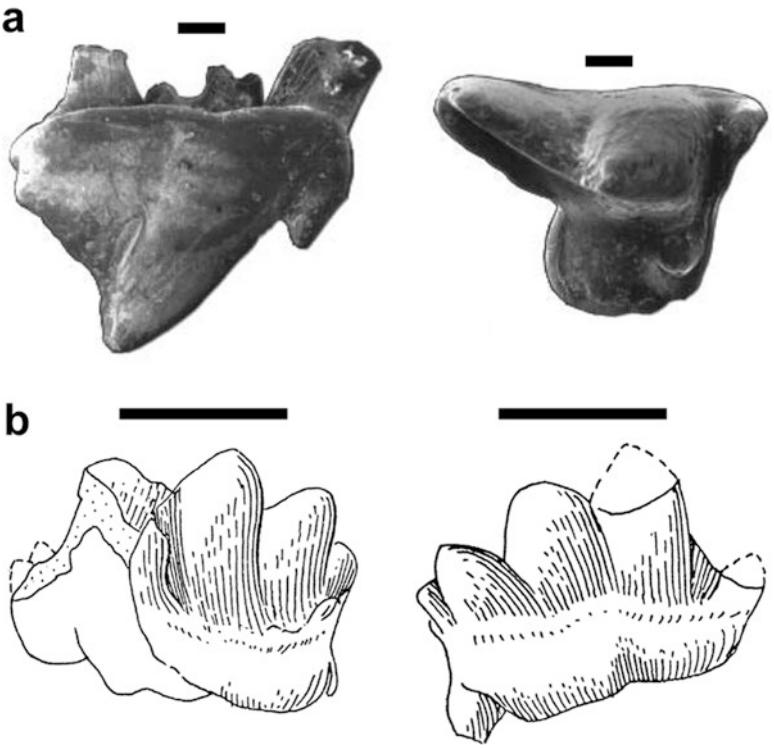

Fig. 11.11 Mammaliaformes (**a**) *Tikitherium copei*; SEM photographs of upper left molariform in labial and occlusal views. Scale bars = 200 μm. (**b**) *Gondwanadon tapani* line drawing of lower right molariform in lingual and labial views. Scale bars = 1 mm. (**a**) from Datta (2005) and (**b**) from Datta and Dass (1996)

et al. 2015). The relationships of most morganucodontans have not been tested phylogenetically. Additionally, there are different opinions regarding the interrelationships of the few morganucodontans that have been cladistically analysed (e.g., Kielan-Jaworowska et al. 2004; Gaetano and Rougier 2012). Morganucodontans are the most abundant and diverse mammaliaforms during the Triassic, particularly the Rhaetian, and they continue to be well represented during the Early and Middle Jurassic.

Originally listed as a morganucodontan, *Tikitherium* (Fig. 11.11b) is now considered closely related to the docodontan clade (Datta 2005; Luo and Martin 2007). Unlike the labiolingually compressed cheek teeth of morganucodontans with mesiodistally aligned main cusps, *Tikitherium* and docodontans present more complex postcanines with labiolingually expanded crowns and a triangular placement of the cusps (Datta 2005; Luo and Martin 2007). *Delsatia* and *Woutersia* from the Rhaetian of France have been interpreted to be basal to *Tikitherium*, but still closely related to docodontans (Luo and Martin 2007). However, it has been proposed that *Woutersia* (including two species) and *Delsatia* (monospecific) might, in fact, represent different teeth of the same taxon due to morphological

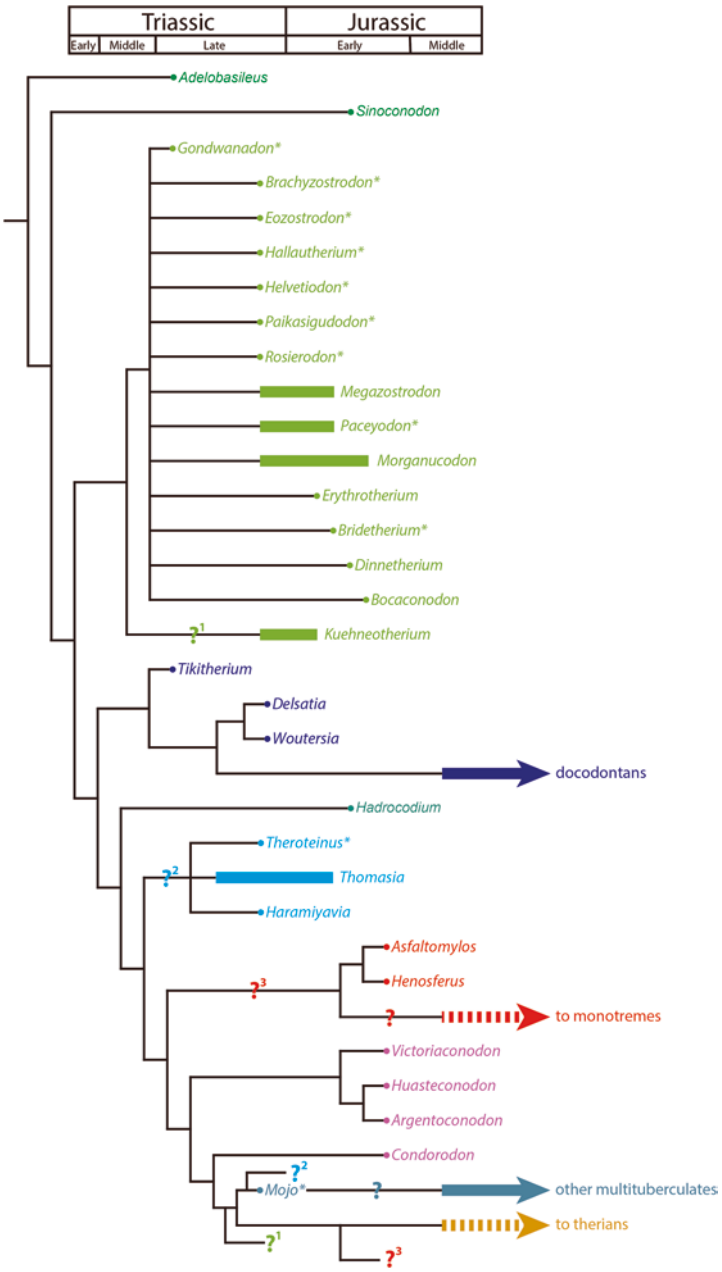

Fig. 11.12 Phylogenetic relationships of mammaliaforms, plotted against the time scale. The topology is the result of manually assembling different cladistics analysis as well as including several taxa that were never analysed phylogenetically. Taxa from the Kota Formation (India) have not been included due to their probably Early Cretaceous age (see text). *Question marks* followed by superscript numbers are employed to represent the alternative positions of certain taxa. Taxa not included in cladistics analysis are marked with an *asterisk*

similarities and co-occurrence (Kielan-Jaworowska et al. 2004). This Triassic radiation of stem-docodontans would precede the radiation and initial diversification of the docodont clade in the Middle Jurassic, when some representatives of this group developed morphological adaptations for swimming (Martin and Nowotny 2000; Martin 2005, 2006; Ji et al. 2006).

The single record of *Thomasia hahni* from the Rhaetian of Halberstadt, Germany (Hahn 1973; Butler and Macintyre 1994) is the oldest member of the contested Haramiyida. Four additional taxa including morganucodontans, haramiyidans, and the oldest "symmetrodont" (identified as *Kuehneotherium* sp.; see below) come from Norian to Rhaetian Laurasian units (Jenkins et al. 1997; Swilo et al. 2014; Clemmensen et al. 2015) (Fig. 11.10).

By the Rhaetian, the number of mammaliaform taxa increased greatly, with 15 genera and at least 20 species identified. This time is clearly dominated by the abundant and diverse morganucodontans (9 genera) whereas haramiyidans, docodontans and related taxa, "symmetrodontans", and tentatively multituberculates, are minor components of the fossil assemblages (Figs. 11.10 and 11.12). Haramiyidans are represented in the Rhaetian by two genera and at least five species. These taxa are the earliest known mammaliaforms with complex quadrangular postcanines with multiple rows of aligned cusps (Fig. 11.13a), a morphology independently acquired in some non-mammaliaform cynodonts. This condition is interpreted as an adaptation to omnivory or herbivory, and contrasts with that of other basal mammaliaforms which have labiolingually compressed molariforms and mesiodistally aligned cusps, or a triangular cusp pattern, suggestive of a more insectivorous or carnivorous diet (Luo et al. 2015). The phylogenetic placement of haramiyidans is currently under debate. Some authors proposed that haramiyidans represent the basal stock of taxa that gave rise to multituberculates, as part of the clade Allotheria and nested within the mammalian crown-group (Zheng et al. 2013; Bi et al. 2014). Other researchers hypothesized instead that haramiyidans are basal mammaliaforms, outside crown-Mammalia, whereas multituberculates are members of the mammalian clade (Zhou et al. 2013; Luo et al. 2015) (Fig. 11.12).

Multituberculates are rodent-like forms that constitute an important component of mammaliaform assemblages from the Middle Jurassic and the remainder of the Mesozoic (Kielan-Jaworowska et al. 2004). It has been proposed that the Rhaetian witnessed the first appearance of this successful clade (Hahn et al. 1987) that survived the K-T extinction, becoming extinct only in the Eocene (Kielan-Jaworowska et al. 2004). This early record consists of a partial isolated tooth of *Mojo usuratus* (Hahn et al. 1987). The fragmentary nature of the specimen, together with the large temporal gap between this record and that of the first undisputed multituberculate in the Middle Jurassic, make the presence of this lineage in the Rhaetian uncertain (Kielan-Jaworowska et al. 2004). Another putative early record of a multituberculate, *Indobaatar zofiae*, was described from the problematic Kota Formation of India (Parmar et al. 2013).

A wide array of poorly known taxa with a reversed-triangle molar pattern is informally known as "symmetrodontans" (Fig. 11.13b). Their molariforms have been interpreted as precursors that led to the evolution of the tribosphenic pattern; however, both the "symmetrodontan" and the tribosphenic molariform structure have proven to be

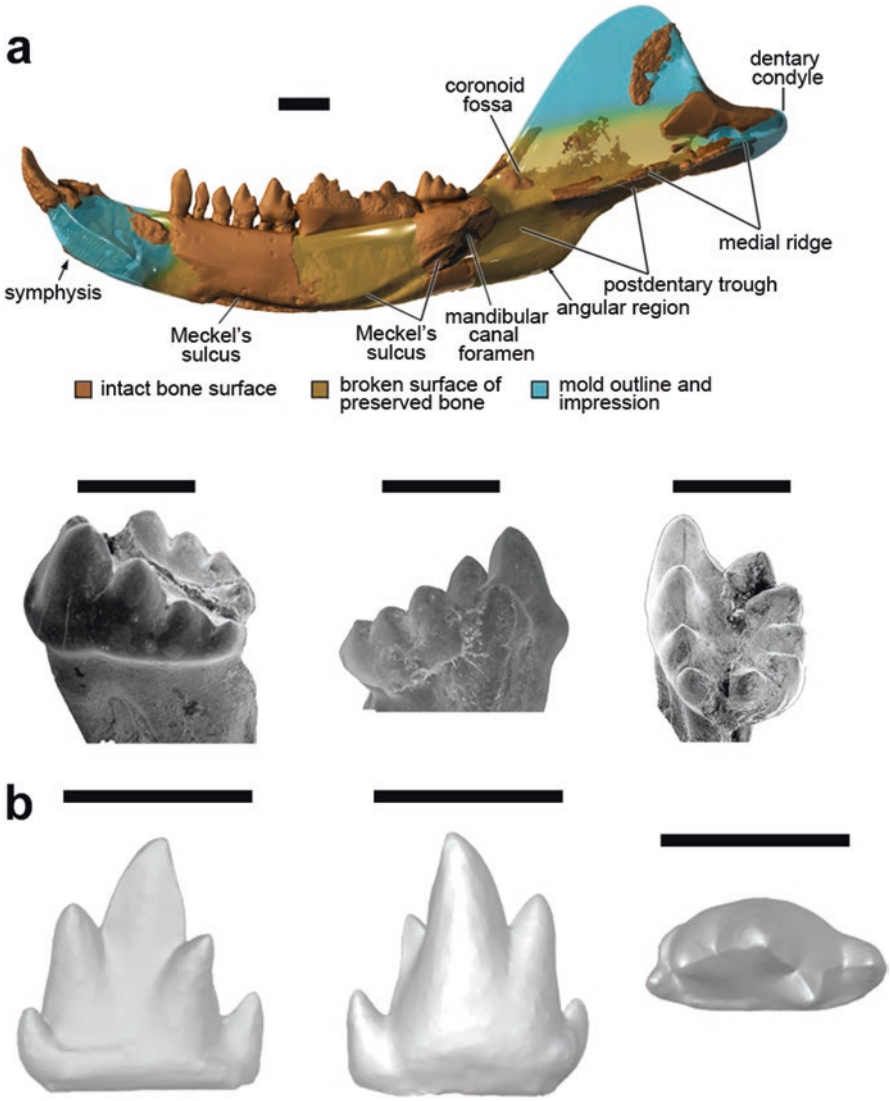

Fig. 11.13 Mammaliaformes. (**a**) Haramiyidan *Haramiyavia*. Composite reconstruction of the right lower jaw in medial view (*dark red*: original bone with intact periosteal surface; *brown*: broken surface of preserved bone or remnant of bone; *light blue*: morphologies preserved in mold outlines or clear impression). Scale bar = 5 mm. Scanning electron microscophy photographs of left lower molariform (m3) in lingual, labial, and occlusal views. Scale bar = 1 mm. (**b**) "Symmetrodontan" *Kuehneotherium*. Computed tomography scans of a right lower molariform in lingual, labial, and occlusal views. Scale bar = 1 mm. (**a**) From Luo et al. (2015), (**b**) from Conith et al. (2016)

homoplasic throughout mammaliaform phylogeny (Kielan-Jaworowska et al. 2004; Luo 2007; Davis 2011). *Kuehneotherium* is the oldest "symmetrodontan", known from the late Norian—early Rhaetian of Greenland (Jenkins et al. 1994; Clemmensen et al. 2015). This taxon is also represented by at least two species recorded in Rhaetian formations from France, Luxemburg, and the United Kingdom (Fraser et al. 1985; Sigogneau-Russell and Hahn 1994; Godefroit and Sigogneau-Russell 1995, 1999; Whiteside et al. 2016). Additionally, *Kuehneotherium* has been discovered in different quarries of Early Jurassic (Hettangian) fissure-filling deposits in the United Kingdom (Kermack et al. 1968, 1973; Säilä 2005; Gill et al. 2014; Whiteside et al. 2016). *Kuehneotherium* is regarded as a basal mammaliaform, phylogenetically nested among morganucodontans by some authors (Kielan-Jaworowska et al. 2004) but considered closely related to cladotherians by others (Rougier et al. 2007).

The passage from the Triassic to the Early Jurassic is accompanied by a relative decline in haramiyidan diversity, whereas there is an increase in the diversity of "symmetrodontans" and the first occurrence of derived "triconodonts" ("amphilestids" and eutriconodontans, *sensu* Gaetano and Rougier 2011), and australosphenidans (Fig. 11.14). *Sinoconodon*, regarded as the basalmost mammaliaform, has also been found in Early Jurassic rocks (Crompton and Sun 1985; Crompton and Luo 1993). *Thomasia* is the only recognized haramiyidan in Early Jurassic outcrops. Haramiyidans are known from the Norian to the Middle-Late Jurassic (Zheng et al. 2013; Zhou et al. 2013; Bi et al. 2014). Morganucodontans, mainly represented in Europe during the Triassic (except for the Indian *Gondwanadon*), are also well represented in Gondwana during the Early Jurassic. With 10 identified genera, morganucodontans are still major components in Early Jurassic assemblages from China, the United Kingdom, the United States, South Africa, Lesotho, and India. During the Early Jurassic, "symmetrodontans" are for the first time recognized in Gondwana, represented by six different genera; a remarkable difference when compared to the single known genus from the Triassic. However, it is important to bear in mind that *Delsatia* and *Woutersia* from the Rhaetian of France, interpreted as stem-docodontans, could also be considered as "symmetrodontans" on a morphological basis (Butler 1997; Sigogneau-Russell and Godefroit 1997; Kielan-Jaworowska et al. 2004; Luo and Martin 2007). Derived "triconodonts" were recorded in Early Jurassic outcrops from South and North America and India. This distribution suggests that the diversification of these forms was already ongoing by the end of the Early Jurassic, and should have started before the Pliensbachian. The simple plesiomorphic morphology of derived "triconodont" molariforms (labiolingually compressed tooth and mesiodistally aligned main cusps), hampers comparisons with other taxa bearing more specialized dentition. Despite a comparable basic structure of molariforms, derived "triconodonts" (Fig. 11.14a) are not nested among the morganucodontans, but in a more derived clade than docodontans, with some authors including them in the crown-group Mammalia (Luo et al. 2002, 2007; Meng et al. 2006; Luo 2007; Gaetano and Rougier 2011, 2012). Two closely related taxa that come from a single locality in Argentina are the oldest representatives of Australosphenida (Fig. 11.14b). There has been some controversy on the phylogenetic relationships of Mesozoic austra-

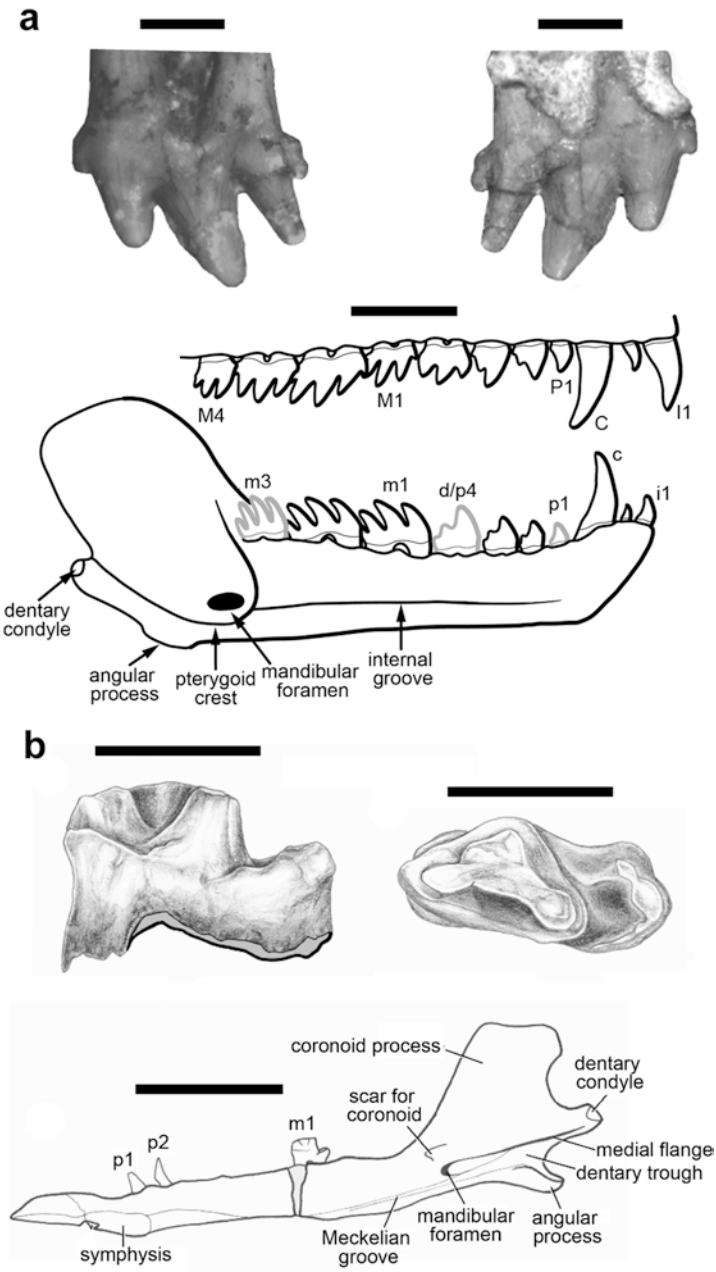

Fig. 11.14 Mammaliaformes. (**a**) "Triconodont" *Argentoconodon fariasorum*, upper left molariform (M2) of the holotype in labial and lingual views. Scale bar = 1 mm. Reconstruction of the lower jaw and upper and lower dentition in medial view (teeth in *grey* are not presently known). Scale bar = 5 mm. (**b**) Australosphenidan *Henosferus molus*, right lower molariform (m1) of the holotype in lingual and occlusal views. Scale bar = 1 mm; right lower jaw of the holotype in medial view. Scale bar = 5 mm. (**a**) from Gaetano and Rougier (2011) and (**b**) from Rougier et al. (2007)

losphenidans, which have been alternatively allied with monotremes or therians (Rougier et al. 2007). Although considered not functionally tribosphenic (Davis 2011), australosphenidans represent a Gondwanan radiation of tribosphenic-like forms (Rougier et al. 2007; Luo 2007). Their temporal and geographic distribution contradicts the traditional view that tribosphenic mammals had a single origin on the northern continents, and then moving to southern landmasses (Luo et al. 2001; Luo 2007). Moreover, the age of the oldest australosphenidans places the origin of the crown-group Mammalia (if related to monotremes) and the therian clade as early as the Early Jurassic, just a few million years after the occurrence of the first mammaliaforms.

Considering that mammaliaform ancestry has been inferred to be among South American brasilodontids (Liu and Olsen 2010; Ruta et al. 2013; Martinelli et al. 2016, 2017a) and that one of the places where the oldest known mammaliaforms (Carnian) were found is in India, it is possible that the history of the lineage that ultimately led to mammals began in Gondwana. In this scenario, *Adelobasileus* could represent a radiation into Laurasia of forms very closely related to mammaliaforms. On the other hand, what we know about the Triassic history of this clade is almost entirely a Laurasian tale. During the Norian and Rhaetian, the diversification of mammaliaforms occurred in Europe, where 16 genera and a number of additional putative different taxa have been identified in 18 localities (Table 11.1). This record is mostly represented by isolated teeth, except for a few more complete but still fragmentary discoveries (Kielan-Jaworowska et al. 2004). The fact that cynodonts are mostly found in Gondwana from Lopingian to Norian times, contrasts with their exclusive Laurasian (particularly European) record during the latest Norian and Rhaetian. In the Early Jurassic, cynodonts have a more widespread distribution. In Laurasia, they are represented in China, Europe, and North America. Additionally, the Gondwanan faunal assemblages from Africa, India, and South America have also provided cynodont remains. It is interesting to note that non-mammaliaform cynodonts and mammaliaforms have been discovered in Early Jurassic localities from Africa (South Africa and Lesotho) (Crompton 1964; Gow 1981; 1986), whereas in the remaining Gondwanan landmasses only mammaliaforms are represented.

The Early Jurassic mammaliaform faunas discussed above include a relatively rich assemblage that has been found in the Kota Formation from the Paikasigudem locality in India (Datta 1981; Yadagiri 1984, 1985; Prasad and Manhas 1997, 2002; Vijaya and Prasad 2001; Parmar et al. 2013). However, the age of this unit has been a matter of controversy. Some authors have proposed an Early Jurassic age on the basis of its fossil fish (King 1881; Robinson 1967; Jain 1973, 1980) and a pterosaur (Jain 1974). Others suggested an early Middle Jurassic age on the basis of the presence of the ostracod *Darwinula* (Govindan 1975; Misra and Satsangi 1979). More recently, comparisons of the Kota Formation faunal assemblage with that of coeval horizons and of the underlying Dharmaram Formation led to the conclusion that its age ranged from the Early Jurassic (Sinemurian) to the Middle Jurassic (?Aalenian) (Bandyopadhyay and Roychowdhury 1996; Bandyopadhyay and Sengupta 2006). On the other hand, the palynological analysis of the Upper Member of the Kota Formation showed that this was a transgressive lithological unit, deposited during the late Middle Jurassic to Early Cretaceous (Vijaya and Prasad 2001). The mammaliaform-bearing levels

(Paikasigudem locality) are interpreted as Early Cretaceous (late Hauterivian—early Barremian). According to Vijaya and Prasad (2001), this is the only locality of the Kota Formation from which a diverse microvertebrate assemblage has been recovered, including semionotid and elasmobranch fishes, sphenodontids, lizards, ornithischian and theropod dinosaurs, and mammaliaforms. This vertebrate diversity includes forms closely associated with taxa recorded in Late Jurassic or Cretaceous units (Vijaya and Prasad 2001). In this scenario, Vijaya and Prasad (2001) suggest that an Early Cretaceous age for the Paikasigudem locality levels of the Kota Formation would be more in line with the present knowledge than an Early Jurassic age.

11.3 Cynodonts and Biostratigraphy

Cynodonts have an important value as biostratigraphic markers, as similar taxa are represented in different faunas from the same or different landmasses (Abdala and Ribeiro 2010). Concerning the Late Triassic of Gondwana, forms such as the herbivorous *Massetognathus* (Fig. 11.15) and the carnivorous *Chiniquodon* are represented in the early Carnian Chañares fauna from Argentina and *Dinodontosaurus* AZ of the Santa Maria Formation in Brazil (Langer et al. 2007). *Chiniquodon* was more recently documented in faunas from Madagascar and Namibia (Abdala and Smith 2009; Kammerer et al. 2010), and an undescribed chiniquodontid with a similar dentition is also known in the *Santacruzodon* AZ of southern Brazil (Abdala et al. 2001). *Chiniquodon* is even known from the late Carnian-early Norian Ischigualasto fauna from Argentina (Bonaparte 1966; Martinez and Forster 1996; Abdala and Giannini 2002) and is thus one of the longest-lived cynodonts (Abdala and Ribeiro 2010). Recent publications reported the presence of *Aleodon* and *Scalenodon* in the *Dinodontosaurus* AZ fauna from Brazil (Martinelli et al. 2017b; Melo et al. 2017). The probainognathian *Aleodon* was previously documented in Tanzania and Namibia (Crompton 1955; Abdala and Smith 2009), whereas the traversodontid *Scalenodon* was known from Tanzania (Crompton 1955). The traversodontid *Menadon*, first reported from the Makay Formation of Madagascar, was also described for the *Santacruzodon* AZ (Flynn et al. 2000; Melo et al. 2015). This AZ was recently dated to 236.1 Ma (Philipp et al. 2013), whereas the lower levels of the Chañares Formation, with concentrations of fossils in concretions (Mancuso et al. 2014), were dated to 236.3 Ma. The non-fossiliferous top levels of this unit date to 233.7 Ma (Marsicano et al. 2016). These absolute dates point to a temporal correlation of the Santa Cruz do Sul and Chañares faunas. The traversodontid *Exaeretodon* (Fig. 11.16a) is known from the late Carnian-early Norian Ischigualasto Formation from Argentina, the Brazilian *Hyperodapedon* AZ, and the lower Maleri fauna of India (Bonaparte 1962; Chatterjee 1982; Abdala et al. 2002). Norian and Rhaetian taxa are also shared by geographically close faunas from Europe. Thus, teeth of the haramiyid *Thomasia* have been recovered from formations in Germany, France, Belgium, Luxemburg, Switzerland, and the United Kingdom (Kielan-Jaworowska et al. 2004). Sectorial toothed non-mammaliaform cynodonts are also represented in

Fig. 11.15 Chañares landscape in the Carnian. The traversodontid cynodont *Massetognathus* at the front and the proterochampsid *Chanaresuchus* behind. Art by Jorge Herrmann

different European countries. *Gaumia* is known from Luxemburg and Belgium; *Tricuspes* is documented in those countries as well as in Germany and France, and *Pseudotriconodon* from Luxemburg, Belgium, France, and perhaps the United States (Sigogneau-Russell and Hahn 1994; Godefroit and Battail 1997; Sues 2001). Taxa only represented by postcanines with a simple pattern (i.e., a single large cusp aligned with anterior and posterior accessory cusps and without a cingulum) such as *Tricuspes* and *Pseudotriconodon*, should be considered with caution until better specimens come to light. The tritylodontid *Oligokyphus* has been reported in the uppermost Triassic of Germany and eastern Canada, and the Lower Jurassic of the United Kingdom, China, and western United States (Kühne 1956; Sues 1985b; Luo and Sun 1994; Fedak et al. 2015). In the Norian, the same mammaliaform genera appear in different faunas. The iconic fossil *Morganucodon* (Fig. 11.16c) is represented by isolated teeth from the Upper Triassic of France as well as the Lower Jurassic of the United Kingdom, the United States, and China (Debuysschere et al. 2015). The best representation of this form is indeed in the United Kingdom, where hundreds of fragmentary specimens allowed for a detailed description of the taxon (Kermack et al. 1973, 1981; Jenkins and Parrington 1976). From China, a couple of nearly-complete skulls of *Morganucodon* are known (Kermack et al. 1981; Luo et al. 1995). Another Laurasian shared form is *Paceyodon* known from the Rhaetian

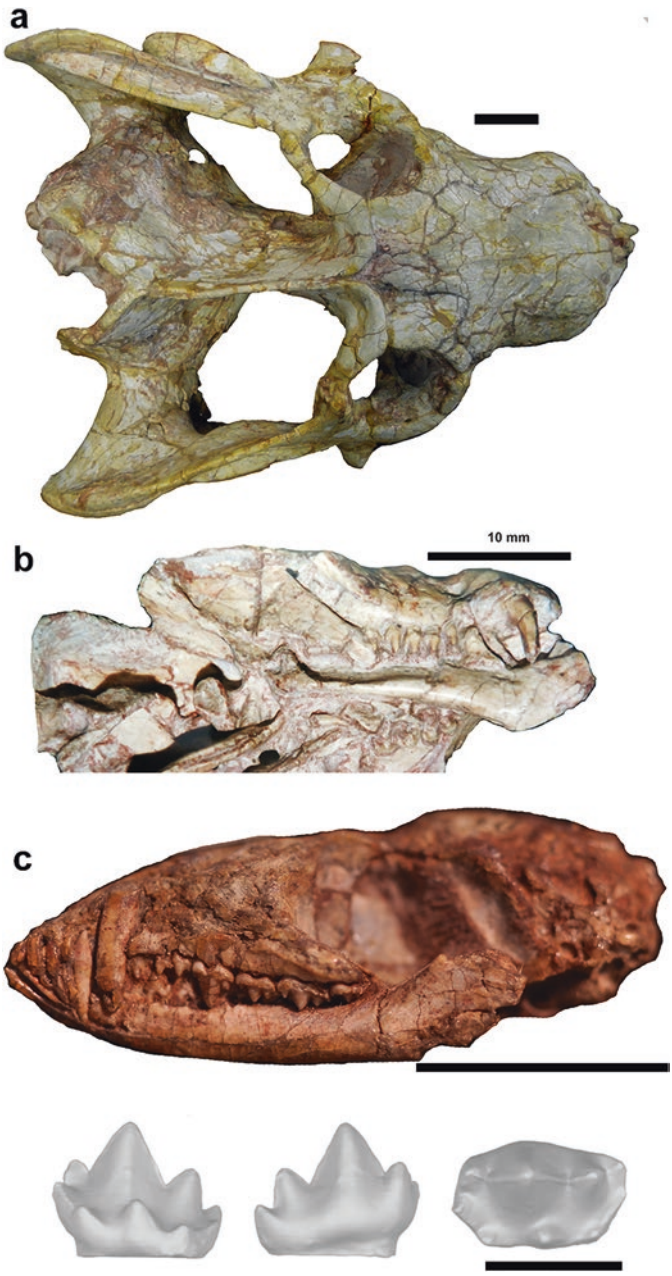

Fig. 11.16 Cynodonts and biostratigraphy. (**a**) Dorsal view of *Exaeretodon* skull (MCP 1522 PV). Scale = 30 mm. (**b**) Lateral view of *Pachygenelus* skull (BP/1/5691). Scale bar = 10 mm. (**c**) Lateral view of *Morganucodon* skull (CUP 2320) (scale bar = 10 mm) and computed tomography scans of a right lower molariform (m4) of *Morganucodon* in lingual, labial, and occlusal views (scale bar = 1 mm). Photography of skull of *Morganucodon* by Zhe-Xi Luo; *Morganucodon* tooth from Conith et al. (2016)

of France and the Early Jurassic of the United Kingdom (Debuysschere et al. 2015). The Laurasia-Gondwana connections are provided by the tritheledontid *Pachygenelus* (Fig. 11.16b), which is known from Early Jurassic localities in South Africa and Canada (Shubin et al. 1991, Sues and Olsen 2015). The mammaliaform *Paikasigudodon* is represented in the Rhaetian of France and in the questionably Lower Jurassic Kota Formation from India, and *Megazostrodon* has been reported in the Rhaetian of France and the Lower Jurassic of southern Africa (Debuysschere et al. 2015).

11.4 Late Triassic Pulses of Cynodont Diversity

In contrast with the approximately 20 taxa represented in the Anisian, mostly from southern and eastern Africa, and the one isolated record from the Ladinian of Germany, there are 68 cynodonts represented in ~35 localities in the Late Triassic, highlighting the notable gap in the Ladinian record of this group. The fauna from the Chañares Formation in Argentina and the *Dinodontosaurus* AZ from Brazil were traditionally considered Ladinian in age, but recent dating of the beds from the Chañares Formation shows they are early Carnian (Marsicano et al. 2016). In the early Carnian there are nine cynodonts recorded in faunas from Argentina and Brazil. Also in the early Carnian *Santacuzodon* AZ from Brazil and the Makay Formation from Madagascar, there are five taxa. In the late Carnian to early Norian the number of taxa increases to 17, and the diversity decreases to 12 in the late Norian. The cynodont record in the Carnian is mostly represented in Gondwana with a few exceptions such as the traversodontid *Boreogomphodon* and the mammaliaform *Adelobasileus* (Figs. 11.3, 11.7, and 11.10). A great diversification of cynodonts occurs in the Norian and Rhaetian, with 25 genera documented. The geography of cynodont Norian record shows some interesting changes, with a poor representation of traversodontids (with only two records in Gondwana and one in Laurasia; Fig. 11.3), whereas probainognathians are well represented in both subcontinents (Fig. 11.7) but mammaliaforms are only known from Laurasia at this age (Fig. 11.10). In the Early Jurassic there are 35 taxa represented (not including the record of the Kota Formation of India). The taxonomic diversity of Laurasia duplicates that of Gondwana, with non-mammaliaform cynodonts (tritylodontids and tritheledontids) only represented in southern Africa in the latter paleocontinent, and tritheledontid in the ?late Norian-?Early Jurassic *Riograndia* AZ from Brazil. The Late Triassic-Early Jurassic transition is thus represented by a temporal and geographic trend in cynodont distribution: in the Carnian, they are mostly represented in Gondwana (although the terrestrial Carnian record of Laurasia is scarce), in the Norian-Rhaetian cynodonts are distributed almost equally in Laurasia and Gondwana and by the Early Jurassic the record is clearly best represented in Laurasia (Figs. 11.3, 11.7, and 11.10).

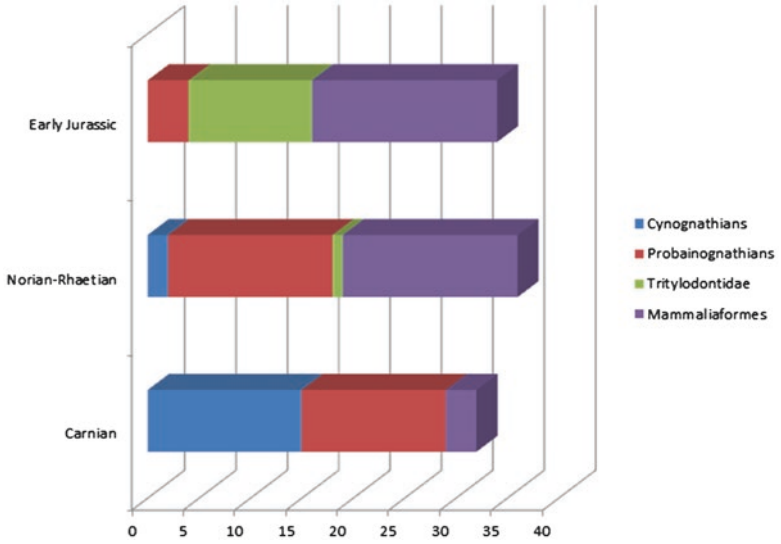

Fig. 11.17 Compared abundance of different cynodont clades during the Carnian, Norian-Rhaetian, and Early Jurassic

11.5 Taxonomic Diversity of Cynodonts and Dinosauromorphs in the Late Triassic/Early Jurassic Transition

Two lineages can be highlighted as key at the end of the Triassic for different reasons. On one hand, cynodonts represent the climax of the non-mammaliaform history of the synapsid lineage, with several groups represented and, in addition, the first members of the Mammaliaformes, whose basal representatives features some characteristic that are main landmarks in mammalian descendants (Kielan-Jaworowska et al. 2004). On the other hand, a major revolution develops in the archosaur branch of the Tree of Life, with the first records followed by a reasonably rapid diversification of the major lineages of dinosaurs (Barrett et al. 2009; Langer et al. 2010). During the Late Triassic derived cynodonts (Eucynodontia) are exemplified by the diverse and successful traversodontids, basal probainognathians, a good diversity of small tritheledontids, including the closely related brasilodontids, the first record of tritylodontids, and a moderate initial diversity of mammaliaforms. By the Early Jurassic, tritylodontid diversification is a major novelty, accompanied by the last tritheledontids and the increasing diversity of mammaliaform groups (Fig. 11.17). On the archosaur line, the Late Triassic saw the diversification and extinction of basal dinosauriforms, and the first records of the three major lineages of dinosaurs: Sauropodomorpha, Theropoda, and Ornithischia (Langer et al. 2010; Brusatte et al. 2010), with considerable diversity of the first group especially in the Norian and Early Jurassic. A comparison of taxonomic diversity of cynodonts and

dinosauromorphs during the Late Triassic-Early Jurassic transition show very close values for these groups. Cynodonts were represented by 74 taxa and dinosauromorphs by 60 in the Late Triassic, whereas the values come closer in the Early Jurassic where cynodonts are known by 41 taxa and dinosaurs by 45. Even when this quite similar taxonomic diversity, the ecological representation for each group was quite different as the major diversity at the Norian and Early Jurassic was represented by medium to large Sauropodomorpha (Barrett et al. 2009; Langer et al. 2010), whereas cynodont diversity was mostly characterized by tiny probainognathians (including mammaliaforms) and only a few medium-sized tritylodontids having a maximum skull length of ~26 cm, with a body size definitively smaller than most sauropodomorphs documented at that time.

11.6 Conclusions

The Upper Triassic was a pivotal time in the evolution of the mammalian lineage. Eucynodonts underwent a remarkable diversification, first with a good representation of herbivorous traversodontids that were particularly prosperous in Gondwana, and towards the end of the Triassic with small carnivorous members of the probainognathians. In the Early Jurassic the only non-mammaliaform cynodonts that remained diverse and abundant in some faunas were the rodent-like tritylodontids, a nearly Laurasian group that replaced the Triassic traversodontids. Mammaliaforms, first documented in the Carnian, had an unprecedented heterogeneity of morphologies at the beginning of the Jurassic, with at least nine groups showing disparate variability in dental morphology. This was indeed the time in which "mammalness" started to manifest strongly in therapsids. In the Late Triassic-Early Jurassic, the therapsid-to-archosaur transition took place, in which non-mammaliaform cynodonts started to fade away and dinosaurs started the road to their dominion for the rest of the Mesozoic.

Acknowledgments This research was possible through funds provided by the National Research Foundation of South Africa to FA, PICT 2013-2701 and PIP 11220150100760CO to LCG, and PICT 2014-1921 to V. Krapovicas. We are grateful to Lawrence Tanner for the invitation to participate in this volume. Curators and collection managers allowed access to fossil collections. Lucinda Backwell helped with language correction. Reviews by Spencer Lucas and Hans-Dieter Sues have been very helpful. Christophe Hendrickx and Zhe-Xi Luo provided digital photos of specimens. Blair McPhee generously checked the list of Late Triassic-Early Jurassic dinosauromorphs compiled by FA. This is LCG's R-221 contribution to the IDEAN.

References

Abdala F (2007) Redescription of *Platycraniellus elegans* (Therapsida, Cynodontia) from the Lower Triassic of South Africa, and the cladistic relationships of eutheriodonts. Palaeontology 50:591–618

Abdala F, Giannini NP (2000) Gomphodont cynodonts of the Chañares Formation: the analysis of an ontogenetic sequence. J Vert Paleontol 20:501–506

Abdala F, Giannini NP (2002) Chiniquodontid cynodonts: systematic and morphometric considerations. Palaeontology 45:1151–1170

Abdala F, Ribeiro AM (2010) Distribution and diversity patterns of Triassic cynodonts (Therapsida, Cynodontia) in Gondwana. Palaeogeogr Palaeoclimatol Palaeoecol 286:202–217. https://doi.org/10.1016/j.palaeo.2010.01.011

Abdala F, Smith RMH (2009) A middle Triassic cynodont fauna from Namibia and its implications for the biogeography of Gondwana. J Vert Paleontol 29:837–851

Abdala F, Ribeiro AM, Schultz CL (2001) A rich cynodont fauna of Santa Cruz do Sul, Santa Maria Formation (Middle–Late Triassic), southern Brazil. Neues Jahrb Geol P M 2001:669–687

Abdala F, Barberena MC, Dornelles J (2002) A new species of the traversodontid cynodont Exaeretodon from the Santa Maria Formation (Middle/Late Triassic) of southern Brazil. J Vert Paleontol 22:313–325

Abdala F, Damiani R, Yates A, Neveling J (2007) A non-mammaliaform cynodont from the Upper Triassic of South Africa: a therapsid Lazarus taxon? Palaeontol Afr 42:17–23

Abdala F, Martinelli AG, Soares MB, de la Fuente M, Ribeiro AM (2009) South American Middle Triassic continental faunas with amniotes: biostratigraphy and correlation. Palaeontol Afr 44:83–87

Abdala F, Marsicano CA, Smith RHM, Swart R (2013) Strengthening western Gondwanan correlations: a Brazilian Dicynodont (Synapsida, Anomodontia) in the Middle Triassic of Namibia. Gondwana Res 23:1151–1162. https://doi.org/10.1016/j.gr.2012.07.011

Bandyopadhyay S, Roychowdhury TK (1996) Beginning of the continental Jurassic in India: a palaeontological approach. Mus North Arizona Bull 60:371–378

Bandyopadhyay S, Sengupta DP (2006) Vertebrate faunal turnover during the Triassic–Jurassic transition: an Indian scenario. In: Harris JD, Lucas SG, Kirkland JD, Milner ARC (eds) Terrestrial Triassic–Jurassic transition. New Mexico Mus Nat Hist Sci Bull 37, New Mexico, pp 77–85

Barboni R, Dutra TL (2013) New "flower" and leaves of Bennettitales from southern Brazil and their implication in the age of the lower Mesozoic deposits. Ameghiniana 50:14–32

Barrett PM, McGowan AJ, Page V (2009) Dinosaur diversity and the rock record. Proc R Soc B 276:2667–2674

Battail B (1991) Les Cynodontes (Reptilia, Therapsida); une phylogenie. Bull Mus Natl Hist Nat C 13:17–105

Battail B (2005) Late Triassic traversodontids (Synapsida: Cynodontia) in southern Africa. Palaeontol Afr 41:67–80

Bi S, Wang Y, Guan J, Sheng X, Meng J (2014) Three new Jurassic euharamiyidan species reinforce early divergence of mammals. Nature 514:579–584. https://doi.org/10.1038/nature13718

Bonaparte JF (1962) Descripción del cráneo y mandíbula de *Exaeretodon frenguellii*, Cabrera, y su comparación con Diademodontidae, Tritylodontidae y los cinodontes sudamericanos. Pub Mus Mun Cien Nat Trad Mar del Plata 1:135–202

Bonaparte JF (1963) Descripción de *Ischignathus sudamericanus* n. gen. n. sp., nuevo cindonte gonfodonte del Triásico Medio Superior de San Juan, Argentina (Cynodontia-Traversodontidae). Acta Geol Lill 4:111–128

Bonaparte JE (1966) *Chiniquodon* Huene (Therapsida-Cynodontia) en el Triásico de Ischigualasto, Argentina. Acta Geol Lill 8:157–169

Bonaparte JF (1972a) *Cromptodon mamiferoides*, Galesauridae de la Formación Río Mendoza, Mendoza, Argentina (Therapsida–Cynodontia). Ameghiniana 9:343–353

Bonaparte JF (1972b) Los tetrápodos del sector superior de la Formación Los Colorados, La Rioja, Argentina (Triásico Superior). Opera Lilloana 22:1–183
Bonaparte JF, Barberena MC (2001) On two advanced carnivorous cynodonts from the Late Triassic of southern Brazil. Bull Mus Comp Zool 156:59–80
Bonaparte JF, Ferigolo J, Ribeiro AM (2001) A primitive Late Triassic 'ictidosaur' from Rio Grande do Sul, Brazil. Palaeontology 44:623–635
Bonaparte JF, Martinelli AG, Schultz CL, Rubert R (2003) The sister group of mammals: small cynodonts from the Late Triassic of southern Brazil. Rev Bras Paleontol 5:5–27
Bonaparte JF, Martinelli AG, Schultz CL (2005) New information on *Brasilodon* and *Brasilitherium* (Cynodontia, Probainognathia) from the Late Triassic of southern Brazil. Rev Bras Paleontol 8:25–46
Bonaparte JF, Schultz CL, Soares MB (2006) A new non-mammalian cynodont from the Middle Triassic of southern Brazil and its implications for the ancestry of mammals. Bull New Mex Mus Nat Hist Sci 37:599–607
Bordy E, Scisio L, Abdala F, McPhee B, Choiniere J (2017) First Lower Jurassic vertebrate burrow from southern Africa (upper Elliot Formation, Karoo Basin, South Africa). Palaeogeogr Palaeoclimatol Palaeoecol 468:362–372. https://doi.org/10.1016/j.palaeo.2016.12.024
Botha J, Abdala F, Smith R (2007) The oldest cynodont: new clues on the origin and diversification of the Cynodontia. Zool J Linnean Soc 149:477–492
Botha-Brink J, Abdala F (2008) A new cynodont record from the *Tropidostoma* Assemblage Zone of the Beaufort Group: implications for the early evolution of cynodonts in South Africa. Palaeontol Afr 43:1–6
Brusatte SL, Nesbitt SJ, Irmis RB, Butler RJ, Benton MJ, Norell MA (2010) The origin and early radiation of dinosaurs. Earth-Sci Rev 101:68–100
Butler PM (1997) An alternative hypothesis on the origin of docodont molar teeth. J Vert Paleontol 17:435–439
Butler PM, MacIntyre GT (1994) Review of the British Haramiyidae (?Mammalia, Allotheria), their molar occlusion and relationships. Phil Trans R Soc Lond 345:433–458
Chatterjee S (1982) A new cynodont reptile from the Triassic of India. J Paleontol 56:203–214
Cisneros JC (2008) Phylogenetic relationships of procolophonid parareptiles with remarks on their geological record. J Syst Palaeontol 6:345–366
Clark JM, Hopson JA (1985) Distinctive mammal-like reptile from Mexico and its bearing on the phylogeny of the Tritylodontidae. Nature 315:398–400
Clemmensen L, Milàn J, Schultz Adolfssen J, Jarl Estrup E, Frobose N, Klein N, Mateus O, Wings O (2015) The vertebrate-bearing Late Triassic Fleming Fjord Formation of central East Greenland revisited: stratigraphy, palaeoclimate and new palaeontological data. In: Kear BP, Lindgren J, Hurum JH, Milàn J, Vajda V (eds) Mesozoic Biotas of Scandinavia and its Arctic Territories, vol 434. Geological Society, Special Publications, London, pp 31–47. https://doi.org/10.1144/SP434.3
Conith AJ, Imburgia MJ, Crosby AJ, Dumont ER (2016) The functional significance of morphological changes in the dentitions of early mammals. J Roy Soc Interface 20160713. https://doi.org/10.1098/rsif.2016.0713
Crompton AW (1955) On some Triassic cynodonts from Tanganyika. Proc Zool Soc Lond 125:617–669
Crompton AW (1964) A preliminary description of a new mammal from the Upper Triassic of South Africa. Proc Zool Soc Lond 142:441–452
Crompton AW (1972) Postcanine occlusion in cynodonts and tritylodonts. Bull Brit Mus (Nat Hist) Geol 21:29–71
Crompton AW, Ellenberger F (1957) On a new cynodont from the Molteno Beds and the origin of the tritylodontids. Ann S Afr Mus 44:1–13
Crompton AW, Luo Z-X (1993) Relationships of the Liassic mammals *Sinoconodon, Morganucodon,* and *Dinnetherium*. In: Szalay FS, Novacek MJ, McKenna MC (eds) Mammal

phylogeny: mesozoic differentiation, multituberculates, monotremes, early therians, and marsupials. Springer, New York, pp 30–44
Crompton AW, Sun A-L (1985) Cranial structure and relationships of the Liassic mammal *Sinoconodon*. Zool J Linnean Soc 85:99–119
Datta PM (1981) The first Jurassic mammal from India. Zool J Linn Soc Lond 73:307–312
Datta PM (2005) Earliest mammal with transversely expanded upper molar from the Late Triassic (Carnian) Tiki Formation, South Rewa Gondwana Basin, India. J Vert Paleontol 25:200–207
Datta PM, Das DP (1996) Discovery of the oldest fossil mammal from India. India Min 50:217–222
Datta PM, Das DP (2001) *Indozostrodon simpsoni*, Gen. et sp. nov., an early Jurassic megazostrodontid mammal from India. J Vert Paleontol 21:528–534
Datta PM, Das DP, Luo Z (2004) A Late Triassic dromatheriid (Synapsida: Cynodontia) from India. Ann Carnegie Mus 73:72–84
Davis BM (2011) Evolution of the tribosphenic molar pattern in early mammals, with comments on the "dual-origin" hypothesis. J Mamm Evol 18:227–244
Debuysschere M, Gheerbrant E, Allain R (2015) Earliest known European mammals: a review of the Morganucodonta from Saint-Nicolas-de-Port (Upper Triassic, France). J Sys Palaeontol 13:825–855. https://doi.org/10.1080/14772019.2014.960486
Erwin DH (1994) The Permo-Triassic extinction. Nature 367:231–236
Fedak T, Sues H-D, Olsen PE (2015) First record of the tritylodontid cynodont *Oligokyphus* and cynodont postcranial bones from the McCoy Brook Formation of Nova Scotia, Canada. Can J Earth Sci 52:244–249. https://doi.org/10.1139/cjes-2014-0220
Flynn JJ, Parrish JM, Rakotosamimanana B, Ranivoharimanana L, Simpson WF, Wyss AR (2000) New traversodontids (Synapsida: Eucynodontia) from the Triassic of Madagascar. J Vert Paleontol 20:422–427
Fraser NC, Walkden GM, Stewart V (1985) The first pre-Rhaetic therian mammal. Nature 314:161–162
Fröbisch J (2008) Global taxonomic diversity of anomodonts (Tetrapoda, Therapsida) and the terrestrial rock record across the Permian–Triassic boundary. PLoS One 3(11):e3733. https://doi.org/10.1371/journal.pone.0003733
Gaetano LC, Rougier GW (2011) New materials of *Argentoconodon fariasorum* (Mammaliaformes, Triconodontidae) from the Jurassic of Argentina and its bearing on triconodont phylogeny. J Vert Paleontol 31:829–843
Gaetano LC, Rougier GW (2012) First amphilestid from South America: a molariform from the Jurassic Cañadón Asfalto Formation, Patagonia, Argentina. J Mamm Evol 19:235–248
Gaetano LC, Mocke H, Abdala F, Hancox PJ (2012) Complex multicusped postcanine teeth from the Lower Triassic of South Africa. J Vert Paleontol 32:1411–1420
Gaetano LC, Abdala F, Govender R (2017) The postcranial skeleton of the Lower Jurassic *Tritylodon longaevus* from southern Africa. Ameghiniana 54:1–35. https://doi.org/10.5710/AMGH.11.09.2016.3011
Gill PG, Purnell MA, Crumpton N, Robson Brown K, Gostling NJ, Stampanoni M, Rayfield EJ (2014) Dietary specializations and diversity in feeding ecology of the earliest stem mammals. Nature 512:303–305
Godefroit P (1999) New traversodontid (Therapsida, Cynodontia) teeth from the Upper Triassic of Habay-la-Vieille (southern Belgium). Paläontol Z 73:385–394
Godefroit P, Battail B (1997) Late Triassic cynodonts from Saint Nicolas de Port (northeastern France). Geodiversitas 19:567–631
Godefroit P, Sigogneau-Russell D (1995) Cynodontes et mammifères primitifs du Trias Supérieur, en region Lorraine et Luxembourgeoise. Bull Soc belge Géol 104:9–21
Godefroit P, Sigogneau-Russell D (1999) Kuehneotheriids from Saint-Nicholas-de-Port (Late Triassic of France). Geolog Belg 2:181–196
Govindan A (1975) Jurassic fresh water ostracods from the Kota limestone of India. Palaeontology 18:207–216

Gow CE (1980) The dentitions of the Tritheledontidae (Therapsida: Cynodontia). Proc R Soc Lond B 208:461–481
Gow CE (1986) A new skull of *Megazostrodon* (Mammalia: Triconodonta) from the Elliot Formation (Lower Jurassic) of southern Africa. Palaeontol Afr 6:13–23
Gow CE, Hancox PJ (1993) First complete skull of the Late Triassic *Scalenodontoides* (Reptilia, Cynodontia) from southern Africa. New Mexico Mus Nat Hist. Sci Bull 3:161–168
Grine FE (1977) Postcanine tooth function and jaw movement in the gomphodont cynodont *Diademodon* (Reptilia; Therapsida). Paleontol Afr 20:123–135
Hahn G (1973) Neue Zähne von Haramiyiden aus der Deutschen Ober-Trias und ihre Beziehungen zu den Multituberculaten. Palaeontogr Abt A 142:1–15
Hahn G, Lepage JC, Wouters G (1987) Ein Multituberculaten-Zahn aus der Ober-Trias von Gaume (S-Belgien). Bull Soc belg Géol 96:39–47
Hahn G, Lepage JC, Wouters G (1988) Traversodontiden zaehne (Cynodontia) aus der ober Trias von Gaume (Sued Belgien). Bull Inst R Sci Nat Belg Sci Terre 58:177–186
Hahn R, Hahn G, Godefroit P (1994) Zur Stellung der Dromatheriidae (Ober-Trias) zwischen den Cynodontia und den Mammalia. Geol et Palaeontol 28:141–159
Hopson JA (1971) Postcanine replacement in the gomphodont cynodont *Diademodon*. Zool J Linnean Soc 50:1–21
Hopson JA (1984) Late Triassic traversodont cynodonts from Nova Scotia and southern Africa. Palaeontol Afr 25:181–201
Hopson JA (1985) Morphology and relationships of *Gomphodontosuchus brasiliensis* von Huene (Synapsida, Cynodontia, Tritylodontoidea) from the Triassic of Brazil. Neues Jahrb Geol P M 1985:285–299
Hopson JA, Kitching JW (2001) A probainognathian cynodont from South Africa and the phylogeny of non-mammalian cynodonts. Bull Mus Comp Zool 156:5–35
Hopson JA, Sues H-D (2006) A traversodont cynodont from the Middle Triassic (Landian) of Baden-Württemberg (Germany). Paläontol Z 80:124–129
Hu Y-M, Meng J, Clark JM (2009) A new tritylodontid from the Upper Jurassic of Xinjiang, China. Acta Paleontol Pol 54:385–391. https://doi.org/10.4202/app.2008.0053
Huttenlocker AK, Sidor CA (2016) The first karenitid (Therapsida, Therocephalia) from the upper Permian of Gondwana and the biogeography of Permo-Triassic therocephalians. J Vert Paleontol 36(4):e1111897. https://doi.org/10.1080/02724634.2016.1111897
Jain SL (1973) New specimens of Lower Jurassic holostean fishes from India. Palaeontology 16:149–177
Jain SL (1974) Jurassic pterosaur from India. Geol Soc Ind 15:330–335
Jain SL (1980) The continental Lower Jurassic fauna from the Kota Formation. In: Jacobs LL (ed) Aspects of vertebrate history. Museum of Northern Arizona Press, Flagstaff, pp 99–123
Jenkins FA Jr, Parrington FR (1976) The postcranial skeletons of the Triassic mammals *Eozostrodon*, *Megazostrodon* and *Erythrotherium*. Phil Trans R Soc Lond 273:387–431
Jenkins FA Jr, Shubin NH, Amaral WW, Gatesy SM, Schaff CR, Clemmensen LB, Downs WR, Davidson AR, Bonde N, Osbaeck F (1994) Late Triassic continental vertebrates and depositional environments of the Fleming Fjord Formation, Jameson Land, East Greenland. Medd Grøn 32:3–25
Jenkins FA Jr, Gatesy SM, Shubin NH, Amaral WW (1997) Haramiyids and Triassic mammalian evolution. Nature 385:715–718
Ji Q, Luo Z-X, Yuan C-X, Tabrum AR (2006) A swimming mammaliaform from the Middle Jurassic and ecomorphological diversification of early mammals. Science 311:1123–1127
Joachimski MM, Lai X, Shen S, Jiang H, Luo G, Chen B, Chen J, Sun Y (2012) Climate warming in the latest Permian and the Permian–Triassic mass extinction. Geology 40:195–198. https://doi.org/10.1130/G32707.1
Kammerer CF (2016) A new taxon of cynodont from the *Tropidostoma* Assemblage Zone (Upper Permian) of South Africa, and the early evolution of Cynodontia. Spec Pap Paleontol 2:387–397. https://doi.org/10.1002/spp2.1046

Kammerer CF, Flynn JJ, Ranivoharimanana L, Wyss AR (2010) The first record of a probainognathian (Cynodontia: Chiniquodontidae) from the Triassic of Madagascar. J Vert Paleontol 30:1889–1894
Kammerer CF, Flynn JJ, Ranivoharimanana L, Wyss AR (2012) Ontogeny in the Malagasy traversodontid *Dadadon isaloi* and a reconsideration of its phylogenetic relationships. Fieldiana Life Earth Sci 5:112–125. https://doi.org/10.3158/2158-5520-5.1.112
Kemp TS (1980) Aspects of the structure and functional anatomy of the Middle Triassic cynodont *Luangwa*. J Zool 191:193–239
Kemp TS (1983) The relationships of mammals. Zool J Lin Soc 77:353–384
Kemp TS (2005) The origin and evolution of mammals. Oxford University Press, Oxford. 331 pp
Kermack DM, Kermack KA, Musset F (1968) The Welsh pantothere *Kuehneotherium praecursoris*. Zool J Linnean Soc 47:407–423
Kermack KA, Mussett F, Rigney HW (1973) The lower jaw of *Morganucodon*. Zool J Linnean Soc 53:87–175
Kermack KA, Musset F, Rigney HW (1981) The skull of *Morganucodon*. Zool J Linnean Soc 71:1–158
Kielan-Jaworowska Z, Cifelli R, Luo Z-X (2004) Mammals from the age of dinosaurs: origin, evolution and structure. Columbia University Press, New York
King W (1881) The geology of the Pranhita–Godavari valley. Mem Geol Surv Ind 18:151–311
Kühne WG (1956) The Liassic therapsid *Oligokyphus*. Trustees of the British Museum, London. 149 pp
Langer MC, Ribeiro AM, Schultz CL, Ferigolo J (2007) The continental tetrapod bearing Triassic of south Brazil. Bull New Mexico Mus Nat Hist Sci 41:201–218
Langer MC, Ezcurra MD, Bittencourt JS, Novas FE (2010) The origin and early evolution of dinosaurs. Biol Rev 85:55–110
Li C, Wu X-C, Rieppel O, Wang L, Zhao L (2008) An ancestral turtle from the Late Triassic of Southwestern China. Nature 456:97–501
Liparini A, Oliveira TV, Pretto FA, Soares MB, Schultz CL (2013) The lower jaw and dentition of the traversodontid *Exaeretodon riograndensis* Abdala, Barberena & Dornelles, from the Brazilian Triassic (Santa Maria 2 Sequence, *Hyperodapedon* Assemblage Zone). Alcheringia 37:331–337
Liu J, Abdala F (2014) The taxonomy and phylogeny of Traversodontidae. In: Kammerer C, Angielczyk K, Frobisch J (eds) Early evolutionary history of the synapsida. Vertebrate paleobiology and paleoanthropology series. Springer, Dordrecht, pp 255–279
Liu J, Olsen P (2010) The phylogenetic relationships of Eucynodontia (Amniota, Synapsida). J Mammal Evol 17:151–176
Liu J, Sues H-D (2010) Dentition and tooth replacement of *Boreogomphodon* (Cynodontia: Traversodontidae) from the Upper Triassic of North Carolina, USA. Vert Palasiat 48:169–184
Lucas SG, Hunt AP (1990) The oldest mammal. New Mex J Sci 30:41–49
Lucas SG, Luo Z-X (1993) *Adelobasileus* from the Upper Triassic of West Texas: the oldest mammal. J Vert Paleontol 13:309–334
Luo Z (1994) Sister-group relationships of mammals and transformations of diagnostic mammalian characters. In: Fraser NC, Sues H-D (eds) The shadow of the dinosaurs: early Mesozoic tetrapods. Cambridge University Press, Cambridge, pp 98–128
Luo Z-X (2007) Transformation and diversification in early mammal evolution. Nature 450:1011–1019
Luo Z-X, Martin T (2007) Analysis of molar structure and phylogeny of docodont genera. Bull Carnegie Mus Nat Hist 39:27–47
Luo Z, Sun A-L (1994) *Oligokyphus* (Cynodontia: Tritylodontidae) from the Lower Lufeng Formation (Lower Jurassic) of Yunnan, China. J Vert Paleontol 13:447–482
Luo Z, Wu X (1994) Small tetrapods from the Lower Lufeng Formation, Yunnan, China. In: Fraser NC, Sues H-D (eds) In the shadow of dinosaurs: early Mesozoic tetrapods. Cambridge University Press, Cambridge, pp 251–270

Luo Z, Lucas SG, Li J, Zhen S (1995) A new specimen of *Morganucodon oehleri* (Mammalia, Triconodonta) from the Liassic Lower Lufeng Formation of Yunnan, China. Neues Jahrb Geol P M 11:671–680

Luo Z-X, Cifelli RL, Kielan-Jaworowska Z (2001) Dual origin of tribosphenic mammals. Nature 409:53–57

Luo Z-X, Kielan-Jaworowska Z, Cifelli RL (2002) In quest for a phylogeny of Mesozoic mammals. Acta Palaeontol Pol 47:1–78

Luo Z-X, Chen P-J, Li G, Chen M (2007) A new eutriconodont mammal and evolutionary development of early mammals. Nature 446:288–293

Luo Z-X, Gatesy SM, Jenkins FA Jr, Amaral WW, Shubin N (2015) Mandibular and dental characteristics of Late Triassic mammaliaform Haramiyavia and their ramifications for basal mammal evolution. Proc Nat Acad Sci U S A 112:E7101–E7109. https://doi.org/10.1073/pnas.1519387112.

Mancuso AC, Gaetano LC, Leardi JM, Abdala F, Arcucci AB (2014) The Chañares Formation: a window to a Middle Triassic tetrapod community. Lethaia 47:244–265

Marsicano CA, Irmis RB, Mancuso AC, Mundile R, Chemale F (2016) The precise temporal calibration of dinosaur origins. Proc Natl Acad Sci USA 113:509–513. https://doi.org/10.1073/pnas.1512541112. PMID: 26644579

Martin T (2005) Postcranial anatomy of *Haldanodon exspectatus* (Mammalia, Docodonta) from the Late Jurassic (Kimmeridgian) of Portugal and its bearing for mammalian evolution. Zool J Linnean Soc 145:219–248

Martin T (2006) Early mammalian evolutionary experiments. Science 311:1109–1110

Martin T, Nowotny M (2000) The docodont *Haldanodon* from the Guimarota mine. In: Martin T, Krebs B (eds) Guimarota: a Jurassic ecosystem. Verlag Dr. Friedrich Pfeil, Munich, pp 91–96

Martinelli AG, Soares MB (2016) Evolution of South American non-mammaliaform cynodonts (Therapsida, Cynodontia). Contrib MACN 6:183–197

Martinelli AG, Soares MB, Schwanke C (2016) Two new cynodonts (Therapsida) from the Middle-Early Late Triassic of Brazil and comments on South American Probainognathians. PLoS One 11(10):e0162945. https://doi.org/10.1371/journal.pone.0162945

Martinelli AG, Eltink E, Da-Rosa AAS, Langer MC (2017a) A new cynodont from the Santa Maria Formation, south Brazil, improves late Triassic probainognathian diversity. Pap Palaeontol 3:401. https://doi.org/10.1002/spp2.1081

Martinelli AG, Kammerer CF, Melo TP, Paes Neto VD, Ribeiro AM, Da-Rosa ÁAS, Schultz CL, Soares MB (2017b) The African cynodont *Aleodon* (Cynodontia, Probainognathia) in the Triassic of southern Brazil and its biostratigraphic significance. PLoS One 12(6):e0177948. https://doi.org/10.1371/journal.pone.0177948

Martinez RN, Forster CA (1996) The skull of *Probelesodon sanjuanensis*, sp. nov., from the Late Triassic Ischigualasto Formation of Argentina. J Vert Paleontol 16:285–291

Martinez RN, May CL, Forster CA (1996) A new carnivorous cynodont from the Ischigualasto Formation (Late Triassic, Argentina), with comments on eucynodont phylogeny. J Vert Paleontol 16:271–284

Martinez RN, Sereno PC, Alcober OA, Colombi CA, Renne PR, Montañez IP, Currie BS (2011) A Basal dinosaur from the dawn of the dinosaur era in southwestern Pangaea. Science 331:206–210. https://doi.org/10.1126/science.1198467

Martinez RN, Fernandez E, Alcober OA (2013) A new non-mammaliaform eucynodont from the Carnian-Norian Ischigualasto Formation, northwestern Argentina. Rev Bras Paleontol 16:61–76

Matsuoka H, Kusuhashi N, Corfe IJ (2016) A new Early Cretaceous tritylodontid (Synapsida, Cynodontia, Mammaliamorpha) from the Kuwajima Formation (Tetori Group) of central Japan. J Vert Paleontol 36(4):e1112289. https://doi.org/10.1080/02724634.2016.1112289

Melo TP, Abdala F, Soares MB (2015) The Malagasy cynodont *Menadon besairiei* (Cynodontia; Traversodontidae) in the Middle–Upper Triassic of Brazil. J Vert Paleontol e1002562. doi:https://doi.org/10.1080/02724634.2014.1002562

Melo TP, Martinelli AG, Soares MB (2017) A new gomphodont cynodont (Traversodontidae) from the Middle–Late Triassic *Dinodontosaurus* assemblage zone of the Santa Maria Supersequence, Brazil. Palaeontology 60:571–582. https://doi.org/10.1111/pala.12302

Meng J, Hu Y-M, Wang Y, Wang X, Li C (2006) A Mesozoic gliding mammal from northeastern China. Nature 444:889–893

Misra RS, Satsangi PP (1979) Ostracodes from Kota Formation. Geol Surv Ind, Miscel Publ 45:81–88

Oliveira TV, Schultz CL, Soares MB (2010) *Trucidocynodon riograndensis* gen. nov. et sp. nov. (Eucynodontia), a new cynodont from the Brazilian Upper Triassic (Santa Maria Formation). Zootaxa 2382:1–71

Ottone EG, Monti M, Marsicano CA, de la Fuente MS, Naipauer M, Armstrong R, Mancuso AC (2014) A new Late Triassic age for the Puesto Viejo Group (San Rafael depocenter, Argentina): SHRIMP U–Pb zircon dating and biostratigraphic correlations across southern Gondwana. J S Am Earth Sci 56:186–199

Pacheco CP, Martinelli AG, Pavanatto AEB, Soares MB, Dias-da-Silvaa S (2017) *Prozostrodon brasiliensis*, a probainognathian cynodont from the Late Triassic of Brazil: second record and improvements on its dental anatomy. Hist Biol. https://doi.org/10.1080/08912963.2017.1292423

Parmar V, Prasad GVR, Kumar D (2013) The first multituberculate mammal from India. Naturwissenschaften 100:515–523. https://doi.org/10.1007/s00114-013-1047-0

Philipp RP, Closs H, Schultz CL, Basei M, Horn BLD, Soares MB (2013) Proveniência por U-Pb LA-ICP-MS em zircão detrítico e idade de deposição da Formação Santa Maria, Triássico da Bacia do Paraná, RS: evidências da estruturação do Arco do Rio Grande. In: VIII Symposium International on Tectonics–XIV Simpósio Nacional de Estudos Tectônicos, 2013. Anais VIII Symposium International on Tectonics–XIV Simpósio Nacional de Estudos Tectônicos, Cuiabá, Mato Grosso. pp 154–157

Prasad GVR, Manhas BK (1997) A new symmetrodont mammal from the Lower Jurassic Kota Formation, Pranhita-Godavari valley, India. Geobios 30:563–572

Prasad GVR, Manhas BK (2002) Triconodont mammals from the Jurassic Kota Formation of India. Geodiversitas 24:445–464

Ray S (2015) A new Late Triassic traversodontid cynodont (Therapsida, Eucynodontia) from India. J Vert Paleontol 35:e930472. https://doi.org/10.1080/02724634.2014.930472

Ribeiro AM, Abdala F, Bertoni RS (2011) Traversodontid cynodonts (Therapsida-Eucynodontia) from two Upper Triassic localities of the Paraná Basin, southern Brazil. Ameghiniana 48(Suppl):R111

Robinson PL (1967) The Indian Gondwana formations a review. First International Symposium on Gondwana Stratigraphy, I. U. G. S., South America, pp 201–268

Rohn R, Dutra TL, Cabral MVB (2014) Conchostráceos como evidência de níveis jurássicos na Formação Caturrita, Faxinal do Soturno, Rio Grande do Sul, Brasil. Geol USP, Sér Cient 14:3–20

Rougier GW, de la Fuente M, Arcucci AB (1995) Late Triassic turtles from South America. Science 268:855–858

Rougier GW, Martinelli AG, Forasiepi AM, Novacek MJ (2007) New Jurassic mammals from Patagonia, Argentina: a reappraisal of australosphenidan morphology and interrelationships. Am Mus Novit 3566:1–54

Rowe T (1988) Definition, diagnosis and origin of Mammalia. J Vert Paleontol 8:241–264

Rowe T (1993) Phylogenetic systematics and the early history of mammals. In: Szalay FS, Novacek MJ, McKenna MC (eds) Mammal phylogeny. Mesozoic differentiation, multituberculates, monotremes, early therians, and marsupials. Springer, New York, pp 129–145

Rubidge BS, Sidor CA (2001) Evolutionary patterns among Permo-Triassic therapsids. Ann Rev Ecol Syst 32:449–480

Ruta M, Botha-Brink J, Mitchell SA, Benton MJ (2013) The radiation of cynodonts and the ground plan of mammalian morphological diversity. Proc R Soc B 280:20131865. https://doi.org/10.1098/rspb.2013.1865

Säilä LK (2005) A new species of the sphenodontian reptile *Clevosaurus* from the Lower Jurassic of South Wales. Palaeontology 48:817–831
Schoch RR, Sues H-D (2015) A Middle Triassic stem-turtle and the evolution of the turtle body plan. Nature 523:584–587
Shubin NH, Crompton AW, Sues H-D, Olsen PE (1991) New fossil evidence on the sister-group of mammals and early Mesozoic faunal distributions. Science 251:1063–1065
Sidor CA, Hancox PJ (2006) *Elliotherium kersteni*, a new tritheledontid from the Lower Elliot Formation (Upper Triassic) of South Africa. J Paleontol 80:333–342
Sidor CA, Hopson JA (in press) *Cricodon metabolus* (Cynodontia: Gomphodontia) from the Triassic Ntawere Formation of northeastern Zambia: patterns of tooth replacement and a systematic review of the Trirachodontidae. J Vert Paleontol
Sigogneau-Russell D, Godefroit P (1997) A primitive docodont (Mammalia) from the Upper Triassic of France and the possible therian affinities of the order. C R Acad Sci 324:135–140
Sigogneau-Russell D, Hahn G (1994) Late Triassic microvertebrates from central Europe. In: Fraser NC, Sues H-D (eds) In the shadow of the dinosaurs: early Mesozoic tetrapods. Cambridge University Press, Cambridge, pp 197–213
Smith RMH, Kitching JW (1997) Sedimentology and vertebrate taphonomy of the *Tritylodon* Acme Zone: a reworked paleosol in the Early Jurassic Elliot Formation, Karoo Supergroup, South Africa. Palaeogeogr Palaeoclimatol Palaeoecol 131:29–50
Soares MB, Schultz CL, Horn BLD (2011) New information on *Riograndia guaibensis* Bonaparte, Ferigolo and Ribeiro, 2001 (Eucynodontia, Tritheledontidae) from the Late Triassic of southern Brazil: anatomical and biostratigraphic implications. An Acad Bras Cienc 83:329–354
Sues H-D (1985a) The relationships of the Tritylodontidae (Synapsida). Zool J Lin Soc 85:205–217
Sues H-D (1985b) First record of the tritylodontid *Oligokyphus* (Synapsida) from the Lower Jurassic of western North America. J Vert Paleontol 5:328–335
Sues H-D (2001) On *Microconodon*, a Late Triassic cynodont from the Newark Supergroup of eastern North America. Bull Mus Comp Zool Harvard Univ 156:37–48
Sues H-D, Fraser NC (2010) Triassic life on land: the great transition. Columbia University Press, New York. 236 pp
Sues H-D, Hopson JA (2010) Anatomy and phylogenetic relationships of *Boreogomphodon jeffersoni* (Cynodontia, Gomphodontia) from the Upper Triassic of Virginia. J Vert Paleontol 30:1202–1220. https://doi.org/10.1080/02724634.2010.483545
Sues H-D, Jenkins FA Jr (2006) The postcranial skeleton of *Kayentatherium wellesi* from the Lower Jurassic Kayenta Formation of Arizona and the phylogenetic significance of the postcranial features of tritylodontid cynodonts. In: Carrano MT, Gaudin TJ, Blob RW, Wible JR (eds) Amniote paleobiology. Perspectives on the evolution of mammals, birds and reptiles. Chicago University Press, Chicago, pp 114–152
Sues H-D, Olsen PE (2015) Stratigraphic and temporal context and faunal diversity of Permian-Jurassic continental tetrapod assemblages from the Fundy rift basin, eastern Canada. Atlantic Geol 5:139–205
Sues H-D, Hopson JA, Shubin NH (1992) Affinities of ?*Scalenodontoides plemmyridon* Hopson, 1984 (Synapsida, Cynodontia) from the Upper Triassic of Nova Scotia. J Vert Paleontol 12:168–171
Sues H-D, Olsen PE, Carter JG (1999) A Late Triassic traversodont cynodont from the Newark Supergroup of North Carolina. J Vert Paleontol 19:351–354
Swilo M, Niedzwiedzki G, Sulej T (2014) Mammal-like tooth from the Upper Triassic of Poland. Acta Palaeontol Pol 59:815–820
Tatarinov LP, Matchenko EN (1999) A find of an aberrant tritylodont (Reptilia, Cynodontia) in the Lower Cretaceous of the Kemerovo Region. Paleontol J 33:422–428
Vijaya, Prasad GVR (2001) Age of the Kota Formation, Pranhita-Godavari Valley, India: a palynological approach. J Palaeontol Soc Ind 46:77–93
von Huene F (1928) Ein Cynodontier aus der Trias Brasiliens. Cbl Min Geol Paläont Abt B 1928:251–270

Watabe M, Tsubamoto T, Tsogtbaatar K (2007) A new tritylodontid synapsid from Mongolia. Acta Palaeontol Pol 52:263–274

Whiteside DI, Duffin CJ, Gill PG, Marshall JEA, Benton MJ (2016) The Late Triassic and Early Jurassic fissure faunas from Bristol and South Wales: stratigraphy and setting. Palaeontol Pol 67:257–287

Wible JR (1991) Origin of mammalia: the craniodental evidence reexamined. J Vert Paleontol 11:1–28

Yadagiri P (1984) New symmetrodonts from Kota Formation (Early Jurassic), India. J Geol Soc Ind 25:514–621

Yadagiri P (1985) An amphidontid symmetrodont from the Early Jurassic Kota Formation, India. Zool J Linn Soc Lond 85:411–417

Zheng X, Bi S, Wang X, Meng J (2013) A new arboreal haramiyid shows the antiquity and Jurassic diversity of crown mammals. Nature 500:199–202

Zhou C-F, Wu S, Martin T, Luo Z-X (2013) A Jurassic mammaliaform and the earliest mammalian evolutionary adaptations. Nature 500:163–167

Chapter 12
Late Triassic Nonmarine Vertebrate and Invertebrate Trace Fossils and the Pattern of the Phanerozoic Record of Vertebrate Trace Fossils

Adrian P. Hunt, Spencer G. Lucas, and Hendrik Klein

Abstract The diverse ichnofaunas of the Late Triassic have been studied for almost 200 years. During the Late Triassic, facies favorable for the preservation of trace fossils were the result of low sea levels, monsoonal climates and the development of extensive depositional basins as Pangea began to fragment. The most abundant vertebrate trace fossils in the Late Triassic are tetrapod tracks, including *Brachychirotherium, Chirotherium,* "*Parachirotherium,*" *Synaptichnium, Atreipus, Grallator, Eubrontes, Banisterobates, Trisauropodiscus, Evazoum, Tetrasauropus, Pseudotetrasauropus, Eosauropus, Apatopus, Batrachopus, Rhynchosauroides, Gwyneddichnium, Procolophonichnium, Chelonipus, Brasilichnium* and *Dicynodontipus.* There are five tetrapod footprint biochrons of Triassic age that can be identified across the Pangaean footprint record. Coprolites are the second most abundant vertebrate trace fossils in the Late Triassic and include *Heteropolacopros, Alococoprus, Dicynodontocopros, Liassocoprus, Saurocoprus, Strabelocoprus, Malericoprus, Falcatocoprus* and *Revueltobromus.* Coprolites are useful in biochronology in the Late Triassic. Consumulites, dentalites (new term for bite marks), and burrows are moderately common in the Late Triassic. Nests and gastroliths are rare. All groups of vertebrate trace fossils demonstrate different diversity and abundance patterns through the Phanerozoic. Most vertebrate trace fossils have their earliest occurrences in the Devonian. The early Permian is an acme for both tracks and coprolites. The Late Triassic yields abundant tracks and coprolites, and tracks

A.P. Hunt (✉)
Flying Heritage and Combat Armor Museum, 3407 109th St SW, Everett, WA, 98204, USA
e-mail: adrianhu@flyingheritage.com

S.G. Lucas
New Mexico Museum of Natural History and Science, 1801 Mountain Road N.W., Albuquerque, NM 87104-1375, USA
e-mail: spencer.lucas@state.nm.us

H. Klein
Saurierwelt Paläontologisches Museum, Alte Richt 7, Neumarkt, D-92318, Germany
e-mail: Hendrik.Klein@combyphone.eu

© Springer International Publishing AG 2018

L.H. Tanner (ed.), *The Late Triassic World*, Topics in Geobiology 46,
https://doi.org/10.1007/978-3-319-68009-5_12

are also common in the Early Jurassic. The Jurassic and Cretaceous represent the times with the greatest diversity of vertebrate traces (tracks, coprolites, consumulites, dentalites, nests and gastroliths). The Quaternary also represents a time of vertebrate ichnological diversity (tracks, coprolites, regurgitalites, nests and burrows).

Keywords Late Triassic • Nonmarine trace fossils • Tracks • Coprolites • Bromalites • Ichnofacies • Biostratigraphy • Ichnotaxonomy

12.1 Introduction

Buckland (1829) first mentioned vertebrate trace fossils from the Late Triassic, and, subsequently this time period became recognized for its rich ichnofaunas, notably of tetrapod tracks. The primary purpose of this paper is to review the fossil record of vertebrate trace fossils from the Late Triassic. We believe that there is value in a holistic approach to the study of vertebrate trace fossils to provide context for the study of the evolution and ecology of Late Triassic faunas (cf. Hasiotis et al. 2007; Hunt and Lucas 2007b, 2016d). We also believe that there is importance in understanding the pattern of the Phanerozoic record of vertebrate trace fossils and its biases. Thus, we provide a preliminary discussion of that dataset that we hope will stimulate other workers to analyze further this important aspect of the fossil record.

12.2 Triassic World

Today, rocks of Triassic age (about 201–252 million years ago) are recognized on all of the continents (e. g., Sherlock 1948; Kummel 1979). These are mostly sedimentary rocks consisting dominantly of shallow-water carbonates of marine origin and siliciclastic red beds of nonmarine origin. These rocks represent a record of sedimentation on and around the vast Pangean supercontinent and tell the tale of its final union and the initiation of its subsequent fragmentation. The Triassic was a time of great continental emergence due to a combination of widespread epeirogenic uplift and relatively low sea-level (Embry 1988, 1997).

At the onset of the Triassic, the world's continents were assembled into a single supercontinent called Pangea. The rest of the globe comprised a single vast ocean called Panthalassa, with a westward-extending arm named Tethys. The supercontinent drifted northward and rotated clockwise throughout the Triassic, so there was considerable latitudinal spread to the landmass, which was nearly symmetrical about the equator. However, no sooner had the supercontinent been assembled than significant fragmentation began. Thus, Gondwana and Laurussia began to separate in Late Triassic time with the onset of rifting in the Gulf of Mexico basin (Lucas

2000). Most Triassic sedimentation took place in one of three types of basins: foreland, fore-arc, or extensional (Lucas and Orchard 2013). Most of the Pangean marginal basins were part of an array of arc-trench systems that surrounded much of the supercontinent. A good example is the complex Cordilleran basin of western North America, in which deposition took place between an offshore island arc and the continental margin. In the western United States portion of this basin, 1.2 km of siliciclastic red beds were shed to the northwest and interfinger with marine carbonates deposited in the arc-trench system (Lucas 2000). Of the (mostly Late Triassic) extensional basins, perhaps the best studied is the Newark basin in the eastern United States. This was a dip–slip-dominated half graben in which about 7 km of fluvial and lacustrine Upper Triassic–Lower Jurassic sediments accumulated. There were also other types of Triassic extensional basins more complex than the Newark half grabens, such as those of the Germanic basin system of northwestern Europe.

Early Mesozoic plate reorganization was apparently associated with the development of new seafloor-spreading axes, which caused a general reduction of ocean basin volume during the Triassic. Pangea was very emergent and, because of its high freeboard, the Triassic was a time of relatively low sea-level, which may be termed a first-order Pangean global lowstand (Embry 1988, 1997).

Triassic climates marked the transition from the late Paleozoic icehouse to the mid-late Mesozoic greenhouse (Tanner 2017). During the Triassic, there were no glacial ages, and there is no evidence of pack ice in the boreal or austral realms. The Triassic was thus a time of increased warmth with relatively wide subtropical dry (desert) belts at 10°–30° latitude, as attested to by the broad latitudinal distribution of Triassic evaporites. There was also strong east–west climatic asymmetry across Pangea, with eastern Pangea (at least between latitudes 40°S and 40°N) being relatively warmer and wetter because of the presence of Tethys and the absence of an Atlantic Ocean to facilitate oceanic heat exchange. With the Pangean landmass centered near the equator during the Triassic, and a prominent Tethyan bight, climate models suggest that seasonality was monsoonal. Hence, there were only two seasons, wet and dry. The abundant rainfall was concentrated in the summer months, and there was little annual temperature fluctuation.

The terrestrial trace fossil record of the Late Triassic is extensive. Low sea levels, monsoonal climates and the development of extensive depositional basins as Pangaea began to fragment during the Late Triassic all created facies in which terrestrial trace fossil preservation was favored.

12.3 Tetrapod Footprints

An extensive record of tetrapod footprints is known from many Late Triassic localities on all of the continents except Antarctica (Fig. 12.1). Here, we begin with a brief review of what we regard as the valid ichnogenera of Late Triassic tetrapod footprints. We follow with a review of the Late Triassic footprint assemblages and then put these into their biostratigraphic and ichnofacies contexts.

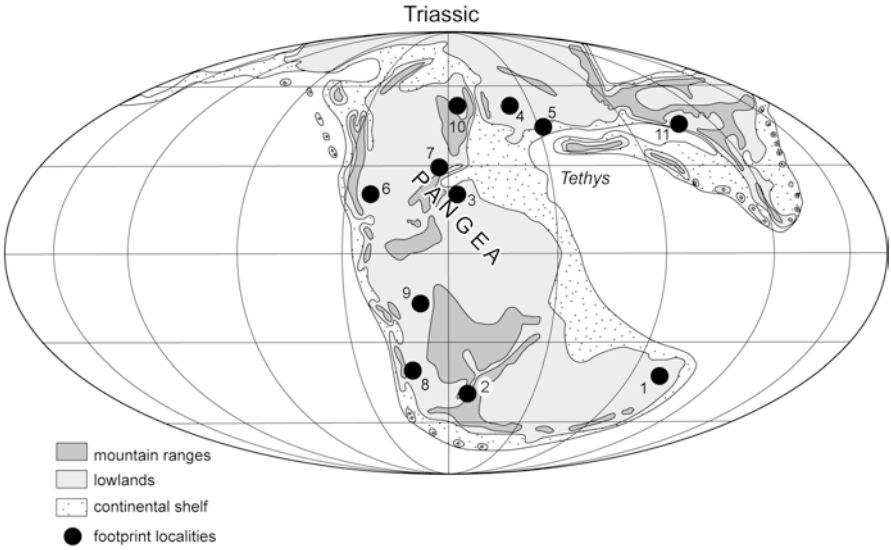

Fig. 12.1 Distribution of principal Late Triassic tracksites on Pangea (from Lucas 2007, updated). Locations are: (1) Sydney Basin, Australia; (2) Karoo Basin, South Africa; (3) Argana Basin, Morocco; (4) western Europe, (5) Italy; (6) Chinle Basin, western United States; (7) Newark Basin, New Jersey-Pennsylvania; (8) Argentina; (9) Brazil; (10) East Greenland; (11) China. Base map after Wing and Sues (1992)

12.3.1 Ichnotaxonomy

12.3.1.1 Archosaur Footprints

***Brachychirotherium* Beurlen 1950**

Type ichnospecies: *Brachychirotherium hassfurtense* Beurlen 1950.

Additional ichnospecies: *B. eyermani*, *B. thuringiacum.*

Distribution: Upper Triassic Germany, Italy, Morocco, Greenland, USA (Chinle Group, Newark Supergroup), Argentina.

Description: *Brachychirotherium* are pentadactyl, broad pes imprints with short, clumsy digits and thin, short claws (Figs. 12.2a and 12.3a–d). Digit proportions of the anterior digit group are III > II > IV > I. Digit V is preserved only as an oval basal pad posterolateral to the anterior digit group, without the phalangeal part, and laterally spread in the type ichnospecies, but, on the axis of digit IV in stratigraphically younger forms such as *Brachychirotherium parvum* (compare Fig. 12.3a with Fig. 12.3c, d). Creases between rounded phalangeal and metatarsophalangeal pads are indistinct. The manus is much smaller and of similar shape. Digits I and V in the imprints can be missing. Remarkable is the occurrence of tridactyl versions due to different substrate conditions. Rare trackways from the Chinle Group of North America show a narrow pattern with pes imprints that are slightly rotated outward (Fig. 12.4a).

Fig. 12.2 Late Triassic tetrapod footprint ichnotaxa. (**a**) *Brachychirotherium hassfurtense*, pes imprint, lectotype of Karl and Haubold (1998), from the Hassberge Formation (Carnian) of Germany. (**b**) *Parachirotherium* cf. *P. postchirotherioides*, pes manus-set from the Timezgadiouine Formation (T5, Carnian) of the Argana Basin, Morocco. (**c**) *Atreipus* isp. Pes-manus set from the Hassberge Formation (Carnian) of Germany. (**d**) *Grallator cursorious*, Redonda Formation (Norian-Rhaetian), east-central New Mexico. (**e**) *Evazoum sirigui*, artificial cast of holotype; original from Montemarcello Formation of La Spezia, Italy. (**f**) *Apatopus lineatus*, set from holotype trackway, Passaic Formation (Newark Supergroup, Norian) of New Jersey. (**g**) *Rhynchosauroides* isp. from Redonda Formation (Norian-Rhaetian) of east-central New Mexico. (**h**) *Dicynodontipus* isp. ("*Callibarichnus ajestarani*") from Vera Formation (Carnian) of Argentina. (**i**) *Gwyneddichnium majore* from Passaic Formation (Newark Supergroup, Norian) of New Jersey. I from Lucas et al. (2014)

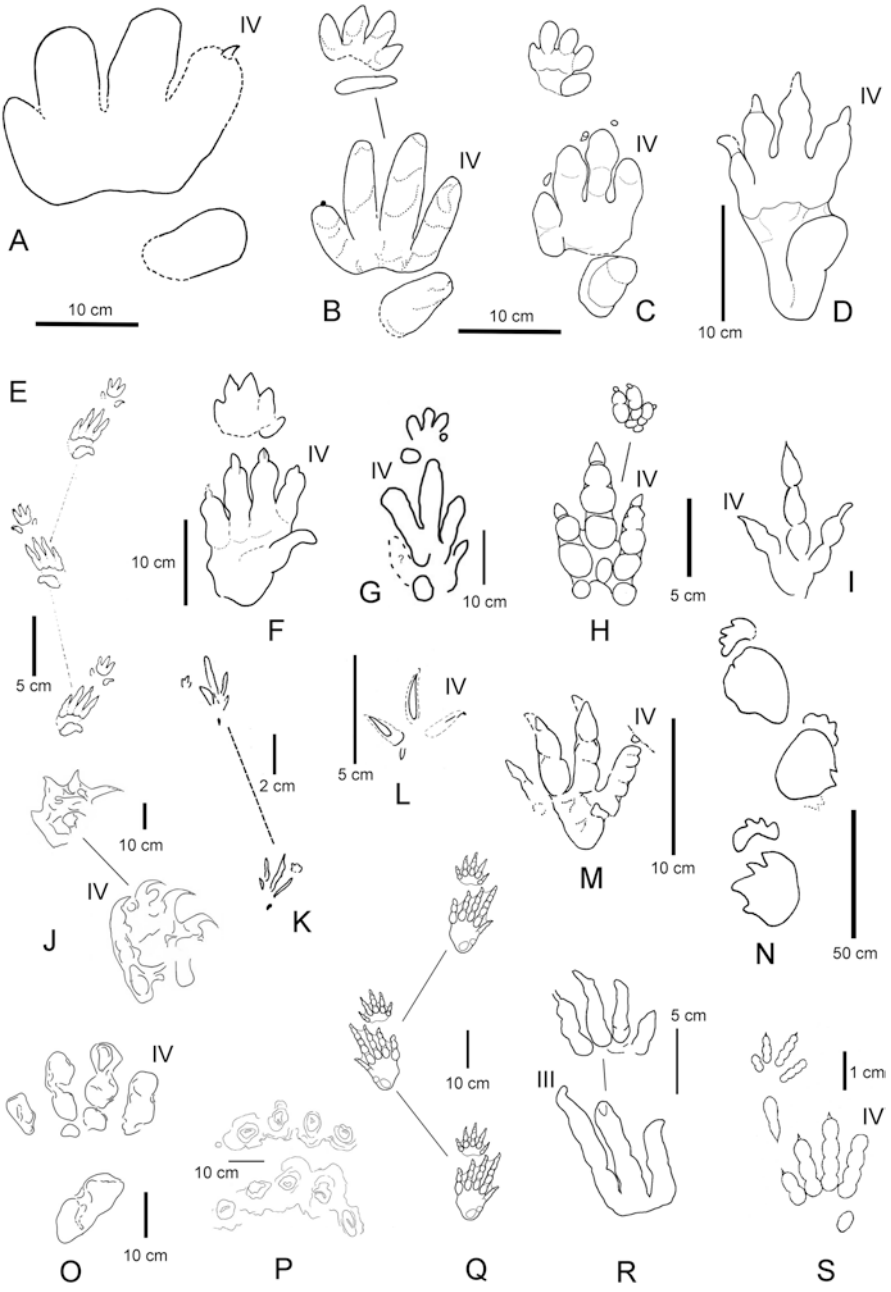

Fig. 12.3 Late Triassic tetrapod footprint ichnotaxa as sketches. (**a**) *Brachychirotherium hassfurtense*, lectotype from Hassberge Formation (Carnian) of Germany. (**b**) *B. thuringiacum*, holotype from Hassberge Formation (Carnian) of Germany. (**c**) *B. parvum*, from Passaic Formation (Norian) of New Jersey. (**d**) *B. eyermani*, holotype from Passaic Formation (Norian), New Jersey.

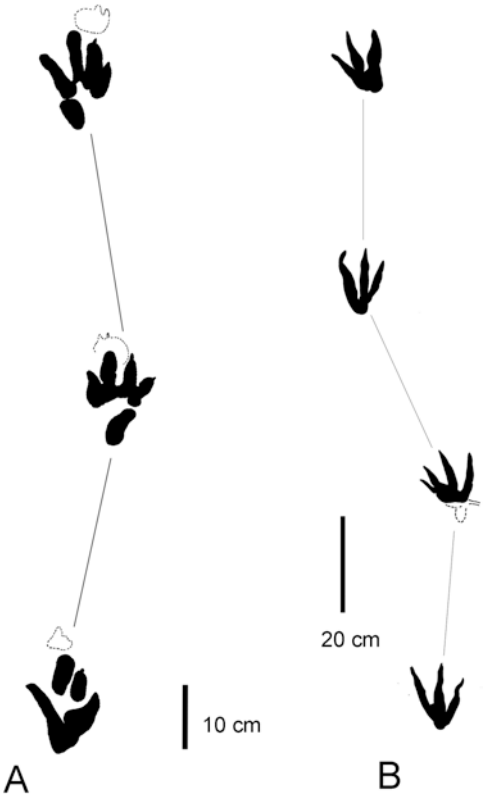

Fig. 12.4 Trackways of archosaurs from the Redonda Formation (Chinle Group, Norian-Rhaetian) of east-central New Mexico as sketches. (**a**) *Brachychirotherium parvum*. (**b**) *Evazoum sirigui*. From Lucas et al. (2010b)

Fig. 12.3 (continued) (**e**) *Chirotherium lulli*, holotype trackway from Passaic Formation (Norian) of New Jersey. (**f**) *Chirotherium wondrai*, holotype from Steigerwald Formation (Carnian) of Germany. (**g**) *Parachirotherium* cf. *P. postchirotherioides* from Timezgadiouine Formation (T5, Carnian) of the Argana Basin, Morocco. (**h**) *Atreipus milfordensis*, composite, from Passaic Formation (Norian) of New Jersey. (**i**) *Grallator* isp. from Rock Point Formation of Colorado. (**j**) *Tetrasauropus unguiferus*, pes-manus set of holotype trackway from Lower Eliott Formation (Norian-Rhaetian) of Lesotho, southern Africa. (**k**) *Banisterobates boisseaui*, holotype from Dry Fork Formation (Carnian) of Virginia. (**l**) *Trisauropodiscus aviforma*, from Lower Eliott Formation (Norian-Rhaetian) of Lesotho, southern Africa. (**m**) *Evazoum sirigui*, holotype, pes imprint from Montemarcello Formation (Carnian) of La Spezia, Italy. (**n**) *Eosauropus cimarronensis*, from Sloan Canyon Formation of New Mexico. (**o**) *Pseudotetrasauropus bipedoida*, holotype, from Lower Eliott Formation (Norian-Rhaetian) of Lesotho, southern Africa. (**p**) *Pentasauropus incredibilis*, from Lower Eliott Formation (Norian-Rhaetian) of Lesotho, southern Africa. (**q**) *Apatopus lineatus*, trackway reconstruction by Baird (1957) from Passaic Formation (Norian-Rhaetian) of New Jersey. (**r**) *Apatopus lineatus*, holotype set from Passaic Formation (Norian-Rhaetian) of New Jersey. (**s**) ?*Batrachopus*, from Passaic Formation (Norian-Rhaetian), New Jersey. After Haubold (1971b), Karl and Haubold (1998), Gaston et al. (2003), Nicosia and Loi (2003), D'Orazi-Porchetti and Nicosia (2007), Klein and Lucas (2010a), Lagnaoui et al. (2012)

Remarks: The ichnogenus *Brachychirotherium* was introduced by Beurlen in 1950 based on material from the Coburger Sandstein of the Hassberge Formation (Upper Triassic, Carnian) in Germany. Subsequently, the name was used informally by Baird (1957) and Haubold (1967, 1971a) in their classifications of chirotheriids by the term "Brachychirotherian Group" for forms with a broad sole surface and short, clumsy digits. Haubold (1971b) confirmed the validity of the ichnogenus and added small footprints of similar shape from the Lower-Upper Triassic. From the Upper Triassic he proposed the new combinations *B. parvum*, *B. eyermani* and *B. thuringiacum*. Karl and Haubold (1998), in their revision of the type material from the German Upper Triassic, recognized problems when applying the diagnosis of *Brachychirotherium* to Lower-Middle Triassic forms.

Klein and Haubold (2004) demonstrated extensive extramorphological variation of footprints of the ichnogenus *Synaptichnium* from Middle Triassic deposits of Germany, showing a transition to a very brachychirothere-like shape. They concluded that the ichnogenus should be restricted to the Upper Triassic material and that "*Brachychirotherium*" from stratigraphically older strata might represent other ichnogenera, including *Synaptichnium*. Hunt and Lucas (2007a) referred all *Brachychirotherium* material from the Upper Triassic to the ichnospecies *B. parvum*. Ichnospecies presently considered as valid by us are *B. hassfurtense* (type ichnospecies) and *B. thuringiacum* from the Carnian-Norian of Germany as well as *B. parvum* from the Newark Supergroup and Chinle Group (Carnian-Norian) of North America.

Trackmaker: *Brachychirotherium* has been attributed to crocodylian stem and crocodylomorph archosaurs. In particular, aetosaurs such as *Typothorax coccinarum* (Lucas and Heckert 2011), but also rauisuchians such as *Postosuchus* and even sphenosuchids have been discussed (Karl and Haubold 1998; Klein et al. 2006; Avanzini et al. 2010b; Lucas and Heckert 2011; Lucas et al. 2010b). The narrow trackway pattern of *Brachychirotherium*, one of the most plausible arguments against an aetosaur interpretation, has been partly refuted by demonstrating a possible narrow gauge of *Typothorax* derived from skeletal anatomy (Heckert et al. 2010; Lucas and Heckert 2011).

***Chirotherium* Kaup** 1835

***Chirotherium lulli* Baird** 1957

Distribution: Passaic Formation of Newark Supergroup, North America.

Description: Trackways with pentadactyl pes (length 4.4 cm) and manus imprints of chirotheriid shape (Fig. 12.3e). The stride length is 23.2 cm, and the pace angulation 150°. Pes and manus imprints are turned outward by 29° relative to the midline. Pes imprints long and slender. The anterior digit group shows the digit proportions III > IV > II > I and an oblique cross axis angle of 68° (Baird 1957). Digit V is positioned posterolaterally. It has an oval basal pad and a restricted phalangeal portion, which is curved backward. Acuminate claws are visible on digits I–IV. The overall shape of the pes imprint is long and slender. Phalangeal and metatarsophalangeal pads are distinct. The rounded manus, which is positioned anterior to the pes, is indistinct, but digit III seems to be the longest.

Remarks: *Chirotherium lulli* was introduced by Baird (1957) based on footprints from the Passaic Formation of the Newark Supergroup at Milford, New Jersey. The assignment of the ichnospecies to *Chirotherium* was followed by Haubold (1971a, b). However, this is presently being re-evaluated by some of the authors.

The functionally tetradactyl anterior digit group, with a robust digit I, the oblique cross axis and the strongly outward rotated orientation in the trackway, are different from all other ichnospecies of *Chirotherium*. There is a slight similarity to conservative forms from the Lower-Middle Triassic such as *Synaptichnium diabloense,* and it cannot be excluded that some *Synaptichnium*-like forms range into the Upper Triassic. This is indicated also by some isolated material from the Upper Triassic Timezgadiouine Formation of Morocco (Lagnaoui et al. 2012).

***Chirotherium wondrai* Heller** 1952

Distribution: Ansbacher Sandstein, Steigerwald Formation (Upper Triassic, Carnian), Germany.

Description: These are pentadactyl pes (up to 20 cm in length) and manus imprints of typical chirotheriid shape (Fig. 12.3f). In the pes, digit III is longest, followed by II, IV and I. Digit V has a massive oval basal pad that is extended into a broad posterior end of the track, and a thinner, slightly recurved phalangeal portion. Anterior digits I–IV are robust, with rounded pads and elongate, triangular claws. The posterior margin of the digit group I–IV is sharp and straight. The manus is rounded, showing short digits with tapering distal ends. Digit III is longest. No trackways are known thus far.

Remarks: *Chirotherium wondrai* was described by Heller (1952) from the Ansbacher Sandstein of the Steigerwald Formation (Upper Triassic, Carnian) of Germany. It is the only occurrence known. Following this author, Haubold (1971a, b) also assigned these footprints to *Chirotherium*. However, an ongoing review of the ichnogenus indicates a determination as chirotheriids *incertae sedis*. This is based on the functionally tetradactyl anterior portion of the pes with a robust digit I, whereas in *Chirotherium* the anterior pes is functionally tridactyl, and digit I is thinner than the other digits.

"*Parachirotherium*" cf. "*P.*" *postchirotherioides* (Rehnelt 1950**)**

Distribution: Benk Formation (Keuper, Middle Triassic, Ladinian) of northern Bavaria, Germany; Timezgadiouine Formation (T5, Upper Triassic, ?Carnian) of the Argana Basin, Morocco.

Description: Small to medium-sized (10–20 cm length) pentadactyl pes imprints with a pronounced, nearly symmetrical digit group II–IV in which digit III is longest and IV is slightly longer than II (Figs. 12.2b and 12.3g). Digit I is short, thin and strongly shifted posteriorly, and digit V is posterolaterally positioned and strongly reduced to an elongate oval or slightly outward-curved impression. Claws on digits I–IV are elongate triangular and sharp. The manus is small, if completely preserved, pentadactyl, with digit III longest, IV and V strongly reduced and laterally spread, and I short and thin, with small acuminate claws. Trackways have a stride length of 66 cm and a pace angulation of 170°. Manus imprints are more strongly turned outward compared with the pes imprints and relative to the midline.

Remarks: The ichnospecies was erected based on material from the Middle Triassic Benk Formation (Ladinian) of Germany by Rehnelt (1950) and described as *Dinosaurichnium postchirotherioides*. Kuhn (1958a) referred it to his new ichnogenus *Parachirotherium*. Haubold and Klein (2000, 2002) considered *Parachirotherium* as valid, however, they demonstrated that in complete trackways, these imprints show variation between pentadactyl and tridactyl (grallatorid) morphology as well as an occasional lack of the manus impression, indicating facultative bipedality of the trackmaker.

The general morphology of the pes and manus imprints match the diagnosis of the ichnogenus *Chirotherium* in the pronounced pedal digit group II–IV, with digit III being longest, and the strongly reduced and thinner digit I. Especially in *C. barthii* there are other congruent features such as the backward shift of pedal digit I and the short and laterally spread digits IV and V in the manus. Morphologically, a transition from *C. barthii* to *Sphingopus* and *Parachirotherium* morphotype imprints, sometimes being indistinguishable, has been documented from Middle Triassic deposits of Germany and Italy (Haubold and Klein 2002; Avanzini and Wachtler 2012). The only Late Triassic record of this ichnotaxon is from Morocco (Lagnaoui et al. 2012, 2016).

Synaptichnium **Nopcsa 1923**

Type ichnospecies: *Synaptichnium pseudosuchoides* 1923.

Distribution: Lower-Middle Triassic of Europe (Buntsandstein-Muschelkalk and coeval strata in Germany, France, Great Britain, The Netherlands, Spain, Italy and Poland) and North America (Moenkopi Group); Upper Triassic of Morocco.

Description: Relatively small (up to 10 cm pes length) ectaxonic pes imprints with digits increasing in length from I–IV, and digit IV being longest or subequal in length with digit III. Digit V antero-laterally directed, straight, or slightly backward curved. Manus smaller, but relatively large for chirotheriids, with digit III being longest. Sharp claws are present on digits I–IV. The single Upper Triassic specimen from Morocco is a very small, ectaxonic left pes impression, preserved with the anterior digit group I–IV (0.9 cm in length), in which digit IV is subequal in length to digit III, and there are small claw traces. Digit V and the manus imprint are missing.

Remarks: Lagnaoui et al. (2012) described an isolated occurrence as the first Late Triassic record of *Synaptichnium* from the Timezgadiouine Formation (T5, Carnian) of the Argana Basin, Morocco. The specimen is distinguished from morphologically similar *Batrachopus* by the digit proportions. In *Batrachopus*, digit III is longest (see below).

Trackmaker: Archosauriformes, either crocodylian-stem members or archosaurs more basal to the crown group.

Atreipus **Olsen and Baird** 1986

Type ichnospecies: *Atreipus milfordensis* (Bock 1952)

Distribution: Lockatong and Passaic formations of the Newark Supergroup (lithostratigraphy of Weems et al. 2016), in the Newark, Gettysburg, Dan River and Fundy basins of eastern North America; Rock Point Formation, Chinle Group of the western USA (Lucas et al. 2006a); Steigerwald and Hassberge formations (Keuper, Carnian-Norian) of Germany (Haubold and Klein 2002); Carnian of

Ardèche region, France (Courel and Demathieu 2000); Travenanzes Formation (Carnian) of northern Italy (D'Orazi-Porchetti et al. 2008); Timezgadiouine Formation (T5-T6, Upper Triassic, Carnian) of the Argana Basin, Morocco (Lagnaoui et al. 2012, 2016). Depending on the different evaluation of the ichnotaxonomy, some researchers identify *Atreipus-Grallator* plexus footprints as early as the Middle Triassic (Anisian-Ladinian) in different formations of Germany and France (Haubold and Klein 2002).

Description: Trackway of a quadruped with a relatively small (12–17 cm long), tridactyl, tulip-shaped pes in which digit III is longest and the digits are thick, with oval metatarsophalangeal pads (Figs. 12.2c and 12.3h). The manus impression is small, tridactyl or tetradactyl-pentadactyl and digitigrade.

Remarks: Without the manus impression, the pes impression of *Atreipus* would readily be assigned to *Grallator*. However, the manus is of chirothere morphology. Haubold and Klein (2000, 2002) described footprints from the Middle Triassic (Ladinian) Benk Formation, formerly assigned to "*Coelurosaurichnus,*" as *Atreipus* and proposed the plexus *Atreipus-Grallator* for trackways of facultative bipeds from this unit. The ichnogenus has a broad geographic distribution in North America in strata of Carnian-Norian age (Olsen and Baird 1986; Lucas et al. 2006a).

Trackmaker: Olsen and Baird (1986) provided a lengthy discussion of the trackmaker of *Atreipus* to conclude that it was most likely made by an early ornithischian dinosaur, a conclusion also advocated by Szajna and Hartline (2003). However, tracks of *Atreipus* have been attributed to a theropod dinosaur (e.g., Thulborn 1990), and Haubold and Klein (2000) attributed them to a dinosauromorph foot form that is a precursor to the theropod foot form of *Grallator*. Another possibility, mentioned by Lucas and Sullivan (2006), is that a dinosauriform such as *Silesaurus* (see Dzik 2003) may have been the *Atreipus* trackmaker. Probably, a dinosaur or a tetrapod close to a dinosaur (dinosauriform or dinosauromorph) made the track called *Atreipus*, even if stem-crocodylian archosaurs such as *Poposaurus* were able to produce tridactyl pes imprints similar to *Atreipus* (Farlow et al. 2014). However, *Poposaurus* was a biped and left no manus impression. Indeed, it is possible that both dinosauromorphs and dinosaurs made these tracks.

Given the absence of dinosauromorphs as body fossils after the Carnian, and the arguments of Olsen and Baird (1986), it cannot be excluded that the *Atreipus* trackmaker in the Norian of Pennsylvania documented by Lucas and Sullivan (2006) was an ornithischian dinosaur. If this is correct, then ornithischians were locally abundant during Norian time in what is now the Newark basin, refuting the suggestion of Parker et al. (2005) and Nesbitt et al. (2007), based on a reappraisal of the bone record, that there were no Triassic ornithischians in North America.

***Grallator* E. Hitchcock, 1858**

Type ichnospecies: *Grallator cursorius* E. Hitchcock, 1858

Distribution: *Grallator* is almost ubiquitous in Late Triassic tracksites of the Chinle Group in the western USA, of the Newark Supergroup in eastern North America and in western Europe (e.g., Conrad et al. 1987; Lockley and Hunt 1993, 1995, 1999; Lockley et al. 1993, 1996; Gand et al. 2000, 2005; Haubold and Klein 2000; Szajna and Hartline 2003; Gaston et al. 2003; Lockley and Eisenberg 2006;

Lucas et al. 2006b). Further occurrences are in Greenland (Milàn and Bromley 2006; Milàn et al. 2004, 2006; Gatesy et al. 1999), South America (Brazil) (Silva et al. 2008c), southern Africa (Ellenberger 1972) and China (Xing et al. 2013).

Description: Trackway of a biped with small to medium-sized (4–15 cm long) tridactyl pes impressions with slender digits and tapering claws (Figs. 12.2d and 12.3i). Digit III significantly longer than digits II and IV, which are of subequal length, thus differing from the pattern in tridactyl versions of the chirotheroid type. Phalangeal pads are often well preserved. Trackway pattern with high pace angulation (up to 175°) and stride lengths up to 117 cm in specimens of 8–9 cm pes length.

Remarks: *Grallator* is a common tetrapod footprint at most Late Triassic footprint localities.

Trackmaker: *Grallator* is widely regarded as the footprint of a relatively small theropod dinosaur such as *Coelophysis* (Olsen et al. 1998).

***Eubrontes* E. Hitchcock, 1845**

Type ichnospecies: *Eubrontes giganteus* E. Hitchcock, 1845.

Description: Trackway of a biped of relatively large size (pes >25 cm long). The pes impression is broad and tridactyl with a relatively short digit III, and a hallux that is rarely, if ever, impressed. Divarication of outer digits averages 25°–40°.

Distribution: *Eubrontes* tracks are well known from Lower Jurassic strata, especially in southern Africa, Western Europe, eastern North America and the American Southwest, and some have advocated that the lowest occurrence (LO) of *Eubrontes* corresponds to the Triassic-Jurassic boundary. However, there are well documented Late Triassic records of *Eubrontes* in Australia, southern Africa, western Europe, Greenland and North America (Lucas et al. 2006a). Indeed, the LO of *Eubrontes* in the Newark Supergroup of eastern North America, long considered to be equivalent to the base of the Jurassic, is demonstrably of Late Triassic age (Lucas and Tanner 2007a, b, 2015).

Remarks: Several authors have argued (most recently Rainforth 2005) that *Eubrontes* and the smaller *Grallator* should be the same ichnogenus, as they are only reliably distinguished on the basis of size. While we agree with this in general, we still use *Eubrontes* here because of the biostratigraphic significance that has been attached to this ichnogenus, understood as a *Grallator*-like pes imprint larger than 25 cm long. *Eubrontes* as used here, also encompasses other large grallatorid ichnotaxa from the Triassic-Lower Jurassic, such as *Kayentapus, Dilophosauripus* and *Gigandipus*, considered by some authors as distinct from *Eubrontes,* as well as several forms described under separate names from the Elliot Formation of South Africa (Ellenberger 1970, 1972, 1974). Full agreement on the synonymy of these ichnogenera has not been reached.

Trackmaker: There is virtually universal agreement that the *Eubrontes* trackmaker was a relatively large, early Mesozoic theropod dinosaur, such as the ceratosaur *Dilophosaurus*. Weems (2003) argued that a *Plateosaurus*-like prosauropod was the *Eubrontes* trackmaker, but the disparity between prosauropod foot structure and *Eubrontes* tracks is so great that we dismiss Weems's contention, as have others.

***Banisterobates* Fraser and Olsen 1996**

Type ichnospecies: *Banisterobates boisseaui* Fraser and Olsen 1996 monotypic.

Distribution: Dry Fork Member of Stockton Formation (Upper Triassic, Carnian) of Dan River Group, Virginia, USA (Fraser and Olsen 1996).

Description: The single known specimen is a trackway with three successive tetradactyl pes imprints and associated manus imprints of a very small individual (pes length 1.8–2.5 cm) (Fig. 12.3k). The stride length is 12.2 cm, and the pace angulation 146°. Imprints are moderately rotated outward relative to the midline. In the mesaxonic pes, digit I is strongly reduced, and digit III is longest. The manus is poorly preserved, showing three short digit impressions (Fraser and Olsen 1996).

Remarks: The combination of a grallatorid pes with a manus impression resembles the ichnogenus *Atreipus* (see above), however, the latter lacks a digit I impression. The presence of a distinct hallux trace justifies maintaining *Banisterobates* as a valid ichnogenus, even if a relationship of morphological peculiarities to the very small size and ontogenetic growth of the trackmaker cannot be excluded.

Trackmaker: A small dinosauromorph, either a juvenile individual or representative of a small adult species can be considered as the most probable trackmaker.

***Trisauropodiscus* Ellenberger** 1972

Type ichnospecies: *Trisauropodiscus aviforma.*

Distribution: Lower Elliot Formation (Upper Triassic) Lesotho, southern Africa.

Description: *Trisauropodiscus* are small (4–5 cm length), tridactyl-tetradactyl pes imprints of bird-like shape (Fig. 12.3l). Digit I (hallux) is partly posteriorly oriented. Digits are slender with sharp distal ends.

Remarks: Ellenberger (1972) introduced the ichnogenus based on trackways and numerous isolated imprints from the Lower Elliot Formation of Lesotho, southern Africa.

Trackmaker: The avian affinity is doubtful. The Upper Triassic age suggests a non-avian theropod with very bird-like feet.

***Evazoum* Nicosia and Loi** 2003

Type ichnospecies: *Evazoum sirigui* Nicosia and Loi 2003.

Distribution: Montemarcello Formation (Carnian) of La Spezia (Italy) (Nicosia and Loi 2003); Chinle Group (Norian-Rhaetian) of North America (Lockley and Lucas 2013; Lockley et al. 2006b; Lucas et al. 2010b); Hassberge Formation (Kieselsandstein, Carnian) of southern Germany (Haderer 2015); Fleming Fjord Formation (Norian-Rhaetian) of East Greenland (Lallensack et al. 2017).

Description: Trackways with small to medium-sized tri- and tetradactyl pes imprints (functionally tridactyl) with digit III being longest, II and IV being shorter and subequal in length or IV slightly longer than II but relatively longer relative to digit III compared with *Grallator* (Figs. 12.2e and 12.3m). Sharp claw marks are present on all digits. Digits II–IV are straight, and digit I is often curved inward. All digits show variably developed phalangeal pads. A distinct metatarso-phalangeal pad is present behind digits II and IV. Trackways have relatively large pace angulations, ranging between 140° and 170° (Fig. 12.4b).

Remarks: Nicosia and Loi (2003) described the ichnogenus *Evazoum* based on material from the Upper Triassic (Carnian) of La Lerici, Italy. These are tetradactyl imprints of a biped or facultative biped. Lockley et al. (2006b) re-assigned tri- to pentadactyl imprints and trackways of a biped from the Redonda Formation of the

Chinle Group in east-central New Mexico to this ichnogenus. The footprints from New Mexico were formerly assigned to *Pseudotetrasauropus* (see Lockley et al. 2001, 2006b; Lucas et al. 2010b), an ichnogenus known from the Upper Triassic of southern Africa (Ellenberger 1970, 1972; D'Orazi-Porchetti and Nicosia 2007). *Pseudotetrasauropus* are tetra-pentadactyl large imprints of chirothere-like shape. Trackways lack manus imprints. The trackmaker was therefore generally considered to be a biped. In contrast with these interpretations, Klein et al. (2006) considered the tracks assigned to *Evazoum* from the Redonda Formation as extramorphological variations of *Brachychirotherium*, because in some cases a transition from typical *Brachychirotherium* to *Evazoum* can be observed. For discussion of ichnotaxonomic problems resulting from these footprints and a justification of the validity of *Evazoum* see Lucas et al. (2010b).

Trackmaker: *Evazoum* is generally considered to be the footprint of a prosauropod dinosaur such as *Plateosaurus* (Lockley et al. 2006b; Lucas et al. 2010b), but see D'Orazi-Porchetti et al. (2008) for alternative interpretations.

***Eosauropus* Lockley et al. 2006**

Type ichnospecies: *Eosauropus cimarronensis* Lockley et al. 2006.

Distribution: Chinle Group (Norian-Rhaetian), North America; Upper Triassic Fleming Fjord Formation (Norian-Rhaetian), Greenland; Xujiahe Formation (Norian-Rhaetian), China.

Description: *Eosauropus* are relatively narrow trackways of a large quadruped (Fig. 12.3n). Characteristic features are strong heteropody and short steps and stride. The pes imprint has a "sauropod-like" shape. It is tetradactyl to pentadactyl, elongate, oval and shows marked claws that are strongly rotated outward. The manus is transversely elongate with four to five outwardly-rotated digit traces and with a concave posterior margin (Lockley et al. 2006a).

Remarks: The ichnogenus was introduced by Lockley et al. (2006a) based on material from the Chinle Group of New Mexico. Similar trackways were reported from China (Xing et al. 2014b). Recently, "sauropod-like" trackways described from the Upper Triassic of Greenland as *Tetrasauropus* (Jenkins et al. 1994; Lockley and Meyer 2000) were re-assigned to *Eosauropus* (Lallensack et al. 2017).

Trackmakers: *Eosauropus* is considered to be the footprint of sauropodomorphs, possibly basal sauropods.

***Tetrasauropus* Ellenberger 1972**

Type ichnospecies: *Tetrasauropus unguiferus* Ellenberger 1972.

Distribution: Lower Elliot Formation (Upper Triassic) Lesotho, southern Africa.

Description: *Tetrasauropus* are large (40–50 cm pes length) pes and manus imprints (Fig. 12.3j). These are plantigrade and tetradactyl, with strong entaxony. Trackways show the long axis of the pes nearly parallel to the midline. Prominent, strongly inward bent claws are present. The manus is smaller and has four digits. Its position is anterolateral to the pes imprint.

Remarks: The ichnogenus was erected by Ellenberger (1972) based on material from the Lower Elliot Formation of Lesotho, southern Africa. It was confirmed by D'Orazi-Porchetti and Nicosia (2007), who also re-evaluated morphologically similar tetradactyl footprints that have been described from this region under various

ichnogenus names (Ellenberger 1972; see below). Subsequently, *Tetrasauropus* was partly identified also from Upper Triassic (Norian-Rhaetian) strata of Switzerland and Greenland (Furrer 1993; Jenkins et al. 1994; Lockley and Meyer 2000; Meyer et al. 2013; Sulej et al. 2014). Their correct assignment, however, is doubtful. *Tetrasauropus* from Greenland was recently re-assigned to *Eosauropus* (Lallensack et al. 2017; see also Clemmensen et al. 2016).

Trackmaker: Sauropodomorpha have been considered as the trackmakers by most researchers (Lockley and Meyer 2000; D'Orazi-Porchetti and Nicosia 2007).

***Pseudotetrasauropus* Ellenberger 1972**

Type ichnospecies: *Pseudotetrasauropus bipedoida* Ellenberger 1972.

Distribution: Lower Elliot Formation (Upper Triassic), Lesotho, southern Africa; ?Upper Triassic, southwestern France.

Description: Large tetradactyl-pentadactyl footprints of a biped showing straight, anteriorly oriented digits with rounded distal ends (Fig. 12.3o). Digit V, if present, preserved with a basal pad only, and positioned in line with digit IV. Trackways with pes imprints being rotated inward or outward.

Remarks: Ellenberger (1972) originally described *Pseudotetrasauropus* from the Lower Elliot Formation of Lesotho (southern Africa). The ichnogenus was also identified from the Chinle Group (Late Triassic) of New Mexico (see Lucas et al. 2010b for ichnotaxonomic overview), however, specimens from this latter region were later referred to *Evazoum* (see above). Other possible occurrences are in the Upper Triassic of southwestern France (Ellenberger 1965; Ellenberger et al. 1970; Gand et al. 2000). Olsen and Galton (1984) considered *Pseudotetrasauropus* as a bipedal *Brachychirotherium*. The similarity of pes imprints with *Brachychirotherium* based on the digit proportions is remarkable, however, *Brachychirotherium* is clearly the footprint of a quadruped. D'Orazi-Porchetti and Nicosia (2007) confirmed *Pseudotetetrasauropus* as a valid ichnogenus.

Trackmaker: *Pseudotetrasauropus* is mostly interpreted as a sauropodomorph footprint.

***Pentasauropus* Ellenberger 1972**

Type ichnospecies: *Pentasauropus incredibilis* Ellenberger 1972.

Distribution: Lower Elliot Formation (Upper Triassic), Lesotho, southern Africa.

Description: Trackways of large tetrapods showing low heteropody (Fig. 12.3p). Pentadactyl pes and manus imprints preserved only as rounded distal ends of digits that are arranged in an arc-like pattern. Sometimes, a rounded sole can be observed. Trackways relatively broad with reduced pace angulation and pes and manus orientation being forward or inward.

Remarks: Ellenberger (1972) introduced *Pentasauropus* together with numerous new ichnotaxa from the Lower Elliot Formation of Lesotho, southern Africa. A re-examination by D'Orazi-Porchetti and Nicosia (2007) confirmed *Pentasauropus* as a valid ichnogenus.

Trackmaker: Considered were, for example, sauropodomorphs and therapsids (Lockley and Meyer 2000; D'Orazi-Porchetti and Nicosia 2007).

***Apatopus* Baird 1957**

Type ichnospecies: *Apatopus lineatus* (Bock 1952), monotypic.

Distribution: Passaic, Stockton and Lockatong formations (Newark Supergroup, Carnian-Norian), Chinle Group (North America); Hassberge Formation (Coburger Sst., Carnian), southern Germany; Carnian of Northern Italy and Poland; Timezgadiouine Formation (T5, Upper Triassic, Carnian) of the Argana Basin, and unnamed Carnian unit of the Ourika Basin, Morocco; Norian of Thailand.

Description: Small to medium-sized pentadactyl pes and manus imprints, mostly showing faintly impressed, indistinct phalangeal pads (Figs. 12.2f and 12.3q, r). Digits with sharp claws, often distally extended into scratches and furrows, indicating a transition to swim tracks. A few specimens with skin texture are known (Klein and Lucas 2013). Pes imprints are elongate and slender, plantigrade to semiplantigrade. In the pes imprint, digits increase in length from I–IV, and digit IV is longest or subequal in length with III. Digit IV is often faintly impressed or even missing. Digit V is straight and antero-laterally extended, posteriorly often running into a "heel." Digits with well-developed articular swellings and sharp claws. Manus pentadactyl, semiplantigrade, short, rounded and symmetrical around digit III, which is longest; position in the trackway anterior or slightly medial to the pes. Trackways show pes imprints more strongly rotated outward than the manus and a relatively low pace angulation (108°–120°) (Klein and Lucas 2013).

Remarks: The ichnogenus *Apatopus* was introduced by Baird (1957), with the type ichnospecies *A. lineatus*. The material from the Passaic Formation of New Jersey was originally described by Bock (1952) as *Otozoum lineatum*. Baird (1957) recognized the distinctive morphology, with the pes showing digits that increase in length from I to IV and with a long, straight and anterolaterally directed digit V. He also noticed the crocodylian-like overall shape of the imprints and webbing between digits. The webbing, however, could not be confirmed during the re-examination of the type material and the revision of the ichnogenus (Klein and Lucas 2013). Similar structures appeared to be extramorphological due to substrate conditions rather than anatomically based features.

Klein and Lucas (2013) also stressed the crocodylian-like overall-shape, recognizing a relationship with the semi-aquatic lifestyle of the trackmaker, which probably were phytosaurs. A distinct similarity with the shape of some chirotherian footprints (*Synaptichnium*) from the Lower-Middle Triassic was documented by these authors, who concluded that evolutionary developments reflecting a change in adaptation from terrestrial to semi-aquatic lifestyle within Phytosauria, similar to those in crocodylians, is indicated by *Apatopus*. Thus far *Apatopus lineatus* has been described from North America (New Jersey, Pennsylvania, Utah) (Baird 1957, 1986; Olsen and Huber 1998; Olsen and Rainforth 2001; Foster et al. 2000, 2003), Europe (Germany, Poland, Italy) (Dalla Vecchia 1996; Avanzini et al. 2007; Sulej et al. 2011; Klein and Lucas 2013), North Africa (Argana and Ourika basins, Morocco) (Biron and Dutuit 1981; Lagnaoui et al. 2012, 2016) and Southeast Asia (Thailand) (Le Loeuff et al. 2009). See also Klein and Lucas (2013) for an overview.

Trackmaker: *Apatopus* footprints most probably were produced by phytosaurs. This has been convincingly demonstrated by Padian et al. (2010). See also Klein and Lucas (2013). Phytosaurs, similar to modern crocodylians, had a semi-aquatic lifestyle. This explains also the rare occurence of *Apatopus* in the Triassic tetrapod footprint

record, which is obviously due to the minor preservation potential of tetrapod footprints in subaqueous environments.

***Batrachopus* Hitchcock** 1845

Type ichnospecies: *Batrachopus deweyi* (Hitchcock 1843).

Distribution: Upper Triassic-Lower Jurassic of Newark Supergroup, Upper Triassic Chinle Group and Moenave Formation, North America; ?Lower Cretaceous of southeast Asia (Thailand) (Olsen and Padian 1986; Klein and Lucas 2010b; Le Loeuff et al. 2009).

Description: *Batrachopus* are trackways of a quadruped with relatively low pace angulation (Fig. 12.3s). Pes imprints are functionally tetradactyl and digitigrade, with moderately spread digits. Digit III is longest, and digit I shortest. Digit V is reduced to an oval pad posterior to and nearly in line with digit III. The manus is pentadactyl and shows a wide digit divarication. It is strongly rotated outward relative to the pes, with digit V pointing backward.

Remarks: The overall morphology of *Batrachopus* is similar to that of chirotheres in the relatively compact anterior digit group I–IV in the pes. Contrary to chirotheres, however, pedal digit V is mostly absent or strongly reduced. Furthermore, the manus shows a larger outward rotation. Thus far, the Triassic record of this ichnogenus is restricted to specimens from the Newark Supergroup of North America (Olsen and Padian 1986). Purported occurrences in the Middle-Upper Triassic of Europe and South America have been referred to *Brachychirotherium* or have been re-dated to a younger stratigraphic age (Klein and Lucas 2010b).

Trackmaker: For Triassic *Batrachopus*, small terrestrial sphenosuchian crocodylomorphs, similar to *Terrestrisuchus* and *Hesperosuchus*, their skeletons known from Upper Triassic deposits of Europe and North America, have to be considered (Klein and Lucas 2010b).

12.3.1.2 Non-archosaur Footprints

***Rhynchosauroides* Maidwell** 1911

Type ichnospecies: *Rhynchosauroides rectipes* Maidwell 1911.

Distribution: Upper Permian, Lower-Upper Triassic, Upper Jurassic, Europe, North America, South America (Argentina, Brazil), North Africa (Morocco).

Description: Relatively broad trackways of a small quadruped with low pace angulation (70°–130°). In most cases, the pes oversteps the manus laterally, however, position of the manus anterior to the pes is also known from some trackways (Figs. 12.2g and 12.5a). This variability of the trackway pattern is obviously controlled by the velocity of movement. The pentadactyl pes imprints are digitigrade. They show long and very slender digits that increase in length from I–IV, with digit IV being the longest. Digits are often curved inward. Tiny, sharp claws are present on all digits. Digit V, if preserved, is positioned posterolateral to the other digits and short. The manus is similar in shape, but shorter and rather semi-plantigrade or plantigrade. Well-preserved specimens show rounded pads and impressions of the scales. Occasionally, tail drag marks are preserved (Haubold 1966, 1971a, b; Klein and Niedźwiedzki 2012).

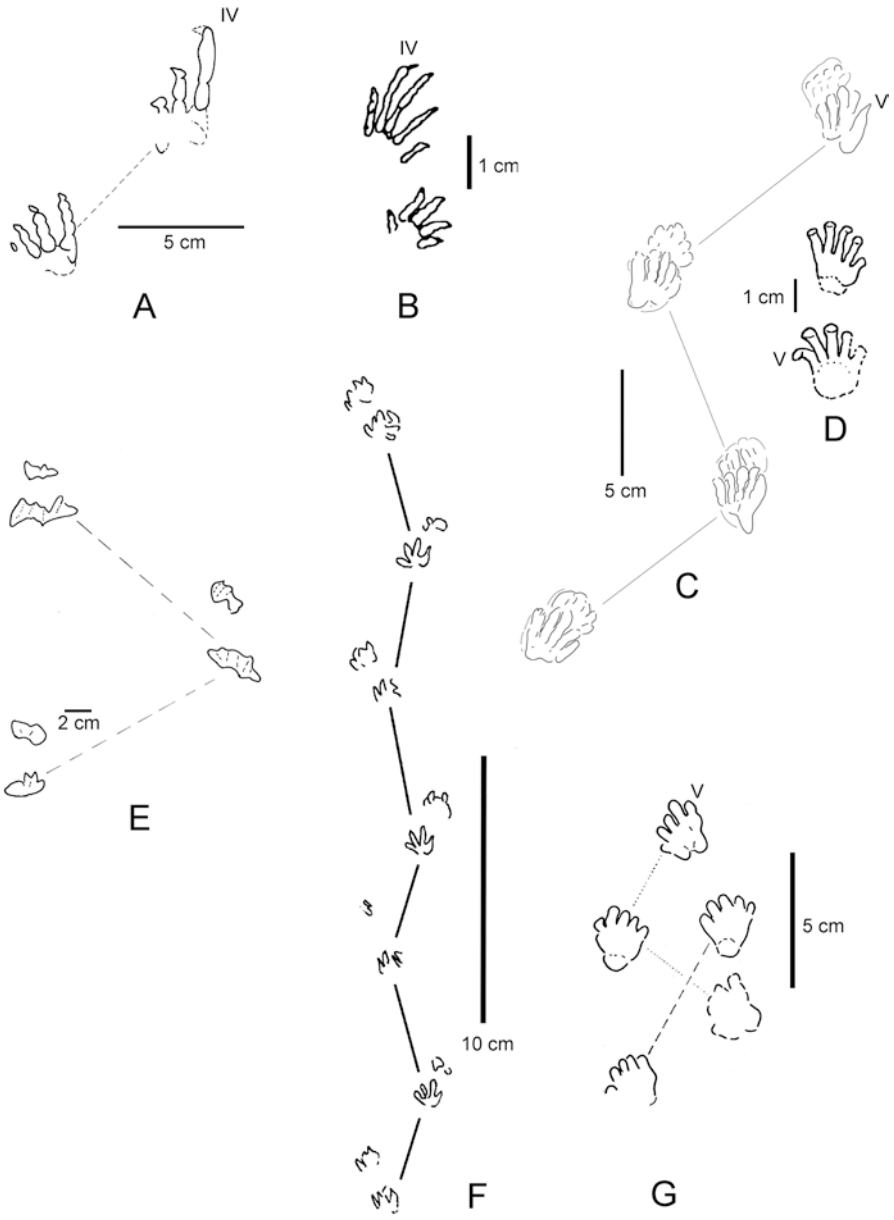

Fig. 12.5 Late Triassic tetrapod footprint ichnotaxa as sketches. (**a**) *Rhynchosauroides hyperbates* from Passaic Formation (Norian) of New Jersey. (**b**) *Gwyneddichnium majore* from Passaic Formation (Norian) of New Jersey. (**c**) *Procolophonichnium lockleyi*, holotype trackway from Hassberge Formation (Carnian) of Germany. (**d**) *Procolophonichnium* isp. from Passaic Formation (Norian) of New Jersey. (**e**) *Chelonipus torquatus* from Stuttgart Formation (Carnian) of Germany. (**f**) *Brasilichnium* isp. from Rock Point Formation (Chinle Group) of Colorado. (**g**) *Dicynodontipus* isp. ("*Gallegosichnus garridoi*") from Vera Formation (Carnian) of Argentina. From Haubold (1971b), Lockley et al. (2004), Klein and Lucas (2010a), Klein et al. (2015a, b)

Remarks: *Rhynchosauroides* footprints often occur on trampled surfaces in mass accumulations, together with scratch marks of the same trackmaker. They were originally described and named by Maidwell (1911), based on material from the Middle Triassic of Great Britain. Up to the present they have been documented from the majority of Triassic footprint assemblages in the global record, often associated with archosaur footprints such as chirotheres or grallatorids. In some marginal marine associations, for example, in the Middle Triassic tidal flat deposits of the Muschelkalk (Anisian-Ladinian) of the Germanic Basin, they are the dominant tetrapod footprints (Demathieu and Oosterink 1983; Diedrich 2008). However, in the Late Triassic they are less abundant, only occasionally being frequent, for example, at some Chinle Group localities.

Trackmaker: Contrary to the name given by Maidwell (1911), *Rhynchosauroides* cannot be attributed to rhynchosaurs, instead being the footprints of lepidosauromorph and/or archosauromorph trackmakers (Avanzini and Renesto 2002). Their long stratigraphic range, with the oldest record known from the late Permian of northern Italy (Conti et al. 1977), and the youngest from the Late Jurassic of Spain (Avanzini et al. 2010a), suggests different trackmakers with similar foot morphologies.

***Gwyneddichnium* Bock, 1952**

Type ichnospecies: *Gwyneddichnium majore* Bock, 1952

Distribution: Middle Triassic of Germany; Upper Triassic strata of the Newark Supergroup in the eastern USA (Pennsylvania and New Jersey); and the Upper Triassic Chinle Group in the western USA (New Mexico, Colorado and Utah).

Description: Footprints of a quadruped in which the manus and pes are pentadactyl and mesaxonic, the pes is substantially larger than the manus, digits are thin, long, straight to slightly curved, have nodular phalangeal pad impressions and terminate in claws (Figs. 12.2i and 12.5b). Differs from the most similar, lacertoid ichnogenus *Rhynchosauroides* in the digit proportions, with digits III > II ≥ IV > I in *Gwyneddichnium*, whereas in *Rhynchosauroides* the proportions are IV > III > II > I. Also, the digits in *Rhynchosauroides* are thicker and display a greater curvature, whereas the digits of *Gwyneddichnium* are nearly straight or only slightly curved. Digit V in *Rhynchosauroides* is strongly recurved laterally, whereas in *Gwyneddichnium* digit V is often nearly parallel to digit IV.

Remarks: The distinctiveness of *Gwyneddichnium* as an ichnogenus has never been questioned. The most similar, co-eval ichnogenus, *Rhynchosauroides,* is ectaxonic rather than mesaxonic, and differs in several features, as noted above. A peculiarity of *Gwyneddichnium* appears to be the nodular shape of the phalangeal pads in a relatively widely separated arrangement with thin interpad spaces.

Lucas et al. (2014) revised *Gwyneddichnium,* recognizing one ichnospecies (*G. majore*) as valid. Lockley et al. (1991) drew a distinction between what they considered to be walking and swimming traces of *Gwyneddichnium*. This is the distinction between trackways indicating quadrupedal progression, with separated digits and bipedal (pes only) tracks with interdigital webbing. Lockley (2006: 172) claimed that this webbing is "suggestive of an aquatic track maker." Certainly, it suggests an aquatic or amphibious habitus for the trackmaker, but it is possible to question

whether the tracks were made while swimming and should be called "swim tracks." The imprint of interdigital webbing could also be left by pressing on the substrate while walking or reflect an incomplete trackway, as only the pes impressions appear to be preserved.

The ichnogenus *Gwyneddichnium* is mostly confined to Upper Triassic strata of the Newark Supergroup (eastern USA) and the Chinle Group (American Southwest). It is widely recognized as a characteristic ichnotaxon of Late Triassic tetrapod footprint ichnoassemblages (e.g., Lucas 2007). A single occurrence in the Germanic Basin of Germany extends its temporal range back to the Middle Triassic (Lucas et al. 2014). This is in congruence with the occurrence of tanystropheids, a candidate trackmaker known from body fossils from Middle and Upper Triassic deposits (see below).

Trackmaker: Originally, Bock (1952: 418) inferred that *Gwyneddichnium* was likely made by a trackmaker that was "probably close to the small pseudosuchians." Haubold (1986) adopted a similar, rather generalized position, inferring that the trackmaker was an undifferentiated pseudosuchian or ornithosuchian. Description of "*Tanytrachelos*" (a synonym of *Gwyneddosaurus*) from the Newark Supergroup by Olsen (1979) based on extensive and articulated material, provided a plausible trackmaker for *Gwyneddichnium.* As Olsen and Flynn (1989) argued, the morphology of the feet of "*Tanytrachelos*" is an excellent match for the footprints assigned to *Gwyneddichnium*.

Lockley (2006) noted that Colbert and Olsen (2001) had implied that drepanosaurs could be possible trackmakers of *Gwyneddichnium* because the body fossils of this group are more common than those of "*Tanytrachelos*." However, given an extensive review of drepanosaur anatomy by Renesto et al. (2010), this suggestion now seems unlikely.

***Procolophonichnium* Nopcsa 1923**

Type ichnospecies: *Procolophonichnium nopcsai* Kuhn 1963.

Distribution: Late Permian, Early Triassic–Late Triassic of South Africa, North Africa, France, Germany, The Netherlands, northern Italy and Poland. In the Upper Triassic, in particular, in the Hassberge Formation (Carnian) of Germany and in the Passaic Formation (Norian) of New Jersey.

Description: *Procolophonichnium* are small (1.5–3.5 cm pes length), pentadactyl, semi-plantigrade to plantigrade footprints of small quadrupedal tetrapods (Fig. 12.5c, d). In both pes and manus, digits increase in length from I–IV, with digit IV being subequal in length with digit III, and digit V subequal in length with digit II. The manus is slightly smaller than the pes and positioned anterior to the latter. Sometimes, the manus is overprinted by the pes at the posterior end. Trackways of Late Triassic forms (3.0 cm pes length) have a pace angulation of 91°–110° and strides of 15–20 cm. In these, both pes and manus imprints are rotated inward relative to the midline, and digits are subparallel, with robust rounded pads and tiny claws. An elongate heel is a particular feature of *Procolophonichnium lockleyi*.

Remarks: The ichnogenus was originally described based on material from ?Lower Triassic deposits of South Africa (von Nopcsa 1923; Kuhn 1963; Klein et al. 2015a, b). Middle Triassic representatives from the Germanic Basin have been

described from abundant material (Demathieu and Oosterink 1983; Klein et al. 2015a, b). Upper Triassic *Procolophonichnium* isp. was described by Baird (1986) from the Passaic Formation (Newark Supergroup) of New Jersey. Klein et al. (2015a, b) introduced a new ichnospecies, *Procolophonichnium lockleyi,* based on longer trackways from the Hassberge Formation (Carnian) of southern Germany.

Trackmaker: Procolophonids or therapsids (Klein et al. 2015a, b).

Chelonipus Rühle von Lilienstern 1939

Type ichnospecies: *Chelonipus torquatus* Rühle von Lilienstern, 1939

Distribution: Known from the Early Triassic of Wyoming and Utah (USA), from the Middle and Late Triassic of Germany and possibly the Late Triassic of Spain (Lichtig et al. 2017).

Description: Tracks of a quadruped that are always nearly in parallel rows, with the manus and pes tracks of one side of the body forming nearly straight lines, one following the other in an understep ranging from an extreme, full understep by which the fore foot is overstepped by the hind foot of the next cycle of steps, to a more standard understep walk in which the hind foot is placed just behind the fore foot of the same series of steps. The broad, arched manus has the longest digit being digit III or IV, and the pes often has a rounded plantar surface and relatively longer digits compared to the manus (Fig. 12.5e).

Remarks: The extreme understep walk of turtles is likely the basis for the variation in turtle tracks given the name *Chelonipus plieningeri* (Haubold 1971a). As such, *C. plieningeri* is best considered a synonym of *C. torquatus* based on extramorphological/gait variation (Lichtig et al. 2017).

In *Chelonipus,* the correct identification of pes and manus imprints has been debated. While Rühle von Lilienstern (1939), in his first description of *C. torquatus,* considered the anterior imprint of a set as the pes overstepping the manus, this was questioned and re-interpreted by Haubold (1971a, b) as a reverse arrangement, with the manus being continuously positioned anterior to the pes. In contrast, Avanzini et al. (2005) followed Rühle von Lilienstern (1939) based on experiments with recent forms, and Lichtig et al. (2017) endorse the conclusion that the *C. torquatus* type trackway shows the pes overstepping the manus.

Lichtig et al. (2017) have recently revised and reviewed *Chelonipus*. The only Late Triassic records are the type of *C. plieningeri*, based on a trackway from the Upper Triassic Middle Keuper (Stuttgart Formation) of Feuerbacher Heide near Stuttgart in southwestern Germany. Originally described by Plieninger (1838) and Meyer and Plieninger (1844), it was incorrectly attributed to a coelurosaurian dinosaur by von Huene (1932). A further Late Triassic record comes from the Keuper (Upper Triassic) of Spain (Márquez-Aliaga et al. 1999). This is a single track and of uncertain origin, but Avanzini et al. (2005) and Lichtig et al. (2017) suggest that a turtle was the most likely trackmaker.

Trackmaker: A *Proganochelys*-like turtle (Lichtig et al. 2017).

Brasilichnium **Leonardi** 1981

Type ichnospecies: *Brasilichnium elusivum* Leonardi 1981.

Distribution: Upper Triassic-Lower Jurassic of North America (Chinle Group, Wingate, Moenave and Navajo formations) and ?Upper Triassic of southern Africa (Elliot Formation, Stormberg Group) Jurassic-Cretaceous (Botucatu Formation) of Brazil.

Description: Small footprints of a quadrupedal tetrapod that show a distinctive size difference between the smaller manus and the larger pes impressions (Fig. 12.5f). Imprints are tetradactyl. The pes is semiplantigrade, wider than long and ectaxonic. Digits are short and rounded, digit V of the pes being laterally separated from the other digits.

Remarks: The ichnogenus *Brasilichnium* was originally described from the Jurassic-Cretaceous Botucatu Formation of the Paraná Basin, Brazil, by Leonardi (1981) and has more recently been revised by Fernandes and Carvalho (2008). From the Upper Triassic, trackways are known from the Redonda Formation (Chinle Group) and from the lower Wingate Formation of New Mexico and Colorado, respectively (Klein et al. 2006; Lockley et al. 2004; Lucas et al. 2010b). Other *Brasilichnium* records may be partly hidden in the material of Ellenberger (1972, 1974, 1975) from the Stormberg Group of southern Africa.

Trackmaker: Non-mammalian and/or basal mammalian synapsids.

***Dicynodontipus* Rühle v. Lilienstern** 1944

Type ichnospecies: *Dicynodontipus geinitzi* (Hornstein 1876).

Distribution: Upper Permian of northern Italy, Lower-Middle Triassic of Germany, Poland, Italy, Upper Triassic (Carnian) of Argentina (Conti et al. 1977; Haubold 1971a; Marsicano and Barredo 2004; Melchor and De Valais 2006; Klein and Niedźwiedzki 2012).

Description: The best-preserved specimens from the Vera Formation (Carnian) of Argentina are small pentadactyl pes and manus imprints of similar shape, 3.6–5.5 cm in length and 3.5–4.3 cm in width, and some are smaller (Melchor and De Valais (2006). They show short digit impressions and a large subcircular to subtriangular sole (Figs. 12.2h and 12.5g). The manus is slightly smaller than the pes. Claws are often absent or indistinctly preserved. The sole is separated from the digits by a distinct crease. Trackways have a pace angulation of 95°–150° (Melchor and De Valais 2006).

Remarks: Different names have been introduced for this footprint morphology, especially for the material from Argentina: *Gallegosichnus, Calibarichnus*, *Palaciosichnus*, and *Stipanicichnus* (Casamiquela 1964, 1975). These ichnogenera were synonymized with *Dicynodontipus* by Melchor and De Valais (2006). Domnanovich and Marsicano (2006) list the names of Casamiquela (1964, 1975) in quotation marks, whereas Domnanovich et al. (2008) describe these as valid ichnotaxa. Presently, strong similarities with *Dicynodontipus* lead us to follow Melchor and De Valais (2006). The presence of different ichnotaxa cannot be excluded completely, however, but presently their distinction is based on weak evidence, and the supposed distinctive features are probably extramorphological, not anatomical.

Trackmaker: *Dicynodontipus* are generally considered as the footprints of therapsid synapsids (Haubold 1971a, b).

12.3.2 Footprint Ichnoassemblages

12.3.2.1 North America

In western North America, Late Triassic tetrapod footprint assemblages are widely distributed in deposits of the Chinle Group, in particular in the Rock Point, Sloan Canyon and Redonda formations, and in the lower Wingate Formation (Wingate Sandstone) of the southwestern United States in Colorado, Utah, Arizona and New Mexico (e.g., Lucas et al. 2006a). On the northern Colorado Plateau, the Rock Point Formation near Dinosaur National Monument yielded *Brachychirotherium parvum*, *Apatopus lineatus*, *Eosauropus cimarronensis*, *Evazoum sirigui*, *Grallator* isp., *Rhynchosauroides* isp., *Gwyneddichnium majore* and small, mammal-like tracks (Lockley et al. 1992; Lockley and Hunt 1995; Lucas et al. 2014). The Rock Point Formation and partly the lower Wingate Formation (Wingate Sandstone) above the Chinle Group near Gateway, Colorado, have provided archosaur footprints, including the theropod ichnogenus *Grallator*, as well as *Brachychirotherium parvum*, *Eosauropus cimarronensis* and *Evazoum gatewayensis*, the latter being attributed to sauropodomorphs. Non-archosaur footprints are known by small lacertoid *Rhynchosauroides* and by *Brasilichnium*, which are considered to have been made by lepidosauromorphs/archosauromorphs and mammal-like forms, respectively (Gaston et al. 2003; Lockley et al. 2004; Lockley and Lucas 2013; Lucas et al. 2006a, b).

Other assemblages come from the Rock Point Formation in the Glen Canyon area in southern Utah, with *Atreipus* isp. (Lockley et al. 1998); from the Sloan Canyon Formation at Peacock Canyon and Sloan Canyon in northern and northeastern New Mexico, including the type of *Eosauropus cimarronensis* (Lockley and Hunt 1993, 1995; Lockley et al. 2001; Hunt and Lucas 2003); and from the Redonda Formation in east-central New Mexico (Hunt et al. 1989a, 1993a, 2000, 2001; Lockley et al. 2000, 2006a, b; Hunt and Lucas 2007a, b; Klein et al. 2006; Lucas et al. 2001, 2010b). The Redonda Formation has yielded a rich tetrapod ichnofauna (Fig. 12.6a–e). Most abundant are *Brachychirotherium parvum*, *Evazoum sirigui* and *Grallator cursorius*. Less frequent are *Rhynchosauroides* isp., *Gwyneddichnium majore* and *Brasilichnium elusivum*. There are numerous other Late Triassic tracksites in Wyoming, Colorado, southern and eastern Utah, Arizona, New Mexico, Oklahoma and Texas (e.g., Foster et al. 2000, 2003; Hunt and Lucas 2001, 2006b, 2007c; Lockley and Eisenberg 2006; Lockley and Milner 2006; see also Lockley and Hunt 1995 and Hunt and Lucas 2007a for overviews). In western North America, the oldest Late Triassic record comes from the Garita Creek Formation of New Mexico and is late Carnian in age (Hunt and Lucas 2001).

In the eastern part of North America, the great rift basins with deposits of the Newark Supergroup (Triassic-Jurassic) have yielded rich Late Triassic tetrapod ichnofaunas, especially from the Stockton, Lockatong and Passaic formations in the Newark Basin of New York, New Jersey and Pennsylvania, the Stockton Formation of the Deep River Basin of North Carolina, the Dan River Basin of Virginia and North Carolina, and the Wolfville Formation in the Fundy Basin of Nova Scotia, Canada (the Newark Supergroup lithostratigraphy used here follows Weems et al. 2016).

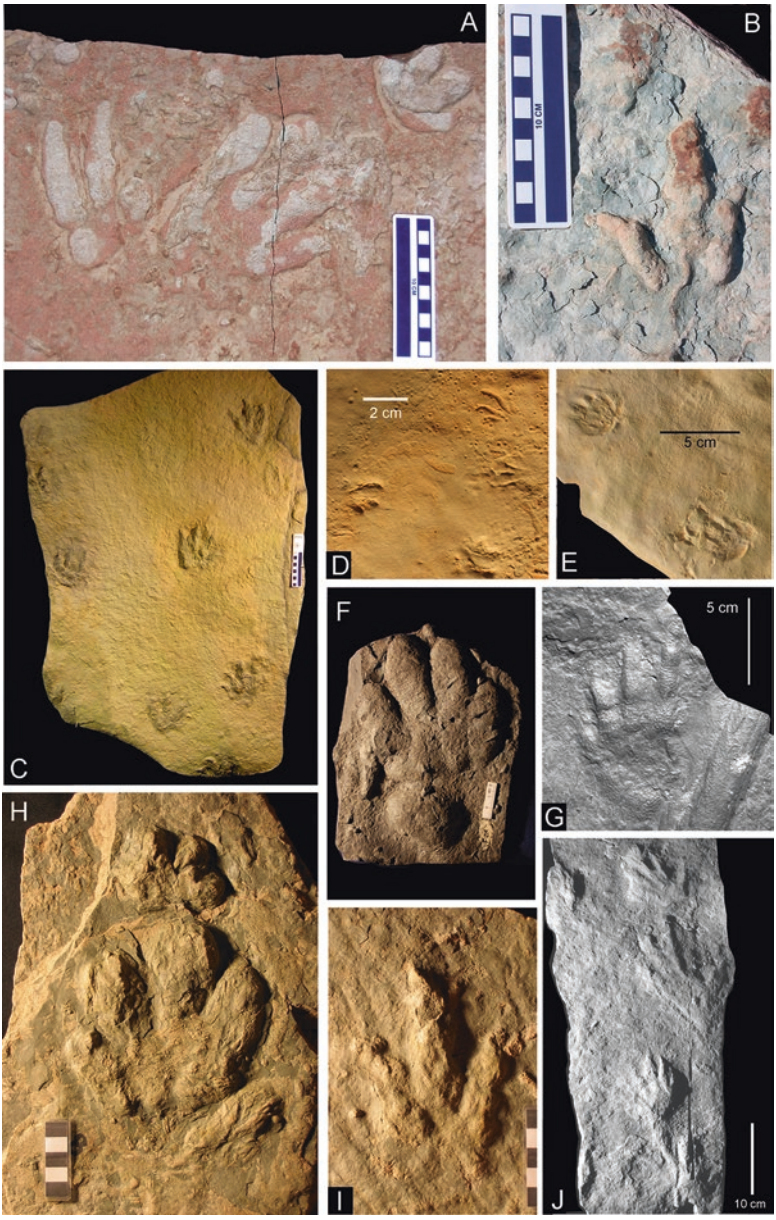

Fig. 12.6 Characteristic Late Triassic tetrapod footprint assemblages. (**a**–**e**) Redonda Formation (Norian-Rhaetian) of Mesa Redonda and Apache Canyon, east central New Mexico. (**f**, **g**) Passaic Formation (Newark Supergroup, Norian-Rhaetian) of eastern North America. (**h**–**j**). Hassberge Formation (Carnian) of Germany. (**a**) *Brachychirotherium parvum* pes-manus set (*right*), *Evazoum sirigui* (*left*). (**b**) *Grallator cursorius*. (**c**). *Evazoum sirigui* artificial cast with trackways. (**d**) *Rhynchosauroides* isp. (**e**) *Brasilichnium elusivum* artificial cast. (**f**) *Brachychirotherium parvum*. (**g**) *Apatopus lineatus*. (**h**) *Brachychirotherium thuringiacum*. (**i**) *Atreipus-Grallator* isp. (**j**) *Apatopus lineatus*. From Klein et al. (2006), Lucas et al. (2010b), Klein and Lucas (2013)

From the Passaic Formation, the classical assemblages of Bock (1952) and Baird (1954, 1957) are well known with *Brachychirotherium parvum*, *B. eyermani*, *Chirotherium lulli*, *Apatopus lineatus*, *Atreipus milfordensis*, *Grallator* isp., *Gwyneddichnium majore* and *Rhynchosauroides* isp. (Fig. 12.6f, g). Other reports from these units with similar assemblages were given by Olsen (1980), Olsen and Baird (1986), Olsen and Flynn (1989), Fraser and Olsen (1996), Szajna and Silvestri (1996), Szajna and Hartline (2003), Lucas and Sullivan (2006), Sues and Olsen (2015) and, in a comprehensive revision of the ichnogenus *Gwyneddichnium,* by Lucas et al. (2014). The oldest Late Triassic (Carnian) tetrapod ichnofauna in North America comes from the Stockton Formation of the Deep River Basin in North Carolina (Olsen and Huber, 1998). The assemblage is composed of tridactyl to pentadactyl footprints that are similar to the ichnogenus *Parachirotherium*, characteristic of Middle-Upper Triassic (Ladinian-Carnian) ichnofaunas from Germany and Morocco (Haubold and Klein 2000; Lagnaoui et al. 2012; Klein and Kneidl 2015).

12.3.2.2 South America

From the Los Colorados Formation (Norian) of northwestern Argentina, small pes and manus imprints of *Brachychirotherium* were described (Leonardi and De Oliveira 1990; Leonardi 1994; Arcucci et al. 2004; Melchor and De Valais 2006). Therapsid footprints similar to *Dicynodontipus*, as well as chirotheriid, grallatorid and *Tetrasauropus*- or *Eosauropus*-like footprints and trackways are documented from the Portezuelo Formation (Carnian) of the Cuyana Basin in San Juan Province of western Argentina (Marsicano and Barredo 2004). A unique assemblage dominated by the footprints of therapsids comes from the Vera Formation (Carnian) of Los Menucos of Río Negro Province, Argentina. It includes trackways that were assigned to different new ichnotaxa by Casamiquela (1964, 1975) but referred to *Dicynodontipus* by Melchor and De Valais (2006) (but see Domnanovich and Marsicano 2006; Domnanovich et al. 2008).

Brazil also has a few Late Triassic footprint sites. Silva et al. (2008a, b) described lacertoid *Rhynchosauroides* footprints from the Santa Maria Formation of southern Brazil, introducing a new ichnospecies. From the same unit, Silva et al. (2008b) documented imprints of theromorphoid or *Procolophonichnium*-like shape, which they assigned to *Dicynodontipus* and another new ichnospecies. The Santa Maria Formation also yielded theropod footprints that can be assigned to the ichnogenus *Grallator* (Silva et al. 2008c). Extramorphological variation and influence of the substrate, not the anatomy of the trackmaker, is obviously responsible for many features observed in these footprints. *Eubrontes* isp. with large footprints (up to 43 cm length) come from the Caturrita Formation of Rio Grande do Sul (Silva et al. 2012). After Lucas (2010), the Late Triassic age of the Caturrita Formation is well established by its tetrapod body fossils, so this could be another Late Triassic record of *Eubrontes* (cf. Lucas et al. 2006a). Recently the age of the Caturrita Formation was debated and a Lower Jurassic age cannot be completely excluded (Silva et al. 2012). Paleofloristic studies (Barboni and Dutra 2013) support a Lower Jurassic age at least for the top of the Caturrita Formation.

12.3.2.3 Europe

In Europe, the Germanic Basin has a large number of important Late Triassic localities in Germany. From the Hassberge Formation of southern Germany the type material of *Brachychirotherium* has been described, with the ichnospecies *B. hassfurtense* (type ichnospecies) and *B. thuringiacum* (Rühle von Lilienstern 1938; Beurlen 1950; Karl and Haubold 1998). From the same unit, *Atreipus-Grallator*, *Apatopus lineatus*, *Rhynchosauroides* isp. and *Procolophonichnium lockleyi* are known (Haubold and Klein 2002; Klein and Lucas 2013; Klein et al. 2015a, b) (Fig. 12.6h–j). The Grabfeld, Stuttgart, Steigerwald and Löwenstein formations (Carnian-Norian) of the German Keuper contain the ichnotaxa *Brachychirotherium thuringiacum*, *Chirotherium wondrai*, cf. *Parachirotherium postchirotherioides*, *Atreipus-Grallator*, *Evazoum* isp., *Apatopus lineatus*, *Rhynchosauroides* isp. and *Chelonipus torquatus* (Heller 1952; Kuhn 1956, 1958b; Haubold 1971a; Haubold and Klein 2002; Haderer 1990, 1996, 2012, 2015; Hofbauer and Klein 2013; Klein and Lucas 2013; Klein and Kneidl 2015; Lichtig et al. 2017).

In the Tatra Mountains of Poland and Slovakia, tridactyl theropod footprints assigned to *Grallator-Eubrontes* have been found in the Rhaetian Tomanóva Formation (Niedźwiedzki 2011). Footprints of similar type and age are known from the Rhaetian Höganäs Formation of southern Sweden (Gierlinski and Ahlberg 1994).

Great Britain, along the coast of Wales, yielded footprints from deposits of the Mercia Mudstone Group that can be assigned to the *Grallator-Eubrontes* plexus. Other footprints from this unit are similar to the ichnogenera *Evazoum*, *Eosauropus* and *Pseudotetrasauropus* (Lockley et al. 1996; Lockley and Meyer 2000).

Contrary to the abundant localities with Middle Triassic footprint assemblages, France has few Late Triassic sites. One is in the Peyzac (Ardeche) region and probably Carnian in age. Ichnotaxa from this locality can be assigned to *Atreipus-Grallator*. They have been described by Courel and Demathieu (2000) and Gand et al. (2005). Tetradactyl footprints similar to *Pseudotetrasauropus* from southern Africa (Ellenberger 1970, 1972) were discovered, together with tridactyl imprints of the *Grallator-Eubrontes*-plexus, in Norian sediments near the city of La Grand-Combe in southern France (Gand et al. 2000). Similar tracks from Norian-Rhaetian (Keuper) deposits come from surfaces close to the city of Anduze (Ellenberger 1965; Ellenberger et al. 1970). Unfortunately, these tracks were destroyed some years ago by river flooding (Ellenberger, pers. com.). Spain has very few Late Triassic sites.

In Switzerland, Late Triassic assemblages occur in the Swiss Alps in the canton of Graubünden, in deposits belonging to the Hauptdolomit Group and the Kössen Formation (Norian-Rhaetian). The largest surface is in the Diavel Formation of the Hauptdolomit Group and is exposed in the Swiss National Park. It shows 13 trackways similar to *Eubrontes* with large (up to 30 cm length) tridactyl pes imprints. Associated are very large tetradactyl footprints (60 cm pes length) and a longer trackway with short steps. These have been compared to *Tetrasauropus,* and similar footprints considered to have been made by sauropodomorphs (Furrer 1993;

Lockley and Meyer 2000). The trackways lack traces of the manus. Similar trackways, but partly with a preserved manus impression, have been documented from the same units, together with tridactyl grallatorids, at adjacent localities in the Swiss National Park and in the Parc Ela (Furrer and Lozza 2008; Meyer et al. 2013).

Brachychirotherium from Jaén and tridactyl footprints of the *Grallator-Eubrontes* plexus from Soria have been described (Pérez-López 1993; Pascual Arribas and Latorre Macarrón 2000; Díaz-Martínez et al. 2015). In particular, the age of the former site is uncertain, tentatively Carnian-Rhaetian, but also a Middle Triassic age cannot be excluded. The latter locality is probably Rhaetian in age.

In Italy, an assemblage from Tuscany was described by von Huene (1941), with several new ichnotaxa that all can be considered as synonyms of existing forms. Among them is "*Coelurosaurichnus,*" which is a synonym of *Grallator*. The ichnofauna consists of poorly preserved chirotheres, grallatorids and small lacertoid footprints. *Brachychirotherium* was described from the lower-middle Carnian Val Sabbia Sandstone of Brescia (Petti et al. 2009). Other Late Triassic footprints come from the Friuli region. From the Dolomia Principale (Norian), tridactyl footprints of the *Grallator-Eubrontes* plexus were described, together with tri-pentadactyl imprints and trackways of quadrupeds of uncertain affinities (Dalla Vecchia and Mietto 1998; Marzola and Dalla Vecchia 2014). Upper Carnian deposits in Friuli yielded *Apatopus lineatus* (Dalla Vecchia 1996; Avanzini et al. 2007; Klein and Lucas 2013). Carnian strata of the Montemarcello Formation along the coast of La Spezia provided the type material of *Evazoum sirigui*, as well as *Brachychirotherium* isp., indeterminate chirotheriids and grallatorid tridactyl footprints (Nicosia and Loi 2003). Further discoveries of footprints have been documented from the Dolomia Principale unit (Norian) of the Monte Pasubio region of northeastern Italy. These are small and large tridactyl theropod imprints of the *Grallator-Eubrontes* plexus, as well as large tetradactyl imprints and others showing an associated manus, all of uncertain affinity (Belvedere et al. 2008). From the Travenanzes Formation (Carnian) in the Southern Alps, southwest of the city of Bolzano, large tridactyl theropod footprints (*Eubrontes*) have been described (Bernardi et al. 2013). From the same unit, *Atreipus* and *Evazoum* have been reported (D'Orazi-Porchetti et al. 2008).

12.3.2.4 North Africa

The Timezgadiouine Formation of the Argana Basin of Morocco, in particular the Irohalene Member (T5), in addition to fossils of vertebrate skeletons, has a rich ichnofauna. Biron and Dutuit (1981) described numerous footprints from Irohalene, assigning them to several new ichnotaxa. These are tridactyl-pentadactyl imprints of small to large size. Lagnaoui et al. (2012, 2016) re-located the sites of Biron and Dutuit (1981) and found abundant new material, which was well preserved. Furthermore, while prospecting Irohalene Member outcrops in the Argana Basin, they discovered new tracksites with a similar ichnofauna. Lagnaoui et al. (2012, 2016) gave the following list of ichnotaxa: *Atreipus-Grallator*, *Eubrontes* isp., *Parachirotherium* cf. *P. postchirotherioides*, *Parachirotherium* isp., *Brachychirotherium* isp., *Synaptichnium*

isp., *Apatopus lineatus*, *Rhynchosauroides* ispp. and *Atreipus-Grallator*. *Apatopus lineatus* and *Atreipus-Grallator* were also listed for the overlying Tadart Ouadou Member (T5) (Lagnaoui et al. 2012). Biron and Dutuit (1981) also described a tetrapod ichnofauna from the Ourika Basin, Morocco, illustrating *Apatopus lineatus* as well as chirotheriid imprints and small lacertoid tracks. These authors proposed several new ichnotaxa, but their validity is doubtful, so this ichnofauna is in need of revision.

12.3.2.5 Southern Africa

In southern Africa, Norian-?Rhaetian ichnofaunas of the Lower Elliot Formation (Stormberg Group) are some of the most important Late Triassic assemblages in the global record. Ellenberger (1970, 1972) documented extensive material with trackways and isolated footprints from Lesotho. A large number of new ichnotaxa was introduced by this author, many of these being *nomina dubia* or synonyms of others known from North America and Europe. Ichnogenera that found general acceptance are *Pseudotetrasauropus*, *Tetrasauropus* and *Pentasauropus*. They have subsequently been identified from localities elsewhere, but many of these records were later referred to *Evazoum* and *Eosauropus*. D'Orazi-Porchetti and Nicosia (2007) furthermore considered *Paratetrasauropus* and *Sauropodopus* as valid ichnogenera, while others were re-assigned to *Brachychirotherium*. Large and small tridactyl theropod footprints from Lesotho that were given numerous names (Ellenberger 1970, 1972) can be re-assigned to the *Grallator-Eubrontes* plexus. Other footprints, possibly present on the surfaces of Lesotho, are lacertoid (?*Rhynchosauroides*) tracks and some mammaloid *Brasilichnium*-like tracks described and differently named by Ellenberger (1972), but this evaluation is tentative and based only on illustrations in his paper.

12.3.2.6 Greenland

The Ørsted Dal Member of the Fleming Fjord Formation (Norian) in East Greenland has recently yielded surfaces trampled by hundreds of small tetradactyl pes (4–4.5 cm length) and manus imprints assigned to cf. *Brachychirotherium* (Klein et al. 2015b). Digit V is missing, possibly due to the very small size (ontogenetic feature). The track-bearing unit has also provided tracks of the *Grallator-Eubrontes* plexus (Milàn and Bromley 2006; Milàn et al. 2004, 2006; Gatesy et al. 1999) and trackways with large pes and manus imprints that formerly were assigned to *Tetrasauropus* (Jenkins et al. 1994; Lockley and Meyer 2000). The re-examination of these footprints, together with new material, by Lallensack et al. (2017) has shown that they can be referred to *Eosauropus*. Other footprints found at the same locality are *Evazoum* isp. (Lallensack et al. 2017). For an overview also see Clemmensen et al. (2016).

The Fleming Fjord Formation is also well known for tetrapod skeletons. Thus far, temnospondyls, possible sphenodonts, lepidosaurs, turtles, phytosaurs, ?rauisuchians, aetosaurs, pterosaurs, prosauropods, theropods, and mammals are known

(Jenkins et al. 1994; Mateus et al. 2014; Sulej et al. 2014). If *Brachychirotherium* is truly an aetosaur track, this would correspond to the osteological record of these archosaurs (Heckert et al. 2010; Lucas and Heckert 2011).

12.3.2.7 Other Regions

Late Triassic (probably Carnian) tetrapod footprints have been described from the Sydney Basin in eastern Australia. They occur in the Blackstone Formation of the Ipswich Coal Measures in southeastern Queensland. These are very large (43 cm long) tridactyl pes imprints similar to *Eubrontes* that are part of a trackway with 2 m stride length (Staines and Woods 1964; Bartholomai 1966; Lucas et al. 2006a). Small theropod tracks that can be assigned to *Grallator* have been reported from the same unit (Thulborn 1998).

In China, the Baoding Formation (Norian-Rhaetian) of Sichuan Province in the southwestern part of the country shows a surface with very large chirotheriid pes imprints (up to 43.5 cm pes length), including a partial trackway (Xing et al. 2014a). A manus imprint is missing. They have been assigned to cf. *Chirotherium*, based on the digit proportions, with digit III longest. In contrast to the typical Late Triassic *Brachychirotherium* they show an elongated digit V with phalangeal pads. Associated with these tracks is an isolated, large (27 cm length), possible theropod track resembling the ichnogenus *Eubrontes*. Other Late Triassic (Norian-Rhaetian) records from China come from the Sichuan Basin with small and large grallatorids, mammal-like footprints and an indeterminate archosaur trackway similar to *Eosauropus*, all from the Xujiahe Formation (Xing et al. 2013, 2014b).

12.3.3 Biostratigraphy and Biochronology

Lucas (2007) reviewed the Phanerozoic record of tetrapod tracks (Devonian-Neogene) and noted that three principal factors limit their use in biostratigraphy and biochronology (palichnostratigraphy): (1) invalid ichnotaxa based on extramorphological variants; (2) slow apparent evolutionary turnover rates; and (3) facies restrictions. The ichnotaxonomy of tetrapod footprints has generally been oversplit, largely due to a failure to appreciate extramorphological variation. Thus, many tetrapod footprint ichnogenera, and most ichnospecies, are useless "phantom" taxa that confound biostratigraphic correlation and biochronological subdivision. Tracks rarely allow identification of a genus or species known from the body fossil record. Indeed, almost all tetrapod footprint ichnogenera are equivalent to a body-fossil-based family or a higher taxon (order, superorder, etc.). This means that ichnogenera necessarily have much longer temporal ranges and therefore slower apparent evolutionary turnover rates than do body fossil genera. Because of this, footprints cannot provide as refined a subdivision of geological time as do body fossils. The tetrapod footprint record is also much more facies controlled than the tetrapod body

fossil record. The relatively narrow facies window for track preservation, and the fact that tracks are almost never transported, redeposited or reworked, limits the facies that can be correlated with any track-based biostratigraphy (Lucas 2007).

There is much literature on Triassic tetrapod footprint biostratigraphy, especially based on the European and North American records. The most comprehensive earlier publications are those of Demathieu (e.g., Demathieu 1977, 1982, 1984, 1994; Demathieu and Haubold 1972, 1974), who established the presence of three different Triassic footprint assemblages in Europe that Lucas (2007) validated. These are the chirothere assemblage of Olenekian-early Anisian age (early-Middle Triassic), the dinosauromorph assemblage of late Anisian-Ladinian age (late Middle Triassic) and the dinosaur assemblage of Carnian-Rhaetian age (Late Triassic). Lucas (2007) suggested that a fourth footprint assemblage, based on earliest Triassic dicynodont footprints from Gondwana, may also be discernable.

The composition and distribution of Triassic tetrapod footprint assemblages reflect ecological/taphonomic peculiarities as well as different directions and stages in the evolutionary development of the locomotor apparatus of some tetrapod groups. In particular, some archosaur footprints show a limited vertical (stratigraphic) range. Their occurrences are restricted to distinct time intervals, thus demarcating distinct biochronological units (Lucas 2003, 2007; Hunt and Lucas 2007b; Klein and Haubold 2007).

Between the late Olenekian/Anisian and the Norian the development of the tridactyl mesaxonic foot and bipedal gait of dinosaurs is reflected by the footprint record and can be followed in a functional evolutionary succession: *Chirotherium–Sphingopus–Parachirotherium–Atreipus–Grallator* (Haubold and Klein 2000, 2002). This has been used for biostratigraphy and biochronology by Klein and Haubold (2007). Thus, *Chirotherium* spans the Olenekian–Anisian, *Sphingopus* the Anisian–Ladinian, *Parachirotherium* the Ladinian, *Atreipus* the Carnian–Norian and *Grallator* the Norian–Rhaetian interval.

Klein and Haubold (2007) discriminated six biochrons (I–VI) by the range of archosaur footprint assemblages. The beginning of each is marked by the first appearance datum (FAD) of a characteristic index ichnotaxon (in bold): **I.** ***Protochirotherium***, Late Induan–Olenekian; **II.** ***Chirotherium*****,** *Rotodactylus*, *Isochirotherium*, *Synaptichnium* ("*Brachychirotherium*"), Late Olenekian–Anisian; **III.** ***Sphingopus****–Atreipus–Grallator*, *Rotodactylus*, *Isochirotherium*, *Synaptichnium* ("*Brachychirotherium*"), Late Anisian–Ladinian; **IV.** ***Parachirotherium****–Atreipus–Grallator*, *Synaptichnium* ("*Brachychirotherium*"), Late Ladinian; **V.** ***Atreipus****–Grallator*, *Brachychirotherium*, Carnian–Norian and **VI.** ***Grallator****–Eubrontes*, *Brachychirotherium*, Norian–Rhaetian.

Lucas (2003, 2007) recognized five Triassic footprint assemblages: (**1**) Dicynodont tracks, earliest Triassic; (**2**) Chirothere, Olenekian–Anisian; (**3**) *Procolophonichnium–Rhynchosauroides*, Anisian–Ladinian; (**4**) Dinosauromorph, Ladinian–Carnian; and (**5**) Dinosaur, Carnian–Rhaetian. In this scheme, (**2**) corresponds to **II** and **III**, (**3**) to **III**, (**4**) to **IV**, and (**5**) to **V** and **VI** of Klein and Haubold (2007). Hunt and Lucas (2007b) proposed five assemblages: (**1**) Dicynodont tracks, earliest Triassic; (**2**) Chirothere, Olenekian–early Anisian; (**3**) Dinosauromorph, late

Anisian–Ladinian; (**4**) Tridactyl dinosaur, Carnian–early Norian; and (**5**) Sauropodomorph, late Norian–Rhaetian.

In addition to Lucas (2003, 2007), Hunt and Lucas (2007b) recognize a sauropodomorph track assemblage in the Late Norian–Rhaetian based on the taxa *Evazoum* and *Eosauropus* (see above), purportedly first appearing in the late Norian. This is contrary to Klein et al. (2006) and Klein and Haubold (2007), who considered the footprints of *Evazoum* to be extramorphological variants of *Brachychirotherium*, a crurotarsan track characteristic of the entire Late Triassic. Furthermore, *Evazoum* was first described from the Carnian of Italy by Nicosia and Loi (2003), thus indicating an earlier appearance.

Independent of further subdivisions proposed by various authors, we follow Klein and Lucas (2010a) and recognize five tetrapod footprint biochrons of Triassic age that can be identified across the Pangaean footprint record (Fig. 12.7):

1. Earliest Triassic dicynodont footprints. These tracks are from strata of the *Lystrosaurus* assemblage zone and thus are of Lootsbergian (= latest Changshingian-Induan) age (Lucas 1998). However, there are only a few records of this assemblage and they are restricted to Gondwana, so it needs further documentation before its Pangaea-wide significance can be established.
2. *Protochirotherium* is characteristic of strata of Nonesian age (=Olenekian). Morphologically, and based on its temporal distribution, it can be considered as the hypothetical "root" of later locomotory developments in archosaurs. Associated forms are *Rhynchosauroides*, *Procolophonichnium* and footprints of temnospondyls.
3. The appearance of *Chirotherium barthii* and *C. sickleri*, *Rotodactylus*, *Isochirotherium* and *Synaptichnium* ("*Brachychirotherium*") roughly demarcates the Nonesian-Perovkan (late Olenekian-Anisian) transition. *Chirotherium barthii* and *C. sickleri* disappear during the Anisian. The range of the other ichnotaxa spans most of the Middle Triassic (Perovkan-Berdyankian = Anisian-Ladinian) together with *Rhynchosauroides*, *Procolophonichnium*, dicynodont and temnospondyl footprints that continue from the Nonesian. *Rotodactylus* and *Isochirotherium* disappear before the end of the Berdyankian (Ladinian).
4. The appearance of tridactyl footprints and quadrupedal to bipedal trackways of the *Atreipus-Grallator* type ("*Coelurosaurichnus*") demarcates the late Perovkan-Berdyankian (= late Anisian-Ladinian) as do pentadactyl footprints of *Sphingopus* and *Parachirotherium*. Other ichnotaxa continue from the Nonesian (see above).
5. *Brachychirotherium* (*sensu stricto*) appears at the beginning of the Otischalkian (= early Carnian). It is a characteristic ichnotaxon of the Late Triassic, together with *Atreipus-Grallator* (quadrupedal to bipedal trackways), *Grallator* and *Eubrontes* (bipedal trackways). The stratigraphic upper limit of *Brachychirotherium* is the Triassic-Jurassic boundary (end of the Apachean); there is no evidence of *Brachychirotherium* in post-Triassic strata (Lucas and Tanner 2007a, b; Lucas et al. 2012c). The same is true for other chirotheres, and for *Apatopus*, *Procolophonichnium* and *Gwyneddichnium*. The range of *Rhynchosauroides* continues into the Jurassic (Avanzini et al. 2010a), and the same is true of *Batrachopus* and the mammal-like forms, as might be expected.

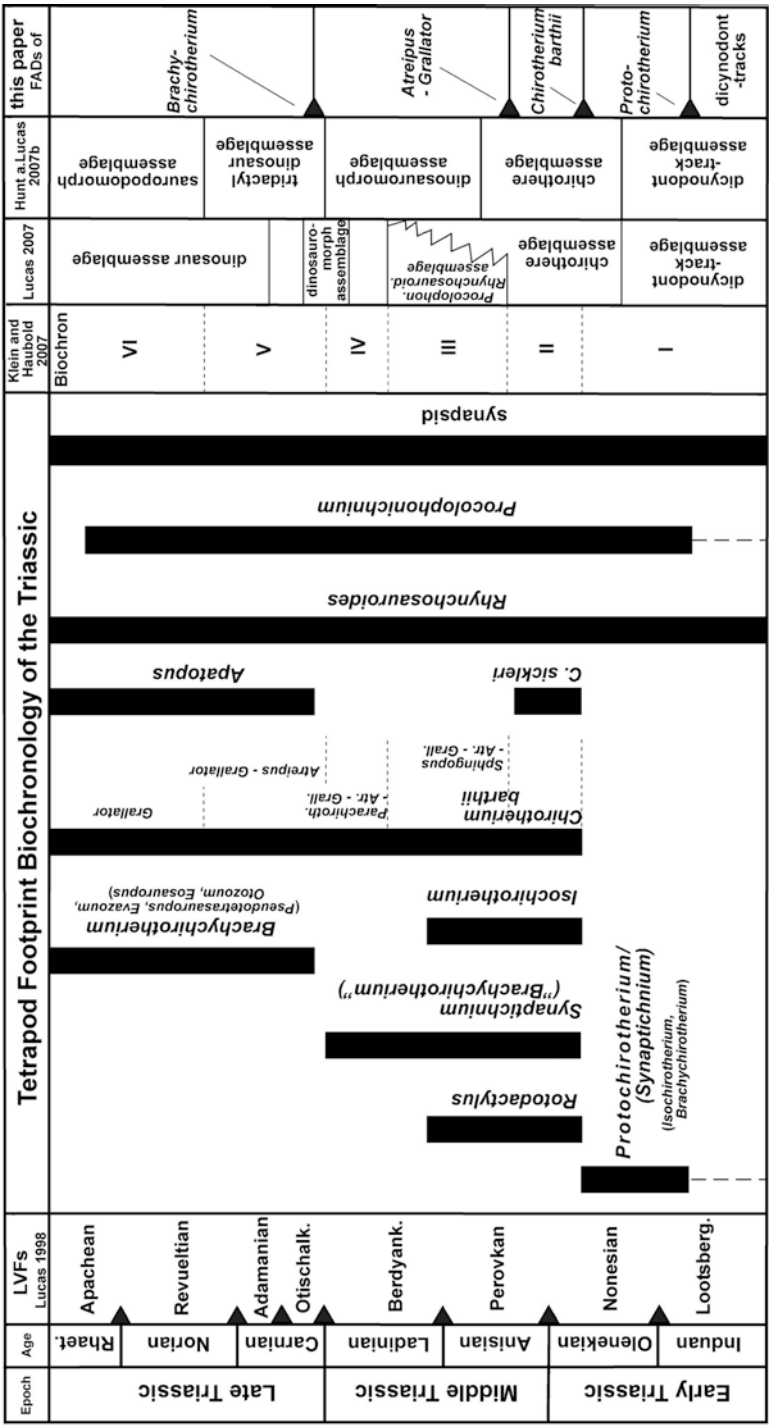

Fig. 12.7 Tetrapod footprint biostratigraphy and biochronology of the Triassic. From Klein and Lucas (2010a)

Rhynchosauroides and *Procolophonichnium*, as well as some dicynodont and temnospondyl footprints, have a long stratigraphic range. They span the complete Triassic Period, with early roots in the late Permian, therefore, they are of less utility for biostratigraphy as long as their taxonomy is unclear, as is the case presently. Their dominance in some assemblages (see above) is extremely facies-controlled and biased by ecological and taphonomic effects. *Rhynchosauroides* and *Procolophonichnium* trackmakers obviously frequented some Anisian–Ladinian carbonate tidal flats (assemblage 3 of Lucas 2003, 2007; Demathieu and Oosterink 1983, 1988; Diedrich 2008), an environment that archosaurs (chirothere trackmakers) mostly avoided. However, a few chirotheres are present as well (Demathieu and Oosterink 1983, 1988) and, on the other hand, *Rhynchosauroides* is common at least on some fluvial-lacustrine surfaces of the Early through Late Triassic (Demathieu 1966; Haubold 1971a, b).

Evolutionary, rather than facies-controlled, signals from footprints are suitable to demarcate distinct time intervals in the Triassic and to outline a coarse biostratigraphy and biochronology of the Triassic. This footprint biochronology identifies five intervals of Triassic time, which is less resolution than the eight land-vertebrate faunachrons of Triassic age based on tetrapod body fossils.

12.3.4 Ichnofacies and Ichnocoenoses

12.3.4.1 Introduction

Hunt and Lucas (2007d, 2016a) provided a discussion of terminology relevant to the study of tetrapod footprint ichnofacies. An ichnocoenosis can be defined as a trace fossil assemblage produced by a biological community that can be characterized by morphological criteria (independent of depositional environment or biological affinities) (e.g., Bromley 1996; McIlroy 2004; Hunt and Lucas 2007d). Seilacher (1964: 303) introduced the term ichnofacies for "general trace associations, or types of ichnocoenoses, representing certain facies with a long geologic range." Subsequently, Hunt and Lucas (2007d) defined five archetypal tetrapod footprint ichnofacies for nonmarine environments: *Chelichnus*, *Grallator*, *Brontopodus*, *Batrachichnus* and *Characichnos* ichnofacies (Table 12.1). The following review is principally based on Hunt and Lucas (2006b, 2007d, e, 2016a).

12.3.4.2 *Batrachichnus* Ichnofacies

Hunt and Lucas (2007d) proposed the *Batrachichnus* ichnofacies for ichnofaunas in which the majority of tracks are of quadrupedal carnivores with a moderate-high diversity (four to eight ichnogenera). This ichnofacies represents tidal flat-fluvial plain environments from the Devonian to the Cretaceous. Hunt and Lucas (2006b, 2007d) recognized two ichnocoenoses of this ichnofacies in the Triassic (Table 12.1).

Table 12.1 Archetypal vertebrate ichnofacies and representative ichnocoenoses of the Triassic

Archetypal Vertebrate Ichnofacies	Main ichnotaxa	Triassic ichnocoenoses	Environment
Chelichnus	Low diversity ichnofaunas (typically less than 4 ichnogenera) with most tetrapod tracks that have sub-equant shape with manual and pedal impressions of subequal size and with short digit impressions	*Brasilichnium* (Late Triassic-Early Jurassic)	Eolian (crossbedded dune facies)
Batrachichnus	Majority of tracks are quadrupedal carnivores with medium-high diversity (4–8 ichnogenera)	*Chirotherium* (Early-Middle Triassic) *Apatopus* (Late Triassic)	Tidal flat-alluvial plain
Brontopodus	Tracks are principally terrestrial herbivore with small percentage (generally >10%) of terrestrial carnivore tracks with medium-high diversity (4–8 ichnogenera)	*Dicynodontipus* (Early Triassic) *Therapsipus* (Middle Triassic) *Procolophonichnium* (Middle Triassic) *Brachychirotherium* (Late Triassic) *Evazoum* (Late Triassic)	Coastal plain (clastic or carbonate marine shoreline)
Grallator	Medium-high diversity (typically 5–8 ichnogenera) with tracks (usually dominant) of tridactyl avian or non-avian theropods	*Grallator* (Late Triassic)	Lacustrine margin
Characichnus	Swimming traces including parallel scratch marks and fish swimming trails (*Undichna*)	Unnamed (Early-Late Triassic)	Shallow aquatic

From Hunt and Lucas (2007e)

Hunt and Lucas (2007d) named the *Chirotherium* ichnocoenosis for the well-studied Early-Middle Triassic ichnofaunas of Europe and North America that are dominated by *Chirotherium* tracks (e.g., Peabody 1948; Haubold 1971a; Lucas et al. 2003). Other common ichnotaxa are *Rotodactylus*, *Rhynchosauroides*, *Isochirotherium* and *Synaptichnium*. Hunt and Lucas (2006b) recognized a distinctive and pervasive ichnocoenosis throughout much of the Upper Triassic portion of the Newark Supergroup in eastern North America assigned to the *Apatopus* ichnocoenosis. Ichnofaunas of this ichnocoenosis lack *Evazoum* and *Eosauropus*, contain less than 50% *Brachychirotherium* and *Grallator* and are characterized by ichnotaxa that are rare or absent elsewhere, including *Apatopus* and *Gwyneddichnium*.

12.3.4.3 *Brontopodus* Ichnofacies

Hunt and Lucas (2007d) proposed the *Brontopodus* ichnofacies for medium diversity ichnofaunas in which the majority of tracks are of terrestrial herbivores with a small quantity (generally >10%) of terrestrial carnivore tracks. This ichnofacies includes coastal plain-marine shoreline environments and some lacustrine shorelines, and it ranges from late Permian to Recent in age. Hunt and Lucas (2006b, 2007d, e) recognized five ichnocoenoses within this ichnofacies in the Triassic (Table 12.1). The oldest ichnocoenosis within the *Brontopodus* ichnofacies occurs in the earliest Triassic (possibly restricted to the Induan) and is characterized by dicynodont footprints in southern Africa, Antarctica and Australia (Watson 1960; MacDonald et al. 1991; Retallack 1996). Hunt and Lucas (2006b) termed this the *Dicynodontipus* ichnocoenosis.

The majority of Early Triassic to early Middle Triassic ichnofaunas represent the *Chirotherium* ichnocoenosis of the *Batrachichnus* ichnofacies. However, a small number of localities are dominated by therapsid tracks. Hunt and Lucas (2006b) termed this the *Therapsipus* ichnocoenosis for the therapsid ichnotaxon from the Moenkopi Group of Arizona (Hunt et al. 1993b). Herein, we recognize a new ichnocoenosis in the Anisian carbonate tidal flats of Germany and the Netherlands. This *Procolophonichnium* ichnocoenosis represents a temporal equivalent of the red-bed *Chirotherium* ichnocoenosis (Lucas 2007). This ichnocoenosis is dominated by tracks of *Procolophonichnium* and *Rhynchosauroides* with only rare chirothere tracks (Demathieu and Oosterink 1983, 1988; Diedrich 1998, 2000, 2002a, b; Lucas 2007).

12.3.4.4 *Grallator* Ichnofacies

Hunt and Lucas (2007d) proposed the *Grallator* ichnofacies for medium to high diversity ichnofaunas (five to eight ichnogenera) dominated by tracks of tridactyl avian and non-avian theropods (usually dominant) or of other habitual bipeds. Tracks of bipedal and quadrupedal ornithischians, sauropods and herbivorous mammals are also locally common in this ichnofacies. This ichnofacies extends from the Late Triassic to the Recent and often characterizes lacustrine margin environments.

Hunt and Lucas (2007d) recognized a *Grallator* ichnocoenosis in the Late Triassic. There are many Late Triassic ichnofaunas in which the most abundant (>50%) ichnogenus is *Grallator*. Notable ichnofaunas occur at the very top of the Chinle Group or in the overlying Wingate Sandstone in Colorado (Gaston et al. 2003; Lucas et al. 2006b); other prominent examples are in Wales, France, Germany, Italy, Switzerland and Greenland (Lockley and Meyer 2000: Figs. 4.4, 4.10, and 4.14). Hunt and Lucas (2006b) noted that there is potential to subdivide the *Grallator* ichnocenosis. For example, on the Colorado Plateau, the upper and lower Wingate Sandstone have different sub-ichnocoenoses: a lower *Eosauropus* subichnocoenosis includes *Brasilichnium*, *Brachychirotherium*, and *Eosauropus*, and an upper *Otozoum* sub-ichnocoenosis includes *Eubrontes*, *Batrachopus* and *Otozoum* (Lucas et al. 2006a, c, d).

12.3.4.5 *Chelichnus* Ichnofacies

Hunt and Lucas (2007d) proposed the *Chelichnus* ichnofacies for ichnofaunas that have a low diversity (fewer than five ichnogenera) of tetrapod tracks in which manus and pes tracks are equant in shape, of subequal size and have short digit impressions. This ichnofacies is recurrent on dune faces in eolian environments, and it extends from the early Permian to the Early Jurassic. Hunt and Lucas (2007d) redefined the *Brasilichnium* ichnofacies of Lockley et al. (1994) as an ichnocoenosis of this ichnofacies (Table 12.1). *Brasilichnium* is abundant in the Early Jurassic Navajo Sandstone and coeval Aztec Sandstone in western North America (Utah, California, Colorado). The *Brasilichnium* ichnocoenosis is also locally present in the lower Wingate Sandstone in western Colorado (Schultz-Pittman et al. 1996; Hunt and Lucas 2006b).

12.3.4.6 *Characichnos* Ichnofacies

Hunt and Lucas (2007d) proposed the *Characichnos* ichnofacies for medium diversity ichnofaunas in which the majority of tracks are tetrapod swimming traces (parallel scratch marks) and fish swimming trails (*Undichna*). This ichnofacies represents shallow lacustrine (and tidal) environments. Swimming traces are notable in various Triassic units in the western United States, including the Moenkopi Group (Lower-Middle Triassic) and equivalent strata in Arizona, Utah, Wyoming and New Mexico (e.g., Peabody 1948; Boyd and Loope 1984; McAllister and Kirby 1998; Schultz et al. 1994; Lucas et al. 2003; Mickleson et al. 2006a, b) and the Chinle Group (Upper Triassic) in Arizona and New Mexico (e.g., Hunt et al. 1993a; Hunt and Lucas 2006b). There is no named ichnocoenosis of this ichnofacies in the Triassic.

12.3.4.7 Late Triassic Ichnocoenoses

There are thus five ichnocoenoses present in the Late Triassic: *Evazoum*, *Brachychirotherium* (*Brontopodu*s ichnofacies), *Grallator* (*Grallato*r ichnofacies), *Apatopus* (*Batrachichnus* ichnofacies) and *Brasilichnium* (*Chelichnus* ichnofacies). The *Apatopus* ichnocoenosis is geographically restricted to eastern North America (although *Apatopus* occurs at one locality in Utah: Foster et al. 2003) and probably environmentally controlled by the distribution of large rift lakes.

The *Evazoum* ichnocoenosis is principally restricted to western North America, where it is replaced in the uppermost Chinle, Wingate and Sheep Pen formations (latest Triassic) by the *Grallator* ichnocoenosis. The Shay Canyon tracksite in Utah pertains to the *Brachychirotherium* ichnocoenosis and is stratigraphically low in the upper Chinle. It may represent a lateral equivalent of the *Evazoum* ichnoceonosis or it may be stratigraphically lower, which would suggest a temporal progression of ichnocoenoses from *Brachychirotherium* to *Evazoum* to *Grallator* (Hunt and Lucas

2006b). The ichnofaunas of the lower Chinle are poorly known but include *Brachychirotherium*, lack *Evazoum*, and several include *Barrancapus* (Hunt and Lucas 2006a). These ichnofaunas may represent the *Brachychirotherium* ichnocoenosis (possibly a *Barrancapus* sub-ichnocoenosis). *Barrancapus* appears to be a potential index ichnotaxon of the Barrancan sub-lvf (land-vertebrate faunachron) of the Revueltian lvf. *Eosauropus* and *Evazoum* are index ichnotaxa of the Apachean lvf (Hunt and Lucas 2006b, 2007c).

12.4 Vertebrate Coprolites

Like tetrapod footprints, vertebrate coprolites are broadly distributed in Upper Triassic strata on all of the continents except Australia and Antarctica (Fig. 12.8). Here, we begin with a brief review of their ichnotaxonomy, followed by discussion of the use of vertebrate coprolites in Late Triassic biostratigraphy/biochronology and in the recognition of ichnofacies. In the ichnotaxonomy we have provided information on the entire temporal ranges of ichnotaxa even if they extend beyond the Late Triassic.

12.4.1 Ichnotaxonomy

12.4.1.1 Fish

***Heteropolacopros* Hunt et al.** 1998

Type ichnospecies: *Heteropolacopros texaniensis* Hunt et al. 1998

Distribution: Late Mississippian: Beeman Formation (late Missourian), New Mexico, USA; Conemaugh Group (Formation), West Virginia, USA; Early Permian: Cutler Group, New Mexico, USA; Abo Formation, New Mexico, USA: Late Permian: "Magnesian Limestone," France: Middle Triassic: Anton Chico Formation of the Moenkopi Group (Anisian), New Mexico, USA; (Perovkan and Berdyankian), Russia; (Perovkan) Mollo-Khara-Bala-Kantemir locality, Kazakhstan: Late Triassic: Irohalene Member of the Timezgadiouine Formation (Otischalkian), Argana Basin, Morocco; Colorado City Formation (Otischalkian: Carnian), Texas, USA; Blue Mesa Member of the Petrified Forest Formation (Adamanian), Arizona, USA; Bluewater Creek Formation (Adamanian), Arizona, USA; Bluewater Creek Formation (Adamanian), New Mexico, USA; Tecovas Formation (Adamanian: Carnian), Texas, USA; Huai Hin Lat Formation (Carnian-Norian), Huai Nam Aun, Chaiyaphum Province, Thailand; Cobert Canyon Sandstone Bed of the Baldy Hill Formation (Revueltian), Colorado, USA; Bull Canyon Formation (Revueltian), New Mexico, USA; Redonda Formation (Apachean), New Mexico, USA.

Description: A microspiral heteropolar coprolite that is small (usually less than 4 cm long) with 3–4 coils forming less than 50% of the length. The posterior spire

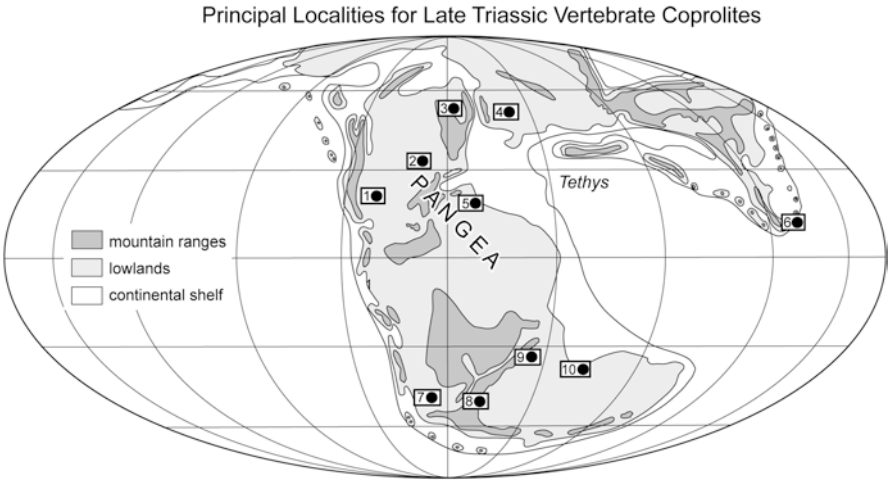

Fig. 12.8 Distribution of principal Late Triassic coprolite localities: (**1**) Western North America; (**2**) Eastern North America; (**3**) Greenland; (**4**) Western and central Europe; (**5**) Morocco; (**6**) Thailand; (**7**) Argentina; (**8**) South Africa; (**9**) Madagascar; (**10**) India. Base map after Wing and Sues (1992). Modified after Hunt et al. (2013a, b)

is wider than the first coil (always less than one third of the total length) and gradually decreases in diameter both up and down the long axis (the tip comes to a rounded point), and the posterior spire gradually tapers to a rounded tip (Fig. 12.9).

Discussion: This ichnospecies is very long ranging and somewhat variable in morphology and is in need of a taxonomic revision.

Tracemaker: Heterospiral coprolites are produced by valvular intestines. The phylogenetic distribution of valvular intestines is not totally understood. McAllister (1987) presented evidence that that some or all agnathans, placoderms, dipnoans, actinistians and chondrichthyans have valvular intestines. Only two fossil actinopterygians have evidence of this structure, and McAllister (1987) hypothesized that this group progressively reduced the valvular intestine, and teleosts do not exhibit this kind of structure. Dipnoans probably produced amphipolar coprolites (Hunt and Lucas 2012b), and Late Triassic heteropolar coprolites represent chondrichthyans.

***Liassocopros* Hunt et al.** 2007

Type ichnospecies: *Liassocopros hawkinsi* Hunt et al. 2007

Distribution: Late Mississippian: Beeman Fomation (late Missourian), New Mexico, USA; Early Permian: Oklahoma, USA; Rotliegend, France: Middle Triassic: Potrerillos, Cacheuta and Río Blanco formations (Berdyankian?), Cuyana Basin, Argentina: Late Triassic: Lower Maleri Formation (upper Carnian), Maleri, India; Huai Hin Lat Formation at Huai Nam Aun (Carnian), Chaiyaphum Province, Thailand; Westbury Formation (Penarth Group), England (Rhaetian): Lower Liassic: (Hettangian-Lower Pliensbachian) of Lyme Regis, England.

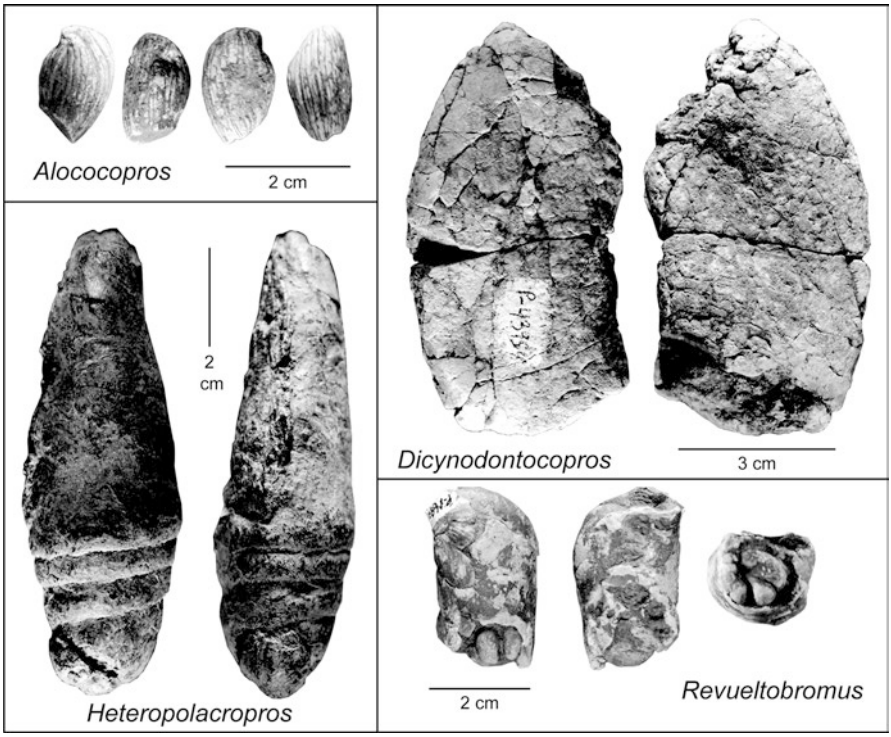

Fig. 12.9 Typical Late Triassic coprolite genera. *Alococopros* (Hunt et al. 2013a: fig. 5L–O). *Dicynodontocopros* (Hunt et al. 2013a: fig. 7N–P). *Heteropolacopros* (Hunt et al. 2013a: fig. 6R–S). *Revueltobromus* (Hunt et al. 2013a: fig. 8N–P)

Description: A microspiral heteropolar coprolite that tends to be large (>5 cm long) with a small number (<3) of wide coils.

Discussion: This is a very long ranging ichnospecies that may be in need of taxonomic revision.

Tracemaker: This heteropolar coprolite was produced by a chondrichthyan.

***Saurocopros* Hunt et al. 2007**

Type ichnospecies: *Saurocopros bucklandi* Hunt et al. 2007

Distribution: Late Triassic: ?Lower Maleri Formation (upper Carnian) near Maleri, India; Carnian-Norian Huai Hin Lat Formation at Huai Nam Aun in Chaiyaphum Province, Thailand; Rhaetian Westbury Formation (Penarth Group) of England; Lower Liassic (Hettangian-Lower Pliensbachian) of Lyme Regis, England.

Description: Microspiral heteropolar coprolite that differs from *Malericopros* in being tapered below the spiral demarcation and from *Heteropolacopros* in having a small number of wide spirals (typically 3) at the anterior end (Fig. 12.10).

Discussion: Hunt et al. (2007) named this coprolite in recognition that Buckland (1835: 227, pl. 28, Figs. 6, 7, 9) termed this morphology "Sauro-coprolites," and they noted that it does not pertain to a reptile.

Tracemaker: *Saurocopros* is a chondrichthyan coprolite.

***Strabelocoprus* Hunt et al.** 2012a

Type ichnospecies: *Strabelocoprus pollardi* Hunt et al. 2012a

Distribution: Late Triassic: Penarth Group (Rhaetian), England: Early Jurassic: Lower Liassic (Hettangian-Lower Pliensbachian), Lyme Regis, England.

Description: Heteropolar, microspiral coprolite with a small number of coils (<3) in lateral view, exhibiting very wide spirals in posterior view. It has a width that exceeds half of its length (Fig. 12.10).

Discussion: This distinctive ichospecies seems to be a good indicator of the Rhaetian-Pliensbachian.

Tracemaker: This form of coprolite was produced by a chondrichthyan.

***Malericopros* Hunt et al.** 2007

Type ichnospecies: *Malericopros matleyi* Hunt et al. 2007

Distribution: Late Permian: "Magnesian Limestone," France. Late Triassic: ?Lower Maleri Formation (upper Carnian) near Maleri, India.

Description: Microspiral heteropolar coprolite with a maximum diameter that is posterior to the anterior coil (Fig. 12.10).

Discussion: This ichnospecies was originally described from the Upper Triassic of India.

Tracemaker: *Malericoprus* was produced by a chondrichthyan.

12.4.1.2 Tetrapods

***Alococopros* Hunt et al.** 2007

Type ichnospecies: *Alococopros triassicus* Hunt et al. 2007

Distribution: Early Triassic: Arcadia Formation (Lootsbergian), Queensland, Australia; Middle Triassic: (Perovkan and Berdyankian), Russia; (Perovkan) Mollo-Khara-Bala-Kantemir locality, Kazakhstan; Late Triassic: Colorado City Formation (Otischalkian: Carnian); Tecovas Formation (Adamanian: Carnian); Bluewater Creek Formation (Adamanian: Carnian), New Mexico, USA; Cobert Canyon Sandstone Bed of the Baldy Hill Formation (Revueltian: Norian), Colorado; Bull Canyon Formation (Revueltian: Norian), New Mexico, USA; Redonda Formation (Apachean: Norian), New Mexico, USA; Late Cretaceous: Kirtland Formation (Campanian), New Mexico, USA; Naashoibito Member of the Ojo Alamo Formation (Maastrichtian), New Mexico, USA: Paleocene: Nacimiento Formation (Puercan), New Mexico, USA; Late Eocene: Aksyir svita, Zaysan Basin, Kazakhstan.

Description: Complete specimens are arcuate in lateral view and sub-rounded in cross-section with regularly spaced, thin, longitudinal grooves. It is common for specimens to be conjoined (Fig. 12.9).

Discussion: This ichnospecies is currently only known from the Triassic to the Eocene. The specimens referred to this ichnospecies from the Early Permian of New Mexico have widely spaced, coarse grooves (Cantrell et al. 2012: fig. 2C–J) and represent a different ichnotaxon. Later Mesozoic and Early Tertiary occurrences appear to represent this ichnospecies (e.g., Lucas et al. 2012a; Suazo et al. 2012).

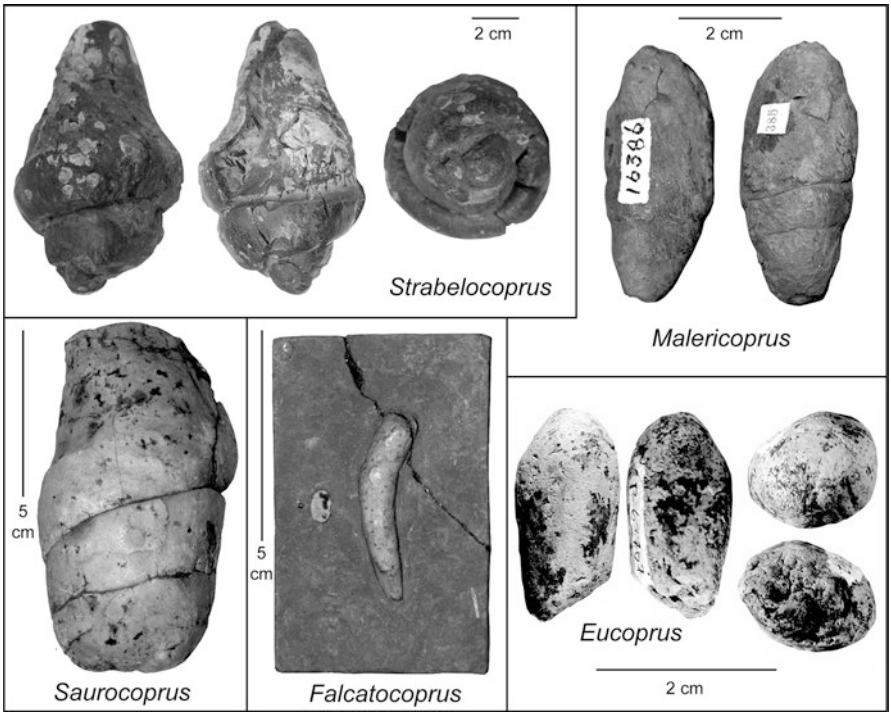

Fig. 12.10 Typical Late Triassic coprolite genera. *Strabelocoprus* (Hunt et al. 2012a: fig. 4A–C). *Malericoprus* (Hunt et al. 2012b: fig. 1T–U). *Saurocoprus* (Hunt et al. 2012c: fig. 1H). *Falcatocoprus* (Hunt et al. 2012f: fig. 1K). *Eucoprus* (Hunt et al. 2013a: fig. 2E–H)

Tracemaker: Northwood (2005) noted that longitudinal intestinal rugae, which would produce striated feces, occur in both amphibians and reptiles, but argued that *Alococopros triassicus* (her "longitudinally striated coprolites") represent archosauromorphs, because: (1) this ichnotaxon first occurs in the Early Triassic; (2) some extant reptiles have longitudinal rugae; and (3) they resemble extant crocodile feces (Young 1964). This is a reasonable hypothesis with Late Triassic forms produced by crocodylomorphs and later examples by crocodylians.

***Revueltobromus* Hunt and Lucas 2016d**

Type ichnospecies: *Revueltobromus complexus* Hunt and Lucas 2016d

Distribution: Bull Canyon Formation (Norian: Revueltian) of eastern New Mexico, USA.

Diagnosis: Bromalite that differs from others in being composed of small, striated and lunate pellets within a thin cylindrical sheath (Fig. 12.9).

Description: *Revueltobromus complexus* is a complex specimen that consists of small *Alococopros*-like specimens (lunate, striated) encased in an apatitic sheath that covers one end (Hunt et al. 2013a: fig. 8N–Q). The holotype (NMMNH P-16204) is 35 mm long and ovoid in cross section (20 by 17 mm). The 1.9 mm-thick outer layer surrounds the lunate pellets.

Discussion: Because this ichnotaxon apparently comprises multiple coprolite-like pellets (*Alococoprus triassicus*) within a structure, it cannot represent an evacuated bromalite. Thus, this ichnotaxon probably represents an evisceralite or a section of the gastrointestinal tract preserved outside the body cavity (*sensu* Hunt and Lucas 2012a). Conjoined specimens of *Alococopros* (usually twice the size of the components of *Revueltobromus*) occur at other localities (e.g., Suazo et al. 2012: figs. 7A–G).

Tracemaker: Given the similarity to *Alococoprus*, it is likely that *Revueltobromus* was produced by a crocodylomorph.

***Dicynodontocopros* Hunt et al.** 1998

Type ichnospecies: *Dicynodontocopros maximus* Hunt et al. 1998

Distribution: Middle Triassic: (Perovkan and Berdyankian), Russia; Middle Triassic (Perovkan) Mollo-Khara-Bala-Kantemir locality, Kazakhstan; Potrerillos, Cacheuta and Río Blanco formations (Berdyankian?), Cuyana Basin, Argentina: Late Triassic: Colorado City Formation (Otischalkian: Carnian), Texas, USA; Tecovas Formation (Adamanian: Carnian), Texas, USA; Bluewater Creek Formation (Adamanian: Carnian), Arizona, USA; Blue Mesa Member of the Petrified Forest Formation (Adamanian: Carnian), Arizona, USA; Bluewater Creek Formation (Adamanian: Carnian), New Mexico, USA.

Description: Large vertebrate coprolites (up to 10 cm long), often dark gray in color, preserving up to four loose coils, often containing large (up to 4 mm in diameter) blebs of carbonaceous plant debris, having a slightly arcuate long axis with one end broadly rounded and the other coming to an acute tip, with a maximum width-to-length ratio of about 45–50% (Fig. 12.9).

Discussion: This ichnotaxon is most abundant at the *Placerias* quarry in northeastern Arizona, USA (Hunt et al. 1998, 2013a).

Tracemaker: *Dicynodontocopros maximus* is the coprolite of a dicynodont (principally *Placerias* during the Late Triassic) (Hunt et al. 1998). It is a proxy for several localities where dicynodont bones are lacking (e.g., western New Mexico).

***Falcatocopros* Hunt et al.** 2007

Type ichnospecies: *Falcatocopros* oxfordensis Hunt et al. 2007

Distribution: Late Triassic: Blue Mesa Member of Petrified Forest Formation (Chinle Group) (Late Triassic: Adamanian: Carnian), Arizona, USA; Rhaetian Westbury Formation (Penarth Group), England; Late Jurassic: Oxford Clay (Oxfordian), England.

Description: Differs from other coprolite ichnogenera in being long, narrow and arcuate in lateral view, rounded to sub-rounded in cross section with a width that gradually decreases from one end to the other (Fig. 12.10).

Discussion: This ichnospecies ranges from the Late Triassic to Late Jurassic. It is uncommon, and probably, at least in part, the result of a taphonomic artifact related to its slender morphology that would render it susceptible to mechanical breakage.

Tracemaker: This ichnotaxon is presumed to be have been produced by an unidentified tetrapod.

***Eucoprus* Hunt and Lucas** 2012b

Type ichnospecies: *Eucoprus cylindratus* Hunt and Lucas 2012b

Distribution: Early Triassic: Arcadia Formation (Lootsbergian), Queensland, Australia; Tecovas Formation (Adamanian), Texas, USA; Bull Canyon Formation (Revueltian: Norian), New Mexico, USA; Redonda Formation (Apachean: late Norian) of New Mexico, USA; Late Cretaceous: Kirtland Formation (Campanian), New Mexico, USA; Naashoibito Member of the Ojo Alamo Formation (Maastrichtian), New Mexico, USA: Paleocene: Nacimiento Formation (Puercan and Torrejonian), New Mexico, USA: Eocene: San Jose Formation (Wasatchian), New Mexico, USA; lower part of the Aksyir svita (late Eocene), Zaysan Basin of northeastern Kazakstan.

Description: Coprolite that is cylindrical in shape, with rounded ends and contains no osseous inclusions (Fig. 12.10).

Discussion: This ichnospecies is probably much more widespread than has been currently documented.

Tracemaker: *Eucoprus* was produced by a wide variety of carnivorous tetrapods based on its long stratigraphic range.

12.4.2 Coprolite Ichnoassemblages

12.4.2.1 Western United States

Vertebrate coprolites are common and locally abundant in strata of the Upper Triassic Chinle Group in the western United States (Hunt and Lucas 1989, 1993a, c; Murry 1989; Murry and Long 1989; Hunt et al. 1998; Heckert et al. 2005). The oldest, Otischalkian, specimens are restricted to West Texas and Wyoming. Adamanian samples are the most abundant, followed by Revueltian. Apachean coprolites are only abundant in eastern New Mexico.

Vertebrate coprolites are common in Adamanian localities in northeastern Arizona. Heckert et al. (2002) described coprolites from the Shinarump Formation or lowermost Cameron Formation near Cameron. Coprolites, including multiple specimens of *Dicynodontocopros maximus*, are abundant in the Bluewater Creek Formation at the *Placerias* quarry near St. Johns (e.g., Camp and Welles 1956; Kaye and Padian 1994; Hunt et al. 1998). Coprolites, including *Dicynodontocopros maximus*, occur in the Blue Mesa Member of the Petrified Forest in the Blue Hills, also near St. Johns (e.g., Norman et al. 2009; Hunt et al. 2013a: fig. 7N–Q).

Adamanian coprolites are common at Petrified Forest National Park in the Blue Mesa Member of the Petrified Forest Formation (Murry and Long 1989; Hunt and Santucci 1994; Hunt et al. 1998, 2012d; Wahl et al. 1998; Heckert 2001, 2004). A notable locality is the "Dying Grounds," which is a fossiliferous horizon high in the Blue Mesa Member near Blue Mesa (e.g., Murry and Long 1989; Heckert 2001, 2004). Hunt et al. (1998) noted that *Heteropolacopros texaniensis* occurs in the Blue Mesa Member at the Park. Hunt et al. (2012f: fig. 2A) described *Falcatocopros oxfordensis* from an unknown Blue Mesa locality.

The USNM collection includes *Heteropolacopros* and indeterminate coprolites from a sample collected near Petrified Forest National Park, presumably from the Blue Mesa Member (Hunt et al. 2012b).

Significant accumulations of coprolites occur in the lower part of the Revueltian Painted Desert Member at Petrified Forest National Park at localities that include Dinosaur Hill (Hunt and Lucas 1993c). Coprolites are also common in the Revueltian Owl Rock Formation at Ward Terrace (Kirby 1989). Lipman and McLees (1940) described a new species of fossil bacteria from a coprolite from an unknown locality in Arizona.

Ash (1978) described a large number of coprolites from a lacustrine mudstone unit in the Adamanian Bluewater Creek Formation of western New Mexico (Hunt et al. 2013a). The sample includes *Dicynodontocopros maximus*, *Heteropolacopros texaniensis* and *Alococopros triassicus* (Hunt et al. 2013a). Weber and Lawler (1978) analyzed the lipid content of a sample of these coprolites. Other localities in the Bluewater Creek Formation yield abundant coprolites, including specimens of *Dicynodontocopros maximus* (Heckert and Lucas 2003; Hunt et al. 2013a: figs. 8D–M).

Adamanian coprolites occur in several other stratigraphic units in New Mexico, including the Los Esteros Member of the Santa Rosa Formation, Garita Creek Formation, lower Petrified Forest Formation and Salitral Formation (Hunt and Lucas 1988, 1990, 1993b; Hunt et al. 1989b). The Revueltian Bull Canyon Formation of east-central New Mexico yields large coprofaunas (Lucas et al. 1985; Hunt 1994, 2001; Hunt et al. 2013a: figs. 8N–T, 10A–H). Lucas et al. (1985) described three morphologies of coprolites: (1) longitudinally furrowed specimens that represent *Alococopros triassicus* (Lucas et al. 1985: fig. 7M–R); (2) small specimens with a rod-like to oval morphology (>90% of sample) (Lucas et al. 1985: fig. 7A–L); and (3) large, irregularly shaped forms with numerous inclusions (fish scales, bone fragments) (Lucas et al. 1985: fig. 7S–U).

The most extensive coprolite locality is in Revuelto Creek (NMMNH locality 1) and yields *Eucoprus cylindratus*, *Alococopros trassicus*, a heteropolar form similar to *Heteropolacopros*, coiled coprolites and comma-shaped specimens (Hunt et al. 2013a). Coprolites are also present at other Revueltian localities in New Mexico, including the upper Petrified Forest Formation in the San Ysidro area (Hunt and Lucas 1990) and Chama Basin (Hunt and Lucas 1993b), and the Trujillo Formation (Hunt 1991a) and Correo Sandstone Member of the Petrified Forest Formation at Mesa Gigante and in the Hagan Basin (Hunt and Lucas 1993b). The Apachean Redonda Formation of east-central New Mexico yields numerous coprolites. The largest concentration is at the Gregory quarry (NMMNH locality 485) in Apache Canyon (Hunt et al. 2013a: figs. 8U–KK, 11). This large sample includes the holotype and other specimens of *Eucoprus cylindratus* (Hunt and Lucas 2012b: fig. 4), *Alococopros* sp. as well as *Heteropolacopros texaniensis* and other heteropolar forms. Coprolites occur associated with skeletons of *Coelophysis* in the Apachean Rock Point Formation at Ghost Ranch (Rinehart et al. 2005a, b, 2009).

Vertebrate coprolites are common in the Upper Triassic strata of West Texas. Otischalkian coprolites occur in the Colorado City Formation near Midland (Elder 1978, 1987; Hunt et al. 2013a, b: Figs. 2AA-GG, LL-MM, 5A–I) and are particu-

larly abundant at Otis Chalk quarries 1 and 2. These samples include *Heteropolacopros texaniensis* (Elder 1978: pl. 14, fig. 1a; Hunt et al. 2013a: Figs. 2AA-GG, LL-MM), *Alococopros triassicus* (Elder 1978: pl. 14, fig. 1b; Hunt et al. 2013a: fig. 5H–I) and *Dicynodontocopros maximus* (Hunt et al. 2013a).

Case (1922) recognized three coprolite forms from the Adamanian Tecovas Formation of West Texas that include the holotype and referred specimens of *Heteropolacopros texaniensis* (Case 1922: fig. 33A–B; Hunt et al. 1998: fig. 2C–L). Other specimens from the Tecovas include the holotype of *Dicynodontocopros maximus* (Hunt et al. 1998: fig. 2A–B) and specimens of *Alococopros triassicus* Case (1922: fig. 33C–D; Hunt et al. 2007, 2013a). Localities in the badlands north of Amarillo include the extremely fossiliferous Rotten Hill bonebed (Lucas et al. 2016). This locality is in the Tecovas Formation and has yielded a large sample of coprolites (Hunt et al. 2013a; Lucas et al. 2016: fig. 10). Like most Adamanian coprolite faunas in the Chinle Group, this collection includes *Heteropolacopros* and *Alococopros* as well as *Eucoprus* (Hunt et al. 2013a; Lucas et al. 2016).

Specimens of *Heteropolacopros* and *Alococopros triassicus* from the Purgatoire River Valley of Colorado probably derive from the Revueltian Cobert Canyon Sandstone Bed of the Baldy Hill Formation (Hunt et al. 2012b). The largest broken specimen is 89 mm long and is the largest known nonmarine Triassic coprolite (Hunt et al. 2012b: fig. 2A). Coprolites also occur in fish beds of the Apachean Rock Point Formation in the southwestern part of the state.

Parrish (1999) reported abundant coprolites from the Adamanian Monitor Butte Formation in southern Utah. DeBlieux et al. (2006: figs. 9A–C) illustrated numerous coprolites from the Petrified Forest Formation of Zion National Park in southern Utah that may be either Adamanian or Revueltian in age. Coprolites are common in a laterally extensive interval in the upper Apachean Bell Springs Formation at Dinosaur National Monument (Hunt et al. 1993c). Coprolites occur on the main track bed at the Shay Canyon tracksite (Rock Point Formation) in southeastern Utah (Lockley 1986; Lockley and Hunt 1995: fig. 3.8).

Coprolites are locally common in the Popo Agie Formation of Wyoming (e.g., High et al. 1969; Hunt et al. 1998, 2013a: fig. 5Q–T).

12.4.2.2 Eastern United States

The Newark Supergroup ranges in age from Middle Triassic to Early Jurassic. However, there are very few references to Newark coprolites, though it seems that they are most common in the Carnian and Jurassic strata (e.g., Olsen 1988; Olsen et al. 1989, 2003, 2005a, b; Olsen and Flynn 1989; Olsen and Huber 1997, 1998; Olsen and Rainforth 2001; Gilfillian and Olsen 2000; Hunt et al. 2007). Gilfillian and Olsen (2000) noted that coprolites are the most common trace fossils in the fish-bearing lacustrine units of the Newark and that large specimens probably derive from coelacanths.

Olsen (1988) noted abundant Carnian coprolites in the Lockatong Formation from several localities (see also Olsen et al. 1989; Olsen and Flynn 1989; Olsen and Rainforth 2001; Jenkins in Häntzschel et al. 1968). Other Carnian localities include

the Stockton Formation in North Carolina (Olsen and Huber 1998: table 1) and the Doswell Formation of Virginia (Weems 1980).

12.4.2.3 Greenland

Milàn et al. (2012) provided a preliminary description of an extensive coprolite ichnofauna from the basal Rhaetian part of the Kap Stewart Formation of Jameson Land. Subsequently, Hansen et al. (2015) described over 300 coprolites from this locality, representing a variety of morphotypes.

12.4.2.4 South America

Hollocher et al. (2005) described the chemistry and mineralogy of a small sample of coprolites from the Ischigualasto Formation of Argentina (see also Contreras 1995). Mancuso et al. (2013) described four morphotypes from the Triassic Potrerillos, Cacheuta and Río Blanco formations of the Cuyana Basin that may be Carnian in their upper part based on pollen (see also Hunt et al. 2007).

The oldest known latrinites (sensu Hunt and Lucas 2012a) occur in the Chañares Formation in Argentina, which may range up into the early Carnian (Fiorelli et al. 2013). The latrinites are attributed to kannemeyeriiform dicynodonts and indicate communal latrines and probably gregarious behavior. Langer (2005) noted that coprolites were collected from the lower Caturrita Formation (Adamanian) of Brazil.

12.4.2.5 Europe

Coprolites are very common in the bone beds of the Westbury Formation in southwestern England, and many specimens are preserved in museum collections (e.g., Buckland 1835; Duffin 1979; Storrs 1994; Martill 1999; Swift and Duffin 1999; Gallois 2007; Hunt et al. 2012a, b: Fig. 12.12). There are more than half a dozen morphotypes in the Westbury coprofaunas, including both spiral (amphipolar and heteropolar) and nonspiral forms, *Liassocopros hawkinsi*, *Saurocopros bucklandi* and *Strabelocoprus pollardi* (Duffin 1979; Swift and Duffin 1999; Hunt et al. 2007, 2012a, b, c, 2013b: fig. 12). Klompmaker et al. (2010) noted coprolites in Rhaetian shale in the Netherlands.

Zatoń et al. (2015) described the composition of a small sample of four morphotypes of coprolites from the Zbąszynek beds (Woźniki Formation) of Norian age in Poland. These specimens were produced by carnivores but include inclusions of plant material.

Upper Norian (Revueltian) sediments of the Lipie Śląskie clay-pit near Lubliniec yield abundant large coprolites (Bajdek et al. 2014). These coprolites include plant debris and are attributed to a dicynodont that is common at this locality (Bajdek et al. 2014).

Qvarnström et al. (2017) studied two coprolites from the upper Carnian locality of Krasiejów using synchrotron microtomography. One preserved beetle remains, and the other a partly articulated fish and fragments of bivalves. Qvarnström et al. (2016: fig. 3J) illustrated fibrous elements in association with bone inclusions in a carnivorous vertebrate coprolite from the Late Triassic of Poland.

Coprolites are common in the Rhaetic bone beds of Switzerland (e.g., Fluckiger 1858). Fraas (1891) reported common spiral coprolites from the German "Keuper," which he attributed to sharks. The Stuttgart Formation (middle Carnian) includes coprolites (Schoch 2002).

12.4.2.6 Africa

Anderson et al. (1998) noted that coprolites are very rare in the Molteno Formation of South Africa.

12.4.2.7 Asia

The Carnian-Norian Huai Hin Lat Formation at Huai Nam Aun in Chaiyaphum Province, Thailand, has yielded abundant coprolites (Laojumpon et al. 2012). Laojumpon et al. (2012) recognize seven different morphotypes, including *Liassocopros hawkinsi* and *Saurocopros bucklandi*.

Coprolites were recognized in the Otischalkian-Adamanian Maleri Formation in India more than 150 years ago and are locally common (Oldham 1859; King 1881; Aiyengar 1937; Matley 1939; Sohn and Chatterjee 1979; Jain 1983; Vijaya et al. 2009). Most fossils, including coprolites, derive from the Otischalkian portion of the Maleri Formation (Hunt et al. 2007). Coprolites include *Malericopros matleyi*, *Heteropolacopros texaniensis*, *Liassocopros hawkinsi* and probably *Saurocopros bucklandi*, as well as amphipolar forms (Matley 1939; Jain 1983; Hunt et al. 2007; Vijaya et al. 2009).

12.4.3 Biostratigraphy and Biochronology

Vertebrate coprolites are of biochronological utility (e.g., Hunt 1992; Hunt et al. 1998, 2005a, 2007, 2013a, b). However, as noted above, vertebrate ichnotaxa almost always correspond to higher level taxonomic groups of body fossils. Thus, footprint ichnogenera are commonly only equivalent to the "family" level of body fossils (Lucas 2007). Coprolites probably represent, in most cases, even higher level taxonomic levels ("order" or above) (Hunt et al. 2007, 2013a). However, coprolite ichnotaxa do have defined stratigraphic ranges that parallel the stratigraphic ranges of the producing animals, so the coprolites have some utility in biostratigraphy and biochronology (Hunt and Lucas 2005; Hunt et al. 2007, 2013a, b).

Hunt et al. (1998) first applied binomial nomenclature to Triassic coprolites. Subsequently, we, and co-authors have named several other ichnotaxa that have been utilized by a number of workers (e.g., Duffin 2010; Laojumpon et al. 2012). However, others have been reluctant to apply a binomial nomenclatural scheme to coprolites based on the misconception that feces are not distinguishable, even though wildlife biologists routinely track the distribution of extant taxa based on the distinct morphologies of their feces (e.g., Stuart and Stuart 2000; Chame 2003; Angom et al. 2012). Some of the most biochronologically important ichnotaxa for the Triassic are (Fig. 12.11):

1. *Hyronocopros amphipola* is common in the Permian and apparently has its last occurrence in the Middle Triassic (Hunt et al. 2013a).
2. *Alococopros triassicus* is abundant and characteristic of the Triassic, although there are reported occurrences from the Permian to the Cretaceous (Cantrell et al. 2012; Suazo et al. 2012). Permian occurrences may represent a different ichnotaxon with wider spaced grooves.
3. *Dicynodontocopros maximus* ranges from the Middle to the Late Triassic (upper Carnian) and it occurs in some faunas as the only evidence of the presence of dicynodonts (e.g., Chinle Group of West Texas and western New Mexico).
4. *Heteropolacopros texaniensis* first occurs in the Pennsylvanian, and it is abundant in the Carnian but rare in the Norian and absent in the Rhaetian.
5. The first occurrence of *Strabelocoprus pollardi* is in the Rhaetian, and the coprolite faunas of this age lack *Heteropolacopros texaniensis.*

The base of the Late Triassic is marked by the last occurrence of *Hyronocopros* and the first appearance of *Saurocopros* (Fig. 12.11). The end of the Carnian coincides with the last occurrence of *Dicynodontocopros* and *Malericopros* and a marked decrease in the abundance of *Heteropolacopros* and *Alococopros.* The start of the Rhaetian coincides with the last occurrence of *Heteropolacopros* and the first occurrence of *Strabelocoprus.* There is no apparent change in coprolites across the Triassic/Jurassic boundary (Fig. 12.11).

12.4.4 Ichnofacies

Coprolites are trace fossils and thus facies fossils. Hunt and co-workers (Hunt et al. 1994a, 1998, 2007, 2013a; Hunt and Lucas 2007d) recognized four Late Triassic coprolite ichnocoenoses, and there is also a long-ranging association of heterospiral coprolites that encompasses this time interval (Hunt et al. 2013a, 2015b).

There are three possible approaches to describing coprolite ichnofacies. First, there is a sophisticated scheme of archetypal (Seilacherian) ichnofacies that principally incorporate invertebrate ichnotaxa (see recent reviews in Buatois and Mángano 2011 and MacEachern et al. 2012). The pervasive association of heteropolar coprolites in shallow marine environments could be considered an archetypal ichnofacies. Second, Hunt and Lucas (2007d, 2016a) defined a set of vertebrate archetypal ich-

nofacies that are based on tracks. The principal difference from the Seilacherian ichnofacies is that the vertebrate ichnofacies includes the identity of the tracemaker as well as its behavior in their definition. Third, we could propose a parallel ichnofacies system just for coprolites. A challenge to this approach is that it is only in the last 20 years that there has been application of binomial nomenclature to coprolites and an increased volume of literature, so there are relatively few potential name bearers (Hunt et al. 1998, 2012d).

We have decided to take a conservative approach and name two ichnofacies within the Seilacherian scheme. The first recognizes the widespread occurrence of large accumulations of spiral coprolites, principally in shallow marine environments, and the second that coprolites are a substrate for other kinds of trace fossils. Subsequently, the former could be incorporated in the vertebrate ichnofacies model by recognizing that spiral coprolites are principally produced by chondrichthyans.

12.4.4.1 *Crassocoprus* Ichnofacies

Definition: Buckland (1829, 1835) largely based his definition of coprolites on the recognition that heteropolar "bezoar stones" from the Early Jurassic of Lyme Regis in southwestern England represented fossil feces. Heteropolar coprolites occur in large numbers in shallow marine strata from the Mississippian to the Eocene (e.g., Hunt et al. 2015b).

We formally define the *Crassocoprus* ichnofacies to include marine trace fossil ichnocoenoses dominated by heteropolar coprolites and that include coprolites of low to moderate ichnodiversity. Shale substrates typify the *Crassocoprus* ichnofacies. The name is for *Crassocoprus*, a macrospiral heteropolar coprolite from the Pennsylvanian that is attributed to a chondrichthyan (Hunt et al. 2012g).

Discussion: Heteropolar coprolites date back to the Devonian and become abundant during the Pennsylvanian (Hunt and Lucas 2016b). Principal large samples of heteropolar coprolites (shallow marine setting unless indicated otherwise) occur in the:

1. Middle-Late Mississippian
   Wardie, Midlothian, Scotland (Middle Mississippian: Viséan) (Buckland 1835; Sumner 1991)
   Anstruther, Fife, Scotland (Middle Mississippian: Viséan) (Sumner 1991).
   Bearsden, East Dunbartonshire, Scotland (Late Mississippian: Serpukhovian) (Clark 1989)
2. Late Pennsylvanian
   Park and Chaffee Counties, Colorado, USA (Johnson 1934).
   Bassam Park, Colorado, USA (Houck et al. 2004)
   Morgantown, West Virginia, USA (Price 1927)
   Sacramento Mountains, New Mexico, USA (Hunt et al. 2012g)
3. Early Permian
   Manhattan, Kansas, USA (Williams 1972; McAllister 1985)

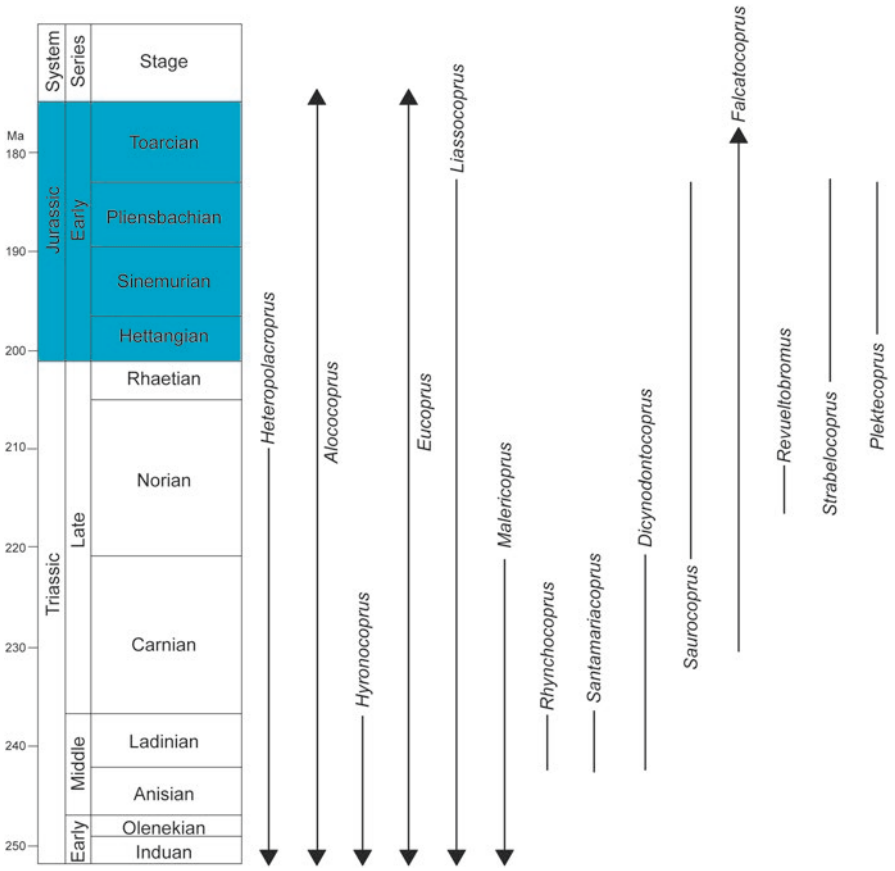

Fig. 12.11 Vertebrate coprolite biostratigraphy and biochronology of the Triassic

4. Middle/Late Permian
   Southern Brazil – lacustrine (Dentzien-Dias et al. 2012a)
5. Late Permian/Early Triassic
   European Russia – nonmarine (Niedźwiedzki et al. 2016b)
6. Early Jurassic
   Lyme Regis, England (Buckland 1835; Hunt et al. 2012a)
7. Late Cretaceous
   Southern England, Western Europe (Hunt et al. 2015b)
8. Middle-Late Eocene
   Northern Germany (Diedrich and Felker 2012)
   Alabama, USA (Stringer and King 2012)

12.4.4.2 *Gaspeichnus* Ichnofacies

Definition: Feces provide a source of food for some insects and vertebrates. Coprolites also undergo bioerosion and are the subject of accidental contact by vertebrates. Therefore, coprolites preserve a variety of traces reflecting vertebrate dentalites, vertebrate footprints and invertebrate borings. We formally define the *Gaspeichnus* ichnofacies to include marine and nonmarine trace fossil ichnocoenoses of low diversity dominated by macroscopic borings and vertebrate dentalites and footprints that utilize coprolites as a substrate. The name is for *Gaspeichnus,* a sinuous coprolite boring from the Devonian (see the Appendix).

Discussion: Tapanila et al. (2004: fig. 3C–E) described flask-shaped borings in both bone and coprolites from the Cretaceous-Eocene of Mali. The coprolite borings have more narrow openings and typically exhibit sculpturing in the basal walls that consist of chevron-shaped grooves arranged in concentric to spiraled whorls, and Tapanila et al. (2004: fig. 3D–F) assigned them to *Gastrochaenolites ornatus* Kelly and Bromley, 1984. These are putative bivalve borings and individual coprolites have multiple examples (Tapanila et al. 2004: fig. 3C).

Dentzien-Dias et al. (2012a: fig. 11c) described an amphipolar coprolite with an invertebrate boring from the Rio do Rasto Formation (Middle/Upper Permian) in southern Brazil. The boring has smooth margins and a cylindrical shape and is interpreted as an indeterminate invertebrate boring.

Wahl et al. (1998) suggested that small holes in Late Triassic coprolites from Arizona, USA were produced by insects, such as dipteran larvae. There are several putative examples of coprophagy traces of dung beetles in the Cretaceous and early Tertiary of the USA (Bradley 1946; Chin and Gill 1996).

Antunes et al. (2006) described Miocene mammalian footprints preserved in coprolites from Portugal. Three coprolites from different stratigraphic horizons yielded: (1) a tridactyl footprint that can be ascribed to a right foot of the rhinoceros *Hispanotherium matritensis;* (2) a tridactyl, left foot impression of a perissodactyl, possibly an *Anchitherium*-like equid; and (3) a didactyl track from a small-sized ruminant, most probably a cervid, genus *Procervulus*. The tridactyl coprolites may have been produced by the animals that stepped on them.

Two coprolites from the Miocene Chesapeake Group of the Calvert Cliffs, Maryland, USA preserve dentalites of sharks (Godfrey and Smith 2010). The shark impressions are of partial dental arcades and could result from: (1) aborted coprophagy, (2) benthic or nektonic exploration, or (3) predation.

Godfrey and Palmer (2015) described a coprolite bitten by a gar from South Carolina, USA. The coprolite derives from a thick lag deposit that includes a mixture of Late Cretaceous, early Paleocene, and Plio-Pleistocene taxa.

Recent studies have also highlighted that coprolites contain diverse body fossils of delicate and rare organisms (Dentzien-Dias et al. 2013, 2017; Qvarnström et al. 2016, 2017). These include vertebrate soft tissues (e.g. muscle tissue and hairs) and parasites (Qvarnström et al. 2017).

12.5 Other Vertebrate Trace Fossils

12.5.1 Consumulites

The majority of tetrapod consumulites described from the Late Triassic pertain to phytosaurs or theropods in the United States and India. Two phytosaur skeletons of *Pseudopalatus pristinus* from the Revueltian (Norian) Bull Canyon Formation of eastern New Mexico, USA, preserve consumulites (Hunt 1991b, 1994, 2001; Hunt and Lucas 2016d). NMMNH P-20852 is a skull and skeleton of a dolichorostral (*sensu* Hunt 1989) (female) phytosaur with preserved consumulites consisting of a proximal pubis of a smaller phytosaur and a series of centra of the sphenosuchian *Vancleavea campi*. NMMNH P-4979 is an altirostral (male) phytosaur skeleton that includes as an evident consumulite a small series of dorsal centra of the metoposaurid amphibian *Apachesaurus gregorii*.

Chatterjee (1978) described two associated skeletons of the phytosaur *Parasuchus* from the lower Maleri Formation (Carnian) of India. Each specimen contains a small bipedal archosaur in the stomach, the bones of which are more or less articulated and well preserved, except for the caudal region. The left specimen "… shows a few skull bones of a rhynchosaur in its stomach" (Chatterjee 1978: 111). Subsequently, Chatterjee (1980) described the small reptile as *Malerisaurus robinsoni,* which may be a synonym of *Trilophosaurus buettneri* (Spielmann et al. 2006).

Three kinds of bromalites are associated with skeletons of the theropod dinosaur *Coelophysis bauri* in the Apachean Rock Point Formation at Ghost Ranch in northern New Mexico, USA (Rinehart et al. 2005a, b, 2009; Nesbitt et al. 2006; Hunt and Lucas 2016d). Bromalite material was found in area of the mouth of NMMNH P-44551, a skull and incomplete neck, which is presumed to belong to the postcranial skeleton NMMNH P-44552 (Rinehart et al. 2009: fig. 119E, F). This specimen contains numerous bone fragments, in a dark reddish brown matrix that is less granular than that of coprolites associated with the *Coelophysis* and darker in color than the surrounding siltstone (Rinehart et al. 2009). The exact location relative to the skull is unclear (Rinehart et al. 2009: fig. 119E, F), and it could be within the oral cavity and thus an oralite (*sensu* Hunt and Lucas 2012a) or an expelled regurgitalite. Whatever its location, the presence of matrix suggests that the bromalite represents regurgitated material. This specimen includes small premaxillary and other teeth of *Coelophysis* (Rinehart et al. 2009: fig. 119F).

Three specimens of *Coelophysis bauri* from NMMNH block C-8-82 have bromalitic material directly associated with articulated skeletal material (Rinehart et al. 2005a, b, 2009). These specimens have indistinct structure and a granular matrix. Some specimens occur between the ischia and the proximal caudal vertebrae and apparently represent incorporeal pelletites (pelletized bromalites preserved within the gastrointestinal tract: Hunt and Lucas 2012a), whereas others are coprolites (excorporeal pelletites: Hunt and Lucas 2012a) that are posteroventral to the proximal caudal vertebrae (Rinehart et al. 2009). These specimens include apparent fish

scale debris and bones of juvenile *Coelophysis* (Rinehart et al. 2009). Two skeletons in the AMNH collection preserve putative demalites (skeletal material preserved within the body cavity of a vertebrate *sensu* Hunt and Lucas 2012a) (Colbert 1989, 1995; Nesbitt et al. 2006).

The neotype of *Coelophysis bauri* (AMNH FR 7224) consists of a nearly complete, mediolaterally crushed skeleton and the abdominal cavity that apparently contains disarticulated skeletal remains concentrated in the posterodorsal region and articulated remains in the anteroventral region, of which only the latter are demalites (Nesbitt et al. 2006). These specimens apparently represent a gastrolite consisting of specimens of *Hesperosuchus* (Nesbitt et al. 2006). Putative demalites associated with a second skeleton (AMNH FR 7223) are probably actually lying underneath the skeleton (Nesbitt et al. 2006). Colbert (1989, 1995) originally interpreted putative demalites as specimens of *Coelophysis,* but only one is actually a cololite, and it contains elements of *Hesperosuchus* (Nesbitt et al. 2006).

However, Rinehart et al. (2009) found specimens in a coprolite that included carpal and manual bones indistinguishable from those of a small juvenile *Coelophysis* and a regurgitalite that contains two laterally compressed finely serrated teeth in a jaw fragment and a premaxilla fragment with one complete, premaxillary tooth. The teeth are morphologically identical (including the denticle count) to those of a small *Coelophysis* (Rinehart et al. 2009). Thus, the most parsimonious interpretation of the small, apparent *Coelophysis* teeth, manual, and carpal elements in the coprolite and regurgitalite is that cannibalism occurred in this species (Rinehart et al. 2009).

An undescribed skeleton of a new paracrocodylomorph from the Upper Triassic (Neshanician: Norian) of North Carolina, USA, preserves diverse bones as a gastrolite (Lucas et al. 1998; Sues et al. 2003). These elements, some bearing tooth marks, include osteoderms of a small stagonolepidid archosaur (*Aetosaurus* sp.), a snout, left coracoid and humerus of a traversodont cynodont (*Plinthogomphodon herpetairus*), two articulated phalanges of a large dicynodont, and a fragment of an unidentified ?temnospondyl bone (Sues et al. 2003).

Jurassic ichthyosaur skeletons commonly preserve consumulites (e.g., Pollard 1968; Hunt et al. 2012a), but there are few reports from the Early (Buchy et al. 2004), Middle (Rieber 1970; Brinkmann 2004) or Late Triassic (Camp 1980; Cheng and Chen 2007; Druckenmiller et al. 2014). The three Late Triassic occurrences are distinctive in that the stomach contents consist of a mix of vertebrate and mollusk shell fragments (*Guizhouichthyosaurus tangae*: Cheng and Chen 2007; *Shonisaurus popularis*: Camp 1980; indeterminate shonosaurian: Druckenmiller et al. 2014). In contrast, gastrolites reported from other Triassic ichthyosaurs consist of cephalopod hooklets (Rieber 1970; Brinkmann 2004; Buchy et al. 2004), more typical of Jurassic and later ichthyosaurs (Druckenmiller et al. 2014). Late Triassic ichthyosaurs show substantial variation in dentition and body size and may have occupied a wider range of predatory guilds than their Jurassic and Cretaceous counterparts (Callaway and Massare 1990; Druckenmiller et al. 2014).

12.5.2 Dentalites (Bite Marks)

One hindrance to the growth of vertebrate ichnology continues to be the continued use in the technical literature of imprecise, undefined, vernacular terms such as tracks, dung, bite mark and burrow (Hunt et al. 2013b; Hunt and Lucas 2016d). To this end we propose the term dentalite (from the Latin *dentes,* for teeth and Greek *lithos,* for rock) to encompass all traces produced on a substrate (normally bone, but could be vegetation or even coprolite: Antunes et al. 2006; Lucas 2016) by the teeth or oral cavity of a vertebrate. This term could also be applied to marks left by the jaw apparatus of invertebrates (e.g., echinoid dentalites on crinoids: Baumiller et al. 2010; Gorzelak et al. 2012).

There are relatively few published records of dentalites from the Late Triassic. The most common taxa with dentalites are dicynodonts from South and North America and Europe, and paracrocodylomorphs with several records from North America.

A femur of a dicynodont similar to *Ischigualastia* (Lucas and Hunt 1993), from the upper part of the Los Esteros Member (Adamanian: Carnian) of the Santa Rosa Formation in north-central New Mexico, USA, has multiple tooth marks (Rinehart et al. 2006; Hunt and Lucas 2016d: fig. 17C, D; Fig. 12.12c, d). There are 11 tooth marks on the anterior surface of the distal end and approximately 15 smaller, poorly-preserved tooth marks on the corresponding posterior surface of the femur. Hunt and Lucas (2016d) assigned these traces to *Heterodontichnites hunti* (Rinehart et al. 2006).

Budziszewska-Karwowska et al. (2010) described bite marks on a dicynodont tibia from the Norian Woźniki Limestone of Zawiercie, Kraków-Częstochowa Upland, Southern Poland. The bone has longitudinal dentalites on the anterior side of its shaft, as well as a row of small oval pits that are interpreted to represent the scavenging of more than one carnivore.

Norian strata of the Lipie Śląskie clay pit in southern Poland yield six small dicynodont bones with dentalites (Dzik et al. 2008; Niedźwiedzki et al. 2010). These traces are assigned to *Linichnus serratus, Knethichnus parallelum* and *Nihilichnus nihilicus* and attributed to theropod dinosaurs (Niedźwiedzki et al. 2010). Dentalites also occur on ribs of the dicynodont *Jachaleria candelariensis* from the Carnian Caturrita Formation of Brazil (Braunn et al. 2001; Vega-Dias et al. 2004).

Drumheller et al. (2014) described two partial femora of paracrocodylomorphs ("rauisuchia") from northern New Mexico, USA, with dentalites interpreted to be from phytosaurs. One specimen is the proximal three fifths of a femur from an unknown locality near Ghost Ranch in Rio Arriba County but presumed to be from the Revueltian (Norian) Petrified Forest Formation. It includes an embedded tooth and healed and unhealed tooth marks. The other specimen is a proximal femur from the Adamanian (Carnian) lower Chinle Group (Bluewater Creek Formation or Blue Mesa Member of Petrified Forest Formation) that preserves an embedded tooth and unhealed dentalites (Heckert and Lucas 2002; Drumheller et al. 2014).

The holotype skeleton of the crocodylomorph archosaur *Dromicosuchus grallator* from the Upper Triassic (Neshanician: Norian) of North Carolina, USA, preserves apparent dentalites to the head and neck (Lucas et al. 1998; Sues et al. 2003).

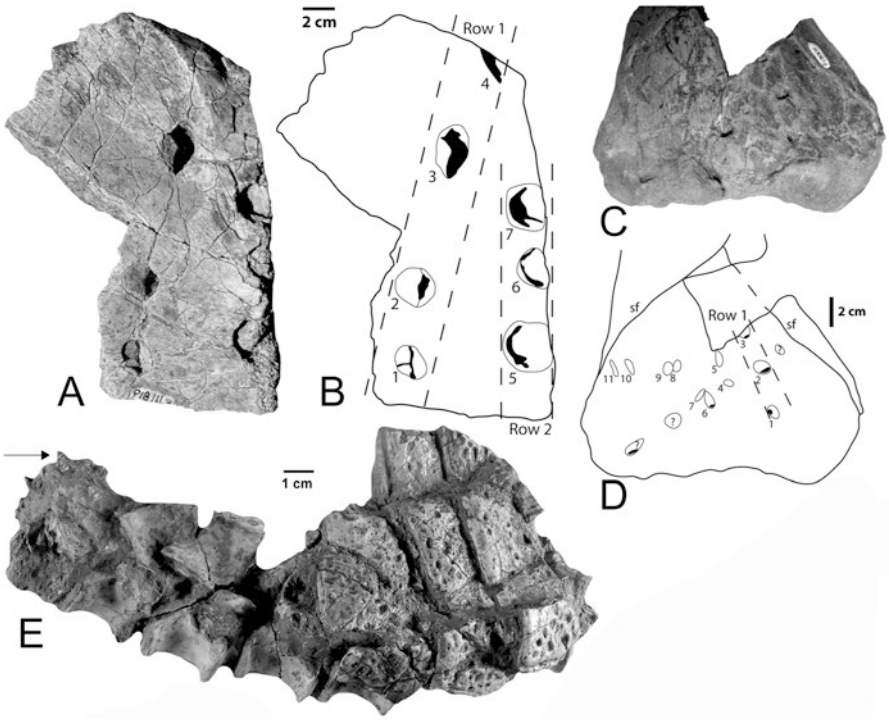

Fig. 12.12 Dentalites (bite marks) from the Late Triassic of New Mexico, USA. (**a**, **b**) NMMNH P-18111 from the Lamy amphibian quarry, 12 cm-long *Koskinodon perfecta* clavicle fragment with holotype bite marks of *Heterodontichnites hunti*. (**a**) Interior surface. (**b**) Sketch showing the tooth mark numbers and rows (after Rinehart et al. 2006: fig. 1C). (**c**, **d**) NMMNH P-13001 from locality L-1410, a left dicynodont femur of *Ischigualastia* sp. with bite marks of *Heterodontichnites hunti*. (**c**) Tooth marks on the anterior distal surface. (**d**) Sketch showing the toothmark numbers and spiral fractures (after Rinehart et al. 2006: fig. 2C). *sf* spiral fracture. (**e**) NMMNH P-16932, topotype skeleton of *Revueltosaurus callenderi* from the Bull Canyon Formation (NMMNH L-467), dorsal vertebral column in lateral view. Note on left the truncation of the last two neural spines, bite marks on last centrum and isolated carnivore tooth (marked by *arrow*). From Hunt and Lucas (2016: fig. 17)

The left third to fifth cervical osteoderms of the sphenosuchian are largely destroyed, leaving a gap in the cervical armor, and the posterior region of the otherwise well preserved left mandibular ramus appears to have been crushed. These bites are attributed to a paracrocodylomorph whose skeleton was found immediately above the *Dromicosuchus* skeleton, and it is inferred that the two animals died and were buried together during the act of predation (Sues et al. 2003).

The topotype skeleton of *Revueltosaurus callenderi* from the Revueltian (Norian) Bull Canyon Formation of eastern New Mexico, USA, preserves evidence of having been bitten (Hunt 1994; Hunt et al. 2005b: figs. 1A–B, 5A; Hunt and Lucas 2016d: fig. 17E–F; Fig. 12.12e). There are three indications of the biting: (1) two posterior dorsal vertebrae have truncated neural spines; (2) the centrum of the most posterior

is heavily pitted as though it has received multiple bites; and (3) a laterally compressed and serrated tooth, oriented medioposteriorly, is affixed to the posteriormost neural arch (Hunt and Lucas 2016d).

The only record of dentalites on a Late Triassic amphibian is a clavicle fragment of *Koskinonodon perfecta* from the Lamy Amphibian Quarry of north-central New Mexico that preserves seven tooth marks on its medial surface (Rinehart et al. 2006; Hunt and Lucas 2016d: fig. 17A–B; Fig. 12.12a, b). This specimen is from the Garita Creek Formation (Adamanian: Carnian). The tooth marks are arranged in two rows and were made by blade-like and rounded teeth that are interpreted to have been made by a phytosaur. Rinehart et al. (2006) named these dentalites *Heterodontichnites hunti.*

12.5.3 Nests

Hasiotis and Martin (1999; also see Hasiotis 2002; Hasiotis et al. 2004) described pits in the Upper Agate Bridge Bed of the Sonsela Member of the Petrified Forest Formation, Chinle Group (Adamanian: Carnian) at Petrified Forest National Park in northeastern Arizona (Fig. 12.13). They interpreted them as nests, and, subsequently, Hasiotis (2002: 123, figs. A, B) attributed the smaller pits to turtles and the larger pits to phytosaurs. However, all these putative nests are demonstrably weathering pits, not of biogenic origin (Lucas and Hunt 2006).

Large depressions with raised rims occur in the Monticello Formation (Tuvalian: late Carnian) of northeastern Italy and Avanzini et al. (2007) interpreted them as vertebrate nests.

These are syndepositional features, and vertebrate tracks occur in superjacent strata. However, there is no compelling reason to believe that these depressions represent nests or even that they are biogenic in origin.

Mussaurus patagonicus is a prosauropod from the late Norian Laguna Colorada Formation (El Tranquilo Group) of Patagonia, Argentina (Bonaparte and Vince 1979). The holotype and subsequent specimens are extremely young individuals and were found in close association with two complete eggs and eggshell fragments (Bonaparte and Vince 1979; Pol and Powell 2007). Eggshell fragments in close association with skeletons of hatchlings provide strong circumstantial evidence of a nest, even though there is no actual nest structure or arrangement of the preserved eggs.

12.5.4 Burrows

Fossil vertebrate burrows are relatively uncommon in the Late Triassic. Casts of lungfish burrows occur locally in the Upper Triassic Redonda Formation (Apachean) at Mesa Redonda, Quay County, New Mexico, USA (Gobetz et al. 2006; Lucas et al. 2010b; Hunt and Lucas 2016d; Fig. 12.14a, b). About 20 casts are densely

Fig. 12.13 Putative reptile "nest" at Petrified Forest National Park, Arizona, USA (NMMNH locality 6756). Trapezoidal pit undergoing mechanical weathering below varnished surface (Lucas and Hunt 2006: fig. 4C)

concentrated over an area of about 5 m^2. They vary in morphology from cylindrical in cross section with helical structure to flask-shaped to very shallow excavations that widen upward. Lucas et al. (2010b) named these *Redondarefugium abercrombieorum* and interpreted them as lungfish estivation burrows.

Other reported lungfish burrows occur in the lower Chinle Group (Adamanian: Carnian) of southeastern Utah and southwestern Colorado, USA (Hasiotis and Hannigan 1991) and western New Mexico (Dubiel et al. 1987). McAllister (1989) disputed the identification of the burrows from near Fort Wingate, New Mexico described by Dubiel et al. (1987), based on dissimilarities to known lungfish burrows. Tanner and Lucas (2007) presented compelling arguments that these structures are rhizoliths.

Hasiotis et al. (2004) reported complex burrows from the Owl Rock Formation of the Chinle Group (Revueltian: Norian) in southeastern Utah. These burrows are characterized by short, interconnected horizontal tunnels, vertical shafts, spiral shafts, and chambers that form a complex network. (Hasiotis et al. 2004: figs. 4A–D). Burrow diameter ranges from 4 to 15 cm. Hasiotis et al. (2004) postulated that the architecture and surficial burrow morphologies indicate that the tracemaker was a vertebrate similar in anatomy and behavior to mammal-like reptiles and mammals.

Two morphotypes of large vertebrate burrows occur in the Cancha de Bochas Member of the Ischigualasto Formation and Los Colorados Formation of northwestern Argentina (Colombi et al. 2012). The morphotypes are characterized by a network of tunnels and shafts. Morphotype 1 from the Ischigualasto Formation is interpreted as being produced by small cynodonts (e.g., *Probelesodon*, cf. *Probainognathus* or *Ecteninion*). The larger morphotype 2 burrows from the Los

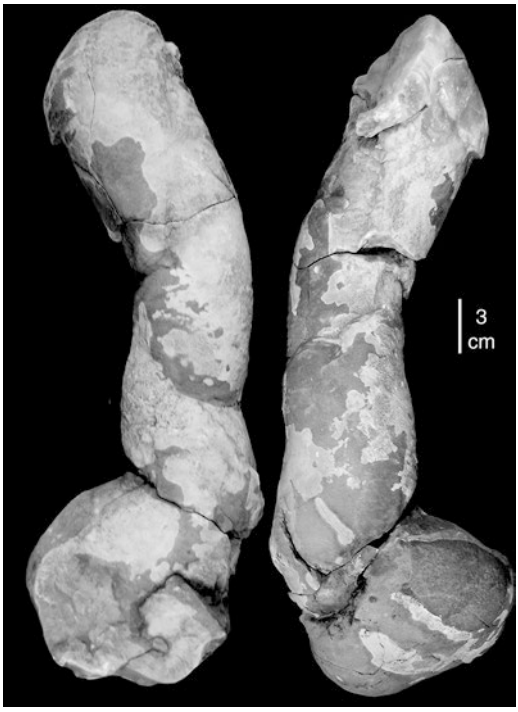

Fig. 12.14 Holotype burrow of *Redondarefugium abercrombieorum*, NMMNH P-50409 (Lucas et al. 2010b: fig. 17A–B)

Colorados Formation are too large to be produced by cynodonts and may represent burrows of sub-adult archosaurs (Colombi et al. 2012).

Tałanda et al. (2011) described a vertebrate burrow system in Upper Triassic (Norian) fluvial strata of the Holy Cross Mountains in central Poland. This is interpreted as burrows of cynodonts.

12.5.5 Gastroliths

Gastroliths are rare in ichthyosaurs, but the holotype skeleton of *Panjiangsaurus epicharis* from the lower Carnian Xiaowa Formation of China contains more than 150 specimens in two clusters (Cheng et al. 2006). Other specimens of *Panjiangsaurus epicharis* do not preserve gastroliths, which Cheng et al. (2006) suggest is a taphonomic artifact.

Weems et al. (2007) described four occurrences of exoliths ("gastrolith-like stones") from the Norian Passaic Formation of northern Virginia, USA. They are not associated with skeletal remains, yet Weems et al. (2007) consider that it is most parsimonious to interpret them as gastroliths based on: (1) "typical" gastrolith microscopic surface texture; (2) evidence of pervasive surface wear that has secondarily removed variable amounts of thick weathering rinds typically found on these

stones; and (3) a width/length-ratio modal peak that is more strongly developed than in any population of fluvial or fanglomerate clasts found in this region. Furthermore, they interpret these stones as gastroliths of prosauropods whose bones are absent from the Late Triassic of North America (Weems et al. 2007). Nevertheless, we are skeptical that these specimens represent gastroliths.

12.6 Terrestrial Invertebrate Trace Fossils

A diverse literature documents various Upper Triassic ichnoassemblages of nonmarine invertebrate traces, many of them listed by Lucas et al. (2010b: table 7). Most of these ichnoassemblages belong to the *Scoyenia* ichnofacies, notable examples being from the Chinle Group in the western USA (e. g., Gillette et al. 2003; Lucas et al. 2010b), the Newark Supergroup in the eastern USA (e.g., Metz 1995, 1996, 2000), from Greenland (e.g., Bromley and Asgaard 1979), from the Keuper strata of Western Europe (e.g., Schlirf et al. 2001) and from Argentina (e.g., Melchor et al. 2001). Nonmarine Upper Triassic red beds of river floodplains or clastic lake margins appear to have invertebrate ichnoassemblages typical of the *Scoyenia* ichnofacies that only vary somewhat in diversity and overall composition. These ichnoassemblages are dominated by shallow grazing traces and burrows (such as *Cochlichnus*, *Gordia, Helminthopsis, Helminthoidichnites, Palaeophycus, Planolites, Scoyenia, Skolithos, Taenidium* and *Treptichnus*) and by arthropod walking traces (such as *Diplichnites*).

Lake margin ichnoassemblages of the Late Triassic appear to be more variable and include *Lockeia*-dominated ichnoassemblages, such as that from lake-margin facies of the Redonda Formation in New Mexico, USA (Lucas et al. 2010b). These contrast with other Late Triassic lake margin ichnoassemblages, which are much more diverse and either lack *Lockeia* or have it as an uncommon constituent (e. g., Metz 2000; Schlirf et al. 2001; Melchor 2004). Some of these lake-margin paleoenvironments, such as lacustrine delta deposits in Argentina, yield ichnofossils of the *Mermia* ichnofacies, though notably from relatively distal portions of the lake margin (Melchor 2004). The abundance of *Lockeia* in some Late Triassic ichnoassemblages probably indicates particular types of lake conditions that differed in one or more factors from the other lakes thus far documented in the trace fossil record of Upper Triassic lake margins.

Late Triassic trace fossils in woody substrates are archetypal of the *Paleoscolytus* ichnofacies of Lucas (2016), as they include the type material of *Paleoscolytus* from the Upper Triassic of Arizona (Walker 1938) (Fig. 12.15). The hypothesized bee's nests in Late Triassic wood in Arizona are actually arthropod borings in the fungal rot *Polyporites* (Lucas et al. 2010a), and pertain to the ichnogenus *Xylokrypta* (Tapanila and Roberts 2012). The oldest osteophagic evidence is in the Middle and Late Triassic of Argentina (Paes Neto et al. 2016), and geologically younger examples occur in that country (e.g., Pirrone et al. 2014; Pirrone and Buatois 2016). Late Triassic records of arthropod borings in bone (cf. Britt et al. 2008: table 1) represent the *Cubiculum* ichnofacies of Lucas (2016). Nevertheless, substrate-based invertebrate traces of the Late Triassic remain greatly understudied.

Fig. 12.15 Holotype *of Paleoscolytus divergens* Walker 1938 (USNM 95872) from the Blue Mesa Member of the Petrified Forest Formation (Adamanian: late Carnian), Petrified Forest National Park, Arizona, USA

An important point is that Late Triassic nonmarine invertebrate ichnoassemblages appear very similar in composition and ichnofacies to Permian, Early-Middle Triassic and to Jurassic ichnoassemblages. This suggests a continuity of the trace-making invertebrate communities through Late Triassic time. The traces thus identify no important evolutionary or ecological breakthroughs in the terrestrial invertebrate communities during the Late Triassic.

12.7 Phanerozoic Record of Vertebrate Trace Fossils

12.7.1 Tracks

The majority of vertebrate trace fossils are tracks. Lucas (2007) provided a useful recent review of the vertebrate track record. Lockley and Hunt (1995: fig. 1.2) provided an overview of the stratigraphic age of tracksites in the western United States, which has the most studied and arguably the richest record of fossil tracks. In general, tracks are first common in the Pennsylvanian. They are notably abundant in the early Permian, Late Triassic-Early Jurassic, Early-Late Cretaceous and to a lesser extent in the Pleistocene.

Hunt et al. (2005c) presented a model of the preservation of tracks based on four premises: (1) tracks will only be common when terrestrial tetrapods are abundant; (2) increasingly complex vegetation, increased terrestrial ground cover and increased sediment binding took place through the Phanerozoic; (3) tetrapod tracks will be more common when ground cover is less extensive; and (4) the preservation potential of tetrapod tracks increases with body size—larger tracks have higher preservational potential. Thus, Hunt et al. (2005c) identified four temporal phases in

the taphonomy of tetrapod tracks: (1) Devonian—few tracks, because terrestrial tetrapods are rare and the relative lack of plant ground cover resulted in frequent reworking of terrestrial surfaces; (2) Carboniferous-Triassic—many tracks because terrestrial tetrapods are common and increased ground cover reduced the reworking of terrestrial surfaces; (3) Jurassic-Cretaceous—tracks are numerous and preserved in more diverse sedimentary environments because many terrestrial animals are very large, even though ground cover is increased; and (4) Cenozoic—increased ground cover, especially after the diversification of grasses, resulted in less unvegetated areas where tracks can be preserved with a few notable exceptions such as lacustrine margins. This model provides a useful framework, but clearly other factors influence the track record. In addition, the larger size of Quaternary mammals would suggest a fifth acme of tracks.

There are apparently three principal acme zones for track preservation: (1) Early Permian; (2) Late Triassic-Early Jurassic; and (3) Cretaceous. Tracks are facies fossils, and certain environments are more conducive to preservation than others. The Early Permian and Late Triassic-Jurassic both exhibit semi-arid fluvial (and to a lesser extent lacustrine) redbeds, and it is probable that intermittent moisture may be considered an important factor in track preservation. At a fundamental level, track preservation requires a wet substrate that then dries (and is buried), and this is best accomplished in a semi-arid environment or on a shoreline (i.e., intermittently wet settings). Semi-arid conditions also result in low vegetation density, which would provide larger areas for potential track preservation and episodic sedimentation to preserve prints. Tectonically, the early Permian and Late Triassic-Early Jurassic represent periods of relative tectonic quiescence, with the stasis of Pangea and, subsequently, its initial break up. The Late Triassic-Early Jurassic formation of rift valleys floored by lakes is also important in the preservation of tracks, notably on the western margin of the Atlantic.

The Cretaceous track acme occurs in a very different context of enhanced tectonic activity and wetter climates. During the early Permian and Late Triassic-Early Jurassic, small tracks about 1 cm in length are common, and there is a wide size range of preserved tracks. In general, Cretaceous tracks represent dinosaurs, and are mostly of large size (>10 cm long). In this acme it may be absolute size rather than optimum environmental conditions that it is more important in the large volume of preserved tracks. However, if size alone resulted in abundant tracks, the record for the Jurassic should be much more extensive. We are not naïve enough to believe that semi-arid conditions alone produced the earlier acme zone, and large animals the second, but it is clear that there are patterns in the track record that require further analysis.

12.7.2 Coprolites

Hunt et al. (2012d) provided an overview of the fossil record of coprolites. The earliest vertebrate coprolites are Late Ordovician in age (Aldridge et al. 2006). The few Silurian coprolites include argillaceous scroll coprolites and non-spiral forms

comprised of macerated fish debris, with minimal interstitial groundmass (Gilmore 1992; Hunt and Lucas 2016b). Groundmass-rich cylindrical coprolites, some spiral in morphology, become common in the Devonian (Hunt and Lucas 2016b). Mississippian and Pennsylvanian coprofaunas represent the first widespread occurrence of vertebrate coprolites in the northern continents. A more global vertebrate coprolite record from the Permian includes records from the Gondwana continents (Hunt and Lucas 2013). The early Permian and Late Triassic are acme zones for coprolites in redbeds (Hunt and Lucas 2005; Hunt et al. 2013a). Niedźwiedzki et al. (2016b) noted changes in the coprolite ichnofaunas across the Permian/Triassic boundary. Jurassic coprolites are locally common, but few have been described, with the notable exception of those from the Lias of England (Hunt and Lucas 2014). Cretaceous and Tertiary coprolites are common, but have been relatively poorly studied (Hunt and Lucas 2016c). Pleistocene coprolites are locally common, particularly in cave faunas (Hunt et al. 2007, 2012d).

The coprolites of carnivorous animals dominate the fossil record in both aquatic and terrestrial ichnofaunas (Hunt et al. 1994a). This is because carnivore digestion results in excrement that is both unattractive to other organisms and is also chemically predisposed for rapid lithification (e.g., Hunt et al. 1994a, b; Hollocher and Hollocher 2012). Such biases must be taken into account when utilizing coprolites for broad ecological analyses (e.g., Niedźwiedzki et al. 2016a, b).

The first herbivore coprolites occur in the Middle Triassic of South America (Fiorelli et al. 2013; Hunt et al. 2013a). Three are several records of Late Triassic dicynodont coprolites (Hunt et al. 1998, 2013a; Bajdek et al. 2014), but other pre-Pleistocene occurrences of herbivore coprolites are uncommon (e.g., Chin 2007), and some are probably misidentified (Chin and Kirkland 1998; Hunt and Lucas 2014). Herbivore coprolites are abundant in the Pleistocene of the arid western United States (see review in Hunt and Lucas 2007b).

There are significant taxonomic biases in the coprolite record. Hunt et al. (2015b) noted that heterospiral coprolites of chondrichthyans are especially abundant in marine environments from the Mississippian to at least the Eocene (e.g., Hunt et al. 2012g; Diedrich and Felker 2012). Late Cretaceous-Paleogene phosphorene's yield coprolites over a wide area from northwest Africa to the Middle East (Hunt and Lucas 2016c).

Hunt and Lucas (2016c) noted that there is limited change in coprolite morphotype across the Cretaceous/Tertiary boundary in nonmarine environments (cf. Suazo et al. 2012). Thus, for example, *Alococopro*s and *Eucoprus* extend across the boundary, and there is no significant change in the overall median size of coprolites (except for the loss of the rare putative tyrannosaurid coprolites). This suggests that ornithischian and non-avian theropod coprolites are not commonly preserved in the Cretaceous and that most small carnivore coprolites in nonmarine environments in the late Mesozoic and early Tertiary probably represent crocodylomorphs, which do not demonstrate significant changes across the boundary (Markwick 1998; Sullivan 1987; Vasse and Hua 1998).

Later in the Tertiary, coprolites in nonmarine environments are more diverse and are principally attributable to carnivorous mammals. In the late Pliocene and

Pleistocene, *Hyaenacoprus bucklandi* in particular, and hyaena coprolites in general, are particularly common in the Old World from Europe to China (e.g., Diedrich 2012b; Hunt et al. 2012a, d; and references therein).

12.7.3 Regurgitalites

Hunt (1992) coined the term regurgitalite to encompass all trace fossils that result from manipulated or digested/partially digested food material egested via the oral cavity. Subsequently, Hunt and Lucas (2012a) introduced the terms ejectalite for regurgitalites that have been manipulated in the mouth or undergone partial digestion (e.g., deriving from the oral cavity or gastrointestinal tract anterior to the stomach) and ekrhexalite for regurgitalites that derive from the stomach. They also defined ornithoregurgitalites for regurgitalites produced by birds and more specifically strigilite for fossil owl pellets. Hunt and Lucas (2012a) also introduced terms to cover accumulations of regurgitalites, with the umbrella name purgolite. These include accretionary purgolite for an accumulation that results from accumulation due to physical, rather than biological processes (e.g., hydrodynamic) and ethological purgolite for those that result from the behavior of an organism (e.g., strigilites accumulated under a perch).

Vertebrate regurgitalites are rarely identified in the fossil record. One reason is that regurgitation is only common in a few discrete taxonomic groups (e.g., fish—Sims et al. 2000; Brunnschweiler et al. 2005; birds—Andrews 1990). More important has been a lack of investigation and recognition. Regurgitalites can be identified by: (1) discrete accumulation of hard parts and other indigestible components such as fur; (2) paucity of groundmass; (3) corrosion of skeletal elements; (4) breakage of elements; (5) skeletal representation comparable to Recent regurgitalites; and (6) bite marks (Hunt 1992; Hunt and Lucas 2012a). Almost all of the identified regurgitalites occur in four sedimentary environments: (1) shallow marine; (2) lacustrine; (3) fluvial; and (4) caves (Hunt et al. 2015a).

The majority of reported regurgitalites are from shallow marine environments, and most were produced by fish (Hunt et al. 2015a). Salamon et al. (2014: figs. 6, 7) report a regurgitalite from the Devonian and nine from the Mississippian composed of shell fragments. Angular shell fragment debris may indicate the presence of durophagous fish and thus the distribution of such material should likely parallel that of shell-rich regurgitalites (Oji et al. 2003; Salamon et al. 2014). This seems to be the case in the Devonian to the Mississippian (Salamon et al. 2014: fig. 7). Thus, based on the work of Oji et al. (2003) we could predict a rise in such regurgitalites in the Paleogene and a major increase in the Neogene.

Regurgitalites are notable in several Carboniferous units of the USA including: (1) Desmoinesian Carbondale Formation, Indiana—Zangerl and Richardson (1963), Elder (1985); (2) Chesterian Tyler Formation, Montana—Hunt et al. (2012e); and (3) the Missourian Atrasado Formation at the Kinney Brick Quarry and Tinajas Lagerstätten—Hunt et al. (2012h, i). Named regurgitalites from these units are

Ostracobromus snowyensis and *Conchobromus kinneyensis* (Hunt et al. 2012e, h, i), which contain abundant oconchostracans and ostracodes respectively.

Salamon et al. (2012) described a number of putative regurgitalites from the Middle Triassic Gogolin Formation in southern Poland. These are composed of angular bivalve fragments and broken crinoid ossicles. Other putative occurrences of regurgitalites are in the Late Cretaceous of Kansas (Everhart 2005), the Early Jurassic-Early Cretaceous of Europe (Vallon 2012) and the Pleistocene of Canada (Hunt and Lucas 2007b).

Lacustrine regurgitalites occur in shallow facies of multiple Eocene units of the western USA and British Columbia, Canada (e.g., Green River, Coldwater, Florissant formations). Wilson (1987) speculated that the regurgitalites from Canada may pertain to birds, not fish. Buskirk et al. (2015) described a variety of bromalites from Florissant, including probable regurgitalites.

There are no convincing regurgitalites described from fluvial environments before the Tertiary. Owl strigilites occur in several localities in the Tertiary of the USA, including the Zia Sandstone of New Mexico (Gawne 1975), the Chadron Formation of South Dakota (Hunt and Lucas 2007b) and the White River Formation of Wyoming (Lucas et al. 2012b), the latter within a purgolite. There are very few convincing examples of Tertiary paleontological microvertebrate accumulations that comprise bones derived from raptor regurgitations (Lucas et al. 2012b; but see Czaplewski 2011). Many Pleistocene cave deposits and some archeological sites yield bone accumulations derived from raptor, notably owl, regurgitations (e.g., Andrews 1990; Hunt and Lucas 2007b).

In summary, most identified vertebrate regurgitalites were produced by fish or birds and are preserved in limited environmental settings. Thus, the fossil record of regurgilatiltes is strongly controlled both by taxonomic and taphonomic factors. Regurgitalites have diverse utility, including providing evidence of the evolution of predation and digestion, data for the analysis of taphonomy and sedimentary environments and acting as proxies for the presence of biotaxa.

12.7.4 Consumulites

Hunt and Lucas (2012a) coined the term consumulite to encompass all fossilized ingested food material preserved within the body cavity. They also redefined existing terms and introduced new ones to provide a refined terminology for all consumulites including oralite (food material preserved wholly or partially within the oral cavity), esophogalite (digested food material preserved in the gastrointestinal tract anterior to the stomach), gastrolite (wholly or partially digested food material preserved in the stomach), cololite (digested food material preserved in the gastrointestinal tract posterior to the stomach), intestinelite (cololite preserved in the intestines), evisceralite (cololite that is a preserved segment of infilled fossilized intestines preserved independently of (exterior to) a carcass), enterospira (cololite preserved in a spiral valve) and incorporeal pelletite (pelletite preserved within the body cavity) (Hunt and Lucas 2012a).

There are a number of studies of individual consumulites that are unusual or provide refined information about diet (e.g., Pollard 1968; Sato and Tanabe 1998; Cavin 1999; Molnar and Clifford 2001; Richter and Baszio 2001; Varricchio 2001; Kear et al. 2003; Kriwet et al. 2008; O'Keefe et al. 2009; Diedrich 2012a), but the vast majority of specimens are undoubtedly undescribed. Obviously, a consumulite cannot be recognized, with the rare exception of evisceralites (e.g., Seilacher et al. 2001), unless a complete or partially articulated skeleton is preserved.

Consumulites are principally recorded from fish, marine reptiles and large terrestrial tetrapods (notably dinosaurs). The vast majority of all complete articulated fossil skeletons are fish, so it is unsurprising that most consumulites occur in fish. Many fish skeletons occur in Lagerstätten or are concentrated in specific environmental settings (notably lagoons or lakes—Mississippian Bear Gulch Limestone, Eocene Green River Formation, USA, etc.). There is a similar situation with marine reptiles, notably ichthyosaurs of all ages, but particularly in the Early Jurassic (e.g., Lyme Regis, England, Holzmaden, Germany). Consumulites in terrestrial tetrapods appear to be most common, or at least more reported, in larger-bodied taxa such as dinosaurs. This may in part reflect interest in dinosaurs or the fact that consumulites may be more prominent and recognizable in larger carcasses.

12.7.5 Dentalites (Bite Marks)

The study of tooth marks on fossil bone goes back to the work of Buckland (1822, 1824) on hyena damage to bones of the Pleistocene fauna of Kirkdale Cave. Lucas (2016) briefly reviewed the fossil record of bite marks. Some of the oldest tetrapod bones, of Late Devonian age, bear apparent tooth marks (Shubin et al. 2004). Well-documented Permian (Reisz and Tsuji 2006) and Triassic tooth marks have been published, the latter the basis of two ichnotaxa, i.e., *Mandaodonites* and *Heterodontichnites* (Cruickshank 1986; Rinehart et al. 2006). There is a diverse literature on dentalites in Jurassic-Cretaceous dinosaur bones reviewed by Fiorillo (1991), Hunt et al. (1994b), Chin (1997), Jacobsen (1998), Tanke and Currie (1998), and Tanke and Rothschild (2002).

Dentalites on Mesozoic aquatic vertebrate bone (fishes, marine reptiles) have a diverse literature (e.g., Zammit and Kear 2011, and references cited therein). Cenozoic dentalites are less studied, but have been the basis of the ichnogenera *Machichnus*, *Linichnus*, and *Knethichnus* (Mikuláš et al. 2006; Jacobsen and Bromley 2009). Dentalites are important archives of various kinds of behavior, including predation, scavenging, intraspecific (agonistic) interactions, and bone utilization for other purposes, including mineral extraction and tooth sharpening (e.g., Schwimmer et al. 1997; Everhart 2004). Crocodiles have long been known to modify bone (von Nopcsa 1902; Weigelt 1927). The actualistic database for understanding dentalites in modern bone is quite extensive, especially for crocodilian damage to bone, and there is a diverse literature on fossil bite marks on bone attributed to

crocodilians (e.g., Carpenter and Lindsey 1980; Webb and Manolis 1983; Buffetaut 1983; Erickson 1984; Schwimmer 2002; Forrest 2003; Avilla et al. 2004; Njau and Blumenschine 2006; Westaway et al. 2011).

Bromley and Jacobsen (2008) have recently outlined research designed to produce an ichnotaxonomy of dentalites. They favor naming dentalites based on the damage of a single tooth and regard multiple tooth marks as compound trace fossils. However, this suggestion fails to recognize the significance of heterodonty and the variation in single dental configurations (arcades) (Lucas 2016). Thus, the ideal ichnotaxobase is the tooth marks of an entire dental arcade, and anything less than that should be regarded as extramorphological variants (Lucas 2016). What is now needed is a dentalite ichnology beginning with diverse documentation of the fossil record, compilation, and synthesis of the entire record, rigorous ichnotaxonomy and determination of analytical criteria for establishing inferences about the diverse behaviors archived by tooth mark ichnofossils (Lucas 2016). Lucas (2016) recently named the *Cubiculum* ichnofacies for modifications to bone, including dentalites.

Hunt (1984, 1987) first predicted that dentalites should be relatively uncommon prior to the Cenozoic. Less derived, non-mammalian vertebrates lack the dental occlusion necessary for fine manipulation of prey or bone crushing. Thus, non-mammalian tooth-to-bone contact is essentially always accidental and was predicted to be less common in the Mesozoic than in the Cenozoic, when mammalian carnivores came to dominate terrestrial faunas (Hunt 1984, 1987). Fiorillo (1991) tested this hypothesis and concluded that bite marks are uncommon in the Mesozoic. Although there is only a small data set, it seems that dentalites are relatively less common in the Paleozoic than the Mesozoic. This may be caused by several factors, including: (1) the evolution of laterally compressed teeth in terrestrial predators, which would penetrate through soft tissue to bone more effectively; (2) the development of a more upright gait among predators that would provide for more three dimensional predation—more opportunity for biting of the dorsal as well as lateral regions; and (3) increased body size of prey that would invite more extensive scavenging of carcasses than is feasible with small-bodied prey. Dentalites are underreported in the Tertiary but abundant in the Quaternary (e.g., Binford 1981; Brain 1981). Tertiary dentalites include records from the Paleocene of the USA (Secord et al. 2002), Eocene of England (Vasileiadou et al. 2007) and Antarctica (Hospitaleche 2016), and Oligocene of France (Laudet and Fosse 2001) and the USA (LaGarry 1997, 2004).

12.7.6 Nests

Lucas and Hunt (2006) defined a nest as the structure made by, or the place chosen by, an animal for spawning, breeding and/or laying eggs and sheltering young. The nests of extant birds are most familiar and are usually constructed from organic material, so they have little chance of being preserved in the rock/fossil record (cf. Zasadil and Mikuláš 2004). However, some birds such as ostriches do build nests

that involve the modification of sediment by scraping, building mounds or burrowing (Coombs 1989), and these are nests that can be preserved in the geological record. Some other extant egg-laying tetrapods also construct nests by sediment modification, including some turtles, crocodiles and lizards (e.g., Coombs 1989; Brannen and Bishop 1993; Carpenter 1999; Mazzotti 2003; Jessop et al. 2004). The fossil record of *bona fide* tetrapod nests is mostly that of dinosaurs and extends back to the Late Triassic (Carpenter and Alf 1994; Moratalla and Powell 1994; Carpenter 1999). Other kinds of tetrapod nests in the literature are mostly those of turtles (e.g., Buckman 1859; Bishop et al. 1997; Carpenter 1999).

Dinosaur nests dominate the literature on fossil tetrapod nests, which date back to the Late Triassic of Argentina (Bonaparte and Vince, 1979). Jurassic dinosaur nests are few in number (Hirsch et al. 1979; Kitching 1979; Mateus et al. 1997; Carpenter 1999), and most known dinosaur nests are of Cretaceous age (Carpenter and Alf 1994). Dinosaur nests are sometimes recognized by the preservation of a nest structure, such as bowl-shaped patches of green mudstone (Horner and Makela 1979) or a raised rim of sediment that is preferentially cemented (Varricchio et al. 1999). Regularly arranged eggs, usually in circular or spiral clutches, are also generally taken as compelling evidence of a nest, as are aggregations of eggshell fragments or the bones/skeletons of hatchling dinosaurs (Lucas and Hunt 2006).

Lucas and Hunt (2006) contended that in the absence of egg or hatchling association, that it is impossible to be certain that any preserved structure is a tetrapod nest. Indeed, even an aggregation of eggshell fragments (e.g., Hirsch et al. 1979: fig. 6) may not be compelling evidence of a nest because sedimentary transport and accumulation may be what caused such an aggregation (Lucas and Hunt 2006). Structures with raised rims concentrated in small areas can be of inorganic origin, so we argue that identification of a structure as a fossil tetrapod nest is speculative at best if there is no clear association of eggs, eggshells or hatchling bones/skeletons with the structure (Lucas and Hunt 2006).

Late Pleistocene nests, notably of rodents such as those of pack rats, are abundant in North America and other areas (e.g., Hunt et al. 2012f; Tweet et al. 2012). The nests of large ratites are also locally common in areas such as New Zealand.

Overall, the acme for nest preservation is in the Mesozoic, which is a result of taxonomic and taphonomic factors. Nesting behavior evolved in the Dinosauria, and the large size of many of their genera resulted in nest structures of large size, which had an elevated chance of survival into the fossil record.

12.7.7 Burrows

There is limited evidence of vertebrate burrowing from the Devonian through the Permian (Hasiotis et al. 2007). The ichnofossil record of vertebrate burrows extends as far back as the Early Devonian. The earliest vertebrate ichnofossils are interpreted as lungfish burrows (Allen and Williams 1981). Upper Devonian burrows occur at several localities worldwide (O'Sullivan et al. 1986; Benton 1988;

McAllister 1992; Hasiotis 2002). These flask-shaped burrows are attributed to the estivation behavior of lungfish and are interpreted as a response to seasonal droughts (Romer and Olson 1954; Hasiotis 2002). Similar Carboniferous-age burrows have also been attributed to lungfishes (Carroll 1965; Benton 1988). Lungfish burrows are also common in the early Permian (e.g., Romer and Olson 1954; Berman 1976, 1979, 1993; Lucas et al. 2013).

A second morphology of Devonian burrow is *Cornulatichnus*, a near vertical conical burrow that is attributed to the open shelter burrow of an eel-like fish (Carroll and Trewin 1995). The oldest tetrapod burrow is from the Mississippian (Visean) Hometown Member of the Mauch Chunk Formation of Pennsylvania, USA (Fillmore et al. 2012).

The Permian record includes more diverse and complex burrow systems (Olson and Bolles 1975; Smith 1987; Hembree et al. 2004, 2005; Fillmore et al. 2012). For example, the Permian of Kansas has yielded nearly vertical, downward tapering burrows (*Torridorefugium eskridgensis*) interpreted as estivation burrows of lysorophid amphibians (Hembree et al. 2004, 2005). Helical burrows, containing skeletal remains of therapsids, occur in the Permian interval of the South African Beaufort Group (Smith 1987). Other large tetrapod burrows occur in the Middle Triassic of Argentina (Krapovickas et al. 2013).

At the beginning of the Mesozoic, the diversity and complexity of burrowing increases as tetrapods diversified and mammals rapidly evolved (e.g., Groenewald et al. 2001; Damiani et al. 2003; Miller et al. 2001; Hasiotis et al. 2004, 2007; Loope 2006; Lucas et al. 2006b; Dentzien-Dias et al. 2007, 2008, 2012b; Tanner and Lucas 2009).

There is a fairly sparse record of North American Cenozoic vertebrate (mostly rodent) burrows of Oligocene-Pleistocene age (Voorhies 1975). The best known are *Daimonelix,* which are the helical burrows of a primitive beaver from the lower Miocene of Nebraska, Wyoming and South Dakota, USA (Barbour 1892; O'Harra 1920; Schultz 1942; Martin and Bennett 1977). Gobetz (2006; Gobetz and Martin 2006), described Miocene mylagaulid and geomyid rodent burrows (*Alezichnos*) from Colorado and Nebraska, USA. Morgan and Lucas (2000: fig. 3G–H) described two complete and four partial likely rodent burrows from near the top of the Pliocene (Blancan) Loma Barbon Member of the Arroyo Ojito Formation, New Mexico, USA, and others have been found subsequently.

There are several records of Cenozoic burrows from South America. Large meniscate burrows (*Nagtuichnus meuleni*) occurring in late Miocene and Holocene eolian deposits from Argentina were probably produced by pink fairy armadillos or pichiciegos (*Chlamyphorus truncatus*) (Melchor et al. 2012). Frank et al. (2012 and references cited therein) described the largest vertebrate burrows, some greater than 2 m in diameter. These enormous burrows occur in the four southeastern states of Brazil and were probably produced by ground sloths or giant armadillos (Frank et al. 2012).

Clearly, the record of burrows has a strong taxonomic influence. The distribution and evolution of groups such as nonmarine lungfish, mammal-like reptiles and rodents strongly effects the distribution and abundance of burrows. However, the

pattern of burrowing behavior may have other influences. For example, the global early Mesozoic appearance of tetrapod burrows has been hypothesized as a behavioral adaptation evolved by terrestrial vertebrates as protection against extreme climatic conditions created during the tectonic assembly of, and by the paleolatitudinal setting of, the supercontinent Pangea (e.g., Colombi et al. 2012; Krapovickas et al. 2013). Low to mid-latitude Pangean climates are interpreted as having been highly seasonal in nature and characterized by long dry periods and a short wet season.

12.7.8 Gastroliths

Wieland (1906) first utilized the term "gastrolith" to apply to swallowed stones in fossil and Recent vertebrates (Wings 2007). Wings (2007: 2) broadened the concept to be "a hard object of no calorific value (e.g., a stone, natural or pathological concretion) which is, or was, retained in the digestive tract of an animal." He proposed two categories of vertebrate gastroliths: (1) patho-gastroliths, for pathological stones formed in the stomach; and (2) geo-gastroliths, for swallowed sediment particles. Geo-gastroliths, hereafter called gastroliths, function in different taxa either to assist in mechanical diminution of food or for ballast in aquatic vertebrates (Wings 2004, 2007; Currie 1981; Taylor 1993).

The fossil record of gastroliths is very taxonomically dependent. The principal taxa that preserve gastroliths include elasmosaurid plesiosaurs, pinnipeds (seals and sea lions), crocodilians, several clades of dinosaurs (e.g., non-avian theropods, prosauropods, sauropods, psittacosaurs, ankylosaurs, stegosaurs, iguanodonts, hadrosaurs), and many taxa of birds, including ratites, song birds and 20 other orders (Baker 1956; Whittle and Everhart 2000; Wings 2004). In addition, as noted above, fossil skeletons of other taxa such as ichthyosaurs, amphibians and protorosaurian reptiles occasionally contain gastroliths (Warren and Hutchinson 1987; Munk and Sues 1993; Cheng et al. 2006).

Skeletons of late Permian nonmarine (e.g., *Protorosaurus:* Munk and Sues 1993) and marine (*Hovasaurus*: Currie 1981) tetrapods contain gastroliths. There are older sparse records from fish (e.g., Devonian: Trewin 1986). Triassic gastroliths occur in a variety of taxa, including a rhytidosteid amphibian and the ichthyosaur *Panjiangsaurus* (Warren and Hutchinson 1987; Cheng et al. 2006). The Mesozoic is the acme for described gastroliths, with multiple reports from plesiosaurs (e.g., Brown 1904; Darby and Ojakangas 1980; Everhart 2000) and dinosaurs (e.g. sauropodomorphs—Christiansen 1996; psittacosaurids—Xu 1997; Kobayashi and Lü 2003; *Caudipteryx zoui*—Ji et al. 1998). There are also reports from other taxa (e.g., chondrichthyans—Moodie 1912). The apparent abundance of Mesozoic gastroliths is clearly in part taxonomic but it may also be partially an artifact as there is a relationship between the size of the host and the size of a gastrolith—large, easily identifiable gastroliths only occur in large animals. The only Tertiary mammals with gastroliths are pinnipeds (e.g., Pandeli et al. 1998). Tertiary (and Mesozoic) crocodiles contain gastroliths (e.g., Langston and Rose 1978).

12.7.9 Discussion

The fossil record of vertebrate traces fossils has distinct acme zones (Fig. 12.16). Most vertebrate trace fossils have their earliest occurrences in the Devonian. The exceptions are coprolites, whose earliest record is in the Late Ordovician, and nests, which are not recorded before the Late Triassic. The Mississisippian-Pennsylvanian has increased numbers of trace fossils (notably tracks, coprolites, dentalites and burrows). The Early Permian is an acme for both tracks and coprolites. The Late Triassic yields abundant tracks and coprolites, and tracks are also common in the Early Jurassic. The Jurassic and Cretaceous represent the time periods with the greatest apparent diversity of traces (tracks, coprolites, consumulites, dentalites,

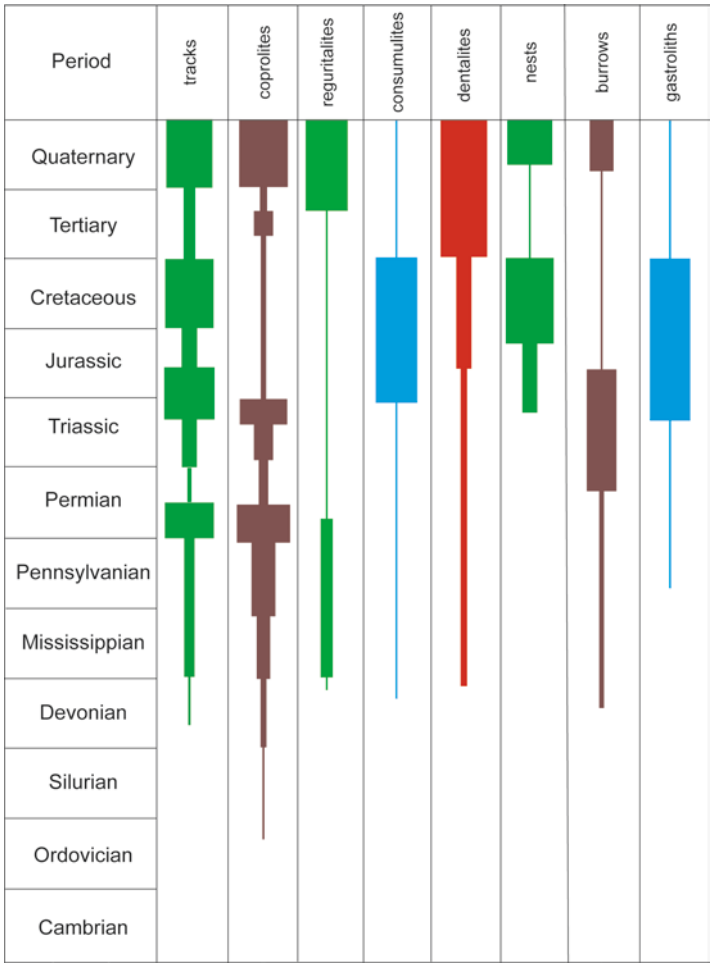

Fig. 12.16 Stratigraphic distribution of vertebrate trace fossils through the Phanerozoic

nests and gastroliths). The Quaternary also represents a time of ichnological abundance (tracks, coprolites, regurgitalites, nests and burrows).

In the early-mid Paleozoic, there were generally high sea levels, low tetrapod diversity, wet greenhouse climates and thus relatively few vertebrate traces. The late Paleozoic and Quaternary acmes for trace fossils were during times of generally low sea level and seasonal climates. The Jurassic-Cretaceous acme does not fit this model, and we believe that large body size (increased recognition) and a disproportionate amount of study of the dinosaur fossil record biases the trace fossil record. The latter we attribute to the Taxophile Effect—a term we introduce to recognize bias introduced by a disproportionate volume of research on a popular taxonomic group. Thus, many dinosaur dentalites warrant individual papers, whereas most Tertiary dentalite records are merely noted within the text of taxonomic descriptions.

Other factors that influence the pattern of the fossil record of vertebrate traces fossils include: (1) taxonomy—regurgitalites, gastroliths and burrows are notably restricted to a small number of taxonomic groups, which control the stratigraphic range of these traces; (2) functional morphology—e.g., the more efficient dental occlusion of mammals resulted in increased dentalites as this Class diversified; and (3) ethology—burrows, nests and regurgitalites reflect specific behaviors.

Acknowledgments We thank those in charge of collections in North and South America, Europe and Asia who have allowed us access to collections over the years to study vertebrate trace fossils. Paula Denzien-Dias and Larry Tanner provided insightful and helpful reviews.

Appendix

Systematic Ichnotaxonomy

Gaspeichnus, ichnogen. nov.

Type ichnospecies: *Gaspeichnus complexus*.
Included ichnospecies: Known only from the type ichnospecies.
Etymology: From the Gaspé Peninsula and the Greek *ichnos* (trace).
Distribution: Late Devonian to Early Triassic.
Diagnosis: Elongate and irregularly sinuous borings of small size (diameter 0.1–0.2 mm) with irregular width in a coprolite substrate.
Discussion: This is possibly the oldest example of coprophagy and is certainly the oldest example of coprolite modification by another organism.

Brachaniec et al. (2015: fig. 6A–B) reported sinuous surface borings of Early Triassic coprolites from Poland that we refer to *Gaspeichnus.* They noted that *Gaspeichnus* occurs in 57% of the coprolites that contain fossils.

The size and sinuosity are similar to the morphology of nematode trails, although *Gaspeichnus* is more irregular in its undulations (Moussa 1970; Baliński et al. 2013; Brachaniec et al. 2015). We tentatively interpret *Gaspeichnus* as being produced by a nematode. The coprolite substrate alone differentatiates it from other sinuous trace fossils.

Fig. 12.17 Holotype of *Gaspeichnus complexus* Hunt et al. (2017) (RSM 2002.59.166) from the Upper Devonian Escuminac Formation of Quebec, Canada

Gaspeichnus complexus, ichnosp. nov. (Fig. 12.17)

Holotype: RSM 2002. 59.166, coprolite with borings.

Etymology: From Latin *complexus* in allusion to the complicated structure of the borings.

Type locality: Escuminac Bay, Gaspé Peninsula, Quebec, Canada.

Type horizon: Escuminac Formation (Upper Devonian).

Distribution: As for ichnogenus.

Referred specimens: None.

Diagnosis: As for ichnogenus.

Description: RSM 2002. 59.166 is a vertebrate coprolite of approximately cylindrical shape with an irregular margin. It is 22 mm long and 6 mm wide. It contains two elongate and sinuous borings that do not overlap. The borings vary in width from 0.1 to 0.2 mm in width and from 8 to 12 mm in length. The sinuosity is irregular.

Discussion: The Escuminac Formation yields a diverse bromalite ichnofauna that has been described by McAllister (1996).

References

Aiyengar KN (1937) A note on the Maleri beds of Hyderabad State (Deccan) and the Tiki beds of south Rewa. Rec Geol Surv India 71:401–406

Aldridge RJ, Gabbott SE, Siveter LJ, Theron JN (2006) Bromalites from the Soom Shale Lagerstätte (Upper Ordovician) of South Africa: palaeoecological and palaeobiological implications. Palaeontology 49:857–871

Allen JRL, Williams BPJ (1981) *Beaconites antarcticus*: a giant channel-associated trace fossil from the Lower Old Red Sandstone of South Wales and the Welsh Borders. Geol J 16:255–269

Anderson JM, Anderson HM, Cruickshank ARI (1998) Late Triassic ecosystems of the Molteno lower Elliot biome of southern Africa. Palaeontology 41:387–421

Andrews P (1990) Owls, caves and fossils: predation, preservation and accumulation of small mammal bones in caves, with an analysis of the Pleistocene cave faunas from Westbury-Sub-Mendip, Somerset, U.K. University of Chicago Press, Chicago

Angom S, Tuboi C, Hussain SA (2012) Nest morphometry of Indian wild boar (*Sus scrofa*), its occurrence and reuse by Eld's deer or Sangai (*Rucervus eldii eldii*) in Keibul Lamjao National Park, Manipur. NeBIO 3:1–7

Antunes MT, Balbino AC, Ginsburg L (2006) Miocene mammalian footprints in coprolites from Lisbon, Portugal. Ann Paléontol 92:13–30
Arcucci AB, Marsicano CA, Caselli AT (2004) Tetrapod association and paleoenvironment of Los Colorados Formation (Argentina): a significant sample from western Gondwana at the end of the Triassic. Geobios 37:557–568
Ash SA (1978) Coprolites. In: Ash, SA (ed) Geology, paleontology and paleoecology of a Late Triassic lake, western New Mexico. Brig Young Univ Geol Stud 25:75–87
Avanzini M, Renesto S (2002) A review of *Rhynchosauroides tirolicus* Abel, 1926 ichnospecies (Middle Triassic: Anisian-Ladinian) and some inferences on *Rhynchosauroides* trackmaker. Riv Italiana Paleontol Strat 108(1):51–66
Avanzini M, Wachtler M (2012) *Sphingopus ladinicus* isp. nov. from the Anisian of the Braies Dolomites (Southern Alps, Italy). Boll Soc Paleontol Italiana 51(1):63–70
Avanzini M, García-Ramos JC, Lires J, Menegon M, Piñuela L, Fernández LA (2005) Turtle tracks from the Late Jurassic of Asturias, Spain. Acta Palaeontol Pol 50(4):743–755
Avanzini M, Dalla Vecchia FM, Mietto P, Piubelli D, Preto N, Rigo M, Roghi G (2007) A vertebrate nesting site in northeastern Italy reveals unexpectedly complex behavior for Late Carnian reptiles. PALAIOS 22:465–475
Avanzini M, Piñuela L, Garcia-Ramos JC (2010a) First report of a Late Jurassic lizard-like footprint (Asturias, Spain). J Iberian Geol 36(2):175–180
Avanzini M, Petti FM, Bernardi M, Tomasoni R (2010b) Crocodile-like footprints from the Upper Triassic (Carnian) of the Italian Southern Alps. New Mexico Mus Nat Hist Sci Bull 51:61–64
Avilla LS, Fernandes R, Ramos DFB (2004) Bite marks on a crocodylomorph from the Upper Cretaceous of Brazil: evidence of social behavior? J Vert Paleontol 24:971–973
Baird D (1954) *Chirotherium lulli*, a pseudosuchian reptile from New Jersey. Bull Mus Comp Zool 111:165–192
Baird D (1957) Triassic reptile footprint faunules from Milford, New Jersey. Bull Mus Comp Zool 117:449–520
Baird D (1986) Some Upper Triassic reptiles, footprints, and an amphibian from New Jersey. Mosasaur 3:125–153
Bajdek P, Owocki K, Niedźwiedzki G (2014) Putative dicynodont coprolites from the Upper Triassic of Poland. Palaeogeogr Palaeoclimatol Palaeoecol 411:1–17
Baker AA (1956) The swallowing of stones by animals. Victorian Nat 73(6):82–95
Baliński A, Sun Y, Dzik J (2013) Traces of marine nematodes from 470 million years old Early Ordovician rocks in China. Nematology 15:567–574
Barboni R, Dutra TL (2013) New "flower" and leaves of Bennettitales from southern Brazil and their implication in the age of the lower Mesozoic deposits. Ameghiniana 50:14–32
Barbour EH (1892) Nature, structure and phylogeny of *Daimonelix*. Geol Soc Amer Bull 8:305–314
Bartholomai A (1966) Fossil footprints in Queensland. Austral Nat Hist 15(5):147–150
Baumiller TK, Salamon MA, Gorzelak P, Mooi R, Messing CG, Gahn FJ (2010) Post-Paleozoic crinoid radiation in response to benthic predation preceded the Mesozoic marine revolution. Proc Natl Acad Sci U S A 107(13):5893–5896
Belvedere M, Avanzini M, Mietto P, Rigo M (2008) Norian dinosaur footprints from the "Strada delle Gallerie" (Monte Pasubio, NE Italy). Studi Trent Sci Nat Acta Geol 83:267–275
Benton MJ (1988) Burrowing by vertebrates. Nature 331:17–18
Berman DS (1976) Occurrence of Gnathorhiza (Osteichthyes: Dipnoi) in aestivation burrows in the lower Permian of New Mexico with description of a new species. J Paleontol 50:1034–1039
Berman DS (1979) *Gnathorhiza bothrotreta* (Osteichthyes: Dipnoi) from the Lower Permian Abo Formation of New Mexico. Ann Carneg Mus 48:211–230
Berman DS (1993) Lower Permian vertebrate localities of New Mexico and their assemblages. New Mex Mus Nat His Sci Bull 2:11–21
Bernardi M, Petti FM, D'Orazi Porchetti S, Avanzini M (2013) Large tridactyl footprints associated with a diverse ichnofauna from the Carnian of the Southern Alps. New Mex Mus Nat Hist Sci Bull 61:48–54

Beurlen K (1950) Neue Fährtenfunde aus der fränkischen Trias. Neu Jahrb Geol Paläontol Monat 1950:308–320
Binford LR (1981) Bones: ancient men and modern myths. Academic Press, New York
Biron PE, Dutuit J-M (1981) Figurations sedimentaires et traces d'activite au sol dans le Trias de la formation d'Argana et de l'Ourika (Maroc). Bull Mus Nat Hist Nat 4e, 3rd ser sec C 4: 399–427
Bishop GA, Marsh NB, Barron J, Pirkle FL, Smith RSU (1997) A Cretaceous sea turtle nest, Fox Hills Formation, Elbert Co., Colorado. Geol Soc Amer Abst Progr 29:104
Bock W (1952) Triassic reptilian tracks and trends of locomotive evolution. J Paleontol 26:395–433
Bonaparte JF, Vince M (1979) El hallazgo del primer nido de dinosaurios Triásicos (Saurischia, Prosauropoda), Triásico Superior de Patagonia, Argentina. Ameghiniana 1:173–182
Boyd DW, Loope DB (1984) Probable vertebrate origin for certain sole marks in Triassic red beds of Wyoming. J Paleontol 58:467–476
Brachaniec T, Niedźwiedzki R, Surmik D, Krzykawski T, Szopa K, Gorzelak P, Salamon MA (2015) Coprolites of marine vertebrate predators from the Lower Triassic of southern Poland. Palaeogeogr Palaeoclimatol Palaeoecol 435:118–126
Bradley WH (1946) Coprolites from the Bridger Formation of Wyoming: their composition and microorganisms. Am J Sci 244:215–239
Brain CK (1981) The hunters or the hunted? University of Chicago Press, Chicago
Brannen NA, Bishop GA (1993) Nesting traces of the loggerhead sea turtle (*Caretta caretta* (Linne)), St. Catherines Island, George: implications for the fossil record. Georgia Geol Soc Guideb 13:30–36
Braunn PR, Fonseca RC, Ferigolo J (2001) Evidências de possível necrofagia em costelas de *Jachaleria candelariensis* (Therapsida, Dicynodontia) do Triássico Superior do Estado do Rio Grande do Sul, Brasil: XVII Congresso Brasieiro Paleontologia. Univeridade Federale do Acre, Resumos, Rio Branca
Brinkmann W (2004) Mixosaurier (Reptilia, Ichthyosauria) mit Quetschzähnen aus der Grenzbitumenzone (Mitteltrias) des Monte San Giorgio (Schweiz, Kanton Tessin). Schweiz Paläont Abhand 124:1–84
Britt BB, Scheetz RD, Dangerfield A (2008) A suite of dermestid beetle traces on dinosaur bone from the Upper Jurassic Morrison Formation, Wyoming, USA. Ichnos 15:59–71
Bromley RG (1996) Trace fossils: biology and taphonomy, 2nd edn. Unwin Hyman, London
Bromley RG, Asgaard U (1979) Triassic freshwater ichnocoenoses from Carlsberg Fjord, East Greenland. Palaeogeogr Palaeoclimatol Palaeoecol 28:39–80
Bromley RG, Jacobsen AR (2008) Ichnotaxa for bite traces of tetrapods: a new area of research or a total waste of time? In: Uchman A (ed) Abstract book and the Intra-Congress Field Trip Guidebook Second International Congress on Ichnology, p 20
Brown B (1904) Stomach stones and food of plesiosaurs. Science 20(501):184–185
Brunnschweiler JM, Andrews PLR, Southall EJ, Pickering M, Sims DW (2005) Rapid voluntary stomach eversion in a free-living shark. J Marine Biol 85:1141–1144
Buatois LA, Mángano MG (2011) Ichnology: organism-substrate interactions in space and time. Cambridge University Press, Cambridge
Buchy M-C, Taugourodeau P, Janvier P (2004) Stomach contents of a Lower Triassic ichthyosaur from Spitzbergen. Oryctos 5:47–55
Buckland W (1822) Account of an assemblage of fossil teeth and bones of elephant, rhinoceros, hippopotamus, bear, tiger and hyaena, and sixteen other animals; discovered in a cave at Kirkdale, Yorkshire, in the year 1821; with a comparative view of five similar caverns in various parts of England, and others on the continent. Phil Trans Roy Soc Lond 112:171–236
Buckland W (1824) Reliquiae diluvianae; or, observations on the organic remains contained in caves, fissures, and diluvial gravel, and on other geological phenomena, attesting the action of an universal deluge. John Murray, London
Buckland W (1829) [A paper by Dr. Buckland]. Proc Geol Soc Lond 1:142–143
Buckland W (1835) On the discovery of coprolites, or fossil faeces, in the Lias at Lyme Regis, and in other formations. Trans Geol Soc Lond 3(Ser 2):223–238

Buckman J (1859) On some fossil reptilian eggs from the Great Oolite of Cirencester. Quart J Geol Soc Lond 16:1067–1110
Budziszewska-Karwowska E, Bujok A, Sadlok G (2010) Bite marks on an Upper Triassic dicynodontid tibia from Zawiercie, Kraków-Częstochowa Upland, southern Poland. PALAIOS 25(6):415–421
Buffetaut E (1983) Wounds on the jaw of an Eocene mesosuchian crocodilian as possible evidence for the antiquity of crocodilian intraspecific fighting behavior. Paläont Zeit 57:43–145
Buskirk BL, Hunt AP, Lucas SG (2015) Who's eating who? Preliminary analysis of enigmatic bromalites from the Eocene Florissant Formation, Colorado. Geol Soc Am Abstr Progr 47(7):346
Callaway JM, Massare JA (1990) The affinities and ecology of Triassic ichthyosaurs. Geol Soc Am Bull 102:409–416
Camp CL (1980) Large ichthyosaurs from the Upper Triassic of Nevada. Palaeontograph Abteil A 170:139–200
Camp CL, Welles SP (1956) Triassic dicynodont reptiles. Mem Univ Calif 13:255–341
Cantrell AK, Suazo TL, Spielmann JA, Lucas SG (2012) Vertebrate coprolites from the Lower Permian (lower Wolfcampian) Gallina Well locality, Joyita Hills, Socorro County, New Mexico. New Mex Mus Nat Hist Sci Bull 57:97–201
Carpenter K (1999) Eggs, nests, and baby dinosaurs. Indiana University Press, Bloomington
Carpenter K, Alf K (1994) Global distribution of dinosaur eggs, nests, and babies. In: Carpenter K, Hirsch KF, Horner JR (eds) Dinosaur eggs and babies. Cambridge University Press, Cambridge, pp 15–30
Carpenter K, Lindsey D (1980) The dentary of *Brachychampsa montana* Gilmore (Alligatorinae: Crocodylidae), a Late Cretaceous turtle-eating alligator. J Paleo 54:1213–1217
Carroll RL (1965) Lungfish burrows from the Michigan coal basin. Science 148:963–964
Carroll S, Trewin NH (1995) *Cornulatichnus*: a new trace fossil from the Old Red Sandstone of Orkney. Scot J Geol 31:37–41
Casamiquela RM (1964) Estudios icnológicos: problemas y métodos de la icnologia con aplicación al estudio de pisadas Mesozoicos (Reptilia, Mammalia) de la Patagonia. Colegio Industrial Pio IX, Buenos Aires
Casamiquela RM (1975) Nuevo material y reinterpretacion de las icnitas Mesozoicas (Neotriasicas) de Los Menucos, Provincia de Rio Negro (Patagonia): 1° Congreso Argentino de Paleontología y Bioestratigrafía (Tucumán, 1974). Actas 1:555–580
Case EC (1922) New reptiles and stegocephalians from the Upper Triassic of western Texas. Carneg Instit Wash Pub 321:1–84
Cavin L (1999) Occurrence of a juvenile teleost, *Enchodus* sp., in a fish gut content from the Upper Cretaceous of Goulmima, Morocco. Spec Pap Palaeontol 60:57–72
Chame M (2003) Terrestrial mammal feces: a morphometric summary and description. Mem Insti Oswaldo Cruz 98(Suppl 1):71–94
Chatterjee S (1978) A primitive parasuchid (phytosaur) reptile from the Upper Triassic Maleri Formation of India. Palaeontology 21(1):83–127
Chatterjee S (1980) *Malerisaurus*, a new eosuchian reptile from the late Triassic of India. Phil Trans Roy Soc Lond Ser B 291:163–200
Cheng L, Chen XH (2007) Gut contents in the Triassic ichthyosaur Panjiangsaurus from the Guanling biota in Guizhou. Geol China 34:61–65
Cheng L, Wings O, Xiaohong C, Sander PM (2006) Gastroliths in the Triassic ichthyosaur *Panjiangsaurus* from China. J Paleontol 80(3):583–588
Chin K (1997) What did dinosaurs eat? Coprolites and other direct evidence of dinosaur diets. In: Farlow JO, Brett-Surman MK (eds) The complete dinosaur. Indiana University Press, Bloomington, pp 371–382
Chin K (2007) The paleobiological implications of herbivorous dinosaur coprolites from the Upper Cretaceous Two Medicine Formation of Montana: why eat wood? PALAIOS 22:554–566
Chin K, Gill BD (1996) Dinosaurs, dung beetles, and conifers: participants in a Cretaceous food web. PALAIOS 11:280–285

Chin K, Kirkland JI (1998) Probable herbivore coprolites from the Upper Jurassic Mygatt-Moore Quarry, western Colorado. Mod Geol 23:249–275
Christiansen P (1996) The evidence for and implications of gastroliths in sauropods (Dinosauria, Sauropoda). Gaia 12:1–7
Clark NDL (1989) A study of a Namurian crustacean-bearng shale from the western Midland Valley of Scotland. Dissertation, University of Glasgow
Clemmensen LB, Milàn J, Adolfssen JS, Estrup EJ, Frobøse N, Klein N, Mateus O, Wings O (2016) The vertebrate-bearing Late Triassic Fleming Fjord Formation of central East Greenland revisited: stratigraphy, palaeoclimate and new palaeontological data. In*:* Kear BP, Lindgren J, Hurum JH, Milàn J, Vajda V (eds) Mesozoic biotas of Scandinavia and its Arctic territories. Geol Soc London Spec Publ 434(1):31–47
Colbert EH (1989) The Triassic dinosaur *Coelophysis*. Mus North Arizona Bull 57:1–160
Colbert EH (1995) The little dinosaurs of Ghost Ranch. Columbia University Press, New York
Colbert EH, Olsen PE (2001) A new and unusual aquatic reptile from the Lockatong Formation of New Jersey (Late Triassic, Newark Supergroup). Am Mus Nov 3334:1–24
Colombi CE, Fernández E, Currie BS, Alcober OA, Martínez R, Correa G (2012) Large-diameter burrows of the Triassic Ischigualasto Basin, NW Argentina: paleoecological and paleoenvironmental implications. PLoS One 7(12):e50662
Conrad K, Lockley MG, Prince NK (1987) Triassic and Jurassic vertebrate-dominated trace fossil assemblages of the Cimarron Valley region: implications for paleoecology and biostratigraphy. New Mexico Geol Soc Guidebook 38:127–138
Conti MA, Leonardi G, Mariotti N, Nicosia U (1977) Tetrapod footprints of the "Val Gardena Sandstone" (North Italy). Their paleontological, stratigraphic and paleoenvironmental meaning. Palaeont Ital NS40:1–91
Coombs WP Jr (1989) Modern analogs for dinosaur nesting and parental behavior. Geol Soc Am Spec Pap 238:21–53
Courel L, Demathieu G (2000) Une nouvelle ichnoespèce *Coelurosaurichnus grancieri* du Trias supérieur de l'Ardèche, France. Geodiversitas 22:35–46
Cruickshank ARI (1986) Archosaur predation on an East African Middle Triassic dicynodont. Palaeontology 29:415–422
Currie PJ (1981) Hovasaurus bolei, an aquatic eosuchian from the upper Permian of Madagascar. Palaeontol Africa 24:99–163
Czaplewski NJ (2011) An owl-pellet accumulation of small Pliocene vertebrates from the Verde Formation, Arizona, USA. Palaeontol Electron 14(3):1–33
D'Orazi-Porchetti S, Nicosia U (2007) Re-examination of some large early Mesozoic tetrapod footprints from the African collection of Paul Ellenberger. Ichnos 14:219–245
D'Orazi-Porchetti S, Nicosia U, Mietto P, Petti FM, Avanzini M (2008) *Atreipus*-like footprints and their co-occurrence with *Evazoum* from the upper Carnian (Tuvalian) of Trentino-Alto Adige. St Trent Sci Nat Acta Geol 83:277–287
Dalla Vecchia FM (1996) Archosaurian trackways in the upper Carnian of Dogna Valley (Udine, Friuli, NE Italy). Nat Nasc 12:5–17
Dalla Vecchia FM, Mietto P (1998) Impronte di rettili terrestri nella Dolomia Principale (Triassico Superiore) delle Prealpi Carniche (Pordenone, Friuli). Atti Ticinesi di Scienze de la Terra 1998 Ser Spec 7:87–107
Damiani R, Modesto S, Yates A, Neveling J (2003) Earliest evidence of cynodont burrowing. Proc Roy Soc Lond 270:1747–1751
Darby DG, Ojakangas RW (1980) Gastroliths from an Upper Cretaceous plesiosaur. J Paleontol 54(3):548–556
DeBlieux DD, Kirkland JI, Smith JA, McGuire J, Santucci VL (2006) An overview of the paleontology of Upper Triassic and Lower Jurassic rocks in Zion National Park, Utah. New Mex Mus Nat Hist Sci Bull 37:490–501
Demathieu G (1966) *Rhynchosauroides petri* et *Sphingopus ferox*, nouvelles empreintes de reptiles de grès a bordure Nord-Est du Massif Central. C R Acad Sci D 263:483–486

Demathieu G (1977) La palichnologie de vertebras. Développement recent et role dans la stratigraphie du Trias. Bull Bur Rech Géol Min 3:269–278
Demathieu G (1982) Archosaurier-Fährtenfaunen der Trias: Die Bedeutung ihrer Ähnlichkeiten und ihrer Verschiedenheiten; ihre mögliche Verwendung im Rahmen der Stratigraphie der Trias. Geol Rundsch 71:741–746
Demathieu G (1984) Une ichnofaune du Trias moyen du Bassin de Lodéve (Hérault, France). Ann Paléontol 70(4):247–273
Demathieu G (1994) Synthèse géologique du Sud-Est de la France. Donées biostratigraphiques. Mém Bur Rech Géol Min 125:63–64
Demathieu G, Haubold H (1972) Stratigraphische Aussagen der Tetrapodenfährten aus der terrestrischen Trias Europas. Geologie 21(7):802–836
Demathieu G, Haubold H (1974) Evolution und Lebensgemeinschaft terrestrischer Tetrapoden nach ihren Fährten in der Trias. Freiberger Forschungsh C 298:51–72
Demathieu G, Oosterink HW (1983) Die Wirbeltier-Ichnofauna aus dem Unteren Muschelkalk von Winterswijk (Die Reptilfährten aus der Mitteltrias der Niederlande). Staringia 7:1–51
Demathieu G, Oosterink HW (1988) New discoveries of ichnofossils from the Middle Triassic of Winterswijk (the Netherlands). Geol Mijnb 67:3–17
Dentzien-Dias PC, Schultz CL, Scherer CM, Lavina EL (2007) The trace fossil record from the Guará Formation (Upper Jurassic?), southern Brazil. Arquiv Mus Nacional Rio de Jan 65(4):585–600
Dentzien-Dias PC, Schultz CL, Bertoni-Machado C (2008) Taphonomy and paleoecology inferences of vertebrate ichnofossils from Guará Formation (Upper Jurassic), southern Brazil. J S Am Earth Sci 25(2):196–202
Dentzien-Dias PC, de Figueiredo AEQ, Horn B, Cisneros JC, Schultz CL (2012a) Paleobiology of a unique vertebrate coprolite concentration from Rio do Rasto Formation (middle/upper Permian), Paraná Basin, Brazil. J South Am Earth Sci 40:53–62
Dentzien-Dias P, de Figueiredo AEQ, Mesa V, Perea D, Schultz C (2012b) Vertebrate footprints and burrows from the Upper Jurassic of Brazil and Uruguay. In: Netto RG, Carmon, NB, Tognoli FMW (eds) Ichnology of Latin America Selected Papers Monografias Da Sociedade Brasileira De Paleontologia 2: 129–139
Dentzien-Dias PC, Poinar G Jr, de Figueiredo AEQ, Pacheco ACL, Horn BLD, Schultz TC (2013) Tapeworm eggs in a 270 million-year-old shark coprolite. PLoS One 8(1):e55007. https://doi.org/10.1371/journal.pone.0055007
Dentzien-Dias P, Poinar G, Francischini H (2017) A new actinomycete from a Guadalupian vertebrate coprolite from Brazil. Hist Biol 29(6):770–776
Díaz-Martínez I, Castanera D, Gasca JM, Canudo JI (2015) A reappraisal of the Middle Triassic chirotheriid *Chirotherium ibericus* Navás, 1906 (Iberian Range, NE Spain), with comments on the Triassic tetrapod track biochronology of the Iberian Peninsula. PeerJ 3:e1044. https://doi.org/10.7717/peerj.1044
Diedrich C (1998) Stratigraphische Untersuchungen der Ichnofaziestypen einer neuen Wirbeltierfährtenfundstelle aus dem Unteren Muschelkalk des Teutoburger Waldes, NW-Deutschland. Neues Jahrb Geol Paläontol Monat 1998:626–640
Diedrich C (2000) Vertebrate track ichnofacies types of the Oolith member (Lower Muschelkalk, Middle Triassic) in the central Teutoburger Wald (NW-Germany) and their stratigraphical, facial and palaeogeographical significance. Zentral Geol Paläontol 1998:925–939
Diedrich C (2002a) Die Wirbeltierfährtenfundstelle Borgholzhausen (Teutoburger Wald, NW-Deutschland) aus der Oolith-Zone (Unterer Muschelkalk, Mitteltrias). Paläontol Z 76:35–56
Diedrich C (2002b) Wirbeltierfährten aus dem Unteren Muschelkalk (Mitteltrias) von Thüringen (SE-Deutschland). Neues Jahr Geol Paläontol Monat 2002:75–91
Diedrich C (2008) Millions of reptile tracks—Early to Middle Triassic carbonate tidal flat migration bridges of Central Europe—reptile immigration into the Germanic Basin. Palaeogeogr Palaeoclimatol Palaeoecol 259:410–423

Diedrich CG (2012a) Stomach and gastrointestinal tract contents in late Cenomanian (Upper Cretaceous) teleosts from black shales of Germany and analysis of fish mortality and food chains in the upwelling-influenced pre-North Sea basin of Europe. New Mex Mus Nat Hist Sci Bull 57:241–253

Diedrich CG (2012b) Typology of Ice Age Spotted Hyena *Crocuta crocuta spelaea* (Goldfuss, 1823) coprolite aggregate pellets from the European Late Pleistocene and their significance at dens and scavenging sites. New Mex Mus Nat Hist Sci Bull 57:369–377

Diedrich CG, Felker H (2012) Middle Eocene shark coprolites from the shallow marine and deltaic coasts of the pre-North Sea Basin in central Europe. New Mex Mus Nat Hist Bull 57:311–318

Domnanovich NS, Marsicano CA (2006) Tetrapod footprints from the Triassic of Patagonia: reappraisal of the evidence. Ameghiniana 43(1):55–70

Domnanovich NS, Tomassini R, Manera De Bianco T, Dalponte M (2008) Nuevos aportes al conocimiento de la icnofauna de tetrápodos del Triásico Superior de Los Menucos (Complejo Los Menucos), provincia de Río Negro, Argentina. Ameghiniana 45(1):211–224

Druckenmiller PS, Kelley N, Whalen MT, McRoberts C, Carter JG (2014) An Upper Triassic (Norian) ichthyosaur (Reptilia, Ichthyopterygia) from northern Alaska and dietary insight based on gut contents. J Vert Paleontol 34(6):1460–1465

Drumheller SK, Stocker MR, Nesbitt SJ (2014) Direct evidence of trophic interactions among apex predators in the Late Triassic of western North America. Naturwiss 101(11):975–987

Dubiel RF, Blodgett RH, Bown TM (1987) Lungfish burrows in the Upper Triassic Chinle and Dolores formations, Colorado Plateau. J Sed Pet 57:512–521

Duffin C (1979) Coprolites: a brief review with reference to specimens from the Rhaetic bone beds of England and South Wales. Mercian Geol 7:191–204

Duffin CJ (2010) Coprolites. In: Lord AR, Davis PG (eds) Fossils from the Lower Lias of the Dorset Coast: Palaeontological Association, field guides to fossils 13, pp 395–400

Dzik J (2003) A beaked herbivorous archosaur with dinosaur affinities from the early Late Triassic of Poland. J Vert Paleontol 23:556–574

Dzik J, Sulej T, Niedźwiedzki G (2008) A dicynodont-theropod association in the latest Triassic of Poland. Acta Palaeontol Polon 53(4):733–738

Elder RL (1978) Paleontology and paleoecology of the Dockum Group, Upper Triassic, Howard County, Texas. Thesis, University of Texas, Austin

Elder RL (1985) Principles of aquatic taphonomy with examples from the fossil record. Dissertation University of Michigan

Elder RL (1987) Taphonomy and paleoecology of the Dockum Group, Howard County, Texas. J Ariz-Nev Acad Sci 22:85–94

Ellenberger P (1965) Découverte de pistes Vertébrés dans le Permien, le Trias et le Lias inférieur, aux abords de Toulon (Var) et d'Anduze (Gard). Compt Rend Acad Sci Paris 260:5856–5859

Ellenberger P (1970) Les niveaux paléontologiques de première apparition des mammifères primordiaux en Afrique du sud et leur ichnologie. Establissement de zones stratigraphiques detaillées dans le Stormberg du Lesotho (Afrique du Sud) (Trias supérieur à jurassique). In: Second Gondwana Symposium, Proceedings and Papers. Council Sci Industr Res Pretoria, pp 343–370

Ellenberger P (1972) Contribution à la classification des Pistes de Vertébrés du Trias: les types du Stormberg d'Afrique du Sud (I). Palaeovert Mem Extraord:1–104

Ellenberger P (1974) Contribution à la classification des Pistes de Vértebrés du Trias: Les types du Stormberg d' Afrique du Sud (II, Les Stormberg Superieur). Palaeovert Mem Extraord, 141 p

Ellenberger P (1975) L'explosion démographique des reptiles quadrupedes a allure de mammiféres dans le Stormberg superieur (Trias) d'Afrique du Sud. Apercu sur leus origine au Permian (France et Karroo). Colloq Int CNRS Paris 218:409–439

Ellenberger F, Ellenberger P, Ginsburg L (1970) Les dinosaures du Trias et du Lias en France et en Afrique du Sud, d'après les pistes qu'ils ont laissées. Bull Soc Géol France 7, XII(1):151–159

Embry AF (1988) Triassic sea level changes: evidence from the Canadian Aarctic archipelago. SEPM Spec Pub 42:249–259

Embry AF (1997) Global sequence boundaries of the Triassic and their identification in the western Canada sedimentary basin. Bull Can Petrol Geol 45:415–433

Erickson BR (1984) Chelonivorous habits of the Paleocene crocodile *Leidyosuchus formidabilis*. Sci Pub Sci Mus Minn New Ser 5:1–9
Everhart MJ (2000) Gastroliths associated with plesiosaur remains in the Sharon Springs Member of the Pierre Shale (late Cretaceous), Western Kansas. Trans Kansas. Acad Sci 103(1–2):58–69
Everhart MJ (2004) Late Cretaceous interaction between predators and prey. Evidence of feeding by two species of shark on a mosasaur. PalArch Vert Paleo Ser 1:1–7
Everhart MJ (2005) Oceans of Kansas: a natural history of the Western Interior Sea. Indiana University Press, Bloomington
Farlow JO, Schachner ER, Sarrazin JC, Klein HK, Currie PJ (2014) Pedal proportions of *Poposaurus gracilis*: convergence and divergence in the feet of archosaurs. Anat Rec 297:1022–1046
Fernandes MA, Carvalho LDS (2008) Revisão diagnóstica para a icnospécie de tetrápode Mesozóico Brasilichnium elusivuum (Leonardi, 1981) (Mammalia) de Formação Botucato, Bacia do Paraná, Brasil. Ameghiniana 45(1):167–173
Fillmore DL, Lucas SG, Simpson EL (2012) Ichnology of the Mississippian Mauch Chunk Formation, eastern Pennsylvania. New Mex Mus Nat Hist Sci Bull 54:1–136
Fiorelli LE, Ezcurra MD, Hechenleitner EM, Argañaraz E, Taborda JR, Trotteyn MJ, Von Baczko MB, Desojo JB (2013) The oldest known communal latrines provide evidence of gregarism in Triassic megaherbivores. Sci Rep 3. https://doi.org/10.1038/srep03348
Fiorillo A (1991) Taphonomy and depositional setting of Careless Creek quarry (Judith River Formation), Wheatland County, Montana, USA. Palaeogeogr Palaeoclimatol Palaeoecol 88:157–166
Fluckiger FA (1858) Über Koprolithen aus Baselland: Schweiz Zeit Pharm 3:189–195
Forrest R (2003) Evidence for scavenging by the marine crocodile *Metriorhynchus* on the carcass of a plesiosaur. Proc Geol Assoc 144:363–366
Foster JR, Hamblin AH, Lockley MG (2000) The oldest evidence of a sauropod dinosaur in the western United States and other important vertebrate trackways from Grand Staircase-Escalante National Monument, Utah. Ichnos 7:169–181
Foster JR, Hamblin AH, Lockley MG (2003) *Apatopus* trackway and other footprints from the Chinle Group of southern Utah: an update. Ichnos 10:165–167
Fraas E (1891) Die Ichthyosaurier der Süddeutschen Trias- und Jura-Ablagerungen. Tubingen, 81 pp
Frank HT, Buchmann FSC, de Lima LG, Fornari M, Caron F, Lopeso RP (2012) Cenozoic vertebrate tunnels in southern Brazil. In: Netto RG, Carmon, NB, Tognoli FMW (eds) Ichnology of Latin America Selected Papers Monografias Da Sociedade Brasileira De Paleontologia 2: 141–157
Fraser NC, Olsen PE (1996) A new dinosauromorph ichnogenus from the Triassic of Virginia: Jeffersonia. Contrib Virg Mus Nat Hist 7:1–17
Furrer H (1993) Dinosaurier im Schweizerischen Nationalpark. Cratschla Ed Spec 1:4–24
Furrer H, Lozza H (2008) Neue Funde von Dinosaurierfährten im Schweizerischen Nationalpark. Cratschla 1:17–21
Gallois RW (2007) The stratigraphy of the Penarth Group (Late Triassic) of the east Devon coast: geoscience in south-west England. Proc Ussher Soc 11:287–297
Gand G, Vianey-Liaud M, Demathieu G, Garric J (2000) Deux nouvelles traces de pas de dinosaures du Trias supérieur de la bordure Cévenole (La Grand-Combe, Sud-Est de la France). Geobios 33:599–624
Gand G, Demathieu G, Grancier M, Sciau J (2005) Les traces dinosauroides du Trias supérieur francais: discrimination, interprétation et comparaison. Bull Soc Géol France 176(1):69–79
Gaston R, Lockley MG, Lucas SG, Hunt AP (2003) *Grallator*-dominated fossil footprint assemblages and associated enigmatic footprints from the Chinle Group (Upper Triassic), Gateway area, Colorado. Ichnos 10:153–163
Gatesy SM, Middleton KM, Jenkins FA, Shubin NH (1999) Three-dimensional preservation of foot movements in Triassic theropod dinosaurs. Nature 399:141–144
Gawne CE (1975) Rodents from the Zia Sand Miocene of New Mexico. Am Mus Novit 2586:1–25

Gierlinski G, Ahlberg A (1994) Late Triassic and Early Jurassic dinosaur footprints in the Höganäs Formation of southern Sweden. Ichnos 3:99–105

Gilfillian AM, Olsen PE (2000) The coelacanth *Diplurus longicaudatus* as the origin of the large coprolites occurring in the Triassic-Jurassic lacustrine strata of eastern North America. Geol Soc Am Abstr Prog 32:20

Gillette L, Pemberton SG, Sarjeant WAS (2003) A Late Triassic invertebrate ichnofauna from Ghost Ranch, New Mexico. Ichnos 10:141–151

Gilmore B (1992) Scroll coprolites from the Silurian of Ireland and the feeding of early vertebrates. Palaeontology 3:319–333

Gobetz KE (2006) Possible burrows of mylagaulids (Rodentia: Aplodontoidea: Mylagaulidae) from the late Miocene (Barstovian) Pawnee Creek Formation of northeastern Colorado. Palaeogeogr Palaeoclimatol Palaeoecol 237:119–136

Gobetz KE, Martin LD (2006) Burrows of a gopher-like rodent, possibly *Gregorymys* (Geomyoidea: Geomyidae: Entoptychinae), from the early Miocene Harrison Formation, Nebraska. Palaeogeogr Palaeoclimatol Palaeoecol 237:305–314

Gobetz KE, Lucas SG, Lerner AJ (2006) Lungfish burrows of varying morphology from the Upper Triassic Redonda Formation, Chinle Group, Eastern New Mexico. New Mex Mus Nat Hist Bull 37:140–146

Godfrey SJ, Palmer BT (2015) Gar-bitten coprolite from South Carolina, USA. Ichnos 22(2):103–108

Godfrey SJ, Smith JB (2010) Shark-bitten vertebrate coprolites from the Miocene of Maryland. Naturwiss 97(5):461–467

Gorzelak P, Salamon MA, Baumiller TK (2012) Predator-induced macroevolutionary trends in Mesozoic crinoids. Proc Natl Acad Sci U S A 109(18):7004–7007

Groenewald GH, Welman J, MacEachern JA (2001) Vertebrate burrow complexes from the Early Triassic *Cynognathus* zone (Driekoppen Formation, Beaufort Group) of the Karoo basin, South Africa. PALAIOS 16:148–160

Haderer F-O (1990) Ein tridactyles Trittsiegel aus dem Stubensandstein (Obere Trias, Nor) des Rühlenbachtales (Württemberg). Stuttgarter Beitr Nat Ser B 160:1–14

Haderer F-O (1996) Archosaurier-Trittsiegel aus dem Stubensandstein (Obere Trias, Nor) von Württemberg (Süddeutschland). Jahr Ges Nat Württ 152:41–45

Haderer F-O (2012) 100 Jahre Saurierfährten aus Stuttgart-Gablenberg und der Erstnachweis der Fährtengattung *Atreipus* Olsen & Baird 1986 im Kieselsandstein (Obere Trias, Karn, Hassberge Formation) von Baden-Württemberg. Jahr Ges Nat Württ 168:29–51

Haderer FO (2015) Erstnachweis der Fährtengattung *Evazoum* Nicosia & Loi 2003 im Kieselsandstein (Obere Trias, Karn, Hassberge-Formation) von Baden-Württemberg. Jh Ges Nat Württemberg 171:191–200

Hansen BB, Milàn J, Clemmensen LB, Adolfssen JS, Estrup EJ, Klein N, Mateus O, Wings O (2015) Coprolites from the Late Triassic Kap Stewart Formation, Jameson Land, East Greenland: morphology, classification and prey inclusions. Geol Soc Lond Spec Pub 434(1):49–69

Häntzschel W, El-Baz F, Amstutz GC (1968) Coprolites: an annotated bibliography. Geol Soc Am Mem 108:1–122

Hasiotis ST (2002) Continental trace fossils. Society of Economic Paleontologists and Mineralogists, Short Course Notes 51, 132 pp

Hasiotis ST, Hannigan RE (1991) Use of periodic acid schiff (PAS) in the identification of possible lungfish burrows in the Upper Triassic Chinle Formation of southeastern Utah and western Colorado. Geol Soc Am Abstr Progr 23:42

Hasiotis ST, Martin AJ (1999) Probable reptile nests from the Upper Triassic Chinle Formation, Petrified Forest National Park, Arizona. In: Santucci VL, McClelland L (eds) National Park Service Paleontological Research, Geologic Resources Division Technical Paper, NPS/NDGRD/GRDTR-99/03. U.S. National Park Service, Washington, pp 85–89

Hasiotis ST, Wellner RW, Martin AJ, Demko TM (2004) Vertebrate burrows from Triassic and Jurassic continental deposits of North America and Antarctica: their paleoenvironmental and paleoecological significance. Ichnos 11:103–124

Hasiotis ST, Platt BF, Hembree DI, Everhart MJ (2007) The trace-fossil record of vertebrates. In: Miller WIII (ed) Trace fossils: concepts, problems, prospects. Elsevier, New York, pp 196–218
Haubold H (1966) Therapsiden- und Rhynchocephalen-Fährten aus dem Buntsandstein Südthüringens. Hercynia NF 3(2):147–183
Haubold H (1967) Eine Pseudosuchier-Fährtenfauna aus dem Buntsandstein Südthüringens. Hallesches Jahrb Mitteld Erdg 8:12–48
Haubold H (1971a) Die Tetrapodenfährten des Buntsandsteins. Paläontol Abh A 4:395–548
Haubold H (1971b) Ichnia Amphibiorum et Reptiliorum fossilium. Encycl Paleoherpetol 18:1–124
Haubold H (1986) Archosaur footprints at the terrestrial Triassic-Jurassic transition. In: Padian K (ed) The beginning of the age of dinosaurs. Cambridge University Press, Cambridge, pp 189–201
Haubold H, Klein H (2000) Die dinosauroiden Fährten *Parachirotherium – Atreipus – Grallator* aus dem unteren Mittelkeuper (Obere Trias: Ladin, Karn, ?Nor) in Franken. Hallesches Jahrb Geowiss B 22:59–85
Haubold H, Klein H (2002) Chirotherien und Grallatoriden aus der Unteren bis Oberen Trias Mitteleuropas und die Entstehung der Dinosauria. Hallesches Jahrb Geowiss B 24:1–22
Heckert AB (2001) The microvertebrate record of the Upper Triassic (Carnian) lower Chinle Group, southwestern U.S.A. and the early evolution of dinosaurs. Dissertation. University of New Mexico
Heckert AB (2004) Late Triassic microvertebrates from the lower Chinle Group (Otischalkian-Adamanian: Carnian), southwestern U.S.A. New Mex Mus Nat Hist Sci Bull 27:1–170
Heckert AB, Lucas SG (2002) Lower Chinle Group (Upper Triassic: Carnian) stratigraphy in the Zuni Mountains, west-central New Mexico. New Mex Mus Nat Hist Sci Bull 21:51–72
Heckert AB, Lucas SG (2003) Triassic stratigraphy in the Zuni Mountains. New Mex Geol Soc Guide 54:245–262
Heckert AB, Lucas SG, Estep JW (2002) Lower Chinle Group (Upper Triassic: Upper Carnian) tetrapods from the vicinity of Cameron, Arizona. New Mex Mus Nat Hist Sci Bull 21:73–76
Heckert AB, Lucas SG, Hunt AP (2005) Triassic vertebrate fossils in Arizona. New Mex Mus Nat Hist Sci Bull 29:16–44
Heckert AB, Lucas SG, Rinehart LF, Celeskey MD, Spielmann JA, Hunt AP (2010) Articulated skeletons of the aetosaur Typothorax coccinarum Cope (Archosauria: Stagonolepididae) from the Upper Triassic Bull Canyon Formation (Revueltian: Early-mid Norian), eastern New Mexico, USA. J Vert Paleontol 30:619–642
Heller F (1952) Reptilienfährten-Funde aus dem Ansbacher Sandstein des Mittleren Keupers von Franken. Geol Bl NO-Bayern 2:129–141
Hembree DI, Martin LD, Hasiotis ST (2004) Amphibian burrows in ephemeral ponds of the Lower Permian Speiser Shalem Kansas: evidence for seasonality in the mid-continent. Palaeogeogr Palaeoclimatol Palaeoecol 203:127–152
Hembree DI, Hasiotis ST, Martin LD (2005) *Torridorefugium eskridgensis* (new ichnogenus and ichnospecies): amphibian aestivation burrows from the lower Permian Speiser Shale of Kansas. J Paleontol 79:583–593
High LR, Hepp DM, Clark T, Picard MD (1969) Stratigraphy of Popo Agie Formation (Late Triassic), Uinta Mountain area, Utah and Colorado. Wyom Geol Soc Guide 16:181–192
Hirsch KF, Young RG, Armstrong HJ (1979) Eggshell fragments from the Jurassic Morrison Formation of Colorado. In: Averett WR (ed) Paleontology and geology of the Dinosaur Triangle. Museum of Western Colorado, Grand Junction, pp 79–84
Hitchcock E (1845) An attempt to name, classify, and describe the animals that made the fossil footmarks of New England. Proc 6th Ann Meet Assoc Amer Geol Nat 6:23–25
Hitchcock E (1858) Ichnology of New England. A report on the sandstone of the Connecticut Valley, especially its fossil footmarks, made to the Government of the Commonwealth of Massachusetts. William White, Printer, Boston, 214 pp
Hofbauer G, Klein H (2013) Ein neuer Blick auf die Langenzenner Fährtenplatte im Museum der Naturhistorischen Gesellschaft Nürnberg. Jahresmitt Naturhist Ges Nürnberg 2012:63–73

Hollocher K, Hollocher TC (2012) Early process in the fossilization of terrestrial feces to coprolites, and microstructure preservation. New Mex Mus Nat Hist Sci Bull 57:79–91
Hollocher KT, Alcober OA, Colombi CE, Hollocher TC (2005) Carnivore coprolites from the Upper Triassic Ischigualasto Formation, Argentina: chemistry, mineralogy, and evidence for rapid initial mineralization. PALAIOS 20:51–63
Horner JR, Makela R (1979) Nests of juveniles provides evidence of family structure among dinosaurs. Nature 82:296–298
Hornstein F (1876) Mitteilung an Prof. Geinitz. Neues Jahrb Mineral Geol Paläontol 1876, 923 pp
Hospitaleche CA (2016) Paleobiological remarks on a new partial skeleton of the Eocene Antarctic penguin Palaeeudyptes klekowskii. Ameghiniana 53(3):269–281
Houck KJ, Fleming J, Guerrero R, Heimink N, Heberton A, Itano W, Titus A, Barrick JE (2004) Paleontology of the Bassam Park fossil beds (Pennsylvanian), San Isabel National Forest, Colorado. Geol Soc Am Abstr Prog 36:413
Hunt AP (1984) Fluvial vertebrate taphonomy: historical perspectives. New Mex J Sci 24(2):26–27
Hunt AP (1987) Phanerozoic trends in nonmarine taphonomy: implications for Mesozoic vertebrate taphonomy and paleoecology. Geol Soc Am Abstr Prog 19:171
Hunt AP (1989) Cranial morphology and ecology among phytosaurs. In: Lucas SG, Hunt AP (eds) Dawn of the age of dinosaurs in the American Southwest. New Mexico Museum of Natural History, Albuquerque, pp 349–354
Hunt AP (1991a) The first tetrapod faunas from the Trujillo Formation (Late Triassic) of east-central New Mexico and their biochronological and paleoecological significance. New Mex Geol 13:93
Hunt AP (1991b) Two phytosaur (Reptilia: Archosauria) skeletons from the Bull Canyon Formation (Late Triassic) of east-central New Mexico. New Mex Geol 13:93
Hunt AP (1992) Late Pennsylvanian coprolites from the Kinney Brick Quarry, central New Mexico, with notes on the classification and utility of coprolites New Mex Bur Mines Mineral Res Bull 138:221–229
Hunt AP (1994) Vertebrate paleontology and biostratigraphy of the Bull Canyon Formation (Chinle Group: Norian), east central New Mexico with revisions of the families Metoposauridae (Amphibia: Temnospondyli) and Parasuchidae (Reptilia: Archosauria). Dissertation, University of New Mexico
Hunt AP (2001) The vertebrate fauna, biostratigraphy and biochronology of the type Revueltian land-vertebrate faunachron, Bull Canyon Formation (Upper Triassic), east-central New Mexico. New Mex Geol Soc Guid 5:123–151
Hunt AP, Lucas SG (1988) Late Triassic fauna from the Los Esteros Member of the Santa Rosa Formation, Santa Fe County, New Mexico and its biochronological implications. New Mex J Sci 28:107–116
Hunt AP, Lucas SG (1989) Late Triassic vertebrate localities in New Mexico. In: Lucas SG, Hunt AP (eds) Dawn of the age of dinosaurs in the American Southwest. New Mexico Museum of Natural History, Albuquerque, pp 72–101
Hunt AP, Lucas SG (1990) Paleontology and biochronology of the Petrified Forest Member of the Upper Triassic Chinle Formation near San Ysidro, Sandoval County, New Mexico. New Mex J Sci 30:17–26
Hunt AP, Lucas SG (1993a) Late Triassic microvertebrate localities in New Mexico (USA): implications for paleoecology. New Mex Mus Nat Hist Sci Bull 3:87–191
Hunt AP, Lucas SG (1993b) Sequence stratigraphy and a tetrapod acme zone during the early Revueltian (Late Triassic: early Norian). New Mex Mus Nat Hist Sci Bull 3:G46
Hunt AP, Lucas SG (1993c) Triassic vertebrate paleontology and biochronology of New Mexico. New Mex Mus Nat Hist Sci Bull 2:49–60
Hunt AP, Lucas SG (2001) The first vertebrate track (*Brachychirotherium*) from the late Carnian Garita Creek Formation, east central New Mexico. New Mex Geol Soc Guid 52:51–52
Hunt AP, Lucas SG (2003) New tetrapod tracksite, Upper Triassic Sloan Canyon Formation, Union County, New Mexico. New Mex Geol 25:53

Hunt AP, Lucas SG (2005) A nonmarine coprolite acme zone in the Permo-Triassic. New Mex Mus Nat Hist Sci Bull 30:123–124
Hunt AP, Lucas SG (2006a) Late Triassic tetrapod tracks from Petrified Forest National Park, Arizona. New Mex Mus Nat Hist Sci Bull 37:221–225
Hunt AP, Lucas SG (2006b) Triassic-Jurassic tetrapod ichnofacies. New New Mex Mus Nat Hist Sci Bull 37:12–22
Hunt AP, Lucas SG (2007a) A new tetrapod ichnogenus from the Upper Triassic of New Mexico, with notes on the ichnotaxonomy of *Rhynchosauroides*. New Mex Mus Nat Hist Sci Bull 41:71–76
Hunt AP, Lucas SG (2007b) Cenozoic vertebrate trace fossils of North America: ichnofaunas, ichnofacies and biochronology. New Mex Mus Nat Hist Sci Bull 42:17–41
Hunt AP, Lucas SG (2007c) Late Triassic tetrapod tracks of western North America. New Mex Mus Nat Hist Sci Bull 40:215–230
Hunt AP, Lucas SG (2007d) Tetrapod ichnofacies: a new paradigm. Ichnos 14:59–68
Hunt AP, Lucas SG (2007e) The Triassic tetrapod track record: ichnofaunas, ichnofacies and biochronology. New Mex Mus Nat Hist Sci Bull 41:78–87
Hunt AP, Lucas SG (2012a) Classification of vertebrate coprolites and related trace fossils. New Mex Mus Nat Hist Sci Bull 57:137–146
Hunt AP, Lucas SG (2012b) Descriptive terminology of coprolites and recent feces. New Mex Mus Nat Hist Sci Bull 57:153–160
Hunt AP, Lucas SG (2013) The fossil record of Carboniferous and Permian vertebrate coprolites. New Mex Mus Nat Hist Sci Bull 60:121–127
Hunt AP, Lucas SG (2014) Jurassic vertebrate bromalites of the western United States in the context of the global record. Volum Jurass 12(2):151–158
Hunt AP, Lucas SG (2016a) The case for archetypal vertebrate ichnofacies. Ichnos 23(3–4):237–247
Hunt AP, Lucas SG (2016b) The most significant record of "middle"- late Paleozoic vertebrate coprolites: Silurian-Carboniferous ichnoassemblages from Scotland. Geol Soc Am Abstr Prog 48(7). https://doi.org/10.1130/abs/2016AM-284166
Hunt AP, Lucas SG (2016c) The record of vertebrate coprolites across the Cretaceous/Paleogene boundary. New Mex Mus Nat Hist Sci Bull 74:79–93
Hunt AP, Lucas SG (2016d) Vertebrate trace fossils from New Mexico and their significance. New Mex Mus Nat Hist Sci Bull 64:9–40
Hunt AP, Santucci VL (1994) Late Triassic coprolites from Petrified Forest National Park. Petrified Forest Nat Park Res Abstr 3:15–16
Hunt AP, Lucas SG, Kietzke KK (1989a) Dinosaur footprints from the Redonda Member of the Chinle Formation (Upper Triassic), eastcentral New Mexico. In: Gillette DD, Lockley MG (eds) Dinosaur tracks and traces. Cambridge University Press, Cambridge, pp 277–280
Hunt AP, Lucas SG, Martini K, Martini L (1989b) Triassic stratigraphy and paleontology, Mesa del Oro, Valencia County, New Mexico. New Mex Geol Soc Guide 40:8–9
Hunt AP, Lockley MG, Lucas SG (1993a) Vertebrate and invertebrate tracks and trackways from Upper Triassic strata of the Tucumcari basin, east-central New Mexico, USA. New Mex Mus Nat Hist Sci Bull 3:199–201
Hunt AP, Santucci VL, Lockley MG, Olson TJ (1993b) Dicynodont trackways from the Holbrook Member of the Moenkopi Formation (Middle Triassic: Anisian), Arizona, USA. New Mex Mus Nat Hist Sci Bull 3:213–218
Hunt AP, Lockley MG, Conrad KL, Paquette M, Chure D (1993c) Late Triassic vertebrates from the Dinosaur National Monument area (Utah, USA) with an example of the utility of coprolites for correlation. New Mex Mus Nat Hist Sci Bull 3:197–198
Hunt AP, Chin K, Lockley MG (1994a) The paleobiology of coprolites. In: Donovan SK (ed) The paleobiology of trace fossils. Wiley, London, pp 221–240
Hunt AP, Meyer CS, Lockley MG, Lucas SG (1994b) Archaeology, toothmarks and sauropod dinosaur taphonomy. Gaia 10:225–231

Hunt AP, Lucas SG, Lockley MG (1998) Taxonomy and stratigraphic and facies significance of vertebrate coprolites of the Upper Triassic, Chinle Group, western United States. Ichnos 5:225–234

Hunt AP, Lucas SG, Lockley MG, Heckert AB (2000) Occurrence of the dinosaurian ichnogenus *Grallator* in the Redonda Formation (Upper Triassic: Norian) of eastern New Mexico. New Mex Mus of Nat Hist Sci Bull 17:39–41

Hunt AP, Lucas SG, Lockley MG, Heckert AB (2001) Comparison of tetrapod faunas inferred from osteological and ichnological data derived from lakeshore facies of the Upper Triassic Redonda Formation, east-central New Mexico. New Mex Geol 23:63

Hunt AP, Lucas SG, Spielmann JA (2005a) Biochronology of early Permian vertebrate coprolites of the American Southwest. New Mex Mus Nat Hist Sci Bull 31:43–45

Hunt AP, Lucas SG, Spielmann JA (2005b) The postcranial skeleton of *Revueltosaurus callenderi* (Archosauria: Crurotarsi) from the Upper Triassic of Arizona and New Mexico, USA. New Mex Mus Nat Hist Sci Bull 29:67–76

Hunt AP, Santucci VL, Lucas SG (2005c) Vertebrate trace fossils from Arizona with special reference to tracks preserved in National Park Service units and notes on the Phanerozoic distribution of fossil footprints. New Mex Mus Nat Hist Sci Bull 29:159–167

Hunt AP, Lucas SG, Spielmann JA, Lerner AJ (2007) A review of vertebrate coprolites of the Triassic with descriptions of new Mesozoic ichnotaxa. New Mex Mus Nat Hist Sci Bull 41:88–107

Hunt AP, Lucas SG, Spielmann JA (2012a) New coprolite ichnotaxa from the Buckland Collection at the Oxford University Museum of Natural History. New Mex Mus Nat Hist Sci Bull 57:115–124

Hunt AP, Lucas SG, Spielmann JA (2012b) The bromalite collection at the National Museum of Natural History (Smithsonian Institution), with descriptions of new ichnotaxa and notes on other significant coprolite collections. New Mex Mus Nat Hist Sci Bull 57:105–114

Hunt AP, Lucas SG, Spielmann JA (2012c) The vertebrate coprolite collection at The Natural History Museum (London). New Mex Mus Nat Hist Sci Bull 57:125–129

Hunt AP, Lucas SG, Milàn J, Spielmann JA (2012d) Vertebrate coprolite studies: status and prospectus. New Mex Mus Nat Hist Sci Bull 57:5–24

Hunt AP, Lucas SG, Spielmann JA, Lockley MG (2012e) Bromalites from the Mississippian Bear Gulch Lagerstätte of central Montana, USA. New Mex Mus Nat Hist Sci Bull 57:71–174

Hunt AP, Santucci VL, Tweet JS, Lucas SG (2012f) Vertebrate coprolites and other bromalites in National Park Service areas. New Mex Mus Nat Hist Sci Bull 57:343–353

Hunt AP, Lucas SG, Spielmann JA, Cantrell A, Suazo T (2012g) A new marine coprofauna from the Beeman Formation (Late Pennsylvanian: Late Missourian), Sacramento Mountains, New Mexico, USA. New Mex Mus Nat Hist Sci Bull 57:193–196

Hunt AP, Lucas SG, Spielmann JA, Suazo T, Cantrell A (2012h) A re-evaluation of Late Pennsylvanian bromalites from the Kinney Brick Quarry Lagerstätte, New Mexico, USA. New Mex Mus Nat Hist Sci Bull 57:185–192

Hunt AP, Lucas SG, Spielmann JA, Cantrell A, Suazo T, Lerner AJ (2012i) Bromalites from the Tinajas Lagerstätte (Late Pennsylvanian: Late Missourian), central New Mexico, USA. New Mex Mus Nat Hist Sci Bull 57:175–183

Hunt AP, Lucas SG, Spielmann JA (2013a) Triassic vertebrate coprolite ichnofaunas. New Mex Mus Nat Hist Sci Bull 61:237–258

Hunt AP, Lucas SG, Cantrell A, Suazo T (2013b) Tracks, dung, bite marks and burrows: imprecision in terminology and a paucity of ichnotaxonomy hinders the development of the study of vertebrate trace fossils. Geol Soc Am Abstr Progr 45(7):326

Hunt AP, Lucas SG, Buskirk BL (2015a) The value of vomit: the fossil record of vertebrate regurgitalites and its significance. Geol Soc Am Abstr Progr 47(7):346

Hunt AP, Lucas SG, Milàn J, Lichtig AJ, Jagt JWM (2015b) Vertebrate coprolites from Cretaceous Chalk in Europe and North America and the shark surplus paradox. New Mex Mus Nat Hist Sci Bull 67:63–68

Jacobsen AR (1998) Feeding behavior of carnivorous dinosaurs as determined by tooth marks on dinosaur bones. Hist Biol 13:17–26
Jacobsen AR, Bromley RG (2009) New ichnotaxa based on tooth impressions on dinosaur and whale bones. Geol Quart 53:373–382
Jain S (1983) Spirally coiled 'coprolites' from the Upper Triassic Maleri Formation, India. Palaeontology 26:813–829
Jenkins FA Jr, Shubin NH, Amaral WW, Gatesy SM, Schaff CR, Clemmensen LB, Downs WR, Davidson AR, Bonde N, Osbaeck F (1994) Late Triassic continental vertebrates and depositional environments of the Fleming Fjord Formation, Jameson Land, east Greenland. Medd Grønland Geosci 32:1–25
Jessop TA, Sumner J, Rudiharto H, Purwandana D, Imansyah MJ, Phillips JA (2004) Distribution, use and selection of nest type by Komodo dragons. Biol Conserv 1117:463–470
Ji Q, Currie PJ, Norell MA, Ji SA (1998) Two feathered dinosaurs from northeastern China. Nature 393:753–761
Johnson JH (1934) A coprolite horizon in the Pennsylvanian of Chafee and Park Counties, Colorado. J Paleo 8:477–479
Karl C, Haubold H (1998) *Brachychirotherium* aus dem Coburger Sandstein (Mittlerer Keuper, Karn/Nor) in Nordbayern. Hallesches Jahrb Geowiss B 20:33–58
Kaup JJ (1835) Über Thierfährten bei Hildburghausen. N Jahrb Min Geol Paläontol 1835:327–328
Kaye FT, Padian K (1994) Microvertebrates from the *Placerias* quarry: a window on Late Triassic vertebrate diversity in the American Southwest. In: Fraser NC, Sues H-D (eds) In the shadow of dinosaurs. Cambridge University Press, Cambridge, pp 362–367
Kear BP, Boles WE, Smith ET (2003) Unusual gut contents in a Cretaceous ichthyosaur. Proc R Soc Lond B Biol Sci 270:206–208
Kelly SRA, Bromley RG (1984) Ichnological nomenclature of clavate borings. Palaeontol 27(4):793–807
King W (1881) The geology of the Pranhita Godavari valley. Mem Geol Surv India 18:151–311
Kirby RE (1989) Late Triassic vertebrate localities of the Owl Rock Member (Chinle Formation) in the Ward Terrace area of northern Arizona. In: Lucas SG, Hunt AP (eds) Dawn of the age of dinosaurs in the American Southwest. New Mexico Museum of Natural History, Albuquerque, pp 12–28
Kitching JW (1979) Preliminary report on a clutch of six dinosaurian eggs from the Upper Triassic Elliott Formation, northern Orange Free State. Palaeontol Africana 22:41–45
Klein H, Haubold H (2004) Überlieferungsbedingte Variation bei Chirotherien und Hinweise zur Ichnotaxonomie nach Beispielen aus der Mittel- bis Ober-Trias (Anisium–Karnium) von Nordbayern. Hallesches Jahrb Geowiss B 26:1–15
Klein H, Haubold H (2007) Archosaur footprints—potential for biochronology of Triassic continental sequences. New Mex Mus Nat Hist Sci Bull 41:120–130
Klein H, Kneidl V (2015) Tetrapodenfährten aus den Estherienschichten (Obertrias, Grabfeld-Formation) der Tongrube Barbaraberg (Speinshart, NO-Bayern)—Profilneuaufnahme. Bildungsmilieu und Hinweise zur Palökologie: Geol Bl NO-Bayern 65(2–4):93–130
Klein H, Lucas SG (2010a) Tetrapod footprints – their use in biostratigraphy and biochronology of the Triassic. In: Lucas SG (ed) The Triassic timescale. Geol Soc London Spec Publ 334: 419–446
Klein H, Lucas SG (2010b) The Triassic footprint record of crocodylomorphs—a critical re-evaluation. New Mex Mus Nat Hist Sci Bull 51:55–60
Klein H, Lucas SG (2013) The Late Triassic ichnotaxon *Apatopus lineatus* (Bock 1952) and its distribution. New Mex Mus Nat Hist Sci Bull 61:313–324
Klein H, Niedźwiedzki G (2012) Revision of the Lower Triassic tetrapod ichnofauna from Wióry, Holy Cross Mountains, Poland. New Mex Mus Nat Hist Sci Bull 56:1–62
Klein H, Lucas SG, Haubold H (2006) Tetrapod track assemblage of the Redonda Formation (Upper Triassic, Chinle Group) in east-central New Mexico—re-evaluation of ichnofaunal diversity from studies of new material. New Mex Mus Nat Hist Sci Bull 37:241–250

Klein H, Lucas SG, Voigt S (2015a) Revision of the ?Permian-Triassic tetrapod ichnogenus *Procolophonichnium* Nopcsa 1923 with description of the new ichnogenus *P. lockleyi*. Ichnos 22:155–176

Klein H, Milán J, Clemmensen LB, Frobøse N, Mateus O, Klein N, Adolfssen JS, Estrup EJ, Wings O (2015b) Archosaur footprints (cf. *Brachychirotherium*) with unusual morphology from the Upper Triassic Flemingfjord Formation (Norian-Rhaetian) of east Greenland. In: Kear BP, Lindgren J, Hurum JH, Milàn J, Vajda V (eds) Mesozoic biotas of Scandinavia and its Arctic territories. Geol Soc London Spec Publ 434:71–85

Klompmaker AA, Herngreen GFW, Oosterink HW (2010) Biostratigraphic correlation, paleoenvironment stress, and subrosion pipe collapse: Dutch Rhaetian shales uncover their secrets. Facies 56:597–613

Kobayashi Y, Lü J-C (2003) A new ornithomimid dinosaur with gregarious habits from the Late Cretaceous of China. Acta Palaeontol Polon 48(2):235–259

Krapovickas V, Mancuso AC, Marsicano CA, Domnanovich NS, Schultz CL (2013) Large tetrapod burrows from the Middle Triassic of Argentina: a behavioural adaptation to seasonal semiarid climate? Lethaia 46(2):154–169

Kriwet J, Witzmann F, Klug S, Heidtke UH (2008) First direct evidence of a vertebrate three-level trophic chain in the fossil record. Proc Roy Soc Lond B Biol Sci 275(1631):181–186

Kuhn O (1956) Eine neue lacertoide Fährte aus dem Sandsteinkeuper Frankens. N Jahrb Geol Paläontol Mh 1956:529–531

Kuhn O (1958a) Die Fährten der vorzeitlichen Amphibien und Reptilien. Bamberg, Meisenbach

Kuhn O (1958b) Zwei neue Arten von *Coelurosaurichnus* aus dem Keuper Frankens. Neu Jahr Geol Paläont Monat 1958:437–440

Kuhn O (1963) Ichnia tetrapodorum. Fossilium Catalogus I Animalia. Ysel Press, Deventer

Kummel B (1979) Triassic. Treatise on invertebrate paleontology, part a, introduction. Fossilization (taphonomy) biogeography and biostratigraphy. Geological Society of America and University of Kansas Press, Lawrence, KS, pp 351–389

LaGarry HE (1997) Geology of the Toadstool Park region of northwestern Nebraska, with the lithostratigraphic revision and redescription of the Brule Formation and remarks on Oligocene bone processing. Dissertation, University of Nebraska, Lincoln

LaGarry HE (2004) Taphonomic evidence of bone processing from the Oligocene of northwestern Nebraska. School Nat Res Institu Agri Natl Res Univf Nebraska-Lincoln Prof Pap 2:1–35

Lagnaoui A, Klein H, Voigt S, Hminna A, Saber H, Schneider JW, Werneburg R (2012) Late Triassic tetrapod-dominated ichnoassemblages from the Argana Basin (Western High Atlas, Morocco). Ichnos 19:238–253

Lagnaoui A, Klein H, Saber H, Fekkak A, Belahmira A, Schneider JW (2016) New discoveries of archosaur and other tetrapod footprints from the Timezgadiouine Formation (Irohalene Member, Upper Triassic) of the Argana Basin, western High Atlas, Morocco—ichnotaxonomic implications. Palaeogeogr Palaeoclimatol Palaeoecol 453:1–9

Lallensack JN, Klein H, Milán J, Wings O, Mateus O, Clemmensen LB (2017) Sauropodomorph dinosaur trackways from the Fleming Fjord Formation of East Greenland: evidence for Late Triassic sauropods. Acta Palaeontol Pol (in press)

Langer M (2005) Studies on continental Late Triassic tetrapod biochronology. I. The type locality of *Saturnalia tupiniquim* and the faunal succession in south Brazil. J South Am Earth Sci 19:205–218

Langston WJ, Rose H (1978) A yearling crocodilian from the middle Eocene Green River Formation of Colorado. J Paleontol 52:122–125

Laojumpon C, Matkhammee T, Wathanapitaksakul A, Suteethorn V, Suteethorn S, Lauprasert K, Srisuk P, Le Loeuff J (2012) Preliminary report on coprolites from the Late Triassic of Thailand. New Mex Mus Nat Hist Sci Bull 57:207–213

Laudet F, Fosse P (2001) Un assemblage d'os grignote par les rongeurs au Paleogene (Oligocene superieur, phosphorites du Quercy). Compt Rend l'Acad Sci Ser IIA Earth Planet Sci 333(3):195–200

Le Loeuff J, Saenyamoon T, Souillat C, Suteethorn V, Buffetaut E (2009) Mesozoic vertebrate footprints of Thailand and Laos. In: Buffetaut E, Cuny G, Le Loeuff J, Suteethorn V (eds) Late Palaeozoic and Mesozoic ecosystems in Southeast Asia. Geol Soc London, Spec Publ 315, pp 245–254

Leonardi G (1981) Novo icnogenero de tetrapode mesozoico da Formacao Botucatu, Araraquara. An Acad Brasil Ci 53(4):793–805

Leonardi G (1994) Annotated atlas of South America tetrapod footprints (Devonian to Holocene). CPRM, Brasilia

Leonardi G, De Oliveira FH (1990) A revision of the Triassic and Jurassic tetrapod footprints of Argentina and a new approach on the age and meaning of the Botucatu Formation footprints (Brazil). Rev Brasileira Geoci 2(1–4):216–229

Lichtig AJ, Lucas SG, Klein H, Lovelace DM (2017) Triassic turtle tracks and the origin of turtles. Hist Biol. https://doi.org/10.1080/08912963.2017.1339037

Lipman CB, McLees E (1940) A new species of sulfur-oxidizing bacteria from a coprolite. Soil Sci 50:429–433

Lockley MG (1986) A guide to dinosaur tracksites of the Colorado Plateau and American Southwest. University of Colorado at Denver, Geology Department Magazine Special Publication, Denver

Lockley MG (2006) Observations on the ichnogenus *Gwyneddichnium* and *Gwyneddichnium*-like footprints and trackways from the Upper Triassic of the western United States. New Mex Mus Nat Hist Sci Bull 37:170–175

Lockley MG, Eisenberg L (2006) A preliminary report on a spectacular dinosaur tracksite in the Chinle Group, Dirty Devil River Valley, Wayne County, Utah. New Mex Mus Nat Hist Sci Bull 37:263–268

Lockley MG, Hunt AP (1993) A new Late Triassic tracksite from the Sloan Canyon Formation, type section, Cimarron Valley, New Mexico. New Mex Mus Nat Hist Sci Bull 3:279–283

Lockley MG, Hunt AP (1995) Dinosaur tracks and other fossil footprints of the western United States. Columbia University Press, New York

Lockley MG, Hunt AP (1999) Dinosaur tracks and other fossil footprints of western North America (revised edition). Columbia University Press, New York

Lockley MG, Lucas SG (2013) *Evazoum gatewayensis*, a new Late Triassic archosaurian ichnospecies from Colorado: implications for footprints in the ichnofamily Otozoidae. New Mex Mus Nat Hist Sci Bull 61:345–353

Lockley MG, Meyer CA (2000) Dinosaur tracks and other fossil footprints of Europe. Columbia University Press, New York

Lockley MG, Milner ARC (2006) Tetrapod tracksites from the Shinarump Formation (Chinle Group, Upper Triassic) of southwestern Utah. New Mex Mus Nat Hist Sci Bull 37:257–262

Lockley MG, Conrad K, Paquette M (1991) Distribution and significance of Mesozoic vertebrate trace fossils in Dinosaur National Monument. In: Plumb G (ed) Univ Wyoming Nat Park Serv Res Cent 15th Ann Rep, pp 85–90

Lockley MG, Conrad K, Paquette M, Hamblin A (1992) Late Triassic vertebrate tracks in the Dinosaur National Monument area. Utah Geol Surv Misc Publ 92(3):383–391

Lockley MG, Santos VF, Hunt AP (1993) A new Late Triassic tracksite from the Sheep Pen Sandstone, Sloan Canyon, Cimarron Valley, New Mexico. New Mex Mus Nat Hist Sci Bull 3:285–288

Lockley MG, Hunt AP, Meyer C (1994) Vertebrate tracks and the ichnofacies concept: implications for paleoecology and palichnostratigraphy. In: Donovan S (ed) The paleobiology of trace fossils. Wiley, London, pp 241–268

Lockley MG, King M, Howe S, Sharp T (1996) Dinosaur tracks and other archosaur footprints from the Triassic of South Wales. Ichnos 5:23–41

Lockley MG, Hunt AP, Meyer C, Rainforth EC, Schultz RJ (1998) A survey of fossil footprint sites at Glen Canyon National Recreation Area (Western USA): a case study in documentation of trace fossil resources at a National Preserve. Ichnos 5:177–211

Lockley MG, Lucas SG, Hunt AP (2000) Dinosaur tracksites in New Mexico: a review. New Mex Mus Nat Hist Sci Bull 17:9–16
Lockley MG, Wright JL, Hunt AP, Lucas SG (2001) The Late Triassic sauropod track record comes into focus: old legacies and new paradigms. New Mexico Geol Soc Guid 52:181–190
Lockley MG, Lucas SG, Hunt AP, Gaston R (2004) Ichnofaunas from the Triassic-Jurassic boundary sequences of the Gateway area, western Colorado: implications for faunal composition and correlations with other areas. Ichnos 11:89–102
Lockley MG, Lucas SG, Hunt AP (2006a) *Eosauropus*, a new name for a Late Triassic track: further observations on the Late Triassic ichnogenus *Tetrasauropus* and related forms, with notes on the limits of interpretation. New Mex Mus Nat Hist Sci Bull 37:192–198
Lockley MG, Lucas SG, Hunt AP (2006b) *Evazoum* and the renaming of northern hemisphere "*Pseudotetrasauropus*": implications for tetrapod ichnotaxonomy at the Triassic-Jurassic boundary. New Mex Mus Nat Hist Sci Bull 37:199–206
Loope DB (2006) Burrows dug by large vertebrates into rain-moistened Middle Jurassic sand dunes. J Geol 114:753–762
Lucas SG (1998) Global Triassic tetrapod biostratigraphy and biochronology. Palaeogeogr Palaeoclimatol Palaeoecol 143:347–384
Lucas SG (2000) The epicontinental Triassic, an overview. Zentral Geol Paläont I(7–8):475–496
Lucas SG (2003) Triassic tetrapod footprint biostratigraphy and biochronology. Albertiana 8:75–84
Lucas SG (2007) Tetrapod footprint biostratigraphy and biochronology. Ichnos 14:5–38
Lucas SG (2010) The Triassic timescale based on nonmarine tetrapod biostratigraphy and biochronology. In: Lucas SG (ed) The Triassic timescale. Geol Soc London Spec Publ 334, pp 447–500
Lucas SG (2016) Two new, substrate-controlled nonmarine ichnofacies. Ichnos 23(3–4):248–261
Lucas SG, Heckert AB (2011) Late Triassic aetosaurs as the trackmaker of the tetrapod footprint ichnotaxon *Brachychirotherium*. Ichnos 18(4):197–208
Lucas SG, Hunt AP (1993) A dicynodont from the Upper Triassic of New Mexico and its biochronological significance. New Mex Mus Nat Hist Sci Bull 3:321–325
Lucas SG, Hunt AP (2006) Reappraisal of "reptile nests" from the Upper Triassic Chinle Group, Petrified Forest National Park, Arizona. New Mex Mus Nat Hist Sci Bull 37:155–159
Lucas SG, Orchard MJ (2013) Triassic: reference module in earth systems and environmental sciences. Elsevier, Oxford. https://doi.org/10.1016/B978-0-12-409548-9.02872-4
Lucas SG, Sullivan RM (2006) Tetrapod footprints from the Upper Triassic Passaic Formation near Graterford, Montgomery County, Pennsylvania. In: Harris JD, Lucas SG, Spielmann JA, Lockley MG, Milner ARC, Kirkland JI (eds) The Triassic-Jurassic terrestrial transition. New Mexico Mus Nat Hist Sci Bull 37:251–256
Lucas SG, Tanner LH (2007a) Tetrapod biostratigraphy and biochronology of the Triassic–Jurassic transition on the southern Colorado Plateau, USA. Palaeogeogr Palaeoclimatol Palaeoecol 244:242–256
Lucas SG, Tanner LH (2007b) The nonmarine Triassic-Jurassic boundary in the Newark Supergroup of eastern North America. Earth Sci Rev 84:1–20
Lucas SG, Tanner LH (2015) End Triassic nonmarine biotic events. J Palaeogeogr 4:331–340
Lucas SG, Oakes W, Froehlich JW (1985) Triassic microvertebrate locality, Chinle Formation, east-central New Mexico. New Mex Geol Soc Guide 36:205–212
Lucas SG, Heckert AB, Huber P (1998) *Aetosaurus* (Archosauromorpha) from the Upper Triassic of the Newark Supergroup, eastern United States, and its biochronological significance. Palaeontology 41:1215–1230
Lucas SG, Hunt AP, Lockley MG (2001) Tetrapod footprint ichnofauna of the Upper Triassic Redonda Formation, Chinle Group, Quay County, New Mexico. New Mex Geol Soc Guid 52:177–180
Lucas SG, Heckert AB, Hunt AP (2003) Tetrapod footprints from the Middle Triassic (Perovkan-early Anisian) Moenkopi Formation, west-central New Mexico. New Mex Geol Soc Guid 54:241–244

Lucas SG, Lockley MG, Hunt AP, Tanner LH (2006a) Biostratigraphic significance of tetrapod footprints from the Triassic-Jurassic Wingate Sandstone on the Colorado Plateau. New Mex Mus Nat Hist Sci Bull 37:109–117

Lucas SG, Gobetz KE, Odier GP, McCormick T, Egan C (2006b) Tetrapod burrows from the Lower Jurassic Navajo Sandstone, southeastern Utah. New Mex Mus Nat Hist Sci Bull 37:147–154

Lucas SG, Lockley MG, Hunt AP, Milner ARC, Tanner LH (2006c) Tetrapod footprint biostratigraphy of the Triassic-Jurassic transition in the American Southwest. New Mex Mus Nat Hist Sci Bull 37:105–108

Lucas SG, Klein H, Lockley MG, Spielmann J, Gierlinski GD, Hunt AP, Tanner LH (2006d) Triassic-Jurassic stratigraphic distribution of the theropod footprint ichnogenus *Eubrontes*. New Mex Mus Nat Hist Sci Bull 37:68–93

Lucas SG, Minter NJ, Hunt AP (2010a) Re-evaluation of alleged bees' nests from the Upper Triassic of Arizona. Palaeogeogr Palaeoclimatol Palaeoecol 286:194–201

Lucas SG, Spielmann JA, Klein H, Lerner AJ (2010b) Ichnology of the Upper Triassic Redonda Formation (Apachean) in east-central New Mexico. New Mex Mus Nat Hist Sci Bull 47:1–75

Lucas SG, Spielmann JA, Hunt AP, Emry RJ (2012a) Crocodylian coprolites from the Eocene of the Zaysan Basin, Kazakstan. New Mex Mus Nat Hist Sci Bull 57:319–324

Lucas SG, Emry RJ, Kraine K, Hunt AP, Spielmann JA (2012b) Strigilites (fossilized owl pellets) from the Oligocene of Wyoming. New Mex Mus Nat Hist Sci Bull 57:325–335

Lucas SG, Tanner LH, Kozur HW, Weems RE, Heckert AB (2012c) The Late Triassic timescale: age and correlation of the Carnian-Norian boundary. Earth Sci Rev 114:1–8

Lucas SG, Krainer K, Chaney DS, DiMichele WA, Voigt S, Berman DS, Henrici AC (2013) The lower Permian Abo Formation in central New Mexico. New Mex Mus Nat Hist Sci Bull 59:161–179

Lucas SG, Szajna MJ, Lockley MG, Fillmore DL, Simpson EL, Klein H, Boyland J, Hartline BW (2014) The Middle-Late Triassic tetrapod footprint ichnogenus *Gwyneddichnium*. New Mex Mus Nat Hist Sci Bull 62:135–155

Lucas SG, Rinehart LF, Heckert AB, Hunt AP, Spielmann JA (2016) Rotten Hill: a Late Triassic bonebed in the Texas Panhandle, USA. New Mex Mus Nat Hist Sci Bull 72:1–99

MacDonald DIM, Isbell JL, Hammer WR (1991) Vertebrate trackways from the Triassic Fremouw Formation, Queen Alexandra Range, Antarctica. Antarctic J United States 26:20–22

MacEachern JA, Bann KL, Gingras MK, Zonneveld J, Dashtgard SE, Pemberton SG (2012) The ichnofacies paradigm. In: Knaust D, Bromley RG (eds) Trace fossils as indicators of sedimentary environments. Elsevier developments in sedimentology, vol 64. Elsevier, Amsterdam, pp 103–138

Maidwell FT (1911) Notes on footprints from the Keuper of Runcorn Hill. Proc Liverpool Geol Soc 11:140–152

Mancuso AC, Marsicano C, Palma R (2013) Vertebrate coprolites from the Triassic of Argentina (Cuyana Basin). Ameghiniana 41(3):347–354

Markwick PJ (1998) Crocodilian diversity in space and time: the role of climate in paleoecology and its implication for understanding K/T extinctions. Paleobiology 24:470–497

Márquez-Aliaga A, García-Forner A, Martínez C, Villena JA (1999) "Colección icnofósiles" del Museo de Geología de la Universidad de Valencia. Temas Geológico−Mineros ITGE 26:413–414

Marsicano CA, Barredo SP (2004) A Triassic tetrapod footprint assemblage from southern South America: palaeobiogeographical and evolutionary implications. Palaeogeogr Palaeoclimatol Palaeoecol 203:313–335

Martill DM (1999) Bone beds of the Westbury Formation. In: Swift A, Martill DM (eds) Fossils of the Rhaetian Penarth Group. Palaeontological Association field guides to fossils 9, pp 239–250

Martin LD, Bennett DK (1977) The burrows of the Miocene beaver *Palaeocaster*, western Nebraska. Palaeogeogr Palaeoclimatol Palaeoecol 22:173–193

Marzola M, Dalla Vecchia FM (2014) New dinosaur tracks from the Dolomia Principale (Upper Triassic) of the Carnic Prealps (Friuli-Venezia Giulia, NE Italy). Boll Soc Paleontol Italiana 53(1):1–18

Mateus I, Mateus H, Telles Antunes M, Mateus O, Taquet P, Ribeiro V, Manuppella G (1997) Couvée, oeufs et embryone d'un dinosaur théropode du Jurassique supérieur de Lourinhã (Portugal). Comptes Rendus Acad Sci Terre Planèt 325:71–78

Mateus O, Clemmensen L, Klein N, Wings O, Frobøse N, Milán, J, Adolfssen JS, Estrup E (2014) The Late Triassic of Jamesonland revisited: new vertebrate findings and the first phytosaur from Greenland. In: Maxwell E, Miller-Camp J (eds) Society of vertebrate paleontology 74th meeting, Berlin, Program and Abstracts, p 182

Matley C (1939) On some coprolites from the Maleri Beds of India. Records Geol Surv India 74:35–547

Mazzotti FJ (2003) American crocodiles (*Crocodylus acutus*) in Florida: Gainesville, Document WEC 38, Department of Wildlife Ecology and Conservation Department, Florida Cooperative Extension Service, Institute of Flood and Agricultural Sciences, University of Florida

McAllister JA (1985) Reevaluation of the origin of spiral coprolites. Univ Kansas Palaeontol Contrib 114:1–12

McAllister JA (1987) Phylogenetic distribution and morphological reassessment of the intestines of fossil and modern fishes. Zool Jahrb Abtheil Anat Ontog Thiere 115:281–294

McAllister JA (1989) Lungfish burrows in the Upper Triassic Chinle and Dolores formations, Colorado Plateau–comments on the recognition criteria of fossil lungfish burrows. J Sed Petr 58:365–369

McAllister JA (1992) *Gnathorhiza* (Dipnoi): life aspects, and lungfish burrows. In: Mark-Kurik E (ed) Fossil fishes as living animals. Academy of Sciences of Estonia, Institute of Geology, Tallinn, pp 91–105

McAllister JA (1996) Coprolites. In: Schultze H-P, Cloutier R (eds) Devonian fishes and plants of Miguasha, Quebec, Canada. Verlag Dr Friedrich Pfeil, München, pp 328–347

McAllister JA, Kirby J (1998) An occurrence of reptile subaqueous traces in the Moenkopi Formation (Triassic) of Capital Reef National Park, south central Utah, USA. J Penn Acad Sci 71:174–181

McIlroy D (2004) Some ichnological concepts, methodologies, applications and frontiers. In: McIlroy D (ed) The application of ichnology to paleoenvironmental and stratigraphic analysis. Geol Soc London Spec Publ, vol 228, pp 3–27

Melchor RN (2004) Trace fossil distribution in lacustrine deltas: examples from the Triassic rift lakes of the Ischigualasto-Villa Unión basin, Argentina. In: McIlroy D (ed), The application of ichnology to palaeoenvironmental and stratigraphic analysis. Geol Soc London Spec Publ 228, pp 335–354

Melchor RN, De Valais S (2006) A review of Triassic tetrapod track assemblages from Argentina. Palaeontology 49(2):355–379

Melchor RN, Genise JF, Verde M (2001) Invertebrate trace fossils from Triassic continental successions of San Juan Province, Argentina. Asociación Paleontológica Argentina, Publicación Especial 7:127–131

Melchor RN, Genise JF, Umazano AM, Superina M (2012) Pink fairy armadillo meniscate burrows and ichnofabrics from Miocene and Holocene interdune deposits of Argentina: palaeoenvironmental and palaeoecological significance. Palaeogeogr Palaeoclimatol Palaeoecol 350:149–170

Metz R (1995) Ichnologic study of the Lockatong Formation (Late Triassic), Newark Basin, southwestern Pennsylvania. Ichnos 4:43–51

Metz R (1996) Newark Basin ichnology: the Late Triassic Perkasie Member of the Passaic Formation, Sanatoga, Pennsylvania. Northeastern Geol Environ Sci 18:118–129

Metz R (2000) Triassic trace fossils from lacustrine shoreline deposits of the Passaic Formation, Douglasville, Pennsylvania. Ichnos 7:253–266

Meyer HV, Plieninger T (1844) Beiträge zur Paläontologie Württembergs, die fossilen Wirbeltierreste aus den Triasgebilden. Schweizerbart, Stuttgart

Meyer CA, Marty D, Thüring B, Stecher R, Thüring S (2013) Dinosaurierspuren aus der Trias der Bergüner Stöcke (Parc Ela, Kanton Graubünden, SE Schweiz). Mitt Naturf Ges beider Basel 14:135–144

Mickleson DL, Huntoon J, Kvale EP (2006a) The diversity and stratigraphic distribution of pre-dinosaurian communities from the Triassic Monekopi Formation. New Mex Mus Nat Hist Sci Bull 34:132–137

Mickleson DL, Milner ARC, Deblieux DD, McGuire JL (2006b) The oldest Early Triassic fossil vertebrate footprints in North America, from Zion National Park, Utah. New Mex Mus Nat Hist Sci Bull 34:141–144

Mikuláš R, Kadlecová E, Fejfar O, Dvořák Z (2006) Three new ichnogenera of biting and gnawing traces on reptilian and mammalian bones: a case study from the Miocene of the Czech Republic. Ichnos 13:113–127

Milàn J, Bromley RG (2006) True tracks, undertracks and eroded tracks, experimental work with tetrapod tracks in laboratory and field. Palaeogeogr Palaeoclimatol Palaeoecol 231:253–264

Milàn J, Clemmensen LB, Bonde N (2004) Vertical sections through dinosaur tracks (Late Triassic lake deposits, East Greenland)—undertracks and other surface deformation structures revealed. Lethaia 37:285–296

Milàn J, Avanzini M, Clemmensen LB, Garciá-Ramos JC, Piñuela L (2006) Theropod foot movement recorded by Late Triassic, Early Jurassic and Late Jurassic fossil footprints. New Mex Mus Nat Hist Sci Bull 37:352–364

Milàn J, Clemmensen LB, Adolfssen JS, Estrup EJ, Frobøse N, Klein N, Mateus O, Wings O (2012) A preliminary report on coprolites from the Late Triassic part of the Kap Stewart Formation, Jameson Land, East Greenland. New Mex Mus Nat Hist Sci Bull 57:203–205

Miller MF, Hasiotis ST, Babcock LE, Isbell JL, Collinson JW (2001) Tetrapod and large burrows of uncertain origin in Triassic high paleolatitude floodplain deposits, Antarctica. PALAIOS 16:218–232

Molnar RE, Clifford HT (2001) An Ankylosaurian cololite from the Lower Cretaceous of Queensland, Australia. In: Carpenter K (ed) The armored dinosaurs. Indiana University Press, Bloomington, pp 399–412

Moodie R (1912) The 'stomach stones' of reptiles. Science 35:377–378

Moratalla JJ, Powell JE (1994) Dinosaur nesting patterns. In: Carpenter K, Hirsch KF, Horner JR (eds) Dinosaur eggs and babies. Cambridge University Press, Cambridge, pp 37–46

Morgan GS, Lucas SG (2000) Pliocene and Pleistocene vertebrate faunas from the Albuquerque Basin, New Mexico. New Mex Mus Nat Hist Bull 16:217–240

Moussa MT (1970) Nematode fossil trails from the Green River Formation (Eocene) in the Uinta basin, Utah. J Paleontol 44(2):304–307

Munk W, Sues HD (1993) Gut contents of *Parasaurus* (Pareiasauria) and *Protorosaurus* (Archosauromorpha) from the Kupferschiefer (Upper Permian) of Hessen, Germany. Paläontol Z 67:169–176

Murry PA (1989) Geology and paleontology of the Dockum Formation (Upper Triassic), West Texas and eastern New Mexico. In: Lucas SG, Hunt AP (eds) Dawn of the age of dinosaurs in the American Southwest. New Mexico Museum of Natural History and Science, Albuquerque, pp 102–144

Murry PA, Long RA (1989) Geology and paleontology of the Chinle Formation, Petrified Forest National Park and vicinity, Arizona and a discussion of vertebrate fossils of the southwestern Upper Triassic. In: Lucas SG, Hunt AP (eds) Dawn of the age of dinosaurs in the American Southwest. New Mexico Museum of Natural History and Science, Albuquerque, pp 29–64

Nesbitt SJ, Turner AH, Erickson GM, Norell MA (2006) Prey choice and cannibalistic behavior in the theropod *Coelophysis*. Biol Lett 2:611–614

Nesbitt SJ, Irmis RB, Parker WG (2007) A critical re-evaluation of the Late Triassic dinosaur taxa of North America. J Syst Palaeontol 5:209–243

Nicosia U, Loi M (2003) Triassic footprints from Lerici (La Spezia, northern Italy). Ichnos 10:127–140
Niedźwiedzki G (2011) A Late Triassic dinosaur-dominated ichnofauna from the Tomanóva Formation of the Tatra Mountains, Central Europe. Acta Palaeontol Pol 56(2):291–300
Niedźwiedzki G, Gorzelak P, Sulej T (2010) Bite traces on dicynodont bones and the early evolution of large terrestrial predators. Lethaia 44:87–92
Niedźwiedzki G, Bajdek P, Owocki K, Kear BP (2016a) An Early Triassic polar predator ecosystem revealed by vertebrate coprolites from the Bulgo Sandstone (Sydney Basin) of southeastern Australia. Palaeogeogr Palaeoclimatol Palaeoecol 464:5–15
Niedźwiedzki G, Bajdek P, Qvarnström M, Sulej T, Sennikov AG, Golubev VK (2016b) Reduction of vertebrate coprolite diversity associated with the end-Permian extinction event in Vyazniki region, European Russia. Palaeogeogr Palaeoclimatol Palaeoecol 450:77–90
Njau JK, Blumenschine RJ (2006) A diagnosis of crocodile feeding traces on larger mammal bone, with fossil examples from the Plio-Pleistocene Olduvai basin, Tanzania. J Hum Evol 50:142–162
Norman JR, Heckert AB, Krzyzanowski SE, Rinehart LF, Lucas SG (2009) New microvertebrate faunal assemblage from the Upper Triassic Blue Mesa Member of the Petrified Forest Formation in the Blue Hills, east-central Arizona. Geol Soc Am Abstr Prog 41:103
Northwood C (2005) Early Triassic coprolites from Australia and their palaeobiological significance. Palaeontology 48:49–68
O'Harra CC (1920) The White River Badlands. South Dak School Mines Bull 13:1–181
O'Keefe FR, Street HP, Cavigelli JP, Socha JJ, O'Keefe RD (2009) A plesiosaur containing an ichthyosaur embryo as stomach contents from the Sundance Formation of the Bighorn Basin, Wyoming. J Vert Paleontol 29:1306–1310
O'Sullivan MJ, Cooper MA, MacCarthy IAJ, Forbes WH (1986) The palaeoenvironment and deformation of *Beaconites*-like burrows in the Old Red Sandstone at Gortnabinna, SW Ireland. J Geol Soc Lond 143:897–906
Oji T, Chigusa Ogaya C, Sato T (2003) Increase of shell-crushing predation recorded in fossil shell fragmentation. Paleobiology 29(4):520–526
Oldham T (1859) On some fossil fish-teeth of the genus *Ceratodus*, from Maleri, south of Nagpur. Mem Geol Surv India 1:295–309
Olsen PE (1979) A new aquatic eosuchian from the Newark Supergroup (Late Triassic-early Jurassic) of North Carolina and Virginia. Postilla 176:1–14
Olsen PE (1980) A comparison of the vertebrate assemblages from the Newark and Hartford basins (Early Mesozoic, Newark Supergroup) of eastern North America. In: Jacobs LL (ed) Aspects of vertebrate history. Museum of Northern Arizona Press, Flagstaff, pp 35–53
Olsen PE (1988) Paleontology and paleoecology of the Newark Supergroup (early Mesozoic, eastern North America). In: Manspeizer W (ed) Triassic-Jurassic rifting and the opening of the Atlantic Ocean. Elsevier, Amsterdam, pp 185–230
Olsen PE, Baird D (1986) The ichnogenus *Atreipus* and its significance for Triassic biostratigraphy. In: Padian K (ed) The beginning of the age of dinosaurs. Cambridge University Press, Cambridge, pp 61–87
Olsen PE, Flynn J (1989) Field guide to the vertebrate paleontology of Late Triassic rocks in the southwestern Newark Basin (Newark Supergroup, New Jersey and Pennsylvania). The Mosasaur 4:1–35
Olsen PE, Galton PM (1984) A review of the reptile and amphibian assemblages from the Stormberg of southern Africa, with special emphasis on the footprints and the age of the Stormberg. Palaeontol Africana 25:87–110
Olsen PE, Huber P (1997) Stop 3: Triangle Brick Quarry. In: Clark TW (ed) TRIBI: Triassic Basin initiative, abstracts with programs and field trip guidebook. Duke University, Durham, pp 22–29
Olsen PE, Huber P (1998) The oldest Late Triassic footprint assemblage from North America (Pekin Formation, Deep River Basin, North Carolina, USA). Southeast Geol 38:77–90

Olsen PE, Padian K (1986) Earliest records of *Batrachopus* from the southwestern United States, and a revision of some Early Mesozoic crocodylomorph ichnogenera. In: Padian K (ed) The beginning of the age of dinosaurs. Cambridge University Press, Cambridge, pp 259–273
Olsen PE, Rainforth EC (2001) The "Age of Dinosaurs" in the Newark Basin, with special reference to the Lower Hudson Valley. NewYork State Geol Assoc Guid, pp 59–176
Olsen PE, Schlische RW, Gore PJW (eds) (1989) Tectonic, depositional, and paleoecological history of Early Mesozoic rift basins, eastern North America: International Geological Congress Field Trip Guidebook T351. American Geophysical Union, Washington, 174 p
Olsen PE, Smith JB, McDonald NG (1998) Type material of the type species of the classic theropod footprint genera *Eubrontes*, *Anchisauripus*, and *Grallator* (Early Jurassic, Hartford and Deerfield basins, Connecticut and Massachusetts, U. S. A.) J Vert Paleontol 18:586–601
Olsen PE, Whiteside JH, Huber P (2003) Causes and consequences of the Triassic-Jurassic mass extinction as seen from the Hartford Basin. In: Brady JB, Cheney JT (eds) Guidebook for field trips in the Five College Region, 95th New England Intercollegiate Geological Conference. Department of Geology, Smith College, Northampton, pp B5-1-B5-41
Olsen PE, Whiteside J, Fedak T (2005a) The Triassic-Jurassic faunal and floral transition in the Fundy Basin, Nova Scotia. Atlant Geosc Soc Spec Publ 26:1–53
Olsen PE, Whiteside JH, LeTourneau P, Huber P (2005b) Jurassic cyclostratigraphy and paleontology of the Hartford Basin. In: Skinner BJ, Philpotts AR (eds) 97th New England Intercollegiate Geological Conference: New Haven, Department of Geology and Geophysics, Yale University, pp A4-1–A4-51
Olson E, Bolles K (1975) Permo-Carboniferous fresh water burrows. Fieldiana Geol 33:271–290
Padian K, Li C, Pchelnikova J (2010) The trackmaker of *Apatopus* (Late Triassic, North America) implications for the evolution of archosaur stance and gait. Palaeontology 53:175–189
Paes Neto VD, Parkinson AH, Pretto FA, Soares MB, Schwanke C, Schultz CL, Kellner AW (2016) Oldest evidence of osteophagic behavior by insects from the Triassic of Brazil. Palaeogeogr Palaeoclimatol Palaeoecol 453:30–41
Pandeli E, Vannucchi P, Monechi S (1998) Possible crystalline gastroliths of large marine Vertebrata from Oligocene pelitic sediments of the Northern Apennines, Italy. Geology 26(9):775–778
Parker WG, Irmis RB, Nesbitt SJ, Martz JW, Browne LS (2005) The pseudosuchian *Revueltosaurus callenderi* and its implications for the diversity of early ornithischian dinosaurs. Proc R Soc Lond B 272:963–969
Parrish JM (1999) Small fossil vertebrates from the Chinle Formation (Upper Triassic) of southern Utah. Utah Geol Surv Misc Publ 99-1:45–50
Pascual Arribas C, Latorre Macarrón P (2000) Huellas de *Eubrontes* y *Anchisauripus* en Carrascosa de Arriba (Soria, España). Bol Geol Min 111(1):21–32
Peabody FE (1948) Reptile and amphibian trackways from the Moenkopi Formation of Arizona and Utah. Univ Calif Pub Bull Depart Geol Sci 27:295–468
Pérez-López A (1993) Estudio de las huellas de reptil, del icnogénero *Brachychirotherium*, encontradas en el Trias subbético de Cambil. Est Geol 49:77–86
Petti FM, Avanzini M, Nicosia U, Girardi S, Bernardi M, Ferretti P, Schirolli P, Dal Sasso C (2009) Late Triassic (Early-Middle Carnian) chirotherian tracks from the Val Sabbia Sandstone (eastern Lombardy, Brescian Prealps, northern Italy). Riv Italiana Paleontol Strat 115:277–290
Pirrone CA, Buatois LA (2016) Bioeroded dinosaur bones: novel signatures of necrophagous activity in a cretaceous continental environment. Ichnos 23:340–348
Pirrone CA, Buatois LA, González Riga B (2014) A new ichnospecies of *Cubiculum* from Upper Cretaceous dinosaur bones in Western Argentina. Ichnos 21:251–260
Plieninger T (1838) Tierfährten in der Keuperformation bei Stuttgart. Neu Jahrb Min Geol 1838:536–537
Pol D, Powell JE (2007) Skull anatomy of *Mussaurus patagonicus* (Dinosauria: Sauropodomorpha) from the Late Triassic of Patagonia. Hist Biol 19:125–144
Pollard JE (1968) The gastric contents of an ichthyosaur from the Lower Lias of Lyme Regis, Dorset. Palaeontology 11:376–388

Price PH (1927) The coprolite horizon of the Conemaugh Series in and around Morgantown. West Virginia Annals Carnegie Mus 17:211–254
Qvarnström M, Niedźwiedzki G, Žigaitė Ž (2016) Vertebrate coprolites (fossil faeces): an under-explored Konservat-Lagerstätte. Earth Sci Rev 162:44–57
Qvarnström M, Niedźwiedzki G, Tafforeau P, Žigaitė Ž, Ahlberg PE (2017) Synchrotron phase-contrast microtomography of coprolites generates novel palaeobiological data. Sci Rep 7:2723. https://doi.org/10.1038/s41598-017-02893-9
Rainforth EC (2005) Ichnotaxonomy of the fossil footprints of the Connecticut Valley (Early Jurassic, Newark Supergroup, Connecticut and Massachusetts). Dissertation, Columbia University
Rehnelt K (1950) Ein Beitrag über Fährtenspuren im unteren Gipskeuper von Bayreuth. Ber Naturwiss Ges Bayreuth 1950:27–36
Reisz RR, Tsuji LA (2006) An articulated skeleton of *Varanops* with bite marks: the oldest known evidence of scavenging among terrestrial vertebrates. J Vert Paleontol 26:1021–1023
Renesto S, Spielmann JA, Lucas SG, Tarditi Spagnoli G (2010) The taxonomy and paleobiology of the Late Triassic (Carnian-Norian: Adamanian-Apachean) drepanosaurs (Diapsida: Archosauromorpha: Drepanosauromorpha). New Mex Mus Nat Hist Sci Bull 46. 81 p
Retallack GJ (1996) Early Triassic therapsid footprints from the Sydney basin, Australia. Alcheringa 20:301–314
Richter G, Baszio S (2001) First proof of planctivory/insectivory in a fossil fish: *Thaumaturus intermedius* from the Eocene Lake Messel (FRG). Palaeogeogr Palaeoclimatol Palaeoecol 173(1):75–85
Rieber H (1970) Phragmoteuthis? ticinensis sp. nov., ein Coeloidea-Rest aus der Grenzbitumenzone (Mittlere Trias) des Monte San Giorgio (Kanton Tessin, Schweiz). Paläontol Z 44:32–40
Rinehart LF, Hunt AP, Lucas SG, Heckert AB (2005a) Coprolites and cololites from the Late Triassic theropod dinosaur *Coelophysis bauri*, Whitaker quarry, Rio Arriba County, New Mexico. New Mex Geol 27:53
Rinehart LF, Hunt AP, Lucas SG, Heckert AB, Smith J (2005b) New evidence for cannibalism in the Late Triassic (Apachean) dinosaur *Coelophysis bauri* (Theropoda: Ceratosauria). J Vert Paleontol 25(3):105
Rinehart LF, Lucas SG, Spielmann JA (2006) Bite marks on tetrapod bones from the Upper Triassic Chinle Group representing a new ichnogenus. New Mex Mus Natl Hist Sci Bull 37:160–163
Rinehart LF, Lucas SG, Heckert AB, Spielmann JA, Celeskey MD (2009) The paleobiology of *Coelophysis bauri* (Cope) from the Upper Triassic (Apachean) Whitaker quarry, New Mexico, with detailed analysis of a single quarry block. New Mex Mus Nat Hist Sci Bull 45:1–260
Romer AS, Olson EC (1954) Aestivation by Permian lungfish. Brevoria 30:1–8
Rühle von Lilienstern H (1938) Fährten aus dem Blasensandstein (km 4) des Mittleren Keupers von Südthüringen. Neu Jahrb Min Geol Paläontol B 80:63–71
Rühle von Lilienstern H (1939) Fährten und Spuren im *Chirotherium*-Sandstein von Südthüringen. Fortschr Geol Paläontol 12(40):293–387
Rühle von Lilienstern H (1944) Eine Dicynodontierfährte aus dem Chirotherium-Sandstein von Heßberg bei Hildburghausen. Paläontol Z 23:368–385
Salamon MA, Niedźwiedzki R, Gorzelak P, Lach R, Surmik D (2012) Bromalites from the Middle Triassic of Poland and the rise of the Mesozoic Marine Revolution. Palaeogeogr Palaeoclimatol Palaeoecol 321:142–150
Salamon MA, Gorzelak P, Niedźwiedzki R, Trzęsiok D, Baumiller TK (2014) Trends in shell fragmentation as evidence of mid-Paleozoic changes in marine predation. Paleobiology 40(1):14–23
Sato T, Tanabe K (1998) Cretaceous plesiosaurs ate ammonites. Nature 394:629–630
Schlirf M, Uchman A, Kümmel M (2001) Upper Triassic (Keuper) non-marine trace fossils from the Hassberge area (Franconia, south-eastern Germany). Paläontol Z 75:71–96

Schoch RR (2002) Stratigraphie und Taphonomie wirbeltierreicher Schichten im Unterkeuper (Mitteltrias) von Vellberg (SW-Deutschland). Stuttgart Beiträg Natur Serie B (Geol Paläontol) 318:1–30

Schultz C (1942) A review of the *Daimonelix* problem. Nebrask Univ Stud Sci Tech 2:1–30

Schultz RJ, Lockley MG, Hunt AP (1994) New tracks from the Moenkopi Formation at Glen Canyon National Recreation Area. In: Santucci VL (ed) The paleontological resources of the National Parks. National Park Service Technical Report NPS/NRPO/NRTR-95/16, pp 60–63

Schultz-Pittman RJ, Lockley MG, Gaston R (1996) First reports of synapsid tracks from the Wingate and Moenave formations, Colorado Plateau region. Mus North Arizon Bull 60:271–273

Schwimmer DR (2002) King of the crocodylians: the paleobiology of *Deinosuchus*. Indiana University Press, Bloomington

Schwimmer DR, Stewart JD, Williams GD (1997) Scavenging by sharks of the genus Squalicorax in the Late Cretaceous of North America. PALAIOS 12:71–83

Secord R, Gingerich PD, Bloch JI (2002) *Mylanodon rosei*, a new metacheiromyid (Mammalia, Palaeanodonta) from the late Tiffinian (late Paleocene) of northwestern Wyoming. Contrib Mus Paleontol Univ Mich 30(15):385–399

Seilacher A (1964) Biogenic sedimentary structures. In: Imbrie J, Newell N (eds) Approaches to paleoecology. Wiley, New York, pp 296–316

Seilacher A, Marshall C, Skinner HCW, Tsuihiji T (2001) A fresh look at sideritic "coprolites". Paleobiology 27:7–13

Sherlock RL (1948) The Permo-Triassic formations. Hutchinson's Scientific and Technical Publ, London

Shubin NH, Daeschle EB, Coates MI (2004) The early evolution of the tetrapod humerus. Science 304:90–93

Silva RC, Ferigolo J, Carvalho IS, Fernandes ACS (2008a) Lacertoid footprints from the Upper Triassic (Santa Maria Formation) of Southern Brazil. Palaeogeogr Palaeoclimatol Palaeoecol 262:140–156

Silva RC, Carvalho IS, Fernandes ACS, Ferigolo J (2008b) Pegadas teromorfóides do Triássico Superior (Formação Santa Maria) do Sul do Brasil. Rev Brasileira Geoci 38:98–113

Silva RC, Carvalho IS, Fernandes ACS (2008c) Pegadas de dinossauros do Triássico (Formação Santa Maria) do Brasil. Ameghiniana 45:783–790

Silva RC, Barboni R, Dutra T, Godoy MM, Binotto RB (2012) Footprints of large theropod dinosaurs and implications on the age of Triassic biotas from southern Brazil. J South Am Earth Sci 39:16–23

Sims DW, Andrews PLR, Young JZ (2000) Fish behaviour: stomach rinsing in rays. Nature 404:566

Smith RMH (1987) Helical burrow casts of therapsid origin from the Beaufort Group (Permian) of South Africa. Paleogeogr Palaeoclimatol Palaeoecol 60:155–170

Sohn IG, Chatterjee S (1979) Freshwater ostracodes from Late Triassic coprolite in central India. J Paleontol 53:578–586

Spielmann JA, Lucas SG, Hunt AP, Heckert AB (2006) Reinterpretation of the holotype of *Malerisaurus langstoni*, a diapsid reptile from the Upper Triassic Chinle Group of West Texas. New Mex Mus Nal Hist Sci Bull 37:543–547

Staines HRE, Woods J (1964) Recent discovery of Triassic dinosaur footprints in Queensland. Aust J Sci 27:55

Storrs GW (1994) Fossil vertebrate faunas of the British Rhaetian (latest Triassic). Zool J Linnaean Soc 112:217–259

Stringer GL, King L (2012) Late Eocene shark coprolites from the Yazoo Clay in northeastern Louisiana. New Mex Mus Nat Hist Sci Bull 57:275–309

Stuart C, Stuart T (2000) A field guide to the tracks and signs of Southern and East African wildlife. Struick Nature (Random House Struick), Cape Town

Suazo T, Cantrell A, Lucas SG, Spielmann JA, Hunt AP (2012) Coprolites across the Cretaceous/Tertiary boundary, San Juan basin, New Mexico. New Mex Mus Nat Hist Sci Bull 57:263–274

Sues H-D, Olsen PE (2015) Stratigraphic and temporal context and faunal diversity of Permian-Jurassic continental tetrapod assemblages from the Fundy rift basin, eastern Canada. Atl Geol 51:139–205

Sues HD, Olsen PE, Carter JG, Scott DM (2003) A new crocodylomorph archosaur from the Upper Triassic of North Carolina. J Vert Paleontol 23(2):329–343

Sulej T, Bronowicz R, Talanda M, Niedzwiedzki G (2011 for 2010) A new dicynodont-archosaur assemblage from the Late Triassic (Carnian) of Poland Earth Env Sci Trans R Soc Edinburgh 101:261–269

Sulej T, Wolniewicz A, Bonde N, Błażejowski B, Niedźwiedzki G, Tałanda M (2014) New perspectives on the Late Triassic vertebrates of East Greenland: preliminary results of a Polish-Danish palaeontological expedition. Polish Polar Res 35:541–552

Sullivan RM (1987) A reassessment of reptilian diversity across the Cretaceous-Tertiary boundary. Contrib Sci Nat Hist Mus Los Angeles Count 391:1–26

Sumner D (1991) Palaeobiology, taphonomy and diagenesis of a Lower Carboniferous fish fauna. Dissertation, University of St. Andrews

Swift A, Duffin CJ (1999) Trace fossils. In: Swift A, Martill DM (eds) Fossils of the Rhaetian Penarth Group. Palaeontological Association Field Guides to Fossils 9: 239–250

Szajna MJ, Hartline BW (2003) A new vertebrate footprint locality from the Late Triassic Passaic Formation near Birdsboro, Pennsylvania. In: Le Tourneau PM, Olsen PE (eds) The great rift valleys of Pangaea in eastern North America, vol 2. Columbia University Press, New York, pp 264–272

Szajna MJ, Silvestri SM (1996) A new occurrence of the ichnogenus *Brachychirotherium*: implications for the Triassic-Jurassic mass extinction event. In: Morales M (ed) The continental Jurassic. Mus N Arizona Bull 60:275–283

Tałanda M, Dzięcioł S, Sulej T, Niedźwiedzki G (2011) Vertebrate burrow system from the Upper Triassic of Poland. PALAIOS 26(2):99–105

Tanke DH, Currie PJ (1998) Head-biting behavior in theropod dinosaurs: paleopathological evidence. Gaia 15:167–184

Tanke DH, Rothschild BM (2002) Dinosores: an annotated bibliography of dinosaur paleopathology and related topics, 1838–2001. New Mex Mus Natl Hist Sci Bull 20:1–96

Tanner LH (2017) Climates of the Late Triassic: perspectives, proxies and problems. In: Tanner LH (ed) The Late Triassic world: earth in a time of transition. Topics in geobiology. Springer, New York (this volume)

Tanner LH, Lucas SG (2007) Origin of sandstone casts in the Upper Triassic Zuni Mountains Formation, Chinle Group, Fort Wingate, New Mexico. New Mex Mus Nat Hist Sci Bull 40:209–214

Tanner LH, Lucas SG (2009) Tetrapod trace fossils from lowermost Jurassic strata of the Moenave Formation, northern Arizona, USA. Volum Jurass 6:133–141

Tapanila L, Roberts EM (2012) The earliest evidence of holometabolan insect pupation in conifer wood. PLoS One 7(2):e31668

Tapanila L, Roberts EM, Bouare ML, Sissoko F, O'Leary MA (2004) Bivalve borings in phosphatic coprolites and bone, Cretaceous–Paleogene, northeastern Mali. PALAIOS 19(6):565–573

Taylor MA (1993) Stomach stones for feeding or buoyancy? The occurrence and function of gastroliths in marine tetrapods. Philos Trans R Soc Lond Ser B Biol Sci 341(1296):163–175

Thulborn RA (1990) Dinosaur tracks. Chapman and Hall, London

Thulborn T (1998) Australia's earliest theropods: footprint evidence in the Ipswich Coal Measures (Upper Triassic) of Queensland. Gaia 15:301–311

Trewin NH (1986) Palaeoecology and sedimentology of the Achanarras fish bed of the Middle Old Red Sandstone, Scotland. Trans Roy Soc Edinburgh Earth Sci 77:21–46

Tweet JS, Santucci VL, Hunt AP (2012) An inventory of packrat (*Neotoma* spp.) middens in National Park Service areas. New Mex Mus Nat Hist Sci Bull 57:355–368

Vallon LR (2012) Digestichnia (Vialov, 1972)—an almost forgotten ethological class for trace fossils. New Mex Mus Nat Hist Sci Bull 57:131–135

Varricchio DJ (2001) Gut contents from a Cretaceous tyrannosaurid: implications for theropod dinosaur digestive tracts. J Paleontol 75(2):401–406
Varricchio DJ, Jackson F, Trueman C (1999) A nesting trace with eggs for the Cretaceous theropod dinosaur *Troodon formosus*. J Vert Paleontol 19:91–100
Vasileiadou K, Hooker JJ, Collinson ME (2007) Taphonomic evidence of a Paleogene mammalian predator–prey interaction. Palaeogeogr Palaeoclimatol Palaeoecol 243(1):1–22
Vasse D, Hua S (1998) Diversité des crocodiliens du Crétace Supérieur et du Paléogene: Influences et limites de la crise Maastrichtien-Paléocéne et des "Terminal Eocene Events". Oryctos 1:65–77
Vega-Dias C, Maisch MW, Schultz CI (2004) A new phylogenetic analysis of Triassic dicynodonts (Therapsida) and the systematic position of Jachaleria candelariensis from the Upper Triassic of Brazil. Neues Jahr Geol Pälontol Abhand 231:145–162
Vijaya, Prasad GVR, Singh K (2009) Late Triassic palynoflora from the Pranhita–Godavari Valley, India: evidence from vertebrate coprolites. Alcheringa 33:91–111
von Huene F (1932) Die fossile Reptil-Ordnung Saurischia, ihre Entwicklung und Geschichte. Monogr Geol Paläontol 1(4):1–361
von Huene F (1941) Die Tetrapoden-Fährten im toskanischen Verrucano und ihre Bedeutung. N Jahrb Geol Paläontol Ser B 86:1–34
von Nopcsa F (1902) Über das Vorkommen der Dinosaurier von Szentpéterfalva. Zeit Deutsch Geolog Gesell 54:34–39
von Nopcsa F (1923) Die Familien der Reptilien. Fortschr Geol Paläontol 2:1–210
Voorhies MR (1975) Vertebrate burrows. In: Frey RW (ed) The study of trace fossils: a synthesis of principles, problems, and procedures in ichnology. Springer, New York, pp 325–350
Wahl AM, Martin AJM, Hasiotis ST (1998) Vertebrate coprolites and coprophagy traces, Chinle Formation (Late Triassic), Petrified Forest National Park, Arizona. National Park Service Paleontological Research, Technical Report NPS/NRGRD/GRDTR–98/01 (Eds VL Santucci & L. McClelland). National Park Service, Geological Resources Division, Lakewood, CO, pp 144–148
Walker MV (1938) Evidence of Triassic insects in the Petrified Forest National Monument, Arizona. Proc U S Nat Mus 85:137–141
Warren AA, Hutchinson MN (1987) The skeleton of a new hornless rhytidosteid (Amphibia, Temnospondyli). Alcheringa 11(4):291–302
Watson DMS (1960) The anomodont skeleton. Trans Zool Soc Lond 29:131–208
Webb GJW, Manolis SC (1983) *Crocodylus johnstoni* in the McKinlay River area N. T. V.: abnormalities and injuries. Aust Wildlife Res 10:407–420
Weber DJ, Lawler GC, (1978) Lipid components of the coprolites. In: Ash S (ed) Geology, paleontology and paleoecology of a Late Triassic lake, western New Mexico. Brigham Young Univ Geol Stud 25:75–87
Weems RE (1980) An unusual newly discovered archosaur from the Upper Triassic of Virginia, USA. Trans Am Phil Soc 70:1–53
Weems RE (2003) *Plateosaurus* foot structure suggests a single trackmaker for *Eubrontes* and *Gigandipus* footprints. In: LeTourneau PM, Olsen PE (eds) The great rift valleys of Pangea in eastern North America, vol 2. Columbia University Press, New York, pp 293–313
Weems RE, Culp MJ, Wings O (2007) Evidence for prosauropod dinosaur gastroliths in the Bull Run Formation (Upper Triassic, Norian) of Virginia. Ichnos 14(3–4):271–295
Weems RE, Tanner LH, Lucas SG (2016) Synthesis and revision of the lithostratigraphic groups and formations in the upper Permian?-Lower Jurassic Newark Supergroup of eastern North America. Stratigraphy 13:111–153
Weigelt J (1927) Recent vertebrate carcasses and their paleobiological implications. University of Chicago Press, Chicago
Westaway C, Thompson JC, Wood WB, Njau J (2011) Crocodile ecology and the taphonomy of early Australasian sites. Environ Archaeol 16:124–136

Whittle CH, Everhart MJ (2000) Apparent and implied evolutionary trends in lithophagic vertebrates from New Mexico and elsewhere. New Mex Mus Nat Hist Sci Bull 17:75–82
Wieland GR (1906) Dinosaurian gastroliths. Science 23(595):819–821
Williams ME (1972) The origin of "spiral coprolites". Univ Kansas Palaeont Contrib 59:1–19
Wilson MVH (1987) Predation as a source of fish fossils in Eocene lake sediments. PALAIOS 2:497–504
Wing SL, Sues H-D (1992) Mesozoic and early Cenozoic terrestrial ecosystems. In: Behrensmeyer AK, Damuth JD, DiMichele WA, Potts R, Sues H-D, Wing SL (eds) Terrestrial ecosystems through time. University of Chicago Press, Chicago, pp 327–416
Wings O (2004) Identification, distribution, and function of gastroliths in dinosaurs and extant birds with emphasis on ostriches (*Struthio camelus*). Dissertation, University of Bonn
Wings O (2007) A review of gastrolith function with implications for fossil vertebrates and a revised classification. Acta Palaeontol Polon 52:1–16
Xing LD, Klein H, Lockley MG, Chen W, Ye Y, Matsukawa M, Zhang JP (2013) Earliest records from China of theropod and mammal–like tetrapod footprints in the Late Triassic of Sichuan Basin. Vert PalasiAtica 51(3):184–198
Xing LD, Klein H, Lockley MG, Kan Z, Zhang J, Peng G, Ye Y (2014a) First chirothere and possible grallatorid footprint assemblage from the Upper Triassic Baoding Formation of Sichuan Province, southwestern China. Palaeogeogr Palaeoclimatol Palaeoecol 412:169
Xing LD, Peng GZ, Marty D, Ye Y, Klein H, Li JJ, Gierliński GD, Shu CK (2014b) An unusual trackway of a possibly bipedal archosaur from the Late Triassic of the Sichuan Basin, China. Acta Palaeontol Pol 59(4):863–871
Xu X (1997) A new psittacosaur (*Psittacosaurus mazongshanensis*, sp. nov.) from Mazongshan Area, Gansu Province, China. In: Dong Z (ed) Sino-Japanese Silk Road dinosaur expedition. China Ocean Press, Beijing, pp 48–67
Young CC (1964) New fossil crocodiles from China. Vert Palasiatica 8:190–208
Zammit M, Kear BJ (2011) Healed bite marks on a Cretaceous ichthyosaur. Acta Palaeontol Polon 56:859–863
Zangerl R, Richardson ES (1963) The paleoecological history of two Pennsylvanian black shales. Fieldiana Geol Mem 4:1–352
Zasadil B, Mikuláš R (2004) A probable fossil bird nest, ?*Eocavum* isp., from the Miocene wood of the Czech Republic. In: Abstract book 4th international bioerosion workshop. Prague. Institute of Geology, Academy of Sciences of the Czech Republic, pp 49–51
Zatoń M, Niedźwiedzki G, Marynowski L, Benzerara K, Pott C, Cosmidis J, Krzykawski T, Filipiak P (2015) Coprolites of Late Triassic carnivorous vertebrates from Poland: an integrative approach. Palaeogeogr Palaeoclimatol Palaeoecol 430:21–46

Chapter 13
Flora of the Late Triassic

Evelyn Kustatscher, Sidney R. Ash, Eugeny Karasev, Christian Pott, Vivi Vajda, Jianxin Yu, and Stephen McLoughlin

Abstract The Triassic was a time of diversification of the global floras following the mass-extinction event at the close of the Permian, with floras of low-diversity and somewhat uniform aspect in the Early Triassic developing into complex vegetation by the Late Triassic. The Earth experienced generally hothouse conditions with low equator-to-pole temperature gradients through the Late Triassic. This was also the time of peak amalgamation of the continents to form Pangea. Consequently, many plant families and genera were widely distributed in the Late Triassic. Nevertheless,

E. Kustatscher (✉)
Museum of Nature South Tyrol, Bindergasse 1, 39100 Bozen/Bolzano, Italy

Department für Geo– und Umweltwissenschaften, Paläontologie und Geobiologie, Ludwig–Maximilians–Universität, and Bayerische Staatssammlung für Paläontologie und Geologie, Richard–Wagner–Straße 10, 80333 Munich, Germany
e-mail: Evelyn.Kustatscher@naturmuseum.it

S.R. Ash
Department of Earth and Planetary Sciences, Northrop Hall, University of New Mexico, Albuquerque, NM 87131, USA
e-mail: sidash@aol.com

E. Karasev
Borissiak Paleontological Institute, Russian Academy of Sciences, Profsoyuznaya 123, Moscow 117647, Russia
e-mail: karasev@paleo.ru

C. Pott
Palaeobiology Department, Swedish Museum of Natural History, P.O. Box 50007, SE-104 05 Stockholm, Sweden

LWL-Museum of Natural History, Westphalian State Museum and Planetarium, Sentruper Straße 285, 48161 Münster, Germany
e-mail: christian.pott@lwl.org

V. Vajda • S. McLoughlin
Palaeobiology Department, Swedish Museum of Natural History, P.O. Box 50007, SE-104 05 Stockholm, Sweden
e-mail: Vivi.Vajda@nrm.se; steve.mcloughlin@nrm.se

J. Yu
State Key Laboratory of Biogeology and Environmental Geology, China University of Geosciences, Wuhan, P.O. Box 430074, P.R. China
e-mail: yujianxin@cug.edu.cn

© Springer International Publishing AG 2018

L.H. Tanner (ed.), *The Late Triassic World*, Topics in Geobiology 46,
https://doi.org/10.1007/978-3-319-68009-5_13

two major floristic provinces are recognizable during this interval—one in the Southern Hemisphere (Gondwana) and another in the Northern Hemisphere (Laurussia); these being largely separated by the Tethys Ocean and a palaeotropical arid belt. Regional variations in topography, climate and light regime imposed further constraints on the distribution of plant groups in the Late Triassic such that two floristic sub-provinces are recognizable within Gondwana, and nine within Laurussia based on the plant macrofossil and dispersed spore-pollen records. In a broad sense, the Late Triassic saw the diversification of several plant groups that would become important components of younger Mesozoic floras (e.g., Bennettitales, Czekanowskiales, Gnetales and several modern fern and conifer families). The representation of these groups varied not only geographically, but waxed and waned through time in response to climatic pulses, such as the Carnian Pluvial Event. Significant turnovers are apparent in both macrofossil- and palyno-floras across the Triassic–Jurassic boundary, especially in the North Atlantic and Gondwanan regions. The geographic and temporal variations in the floras have necessitated the establishment of numerous regional palynozonation schemes that are tentatively correlated in this study. Major plant macrofossil assemblages of the Late Triassic world are also placed in a stratigraphic context for the first time. The Late Triassic floras also record the re-diversification of insect faunas based on a broad array of damage types preserved on leaves and wood. By the Late Triassic, all modern terrestrial arthropod functional feeding groups were established, and several very specialized feeding traits and egg-laying strategies had developed. Although age constraints on various fossil assemblages need to be improved, this study provides the first global overview of the temporal and geographic distributions of Late Triassic floras, and establishes a basis for future targeted research on Triassic phytogeography and phytostratigraphy.

Keywords Non-marine ecosystems • Palaeoclimate • Plant fossils • Palynomorphs • Palaeo-provinces • Mass-extinction • Plant-animal interactions

13.1 Introduction

The Triassic, spanning the interval from 252 to 201 million years (Myr) ago, was a crucial period in the evolution of non-marine ecosystems. It witnessed the recovery of terrestrial ecosystems following the end-Permian mass extinction and saw a proliferation of new fern and gymnosperm families and genera that peaked in the Late Triassic before another global biotic crisis at the end of the period (Anderson et al. 1999; Willis and McElwain 2002; Vajda and Bercovici 2014). The continents reached their maximum phase of amalgamation, forming the supercontinent Pangaea (Fig. 13.1), which began to break up towards the end of the Triassic when rifting started in the North Atlantic region. The continued northward drift of the Cimmerian continental blocks progressively closed the Palaeotethys Ocean and opened the Neotethys Ocean at this time. The most significant Late Triassic convergent event, the Indosinian orogeny, occurred as a result of the consolidation of the South China and North China blocks, and the opening of the so-called

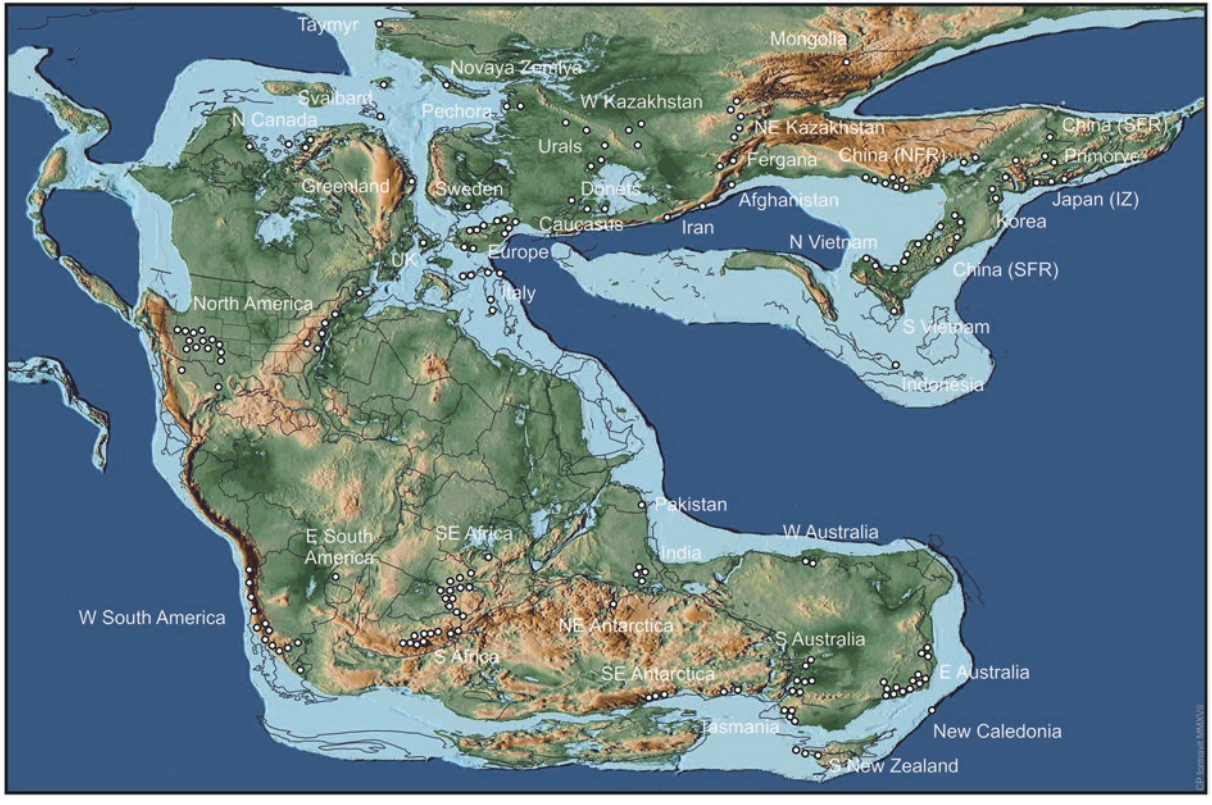

Fig. 13.1 Palaeogeographic world map showing the distribution of major Upper Triassic plant assemblages. Base map: PALEOMAP Project, C. R. Scotese, Arlington, Texas, USA

Mongol-Okhotsk Ocean (Golonka 2007). The climate was warm with no polar ice-caps, although the variation in photoperiod regime imposed some latitudinal constraints on the composition of vegetation belts, and the equable conditions were interrupted by several global and regional climate perturbations (Preto et al. 2010 and references therein). Moreover, the Triassic in general was a period of exceptional sea-level lowstand in comparison with the Palaeozoic.

The Triassic is delineated by two of the five major mass extinctions in Earth history, the end-Permian Event (EPE) and the end-Triassic Event (ETE), owing to which the Triassic flora differs markedly from preceding and succeeding floras. Thus, it was a time of transition and of great changes in the composition of the global flora although our understanding of this transformation of plant communities is challenged by the scattered palaeontological record.

Past phytogeographic studies of the Triassic have used a diverse range of terms to denote floristic regions. In this chapter, we aim to rationalize the nomenclature applied to these regions and better define the relationships between areas based on shared taxa. We apply the term 'assemblage' to a suite of fossils derived from a particular bed. Thus, several assemblages constitute a local 'flora', multiple floras from related areas comprise a floristic 'subprovince', and two or more subprovinces make up a floristic 'province', the last of these categories being of continental or pancontinental scale. Available space constrains us from documenting the finer details of every studied Triassic flora. Nevertheless, we provide the first summary of the succession of Late Triassic plant assemblages globally (Tables 13.1 and 13.2) in order to elucidate phytostratigraphic patterns that might be related to variations in palaeoclimate and/or evolutionary processes. Although this contribution focuses on the macrofloral record, brief details on the complementary dispersed spore-pollen successions are also included because palynology provides the basis for the biostratigraphical framework of many of the continental successions. Pollen and spores also provide insights into the vegetation and climatic signals owing to their abundant presence in near-shore marine successions. This review is a first step towards a better understanding of the composition and distribution of the Late Triassic floras through time.

13.2 Late Triassic Floras of North America

Late Triassic plant fossils occur in five widely separated parts of North America: in a string of narrow rift basins along the eastern seaboard of the United States, adjacent parts of Canada, the desert southwest of the United States and on some of the Arctic islands of Canada and in northwestern and northeastern Mexico (Figs. 13.1 and 13.2, Table 13.1). The known floras are restricted to the Carnian and early Norian stages, whereas Rhaetian floral assemblages are unknown in North America. Since the Late Triassic flora of Greenland is more closely related palaeogeographically to the Late Triassic floras of northern Europe, it is discussed within the European section of this chapter, whereas the floras of the Canadian Arctic are discussed here. The nomenclature of the Upper Triassic strata in eastern North America that is used here follows that recently proposed by Weems, et al., 2016 and approved by the U.S. Geological Survey.

Table 13.1 Stratigraphic distribution of selected Triassic units hosting plant macrofossil assemblages according to the major phytogeographic subprovinces recognized in this study

Age Ma		Chinle/Dockum - Newark Subprov.	Arctic Canada - N. Atlantic - C. Europe	Western Tethyan Subprovince	Siberian - Middle Asian Subprovince	Northern E. Asian Subprov.	Southern E. Asian Subprov.	Ipswich Flora (south Gondwana)	Onslow Flora (north Gondwana)
LATE TRIASSIC	201.3 ±0.2		Bjuv Mbr Kap Stewart Grp Schilfsandstein fl.		Central Pamir & Afghanistan floras		Yangbaichong Fm Sanqiutian Fm	Raceview Fm Aberdare Cgl	Parsora Fm
	Rhaetian		Vallåkra Mbr Tatra Mts flora Seinstedt flora Bayreuth flora east-central		Nayband Fm Novorayskaya Fm Aktash and Tashkutan fms	Dongfeng flora	Wenbinshan flora Tonkin flora	Callide C.M.	La Ternera & El Puquen floras
	c. 208.5		Axel Heiberg Island flora Ørsted Dal Mbr		Aghdarband flora				Los Colorados Fm
	Norian		Sverdrup Basin fl. Seefeld flora Upper Silesian flora	Giffoni & Filettino floras	Protopivskaya Fm Nemtsov Fm Kozyrevskaya Fm	Malugou Fm Primorye floras Amba Fm	Dakeng Fm Badong Fm Nariwa flora Anyuan Fm Daqing Fm	Leigh Creek C.M. (Telford Basin)	Tiki Fm McKelvey Mbr (Flagstone Bench Fm)
		Dockum Grp flora Chinle Fm flora	Flatsalen Fm				Hsuchiaho Fm		Cacheuta Fm
	c. 227	Lockatong Fm flora				Imalinovo flora		Tarong C.M. Lashly, Falla, Section Peak fms	
		Santa Clara Fm fl. Stockton Fm flora	De Geerdalen Fm Lunz flora Neuewelt flora	Bergamasc Alps flora Monte Pora, Dogna & Raibl floras	Chelyabinsk Basin flora Nikolaevka flora		Momonoki and Aso fms	Blackstone Fm Red Cliff C.M.	Ischigualasto Fm Quilacoya Mbr Santa Maria Fm
	Carnian	Doswell Fm flora	Krasiejów flora	Karavanke Mts Heiligkreuz Fm Rio del Lago Fm	western and eastern Urals floras	Sad-Gorod Fm	Indonesian floras Daqiaodi Fm Jiuligang Fm Jiapeila Fm	Brady Fm Molteno Fm Tivoli Fm	Potrerillos Fm Cortaderita Fm Barreal Fm El Tranquilo Grp
	c. 237				Madygen flora				

Table 13.2 Tentative correlation of selected Late Triassic palynozonation schemes erected within the major phytogeographic subprovinces recognized in this study

Data sourced from numerous studies: Chinle/Dockum–Newark subprovinces (Cornet 1977a; Litwin et al. 1991; Reichgelt et al. 2013); Arctic Canada–North Atlantic/Central European subprovinces (Lund 1977; Kürschner and Herngreen 2010; Vigran et al. 2014; Paterson and Mangerud 2015); Western Tethyan Subprovince (Roghi et al. 2010); Siberian–Middle Asian subprovinces (Odintsova 1977; Romanovskaya and Vasilieva 1990; Ghavidel-Syooki et al. 2015); Northern East Asian Subprovince (Peng et al. 2017b); Southern East Asian Subprovince (Wang et al. 2010); South Gondwana (Helby et al. 1987; de Jersey and Raine 1990); North Gondwana (Helby et al. 1987; Tripathi et al. 2005)

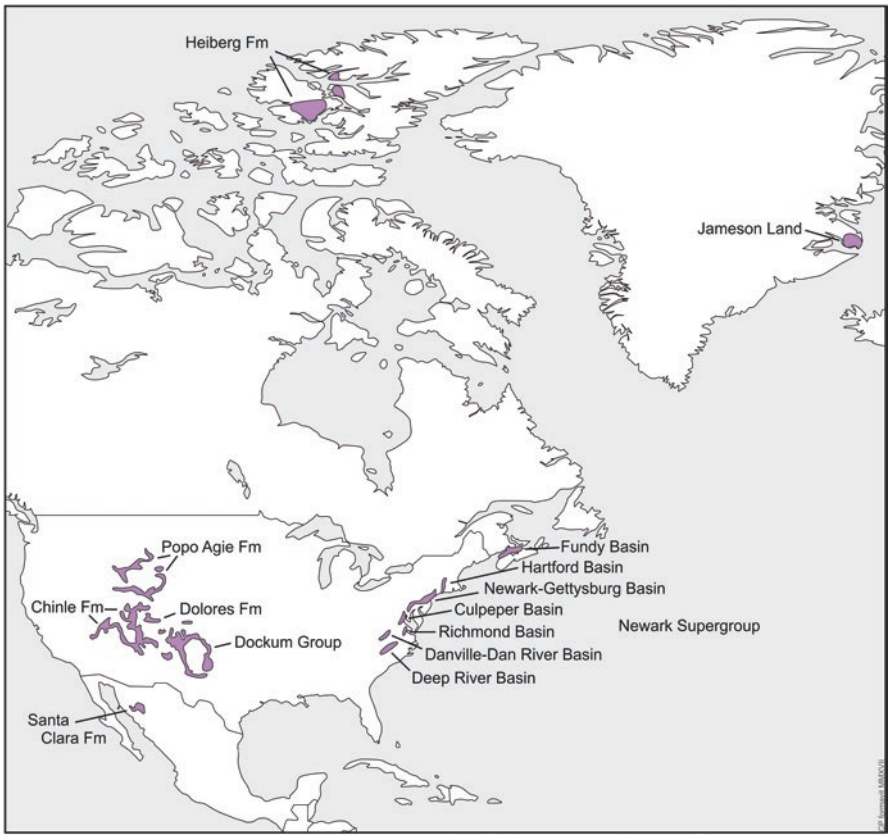

Fig. 13.2 Areas with major Upper Triassic plant assemblages in Arctic Canada, the US and northern Mexico

13.2.1 Carnian Floras of North America

The Carnian floras of North America occur in the basal coal-bearing Doswell Formation of the Newark Supergroup in the Richmond rift basin in Virginia, in a clay quarry excavated into the Stockton Formation in the Chatham Basin of North Carolina and in the Gettysburg Basin in Pennsylvania (Wanner and Fontaine, in Ward 1900). The plant fossils associated with the coal deposits in the Doswell Formation soon began to attract attention after they were first reported by William MacClure (1817). However, the fossils were not systematically investigated until William Fontaine began his work on them in the early 1880s. Subsequently, he (Fontaine 1883) described 18 genera in the Doswell flora including several ferns (*Acrostichides, Lonchopteris* [*Cynepteris*], *Mertensides*), conifers (*Cheirolepis*), bennettitaleans (*Ctenophyllum*, *Pterophyllum*, *Sphenozamites*) and ginkgophytes (*Baiera*).

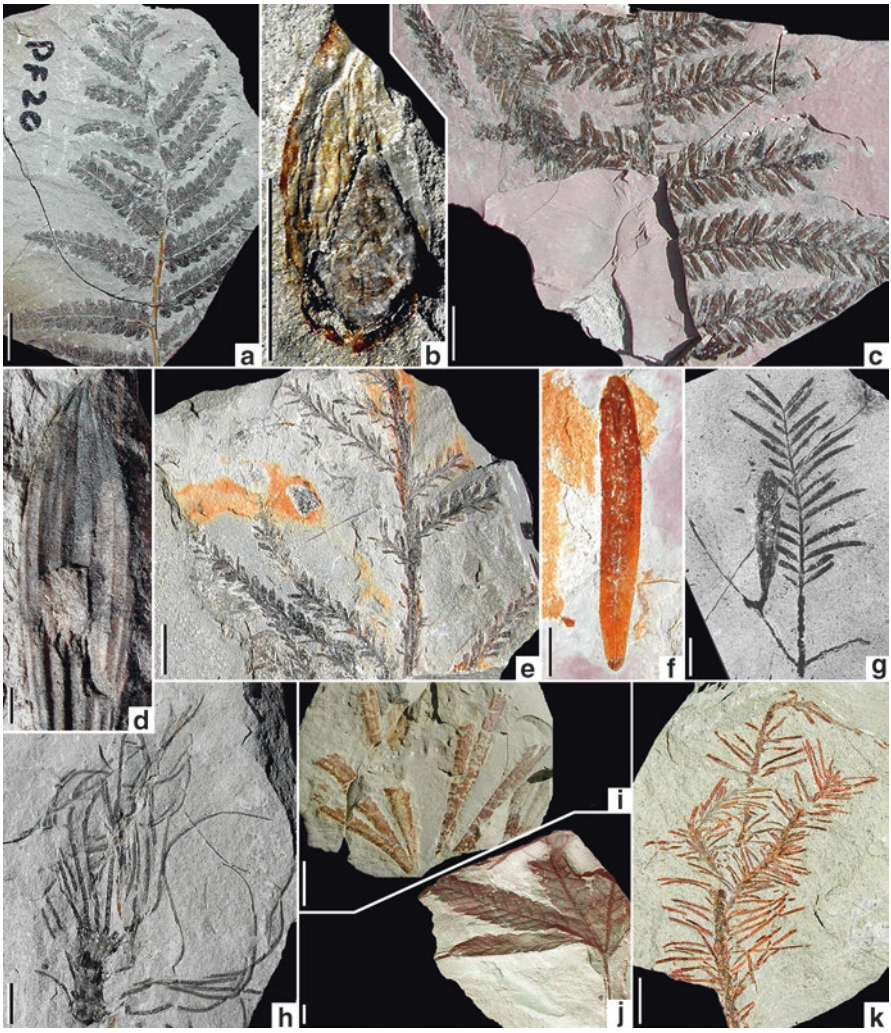

Plate 13.1 Upper Triassic plants from North America. (**a**) *Cynepteris lasiophora*, Petrified Forest National Park, Arizona, Norian. (**b**) *Samaropsis* sp., Fort Wingate, New Mexico, Norian. (**c**) *Sanmiguelia lewisii*, Petrified Forest National Park, Arizona, Norian. (**d**) *Palodurophyton quanahensis*, Palo Duro Canyon, Texas, Norian. (**e**) *Pagiophyllum* sp., Fort Wingate, New Mexico, Norian. (**f**) *Fraxinopsis patharrisiae*, Palo Duro Canyon, Texas, Norian. (**g**) *Neocalamites* sp., Petrified Forest National Park, Arizona, Norian. (**h**) *Ginkgoites watsoniae*, Petrified Forest National Park, Arizona, Norian. (**i**) *Clathropteris walkerii*, Petrified Forest National Park, Arizona, Norian. (**j**) *Dechellyia gormanii*, Canyon de Chelly, Arizona, Norian. (**k**) *Dinophyton spinosus*, Petrified Forest National Park, Arizona, Norian. Scale bar = 10 mm in each image

In contrast to the plant assemblage preserved in the underlying Doswell Formation, the Stockton flora is not associated with coal deposits although cuticles are preserved on some specimens. The flora that occurs in the Stockton Formation was discovered in the Gettysburg Basin, Pennsylvania in the late nineteenth century and first described by Wanner and Fontaine (in Ward 1900). Much later additional Carnian-age plant assemblages were collected from the same rift basin by several workers including Wilhelm Bock (1969), Bruce Cornet (1977b) and Brian Axsmith (1989). Most of the taxa these workers found commonly occur in the Newark Supergroup at other localities and included the conifers *Cheirolepis, Glyptolepis, Pagiophyllum, Palissya* and *Podozamites*, the cycads/bennettitaleans Cycadospadix, Eoginkgoites, Nilssonia and Zamites, and the enigmatic gymnosperm *Dinophyton* (Plate 13.1k). A new era in the study of the Carnian flora really began when a report on the plant fossils in the Stockton Formation in the Chatham Basin was published by Hope and Patterson in 1969. Other workers who soon joined Hope in the study of this flora were Ted Delevoryas (Delevoryas and Hope 1971, 1975, 1981, 1987), Brian Axsmith and Tom Taylor (see Axsmith et al. 1995 for more details). An unpublished review of the Stockton flora from the Chatham Basin (Mickle et al. 2000) lists 25 taxa. Since then, two additional genera have been described (Axsmith et al. 2001; Pott and Axsmith 2015) so that the known diversity of the assemblage now includes 27 genera, eight of which seem to be restricted to that deposit (e.g., *Leptocycas*, *Metridiostrobus, Pekinopteris*), the rest are relatively common in other Upper Triassic floras.

It is currently uncertain exactly how many genera are present in the Carnian successions of the Richmond, Chatham and Gettysburg basins, since Fontaine's and Wanner's identifications have never been critically re-evaluated. However, a quick comparison between the fossil lists in each plant assemblage suggests that nearly all of the genera in the Doswell Formation also occur in the overlying Stockton Formation, so it is probable that the Carnian flora of the Newark Supergroup consists of about 30 genera. Sphenophytes (*Equisetites*, *Neocalamites*) and ferns (*Clathropteris*, *Danaeopsis*, *Lonchopteris* [= *Cynepteris*], *Mertensides*, *Pekinopteris*, *Phlebopteris*) are particularly well represented in the flora, whereas the cycads/bennettitaleans (*Cycadospadix*, *Leptocycas*, *Otozamites*, *Williamsonia*, *Zamites*) and conifers (*Compsostrobus*, *Metridiostrobus*, *Pagiophyllum*, *Voltzia*) are abundant. Collectively, the Carnian flora of North America appears to closely resemble the succeeding Norian flora of that continent.

The age of the plant fossils found in the Santa Clara Formation in Sonora (northwestern Mexico) is somewhat uncertain, ranging as it does from ?Carnian to Norian (see Weber 1995, 1996, 1999). Most of the fossil plants are typical Late Triassic sphenophytes (*Equisetites, Neocalamites*), ferns (*Asterotheca*), cycads/bennettitaleans (*Laurozamites*, *Pterophyllum*, *Ctenophyllum*), ginkgophytes and conifers. Some additional plants in this flora are of uncertain relationship, such as *Marcouia*, or putative angiosperm precursors, such as *Scoresbya* and *Sonoraphyllum*.

The palynoflora in the Carnian succession in the Chatham Basin in the eastern United States is rich and well preserved (e.g., Schultz and Hope 1973; Cornet 1977a; Dunay and Fisher, 1979; Fisher and Dunay 1984; Cornet and Olsen 1985; Traverse 1986; Litwin et al. 1991; Litwin and Ash 1993) and has been subdivided in two palynozones: the Chatham-Taylorsville palynofloral Zone and the overlying

New Oxford-Lockatong palynofloral Zone (Cornet 1977a; Cornet and Olsen 1985); in the Chinle Formation to the informal palynomorph zones I and II *sensu* Litwin et al. (1991). *Patinasporites densus* and *Vallasporites ignacii* dominate the Carnian palynofloras. The informal palynomorph zone I *sensu* Litwin et al. (1991) is characterized by abundant taeniate bisaccate taxa (Litwin et al. 1991). The Chatham-Taylorsville palynofloral Zone is characterized by the overlapping ranges of *Patinasporites densus*, *Striatoabieites aytugii*, *Triadispora verrucata*, *Protodiploxypinus doubingeri, Plicatisaccus badius* and *Lagenella martinii.* The informal palynomorph zone II includes the more diverse and abundant palynological assemblages, and is characterized by the FOs (first occurrences) of *Camerosporites rudis*, *Enzonalasporites vigens*, *Heliosaccus dimorphus*, *Ovalipollis ovalis*, *Pseudoenzonalasporites summus* and other taxa (e.g., *Alisporites* spp., *Cycadopites stonei*, *Guthoerlisporites cancellosus*). The coeval New Oxford-Lockatong palynoflora Zone is dominated by *Patinasporites densus*, *Vallisporites ignacii*, *Alisporites parvus* and *Triadispora* spp. Most of the palynomorphs correlate with taxa in Carnian assemblages in Western Europe and Australia (Litwin et al. 1991).

13.2.2 Norian Floras of North America

Plant macrofossils of Norian age occur in the lower part of the Newark Supergroup in both the Chatham and Danville rift basins along the eastern seaboard of the United States as well as in the lower part of the Chinle-Dockum beds in the desert southwest of the United States. They were first described from what is now called the Passaic Formation in the Chatham rift basin by Ebenezer Emmons (1856, 1857) who reported that they came from coal prospects "…many hundreds of feet…" above the coal-bearing strata in the Carnian Doswell Formation from which Fontaine was to later (1883) make his collections. Eventually, Fontaine (in Ward 1900) redescribed Emmons' collection and reported that the Passaic flora includes 24 genera including sphenophytes (*Equisetites*), ferns (*Laccopteris* [=*Phlebopteris*], *Lonchopteris* [=*Cynepteris*], *Pseudodaneosis*, *Sphenopteris*), conifers (*Abietites*, *Cephalotaxopsis*, *Pagiophyllum*; Plate 13.1e), cycads/bennettitaleans (*Anomozamites*, *Ctenophyllum*, *Otozamites*) and ginkgophytes (*Baiera*).

Starting in the late 1970s, important collections of Norian plant fossils, insects and fish remains were described by Fraser et al. (1996) and Axsmith et al. (1997, 2013) from the Lockatong Formation in the Solite clay quarry in the Danville rift basin on the border between North Carolina and Virginia. A floral list published by Fraser et al. (1996) indicated that the Lockatong flora included about 30 genera (including at least 10 new taxa), such as sphenophytes (*Neocalamites*, Plate 13.1g), ferns (*Cynepteris*, *Dictyophyllum*, *Wingatea*), ginkgophytes (*Sphenobaiera,* Plate 13.1h, *Metreophyllum*), cycads/bennettitaleans (*Otozamites*, *Pterophyllum*, *Zamiostrobus*, *Zamites*), together with many conifers (*Cheirolepis*, *Palissya*, *Podozamites*) and several enigmatic forms (*Brunswickia*, *Dinophyton*, *Edenia*, *Fraxinopsis* Plate 13.1f, *Pannaulika*). Several (*Edenia*, *Pannaulika*) seem to occur only at this locality.

The Norian plant fossils that occur in the desert southwest of the United States occur principally in the lower one-third of the Chinle Formation (Shinarump and Blue Mesa Members) and the Dockum Group (Garita Creek and Trujillo formations: Chinle Group of some authors), although it is noted that the basal units of both the Chinle and Dockum are considered Carnian if the 'short' Norian time scale is accepted (cf. Lucas et al. 2012). The fossil assemblages, here referred to as the Chinle-Dockum flora, were not documented until 1941 when Lyman Daugherty (Daugherty 1941) described more than 40 genera based on compressed leaves, stems, and reproductive structures of lycophytes, sphenophytes, ferns, conifers and cycads/bennettitaleans that mostly came from the Chinle Formation in Petrified Forest National Park, Arizona. Since then elements of the Chinle-Dockum flora have been found at several dozen localities in northern Arizona, southern Utah, northern New Mexico and west Texas. Probably the most well-known of all these localities are still those in Petrified Forest National Park where literally hundreds, if not thousands of highly coloured silicified conifer (pycnoxylic) logs (up to 40 m in length and 2 m in diameter) are exposed on the surface of the desert (Ash 2005; Sadler et al. 2015). In addition, amber, charcoal, and burned logs have been found in the park, together with a rich palynoflora (Litwin and Ash 1991; Reichgelt et al. 2013).

Most genera in the Chinle-Dockum flora are represented by a single species; only the common form genera, such as C*ladophlebis* and *Pagiophyllum* (Plate 13.1e), seem to be represented by more than one species (Ash 1989). The components of this flora represent all major groups of vascular land plants except the angiosperms. Given the abundance of petrified conifer (pycnoxylic) logs found in the Chinle-Dockum beds, it is not especially surprising that about one-third of the compressed flora is coniferous (*Agathoxylon*, *Elatocladus*, *Pagiophyllum*, *Pelourdea*). The cycads/bennettitaleans are next in order of abundance with about 13 genera (*Nilssonia*, *Nilssoniopteris*, *Williamsonia*, *Weltrichia*, *Zamites*) followed by the ferns with about eight genera (*Clathropteris* Plate 13.1i, *Cynepteris* Plate 13.1a, *Phlebopteris*, *Todites*; Ash 1969, 1975; Ash et al. 1982). Although there are only five sphenophyte genera (*Neocalamites*, *Equisetites*, *Schizoneura*) in the flora, their remains, especially stem casts, are very common and more widely distributed than most other taxa in the flora suggesting generalist ecological niches in a wide range of habitats. Other plant groups, such as the ginkgophytes and gnetopsids are represented only by two to three genera each (*Ginkgoites* and *Dechellyia*; Plate 13.1j) and several seed plants were represented by dispersed seeds (Plate 13.1b) and cones (Plate 13.1d) of uncertain relationships.

Some of the plant macrofossils are so unusual and/or incomplete that they are difficult to classify with any assurance. One of the most contentious of these is *Sanmiguelia* (Plate 13.1c), a monopodial plant that was a little less than a metre tall and bore large, palm-like, pleated leaves on its non-woody stem. Apparently, it grew extensively along the shores of rivers and lakes throughout the desert southwest during the Norian and Rhaetian ages of the Late Triassic and during the Hettangian age of the Early Jurassic in southwestern Utah (Ash and Hasiotis 2013). Another genus that is difficult to classify is *Dechellyia*. It consists of a leafy shoot bearing long, narrow, opposite, decussate leaves and winged seeds with a narrowly elliptical wing that are borne in pairs at the ends of short stalks attached to the base of the main

rachis of the leaf. The opposite-decussate leaves and the characters of the associated pollen are shared with all extant Gnetales, whereas winged seeds are present only in *Welwitschia* (Crane 1985). Until more material is found, it will be impossible to determine the systematic relationships of these enigmatic plants. At present, the Chinle-Dockum plant assemblage includes approximately 60 well-defined genera incorporating about 70 species based on plant megafossils, i.e., compressed leaves, leafy shoots, and reproductive structures and permineralized axes (Ash 1989, and personal observations).

The Chinle-Dockum (Carnian-Norian) and the Newark (Carnian–Norian) floras share many genera and species. However, each flora also contains a few distinctive genera, such as *Dechellyia* and *Sanmiguelia* that occur only in the Chinle-Dockum flora, and *Edenia* and *Leptocycas* that are restricted to the Newark flora (Axsmith et al. 2013; Delevoryas and Hope 1971). The presence of *Fraxinopsis* in both the Chinle-Dockum and the Newark floras (Axsmith et al. 1997; Ash 2011) and *Schizoneura* in the Chinle-Dockum floras (Ash 1986) suggest that there was some floral interchange between North America, Europe and Gondwana during the Late Triassic or earlier. It appears that the Newark flora generally grew in a more humid climate than the Chinle flora, since minable coal deposits occur in the Carnian and the lower part of the Norian beds of the Newark Supergroup but not in the Chinle-Dockum beds. Furthermore, many of the leaves in the Newark Supergroup are much larger than those of the same genera in the Chinle-Dockum flora. This is particularly true for the ferns (e.g., *Clathropteris, Phleboteris*) and some of the bennettitaleans (e.g., *Sphenozamites*). Consequently, it appears that the climate was much more humid along what is now the eastern seaboard of North America. Although the climatic changes along the eastern seaboard of North America were due to continental drift, the changes in the desert southwest were probably caused by orogeny and elevation changes in eastern California (Nordt et al. 2015).

The Norian portion of the Newark Supergroup found in the rift basins along the eastern seaboard of North America contains a moderately diverse palynoflora (Cornet 1977a; Cornet and Olsen 1985; Litwin et al. 1991). The Norian is divided into two main palynozones, separated from the Carnian palynofloras by a transitional zone (Cornet 1977a; Weems et al. 2016), i.e., the Lower Passaic-Heidlersburg Zone and the Manassas-Upper Passaic Zone (Cornet and Olsen 1985). The former zone is distinguished by the presence of *Camerosporites verrucosus* together with abundant large and varied pollen grains including *Alisporites opii*, *Patinasporites densus*, *Vallasporites ignacii* and *Triadispora* spp. The Manassas-Upper Passai Zone is characterized by the first occurrence of *Corollina torosus* and *Granuloperculatispollis rudis* in combination with the ongoing presence of the previously appeared pollen (Cornet and Olsen 1985).

The Norian (and Rhaetian?) corresponds in the Chinle Formation to parts of the informal palynomorph zones II and III, divided by a transitional zone. The informal palynomorph zone III has lately been divided into two subzones, IIIa and IIIb (Reichgelt et al. 2013). The palynoflora of the Norian is generally rich and diverse with more than 100 species (Dunay and Traverse 1971; Fisher and Dunay 1984; Litwin et al. 1991; Lucas et al. 2012). Zone II has a high diversity but low spore

abundance, high dominance of bisaccates and with *Cordaitina minor*, *Protodiploxypinus* spp. and *Angustisaccus reniformis* as characteristic elements (Reichgelt et al. 2013). In zone IIIa palynofloral diversity drops significantly and several pollen types disappear from the record. The spores increase in abundance and diversity (*Osmundacidites, Todisporites, Dictyophyllidites, Froelichsporites*). Characteristic elements of this zone are *Klausipollenites gouldii*, *Pretricolpipollenites bharadwajii*, *Araucariacites* sp., *Todisporites major* and *Dictyophyllidites harrisii*. The abundance of *Klausipollenites gouldii* remains high also in the zone IIIb (>50%), the general pollen diversity increases again (*Klausipollenites, Patinasporites, Colpectopollis, Cordaitina, Protodiploxypinus*) and the spore abundance drops. *Patinasporites densus* also becomes abundant. Additional characteristic elements of this zone are *Froelichsporites traverse* and *Colpectopollis ellipsoideus* (Litwin et al. 1991; Reichgelt et al. 2013). Thus, these two Norian palynofloras not surprisingly reflect the change in climate that occurred in the desert southwest of North America as a consequence of strong orogenic activity in eastern California (Nordt et al. 2015).

The late Norian flora of the Sverdrup Basin (eastern Canadian Arctic Archipelago) reflects a high-latitude vegetation that lived close to the border with Europe and Siberia and contains elements of both regions. The flora includes 25 genera of plant macrofossils from 11 localities. The diversity at most of the localities is relatively low (only a few species). In total, the flora is characterized by abundant sphenophytes (*Equisetites*, *Neocalamites*) and ferns (*Camptopteris*, *Cladophlebis*, *Clathropteris*, *Marattiopsis*, *Phlebopteris*, *Todites*) and less abundant bennettitaleans (*Anomozamites*, *Pterophyllum, Ptilophyllum*), ginkgophytes (*Ginkgo*, *Sphenobaiera*), Czekanowskiales (*Czekanowskia*) and conifers (*Pelourdea*, *Podozamites*, *Stachyotaxus*, *Swedenborgia*), together with tree trunks (*Araucarioxylon*, *Mesembrioxylon*). The floral composition (large horsetails, ginkgophytes, *Camptopteris* and *Clathropteris*) and the presence of coal beds indicate that the plants grew in a relatively warm climate with abundant rainfall and well-developed seasons (well-developed growth rings; Ash and Basinger 1991). Also from Canada is the Norian flora of east-central Axel Heiberg Island. This flora is dominated by bennettitalean leaves (*Anomozamites*, *Pterophyllum*, *Vardekloeftia*) and conifer shoots (*Podozamites*) with only a few sphenophyte (*Neocalamites*), fern (*Dictyophyllum, Todites*), seed fern (*Lepidopteris*), Czekanowskiales (*Czekanowskia*) and ginkgophyte (*Ginkgoites*) remains, suggesting a drier climate and/or palaeoenvironment than proposed on studies of the Norian floras of Axel Heiberg and Ellesmere islands (Vavrek et al. 2007). Alternatively, a Rhaetian age might be considered for this flora.

13.3 Late Triassic Floras of Europe and Greenland

Late Triassic floras are widely distributed in Europe and Greenland (these two landmasses being juxtaposed as part of northern Pangea at that time) and they have been grouped historically into three sectors, the Central European Basin (known also as

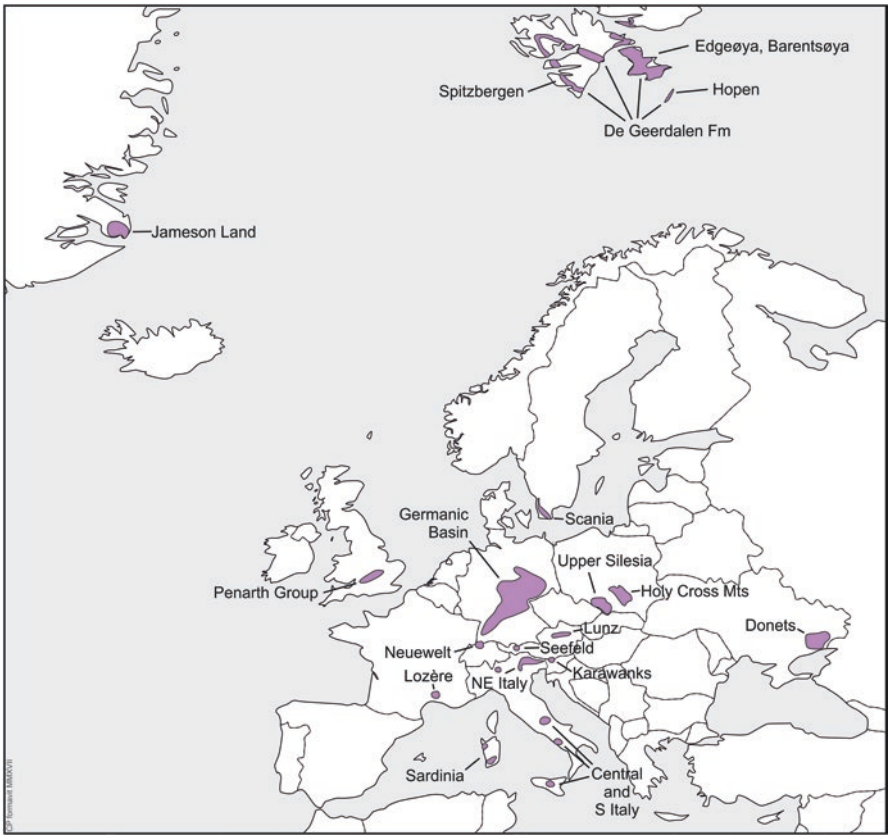

Fig. 13.3 Areas with major Upper Triassic plant assemblages in Europe, Svalbard and Greenland

the Germanic Basin) and the northern Alpine belt, the Southern Alps and the higher latitude Scandinavia-Greenland area (Figs. 13.1 and 13.3, Table 13.1). These sectors host floras with subtly different compositions. This area also includes the type section for the Triassic–Jurassic boundary, at the Kuhjoch Section in the Karwendel Mountains (Northern Calcareous Alps, Austria; e.g., Ogg et al. 2008). The Triassic–Jurassic boundary is dated radiometrically to 201.3 ± 0.2 Ma, and is defined on the First Appearance Datum (FAD) of the ammonite *Psiloceras spelae tirolicum.* In the continental realm, this coincides with the FAD of the gymnosperm pollen-taxon *Cerebropollenites thiergarthii* (Kürschner et al. 2007; Ogg et al. 2008; Von Hillebrandt et al. 2008).

The most famous floras of the Central European Basin (mostly Germany) are the Schilfsandstein flora and the Germanic Basin 'Rhaeto-Liassic' flora (e.g., Schenk 1867; Gothan 1914; Frentzen 1922; Weber 1968; Kirchner 1992; Kelber and Hansch 1995; Kelber 1998, 2000; Pott et al. 2016a). The Alpine floras host plant assemblages of all stages of the Late Triassic (e.g., Schenk 1866–1867; Stur 1868, 1885; Leuthardt 1903; Kräusel and Leschik 1955; Kräusel and Schaarschmidt 1966; Dobruskina 1993, 1994; Pott 2007; Pott et al. 2007d, 2008a; Pott and Krings 2010;

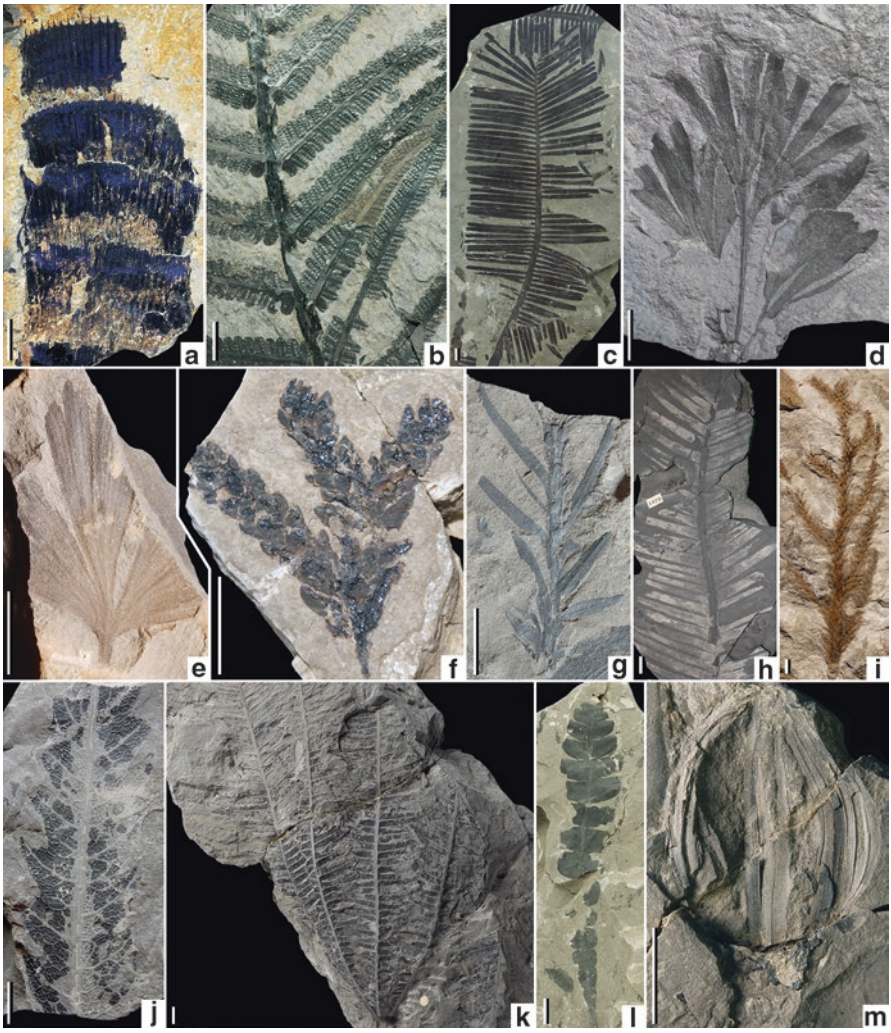

Plate 13.2 Upper Triassic plants from Europe. (**a**) *Equisetites arenaceus*, Lunz, Austria, Carnian. (**b**) *Asterotheca merianii*, Lunz, Austria, Carnian. (**c**) *Pterophyllum filicoides*, Lunz, Austria, Carnian. (**d**, **e**) *Ginkgoites* sp., Edgeøya, Svalbard, Carnian. (**f**) *Voltzia* sp., Seefeld, Austria, Norian. (**g**) *Elatocladus* sp., Rögla, Sweden, Rhaetian. (**h**) *Nilssonia pterophylloides*, Bjuv, Sweden, Rhaetian. (**i**) *Voltzia coburgensis*, Ziegelanger, Germany, Rhaetian. (**j**) *Dictyophyllum exile*, Rögla, Sweden, Rhaetian. (**k**) *Thaumatopteris schenkii*, Stabbarp, Sweden, Hettangian. (**l**) *Wielandiella angustifolia*, Jameson Land, Greenland, Rhaetian. (**m**) *Wielandiella angustifolia*, Jameson Land, Greenland, Rhaetian. Scale bar = 10 mm in each image

Kustatscher et al. 2011; Petti et al. 2013; Dalla Vecchia 2000) including historically famous plant suites, such as the Lunz, Neuewelt and Raibl plant assemblages. Additional Carnian floras occur in Slovenia (Dobruskina 2001) and Poland (Pacyna 2014), Norian floras in Poland (Barbacka et al. 2012; Pacyna 2014) and the Apennines (Dalla Vecchia 2000), and Rhaetian floras in France (Lozere: de Saporta

1873–1891; Depape and Doubinger 1963), England (Worchstershire and Bristol: Harris 1938, 1957) and Poland (Schmidt 1928). The Late Triassic floras of the Scandinavia–Greenland sector are documented from relatively few areas but host rich and highly diverse plant assemblages, that reflect extensive wetland systems developed in narrow basins that opened up during initial rifting across the North Atlantic region (e.g., Svalbard, southern Sweden, Greenland; Harris 1931a, 1932a, b, 1935, 1937; Pott and McLoughlin 2009, 2011; Pott 2014a, b).

13.3.1 Carnian Floras of Europe

The Carnian floras of Europe (Lunz, Neuewelt, Monte Pora, Raibl, several localities in Germany, Svalbard) are diverse and reflect generally humid conditions and swampy fluvial to deltaic depositional environments (e.g., Dobruskina 1994; Kelber and Hansch 1995; Pott et al. 2008b). The Carnian flora of Lunz is one of the most diverse Late Triassic floras currently known from the Northern Hemisphere (Pott and Krings 2010). The swampy depositional environment is reflected by coals and carbonaceous shales hosting abundant plant fossils referable to a great diversity of species belonging to numerous plant groups. Ferns (including Matoniaceae, Gleicheniaceae, Marattiaceae; Plate 13.2b), cycads/bennettitaleans (*Nilssonia*, *Nilssoniopteris*, *Pseudoctenis*, *Pterophyllum*; Plate 13.2c) are very abundant, whereas sphenophytes (*Equisetites*, *Neocalamites*; Plate 13.2a), conifers (*Elatocladus*) and putative ginkgophytes (*Arberophyllum*, *Ginkgoites*) are less common (e.g., Dobruskina 1994, 1998; Pott et al. 2007a, b, c, d, 2008a, b, c, in press; Pott and Krings 2010 and references therein). The Lunz flora is especially well known for its abundant and diverse bennettitaleans that are among the earliest representatives of that group. The material includes excellently preserved reproductive structures that play a key role in understanding the phylogeny of the group (Pott 2016; Pott et al. 2017).

The flora of Neuewelt in Basel (Switzerland; Kräusel and Leschik 1955; Kräusel and Schaarschmidt 1966) is slightly less diverse but incorporates abundant sphenophytes, ferns and bennettitaleans, whereas conifers are scarce. The Schilfsandstein flora (Germany) is dominated by sphenophytes (*Equisetites*, *Neocalamites*) and ferns (*Asterotheca*, *Cladophlebis*); conifers (*Swedenborgia*, *Voltzia*) and bennettitaleans (*Pterophyllum*) are rare. The succession hosting this flora incorporates multiple palaeosol layers with successive generations of horsetail (*Equisetites*) shoots and roots; the roots of one generation cut through the plant remains of the previous (underlying) generation (Kelber and Hansch 1995). The plant assemblages from Lunz and the Germanic Basin are considered autochthonous or parautochthonous based on the presence of abundant large, randomly oriented and well-preserved leaves, the presence of extensive, monotypic accumulations of ferns, and the occurrence of *in situ* sphenophyte rhizomes (Kelber and Hansch 1995; Pott et al. 2008a, b). Monotypic associations of ferns and sphenophytes, together with palynological signatures, suggest that

these floras grew in a humid environment (e.g., Pott et al. 2008a, b; Mueller et al. 2016a).

Some other Alpine floras differ noticeably in composition from the Lunz assemblages suggesting important local to regional environmental influences on the composition of the fossil assemblages. These include plant assemblages of the Italian Mount Pora (Bergamasc Alps), Dogna and Raibl (Julian Prealps), which are not as diverse as the better known coeval floras of the northern Alps and the Central European Basin and are dominated by gymnosperms (*Pterophyllum*, *Ptilozamites*, *Sagenopteris*, *Voltzia*; Plate 13.2f), although various sphenophytes (*Equisetites*) and ferns (*Chiropteris*, *Danaeopsis*) are also preserved, together with enigmatic plant remains, such as *Phylladelphia* (Schenk 1866–1867; Stur 1868, 1885; Dobruskina 2001; Kustatscher and Van Konijnenburg-van Cittert 2008). The Raibl and Dogna floras are dominated by conifers but, in the former, they belong to the voltzialeans (*Voltzia*, Bronn 1858; Stur 1885; Dobruskina 2001), whereas in the latter they are attributable to the cheirolepidiaceans (Roghi et al. 2006a). *Brachyphyllum* and *Pelourdea* are the most abundant taxa in the Monte Pora plant assemblages. This might reflect a palaeovegetation adapted to less humid environments and/or a taphonomic bias owing to longer transport distances before deposition of the plant remains. A small Carnian plant assemblage from the Karavanke Mountains (Slovenia) has yielded a few conifer remains (*Desmiophyllum*, *Voltzia;* Dobruskina 2001). The fossil flora of the Carnian Prealps is dominated by *Brachyphyllum*, *Pagiophyllum* and *Pelourdea* (Dalla Vecchia 2000, 2012), and that of the Bergamasc Alps by unidentified conifer shoots (Andrea Tintori, pers. comm. 2016). The plant assemblages from the famous Carnian Krasiejów fossiliferous locality (southwestern Poland) are generally poor in species and consist mainly of poorly studied leaves, leafy shoots, seeds and cone scales of conifers (*Desmiophyllum*, *Glyptolepis*, *Pachylepis*, *Pseudohirmerella*, *Voltzia*) and rare remains of ferns (*Sphenopteris*) and bennettitaleans (*Pterophyllum*; Dzik and Sulej 2007; Pacyna 2014).

Carnian strata of Europe have also yielded important amber discoveries. These derive mostly from the Heiligkreuz Formation in the eastern Dolomites and from the Rio del Lago Formation in the Julian Alps (Koken 1913; Zardini 1973; Wendt and Fürsich 1980; Gianolla et al. 1998; Roghi et al. 2005, 2006b) but amber has been found also in the Schilfsandstein of Switzerland and Germany (Soom 1984; Kelber 1990; Schönborn et al. 1999), the Raibler Schichten and the Lunz flora of Austria (Pichler 1868; Sigmund 1937; Vávra 1984) and the Sándorhegy Formation of Hungary (Budai et al. 1999). This unusually high abundance of amber in the fossil record has been linked to the environmental stresses imposed on the plants by the Carnian Pluvial Event (Gianolla et al. 1998; Roghi et al. 2006b).

The Carnian palynological record in Europe expresses a major floristic change characterised by a significant increase in the Circumpolles-group. Circumpolles is an interesting group that increased in abundance and diversity around the Ladinian–Carnian boundary and includes taxa such as *Duplicisporites*, *Paracirculina* and *Camerosporites*, all having supposed cheirolepidiaceous affinities (Zavialova and

Roghi 2005). The group is of great interest to evolutionary palaeontologists as it seems to have diversified through the Late Triassic to produce pollen grains of varied morphologies, and especially so during the Carnian. Its radiation coincides with an arid phase during the early Carnian. The early Carnian palynological assemblages are dominated by xeromorphic elements including taeniate bisaccate pollen and *Triadispora* (Kürschner and Herngreen 2010). The FADs of several characteristic sporomorphs, including *Camerosporites secatus*, *Enzonalasporites vigens*, *Triadispora verrucata* and *Vallasporites ignacii* are recorded during this period. The palynoflora registers a maximum in diversity and a dominance of spores (*Leschikisporis*, *Calamospora*, *Deltoidospora*, *Dictyophyllidites*) during the middle Carnian, in correspondence with the Carnian Pluvial Event (e.g., Simms and Ruffel 1989, 1990; Olsen and Kent 2000; Hochuli and Frank 2000; Roghi 2004; Breda et al. 2009; Kozur and Bachmann 2010; Preto et al. 2010; Arche and Lopez-Gomez 2014; Dal Corso et al. 2015; Mueller et al. 2016b). During the late Carnian, diversity began to decline and cheirolepidiacean pollen experienced further diversification. The entire Carnian was assigned to the *Camerosporites secatus* Zone by Herngreen (2005) and Kürschner and Herngreen (2010); this biozone is defined by the FADs of *Camerosporites secatus*, *Enzonalasporites vigens*, *Triadispora verrucata* and *Vallasporites ignacii* and the first common occurrence of *Ovalipollis pseudoalatus*. The lower part of this zone is assigned to the *Triadispora verrucata* Subzone, which corresponds to zones 12 and 13 of Heunisch (1999), the *Porcellispora longdonensis* Zone of Orłowska-Zwolińska (1984) and the *Concentricisporites bianulatus* assemblage of Roghi (2004). The middle part of the *Camerosporites secatus* Zone is named *Aulisporites astigmosus* Subzone; it correlates to zone 14 of Heunisch (1999), the *Aulisporites astigmosus* Zone of Orłowska-Zwolińska (1984), the *Aulisporites astigmosus* assemblage and the *Lagenella martinii* Assemblage of Roghi et al. (2010). The upper Carnian, is represented by zone 15 of Heunisch (1999), the lower part of the *Corollina meyeriana* Zone of Orłowska-Zwolińska (1984) and the *Granuloperculatipollis rudis* Assemblage of Roghi et al. (2010). This interval was not assigned to any subzone by Herngreen (2005) and Kürschner and Herngreen (2010).

Carnian floras of the Scandinavia-Greenland region are known from Svalbard and the Barents Sea (Figs. 13.1 and 13.3, Table 13.1). Svalbard comprises an archipelago of nine main islands with extensive exposures of Upper Triassic successions, including fossiliferous sandstones, siltstones and shales (Vajda and Wigforss-Lange 2009; Vigran et al. 2014). The most extensive Upper Triassic successions hosting plant remains are attributed to the Carnian De Geerdalen Formation and are represented by non-marine delta plain deposits (Klausen and Mørk 2014). Detailed palynological studies through the Upper Triassic successions have revealed variations in the miospore/dinoflagellate cyst ratios that were responses to variations in climate and sea-level. The assemblages document increased marine influences during the Late Triassic in this region (Hochuli and Vigran 2010; Vigran et al. 2014). The

Svalbard flora is dominated by ferns (*Asterotheca*, *Cladophlebis*, *Clathropteris*, *Danaeopsis*, *Dictyophyllum*, *Phlebopteris*, *Sphenopteris*), bennettitaleans (*Nilssoniopteris*, *Pterophyllum*) and seed ferns (*Paratatarina*, *Ptilozamites*, *Sagenopteris*) but sphenophytes (*Equisetites*, *Neocalamites*) and ginkgophytes are also well represented. Pott and Launis (2015), McLoughlin and Strullu-Derrien (2016), Pott (2016) and Pott et al. (2016b) identified 26 species in the late Carnian (to possibly early Norian) flora of Svalbard, Vassilevskaja (1972) reported a similar flora from Franz Josef Land. Common genera include the sphenophyte *Neocalamites*, the osmundaceous fern *Asterotheca*, possible peltasperms *Paratatarina* and *Glossophyllum*, ginkgophytes *Arberophyllum*, *Ginkgoites* (Plate 13.2d, e) and *Sphenobaiera*, and several species of the bennettitalean foliage *Pterophyllum*. Dipteridaceae occur only in the uppermost fossiliferous beds. Gothan (1910) reported woods with indistinct growth rings from the Svalbard flora, suggesting only weakly seasonal growth conditions.

Vassilevskaja (1972) argued that there were strong similarities between the Svalbard Carnian flora and assemblages of the Alpine region but notable differences from the coeval floras of central Europe and the slightly younger floras of Sweden and Greenland. Recent studies of the Late Triassic floras of the Svalbard Archipelago have partially supported these interpretations, with several taxa shared between the Svalbard, Lunz and Neuewelt floras (Launis et al. 2014; Pott 2014b). Pott (2014b) argued that the distinctive floristic North Atlantic Subprovince hypothesized for Rhaetian floras (Pott and McLoughlin 2009, 2011) within Dobruskina's (1994) Siberian and European-Sinean palaeofloral areas, was already established by the Carnian.

Extensive palynostratigraphic studies both onshore and, in recent years, from subsurface strata of the Barents Sea have established four Upper Triassic palynoassemblage zones that document the existence of a succession of four distinct, high-diversity palynofloras in this region (Vigran et al. 2014; Paterson and Mangerud 2015). Svalbard Carnian assemblages are represented by the *Aulisporites astigmosus* Composite Assemblage Zone of early to mid-Carnian age (Table 13.2). Assemblages attributable to this zone are typified by the high relative abundance of the trilete spores *Aulisporites astigmosus* and *Deltoidospora toralis* and the acme of monolete spores including *Leschikisporis aduncus*. The zone is further defined on the FADs of *Ricciisporites tuberculatus* and *Camarozonosporites rudis* (Vigran et al. 2014). The succeeding *Rhaetogonyaulax* spp. Composite Assemblage Zone (Table 13.2) has been dated to late Carnian–early Norian. This zone is defined within nearshore marine deposits and is characterized by a high relative abundance of the dinoflagellate cyst *Rhaetogonyaulax rhaetica*, together with abundant spores and bisaccate pollen, such as *Protodiploxypinus* and *Ovalipollis pseudoalatus*. Taxa defining the zone include a combination of dinoflagellate cysts and pollen, with key FADs of the dinoflagellates *R. rhaetica* and *R. arctica* and last occurrence datums (LADs) of several bisaccate pollen taxa, such as *Protodiploxypinus gracilis* and *Staurosaccites quadrifidus*.

13.3.2 Norian Floras of Europe

Exposures of Norian strata yielding plant fossils are known from the Alps (Bergamasc Prealps, Carnian Prealps; Northern Calcareous Alps), Apennines (Italy) and Silesia (Poland) (Figs. 13.1 and 13.3, Table 13.1). Norian floras in Europe generally have low taxonomic diversity and are dominated by conifers (reaching 80–90% of the assemblages: Dobruskina 1993, 1994; Dalla Vecchia 2000; Dalla Vecchia and Selden 2013; Pacyna 2014; Kustatscher et al. 2017), whereas cycads/bennettitaleans, lycophytes, sphenophytes and seed ferns are rare (Dobruskina 1993). The Seefeld flora is dominated by conifers of both voltzialean and cheirolepidiacean affinity (Plate 13.2e), in association with probable cycads (*Taeniopteris*) and lycophytes (e.g., *Lepacyclotes*; Dobruskina 1993, 1994; Kustatscher et al. 2017). The two small plant assemblages from the Appenines, i.e., Giffoni (Salerno) and Filettino (Frosinone), have yielded bennettitaleans (*Pterophyllum*) and conifers (*Araucarites, Brachyphyllum*, *Podozamites*, *Voltzia*; Dalla Vecchia 2000). The Upper Silesian flora (Poland) is dominated by conifers (*Brachyphyllum*) associated with sparse horsetails (*Equisetites*), ferns (*Cladophlebis*, *Clathropteris*), bennettitaleans (*Pterophyllum*) and Czekanowskiales (Pacyna 2014). In some localities, *Pachylepis*-type seed scales, matching the cuticles of the *Brachyphyllum* shoots, and putative fragments of *Czekanowskia* and ginkgophyte leaves are also preserved. Even a liverwort, *Palaeohepatica*, was described but never figured from this flora (Pacyna 2014).

The fragmentary nature of most of the Norian plant remains and the preservation of the cuticles in the Seefeld flora suggest that, in most cases, the plant remains were subjected to extensive transport. The thick cuticle and the sunken stomata protected by papillae suggest that the plants grew in stressed environments, such as small carbonate islands with thin soils and low groundwater levels and/or under arid conditions (Kustatscher et al. 2017). This may be true for most of the Norian plant assemblages of Europe with the exception of the Polish flora, which incorporates various ferns and a putative bryophyte, both considered hygrophytic plant groups. This suggests that the Polish flora grew under moister environmental conditions favoured by Poland's higher palaeolatitude, and/or the Polish assemblages were subjected to shorter transport before deposition.

During the Norian, the Circumpolles-producers became progressively more prominent in the vegetation, which is reflected in their high abundance. Generally, the palynofloral diversity decreases by about 50% between the early Carnian and the Norian (Kürschner and Herngreen 2010). Carnian hold-overs (*Duplicisporites* spp., Enzonalasporites spp. and *Camerozonosporites* spp.) remain common in lower Norian successions (Cirilli 2010). Difficulties assessing the Norian palynological record include the absence of continental deposits that can be readily correlated with marine successions and also the fact that Norian and lower Rhaetian assemblages are generally rather homogeneous. Owing to the incomplete Norian palynological record, considerable uncertainty exists about the ranges of so-called 'typical' Rhaetian sporomorphs (e.g., *Cornutisporites* spp., *Limbosporites lundbladii*, *Perinosporites thuringiacus*, *Rhaetipollis germanicus*, *Semiretisporis* spp., *Triancoraesporites* spp. and *Zebrasporites* spp.), for which a late Norian appear-

ance cannot be excluded (Kürschner and Herngreen 2010). The Norian successions are attributed by Herngreen (2005) to the *Granuloperculatipollis rudis* Zone, based on the FAD of the marker species and the abundance of *Classopollis meyeriana* and *C. zwolinskae*. This zone corresponds to zones 16–17 of Heunisch (1999), the middle–upper part of the *Corollina meyeriana* Zone of Orłowska-Zwolińska (1984) and the upper part of the *Granuloperculatipollis rudis* assemblage of Roghi et al. (2010).

In Svalbard, the Norian Flatsalen Formation incorporates predominantly shallow marine deposits and, consequently, does not preserve abundant plant macrofossils. However, well-preserved Norian palynological assemblages from this unit are assigned to the *Limbosporites lundbladii* Composite Assemblage Zone (Vigran et al. 2014; Table 13.2), which is typified by a dominance of spores (especially spikes of *Annulispora* spp. and *Deltoidospora* spp.), together with diverse representatives of the fern spore *Kyrtomisporis*. This zone is defined by the FADs of *Limbosporites lundbladii* and *Rogalskaisporites barentzii*, and the regular occurrence of *Ricciisporites umbonatus*, *Cingulizonates rhaeticus*, *Granuloperculatipollis rudis* and *Quadraeculina anellaeformis*. Owing to the nearshore marine depositional setting of the Flatsalen Formation, the palynoassemblages include dinoflagellates, mainly *Heibergella* spp., *H. asymmetrica* and *Rhaetogonyaulax rhaetica*, which aid regional correlation. Palynostratigraphic studies have also noted the inception of cheirolepidiacean conifers (commonly an indicator of drier and/or saline influences) and a relative increase in the abundance of gymnosperms producing bisaccate pollen in this interval (Paterson and Mangerud 2015).

Strata of this age in southern Sweden are assigned to the Kågeröd Formation and occur mostly in the subsurface as red-beds devoid of plant material. Similarly, the Norian–lower Rhaetian Ørsted Dal Member (Fleming Fjord Formation) of East Greenland consists of fluvial and lacustrine red, marly mudstones, grey sandstones and carbonates that lack plant fossils (Surlyk 2003). In the Alpine area, the Norian succession is characterized by dolomitic strata that are also poor in palynomorphs.

13.3.3 Rhaetian Floras of Europe and Greenland

Several of the most important latest Triassic assemblages (Fig. 13.3, Table 13.1) were assigned historically to 'Rhaeto-Liassic' floras because, in early studies, the distinctions between the Rhaetian and Early Jurassic successions were difficult to resolve. A more detailed stratigraphic resolution of the Triassic–Jurassic transition in continental successions of Europe and Greenland has been achieved in recent years utilizing palynofloral (e.g., Lindström and Erlström 2006; Larsson 2009; Vajda et al. 2013; Vigran et al. 2014; Lindström et al. 2017), macrofloral (e.g., McElwain et al. 2009; Pott and McLoughlin 2009, 2011; Pott et al. 2016b), stable isotope (e.g., Hesselbo et al. 2002) and magnetostratigraphic data (e.g., Lord et al. 2014), and this has facilitated a better understanding of the significant changes in the vegetation across this boundary.

The Bayreuth flora (Oberfranken, Germany) includes one of the most famous 'Rhaeto-Liassic' floras (Weber 1968). The richest Rhaetian plant assemblage restudied recently is that from Wüstenwelsberg (e.g., Kelber and Van Konijnenburg-van Cittert 1997; Bonis et al. 2010; Zavialova and Van Konijnenburg-van Cittert 2011; Van Konijnenburg-van Cittert et al. 2014, 2016; Pott et al. 2016a). The sandstone quarry at Wüstenwelsberg is well known for its rich and diverse flora, including lycophytes (*Selaginellites*), sphenophytes (*Equisetites*), ferns (e.g., *Cladophlebis*, *Clathropteris*, *Dictyophyllum*, *Marattia*, *Phlebopteris*, *Todites*, *Thaumatopteris*), seed ferns (*Ctenozamites*, *Lepidopteris*, *Pachypteris*, *Ptilozamites*, *Rhapidopteris*), cycads/bennettitaleans (*Anomozamites*, *Ctenis*, *Nilssonia*, *Nilssoniopteris*, *Pseudoctenis*, *Pterophyllum*), ginkgophytes (*Ginkgoites*, Schmeissneria) and conifers (*Desmiophyllum*, *Elatocladus*, *Palissya*, *Stachytaxus*, *Schizolepis, Voltzia*; Plate 13.2i). Cycads/bennettitaleans are very abundant but *Voltzia* is apparently absent; so too is *Hirmerella*, one of the most prominent taxa of the 'Rhaeto-Liassic flora of Bayreuth' (Gothan 1914; Kirchner 1992; Bonis et al. 2010). The Rhaetian Seinstedt plant assemblage is also a diverse and hygrophytic flora (Barth et al. 2014).

The Polish Rhaetian flora of Upper Silesia and the Tatra Mountains is of low diversity and consists mostly of fragments of sphenophytes (*Neocalamites*), ferns (*Cladophlebis*, *Clathropteris*), seed ferns (*Lepidopteris*, *Peltaspermum*), cycads/bennettitaleans (*Pterophyllum*, *Taeniopteris*), Czekanowskiales (*Czekanowskia*), ginkgophytes (*Ginkgoites*) and conifers (*Brachyphyllum*, *Pagiophyllum*, *Palissya*, *Widdringtonites*, Cheirolepidiaceae) (Barbacka 1991; Reymanówna and Barbacka 1981; Wawrzyniak and Ziaja 2009; Pacyna 2014).

Rhaetian and Early Jurassic floras in Skåne (southern Sweden) derive from the coal-rich Bjuv Member (upper Rhaetian) and Helsingborg Member (Hettangian) of the Höganäs Formation, but a few plants have also been recovered from the underlying Vallåkra Member (lower Rhaetian). The plant remains are abundant and exceptionally well preserved. A wealth of fossils has been collected and curated over the past century in association with bituminous coal mining (more than 28,000 specimens are curated in the collections of the Swedish Museum of Natural History alone). Rhaetian–Hettangian plant assemblages of southern Sweden, similarly to the Rhaeto-Liassic floras of the Central European Basin, were treated as a single flora in many early taxonomic studies because the uppermost Triassic and lowermost Jurassic successions were difficult to distinguish lithologically, problematic to trace laterally, and the depositional environment was represented by relatively consistent floodplain settings across the boundary interval. A consistent lithostratigraphic framework did not develop for the region until the mid-twentieth century (Troedsson 1943, 1950, 1951). The floras are preserved in deltaic and coastal plain deposits that locally also host fossils of fishes, amphibians and dinosaur trackways (Nilsson 1946; Troedsson 1951; Vajda et al. 2013). This wealth of fossil plant material has been the subject of numerous taxonomic studies over the past two centuries (Nilsson 1820; Nathorst 1876a, b, 1878a, b, c, 1879, 1880, 1886, 1888, 1902, 1909a, b, 1913; Halle 1908; Johansson 1922; Lundblad 1949, 1950, 1959a, b; Pott and McLoughlin 2009, 2011; Pott 2014a).

Although around 445 taxa have been recorded from the Rhaetian–Early Jurassic floras of Skåne, accurate measures of diversity are difficult to obtain without wholesale revision of the historical fossil collections because various authors have adopted different approaches to the delimitation of taxa. For example, Lundblad (1959a) re-assessed the taxonomy of several *Ginkgo* taxa described by Nathorst (1878c, 1886), synonymizing some forms, and emphasized that morphological characteristics for taxonomical delinations of *Ginkgo* species need to be combined with cuticular analyses. Further, Pott and McLoughlin (2009), in an analysis of bennettitalean foliage from the various Scanian localities, reduced the around 50 taxa of this group reported previously to just 10 clearly demarcated species attributable to *Pterophyllum* and *Anomozamites*, of which only five were recorded with confidence from Rhaetian strata. Overall, the Skåne Rhaetian floras include a diverse array of plant groups including bryophytes, lycophytes, sphenophytes (*Equisetites*, *Neocalamites*), ferns (*Camptopteris*, *Dictyophyllum* Plate 13.2j, *Phlebopteris*, *Thaumatopteris* Plate 13.2k, *Todites*), bennettitaleans (*Anomozamites*, *Pterophyllum*), cycads (*Nilssonia*; Plate 13.2h), seed ferns (*Lepidopteris*, *Ptilozamites*, *Sagenopteris*), ginkgophytes (*Baiera*, *Ginkgo*, *Ginkgoites*, *Sphenobaiera*) and conifers (*Cyparissidium*, *Elatocladus* Plate 13.2g, *Stachyotaxus*, *Palissya*). Quantitatively, sphenophyte stems and foliage of ferns, conifers and bennettitaleans tend to dominate the Rhaetian assemblages of Skåne (Pott and McLoughlin 2009, 2011). The overall composition of the flora suggests a multi-storey vegetation with ferns, sphenophytes and lycophytes dominating the under-storey, conifers and ginkgoaleans the upper-storey, and a range of bennettitaleans, cycads and seed-ferns constituting plants of intermediate stature.

Many of the genera and species in the Skåne deposits are shared with the Rhaetian flora of Jameson Land (East Greenland), and Lundblad (1950, 1959a) noted a disjunction in Skåne between the composition of latest Triassic assemblages (assigned to the *Lepidopteris* Zone) of the Bjuv Member and the succeeding earliest Jurassic assemblages of the Helsingborg Member (assigned to the *Thaumatopteris* Zone) that is matched in the Greenland succession. The first appearances of several fern and gymnosperm species, notably *Thaumatopteris schenkii* (Plate 13.2k), *Pterophyllum subequale*, *Anomozamites gracilis*, *Dictyophyllum nilssonii*, *Sagenopteris nilssoniana*, *Ginkgoites marginatus*, *Baiera taeniata*, *Czekanowskia rigida*, *Podozamites distans*, and *Palissya braunii* characterize basal Jurassic strata in Skåne and signify an important change in the flora. Further, a stratigraphic interval of a few metres in the uppermost Rhaetian strata is typified by great abundances of the enigmatic gymnosperm pollen *Ricciisporites tuberculatus*. This taxon ranges from the Norian to the Sinemurian but has a pronounced acme in the upper Rhaetian of Northwest Europe (Kürschner et al. 2014; Peterffy et al. 2016). The acme provides a useful biostratigraphic marker for the end-Triassic biotic crisis interval in both the East Greenland and Skåne successions (Pedersen and Lund 1980; Mander et al. 2013; Vajda et al. 2013). The *Ricciisporites*-rich zone is succeeded by a short interval dominated by fern (mainly *Deltoidospora*) spores. In Skåne, as in East Greenland, this stratigraphic package is identified as a transitional interval (Larsson 2009; Vajda et al. 2013) that possibly incorporates fossils of the recovery vegetation following the end-Triassic crisis.

Fossiliferous strata in Jameson Land and nearby Traill Island (East Greenland) were first mentioned by William Scoresby Jnr. The coal layers were first considered to be Carboniferous (Jameson 1823), later Cenozoic (Heer 1868) and finally Rhaetian in age (Hartz 1896). Harris (1926, 1931a, 1932a, b, 1935, 1937, 1946) undertook the most intensive studies of the Primulaelv Formation floras (Kap Stewart Group) from the Hurry Inlet and Klitdal areas (Pedersen 1976; Surlyk 2003; McElwain et al. 2007). Harris described around 200 species of fossil plants, many of them represented by specimens with excellent preservation yielding cuticular details (Plate 13.2l, m). As in Skåne, Harris (1937) recognized two stratigraphically distinct floras in this region, a lower *Lepidopteris* flora, and an upper *Thaumatopteris* flora. Only a few species are common to both floras but there are great similarities at family level (McElwain et al. 2009). Bennettitales, cycads, ginkgophytes and conifers dominate both floras. The transition from the Rhaetian to the Lower Jurassic is marked by the inception of several fern and gymnosperm taxa, especially *Thaumatopteris schenkii*, *Pterophyllum subequale*, *Anomozamites gracilis*, *Dictyophyllum nilssonii*, *Sagenopteris nilssoniana*, *Ginkgoites marginatus*, *Baiera taeniata*, *Czekanowskia rigida*, *Podozamites distans* and *Palissya braunii*.

Harris (1937) assigned the *Lepidopteris* Zone to the Rhaetian and *Thaumatopteris* Zone to the Early Jurassic based on correlations with the fossil floras of southern Sweden and southern Germany (e.g., the Grenzschichten flora). These ages were later confirmed by palynostratigraphy and stable isotope signatures (Pedersen and Lund 1980; Hesselbo et al. 2002). These palynological studies have provided more detailed insights into the floristic transition in East Greenland; the most important of these being the study by Pedersen and Lund (1980) who identified well-preserved and rich miospore assemblages dominated by gymnosperm pollen in the Rhaetian and Hettangian siliciclastic successions exposed along Hurry Inlet. In general terms, these assemblages matched the composition of the macrofloras documented by Harris in the 1930s. Pedersen and Lund (1980) grouped the assemblages into two 'microflora zones' (Microflora Zone 1 and Zone 2), which essentially are equivalent to the *Lepidopteris* (Rhaetian) and *Thaumatopteris* (Hettangian) macrofloral zones of Harris (1937), respectively. Zone 1 is characterized by abundant *Ricciisporites tuberculatus,* and the presence of *Limbosporites lundbladii*, *Rhaetipollis germanicus*, *Heliosporites altmarkensis*, *Ovalipollis ovalis* and *Apiculatisporis parvispinosus.* It is correlated to the northwest European *Rhaetipollis-Limbosporites* Zone of early Rhaetian age (Lund 1977), the *Rhaetipollis germanicus* Zone of Herngreen (2005), zones 18–20 of Heunisch (1999) and the *Ricciisporites tuberculatus* Composite Assemblage Zone of Vigran et al. (2014) and Orłowska-Zwolińska (1984) (Table 13.2). The latter is defined mainly on the high relative abundance of *L. lundbladii* and *Cingulizonates rhaeticus*, together with *Chasmatosporites* spp. and *R. tuberculatus.* Several of these taxa, e.g., *L. lundbladii* and *R. tuberculatus*, together with the dinoflagellate cysts *Rhaetogonyaulax rhaetica*, *Suessia swabiana* and *S. mutabilis*, also have their LADs within this zone.

Pedersen and Lund (1980) subdivided Microfloral Zone 1 into three sub-zones (Lower, Middle and Upper). 'Zone 1 Lower' is distinguished from the succeeding subzones mainly by the presence of '*Vesicaspora*' *fuscus* and more common

Fig. 13.4 Areas with major Upper Triassic plant assemblages in easternmost Europe and Asia (except India)

Ovalipollis ovalis. 'Zone 1 Middle' is defined by the acme of *Limbosporites lundbladii*, includes the dominance of *Deltoidospora toralis* and *Uvaesporites reissingeri*, and the presence of *Polypodiisporites polymicroforatus*, *Araucariacites* spp. and a spike of *R. tuberculatus* in the upper part of this sub-zone. The coeval *R. tuberculatus* Composite Assemblage Zone in Svalbard (Fig. 13.4) is also characterized by a high abundance of the nominal taxon. 'Zone 1 Upper' is distinguished from the preceding sub-zones based on the occurrence of *Vesicaspora fuscus* and the common presence of *Ovalipollis ovalis*. This sub-zone is also characterized by a highly diverse miospore assemblage with high relative abundances of *Deltoidospora toralis, Baculatisporites comaumensis*, *Vitreisporites bjuvensis*, *Araucariacites* spp., *Classopollis* spp. and *Ricciisporites tuberculatus*. At the Triassic–Jurassic transition, palynofloral diversity declines by about 20%, mainly as a result of a decrease in the number of spore species (Kürschner and Herngreen 2010). The Hettangian Miospore Zone 2 palynomorph species richness is similar to that prior to the Rhaetian. Zone 2 is characterized by the absence (or rarity) of some taxa diagnostic

of Zone 1, and the appearance of various gymnosperm pollen, and fern and lycophyte spores, such as *Cerebropollenites thiergartii*, *Heliosporitesaltmarkensis*, *Trachysporites asper*, *Lycodopiumsporites semimuris*, *Deltoidospora crassexina*, *Iraquispora laevigata* and *Schismatosporites ovalis*.

The end-Triassic biotic crisis has an ambiguous palynofloral signal in Europe and Greenland. Some studies indicate only minor changes in the palynoflora (Lund 1977; Achilles 1981; Batten and Koppelhus 1996; Bonis et al. 2009a, b; Kürschner and Herngreen 2010; Götz et al. 2011). Others (Pedersen and Lund 1980; Lindström and Erlström 2006; Van de Schootbrugge et al. 2007; Larsson 2009; Vajda et al. 2013; Lindström 2016) have indicated a significant floral turnover and a spike in the pollen *Ricciisporites tuberculatus* across the Triassic–Jurassic transition. Although some floristic modifications and $\delta^{13}C$ isotope excursions might be related to facies changes around the boundary (Brenner 1986; Heunisch 1999), the significant turnover in palynomorph taxa in correspondence with changes in the plant macrofossil assemblages (Harris 1937; Lundblad 1959b; McElwain et al. 2009) and a spike in *R. tuberculatus*, matching equivalent surges in disaster taxa during other Earth crises (Visscher et al. 1996; Vajda et al. 2001; Vajda and McLoughlin 2004, 2007; Vajda and Bercovici 2014), suggests a marked disruption to the vegetation, at least in the North Atlantic sector. High-resolution palynological studies in widely separated basins will be necessary to obtain a clear picture of the regional patterns of floristic turnover across this boundary.

Silicified and sideritized fossil wood is preserved in both the East Greenland and the Skåne floras (Clemmensen 1976; S. McLoughlin pers. obs.). Despite the apparently wide distribution of fossil woods in the region, few palaeoxylological studies have been undertaken. One exception is a silicified (permineralized) peat block recovered from the island of Hopen (Svalbard Archipelago), which has yielded a remarkable array of three-dimensionally preserved autochthonous roots and stems of lycophytes and bennettitaleans, and parautochthonous sporangia, spores, pollen and leaves from various pteridophytes and gymnosperms (Selling 1944, 1945; Strullu-Derrien et al. 2012; McLoughlin and Strullu-Derrien 2016). Future studies on fossil woods from the Late Triassic of these regions offer considerable opportunities for analysis of biotic interactions (arthropod borers and fungal damage) and palaeoclimates (via growth-ring analysis) that can be compared and contrasted with equivalent parameters from the Early Jurassic of the same areas (Vajda et al. 2016; McLoughlin and Bomfleur 2016).

13.4 Late Triassic Floras of Easternmost Europe and Asia (Except China and Eastern Asia)

The major regions hosting Upper Triassic fossiliferous strata in easternmost Europe and Asia lie in the territory of the former Soviet Union (Figs. 13.1 and 13.4, Table 13.1), attributed by Dobruskina (1994) to the Middle Asian and East Asian sectors (Middle Asian and East Asian floristic subprovinces). The East Asian

Subprovince includes the Donets Basin, Fore-Caucasus, Kazakhstan and Southern Fergana, Southern Urals and Caspian Depression, whereas the Middle Asian Subprovince comprises the Pechora Basin, eastern Urals, and eastern and northern Siberia (Fig. 13.6). Floras of the Middle Asian floristic Subprovince are characterized by a dominance of peltasperms, the presence of marattiacean ferns, rare cycadocarpidiacean conifers and a lack of Dipteridaceae. The East Asian Subprovince (Primorye included) is characterized by numerous dipteridacean ferns and cycadocarpidiacean conifers whereas marattiacean ferns and peltasperms are virtually absent.

Palynological studies of Upper Triassic deposits in the territory of the former Soviet Union are scattered and no synthetic palynozonation scheme has been established. The best-studied miospore assemblages derive from the European part of Russia, Donetsk Basin, Western Caucasus and Siberia. No palynological studies have been carried out on the Upper Trassic strata of Primorye.

13.4.1 Carnian Floras of Easternmost Europe and Asia (Except China and Eastern Asia)

Carnian floras are well represented across easternmost Europe and north and central Asia (Figs. 13.1 and 13.3, Table 13.1). The richest and best-studied Carnian floras from this region derive from the lower part of the Protopivskaya Formation of the Donets Basin (Stanislavsky 1965, 1971, 1973, 1976), Kalachevskaya Formation of the Pechora Basin (Kirichkova 2011; Kirichkova and Esenina 2014), eastern Urals (Vladimirovich 1959, 1965, 1967; Kirichkova 1990), southern Fergana and Kazakhstan (Turutanova-Ketova 1931; Brick 1941; Sixtel 1960; Dobruskina 1995) and southern Primorye (Kryshtofovich 1912; Srebrodolskaya 1960; Shorokhova 1975a; Shorokhova and Srebrodolskaya 1979; Volynets and Shorokhova 2007; Volynets et al. 2008).

Peltasperms (e.g., *Lepidopteris*, *Peltaspermum*, *Scytophyllum*; Plate 13.3h) reach their maximum abundance and diversity in the Middle Asian Subprovince during this interval, especially in assemblages close to the Urals. The floras of the Donbass, Urals and Central Asia are composed of up to 30% peltasperm remains. Apart from various spore-producing plants (Plate 13.3b), the Madygen flora also contains seed ferns (*Peltaspermum*, *Ptilozamites*, *Scytophyllum*, *Vittaephyllum*; Plate 13.3c) among its most common elements (Dobruskina 1995; Moisan et al. 2011; Moisan and Voigt 2013). The Carnian assemblages of the western and eastern part of the Urals contain *Scytophyllum*-type leaves suggesting that the Ural Mountains were not an impassable barrier for peltasperms during the Late Triassic (Dobruskina 1994), whereas the floras of the East Asian Subprovince lack peltasperms. *Glossophyllum*-type leaves are the common element in the Carnian floras of the Central European and Middle Asian subprovinces. Dobruskina (1994) referred her lanceolate leaves of *Glossophyllum* to the ginkgophytes, but at least some of them may alternatively belong to pteridosperms. Czekanowskiales are restricted to northern latitudes. They may have radiated from the mountains of the Ural-Tien Shan

region to Primorye, Japan and Mongolia during the Carnian and to the eastern side of the Urals during the Norian (Dobruskina 1994; Volynets and Shorokhova 2007).

Marattiacean ferns (e.g., *Danaeopsis*, *Marattiopsis*, *Rhinipteris*) were important during the Carnian in the Urals, Caucasus and Central Asia, but were absent from the eastern Urals, Taimyr and Primorye. Dobruskina (1994) related this distribution to the migration of families from the west of Eurasia, up to the geographic barrier posed by the Ural Mountains. Dipteridaceae spread at lower latitudes of the East Asian Subprovince, being represented in such deposits as the Sad-Gorod Formation of the Primorye (Volynets and Shorokhova 2007), whereas they are rare or absent in the continental interior. The fact that one of the oldest Northern Hemisphere records comes from the Ladinian deposits of Japan (*Dictyophyllum*; Plate 13.3a) might indicate that the family originated in and spread from the East Asian sector. Sphenophytes are numerous but taxonomically monotonous; they are represented by three genera only (*Neocalamites*, *Annulariopsis*, *Schizoneura*) and occupy a subordinate position in relation to other plant groups in the southern latitudes of the Central European and Middle Asian Subprovince. However, they constitute a significant component of several assemblages in the northern part of the Chelyabinsk Basin and the Southern Urals (Kirichkova 1969) and in the Bukobay Formation of the Ilek River Basin (Brick 1952). Bryophytes (*Muscites*, *Ricciopsis*) and lycophytes (*Annalepis*, *Ferganodendron*, *Isoetites*, *Mesenteriophyllum*, *Pleuromeiopsis*) are rare, although Moisan et al. (2012b) and Moisan and Voigt (2013) described a few new taxa from the Madygen locality of South Fergana. The peculiar composition of this flora has been attributed to its special palaeoenvironmental setting; the plants grew in rather humid environments of alluvial plains, delta plains and shallow lacustrine environments near the northern limits of the Tethys Ocean during the Carnian (Kochnev 1934; Brick 1936; Sixtel 1961, 1962; Dobruskina 1995; Moisan et al. 2011).

Conifers constitute a subordinate component of most northern and central Asian Carnian floras, and only at Nikolaevka (Donets Basin) do they reach more than 30% of all plant remains (Stanislavsky 1976). Primitive voltzialean conifers were gradually replaced by more advanced groups (e.g., *Pachylepis*, *Schizolepis*, *Stachyotaxus*; Dobruskina 1994). Conifers (*Cycadocarpidium*, *Podozamites*; Plate 13.3f) were widely distributed in the southern latitudes of the East Asian sector. The dominance of coniferous genera changes from west to east and is probably linked to the provincialism of the Carnian floras (Dobruskina 1994). The relative abundance of cycads/bennettitaleans increased towards the south; they are the most abundant group in the Carnian flora of Primorye (up to 50%; Volynets and Shorokhova 2007). This is mainly a consequence of the great abundance of *Taeniopteris* remains, whereas *Otozamites* and *Pseudoctenis* leaves (Plate 13.3d) are rare. Moisan et al. (2011) noted the first occurrence of *Pseudoctenis* and *Pterophyllum* (Plate 13.3e) from central Asia (Madygen flora).

A rich and well-preserved palynological assemblage was first described by Yaroshenko (1978) from marine deposits of Western Ciscaucasia containing bivalves, ammonoids and brachiopods of Carnian age. The assemblage is characterized by a high relative abundance of *Camerosporites secatus*, *Alisporites australis*

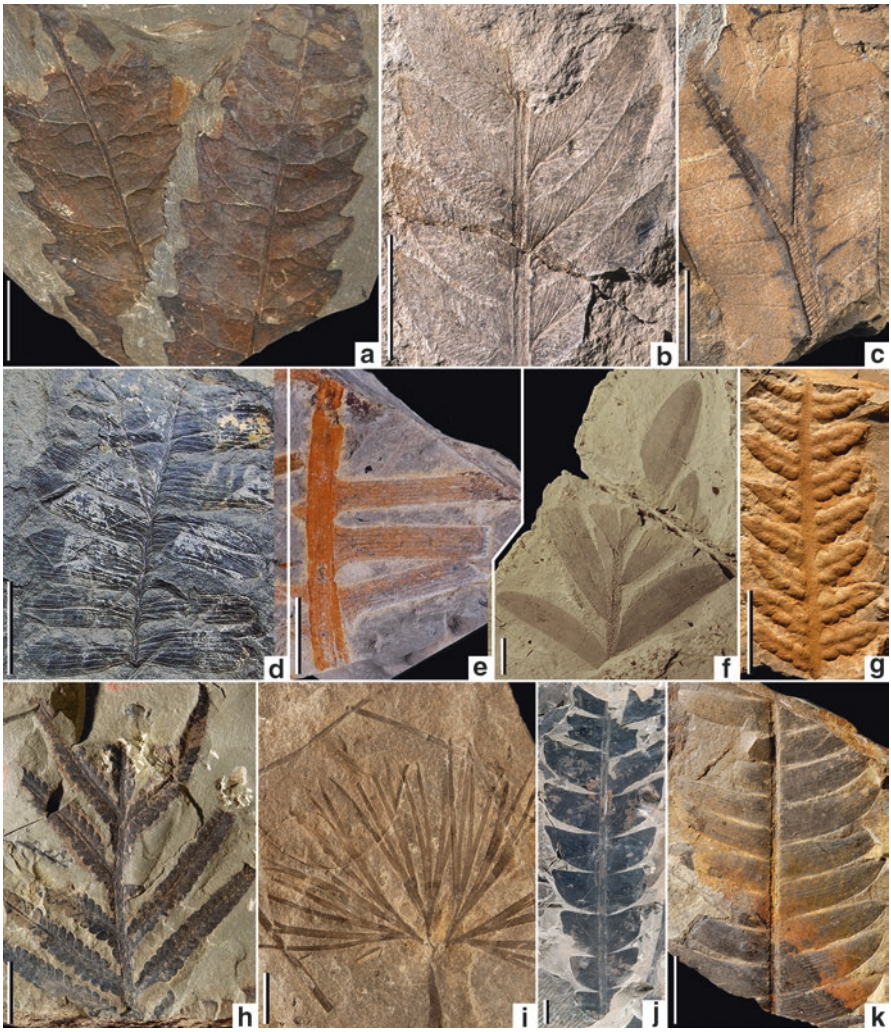

Plate 13.3 Upper Triassic plants from Asia. (**a**) *Dictyophyllum kryshtofovichii*, Razdol'naya River basin, Primorye, Russia, Norian. (**b**) *Cladophlebis* sp., Madygen, Kyrgyzstan, Carnian. (**c**) *Vittaephyllum hirsutum*, Madygen, Kyrgyzstan, Carnian. (**d**) *Pseudoctenis mongugaica*, Filipovka River basin, Primorye, Russia, Carnian. (**e**) *Pterophyllum* sp., Madygen, Kyrgyzstan, Carnian. (**f**) *Podozamites* sp., Madygen, Kyrgyzstan, Carnian. (**g**) *Gleichenites* sp., Dharbid Khun, Iran, Rhaetian. (**h**) *Lepidopteris ottonis*, Apuntal, Iran, Rhaetian. (**i**) *Baiera muensteriana*, Dharbid Khun, Iran, Rhaetian. (**j**) *Anomozamites polymorpha*, Aghusbin, Iran, Rhaetian. (**k**) *Pterophyllum nathorstii*, Apuntal, Iran, Rhaetian. Scale bar = 10 mm in each image

and *Dictyophyllidites* spp., and the FAD of *Auritulinasporites scanicus* and *Granosaccus tkhachensis*. Ilyina and Egorov (2016) noted that the continental strata of the transitional continental-marine deposits of northern Middle Siberia were characterized by a significant representation of *Ovalipollis*, *Ricciisporites* and *Minutosaccus* pollen grains, and *Kyrtomisporis*, *Tigrisporites* and *Limbosporites*

spores (Romanovskaya and Vasilieva 1990). Carnian pollen assemblages differ significantly from those of the western and eastern slopes of the Ural Mountains of the Middle Asian Subprovince. The pollen assemblages from the Protopivskaya Formation of the Donetsk Basin are characterized by *Tigrisporites*, *Limbosporites*, *Aratrisporites*, *Minutosaccus*, *Ovalipollis* and *Ricciisporite*s (Semenova 1970, 1973; Gluzbar 1973). It is noteworthy that the Carnian assemblage of the Donetsk Basin is poorly correlated with coeval assemblages of the eastern part of the Pechora Basin (Chalyshev and Variukhina 1966; Variukhina 1971), West Siberia (Malyavkina 1964), Franz-Josef Land (Fefilova 2005) and Kazakhstan (Sakulina 1973) but are similar to the Middle Keuper assemblages of Western Europe (Gluzbar 1973). A review of the palynological assemblages from the territory of former Soviet Union identified the *Ovalipollis-Dictyophyllidites-Enzonalasporites-Porcellispora longdonensis* assemblage as characteristic for the Carnian of the East European platform and Southern Kazakhstan (Romanovskaya and Vasilieva 1990). Romanovskaya and Vasilieva (1990) also proposed several regional assemblages (Table 13.2): the *Aratrisporites-Disaccites-Dictyophyllidites-Ovalipollis* association for the Pechora Basin, the *Disaccites-Osmundacidites-Aratrisporites-Dictyophyllidites-Punctatosporites walkomi-Striatites* association for the Chelyabinsk Basin, the *Duplexisporites-Lycopodiacidites kuepperi-Cingulizonates delicatus-Chasmatosporites* association for eastern Taymir and the *Dictyophyllidites-Osmundacidites-Chasmatosporites-Cingulizonates delicatus-Neoraistrickia taylorii* association for the Arctic regions.

13.4.2 Norian–Rhaetian Floras of Asia (Except China and Eastern Asia)

Norian and Rhaetian floras of easternmost Europe and northern and central Asia (Figs. 13.1 and 13.4, Table 13.1) are discussed together, because, in most cases, the continental deposits of these ages are difficult to correlate with well-dated marine sequences (Dobruskina 1980; Markevich and Zakharov 2004). Norian continental deposits are common in many regions of easternmost Europe and northern and central Asia, especially from Primorye (Shorokhova 1975b; Shorokhova and Srebrodolskaya 1979; Volynets and Shorokhova 2007). They are preserved in the upper part of the Protopivskaya Formation of the Donets Basin (Stanislavsky 1976), the upper part of the Nemtsov Formation of central Siberia, the Kozyrevskaya Formation of the eastern Urals and the Amba Formation of Primorye (Kirichkova 1962, 1969, 2011; Volynets and Shorokhova 2007). Rhaetian continental facies with plant remains are completely absent from some areas. Rhaetian plant assemblages are interpreted to be present in the Novorayskaya Formation of the Donets Basin (Stanislavsky 1971) and the Aktash and Tashkutan formations of central Asia (Genkina 1964; Gomolitzky 1993; Sixtel 1960).

The Norian–Rhaetian was a time of optimum development of cycads and bennettitaleans. Cycad/bennettitalean remains typically constitute 35–50% of specimens in leaf-dominated assemblages of this sector and are particularly rich in the Rhaetian Novorayskaya Formation of the Donbass region. Volynets et al. (2008) also noted that the Imalinovo plant assemblage (early Norian) of Primorye is rich in *Otozamites*, *Pseudoctenis* and many remains of *Ctenis*, *Drepanozamites*, *Nilssonia* and *Pterophyllum*. An especially large number of cycads/bennettitaleans is known from the Rhaetian Novorayskaya Formation of Donbass.

There are almost no ferns of Palaeozoic aspect in the Norian–Rhaetian floras. However, Mesophytic marattialean fern families, Osmundaceae (*Todites*), Matoniaceae (*Phlebopteris*) and Dipteridaceae (e.g., *Camptopteris*, *Clathropteris*, *Dictyophyllum*) are widely distributed in the Novorayskaya Formation of Donbass (Stanislavsky 1971), in the Eastern Caucasus (Vakhrameev et al. 1977) and in Central Asia (Issyk-Kul and Kavak-Tau) (Turutanova-Ketova 1931). Primorye is known for its unusual occurrences of endemic fern species attributable to *Acrostichopteris* (Shorokhova 1975a).

Ginkgoales and Czekanowskiales are geographically widespread in central and northern Asia during this time. Ginkgoales are represented by *Allicospermum*, *Baiera*, *Ginkgoites*, *Sphenobaiera* and leaves of Umaltolepidiaceae (*Pseudotorellia*), which are also typical of the Early Jurassic assemblages. New conifer genera (e.g., *Fraxinopsis*, *Palaeotaxus*, *Palissya*, *Storgaardia*) appeared in the Rhaetian and coexisted with forms that appeared earlier in the Norian. Peltasperms decrease in abundance, and in Central Asia are they virtually absent. Only *Ctenozamites*, *Ptilozamites* and *Lepidopteris* are found on the eastern slope of the Polar Urals (Dobruskina 1994). Leaves of *Thinnfeldia* and the endemic pteridosperms *Imania* and *Tudovakia* were described from Primorye (Volynets et al. 2008; Krassilov and Shorokhova 1970). The species diversity and relative abundance of sphenophytes decreases in the Norian–Rhaetian floras of central and northern Asia.

Rhaetian plant assemblages are also known from localities in central Pamir and Afghanistan (Prynada 1934; Sixtel 1960; Vakhrameev et al. 1978). These consist mainly of cycads and bennettitaleans (*Anomozamites*, *Nilssonia*, *Otozamites*, *Pterophyllum*, *Taeniopteris*), conifers (*Pelourdea*) and ferns (*Clathropteris*, *Dictyophyllum*, *Thaumatopteris*). The Nayband Formation of Central-East Iran has also yielded 19 genera (31 species) of sphenophytes (*Equisetites*), ferns (*Cladophlebis*, *Clathropteris*, *Dictyophyllum*, *Gleichenites* Plate 13.3g, *Phlebopteris*, *Todites*), seed ferns (*Scytophyllum*, *Lepidopteris;* Plate 13.3h), cycads/bennettitaleans (*Androstrobus*, *Dictyozamites*, *Nilssonia*, *Nilssoniopteris*, *Pterophyllum* Plate 13.3k, *Anomozamites* Plate 13.3j, *Weltrichia*, *Williamsonia*), ginkgophytes (*Ginkgoites*, *Baiera;* Plate 13.3i) and conifers (*Elatocladus*, Krasser 1891; Kilpper 1964, 1971; Fakhr 1977; Schweitzer 1977, 1978; Schweitzer and Kirchner 1995, 1996, 1998, 2003; Schweitzer et al. 1997, 2000, 2009; Vaez-Javadi 2012, 2013a, b). The Norian–Rhaetian flora from Aghdarband (northeast Iran) is dominated by cycads/bennettitaleans (*Pterophyllum*, *Taeniopteris*) and conifers (*Pagiophyllum*, *Podozamites*, *Stachytaxus*) with a few horsetails (*Neocalamites*),

ferns (*Cladophlebis*) and ginkgophytes (*Sphenobaiera*) (Boersma and Van Konijnenburg–van Cittert 1991).

Extensive palynostratigraphic studies of Norian and Rhaetian marine deposits have been undertaken in Western Caucasia. Yaroshenko (2007) noted strong similarities between the Rhaetian palynofloras of this region and the *Rhaetipollis germanicus-Ricciisporites tuberculatus* Zone of Western Europe, particularly in the abundance of *Ricciisporites tuberculatus* (87%) with abundant *Rhaetipollis germanicus*. The palynoflora from the Salgir Formation of the Crimean Peninsula (Bolotov et al. 2004) closely resembles that of western and eastern Ciscaucasia (Yaroshenko 2007). The Triassic deposits of southern Kazakhstan have yielded *Deltoidospora* spp., *Dictyophyllidites* spp., *Kyrtomisporites speciosus*, *Chasmatosporites* among others (Table 13.2) but lack the characteristic Rhaetian taxa *Riccisporites tuberculatus* and *Rhaetipollis germanicus* (Vinogradova and Tsaturova 2005).

The *Thuringiatriletes* Assemblage Zone (Table 13.2) typifies the Norian deposits of the Siberian Platform. This assemblage is characterized by the high abundance of *Thuringiatriletes microverrucatus* and *Zebrasporites laevigatus* and its co-occurrence with *Cingulatisporites bulbifera* and *Camptotriletes echinatus* (Odintsova 1977). The Rhaetian strata of the Donets Basin are characterized by *Cornutisporites seebergensis, Triancoraesporites ancorae, T. reticulatus*, *Zebrasporites laevigatus*, *Z. interscriptus*, *Cingulatizonates insignis*, *Ricciisporites tuberculatus* and *Limbosporites* spp. (Semenova 1970, 1973). The most typical forms in the Norian and Rhaetian assemblages of Siberia are representatives of typical European genera, such as *Cingulatizonates*, *Chasmatosporites*, *Lycopodiumsporites*, *Ovalipollis*, *Tigrisporites*, *Zebrasporites*, *Aratrisporites*, and *Triancoraesporites ancorae*, along with numerous saccate pollen grains of gymnosperms (Odintsova 1977; Yaroshenko 2007).

Romanovskaya and Vasilieva (1990) proposed two miospore associations for the European sector of Russia (Table 13.2). The lower miospore assemblage includes *Circulina* spp., *Punctatosporites walkomii, Dictyophyllidites* spp., *Cingulizonates* spp., *Camarozonotriletes rudis*, whereas the upper assemblage includes *Dictyophyllidites* spp., *Ricciisporites tuberculatus*, *Chasmatosporites* spp. and *Triancoraesporites*.

13.5 Late Triassic Floras of China and Eastern Asia

The first studies of Late Triassic floras from this region were carried out by European scholars, such as Schenk (1883, 1884) and von Richthofen (1882), working on the Upper Triassic Xujiahe (=Hsuchiaho) Formation in Guangyuan (northern Sichuan Basin). In the early to mid-twentieth century, Sze (1933) and Sze and Lee (1952) published on the fossil flora of the Sichuan Basin, followed later by Yang (1978) and Hsü et al. (1979).

The Late Triassic floras of China (Figs. 13.1 and 13.4, Table 13.1) can be segregated into Southern-type floras (=Southern East Asia Subprovince; i.e.,

Dictyophyllum-Clathropteris flora) and Northern-type floras (=Northern East Asia Subprovince; i.e., *Danaeopsis-Bernouillia* [=*Symopteris*] flora), which correspond to the southern and northern China tectonic regions, respectively. Floras of the Southern East Asia Subprovince are widely distributed in South China, extending south to Indonesia and north to a small area of eastern northeast China. This subprovince is mainly represented by the Xujiahe (Hsuchiaho) flora (Li 1964; Ye and Liu 1986) and Baoding flora of Sichuan (Hsü et al. 1979), the Shaqiao flora of Hunan (Zhou 1989) and the Tianqiaoling flora of Jilin (Sun 1993). The Southern East Asia Subprovince can be divided into three suites based on their distinctive floristic characters (see below) with age constraints provided by associated marine fossil faunas. The Northern East Asia Subprovince is widely distributed in North China, southern Northeast China and northern Northwest China. The floras are represented by the Yenchang (Yanchang) flora of northern Shaanxi (P'an 1936; Sze 1956a; Huang et al. 1980) and the Xiaohekou flora of Hunjiang (Jilin: Mi 1977), among others (Table 13.1). Unfortunately, it has so far been impossible to assign these floras to different stages with confidence. The boundary between the two floristic subprovinces follows a rough line from Kuqa in Xinjiang to Nanzhang in Hubei (Li et al. 1991). Mixed assemblages characterized by elements of both the Southern East Asia Subprovince and Northern East Asia Subprovince exist close to this line.

High-resolution stratigraphical schemes are presently lacking for the Chinese terrestrial successions. This is mainly due to the enormous thicknesses of strata, making detailed palynostratigraphy an expensive and time-consuming task. However, pollen and spore assemblages have been employed for broad-scale stratigraphic and palaeoenvironmental reconstructions. A general feature of the Carnian and Norian assemblages is the abundant occurrence of *Dictyophyllidites harrisii*, *Alisporites* spp., *Cyclogranisporites* spp. and in places *Aratrisporites* spp. (Peng et al. 2017b).

No reliably dated Late Triassic plants have yet been found in southern Tibet, although some poor coal layers are present in the Norian Langjixue Group of Xiukang, south of the Yarlung Zangbo River (Sun 1993). However, Peng et al. (2017a) recovered Upper Triassic palynoassemblages from mostly marine strata at Tulong, Nyalam County, southern Xizang (Tibet), that are referable to three Middle to Late Triassic zones more characteristic of the Gondwanan Onslow Subprovince: viz., the *Staurosaccites quadrifidus* Assemblage Zone (late Anisian to early Norian), the *Dictyophyllidites harrisii* Assemblage Zone (early Norian), and the *Craterisporites rotundus* Assemblage Zone (middle to late Norian). This region of southern Tibet was part of Gondwana during the Late Triassic. The local palynoflora reveals a marked rise of *Classopollis* (Cheirolepidiace) pollen in the Rhaetian that might reflect a more xeric vegetation under a torrid and arid (or subarid) climate in this region compared with other parts of China. Adjacent regions of southern Tibet (Lhasa Block) and central Tibet (Qiangtang Block) belong to the Cimmerian terranes but have not yet yielded productive Late Triassic palynofloras. Further studies will be required to assess whether their phytogeographic affinities lie more closely with Gondwana or with the Southern East Asian terranes.

Plate 13.4 Upper Triassic plants from China. (**a**) *Clathropteris platyphylla*, Zigui, Hubei, China, Carnian. (**b**) *Gleichenites* sp. cf. *G. nitida*, Nanzhang, Hubei, China, Carnian. (**c**) *Anthrophyopsis* sp., Guangyuan, Sichuan, China, Norian. (**d**) *Symopteris* (*Bernoullia*) *zeilleri*, Jimusaer, Xinjiang, China, Carnian. (**e**) *Clathropteris meniscioides*, Hechuan, Chongqing, China, Norian. (**f**) *Dictyophyllum* sp. cf. *D. nathorstii*, Lufeng, Yunnan, China, Norian. (**g**) *Symopteris* (*Bernoullia*) sp., Jimusaer, Xinjiang, China, Carnian. (**h**) *Danaeopsis fecunda*, Jimusaer, Xinjiang, China, Carnian. Scale bar = 10 mm in each image

Also of Late Triassic age, although not more precisely dated, are some remains of *Leptostrobus* from the Amisan Formation and wood remains (*Agathoxylon*, *Cedroxylon*, *Phyllocladoxylon*, *Xenoxylon*) from the Nampo Group of Korea. The Daedong flora of Korea includes rich assemblages of sphenophytes (*Neocalamites*), ferns (*Clathropteris*, *Dictyophyllum*, *Hausmannia*, *Todites*), seed ferns (*Ctenozamites*), cycads/bennettitaleans (*Anomozamites*, *Ctenis*, *Nilssonia*, *Otozamites*, *Pseudoctenis*, *Pterophyllum*, *Taeniopteris*), ginkgophytes (*Baiera*, *Sphenobaiera*), Czekanowskiales (*Czekanowskia*) and conifers (*Cycadocarpidium*, *Elatocladus*, *Podozamites*) (Yabe 1905; Kawasaki 1925, 1926, 1939; Kimura and Kim 1984, 1988, 1989; Kim and Kimura 1988; Kim 1989, 1993; Kim et al. 2002, 2005).

13.5.1 Carnian Floras of China and Eastern Asia

Carnian deposits of the Southern East Asia Subprovince (Figs. 13.4 and 13.6, Table 13.1) host plant assemblages attributed to the *Abropteris-Pterophyllum longifolium* Flora ('Assemblage'). This flora incorporates plant assemblages from the Daqiaodi Formation of Yongren, Yunnan and Yunnan-Sichuan border area, the Jiuligang Formation of Nanzhang, Hubei, and the Jiapeila Formation of Tibet (Zhou and Zhou 1983; Meng 1983, 1990). The flora includes the sphenophyte *Equisetites*, the ferns *Abropteris*, *Yungjenophyllum*, *Asterotheca*, *Miscopteris*, *Stenopteris, Angiopteris Clathropteris* (Plate 13.4a) and *Danaeopsis* (Plate 13.4h), the seed ferns *Sagenopteris*, *Thinnfeldia* and *Ctenozamites*, and the cycads/bennettitaleans *Pterophyllum* and *Paradrepanozamites*. The assemblage bears some resemblance to the Carnian Schilfsandstein flora of Western Europe (Zhou and Zhou 1983).

The Indonesian Carnian flora is dominated by sphenophytes (Kon'no 1972; Vakhrameev et al. 1978; *Annulariopsis*, *Neocalamites*, *Neocalamostachys*), ferns (*Clathropteris*, *Dictyophyllum*, *Cladophlebis*, *Todites*) and cycads/bennettitaleans (*Dictyozamites*, *Otozamites*). Carnian floras are also known from Japan; i.e., the Yamaguti plant assemblages from the Momonoki and Aso formations of the Mine Group (Ôishi 1932a, b, 1940; Ôishi and Takahashi 1936; Takahashi 1951). The ferns (*Cladophlebis*, *Clathropteris*, *Todites*), conifers (*Podozamites*) and cycads/bennettitaleans (*Cycadocarpidium*, *Nilssonia*, *Taeniopteris*) are the most abundant groups, whereas sphenophytes (*Neocalamites*, *Equisetites*, *Equisetostachys*) are rare (Volynets and Shorokhova 2007).

13.5.2 Norian Floras of China and Eastern Asia

Norian deposits of the East Asia Subprovince (Figs. 13.1, 13.4, and 13.6, Table 13.1) host the *Dictyophyllum-Drepanozamites* flora ('Assemblage') or the *Dictyophyllum-Cycadocarpidium* flora ('Assemblage') (Sun 1987). These floras are represented mainly by the fossil assemblages of the Hsuchiaho (Xujiahe) Formation of Sichuan, the Daqing Formation of the Sichuan-Yunnan border area, the Anyuan Formation of Hunan and Jiangxi, the Badong Formation of eastern Tibet, the Dakeng Formation of Fujian and the Malugou Formation of Tianqiaoiin (Jilin) (Sun 1987). The main elements of the flora are ferns (e.g., *Clathropteris* Plate 13.4e, *Dictyophyllum* Plate 13.4f, *Hausmannia*, *Reteophlebis*, *Gleichenites* Plate 13.4b), cycads/bennettitaleans (e.g., *Anomozamites*, *Cycadocarpidium*, *Doratophyllum*, *Drepanozamites*, *Pterophyllum*) and conifers (e.g., *Podozamites*). The bennettitaleans are particularly diverse and, among the ferns, Dipteridaceae is especially abundant. Sphenophytes are also abundant but of low diversity. Conifers are rare and represented mainly by large-leafed taxa (e.g., *Ferganiella* and *Podozamites*). Ginkgophytes are represented by some species of *Glossophyllum* and the Czekanowskiales by *Czekanowskia* (Wang et al. 2010).

These Norian floras closely resemble the Nariwa flora of Japan and some coeval floras of Eurasia (Zhou and Zhou 1983; Volynets and Shorokhova 2007). The Nariwa flora includes abundant ferns (*Cladophlebis*, *Goeppertella*, *Marattiopsis*, *Thaumatopteris*) and cycads/bennettitaleans (*Nilssonia*, *Otozamites*, *Pterophyllum*, *Taeniopteris*); sphenophytes (*Annulariopsis*, *Neocalamites*), ginkgophytes (*Baiera*, *Ginkgoites*, *Sphenobaiera*), seed ferns (*Ptilozamites*, *Sagenopteris*), conifers (*Pityophyllum, Elatocladus*, *Pityophyllum*, *Podozamites*) and Czekanowskiales (*Ixostrobus*) are rare (Ôishi 1932a; Ôishi and Takahashi 1936; Volynets and Shorokhova 2007).

13.5.3 Rhaetian Floras of China and Eastern Asia

Rhaetian successions of eastern Asia are typified by the *Ptilozamites-Anthrophyopsis* flora ('Assemblage') from the Yangbaichong Formation of Shaqiao (Hunan; Zhou 1989), which contains mainly *Clathropteris*, *Cycadocarpidium*, *Nilssoniopteris*, *Pterophyllum*, *Ptilozamites*, *Podozamites*, *Stalagma* and *Todites* (Figs. 13.1, 13.4, and 13.6, Table 13.1). This flora resembles closely that of the *Lepidopteris* Zone of eastern Greenland and Germany. The Sanqiutian Formation flora of the Anyuan Group (Jiangxi) and the Wenbinshan flora of Fujian also have similar content (Zhou 1978). Recently, some plants were found from the Dongfeng area (Jilin) in which *Anthrophyopsis* (Plate 13.4c) occurs associated with *Neocalamites* and *Cycadocarpidium*; these fossils may represent a Rhaetian assemblage. Floras of the Northern East Asia Subprovince cannot be attributed confidently to any stage. They contain more than 100 species belonging to about 50 genera whose main representatives are the sphenophyte *Equisetites*, the ferns *Danaeopsis*, *Bernouillia* (=*Symopteris*) and *Todites*, the seed fern *Thinnfeldia*, the ginkgophytes *Glossophyllum*, *Ginkgoidium* and *Ginkgoites* and the cycads/bennettitaleans *Sinozamites* and *Sphenozamites* (Zhou and Zhou 1983).

Rich Rhaetian floras with abundant sphenophytes (*Annulariopsis*, *Equisetites*, *Neocalamites*), ferns (*Cladophlebis*, *Clathropteris*, *Dictyophyllum*, *Marattiopsis*, *Sphenopteris*, *Todites*), seed ferns (*Sagenopteris*), cycads/bennettitaleans (*Ctenis*, *Nilssonia*, *Pterophyllum*, *Taeniopteris*), ginkgophytes (*Baiera*) and conifers (*Cycadocarpidium*, *Elatocladus*, *Podozamites*) were also described from Tonkin, Vietnam (Zeiller 1903; Akagi 1954) and Japan (Ôishi 1930, 1931, 1932a, b; Ôishi and Takahashi 1936). The cycads/bennettitaleans and conifers in these assemblages closely resemble those of the middle Norian flora of the Primorye region (Volynets and Shorokhova 2007).

Based on palynology of the Junggar Basin, Northwestern China (Sha et al. 2011, 2015), the Triassic–Jurassic boundary is placed at the last appearance datum of the pollen taxon *Lunatisporites rhaeticus*. The transition is characterized by a turnover from a vegetation dominated by lycophytes (*Aratrisporites*-producers) and seed ferns (*Alisporites*-producers) to an Early Jurassic flora dominated by *Lycopodiumsporites*-producers, Taxodiaceae (*Perinopollenites*) and Pinaceae (*Pinuspollenites*).

13.6 Late Triassic Floras of the Southern Hemisphere

The Late Triassic floras of those southern landmasses (Figs. 13.1, 13.5, and 13.6, Table 13.1) that were formerly united into the supercontinent Gondwana are characterized by broad compositional similarities at generic and, in some cases, specific level (Retallack 1987; Srivastava and Manik 1991; Anderson et al. 1999; Hill et al. 1999; Artabe et al. 2003; Escapa et al. 2011; and references therein). The Late Triassic saw the climax of the *Dicroidium*-dominated flora of Gondwana—a floristic association that had essentially supplanted the *Glossopteris* flora in diversity and geographic extent across the middle and high latitudes of the Southern Hemisphere after the end-Permian mass extinction (McLoughlin 2001, 2011). Despite the wide distribution and richness of austral Late Triassic floras (Figs. 13.1 and 13.6, Table 13.1), most data comes from a few well-studied assemblages that are widely separated within the former supercontinent. Moreover, the scarcity of marine strata and radiometrically dated ash beds intercalated with the plant-bearing intervals in Gondwana has greatly hindered precise dating of many Late Triassic plant assemblages in that region. This overview of the Gondwanan Late Triassic floras outlines the general representation of plant groups and broad-scale geographic and temporal variations in the palaeovegetation. Foremost among the sources of data for this overview is the series of monographs dealing with the Molteno Formation flora of South Africa produced by Anderson and Anderson (1983, 1985, 1989, 2003, 2008), which also incorporates data from other southern continents.

13.6.1 Carnian Floras of the Southern Hemisphere

Carnian floras are well represented across Gondwana, although in some areas they have been inadequately studied. By far the richest and best-studied Gondwanan Carnian flora is that of the Molteno Formation of the Karoo Basin, South Africa, from which some 30,000 catalogued rock slabs have been recovered from around 100 assemblages. From this vast collection, Anderson and Anderson (1983, 1985, 1989, 2003, 2008, in press) have documented over 200 species of vegetative organs. Based on a generalized inverse Gaussian-Poison distribution of fossil records, they estimated that the identified fossil diversity equates to an original vegetation containing over 2000 species of plants. Foremost among the constituents of the Molteno Formation flora are the remains of Umkomasiales (=Corystospermales), particularly the foliage attributed to various species of *Dicroidium* (Plate 13.5c–e). Of the 21 species of *Dicroidium* recognized throughout the Triassic of Gondwana, at least seven occur in the Carnian of the Karoo Basin. Remains of these species typically constitute more than 90% of specimens in leaf-dominated assemblages. Moreover, leaves attributed to several other taxa across Gondwana (viz., *Johnstonia*, *Dicroidiopsis*, *Diplasiophyllum*, *Zuberia*, *Xylopteris*, *Tetraptilon* and *Hoegia*) undoubtedly belong in *Dicroidium* on the basis of consistency in leaf architecture,

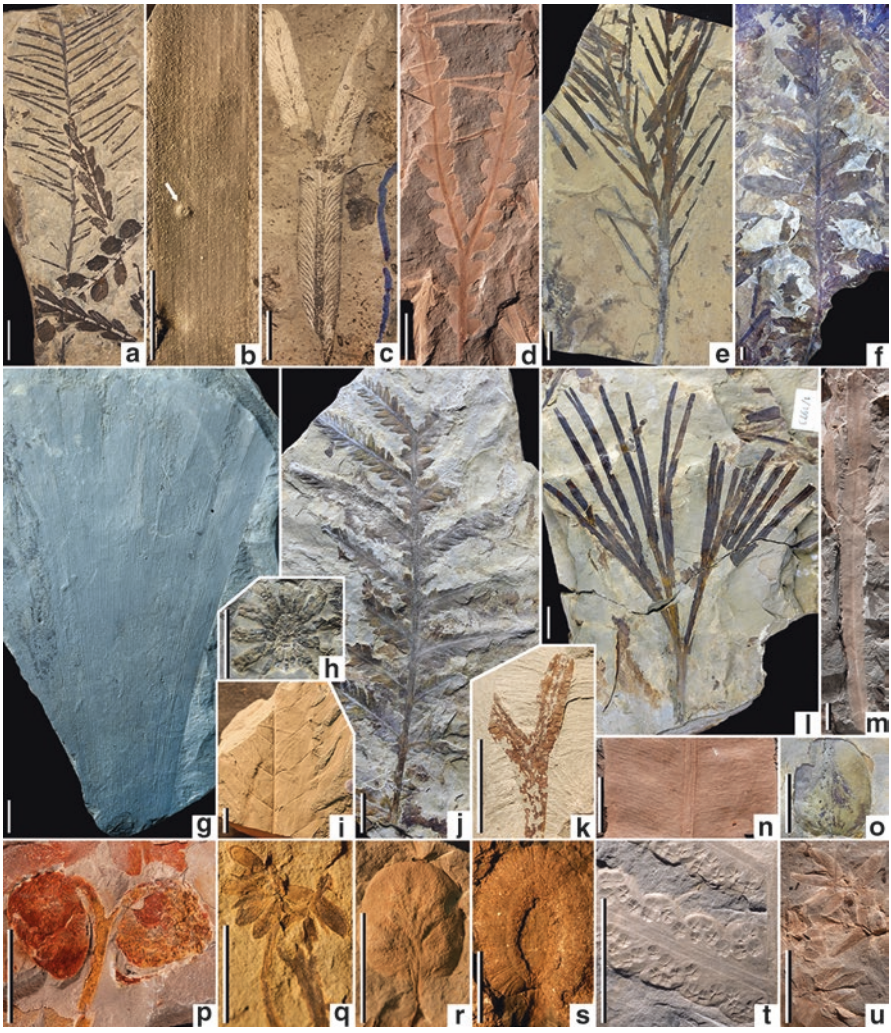

Plate 13.5 Upper Triassic plants from Gondwana. (**a**) *Rissikia media*, Mount Bumstead, Antarctica, Late Triassic. (**b**) *Heidiphyllum elongatum*, leaf with arthropod piercing-and-sucking damage (*arrowed*), Transantarctic Mountains, Antarctica, Late Triassic. (**c**) *Dicroidium dutoitii*, Allan Nunatak, Australia, Late Triassic. (**d**) *Dicroidium odontopteroides,* Dinmore, Ipswich Basin, Australia Carnian–Norian. (**e**) *Dicroidium elongatum*, Birds River, Karoo Basin, South Africa, Carnian. (**f**) *Scytophyllum neuburgianum*, Argentina, El Tranquilo Group, Carnian. (**g**) *Rochipteris etheridgei*, Leigh Creek Coal Measures, Telford Basin, Australia,?Carnian. (**h**) *Equisetites* sp., Birds River, Karoo Basin, South Africa, Carnian. (**i**) *Dictyophyllum rugosum*, Ipswich Basin, Australia, Carnian–Norian. (**j**) *Lepidopteris stormbergensis* Birds River, Karoo Basin, South Africa, Carnian. (**k**) Thalloid liverwort (Hepaticopsida); Barbers Mine, Fingal, Tasmania, Late Triassic. (**l**) *Sphenobaiera schenkii*, Birds River, Karoo Basin, South Africa, Carnian. (**m**) *Linguifolium tenisonwoodsi*, Dinmore, Ipswich Basin, Australia, Carnian–Norian. (**n**) *Taeniopteris lentriculiformis,* Dinmore, Ipswich Basin, Australia, Carnian–Norian. (**o**) Seed of *Fanerotheca papilioformis*, Birds River, Karoo Basin, South Africa, Carnian. (**p**) *Umkomasia simmondsii,* Dinmore, Ipswich Basin, Australia, Carnian–Norian. (**q**) *Pteruchus minor* Slacks Creek, Ipswich Basin, Australia, Carnian–Norian. (**r**) Single cupule of *Hamshawvia longipedunculata*, Denmark Hill, Ipswich Basin, Australia, Carnian–Norian. (**s**) *Fredlindia moretonensis*, Denmark Hill, Ipswich Basin, Australia, Carnian–Norian. (**t**) *Asterotheca* sp.*,* Dinmore, Ipswich Basin, Australia, Carnian–Norian. (**u**) *Antevsia mazenodensis,* Dinmore, Ipswich Basin, Australia, Carnian–Norian. Scale bar = 10 mm in each image

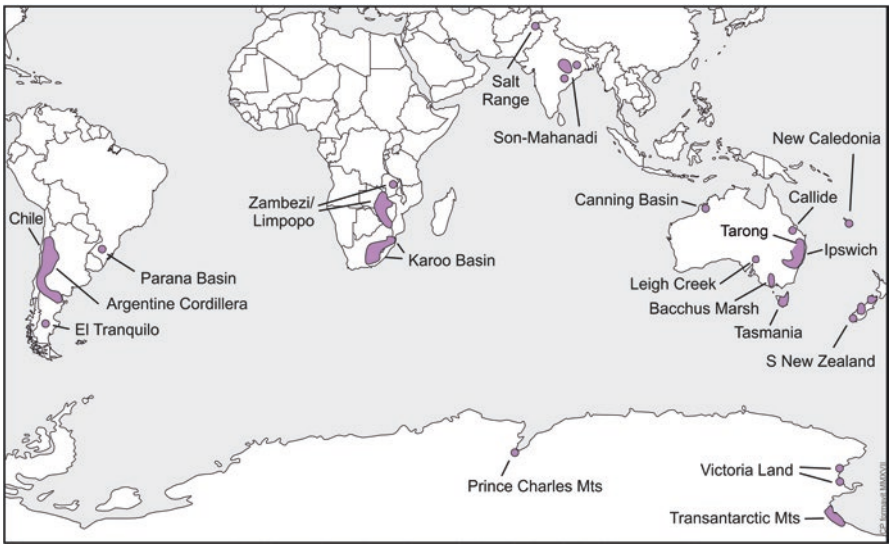

Fig. 13.5 Areas with major Upper Triassic plant assemblages in the Southern Hemisphere and India (Gondwana)

venation style, cuticular micromorphology and examples of hybridism (Anderson and Anderson 1983). Such examples of taxonomic inflation may account for relatively high apparent generic diversity in some Late Triassic Gondwanan assemblages (Colombi and Parrish 2008; Pattemore 2016a, b).

Among other gymnosperms that co-dominate or are important components of the Molteno Formation flora in terms of relative abundance are Peltaspermales (*Lepidopteris*: Plate 13.5j), Ginkgoales/Hamshawviales (*Ginkgo*, *Sphenobaiera*: Plate 13.5l), voltzialean and pinalean conifers (*Heidiphyllum* and associated genera: Plate 13.5b), and Matatiellales (*Dejerseya* and possibly *Linguifolium*: Plate 13.5m). Various other enigmatic seed fern families (e.g., Petriellales Plate 13.5g, Alexiales, Hlatimbiales), putative podocarp and pinalean conifers (e.g., *Pagiophyllum*, *Rissikia*: Plate 13.5a), Bennettitales (*Halleyoctenis*), Pentoxylales (*Taeniopteris*: Plate 13.5n), Gnetopsida (*Gontriglossa*, *Yabeiella* and related taxa) and Cycadales (*Pseudoctenis*, *Jeanjacquesia*) represent subordinate gymnospermous components of the Carnian flora. Extensive and detailed documentation of physical attachments and organ associations has enabled confident linkages between the various dispersed sterile and fertile parts (Plate 13.5o–u) belonging to many of the plant groups represented in this flora (Anderson and Anderson 1989, 2003). Sphenophytes are represented by eight genera and 23 species of fertile and sterile organs (mostly schizoneurid and equisetacean genera; Plate 13.5h) in the Molteno Formation flora. They are locally abundant, especially in lake-margin and floodplain wetland facies. Ferns are represented by around 16 genera and 37 species in this flora (dominantly members of Osmundaceae and Dipteridaceae; Plate 13.5i, t) and represent rare to moderately common elements of the Carnian understorey vegetation. Bryophytes

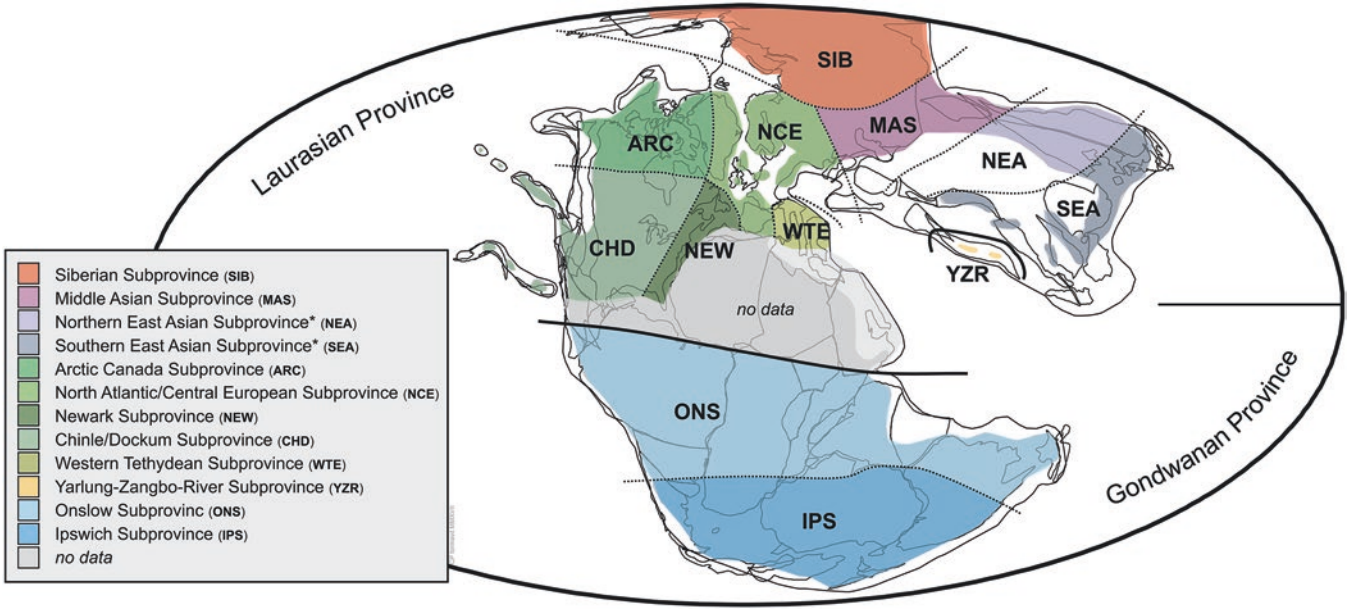

Fig. 13.6 Palaeogeographic map showing floral zonation in the Late Triassic. Distribution of Onslow Subprovince and Ipswich Subprovince based on palynofloras (after Foster et al. 1994; Césari and Colombi 2013). Note: NEA and SEA are commonly referred to as Northern and Southern Floristic Region of China, respectively. Basemap: PALEOMAP Project, C. R. Scotese, Arlington, Texas, USA

(Plate 13.5k) and lycophytes are rare components of this fossil flora, although this may be an artefact of poor preservational potential owing to their diminutive size and soft tissues.

Elsewhere in Gondwana, Carnian plant assemblages show strong similarities to the Molteno Formation flora in terms of taxonomic representation (at least at generic level) and relative group abundance. Any deviations appear to be linked mostly to differences in depositional environment and less intense sampling. In Argentina, Spalletti et al. (1999) assigned the bulk of Carnian-age plant assemblages to their *Yabeiella brackebuschiana-Scytophyllum neuburgianum-Rhexoxylon piatnitzkyi* (BNP) Biozone. This biozone differed little in generic representation and relative abundance from the preceding (Middle Triassic) flora, but its inception was marked by the turnover in key species of *Scytophyllum* (Peltaspermales; Plate 13.5f) and *Yabeiella* (?Gnetales) (Morel et al. 2003). Key Gondwanan floras of this age outside South Africa include those of the Blackstone Formation and Red Cliff Coal Measures in Australia (Walkom 1917; Jones and de Jersey 1947; Flint and Gould 1975) and Brady Formation and New Town Coal Measures in Tasmania (Johnston 1886, 1887, 1894, 1896). In Argentina, Carnian floras are known from the Barreal and Cortaderita formations in the Barreal Basin (Bonetti 1963), the Ischigualasto Formation in the Ischigualasto Basin (Archangelsky 1968), the Potrerillos Formation in the Cuyo Basin (Jain and Delevoryas 1967; Spalletti et al. 2005) and the El Tranquilo Group in southern Argentina (Jalfin and Herbst 1995; Crisafulli and Herbst 2011). Additional Carnian floras in South America come from the Quilacoya Member in Chile (Nielsen 2005) and the Santa Maria Formation (Paraná Basin) in Brazil (Barboni and Dutra 2015; Barboni et al. 2016). In Antarctica, the Lashly, Falla and Section Peak formations all possibly extend from the Carnian to the Norian or Rhaetian (Bomfleur et al. 2011b, 2012, 2013a, b, 2014a, b; Escapa et al. 2011).

Palynology is the main tool for dating the Upper Triassic continental successions and half a century of intensive palynological investigations related mainly to hydrocarbon prospecting have resulted in the development of detailed palynostratigraphical schemes particularly for Australia (De Jersey 1975; Helby et al. 1987; Price 1997). As a consequence of the initiation of Pangean break-up and more latitudinally differentiated climate regimes, floristic provincialism became more pronounced in the Late Triassic resulting in two Gondwanan palynofloral provinces and a zone of intermediate or transitional assemblages (Table 13.2). The so-called Ipswich 'Microflora' represents the Late Triassic southern polar vegetation; these temperate floras spanning present-day eastern Australia, New Zealand and most of Antarctica (de Jersey and Raine 1990; Farabee et al. 1990; Zhang and Grant-Mackie 2001). The warm temperate Carnian floras belong to the Onslow 'Microflora' represented and extending across northern Australia (including Timor), along the western Tethys coasts, to westernmost Gondwana. The Onslow Microflora is distinguished by its higher diversity and a greater number of species shared with the Tethyan region. Consequently, different palynostratigraphical zonation schemes exist for these subprovinces (Table 13.2). Importantly, some Australian Carnian successions incorporate shallow marine strata allowing correlation with dinoflagellate, conodont and ammonite zones (Helby et al. 1987).

The Carnian successions in Western Australia are represented by the *Samaropollenites speciosus* Oppel Zone (Helby et al. 1987; Fig. 13.4) and dominated by the *Falcisporites* pollen complex, probably produced by *Dicroidium* (Umkomasiales [=Corystospermales]) plants. This zone is correlated with the *Craterisporites rotundus* Zone (Table 13.2) in deposits of eastern and southern Australia, New Zealand and parts of India and China. The latter zone is defined on the FAD of the nominal taxon and characterised by the high relative abundances of the bisaccate pollen *Falcisporites australis* and the fern spore taxon *Striatella seebergensis.*

Argentinean Carnian continental deposits are world renowned for hosting important vertebrate fossils and a need for accurate dating has spurred interest in palynological studies of these successions. The Paso Flores and Comallo formations in northern Patagonia host assemblages of late Carnian–early Norian age, which are coeval with those of the *Craterisporites rotundus* Oppel Zone of eastern Australia (Zavattieri et al. 1994; Zavattieri and Mego 2008). These assemblages are characterized by the absence of typical Tethyan taxa otherwise present in the Onslow Microflora. However, in the light of new results from the Ischigualasto Formation, this might be re-evaluated by future high-resolution studies. The Ischigualasto Formation is one of the few South American continental Triassic units constrained by reliable radioisotopic dating. Dated beds from near the base and top of the unit yield ages of ~231.4 and ~225.9 Ma, respectively (Rogers et al. 1993; Martínez et al. 2011), placing the formation in the upper Carnian to lower Norian (Fig. 13.3). New palynological results from the Ischigualasto Formation (Césari and Colombi 2016) reveal the presence of typical Tethyan taxa showing that spore-pollen suites from westernmost Gondwana belong to the warm temperate Onslow palynoflora and not to the Ipswich palynoflora (Césari and Colombi 2013). This assignment is evidenced by the presence of pollen and spores previously found only outside Argentina, such as *Cadargasporites granulatus*, *Cycadopites stonei*, *Enzonalasporites vigens*, *Ovalipollis pseudoalatus*, *O. ovalis*, *Patinasporites densus*, *Quadraeculina anellaeformis*, *Samaropollenites speciosus* and *Staurosaccites quadrifidus*.

13.6.2 Norian Floras of the Southern Hemisphere

Although the Norian spans more than 18 million years on the current international chronostratigraphic chart (Cohen et al. 2013), surprisingly few macrofloras of this age have been documented from Gondwana (Table 13.1). In part, this may be a consequence of poor age constraints on many of the assemblages, such that any newly discovered macroflora having broad similarities to that of the Molteno Formation is automatically assigned to the Carnian. Exceptions to this are the macrofloras of the Cacheuta Formation in Argentina (Cuyo Basin: Frenguelli 1948, Morel et al. 2011), the Tiki Formation in India (Maheshwari et al. 1978, Srivastava and Pal 1983; Pal 1984), and the Flagstone Bench Formation in East Antarctica (Cantrill et al. 1995; McLoughlin and Drinnan 1997; McLoughlin et al. 1997). It is possible that part of

the well-studied Blackstone Formation of the Ipswich Basin, eastern Australia, also extends to the Norian based on palynostratigraphic data (de Jersey 1975; Helby et al. 1987). However, Pattemore (2016b) has argued that one of the key assemblages from the Ipswich Basin (the Dinmore assemblage) traditionally assigned to the Blackstone Formation may instead derive from the underlying Tivoli Formation (Carnian). Other plant-rich units across Gondwana may also be of Norian age, based on palynostratigraphic dating, but their macrofossil floras have not yet been investigated in detail. Examples of these include portions of the Leigh Creek Coal Measures preserved within the Copley and Telford basins of central South Australia (Barone-Nugent et al. 2003), the upper part of the Tarong Coal Measures of southern Queensland (Jell 2013; Pattemore 2016a), and the lower part of the Callide Coal Measures of central Queensland (Australia: Jell and McKellar 2013).

Norian macrofossil floras from Gondwana, like those of the Carnian, are dominated by the remains of Umkomasiales and voltzialean conifers. A broad range of accessary gymnosperms, ferns and sphenophytes are also present in these floras. Clubmosses remain scarce as macrofossils, but diverse assemblages of megaspores in strata of this age attest to a rich but cryptic representation of herbaceous heterosporous lycophytes (Dettmann 1961; Cantrill and Drinnan 1994) that, as a group, persisted into the Jurassic as subsidiary elements of the vegetation (McLoughlin et al. 2014). In Argentina, the *Dicroidium odontopteroides-D. lancifolium* (OL) Biozone of Spalletti et al. (1999) probably equates to the Norian. The nominal species reach their acme in this biozone, whereas other Umkomasiales, and most other seed-plants, become subordinate, with the exception of *Yabeiella*, which persisted with equivalent abundance from the preceding biozone (Morel et al. 2003).

The most studied Norian palynological assemblages in Gondwana are those of Australia. There, detailed and well-dated spore-pollen zonation schemes have been tied to dinoflagellate zonations. In eastern Australia, Norian palynofloras are represented by the '*Aratrisporites* Assemblage' which includes the *Polycingulatisporites crenulatus* Zone in its upper part, the same zone that represents this interval in New Zealand (Table 13.2). The base of the *P. crenulatus* Oppel Zone is characterized by the FAD of *P. crenulatus* and a decline in abundance of the previously dominant bisaccate *Falcisporites*, together with a significant increase in *Classopollis* species. In Western Australia, the Norian warm temperate Onslow flora is represented by the *Minutosaccus crenulatus* Oppel Zone (Table 13.2) characterized by a decline in typical Tethyan taxa, such as *Enzonalasporites vigens* and *Samaropollenites speciosus.*

13.6.3 Rhaetian Floras of the Southern Hemisphere

Rhaetian floras are poorly documented from the Gondwanan continents (Table 13.1). Spalletti et al. (1999) attributed latest Triassic floras (Los Colorados Formation and equivalents) of Argentina to their *Dictyophyllum tenuiserratum-Linguifolium arctum-Protocircoporoxylon marianaensis* (DLM) Biozone. They noted the importance of *Linguifolium* and voltzialean conifers associated with the last occurrences of *Dicroidium* in this zone. They also reported initial sporadic occurrences of

cheirolepid conifers, together with osmundacean and dipteridacean ferns of Jurassic aspect in this interval. Other plant fossil assemblages possibly of Rhaetian age occur in Chile (La Ternera and El Puquen floras: Solms-Laubach 1899; Brüggen 1918; Herbst and Troncoso 2000), India (Parsora Formation: Bose 1974; Pal 1985; Ghosh et al. 2016), and eastern Australia (Raceview Formation and Aberdare Conglomerate: Jell 2013; Jell et al. 2013), but precise age constraints are scarce. In general, these floras are consistent with the Argentine assemblages in hosting the last representation of *Dicroidium* and *Linguifolium* before an influx of cheirolepid conifers and bennettitaleans at the Triassic–Jurassic transition. The upper part of the Callide Coal Measures in eastern Australia apparently hosts a rich Rhaetian flora but, to date, only a few species (e.g., *Dicroidium feistmantelii*, *Taeniopteris taeniopteroides*) have been documented (Pattemore 2016b).

Some regions, such as New Zealand and New Caledonia, possibly host Rhaetian floras that are potentially important for understanding the structure of the maritime-influenced vegetation along the Panthalassan margin at the end of the Triassic. However, these floras remain poorly studied and dated. The few Triassic plant remains recorded from New Caledonia are mostly represented by coniferous/pteridospermous fossil woods from the Moindou and Baie de St. Vincent regions (Loubiere 1936; Lanteaume 1950; Boureau 1954, 1955, 1957; Salard 1968; Vozenin-Serra and Salard-Cheboldaeff 1992). The ages of these fossil woods are poorly constrained, although some from the Moindou region are probably Carnian–Norian rather than Rhaetian in age. Others, previously considered Triassic, may be as old as Permian (Vozenin-Serra and Salard-Cheboldaeff 1992). Retallack (1985) described Smithian to Rhaetian floras of the Murihiku Supergroup from the Southland Syncline (Southland) and the Kawhia Syncline (North Island). These constitute mostly fragmentary foliage impressions preserved in marine sediments, but are otherwise similar to coeval assemblages from eastern Australia. A total of 54 plant macrofossil taxa have been identified from the New Zealand Triassic and, as in other Gondwanan regions, the makeup of individual assemblages appears to be strongly influenced by local sedimentary facies and the environmental setting of the parent flora within regional-scale depositional tracts (Retallack 1987).

This dearth of studies on Gondwanan Rhaetian floras is unfortunate given their importance in assessing floristic changes across the Triassic–Jurassic boundary. Palynological data provide the best insights into changes in the vegetation at the close of the Triassic.

Australian and New Zealand Rhaetian palynofloral successions are dominated by *Falcisporites* species and *Densoisporites psilatus* together with a range of ornate trilete spores (Zhang and Grant-Mackie 2001; Akikuni et al. 2010). The appearance of *Classopollis* in the lower part of the local New Zealand stage Otapirian has, traditionally, been used to correlate this stage to the Rhaetian (Marwick 1953). This feature is consistent with the increase in relative abundance in the Circumpolles Group, and specifically *Classopollis*, in the Northern Hemisphere, while many of the characteristic Triassic palynotaxa declined dramatically across the T–J boundary in the New Zealand succession (de Jersey and Raine 1990) as they do globally. The Triassic–Jurassic transition in both Australia and in New Zealand is character-

ized by a marked increase in the proportion of *Classopollis* and *Perinopollenites* pollen and a great decline of *Falcisporites* suggesting that Umkomasiaceae were replaced by Cheirolepidiaceae and Cupressaceae as the dominant arborescent components of the vegetation (Helby et al. 1987; Burger 1994; de Jersey and Raine 1990; Akikuni et al. 2010; de Jersey and McKellar 2013). There were also significant changes in the understorey components of the vegetation evidenced by the loss of several key Triassic fern/bryophyte spore taxa and the replacement among the lycophytes of *Densoisporites* by *Retitriletes* (de Jersey and Raine 1990; Zhang and Grant-Mackie 2001; Akikuni et al. 2010). The regional Rhaetian palynological zonations differ in that the Western Australian zonation scheme includes the transitional Triassic–Jurassic boundary *Ashmoripollis reducta* Oppel Zone (extending through the basal Hettangian; Table 13.2) characterized by the consistent presence of the very distinctive nominal taxon and the FAD of *Zebrasporites interscriptus*. In eastern Australia, the equivalent interval is represented by the upper part of the *Polycingulatisporites crenulatus* Zone and in New Zealand by the *Foveosporites moretonensis* Zone (Table 13.2), representing the local Otapirian stage, and followed by the Hettangian *Retitriletes austroclavatidites* Zone. In both Australian provinces, most of the Hettangian is represented by the *Classopollis torosus* Zone and the differences between New Zealand and Australia are probably due mainly to alternative taxonomic approaches by the palynologists working on the respective floras because the palynofloras from the Hettangian onwards are very similar in Australia and New Zealand and consistently include both *Classopollis* and *Retitriletes* species (Vivi Vajda pers. obs.).

As yet, no study has undertaken a detailed assessment of the contemporaneous plant macrofossil turnover at the T–J transition in Gondwana but, on a broad scale, the dominant elements of the Late Triassic flora (viz., *Dicroidium*, *Lepidopteris*, *Heidiphyllum*, *Linguifolium*, *Dejerseya*, *Yabeiella*) are entirely absent from the Early Jurassic floras (Hill et al. 1999; Anderson et al. 1999). They are replaced in the Early Jurassic by floras dominated by scale-leafed cheirolepid and araucarian conifers, Bennettitales, Caytoniales and Pentoxylales (Gould 1975; Tidwell et al. 1987; McLoughlin and Hill 1996; Bromfield et al. 2007; McLoughlin and Pott 2009; Bomfleur et al. 2011a; Pattemore 2016b). This change attests to a major extinction and reorganization of plant communities around the Triassic–Jurassic boundary, a change also apparent in the palynofloras (Helby et al. 1987). From this time onwards until the rapid fragmentation of Gondwana in the Cretaceous, a world emerges with a more homogenous (cosmopolitan) flora.

13.7 Discussion

13.7.1 Climate Considerations

The climate of the Triassic in a general sense was warm with dry continental interiors and no polar icecaps. The aggregation of the Pangaean supercontinent (Figs. 13.1 and 13.6), which was completed during the Triassic, gave rise to a strong global

monsoon regime (e.g., Robinson 1973; Mutti and Weissert 1995; Loope et al. 2004; Wang 2009). This generated three broad climatic regions with ill-defined latitudinal distributions. The tropical belt spanning the western margin of the Tethys Ocean and the central part of Pangaea, together with the horse latitudes (those atmospheric zones typified by subtropical highs) were characterized by a broad arid belt with dry conditions persisting throughout the entire year (Preto et al. 2010). The coasts of eastern Laurussia, Gondwana and the western coasts of Pangaea would have been subjected to seasonally wet and dry periods (Parrish and Peterson 1988; Dubiel et al. 1991; Mutti and Weissert 1995) and the more polar areas by warm and wet climates (evidenced by palaeosols and fossil floras up to 85°N and S; Robinson 1973; Taylor 1989; Retallack 1999; Kidder and Worsley 2004). However, other authors have suggested a more pronounced zonal climatic pattern with a narrow equatorial humid zone, an arid belt extending up to 30° and, beyond that, northwards and southwards humid temperate climates (e.g., Kent and Olsen 2000; Olsen and Kent 2000).

Climatic oscillations were superimposed on the general climate belts during the 50 million years of the Triassic. Humid episodes were experienced throughout the Triassic with the most pronounced documented during the Carnian. The increase in rainfall during the 'Carnian Pluvial Event' (CPE), documented worldwide, constitutes the most distinctive climate change within the Triassic (Gianolla et al. 1998; Hochuli and Frank 2000; Preto and Hinnov 2003; Hornung and Brandner 2005; Hochuli and Vigran 2010). This contributed to a suite of environmental changes and biotic turnover (Simms and Ruffel 1989, 1990; Simms et al. 1995) including an increase in deposition of coarse siliciclastics in the western Tethys (e.g., Schilfsandstein) and the development of coal seams (e.g., Lunz, Svalbard, Skåne, Australia, South Africa; e.g., Köppen and Wegener 1924). The different hypotheses providing a causal mechanism for this event include changes in atmospheric or oceanic circulation driven by plate tectonics (Hornung and Brandner 2005), a peak of the global monsoon due to maximum continental aggregation (Parrish 1993; Colombi and Parrish 2008) or triggering by the eruption of a large igneous province (e.g., Furin et al. 2006; Greene et al. 2009a, b; Preto et al. 2010 and ref. therein). The remainder of the Late Triassic seems to have been climatically stable. The trend from humid to arid observed, for example, in the Newark Basin, has been attributed to the northwards drift of the North American continent (Smoot and Olsen 1988; Kent and Olsen 2000; Olsen and Kent 2000). In contrast, the abrupt change from a humid climate to an arid climate in the desert southwest of the United States during the lower Norian Stage is thought by some to be the result of orogeny and elevation changes brought about by the uplift of the Cordilleran magmatic arc in eastern California (Nordt et al. in). However, some other indications exist for minor or regional climatic changes. This includes the shift from red-beds rich in gypsum or other aridity indices to plant-rich and coal-bearing paralic sediments in the early to mid-Rhaetian (Hallam 1985) as well as small late Carnian (Mazza et al. 2010; Tanner and Lucas 2007) and late Norian climate changes (Berra et al. 2010; Haas et al. 2012). The end-Triassic biotic crisis appears to have occurred at a time of relatively high humidity, especially in the northern Tethyan realm (Preto et al. 2010), in

northern Europe (Vajda and Wigforss-Lange 2009) and in southern Gondwana based on the distribution of fluvial and paludal strata (Turner et al. 2009).

13.7.2 Floristic Provincialism

The Permian world initiating at the peak of the Late Palaeozoic Ice Age and terminating with marked global warming (Fielding et al. 2008) was characterized by strong floristic provincialism (Meyen 1987). That provincialism apparently became less pronounced after the end-Permian mass extinction. Essentially two floral provinces remained (Fig. 13.6), the Gondwana Province encompassing all regions in the Southern Hemisphere (together with at least part of the Cimmerian rifted terranes), and the Laurussian Province spanning the continental masses of the Northern Hemisphere, e.g. North America, Europe and Asia including China (Dobruskina 1994; Vakhrameev et al. 1970, 1978). An equatorial belt encompassing the northern regions of Gondwana (i.e., northern South America, North Africa and Arabia; Fig. 13.6) has yielded very little data with respect to Late Triassic plant macrofossils. This region provides considerable scope for future palaeobotanical research that will have a strong bearing on our understanding of the degree of taxonomic mixing between the two major floristic provinces of the Late Triassic.

The Late Triassic floras of the southern landmasses are rather uniform (see above), whereas the vegetation in the Northern Hemisphere was less homogeneous. Consequently, several floristic subprovinces are apparent in the latter region (Fig. 13.6), although linked by broad areas hosting mixed or 'transitional' floras. A North Atlantic sub-province was proposed for the coastal plains of southern Sweden (Skåne), eastern Greenland (Jameson Land) and northern central Europe (Poland: Reymanówna 1963; Harris 1926, 1931b; Pott and McLoughlin 2009; Pott 2014a). This subprovince was originally recognized based on Rhaetian floras, but was probably already established during the Carnian (Pott 2014b).

Vakhrameev et al. (1970, 1978) and Krassilov and Shorokhova (1975) divided Eurasia into two palaeolatitudinally distinct Late Triassic floristic regions that became more distinct during the Norian–Rhaetian. The northern area (Siberian palaeoprovince or Arctotriassic geoflora = Siberian Subprovince herein) was characterized by an extra-tropical, temperate climate and dominated by *Phoenicopsis*. The more southern, subtropical areas (historically referred to the European-Sinian palaeoprovince or Mediotriassic geoflora) were dominated by *Lepidopteris* and *Goeppertella*. Dobruskina (1994) proposed dividing these two floristic subprovinces into three zones or sectors delimited by longitude: (i) European (=North Atlantic/Central European Subprovince), (ii) Middle Asian (=Middle Asian Subprovince) and (iii) East Asian (=East Asian Subprovince) sectors. She considered these sectors to be centres of dominance or emergence and spread of the most important Late Triassic plant groups. The Middle-Asian Subprovince includes the Donets Basin, Fore-Caucasus, Kazakhstan and Southern Fergana, Southern Urals and Caspian Depression (Fig. 13.6) and is characterized by the dominance of pelta-

sperms, presence of marattiacean ferns and Cycadocarpidiaceae and a lack of Dipteridaceae. The Siberian Subprovince (Fig. 13.6) comprises the Pechora Basin, Eastern Urals, and Eastern and Northern Siberia (Dobruskina 1994). The Northern and Southern East Asian subprovinces (Primorye included; Fig. 13.6) are characterized by numerous dipteridacean ferns and cycadocarpidiacean conifers during the Carnian; marattiacean ferns and peltaspermalean seed ferns are virtually absent from the East Asian sector. The North American continent is divided into the Chinle/Dockum Subprovince, the Arctic Canada Subprovince (with some shared characters with the Siberian floras), and the floras of the Newark Supergroup Subprovince (Fig. 13.6), which have characteristics shared with both the North Atlantic/Central European Subprovince and the Chinle/Dockum Subprovince.

Sun (1987, 1993) divided China into three Late Triassic floristic subprovinces based on the taxonomic composition and palaeogeographic position of the various floras. The Northern Floristic Region (=Northern East Asia Subprovince) corresponds to vegetation (*Danaeopsis-Bernouillia* [=*Symopteris*] flora) occupying the subtropical–temperate zone or the coastal temperate zone with a warm and humid climate. It comprises floras from more than 20 localities in northern China, including Yanchang of Shaanxi, Tianzhu of Gansu (Sze 1960), Muriof Qinghai (He 1980), Xiaoquangou (Hu and Gu 1987), Manas and Haojiagou of Xinjiang (Sze 1956b; Deng et al. 2001), and Xiaohekou of Jilin. Typical Northern East Asia Subprovince plants are *Glossophyllum*, *Danaeopsis*, *Bernouillia* (=*Symopteris* Plate 13.4d, g) and *Sphenobaiera*. The boundary with the Southern East Asia Subprovince lies roughly along the line of the South Tianshan Qinling-Dabie Mountains (Fig. 13.6). The Southern East Asia Subprovince covers almost the entirety of southern China (except for southern Tibet) and southern Northwest China. More than 30 localities have yielded floras of this type in southern China, including Baoding and Xujiahe in Sichuan, Yipinglang in Yunnan (Li et al. 1976), Baqen-Amdo in eastern Tibet (Wu and Pu 1982), Shazhengxi in Hubei (Wu et al. 1980), Shaqiao in Hunan (Zhou 1989), Dakeng-Wenbinshan in Fujian (Zhou 1978), Jieza in Yushu (Qinghai: He 1980) and the Tianqiaoling flora of Jilin (Sun 1979, 1981, 1993). The Tianqiaoling flora closely resembles the Nariwa and Yamaguchi floras of Japan (Norian or Carnian–Norian), and the Mongugai flora of Primorye, Russia (Carnian–Norian). This may be related to the fact that it was palaeogeographically close to the Japanese localities during the Triassic (Wang et al. 1986; Zhang 1990; Shao et al. 1992; Yin and Ling 1986; Sun 1979, 1981, 1987, 1990, 1993) but later became separated and drifted northwards. The plant remains of the Southern East Asia Subprovince (*Dictyophyllum-Clathropteris* flora) reflect a rich tropical–subtropical vegetation (more than 80 genera and 160 species), although there are some differences in the composition of assemblages between the eastern and western parts of the region. This flora is dominated by cycads/bennettitaleans (*Anomozamites*, *Anthrophyopsis*, *Ctenis, Ctenozamites*, *Cycadocarpidium*, *Drepanozamites*, *Doratophyllum*, *Nilssonia*, *Nilssoniopteris*, *Otozamites*, *Pseudoctenis*, *Pterophyllum*) and dipteridacean ferns (*Abropteris*, *Clathropteris*, *Dictyophyllum*, *Goeppertella*, *Thaumatopteris*, *Yungjenophyllum*). Seed ferns (e.g., *Ptilozamites*) are rare.

The Yarlung-Zangbo-River Subprovince (Fig. 13.6) is represented by plant assemblages from the coal-beds of the Norian Lanjixue Group of Xiukang near Lhasa, south of the Yarlung Zangbo River (Sun 1993). Palaeogeographically, this area belonged to the Gondwanan Province during the Late Triassic (24.3°S), and the plant remains are affiliated with Gondwanan assemblages dominated by *Pagiophyllum*, *Elatocladus* and *Dicroidium* (Sukh-Dev 1987). In the transition zone between the Northern East Asia Subprovince and Southern East Asia Subprovince there is also a belt of mixed floras, such as the Xiaoquangou flora of Xinjiang, the Xujiahe, Baoding and Wolunggang floras and the Nanzhang flora of western Hubei (Hu 1986; Hu and Gu 1987). These floras contain a mixture of 'Northern-type' elements, such as *Asterotheca*, *Bernouillia* (= *Symopteris*), *Danaeopsis*, *Glossophyllum*, *Neocalamites, Thinnfeldia* and *Todites*, and 'Southern-type' elements, such as *Dictyophyllum* and *Hausmannia* (Meng 1983, 1992; Chen et al. 1979a, b, c, 1985). The existence of these mixed floras suggests that northern China was probably connected with southern China from the early Late Triassic onwards. The Tethys Ocean probably remained only to the south of the western Qinling Mountains, and regressed by the end of Late Triassic, giving origin to huge tracts of exposed land facilitating the migration and mixing of plants from the Northern and Southern East Asia subprovinces.

Two Late Triassic palynofloral provinces have been defined for China; the North and South China provinces, first defined by Qu et al. (1983) and subsequently described by many authors (see Peng et al. 2017b and references therein). The South China province is characterized by the presence of key taxa, such as *Ovalipollis*, *Rhaetipollis* and *Camerosporites*. The North China Province is typified by Late Triassic cosmopolitan taxa, such as *Apiculatisporis* and *Striatella seebergensis* along with *Ovalipollis* and *Kyrtomisporites* (Peng et al. 2017b). The presence of *Ricciisporites* has been claimed for both Provinces but, so far, no illustrations have been presented.

During the Late Triassic, Pangea began its initial fragmentation segregating the Northern and Southern Hemisphere landmasses divided by the broad Tethys Ocean. In addition, the broad latitudinal spread of the landmasses by the Carnian, imposed significant floral provincialism (Buratti and Cirilli 2007). The Gondwana Province is generally divided in two subprovinces (Fig. 13.6), based mostly on differences in palynomorph assemblages. This Late Triassic provincialism has necessitated the establishment of separate palynological zonation schemes in Western and eastern Australia (Table 13.2): the southeastern Australian 'Ipswich-type' (=Ipswich Subprovince) and northwestern Australian 'Onslow-type' (=Onslow Subprovince) floras (Dolby and Balme 1976) with a few intervening 'mixed' or 'intermediate' palynofloras (Foster et al. 1994). The Onslow Subprovince generally has a slightly higher diversity and includes a greater proportion of equatorial (European) taxa. The lower-diversity Ipswich Subprovince is dominated by *Falcisporites* (Umkomasiales) species. These two subprovinces can be traced across Gondwana and appear to have been constrained by palaeolatitude (Dolby and Balme 1976; Césari and Colombi 2013). The Ipswich Subprovince is distributed from about 90° to 40°S palaeolatitude, whereas the Onslow Subprovince flanked the Tethyan mar-

gin of Gondwana, extending to central South America at palaeolatitudes of around 45° to 20°S (Fig. 13.6). The contrasting compositions of the palynofloristic subprovinces probably reflect the Onslow Subprovince's proximity to the Laurussian Province (facilitating floristic interchange) and warmer climates supporting higher plant diversity. The Ipswich Subprovince appears to have hosted cooler and perhaps more humid climates supporting umkomasialean-dominated deciduous-forest biomes. Although this latitudinally defined provincialism is marked in the palynofloras, no such distinct variations have yet been recognized in the plant macrofossil floras.

However, it is possible that the contrasting opinions concerning the age of some Gondwanan fossil floras, e.g., that of the Parsora Formation of central India treated as Early Jurassic by Mukherjee et al. (2012) but Norian–Rhaetian by Ghosh et al. (2015, 2016), relate to equatorial influences endowing the composition of the flora with an apparently younger aspect than its true age. Within the Triassic Gondwanan Province, local palaeoenvironmental changes also imposed significant influences on the vegetation structure and, together with taphonomic sorting, played an important role in determining the composition of individual plant fossil assemblages (Retallack 1977; Cairncross et al. 1995; Anderson et al. 1998; Spalletti et al. 2005). Retallack (1977) noted several contrasting plant-community associations in the Triassic of eastern Australia that potentially obscure straightforward biostratigraphic signals based on taxon ranges in the plant fossil assemblages. Moreover, Spalletti et al. (2005) recognized 16 macrofloral taphocenoses representing diverse combinations of gymnosperm and pteridophyte taxa with various taphonomic influences within the continental Upper Triassic Potrerillos Formation of Argentina. In a similar manner, Cairncross et al. (1995) linked fossil faunal and floral associations with sedimentological data to interpret palaeoenvironmental settings that were eventually developed into seven habitat (mostly plant community) reconstructions for the Molteno Formation (South African) biotas (Anderson et al. 1998). These habitats ranged from riparian forests and sandbar meadows to floodplain woodlands and marsh communities. Given the taxonomic similarities evident in plant macrofossil assemblages across the Southern Hemisphere, equivalent discrete palaeocommunities to those of the Molteno Formation biotas were probably represented throughout Gondwana during the Late Triassic.

13.7.3 Animal-Plant Interactions

The study of arthropod-plant-fungal interactions has become a burgeoning field of research in recent years. Consequently, many more examples of biotic linkages in Triassic continental fossil assemblages are likely to be forthcoming in the near future. Prior to the 1980s there were few reports of feeding damage or oviposition scars on Triassic plants from Gondwana. Subsequent reports, have come from all major regions of the supercontinent (Wappler et al. 2015). By the Late Triassic, insect faunas appear to have recovered from the end-Permian mass extinction, with a major expansion of herbivory in Gondwana. Preliminary results indicate that the Late Triassic radiation of arthropod herbivores targeted a broad range of plants

including ferns, seed ferns, cycads/bennettitaleans, ginkgophytes, gnetaleans and conifers and was essential in the trophic modernization of terrestrial plant-animal interactions especially in external foliage feeding, piercing-and-sucking, galling, leaf mining and seed predation (Labandeira 2006). For terrestrial ecosystems, most of the functional feeding groups (FFG) had been established by the Pennsylvanian but all were clearly present in the early Late Triassic, when the herbivores of land plants became trophically modern (Labandeira 2006). Key evidence of interactions has come from the Molteno Formation (Carnian, South Africa), where 79 damage types were identified on around 220 plant taxa including liverworts, lycophytes, sphenophytes, ferns, peltasperms, umkomasialeans, hamshawvialeans, ginkgophytes, cycads, bennettitaleans, voltzialean conifers and gnetaleans (Anderson and Anderson 1983, 1985, 2003; Scott et al. 2004; Labandeira and Anderson 2005). Other fossil floras have provided evidence of specialized feeding traits or egg-laying strategies. For example, galls and oviposition damage have been reported on a range of ferns, conifers, Umkomasiales and cycads/bennettitaleans from the Blackstone Formation (Carnian) of Australia (Tillyard 1922; Webb 1982), La Ternera and Las Breas formations (probable Rhaetian) of Chile (Gallego et al. 2003, 2004; Gnaedinger et al. 2007, 2008, 2014) and the Parsora Formation (Rhaetian) of India (Ghosh et al. 2015). Adami-Rodrigues et al. (2008) reported various complex herbivory patterns of fossil leaves from the Laguna Colorado Formation (Norian) of Argentina. Rozefelds and Sobbe (1987) and McLoughlin (2013) illustrated early mining traces on *Heidiphyllum* (conifer) and *Ginkgoites* leaves from the Blackstone or Tivoli Formation of Australia. Archangelsky and Brett (1961) identified putative arthropod boring traces and frass within *Rhexoxylon* (Umkomasiales) wood from the Ischigualasto Formation of Argentina. Finally, we illustrate (Plate 13.5b) an additional form of probable piercing-and-sucking damage on *Heidiphyllum* (conifer) leaves from an unspecified Upper Triassic deposit in the Transantarctic Mountains, Antarctica. Many of these same feeding and egg-laying strategies persisted beyond the end-Triassic mass extinction into the Jurassic of the Southern Hemisphere, albeit associated with new plant groups in many cases (McLoughlin et al. 2015). In addition, various forms of interactions between seed-plants and fungi have been detected in Middle to Late Triassic woods and leaves from Antarctica (Stubblefield and Taylor 1986; Bomfleur et al. 2013a; Harper et al. 2016).

Evidence of Late Triassic plant-animal interactions are not restricted to the Southern Hemisphere, although they are less well described from Northern Hemisphere assemblages. In North America, only a few plant fossil assemblages of the Chinle Formation (Norian) in the desert southwest of the United States have yielded plant-insect interactions. This evidence consists of empty and frass-filled tunnels and chambers in petrified wood (Walker 1938; Ash 2000; Creber and Ash 2004; Lucas et al. 2010) and several types of leaf damage, including marginal and non-marginal feeding traces and leaf galls (Ash 1997, 1999, 2000, 2001, 2014; Ash and Savidge 2004). Several more irregular patterns of degradation in these woods were generated by fungal degradation (Tanner and Lucas 2013).

Few Late Triassic plant assemblages of Europe have been analysed for plant-animal interactions. One of these few examples is the deposition of insect (probable

odonatan) eggs and ovipositional damage on bennettitalean leaves from the Carnian flora of Lunz, accompanied by mining-structures, and marginal and non-marginal feeding traces on *Nilssoniopteris* leaves (Pott et al. 2008c; Meller et al. 2011; Wappler et al. 2015). Borings in *Dadoxylon* woods and possible oviposition scars on *Equisetites* have been mentioned from the Carnian of Germany (Linck 1949; Roselt 1954; Grauvogel-Stamm and Kelber 1996; Wappler et al. 2015). Possible oviposition scars on *Podozamites* were also indicated from the Rhaetian of Sweden (Nathorst 1876a, 1878b; Wappler et al. 2015). A very special type of plant-animal interaction is represented by the arthropods (nematoceran fly and mites) and microorganisms that were discovered in the Carnian amber of the Dolomites (Roghi et al. 2005; Schmidt et al. 2006, 2012) and of Germany (Schönborn et al. 1999).

Few studies have been carried out on arthropod-plant-fungal interactions in the Late Triassic fossil biotas of the North Atlantic sector (Greenland, Sweden and Svalbard). Pott and McLoughlin (2009) reported indentations in the adaxial cuticle of *Anomozamites angustifolium* leaves from the Rhaetian of Skåne that might represent wound callouses of piercing-and-sucking insects. Steinthorsdottir et al. (2015) documented putative odonatan endophytic oviposition scars referable to the ichnogenus *Paleoovoidus* on ginkgoalean (*Ginkgoites*, *Sphenobaiera*, *Baiera*) leaves across the Triassic–Jurassic transition in East Greenland. They noted that examples of such leaf damage are more abundant below than above the Triassic–Jurassic transition, possibly reflecting a turnover in insect faunas at the close of the Triassic. McLoughlin and Strullu-Derrien (2016) documented interactions of chytrid fungi and bacteria infecting some parenchymatous bennettitalean root cells in a silicified peat from Hopen, Svalbard. Various other fungi and fungi-like remains are scattered through the detrital matrix of this peat. Cavities excavated through some roots (especially cortical cells) and through patches of compacted plant detritus contain abundant coprolites that were probably produced by sapro-xylophagous oribatid mites (Strullu-Derrien et al. 2012). A few larger coprolites containing leaf fragments attest to the presence of unidentified invertebrate folivores in the Carnian ecosystem of Hopen (McLoughlin and Strullu-Derrien 2016).

Vasilenko (2009) reported an assemblage of damaged leaves and stems from the Madygen flora of southern Fergana. The assemblage includes leaf mines, traces of feeding on leaf tissues (margin feeding), and traces of damage of ambiguous nature (some of them may be insect-eggs). The author considered the diversity of damage types at Madygen similar to known associations of damage traces from the Triassic of Germany and South Africa (Vasilenko 2009). Moisan et al. (2012a) identified and illustrated odonatan (dragonfly) oviposition scars on leaves of two lycopsid species of *Isoetites* from Madygen. Plant-animal interactions in the Late Triassic floras of China are rare but crescentic bite marks on *Mixopteris* and intense skeletonization of *Dictyophyllum* fronds were described from the Late Triassic strata of Yunnan Province (Hsü et al. 1974; Feng et al. 2014). The plant-animal interactions documented so far indicate that the diversity in damage types was vastly greater than had been described in the twentieth century, and was probably higher than that recognized for the Permian and Early Jurassic (Vasilenko 2009; Wappler et al. 2015).

13.8 Concluding Remarks

The transition from palaeophytic plant assemblages (Korvunchana/*Pleuromeia* flora) to mesophytic ones (*Scytophyllum*, *Lepidopteris* and *Thaumatopteris* floras) occurred during the Ladinian and Carnian in many areas (Kryshtofovich 1957; Meyen 1970; Dobruskina 1988). Indeed, several Palaeozoic *bauplans*, such as the arborescent sphenophytes (*Equisetites*) and the winged seeds (*Fraxinopsis*, *Samaropsis*) are still represented in the Late Triassic plant assemblages. Key plant groups, such as the Bennettitales, Gnetales and modern fern and conifer (Pinaceae, Taxodiaceae, Araucariaceae, Cheirolepidiaceae) families, originated during this span of time. Further, some enigmatic plants putatively related to angiosperms (e.g., *Furcula*, *Imania*, *Marcouia*, *Phylladelphia*, *Sanmiguelia*) developed during the Late Triassic although superficially angiosperm-like pollen grains have been described from strata as old as the Middle Triassic (Hochuli and Feist-Burkhardt 2013; Herendeen et al. 2017).

Although the Late Triassic saw important evolutionary innovations and plant diversification, our understanding of floristic change is constrained by the geographically and stratigraphically irregular distribution of fossil assemblages. Norian floras, for example, are rare and relatively uniform in Europe but floras of this age are the best-represented of the Late Triassic floras in North America. Rhaetian floras, on the other hand, are apparently absent from North America but are widespread and host diverse taxa in Europe and Greenland. In several areas, such as Russia and Gondwana, it is difficult to distinguish between Norian and Rhaetian floras with confidence. Our understanding of the change in diversity and composition of the plant communities through the Late Triassic, thus, remains at an early stage of development and great opportunities exist for future researchers to document additional fossil assemblages from poorly sampled regions and stratigraphic intervals, and to integrate the available data into regional syntheses of plant evolution, phytogeography and palaeoclimatology. The composition of the various fossil assemblages show that the Triassic floras are indeed much more homogeneous than those of the Permian on a global scale. Although several floristic provinces and subprovinces have been recognized by various authors, our global analysis identifies just two major provinces: Gondwana and Laurussia (Fig. 13.6). Within these provinces, variations in taxonomic representation and group abundance were mainly imposed by climatic and regional environmental conditions, and these define several floristic subprovinces (Fig. 13.6, Table 13.1), typically with diffuse boundaries. Similar regional variations are evident in the palynofloras (Table 13.2) and, together with diachronous inceptions of some key taxa, this has necessitated the establishment of numerous regional palynostratigraphic schemes (Table 13.2).

Finally, we note that many plant families and genera were widely distributed in the Late Triassic, at least in the respective hemispheres. The fact that it is still difficult to distinguish between Norian and Rhaetian floras (e.g., within Asia and Gondwana) based on family- or genus-level floral composition, that the Chinle-Dockum (Carnian) flora and the Newark (Carnian–Norian) flora share many taxa,

and that the Primorye flora is very similar to the floras of Tonkin, Japan and the German Keuper shows how closely related the regions are at higher taxonomic levels. A clearer picture of phytogeographic relationships and levels of endemism will likely emerge with improved systematic appraisal of the floras and when area relationships are analysed at species-level.

Acknowledgements We want to thank Lawrence (Larry) Tanner for the organization of this book as well as Brian Axsmith and Spencer Lucas for their constructive reviews. Part of the material was studied by Evelyn Kustatscher under the projects 'Taxonomic revision of the Carnian (Upper Triassic) conifers from the historical Raibl flora from Northern Italy' (AT-TAF2999) and 'Palaeozoic relict and "modern" Mesozoic ferns in the Ladinian and Carnian floras of Europe' (DE-TAF239, AT-TAF236, SE-TAF149), which received funding through SYNTHESYS, which was made available by the European Community-Research Infrastructure Action under the FP7 'Structuring the European Research Area' Programme. Evelyn Kustatscher acknowledges also financial support from the Alexander von Humboldt-Foundation (3.3-ITA/1141759STP). This paper is also part of the IGCP 630 cooperation project 'Permian-Triassic climatic and environmental extremes and biotic response'. Eugeny Karasev thanks E.B. Volynets (Institute of Biology and Soil Sciences) for photos of fossil plants from the Late Triassic of Primorye. Eugeny Karasev received funding from the subsidy allocated to Kazan Federal University (#5.2192.2017/4.6) for the state assignment in the sphere of scientific activities. Christian Pott acknowledges funding from the German and Swedish Research Councils (DFG KR2125/3, VR 2012-4375) and from the 'Friends of the Swedish Museum of Natural History' (Riksmusei Vänner, Stockholm) and funding through SYNTHESYS (AT-TAF 467). Vivi Vajda acknowledges support from UNESCO grant IGCP 632 and the Swedish Research Council grant VR 2015-4264. Financial support to Stephen McLoughlin by the Swedish Research Council (VR grant 2014-5234) and National Science Foundation (project #1636625) is gratefully acknowledged.

References

Achilles H (1981) Die Rhaetische and Liassische Microflora Frankens. Palaeontographica B 179:1–86

Adami-Rodrigues K, Gnaedinger S, Gallego OF (2008) Registro de interações inseto-planta do grupo El Tranquilo (Triássico Superior) Provincia de Santa Cruz, Patagonia Argentina [Abstract 1]. In: Boardman DR (ed) Simpósio Brasileiro de Paleobotânica e Palinologia Boletim de Resumos. Florianópolis, Asociación Latinoamericana de Paleobotánica y Palinología 1:482

Akagi T (1954) On the Triassic Plants from the Homgay Coalfield, in Tonkin, Indo–China. Natural Science Report, Oehanomizu Univ 5(1):153–174

Akikuni K, Hori R, Vajda V et al (2010) Stratigraphy of Triassic–Jurassic boundary sequences from the Kawhia coast and Awakino gorge, Murihiku Terrane, New Zealand. Stratigraphy 7:7–24

Anderson JM, Anderson HM (1983) Palaeoflora of southern Africa, Molteno Formation (Triassic) 1. (Part 1. Introduction; Part 2. *Dicroidium*). A.A. Balkema, Rotterdam

Anderson JM, Anderson HM (1985) Palaeoflora of southern Africa. Prodromus of South African megafloras Devonian to Lower Cretaceous. A.A. Balkema, Rotterdam

Anderson JM, Anderson HM (1989) Palaeoflora of southern Africa, Molteno Formation (Triassic) 2. Gymnosperms (excluding *Dicroidium*). A.A Balkema, Rotterdam

Anderson JM, Anderson HM (2003) Heyday of the gymnosperms: systematics and biodiversity of the Late Triassic Molteno fructifications. Strelitzia 15:1–398

Anderson HM, Anderson JM (2008) Molteno ferns: Late Triassic biodiversity in southern Africa. South African National Biodiversity Institute, Pretoria. Strelitzia 21:1–258

Anderson HM, Anderson JM (in press) Molteno sphenophytes: Late Triassic biodiversity in southern Africa. Paleontologia Africana
Anderson HM, Anderson JM, Cruickshank ARI (1998) Late Triassic ecosystems of the Molteno/Lower Elliot biome of southern Africa. Palaeontology 41:387–421
Anderson JM, Anderson HM, Archangelsky S et al (1999) Patterns of Gondwana plant colonisation and diversification. J Afr Earth Sci 28:145–167
Archangelsky S (1968) Studies on Triassic fossil plants from Argentina. IV. The leaf genus *Dicroidium* and its possible relation to *Rhexoxylon* stems. Palaeontology 11:500–512
Archangelsky S, Brett DW (1961) Studies on Triassic fossil plants from Argentina. I. *Rhexoxylon* from the Ischigualasto Formation. Phil Trans R Soc Lond B 244:1–19
Arche A, Lopez-Gomez JL (2014) The Carnian Pluvial Event in Western Europe: new data from Iberia and correlation with the Western Neotethys and Eastern North America–NW Africa regions. Earth-Sci Rev 128:196–231
Artabe AE, Morel EM, Spalletti LA (2003) Caracterización de las provincias fitogeográficas triásicas del Gondwana extratropical. Ameghiniana 40:387–405
Ash SR (1969) Ferns from the Chinle Formation (Upper Triassic) in the Fort Wingate area, New Mexico. U.S. Geol Surv Prof Paper 613D:1–40
Ash SR (1975) *Zamites powelli* and its distribution in the Upper Triassic of North America. Palaeontographica 149B:139–152
Ash SR (1986) First record of the Gondwana plant *Schizoneura* (Equisetales) in the Upper Triassic of North America. In: Weber R (ed) 3d Congreso Latinoamericano Paleontologia, Simposio sobre flores del Triasico Tardio su fitogeografia y paleoecologia. Universidad Nacional. Autonoma Mexico, Instituto Geologia, Memoria, pp 59–65
Ash SR (1989) A catalog of Upper Triassic plant megafossils of the western United States through 1988. In: Lucas SG, Hunt AP (eds) Dawn of the age of dinosaurs in the American Southwest. New Mexico Museum of Natural History, Albuquerque, pp 189–222
Ash SR (1997) Evidence of arthropod-plant interactions in the Upper Triassic of the southeastern United States. Lethaia 29:237–248
Ash SR (1999) An Upper Triassic *Sphenopteris* showing evidence of insect predation from Petrified Forest National Park, Arizona. Int J Plant Sci 160:208–215
Ash SR (2000) Evidence of oribatid mite herbivory in the stem of a Late Triassic tree fern from Arizona. J Paleontol 74:1065–1071
Ash SR (2001) New cycadophytes from the Upper Triassic Chinle Formation in the southwestern United States. PaleoBios 21:15–28
Ash SR (2005) A new Upper Triassic flora and associated invertebrate fossils from the basal beds of the Chinle Formation, near Cameron, Arizona. PaleoBios 25:17–34
Ash SR (2011) Anomalous occurrence of the Gondwanan winged seed *Fraxinopsis* in a new Late Triassic (Norian) flora from west Texas, USA. Rev Palaeobot Palynol 166:94–106
Ash SR (2014) Contributions to the Upper Triassic Chinle flora in the American southwest. Palaeobiogeogr Palaeoclimatol Palaeoecol 94:279–294
Ash SR, Basinger JF (1991) A high latitude Upper Triassic flora from the Heiberg Formation, Sverdrup Basin, Arctic Archipelago. Contrib Can Paleont Geol Surv Canada Bull 412:101–131
Ash SR, Hasiotis ST (2013) New occurrences of the controversial Late Triassic plant fossil *Sanmiguelia* Brown and associated ichnofossils in the Chinle Formation of Arizona and Utah. N Jb Geol Paläont Abh 268(1):65–82
Ash SR, Savidge RA (2004) The bark of the Late Triassic *Araucarioxylon arizonicum* tree from the Petrified Forest National Park, Arizona. IAWA J 25:349–368
Ash SR, Litwin R, Traverse AT (1982) The Upper Triassic fern *Phlebopteris smithii* (Daugherty) Arnold and its spores. Palynology 6:203–219
Axsmith B (1989) Upper Triassic *Dinophyton* Zone plant fossils from the Stockton Formation in southeastern Pennsylvania. The Mosasaur. J Delaware Valley Paleont Soc 4:45–47
Axsmith B, Taylor TN, Delevoryas T et al (1995) A new species of *Eoginkgoites* from the Upper Triassic of North Carolina, USA. Rev Palaeobot Palynol 85:189–198

Axsmith B, Taylor TN, Fraser NC et al (1997) An occurrence of the Gondwanan plant *Fraxinopsis* in the Upper Triassic of eastern North America. Mod Geol 21:299–308

Axsmith B, Krings M, Taylor TN (2001) A filmy fern from the Upper Triassic of North Carolina (USA). Am J Bot 88:1558–1567

Axsmith B, Fraser NC, Corso T (2013) A Triassic seed with an angiosperm-like wind dispersal mechanism. Palaeontology 56:1173–1177

Barbacka M (1991) *Lepidopteris ottonis* (Goepp.) Schimp. and *Peltaspermum rotula* Harris from the Rhaetian of Poland. Acta Palaeobot 31:23–47

Barbacka M, Pacyna G, Ziaja J et al (2012) The new type of Late Triassic ovulate scales associated with *Brachyphyllum*-like leaves. In: Nishida H, Saito T, Takahara H (eds) 13th International Palynological Congress, 9th International Organisation of Palaeobotany Conference, Japanese Journal of Palynology, 58(special volume):11

Barboni R, Dutra TL (2015) First record of *Ginkgo*-related fertile organs (*Hamshawvia*, *Stachyopitys*) and leaves (*Baiera*, *Sphenobaiera*) in the Triassic of Brazil, Santa Maria formation. J South Am Earth Sci 63:417–435

Barboni R, Dutra TL, Faccini UF (2016) *Xylopteris* (Frenguelli) Stipanicic and Bonetti in the Middle–Upper Triassic (Santa Maria Formation) of Brazil. Ameghiniana 53:599–622

Barone-Nugent E, McLoughlin S, Drinnan AN (2003) Two new species of *Rochipteris* from Upper Triassic (Carnian–Norian) strata of the Leigh Creek and Ipswich basins, Australia. Rev Palaeobot Palynol 123:273–287

Barth G, Franz M, Heunisch C et al (2014) Late Triassic (Norian–Rhaetian) brackish to fresh water habitats at a fluvial–dominated delta plain (Seinstedt, Lower Saxony, Germany). Palaeobiodiv Palaeoenviron 94:495–528

Batten DJ, Koppelhus EB (1996) Biostratigraphic significance of uppermost Triassic and Jurassic miospores in Northwest Europe. In: Jansonius J, McGregor DC (eds) Palynology: principles and applications. Amer Assoc Strat Palynol Found 2:7957806

Berra F, Jadoul F, Anelli A (2010) Environmental control on the end of the Dolomia Principale/ Hauptdolomit depositional system in the central Alps: coupling sea level and climate changes. Palaeogeogr Palaeoclimatol Palaeoecol 290:138–150

Bock W (1969) The American Triassic flora and global distribution. Geol Center Res Ser 3/4:1–406

Boersma M, Van Konijnenburg–van Cittert JHA (1991) Late Triassic plant megafossils from Aghdarband (NE Iran). In: Rutter AW (ed) The Triassic of Aghdarband (Agharband) NE–Iran, and its pre–Triassic Frame. Abh Geol Bundesanst 38:223–252

Bolotov SN, Panov DI, Yaroshenko OP (2004) New data on palynological characteristics of Triassic and Liassic of Bordak river Basin (Mountain Crimea). Bull Moscow Nat Soc Geol Sect 29(3):13–19. (in Russian)

Bomfleur B, Pott C, Kerp H (2011a) Plant assemblages from the Shafer Peak Formation (Lower Jurassic), North Victoria Land, Transantarctic Mountains. Antarct Sci 23:188–208

Bomfleur B, Taylor EL, Taylor TN et al (2011b) Systematics and paleoecology of a new peltaspermalean seed fern from the Triassic polar vegetation of Gondwana. Int J Plant Sci 172:807–835

Bomfleur B, Escapa IH, Taylor EL et al (2012) Modified basal elements in *Dicroidium* fronds (Corystospermales). Rev Palaeobot Palynol 170:15–26

Bomfleur B, Decombeix A-L, Escapa IH et al (2013a) Whole-plant concept and environment reconstruction of a *Telemachus* conifer (Voltziales) from the Triassic of Antarctica. Int J Plant Sci 174:425–444

Bomfleur B, Escapa IH, Taylor EL, Taylor TN (2013b) A reappraisal of *Neocalamites* and *Schizoneura* (fossil Equisetales) based on material from the Triassic of East Antarctica. Alcheringa 37:1–17

Bomfleur B, Decombeix A-L, Schwendemann AB et al (2014a) Habit and ecology of the Petriellales, an unusual group of seed plants from the Triassic of Gondwana. Int J Plant Sci 175:1062–1075

Bomfleur B, Klymiuk AA, Taylor EL et al (2014b) Diverse bryophyte mesofossils from the Triassic of Antarctica. Lethaia 47:120–132

Bonetti MIR (1963) Contribución al conocimiento de la flora fósil de Barreal. Dpto de Calingasta (provincial de San Juan), Facultad de Ciencias Exactas Fisicas y Naturales, Universidad de Buenos Aires

Bonis NR, Kürschner WM, Krystyn L (2009a) A detailed palynological study of the Triassic-Jurassic transition from key sections in the Eiberg Basin (Northern Calcareous Alps, Austria). Rev Palaeobot Palynol 156:376–400

Bonis NR, Ruhl M, Kürschner WM (2009b) Climate change driven black shale deposition during the end-Triassic in the western Tethys. Palaeogeogr Palaeoclimatol Palaeoecol 290(1–4):151–159

Bonis NR, Kürschner WM, Van Konijnenburg-van Cittert JHA (2010) Changing CO_2 conditions during the end-Triassic inferred from stomatal frequency analysis on *Lepidopteris ottonis* (Goeppert) Schimper and *Ginkgoites taeniatus* (Braun) Harris. Palaeogeogr Palaeoclimatol Palaeoecol 295:146–161

Bose MN (1974) Triassic floras. In: Surange KR, Lakhanpal RN, Bharadwaj DC (eds) Aspects and appraisal of Indian palaeobotany. Birbal Sahni Institute of Palaeobotany, Lucknow, pp 258–293

Boureau E (1954) Découverte du genre *Homoxylon* Sahni dans les terrains secondaires de la Nouvelle Calédonie. Mém Mus Natn Hist Nat Sér C 3(2):129–143

Boureau E (1955) Etude paléoxylogique de la Nouvelle Calédonie.1. Sur un *Homoxylon australe* n.sp., bois fossile du Marais de Mara. Bull Mus Nat Hist Nat Sér 2, 27(4):341–346

Boureau E (1957) Sur certaines espèces homoxylées à ponctuations aréolées scalariformes des flores vivantes et fossiles du Mésozoïque de Nouvelle Calédonie. Proc Eighth Pacific Sci Congr 4:346–347

Breda A, Preto N, Roghi G et al (2009) The Carnian Pluvial Event in the Tofane área (Cortina d'Ampezzo, Dolomites, Italy). Geo Alp 6:80–115

Brenner W (1986) Bemerkungen zur Palynostratigraphy der Rhaet-Lias Grenze in SW Deutschland. N Jb Geol Pal Abh 173(131):166

Brick MI (1936) The first finding of the Lower Triassic flora in Middle Asia. Trans Geol Inst USSR Acad Sci 5:161–174. (in Russian)

Brick MI (1941) Mezozojskaja flora Kamysh-Bashi (mezhdurech'e Isfara-Soh) (The Mesozoic flora of Kamyshbashy (the interfluve Isfara and Sokh)). UzGIZ, Tashkent. (in Russian)

Brick MI (1952) Iskopaemaja flora i stratigrafija nizhnemezozojskih otlozhenij bassejna srednego techenija r. Ilek v Zapadnom Kazahstane (The fossil flora and the stratigraphy of the Lower Mesozoic sediments of the middle stream of the Ilek River Basin in western Kazakhstan). Gosgeoltechizdat, Moscow. (in Russian)

Bromfield K, Burrett CF, Leslie RA, Meffre S (2007) Jurassic volcaniclastic—basaltic andesite—dolerite sequence in Tasmania: new age constraints for fossil plants from Lune River. Austr J Earth Sci 54:965–974

Bronn HG (1858) Beiträge zur triasischen Fauna und Flora der bituminösen Schiefer von Raibl, nebst Anhang über die Kurr'sche Sippe *Chiropteris* aus dem Lettenkohlen-Sandsteine. E. Schweitzerbart'sche Verlagshandlung und Druckerei, Stuttgart

Brüggen J (1918) Informe sobre el carbón de La Ternera (Copiapó). Soci Nac Minería, bol 29, Serie 3:486–496

Budai T, Császá RG, Csillag G et al (1999) A Balaton-Felvidék Földtana. Geological Institute of Hungary, Budapest

Buratti N, Cirilli S (2007) Microfloristic provincialism in the Upper Triassic Circum–Mediterranean area and paleogeographic implication. Geobios 40:133–142

Burger D (1994) Palynological studies of the Bundamba Group and Walloon Coal Measures in the Clarence-Moreton Basin. In: Wells AT, O'Brien PE (eds) Geology and petroleum potential of the Clarence-Moreton Basin, New South Wales and Queensland. Austral Geol Surv Org, Bull 241:164–180

Cairncross B, Anderson JM, Anderson HM (1995) Palaeoecology of the Triassic Molteno Formation, Karoo Basin, South Africa—sedimentological and palaeoecological evidence. South Afr J Geol 98:452–478

Cantrill DJ, Drinnan AN (1994) Late Triassic megaspores from the Amery Group, Prince Charles Mountains, East Antarctica. Alcheringa 18:71–78

Cantrill DJ, Drinnan AN, Webb JA (1995) Late Triassic plant fossils from the Prince Charles Mountains, East Antarctica. Antarct Sci 7:51–62
César SN, Colombi CE (2013) A new Late Triasssic phytogeographical scenario in westernmost Gondwana. Nat Commun 4:1889
César SN, Colombi CE (2016) Palynology of the Late Triassic Ischigualasto Formation, Argentina: Paleoecological and paleogeographic implications. Palaeogeogr Palaeoclimatol Palaeoecol 449:365–384
Chalyshev VI, Variukhina LM (1966) Triassic biostratigraphy of the Pechora region. Nauka, Moscow. (in Russian)
Chen Y, Duan S-Y, Zhang Y-C (1979a) New species of Late Triassic plants from Yanbian Sichuan I. Acta Bot Sin 21:57–63
Chen Y, Duan S-Y, Zhang Y-C (1979b) New species of Late Triassic plants from Yanbian Sichuan II. Acta Bot Sin 21:186–190
Chen Y, Duan S-Y, Zhang Y-C (1979c) New species of Late Triassic plants from Yanbian Sichuan III. Acta Bot Sin 21:269–273
Chen Y, Duan S-Y, Zhang Y-C (1985) A preliminary study of Late Triassic plants from Qinghe of Yanbian District, Sichuan Province. Acta Bot Sin 27:318–325
Cirilli S (2010) Upper Triassic lowermost Jurassic palynology and palynostratigraphy: a review. Geol Soc Lond Spec Publ 334:285–314
Clemmensen LB (1976) Tidally influenced deltaic sequences from the Kap Stewart Formation (Rhaetic-Liassic, Scoresby Land, East Greenland). Bull Geol Soc Denmark 25:1–13
Cohen KM, Finney SC, Gibbard PL et al (2013) The ICS International Chronostratigraphic Chart. Episodes 36:199–204
Colombi CE, Parrish JT (2008) Late Triassic environmental evolution in southwestern Pangea: plant taphonomy of the Ischigualasto Formation. Palaios 23:778–795
Cornet B (1977a) The palynostratigraphy and age of the Newark Supergroup. Dissertation, Pennsylvania State University, University Park, PN, 505 p
Cornet B (1977b) Preliminary investigations of two Triassic conifers from York County, Pennsylvania. In: Romans RC (ed) Geobotany. Plenum Publishing Corporation, New York, pp 165–172
Cornet B, Olsen PE (1985) A summary of the biostratigraphy of the Newark Supergroup of eastern North America. In: Weber R (ed) 3rd Congreso Latinoamericano de paleontologia. Simposio sobre floras del Triasico Tardio, su fitogeografia y paleoecologia. Instituto de Geologia Universidad Nacional Autonoma de Mexico, Memoria, pp 67–81
Crane PR (1985) Phylogenetic analysis of seed plants and the origin of angiosperms. Ann Missouri Bot Garden 72:716–793
Creber GT, Ash SR (2004) The Late Triassic *Schilderia adamanica* and *Woodworthia arizonica* trees of the Petrified Forest National Park, Arizona, USA 47:21–38
Crisafulli A, Herbst R (2011) La flora triásica del grupo El Tranquilo, provincia de Santa Cruz (Patagonia): leños fósiles. Ameghiniana 48:275–288
Dal Corso J, Gianolla P, Newton RJ et al (2015) Carbon isotope records reveal synchronicity between carbon cycle perturbation and the 'Carnian Pluvial Event' in the Tethys realm (Late Triassic). Global Planet Change 127:79–90
Dalla Vecchia FM (2000) Macrovegetali terrestri nel Mesozoico Italiano: un'ulteriore evidenza di frequenti emersioni. Natura Nascosta 20:18–35
Dalla Vecchia FM (2012) Il Friuli 215 milioni di anni fa: gli straordinari fossili di Preone, finestra su di un mondo scomparso. Comune di Preone
Dalla Vecchia FM, Selden PA (2013) A Triassic spider from Italy. Acta Palaeont Pol 58:325–330
Daugherty LH (1941) The Upper Triassic flora of Arizona. Carnegie Institution of Washington Publication 526:1–108
de Jersey NJ (1975) Miospore zones in the lower Mesozoic of southeastern Queensland. In: Campbell KSW (ed) Gondwana geology. ANU Press, Canberra, pp 159–172
de Jersey NJ, McKellar JL (2013) The palynology of the Triassic–Jurassic transition in southeastern Queensland, Australia, and correlation with New Zealand. Palynology 37:77–114

de Jersey NJ, Raine JI (1990) Triassic and earliest Jurassic miospores from the Murihiku Supergroup, New Zealand. New Zealand Geol Surv Paleont Bull 62:1–164
de Saporta G (1873–1891) Paléontologie Française. Ser. 2, Vegetaux. Plantes jurassiques: 1–4, Paris
Delevoryas T, Hope RC (1971) A new Triassic cycad and its phylletic implications. Postilla 150:1–21
Delevoryas T, Hope RC (1975) *Voltzia andrewsii*, n. sp., an Upper Triassic seed cone from North Carolina, U.S.A. Rev Palaeobot Palynol 166:94–106
Delevoryas T, Hope RC (1981) More evidence for conifer diversity in the Upper Triassic of North Carolina. Am J Bot 68:1003–1007
Delevoryas T, Hope RC (1987) Further observations on the Late Triassic conifers *Compsostrobus neotericus* and *Voltzia andrewsii*. Rev Palaeobot Palynol 51:59–64
Deng S, Lu Y, Fan R et al (2001) The Jurassic System of Northern Xinjiang, China. Univ Science and Technology of China Press, Hefei
Depape G, Doubinger J (1963) Flores triasiques de France, Colloques sur le Trias de la France et les regions limitrophes. Mem Bureau Rech Geol Minéres 15:507–523
Dettmann ME (1961) Lower Mesozoic megaspores from Tasmania and South Australia. Micropaleontology 7:71–86
Dobruskina IA (1980) Stratigraficheskoe polozhenie floronosnyh tolshh triasa Evrazii. (Stratigraphical position of Triassic plant-bearing beds of Eurasia). Trudy GIN AN SSSR, Moscow. (in Russian)
Dobruskina IA (1988) The history of land plants in the northern hemisphere during the Triassic with special reference to the floras of Eurasia. Geol Paläont Mitt 15:1–12
Dobruskina IA (1993) First data of the Seefeld conifer flora (Upper Triassic, Tyrol, Austria). In: Lucas SG, Morales M (eds) The Nonmarine Triassic, New Mexico Mus Nat Hist Sci Bull 3:113–115
Dobruskina IA (1994) Triassic Floras of Eurasia. Österr Akad Wissensch, Schriftenreihe Erdwiss Kommiss 10:1–422
Dobruskina IA (1995) Keuper (Triassic) Flora from Middle Asia (Madygen, Southern Fergana). New Mexico Museum of Natural History and Science, Albuquerque
Dobruskina IA (1998) Lunz flora in the Austrian Alps: a standard for Carnian floras. Palaeogeogr Palaeoclimatol Palaeoecol 143:307–345
Dobruskina IA (2001) Upper Triassic Flora from “Raibl beds” of Julian Alps (Italy) in Karavanke Mts. (Slovenia). Geologija 44:263–290
Dolby JH, Balme BE (1976) Triassic palynology of the Carnarvon Basin, Western Australia. Rev Palaeobot Palynol 22:105–168
Dubiel RF, Parrish JT, Parrish JM et al (1991) The Pangean megamonsoon: evidence from the Upper Triassic Chinle Formation, Colorado Plateau. Palaios 6:347–370
Dunay RE, Fisher MJ (1979) Palynology of the Dockum Group (Upper Triassic), Texas, U.S.A. Rev Paleobot Palynol 28:61–92
Dunay RE, Traverse A (1971) Preliminary report on Triassic spores and pollen of the Dockum Group, Texas panhandle. Geosci Man 3:65–68
Dzik J, Sulej T (2007) A review of the early Late Triassic Krasiejów biota from Silesia, Poland. Palaeontol Pol 64:3–27
Emmons E (1856) Geological Report of the midland counties of North Carolina. George P. Putnam & Company, New York and Henry D. Turner, Raleigh
Emmons E (1857) American geology, Part 6. Sprague & Company, Albany
Escapa IH, Taylor EL, Cuneo R et al (2011) Triassic floras of Antarctica: plant diversity and distribution in high paleolatitude communities. Palaios 26:522–544
Fakhr MS (1977) Contribution a l’étude de la flore Rhéto–Liasique de la formation de Shemshak de l'Elbourz (Iran). Mém Section Sci 5:1–178
Farabee MJ, Taylor IL, Taylor TN (1990) Correlation of Permian and Triassic palynomorph assemblages from the central Transantarctic Mountains, Antarctica. Rev Palaeobot Palynol 65:257–265

Fefilova LA (2005) Upper Triassic palynoassemblages of Franz-Iosef land. In: Afonin SA, Tokarev PI (eds) Proceedings of XI All-Russian palynological conference "Palynology: Theory & applications" (27 september – 1 october 2005). PIN RAS, Moscow, pp 266–267. (in Russian)
Feng Z, Su T, Yang JY et al (2014) Evidence for insect-mediated skeletonization on an extant fern family from the Upper Triassic of China. Geology 42:407–410
Fielding CR, Frank TD, Isbell JL (2008) The late Paleozoic ice age—a review of current understanding and synthesis of global climate patterns. In: Fielding CR, Frank TD, Isbell JL (eds) Resolving the Late Paleozoic Ice Age in Time and Space. Geological Society of America Special Paper 441:343–354
Fisher MJ, Dunay RE (1984) Palynology of the Petrified Forest Member of the Chinle Formation (Upper Triassic), Arizona, U.S.A. Pollen et Spores 26:241–284
Flint JCE, Gould RE (1975) A note on the fossil megafloras of the Nymboida and Red Cliff Coal Measures, southern Clarence-Moreton Basin, NSW. J Proc R Soc New South Wales 108:70–74
Fontaine WM (1883) Contributions to the knowledge of the older Mesozoic flora of Virginia. U.S. Geol Surv Monogr 6:1–144
Foster CB, Balme BE, Helby R (1994) First record of Tethyan palynomorphs from the Late Triassic of Antarctica. AGSO J Austral Geol Geophys 15:239–246
Fraser NC, Grimaldi DA, Olsen PE, Axsmith B (1996) A Triassic Lagerstätte from eastern North America. Nature 380:615–619
Frenguelli J (1948) Estratigrafía y edad del Ilamado "Rético" en la Argentina. Soc Argent Estud Geogr 8:159–309
Frentzen K (1922) Beiträge zur Kenntnis der fossilen Flora des südwestlichen Deutschland. II. Lettenkohlen- und Schilfsandsteinflora. Jb Mitt Oberrh Geol Ver 11:1–14
Furin S, Preto N, Rigo M et al (2006) A high-precision U-Pb zircon age from the Triassic of Italy: implications for the Carnian rise of calcareous nannoplankton and dinosaurs. Geology 34:1009–1012
Gallego OF, Gnaedinger S, Kirsten O et al (2003) Primera cita de trazas fósiles de insectos en hojas del Pérmico de Uruguay y Triásico de Chile. Univ Nacl Nordeste. Comun Cient Tecnol Biol B032:1–4
Gallego OF, Gnaedinger S, Labandeira CC et al (2004) Permian and Triassic insect traces on fossil leaves from Uruguay and Chile. International Congress on Ichnology ICHNIA Abstract Book 1:35
Genkina RZ (1964) *Cycadocarpidium* Nathorst and *Fraxinopsis* Wieland from the Aktash Formation sediments of the Upper Triassic of the southern coast of Issyk-Kul in Kirghizia. In: Biostratigraphy and palaeogeography of the Meso-Kainozoic of the oil and gaz promising areas of the south east of the USSR. Nauka, Moscow, pp 69–78. (in Russian)
Ghavidel-Syooki M, Yousefi M, Shekarifard A, Mohnhoff D (2015) Palynostratigraphy, palaeogeography and source rock evaluation of the Nayband Formation at the Parvadeh area, Central Iran, Iran. J Sci Islamic Rep Iran 26:241–263
Ghosh AK, Tewari R, Agnihotri D et al (2015) Gondwana formations of South Rewa and upper Narmada basins, Central India. Birbal Sahni Institute of Palaeobotany, Lucknow
Ghosh AK, Kar R, Chatterjee R (2016) Reassessment of the macroflora of the Parsora Formation with remarks on the age connotation. J Palaeont Soc India 61:225–238
Gianolla P, Ragazzi E, Roghi G (1998) Upper Triassic amber from the Dolomites (Northern Italy). A paleoclimatic indicator? Riv Ital Pal Strat 93:331–347
Gluzbar EA (1973) Correlation of several lower Mesozoic geological sections of Europe based on palynological data. In: Chlonova AF (ed) Palynology of mesophyte. Proc Int Palynol Conf, 3rd, Nauka, Moscow, pp 44–48. (in Russian)
Gnaedinger SC, Adami-Rodrigues K, Gallego OF (2007) Evidencias de trazas de oviposición de insectos (Odonata) en hojas del Triásico de Chile. Ameghiniana 44:94R
Gnaedinger SC, Adami-Rodrigues K, Gallego OF (2008) Insect egg ovipositions on leaves from the Upper Triassic from northern Chile [Abstract 86]. In: Boardman DR (ed) Simpósio Brasileiro de Paleobotânica e Palinologia, Florianópolis: Asociación Latinoamericana de Paleobotánica y Palinología, Abstract book

Gnaedinger SC, Adami-Rodrigues K, Gallego OF (2014) Endophytic oviposition on leaves from the Late Triassic of northern Chile: ichnotaxonomic, palaeobiogeographic and palaeoenvironment considerations. Geobios 47:221–236
Golonka J (2007) Late Triassic and Early Jurassic palaeogeography of the world. Palaeogeogr Palaeoclimatol Palaeoecol 244:297–307
Gomolitzky NP (1993) On the question of the age of the continental Aktash Formation of the Soguti (Issyk-Kul), previously considered to be Upper Triassic. The Nonmarine Triassic: Bulletin 3:151
Gothan W (1910) Die fossilen Holzreste von Spitzbergen. Kung Sven Vetenskap Handl 45(8):565
Gothan W (1914) Die unter-liassische (rhätische) Flora der Umgegend von Nürnberg. Abh Naturhist Ges Nürnberg 19:91–186
Götz AE, Ruckwied K, Barbacka M (2011) Palaeoenvironment of the Late Triassic (Rhaetian) and Early Jurassic (Hettangian) Mecsek Coal Formation (south Hungary): implications from macro and microfloral assemblages. Palaeobiodiv Palaeoenviron 91:75–88
Gould RE (1975) The succession of Australian pre-Tertiary megafossil floras. Bot Rev 41:453–483
Grauvogel-Stamm L, Kelber K-P (1996) Plant-insect interactions and coevolution during the Triassic in Western Europe. Paleont Lombarda Nov Ser 5:5–23
Greene A, Scoates JS, Weis D et al (2009a) Geochemistry of Triassic flood basalts from the Yukon (Canada) segment of the accreted Wrangellia oceanic plateau. Lithos 110:1–19
Greene A, Scoates JS, Weis D et al (2009b) Melting history and magmatic evolution of basalts and picrites from the accreted Wrangellia oceanic plateau, Vancouver Island. Can J Petrol 50:467–505
Haas J, Budai T, Raucsik B (2012) Climatic controls on sedimentary environments in the Triassic of the Transdanubian Range (Western Hungary). Palaeogeogr Palaeoclimatatol Palaeoecol 353:31–44
Hallam A (1985) A review of Mesozoic climates. J Geol Soc 142:433–445
Halle TG (1908) Zur Kenntnis der Mesozoischen Equisetales Schwedens. Kung Sven Vetenskap Handl 43:1–40
Harper CJ, Taylor TN, Krings M et al (2016) Structurally preserved fungi from Antarctica: diversity and interactions in late Palaeozoic and Mesozoic polar forest ecosystems. Antarct Sci 28:153–173
Harris TM (1926) The Rhaetic flora of Scoresby Sound East Greenland. Medd om Grønland 68:44–148
Harris TM (1931a) The fossil flora of Scoresby Sound, East Greenland. 1. Cryptogams. Medd om Grønland 85(2):1–102
Harris TM (1931b) Rhaetic floras. Biol Rev 6:133–162
Harris TM (1932a) The fossil flora of Scoresby Sound, East Greenland. 2. Description of seed plants Incertae sedis together with a discussion of certain cycadophyte cuticles. Medd om Grønland 85(3):1–112
Harris TM (1932b) The fossil flora of Scoresby Sound East Greenland. 3. Caytoniales and Bennettitales. Medd om Grønland 85(5):1–333
Harris TM (1935) The fossil flora of Scoresby Sound, East Greenland. 4. Ginkgoales, Coniferales, Lycopodiales and isolated fructifications. Medd om Grønland 112(1):1–176
Harris TM (1937) The fossil flora of Scoresby Sound, East Greenland. Part 5: stratigraphic relations of the plant beds. Medd om Grønland 112:1–114
Harris TM (1938) The British Rhaetic flora. British Museum
Harris TM (1946) Liassic and Rhaetic plants collected in 1936–38 from East Greenland. Medd om Grønland 114(9):1–41
Harris TM (1957) A Liasso–Rhaetic flora in South Wales. Proc R Soc 147B:289–308
Hartz N (1896) Planteforsteninger fra Cap Stewart i Øst-grønland. Medd om Grønland 19:215–247
He Y (1980) Upper Triassic stratigraphy of Qinghai. J Strat 4(4):293–300. (in Chinese)
Heer O (1868) Flora Fossilis Arctica 1. Die fossile Flora der Polarländer. Schulthess, Zurich
Helby R, Morgan R, Partridge AD (1987) A palynological zonation of the Australian Mesozoic. Assoc Austral Palaeont Mem 4:1–94

Herbst R, Troncoso A (2000) Las Cycadophyta del Triásico de las Formaciones La Ternera y El Puquén (Chile). Ameghiniana 37:283–292
Herendeen PS, Friis EM, Pedersen KR et al (2017) Palaeobotanical redux: revisiting the age of the angiosperms. Nat Plants 17015(8 p):3
Herngreen GFW (2005) Triassic sporomorphs of NW Europe: taxonomy, morphology and ranges of marker species with remarks on botanical relationship and ecology and comparison with ranges in the Alpine Triassic. Kenniscentrum Biogeology (UU/TNO)—TNO report, NITG 04–176-C, Ned Inst Toegepaste Geowet TNO, Utrecht
Hesselbo SP, Robinson SA, Surlyk F et al (2002) Terrestrial and marine extinction at the Triassic-Jurassic boundary synchronized with major carbon-cycle perturbation: a link to initiation of massive volcanism? Geology 30:251–254
Heunisch C (1999) Die Bedeutung der Palynologie für Biostratigraphie und Fazies in der Germanischen Trias. In: Hauschke N, Wilde V (eds) Trias, Eine ganz andere Welt, Mitteleuropa im frühen Erdmittelalter. Pfeil Verlag, München, pp 207–220
Hill RS, Truswell EM, McLoughlin S et al (1999) The evolution of the Australian flora: fossil evidence. Flora of Australia, 2nd edn, vol 1 (Introduction), pp 251–320
Hochuli PA, Feist-Burkhardt S (2013) Angiosperm-like pollen and *Afropollis* from the Middle Triassic (Anisian) of the Germanic Basin (Northern Switzerland). Front Plant Sci 4:344. https://doi.org/10.3389/fpls.2013.00344
Hochuli PA, Frank SM (2000) Palynology (dinoflagellate cysts, spore-pollen) and stratigraphy of the Lower Carnian Raibl Group in the Eastern Swiss Alps. Eclog Geol Helv 93:429–443
Hochuli PA, Vigran JO (2010) Climate variations in the Boreal Triassic—Inferred from palynological records from Barents Sea. Palaeogeogr Palaeoclimatol Palaeoecol 290:20–42
Hope RC, Patterson OF III (1969) Triassic flora from the Deep River Basin, North Carolina. North Carolina Department of Conservation, Division of Mineral Resources, Special Publication 3:1–22
Hornung T, Brandner R (2005) Biostratigraphy of the Reingraben Turnover (Hallstatt Facies Belt): local black shale events controlled by the regional tectonics, climatic change and plate tectonics. Facies 51:460–479
Hsü J, Chu C-N, Chen Y et al (1974) New genera and species of the Late Triassic plants from Yungjen, Yunnan I. Acta Bot Sin 16:266–278
Hsü J, Zhu J, Chen Y, Hu Y et al (1979) Late Triassic Baoding flora of China. Science Press, Beijing. (in Chinese)
Hu Y (1986) Phytogeography and distribution characters of the fossil plants from Xinjiang. In: Palaeontological Society of China (ed) Abstract of symposium on paleoecology, paleogeography and paleoclimate 14th annual conventions of Palaeontological Society of China. Nanjing, pp 23–24. (in Chinese)
Hu Y, Gu D (1987) Plant fossils from the Xiaoquangou Group of the Xinjiang and its flora and age. Bot Res 2:207–234. (in Chinese with English abstract)
Huang Z, Zhou H (1980) Fossil plants. In: Institute of Geology, Chinese Academy of Geological Sciences (ed) Mesozoic stratigraphy and palaeontology Palaeont of Shaanxi-Gansu-Ningxia Basin, vol 1. Geological Publishing House, Beijing, pp 43–198. (in Chinese)
Ilyina NV, Egorov AY (2016) The Upper Triassic of northern Middle Siberia: stratigraphy and palynology. Polar Res 27(3):372–392. https://doi.org/10.1111/j.1751-8369.2008.00083.x
Jain RK, Delevoryas T (1967) A Middle Triassic flora from the Cacheuta Formation, Minas de Petroleo, Argentina. Palaeontology 10:564–589
Jalfin G, Herbst R (1995) La flora triásica del Grupo El Tranquilo, provincia de Santa Cruz (Patagonia). Estrat. Ameghiniana 32:211–229
Jameson I (1823) List of specimens of rocks brought from the eastern coast of Greenland. In: Scoresby W Jr (ed) Journal of a Voyage to the Northern Whale-fishery Including Researches and Discoveries on the Eastern Coast of West Greenland, Made in the Summer of 1822, in the Ship Baffin of Liverpool. Archibald Constable and Co., Edinburgh, pp 399–408
Jell PA (2013) Tarong Basin. In: Jell PA (ed) Geology of Queensland. Geological Survey of Queensland, Brisbane, pp 396–397

Jell PA, McKellar JL (2013) Callide Basin. In: Jell PA (ed) Geology of Queensland. Geological Survey of Queensland, Brisbane, p 398
Jell PA, McKellar JL, Draper JJ (2013) Clarence-Moreton Basin. In: Jell PA (ed) Geology of Queensland. Geological Survey of Queensland, Brisbane, pp 542–546
Johansson N (1922) Die rhätische Flora der Kohlengruben bei Stabbarp und Skromberga in Schonen. Kungl Svenska Vetenskap Handl 63:1–78
Johnston RM (1886) General observations regarding the classification of the upper Palaeozoic and Mesozoic rocks of Tasmania, together with a full description of all the known Tasmanian coal plants, including a considerable number of new species. Pap Proc R Soc Tasmania 1885:343–387
Johnston RM (1887) Fresh contribution to our knowledge of the plants of Mesozoic age in Tasmania. Pap Proc R Soc Tasmania 1886:160–185
Johnston RM (1894) Further contributions to the history of the fossil flora of Tasmania. Part 1. Pap Proc R Soc Tasmania 1893:170–178
Johnston RM (1896) Further contributions to the history of the fossil flora of Tasmania. Parts 1 and 2. Pap Proc R Soc Tasmania 95:57
Jones OA, de Jersey NJ (1947) The flora of the Ipswich Coal Measures: morphology and succession. Pap Dep Geol Univ Queensl 3(3):1–88
Kawasaki S (1925) Some older Mesozoic plants in Korea. Bull Geol Surv Korea 4:1–71
Kawasaki S (1926) Addition to the older Mesozoic plants in Korea. Bull Geol Surv Korea 4:1–35
Kawasaki S (1939) Second addition to the older Mesozoic plants in Korea. Bull Geol Surv Korea 4:1–69
Kelber K-P (1990) Die versunkene Pflanzenwelt aus den Deltasümpfen Mainfrankens vor 230 Millionen Jahren. Beringeria 1:1–67
Kelber K-P (1998) Phytostratigraphische Aspekte der Makrofloren des süddeutschen Keupers. Documenta naturae 117:89–115
Kelber K-P (2000) Zur Pflanzenwelt des Keupers. In: Brunner K, Hinkelbein K (eds) 1:50000 Erläuterungen zum Blatt Heilbronn und Umgebung, pp 78–95
Kelber K-P, Hansch W (1995) Keuperpflanzen. Die Enträtselung einer über 200 Millionen Jahre alten Flora. Museo 11:1–157
Kelber K-P, Van Konijnenburg-van Cittert JHA (1997) A new Rhaetian Flora from the neighbourhood of Coburg (Germany): preliminary results. Medd Nederlands Instit Toegepaste Geowet 58:105–113
Kent DV, Olsen PE (2000) Magnetic polarity stratigraphy and paleolatitude of the Triassic Jurassic Blomidon Formation in the Fundy basin (Canada): implications for early Mesozoic tropical climate gradients. Earth Planet Sci Lett 179:311–324
Kidder DL, Worsley TR (2004) Causes and consequences of extreme Permo–Triassic warming to globally equable climate and relation to Permo–Triassic extinction and recovery. Palaeogeogr Palaeoclimatol Palaeoecol 203:207–237
Kilpper K (1964) Über eine Rhät/Lias-Flora aus dem nördlichen Abfall des Alburs-Gebirges in Nord-Iran. Teil 1: Bryophyta und Pteridophyta. Palaeontographica 114B:1–78
Kilpper K (1971) Über eine Rhät/Lias-Flora aus dem nördlichen Abfall des Alburs-Gebirges in Nord-Iran. Teil II: Ginkgophyten-Belaubungen. Palaeontographica B133:89–102
Kim JH (1989) New fossil plants from the Nampo Group (Lower Mesozoic), Korea. Geosci J 5:173–180
Kim JH (1993) Fossil plants from the Lower Mesozoic Daedong Supergroup in the Korean Peninsula and their phytogeographical and paleogeographical significance in East and Southeast Asia. PhD thesis, Kyushu University, 315 p
Kim JH, Kimura T (1988) *Lobatannularia nampoensis* (Kawasaki) Kawasaki from the Upper Triassic Baegunsa Formation, Nampo Group, Korea. Proc Jap Acad Ser B 64:221–224
Kim JH, Kim H-S, Lee B-J et al (2002) A new species of *Leptostrobus* from the Upper Triassic Amisan Formation of the Nampo Groups in Korea. J Korean Earth Sci Soc 23:30–37
Kim K, Jeong EK, Kim JH et al (2005) Coniferous fossil woods from the Jogyeri Formation (Upper Triassic) of the Nampo-Group, Korea. IAWA J 26:253–265

Kimura T, Kim BK (1984) General review on the Daedong flora, Korea. Bull Tokyo Gakugei Univ 36:201–236
Kimura T, Kim BK (1988) New taxa in the Late Triassic Daedong Flora, South Korea Part 1. Trans Proc Palaeont Soc Japan 152:603–624
Kimura T, Kim BK (1989) New taxa in the Late Triassic Daedong Flora, South Korea. Part 2. Trans Proc Palaeont Soc Japan 155:141–158
Kirchner M (1992) Untersuchungen an einigen Gymnospermen der fränkischen Rhät-Lias-Grenzschichten. Palaeontogr B 224:17–91
Kirichkova AI (1962) Rod *Cladophlebis* v nizhnemezozojskih otlozhenijah Vostochnogo Urala (The genus *Cladophlebis* in the Lower Mesozoic sediments of the Eastern Urals). Trudy VNIGRI, Paleontol Sbornik 196:495–544. (in Russian)
Kirichkova AI (1969) Materialy k izucheniju nizhnemezozojskoj flory Vostochnogo Urala (The materials for the study of the Lower Mesozoic flora of the Eastern Urals). Trudy VNIGRI, Paleontol Sbornik 268:270–349. (in Russian)
Kirichkova AI (1990) Taksonomicheskaja revizija nekotoryh triasovyh rastenij Vostochnogo Urala (Taxonomic revision of some Triassic plants of the Eastern Urals). Bot Zhurn 75:1288–1294. (in Russian)
Kirichkova AI (2011) Fitostratigrafija opornyh razrezov i problema korreljacii triasa Zapadnoj Sibiri (Western Siberian Triassic—phyto stratigraphy and correlation of key sequences). Neftegasovya geologya. Teorya i practika 6(3):1–40. (in Russian)
Kirichkova AI, Esenina AV (2014) Stratotipicheskie i opornye razrezy srednego-nizy verhnego triasa Timano-Pechorskoj neftegazonosnoj provincii: litologija, facial'nye osobennosti (Stratotypical and key sections of the Lower Triassic of the Timan-Pechora province: lithology and facial features). Neftegasovya geologya. Teorya i practika 9(3):1–26. (in Russian)
Klausen TG, Mørk A (2014) The Upper Triassic paralic deposits of the De Geerdalen Formation on Hopen: outcrop analog to the subsurface Snadd Formation in the Barents Sea. Am Assoc Petrol Geol Bull 98:1911–1941
Kochnev EA (1934) On the study of Jurassic coal-bearing deposits of Fergana. Materials on geology of coal deposits of Middle Asia, pp 5–6. (in Russian)
Koken E (1913) Kenntnis der Schichten von Heiligenkreuz (Abteital, Südtirol). Abh k k geol Reichsanst 16:1–43
Kon'no E (1972) A new *Chiropteris* and other fossil plants from the Heian System, Korea. Jap J Geol Geogr 16:105–114
Köppen W, Wegener A (1924) Die Klimate der geologischen Vorzeit. Borntraeger, Berlin
Kozur HW, Bachmann GH (2010) The Middle Carnian wet intermezzo of the Stuttgart formation (Schilfsandstein), Germanic basin. Palaeogeogr Palaeoclimatol Palaeoecol 290:107–119
Krasser F (1891) Über die fossile Flora der rhätischen Schichten Persiens. Sitzungsber math naturwiss Ges 100:413–432
Krassilov VA, Shorokhova SA (1970) New Triassic plants from the Iman River (Primorye) Basin and some problems of the morphogenesis of the Mesozoic Pteridophyllum. In: Triassic invertebrates and plants of the East of the USSR, Vladivostok, pp 98–121. (in Russian)
Krassilov VA, Shorokhova SA (1975) Triasovye geoflory i nekotorye obshhie principy paleofitogeografii (Triassic geofloras and some general principles of palaeophytogeography). Trudy DVNTS, biol pochv Inst AN SSSR 27:7–16. (in Russian)
Kräusel R, Leschik G (1955) Die Keuperflora von Neuewelt bei Basel: Koniferen und andere Gymnospermen. Schweiz Paläont Abh 71:1–27
Kräusel R, Schaarschmidt F (1966) Die Keuperflora von Neuewelt bei Basel–IV. Pterophyllen und Taeniopteriden. Schweiz Paläontol Abh 84:3–44
Kryshtofovich AN (1912) Rastitel'nye ostatki mezozojskih uglenosnyh otlozhenij vostochnogo sklona Urala. (The plant remains of the Mesozoic coal-bearing sediments of the eastern slope of the Urals) Izv. geol. com, St.-Petersbourg. (in Russian)
Kryshtofovich AN (1957) Palaeobotany. Gostoptechisdat. (In Russian)

Kürschner WM, Herngreen GW (2010) Triassic palynology of central and northwestern Europe: A review of palynofloral diversity patterns and biostratigraphic subdivisions. In: Lucas SG (ed) The Triassic Timescale. Geological Society, London, Special Publications 334:263–283

Kürschner WM, Bonis NR, Krystyn L (2007) Carbon–isotope stratigraphy and palynostratigraphy of the Triassic–Jurassic transition in the Tiefengraben section—Northern Calcareous Alps (Austria). Palaeogeogr Palaeoclimatol Palaeoecol 244:257–280

Kürschner WM, Mander L, McElwain J (2014) A gymnosperm affinity for *Ricciisporites tuberculatus* Lundblad: implications for vegetation and environmental reconstructions in the Late Triassic. Palaeobiodiver Palaeoenvir 94:29–305

Kustatscher E, Van Konijnenburg-van Cittert JHA (2008) Considerations on *Phylladelphia strigata* Bronn from the historical Raibl flora (Carnian, lower Upper Triassic, Italy). Geo Alp 5:69–81

Kustatscher E, Bizzarini F, Roghi G (2011) Plant fossils in the Cassian Beds and other Carnian formations of the Southern Alps (Italy). Geo Alp 8:146–155

Kustatscher E, Daxer C, Krainer K (2017) Plant fossils from the Norian Seefeld Formation (Late Triassic) of the Northern Calcareous Alps (Tyrol, Austria). N Jb Geol Pal Abh 283(3):335–346

Labandeira CC (2006) The four phases of plant-arthropod associations in deep time. Geologica Acta 4:409–438

Labandeira CC, Anderson JM (2005) Insect leaf-mining in Late Triassic gymnospermous floras from the Molteno Formation of South Africa. Geol Soc Am Abstr Prog 37:15

Lanteaume M (1950) *Dadoxylon* (*Araucarioxylon*) *boureaui* n.sp. Bois silicifé mésozoïque de Nouvelle Calédonie. Bull Soc Géol France, 5ème série 20:33–38

Larsson LM (2009) Palynostratigraphy of the Triassic–Jurassic transition in southern Sweden. GFF 131:147–163

Launis A, Pott C, Mørk A (2014) A glimpse into the Carnian: Late Triassic plant fossils from Hopen, Svalbard. Norw Petrol Direct Bull 11:129–136

Leuthardt F (1903) Die Keuperflora von Neuewelt bei Basel—I. Teil Phanerogamen. Abh Schweiz Paläontol Ges 30:1–23

Li P (1964) Fossil plants from the Hsuchiaho Series of Kwangyuan, northern Szechuan. Mem Inst Geol Palaeont, Acad Sinica 3:101–178. (in Chinese with English summary)

Li P, Cao Z, Wu S (1976) Mesozoic plants of Yunnan. In: Nanjing Institute of Geology and Palaeontology, Academia Sinica (eds) Mesozoic fossils of Yunnan, vol 1. Science Press, Beijing, pp 87–160. (in Chinese)

Li J, Zhen B, Sun G (1991) First discovery of Late Triassic florule in Wusitentag-Karamiran area of Kulun Mountain of Xinjiang. Xinjiang Geol 9:50–58. in Chinese with, English abstract

Linck O (1949) Fossile Bohrgänge (*Anobichnium simile* n. g. n sp.) an einem Keuperholz. N Jb Min Geol Paläont 90B:180–185

Lindström S (2016) Palynofloral patterns of terrestrial ecosystem change during the end—Triassic event—a review. Geol Mag 153:223–251

Lindström S, Erlström M (2006) The late Rhaetian transgression in southern Sweden: Regional (and global) recognition and relation to the Triassic–Jurassic boundary. Palaeogeogr Palaeoclimatol Palaeoecol 241:339–372

Lindström S, van de Schootbrugge B, Hansen KH et al (2017) A new correlation of Triassic–Jurassic boundary successions in NW Europe, Nevada and Peru, and the Central Atlantic Magmatic Province: a time-line for the end-Triassic mass extinction. Palaeogeogr Palaeoclimatol Palaeoecol 478:80–102. https://doi.org/10.1016/j.palaeo.2016.12.025

Litwin R, Ash SR (1991) First early Mesozoic amber in the western hemisphere. Geology 19:273–276

Litwin RJ, Ash SR (1993) Revision of the biostratigraphy of the Chatham Group (Upper Triassic), Deep River basin, North Carolina, USA. Rev Palaeobot Palynol 77:75–95

Litwin RJ, Traverse A, Ash SR (1991) Preliminary palynological zonation of the Chinle Formation, southwestern U.S.A., and its correlation with the Newark Supergroup (eastern U.S.A.) Rev Palaeobot Palynol 68:269–287

Loope DB, Steiner MB, Rowe CM et al (2004) Tropical westerlies over Pangaean sand seas. Sedimentology 51:315–322

Lord GS, Solvi KH, Ask M, Mork A, Hounslow MW, Paterson NW (2014) The Hopen Member: a new member of the Triassic De Geerdalen Formation, Svalbard. Norweg Petrol Direct Bull 11:81–96

Loubiere A (1936) Sur la structure d'un bois silicifié de Nouvelle Calédonie. Bull Bot Soc France 82:620–624

Lucas SG, Minter NJ, Hunt AP (2010) Re-evaluation of alleged beesevaluation of alleged0–624turic of Arizona. Palaeogeogr Palaeoclimatol Palaeoecol 286:194–201

Lucas SG, Tanner LH, Kozur HW et al (2012) The Late Triassic timescale: age and correlation of the Carnian–Norian boundary. Earth-Sci Rev 114:1–18

Lund JJ (1977) Rhaetic to Lower Liassic palynology of the onshore south-eastern North Sea Basin. Geol Surv Denmark II Ser 109:1–129

Lundblad AB (1949) De geologiska resultaten från borrningarna vid Höllviken Del 4: On the presence of *Lepidopteris* in cores from "Hollviken II". Sver Geol Undersök Ser C 506(43):1–17

Lundblad AB (1950) Studies in the Rhaeto–Liassic floras of Sweden. I. Pteridophyta, Pteridospermae and Cycadophyta from the mining district of NW Scania. Kungl Svenska Vetenskap Handl, Fjärde Ser 1:1–82

Lundblad AB (1959a) Studies in the Rhaeto–Liassic floras of Sweden. II:1. Ginkgophyta from the mining district of NW Scania. Kungl Svenska Vetenskap Handl, Fjärde Ser 6:1–38

Lundblad AB (1959b) Rhaeto–Liassic floras and their bearing on the stratigraphy of Triassic–Jurassic rocks. Stockholm. Contrib Geol 3:83–102

MacClure W (1817) Observations on the geology of the United States of America, to accompany geologic map. Am Phil Soc Trans 6:411–428

Maheshwari HK, Kumaran KPN, Bose MN (1978) The age of the Tiki Formation: with remarks on the miofloral succession in the Triassic Gondwanas of India. Palaeobotanist 25:254–265

Malyavkina VS (1964) Spores and pollen of Triassic deposits of West-Siberian lowland. Nedra, Leningrad. (in Russian)

Mander L, Kürschner WM, McElwain JC (2013) Palynostratigraphy and vegetation history of the Triassic–Jurassic transition in East Greenland. J Geol Soc Lond 170:37–46

Markevich PV, Zakharov VD (eds) (2004) Triassic and Jurassic of the Sikhote-Alin: Book 1. Terrigenous assemlage. Dal'nauka, Vladivostok. (in Russian)

Martínez RN, Sereno PC, Alcober OA et al (2011) A basal dinosaur from the dawn of the dinosaur era in southwestern Pangaea. Science 331:206–210

Marwick J (1953) Divisions and faunas of the Hokmui System (Triassic and Jurassic). Paleont Bull N Z Geol Surv 21:1–114

Mazza M, Furin S, Spötl C et al (2010) Generic turnovers of Carnian/Norian conodonts: climatic control or competition? Palaeogeogr Palaeoclimatol Palaeoecol 290:120–137

McElwain JC, Popa ME, Hesselbo SP et al (2007) Macroecological responses of terrestrial vegetation to climatic and atmospheric change across the Triassic/Jurassic boundary in East Greenland. Paleobiology 33:547–573

McElwain JC, Wagner PJ, Hesselbo SP (2009) Fossil plant relative abundances indicate sudden loss of Late Triassic biodiversity in East Greenland. Science 324:1554–1556

McLoughlin S (2001) The breakup history of Gondwana and its impact on pre-Cenozoic floristic provincialism. Aust J Bot 49:271–300

McLoughlin S (2011) *Glossopteris*: insights into the architecture and relationships of an iconic Permian Gondwanan plant. J Bot Soc Bengal 65:93–106

McLoughlin S (2013) Claystone textbooks. Aust Age Dinosaurs Mag 10:40–49

McLoughlin S, Bomfleur B (2016) Biotic interactions in an exceptionally well preserved osmundaceous fern rhizome from the Early Jurassic of Sweden. Palaeogeogr Palaeoclimatol Palaeoecol 464:86–96

McLoughlin S, Drinnan AN (1997) Fluvial sedimentology and revised stratigraphy of the Triassic Flagstone Bench Formation, northern Prince Charles Mountains, East Antarctica. Geol Mag 134:781–806

McLoughlin S, Hill RS (1996) The succession of Western Australian Phanerozoic floras. In: Hopper SD, Chappill JA, Harvey MS, George AS (eds) Gondwanan heritage: past, present and future

of the Western Australian Biota (Proceedings of the Conference on Systematics, Evolution and Conservation of the Western Australian Biota, Perth, 1993). Surrey Beatty, Sydney, pp 61–80
McLoughlin S, Pott C (2009) The Jurassic flora of Western Australia. GFF 131:113–136
McLoughlin S, Strullu-Derrien C (2016) Biota and palaeoenvironment of a high middle-latitude Late Triassic peat-forming ecosystem from Hopen, Svalbard Archipelago. In: Kear BP, Lindgren J, Hurum JH et al (eds) Mesozoic Biotas of Scandinavia and its Arctic Territories. Geol Soc London Spec Pub 434:87–112
McLoughlin S, Lindström S, Drinnan AN (1997) Gondwanan floristic and sedimentological trends during the Permian-Triassic transition: new evidence from the Amery Group, northern Prince Charles Mountains, East Antarctica. Antarct Sci 9:281–298
McLoughlin S, Jansson IM, Vajda V (2014) Megaspore and microfossil assemblages reveal diverse herbaceous lycophytes in the Australian Early Jurassic Flora. Grana 53:22–53
McLoughlin S, Martin SK, Beattie R (2015) The record of Australian Jurassic plant-arthropod interactions. Gondwana Res 27:940–959
Meller B, Ponomarenko AG, Vasilenko DV et al (2011) First beetle elytra, abdomen (Coleoptera) and a mine trace from Lunz (Carnian, Late Triassic, Lunz-am See, Austria) and their taphonomical and evolutionary aspects. Palaeontology 54:97–110
Meng F (1983) New materials of fossil plants from Jiuligang Formation of Jingmen-Dangyang Basin, Western Hubei. Prof Pap Strat Palaeont 10:223–238
Meng F (1990) Some pteridosperms from Western Hubei in Late Triassic and their evolutionary tendency. Acta Bot Sin 32:317–322
Meng F (1992) New genus and species of fossil plants from Jiuligang Formation in Western Hubei. Acta Palaeont Sin 31:703–707
Meyen SV (1970) Permian floras. Trans Geol Inst USSR Acad Sci N208:111–157. (in Russian)
Meyen SV (1987) Fundamentals of palaeobotany. Chapman and Hall, London. 432 pp
Mi J (1977) Late Triassic plants and strata from Hunjiang of Jilin Province. J Changchun Coll Geo1 3:2–12. (in Chinese)
Mickle JE, Gensel P, Wheeler E (2000) 17th MPC Field Trip Guidebook: Boren Clay Products, Gulf, North Carolina, May 7, 2000. Department of Biology, UNC-Chapel Hill, 20 p. (Unpublished)
Moisan P, Voigt S (2013) Lycophytes from the Madygen Lagerstätte (Middle to Late Triassic, Kyrgystan, Central Asia). Rev Palaeobot Palynol 192:42–64
Moisan P, Voigt S, Pott C et al (2011) Cycadalean and bennettitalean foliage from the Triassic Madygen Lagerstätte (SW Kyrgyzstan, Central Asia). Rev Palaeobot Palynol 164:93–108
Moisan P, Labandeira CC, Matushkina NA, Wappler T, Voigt S, Kerp H (2012a) Lycopsid–arthropod associations and odonatopteran oviposition on Triassic herbaceous *Isoetites*. Palaeogeogr Palaeoclimatol Palaeoecol 344–345:6–15
Moisan P, Voigt S, Schneider JW et al (2012b) New fossil bryophytes from the Triassic Madygen Lagerstätte (SW Kyrgyzstan). Rev Palaeobot Palynol 187:29–37
Morel EM, Artabe AE, Spalletti LA (2003) Triassic floras of Argentina: biostratigraphy, floristic events and comparison with other areas of Gondwana. Alcheringa 27:231–243
Morel EM, Artabe AE, Martínez LCA et al (2011) Megafloras Mesozoicas. Relatorio del XVIII Congreso Geológico Argentino, Neuquén, pp 573–578
Mueller S, Hounslow MW, Kürschner WM (2016a) Integrated stratigraphy and palaeoclimate history of the Carnian Pluvial Event in the Boreal realm; new data from the Upper Triassic Kapp Toscana Group in central Spitsbergen (Norway). J Geol Soc 173:186–202. https://doi.org/10.1144/jgs2015-028
Mueller S, Krystyn L, Kürschner WM (2016b) Climate variability during the Carnian Pluvial Phase: a quantitative palynological study of the Carnian sedimentary succession at Lunz am See, Northern Calcareous Alps, Austria. Palaeogeogr Palaeoclimatol Palaeoecol 441:198–211
Mukherjee D, Ray S, Chandra S et al (2012) Upper Gondwana succession of the Rewa Basin, India: understanding the interrelationship of lithologic and stratigraphic variables. J Geol Soc India 79:563–575
Mutti M, Weissert H (1995) Triassic Monsoonal Climate and its signature in Ladinian—Carnian carbonate platforms (Southern Alps, Italy). J Sed Res B65:357–367

Nathorst AG (1876a) Anmärkningar om den fossilen floran vid Bjuf i Skåne. Öfversigt af Kongl Vetenskaps-Akad Förh 1:29–41
Nathorst AG (1876b) Bidrag till Sveriges fossila flora. Växter från rätiska formationen vid Pålsjö i Skåne. Kongl Vetenskaps-Akad Förh 14:1–82
Nathorst AG (1878a) Om floran i Skånes kolförande bildningar. Sver Geol Undersök Ser C 27:1–52
Nathorst AG (1878b) Beiträge zur fossilen Flora Schwedens. Über einige rhätische Pflanzen von Pålsjö in Schonen. Schweitzerbart'sche Verlagsbuchhandlung, Stuttgart
Nathorst AG (1878c) Bidrag till Sveriges fossila flora. II. Floran vid Höganäs och Helsingborg. Kungl Svenska Vetenskapsakad Handl 16(7):1–53
Nathorst AG (1879) Om floran i Skånes kolförande bildningar. Sver Geol Undersök Ser C 33:53–82
Nathorst AG (1880) Om de växtförande lagren i Skånes kolförande bildningar och deras plats i Lagerföljden. Geol Fören Stockholm Förhand 62:274–284
Nathorst AG (1886) Om floran i Skånes kolförande bildningar. Sver Geol Undersök Ser C 85:83–131
Nathorst AG (1888) Nya anmärkningar om *Williamsonia*. Kongl Vetenskaps-Akad Förh 6:359–365
Nathorst AG (1902) Beiträge zur Kenntnis einiger mesozoischen Cycadophyten. Kungl Svenska Vetenskapsakad Handl 36:1–28
Nathorst AG (1909a) Über die Gattung *Nilssonia* Brongn. mit besonderer Berücksichtigung schwedischer Arten. Kungl Svenska Vetenskapsakad Handl 43:3–37
Nathorst AG (1909b) Paläobotanische Mitteilungen 8. Über *Williamsonia, Wielandia, Cycadocephalus* und *Weltrichia*. Kungl Svenska Vetenskapsakad Handl 45:3–37
Nathorst AG (1913) How are the names *Williamsonia* and *Wielandiella* to be used? A question of nomenclature. Geol Fören Stockholm Förhand 35:361–366
Nielsen SN (2005) The Triassic Santa Juana Formation at the lower Biobío River, south central Chile. J South Am Earth Sci 19:547–562
Nilsson S (1820) Om försteningar och aftryck af tropiska trädslag, blad, ormbunkar och rörväxter m. m. samt trädkol funna i ett sandstenslager i Skåne. Kungl Svenska Vetenskapsakad Handl Ser 2:278–285
Nilsson T (1946) A new find of *Gerrothorax rhaeticus* Nilsson, a plagiosaurid from the Rhaetic of Scania. Lunds Universitets Årskrift n.f., avd. 2, 42(1–10):1–42
Nordt L, Atchley S, Dworkin S (2015) Collapse of the Late Triassic megamonsoon in western equatorial Pangea, present American Southwest. Geol Soc Am Bull 127:1798–1815
Odintsova MM (1977) Palynology of the Early Mesozoic of the Siberian platform. Nauka Sib otd AN SSSR, Novosibirsk. (in Russian)
Ogg JG, Ogg G, Gradstein FM (2008) The concise Geologic Time Scale 2008. Cambridge University Press, Cambridge
Ôishi S (1930) Notes on some fossil plants from the. Upper Triassic beds of Nariwa, Provo Bitchu. Japan. Inst Geol Palaeont Tôhoku Imp Uni Sendai, pp 49–58
Ôishi S (1931) Rhaetic plants from Province Nagato (Yamaguchi Prefecture), Japan. J Faculty of Science, Hokkaido Imperial University, ser 4 Geol Min 2(1):51–68
Ôishi S (1932a) Rhaetic Plants from Province Nagato (Yamaguchi Prefecture). J Fac Sci Hokkaido Imp Univ Ser 4 Geol Min 2:51–68
Ôishi S (1932b) The Rhaetic plants from the Nariwa Distric, Prov. Bitchû (Okayama Prefecture), Japan. J Fac Sci Hokkaido Imp Univ Ser 4 Geol Min 1:271–310
Ôishi S (1940) The Mesozoic Flora of Japan. J Fac Sci Hokkaido Imp Univ Ser 4 5:123–480
Ôishi S, Takahashi E (1936) Rhaetic plants from Nagato (a Supplement). J Fac Sci Hokkaido Imp Univ Ser 4 4:113–133
Olsen PE, Kent DV (2000) High resolution early Mesozoic Pangean climatic transect in lacustrine environments. Zentralbl Geol Paläont 11–12:1475–1496
Orłowska-Zwolińska T (1984) Palynostratigraphy of the Buntsandstein in sections of western Poland. Acta Pal Pol 29:161–194
P'an CH (1936) Older Mesozoic plants from North Shensi. Palaeont Sinica 4(2):1–49
Pacyna G (2014) Plant remains from the Polish Triassic. Present knowledge and future prospects. Acta Palaeobot 54:3–33

Pal PK (1984) Triassic plant megafossils from the Tiki Formation, South Rewa Gondwana Basin, India. Palaeobotanist 32:235–309
Pal PK (1985) Palaeobotany and stratigraphy of the Dhaurai Hill beds, South Rewa Gondwana Basin, India. Geophytology 15:224–225
Parrish JT (1993) Climate of the supercontinent Pangea. J Geol 101:215–233
Parrish JT, Peterson F (1988) Wind directions predicted from global circulation models and wind directions determined from eolian sandstones of the western United States: a comparison. Sed Geol 56:261–282
Paterson NW, Mangerud G (2015) Late Triassic (Carnian – Rhaetian) palynology of Hopen, Svalbard. Rev Palaeobot Palynol 220:98–119
Pattemore GA (2016a) The structure of umkomasiacean fructifications from the Triassic of Queensland. Acta Palaeobot 56:17–40
Pattemore GA (2016b) Megaflora of the Australian Triassic–Jurassic: a taxonomic revision. Acta Palaeobot 56:121–182
Pedersen KR (1976) Fossil floras of Greenland. In: Escher A, Watt WS (eds) Geology of Greenland. Geological Survey of Greenland, Copenhagen, pp 519–535
Pedersen KR, Lund JJ (1980) Palynology of the plant-bearing Rhaetian to Hetangian Kap Stewart Formation, Scoresby Sund, East Greenland. Rev Palaeobot Palynol 31:1–69
Peng J, Li J, Li W, Slater SM, Zhu H, Vajda V (2017a) Triassic to Early Jurassic vegetation change of the Tarim Basin, Xinjiang, China, based on palynology. Palaeobiol Palaeoenviron XX: xxx–xxx DOI 10.1007/s12549-017-0279-y
Peng J, Li J, Slater SM, Li W, Zhu H, Vajda V (2017b) Middle to Late Triassic palynofloras from southern Xizang (Tibet), China and their bearing on biostratigraphy and palynofloral provinces. Alcheringa XX: xxx–xxx
Peterffy O, Calner M, Vajda V (2016) Early Jurassic cyanobacterial mats—a potential response to reduced biotic activity in the aftermath of the Triassic mass extinction event. Palaeogeogr Palaeoclimatol Palaeoecol 464:76–85
Petti FM, Bernardi M, Kustatscher E et al (2013) Diversity of continental tetrapods and plants in the Triassic of the Southern Alps: ichnological, paleozoological and paleobotanical evidence. New Mex Mus Nat Hist Sci Bull 61:458–484
Pichler A (1868) Beiträge zur Geognosie Tirols. XI. Fossiles Harz. Jb k k Geol Reichsanst 18:45–52
Pott C (2007) Cuticular analysis of gymnosperm foliage from the Carnian (Upper Triassic) of Lunz, Lower Austria. PhD thesis, University Münster, 274 p
Pott C (2014a) A revision of *Wielandiella angustifolia*: a shrub-sized bennettite from the Rhaetian–Hettangian of Scania, Sweden, and Jameson Land, Greenland. Int J Plant Sci 175:467–499
Pott C (2014b) The Upper Triassic flora of Svalbard. Acta Pal Pol 59:709–740
Pott C (2016) *Westersheimia pramelreuthensis* from the Carnian (Upper Triassic) of Lunz, Austria: more evidence for a unitegmic seed coat in early Bennettitales. Int J Plant Sci 177:771–791
Pott C, Axsmith BJ (2015) *Williamsonia carolinensis* sp. nov. and associated *Eoginkgoites* foliage from the Upper Triassic Pekin Formation, North Carolina: implications for early evolution in the Williamsoniaceae (Bennettitales). Int J Plant Sci 176:174–185
Pott C, Bouchal JM, Yousif R, Bomfleur B (In press) Ferns and fern allies from the Carnian (Upper Triassic) flora of Lunz am See, Lower Austria: A melting pot of Mesozoic fern vegetation. Palaeontographica B XX:xxx–xxx
Pott C, Krings M (2010) Gymnosperm foliage from the Upper Triassic of Lunz, Lower Austria: an annotated checklist and identification key. Geo Alp 7:19–38
Pott C, Launis A (2015) *Taeniopteris novomundensis* sp. nov.—"cycadophyte" foliage from the Carnian of Switzerland and Svalbard reconsidered: how to use *Taeniopteris*? N Jb Geol Pal Abh 275:19–31
Pott C, McLoughlin S (2009) Bennettitalean foliage in the Rhaetian–Bajocian (latest Triassic–Middle Jurassic) floras of Scania, southern Sweden. Rev Palaeobot Palynol 158:117–166
Pott C, McLoughlin S (2011) The Rhaetian Flora of Rögla, Northern Scania, Sweden. Palaeontology 54:1025–1051

Pott C, Krings M, Kerp H (2007a) The first record of *Nilssoniopteris* (Gymnospermophyta, Bennettitales) from the Carnian (Upper Triassic) of Lunz, Lower Austria. Palaeontol Palaeont 50:1299–1318

Pott C, Van Konijnenburg-van Cittert JHA, Kerp H et al (2007b) Revision of the *Pterophyllum* species (Cycadophytina: Bennettitales) in the Carnian (Late Triassic) flora from Lunz, Lower Austria. Rev Palaeobot Palynol 147:3–27

Pott C, Kerp H, Krings M (2007c) Morphology and epidermal anatomy of *Nilssonia* (cycadalean foliage) from the Upper Triassic of Lunz (Lower Austria). Rev Palaeobot Palynol 143:197–217

Pott C, Kerp H, Krings M (2007d) *Pseudoctenis cornelii* nov. spec. (cycadalean foliage) from the Carnian (Upper Triassic) of Lunz, Lower Austria. Ann Naturhist Mus Wien 109A:1–17

Pott C, Kerp H, Krings M (2008a) Sphenophytes from the Carnian (Upper Triassic) of Lunz am See, Lower Austria. Jahrb Geol Bundesanstalt Wien 148:183–199

Pott C, Krings M, Kerp H (2008b) The Carnian (Late Triassic) flora from Lunz in Lower Austria: palaeoecological considerations. Palaeoworld 17:172–182

Pott C, Labandeira CC, Krings M, Kerp H (2008c) Fossil insect eggs and ovipositional damage on bennettitalean leaf cuticles from the Carnian (Upper Triassic) of Austria. J Paleont 82:778–789

Pott C, Schmeißner S, Dütsch G et al (2016a) Bennettitales in the Rhaetian flora of Wüstenwelsberg, Bavaria, Germany. Rev Palaeobot Palynol 232:98–118

Pott C, Van der Burgh J, Van Konijnenburg-van Cittert JHA (2016b) New ginkgophytes from the Upper Triassic–Lower Cretaceous of Spitsbergen and Edgeøya (Svalbard, Arctic Norway): the history of Ginkgoales on Svalbard. Int J Plant Sci 177:175–197

Pott C, Fischer T, Aschauer B (2017) *Lunzia austriaca*—a bennettitalean microsporangiate structure with Cycadopites-like in situ pollen from the Carnian (Upper Triassic) of Lunz, Austria. Grana 56:321–338

Preto N, Hinnov LA (2003) Unravelling the origin of shallow-water cyclothems in the Upper Triassic Dürrenstein Fm. (Dolomites, Italy). J Sed Res 73:774–789

Preto N, Kustatscher E, Wignall PB (2010) Triassic climates—state of the art and perspectives. Palaeogeogr Palaeoclimatol Palaeoecol 291:1–10

Price PL (1997) Permian to Jurassic palynostratigraphic nomenclature of the Bowen and Surat Basins. In: Green PM (ed) The Surat and Bowen Basins, South-east Queensland. Queensland Minerals and Energy Review Series, Queensland Department of Mines and Energy, Brisbane, pp 137–178

Prynada VD (1934) Ancient Mesozoic plants of Pamir. Tadzhik integrated expedition of 1932. Reports of the expedition. Geology of Pamir. Union Expeditional Committee GGGGU, Acad Sci USSR, Leningrad Department 9:1–100. (in Russian)

Qu LF, Yang JD, Bai YH, Zhang ZL (1983) A preliminary discussion on the characteristics and stratigraphic division of Triassic spores and pollen in China. Bull Chin Acad Geol Sci 5:81–94. (in Chinese with English abstract)

Reichgelt T, Parker WG, Martz JW et al (2013) The palynology of the Sonsela Member (Late Triassic, Norian) at Petrified Forest National Park, Arizona, USA. Rev Palaeobot Palynol 189:75–95

Retallack GJ (1977) Reconstructing Triassic vegetation of eastern Australasia: a new approach for the biostratigraphy of Gondwanaland. Alcheringa 1:247–278

Retallack GJ (1985) Triassic fossil plant fragments from shallow marine rocks of the Murihiku Supergroup, New Zealand. J Roy Soc New Zealand 15:1–26

Retallack GJ (1987) Triassic vegetation and geography of the New Zealand portion of the Gondwana supercontinent. In: Elliot DH, Collinson JW, McKenzie GD et al (eds) Gondwana Six: stratigraphy and paleontology. Amer Geophys Union, Geophys Monograph 41:29–39

Retallack GJ (1999) Postapocalyptic greenhouse paleoclimate revealed by earliest Triassic paleosols in the Sydney Basin, Australia. GSA Bull 111:52–70

Reymanówna M (1963) The Jurassic flora of Grojec near Cracow in Poland. Part I. Acta Palaeobot 4:9–48

Reymanówna M, Barbacka M (1981) *Lepidopteris ottonis* (Goeppert) Schimper z Wyżyny Śląsko-Krakowskiej i obrzeżenia Gór Świętokrzyskich (*Lepidopteris ottonis* (Goepp.) Schimp. from

Śląsko-Krakowska Highland and Holy Cross Mountains). In: Fauna i flora triasu obrzeżenia Gór Świętokrzyskich i Wyżyny Śląsko-Krakowskiej. Materiały V Krajowej Konferencji Paleontologicznej, Kielce-Sosnowiec, pp 79–84. (in Polish)

Robinson PL (1973) Paleoclimatology and continental drift. In: Tarling DH, Runcorn SK (eds) Implications of continental drift to the earth sciences. Academic Press, London, pp 449–476

Rogers RR, Swisher CC, Sereno PC et al (1993) The Ischigualasto tetrapod assemblage (Late Triassic, Argentina) and $^{40}Ar/^{39}Ar$ dating of dinosaur origins. Science 260:794–797

Roghi G (2004) Palynological investigations in the Carnian of the Cave del Predil area (Julian Alps, NE Italy). Rev Palaeobot Palyn 132:1–35

Roghi G, Coppellotti O, Ragazzi E (2005) Fossil microorganisms in Triassic amber of the Dolomites. Rend Soc Paleont Ital 2:209–217

Roghi G, Kustatscher E, Van Konijnenburg-van Cittert JHA (2006a) Late Triassic plants from Julian Alps (Italy). Boll Soc Paleont Ital 45:133–140

Roghi G, Ragazzi E, Gianolla P (2006b) Triassic amber of the Southern Alps (Italy). Palaios 21:143–154

Roghi G, Gianolla P, Minarelli L et al (2010) Palynological correlation of Carnian humid pulses throughout western Tethys. Palaeogeogr Palaeoclimatol Palaeoecol 290:89–106

Romanovskaya GM, Vasilieva NS (1990) Palynostratigraphy of Triassic deposits. In: Panova LA, Oshurkova MV, Romanovskaya GM (eds) Practical palynostratigraphy. Nedra, Leningrad, pp 81–102. (in Russian)

Roselt G (1954) Ein neuer Schachtelhalm aus dem Keuper und Beiträge zur Kenntnis von *Neocalamites meriani* Brongn. Geologie 3:617–643

Rozefelds AC, Sobbe I (1987) Problematic insect leaf mines from the Upper Triassic Ipswich Coal Measures of southeastern Queensland, Australia. Alcheringa 11:51–57

Sadler C, Parker WG, Ash SR (2015) Dawn of the dinosaurs. The Late Triassic in the American Southwest. Petrified Forest Museum Association, Petrified Forest, Arizona, p 124

Sakulina GV (1973) Middle and Late Triassic miospores from South-Eastern Kazakhstan. In: Chlonova AF (ed) Palynology of mesophyte. Proc Int Palynol Conf, 3rd, Nauka, Moscow, pp 33–38. (In Russian)

Salard M (1968) Contribution à la connaissance de la flore fossile de la Nouvelle Calédonie. Palaeontographica B 124:1–44

Schenk A (1866–1867) Über die Flora der schwarzen Schiefer von Raibl. Würzb naturwiss Zeitschr 6:10–20

Schenk A (1867) Bemerkungen über einige Pflanzen der Lettenkohle und des Schilfsandsteines. Würzb naturwiss Zeitschr 6:49–63

Schenk A (1883) Jurassische Pflanzen. In: von Richthofen F (ed) China, vol 4. Studien Verlag von Dietrich Reimer, Berlin, pp 245–269

Schenk A (1884) Die Wahrend der Reise des Grafen Bela Szechenyi in China Gesammelten fossilen Pflanzen. Palaeontographica B 31:163–182

Schmidt M (1928) Die Lebewelt unserer Trias. Hohenlohe'sche Buchhandlung, Öhringen

Schmidt AR, Ragazzi E, Coppellotti O, Roghi G (2006) A microworld in Triassic amber. Nature 444:835

Schmidt AR, Jancke S, Lindquist EE et al (2012) Arthropods in amber from the Triassic Period. PNAS 109(37):14796–14801

Schönborn W, Dörfelt H, Foissner W et al (1999) A fossilized microcenosis in Triassic amber. J Eukaryot Microbiol 46(6):571–584

Schultz G, Hope RC (1973) Late Triassic microfossil flora from the Deep River Basin, North Carolina. Palaeontographica B 141:63–88

Schweitzer HJ (1977) Die räto-jurassischen Floren des Iran und Afghanistans. 4. Die rätische zwitterblüte *Irania hermaphroditica* nov. sp. und ihre Bedeutung für die Phylogenie der Angiospermen. Palaeontographica B 161:98–145

Schweitzer HJ (1978) Die rhäto-jurassischen Floren des Iran und Afghanistans: 5. *Todites princeps, Thaumatopteris brauniana* und *Phlebopteris polypodioides*. Palaeontographica B 168:17–60

Schweitzer H-J, Kirchner M (1995) Die rhäto-jurassischen Floren des Iran und Afghanistans. 8. Ginkgophyta. Palaeontographica B 237:1–58
Schweitzer H-J, Kirchner M (1996) Die rhäto-jurassischen Floren des Iran und Afghanistans. 9. Coniferophyta. Palaeontographica B 238:77–139
Schweitzer H-J, Kirchner M (1998) Die rhäto-jurassischen Floren des Iran und Afghanistans. 11. Pteridospermophyta und Cycadophyta I. Cycadales. Palaeontographica B 248:1–85
Schweitzer H-J, Kirchner M (2003) Die rhäto-jurassischen Floren des Iran und Afghanistans 13. Cycadophyta. III. Bennettitales. Palaeontographica B 264:1–166
Schweitzer HJ, Van-Konijnenburg-van Cittert JHA, van der Burg J (1997) The Rhaeto-Jurassic flora of Iran and Afghanistan. 10. Bryophyta, Lycophyta, Sphenophyta, Pterophyta-Eusporangiate and Protoleptosporangiate. Palaeontographica B 243:103–192
Schweitzer HJ, Kirchner M, Van-Konijnenburg-van Cittert JHA (2000) The Rhaeto-Jurassic flora of Iran and Afghanistan. 12. Cycadophyta II. Nilssoniales. Palaeontographica B 279:1–108
Schweitzer HJ, Schweitzer U, Kirchner M et al (2009) The Rhaeto-Jurassic flora of Iran and Afghanistan. 14. Pterophyta-Leptosporangiatae. Palaeontographica B 279:1–108
Scott AC, Anderson JM, Anderson HM (2004) Evidence of plant–insect interactions in the Upper Triassic Molteno Formation of South Africa. J Geol Soc Lond 161:401–410
Selling OH (1944) On cupressoid root remains of Mesozoic age from the Arctic. Arkiv för Botanik 31A(13):1–20
Selling OH (1945) A megaspore from the Mesozoic of Hope Island, Svalbard. Bot Notiser 1:44–48
Semenova EV (1970) Spore and pollen assemblages of deposits of the Jurassic and Triassic Boundary of the Donents Basin. Naukova Dumka, Kiev. (In Russian)
Semenova EV (1973) Correlation of the Upper Triassic of the Donets Basin and some Central European regions according to miospores. In: Chlonova AF (ed) Palynology of mesophyte. Proceedings of the 3rd International Palynological Conference. Nauka, Moscow, pp 42–44. (In Russian)
Sha J, Vajda V, Pan Y et al (2011) The stratigraphy of the Triassic−Jurassic boundary successions of the southern margin of Junggar Basin, northwestern China. Act Geol Sin 85:421–436
Sha J, Olsen PE, Pan Y et al (2015) Triassic−Jurassic climate in continental high-latitude Asia was dominated by obliquity-paced variations (Junggar Basin, Urumqi, China). PNAS 112:3624–3629
Shao J, Tang K, Wang C et al (1992) Structural feature and evolution of the Nadanhada Terrane. Sci China B 35:621–630
Shorokhova SA (1975a) Novye osmundovye paporotniki iz verhnego triasa Primor'ja (New Osmundaceae from the Upper Triassic of Primorye). Paleont Zhurn 4:106–110. (In Russian)
Shorokhova SA (1975b) The Early Mesozoic flora of Primorye and its significance for the stratigraphy. In: Avtoreferat kand. dissertatsii, Moscow, p 21. (In Russian)
Shorokhova SA, Srebrodolskaya IN (1979) Some Triassic plants from Primorye. Trudy biol pochv in ta DVNTS AN SSSR, Vladivostok. (In Russian)
Sigmund A (1937) Die Minerale Niederösterreichs, 2nd edn. Deuticke, Wien-Leipzig
Simms MJ, Ruffel AH (1989) Synchroneity of climatic change and extinctions in the Late Triassic. Geology 17:265–268
Simms MJ, Ruffel AH (1990) Climatic and biotic change in the late Triassic. J Geol Soc Lond 147:321–327
Simms MJ, Ruffel AH, Johnson LA (1995) Biotic and climatic changes in the Carnian (Triassic) of Europe and adjacent areas. In: Fraser NC, Sues HD (eds) In the shadow of the dinosaurs: early mesozoic tetrapods. Cambridge University Press, Cambridge, pp 352–365
Sixtel TA (1960) Stratigrafija kontinental'nyh otlozhenij verhnej permi i triasa Srednej Azii. (The stratigraphy of the continental sediments of the Upper Permian and Triassic of Middle Asia). Trudy Tashkent Univ, Nov Ser, geol. Nauki, Tashkent. (In Russian)
Sixtel TA (1961) The representatives of the *Gigantopteris* and some accompanying plants from the Madygen Formation of Fergana. Paleont J 1:151–158. (in Russian)
Sixtel TA (1962) Flora of the Late Permian and Early Triassic in Southern Fergana. Stratigrafia i Paleontologia Uzbekistana i sopredelnychrayonov, Tashkent, pp 271–414. (in Russian)

Smoot JP, Olsen PE (1988) Massive mudstones in basin analysis and paleoclimatic interpretation of the Newark Supergroup. In: Manspeizer W (ed) Triassic–Jurassic rifting, continental breakup and the origin of the Atlantic Ocean and passive margins. Elsevier, New York, pp 249–274

Solms-Laubach G (1899) Beschreibung der Pfianzenreste von La Ternera. N Jb Min Geol Pal 12:593–609

Soom M (1984) Bernstein vom Nordrand der Schweizer Alpen. Stuttgarter Beitr Naturk, Ser C 18:15–20

Spalletti LA, Artabe AE, Morel E et al (1999) Biozonación paleoflorística y cronoestratigrafía del Triásico Argentino. Ameghiniana 36:419–451

Spalletti LA, Morel EM, Artabe AE et al (2005) Estratigrafía, facies y paleoflora de la sucesión triásica de Potrerillos, Mendoza, República Argentina. Rev Geol Chile 32:249–272

Srebrodolskaya IN (1960) Novye materialy po mongugajskim floram juzhnogo Primor'ja (New data on the Mongugay floras of Southern Primorye). Inf. bull. VSEGEI (24):107–116. (In Russian)

Srivastava SC, Manik SR (1991) Triassic flora of India; a transition. Palaeobotanist 40:244

Srivastava SC, Pal PK (1983) Upper Triassic fossil plants from Son River section near Giar, Shahdol district, M.P, India. Geophytology 13:238

Stanislavsky FA (1965) Ostatki roda *Neocalamites* iz verhnego triasa Doneckogo bassejna (The remains of the genus *Neocalamites* from the Upper Triassic of the Donets Basin). Paleont. Sbornik 2:88–95. (In Russian)

Stanislavsky FA (1971) Iskopaemaja flora i stratigrafija verhnetriasovyh otlozhenij Donbassa (Fossil flora and stratigraphy of Upper Triassic sediments in the Donetz Basin (Rhaetian flora from Raiskoye). Naukova Dumka, Kiev. (In Russian)

Stanislavsky FA (1973) Novyj rod *Toretzia* iz verhnego triasa Donbassa i ego otnoshenie k rodam porjadka Ginkgoales (New genus *Toretzia* from the Upper Triassic of the Donbass and its relations to the genera of the Ginkgoales order). Paleont Zhurn 1:88–96. (In Russian)

Stanislavsky FA (1976) Srednekejperskaja flora Doneckogo bassejna (The Middle Keuper flora of the Donets Basino vremeni). Naukova Dumka, Kiev. (In Russian)

Steinthorsdottir M, Tosolini A-MP, McElwain JC (2015) Evidence for insect and annelid activity across the Triassic-Jurassic transition of east Greenland. Palaios 30:597–607

Strullu-Derrien C, McLoughlin S, Philippe M et al (2012) Arthropod interactions with bennettitalean roots in a Triassic permineralized peat from Hopen, Svalbard Archipelago (Arctic). Palaeogeogr Palaeoclimatol Palaeoecol 348–349:45–58

Stubblefield SP, Taylor TN (1986) Wood decay in silicified gymnosperms from Antarctica. Bot Gaz 147:116–125

Stur D (1868) Beiträge zur Kenntnis der geologischen Verhältnisse der Umgebung von Raibl und Kaltwasser. Jb Geol Reichsans 18:71–122

Stur D (1885) Die obertriadische Flora der Lunzer-Schichten und des bituminösen Schiefers von Raibl. Sitzungsber Kais Akad Wissensch Wien, Math-Naturwiss Klasse 91:93–103

Sukh-Dev (1987) Floristic zones in the Mesozoic formations and their relative age. Palaeobotanist 36:161–167

Sun G (1979) On the discovery of *Cycadocarpidium* from the Upper Triassic of eastern Jilin. Acta Palaeont Sinica 18:312–325. (in Chinese with English abstract)

Sun G (1981) Discovery of Dipteridaceae from Upper Triassic of eastern Jilin. Acta Palaeont Sin 20:459–467. (in Chinese with English abstract)

Sun G (1987) On Late Triassic geofloras in China and principles for palaeophytogeographic regionalization. Acta Geol Sin 61:1–9

Sun G (1990) Correlation on Late Triassic floras from Tianqiaoling of Jilin, China to from Mongugai of S. Primorye, USSR and its geological significance. In: Editorial Committee of 4th Symp. Asian Cont. Pacific Trans Zon (ed) Abstract collections 4th Symp. Asian Cont. Pacific Trans. Zon, Beijing, pp 31–32

Sun G (1993) Late Triassic flora from Tianqiaoling of Jilin, China. Jilin Science and Technology Publishing House, Changchun. (in Chinese with English summary)

Surlyk F (2003) The Jurassic of East Greenland: a sedimentary record of thermal subsidence, onset and culmination of rifting. In: Ineson JR, Surlyk F (eds) The Jurassic of Denmark and Greenland. Geol Surv Denmark Greenland, Copenhagen, pp 659–723
Sze (1933) Fossile Pflanzen aus Shensi, Szechuan and Kueichow. Palaeont Sin A 1(3):1–32
Sze HC (1956a) On the occurrence of the Yenchang Formation in Kuyuan district, Kansu Province. Acta Palaeont Sin 4:285–292. (in Chinese and English)
Sze HC (1956b) The fossil flora of the Mesozoic oil-bearing deposits of the Dzungaria-Basin, northwestern Sinkiang. Acta Palaeont Sin 4:461–467. (in Chinese and English)
Sze HC (1960) Late Triassic plants from Tiencho, Kansu. In: Institute of Geology and Paleontology, Academia Sinica et al (eds) Contribution to Geology of the Chilien Mts. Science Press, Beijing 4:23–26. (in Chinese)
Sze H, Lee H (1952) Jurassic plant from Szechuan. Palaeont Sin A, No. 135(Ser. A., no 3):1–38. (in Chinese with English abstract)
Takahashi E (1951) Descriptive notes on some Mesozoic plants from Province Nagato. J Geol Soc Jap 664:29–33
Tanner LH, Lucas SG (2007) The Moenave Formation: sedimentologic and stratigraphic context of the Triassic–Jurassic boundary in the Four Corners area, southwestern U.S.A. Palaeogeogr Palaeoclimatol Palaeoecol 244:111–125
Tanner LH, Lucas SG (2013) Degraded wood in the Upper Triassic Petrified Forest Formation (Chinle Group), northern Arizona: differentiating fungal rot from arthropod boring. In: Tanner LH, Spielmann JA, Lucas SG (eds) The Triassic system. New Mexico Mus Nat Hist Sci Bull 61:582–582B
Taylor EL (1989) Tree-ring structure in woody axes from the central Transantarctic Mountains, Antarctica. In: Proceedings of the International Symposium on Antarctic Research, China. Ocean Press, Tianjin, pp 109–113
Tidwell WD, Kim J-H, Kimura T (1987) Mid-Mesozoic leaves from near Ida Bay, southern Tasmania, Australia. Pap Proc R Soc Tasmania 121:159–170
Tillyard RJ (1922) Mesozoic insects of Queensland. 9. Orthoptera, and additions to the Protorthoptera, Odonata, Hemiptera and Plannipennia. Proc Linn Soc New South Wales 47:447–470
Traverse A (1986) Palynology of the Deep River Basin, North Carolina. In: Gore PJW (ed) Framework of a Triassic rift basin: the Durham and Sanford sub-basins of the Deep River Basin, North Carolina. Field Trip #3, Society of Economic Paleontologists and Mineralogists Meeting, Raleigh, NC, pp 66–71
Tripathi A, Vijaya, Raychowdhuri AK (2005) Triassic palynoflora from the Mahuli-Mahersop area, Singrauli Coalfield (southern extension), Sarguja district, Chhattisgarh, India. J Palaeont Soc India 50:77–99
Troedsson G (1943) Om gränsen mellan rät och lias i Skåne. Geol Fören Stockholm Förhand 65:271–284
Troedsson G (1950) Om lagerföljden inom Sveriges äldre Mesozoikum. Medd fra Dansk Geol Foren 11:595–597
Troedsson G (1951) On the Höganäs Series of Sweden (Rhaeto-Lias). Skrifter från Mineralogisk-Paleont-Geol Institut Lund 7:1–269
Turner S, Bean LB, Dettmann M, McKellar J, McLoughlin S, Thulborn T (2009) Australian Jurassic sedimentary and fossil successions: current work and future prospects for marine and non-marine correlation. GFF 131:49–70
Turutanova-Ketova AI (1931) Materialy k poznaniju jurskoj flory bassejna oz. Issyk-Kul' v Kirgizskoj SSR (The materials to the knowledge of the Jurassic flora of the Issyk-Kul Basin in the Kirgiz SSR). Trudy Geol Mus AN SSSR 8:311–356. (In Russian)
Vaez-Javadi F (2012) Plant macrofossils from Tiar area, South Amol, dating and correlation with the other florizones of Iran. Geosciences 21(83):229–237. (In Persian)
Vaez-Javadi F (2013a) Triassic and Jurassic floras and climate of central-east Iran. Geological Survey of Iran, Rahi Publication, Tehran, p 254

Vaez-Javadi F (2013b) *Williamsonia iranica* sp. nov. and *Ginkgoites persica* sp. nov. from the Rhaetian of Nayband Formation, Tabas. J Strat Sed Res Esfahan 48(4):25–34. (In Persian)

Vajda V, Bercovici A (2014) The global vegetation pattern across the Cretaceous–Paleogene mass-extinction interval—an integrated global perspective. Global Planet Change 12:29–49

Vajda V, McLoughlin S (2004) Fungal proliferation at the Cretaceous-Tertiary boundary. Science 303:1489

Vajda V, McLoughlin S (2007) Extinction and recovery patterns of the vegetation across the Cretaceous–Palaeogene boundary—a tool for unravelling the causes of the end-Permian mass-extinction. Rev Palaeobot Palynol 144:99–112

Vajda V, Wigforss-Lange J (2009) Onshore Jurassic of Scandinavia and related areas. GFF 131:5–23

Vajda V, Raine JI, Hollis CJ (2001) Indication of global deforestation at the Cretaceous-Tertiary boundary by New Zealand fern spike. Science 294:1700–1702

Vajda V, Calner M, Ahlberg A (2013) Palynostratigraphy of dinosaur footprint-bearing deposits from the Triassic–Jurassic boundary interval of Sweden. GFF 135:120–130

Vajda V, Linderson H, McLoughlin S (2016) Disrupted vegetation as a response to Jurassic volcanism in southern Sweden. In: Kear BP, Lindgren J, Hurum JH, Milàn J, Vajda V (eds) Mesozoic Biotas of Scandinavia and its Arctic Territories. Geological Society, London, Special Publications 434:127–147

Vakhrameev VA, Dobruskina IA, Zaklinskaya EL (1970) Paleozoic and Mesozoic floras of Eurasia and phytogeography of that time. Trans Geol Inst Acad Sci USSR Nauka, Moscow. (In Russian)

Vakhrameev VA, Dobruskina IA, Zhatkova EA, Yaroshenko OP (1977) Verhnetriasovye floronosnye otlozhenija Vostochnogo Predkavkaz'ja (The Upper Triassic plant-bearing beds of Eastern Predkavkazye). Izv AN SSSR Ser Geol 3:62–72. (In Russian)

Vakhrameev VA, Dobruskina IA, Meyen SV et al (1978) Paläozoische und mesozoische Floren Eurasiens und die Phytogeographie dieser Zeit. VEB Gustav Fischer Verlag, Jena

van de Schootbrugge B, Tremolada F, Rosenthal Y et al (2007) End-Triassic calcification crisis and blooms of organic-walled 'disaster species'. Palaeogeogr Palaeoclimatol Palaeoecol 244:126–141

Van Konijnenburg-van Cittert JHA, Kustatscher E, Bauer K et al (2014) A *Selaginellites* from the Rhaetian of Wüstenwelsberg (Upper Franconia, Germany). N Jb Geol Pal Abh 272:115–127

Van Konijnenburg-van Cittert JHA, Kustatscher E, Pott C et al (2016) New data on *Selaginellites coburgensis* from the Rhaetian of Wüstenwelsberg (Upper Franconia, Germany). N Jb Geol Paläont Abh 280:177–181

Variukhina LM (1971) Spores and pollen of red color and coal bearing deposits of Permian and Triassic of north-east of European part of USSR. Nauka, Leningrad. (In Russian)

Vasilenko DV (2009) Traces of plant-arthropod interactions from Madygen (Triassic, Kyrgyzstan): preliminary data. In: Sovremennaya paleontologia: klassicheskie i noveishie metody. PIN RAS, Moscow, pp 9–15. (In Russian)

Vassilevskaja ND (1972) Late Triassic flora of Svalbard. In: Mesozoic deposits of Svalbard. NIIGA, St Petersburg, pp 27–63

Vávra N (1984) Reich an armen Fundstellen: Übersicht über die fossilen Harze Osterreichs. Stuttgarter Beitr Naturk Ser C 18:9–14

Vavrek MJ, Larsson HCE, Rybczynski N (2007) A Late Triassic flora from east-central Axel Heiberg Island, Nunavut, Canada. Can J Earth Sci 44:1653–1659

Vigran J, Mangerud G, Mørk A et al (2014) Palynology and geology of the Triassic succession of Svalbard and the Barents Sea. Norweg Geol Surv Spec Publ 14:1–274

Vinogradova KV, Tsaturova AA (2005) Palynostratigraphy and paleogeography of the Triassic deposits of Southern Mangyshlak. In: Afonin SA, Tokarev PI (eds) Proceedings of XI All-Russian palynological conference "Palynology: Theory & applications", (27 september – 1 october 2005). PIN RAS, Moscow, pp 46–47. (In Russian)

Visscher H, Brinkhuis H, Dilcher DL et al (1996) The terminal Paleozoic fungal event: evidence of terrestrial ecosystem destabilization and collapse. Proc Natl Acad Sci U S A 93:2155–2158

Vladimirovich VP (1959) K izucheniju verhnetriasovoj i nizhnejurskoj flory Vostochnogo Urala (On the study of the Late Triassic–Early Jurassic flora of Eastern Urals). Bot Zhurn 49:458–466. (In Russian)
Vladimirovich VP (1965) Ostatki nekotoryh predstavitelej roda *Thinnfeldia* iz rjetskih otlozhenij Vostochnogo Urala (Remains of some representatives of the genus *Thinnfeldia* from the Rhaetian deposits of the Eastern Urals). Ezhegodnik VPO XVII:238–261. (In Russian)
Vladimirovich VP (1967) Biostratigraphy of the continental Triassic and Jurassic deposits of the Eastern slope of the Urals, northern Kazakhstan and mountaneous part of western Siberia. In: Stratigraphy and palaeontology of the Mesozoic and Palaeogene–Neogene continental deposits of the Asian part of the USSR. Nauka, Moscow, pp 46–56. (In Russian)
Volynets EB, Shorokhova SA (2007) Late Triassic (Mongugai) flora of the Primorye region and its position among coeval floras of Eurasia. Russ J Pac Geol 1(5):482–494. (In Russian)
Volynets E, Shorokhova SA, Ge S (2008) Late Triassic flora of the Partizanskaya River Basin (Southern Primor'e). Stratigr Geol Correl 16(1):47–58. https://doi.org/10.1007/s11506-008-1004-0. (In Russian)
von Hillebrandt A, Krystyn L, Kürschner WM, Bown PR, McRoberts C, Ruhl M, Simms M, Tomasovych A, Urlichs M (2008) A candidate GSSP for the base of the Jurassic in the Northern Calcareous Alps (Kuhjoch section; Karwendel Mountains, Tyrol, Austria). Intern Subcom Jurassic Stratigraphy, Triassic/Jurassic Boundary Working Group Ballot, pp 2–20
von Richthofen F (1882) China. Ergebnisse eigener Reisen und darauf gegründeter Studien. 5 Bände mit Atlas. Band 2: Das nördliche China. Dietrich Reimer, Berlin
Vozenin-Serra C, Salard-Cheboldaeff M (1992) Les bois mineralises Permo-Triasiques de Nouvelle Calédonie. Implications phylogenetique et paleogeographique. Palaeontographica B 225B:1–25
Walker MV (1938) Evidence of Triassic insects in the Petrified Forest National Monument. U.S. Nat Mus Proc 88:137–141
Walkom AB (1917) Mesozoic floras of Queensland. Part 1 continued. The flora of the Ipswich and Walloon Series (c.) Filicales, etc. Geol Surv Queensl Publ 257:1–65
Wang PX (2009) Global monsoon in a geological perspective. Chinese Sci Bull 54:1113–1136
Wang C, Kang B, Zhang H (1986) A discovery of Triassic conodonts in the Nadanhad Range and geological significance. In: Editorial Committee of Contribution for the Project of Plate Tectonics in Northern China (ed) Contributions for the project of plate tectonics in northern China. Geological Publishing House, Beijing, pp 208–213. (in Chinese with English abstract)
Wang YD, Fu BH, Xie XP et al (2010) The terrestrial Triassic and Jurassic Systems in the Sichuan Basin, China. University of Science and Technology of China Press, Hefei. 216 p
Wappler T, Kustatscher E, Dellantonio E (2015) Plant–insect interactions from Middle Triassic (late Ladinian) of Monte Agnello (Dolomites, N-Italy): initial pattern and response to abiotic environmental pertubations. PeerJ 3:e921. https://doi.org/10.7717/peerj.921
Ward LH (1900) The older Mesozoic. In: Status of the Mesozoic floras of the United States. US Geological Survey, Twentieth Annual Report 2:213–768
Wawrzyniak Z, Ziaja J (2009) Wstępne wyniki badań górnotriasowej makroflory Lipia Śląskiego, Polska. Preliminary results of research of the Upper Triassic macroflora from Lipie Śląskie, Poland. In: Krobicki M (ed) Jurassica VIII, Vršatec 09–11.10.2009. Kwartalnik AGH Geologia 35(3/1):105–106
Webb JA (1982) Triassic species of *Dictyophyllum* from eastern Australia. Alcheringa 6:79–91
Weber R (1968) Die fossile Flora der Rhät-Lias-Übergangsschichten von Bayreuth (Oberfranken) unter besonderer Berücksichtigung der Coenologie. Erlanger geol Abh 72:1–73
Weber R (1995) A new species of *Scoresbya* Harris and *Sonoraphyllum* gen. nov. (Plantae incertae sedis) from the Late Triassic of Sonora, Mexico. Rev Mexic Ciencias Geo1 12:94–107
Weber R (1996) Review of *Macropterygium* Schimper ("Cycadophyta", presumed Bennettitales) and a new species from the Upper Triassic of Sonora, Northwestern Mexico. Rev Mexic Ciencias Geo1 13:201–220
Weber R (1997) How old is the Triassic flora of Sonora and Tamaulipas and news on Leonardian floras in Puebla and Hidalgo, Mexico. Rev Mexic Ciencias Geo1 14:225–243

Weber R (1999) New and poorly known ferns from the Santa Clara Formation, Late Triassic, Sonora, NW Mexico, III, Marattiales. *Tranuilia* Herbst: a panamerican dimorphic genus. Rev Mexic Ciencias Geo1 16:172–186
Weems RE, Tanner LH, Lucas SG (2016) Synthesis and revision of the lithostratigraphic groups and formations in the Upper Permian?–Lower Jurassic Newark Supergroup of eastern North America. Stratigraphy 13:111–153
Wendt J, Fürsich FT (1980) Facies analysis and palaeogeography of the Cassian Formation, Triassic, Southern Alps. Riv Ital Paleont Stratigr 85:1003–1028
Willis KJ, McElwain JC (2002) The evolution of plants. Oxford University Press, New York
Wu H, Pu Y (1982) Sporo-pollen assemblage from the Beishan Formation of Hunjiang, Jilin. In: Palynological Society of China (ed) Selected papers for the First Scientific Symposium of the Palynological Society of China. Beijing Science Press, pp 110–115. (in Chinese)
Wu S, Ye M, Li B (1980) Upper Triassic and Lower and Middle Jurassic plants from the Hsiangchi Group, western Hubei. Mem Nanjiang Inst Geol Palaeont Acad Sin 14:63–131. (in Chinese with English abstract)
Yabe H (1905) Mesozoic plants from Korea. J Coll Sci Imp Univ Tokyo, Japan 20:1–59
Yang X (1978) The vegetable kingdom (Mesozoic). In: Chengdu Institute of Geology and Mineral Resources (The Southwest China Institute of Geological Science) (ed) Altas of fossils of Southwest China, Sichuan volumn, (Part II): Carboniferous to Mesozoic. Geological Publishing House, Beijing, pp 469–536. (in Chinese)
Yaroshenko OP (1978) Miospore assemblages and stratigraphy of the Triassic of the Western Caucasus Mountains. Proc Geol Inst Acad Sci USSR, vol 324. Nauka, Moscow. (In Russian)
Yaroshenko OP (2007) Late Triassic palynological flora from western Ciscaucasia. Paleont J 41:1190–1197. https://doi.org/10.1134/S0031030107110172. (In Russian)
Ye M, Liu X (1986) Late Triassic and Early-Middle Jurassic fossil plants from northeastern-Sichuan. Anhui Science and Technology Publishing House, Hefei, p 141. (in Chinese with English abstract)
Yin H, Ling Q (1986) Triassic palaeobiogeographic provincialization of China. In: Palaeotological Society of China (ed) Selected papers 13th and 14th annual conventions of palaeontological Society of China. Anhui Science and technology Publishing House, pp 189–203. (in Chinese with English abstract abstract)
Zardini R (1973) Geologia e fossili attorno a Cortina d'Ampezzo. Ed. Ghedina, Cortina d'Ampezzo.
Zavattieri AM, Mego N (2008) Palynological record of the Paso Flores Formation (Late Triassic) on the southeastern side of the Limay River, Patagonia, Argentina. Ameghiniana 45:483–502
Zavattieri AM, Volkheimer W, Rosenfeld U (1994) Palynology and facies of the Late Triassic of Comallo (Northern Patagonia, Argentina). Zentralbl Geol Palaeontol 1:133–154
Zavialova NE, Roghi G (2005) Exine morphology and ultrastructure of *Duplicisporites* from the Triassic of Italy. Grana 44:337–342
Zavialova NE, Van Konijnenburg-van Cittert JHA (2011) Exine ultrastructure of *in situ* peltasperm pollen from the Rhaetian of Germany and its implications. Rev Palaeobot Palynol 168:7–20
Zeiller R (1903) Flore fossile des Gîtes de Charbon du Tonkin. Études des Gîtes mineraux de la France.
Zhang Q (1990) Triassic and Jurassic Radiolaria fauna in Nadanhada Range, northeast China. Bull Shenyang Inst Geol Miner Resour 21:157–191. in Chinese with English abstract
Zhang W, Grant-Mackie JA (2001) Late Triassic–Early Jurassic palynofloral assemblages from Murihiku strata of New Zealand, and comparisons with China. J R Soc New Zealand 31:575–683
Zhou T (1978) The Mesozoic coal-bearing strata and fossil plants from Fujian Province. Prof Pap Strat Palaeont 4:88–134. (in Chinese)
Zhou Z (1989) Late Triassic plants from Shaqiao, Hengyang, Hunan Province. Palaeont Cathayana 4:131–197
Zhou T, Zhou H (1983) Triassic non-marine strata and flora of China. Bull Chin Acad Geol Sci 5(5):95–108

Chapter 14
Expansion of Arthropod Herbivory in Late Triassic South Africa: The Molteno Biota, Aasvoëlberg 411 Site and Developmental Biology of a Gall

Conrad C. Labandeira, John M. Anderson, and Heidi M. Anderson

Abstract The Carnian Aasvoëlberg 411 (Aas411) site of the Molteno Formation in South Africa provides exceptional data for understanding how plants, their arthropod herbivores and interactions responded to the P-Tr ecological crisis approximately 18 million years earlier. Our study lists six consequences stemming from the P-Tr event. First, Aas411 was one of the most herbivorized of Molteno's 106 sites, consisting of 20,358 plant specimens represented by 111 plant form-taxa that includes 14 whole-plant taxa (WPT); the insect damage consists of 11 functional feeding groups (FFGs), 44 damage types (DTs) and 1127 herbivorized specimens for an herbivory value of 5.54%. Second, the seven most herbivorized hosts, in decreasing importance, were the conifer *Heidiphyllum elongatum*; corystosperm *Dicroidium crassinervis*; ginkgophyte *Sphenobaiera schenckii*, peltasperms *Lepidopteris stormbergensis* and *L. africana* and horsetail *Zonulamites viridensis*. Third, generalized feeding damage and 11 host-specialized associations were present that targeted 39 of 111 plant taxa. Fourth, the *Heidiphyllum elongatum* WPT was most herbivorized, harboring an extensive herbivore component community containing 81.8% of FFGs, 63.6% of DT categories, 40.9% of DT occurrences, and 36.4% of specialized interactions at the site. Fifth, eriophyioid gall DT70 was

C.C. Labandeira (✉)
Department of Paleobiology, National Museum of Natural History, Smithsonian Institution, Washington, DC 20013-7012, USA

Department of Entomology and BEES Program, University of Maryland, College Park, MD 20742, USA

College of Life Sciences, Capital Normal University, Beijing 100048, China
e-mail: labandec@si.edu

J.M. Anderson • H.M. Anderson
Evolutionary Studies Institute, University of the Witwatersrand, Johannesburg 2000, South Africa
e-mail: jmanderson.gondwana@googlemail.com; hmsholmes@googlemail.com

© Springer International Publishing AG 2018

L.H. Tanner (ed.), *The Late Triassic World*, Topics in Geobiology 46,
https://doi.org/10.1007/978-3-319-68009-5_14

host-specialized on *Dicroidium crassinervis*, where it constitutes 70.1% of all Molteno DT70 occurrences and revealing a distinctive developmental ontogeny. Sixth, herbivory levels significantly surpassed those of the Late Permian.

Keywords Carnian • Component community • Damage Type • *Dicroidium crassinervis* • End-Permian extinction • Gondwana • *Heidiphyllum elongatum* • Karoo Basin • Mite gall • Plant–insect interactions

14.1 Introduction

The most consequential event for the Phanerozoic history of life was the end-Permian ecological crisis (P-Tr event) that extinguished numerous, indeed an overwhelming majority, of lineages in the marine and terrestrial realms (Erwin 2006). For the terrestrial realm, most subordinate lineages and many major lineages of plant and arthropod clades experienced a major extinction (Labandeira 2005; Hochuli et al. 2010), although some fungal clades may have had an opposite response (Visscher et al. 1996). This event undoubtedly resulted in permanent removal or degradation of many antagonistic interactions, mutualistic associations and other varied and diffuse relationships (Krassilov and Karasev 2008; Labandeira et al. 2016; Feng et al. 2017). As important as the ravages of the taxonomic extinctions were, the devastation of more ecologically specialist interactions likely was greater (Shcherbakov 2000; Wang et al. 2009; Feng et al. 2017). The demise of particular specialized interactions resulted in a shift from an intricate, developing nexus of inter-organismic relationships present in the Late Permian to the virtual absence of such interactions during the Early Triassic. Terrestrial lineages that survived into the Early Triassic represented a small subset of the previously existing diversity of life and their relationships occurring in the Late Permian (Lopingian) (Labandeira 2006a). Nevertheless, it was these surviving, taxonomically depauperate lineages and their few trophic inter-relationships that sowed the seeds of a recovery. After the 10 million-year-long recovery interval of the Early Triassic (Induan and Olenekian stages) and first part of the Middle Triassic (Anisian Stage), there was by contrast a spectacular flourishing of plant, insect and even fungal lineages and their ecological networks (Labandeira et al. 2016). Many interactions that appeared during the later Triassic were the same types of associations that were extinguished during the Late Permian (Roopnarine and Angielczyk 2015; Labandeira et al. 2016; Feng et al. 2017). The difference was that the Triassic plant, insect and fungal participants originated from different, unrelated clades than those of the Permian (Béthoux et al. 2005; Labandeira 2005; Hochuli et al. 2010; Ponomarenko 2016; Yang et al. 2012), attributable to an ecological sorting process during the P-Tr event (Sidor et al. 2013; Prinzing et al. 2017).

One approach toward understanding this major transformation in the relationships between plants and insects before and after the P-Tr crisis is documentation of insect-induced damage diversity and intensity on Late Permian floras and post-event

successor floras throughout the Triassic (e.g., Prevec et al. 2009; Labandeira et al. 2016). Such an encompassing study would document (i), the Late Permian baseline of ecological interactions; (ii), an ecological decline resulting in depauperate interactions immediately following the P-Tr crisis and into the earlier Triassic; and (iii), the subsequent, post-crisis pattern of ecological recovery and clade diversification during the later Triassic (Roopnarine and Angielczyk 2015; Labandeira et al. 2016). Comparisons between these three intervals—Late Permian, earlier Triassic, and later Triassic—could yield considerably more finer-grained insights than previous, coarser-grained approaches (Labandeira 2006b, 2013a), especially regarding how insect herbivores were finely partitioning host-plant tissues and to what extent insect herbivore guild structure was changed before, soon after, and later in the Triassic after the P-Tr event. There are several levels at which such a comparative analysis can be investigated. At the histological level, one productive method is detailed, qualitative recording of plant tissue types that were being consumed by insects, as revealed by damage on organs such as foliage, stems, seeds and fructifications before and after the event (Labandeira 2013a; Schachat et al. 2014). A second avenue is to assess functional feeding group (FFG) or damage-type (DT) diversity and frequency as well as herbivory level on bulk floras before and after the event, such as the analogous Paleocene–Eocene Thermal Maximum event (Wilf and Labandeira 1999; Wilf et al. 2001, 2006). A third type of examination is to determine the extent of damage diversity of the insect herbivore component community on the most intensely herbivorized host-plant species in a flora before and after the event (Labandeira et al. 2016). An herbivore component community consists of all of the insect herbivore species consuming tissues of a single source plant (Root 1973). Such component communities can reveal varying and differential patterns of herbivory in space and time that accrue from both historical incumbency (Prinzing et al. 2017), as well as the ecological processes favoring partitioning of host-plant tissue types by particular feeding guilds of insect herbivores (Lawton 1982; Futuyma and Mitter 1996).

The current project is part of ongoing documentation of a 35 million-year-long interval from the middle Permian (Guadalupian) to Late Triassic (Carnian) interval designed to evaluate the effect of the P-Tr event for plant–insect interactions in the Karoo Basin of South Africa. To date, one late Permian (Lopingian) site, Clouston Farm, has been assessed (Prevec et al. 2009), although two other Permian localities (Gastaldo et al. 2005) currently are being evaluated. In this contribution, we examine plant–insect interactions for the most specimen-abundant site of all Karoo Basin localities, the Late Triassic Aasvoëlberg 411 (Aas411) site, which is one of a series of Carnian-age localities from the Molteno Formation, in the Karoo Basin of South Africa. The consequences of the P-Tr event will be evident from a comparison of plant–insect interactions of the Aas411 site to equivalent, earlier interactions from Middle Triassic and Late Permian localities (Prevec et al. 2009; Wappler et al. 2015; Labandeira et al. 2016). (Early Triassic localities with sufficient, well preserved plant fossils to study are virtually absent.) Empirical analyses of richly preserved plant–insect interactions across this time interval can provide ecologically robust

data for interpreting the response of the P-Tr event for variously herbivorized plant-host lineages and for diverse feeding guilds of arthropod herbivores in a variety of habitats.

14.2 Early to Late Triassic Plant–Insect Interactions

14.2.1 Overview

During the Permian, the diversity and frequency of plant–insect interactions apparently reached a plateau, based on data from about a dozen time slices during the Cisuralian and Lopingian that represent a variety of habitats in Gondwana and Euramerica (Adami-Rodrigues et al. 2004; Prevec et al. 2009; Schachat et al. 2014; Schachat and Labandeira 2015; Labandeira et al. 2016). This trend was disrupted by the end-Permian (P-Tr) ecological crisis (Ponomarenko 2016), resulting in a reset of the associational clock at the beginning of the Triassic. Previous studies (Shcherbakov 2008b) providing documentation of plant–insect associational diversity indicates that the recovery period was prolonged.

14.2.2 Olenekian and Induan Interactions

After the P-Tr crisis, the Early Triassic was a time of exceedingly diminished diversity on land, as determined by the empirical record (Labandeira 2006a; Chen and Benton 2012) and by ecological model results (Roopnarine and Angielczyk 2007, 2015). Unfortunately, very few deposits provide fossil data that are appropriate for evaluating insect diversity during the Induan and Olenekian stages of the Early Triassic. Exceptions probably include the Solling Formation of the Lower Buntsandstein sequence that contains the Bremke and Fürstenberg floodplain floras in Germany (Kustatscher et al. 2014), and the Newport Formation at Turrimetta Head, in the Sydney Basin of New South Wales in Australia (McLoughlin 2011). The Solling Formation material provides the more insightful glimpse regarding rare herbivory of the two deposits; this deposit records eight, distinctive, DT occurrences from an Early Triassic flora that included some apparently specialized associations. One notable plant host was the fern *Tongchuanophyllum* that exhibits multiple DTs of external foliage feeding, a midveinal gall, and lenticular to ovoidal oviposition scars (Wappler et al. 2015).

Other sporadic examples of insect herbivory have been documented for the Early Triassic. A probable Olenekian-age gall occurs on the pinnae and rachis of the corystosperm *Dicroidium odontopteroides* (McLoughlin 2011), a species that also occurs in the Molteno Formation, is notable for its distinctive physiognomy. This plant host represents one of the few host-specialized associations known from the

Early Triassic. In earlier Induan-age deposits immediately above the P-Tr boundary, the earliest known Triassic herbivory has been described (Lozovsky et al. 2016), which notably includes the earliest known leaf mine (Krassilov and Karasev 2008).

14.2.3 Anisian Interactions

Several lower Middle Triassic localities of Anisian age have been explored worldwide for plant–arthropod interactions. These studies indicate the gradual accumulation of plant–insect interactional diversity within the first 5–10 million years after the P-Tr ecological crisis. One of the most prominent of these associations is the Upper Buntsandstein sequence from the Grès à Voltzia deposits in the northern Voltzia Mountains of northeastern France. Grès à Voltzia associations include exophytic and endophytic oviposition on horsetails, external foliage feeding on the seed plant *Neuropteridium*, and a distinctive host-specialized gall present on the herbaceous conifer *Aethophyllum stipulare* (Grauvogel-Stamm and Kelber 1996). Also found in this deposit were the wings of a tettigoniid orthopteran that mimicked the venation and other surface foliar features of a seed plant (Papier et al. 1997).

Several other examples of insect herbivore associations are known from Anisian deposits. One site is the Dhauari Hill bed of the Parsora Formation, in the South Rewa area of the Gondwana Basin in central India (Ghosh et al. 2015). At this deposit, the Triassic corystosperm *Dicroidium hughesii*—a taxon also recorded in the Anisian Burgersdorp Formation hosted a distinctively spheroidal and heavily walled gall on the host's pinnules. Another significant occurrence is the early Anisian Fremouw Formation of the central Transantarctic Mountains along the Palmer Peninsula in Antarctica (Hermsen et al. 2006). Although this material exhibits rare root detritivory by oribatid mites (Kellogg and Taylor 2004), a cycad specimen of *Antarcticyas schopfi* shows tunneling in thickened cataphyll tissue that may indicate pollination by an unknown beetle (Hermsen et al. 2006; also see Klavins et al. 2005). In the penecontemporaneous Burgersdorp Formation of South Africa, Labandeira (2006a) mentioned a sparse record of herbivory, although these plant–insect interactions await formal description.

14.2.4 Ladinian Interactions

During the Ladinian there was a significant qualitative and quantitative increase in insect herbivory from the earlier level documented in Anisian floras. This expansion of herbivory is best demonstrated by four major occurrences, particularly from Western Europe. The Lower Keuper and Lettenkohle formations of Franconia, Germany, and adjacent Alsace in France and in Switzerland were first mentioned by Heer (1877), who noted likely oviposition scars on the horsetail *Equisetites*.

Oviposition lesions later were documented on the horsetail *Neocalamites* (Roselt 1954). Subsequent studies indicated borings in *Agathoxylon*-type wood (Linck 1949), and particularly several types of margin and hole feeding on *Taeniopteris angustifolia* and *Schizoneura paradoxa* (Geyer and Kelber 1987; Kelber and Geyer 1989). Grauvogel-Stamm and Kelber (1996) documented examples of clustered, endophytic, ellipsoidal to ovoidal oviposition marks on *Equisetites arenaceus* and linear, end-to-end arrays of oviposition on *T. angustifolia*.

A quantitative and intensive study documented a wealth of interactions for the Monte Agnello Site from the Dolomites Region of the Southern Alps in Northern Italy (Wappler et al. 2015; Labandeira et al. 2016). A wide variety of herbivore damage was represented by 20, distinctive DTs that were scored for host plants such as horsetails, ferns including *Neuropteridium*, *Phlebopteris*, *Cladophlebis* and *Thaumatopteris*, the seed-fern *Scytophyllum*, the cycadophytes *Bjuvia* and *Nilssonia*, and the voltzialean conifer *Voltzia*. The repertoire of damage included external foliage feeding, piercing and sucking, leaf mining, and galling, all of which display partitioning of a variety tissue types (see Labandeira 2013a). Of particular note was the component community structure of the seed-fern *Scytophyllum bergeri*, which harbored 11 distinctive DTs within the functional feeding groups (FFGs) of external foliage feeding, piercing and sucking, oviposition, galling and leaf mining, mostly indicating host specialization, and contributing to the most diverse component community known from any Ladinian deposit. The component community of *Scytophyllum bergeri* was compared to that of the Late Permian (Wuchiapingian) conifer *Pseudovoltzia liebeana* from a nearby site, the latter of which harbored a mere four DTs, only one of which, a foliar gall, was a host specialist (Labandeira et al. 2016). This Lopingian to Ladinian contrast in component-community structure provides additional evidence for the demise of the ecological web of herbivore interactions based on single host-plant species resulting from the P-Tr ecological crisis.

Another site with Ladinian plant–insect interactions is the Xinigua Flora of the Santa Maria Formation, from Rio Grande do Sul in southeastern Brazil, which displays borings in *Agathoxylon*-type wood (Minello 1994). Other Ladinian localities represent single occurrences of particular plant–insect associations, but nevertheless provide supplemental evidence documenting the subtle but sustained increase in herbivory throughout this interval. However, it was during the Carnian that a dramatic increase in herbivory has been recorded, particularly in the Karoo Basin of South Africa.

14.2.5 Carnian Interactions

There are five major deposits with diverse floras that have recorded the considerable expansion of plant–insect associations during the Carnian. In addition to the Molteno Formation discussed later in this report, the Lunz Formation of Lunz-am-See in the Northern Calcareous Alps of eastern Austria is characterized by

frequently exquisitely preserved material that is recorded mostly on cycads and bennettitaleans. One notable feature of insect damage at Lunz-am-See are oviposition lesions that retain altered histological features of foliar epidermis and cuticle of the bennettitalean host *Nilssoniopteris haidingeri*, as well as damage that reveals details of egg chlorion and other microstructural features of eggs oviposited endophytically, probably by a dragonfly of the Odonatoptera (Pott et al. 2008). A variety of marginal and nonmarginal feeding also has been recorded on other bennettitalean foliage, but principally on *Nilssoniopteris* (Wappler et al. 2015). Other interaction features of the Lunz-am-See deposit are a probable leaf mine on a frond pinnule of the cycad *Nilssonia* (Meller et al. 2011), and presence of structural defenses in the foliage of the possible ginkgophyte *Glossophyllum florini* (Pott et al. 2007).

From the Blackstone Formation of the Sydney Basin of New South Wales, in Australia, several distinct types of herbivory reveal that stereotyped and host-specific plant–insect associations were present across a broader swath of Gondwanan floras other than just the Molteno Biome. These include distinctive leaf mines (DT71) on the voltzialean broadleaved conifer *Heidiphyllum elongatum* (Tillyard 1922; Rozefelds and Sobbe 1987) and on the ginkgophyte *Ginkgoites* (Wappler et al. 2015). Other interactions likely are endophytic oviposition scars and epiphytic deposition of eggs on the fern *Dictyophyllum* (Webb 1982), interaction types that also occur in the Molteno Biome. In a different environment, Strullu-Derrien et al. (2012) reported interactions that are very rarely described from plants, specifically a community of arthropod detritivores, including oribatid mites that consumed cortical tissues of probable bennettitalean roots. Notably, the permineralized peat of this site—Hopen Island from Svalbard Archipelago of Norway—also preserves root galls, some of which may have been interacting with live tissues of larger root branches. These below-ground interactions compliment the above-ground associations described in other Carnian floras, indicating that the component community of arthropods on bennettitaleans included detritivores and herbivores consuming almost all organs and tissues of their plant hosts.

14.2.6 Norian Interactions

The primary site for Norian plant–insect interactions is the Chinle Formation of Petrified Forest National Park, in northeastern Arizona, USA. The Chinle floras containing these interactions have been radiometrically dated to 220.6–209.9 million years (Ramezani et al. 2014; Sadler et al. 2015), and thus are early Norian in age (Walker et al. 2013) and perhaps the only Late Triassic flora that has been radiometrically dated (Ash, pers. comm.). Multiple stratigraphic members of the Chinle Formation have been examined for virtually all major types of insect herbivory. With the exception of leaf mining and seed predation, all of the major modes of insect herbivore feeding have been found on Chinle plant hosts. These include a variety of external foliage feeding on ferns and seed plants, principally *Cynepteris*, *Sphenopteris*, *Zamites*, *Nilssoniopteris*, *Macrotaeniopteris*, *Marcouia* and

Dechellyia, the latter of which also features a distinctive, polymorphic, foliar gall (Ash 1997, 1999, 2000, 2009, 2014). Oviposition has been recorded for the seed plant *Dechellyia* and the horsetail *Equisetites*. Wood borings, attributed to beetles, have been described for multiple woods such as *Itopsidema* and *Schilderia* but especially *Agathoxylon* (Walker 1938; Ash and Savidge 2004; Creber and Ash 2004; Tapanila and Roberts 2012). Although foliar herbivory from Chinle strata have not been systematically sampled qualitatively and quantitatively, these preliminary inventories of plant hosts and their herbivore damage strongly indicate a continuation of interaction diversity largely established earlier during the Carnian.

Two other Norian localities house significant plant–insect interactional data. Evidence was established for one of the earliest examples of skeletonization from the fossil record, on the fern *Dictyophyllum nathorstii*, in a second site from the Yipinglang flora of Yunnan, in southern China (Feng et al. 2014). Earlier, lunate-shaped bite marks were documented from a species of *Mixopteris* from the same flora (Hsü et al. 1974). From the Laguna Colorada Formation of Santa Cruz, Argentina, a spectrum of herbivory representing many DTs and several major FFGs were documented from this diverse flora (Adami-Rodrigues et al. 2004).

14.2.7 Rhaetian Interactions

Compared to previous plant–insect interaction data, few Rhaetian data are available. One of the best known studies is the likely oviposition scars on the voltzialean conifer *Podozamites* from the Pälsjo site in Scania, Sweden (Nathorst 1876, 1878). The paucity of investigations of Rhaetian plant–insect interactions may be attributable to an absence of studies or could represent the prelude of depressed diversity prior to the terrestrial Triassic–Jurassic extinction event (McElwain et al. 2009). However, additional Gondwanan interactions have been described from younger deposits from the La Ternera Formation of Quebrada la Cachivarita and from the Las Breas Formation near Vicuña, both in Chile. The age of these deposits range from Upper Triassic to Lower Jurassic (Moreno and Gibbons 2007). These deposits reveal, respectively, distinctive oviposition damage on the cycad *Pseudoctenis harringtoniana* and on the probable bennettitalean *Taeniopteris* sp. B (Gnaedinger et al. 2014), both of which resemble damage on their congeneric Molteno hosts.

14.2.8 General Patterns

Although additional global analyses of Triassic plant–insect interactions are sorely needed, there are a few tentative inferences about insect herbivory that can be established. First, virtually nothing is known about plant–insect interactions of the

Early Triassic. This absence may represent either considerable taphonomic loss or the intrinsic lack of insect interactions with plants. Second, interactions for the Anisian, recorded in Western Europe and informally observed in the Karoo Basin, likely represent a very modest increase of generalized associations but minimal specialized associations, except for rare galls and possibly some patterned oviposition marks. Third, there is a significant increase in the diversity and frequency of plant–insect interactions during Ladinian times, including a demonstrable uptick in specialized damage patterns. This is particularly true for sites in Western Europe and eastern Australia. Fourth, there appears to be an overwhelming increase in associational diversity and herbivory levels during the Carnian that is evident in several regions worldwide. And last, based principally on data from the Chinle Formation, it appears that the diversity of interactions equilibrates or perhaps decreases somewhat during the Norian and Rhaetian. However, these conclusions should be tempered by problems in correlation of Triassic strata.

14.3 Methods

14.3.1 Obtaining Associational Data from Aasvoëlberg 411 Specimens

All adequately preserved plant specimens greater than 0.25 cm^2, including foliage, stems, roots and reproductive structures such as cones and seeds were exhaustively examined at the Aasvoëlberg 411 (Aas411) site. When present, fungal damage on plants and the presence of insect body fossils was recorded. Fossil intactness from the Aas411 site ranged from robust to delicate, and specimens often were preserved as single occurrences with considerable intervening matrix, to more dense accumulations with minimal matrix evident, to rare leaf mats of superimposed foliage. Whereas preservation of plant and insect material typically was good, occasionally specimens were exceptionally well preserved and revealed considerable plant anatomical detail as well as specific features of plant response to insect damage. Specimens very infrequently were abraded along their margins, and they almost always significantly exceeded the threshold for detection of arthropod-mediated damage.

The process for the examination of specimens is summarized as follows. An initial, overall evaluation was made of whether plant specimens from the fossil assemblage were sufficiently well preserved for analyses. Because of exceptionally good preservation, virtually all plant material from Aas411, including practically every recognizable leaf, stem, reproductive organ, and rare root mass was selected for data-set inclusion. Pollen organs were not included in the analyses because as a class of organs, they uniformly lacked evidence for herbivory throughout the

Molteno Biome. The principle plant material examined was foliage. The term, foliage, was operationally defined as any photosynthetic organ, including true leaves, scale leaves, pinnules, cataphylls, short shoots, horsetail stems or analogous structures (Schachat et al. 2014). After initial assessment, the specimen number of each fossiliferous slab, beginning with the prefix PRE/F/ was recorded. For each slab, specific plant specimens were assigned a specimen number, separated by a hyphen from the slab number, beginning with a "1" for the first specimen, and continuing until all plant specimens for that slab were numbered. (For example, one particular Aas411 slab that had three plant specimens was designated PRE/F/22051. The third arbitrarily numbered specimen on this slab is PRE/F/22051-3, which is part of a *Dicroidium odontopteroides* leaf that is designated on the ExCel database but not marked on the slab. Importantly, care was taken to recognize parts and counterparts so as to not count plant specimens twice.

Each plant specimen was taxonomically identified to the lowest rank possible. In most cases identification was to the level of species, such as the Linnaean binomial of *Heidiphyllum elongatum* or *Pseudoctenis sanipassiensis*. In other cases, a genus-level designation was used, such as *Sphenobaiera* scale leaf or *Yabeiella* sp. Less commonly, unidentifiable or isolated plant organs were designated as "seed indet. C", "unidentifiable woody axis", "unidentifiable foliage" or an analogous name. Seeds were an important contribution to the plant inventory and most were preserved as dispersed specimens. However, if seeds were encountered dispersed singly, the species name was placed in parentheses, as in *Peltaspermum* (*turbinatum*); however, if the seed was attached to a reproductive structure, its name was left outside of parentheses, as in *Avatia bifurcata*. Major Molteno plant groups were identified by the use of several monographic sources. For formal descriptions and classifications of horsetails, Anderson and Anderson (2017) was used; for ferns, the source was Anderson and Anderson (2008); for *Dicroidium* seed plants, it was Anderson and Anderson (1983, 2003); for seed plants excluding *Dicroidium*, Anderson and Anderson (1989, 2003) was employed; and for seed-plant female and male reproductive material, Anderson and Anderson (2003) and unpublished recent updates were consulted.

Linnaean binomials were used for those Molteno taxa that have been formally monographed taxonomically. However, some groups have not been taxonomically monographed, principally mosses, liverworts, lycopods, specimens of uncertain taxonomic position, several provisional species of seed-plant foliage whose encompassing genera already have been formally established, and approximately 75 additional seed, scale and ovulate morphotypes, the vast majority of which originate from the Aas411 site. As for use of DTs connected with Aas411 described plant taxa and undescribed plant morphotypes, the identification of insect damage was based on the FFG and DT system, informally referred to *Damage Guide* (Labandeira et al. 2007), used in previous studies (Wilf and Labandeira 1999; Wilf et al. 2006; Schachat et al. 2014; Ding et al. 2015). Although most of the DTs at Aas411 were described previously (Labandeira et al. 2007), newly encountered DTs were added to the data base and will be updated in forthcoming version 4 of the *Damage Guide*.

Procedurally, each Aas411 plant specimen was entered as a row into an ExCel database and associated data were expressed in six column fields. The columns were: (i), fossil site designation; (ii), specimen number; (iii), plant-host morphotype; (iv), DT assignments, if any; (v), macrophotography–microphotography log; and (vi), comments. The raw data are presented in Figs. 14.1, 14.2, 14.3, 14.4, 14.5, 14.6, 14.7, 14.8, 14.9, 14.10, 14.11, 14.12, 14.13 and Tables 14.1, 14.2, 14.3. Further analyses of the Aas411 site will await a more integrative meta-analysis of the plant–insect interactions across all 106 localities within the Molteno Biome.

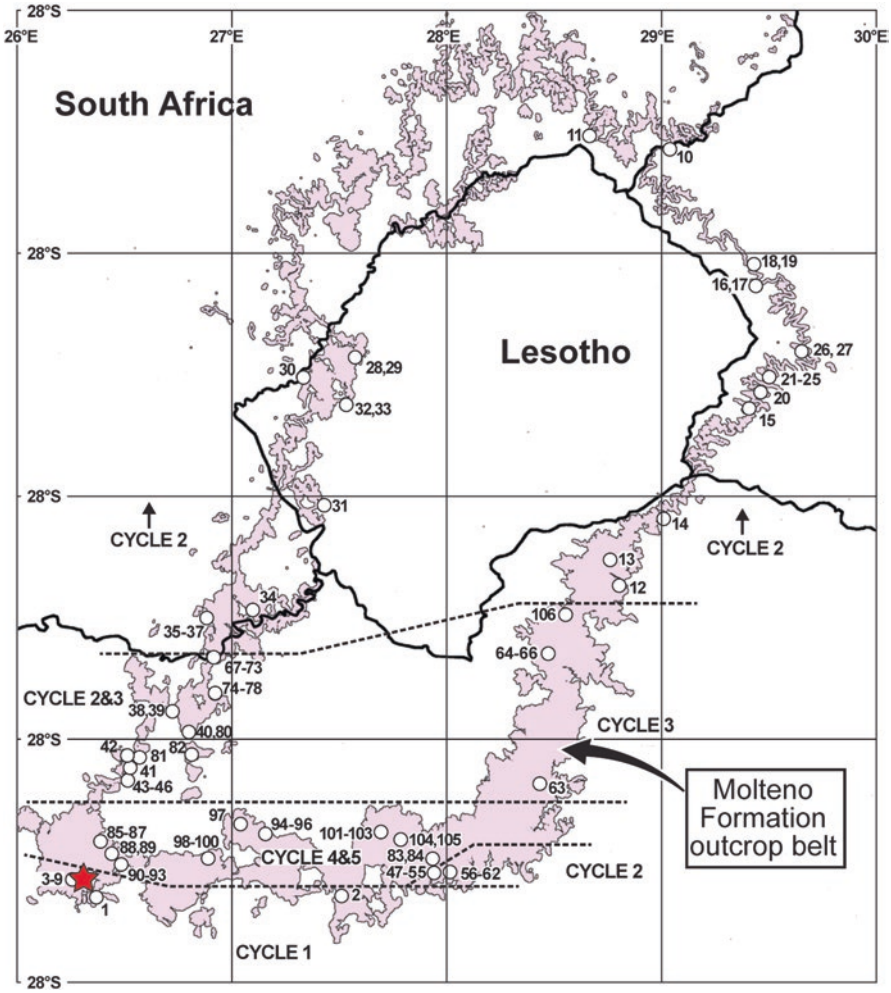

Fig. 14.1 The outcrop belt of the Molteno Formation in the Karoo Basin of South Africa, showing localities numbered in Table 14.1. The Aasvoëlberg 411 (Aas411) site is indicated at the *red star* in the *lower-left* corner, adjacent the Cycle 1 to Cycle 2 boundary

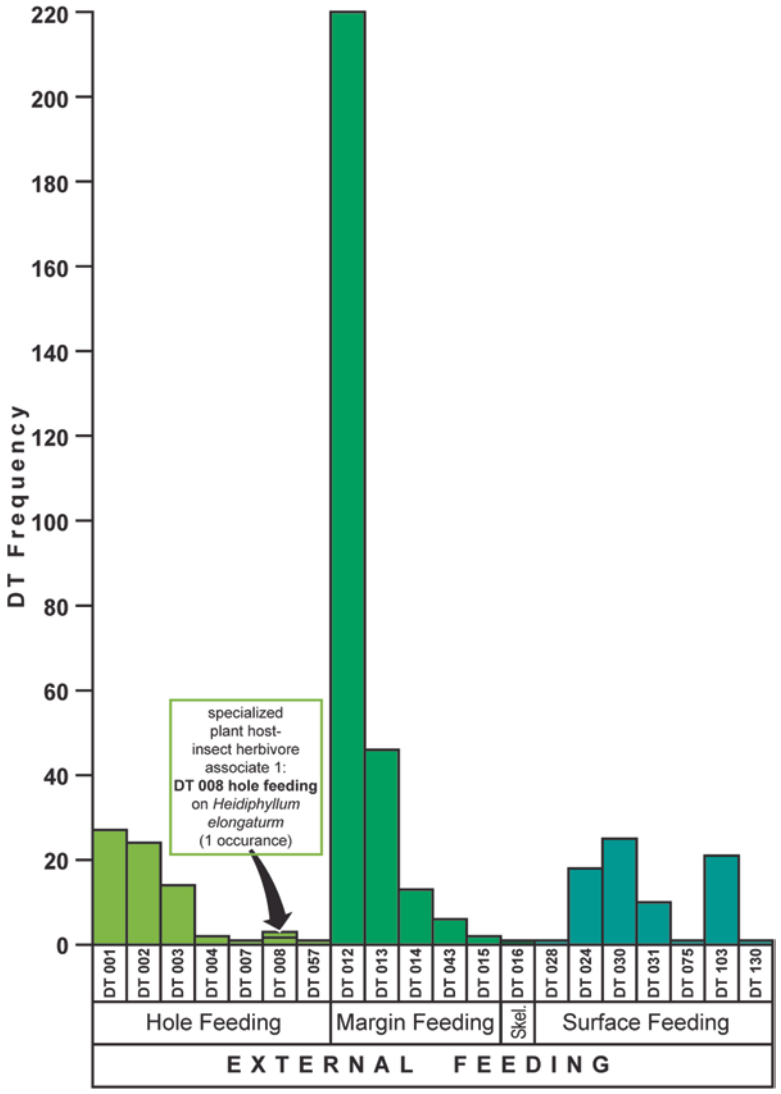

Fig. 14.2 Frequency distribution of external feeding damage types (DTs) by functional feeding group (FFG) and damage type (DT) at the Aasvoëlberg 411 (Aas111) site in the Karoo Basin of South Africa. Note that the only host-specialized association is DT8 slot feeding, a type of hole feeding. The hachured pattern in DT8 indicates the proportion of occurrences present on the host *Heidiphyllum elongatum*. (Also see Table 14.3)

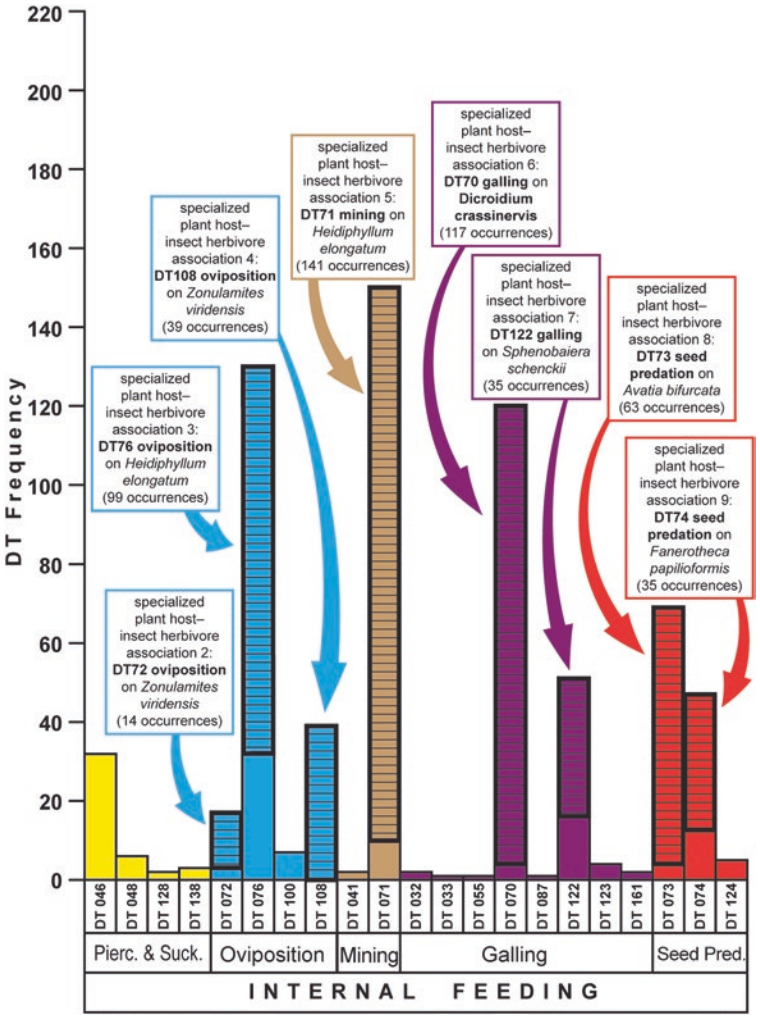

Fig. 14.3 Frequency distribution of internal feeding damage types (DTs) by functional feeding group (FFG) and damage type (DT) at the Aasvoëlberg 411 (Aas411) site in the Karoo Basin of South Africa. Note the abundance of nine host-specialized associations. Such host specializations include three types of oviposition (DT72 on *Zonulamites viridensis*, DT76 on Heidiphyllum *elongatum*, DT108 on *Z. viridensis*), one leaf mining (DT71 on *H. elongatum*), two types of galling (DT70 on *Dicroidium crassinervis*, DT122 on *Sphenobaiera schenckii*) and two types of seed predation (DT73 on *Avatia bifurcata* and DT74 on *Fanerotheca papilioformis*). One additional host-specialized association, DT124 seed predation on *Dordrechtites elongatus*, is not shown for spatial considerations. *Vertical columns with hachured pattern* indicates the proportion of occurrences for the specialized association indicated for a given DT present on a particular plant host. (Also see Table 14.3.)

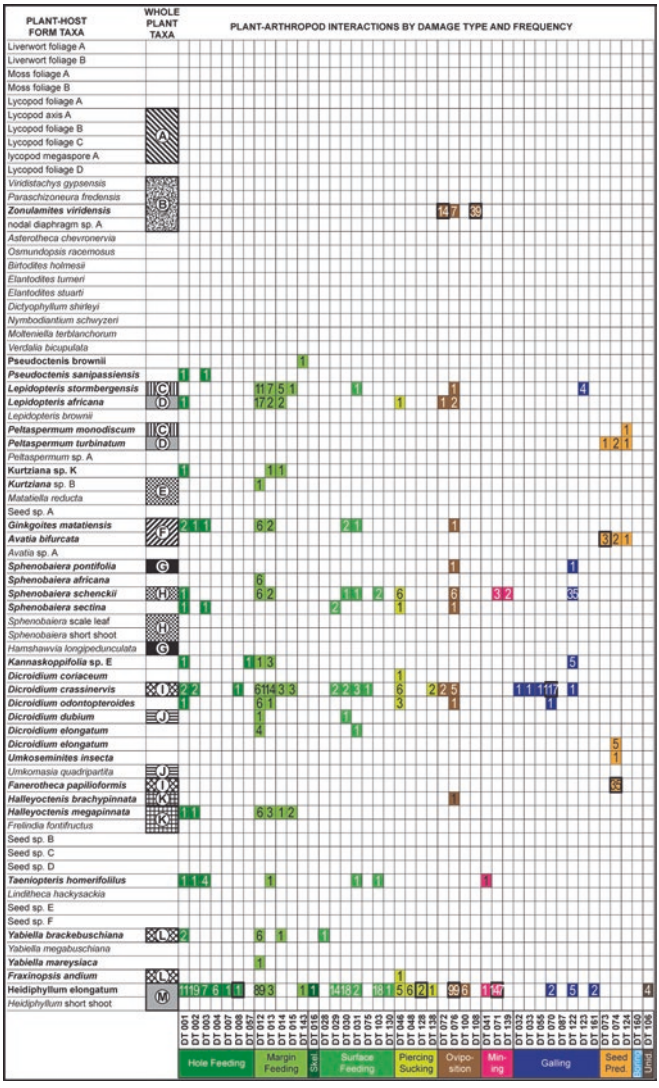

Fig. 14.4 Raw plant–insect interaction data for the Aasvoëlberg 411 site, ordinated by functional feeding group (*colors*) and constituent DTs at *bottom* and plant taxa at *left* with herbivorized hosts in *bold font*. Fifteen whole-plant taxa are indicated at *left* but exclude relevant pollen-organ form taxa. Presence/absence data in *grid* indicate the number of plant specimens with one or more occurrences of the specified DT on a particular plant host. *Cells with thick black* outlines indicate the 11 host-specialist associations indicated in Table 14.3 and in text. Fungal damage DT58 is not shown. Associational data of seven of the most intensely herbivorized of the 14 whole plant taxa (WPT) are provided in Tables 14.2 and 14.3. These data are continued on the folowing page

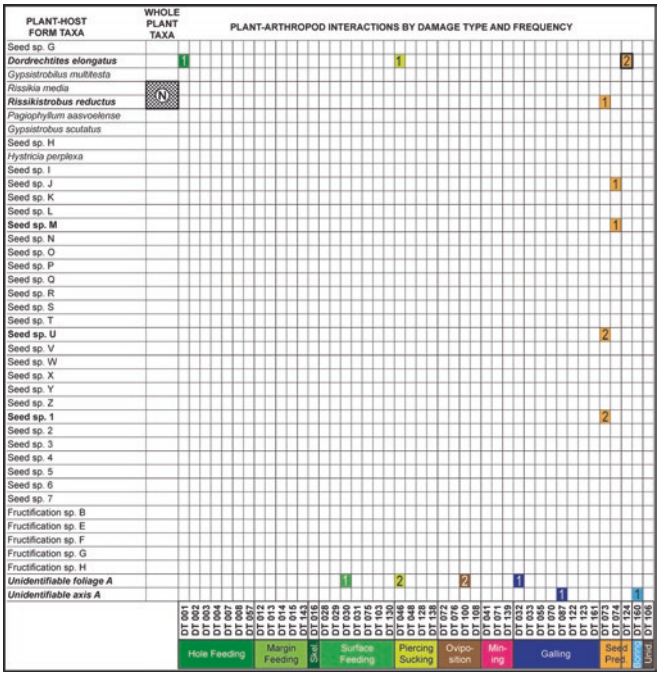

Fig. 14.4 (continued)

14.3.2 Herbivory and its Differentiation from Detritivory

The distinctive types of insect-mediated DTs serves as the basis for categorizing and analyzing herbivory in compressed fossil floras. However, damage on fossil plant specimens initially must be categorized as to whether it is due to detritivory (feeding on dead plant tissues) or attributable to herbivory (feeding on live plant tissues). This separation is accomplished by using five features that occur on live plant tissues and define a particular mode of diagnostic damage (Labandeira 2006a). First, herbivory is indicated for those DTs that have certain distinctive features of size, shape, pervasiveness, and position on the host plant. Second, herbivore damage typically consists of an iterative pattern of stereotyped insect damage that is repeated on a particular host-plant tissue, organ or species. Third are the structural features induced by the plant response to herbivory that typically involve production of teratological tissue, such as callus that involves hypertrophy (increase in cell size) and hyperplasia (increase in cell number). A fourth indicator is the presence of dead tissue occurring along the affected area, including necroses that often are a response of secondary infection by pathogens (Labandeira and Prevec 2014). Last, the occurrence of small, specific, insect-produced features such as small cuspate chew marks along leaf edges or stylet crater marks on surfaces, also are distinctive indicators of herbivory (Johnson and Lyon 1991; Labandeira et al. 2007).

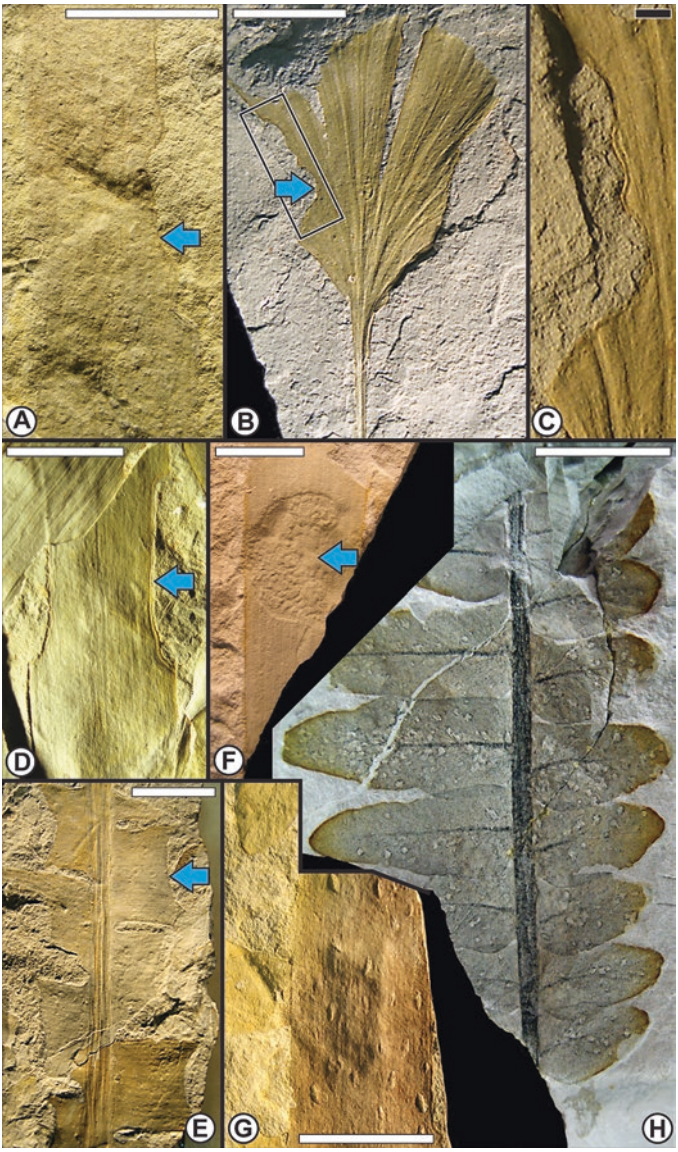

Fig. 14.5 Margin feeding, hole feeding, surface feeding, piercing and sucking and oviposition at the Aasvoëlberg 411 site, from the Late Triassic Molteno Formation of South Africa. (**a**) Cuspate DT12 margin feeding (*blue arrow*) on the conifer *Heidiphyllum elongatum*; PRE/F/12863-6. (**b**) Continuous DT143 margin feeding (*blue arrow*) on the ginkgophyte *Ginkgoites matatiensis*; PRE/F/21065-1. (**c**) Enlargement of DT143 outlined in (**b**). (**d**) Cuspate DT12 margin feeding (*blue arrow*) on *H. elongatum*; PRE/F/21443a-16. (**e**) Pinnule-tip DT13 margin feeding (*blue arrow*) on the cycad *Pseudoctenis* sp.; PRE/F/20636-1. (**f**) Ovoidal DT128 scale impression mark (*blue arrow*) on *H. elongatum*; PRE/F/21912-1. (**g**) Extensive DT76 oviposition on *H. elongatum*; PRE/F/12905-2. (**h**) Extensive DT1 hole feeding on the corystosperm *Dicroidium odontopteroides*; PRE/F/12229-4. *Blue arrows* indicate insect damage; scale bars for all figures: white, 1 cm; black, 1 mm

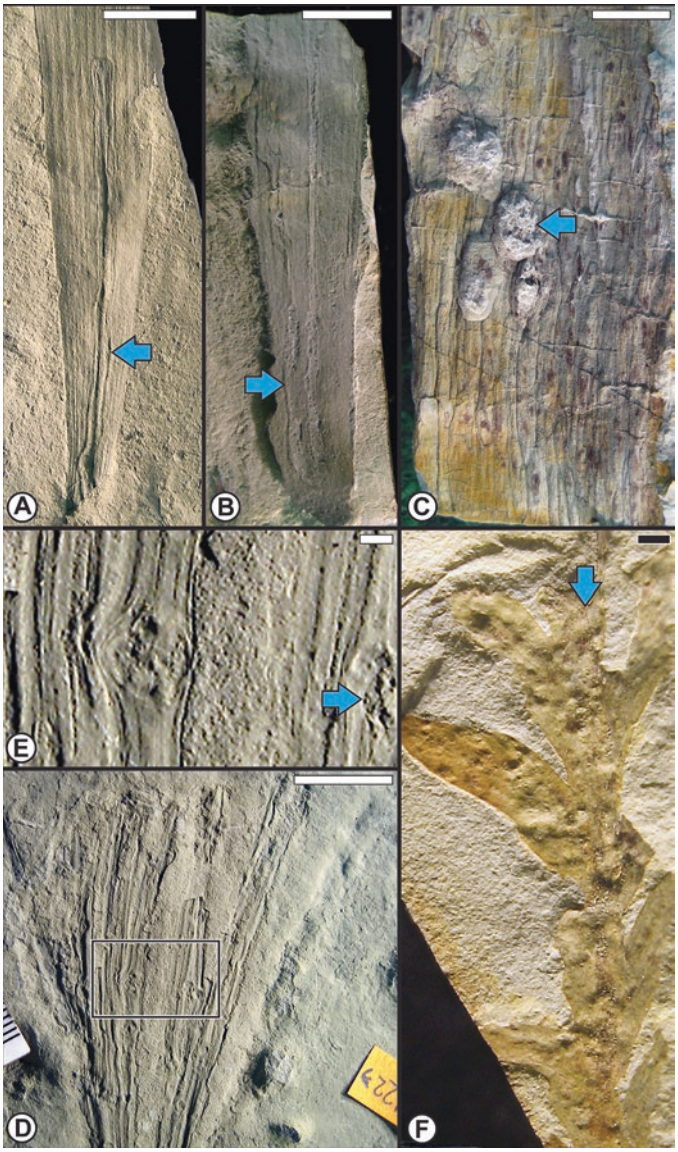

Fig. 14.6 Mining, oviposition and galling at the Aasvoëlberg 411 site, from the Late Triassic Molteno Formation of South Africa. (**a**) A linear leaf mine with the serpentine frass trail of DT71 (*blue arrow*), on *Heidiphyllum elongatum*; PRE/F/21921-2. (**b**) Another distinctive DT71 leaf mine (*blue arrow*) on *H. elongatum*; PRE/F/20710a-1. (**c**) A cluster of deep-seated DT72 oviposition marks on the stem of the horsetail *Zonulamites viridensis*; PRE/F/12047-6. (**d**) The gall DT122 showing distortions in the foliage of the ginkgophyte *Sphenobaiera schenckii*; PRE/F/12857a-23. (**e**) An enlargement of a galled area outlined in (**d**); microscope image. (**f**) Foliage of *Dicroidium crassinervis* with extensive DT122 gall damage; PRE/F/12238b. *Blue arrows* indicate insect damage; scale bars: white, 1 cm; black, 1 mm

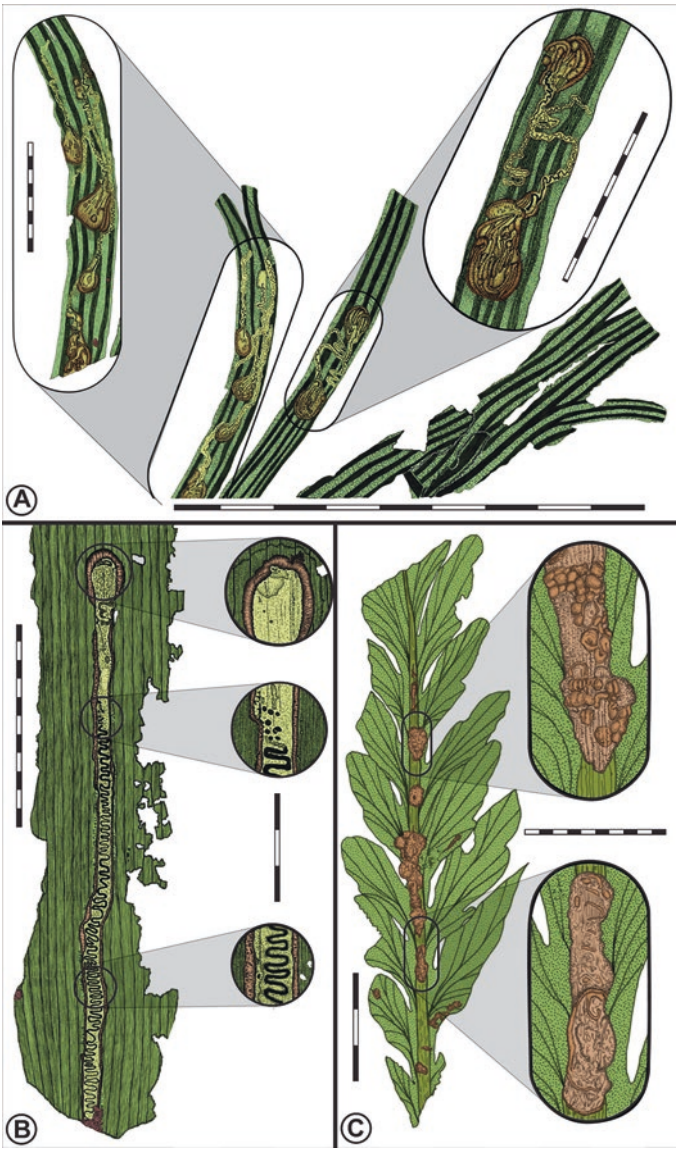

Fig. 14.7 Two mines and a gall on foliage of the dominant plant hosts of the Aasvoëlberg 411 site, as they may have appeared in life during the Carnian. Colorized versions of inked camera-lucida drawings. (**a**) Mine DT139 on *Sphenobaiera schenckii*; PRE/F/12472-1; all scale bars, mm. (**b**) Mine DT71 on *Heidiphyllum elongatum*; PRE/F/1902a, but from sister site of Aas311 (Aasvoëlberg 311); left and right scale bars, mm. (**c**) Gall DT122 on *Dicroidium crassinervis*; PRE/F/21912-2; scale bars: lower left, cm; center-right, mm

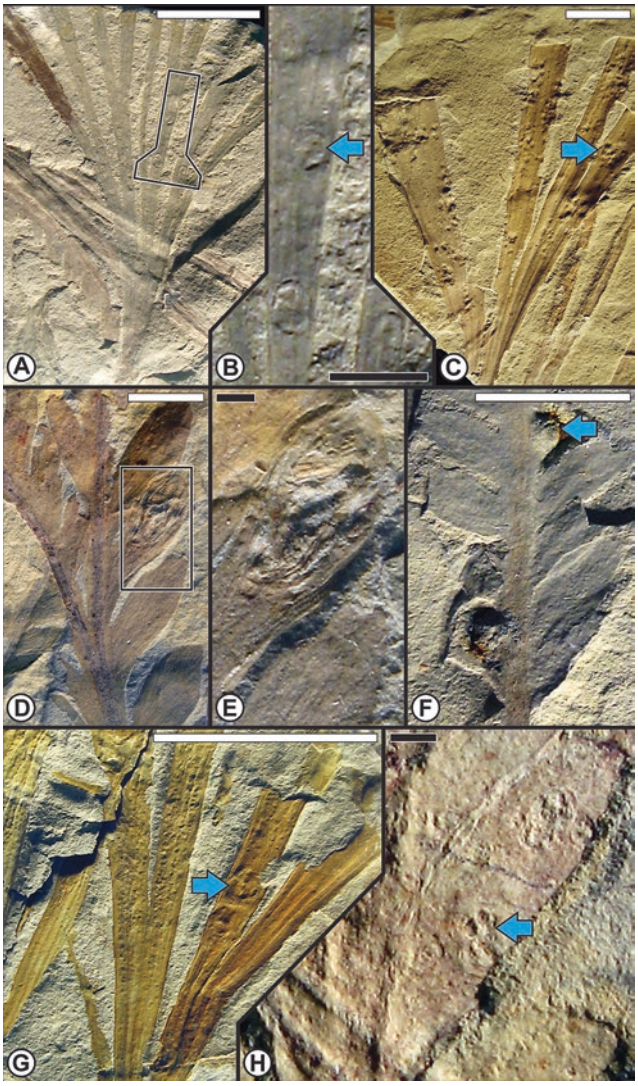

Fig. 14.8 Galling at the Aasvoëlberg 411 site, from the Late Triassic Molteno Formation of South Africa. (**a**) Bulbous DT122 galls on the foliage of the ginkgophyte *Sphenobaiera schenckii*; PRE/F/12103a-1. (**b**) Enlargement of galls (*blue arrow*) from template in (**a**). (**c**) Incipient DT122 galls (*blue arrow*) on the foliage of *S. schenckii*; PRE/F/12254-7. (**d**) An early-stage (immature) expression of the DT70 mite gall on the corystosperm *Dicroidium crassinervis*; PRE/F/12351-1. (**e**) Enlargement of galled pinnule at (**d**), showing surface structure of the galled pinnule. (**f**) An immature, early phase of the DT70 gall on *D. crassinervis*; PRE/F/21923-1. (**g**) An early phase of DT122 galls on its *S. schenckii* host; PRE/F/12396a-2. (**h**) Multiple, DT122 galls on pinnules of *D. crassinervis*; PRE/F/12242-1. *Blue arrows* indicate insect damage; scale bars: white, 1 cm; black, 1 mm

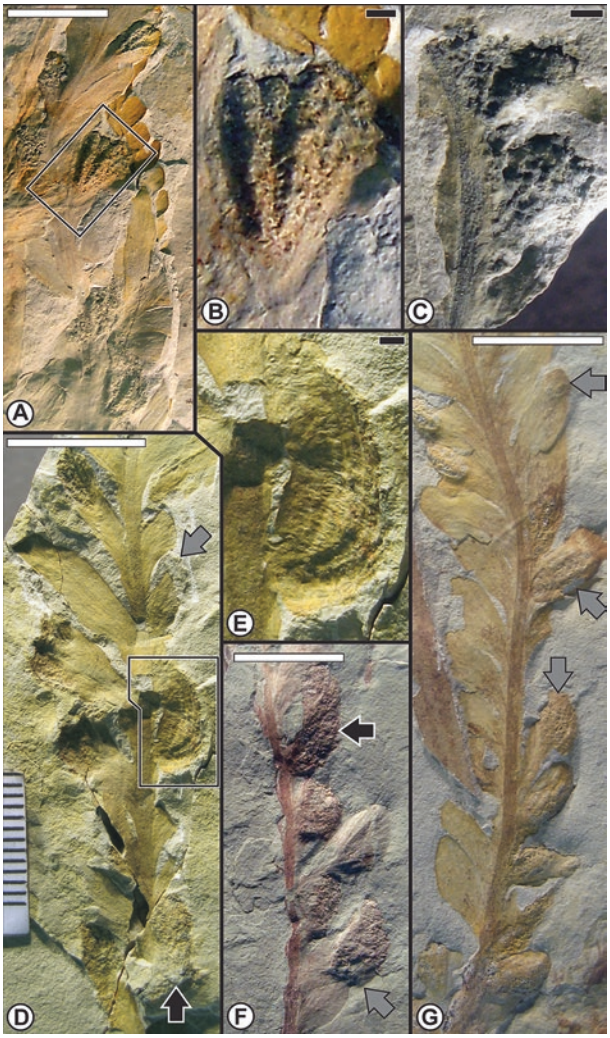

Fig. 14.9 DT70 galls on *Dicroidium crassinervis* at the Aasvoëlberg 411 site, from the Late Triassic Molteno Formation of South Africa. (**a**) Holotype of a mature, pustulose, DT70 gall, showing engulfment of the entire deltoid-shaped leaf and preservation of relict fasciculate venation of pinnule; PRE/F/12392-1. (**b**) Enlargement holotype DT70 gall at template at (**a**); microscope image. (**c**) Mature DT70 gall showing later stage, coarser pustulation on pinnular surface, and galled tissue connecting adjacent pinnules along the rachis; PRE/F/21416-1. (**d**) Approximately nine separate galls on a rachis showing various stages of maturity, ranging from establishment at pinnular tips (*grey arrow*) to an entire pinnule enveloped by gall tissue at the polygonal template (*black arrow*); PRE/F/12389b-1. (**e**) Enlargement of gall outlined in (**d**), showing relict pinnular venation and extensive pustulose surface. (**f**) Four mature (*black arrow*) or mostly mature galls occurring on one side of a rachis; PRE/F/12387a-1. (**g**) A long frond displaying approximately 11 galls ranging from small patches of galled tissue at pinnular tips (*top grey arrow*), to pinnules having a greater extent of galled tissue (*bottom grey arrow*) to near engulfment by galled tissue (*center grey arrow*); PRE/F/20880b. *Black arrows*, mature galls; *grey arrows*, immature damage; scale bars: white, 1 cm; black, 1 mm

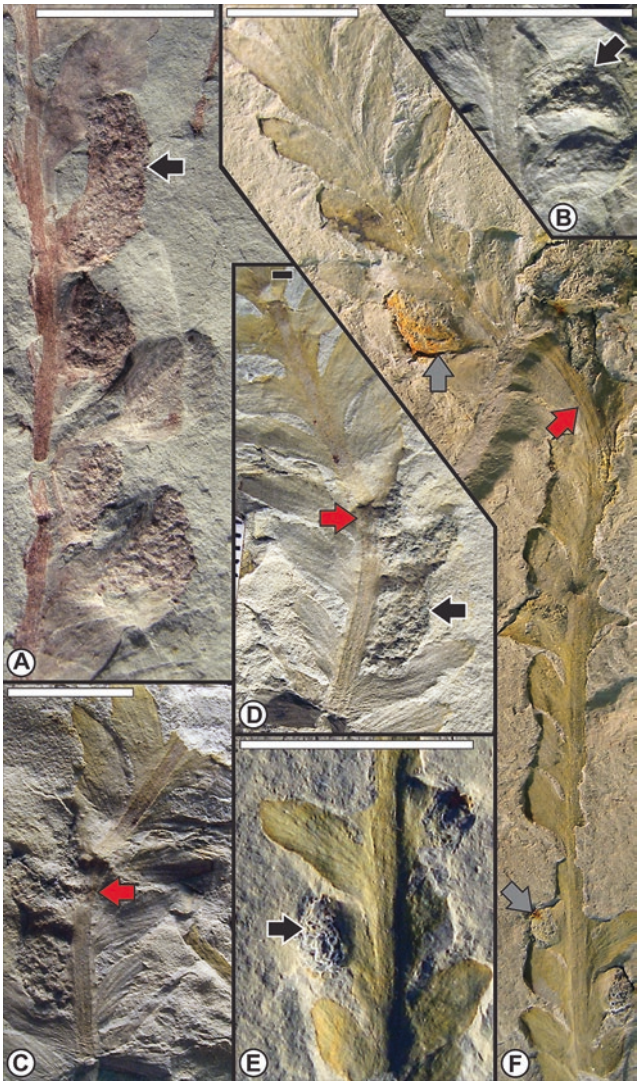

Fig. 14.10 DT70 galls on *Dicroidium crassinervis* at the Aasvoëlberg 411 site, from the Late Triassic Molteno Formation of South Africa. (**a**) Frond consisting of very mature galls, displaying breached pustules that expose inner cavities (*black arrow*); PRE/F/12387b-1, the enlarged counterpart of Fig. 14.8f. (**b**) Gall showing relict pinnular vein structure at *black arrow*; PRE/F/12394-1. (**c**) Portion of frond with five galled pinnules and distinctive teratological bend of the rachis at *red arrow*; PRE/F/12396a-1. (**d**) Another rachis segment with two pinnules, one indicated by a *black arrow* and revealing mature galls, and rachis bend at *red arrow*, representing the counterpart to (**c**); PRE/F/12396b-1. (**e**) Frond segment showing three, half mature galls, the left one (*black arrow*), showing upraised galled tissue; PRE/F/21908a-1. (**f**) Long frond branch with distinctive gall-induced crook at *red arrow* and immature galls (*lower grey arrow*) and more mature galls (*upper grey arrow*); PRE/F/21908-1. *Black arrows*, mature galls; *grey arrows*, immature galls; *red arrows*, rachis bends; scale bars: white, 1 cm; black, 1 mm

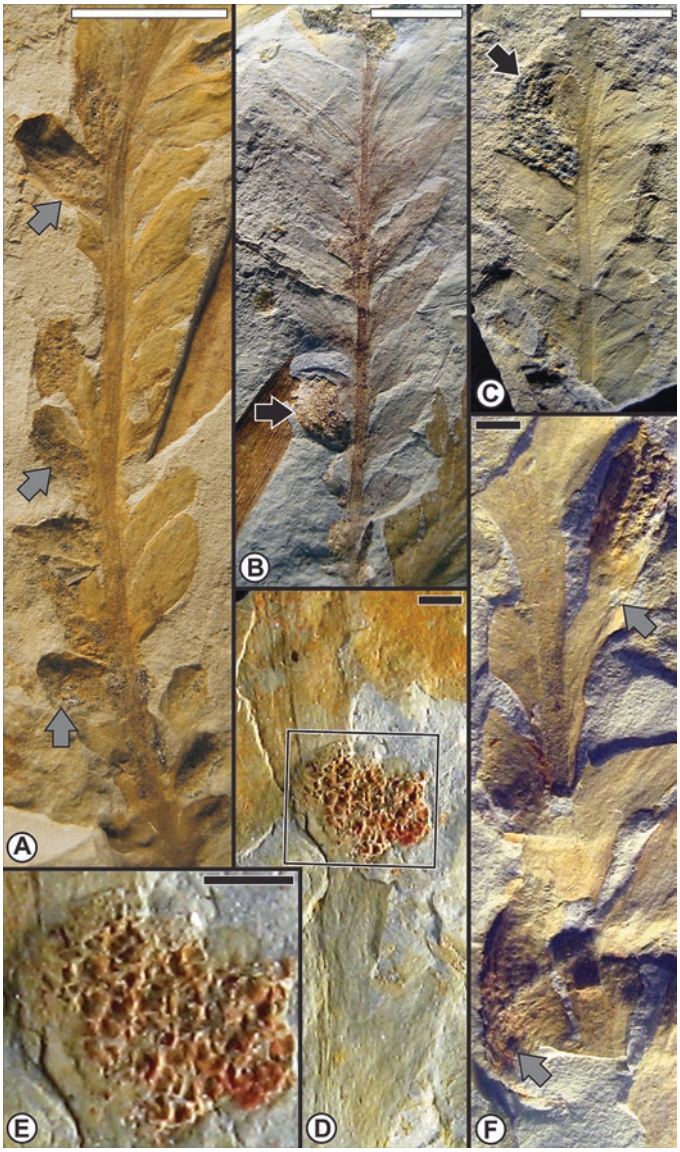

Fig. 14.11 DT70 mite galls on *Dicroidium crassinervis* at the Aasvoëlberg 411 site, from the Late Triassic Molteno Formation of South Africa. (**a**) A long frond segment with 12 galls that vary in the amount of pinnular coverage with galled tissue (*grey arrows*); PRE/F/20880a-1. (**b**) A frond with several incipiently galled pinnules and a highly galled pinnule (*black arrow*) that may have supplied colonizing mites for adjacent pinnules; PRE/F/2144a-1. (**c**) A gall (*black arrow*) with pustules occurring along the primary fasciculate venation of the pinnule; PRE/F/21920b-1. (**d**) A massive spheroidal gall that has obliterated pinnular structures such as veins and margin; PRE/F/21909-1. (**e**) Enlargement of gall surface detail in (d). (**f**) Frond segment bearing several galls, one of which is a mature gall (*bottom grey arrow*), and another immature gall showing the initial colonization of gall mites along pinnular primary veins (*top grey arrow*); PRE/F/21920b-1. *Black arrows*, mature galls; *grey arrows*, immature galls; scale bars: white, 1 cm; black, 1 mm

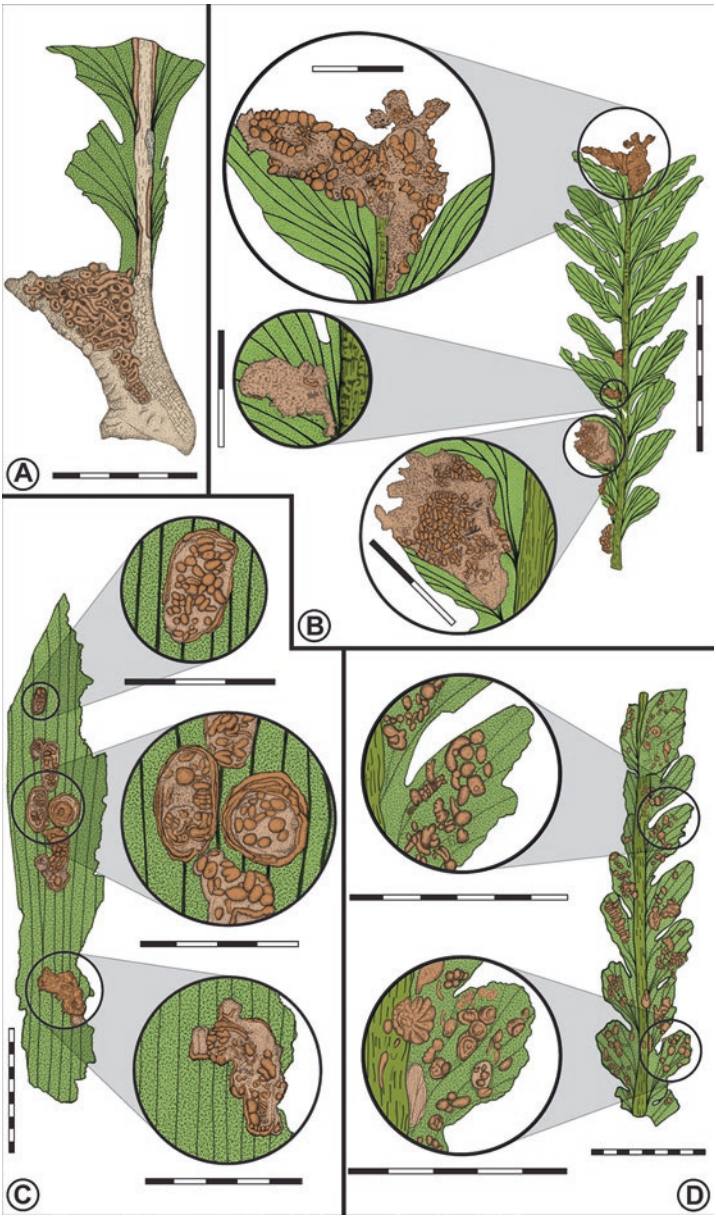

Fig. 14.12 Two galls on foliage of the two dominant plant hosts of the Aasvoëlberg 411 site, as they may have appeared in life during the Carnian. Colorized versions of inked camera-lucida drawings. (**a**) Gall DT70 on *Dicroidium crassinervis*; PRE/F/20883-3; scale bar, mm. (**b**) Gall DT70 on *D. crassinervis*; PRE/F/21144a-7; all scale bars, mm. (**c**) Gall DT122 on *Heidiphyllum elongatum*; PRE/F/12684a-10; all scale bars, mm. (**d**), Gall DT70 on *D. crassinervis*; PRE/F/21050-2; scale bars, mm

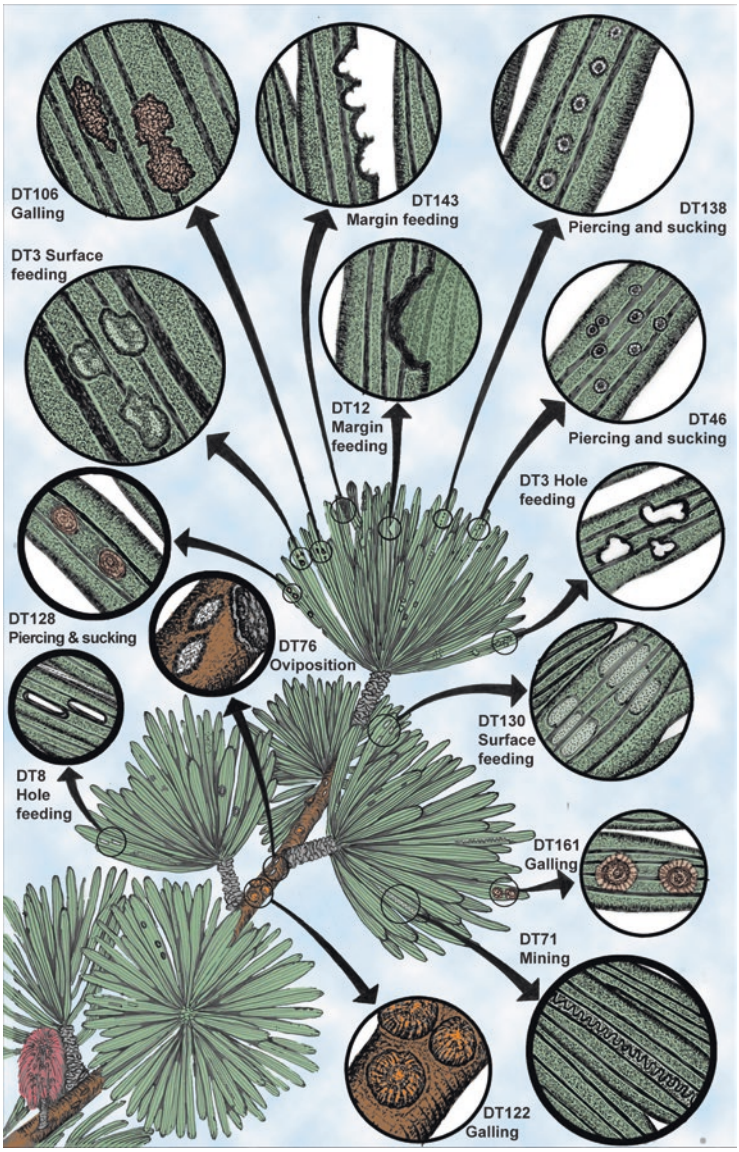

Fig. 14.13 The component herbivore community of the *Heidiphyllum elongatum–Heidiphyllum* short shoot–*Telemachus elongatus–Odyssianthus crenulatus* whole-plant taxon, from the Aasvoëlberg 411 (Aas411) site. DT numbers refer to damage types occurring on *H. elongatum* in Fig. 14.4. Only 14 of the 28 documented interactions (50%) of the *H. elongatum* herbivore component community are shown. Circular insets with thin ring enclosures are generalized interactions while those of thick ring enclosures are host-specialized associations, and match the same convention in Fig. 14.4. The basis of reconstruction is taken from Anderson and Anderson (2003) and Bomfleur et al. (2013)

Table 14.1 Patterns of herbivory throughout the Molteno Formation localities in the Karoo Basin of South Africa

Site name (abbreviation)	Stratigraphic position[a]	Habitat[a]	Whole plant taxa[b]	Dominant functional feeding group[c]	Total DT occurrences	Total plant specimens	Inter action index[d]	Total kinds of DTs	Plant morphotypes
Kenegapoort 111 (Ken111)	106	*Dicroidium* Open Woodland	0	Margin feeding	6	162	0.037	6	6
Navar 111A (Nav111B)	105	Horsetail Marsh	0	[none]	0	31	0	0	1
Navar 111B (Nav111B)	104	Horsetail Marsh	0	Margin feeding	5	212	0.0235	2	7
Cala Road 211 (Cal211)	103	Horsetail Marsh	0	Margin feeding, piercing & sucking	6	178	0.0215	5	3
Cala Road 111A (Cal111A)	102	Horsetail Marsh	1	Margin feeding	18	517	0.1451	6	9
Cala Road 111B (Cal111B)	101	*Dicroidium* Open Woodland	1	Galling	39	990	0.0283	6	12
Birds River 211 (Bir211)	100	*Sphenobaiera* Closed Woodland	1	Margin feeding	13	358	0.0363	7	15
Birds River 311 (Bir311)	99	*Sphenobaiera* Closed Woodland	4	Piercing & sucking	7	245	0.0288	5	20
Birds River 111 (Bir111)	98	*Sphenobaiera* Closed Woodland	9	Seed predation	2501	15,503	0.1598	41	72
Dordrecht 111 (Dor111)	97	*Heidiphyllum* Thicket	0	Margin feeding	5	144	0.0347	4	6
Greenvale 121 (Gre121)	96	*Heidiphyllum* Thicket	2	Hole feeding	104	2966	0.035	12	12
Greenvale 111A (Gre111A)	95	*Sphenobaiera* Closed Woodland	1	Surface feeding	5	281	0.0177	3	15
Greenvale 111B (Gre111B)	94	Horsetail Marsh	4	Oviposition	14	634	0.0220	3	22

(continued)

Table 14.1 (continued)

Site name (abbreviation)	Stratigraphic position[a]	Habitat[a]	Whole plant taxa[b]	Dominant functional feeding group[c]	Total DT occurrences	Total plant specimens	Inter action index[d]	Total kinds of DTs	Plant morphotypes
Boesmanshkoek 111A (Boe111A)	93	[indeterminate]	2	Margin feeding	11	369	0.0298	3	13
Boesmanshkoek 111B (Boe111B)	92	Horsetail Marsh	2	Oviposition	1	148	0.0068	1	9
Boesmanshkoek 111C (Boe111C)	91	*Dicroidium* Open Woodland	1	Margin feeding	22	700	0.0314	6	13
Boesmanshkoek 112 (Boe112)	90	*Dicroidium* Open Woodland	3	Margin feeding	6	1197	0.005	2	18
Cyphergat 111A (Cyp111C)	89	*Dicroidium* Open Woodland	3	Seed predation	168	6377	0.0263	27	32
Cyphergat 111B (Cyp111B)	88	*Heidiphyllum* Thicket	0	Surface feeding	1	180	0.0055	1	2
Molteno 211 (Mol211)	87	*Sphenobaiera* Closed Woodland	1	Oviposition	6	57	0.1052	4	10
Molteno 311 (Mol311)	86	*Sphenobaiera* Closed Woodland	0	Margin feeding	7	112	0.0625	6	5
Molteno 111 (Mol111)	85	*Sphenobaiera* Closed Woodland	0	[no damage]	0	27	0	0	6
Kannaskop 112 (Kan112)	84	*Heidiphyllum* Thicket	3	Piercing & sucking	44	1538	0.0286	9	29
Kannaskop 111 (Kan111)	83	Fern-*Kannaskoppifolia* Meadow	4	Margin feeding	42	2387	0.0176	11	15
Telemachus Spruit 111 (Tel111)	82	*Heidiphyllum* Thicket	3	Margin feeding	99	6681	0.015	14	38
Kommandantskop 111(Kom111)	81	Fern-*Kannaskoppifolia* Meadow	3	Hole feeding	23	1213	0.019	10	20

Vineyard 111 (Vin111)	80	*Dicroidium* Open Woodland	1	Margin feeding	63	2217	0.028	10	14
Elandspruit 111 (Ela111)	79	*Dicroidium* Open Woodland	3	Margin feeding	55	1154	0.0477	10	22
Kraai River 311 (Kra311)	78	*Dicroidium* Open Woodland	0	Galling	43	1387	0.031	6	8
Kraai River 211 (Kra211)	77	*Heidiphyllum* Marsh	1	Oviposition	2	401	0.005	1	2
Kraai River 222 (Kra222)	76	*Heidiphyllum* Marsh	0	[no damage]	0	50	0	0	1
Kraai River 221 (Kra221)	75	[indeterminate]	1	[no damage]	0	38	0	0	5
Kraai River 111 (Kra111)	74	*Dicroidium* Open Woodland	2	Margin feeding	22	2006	0.011	9	21
Lutherskop 111 (Lut111)	73	*Heidiphyllum* Thicket	1	Margin feeding	9	472	0.0191	4	5
Lutherskop 511 (Lut511)	72	*Heidiphyllum* Thicket	1	Surface feeding	28	634	0.0442	11	6
Lutherskop 4112 (Lut4112)	71	*Heidiphyllum* Thicket	1	Oviposition, mining, galling	13	744	0.0164	6	12
Lutherskop 4111 (Lut4111)	70	Horsetail Marsh	0	Surface feeding, oviposition	2	184	0.0109	2	2
Lutherskop 311 (Lut311)	69	*Heidiphyllum* Thicket	6	Mining	206	5784	0.034	23	39
Lutherskop 231 (Lut221)	68	Horsetail Marsh	0	[no damage]	0	46	0	0	3
Lutherskop 211 (Lut211)	67	Horsetail Marsh	1	Margin feeding	7	63	0.1111	4	10
Tina Bridge 121 (Tin121)	66	*Sphenobaiera* Closed Woodland	2	[no damage]	0	80	0	0	13
Tina Bridge 111 (Tin111)	65	Horsetail Marsh	2	Piercing & sucking	3	497	0.0024	1	9
Tina Bridge 111 (Tin131)	64	*Heidiphyllum* Thicket	0	Margin feeding, mining	7	148	0.0405	4	8
Waldeck 111 (Wal111)	63	*Sphenobaiera* Closed Woodland	1	Margin feeding	97	1695	0.0572	12	22

(continued)

Table 14.1 (continued)

Site name (abbreviation)	Stratigraphic position[a]	Habitat[a]	Whole plant taxa[b]	Dominant functional feeding group[c]	Total DT occurrences	Total plant specimens	Inter action index[d]	Total kinds of DTs	Plant morphotypes
Konings Kroon 223 (Kon223)	62	*Dicroidium* Open Woodland	4	Margin feeding	5	517	0.001	4	26
Konings Kroon 222 (Kon222)	61	*Dicroidium* Open Woodland	6	Margin feeding	31	2973	0.0105	13	35
Konings Kroon 211A & 221 (Kon211A & Kon221)	60	Fern-*Kannaskoppifolia* Meadow	2	Margin feeding	36	774	0.0466	10	33
Konings Kroon 211B (Kon211B)	59	*Heidiphyllum* Thicket	0	Hole feeding	1	168	0.006	1	5
Konings Kroon 111A (Kon111A)	58	*Dicroidium* Open Woodland	3	Margin feeding	19	1190	0.016	5	29
Konings Kroon 111B (Kon111B)	57	Horsetail Marsh	0	[no damage]	0	35	0	0	4
Konings Kroon 111C (Kon111C)	56	*Heidiphyllum* Thicket	2	Margin feeding	30	573	0.0526	11	14
Peninsula 111 (Pen111)	55	*Dicroidium* Open Woodland	0	Margin feeding	4	73	0.0548	2	6
Peninsula 321 (Pen321)	54	*Dicroidium* Open Woodland	4	Margin feeding	37	2315	0.0135	9	28
Peninsula 211 (Pen211)	53	*Dicroidium* Open Woodland	1	Margin feeding	3	307	0.0098	2	13
Peninsula 222, 221 (Pen221 & Pen221)	52	*Dicroidium* Open Woodland	0	Margin feeding	7	342	0.0205	3	13
Peninsula 511 (Pen511)	51	Horsetail Marsh	1	Oviposition	10	286	0.0347	7	5
Peninsula 421 (Pen421)	50	*Dicroidium* Open Woodland	2	Margin feeding	22	870	0.0256	13	18

Peninsula 431 (Pen431)	49	*Dicroidium* Open Woodland	0	Margin feeding	7	241	0.0292	3	11
Peninsula 311 (Pen311)	48	*Heidiphyllum* Thicket	1	Margin feeding	36	1785	0.0178	11	20
Peninsula 411 (Pen411)	47	*Heidiphyllum* Thicket	2	Oviposition	234	6807	0.0335	18	18
Klein Hoek 111A (Kle111A)	46	Horsetail Marsh	1	Piercing & sucking, oviposition	1	115	0.0087	1	7
Klein Hoek 111B (Kle111B)	45	[indeterminate]	3	Margin feeding, surface feeding	39	1267	0.0308	9	21
Klein Hoek 111C (Kle111C)	44	*Heidiphyllum* Thicket	3	Oviposition	141	2930	0.0478	17	15
Klein Hoek 211 (Kle211)	43	*Sphenobaiera* Open Woodland	0	[no damage]	0	34	0	0	1
Kullfontein 111 (Kul111)	42	*Sphenobaiera* Closed Woodland	0	[no damage]	0	5	0	0	4
Kappokraal 111 (Kap111)	41	*Dicroidium* Riparian Forest (Immature)	7	Margin feeding	554	1965	0.2819	27	39
Vineyard 211 (Vin211)	40	Horsetail Marsh	0	Oviposition	4	287	0.0134	2	1
Elandspruit 112A (Ela112A)	39	Horsetail Marsh	3	Seed predation	78	1295	0.0593	7	19
Elandspruit 112B (Ela112B)	38	*Heidiphyllum* Thicket	0	Margin feeding	12	546	0.0220	5	5
Nuwejaarspruit 111A (Nuw111A)	37	Horsetail Marsh	2	Oviposition	45	709	0.0634	6	11
Nuwejaarspruit 111B	36	*Dicroidium* Open Woodland	3	Margin feeding	76	2188	0.0347	20	24
Nuwejaarspruit 211 (Nuw211)	35	*Dicroidium* Open Woodland	1	Piercing & sucking	89	763	0.1153	13	13

(continued)

Table 14.1 (continued)

Site name (abbreviation)	Stratigraphic position[a]	Habitat[a]	Whole plant taxa[b]	Dominant functional feeding group[c]	Total DT occurrences	Total plant specimens	Inter action index[d]	Total kinds of DTs	Plant morphotypes
Winnaarspruit 111 (Win111)	34	*Heidiphyllum* Thicket	0	Margin feeding	80	1679	0.0478	17	16
Morija 111-A (Mor111A)	33	*Dicroidium* Open Woodland	2	Margin feeding	39	539	0.0724	3	3
Morija 111-B (Mor111B)	32	*Dicroidium* Open Woodland	2	Margin feeding	59	1628	0.0362	7	14
Qualasi Hill 111 (Qua111)	31	*Dicroidium* Open Woodland	2	Margin feeding	1	235	0.0043	1	11
Makoaneng 111 (Mak111)	30	*Dicroidium* Open Woodland	2	Margin feeding	22	1308	0.0168	7	14
Mazenod 111 (Maz111)	29	*Dicroidium* Riparian Forest (Immature)	2	Margin feeding	73	1041	0.0701	11	22
Mazenod 211 (Maz211)	28	*Dicroidium* Riparian Forest (Immature)	7	Margin feeding	254	2279	0.11	32	34
Mooi River 111 (Moo111)	27	*Dicroidium* Open Woodland	1	Margin feeding, oviposition	2	186	0.0108	2	9
Mooi River 121 (Moo121)	26	*Sphenobaiera* Closed Woodland	0	[no damage]	0	44	0	0	5
Hlatimbe Valley 111 (Hla111)	25	Horsetail Marsh	0	[no damage]	0	287	0	0	2
Hlatimbe Valley 111 (Hla111)	24	*Dicroidium* Riparian Forest (Immature)	3	Margin feeding	11	515	0.037	8	25
Hlatimbe Valley 212 (Hla212)	23	*Dicroidium* Riparian Forest (Immature)	4	Margin feeding	21	723	0.034	10	29
Hlatimbe Valley 213 (Hla213)	22	*Dicroidium* Riparian Forest (Immature)	7	Margin feeding	95	1943	0.0474	19	59

Hlatimbe Valley 311 (Hla311)	21	*Dicroidium* Riparian Forest (Immature)	0	[no damage]	0	10	0	0	5
Umkomaas 111 (Umk111)	20	*Dicroidium* Riparian Forest (Mature)	12	Margin feeding	639	12,788	0.0481	38	109
Champagne Castle 111 (Cha111)	19	*Dicroidium* Open Woodland	0	[no damage]	0	17	0	0	1
Champagne Castle 211 (Cha211)	18	*Dicroidium* Open Woodland	0	[no damage]	0	10	0	0	2
Injasuti Valley 111 (Inj111)	17	*Dicroidium* Open Woodland	1	Margin feeding	2	22	0.091	1	4
Injasuti Valley 211 (Inj211)	16	*Dicroidium* Open Woodland	0	[no damage]	0	55	0	0	5
Sani Pass 111 (San111)	15	*Dicroidium* Riparian Forest (Immature)	4	Margin feeding	34	1340	0.0254	10	33
Mngeni Valley 111 (Mng111)	14	*Dicroidium* Open Woodland	2	Margin feeding	6	398	0.051	1	14
Qachasnek 111 (Qac111)	13	*Heidiphyllum* Thicket	2	Hole feeding	15	2130	0.007	7	11
Matatiele 111 (Mat111)	12	*Dicroidium* Riparian Forest (Immature)	6	Margin feeding	237	6343	0.0365	22	55
Golden Gate 111 (Gol111)	11	*Dicroidium* Riparian Forest (Immature)	2	Margin feeding	119	1326	0.09	17	13
Little Switzerland 111 (Lit111)	10	*Dicroidium* Riparian Forest (Mature)	6	Margin feeding	663	9912	0.0669	31	64
Aasvoëlberg 611 (Aas611)	9	*Heidiphyllum* Thicket	1	Hole feeding, margin feeding, galling	6	229	0.0278	4	7
Aasvoëlberg 111 (Aas111)	8	*Heidiphyllum* Thicket	1	Margin feeding	35	3308	0.0103	12	24
Aasvoëlberg 211 (Aas211)	7	*Heidiphyllum* Thicket	1	Margin feeding	103	2061	0.05	12	16

(continued)

Table 14.1 (continued)

Site name (abbreviation)	Stratigraphic position[a]	Habitat[a]	Whole plant taxa[b]	Dominant functional feeding group[c]	Total DT occurrences	Total plant specimens	Inter action index[d]	Total kinds of DTs	Plant morphotypes
Aasvoëlberg 311 (Aas311)	6	*Heidiphyllum* Thicket	1	Mining	1209	11,677	0.1313	18	18
Aasvoëlberg 411 (Aas411)	5	*Sphenobaiera* Closed Woodland	15	Margin feeding	1127	20,358	0.0554	44	112
Aasvoëlberg 511 (Aas511)	4	*Dicroidium* Open Woodland	0	Surface feeding	5	85	0.0588	3	11
Aasvoëlberg 711 (Aas711)	3	*Sphenobaiera* Closed Woodland	1	Galling	3	47	0.0638	2	5
Askeaton 111 (Ask111)	2	Horsetail Marsh	2	Margin feeding	45	1061	0.0424	8	21
Bamboesberg 111 (Bam111)	1	*Dicroidium* Open Woodland	0	Margin feeding	6	284	0.0211	4	7

[a]In stratigraphic order: the youngest site is Kenegapoort 111 at *top* (site 106) and the oldest site is Bamboesberg (site 1) at *bottom*

[b]The seven primary habitats of the Molteno Biome are illustrated and defined by Anderson and Anderson (2003) and MacRae (1999)

[c]Based on the greatest number of damage-type (DT) occurrences of a functional feeding group (FF) for each site

[d]The interaction index is calculated as the total number of DT occurrences divided by the number of plant specimens examined, providing a number expressing the density of interactions for each site

Table 14.2 Herbivory metrics of the seven most herbivorized whole-plant-taxa of the Late Triassic Aasvoëlberg 411 site, Karoo Basin of South Africa

Whole-plant taxon (WPT)[1] and host affiliation	Functional feeding groups	Number of DTs	DT occurrences	Specialized associations	Importance rank
Heidiphyllum elongatum——*Telemachus acutisquamus*——*Odyssanthus crenulata* (conifer) [WPT: **M**]	9	28	472	4	**1**
Dicroidium crassinervis——*Fanerotheca papilioformis*——*?Petruchus matatimajor* (corystosperm) [WPT: **I**]	7	20	265	2	**2**
Sphenobaiera schenckii——*Sphenobaiera*-short shoot——*Hamshawvia longipeduncu-lata*——*Stachyopitys gypsianthus* (ginkgophyte) [WPT: **H**]	7	11	65	1	**3**
Ginkgoites matatiensis——*Avatia bifurcata*——*Eosteria eosteranthus* (ginkgophyte) [WPT: **F**]	5	11	88	1	**4**
Lepidopteris africana——*Peltaspermum turbinatum*——*Antevsia* sp. (peltasperm) [WPT: **D**]	5	10	30	0	**5**
Lepidopteris stormbergensis——*Peltaspermum monodiscum*——*Antevsia* sp. (peltasperm) [WPG: **C**]	5	8	31	0	**6**
Zonulamites viridensis——nodal diaphragm A–*Viridistachys gypsensis*——*Paraschizo-neura fredensis* (horsetail) [WPT: **B**]	1	3	60	2	**7**

[1]Plant organs forming each whole plant taxon, lettered in Fig. 14.4, are indicated by the WPT designation

Table 14.3 Specialized associations of the five most herbivorized whole-plant-taxa of the Late Triassic Aasvoëlberg 411 site, compared to other relevant Molteno localities, Karoo Basin of South Africa

Whole-plant taxon (WPT)[a] and host affiliation	Specialized Associations						
	Functional Feeding group	Host specialized DT	Aas411 DT occurrences	Total Molteno localities with the DT	Total Molteno DT occurrences	Proportion of FFG DTs at Aas411	Dominant Molteno habitat[b]
Heidiphyllum elongatum——*Telemachus acutisquamus*——*Odyssanthus crenulata* (conifer) [WPT: **M**]	**Hole Feeding**	DT8	1	21	78	1.3%	HT
	Piercing and Sucking	DT128	2	4	40	5.05	HT
	Oviposition	DT76	99	30	472	21.0%	HT
	Mining	DT71	147	23	1271	11.8%	HT
Dicroidium crassinervis——*Fanerotheca papilioformis*——*Petruchus matatimajor* (corystosperm) [WPT: **I**]	**Galling**	DT70	117	12	167	70.1%	DOW
	Seed Predation	DT74	35	10	700	5.0%	DOW
Sphenobaiera schenckii——*Sphenobaiera*-short shoot——*Hamshawvia longipeduncu-lata*——*Stachyopitys gypsianthus* (ginkgophyte) [WPT: **H**]	**Galling**	DT122	35	5	49	71.4%	SCW
Ginkgoites matatiensis——*Avatia bifurcata*——*Eosteria eosteranthus* (ginkgophyte) [WPT: **F**]	**Seed Predation**	DT73	63	7	1130	5.6%	SCW
Zonulamites viridensis—nodal diaphragm A–*Viridistachys gypsensis*—*Paraschizo-neura fredensis* (horsetail) [WPT: **B**]	**Oviposition**	DT72	14	9	38	36.8%	HM
	Oviposition	DT108	39	2	40	97.5%	HM,SCW
Dordrechtites elongatus/*D. mazocirrus* (conifer)	**Seed Predation**	DT124	2	2	13	15.4%	SCW,DRF-I

[a]Whole plant taxa (WPT) are indicated in Fig. 14.4, with their herbivore damage types (DTs) and functional feeding groups (FFGs)

[b]Habitat abbreviations: *DOW* Dicroidium Open Woodland, *HM* Horsetail Marsh, *HT* Heidiphyllum Ticket, *SCW* Sphenobaiera Closed Woodland, *DRF-I* Dicroidium Riparian Forest, immature phase (Anderson and Anderson 2003)

Although the consumption of live plant tissue is quite different from the consumption of dead plant tissue (Brues 1924; Mitter et al. 1988), both types of biological interactions are quite different from physical destruction of plants by the environment, such as leaf damage attributable to wind, water or the impact of gravity (Wilson 1980; Vincent 1990; Vogel 2012). For detritivory, the five classes of evidence listed immediately above typically are absent. For example, detritivory does not produce callus and other teratological plant-response tissues that typically result when insect-induced herbivory targets live plant tissues. Importantly, detritivory almost always lacks the delicate microstructural features of damage, such as veinal stringers and necrotic tissue flaps that occur along the margins or surfaces of herbivorized plant organs.

14.3.3 Functional Feeding Groups, Damage Types and Component Communities

The arthropod damage present at Aas411 was categorized based on the FFG–DT system of Labandeira et al. (2007), consisting of data (Tables 14.2, 14.3; Figs. 14.2, 14.3, 14.4) and illustrations of damage (Figs. 14.5, 14.6, 14.7, 14.8, 14.9, 14.10, 14.11, 14.12, 14.13). A functional feeding group (FFG) is a major mode of insect feeding defined by the way an insect consumes its food and is associated with particular insect mouthpart structure, feeding mode and plant damage pattern (Labandeira 1997, 2002b). A FFG is subdivided into multiple damage types (DTs), each of which is a distinctive, defined pattern of damage that represents the most restrictive level of diagnosis and constitutes the fundamental unit of analysis in this and other such studies (Wilf and Labandeira 1999; Schachat et al. 2014; Ding et al. 2015).

There are, however, a few complexities to this system of insect-damage analysis. Oviposition also is considered a FFG, even though it represents the insertion of eggs into plant tissues by a sword-like abdominal feature, the ovipositor, and technically is not a type of plant consumption. However, oviposition has an abundant and rich fossil record of insect-mediated plant damage and is represented by a wide variety of DTs (Sarzetti et al. 2009; McLoughlin 2011; Gnaedinger et al. 2014), and has been treated as a FFG in this and previous studies. In addition, some DTs are combined into a damage-type suite that has two or more associated DTs that are linked organically to the same insect maker. For example, the base of deciduous gall DT186 has attachments to leaves that exactly match the holes of DT148 that occur on the same host plant of the same deposit, indicating a match that represents a deciduous gall and the dehisced leaf scar from which it originated (Labandeira et al. 2007). Another example of a damage-type suite is the leaf mine DT280 that likely originated from oviposition lesion DT101 on the same leaf taxon, and whose adult feeding damage likely is DT103, also occurring the same host-plant organ (Ding et al. 2014).

Herbivore component communities were established for the major plant hosts at Aas411. A component community consists of all species that trophically are dependent on a single, live, host-plant species (Root 1973). Some Molteno vascular-plant species are a host to herbivores that consist of a single organ, whereas others are designated as a host consisting of a whole plant taxon (WPT) that consists of multiple affiliated plant organs. The component community of each plant host includes all dependent herbivores and their derivative consumers, including predators and parasitoids, as well as saprobes that are trophically linked to that source-plant species through the same food web. Many arthropod herbivores and predators are known for the Molteno Biome in general and Aas411 in particular, as discussed below. In modern component communities, the source plant constitutes approximately 90% of the total component community biomass; insect herbivores account for about 10%; and generally 1% is attributable to consumers of the herbivores (Schmitz 2008). A relevant consideration here is that insect parasites and parasitoids are a feeding guild that did not appear until the Early Jurassic (Labandeira 2002a), and thus are excluded from the component community structure of Molteno plant species, which was characterized by top-to-down regulation by insect and ultimately vertebrate predators.

14.4 The Molteno Formation

14.4.1 Geological Backdrop

The Late Triassic (Carnian) Molteno Formation is a thick, wedge-shaped sequence of conglomerate, sandstone, shale and coal that occupies the eastern limb of the Karoo Basin in South Africa. (Hancox 2000). The Molteno sedimentary package consists of a well exposed, approximately quadrangular outcrop pattern that extends approximately 200 km in an east–west and 450 km in south–north directions (Fig. 14.1). This sedimentary package thickens to 650–600 m from the south (Hancox 2000), adjacent the Triassic sediment source of the then substantial mountains of the Cape Fold Belt, and thins to the north where it is unconformably underlain by the older Middle Triassic (Anisian) Burgersdorp Formation, the uppermost unit of the Beaufort Group. The Molteno Formation conformably intergrades laterally and distally into a red-bed facies of the Lower Elliot Formation (Anderson et al. 1998). The portion of the Karoo Basin housing the Molteno Formation consists of a foreland basin established by tensional tectonism from the break-up of Gondwana. This tectonic separation of landmasses formed a rift between northern Antarctica and South American toward the south from southern Africa, while Gondwana drifted northward during the Triassic.

14.4.2 Lithostratigraphy

Although the lower contact of the Molteno Formation with the Burgersdorp Formation is unconformable, generally the lowermost strata of the Molteno Formation is considered as the first appearance of conglomeratic and coarse-grained sandstone strata, typical of the transition from an earlier phase of suspension-load flow to a later phase of bed-load flow. This switch parallels a distinct change in outcrop color from red and purple to grey and buff hues (Cairncross et al. 1995; Anderson et al. 1998). This marked sedimentologic and color break coincides with a change in the depositional environment from a floodplain of ephemeral streams to a braided-stream system, and is marked by an unconformity that probably is regional in scope. It is likely that this changeover was caused by initiation of an offshore, tensional tectonic regime, occasioned by the rifting of Antarctica and South America from southern Africa. Deposits of the Molteno Formation consist of buff-colored to grey, often yellowish brown and pale bluish to light grey sandstones that interdigitate with grey to olive-grey and reddish brown siltstones and mudstones (Cairncross et al. 1995; Anderson et al. 1998). These strata occasionally contain sedimentary ichnofossils (Turner 1978). Carbonaceous mudstones often are present, but coals are rare, with thermal rank intensity decreasing in a westerly direction (Hancox 2000). After deposition of the Molteno sediments, there was another colorimetric shift in the Lower Elliot Formation, from buff-colored hues and grays to reds and purples, as well as a distinctive change to finer-grained strata that represent a stepwise increase in flooding events (Cairncross et al. 1995; Anderson et al. 1998).

14.4.3 Depositional Environment and Cycles

During the interval of Molteno sedimentation, as the Cape Fold Belt Mountains to the south were eroded to a remnant of their former size, there was a sedimentary wedge of strata that fanned out toward the north and formed a variety of depositional environments (Hancox 2000). These environments consisted of braided and subordinate meandering fluvial systems that consisted of three primary facies. These facies were: (i), channel-fill deposits of coarse grained and upward-fining sequences; (ii), upward-coarsening crevasse splays and sheet-flood strata; and (iii), interspersed laminated lake and waterlogged shales indicating lacustrine or palustrine conditions. The beginning of Molteno sedimentation was characterized by a braided-stream style of fluvial deposition, and small inter-channel bodies of water. By contrast, toward the end of Molteno deposition there was a shift toward meandering-river systems and the establishment of more extensive lakes (Anderson et al. 1998).

The Molteno Formation is subdivided into six, distinctive, sedimentary cycles (Fig. 14.1). Each cycle repeats a fining-upward sequence of sedimentation that resulted from a pulse of mostly fault-controlled uplift (Turner 1975). The uplifts

that produced the sedimentary cycles originated from the south in cycles 1 and 2, and from the southeast for cycles 3 through 6 (Anderson et al. 1998). Each of the six sedimentary cycles in the Molteno Formation typically produced a coarse-grained sandstone to fine-grained sandstone to a siltstone–shale–coal succession that displayed more resistant strata at the base and less resistant strata at the top of each sequence. The sedimentary cycles begin with the Bamboesberg Member representing cycle 1, and end with the Loskop Member of cycle 6. The physical environment and habitat type of a Molteno site are contingent on where in the sedimentary cycle landscape that it occurs. More stable, proximal localities closer to the source area tend to favor mature forests bordering lakes, whereas more distal localities occur along distributary channels that prefer ephemeral vegetation in disturbed environments.

14.4.4 Molteno Localities and the Broader Context

For this and following studies of Molteno plant–insect interactions, the total data-set consists of 106 localities containing 177,297 separately examined plant specimens from which 10,165 interactions have been recorded (Table 14.1). The number of localities for each habitat type, detailed below, are: two localities of Mature Dicroidium Riparian Forest, nine localities of Immature Dicroidium Riparian Forest, 33 of Dicroidium Open Woodland, 15 of Sphenobaiera Closed Woodland, 23 of Heidiphyllum Thicket, 18 of Horsetail Marsh, three of Fern–Kannaskoppia Meadow, and three of indeterminate habitat. These Molteno data represent the most extensive database of plant–insect interactions in the fossil record and will be included with eight Anisian localities and approximately ten Guadalupian and Lopingian Permian localities, all from the Karoo Basin, in future analyses. This broader study will examine the effects on Molteno plant–insect interactions that were inflicted by the P-Tr ecological crisis approximately 35 million-years earlier.

14.4.5 The Aasvoëlberg 411 Site

Of the 106 plant assemblages collected from the Molteno Formation, the Aas411 site is the second most intensively sampled in terms of human labor. Specimens were excavated from Aas411 on 11 separate field trips, covering 40 days and include a total of 512 person-hours splitting slabs on site or back in the lab by John and Heidi Anderson and colleagues. A total of 2535 catalogued slabs originate from Aas411, of which 242 were part/counterpart slabs, that consist of 20,358 examined individual plant specimens averaging to about eight plant specimens per slab. The Aas411 site has the most numerically abundant specimens from the Molteno Formation; the Bir111 (Birds River 111) site is second at 15,503 specimens. All fossil plants from the Molteno Formation currently is housed at the Evolutionary

Studies Institute (ESI) at the University of the Witwatersrand, in Johannesburg, South Africa, under the curation of Dr. Marion Bamford.

Geographically the Aas411 site occurs in the far southwestern corner of the Molteno Formation outcrop belt, in the north-central part of the Eastern Cape Province, approximately 50 km southwest of the town of Molteno, after which the formation is named. Strata of the Aas411 site crop out within the Bamboesberg Member, the stratigraphically lowest of six defined members (cycles) in the formation. Of the 106 sampled plant assemblages, Aas411 is the fourth lowest in the Molteno sequence. Of the seven primary habitats recognized as characterizing the Molteno Biome, Aas411 represents Sphenobaiera Closed Woodland, a habitat which typically occurs along floodplains surrounding lakes.

The fossiliferous stratum yielding the Aas411 material consists of about a two m-thick bed of rhythmically alternating, thinly laminated, yellowish-grey shale to slate with very good cleavage. The strata are significantly altered thermally, resulting from the heating effect of nearby dolerite sills and dikes. Preservation is exclusively in the form of impressions, though with excellent clarity of detail. The local bed from which the specimens originate is exposed intermittently along a grassy hillslope for some 140 m, but its full extent is uncertain, as is its uniformity of thickness and lithology.

The preserved Aas411 flora consists of 30 vegetative species, of which 22 are gymnosperms and eight are non-gymnosperms. The Aas411 flora is dominated by several species each of the corystosperm *Dicroidium* (60%) and the ginkgophyte *Sphenobaiera* (30%), which, together with non-dominant plants, probably represent distinct woodland communities within the Sphenobaiera Closed Woodland habitat that bordered floodplain lakes. Generally, the constituents and preservation of the flora, considering the foliage, cones, scales and seeds, suggest quiescent conditions occurring adjacent to a sizable water body. The insect fauna is composed of a high-diversity cockroaches, beetles and dragonflies which form an association represented by 129 individuals. These informal insect taxa provisionally have been assigned to 30 genera and 43 species across a wide spectrum of 13 orders. The numerical dominance of cockroaches, consisting of 54 individuals, hints at the surrounding woodland having a dense cover with mostly a closed canopy and well-developed leaf litter layer.

14.4.6 Habitats

There are seven distinctive, primary habitats that characterize the floodplain environments of the Molteno Biome (Cairncross et al. 1995; Anderson et al. 1998). These habitats were determined by physiognomic features of the plants, such as abundance patterns, plant growth form, leaf architecture, and recurring plant associations. In addition, features of the environment are relevant for determination of the habitat, such as sedimentologic features of the deposit, indications of climate-based aridity, and inferred water saturation levels in soils (Anderson and Anderson

2003). These seven habitats occupy particular, confined settings on the regional landscape that consist of particular plant associations or monodominant communities that have been determined for 103 of the 106 floras of the Molteno Formation. Floras from three of the Molteno localities have not been assigned to any of the seven habitats.

The climax, or mature, phase of Dicroidium Riparian Forest consists of a multistory, close-canopied, high diversity forest of plant taxa and morphotypes occurring adjacent to active and abandoned and meandering water channels that are superimposed on an earlier Triassic erosional surface. By contrast, the pre-climax, or immature, phase of Dicroidium Riparian Forest is characterized by single story, mostly closed canopy, medium diversity forest adjacent various floodplains. These channels are mostly braided and occur on alluvial flood plains. Dicroidium Open Woodland consists of a low to medium diverse woodland with a considerable intervening open spaces occurring along floodplains bordering water courses that are subject to intermittent sheet flooding. Sphenobaiera Closed Woodland, such as the Aas411 site, is comprised of a moderately diverse woodland with a minimally interrupted canopy that borders lakes and is present on floodplains. Heidiphyllum Thicket represents almost monodominant, dense stands of shrubby coniferous plants and associated lianas rooted in soils with an elevated water table along floodplains or on mid-stream sandbars. Horsetail Marsh consists of highly monodominant stands of horsetails along sandbars in channels, floodplain marshes, and poorly drained wetland soils that surround lakes. Fern–Kannaskoppifolia Meadow is a rare habitat of a low-diversity, mostly herbaceous in form that occupies median channel bars or braided-river sandbars, often in ruderal environments.

Each habitat type has a characteristic spectrum of plant species whose rank-order of abundance is distinctive at the genus level (see Sect. 14.5.14). Preliminary observations indicate that 43 localities and most habitats have produced insect fossils that express different combinations of and dominance of particular insect taxa. Insects of the Molteno Biome are Ephemeroptera (mayflies), Odonatoptera (dragonflies and related forms), Plecoptera (stoneflies), Blattodea (cockroaches), Orthoptera (forms related to grasshoppers and crickets), Hemiptera (cicada-like forms and bugs), Coleoptera (beetles), Neuroptera (lacewings), Hymenoptera (sawflies) and Mecoptera (scorpionflies) (MacRae 1999; Anderson and Anderson 2003). About half of these groups are overwhelmingly are herbivorous or have significant herbivore lineages, and undoubtedly assumed a major role in the plant–insect interactions in the Molteno Biome (Scott et al. 2004; Labandeira 2006a, 2012, 2016).

14.5 Molteno Plant Hosts

14.5.1 Overview

A broad variety of plants characterize the Molteno Flora, collectively representing the most diverse assemblage worldwide of plants from the Late Triassic. The Molteno Flora from the Karoo Basin of South Africa and Lesotho is a Late Triassic

Gondwanan assemblage that is floristically consistent with all of the major groups of cryptogams, ferns, and seed plants that typically occur in other floras of the supercontinent at the genus and frequently the species level. The Molteno Flora represents a rich assemblage of bryophytes (mosses, unpublished data), hepatophytes (liverworts, unpublished data) and lycopods (clubmosses, unpublished data), horsetails (Anderson and Anderson 2017), ferns (Anderson and Anderson 2008) and seed plants (Anderson and Anderson 1983, 1989, 2003). The seed plants represent the majority of the plant lineages present, and include virtually all major Late Triassic taxa of cycads, conifers, peltasperms, diverse ginkgophytes, corystosperms, bennettitaleans and probably gnetaleans. Additional unaffiliated taxa also occur. Based on an assessment of success following five criteria established by Anderson and Anderson (2003), the five most prominent foliage genera, in order of prominence, are the corystosperm *Dicroidium*, the conifer *Heidiphyllum*, the ginkgophyte *Sphenobaiera*, the bennettitopsid *Taeniopteris*, and the ginkgophyte *Kannaskoppifolia*.

14.5.2 Bryophytes

Most Molteno bryophytes currently are undescribed, although a preliminary tally of these rare to uncommon herbaceous taxa indicates that they bore a thallus representing a broad variety of morphologies among mosses, liverworts and an indeterminate taxon. Bryophytes collectively occur in about a fourth of the 106 Molteno localities. Mosses are represented by a single species of undescribed *Muscites* and 12 undescribed species of *Thallites* that are present in 18 localities and predominantly inhabited the immature and mature phases of Dicroidium Open Woodland. Liverworts are equally speciose, comprised of 13 undescribed species of *Marchantites* foliage from 19 localities that occurred on soils principally in Heidiphyllum Thicket and subordinately in the immature and mature phases of Dicroidium Riparian Forest, Dicroidium Open Woodland and Sphenobaiera Closed Woodland. The species of moss foliage primarily inhabited five localities, dominantly in Heidiphyllum Thicket and both developmental phases of Dicroidium Riparian Forest. One undescribed, monospecific genus was present in two localities of Sphenobaiera Closed Woodland, including Aas411. Although modestly diverse, the above four bryophyte genera were present at low frequencies and were an insignificant part of the flora, occurring on or within a few centimeters of the soil surface.

14.5.3 Lycopods

Largely undescribed, herbaceous or small single-stemmed, arborescent lycopods consisted of five undescribed genera and 13 species of stems, foliage and cones informally assigned to a new, undescribed lycopodialean family and the extinct

isoëtalean Pleuromeiaceae. Lycopods occurred in about a tenth of the Molteno localities, are present at significantly lower frequencies than bryophytes, and are represented by six genera and 13 species that formally have not been described. A single undescribed genus of lycopod cone was present at one site of Sphenobaiera Closed Woodland. By contrast, another undescribed genus of lycopod cone is represented by five species that occurred in five localities across a landscape of varied habitats. Lycopod megaspores have been found in two localities, including Aas411. Three genera of lycopod foliage are present at three localities, principally in Sphenobaiera Closed Woodland, all three of which occur at Aas411. A genus of lycopod stems is represented at one site whereas another morphotype of lycopod stems occurs in five localities, including a species at Aas411, amid a broad spectrum of habitats. Like bryophytes, lycopods were present in those localities with the most diverse biotas, especially at Aas411, Umk111 and Bir111. Molteno lycopods represent several new, higher-level taxa not known elsewhere from the Late Triassic and many had distinctive stem morphologies.

14.5.4 Horsetails

Horsetails, or sphenopsids, are one of the plant groups that persistently are present throughout the Molteno Biome, whose stems, foliage and cones were present in 77 of the 106 localities (73%) and occasionally occur in some localities as monodominant or nearly monodominant stands in a variety of habitats (Anderson and Anderson 2017). Molteno horsetails consist of two orders, three families, 13 genera and 37 species representing fertile and sterile taxa. These taxa were present predominantly in the three habitat types of Horsetail Marsh, Heidiphyllum Thicket and Dicroidium Open Woodland. In addition, horsetails form a significant floral component in Fern-Kannaskoppia Meadow, present in all three localities of this distinctive community type, and also are documented in all 11 localities of the immature and mature phases of Dicroidium Riparian Forest. Horsetails are considerably less abundant in the six localities of Sphenobaiera Closed Woodland but are present in all three localities of indeterminate habitat type. Within the mostly wetlands-inhabiting horsetails, there was a considerable diversity of stem architecture, foliage types, reproductive structures and apparently a division between smaller, shorter statured herbaceous forms versus considerably taller, reed-like to arborescent forms.

Horsetails consist of two ordinal-level ranks, Echinostachyales, represented by fertile and sterile material, and Equisetales, affiliated with vegetative material. The Echinostachyales is comprised of the Echinostachyaceae and a second family of uncertain taxonomic status. The Echinostachyaceae consists of the cone genus of *Echinostachys*, represented by one species, and the foliage genera of *Schizoneura* (two species) and *Paraschizoneura* (four species), all of which occur in seven localities. The second family, an extinct, family-level lineage of uncertain position, consists of *Cetistachys*, *Moltenomites* and *Balenosetum*, that uniquely is present only at the Umk111 site. The Equisetales are represented by vegetative and sterile material

and consist of the single extant family, Equisetaceae, but represent extinct taxa housing the six genera of *Kraaiostachys* with one species, *Anisetum* (one species), *Viridistachys* (two species), *Zonulamites* (four species), *Townroviamites* (three species), *Equisetostachys* (nine species), and *Equisetites* (six species), collectively present in 12 localities that include all seven localities containing members of the Echinostachyaceae. For the horsetails of the Molteno Biome, the most speciose horsetail taxa are the vegetative organs of *Zonulamites* and *Equisetostachys* (Anderson and Anderson 2017).

14.5.5 Ferns

The moderately diverse ferns are represented in 50 of the 106 localities (47%) and are the third most abundant vascular plant group, after horsetails and seed plants. Molteno ferns are divided into four major lineages (Anderson and Anderson 2008), the first three of which are extant, although the evolutionary relationship of the fourth, unaffiliated group remains unknown. The first group consists of the eusporangiate Marattiaceae, represented by two species of *Drepanozamites*, and Asterothecaceae consisting of three species of *Asterotheca*. These eusporangiate ferns collectively inhabit six localities, and occur predominantly amid the arborescent vegetation of Dicroidium Riparian Forest and to a lesser extent in Sphenobaiera Closed Forest and Dicroidium Open Woodland. The second major group is affiliated with leptosporangiate Osmundaceae, also representing fertile material, and consists of 12 species of *Osmundopsis*, *Rooitodites*, *Birtodites* and *Elantodites*. The osmundaceous taxa are found in 22 localities, predominantly in Heidiphyllum Thicket and Dicroidium Open Woodland, and subordinately in the remaining five habitats.

A third group of ferns is assigned to the Dipteridaceae and an unaffiliated family. The Dipteridaceae is represented by the three species of *Dictyophyllum* that occur in eight localities, preferring Heidiphyllum Thicket and subordinately the immature and mature phases of Dicroidium Riparian Forest, Sphenobaiera Closed Woodland and Dicroidium Open Woodland. The unassigned family is represented by three species across a broad swath of localities and habitats. The fourth group consists of vegetative material of uncertain taxonomic position that lack spore or sporangial features that would provide an affiliation to a known lineage. The unaffiliated ferns of sterile foliage from the fourth group are *Cladophlebis*, *Sphenophyllum*, *Birmoltia*, *Nymbopteron*, *Parsorophyllum*, *Stormbergia*, *Nymboidiantum*, *Displinites* and *Molteniella* that occur in 47 localities. Habitats colonized by Dipteridaceae ferns are dominantly Dicroidium Open Woodland and Heidiphyllum Thicket, somewhat less so for Dicroidium Riparian Forest, and minor elements in the remaining habitats.

Molteno ferns constitute three or four families, 16 genera and 49 species, inclusive of fertile and vegetative taxa. This spectrum of fern lineages is the product of three ancient fern radiations, consisting of older, late Paleozoic eusporangiate lineages of the Marattiaceae and Asterothecaceae; the basal leptosporangiate lineages

of the Osmundaceae originating during osmundalean radiation of the late Paleozoic to earliest Mesozoic; and an early lineage of the younger still Dipteridaceae that likely originated during the earliest Mesozoic polypodialean radiation (Anderson and Anderson 2008; also see Pryer et al. 2004). Ecologically, all fern groups were distributed in the seven habitats described for the Molteno (MacRae 1999), although they did not prefer overwhelmingly any particular habitat, except perhaps Heidiphyllum Thicket, which appears particularly well populated by fern taxa.

14.5.6 Cycads

Cycad foliage is well represented in the Molteno flora (Anderson and Anderson 1989), although the only known fructification, *Androstrobus*, is indeed rare and represented by two specimens that occur at the Kra311 (Kraai River 311) and Pen321 (Peninsula 321) localities (Anderson and Anderson 2003). Molteno cycad foliage is probably affiliated with Cycadaceae, an extant major lineage of cycads that are basal within the modern clade (Condamine et al. 2015), but extend to the early Mesozoic and possibly late Paleozoic (Anderson et al. 2007). The most diverse Molteno genus is *Pseudoctenis*, a pinnate frond of medium to large size represented by 10 species that occur in 23 of the 106 localities (22%). The habitats in which *Pseudoctenis* resided are Dicroidium Open Woodland and the immature and mature phases of Dicroidium Riparian Forest; although it also is found subordinately in Sphenobaiera Closed Woodland and Fern–Kannaskoppia Meadow. Three, other, less commonly occurring foliage genera are *Jeanjacquesia*, with four species inhabiting four localities; *Ctenis*, consisting of two species found in two localities; and *Moltenia* that consists of four species confined to five localities of Dicroidium Riparian Forest. Localities with the greatest number of cycad species are Hla212 (Hlatimbe 212), Kon211A + Kon221 (Konigs Kroon 211A and 221 combined), and Kon221 (Konigs Kroon 221). Molteno cycads were generally small and had a pachycaul plant form similar to modern cycads, and occurred in all habitats except Horsetail Marsh and Heidiphyllum Thicket.

14.5.7 Conifers

Conifers are richly represented in the Molteno flora and consist of three, perhaps four, family-level groupings (Anderson and Anderson 1989, 2003). Most commonly present is Voltziaceae, a lineage that consists of ubiquitous *Heidiphyllum elongatum* foliage, the affiliated ovulate organ *Telemachus*, and affiliated pollen organ *Odyssianthus*. Vegetative and reproductive material of Voltziaceae occur in 76 of the 106 floras (72%), attributable to the overwhelmingly dominance of *H. elongatum* and associated conspecific reproductive taxa. *Heidiphyllum elongatum* occurs in every Molteno habitat, but especially is prominent in Heidiphyllum Thicket and

Dicroidium Open Woodland; much less so in Sphenobaiera Closed Woodland, the immature and mature phases of *Dicroidium* Riparian Forest and Horsetail Marsh; and rarely in Fern–Kannaskoppifolia Meadow. *Telemachus* consists of ten distinctive species occurring in 28 localities and occurs in approximately in the same proportions and habitats as *H. elongatum*. By contrast, one specimen of *Odyssianthus* was found at Telemachus Spruit (Tel111), a site rich in associated *Telemachus* ovulate material and *H. elongatum* foliage. A probably related, unnamed ovulate fructification has been found only at the Aas411 site. The possibly related, monospecific foliage of *Clariphyllum clarifolium* was found at three localities of the immature and mature phases of Dicroidium Riparian Forest. *Heidiphyllum* and *Clariphyllum* are considered as woody, small to medium-size shrubs with a bamboo like habit (Anderson and Anderson 2003; Barboni and Dutra 2015).

A second group of vegetative and reproductive conifer material, tentatively assigned to Podocarpaceae, consists of the leaf genus *Rissikia*, with two species that occur in 25 localities. Associated with *Rissikia* is the ovulate cone, *Rissikistrobus*, comprised of four species occurring in eight localities, and the pollen cone, *Rissikianthus*, with four species that are found in five localities. The *Rissikia–Rissikistrobus–Rissikianthus* affiliation forms a whole-plant taxon that was a minor member at Aas411, and was present sporadically throughout the Molteno Biome, preferentially inhabiting Dicroidium Riparian Forest. A third conifer group, the Dordrechtitaceae, consists of the ovulate cone *Dordrechtites* with four species and the monospecific male cone *Gypsistrobus* that collectively occur in 28 localities—a lineage exhibiting a habitat preference for Heidiphyllum Ticket, Dicroidium Open Woodland and Dicroidium Riparian Forest, and to a lesser extent Sphenobaiera Closed Woodland, occurring rarely in other habitats. The last group, monospecific *Pagiophyllum*, is another conifer foliage genus also occurring at Aas411; however, this enigmatic taxon has an uncertain taxonomic position. The reconstruction of the *Rissikia–Rissikistrobus–Rissikianthus* source plant is that of a large tree that occurred in wetlands and riparian border habitats (Anderson and Anderson 2003). The parent plant of the Dordrechtitaceae remains unknown, whereas *Pagiophyllum* is reconstructed as a small tree.

14.5.8 Peltasperms

Peltasperms are a major seed-plant group of the Permian to mid Mesozoic whose Mesozoic representatives are characterized by *Lepidopteris* foliage and associated, distinctive *Peltaspermum* ovulate organs and *Antevsia* pollen organs (Anderson and Anderson 1989, 2003). Molteno peltasperms are typified by the common Gondwanan foliage genus *Lepidopteris*, consisting of two species, both of which occur at Aas411. The two species of *Lepidopteris* are found in 37 of the 106 Molteno localities (35%), and are dominant in Dicroidium Open Woodland, less so in the immature and mature phases of Dicroidium Riparian Forest and Sphenobaiera Closed Woodland, and becoming uncommon to insignificant in Heidiphyllum Thicket,

Horsetail Marsh and Fern–Kannaskoppia Meadow. The affiliate ovulate organ, *Peltaspermum*, has been assigned to five species that occur in 30 localities, and is dominant in Dicroidium Open Woodland, less so in the immature and mature phases of Dicroidium Riparian Forest and Heidiphyllum Thicket, and is rare in the remaining localities. All but 8 of the 30 localities that have *Peltaspermum* fructifications also have *Lepidopteris* foliage, thereby indicating conspecificity in association (Anderson and Anderson 2003). The monospecific pollen organ, *Antevsia*, is represented in five localities that are dominated by the immature and mature phases of the Dicroidium Riparian Forest habitat, frequently in association with *Lepidopteris* and *Peltaspermum*. For the Molteno Biome, the *Lepidopteris–Peltaspermum–Antevsia* whole-plant taxon is reconstructed as a medium sized shrub occupying riverine forest (Retallack and Dilcher 1988; Anderson and Anderson 2003).

14.5.9 Corystosperms

Of any Late Triassic plant lineage, it is the Umkomasiales, commonly called corystosperms, which have been the most iconic representative of Late Triassic vegetation throughout Gondwana. The family Umkomasiaceae was the most ubiquitous plant group present in the Molteno Biome (Anderson and Anderson 1983), whose foliage of *Dicroidium* is conspicuously represented in 92 of the 106 localities (87%), the most for any Molteno plant group (Anderson and Anderson 2003). *Dicroidium* consists of species that occur mostly in Dicroidium Open Woodland habitat (36%), less so in Heidiphyllum Thicket, and subordinately in Sphenobaiera Closed Woodland, Horsetail Marsh and the immature and mature phases of Dicroidium Riparian Forest. *Dicroidium* also occurs in all three localities of Fern–Kannaskoppia Meadow. The rarity or absence of *Dicroidium* is most pronounced in Horsetail Marsh and Heidiphyllum Thicket habitats.

Of the nine species of *Dicroidium* foliage in the Molteno Biome, five occur at Aas411. The affiliations between species of *Dicroidium* foliage and seeds that are either dispersed or part of ovulate fructifications are complex, although certain species-level whole-plant taxa can be established in particular localities. Major corystosperm ovulate organs or seeds potentially affiliated with *Dicroidium* foliage are common. They are (i) *Umkomasia* seeds; (ii), the very common *Fanerotheca* (attached ovules)—*Feruglioa* (dispersed seed) complex; (iii), three species of a rare, undescribed seed genus; and (iv), a very rare, additional undescribed seed genus. These four, major seed morphologies probably are affiliated with particular species of *Dicroidium* and the pollen organ *Petruchus* in the same site, but species affiliations remain unknown. *Umkomasia* and *Fanerotheca–Feruglioa* seeds are represented in 53 and 58 of the Molteno localities, respectively, and preferentially occur in Dicroidium Open Woodland, subordinately in the immature and mature phases of Dicroidium Riparian Forest, Sphenobaiera Closed Woodland and Heidiphyllum Thicket; they are much less present in Fern–Kannaskoppia Meadow and Horsetail Marsh. The three species of the less common, undescribed seed is found at 12 local-

ities, and preferentially occurs in both the immature and mature phases of Dicroidium Riparian Forest. Other corystosperm material consists of single site occurrences of foliage and seeds that remain undescribed. The pollen organ affiliated with *Dicroidium* foliage, *Petruchus*, consists of four species that occur in eight localities and preferentially is represented in Dicroidium Riparian Forest and Dicroidium Open Woodland habitats. The whole plant taxon with *Dicroidium* foliage generally is reconstructed as a shrub to large tree; depending on the species, that occupied forest to woodland landscapes (Retallack and Dilcher 1988; Anderson and Anderson 2003).

14.5.10 Ginkgophytes

Ginkgophytes were the most diverse group of plants in the Molteno Biome. The group consists of four or five major lineages or groupings of plants for which foliage and reproductive material are affiliated to various degrees (Anderson and Anderson 1989, 2003). In addition, there are certain genera that likely are ginkgophytes but remain unplaced within the broader ginkgophyte alliance.

The Hamshawviaceae consists of *Sphenobaiera* foliage, *Hamshawvia* ovulate fructifications and *Stachyopitys* pollen organs. *Sphenobaiera* is considered as one of the several most prominent foliage types throughout Gondwana in general and the Molteno Biome in particular, consisting of nine species, excluding short shoot and scale leaf morphotypes, and has been recorded in 56 of 106 localities (53%). This distinctive, mostly lobate leaf with deep incisions ecologically predominates in Dicroidium Open Woodland habitat, but occurs at lesser frequencies in other habitats with mostly woody plant taxa such as Sphenobaiera Closed Woodland, the immature and mature phases of Dicroidium Riparian Forest and in Heidiphyllum Thicket. It is represented sparingly in Horsetail Marsh and Fern–Kannaskoppia Meadow. The ovulate organ, *Hamshawvia*, is considerably rarer and consists of five species from six localities. *Stachyopitys*, the pollen organ, consists of six species occurring in eight localities that has a predilection for woodland and forested habitats. *Sphenobaiera* is reconstructed as a shrub or a tree of medium size that inhabited lake margins, as attested to its presence in Sphenobaiera Closed Woodland along the lakeshore plant communities of Aas411 and Bir111.

The second, major ginkgophyte group is Matatiellaceae, which consists of *Kurtziana* foliage and affiliated *Matatiella* ovulate fructifications. The pollen organ remains unknown. The uncommon to rare leaf genus *Kurtziana* consists of 14 undescribed species occurring in 17 of 106 Molteno localities (16%), and exhibits a preference for occupying the immature and mature phases of Dicroidium Riparian Forest and Heidiphyllum Thicket habitats. *Matatiella* which comprises seven species and is present in 10 localities, exhibits a similar broad range of habitat occupation as the foliage. The *Kurtziana* plant has been reconstructed as a small tree that occupied principally floodplain woodland (Anderson and Anderson 2003).

A third major ginkgophyte group, Avatiaceae, is represented by *Ginkgoites* foliage, *Avatia* ovulate fructifications and seeds, and *Eosteria* pollen organs (Anderson and Anderson 2003). *Ginkgoites* foliage consists of seven Molteno species present in 21 of the 106 localities (20%), and displays a habitat preference for the shrubby to arborescent habitats of Dicroidium Open Woodland, Sphenobaiera Closed Woodland and the immature and mature phases of Dicroidium Riparian Forest, but is rare to absent in other habitats. The affiliated and occasionally very common *Avatia* is monospecific, occurs in 20 localities, and has a preference for Heidiphyllum Thicket, with a much lesser presence in other habitats. The pollen organ, *Eosteria*, consists of two species that occupy only Sphenobaiera Closed Woodland and Heidiphyllum Thicket. The *Ginkgoites–Avatia–Eosteria* whole-plant taxon is reconstructed as a shrub to a tall tree inhabiting floodplain woodland habitats. The very rare foliage of *Paraginkgo*, a second related lineage, occurs only in the two localities of San111 (Sani Pass 111) and Lit111 of Dicroidium Riparian Forest. *Paraginkgo* lacks known, affiliated reproductive organs.

The fourth, major ginkgophyte group, Kannaskoppiaceae, combines *Kannaskoppifolia* foliage with *Kannaskoppia* ovulate fructifications and *Kannaskoppianthus*, pollen organs (Anderson and Anderson 2003). *Kannaskoppifolia* foliage consists of 12 undescribed species occupying 34 of the 106 Molteno localities (32%), and ecologically is best represented in Heidiphyllum Thicket, somewhat less so in Dicroidium Riparian Forest and Dicroidium Open Woodland, and is least present in other habitats. *Kannaskoppia* ovulate fructifications consist of three species occurring in six localities and inhabit a broad swath of habitat types. *Kannaskoppianthus* pollen organs are divided into four species, are present in eight localities, and occur in almost all habitats, but with a strong preference for Heidiphyllum Thicket. The growth form of the *Kannaskoppifolia–Kannaskoppia–Kannaskoppianthus* plant is said to be an herbaceous, ruderal pioneer in a variety of habitats (Anderson and Anderson 2003). An herbaceous habit is a very rare occurrence among gymnosperms.

Within ginkgophytes, the highly polymorphic foliage of *Dejerseya* remains taxonomically unplaced. *Dejerseya lunensis*, the only recognized Molteno species, bears polymorphic foliage that range from very long, linear leaves with entire margins to much shorter, lobate forms to deeply sinuate, lobed foliage. The female reproductive organ affiliated with *Dejerseya* is unclear, and could be a *Matatiella*-like structure or an extremely rare undescribed taxon, Seed sp. A, which occurs in at the Aas411 site. Such an attribution, however, is inconclusive. A more likely affiliation is a species of the rare pollen organ, *Switzianthus* that is found in four localities amid a variety of habitats. Considerably more abundant is monospecific *Dejerseya* foliage, which is found in ten localities and is best represented in habitats of Heidiphyllum Thicket and the immature and mature phases of Dicroidium Riparian Forest. The *Dejerseya* plant is considered a shrub to small tree occupying woodland to forest habitats (Anderson and Anderson 2003).

14.5.11 Bennettitopsids

Although bennettitopsids became one of the most prominent seed-plant groups during the Jurassic and Early Cretaceous, their earliest occurrences were during the Middle and Late Triassic (Pedersen et al. 1989; Anderson et al. 2007). By Late Triassic time, there are early lineages present in a several geographically disparate deposits. For the Molteno Biome, the elongate, entire-margined foliage genus *Taeniopteris*, assigned to the Lindthecaceae (Anderson and Anderson 1989, 2003), was present with nine species. *Taeniopteris* has been found in 45 of the 106 Molteno localities (42.5%), and ecologically was best represented in Dicroidium Open Woodland, much less so in Dicroidium Riparian Forest, Heidiphyllum Thicket and Sphenobaiera Closed Woodland, and is sparse in the remaining habitats. The affiliate ovulate organ of *Taeniopteris* foliage is the monospecific *Lindtheca*, found only at the Aas411 site in Sphenobaiera Closed Woodland. A second, undescribed, ovulate fructification was found only at the Kra111 (Kraai River 111) site, and perhaps is affiliated with *T. anavolans* at this site. The pollen organ affiliated with *Taeniopteris* is unknown. The *Taeniopteris–Lindtheca* plant is reconstructed as a shrub to small tree that commonly occurred in forested and woodland habitats (Anderson and Anderson 2003).

A second lineage of bennettitopsids, attributed to the Fredlindiaceae, is represented by *Halleyoctenis* foliage, affiliated with a *Fredlindia* ovulate fructification and a *Weltrichia* pollen organ, whose dispersed, deciduous, bracts are known separately as *Cycadolepis*. *Halleyoctenis*, a long pinnate frond with oppositely inserted pinnules, is represented by three species that occur in 11 of the 106 Molteno localities (10%) but preferentially are present in Dicroidium Open Woodland, and to a lesser extent in Sphenobaiera Closed Woodland. The affiliated female organ, monospecific *Fredlindia*, is a rather massive, strobilus-like structure that occurs at six localities, principally in Sphenobaiera Closed Woodland and Dicroidium Open Woodland. The male organ, *Weltrichia*, presumably associated with detached *Cycadolepis* bracts found at other localities, consists of two very rare species that occur individually only at the Kon222 (Konigs Kroon 222) and Lit111 localities. The *Cycadolepis*-like bract that bears a pollen sac, Seed sp. B, occurs at Aas411 and also may have originated from a *Weltrichia* pollen organ. Other probable bennettitalean affiliate pollen organs, Seed sp. E and Seed sp. F, also occur at the Aas411 site. The *Halleyoctenis–Fredlindia–Weltrichia* plant is considered a cycad-like, pachycaulous shrub to small tree occupying forest and woodland habitats (Anderson and Anderson 2003).

14.5.12 Gnetophytes

There are three major lineages of the Molteno Biome that are assigned to gnetophytes. These gnetophyte taxa are sparse to very rare and are among the earliest occurrences of this major lineage in the fossil record (Cornet 1996; Anderson et al. 2007). Gnetophytes became prominent during the Late Jurassic to Early Cretaceous, but subsequently declined to their current relictual status. Molteno gnetophyte lineages consist of five foliage genera, two of which have affiliated ovulate fructifications, although pollen organs have not been identified that are attributable to this group.

The Fraxinopsiaceae is the most prominent of the Molteno gnetophyte lineages, and is comprised of two foliage genera. The foliage is comprised of *Taeniopteris*, resembling *Yabeiella* but bearing the affiliated seed *Fraxinopsis*; and the cycad-like *Jungites*, which lacks affiliated reproductive material. *Yabeiella* is the most prominent gnetophyte foliage in the Molteno Biome, occurring in 35 of the106 localities (33%), and has an ecological preference for Dicroidium Open Woodland. *Yabeiella* also occurs in significant numbers in Dicroidium Riparian Forest, Heidiphyllum Thicket and Sphenobaiera Closed Woodland, and is present, albeit rarely, in Horsetail Marsh and Fern–Kannaskoppia Meadow. *Fraxinopsis* consists of three species occurring in 20 localities, three-fourths of which also are *Yabeiella* containing localities. The ecological distribution of this *Fraxinopsis* favored Sphenobaiera Closed Woodland and Dicroidium Riparian Forest habitats. The *Yabeiella–Fraxinopsis* whole-plant reconstruction is a large tree that occurs sparsely in riverine forest (Anderson and Anderson 2003). By contrast, the very rare *Jungites* is an obscure foliage type consisting of one species occurring only at the Umk111 site within mature Dicroidium Riparian Forest.

The Nataligmaceae consists of *Gontriglossa* foliage and *Nataligma* ovulate organs. *Gontriglossa* is a medium-size, *Glossopteris*-resembling leaf consisting of a single species, occurring in eight localities, and displaying an ecological preference for the immature and mature phases of Dicroidium Riparian Forest. The affiliated ovulate fructification, the monospecific *Nataligma*, is found only at the Umk111 site. The *Gontriglossa–Nataligma* whole-plant reconstruction is a sparsely occurring, ruderal plant, presumably herbaceous in growth form, and inhabiting water-margin habitats.

A third gnetophyte lineage, of indeterminate familial affiliation, consists of the foliage genera *Cetiglossa* and *Graciliglossa*, both of which lack affiliated reproductive organs. *Cetiglossa* and *Graciliglossa* each consist of one species that have been found only in the Umk111 site, where they inhabited mature Dicroidium Riparian Forest. The extremely rare *Cetiglossa* is inferred to have been herbaceous undergrowth in riverine forest, whereas the very rare *Graciliglossa* presumably was a slender liana and also was established in riverine forest (Anderson and Anderson 2003).

14.5.13 Taxa of Uncertain Relationships

The Molteno Biome houses numerous taxa of uncertain relationships, principally seed- taxa, but also several other foliage types. The approximately 38 genera of known unaffiliated seeds likely is an under-representation of the true seed diversity, and these will be described and discussed in a subsequent contribution. Other, mostly foliage-based taxa of uncertain relationships, are the possible ginkgophyte *Dejeryseya*–Seed sp. A and *Cetifructus*–Seed sp. H whole-plant taxa; seed taxa belonging to a third, undescribed, possible bennettitalean lineage; and families of uncertain class affiliation: Hlatimbiaceae, Alexaceae and a third, undescribed family. These taxa, representing foliage and female and male reproductive material that currently are difficult to place taxonomically, await additional collected specimens before progress can be made on their taxonomic placement.

14.5.14 General Patterns

Although there are many ways of evaluating the prominence of Molteno plants (Anderson and Anderson 2003), there are three approaches employed below for assessing the omnipresence of Molteno plant taxa at the genus level. The first method simply provides a measure of abundance. In the first method, the abundance of the most commonly occurring genera at the 106 localities is a most commonly used metric. A second method is an overall assessment of success, as used by the FUDAL rating system, as outlined by Anderson and Anderson (2003). A third method is to provide a sense of habitat dominance. For the Molteno flora, the five most abundant taxa, followed by their percentage representation in the 106 floras, are: (i), the most abundant is the voltzialean conifer *Heidiphyllum* (95%); then (ii), the umkomasialean corystosperm *Dicroidium* (90%); (iii), the hamshawvialean ginkgophyte *Sphenobaiera* (30%); (v), the matatiellalean ginkgophyte *Dejerseya* (11%); and (vi) the cycad of indeterminate affinities *Pseudoctenis* (3%). All other Molteno taxa are at abundance levels of 2% or less.

The second mode of evaluation is the FUDAL system was established by Anderson and Anderson in 1989 to provide a measure of success for specified Molteno plant genera. The FUDAL concept was revised by Anderson and Anderson (2003) to provide a more accurate rating system for the prominence of Molteno plant genera. The acronym is an abbreviation for the first letters of frequency, ubiquity, diversity, abundance and longevity for Molteno plant genera. Frequency is the repetitiveness of occurrences of a Molteno genus, as measured directly from the specific distribution of a particular genus in the 85 localities across five Gondwanan continents. Ubiquity is a measure of the general range of specimen occurrence, expressed as the number of the five continental regions across Gondwana in which the genus in question has been recorded. Diversity is a measure of speciation, radiation and variability, as expressed by the number of species of the genus established

for the Gondwanan Triassic. Abundance is a measure of quantity, as determined by the abundance of a particular plant genus in Molteno floras. Longevity is a measure of the duration of the lineage in the 35 internationally recognized biozones in which the genus occurs. Based on these FUDAL criteria, the scores and ranks of the five most prominent Molteno genera are: the corystosperm *Dicroidium* (score of 188, rank of 5), the conifer *Heidiphyllum* (147, 4), the ginkgophyte *Sphenobaiera* (99, 4), the bennettitalean *Taeniopteris* (69, 3), and the ginkgophyte *Kannaskoppia* (62, 3). The first five plant genera in the Molteno ranking approximately parallel the ranking of major plant genera in floras across the Gondwanan Triassic (Anderson and Anderson 2003). This suggests there are supercontinent-wide floristic similarities in the dominance of the same genera.

A habitat-based measure of importance expresses the rank order of the three most abundant Molteno genera in each of the seven habitats (Anderson and Anderson 2003). For the (i), mature phase of Dicroidium Riparian Forest the dominant genera are, in decreasing order of abundance, *Dicroidium*, *Heidiphyllum* and *Sphenobaiera*. For the (ii), immature, or pre-climax, phase of Dicroidium Riparian Forest the analogous ranked taxa are *Dicroidium*, *Heidiphyllum* and horsetails. For (iii), Dicroidium Open Woodland, the respectively ranked taxa are *Dicroidium*, *Heidiphyllum* and *Sphenobaiera*, although the species of *Dicroidium* and *Sphenobaiera* are different than those of the mature phase of Dicroidium Riparian Forest. For (iv), Sphenobaiera Closed Woodland the respective ranked taxa are *Sphenobaiera*, *Dicroidium* and *Heidiphyllum*. For (v), Heidiphyllum Thicket the respective ranked taxa are *Heidiphyllum*, *Dicroidium* and horsetails. For (vi), Fern–Kannaskoppia Meadow the respective ranked taxa are ferns, *Sphenobaiera* and *Dicroidium*. And last, for (vii), Horsetail Marsh the respective ranked taxa are horsetails, *Dicroidium* and ferns. All three evaluative methods indicate that it is the same limited number of plant groups that exhibit prominence in the Molteno Biome, albeit under various combinations and based on different methods of measurement.

14.6 Molteno and Gondwanan Late Triassic Insect Herbivores

14.6.1 Overview

In this section an overview is provided for the major herbivorous mite and insect groups that had interactions with plants or are inferred to have been present during the Carnian Stage in the Karoo Region of South Africa. Because of the regional uniqueness of the Gondwanan biota, the body-fossil record of insects are reviewed for the Karoo Basin of South Africa in particular as well as penecontemporaneous insect faunas from other Gondwanan localities in general (Schlüter 1990; Anderson et al. 1998), principally those of Australia and South America. While the discussion below is not exhaustive, the known, major suspected herbivore mite and insect

groups are covered, many of which had major lineages that experienced ancient evolutionary radiations (Krantz and Lindquist 1979; Whitfield and Kjer 2008). Simultaneously, these taxa provide inferences regarding the ecological structure to Late Triassic plant–insect interactions that now are documented in the Molteno Biota (Scott et al. 2004; Labandeira 2006a). Approximately 3000 insect specimens are known from 43 localities of the Molteno Formation (Schlüter 2003). This material currently is being examined and documented by Torsten Wappler of the Senckenberg Institute in Frankfurt, Germany, and by Olivier Béthoux of the National Museum of Natural History in Paris, France.

14.6.2 Mites

The broader group, Arachnida, to which plant-interacting mites are a member, is virtually absent in Gondwanan deposits. The only formally described occurrence is the predatory araneomorph spider *Triassaraneus andersonorum*, which was described from the Umk111 and Tel111 (Telemachus Spruit 111) localities of the Molteno Formation (Selden et al. 1999, 2009). *Triassaraneus* is a member of the Arachnopulmonata, but no members of another arachnid group, Acariformes, have been found at any Molteno site, an absence attributable to the diminutive size and inconspicuousness of mites, the overwhelmingly dominant phytophagous members of this group. However, oribatid mites are known from their distinctive wood borings, found in the Middle Triassic Fremouw Formation of the Palmer Peninsula of Antarctica (Kellogg and Taylor 2004). More exceptional is the presence of three distinctive genera of plant-feeding mites anatomically preserved in Triassic amber from the late Carnian Heiligkreuz Formation in the Dolomite Alps of northeastern Italy (Sidorchuk et al. 2015). These mites belong to a new superfamilial lineage, Triasacaroidea, associated with amber of the extinct conifer lineage, Cheirolepidiaceae (Sidorchuk et al. 2015). Their occurrence is consistent with earlier estimates of the Eriophyoidea appearing phylogenetically during the late Paleozoic (Krantz and Lindquist 1979).

14.6.3 Odonatopterans

Odonatopterans are dragonflies, damselflies and related archaic Paleozoic and early Mesozoic lineages that are obligately predatory in the adult and subadult stages. However, most odonatopteran females insert eggs by a piercing structure, the ovipositor, which is used to slice into stems and other plant tissues of live vascular plants that typically occur as emergent or slightly submergent positions along bodies of water in terrestrial environments (Wesenberg-Lund 1913; Moisan et al. 2012). The resulting lenticular to ellipsoidal lesions were likely produced by a variety of Molteno odonatopterans, including *Triassoneura andersoni* and two other

congeneric species, of uncertain family assignment (Riek 1976a; Labandeira 2005), as well as the meganisopterid *Triassologus biseriatus* (Riek 1976a), representing a Paleozoic lineage that survived the P-Tr ecological crisis.

Triassic Odonatoptera occur in other Gondwanan continents. A damselfly nymph of Zygoptera, attributable to the form genus, *Samarura*, was recovered from the Late Triassic Aberdare Conglomerate of Queensland, Australia (Rozefelds 1985). From the Late Triassic Ipswich beds, of similar age, the taxon *Triassolestes epiophlebioides* was described by Tillyard and Dunstan (1916); additional conspecific material was illustrated by Rozefelds (1985). Later, Tillyard (1918a, b, 1922, 1923) described three additional genera of Odonatoptera from The Ipswich Beds in Queensland. From South America, Carpenter (1960) erected *Triassothemis mendozensis*, a taxonomically unaffiliated wing, from Cerro Cachueta of Mendoza, Argentina, of Late Triassic age (Gallego and Martins-Neto 1999).

14.6.4 Cockroaches

The presence of various cockroach specimens have been mentioned in several Late Triassic deposits. Besides the Molteno Formation (Riek 1974, 1976a), Late Triassic deposits that bore cockroaches include Australia (Tillyard 1919b, 1937) and South America (Pinto and de Ornellas 1974; Gallego 1997; Gallego and Martins-Neto 1999). Several early to mid-Mesozoic cockroach lineages that possessed long external ovipositors, such as the Mesoblattinidae (Vishniakova 1968; Grimaldi and Engel 2005), likely were responsible for some of the ovipositional damage in Late Triassic plants, particularly those with smaller, circular cross-sectional areas (Meng et al. 2017). These cockroaches were replaced by oothecate forms originating during the Late Jurassic to Early Cretaceous from very modified and reduced ovipositor morphologies (Gao et al. 2017).

14.6.5 Orthopteroids

The most speciose, documented group of herbivorous insects in Late Triassic Gondwana probably were Orthopteroidea (Zherikhin 2002). For the Molteno Formation, approximately 23 species of Orthoptera have been described by Riek (1974, 1976a) and Wappler (1999, 2000a, b). Six species of Haglidae, the relict hump-winged crickets, are known, including: *Hagla contorta*, two undescribed species of *Hagla*, *Zeunerophlebia margueritae*, and two undescribed species of another genus of Haglidae (Wappler 2001). Eight species of the second family of Orthoptera, the extinct Proparagryllacrididae described by Riek (1976a) and Wappler (1999), likely were herbivorous as were *Dordrechtia robusta*, *D. aasvoelbergensis*, *Dordrechtia* sp., *Gryllacrimima johnski*, *Gryllacrimima* sp., and Proparagryllacrididae gen. et sp. indet 1, gen. et sp. indet 2 and gen et sp. 3 (Wappler 1999). The extinct

Xenopteridae is a third family of probable herbivorous Orthoptera that included only *Lutheria dewetii* (Wappler 1999).

The Grylloblattida were another group of orthopteroids that encompassed the extant, relict ice crawlers, that presently have detritivorous feeding habits in cool, north temperate habitats, but during the earlier Mesozoic, this group was considerably more diverse and possibly included herbivorous forms. Molteno Grylloblattida consisted of seven or eight species that were represented primarily by Geinitziidae, consisting of four species of *Fletchitzia*, two undescribed species an undescribed genus of Geinitziidae, and two undescribed species from an indeterminate family of Grylloblattida (Riek 1976a; Wappler 1999). Haughton (1924) earlier described *Protogryllus stormbergensis* as a member of the Gryllidae, which most likely was detritivorous in habits. All Molteno orthopteroid taxa that are suspected herbivores currently are either extinct or relict, and likely were replaced later in the Mesozoic by herbivorous forms that persist to the present day or are ancestors of currently relict lineages.

In other parts of Gondwana, such as Australia and South America, the documented diversity of orthopteroids was considerably less than that of the Karoo Basin. The Late Triassic Blackstone Formation of the Ipswich Basin in southeastern Queensland contains the grasshopper-like Locustopseidae indicated by *Triassolocusta leptoptera* (Tillyard 1922, 1923). The spectacularly large *Mesotitan scullyi*, a member of the Mesotitanidae and assigned to the orthopteroid order Titanoptera occurs in earlier, Middle Triassic deposits at Deewhy in New South Wales, Australia (Tillyard 1925). Recent interpretation of this distinctive group of huge, geochronologically short-lived insects, however, indicate that they likely were insectivorous rather than herbivorous (Zherikhin 2002). In South America, two deposits of late Middle Triassic to Late Triassic age, the Potrellos Formation of Mendoza Province and the Los Rastros Formation of La Rioja Province, preserves several taxa of Orthoptera, including *Hagla* sp. (Haglidae), *Elcana* sp. (Elcanidae), *Nothopamphagopsis* (no family affiliation), and perhaps *Eolocustopsis* sp. (Locustopseidae) (Gallego 1997; Gallego and Martins-Neto 1999). Assuming that the herbivore assignments of these taxa are correct, the varied geographic distribution of orthopteroid taxa across Gondwana, such as those from the Santa Juana Formation in Chile (Gallego et al. 2005), indicates a well-established orthopteroid herbivore insect fauna by Late Triassic times.

14.6.6 Hemipteroids

Piercing-and-sucking hemipteroids currently are a major group of insect herbivores on plants (Pollard 1973). Given their elevated diversity relative to other Late Triassic herbivores, such as mandibulate feeding orthopteroids, hemipteroids likely were a major force in Molteno herbivory. Late Triassic hemipteroids consisted of two major groups: Thysanoptera (thrips) (Childers 1997; Retana-Salazar and Nishida 2007), for which Molteno fossils are lacking, and Hemiptera (other

piercing-and-sucking groups) (Weber 1930; Cobben 1978), which have been rather abundant from the Permian to the present day (Zherikhin 2002). Hemiptera principally consists of six major lineages. They are: (i) Psylloidea, or plant lice; (ii) Aleyrodoidea, or white flies; (iii) Aphidoidea, or aphids; and (iv) Coccoidea, or scale insects and mealy bugs, these four of which collectively constitute the Sternorrhyncha; (v) Auchenorrhyncha, comprising cicadas, plant hoppers and tree hoppers; and (vi) Heteroptera, or true bugs. The Molteno Biome hosted some of these groups, including the sternorrhynchan lineage Protopsyllidiidae, known from a protopsyllidid nymph (Riek 1974, 1976a). The most abundant group within the Molteno Biome were Auchenorrhyncha, represented by Cicadoprosbolidae, consisting of *Prosobolomorpha clara* and *Leptoprosbole lepida*; Scytinopteridae, represented by *Scytinoptera distorta*; Mesogereonidae, with *Triassogereon distinctum*; Dysmorphoptilidae, exemplified by the cicada-like *Tennentsia protuberans*; and Dunstaniidae, an early group of large, hirsute, cicada-like forms exemplified by *Dunstania petrophila* and *Fletcheriana magna* (Riek 1974, 1976a; Labandeira 2005). To date, no Heteroptera have been described from the Molteno Biome. Nevertheless, these eight species of Hemiptera define a broad variety of sizes, shapes, body plans and mouthpart stylet and ovipositor types that likely resulted in partitioning host-plant tissues in intricate ways and employing the same ways as modern hemipterans (Funkhouser 1917; Hori 1971).

For Gondwanan Late Triassic herbivores, the Hemiptera of Australia exhibits the greatest known diversity of any Late Triassic herbivore group, consisting minimally of 33 species that are recorded principally from the Ipswich Basin of southwestern Queensland. The suborder Auchenorrhyncha consisted of the five families of Mesogereonidae that was comprised of five species of *Mesogereon*; the leafhopper-like Cicadellidae with *Mesojassus ipsviciensis*, *Eurymelidium australe* and *Triassojassus proavitus*; Scytinopteridae, occurring as two species of *Mesoscytina*, *Triassoscarta subcostalis*, *Apheloscyta mesocampta*, *Chiliocycla scolopoides*, *Polycytella triassica* and three species of *Mesodiphthera*; the distinctive, fulgoromorph Cixiidae, exemplified by *Mesocixius triassicus*, *Triassocixius australicus* and three species of *Mesocixiodes*; Dunstaniidae, represented by *Dunstania pulcra*, *Dunstaniopsis triassica* and *Paradunstania affinis*; and Ipsviciidae, with *Ipsvicia jonesi*, *I. maculata* and *I. acutipennis* (Tillyard 1918c, 1920, 1921, 1922, 1923; Evans 1971). Late Triassic Auchenorrhyncha were a distinctive group perhaps related to modern Cercopidae, commonly known as froghoppers and spittlebugs. The Heteroptera, or true bugs, have been described as three or four species of *Triassocoris*, members of the Triassocoridae (Tillyard 1923). Collectively, this Australian, Late Triassic assemblage of Hemiptera included xylem, phloem and mesophyll feeders, and probably were engaged in the same or very similar type of feeding as their relatives do today (Hori 1971; Günthart and Günthart 1983; Golden et al. 2006).

There have been considerably fewer occurrences of Hemiptera from strata of similar age in South America. From the Santa Maria Formation at Passo das Tropas in Rio Grande do Sul, Brazil, a wing, *Sanctipaulus mendesi*, was assigned to the fulgoromorph Auchenorrhyncha, and affiliated with the Derbidae (Pinto 1956). In a

somewhat older deposit of the Potreillos Formation of Mendoza Province in Argentina, Gallego (1997) assigned *Mesocixiella* sp. to the Cixiidae, representing another member of the Auchenorrhyncha. At the nearby site of Cerro Cachueta, of younger Triassic age, Tillyard (1926) described *Wielandia rhaetica* and assigned it to the Scytinopteridae. In a review of the Mesozoic insect fauna of Argentina, Gallego and Martins-Neto (1999) mentioned the auchenorrhynchans *Dysmorphoptiloides acostai* of the Dysmorphoptilidae, and *Argentinocicada magna*, *A. minima* and *Potrerillia nervosa* of the Scytinopteridae from Late Triassic sites of west-central Argentina. While these taxa are assigned to lineages that also are found in South Africa, Australia, and South America, they apparently also indicate regional taxonomic differentiation across Gondwana, at least for some insects at the genus level.

14.6.7 Beetles

Permian beetles have been described from the Karoo Basin (Geertsema and Van den Heever 1996; Geertsema et al. 2002), but their affinities lie either with a primitive, paraphyletic lineage to Coleoptera (McKenna et al. 2015), or alternatively as an archaic member of Archostemata, the most basal extant major lineage (Grimaldi and Engel 2005). However, virtually nothing can be said of the finer-grained taxonomic affinities of these or any other Permian beetle lineages, with one exception from north-central China occurring lodged in a complex gallery–tunnel network in a Lopingian conifer host (Feng et al. 2017). Similarly, Early and Middle Triassic beetles, with few exceptions (Grimaldi and Engel 2005; Ponomarenko 2016), also are taxonomically enigmatic, although there are exceptions (Fraser et al. 1996). These Late Triassic exceptions include several identifiable lineages of beetles that are known with some confidence, including Cupedidae (reticulated beetles) of the suborder Archostemata, extinct Trachypachidae of the suborder Adephaga, and Hydrophilidae (water scavenger beetles), Staphylinidae (rove beetles), Artematopodidae (soft-bodied plant beetles), Scirtidae (marsh beetles) and Elateridae (click beetles) of the suborder Polyphaga. Polyphaga are the most diverse, extant major clade, currently representing 85% of all beetle species, and likely were the beetles contributing at least some of the co-associations and herbivory found in the Molteno Biome (Anderson et al. 1999). Independent evidence from plant–insect interaction data suggest, from a process of elimination of potential culprit taxa, that some Late Triassic beetle lineages contributed to a variety of plant damage, including leaf mining (Rozefelds and Sobbe 1987; Labandeira 2006a), wood boring (Walker 1938; Linck 1949; Tapanila and Roberts 2012), and possibly margin and surface feeding (Ponomarenko 2016). Phylogenetic evidence indicates, curiously, that many of the beetle lineages, which would have been responsible for Late Triassic endophytic damage such as leaf mining and wood boring, had not evolved (McKenna et al. 2015). By contrast, several basal polyphagan lineages already were

present, such as the Artematopodidae and Scirtidae that are good herbivore candidates for a variety of external foliage feeding.

For the Late Triassic Molteno Biome, nine beetle taxa have been described, some of which are based on anatomy other than elytra. Molteno beetles include three species of *Ademosyne* in the Permosynidae; *Moltenocupes townrowi* in the Cupedidae; undetermined Ommatinae of the Ommatidae; *Umkomaasia depressa*, possible Carabidae; two species of *Pseudosilphites* that are possible Silphidae (carrion beetles); and an undetermined family (Zeuner 1961; Riek 1974, 1976a; Anderson et al. 1998). Considerably more beetle taxa, approximately 62 species, have been described from the Late Triassic of Australia (Tillyard 1918b, 1923; Tillyard and Dunstan 1923), although these taxonomic assignments remain uncertain and need to be confirmed. From the Middle Triassic Los Rastros Formation of La Rioja Province in Argentina, several taxa have been established, including *Argentinocupes* sp. in Permocupedidae; two species of *Ademosyne* in Ademosynidae; *Tillyardiopsis* sp., possible Curculionidae (weevils); and *Mesostigmodera frenguelli*, possible Buprestidae (metallic wood-boring beetles) from the Middle Triassic Los Rastros Formation of La Rioja Province (Gallego 1997; Gallego and Martins-Neto 1999). As with the Australian beetle material, the South American occurrences need confirmation.

14.6.8 Sawflies

The fossil record of the Symphyta, a group of approximately 14, overwhelmingly plant-associated, basalmost lineages within Hymenoptera are characterized by a diverse repertoire of exophytic and endophytic herbivory, including xylophagy. (The most derived lineage, the parasitoid Orussidae, is the sole nonherbivorous group.) This group collectively is termed sawflies, and their consumption of live plant tissues takes a variety of forms that notably includes external foliage feeding, leaf mining, galling, pith tunneling, seed predation, pollen feeding and wood boring (Blank et al. 2006). The adults are adept in ovipositing eggs in plant tissues and some are implicated in pollination (Burdick 1961). Almost all of the earliest known fossils of Symphyta originate from the Middle Triassic of Central Asia (Rasnitsyn 1969), although two taxa of wings are known from the Late Triassic of Gondwana: one from the Mt. Crosby Formation of southern Queensland, in Australia (Riek 1955), and the other from the Molteno Formation in South Africa (Schlüter 2000). The Molteno specimen is *Moltenia rieki*, found at the Bir111 site, and is identified as a probable member of the Xyelidae (Schlüter 2000). The larval stages provide the overwhelming bulk of plant consumption in sawflies, and their diet probably has the broadest range of functional feeding groups of any larval clade.

14.6.9 Scorpionflies

One of the most taxonomically enigmatic insects of the fossil record is *Mesoses optata*, a broad, incomplete forewing from the Molteno Formation (Riek 1976a). It once was assigned to the "Paratrichoptera" (Shields 1988), a polyphyletic assemblage of antliophoran and amphiesmenopteran stem-group lineages that recently have been reassigned to other insect orders (Schlüter 1997), including Mecoptera (scorpionflies), Diptera (flies), Trichoptera (caddisflies) and Lepidoptera (moths and butterflies). *Mesoses* now is considered an early member of Mesopsychidae, a basal lineage of the Mecoptera that is confined to the early Mesozoic. Notably, *Mesoses* precedes evolutionarily the origin of the long-proboscid condition in successor mesopsychid taxa, such as *Mesopsyche*, *Lichnomesopsyche* and *Vitimopsyche* from the Eurasian Middle Jurassic to Early Cretaceous (Lin et al. 2016). Given the relationship between these long-proboscid scorpionfly taxa and deep-throated gymnosperm fructifications such as the bennettitalean *Weltrichia*, it is highly likely that *Mesoses*, though lacking a long proboscis, was a pollinator feeding on the pollination drops of contemporaneous Molteno fructifications (Anderson and Anderson 1993; Labandeira 2010).

14.6.10 General Patterns

In this survey of described arthropod fossils from the Molteno Biome, eight major mite and insect groups of herbivores have been identified. These herbivore groups were available potentially to produce the 10 major types of arthropod damage on Molteno plants of margin feeding, hole feeding, skeletonization and surface feeding, collectively known as external foliage feeding, as well as internal feeding damage resulting from piercing and sucking, oviposition, mining, galling, seed predation and wood boring. Based on the diversity of body-fossil taxa in each group discussed above, three general patterns emerge. First, the most diverse group, beetles, have an uncertain role in Molteno herbivory due to poor taxonomic assignments and the absence of any dietary and feeding data to make reasoned inferences about what subgroups inflicted particular types of damage. Second, the next, two, equally represented groups, orthopteroids and hemipteroids, would have produced the known damage spectra of external foliage feeding and piercing and sucking, respectively. Third, the remaining groups are either very nondiverse, consisting of very few known taxa, particularly odonatopterans, sawflies, and scorpionflies, or there is the absence of relevant taxa in the Molteno Biome, such as mites, to indicate a reliance of relevant fossils elsewhere in Triassic Gondwanan that would be responsible for a particular type of Molteno herbivory. Certain Late Triassic taxa such as mayflies (Riek 1976b) and lacewings and relatives (Tillyard 1917, 1919a, b) likely lacked interactions with plants. Nevertheless, for the eight plant-interacting groups, such as hemipteroids, there is considerable more diversity of documented insect body-fossil

taxa elsewhere in Gondwana, particularly Australia, than there is in the Karoo Basin. This imbalance suggests the absence of adequate preservation, under-collection of fossils, or more likely a delays in the formal descriptions of fossils in South Africa.

14.7 Plant–Insect Interactions of the Molteno Biota

14.7.1 Overview

Examination of the plant–insect interactions of the 106 localities from the Molteno Biota is part of a broader assessment of the effects of the P-Tr ecological crisis on plants and their insect herbivores. The results of the current study of herbivory at the Aas411 site is part of an ongoing, more detailed, quantitative analyses of existing data which will ferret out generalized and specialized patterns of plant–insect interactions based on host plants, functional feeding groups, damage types, habitats, regional geography, stratigraphic position and other environmental and biotal features of all relevant localities. The broader analysis of the Molteno Biota will be integrated along a 35 million-year-long interval that includes additional earlier Triassic and later Permian deposits. The current, detailed analysis of the most plant-specimen-rich site, the Aas411 site, focuses principally on patterns of host use, host specialization, component community formation, the role of habitat on associational richness, and in particular the biology of gall DT70. Detailed study on the development and other aspects of the biology of gall DT70 will be followed in other contributions from examinations of prominent interactions throughout the Molteno Formation and other Karoo Basin deposits from the Permian to Triassic studied interval.

14.7.2 Molteno Plant–Insect Interactions

The total Molteno data set of 106 stratigraphically ordinated localities that consists of 383 total plant form-species (Table 14.1). Of the total species in the Molteno flora there are 27 bryophytes, 17 lycophytes, 37 sphenophytes, 37 ferns, 22 cycads, 10 peltasperms, 35 corystosperms, 69 ginkgoopsids, 20 bennettitaleans, 13 gnetophytes, 33 coniferophytes and 63 plants of uncertain position that includes foliage and mostly seeds based on published sources (Anderson and Anderson, 1983, 1989, 2003, 2008, 2017) and unpublished updates (J.M. Anderson, H.M. Anderson and C.C. Labandeira, pers. observ.). For all major plant groups except bryophytes, affiliated form-taxa occurring in the same site were associated with 52 separate, whole plant species for the Molteno Biome. These whole-plant taxa consist of multiple, affiliated plant parts such as foliage, female and male reproductive material, and

other plant parts, and were evaluated using a confidence scale of 1–5, with 5 being a direct association such as an attachment or the housing of a seed in an encompassing female fructification. For example, whole-plant taxon suite 13, the *Sphenobaiera schenckii* whole plant taxon, consisted of the *S. schenckii* leaf, *Sphenobaiera* sp. scale leaf, *Sphenobaiera* sp. short shoot, *Hamshawvia longipedunculata* ovulate organ and *Stachyopitys* sp. pollinate organ with a confidence value of 4.5 (Anderson and Anderson 2003; also see Barboni and Dutra 2015). The *Sphenobaiera schenckii* whole-plant taxon occurs at the Kan111 (Kannaskop 111), Nuw111B (Nuwejaarspruit 111B), Gol111 (Golden Gate 111) and Aas411 localities. These unaffiliated plant taxa occur in various and distinct proportions among the seven habitats within the Molteno Biome. The most well represented habitat is Dicroidium Open Woodland, consisting of 33 localities; by contrast, Heidiphyllum Thicket has 23 localities; Horsetail Marsh consists of 18 localities, Sphenobaiera Closed Woodland includes 15 localities, Immature Dicroidium Riparian Forest is attributed to nine localities, Fern-Kannaskoppia Meadow has three localities, Mature Dicroidium Riparian Forest, only has two localities. Three localities that could not be assigned to a particular habitat.

The Molteno database consists 177,297 examined specimens that contain 10,165 separate DT occurrences of herbivory. This ratio corresponds to 5.73% of the specimens that have one or more DTs, a significant level of plant–insect interaction diversity for the early Mesozoic (Labandeira 2006b, 2013b, 2016). Molteno plant–insect interactions consist of two basic groups of FFGs. Some are exophytic in nature, typified by external feeding or consumption from without, represented by hole feeding (13 DTs), margin feeding (6 DTs), skeletonization (2 DTs) and surface feeding (9 DTs). The other major assemblage of functional feeding groups are endophytic in nature, and are characterized by internal feeding or consumption from within, consisting of piercing and sucking (8 DTs), oviposition (10 DTs), mining (7 DTs), galling (15 DTs), seed predation (4 DTs) and borings (2 DTs). Generalized fungal damage was scored as DT58, but was not subdivided into more discrete DTs. This spectrum of 10 functional feeding groups that encompass 76 DTs, of which external feeding is represented by 30 DTs and internal feeding is represented by 46 DTs, is the single highest number of DTs detected in any pre-angiosperm fossil biome examined to date. One site, Aasvoëlberg 311 (Aas311), is the only early Mesozoic site of a possible insect outbreak, specifically insect leaf mining (DT71) on the broadleaved conifer host *Heidiphyllum elongatum* (Labandeira 2012). A comprehensive analysis is being prepared that will assess the effects of the P-Tr ecological crisis on insect herbivory from late Guadalupian and Lopingian floras of, respectively the Middleton Formation and Balfour Formation, to the post-event Anisian Burgersdorp Formation and Carnian Molteno Formation.

A preliminary survey of the plant–insect interactions of the Molteno Biome (Table 14.1) provides basic data regarding the basic ecological context relevant for the plant–insect interactions at each site. Table 14.1 provides a record of site stratigraphic position; habitat; number of whole-plant taxa, if any; dominant functional feeding group; and other data involving the types of and numbers of plant morphotypes/species, DTs and the interaction index. The interaction index is the total num-

ber of DT occurrences divided by the number of plant specimens for each examined site, and serves as a comparative measure of herbivory intensity across all Molteno localities. For these five latter types of data, the localities display a wide range of values that can approach or exceed four orders of magnitude. This wide range of values are: total DT occurrences, ranging from 0 for several localities to 2501 for Bir111; total plant specimens, ranging from 5 for Kullfontein 111 (Kul111) to 20,358 for Aas411; interaction index, ranging from 0 for several localities to 0.2819 for Kappokraal 111(Kap111); total kinds of DTs, ranging from 0 for several localities to 44 for Aas411; and total number of plant species and morphotypes, with as few as 1 for Navar 111 (Nav111), Kraai River 222 (Kra222), Klein Hoek 111A (Kle111A), Vineyard 111 (Vin111) and Champagne Castle (Cha111) to 111 for Aas411. The interaction index is an important measure, and expresses, through the use of presence–absence data, the considerable difference in the incidence of attack on plant specimens from zero to the exceptionally high 28.19% in the case of Kap111. Most Molteno values were in the range of 2.0–6.0%, in accord with typical levels of herbivory in the fossil record of plant–insect interactions (Q. Xu, C. Labandeira and H. Jin, unpublished data).

14.8 Plant–Insect Interactions of the Molteno Aasvoëlberg 411 Site

14.8.1 Overview

The preserved biological diversity of the Molteno Biome has been statistically extrapolated from extant biodiversity from similar environments, indicating a significantly elevated level compared to other, equivalent, Triassic biotas (Anderson et al. 1996). Although not specifically addressed in the Anderson et al. study (1996), plant–insect interactions are an excellent indicator of ecological diversity in terrestrial habitats, and can serve as a measure of biodiversity when expressed as FFGs and DTs (Labandeira 2002b; Carvalho et al. 2014). Each FFG results from insects that bear distinctive mouthpart morphologies engaged in particular modes of feeding (Labandeira 1997). Exophytic interactions representing external feeding are defined by the consumption of plant tissues wherein the insect is positioned outside of the tissue being consumed. Such interactions are synonymous with external foliage feeding that is subdivided into hole feeding, margin feeding, skeletonization and surface feeding FFGs. The frequency distribution of these four external feeding FFGs and their 20 constituent DTs, including the presence of one specialized association, are given in Fig. 14.2 for the Aas411 site.

By contrast, endophytic interactions are defined by the consumption of internal tissues in which feeding occurs, with the entire body or at least the mouthparts embedded within the plant-host tissue. There are two categories of endophytic interactions. One category consists of those interactions in which the body of the con-

sumer lies mostly outside of the tissue, on the plant surface, such as the piercing and sucking and oviposition FFGs. The second type of endophytic interaction is when the consumer is embedded with the plant tissue, which is comprised of the galling, leaf mining, seed predation and borer FFGs. Modern examples of these FFGs, discussed below, are taken from the plant–insect interactional literature, and emphasize vascular plant hosts other than angiosperms that are more anatomically and phylogenetically related to those present during the Carnian. Lastly, host specialized interactions are defined by the presence of a particular damage type that occurs on the same host-plant species or closely-related group of species throughout multiple habitats across the Molteno Biome. The frequency distribution of the five internal feeding FFGs and their 21 constituent DTs, including the distribution of eight specialized associations, are given in Fig. 14.3 for the Aas411 site. The complete host-plant–DT matrix showing the distribution of all FFGs, including the three interactions of a wood boring, an undefined association and fungal damage, is provided in Fig. 14.4.

14.8.2 Exophytic Interactions

Four, major, exophytic FFGs characterize the Molteno Biome. These are the four standard categories of plant–insect interactions that occur in virtually all modern and fossil floras, given sufficient sampling intensity. They are hole feeding (Alford 1991)), margin feeding (Gangwere 1966), skeletonization (Carvalho et al. 2014) and surface feeding (Johnson and Lyon 1991). Typically margin feeding is the most abundant and skeletonization is the least frequent of exophytic FFGs in modern and fossil floras. This pattern of exophytic interactions is repeated for most Molteno localities, and in particular applies for external feeding documented from the Aas411 site (Fig. 14.2).

Hole Feeding: For modern insect herbivores, hole feeding is one of the most ubiquitous and most conspicuous types of feeding (Alford 1991; Johnson and Lyon 1991). At Aas411 there were eight hole-feeding DTs, responsible for 71 occurrences on plant specimens. The most frequently occurring hole feeding is DT1, characterized by small perforations less than 1 mm in maximum diameter, consisting of DT occurrences on 27 plant specimens, and representing 32.4% of all hole-feeding damage. A typical example is DT1 on *Dicroidium odontopteroides* (Fig. 14.5h). Given the variety of hole-feeding that emphasizes the smaller sized holes of DT1, DT2 and DT3 (Labandeira et al. 2007), it is likely that the responsible insect herbivores were small orthopteroids and beetles. These generalized interactions contrast with the presence of stereotypical slot feeding, DT8, on *H. elongatum*, which more likely is attributable to beetle feeding, akin to leaf beetles on the modern fern *Pteris* (Patra and Bera 2007). Distinctive slot feeding occurs in other Molteno localities with abundant *H. elongatum*, and indicates a specialized association. This association occurs in 21 other Molteno localities, predominantly in Heidiphyllum Thicket habitats, and rarely is present at high frequencies, although

the 16 occurrences in Gre-121 is an exception. Consistent with the observation that *H. elongatum* is overwhelmingly the most intensely herbivorized host at Aas411, 57.7% of all damage by hole feeders targeted this host.

Margin Feeding: Margin feeding is the most abundant functional feeding group at Aas411. Margin feeding consists of five DTs that are responsible for 273 occurrences on particular plant specimens, and amounts to 24.6% of all Aas411 associations. The most frequently occurring margin-feeding is DT12, accounting for DTs on 221 plant specimens and representing 81% of all margin feeding. DT12 is characterized by cuspate excisions on foliar margins that do not extend to primary veins or leaf tips. The dominance of margin feeding in general and DT12 in particular is a common pattern seen in many late Paleozoic and early Mesozoic floras, including those of the Molteno Biome. The likely insect culprits of DT12 and other types of margin feeding are medium to large sized orthopteroids, and possibly equally large beetles. Molteno external foliage feeding damage is analogous to damage caused by the nymphs and adults of stick insects and grasshoppers (Floyd 1993; Gangwere 1966), and larvae of owlet and looper moths and common sawflies (Comstock 1939; Welke 1959; Weintraub et al. 1994) on ferns. None of the margin feeding at Aas411 represents a specialized association. The most intensively attacked hosts by margin feeders are *H. elongatum* (Fig. 14.5a,d) and *D. crassinervis* for DT12, representing 34.1% and 29.7% of occurrences, respectively, and subordinately *Lepidopteris stormbergensis* and *L. africana*, representing 16.5% of total margin-feeding DTs. Continuous margin feeding of DT143 is present on *Ginkgoites matatiensis* (Fig. 14.5b,c), and DT13 occurs as the snipped pinnule margins of *Pseudoctenis* sp. (Fig. 14.5e).

Skeletonization: Skeletonization is represented by one occurrence of DT16 on *H. elongatum*. Skeletonization is absent to very rare in Middle Pennsylvanian to Late Triassic floras of Gondwana and Laurasia (Beck and Labandeira 1998; Prevec et al. 2009; Feng et al. 2014) and does not become particularly abundant until the Cenozoic (Wilf and Labandeira 1999).

Surface Feeding: Of the seven surface-feeding DTs at Aas411, the most frequently occurring is DT30, consisting of 25 occurrences on foliage, and representing 32.9% of all surface feeding. The dominance of surface-feeding herbivory, particularly DT29, DT30 and DT103, occurs principally on *H. elongatum* and corresponds to 70% of the total surface-feeding occurrences. DT103, the consumption of surface tissues in the interveinal area between two adjacent, mostly parallel veins, is similar to that of the modern leaf beetle *Aulacoscelis* on the cycad host *Zamia* (Windsor et al. 1999), and other leaf-beetle species on the fern *Pteris* (Patra and Bera 2007). The concentration of these three damage types on *H. elongatum* contrasts with more scattered and fewer occurrences of other surface feeding DTs on other seed-plant taxa at Aas411. The likely culprits for surface feeding on *H. elongatum* are beetles, and perhaps certain orthopteroid clades. However, such surface-feeding lineages would require modified chewing mouthparts for accessing and delaminating surface tissue layers.

14.8.3 Endophytic Interactions

There are six major endophytic interactions that characterize the Molteno Biome in general and Aas411 in particular. These interactions are given in Fig. 14.3, and includes eight specialized associations mapped on some of these endophytic DTs, with the exclusion of borings. The Aas411 site has all six FFGs of piercing and sucking (Weber 1930; Cobben 1978), oviposition (Wesenberg-Lund 1943; Childers 1997), mining (Needham et al. 1928; Hering 1951), galling (Felt 1917; Meyer 1987; Rohfritsch 1992), seed predation (Shepard 1947; Janzen 1971), and borings (Solomon 1995). Collectively, these interactions exhibit a robust partitioning of internal tissues.

Piercing and Sucking: The piercing-and-sucking FFG consists of four DTs that have resulted in damage to 38 plant specimens at Aas411. The most abundant is DT46, consisting of 27 instances on plant specimens and representing 71.1% of all piercing-and-sucking occurrences. DT46 is a generalized interaction consisting of small, isolated puncture marks typically with a surrounding, crater-like rim, analogous to modern punctures produced by thysanopterans (Childers 1997) and hemipterans (Günthart and Günthart 1983). Although stereotypical Molteno piercing-and-sucking damage of scale impression marks by sternorrhynchan hemipterans, such as DT77 or DT158, are absent at Aas411, there are two occurrences of DT128 on *H. elongatum* present at the site. DT128, is a specialized interaction always on *H. elongatum* hosts that also is present at Maz211 (Mazenod 211) with 36 examples, and at the Lut311 (Lutherskop 311) and Win111 (Winnarspruit 111) localities. DT128 is a very distinctive, broadly elliptical scale impression mark characterized by a roughened inner surface, a distinctive bordering rim and an anterior notch (Fig. 14.5f), and closely resembles modern black pineleaf scale, a diaspidid scale insect, on red pine (Johnson and Lyon 1991; also see Maskell 1887). An intermediate specialized association is DT138, which targets particular vascular tissues, whose linear rows of punctures occur along major veins of *H. elongatum* and *D. crassinervis* indicative of feeding on xylem or phloem tissue. The linear tracking of vascular tissue by piercing-and-sucking hemipterans is common in modern plants, and the same DT138 feeding pattern has been recorded on modern pine needles by a typhlocybine leaf hopper (Günthart and Günthart 1983).

Oviposition: Ovipositional damage at Aas411 typically consists of lenticular and less commonly ellipsoidal to circular lesions on the foliage and stems of plants. Endophytic oviposition is characterized by inner disturbed tissue, rarely with evidence for a lodged egg (Labandeira and Currano 2013), and a prominent, surrounding border of callus or other scar tissue. There are four DTs of oviposition, which have left damage on 188 plant specimens. The most frequently occurring is DT76, consisting of 125 DT occurrences on specimens and representing 66.5% of the all oviposition occurrences. The DT76 specialized association accounts for 99 DT examples (52.7%) of damage occurrences that frequently occur on *H. elongatum* (Fig. 14.5g). DT76 lesions are very similar to the modern odonatan *Calopteryx* ovipositing in the stems of emergent semiaquatic plants (Corbet 1999). Analogous

examples of modern DT76 damage include *Ceresa* tree hoppers, terrestrial hemipterans that insert eggs into twigs that result in lenticular oviposition lesions surrounded by scar tissue (Funkhouser 1917), and also by the aquatic water scorpion, *Ranatra*, a hemipteran that oviposits on submerged hydrophyte stems (Wesenberg-Lund 1943).

The specialized interaction, DT72, consists of 14 examples (7.4%) of lenticular lesions whose long axis is oriented parallel to the vasculature of *Zonulamites viridensis* horsetail stems (Fig. 14.6c). The third association is DT108 which occurs again on the horsetail *Zonulamites viridensis*, and is responsible for 39 examples (20.7%) of the damage and closely resembles modern *Stictocephala* tree hopper damage to the tissues of small twigs (Funkhouser 1917; Yothers 1934). A considerable amount of the oviposition damage, particularly DT72 and DT108, overwhelmingly targeted horsetails, particularly *Zonulamites viridensis* (Anderson and Anderson 2017). Although the likely culprit for most ovipositional damage are early lineages of odonatopteran dragonflies, other groups, principally orthopteroids and sawflies, may have been responsible for damage as well. These non-odonatan examples could have inflicted DT100 (e.g. Wesenberg-Lund 1913) and DT101 (e.g. Jurzitza 1974).

Mining: There are 154 mining occurrences at Aas411 that are allocated to three DTs: They are: DT41 (not illustrated), the very rare threadlike and delicate leaf mine with two occurrences (1.3%); the vastly more abundant and robust DT71 (Fig. 14.6a,b), represented by150 occurrences (97.4%); and the very rare DT139 with two occurrences (1.3%). DT41 is a common leaf mine type that is quite abundant in Late Cretaceous and Paleogene biotas where it is generally affiliated with a lepidopteran culprit (Doorenweerd et al. 2015). However, the presence of DT41 in the Late Triassic could be attributed to another major lineage of insects, such as a nematoceran fly (Swezey 1915). By contrast, DT71 is one of the most conspicuous, persistent and abundant of the host-specialized associations throughout the Molteno Biome, of which 1247 DT occurrences are recorded on its host plant, *H. elongatum*. The DT71 interaction is present at 23 Molteno localities, half of which are Heidiphyllum Thicket habitats.

At Aasvoëlberg 311 (Aas311), a sister-site of Aas411, there are 740 occurrences of DT71 on host *H. elongatum*, representing 59.3% of all DT71 Molteno leaf mining occurrences (Fig. 14.7b), and providing some of the best evidence for a pest outbreak in the fossil record (Labandeira 2012). DT71 mines are distinctive, full-depth mines that have a loosely sinusoidal frass trail in early instars that becomes more tightly sinusoidal later instars, but always are characterized by particulate fecal pellets whose size changes with instar molt shifts (Fig. 14.6a,b). The leaf mines occupy the intercostal areas between the major veins of the monocot-like, parallel-veined *Heidiphyllum* leaf; apparently, the smaller veinules embedded in mesophyll were consumed by the mine occupant. Miner emergence frequently occurred at the leaf edge, where an enlargement of the mine may represent a pupation chamber. The DT71 mine closely resembles the mine of extant *Charixena iridoxa*, a plutellid moth from New Zealand that mines the structurally very similar, parallel-veined foliage of the liliaceous monocot *Astelia montana*.

DT139 is a short, serpentine, full depth mine with a large, expansive and rounded terminal chamber that typically has an irregular course between major veins of host *Sphenobaiera schenckii* (Fig. 14.7a). This mine also occurs on other unrelated hosts such as *Paraginkgo antarctica* at Lit111, *H. elongatum* at Win111, *Pseudoctenis fissa* at Kap111 (Kappokraal 111), and *Kannaskoppifolia lacerata* at Kan112 (Kannaskop 112), indicating that occurrences on *S. schenckii* at Aas411 are not host specific. The DT139 mine is similar to a metallic wood-boring beetle mine of modern *Pachyschelus coeruleipennis* (Buprestidae) on the euphorbiaceous angiosperm, *Croton floribundus* (Queiroz 2002; Ding et al. 2014), as well as the leafminer moth mine of modern *Parectopa zorionella* (Gracillariidae) on the rubiaceous angiosperm *Coprosma grandifolia* (Watt 1920). Most likely, however, the DT71 and DT139 leaf-mining associations are likely attributable to an early-derived polyphagan beetle, possibly a buprestoid (metallic wood-boring beetles and relatives) or an elateroid (click beetles and relatives) that resemble other leaf mines in broadleaved conifers from the more recent fossil record (Ding et al. 2014; Donovan et al. 2016).

Galling: Unlike mining, which presents the three types of damage of DT41, DT71 and DT139, the 182 galls at Aas411 are distributed across eight DTs and represent a wide variety of galling strategies. Insect galls are present on the intercostal areas between leaf veins (DT32), on primary leaf veins (DT33), on leaf petioles (DT55), and on small, woody twigs (DT87). Modern DT32 is a common type of gall, made by a variety of modern insect gallers, including the mite "*Eriophyes*" *nalepai* on the polypodialean fern *Nephrolepis biserrata* (Gieshagen 1919). DT33 also is a common gall, made by a cecidomyiid midge on the foliar midrib of the gnetalean, *Gnetum neglectum* (Docters van Leeuwen-Reijnvaan and Docters van Leeuwen 1926). The petiole gall DT55 ranges in shape from a modest petiolar expansion to a considerably more bulbous, broadly ellipsoidal to spheroidal structure (Labandeira et al. 2007), for which the gall of the gall midge *Lasioptera ephedrae* on the gnetalean *Ephedra trifurca* is a structural analog (Felt 1917). Another modern twig gall, very similar to DT55, is produced by a gelechiid moth on the polypodialean fern *Microgramma squamulosa* (Kraus et al. 1993), which is prominently and centrally positioned on the twig axis and has a symmetrical bulbous expansion. As for DT87, a modern example is a gall by a gall midge, also on the epiphytic polypodialean fern *M. squamulosa*, but one that rather results in a projecting bulbous prominence broadly attached along one surface of a twig (Maia and Santos 2011). Each of these gall types are characterized by different micromorphologies of hardened wall tissues, an inner nutritive tissue layer surrounding the larval chamber, and co-optation of host-plant vascular tissue to supply nutrients to gall tissues.

Different, more specialized strategies are represented by galls such as DT123, DT161 and DT122. DT123 is a distinctive gall caused by small insects such as mites, aphids and thrips that display collapse of individual plant cells and unusual foliar thickenings, causing abnormal cupping and enrollment of foliage. Such foliar distortions are analogous to the gall of the phlaeothripid thrips *Jersonithrips galligenus* on the polypodialean fern *Elaphoglossum morani* (Retana-Salazar and Nishida 2007), or to various eriophyid mites in which pinnular cupping is estab-

lished by early stages of mite feeding (Boughton and Pemberton 2011), resulting from styletal modification of epidermal cells into nutritive tissue for nymphal gall-mite feeding (Freeman et al. 2005). DT161, by contrast, is a roughened, circular blister gall with pustulose centers and lineations that radiate to the outer periphery of the gall wall, similar to an eriophyid blister gall on the foliage of a *Carya* (hickory) species (Johnson and Lyon 1991). The two host-specialized galls are DT70 and DT122. The specialized mite gall, DT70 (Figs. 14.8d–f, h, 14.9, 14.10, 14.11, 14.12a,b,d), occurs almost exclusively on *D. crassinervis* and is represented by 167 occurrences in 12 localities throughout the Molteno Biome that represent a broad variety of habitats. At Aas411, DT70, discussed in detail below, consists of 120 occurrences.

The host-specialized gall other than DT70 is DT122. DT122 is a medium sized, bulbous, ellipsoidal gall that is oriented parallel to the venation of the ginkgophyte, *Sphenobaiera schenckii* (Figs. 14.6d,e, 14.7c, 14.8a–c,g). This gall represents a recurring association found in several other localities in the Molteno Biome and occasionally on other hosts, such as *D. crassinervis* (Fig. 14.6f) and *H. elongatum* (Fig. 14.12c), where there evidently is not a host-specialist association. The culprit for this gall remains unknown, but it shares a superficial resemblance to certain galls of the same size, shape and outer surface texture as the pteromalid wasp *Aditrochus* sp. on coigüe, *Nothofagus nitida* (Nothofagaceae), in the southern Andes of South America (Quintero et al. 2014).

Seed Predation: For a function feeding group with few DTs, seed predation has a considerable number of specialized associations. From 121 seed-predation DTs at Aas411, 100, or 82.6%, are associated with the three specialized DTs of DT73, DT74 and DT124. The first damage type, DT73, consists of 63 occurrences (52.1%) of all seed predation at Aas411, and is a lenticular to narrowly ellipsoidal perforation into the central body of *Avatia bifurcata* dispersed seeds. Each DT73 occurrence on a predated seed can have from one to several perforations through the seed central body (Anderson and Anderson 2003; Labandeira 2006a, 2016). *Avatia bifurcata* is affiliated with *Ginkgoites matatiensis* foliage and *Eosteria eosteranthus* pollen organs, the three of which constitute a ginkgoopsid whole-plant taxon. The likely culprit was a heteropteran hemipteroid with a laterally compressed stylet bundle and sheath found in some extant seed-feeding heteropterans (Weber 1930; Cobben 1978) such as Lygaeidae (seed bugs) or Miridae (capsid bugs) that match the cross-sectional aspect ratios of damage to modern flowering plants (Hori 1971; Burdfield-Steel and Shuker 2014).

The second damage type, DT74, is represented by 35 occurrences (28.9%) of the seed predation damage at Aas411. DT74 consists of circular to occasionally slightly and laterally compressed subcircular perforations into the central body of *Fanerotheca papilioformis* dispersed seeds, equivalent to *Feruglioa samaroides* seeds when attached to an ovulate organ. The corystosperm whole-plant taxon consists of *Dicroidium crassinervis* foliage, *Fanerotheca papilioformis* (*Feruglioa samaroides*) seeds and possibly *Pteruchus* sp. pollen organs. The likely culprit of DT74 damage was a hemipteroid different than the fabricator of DT73, also a heteropteran, but with a smaller, circular cross-sectional styletal apparatus common in

some modern taxa (Handley and Pollard 1993) and with a distinctive mode of inflicting damage (Golden et al. 2006).

The third damage type, very rare DT124, is a minor element of seed predation at Aas411. DT124 consists of the major removal of nutritive and embryonic tissues from a *Dordrechtites* cone scale. The affiliation of *Dordrechtites* cone scales, however, remains enigmatic. The seed likely originates from the cone of a coniferalean plant that is known but lacks attribution to foliage; such a source plant has not been identified in the Molteno Biome (Anderson and Anderson 2003). Nevertheless, the culprit of DT124 is very different than those of DT73 and DT74, and shows damage evidence indicating a mandibulate larval insect similar to modern larval sawfly (Bird 1926) or bruchid or other beetle damage on gymnosperm (Bedard 1968) or angiosperm (Shepard 1947) seeds.

Borings: Borings are an extremely rare plant–insect interaction in the Molteno Biome and are represented at Aas411 by one occurrence of DT160. By comparison there are only three other occurrences of borings at Molteno—two instances of DT160 at Bir111 and a single example of DT174 at Lit111. The Aas411 boring consists of a tunnel circular to ellipsoidal in cross section, approximately 5.0 mm in maximum diameter, and oriented parallel to the xylary grain in petioles or twigs.

Other Interactions: There are four instances of damage at Aas411 that are not assigned to any functional feeding group. DT106 probably represents thermal stress or nutrient deficiencies to the leaf margin of *H. elongatum* (Labandeira and Prevec 2014). Also occurring on *H. elongatum* is fungal damage, all of which is allocated to DT58, likely representing primary fungal colonization of the leaf surface. Fungal damage at Aas411 resembles much of the damage found on plants such as the ascomycete *Cephalosporium* that forms necrotic blotches on the polypodialean fern *Pteris* (Schneider 1966).

14.8.4 Herbivory Patterns

From the distribution of the above interaction data on the plant hosts at Aas411 (Fig. 14.4), there are six major patterns that are present. These patterns involve comparisons of plant host, DT, host specialization, component community and other categories within the Aas411 site, and also observations comparing the Aas411 site to other such Molteno localities.

Number of DT Occurrences: There are 1127 DT occurrences on specific plant specimens, based on presence–absence data at Aas411. This value is the sum of all recorded occurrences for each DT that is present on a single, inventoried plant specimen. As these occurrences represent presence–absence data, for a DT occurrence to be recorded on a plant specimen, it must occur at least once, although (unrecorded) multiple occurrences may be present. The FFG abundance data, in decreasing rank, for the number of DTs per FFG is: margin feeding, 286 occurrences; oviposition, 188; galling, 182; leaf mining, 154; seed predation, 121; surface feeding, 76; hole feeding, 66; unidentified DTs, 4; fungi, 3; and skeletonization, 1. The

abundance of margin feeding and virtual absence of skeletonization is expected, as margin feeding typically has the most elevated occurrences of any FFG and skeletonization is very rarely represented in the Paleozoic and Mesozoic. However, it is notable that there is a greater abundance of the endophytic FFGs of piercing and sucking, oviposition, leaf mining, galling, and seed predation, representing 681 DT presence–absence occurrences, over the exophytic FFGs of hole feeding, margin feeding, skeletonization and surface feeding that represent 429 DT presence–absence occurrences. This latter comparison, where endophytic DTs exceed exophytic DTs by a factor of almost 1.6, represents a condition rarely seen in other Molteno localities.

Number of DT Categories: The pattern of DT diversity per FFG is different than that of individual DT occurrences on plant specimens per FFG measured above. For exophytic FFGs, hole feeding is represented by seven DTs, margin feeding by five DTs, skeletonization by one DT and surface feeding by seven DTs for a total of 20 DTs. For endophytic FFGs, piercing and sucking is represented by four DTs, oviposition by four DTs, mining by three DTs, galling by eight DTs, seed predation by three DTs and borings by one DT for a total of 23 DTs. The exophytic to endophytic DT ratio is 1.15 or approaching equivalence and is significantly different than that of the individual DT occurrences. This indicates that modes of feeding on tissues is approximately equivalent under exophytic or endophytic feeding regimes, but the intensity, as measured by individual feeding events that target plant specimens, is substantially greater under endophytic feeding. This also is indicated by the galling FFG having the greatest number of eight DTs at Aas411.

Plant Hosts: Of the 111 plant form-taxa, 35 are combined into 14 separate whole-plant taxa. Of these 14 whole-plant taxa, seven are the principal plant species that are the most herbivorized at Aas411 (Table 14.2). Often multiple organs are herbivorized within a whole-plant taxon, such as foliage, stems and seeds. The ranking of herbivory intensity is provided from evidence of four attributes for each whole-plant taxon. The attributes are: (i), the numbers of functional feeding groups; (ii), the number of DT categories; (iii), the number of individual DT occurrences; and (iv), the number of specialized associations for each whole-plant taxon. The most herbivorized plant host by far (Fig. 14.4; Table 14.3), is the *Heidiphyllum elongatum–Telemachus acutisquamus–Odyssanthus crenulata* whole-plant taxon (Anderson and Anderson 2003; Bomfleur et al. 2013), representing the affiliated foliage, ovulate organ and pollen organ of a prominent voltzialean conifer. (This convention of sequential characterization of whole-plant taxa by their foliage, female organ and male organ taxa will be used for all seed-plant taxa.) The second ranked, most herbivorized taxon is the *Dicroidium crassinervis–Fanerotheca papilioformis–*?*Pteruchus matatimajor* whole plant taxon (Retallack and Dilcher 1988; Anderson and Anderson 2003), an umkomasialean corystosperm. The third most herbivorized whole-plant taxon is the *Sphenobaiera schenckii–Sphenobaiera* short shoot–*Hamshawvia longipeduncula–Stachyopitys gypsianthus* whole-plant taxon, a ginkgophyte (Anderson and Anderson 2003; Barboni and Dutra 2015). These three plant-host taxa at Aas411 also are the three most prominent taxa that parallel in the same rank order the Molteno Biome as a whole (Anderson and Anderson 2003).

Other than the three major herbivorized plant hosts, those whole-plant taxa with significant but less herbivory are three seed plants and a horsetail. The fourth most herbivorized taxon is another ginkgophyte, the *Ginkgoites matatiensis–Avatia bifurcata–Eosteria eosteranthus* whole-plant-taxon (Anderson and Anderson 2003). The fifth most herbivorized taxon, the peltasperm *Lepidopteris africana–Peltaspermum turbinatum–Antevsia mazenodensis* whole-plant-taxon and the sixth most herbivorized taxon, the congeneric peltasperm *Lepidopteris stormbergensis–Peltaspermum monodiscum–Antevsia* sp. whole-plant-taxon, which likely occupied similar habitats (Anderson and Anderson 2003). The seventh most herbivorized taxon is the only plant host with elevated damage that is not a seed plant, and unlike the other six whole-plant taxa, the *Zonulamites viridensis*–nodal diaphragm A–*Viridistachys gypsensis–Paraschizoneura fredensis* whole-plant taxon is a horsetail that has insect damage only as oviposition. These four, less dominant, whole-plant taxa do not follow the same rank order of prominence throughout the entire Molteno Biome, as do the *Heidiphyllum*, *Dicroidium* and *Sphenobaiera* host sequence. Rather, fourth ranked Aas411 *Ginkgoites* occurs as seventh position in the Molteno Biome as a whole, fifth and sixth ranked Aas411 *Lepidopteris* occurs collectively as the eighth Molteno position, and seventh-ranked Aas411 *Zonulamites* is unranked within Molteno Biome (Anderson and Anderson 2003).

Persistent Specialized Associations: One of the features determining the most herbivorized whole-plant taxa at the Aas411 site is the number of specialized associations. Host-specialized interactions are defined by the presence of the same recurring, stereotypical damage type that is present on the same host-plant species or closely-related group of species throughout multiple localities across the Molteno Biome. In addition, host specificity can be assessed by the extent to which the herbivore modifies the tissues of its plant host, which in the case of gallers implies an intimate association that results from the gall extending the limits of its phenotype to include galled host tissues (Stone and Schönrogge 2003). The *Heidiphyllum elongatum* whole-plant-taxon houses the greatest number and most diverse repertoire of host-specialized associations of any Aas411 host plant, or for that matter, of any plant host from a Molteno site (Tables 14.2, 14.3; Figs. 14.2, 14.3, 14.13). These recurring host-specialized associations include DT8 of hole feeding (not figured), DT128 of piercing and sucking (Fig. 14.5f), DT76 of oviposition (Fig. 14.5g), and DT71 of mining (Fig. 14.6a,b). These four, pervasive associations of the *H. elongatum* whole-plant taxon are present at other Molteno localities; in the case of distinctive DT76 oviposition, 30 other Molteno localities have this interaction. For the distinctive, highly host specific leaf mine of DT71, 98.4% occur on the *H. elongatum* whole-plant taxon across Molteno localities. This association has 147 occurrences at Aas411, but is matched by 1124 other occurrences in 22 other localities within the Molteno Biome (Table 14.3).

Four, other, highly stereotyped associations on hosts other than *H. elongatum* are noteworthy (Tables 14.2, 14.3; Figs. 14.2, 14.3, 14.13). One notable, persistent association of specialized damage is the highly stereotyped mite gall DT70, found almost exclusively on the foliage of *D. crassinervis* (Tables 14.2, 14.3; Figs. 14.8d–f, h, 14.9, 14.10, 14.11, 14.12a,b,d). At Aas411 there are 117 occurrences

of DT70 on *D. crassinervis*, but 50 other occurrences are found on the same host at 11 other Molteno localities. A second example are distinctive DT73 seed-predation lesions on *Avatia bifurcata*, the affiliated platysperm seed of *Ginkgoites matatiensis* foliage (Labandeira 2016). Seed damage of DT73 is found on 63 specimens at Aas411, but this DT has 1067 occurrences at six other Molteno localities, of which 1045 *A. bifurcata* seeds show this damage at the Bir111 site. A third example is the characteristic DT72 oviposition lesions in the stems of the horsetail *Zonulamites viridensis* whole-plant taxon (Fig. 14.6c), of which 14 occurrences are present at Aas411, and 30 other occurrences are found in nine other localities across the Molteno Biome on *Z. viridensis* at Gre111B (Greenville 111B), Bir111 and two, other, closely related species of *D. annumensis* from Lit111, Nuwejaarspruit 111A (Nuw111A) and Peninsula 511 (Pen511); and *D. elandensis* at Elandspruit 111 (Ela111), Lutherskop 4111 (Lut4111), Boesmanshkoek 111B, (Boe111B) and Cala Road 111A (Cal111A). Last is the excavation of megagametophytic tissues of DT124 seed predation on *Dordrechtites elongatus*, an unaffiliated pinopsid cone (Anderson and Anderson 2003). This distinctive ovulate reproductive structure has both of its two occurrences at Aas411 that exhibit damage, but also has 11 occurrences with damage in the closely related *D. mazocirrus* at the Maz211 site.

Component Community Structure: The *Heidiphyllum elongatum* whole-plant taxon has the most diverse and balanced component community at Aas411 of any plant host (Tables 14.2, 14.3; Figs. 14.3, 14.13). However, pending additional analyses, the *H. elongatum* whole-plant taxon likely is the most diverse and thoroughly herbivorized plant throughout the Molteno Biome, as it occurs in 78 of the 106 Molteno localities. This whole-plant taxon is represented by nine of the ten FFGs at Aas411, including the unknown FFG of DT106, and displays 28 DTs (Tables 14.2 and 14.3; Fig. 14.13). The only missing FFGs for *H. elongatum* are wood boring and seed predation. As for seed predation, no affiliate seed or female ovulate organ has been assigned to *H. elongatum* at Aas411, assuming that the present *Dordrechtites elongatus* is not the affiliate ovulate organ and neither is the possible affiliate ovulate organ *Telemachus*, which interestingly is absent at Aas411. (See the discussion on page 62 of Anderson and Anderson [2003] for a full discussion of this enigma.) If *Dordrechtites elongatus* is the ovulate organ of *H. elongatum*, as may be suspected, then the highly stereotyped seed-predation association of DT124 would almost complete the tally of ten functional feeding groups contained in the *H. elongatum* whole-plant taxon, five of which would include the host-specialized associations of DT8 hole feeding, DT128 piercing and sucking, DT76 oviposition, DT71 leaf mining and DT124 seed predation. Much of the component community structure of the *Heidiphyllum elongatum* whole-plant taxon is illustrated in Fig. 14.13.

There is considerable structure in the component communities of the remaining whole-plant taxa as well. The *Dicroidium crassinervis* whole-plant taxon is the second most diverse component community at Aas411, housing seven FFGs and 20 DTs that includes hole feeding, margin feeding, piercing and sucking, oviposition, galling and seed predation. The *Sphenobaiera schenckii* whole-plant taxon houses the third most complete component community, containing all the FFGs occurring in *Dicroidium crassinervis*, except for the presence of leaf mining, the absence of

seed predation, and about half of the number of DTs. The *Ginkgoites matatiensis*, *Lepidopteris africana* and *L. stormbergensis* whole-plant taxa have two less, or five FFGs, and 8–11 DTs each. By contrast, the horsetail *Zonulamites viridensis* component community has a very limited component herbivore community, consisting only of one FFG and three DTs of oviposition. This paucity of diverse damage in horsetails is attributable to herbivory that largely is limited to stem tissues embedded with silica deposits and also to the presence of foliage resistant to arthropod consumption (Law and Exley 2011).

Role of Habitat: The dominant habitat for the specialized associations of five of the most herbivorized associations at Aas411 also match the stated site habitat of their plant hosts at other localities across the Molteno Biome. Perhaps not surprisingly, the habitat of the four host-specialized associations representing the distinct FFGs of DT8 hole feeding, DT128 piercing and sucking, DT76 oviposition and DT71 mining of the *H. elongatum* whole-plant-taxon is Heidiphyllum Thicket. Similarly, for the two host-specialized associations of DT70 and DT74, representing two FFGs of the *D. crassinervis* whole-plant taxon, is Dicroidium Open Woodland. The single host-specialized associations of DT122 galling for the *S. schenckii* and DT73 seed predation for the *G. matatiensis* whole-plant-taxa is Sphenobaiera Closed Woodland. Last, the two host-specialized associations of DT72 and DT108 oviposition for *Z. viridensis* is Horsetail Marsh. It appears that because of the host-plant ecological preferences for certain habitats, that their more intimate interactions with insect herbivores also are closely tied to a specific habitat within the Molteno Biome.

14.9 Early Gall History and Gall DT70 on *Dicroidium crassinervis*

14.9.1 Early Arthropod Gall History

Terrestrial fossil galls have their earliest occurrence in a liverwort host from the Middle Devonian of New York state, attributed to an unknown small arthropod (Labandeira et al. 2014). The gall record increases substantially during the Pennsylvanian Period, particularly in Euramerica, in which galls overwhelmingly are hosted on plant axial tissues of the rachises of *Psaronius* tree ferns (Labandeira and Phillips 1996) and the terminal strobili of calamitalean horsetails (van Amerom 1973; Kelber 1988). During the early Permian (Cisuralian), a variety of gall morphologies, representing approximately ten DTs, colonized the foliage of seed plants, particularly in southwestern (Schachat et al. 2014; Schachat and Labandeira 2015) and central-south (Labandeira et al. 2016) Euramerica. This shift toward and expansion of galling on foliage rather than axes such as stems continued in Gondwana until the Lopingian, where almost all occurrences are on glossopterid hosts (Adami-Rodrigues et al. 2004; Prevec et al. 2009; McLoughlin 2011). These plant–gall

interactions largely were eliminated globally at the P-Tr ecological crisis (Labandeira 2006a), as there is minimal evidence from depauperate Early Triassic deposits to suggest the survival of recognizable Permian gall interactions on particular hosts later into the Triassic. An exception includes a midveinal gall on the probable seed fern *Tongchuanophyllum* of the Olenekian Solling Formation in southern Germany (Kustatscher and van Konijnenburg-Van Cittert 2013; Kustatscher et al. 2014). Additionally, a distinctive, circular to broadly ovoidal gall with thick enveloping walls on *Dicroidium odontopteroides*, probably of Olenekian age, have been described from the Newport Formation of the Sydney Basin in Australia (McLoughlin 2011).

Well documented insect damage on Anisian, Ladinian and Carnian Triassic floras throughout Pangaea indicate the re-evolution of the galling habit by several insect lineages on multiple plant hosts. In stark contrast to the Permian, Middle Triassic galling interactions occur on very different plant hosts in Euramerica and Gondwana (Anderson and Anderson 1985, 1989, 2003, 2008, 2017; Visscher et al. 1996; Anderson et al. 2007; Krassilov and Karasev 2009). Similarly, the evolution of new insect groups with potentially newly evolved galler lineages during the Middle Triassic to early Late Triassic is indicated by their body-fossil record (Tillyard 1923; Riek 1974; Gallego 1997; Béthoux et al. 2005; Labandeira 2005). The insect body-fossil record was supplemented by newly appearing lineages of mites (Sidorchuk et al. 2015), sternorrhynchans (Evans 1971; Shcherbakov 2000), thrips (Fraser et al. 1996), beetles (Ponomarenko 2016; also see McKenna et al. 2015), sawflies (Rasnitsyn 1969; Schlüter 2000), and flies (Krzeminski 1992; Shcherbakov et al. 1995). Consequently, the insect body-fossil record indicates that many major insect lineages were present during the Anisian, Ladinian and early Carnian that would have supplied taxa engaged in the galling habit on a broad repertoire of available, newly emerging plant hosts (Larew 1992). The fossil mite record, particularly for those taxa engaged in gall associations with fern and especially conifer hosts, is ancient, based examinations of the fossil record (Sidorchuk et al. 2015), phylogenetic studies (Boczek and Shevchenko 1996; Fenton et al. 2000) and biogeographical inference (Gerson 1996; Oldfield 1996; Lewandowski and Kozak 2008).

During this time interval, evidence for Anisian galling associations comes from the Dont Formation of the Dolomites Region in northeastern Italy, especially DT32 and DT80 galls on cycadophytes, such as *Bjuvia dolomitica*. In the penecontemporaneous Valle San Lucano Flora of the Agordo Formation, also in the Dolomites Region, DT11 galls (erroneously reported as surface feeding) occur on the cycadophyte *Taeniopteris* sp. and DT32 galls have been found on a second cycadophyte, *Nilssonia neuberi* (Labandeira et al. 2016). From the upper Grès à Voltzia, or upper Buntsandstein, beds of the Röt Formation in Alsatian France, there is a distinctive gall on the voltzialean conifer *Aethophyllum stipulare* (Larew 1992; Grauvogel-Stamm and Kelber 1996), presumably of herbaceous habit. This gall is notable for its considerable expansion of anomalous tissue in the peduncular base of the male conifer cone. A second gall affects another conifer at the same site, an undetermined species of *Voltzia*, which resembles a witch's broom deformity, characterized by the bending of shoot axes and extensive proliferation of derivative foliage, similar to a

DT121 aldelgid gall (Grauvogel-Stamm and Kelber 1996; also see Labandeira and Allen 2007, for a Permian example). Notably, no galls have been observed on any plant host among the 1386 plant specimens from the Anisian Burgersdorp Formation of South Africa (Labandeira et al., unpubl. observ.).

Plant material displaying Ladinian galls overwhelmingly originated from the same regions in Western Europe as Anisian galls. Some Ladinian gall associations may have been described as oviposition scars by Grauvogel-Stamm and Kelber (1996). However, the best evidence for Ladinian galls comes from several sites of the Dolomites Region of northeastern Italy (Wappler et al. 2015; Labandeira et al. 2016). One such site contains the Monte Agnello Flora, from the Vulcanites Formation, revealed a DT121 bud gall on the conifer *Voltzia* sp. 1 (Wappler et al. 2015), very similar to the gall on an undetermined species of *Voltzia* from the penecontemporaneous Grès à Voltzia material in Alsatian France mentioned above (Grauvogel-Stamm and Kelber 1996). The diverse gall component of plant–insect interactions from the Monte Agnello Flora also includes the small, nondescript, hemispheroidal, DT80 galls on the fern *Phlebopteris fiemmensis*, cycadophyte *Bjuvia* cf. *dolomitica*, and seed fern *Scytophyllum bergeri* (Wappler et al. 2015; Labandeira et al. 2016). A different species of *Phlebopteris* at Monte Agnello exhibits a DT106 gall likely caused by a mite (Labandeira et al. 2007, 2016). Two other Ladinian floras from the Dolomites Region, the St. Veit–Innerkohlbach and Forcela da Cians floras, contain the seed fern *Ptilozamites sandbergeri* that display generalized, indistinct galls of DT32 and DT80 (Labandeira et al. 2016). Anisian and Ladinian data indicate that gall morphologies, with the exception of the conifer-borne galls, were generalized, hemispherical, well protected and probably single chambered.

During the Carnian, particularly in the early part of the stage, galling insects increased their geographic range and entered into new associations with plant hosts that produced novel gall morphologies. These new gall types were present at different regions, occupied different habitats, and colonized new plant hosts when compared to those of the Middle Triassic. One such gall is a pustulose, compound gall on the net-veined fern *Dictyophyllum bremerense* from the Blackstone Formation of the Sydney Basin in Australia (Webb 1982). A second occurrence comes from the De Geerdalen Formation of Svalbard, Norway, which is a permineralized peat deposit bearing anatomically preserved bennettitalean roots that contain cortex-embedded, single chambered, spheroidal galls with walls having an inner ragged surface and a smooth outer surface (Strullu-Derrien et al. 2012). The broad affinities of the arthropod galler forming this distinctive gall remains unknown. From deposits of about the same age, there are 15 distinctive gall DTs described from the Molteno Formation, about half of which are present at the Aas411 site. These and other Molteno galls indicate a variety of galling strategies, in particular the blister gall DT11; the generalized gall DT34 occurring on secondary veins; small, undistinguished hemispherical galls of DT80; elliptical midveinal expansions of DT85; pustulose, surficial galls of DT107; and the large, bulbous and ellipsoidal galls of DT127. Later during the Triassic, a distinctive, irregularly bulbous gall deformed the pinnules of the probable gnetalean host, *Delchellyia gormani*, from the early

Norian Chinle Formation of the Petrified Forest National Park, in northeastern Arizona (Ash 1972, 1997). The culprit of this gall most likely is a tenthredinoid sawfly, based on details of modern sawfly galls (Bird 1926; Meyer 1987; Zinovjev 2006). These Carnian occurrences of new, distinctive, gall morphotypes collectively suggest a major diversification of the galler FFG that expanded the plant hosts and life habits of mites and insects.

14.9.2 Systematics and Biology of Gall DT70

Ichnogenus ***Pustuleon*** Krassilov, 2008

Etymology: From the Latin, *pustula -ae*, meaning a blister or pimple (feminine).

Type species: *Pustuleon gregarium* Krassilov 2008 (in Krassilov et al. 2008).

Diagnosis: "Dense aggregates of minute distinct ostiolate pustules on or near the stronger veins" (Krassilov et al. 2008, p. 81).

Remarks: Krassilov (2008, p. 81) also states: "Aggregates of minute pustules are induced and then used for egg emplacement by eriophyid mites." (Krassilov et al. 2008, p. 84). Additional comments are: "In extant eriophyid mites, a sting by fundatrix may induce a similar cluster of numerous pustules. Vein twisting by the gall is also typical of cecidogenous eriophyid effects. Occasional black fusiform bodies among the pustules … may represent an adult mite (compare fig. 2c in Westphal 1977). However, it must be admitted that interpretation of the interior structures remains ambiguous because of insufficient preservation of the scanned material."

Ichnospecies ***Pustuleon parvicubiculites*** C.C. Labandeira, J.M. Anderson and H.M. Anderson

Etymology: From the Latin, *parvus -a -um*, meaning little or small (neuter); and from *cubiculum –i*, diminutive form meaning a (small) bedchamber or bedroom, often taken to mean any small chamber The gender is masculine.

Holotype: PRE/F/12392-1; this report: Fig. 14.8a,b; Labandeira 2006a, figs. 36, 38.

Description: A variously shaped foliar epidermal gall distributed in small patches, enlarging to a more robust structure that is well developed along pinnular veins and consisting of a pustulose to ragged surface texture; gall edge irregularly confluent with pinnule margin and often with expanded pinnular base; surface pockmarked with miniscule spheroidal chambers typically 0.1–0.3 mm diameter, occasionally breached, exposing inner cavities and significant, embedded hypertrophic and hyperplasic epidermal tissue appearing as a roughened and abraded surface. Gall ontogeny starts as small patches of small pustules often on tips of pinnules that represent immature galls, later growing to larger areas extending to major portions of pinnules, eventually engulfing an entire pinnule, at which time pustules are visibly larger and occasionally marked by extension of galled tissue along the adjacent rachis and colonization of nearby pinnules.

Measurements: Holotype gall 6.7 mm long measured medially from near the base of the pinnule to pinnule tip, and 5.5 mm across the widest portion of the gall near the pinnule tip; pustules ca 0.1–0.2 mm in longest dimension (Fig. 14.8a,b).

Occurrence: Bamboesberg Member (Cycle 1) of the Molteno Formation, assigned to a Late Triassic age (Anderson and Anderson 2003). Although a search for volcanic strata with zircons is ongoing, short of any absolute dates, the precise age of the Molteno Formation and its duration, remains uncertain. Based on global biostratigraphic correlations (Anderson et al. 2007), a generic age of Late Carnian has been established for the Molteno Formation.

There are 167 occurrences of the DT70 gall on *Dicroidium crassinervis* in 12 Molteno localities. The overwhelmingly majority of specimens with DT70 galls exhibit multiple galls per frond or frond fragment. Frequently, galled fronds exhibit multiple galled pinnules that occasionally are connected along an intervening galled rachis. DT70 galls are found in the following Molteno localities, from oldest to youngest: Aas411, with 117 occurrences discussed in this report; Umk111, with four occurrences; Mazenod 211 (Maz211), with one occurrence; Elandspruit 112B (Ela112B), with one occurrence; Kap111, with two occurrences; Klein Hoek 111C (Kle111C), with six occurrences; Klein Hoek 111B (Kle111B), with five occurrences; Peninsula 421 (Pen421), with three occurrences; Cyphergat 111A (Cyp111A), with three occurrences; and Cala Road 111B (Cal111B), with 23 occurrences (see Table 14.1 for site data). DT70 galls have not been documented at fossil localities other than those of the Molteno Formation, although other, structurally different mite galls co-occurring in the Molteno Formation resemble modern eriophyioid galls. There is no preference of the DT70 gall by habitat, as this gall occurs in five of the seven habitats in the Molteno Biome—Sphenobaiera Closed Woodland, Mature Dicroidium Riparian Forest, Immature Dicroidium Riparian Forest, Heidiphyllum Thicket, and Dicroidium Open Woodland—as well as present in one site whose habitat was indeterminate. These habitats are characterized by the presence of *Dicroidium*, especially *D. crassinervis* and *D. odontopteroides*, as the dominant or subdominant taxon.

Assigned Functional Feeding Group and Damage Type: Galling; DT70 (Labandeira 2006b; Labandeira et al. 2007).

Host Plant: *Dicroidium crassinervis* (Geinitz 1876) Anderson and Anderson 1982, comb. nov. (Umkomasiales: Umkomasiaceae), a corystosperm seed fern. The distribution of DT70 is greatest at Aas411, with 117 occurrences, 70.1% of the total for the entire Molteno Biota. DT70 is present at nine other localities representing 48 additional occurrences. The presence of DT70 at sites other than Aas411 range from one to six occurrences per site, with the exception of Cal111B, where it is represented by 23 occurrences, or about half of the total for the non Aas411 associations in the Molteno Biota.

Host-Plant Specificity: Throughout the Molteno Flora DT70 is found almost always on the single host-plant, *Dicroidium crassinervis*, and is given a value of 3, indicating monospecificity, following the host-specialization categories in Labandeira et al. (2007). The monospecific relationship of the DT70 gall on *D. crassinervis* involves an attack rate of 3.82% (3064/117) for the DT70 gall on *D.*

crassinervis at the Aas411 site. Typically, eriophyoid mites are "highly host specific" according to Oldfield (2005, p. 35).

Inferred Culprit: The damage is most consistent with an eriophyoid mite (Acari: Eriophyoidea). Eriophyoid mites have been documented from penecontemporaneous Triassic amber of northeastern Italy (Sidorchuk et al. 2015). Also see remarks below.

Figured Material*:* DT70 is figured in this report as follows: Fig. 14.8d,e: PRE/F/12351-1; Fig. 14.8f: PRE/F/21923-1; Fig. 14.9a,b: PRE/F/12392-1; Fig. 14.9c: PRE/F/21416-1; Fig. 14.9d,e: PRE/F/12389b; Fig. 14.9f: PRE/12387a-1; Fig. 14.9g: PRE/F/20880a-1; Fig. 14.10a: PRE/F/12387a-1 (different illumination than Fig. 14.9f); Fig. 14.10b: PRE/F/12394-1; Fig. 14.10c: PRE/F/12396a-1; Fig. 14.10d: PRE/F/12396b (counterpart to Fig. 14.10c); Fig. 14.10e: PRE/F/21908a-4; Fig. 14.10f: PRE/F/21908-1; Fig. 14.11a: PRE/F/20880a-1; Fig. 14.11b: PRE/F/21144a-7 (gall detail figured in Fig. 14.12b); Fig. 14.11c: PRE/F/21920b-1; Fig. 14.11d,e: PRE/F/21909-1; Fig. 14.11f: PRE/F/12389a-1; Fig. 14.12a: PRE/F/20883-2; Fig. 14.12b: PRE/F/21144a-7 (photo in Fig. 14.11b); and Fig. 14.12d: PRE/F/21050-2. Previous illustrations: Scott et al. 2004, fig. 2h, erroneously referred to as an "irregular blotch mine"; and Labandeira 2006a, figs. 36 and 38.

Other Material*:* The DT70 gall occurs in 12 localities within the Molteno Biome, represented by a total of 167 specimens, all of which are found on its host, *D. crassinervis*. The Aas411 site accounts of 117, or 70.1%, of all Molteno DT70 occurrences. With the exception of the Cal111B site which has 23 specimens of DT70, the remaining 10 localities have on average three specimens each. The most commonly occurring habitat supporting DT70 on *D. crassinervis* is Dicroidium Open Woodland. To our knowledge DT70 has not been described from any other Gondwanan site of similar age nor from any other site in the fossil record.

Repository*:* Palaeobotanical Collections ("Molteno Room"); Evolutionary Studies Institute of the University of the Witwatersrand; Johannesburg, South Africa.

Remarks*:* The DT70 gall is a histioid gall that results in cellular modification such that an existing, affected organ is histologically changed to produce a new structure of abnormal tissue, typically a gall (Meyer 1987). Histioid galls are classified into cataplasmas or prosoplasmas. Cataplasmic galls have a relatively organized appearance through growth and shape changes, but do not form specific, differentiated tissues (Dreger-Jauffret and Shorthouse 1992). By contrast, cataplasmic galls are less organized than prososplasmic galls, and form anomalous structures from existing tissues by an increase in the number (hyperplasia) and size (hypertrophy) of cells, and often forming one or more layers of parenchymatous cells (Dreger-Jauffret and Shorthouse 1992; Rohfritsch 1992). Accordingly, DT70 is a histioid, cataplasmic gall that did not form an organized, three-dimensional, symmetrical structure, but rather had a disorganized, more two-dimensional configuration of embedded nutritive cells exhibiting a pustulose surface that resulted from mouthpart puncturing of individual cells by arthropods. The arthropod culprits undoubtedly had specialized, piercing and sucking mouthparts consisting of an armature of protractible stylets (Vacante 2016). These punctured cells evidently were transformed

into enlarged, bulbous, nutritive cells by salivary secretions of eriophyoid mites that transformed normal tissues of epidermal and parenchymatous cells into abnormal, galled tissues (De Lillo and Monfreda 2004).

With the exception of galls produced by certain gall midge larvae with specialized mouthparts that puncture individual cells (Rohfritsch 1992), there only are three other piercing-and-sucking arthropod groups capable of producing similar cataplasmic, histioid galls: thrips, sternorrhynchan hemipterans, and mites (Rohfritsch 1992). Galls of thrips are open and not sealed structures, but more typically result in leaf folding or curling along the leaf margin, or otherwise have irregular leaf folding with unsightly teratologic forms, including the production of massive peapod-like structures up to 20 cm long (Meyer 1987; Ananthakrishnan and Raman 1989). Sternorrhynchan hemipterans, such as aphids, scale insects, whiteflies and psyllids, also produce cataplasmic histioid galls, but because their stylate mouthparts differ from thrips and mites, they do not pierce shallowly positioned individual cells of the epidermis that result in eventual tissue necrosis. Rather, sternorrhynchan hemipterans have an intercellular stylet trajectory and target deeper seated vascular tissue, principally phloem, for nutrition rather than consuming large nutritive cells at the surface. Sternorrhynchan hemipterans deposit distinctive, mucilaginous salivary sheaths surrounding the puncture marks. Enlarged, bulbous nutritive cells, whose protoplasts are rich in nutrients, form around the punctures on the epidermal surface, but are not teratologically transformed as are thrips-punctured epidermal cells (Westphal 1992). Eriophyoid mites, in contrast to thrips and sternorrhynchan hemipterans, are ca. 10 times smaller and thus target individual epidermal cells during feeding. The piercing-and-sucking feeding style of mites result in abundant nutritive tissue, occurring as excrescences on surface tissue that consist of individual, bloated nutritive cells or enlarged trichomes. Hyperplasia is common and cellular necroses typically ensue after feeding has terminated (Westphal 1977; Larew 1981). Of these three groups of potential culprits—thrips, sternorrhynchans, and eriophyoid mites—the DT70 gall is consistent with a mite galler. Gall midges of the Cecidomyiidae are a remote possibility, but do not extend to the Late Triassic (Nel and Prokop 2006). As well, thrips and sternorrhynchan hemipterans produce considerably larger and differently structured galls that are reflected in the very different feeding habits than those of eriophyoid mites.

In addition to classification as a histioid cataplasmic gall, DT70 also is considered a cover gall. Cover galls form by an inducer, in this case a mite with piercing mouthparts, which provokes a response from its host *D. crassinervis* by producing of hyperplasic and hypertrophic tissue. This tissue proliferation gradually surrounds and covers the gall mites. This is done by the formation of minute chambers, often with limited access to the outside such as through an ostiole (Meyer 1987). It is strongly suspected that the particular type of cover gall DT70 represents is an erineum gall. Erineum galls are provided with enlarged but small nutritive cells, sometimes in the form of expanded trichomes, but whose contents are activated from stylet punctures of individual cells by mites (Larew 1981). Typical live erineum galls appear reddish to pinkish from mites that attack foliage and are characterized by unsightly bulging of tissues and distortions that can spread to other contiguous

plant organs (Westphal and Manson 1996). A variety of erineum galls occur on ferns, gymnosperms and angiosperms (Castagnoli 1996), some of which are economically important. Common examples include the fern mite *Hemitarsonemus tepidariorum* on the fern, *Pteris* sp., in California (Pritchard 1951); the pear leaf-blister mite *Eriophyes pyri* on pear, *Pyrus communis*, in Lebanon (Talhouk 1969); and *Aceria dactylonyx*, on hīnau, *Elaeocarpus dentatus*, in New Zealand (Lamb 1953). In particular, foliose mite galls, including erinea, that are morphologically very similar to DT70, prominently include *Eriophyes tetratrichus* on basswood, *Tilia platyphyllos* (Tiliaceae). This mite gall has macroscopic similarities to DT70, exhibiting foliar thickening and puffiness along the leaf margin that apparently migrates inwardly to the leaf median axis as the gall matures (von Schlechtendal 1916; Jeppson et al. 1975).

There are several additional defining features of DT70 on *D. crassinervis*, beyond the description above, and including additional figures (Figs. 14.8d–f, 14.9, 14.10, 14.11, 14.12a,b,d), and unfigured material from Aas411. The DT70 gall occasionally is interrupted by larger, bulbous and spheroidal to ellipsoidal features that often are breached to reveal an inner cavity similar to those mentioned by Larew (1981) and illustrated in his plate 4, figure 6. These structures also are similar to the eriophyoid gall on the dryopteridaceous fern *Nephrolepis* sp. (Nalepa 1909). The larger bulbous structures are interpreted as chambers inhabited by mites, whereas the smaller-sized pustules considerably less than 0.1 mm in longest dimension are interpreted as engorged nutritive cells. These features resemble the meristematic surfaces of some eriophyid pouch galls (Arnold 1965). Another major condition of the gall are upraised surfaces aligned between major pinnular veins. In some instances it appears that the incompletely galled pinnular margins exhibit curling. There is no evidence for enlarged pinnular trichomes containing nutritive protoplasts that many modern mite galls have, possibly attributable to the failure of trichome preservation in all examples of galled *D. crassinervis*. A major defining aspect of the gall is the ontogeny of DT70 that involves gall development progressing through four phases. Early galls are (i), small patches on pinnules (Fig. 14.8g, *grey arrows*); that later enlarge to (ii), broader pinnular patches (Fig. 14.9f, *grey arrows*); to (iii), a condition where the entire pinnule is engulfed by a gall (Figs. 14.8a–f, 14.9a, 14.10c, *black arrows*); and finally (iv), adjacent rachis tissue and nearby pinnules are invaded by the gall (Fig. 14.10a, *black arrow*; Fig. 14.12a), that occasionally undergo rachial bending (Figs. 14.9c,d,f, *red arrows*).

14.10 Discussion

During the late Permian (Lopingian), plant–insect interactions of the earlier Wuchiapingian Stage in Gondwana and Euramerica were moderately diverse, indicated by the Clouston Farm flora in KwaZulu-Natal in South Africa (Prevec et al. 2009) and by the Bletterbach flora in northeastern Italy (Labandeira et al. 2016). For the Clouston Farm site, 9772 plant specimens were assessed, consisting of 23 plant

morphotypes, 22 DTs and resulting in a 1.40% level of herbivory, of which 62.5% was generalized and 37.5% specialized (Prevec et al. 2009). The most common insect herbivorized plant was glossopterid morphotype C2a and most pervasive type of insect damage was DT12. For the Bletterbach site, 1531 plant specimens were examined, consisting of 23 plant morphotypes, 16 DTs and resulting in a 1.95% level of herbivory, of which 68.7% was generalized and 31.3% specialized (Labandeira et al. 2016). At Bletterbach, the most common insect herbivorized plant was *Taeniopteris* sp. A, and DT12 was the most prevalent insect damage. The South African and Italian Wuchiapingian floras harbored interactions dominated by the exophytic interactions of hole feeding, margin feeding and surface feeding and much lesser occurrences of the endophytic interactions of piercing and sucking, oviposition and galling. A broad summary for both floras can be expressed as: (i), levels of herbivory were approximately 1.7%; (ii), two-thirds of the interactions were generalized and one-third were specialized; and (iii), the dominant herbivorized plant was a seed plant that had a plurality of DT12 damage (Prevec et al. 2009; Labandeira et al. 2016). The Clouston Farm site, in addition, is notable for a significant amount of oviposition (Prevec et al. 2009), which may express a broader pattern across Gondwanan floras (McLoughlin 2011; Cariglino and Gutiérrez 2011; Labandeira and Currano 2013), that is not present in Euramerican floras.

The Wuchiapingian floras collectively established a baseline level of herbivory that apparently did not change during the Changhsingian Stage of the later Lopingian (Labandeira et al., unpubl. observ.). A sparse, depauperate flora of uppermost Lopingian age, described from the Sokovka site in the Volga Basin of European Russia (Lozovsky et al. 2016), has yielded specimens of the peltasperm *Vjaznikopteris rigida* (Krassilov and Karasev 2008, 2009). At this site specimens of *V. rigida* house a histioid mite gall and a robust, serpentine leaf mine (Krassilov and Karasev 2008), attributable to a beetle and indicating significant endophytic penetration of plant internal tissues immediately prior to the P-Tr ecological crisis. After this Changhsingian prelude was upstaged by the P-Tr event, all available evidence indicates that terrestrial ecosystems were devastated during the ecological crisis (Erwin 2006). This event particularly wreaked havoc on plants (Visscher et al. 1996; Gastaldo et al. 2005), devastated insect lineages (Labandeira 2005; Ponomarenko 2016), and significantly diminished the manifold interactions between these most diverse elements of terrestrial ecosystems (Labandeira and Currano 2013).

In the aftermath of the P-Tr global crisis, former Changhsingian terrestrial ecosystems that were drastically degraded show little evidence of recovery or regeneration during the Induan and Olenekian stages of the Early Triassic. Most plant–insect interactions succumbed to substantial ecological deterioration or otherwise were eliminated. Specialized relationships were especially impacted. Such a conclusion is based on limited, empirical, body-fossil data on Early Triassic plants (Retallack 1995) and insects (Shcherbakov 2000, 2008a; Ponomarenko 2016), but also buttressed by Karoo Basin food-web reconstructions that use trophic network models emphasizing diminished vertebrate ecological response to the P-Tr event that favored generalists (Sidor et al. 2013; Roopnarine and Angielczyk 2007, 2015). This pattern also is consistent with the observation that several major insect lineages experienced extinction at or close to the P-Tr boundary, such as many paleodicty-

opteroid, odonatopteran and orthopteroid lineages. By contrast, uncommon and inconspicuous lineages such as hemipterans (aphids, psyllids, whiteflies and related forms), coleopterans (beetles) and dipterans (true flies) survived and diversified considerably during the subsequent Triassic (Krzeminski 1992; Shcherbakov 2000, 2008a, b; Béthoux et al. 2005). Significantly, minimal plant–insect associational evidence is available from the Early Triassic Induan and Olenekian stages. The few reports available represent questionable assignment to the Olenekian Stage or describe only a few notable interactions (McLoughlin 2011; Kustatscher et al. 2014). These reports indicate that interactions were more negatively affected than the primary plant and insect extinctions at the P-Tr event. Severe reductions of taxa and improperly functioning ecosystems essentially produced a terrestrial dead zone approximately lasting a 5 million-year-long Early Triassic interval during a very inclement greenhouse world characterized by highly elevated CO_2 levels and temperatures that were excessive in continental interiors (Tong et al. 2007; Krassilov and Karasev 2009; Sun et al. 2012).

During the Middle Triassic there is increasing evidence for a major transformation in the relationships between plant hosts and their insect herbivores. This change began during the Anisian Stage and became more pronounced in the Ladinian Stage. During Anisian times there is an uptick in the number and quality of preservation of vascular plant floras, insect faunas and plant–insect interactions in several regions worldwide, particularly Western Europe. In Western Europe, a major regional flora of Anisian age was the Grès à Voltzia flora from upper Buntsandstein strata of the Röt Formation, located in the Vosges Mountains of northeastern France, with lateral equivalents in western Germany (Grauvogel-Stamm and Kelber 1996). Also in Western Europe, several geographically proximal floras of Anisian age occur in the Dont, Richthofen and Agordo formations from the Dolomites Region of northeastern Italy. Collectively these floras document additional plant communities in Western Europe that harbored a variety of plant–insect interactions prior to the buildup of the Alpine Cordillera (Labandeira et al. 2016). Plant–insect associations from the Italian floras indicate a degree of plant–insect interaction heterogeneity that rival those of Lopingian floras.

It was during the Ladinian Stage that several floras worldwide apparently exceeded the diversity of plant–insect interactions that had occurred during the previous Anisian Stage. This seemingly small but discrete increase in the level of plant–insect interaction activity is evident especially in Western Europe, particularly for Ladinian floras from the Lettenkohle Formation in the Alsace Region of northeastern France, and in the Lower Keuper Formation of Franconia, in south-central Germany. The relevant, plant-yielding beds of the German deposits with insect interactions are somewhat older that those found in France, but both deposits house evidence for some of the same interactions, principally margin feeding, oviposition and galling (Grauvogel-Stamm and Kelber 1996). A similar increase in herbivory also is detected in Ladinian-age floras from the Aquatona, Vulcanites, Fernazza and Wengen formations in the Dolomites Region of Northeastern Italy (Wappler et al. 2015; Labandeira et al. 2016). Compared to nearby Anisian floras of the Dolomites, these pooled Ladinian floras from both regions in Western Europe

show elevated percentages of foliage that were herbivorized and a greater proportion of specialized DTs than earlier Anisian floras. Also, some of the earliest examples of leaf mining are absent from the French and German localities, but present in the Italian localities. This presence of leaf-mining DTs in Ladinian northeastern Italy presages expansion of the leaf-mining FFG during the Carnian of Gondwana, as exemplified by Molteno localities such as Aas411.

It was during the Carnian Stage of the Late Triassic that the full recovery and subsequent development of the plant–insect associations apparently becomes evident for the early Mesozoic in the wake of the P-Tr ecological crisis. The prolonged expansion of this plant–insect associational diversity is dramatically manifest in the Molteno Formation of South Africa. In particular, the earliest major deposit of the Molteno sedimentary sequence, the Aas411 site with 20,358 examined specimens, 111 plant form-genera, 14 whole-plant taxa, and representing 10 FFGs, 44 DTs and 11 host-specific associations, displays a qualitative and quantitative quantum increase in associational diversity. In addition, highly diverse, plant–insect component communities were developed, such as the one on *H. elongatum* (Fig. 14.13). Future, additional examination of all 106 plant assemblages in the Molteno Formation as well as earlier Karoo deposits extending to the mid Permian will reveal not only the patterns of insect herbivory within the Molteno Formation based on variables such as site, time, habitat, plant host, FFG, DT, and specialized associations, but also the particularities of response of insect herbivores to the P-Tr ecological crisis approximately 18 million years earlier.

14.11 Summary and Conclusions

This study represents one installment of a continuing study that will examine the consequences of the end-Permian (P-Tr) ecological crisis in the Karoo Basin of South Africa. To partially address this issue, the Aasvoëlberg 411 (Aas411) site of the Late Triassic Molteno Formation was selected in this report to determine the extent and intensity of insect herbivory on all plant material collected toward the beginning of the Molteno depositional sequence. Although preliminary comparisons are made to other, unstudied Molteno localities, the principal focus of this study is to understand how plant hosts, their arthropod herbivores and particularly their shared interactions responded to the ecologically catastrophic events of the P-Tr event approximately 18 million years earlier. Seven general points summarize this study.

1. Response of plant–insect interactions to the end-Permian extinction. Tentative data indicates that by 18 million years after the P-Tr event, herbivory levels were equivalent to or surpassed those of the Late Permian. During the early Carnian Stage of the Late Triassic, insect herbivory had surpassed the level that was established during the Late Permian of southeastern Gondwana and southern Euramerica. This conclusion is based on an evaluation of plant–insect interactions at the Aas411 site from the Molteno Formation, Karoo Basin of South Africa.

2. The spectrum of arthropod herbivory at the Aasvoëlberg 411 (Aas411) site. The Aas411 site has a diverse spectrum and moderately elevated levels of herbivory within the Molteno Biome. At the Aas411 site, 20,358 plant specimens, including foliage, stems and reproductive material was examined representing 111 plant form-genera that includes 14 whole-plant taxa, 11 functional feeding groups (FFGs), and 44 arthropod herbivore damage type (DT) categories and 1127 individual DT feeding occurrences on specimens that were assessed using version 3 of the *Guide to Insect (and Other) Damage Types on Compressed Plant Fossils* (Labandeira et al. 2007). The Aas411 site is one of the more intensely herbivorized localities in the Molteno Biome.

3. The most herbivorized plant hosts at Aas411. The seven most herbivorized hosts at Aas411 are a broad representation of the vascular-plant taxa present at Aas411. Although 39 taxa showed DT evidence of arthropod herbivory on some plant tissue, the seven most herbivorized taxa, in decreasing rank order were the conifer *Heidiphyllum elongatum*; the corystosperm *Dicroidium crassinervis*; the ginkgophyte *Sphenobaiera schenckii*, the peltasperms *Lepidopteris stormbergensis* and *L. africana* and the horsetail *Zonulamites viridensis*. The spectrum of herbivory on these targeted and other less herbivorized plants at Aas411 includes generalized and specialized damage.

4. Specialized insect-herbivore interactions on whole-plant taxon hosts at Aas411. A broad spectrum of generalized feeding damage as well as 11 host-specialized associations were present at Aas411 that targeted 39 of the 111 plant species or morphotype taxa at the site. Host-specialized associations were particular damage types (DTs) of hole feeding, piercing and sucking, oviposition, mining, galling and seed predation that variously targeted whole-plant taxa. The most herbivorized whole-plant taxa with specialized herbivores are: (i), the *Heidiphyllum elongatum–Telemachus acutisquamus–Odyssanthus crenulata* conifer; (ii), the *Dicroidium crassinervis–Fanerotheca papilioformis–*?*Pteruchus matatimajor* corystosperm; (iii), the *Sphenobaiera schenckii–Sphenobaiera* short shoot–*Hamshawvia longipeduncula–Stachyopitys gypsianthus* ginkgophyte; (iv) the *Ginkgoites matatiensis–Avatia bifurcata– Eosteria eosteranthus* ginkgophyte; and (v) the *Zonulamites viridensis*–nodal diaphragm A–*Viridistachys gypsensis–Paraschizoneura fredensis* horsetail.

5. The *Heidiphyllum elongatum* component community at Aas411. The *Heidiphyllum elongatum* whole-plant-taxon is the most herbivorized plant at Aas411. The component herbivore component community is extensive compared with other highly herbivorized whole-plant taxa at the site and is trophically well balanced across FFGs with arthropod herbivores. This Aas411 plant host contains 81.8% (9/11) of all FFGs (including fungal damage), 63.6% (28/44) of all DT feeding categories, 40.9% (461/1127) of all individual DT occurrences, and 36.4% (4/11) of all specialized interactions.

6. Biology of the mite gall DT70. The gall DT70 has a host-specialized association with *Dicroidium crassinervis* at Aas411. At Aas411, DT70 constitutes 70.1% of

all feeding occurrences in the 11 other localities throughout the Molteno Biome where this host-specialist association occurs. The 117 occurrences of DT70 at Aas411 provides sufficient material that allows determination of the plant-host association, anatomical structure, and developmental ontogeny of this distinctive mite gall. This gall is consistent with an assignment to an eriophyioid gall mite culprit.

7. Future work on plant–insect interactions of the Molteno Biome. Future work will evaluate the relationships that the variables of time, habitat, host-plant abundance, insect herbivore abundance, FFG occurrence, DT occurrence and host-specialist associations. Such an assessment will span an interval from the mid Permian to the early Late Permian, including the Molteno Formation. These works will allow better understanding of the evolutionary and ecological dynamics of plant–insect interactions in the wake of the P-Tr event.

Acknowledgements Thanks go to Finnegan Marsh for formatting Figs. 14.1 to 14.13. Pfarelo (Grace) Tshivhandekano provided the images from which Fig. 14.5 to 14.10 were assembled. Jennifer Wood rendered and colorized Figs. 14.11 and 14.12. We thank an anonymous reviewer for constructive comments and Larry Tanner for inviting this contribution. This work is contribution 320 of the Evolution of Terrestrial Ecosystems consortium at the National Museum of Natural History, in Washington, D.C.

References

Adami-Rodrigues K, Iannuzzi R, Pinto ID (2004) Permian plant–insect interactions from a Gondwana flora of Southern Brazil. Foss Strat 51:106–125

Adami-Rodrigues K, Souza PA, Iannuzzi R, Pinto ID (2004) Herbivoria em floras Gonduânicas do Neopaleózoico do Rio Grande do Sul: análise quantitativa. Rev Brasil Paleontol 7:93–202

Alford DV (1991) A colour atlas of pests of ornamental trees, shrubs and flowers. Wolfe Publishing, London, p 448

van Amerom HWJ (1973) Gibt es Cecidien im Karbon bei Calamiten und Asterophylliten? In: Josten KH (ed) Compte Rendu Septième Congrès International de Stratigraphie et de Géologie du Carbonifère. Geologisches Landesamt Nordrhein-Westfalen, Krefeld, Germany, pp 63–83

Ananthakrishnan TN, Raman A (1989) Thrips and Gall dynamics. Leiden, Brill, p 120

Anderson JM, Anderson HM (1983) Palaeoflora of Southern Africa Molteno Formation (Triassic). Volume 1: part 1. Introduction/part 2. Dicroidium. Balkema, Rotterdam, p 227

Anderson JM, Anderson HM (1985) Palaeoflora of Southern Africa: prodromus of South African megafloras, Devonian to Lower Cretaceous. Balkema, Rotterdam, p 423

Anderson JM, Anderson HM (1989) Palaeoflora of Southern Africa Molteno Formation (Triassic). Volume 2: Gymnosperms (*Dicroidium*). Balkema, Rotterdam, p 567

Anderson JM, Anderson HM (1993) Terrestrial flora and fauna of the Gondwana Triassic: Part 2—co-evolution. The Nonmarine Triassic: New Mexico Nat Hist Sci Bull 3:13–25

Anderson JM, Anderson HM (2003) Heyday of the gymnosperms: systematics and biodiversity of the Late Triassic Molteno fructifications. Strelitzia 15:1–398

Anderson HM, Anderson JM (2008) Molteno ferns: Late Triassic biodiversity in Southern Africa. Strelitzia 21:1–258

Anderson HM, Anderson JM (2017) Molteno sphenophytes: Late Triassic biodiversity in Southern Africa. Evol Stud Inst Monogr Ser 1:1–191. pls 180

Anderson JM, Anderson HM, Archangelsky S, Bamford M, Chandra S, Dettmann M, Hill R, McLoughlin S, Rösler O (1999) Patterns of Gondwana plant colonization and diversification. J Afr Earth Sci 145:145–167

Anderson JM, Anderson HM, Cleal CJ (2007) Brief history of the gymnosperms: classification, biodiversity, phytogeography and ecology. Strelitzia 20:1–280

Anderson JM, Anderson HM, Cruickshank ARI (1998) Late Triassic ecosystems of the Molteno/Lower Elliott Biome of southern Africa. Palaeontology 41:387–421

Anderson JM, Anderson HM, Fatti P, Sichel H (1996) The Triassic explosion (?): a statistical model for extrapolating biodiversity based on the terrestrial Molteno Formation. Paleobiology 22:318–328

Anderson JM, Kohring R, Schlüter T (1998) Was insect biodiversity in the Triassic akin to today? A case study from the Molteno Formation (South Africa). Entomol Gen 23:15–26

Arnold BC (1965) Structure and growth of mite-induced galls of *Hoheria sexstylosa* Col. Pac Sci 19:502–506

Ash S (1972) Late Triassic plants from the Chinle Formation in northeastern Arizona. Palaeontology 15:598–618

Ash S (1997) Evidence of arthropod–plant interactions in the Upper Triassic of the southwestern United States. Lethaia 29:239–248

Ash S (1999) An Upper Triassic *Sphenopteris* showing evidence of insect predation from Petrified Forest National Park, Arizona. Internat J Pl Sci 160:208–215

Ash S (2000) Evidence of oribatid mite herbivory in the stem of a Late Triassic tree fern from Arizona. J Paleontol 74:1065–1071

Ash S (2009) A Late Triassic flora and associated invertebrate fossils from the basal beds of the Chinle Formation in Dinnebito Wash, eastcentral Arizona, USA. Palaeontographica Abt B 282:1–37

Ash SR (2014) Contributions to the Upper Triassic Chinle flora in the American Southwest. Palaeobiodiv Palaeoenviron 94:279–294

Ash S, Savidge RA (2004) The bark of the Late Triassic *Araucarioxylon arizonicum* tree from Petrified Forest National Park, Arizona. Internat Assoc Wood Anat J 25:349–368

Barboni R, Dutra TL (2015) First record of *Ginkgo*-related fertile organs (*Hamshawvia*, *Stachyopitys*) and leaves (*Baiera*, *Sphenobaiera*) in the Triassic of Brazil, Santa Maria Formation. J So Am Earth Sci 63:417–435

Beck AL, Labandeira CC (1998) Early Permian insect folivory on a gigantopterid-dominated riparian flora from North-central Texas. Palaeogeogr Palaeoclimat Palaeoecol 142:139–173

Bedard WD (1968) The sugar pine cone beetle. US Dept Agric For Pest Leaf 112:1–6

Béthoux O, Papier F, Nel A (2005) The Triassic radiation of the entomofauna. C R Palevol 4:609–621

Bird RD (1926) The Life History of the Saskatoon Sawfly, *Hoplocampa halcyon* Nort. Master's Thesis, University of Manitoba, Treesbank, Manitoba, pp 21

Blank SM, Schmidt S, Taeger A (eds) (2006) Recent Sawfly research: synthesis and prospects. Goecke & Evers, Keltern, Germany, p 702

Boczek J, Shevchenko VG (1996) Ancient associations: eriophyoid mites on gymnosperms. In: Lindquist EE, Sabelis MW, Bruin J (eds) Eriophyoid mites—their biology, natural enemies and control. Elsevier Science B.V, Amsterdam, pp 217–225

Bomfleur B, Decombeix A-L, Escapa IH, Schwendemann AB, Axsmith B (2013) Whole-plant concept and environment reconstruction of a *Telemachus* conifer (Voltziales) from the Triassic of Antarctica. Int J Plant Sci 174:425–444

Boughton AJ, Pemberton RW (2011) Limited field establishment of a weed biocontrol agent, *Floracarus perrepae* (Acariformes: Eriophyidae), against Old World climbing fern in Florida—a possible role of mite resistant plant genotypes. Environ Entomol 40:1448–1457

Brues CT (1924) The specificity of food plants in the evolution of phytophagous insects. Am Nat 58:127–144

Burdfield-Steel ER, Shuker DM (2014) The evolutionary ecology of the Lygaeidae. Ecol Evol 4:2278–2301
Burdick DJ (1961) A taxonomic and biological study of the genus *Xyela* Dalman in North America. Univ Calif Publ Entomol 17:281–353
Cairncross B, Anderson JM, Anderson HM (1995) Palaeoecology of the Triassic Molteno Formation, Karoo Basin, South Africa—sedimentological and palaeontological evidence. S Afr J Geol 98:452–478
Cariglino B, Gutiérrez PR (2011) Plant-insect interactions in a *Glossopteris* flora from the La Golondrina Formation (Guadalupian–Lopingian), Santa Cruz Province, Patagonia, Argentina. Ameghiniana 48:103–112
Carpenter FM (1960) A Triassic odonate from Argentina. Psyche 67:71–75
Carvalho M, Wilf P, Barrios H, Windsor DM, Currano ED, Labandeira CC, Jaramillo CA (2014) Insect leaf-chewing damage tracks herbivore richness in modern and ancient forests. PLoS One 9(5):e94950
Castagnoli M (1996) Ornamental coniferous and shade trees. In: Lindquist EE, Sabelis MW, Bruin J (eds) Eriophyoid mites—their biology, natural enemies and control. Elsevier Science B.V, Amsterdam, pp 661–671
Chen Z, Benton MJ (2012) The timing and pattern of biotic recovery following the end-Permian mass extinction. Nat Geosci 5:375–383. https://doi.org/10.1038/ngeo1475
Childers CC (1997) Feeding and oviposition injuries to plants. In: Lewis T (ed) Thrips as Crop Pests. CAB International, Wallingford, UK, pp 505–537
Cobben RH (1978) Evolutionary trends in Heteroptera. Part II. Mouthpart-structures and feeding strategies. Meded Landbouwhoesch Wageningen 78(5):1–407
Comstock JA (1939) Studies in Pacific Coast Lepidoptera. Bull Calif Acad Sci 38:34–35
Condamine FL, Nagalingum NS, Marshall CR, Morlon H (2015) Origin and diversification of living cycads: a cautionary tale on the impact of the branching process prior in Bayesian molecular dating. BMC Evol Biol 15:65. https://doi.org/10.1186/s12862-015-0347-8
Corbet PS (1999) Dragonflies: behaviour and ecology of Odonata. Harley Books, Colchester, UK, p 829
Cornet B (1996) A new gnetophytes from the Late Carnian (Late Triassic) of Texas and its bearing on the origin of the angiosperm carpel and stamen. In: Taylor DW, Hickey LJ (eds) Flowering plant origin, evolution and phylogeny. Chapman & Hall, New York, pp 32–67
Creber GT, Ash SF (2004) The Late Triassic *Schilderia adamanica* and *Woodworthia arizonica* trees of the Petrified Forest National Park, Arizona, USA. Palaeontology 47:21–38
De Lillo E, Monfreda R (2004) 'Salivary secretions' of eriophyoids (Acari: Eriophyoidea): first results of an experimental model. Exper Appl Acarol 34:291–306
Ding Q, Labandeira CC, Ren D (2014) Biology of a leaf miner (Coleoptera) on *Liaoningocladus boii* (Coniferales) from the Early Cretaceous of Northeastern China and the leaf-mining biology of possible insect culprit clades. Arthro Syst Phyl 72:281–308
Ding Q, Labandeira CC, Ren D (2015) Insect herbivory, plant-host specialization and tissue partitioning on mid-Mesozoic broadleaved conifers of Northeastern China. Palaeogeogr Palaeoclimatol Palaeoecol 440:259–273
Docters van Leeuwen-Reijnvaan J, Docters van Leeuwen WM (1926) The Zoocecidia of the Netherlands East Indies. Batavia, Drukkerij de Unie, p 601
Donovan MP, Iglesias A, Wilf P, Labandeira CC, Cúneo NR (2016) Rapid recovery of Patagonian plant–insect associations after the end-Cretaceous extinction. Nat Ecol Evol 1:0012. https://doi.org/10.1038/s41559-016-0012
Doorenweerd C, van Nieukerken EJ, Sohn J-C, Labandeira CC (2015) A revised checklist of Nepticulidae fossils (Lepidoptera) indicates an early Cretaceous origin. Zootaxa 3963:295–334
Dreger-Jauffret F, Shorthouse JD (1992) Diversity of gall-inducing insects and their galls. In: Shorthouse JD, Rohfritsch O (eds) Biology of insectinduced galls. Oxford University Press, New York, pp 8–33

Erwin DH (2006) Extinction: how life on Earth nearly ended 250 million years ago. Princeton University Press, Princeton, p 296
Evans JW (1971) Some Upper Triassic Hemiptera from Mount Crosby, Queensland. Mem Queensland Mus 16:145–151
Felt EP (1917) Key to American insect galls. N Y State Mus Bull 200:1–310. pl 1–16
Feng Z, Su T, Yang J, Chen Y, Wei H, Dai J, Guo Y, Liu J, Ding J (2014) Evidence for insect-mediated skeletonization on an extant fern family from the Upper Triassic of China. Geology 42:407–410
Feng Z, Wang J, Rößler R, Ślipiński A, Labandeira CC (2017) Late Permian wood-borings reveal an intricate network of ecological relationships. Nat Commun 8. https://doi.org/10.1038/s41467-017-00696-0
Fenton B, Birch ANE, Malloch G, Lanham PG, Brennan RM (2000) Gall mite molecular phylogeny and its relationship to the evolution of plant host specificity. Expt Appl Acarol 24:831–861
Floyd D (1993) Oreophoetes peruana——a very unconventional stick insect! Amateur Entomol Soc 52:121–124, pl 10
Fraser NB, Grimaldi DA, Olsen PC, Axsmith BA (1996) A Triassic Lagerstätte from eastern North America. Nature 380:615–620
Freeman TP, Goolsby JA, Oxman SK, Nelson DR (2005) An ultrastructural study of the relationship between the mite *Floracarus perrepae* Knihinicki & Boczek (Acariformes: Eriophyidae) and the fern *Lygodium microphyllum* (Lygodiaceae). Austral J Entomol 44:57–61
Funkhouser WD (1917) Biology of the Membracidae of the Cayuga Lake Basin. Cornell Univ Agric Expt Sta Mem 11:173–445
Futuyma DJ, Mitter C (1996) Insect–plant interactions: the evolution of component communities. Phil Trans R Soc Lond B 351:1361–1366
Gallego OF (1997) Hallazgos de insectos Triásicos en la Argentina. Ameghiniana 34:511–516
Gallego OF, Martins-Neto RG (1999) La entomofauna Mesozoica de la Argentina: Estado actual del conocimiento. Rev Soc Argentina 58:86–94
Gallego OF, Martins-Neto RG, Nielsen SN (2005) Conchostracans and insects from the Upper Triassic of the Biobío river ('Santa Juana Formation'), south-central Chile. Rev Geol Chile 32:293–311
Gangwere SK (1966) Relationships between the mandibles, feeding behavior, and damage inflicted on plants by the feeding of certain acridids (Orthoptera). Mich Entomol 1:13–16
Gao T, Shih CK, Labandeira CC, Liu X, Wang ZQ, Che YL, Yin XC, Ren D (2017) Maternal care by Early Cretaceous cockroaches and the early evolution of the oothecate condition. J Syst Entomol (in press)
Gastaldo RA, Adendorff R, Bamford M, Labandeira CC, Neveling J, Sims H (2005) Taphonomic trends of macrofloral assemblages across the Permian–Triassic boundary, Karoo Basin, South Africa. PALAIOS 20:480–498
Geertsema H, van den Heever JA (1996) A new beetle, *Afrocupes firmae* gen. et sp. nov. (Permocupedidae), from the Late Palaeozoic Whitehill Formation of South Africa. So Afr J Sci 92:497–499
Geertsema DE, van Dijk DE, van den Heever JA (2002) Palaeozoic insects of Southern Africa: a review. Palaeont Afr 38:19–25
Geinitz HB (1876) Ueber rhätischen Pflanzen und Thierreste in den Argentinischen Provinzen, La Rioja, San Juan, und Mendoza. Palaeontographica Suppl 3:1–14
Gerson U (1996) Secondary associations: eriophyoid mites on ferns. In: Lindquist EE, Sabelis MW, Bruin J (eds) Eriophyoid mites—their biology, natural enemies and control. Elsevier Science B.V, Amsterdam, pp 227–230
Geyer G, Kelber K-P (1987) Flügelreste und Lebensspuren von Insekten aus dem Unteren Keuper Mainfrankens. Neues Jb Geol Paläontol Abh 174:331–355
Ghosh AK, Kar R, Chatterjee R (2015) Leaf galls on *Dicroidium hughesii* (Feistmantel) Lele from the Triassic of India——a new record. Alcheringa 39:92–98

Gieshagen K (1919) Entwicklungsgeschichte einer Milbengalle an *Nephrolepis biserrata* Schott. Jahr Wiss Bot 58:66–104. pls 2–3
Gnaedinger SC, Adami-Rodrigues K, Gallego OF (2014) Endophytic oviposition on leaves from the Late Triassic of northern Chile: Ichnotaxonomic, palaeobiogeographic and palaeoenvironment considerations. Geobios 47:221–236
Golden M, Follett PA, Wright MG (2006) Assessing *Nezara viridula* (Hemiptera: Pentatomidae) feeding damage in macadamia nuts by using a biological stain. J Econ Entomol 99:822–827
Grauvogel-Stamm L, Kelber K-P (1996) Plant–insect interactions and coevolution during the Triassic in Western Europe. Paleontol Lomb 5:5–23
Grimaldi DA, Engel MS (2005) Evolution of the insects. Cambridge University Press, New York, p 755
Günthart H, Günthart MS (1983) Aguriahana germari (Zett.) (Hom. Auch. Cicadellidae, Typhlocybinae): breeding and specific feeding behavior on pine needles. Mitt Schweizer Entomol Ges 56:33–44
Hancox PJ (2000) The continental Triassic of South Africa. Zb Geol Paläontol 11–12:1285–1324
Handley DT, Pollard JE (1993) Microscopic examination of tarnished plant bug (Heteroptera: Miridae) feeding damage to strawberry. J Econ Entomol 86:505–510
Haughton SH (1924) The fauna and stratigraphy of the Stormberg Series. Ann So Afr Mus 12:323–495
Heer O (1877) Die Vorweltliche Flora der Schweiz. J. Wurster, Zürich, p 182. pls 1–70
Hering EM (1951) Biology of the Leaf Miners. Springer, Dordrecht, p 420
Hermsen EJ, Taylor TN, Taylor EL, Stevenson DM (2006) Cataphylls of the Middle Triassic cycad *Antarcticycas schopfii* and new insights into cycad evolution. Am J Bot 93:724–738
Hochuli PA, Hermann E, Vigran JO, Bucher H, Weissert H (2010) Rapid demise and recovery of plant ecosystems across the end-Permian extinction event. Glob Planet Change 74:144–155
Hori K (1971) Studies on the feeding habits of *Lygus disponsi* Linnavuori (Hemiptera: Miridae) and the injury to its host plants. I. Histological observations of the injury. Appl Entomol Zool 6:84
Hsü J, Chu CN, Chen Y, Tuan SY, YF H, Chu WC (1974) new genera and species of the late Triassic plants from Yungjen, Yunnan I. Acta Bot Sin 16:266–278
Janzen DH (1971) Seed predation by animals. Annu Rev Ecol Syst 2:465–492
Jeppson LR, Keifer HH, Baker EW (1975) Mites Injurious to Economic Plants. University of California Press, Berkeley, Los Angeles and London, p 614. pls 1–74
Johnson WT, Lyon HH (1991) Insects that feed on trees and shrubs, 2nd edn. Cornell University Press, Ithaca, NY, p 560
Jurzitza G (1974) *Antiagrion gayi* (Selys, 1876) und *A. grinsbergsi* spec. nov., zwei Verwechslungsarten aus Chile (Zygoptera: Coenagrionidae). Odonatologica 3:221–239
Kelber K-P (1988) Was ist *Equisetites foveolatus*? In: Hagdorn H (ed) Neue Forschung zur Erdegeschichte von Crailsheim. Sond Gesel Naturk Württemberg 1, pp 166–184
Kelber K-P, Geyer G (1989) Lebensspuren von Insekten an Pflanzen des unteren Keupers. Cour Forsch Inst Senck 109:165–174
Kellogg DW, Taylor EL (2004) Evidence of oribatid mite detritivory in Antarctica during the Late Paleozoic and Mesozoic. J Paleontol 78:1146–1153
Klavins SD, Kellogg DW, Krings M, Taylor EL, Taylor TN (2005) Coprolites in a Middle Triassic cycad pollen cone: evidence for insect pollination in early cycads? Evol Ecol Res 7:479–488
Krantz GW, Lindquist EE (1979) Evolution of phytophagous mites (Acari). Annu Rev Entomol 24:121–158
Krassilov VA, Karasev E (2008) First evidence of plant–arthropod interaction at the Permian–Triassic boundary in the Volga Basin, European Russia. Alavesia 2:247–252
Krassilov VA, Karasev E (2009) Paleofloristic evidence of climate change near and beyond the Permian–Triassic boundary. Palaeogeogr Palaeoclimat Palaeoecol 284:326–336

Krassilov V, Silantieva N, Lewy Z (2008) Traumas on fossil leaves from the Cretaceous of Israel. In: Krassilov V, Rasnitsyn A (eds) Plant–Arthropod interactions in the Early Angiosperm history: evidence from the Cretaceous of Israel. Pensoft/Brill, Sofia/Leiden, pp 7–187

Kraus JE, Montenegro G, Kim AJ (1993) Morphological studies on entomogenous stem galls of *Microgramma squamulosa* (Kauf.) Sota (Polypodiaceae). Am Fern J 83:120–128

Krzeminski W (1992) Triassic and Lower Jurassic stage of Diptera evolution. Mitt Schweiz Entomol Gesel 65:39–59

Kustatscher E, Franz M, Heunisch C, Reich M, Wappler T (2014) Floodplain habitats of braided river systems: depositional environment, flora and fauna of the Solling Formation (Buntsandstein, Lower Triassic) from Bremke and Fürstenberg (Germany). Palaeobiodiv Palaeoenviron 94:237–270

Kustatscher E, van Konijnenburg-Van Cittert JHA (2013) Seed ferns from the European Triassic—an overview. In: Tanner LH, Spielmann JA, Lucas SG (eds) The Triassic System, vol 61. New Mexico Mus Nat Hist Sci Bull, New Mexico, pp 331–344

Labandeira CC (1997) Insect mouthparts; ascertaining the paleobiology of insect feeding strategies. Annu Rev Ecol Syst 28:153–193

Labandeira CC (2002a) The paleobiology of predators, parasitoids and parasites: accommodation and death in the fossil record of terrestrial invertebrates. In: Kowalewski M, Kelley PH (eds) The fossil record of predation. Paleontol Soc Pap 8, pp 211–250

Labandeira CC (2002b) The history of associations between plants and animals. In: Herrera C, Pellmyr O (eds) Plant–animal interactions: an evolutionary approach. Blackwell, Oxford, pp 248–261

Labandeira CC (2005) The fossil record of insect extinction: new approaches and future directions. Am Entomol 51:14–29

Labandeira CC (2006a) Silurian to Triassic plant and insect clades and their associations: new data, a review, and interpretations. Arthro Syst Phylo 64:53–94

Labandeira CC (2006b) The four phases of plant–arthropod associations in deep time. Geol Acta 4:409–438

Labandeira CC (2010) The pollination of mid Mesozoic seed plants and the early history of long-proboscid insects. Ann Mo Bot Gard 97:469–513

Labandeira CC (2012) Evidence for outbreaks from the fossil record of insect herbivory. In: Barbosa P, Letorneau D, Agrawal A (eds) Insect outbreaks revisited. Blackwell, Oxford, pp 269–290

Labandeira CC (2013a) Deep-time patterns of tissue consumption by terrestrial arthropod herbivores. Naturwissenschaften 99:255–264

Labandeira CC (2013b) A paleobiological perspective on plant–insect interactions. Curr Opin Pl Biol 16:414–421

Labandeira CC (2016) Faunal ecology of the Molteno: towards an integrated ecology. In: Anderson JM, Anderson HM (eds) Molteno sphenophytes: Late Triassic biodiversity in southern Africa. Evol Stud Inst Monogr. Ser 1:14

Labandeira CC, Allen EM (2007) Minimal insect herbivory for the Lower Permian Coprolite Bone bed locality of north-central Texas, USA, and comparison to other late Paleozoic floras. Palaeogeogr Palaeoclimatol Palaeoecol 247:197–219

Labandeira CC, Currano ED (2013) The fossil record of plant–insect dynamics. Annu Rev Earth Planet Sci 41:287–311

Labandeira CC, Kustatscher E, Wappler T (2016) Floral assemblages and patterns of insect herbivory during the Permian to Triassic of Northeastern Italy. PLoS One 11(11):e0165205

Labandeira CC, Phillips TL (1996) A Carboniferous petiole gall: insight into early ecologic history of the Holometabola. Proc Natl Acad Sci U S A 93:8470–8474

Labandeira CC, Prevec R (2014) Plant paleopathology and the roles of pathogens and insects. Internat J Paleopathol 4:1–16

Labandeira CC, Tremblay S, Bartowski KE, Hernick LV (2014) Middle Devonian liverwort herbivory and antiherbivore defense. New Phytol 200:247–258
Labandeira CC, Wilf P, Johnson KR, Marsh F (2007) Guide to insect (and other) damage types on compressed plant fossils. Version 3.0, Spring 2007. Smithsonian Institution, Washington, DC, p 25
Lamb KP (1953) New plant galls. II——Description of seven new species of gall-mites and the galls which they cause. Trans R Soc New Zealand 80:371–382. pls. 78–83
Larew HG (1981) A comparative anatomical study of galls caused by the major cecidogenetic groups, with special emphasis on the nutritive tissue. PhD thesis, Department of Entomology, Oregon State University, pp 392
Larew HG (1992) Fossil galls. In: Shorthouse JD, Rohfritsch O (eds) Biology of insect-induced galls. Oxford University Press, New York, pp 50–59
Law C, Exley C (2011) New insight into silica deposition in horsetail (*Equisetum arvense*). BMC Plant Biol 11:112. https://doi.org/10.1186/1471-2229-11-112
Lawton JH (1982) Vacant niches and unsaturated communities: a comparison of bracken herbivores at sites on two continents. J Anim Ecol 51:573–595
Lewandowski M, Kozak M (2008) Distribution of eriophyoid mites (Acari: Eriophyoidea) on coniferous trees. Exp Appl Acarol 44:89–99
Lin X, Shih MJH, Labandeira CC, Ren D (2016) New data from the Middle Jurassic of China shed light on the phylogeny and origin of the proboscis in the Mesopsychidae (Insecta: Mecoptera). BMC Evol Biol 16:1. https://doi.org/10.1186/s12862-015-0575-y
Linck O (1949) Fossile Bohrgänge (*Anobichnium simile* n.g. n.sp.) an einem Keuperholz. Neues Jb Mineral Geol Paläontol 1949:180–185
Lozovsky VR, Balabanov YP, Karasev EV, Novikov IV, Ponomarenko AG, Yaroshenko OP (2016) The terminal Permian in European Russia: Vyaznikovian Horizon, Nedubrovo Member, and Permian–Triassic boundary. Strat Geol Corr 24:364–380
MacRae C (1999) Life etched in stone: fossils of South Africa. Geological Society of South Africa, Johannesburg, p 305
Maia VC, Santos MG (2011) A new genus and species of gall midge (Diptera, Cecidomyiidae) associated with *Microgramma vaccinifolia* (Langsd. & Fisch.) Copel. (Polypodiaceae) from Brazil. Rev Bras Entomol 55:40–44
Maskell WM (1887) An Account of the Insects Noxious to Agriculture and Plants in New Zealand. The Scale-Insects (Coccidae). State Forests and Agricultural Department, Wellington, p 116. pl 23
McElwain JC, Wagner PJ, Hesselbo SP (2009) Fossil plant relative abundances indicate sudden loss of Late Triassic biodiversity in East Greenland. Science 324:1554–1556
McKenna DD, Wild AL, Kojun K, Bellamy CL, Beutel RG, Caterino MS, Farnum CW, Hawks DC, Ivie MA, Jameson ML, Leschen RAB, Marvaldi AE, McHugh JV, Newton AF, Robertson JA, Thayer MK, Whiting MF, Lawrence JF, Ślipiński A, Maddison DR, Farrell BD (2015) The beetle tree of life reveals that Coleoptera survived end-Permian mass extinction to diversify during the Cretaceous terrestrial revolution. Syst Entomol 40:835–880
McLoughlin S (2011) New records of leaf galls and arthropod oviposition scars in Permian–Triassic Gondwanan gymnosperms. Austral J Bot 59:156–169
Meller B, Ponomarenko AG, Vasilenko DV, Fischer TC, Aschauer B (2011) First beetle elytra, abdomen (Coleoptera) and a mine trace from Lunz (Carnian, Late Triassic, Lunz-am-See, Austria) and their taphonomical and evolutionary aspects. Palaeontology 54:97–110
Meng Q, Labandeira CC, Ding Q, Ren D (2017) The natural history of oviposition on a ginkgophyte fruit from the Middle Jurassic of Northeastern China. Ins Sci 24. https://doi.org/10.1111/1744-7917.12506
Meyer J (1987) Plant galls and gall inducers. Gebrüder Borntraeger, Berlin, p 291

Minello LF (1994) As "florestas petrificadas" da região de São Pedro do Sul e Mata, R.S. III—análise morfológica megascópica, afinidades e consideraçõs paleoambentais. Acta Geol Leopold 39:75–91

Mitter C, Farrell B, Wiegmann B (1988) The phylogenetic study of adaptive zones: has phytophagy promoted insect diversification? Am Nat 132:107–128

Moisan P, Labandeira CC, Matushkina N, Wappler T, Voigt S, Kerp H (2012) Lycopsid–dragonfly associations and odonatopteran oviposition on Triassic herbaceous *Isoetites*. Palaeogeogr Palaeoclimatol Palaeoecol 344–345:6–15

Moreno T, Gibbons W (eds) (2007) The geology of Chile. The Geological Society, London

Nalepa A (1909) Eriophyiden. Denk Kaiser Akad Wiss Math-Naturwiss Klasse 84:523–536. pls 2–6

Nathorst AG (1876) Bidrag till Sveriges fossila Flora. Kongl Sven Veten Akad Handl 14:1–82

Nathorst AG (1878) Beiträge zur Fossilen Flora Schwedens. Über Einige Rhätische Pflanzen von Pälsjö in Schonen. E. Schweizerbart'sche Verlagshandlung, Stuttgart, p 82

Needham JG, Frost SW, Tothill BH (1928) Leaf-mining insects. Williams & Wilkins, Baltimore, p 351

Nel A, Prokop J (2006) New fossil gall midges from the earliest Eocene French amber (Insecta, Diptera, Cecidomyiidae). Geodiversitas 28:3754

Oldfield GN (1996) Diversity and host plant specificity. In: Lindquist EE, Sabelis MW, Bruin J (eds) Eriophyoid mites—their biology, natural enemies and control. Elsevier Science B.V, Amsterdam, pp 199–216

Oldfield GN (2005) Biology of gall-inducing Acari. In: Raman A, Schaefer CW, Withers TM (eds) Biology, ecology, and evolution of gall-inducing arthropods, vol 1. Science Publishers, Enfield, NH, pp 35–57

Papier F, Nel A, Grauvogel-Stamm L, Gall J-C (1997) La plus ancienne sauterelle Tettigoniidae, Orthoptera (Trias, NE France): mimétisme ou exaptation? Paläontol Z 71:71–77

Patra B, Bera S (2007) Herbivore damage to ferns caused by a chrysomelid beetle from lower Gangetic Plains of West Bengal, India. Am Fern J 97:19–29

Pedersen KR, Crane PR, Friis EM (1989) The morphology and phylogenetic significance of *Vardekloeftia* Harris (Bennettitales). Rev Palaeobot Palynol 60:7–24

Pinto ID (1956) Artrópodos da Formação Santa Maria (Triássico Superior) do Rio Grande do Sul, cum notícias sôbre alguns restos vegetais. Bol Soc Brasil Geol 5:75–94. pls. 1–4

Pinto ID, de Ornellas LP (1974) A new insect Triassoblatta cargnini Pinto et Ornellas, sp. nov., a Triassic blattoid from Santa Maria Formation, South Brazil. An Acad Brasil Cien 46:515–521

Pollard DG (1973) Plant penetration by feeding aphids (Hemiptera: Aphidoidea): a review. Bull Entomol Res 62:631–714

Ponomarenko AG (2016) Insects during the time around the Permian–Triassic crisis. Paleontol J 50:174–186

Pott C, Krings M, Kerp H (2007) A surface microrelief on the leaves of *Glossophyllum florinii* (?Ginkgoales) from the Upper Triassic of Lunz, Austria. Bot J Linn Soc 153:87–95

Pott C, Labandeira CC, Krings M, Kerp H (2008) Fossil insect eggs and ovipositional damage on bennettitalean leaf cuticles from the Carnian (Upper Triassic) of Australia. J Paleontol 82:778–789

Prevec R, Labandeira CC, Neveling J, Gastaldo RA, Looy CV, Bamford M (2009) Portrait of a Gondwanan ecosystem: a new late Permian fossil locality from KwaZulu-Natal, South Africa. Rev Palaeobot Palynol 156:454–493

Prinzing A, Ozinga WA, Brändle M, Courty PE, Hennion F, Labandeira CC, Parisod C, Pihain M, Bartish IV (2017) Benefits from living together? Clades whose species use similar habitats may persist as a result of eco-evolutionary feedbacks. New Phytol 213:67–82

Pritchard AE (1951) The fern mite. Calif Agric 5:10

Pryer KM, Schuettpelz E, Wolf PG, Schneider H, Smith AR, Cranfill R (2004) Phylogeny and evolution of ferns (monilophytes) with a focus on the early leptosporangiate divergences. Am J Bot 91:1582–1598

Queiroz JM (2002) Distribution, survivorship and mortality sources in immature stages of the Neotropical leaf miner *Pachyschelus coeruleipennis* Kerremans (Coleoptera: Buprestidae). Bras J Biol 62:69–76
Quintero C, Garibaldi LA, Grez A, Polidori C, Nieves-Aldrey JL (2014) Galls of the temperate forest of southern South America: Argentina and Chile. In: Fernandes GW, Santos JC (eds) Neotropical insect galls. Springer, Dordrecht, pp 429–463
Ramezani J, Fastovsky DE, Bowring SA (2014) Revised chronostratigraphy of the lower Chinle Formation strata in Arizona and New Mexico (USA): high precision U-Pb geochronological constraints on the Late Triassic evolution of dinosaurs. Am J Sci 314:981–1006
Rasnitsyn AP (1969) Proiskhozhdenie i ehvolyutsiya nizshikh pereponchatokrylykh [The origin and evolution of lower Hymenoptera]. Tr Paleontol Inst 123:1–196
Retallack GJ (1995) Permian–Triassic life crisis on land. Science 267:77–80
Retallack GJ, Dilcher DL (1988) Reconstructions of selected seed ferns. Ann Missouri Bot Gard 75:1010–1057
Retana-Salazar AP, Nishida K (2007) First gall-inducing thrips on *Elaphoglossum* ferns: a new genus and species of thrips, *Jersonithrips galligenus* from Costa Rica (Insecta, Thysanoptera, Phlaeothripidae). Senck Biol 87:143–148
Riek EF (1955) Fossil insects from the Triassic Beds at Mt. Crosby, Queensland. Austral J Zool 3:654–691
Riek EF (1974) Upper Triassic insects from the Molteno "Formation", South Africa. Palaeontol Afr 17:19–31
Riek EF (1976a) A new collection of insects from the Upper Triassic of South Africa. Ann Natal Mus 22:791–820
Riek EF (1976b) An unusual mayfly (Insecta: Ephemeroptera) from the Triassic of South Africa. Palaeont Afr 19:149–151
Rohfritsch O (1992) Patterns in gall development. In: Shorthouse JD, Rohfritsch O (eds) Biology of insect-induced galls. Oxford University Press, New York, pp 60–86
Roopnarine PD, Angielczyk KD (2007) Trophic network models explain instability of Early Triassic terrestrial communities. Proc R Soc B 274:2077–2086
Roopnarine PD, Angielczyk KD (2015) Community stability and selective extinction during the Permian–Triassic mass extinction. Science 350:90–93
Root RB (1973) Organization of a plant-arthropod association in simple and diverse habitats. The fauna of collards. Ecol Monogr 43:95–124
Roselt G (1954) Ein neuer Schachtelhalm aus dem Keuper und Beiträgezur Kenntnis von Neocalamites meriani Brongn. Geologie 3:617–643
Rozefelds AC (1985) A fossil zygopteran nymph (Insecta, Odonata) from the Late Triassic Aberdare Conglomerate, southeast Queensland. Proc Roy Soc Queensland 96:25–32
Rozefelds AC, Sobbe I (1987) Problematic insect leaf mines from the Upper Triassic Ipswich coal measures southeastern Queensland, Australia. Alcheringa 11:51–57
Sadler C, Parker W, Ash S (2015) Dawn of the Dinosaurs. The Late Triassic in the American Southwest. Petrified Forest Museum Association, Petrified Forest, AZ, p 124
Sarzetti LC, Labandeira CC, Muzón j WP, Cúneo NR, Johnson KR, Genise JF (2009) Odonatan endophytic oviposition from the Eocene of Patagonia: the ichnogenus *Paleoovoidus* and implications for dragonfly behavioral stasis. J Paleontol 83:431–447
Schachat S, Labandeira CC (2015) Evolution of a complex behavior: the origin and initial diversification of foliar galling by Permian insects. Sci Nat 102:14. https://doi.org/10.1007/s00114-015-1266-7
Schachat S, Labandeira CC, Gordon J, Chaney DS, Levi S, Halthore M, Alvarez J (2014) Plant–insect interactions from the Early Permian (Kungurian) Colwell Creek Pond, north-central Texas: the early spread of herbivory in clastic environments. Int J Plant Sci 175:855–890
von Schlechtendal DHR (1916) Eriophyidocecidien die durch Gallmilben verursachten Pflanzengallen. E. Schweizerbart'sche Verlagsbuchhandlung, Stuttgart, pp 295–498. pls 1–28
Schlüter T (1990) Fossil insect localities in Gondwanaland. Entomol Gen 15:61–76

Schlüter T (1997) Validity of the Paratrichoptera—an extinct order related to the Mecoptera, Diptera, Trichoptera or Lepidoptera? Suggestions based on discoveries in the Upper Triassic Molteno Formation of South Africa. Berl Geowiss Abh 25:303–312
Schlüter T (2000) Moltenia rieki n. gen., n. sp. (Hymenoptera: Xyelidae?), a tentative sawfly from the Molteno Formation (Upper Triassic), South Africa. Paläontol Z 74:75–78
Schlüter T (2003) Fossil insects in Gondwana—localities and palaeodiversity trends. Acta Zool Cracovien 46:345–371
Schmitz OJ (2008) Herbivory from individuals to ecosystems. Annu Rev Ecol Evol Syst 39:133–152
Schneider J (1966) Ennemis des fougeres ornementales. Phytoma 18:26–32
Scott AC, Anderson JM, Anderson HM (2004) Evidence of plant–insect interactions in the Upper Triassic Molteno Formation of South Africa. J Geol Soc Lond 161:401–410
Selden PA, Anderson HM, Anderson JM (2009) A review of the fossil spiders (Araneae) with special reference to Africa, and description of a new specimen from the Triassic Molteno Formation of South Africa. Afr Invert 50:105–116
Selden PA, Anderson JM, Anderson HM, Fraser NC (1999) Fossil araneomorph spiders from the Triassic of South Africa and Virginia. J Arachnol 27:401–414
Shcherbakov DE (2000) Permian faunas of Homoptera (Hemiptera) in relation to phytogeography and the Permo–Triassic crisis. Paleontol J 34:A251–S267
Shcherbakov DE (2008a) Insect recovery after the Permian/Triassic crisis. Alavesia 2:125–131
Shcherbakov DE (2008b) On Permian and Triassic insect faunas in relation to biogeography and the Permian–Triassic crisis. Paleontol J 42:15–31
Shcherbakov DE, Lukashevich ED, Blagoderov VA (1995) Triassic Diptera and initial radiation of the order. Int J Dipterol Res 6:75–115
Shepard HH (1947) Insects infesting stored grain and seeds. Univ Minnesota Agric Expt Sta Bull 340:1–31
Shields O (1988) Mesozoic history and neontology of Lepidoptera in relation to Trichoptera, Mecoptera, and angiosperms. J Paleontol 62:251–258
Sidor CA, Vilhena DA, Angielczyk KD, Huttenlocker AK, Nesbitt SJ, Peecook BR, Steyer JS, Smith RMH, Tsuji LA (2013) Provincialization of terrestrial faunas following the end-Permian mass extinction. Proc Natl Acad Sci U S A 110:8129–8133
Sidorchuk EA, Schmidt AR, Ragazzi E, Roghi G, Lindquist EE (2015) Plant-feeding mite diversity in Triassic amber (Acari: Tetrapodili). J Syst Palaeontol 13:129–151
Solomon JD (1995) Guide to insect borers in North American Broadleaf trees and shrubs. US Dept Agric For Serv Agric Hand AH706, Washington DC, p 735
Stone GN, Schönrogge K (2003) The adaptive significance of insect gall morphology. Tr Ecol Evol 18:512–522
Strullu-Derrien G, McLoughlin S, Phillipe M, Mørk A, Strullu DG (2012) Arthropod interactions with bennettitalean roots in a Triassic permineralized peat from Hopen, Svalbard Archipelago (Arctic). Palaeogeogr Palaeoclimatol Palaeoecol 348–349:45–58
Sun Y, Joachimski MM, Wignall PB, Yan C, Chen Y, Jiang H, Wang L, Lai X (2012) Lethally hot temperatures during the Early Triassic greenhouse. Science 338:366–370
Swezey OH (1915) A leaf-mining cranefly in Hawaii. Proc Hawaiian Entomol Soc 3:87–89
Talhouk AMS (1969) Insects and mites injurious to crops in Middle Eastern Countries. Mon Angew Entomol 21:1–239
Tapanila L, Roberts EM (2012) The earliest evidence of holometabolan insect pupation in conifer wood. PLoS One 7:e31668
Tillyard RJ (1917) Mesozoic insects of Queensland. No. 1. Planipennia, Trichoptera, and the new order Protomecoptera. Proc Linn Soc NSW 42:175–200, pls. 7–9
Tillyard RJ (1918a) Mesozoic insects of Queensland. No. 3. Odonata and Protodonata. Proc Linn Soc NSW 43:417–436, pls. 44–45

Tillyard RJ (1918b) Permian and Triassic insects from New South Wales, in the collection of Mr. John Mitchell. Proc Linn Soc NSW 43:720–756, pl. 59
Tillyard RJ (1918c) Mesozoic insects of Queensland. No. 4. Hemiptera Heteroptera: the family Dunstaniidae, with a note on the origin of the Heteroptera. Proc Linn Soc NSW 43:568–592
Tillyard RJ (1919a) Mesozoic insects of Queensland. No. 5. Mecoptera, the new order Paratrichoptera, and additions to Planipennia. Proc Linn Soc NSW 44:194–212
Tillyard RJ (1919b) Mesozoic insects of Queensland. No. 6. Blattodea. Proc Linn Soc NSW 44:358–382
Tillyard RJ (1920) Mesozoic insects of Queensland. No. 7. Hemiptera Homoptera; with a note on the phylogeny of the suborder. Proc Linn Soc NSW 44:857–895
Tillyard RJ (1921) Mesozoic insects of Queensland. No. 8. Hemiptera Homoptera (contd.). The genus Mesogereon; with a discussion of its relationship with the Jurassic Palaeotinidae. Proc Linn Soc NSW 46:270–284, pls. 16–21
Tillyard RJ (1922) Mesozoic insects of Queensland. No. 9. Orthoptera, and additions to the Protorthoptera, Odonata, Hemiptera and Planipennia. Proc Linn Soc NSW 47:447–470, pls. 51–53
Tillyard RJ (1923) Mesozoic insects of Queensland. No. 10. Summary of the Upper Triassic insect fauna of Ipswich, Q. (With an appendix describing new Hemiptera and Planipennia). Proc Linn Soc NSW 48:481–498, pl. 43
Tillyard RJ (1925) A new fossil insect wing from Triassic beds near Deewhy, N.S.W. Proc Linn Soc NSW 50:374–377, pl. 36
Tillyard RJ (1926) Alleged Rhaetic "crane flies" from South America, not Diptera but Homoptera. Am J Sci 5:265–272
Tillyard RJ (1937) A small collection of fossil cockroach remains from the Triassic beds of Mount Crosby, Queensland. Proc Roy Soc Queensland 48:35–40
Tillyard RJ, Dunstan B (1916) Mesozoic and Tertiary insects of Queensland and New South Wales. Description of the fossil insects and stratigraphical features. Queensland Geol Surv Publ 253:1–60, pls. 1–8
Tillyard RJ, Dunstan B (1923) Mesozoic insects of Queensland. Part 1. Introduction and Coleoptera. Queensland Geol Surv Publ 273:1–88, pls. 1–7
Tong J, Zhang S, Zuo J, Xiong X (2007) Events during Early Triassic recovery from the end-Permian extinction. Glob Planet Change 55:66–80
Turner BR (1975) The stratigraphy and Sedimentary History of the Molteno Formation in the Main Karoo Basin of South Africa and Lesotho. Unpublished PhD thesis. Johannesburg: University of the Witwatersrand, pp 314
Turner BR (1978) Trace fossils from the upper Triassic fluviatile Molteno Formation of the Karoo (Gondwana) Supergroup, Lesotho. J Paleontol 52:959–963
Vacante V (2016) The handbook of mites of economic plants: identification, bioecology and control. Commonwealth Agricultural Board International, Wallingford, UK, p 872
Vincent J (1990) Fracture properties of plants. Adv Bot Res 17:235–287
Vishniakova VN (1968) Mesozoic cockroaches with the external ovipositor and peculiarity of their reproduction (Blattodea). In: Rohdendorf BB (ed) Jurassic insects of Karatau. Nauka, Moscow, pp 55–86. (in Russian)
Visscher H, Brinkhuis H, Dilcher DL, Elsik WC, Eshet Y, Looy CV, Rampino MR, Traverse A (1996) The terminal Paleozoic fungal event: evidence of terrestrial ecosystem destabilization and collapse. Proc Natl Acad Sci U S A 93:2155–2158
Vogel S (2012) The life of a leaf. University of Chicago Press, Chicago, p 303
Walker MV (1938) Evidence of Triassic insects in the Petrified Forest National Monument, Arizona. Proc US Natl Mus 85:137–141, pls. 1–4
Walker JD, Geissman JW, Bowring SA, Babcock LE (2013) The Geological Society of America geologic time scale. Geol Soc Am Bull 125:259–272

Wang J, Labandeira CC, Zhang S-F, Bek J, Pfefferkorn HW (2009) Permian *Circulipuncturites discinisporis* Labandeira, Wang, Zhang, Bek et Pfefferkorn gen. et sp. nov. (formerly *Discinispora*) from China, an ichnotaxon of punch-and-sucking insect on Noeggerathialean spores. Rev Palaeobot Palynol 156:277–282

Wappler T (1999) Die Orthopteren (Insekten der Molteno) Formation (Ober–Trias) im Südlichen Afrika. Clausthal Technical University, Diplomarbeit, Clausthal, Germany, p 96

Wappler T (2000a) Triassische Insekten aus dem Karoo-Becken im südlichen Afrika. Arbeit Paläontol. Hannover 28:68–84

Wappler T (2000b) New Orthoptera and Grylloblattida (Insecta) from the Upper Triassic (Carnian) Karoo-System in southern Africa. First Internat Meet Paleoarthropodology (Ribeirão Preto, Brazil), pp. 34–35

Wappler T (2001) Haglidae (Insecta: Orthoptera) aus der obertriassischen Molteno-Formation im südlichen Afrika. N Jb Geol Paläontol Abh 222:329–352

Wappler T, Kustatscher E, Dellantonio E (2015) Plant–insect interactions from Middle Triassic (late Ladinian) of Monte Agnello (Dolomites, NItaly)——initial pattern and response to abiotic environmental perturbations. PeerJ 3:e921. https://doi.org/10.7717/peerj.921

Watt MN (1920) The leaf-mining insects of New Zealand. Part 1——the genus Parectopa (Lepidoptera). Trans Proc N Z Inst 52:439–466, pl 30

Webb JA (1982) Triassic species of *Dictyophyllum* from eastern Australia. Alcheringa 6:79–81

Weber H (1930) Biologie der Hemipteren: Eine Naturgeschichte der Schnabelkerfe. Julius Springer, Berlin, p 543

Weintraub JD, Cook MA, Scoble MJ (1994) Notes on the systematics and ecology of a fern-feeding looper moth, *Entomopteryx amputata* (Lepidoptera: Geometridae). Malayan. Nat J 47:355–367

Welke G (1959) Zur Kenntnis von *Strongylogaster xanthoceros* (Steph.) und *Strongylogaster lineata* (Christ) und ihrer Parasiten. Beitr Entomol 9:233–292

Wesenberg-Lund G (1913) Fortpflanzungsverhältnisse: Paarung und Eiblage der Süsswasserinsekten. Fortschr Naturwiss Forsch 8:161–286

Wesenberg-Lund G (1943) Biologie der Süsswasserinsekten. J. Springer, Berlin, Vienna, p 682

Westphal E (1977) Morphogenese, ultrastructure et etiologie de quelques galles d'eriophyes (Acariens). Marcellia 39:193–375

Westphal E (1992) Cecidogenesis and resistance phenomena in mite-induced galls. In: Shorthouse JD, Rohfritsch O (eds) Biology of insectinduced galls. Oxford University Press, New York, pp 141–156

Westphal E, Manson DCM (1996) Feeding effects on host plants: gall formation and other distortions. In: Lindquist EE, Sabelis MW, Bruin J (eds) Eriophyoid mites—their biology, natural enemies and control. Elsevier Science B.V, Amsterdam, pp 231–242

Whitfield JB, Kjer KM (2008) Ancient rapid radiations of insects: challenges for phylogenetic analysis. Annu Rev Entomol 53:449–472

Wilf P, Labandeira CC (1999) Response of plant-insect associations to Paleocene–Eocene warming. Science 284:2153–2156

Wilf P, Labandeira CC, Johnson KR, Coley PD, Cutter AD (2001) Insect herbivory, plant defense, and early Cenozoic climate change. Proc Natl Acad Sci U S A 98:6221–6226

Wilf P, Labandeira CC, Johnson KR, Ellis B (2006) Decoupled plant and insect diversity after the end-Cretaceous extinction. Science 313:1112–1115

Wilson J (1980) Macroscopic features of wind damage to leaves of *Acer pseudoplatanus* L. and its relationship with season, leaf age, and windspeed. Am Bot 46:303–311

Windsor D, Ness J, Gomez LD, Jolivet PH (1999) Species of *Aulacoscelis* Duponchel and Chevrolat (Chrysomelidae) and *Nomotus* Gorham (Languriidae) feed on fronds of Central American cycads. Coleopt Bull 53:217–231

Yang E, Xu L, Yang Y, Zhang X, Xiang M, Wang C, An Z, Liu X (2012) Origin and evolution of carnivorism in the Ascomycota (fungi). Proc Natl Acad Sci U S A 109:10960–10965

Yothers MA (1934) Biology and control of tree hoppers injurious to fruit trees in the Pacific Northwest. US Dept Agric Tech Bull 402:1–45

Zeuner FE (1961) A Triassic insect fauna from the Molteno beds of South Africa. Proc 11th Congr Entomol 1:303–306

Zherikhin VV (2002) Ecological history of the terrestrial insects. In: Rasnitsyn AP, Quicke DLJ (eds) History of insects. Kluwer, Dordrecht, pp 331–388

Zinovjev AG (2006) Taxonomic position and biology of Potania myrtillifoliae Benson, 1960 (Hymenoptera: Tenthredinidae). In: Blank SM, Schmidt S, Taeger A (eds) Recent sawfly research: synthesis and prospects. Goecke & Evers, Keltern, pp 139–142

Chapter 15
The Missing Mass Extinction at the Triassic-Jurassic Boundary

Spencer G. Lucas and Lawrence H. Tanner

Abstract The Late Triassic was a prolonged episode characterized by high rates of biotic turnover and discrete extinction events due to elevated extinction rates for some biotic groups and low origination rates for many. An end-Triassic mass extinction continues to be cited as one of the "big five" mass extinctions of the Phanerozoic. However, a detailed examination of the fossil record, especially by best-sections analysis, indicates that many of the groups usually claimed to have suffered catastrophic extinction at the end of the Triassic, such as ammonoids, marine bivalves, conodonts and tetrapod vertebrates, experienced multiple extinctions throughout the Late Triassic, not a single mass extinction at the end of the Period. Many other groups were relatively unaffected, whereas some other groups, such as reef communities, were subject to only regional effects. Indeed, the lack of evidence of a collapse of trophic networks in the sea and on land makes the case for an end-Triassic mass extinction untenable. Still, marked evolutionary turnover of radiolarians and ammonoids did occur across the Triassic-Jurassic boundary. The end of the Triassic encompassed temporary disruptions of the marine and terrestrial ecosystems, driven by the environmental effects of the eruption of the flood basalts of the Circum-Atlantic Magmatic Province (CAMP), through outgassing in particular, but these disruptions did not produce a global mass extinction.

Keywords Triassic-Jurassic boundary (TJB) • Mass extinction • Radiolarians • Bivalves • Ammonoids • Conodonts • Land plants • Tetrapods • CAMP volcanism

S.G. Lucas (✉)
New Mexico Museum of Natural History and Science,
1801 Mountain Road N. W., Albuquerque, NM 87104-1375, USA
e-mail: spencer.lucas@state.nm.us

L.H. Tanner
Department of Biological and Environmental Sciences, Le Moyne College, 1419 Salt Springs Road, Syracuse, NY 13214, USA
e-mail: tannerlh@lemoyne.edu

© Springer International Publishing AG 2018

L.H. Tanner (ed.), *The Late Triassic World*, Topics in Geobiology 46,
https://doi.org/10.1007/978-3-319-68009-5_15

15.1 Introduction

The biodiversity crisis at the end of the Triassic (Triassic-Jurassic boundary: TJB) has long been identified as one of the "big five" mass extinctions of the Phanerozoic (Fig. 15.1). Attribution of this level of suddenness and severity to the TJB extinction began during the 1960s, based on literature compilations of families of marine invertebrates. Sepkoski (1982) well-summarized early thinking on the TJB extinction(s) by designating the TJB extinction as one of four mass extinctions events of intermediate magnitude (Late Ordovician, Late Devonian, end-Triassic, end-Cretaceous), less severe than the largest Phanerozoic extinction, which was at the end of the Permian (Fig. 15.1). This identification of a severe and sudden biotic decline at the TJB remained unquestioned for about two decades. Then, Hallam (2002), Tanner et al. (2004) and Lucas and Tanner (2004, 2008, 2015) re-evaluated the stratigraphic and paleontologic data used to indicate a TJB mass extinction, concluding that no single mass extinction took place at the end of the Triassic. However, ignoring this literature and the science behind it, many workers continue to identify a global mass extinction at the TJB, ostensibly as the raison d'être for continued research near or across that time boundary.

Here, we review the magnitude and timing of the extinctions that took place across the TJB. No reliable data document global TJB mass extinction(s) of many significant biotic groups, including foraminiferans, ostracods, brachiopods,

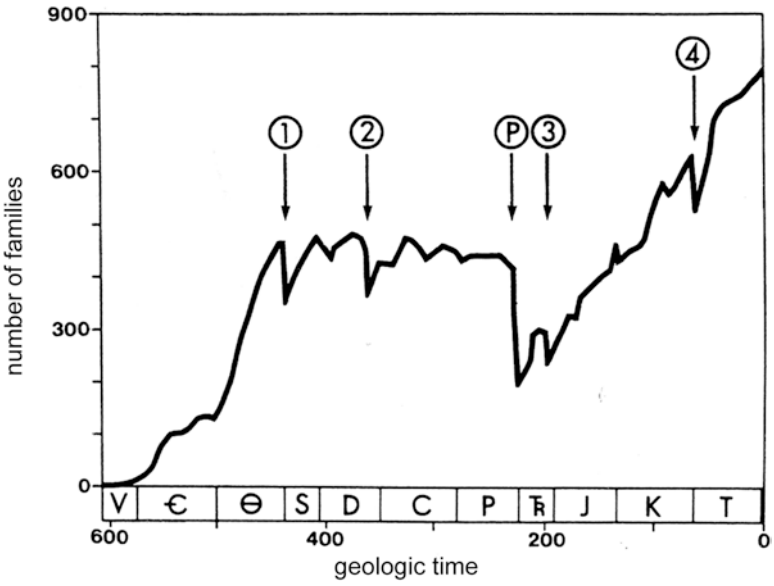

Fig. 15.1 The number of skeletonized families of marine invertebrate compiled from the literature through Phanerozoic time (modified from Sepkoski 1982). Five principal extinction events are marked by *vertical arrows*, each indicated by a significant drop in diversity. These came to be called the "big five extinctions" of current usage

gastropods, arthropods, freshwater and marine fishes and marine reptiles (Hallam 2002; Tanner et al. 2004; Lucas and Tanner 2008; Kelley et al. 2014; Renesto and Dalla Vecchia 2017). Therefore, we focus our discussion on those groups that have been perceived by many as part of a TJB mass extinction, namely radiolarians, conodonts, marine bivalves, reef-building organisms, ammonoids, land plants and terrestrial tetrapods (amphibians and reptiles).

15.2 Chronology

We use the Late Triassic timescale presented by Lucas (2017c), which is very similar to that of Ogg (2012a, b) and Ogg et al. (2014) (Fig. 15.2). The Upper Triassic chronostratigraphic scale consists of one Series, the Upper Triassic, divided into three stages—Carnian, Norian and Rhaetian. Substages of the Carnian and Norian provide much more detailed subdivisions of Late Triassic time than do the relatively long Carnian and Norian stages, and are used here as needed.

Numerical chronology of the Late Triassic is based on very few radioisotopic ages from volcanic ash beds directly related to marine biostratigraphy. The numerical calibration of the Late Triassic favored here is Carnian ~221–237 Ma, Norian ~205–221 Ma and Rhaetian ~201–205 Ma (Fig. 15.1; see Lucas 2017c). The numerical age of the Norian base has been particularly controversial, with many authors using the "long Norian" option and placing that base close to 228 Ma. Lucas et al. (2012) argued for a Norian base close to 220 Ma, and this base has found further support from radioisotopic ages published by Kohút et al. (2017).

Correlation of nonmarine and marine biochronology in the Late Triassic remains imprecise. The correlations used here are those of Lucas and Tanner (2007a), Lucas (2010a), Lucas et al. (2012) and Lucas (2017c). An important point is that for nearly 40 years, placement of the base of the Jurassic in the terrestrial section relied heavily on wholly unsubstantiated palynostratigraphic correlations in the Newark Supergroup strata of eastern North America (see review by Lucas and Tanner 2007b). Correcting this mis-correlation substantially improved understranding of the timing of nonmarine events across the TJB (Lucas and Tanner 2015).

15.3 Methods

Two methods have been used to analyze mass extinctions: (1) the compilation of global diversity from the published literature; and (2) the study of diversity changes based on the actual distribution of fossils in specific stratigraphic sections. These two methods are not totally disjunct, because the global compilations are based on the actual stratigraphic distributions of the fossils in all sections. However, the global compilations contain a serious flaw—their stratigraphic (temporal)

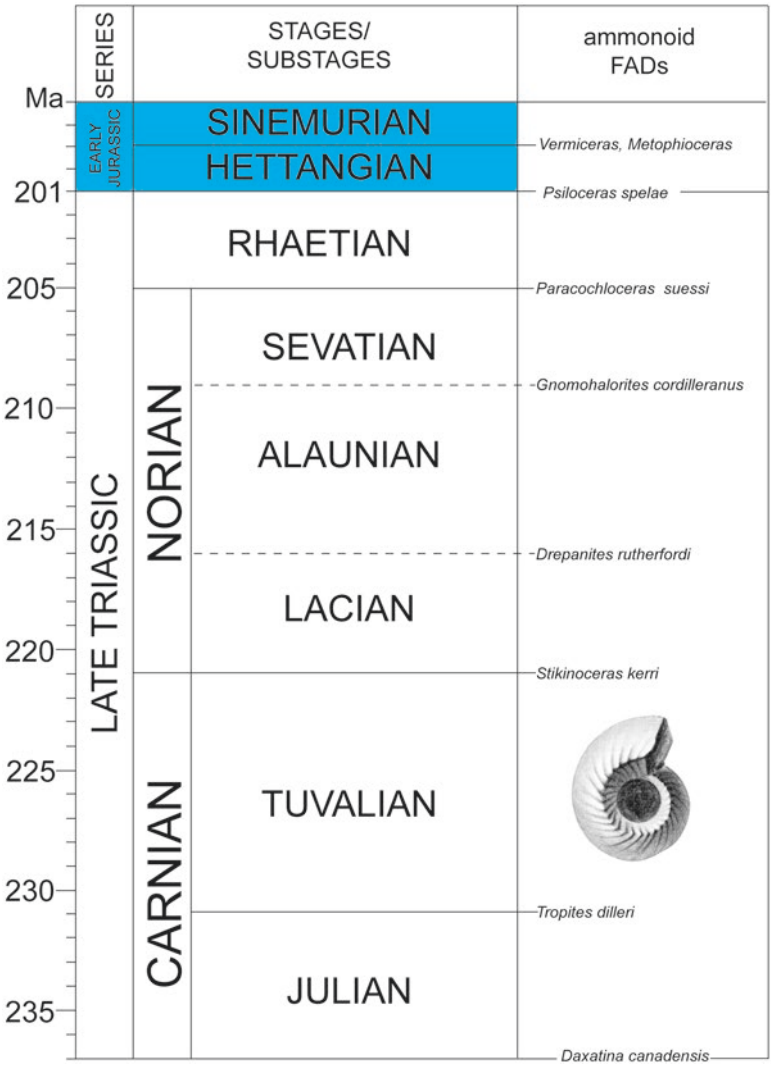

Fig. 15.2 Triassic-Jurassic boundary timescale (after Lucas 2017c)

imprecision (Teichert 1988), which Lucas (1994) termed the compiled correlation effect (CCE). We believe that this imprecision is largely responsible for the concept of a single TJB mass extinction (Lucas and Tanner 2008).

The CCE refers to the fact that the temporal ranges of taxa in literature compilations are only as precise as the correlations, or relative ages, of the taxa compiled. Because most published correlations are at the stage/age level, the temporal resolution of extinction events within these stages/ages cannot be resolved. The result is the artificial concentration of extinctions at stage/age boundaries. Thus, a complex

extinction of significant temporal duration during a stage/age can be made to appear as a mass extinction at the end of the stage/age.

Much of the literature on the TJB extinction has failed to consider the CCE. Thus, for example, the supposedly profound extinction of ammonoids across the TJB reflects a lack of detailed stratigraphic analysis. Literature compilations assume that any ammonoid taxon found in Rhaetian strata has a stratigraphic range throughout the entire Rhaetian (e.g., House 1989). This gives the appearance of a dramatic ammonoid extinction at the end of the Rhaetian, when in fact, ammonoid taxa experienced extinction their most profound extinction earlier, at the end of the Rhaetian (see below).

A relatively recent analysis heavily influenced by the CCE is that of Kiessling et al. (2007), who used the Paleobiology Database (PBDB) to evaluate the TJB extinction. They thus compared one Rhaetian diversity point to one Hettangian point and concluded there was a "true mass extinction" (Kiessling et al. 2007: 220) at the TJB. Indeed, the PBDB continues to be a basis for analyzing changing diversity and extinction (e. g., Alroy 2010; Vazquez and Clapham 2017), though close examination of any part of it reveals it is riddled with taxonomic errors and incorrect reporting of temporal ranges (e.g., Prothero 2015).

Rather than attempt to compile global diversity from the published literature, an alternative approach is to analyze mass extinctions by the "best sections" method (Lucas 2017a, b). Abundantly fossiliferous, well studied, stratigraphically dense and temporally extensive records from a single depositional basin or geographically restricted outcrop area are the "best sections" with which to identify extinctions (Fig. 15.3). These criteria may be somewhat subjective, but within a time interval we think the "best sections" are readily identified as those that have the most continuous and extensive fossil record that encompasses the extinction being studied, as well as the capability of providing geochemical and other geological data relevant to evaluating an extinction. Typically, within a given time interval, a limited number of stratigraphic sections (outcrop areas) will meet these criteria that identify a best section. This is particularly true of nonmarine sections. As an example, consider that most of what we know about dinosaur extinction at the end of the Cretaceous is based on a single, very best section in eastern Montana, USA (e. g. Archibald and MacLeod 2013). That section elucidates many of the accepted details of the extinction of dinosaurs. Other, less complete sections provide data consistent with the best section, which suggests that the pattern documented by the best section is a much broader, and in this case, likely a global pattern.

For the Late Triassic extinctions, marine sections in western Europe (especially Austria) and in the New World (British Columbia, Nevada, Peru) are the very best sections to study marine extinction events across the Triassic-Jurassic boundary (e. g. Lucas et al. 2007a; Hillebrandt et al. 2013) (Fig. 15.4). For the nomarine TJB, the Newark Supergroup sections in New Jersey and Nova Scotia, and the Glen Canyon Group section on the southern Colorado Plateau are the very best sections for examining the tetrapod record across the TJB (Lucas and Tanner 2007a, 2015) (Fig. 15.3).

A strength of the best sections method is that it allows the extinctions identified to be compared directly to changes in facies and other factors recorded in the best

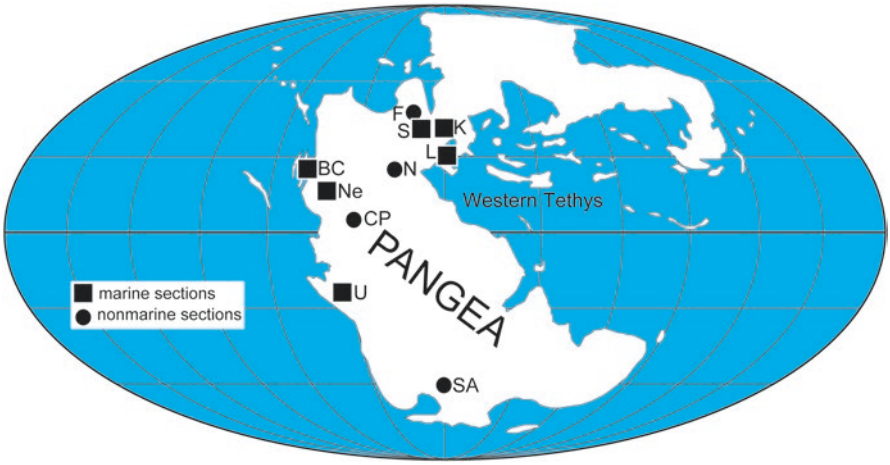

Fig. 15.3 Triassic world map with some of the best sections for studying the Triassic-Jurassic boundary extinctions. Marine sections are: *BC* Sections at Kennecott Point and nearby localities in the Queen Charlotte Islands, British Columbia, Canada, *K* Kuhjoch and other sections in western Austria, *L* Lagonegro basin and other sections in northern Italy, *Ne* New York Canyon, Nevada, USA, *S* St Audrie's Bay, UK, *U* Utcabamba Valley, Peru. Nonmarine sections are: *CP* Southern Colorado Plateau, Arizona-Utah-Colorado, USA, *F* Fissure fills in the United Kingdom, *N* Newark Supergroup sections, especially in the Newark basin, New Jersey, USA, and Fundy basin, Nova Scotia, Canada, *SA* Karoo basin, South Africa

section. Nevertheless, the best sections method has an inherent problem because it may only identify a local or regional extirpation, not a global extinction. Whether a best section captures a global pattern (the microcosm reflects the macrocosm) may be questioned. A good example of such a problem is the claim of a mass extinction of land plants across the TJB based on the section in East Greenland (McElwain et al. 1999 and see below). If less complete, temporally overlapping sections appear to reflect the patterns seen in the best section, this should increase confidence that these are broad patterns. The fact that no other sections reflect the inferred plant extinction at the TJB in East Greenland (see below) indicates that the event is at most of local significance. Indeed, the hypothesis of a widespread extinction based on an extinction seen in a best section can be tested by its presence or absence in temporally equivalent sections. Conversely, if a global mass extinction is posited, and the best section does not capture it, then the identification of that event should be questioned.

Indeed, best sections analysis has already been the source of some problems in analyzing the TJB extinctions. This stems from comparing local events in actual stratigraphic sections to broader global patterns. For example, one of the most studied marine TJB sections is at St. Audrie's Bay in southern England (e.g. Hesselbo et al. 2002, 2004; Hounslow et al. 2004). In this section, there is a major facies change that reflects a substantial marine regression followed by a transgression that began very close to the beginning of the Jurassic. Yet, many studies (e.g., Barras and

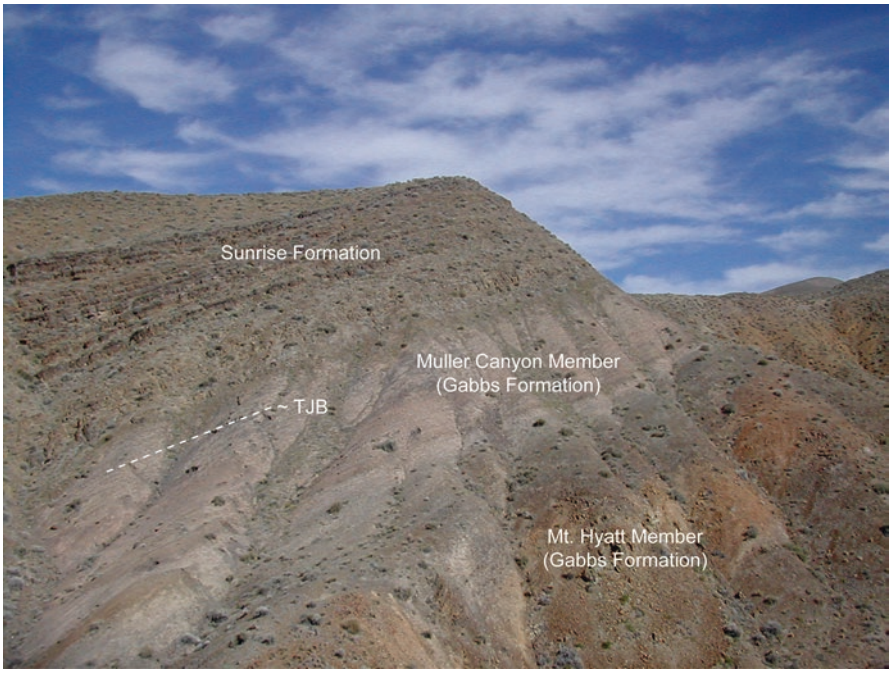

Fig. 15.4 The Triassic-Jurassic boundary section at Ferguson Hill near New York Canyon, Nevada, USA, is the best section for studying ammonoid extinctions across the TJB. The lowest occurrence of *Psiloceras spelae*, and therefore the Jurassic base, is about 8 m below the top of the Muller Canyon Member (see Fig. 15.7)

Twitchett 2007; van de Schootbrugge et al. 2007; Ibarra et al. 2016) have documented biotic changes in the St Audrie's Bay section and inferred that they reflect global events, when in fact they may more simply be explained by profound local facies changes. Indeed, the first question that should be asked of any section crossing the TJB is, are the biotic changes in that section due to the facies changes and not reflective of broader patterns of change? Indeed, many workers have not asked that question (for example, see McRoberts et al. 2012 discussed below) or have concluded there are no significant facies changes in sections where there obviously are (see Hallam et al. 2000). They thus extrapolate what are evidently local, facies driven biotic changes as indicative of broader biotic changes, thus confounding understanding of biotic events across the TJB.

"Best sections" may be new terminology, but the method is the oldest method of identifying mass extinctions. Thus, the first serious scientific advocacy of mass extinction by Georges Cuvier in the 1820s was based heavily on his studies (with Alexandre Brongniart) of the Eocene and younger Cenozoic strata and fossil succession of the environs of Paris (cf. Newell 1963; Rudwick 1997). This was the first "best sections" analysis of mass extinctions. It supported Cuvier's identification of various global extinctions ("catastrophes") of plants and animals in the Cenozoic

strata, though subsequent work revealed these to be only local or regional events. It thus provides a cautionary tale to those who would use a "best section" to posit a global extinction.

Of course, the actual stratigraphic ranges of fossils aggregated in genera or species are not perfect data with which to analyze changing diversity. Incompletely known stratigraphic ranges, taxonomic problems, taphonomic and facies biases, and issues of sampling all undermine our ability to read diversity directly from the fossil record. These problems are faced by those who use the best sections method to analyze changing diversity, and they also affect diversity compilations, which are, of course, ultimately rooted in the stratigraphic range data aggregated from all relevant sections. Nevertheless, "best sections" analysis has long been an important method by which to analyze changing diversity and extinctions. It should be recognized as an important approach to the study of mass extinctions, and a method that does not face all of the caveats associated with compilations of global diversity from the published literature.

In the context of best sections analysis, we note that the Signor-Lipps effect (Signor and Lipps 1982) has been used by some to discount the reliability of actual stratigraphic ranges. This hypothesis suggests that some actual stratigraphic ranges in the fossil record are artificially truncated by incomplete sampling, and statistical methods exist to "complete" these supposedly truncated stratigraphic ranges. However, we regard use of these methods as little more than assumptions that invent data, and prefer to rely on the actual stratigraphic ranges of fossils in well-studied sections. Indeed, the statistical analyses of Ward et al. (2005) and Marshall (2005), which used the same dataset of taxon ranges relevant to the end-Permian extinctions to support different conclusions based on different assumptions, provide a caution to those who would use statistical methods of stratigraphic range estimation to analyze extinctions.

On the other side of this issue, global data sometimes show no extinction of a biotic group across the TJB, whereas well-analyzed local (regional) data show otherwise. Tomašových and Siblík (2007) present an example of this with their excellent documentation of major changes in the brachiopod communities across the TJB in the Northern Calcareous Alps (Austria), whereas global data suggest no substantial extinction of brachiopods at this boundary (Hallam 2002; Tanner et al. 2004). One explanation of this may be that the profound facies change across the TJB that occurs in the Northern Calcareous Alps is correlated to (underlies) the brachiopod changes, but the possibility that this well-analyzed record is a more sensitive determinant of a global change needs to be considered and further evaluated.

15.4 Some History

The development of ideas about end-Triassic extinctions began almost 70 years ago (also see Deng et al. 2005), and we review key aspects of that development here. The first identification of substantial extinctions at the end of the Triassic are found

in publications by Colbert (1949, 1958) and Newell (1956, 1962, 1963). Initially, Newell (1952) presented analyses of diversity changes in marine invertebrates at the generic level that did not identify an end-Triassic extinction (also see Newell 1956). A parallel analysis of changing vertebrate diversity by Simpson (1952) also did not identify an end-Triassic extinction.

However, Newell (1962: 598) later stated that the "second great crisis in animal history occurred at the end of the Triassic Period" (the first was at the end of the Permian). He thus identified major extinctions of amphibians, "primitive reptiles," a 100% extinction of ammonite families and extinctions of some other (unspecified) genera and families of marine animals at the TJB. Newell (1963: 79) went on to state that "the mass extinction on land and sea at the close of the Triassic Period was almost equally significant [as the end Permian extinction]."

Newell (1962, 1963) took his conclusions about tetrapod extinctions on land from earlier publications by Colbert (1949, 1958), who drew attention to the extinction of "labyrinthodont" amphibians and "thecodont" reptiles at the end of the Triassic. Furthermore, Newell identified dinosaurs as replacing the "thecodonts" across the Triassic-Jurassic boundary.

In a more detailed analysis, Newell (1967, fig. 2) drew attention to the ammonite extinction at the end of the Triassic. However, his diagram, based on House (1963), actually showed the major collapse of ammonoid diversity taking place at the Norian-Rhaetian boundary, not at the end of the Triassic. Newell (1967) also identified a substantial extinction of brachiopods at the end of the Triassic. He stated that an analysis of family level diversity indicated 35% extinction of families at the end of the Triassic, compared to 50% extinction at the end of the Permian and 26% extinction at the end of the Cretaceous. Also, although Newell (1967) discussed various possible causes of mass extinctions, including climate changes and changes in the distribution of land and sea, he posited no specific cause(s) of the end-Triassic extinctions.

Tappan (1968) endorsed Newell's (1967) identification of a mass extinction at the end of the Triassic. Bakker (1977) analyzed terrestrial tetrapod mass extinctions and identified an extinction of large herbivores (rhynchosaurs, aetosaurs and dicynodonts) during the Late Triassic, which is the boundary between his "dynasties" IV and V. He also concluded that there was a co-eval extinction of aquatic marine tetrapods during the Late Triassic. Bakker (1977) argued that this and the other tetrapod extinctions were caused by major marine regressions correlated with a global decrease in orogenic activity (the "Haug effect" of Johnson 1971).

Hallam (1981) identified a major extinction of marine bivalves across the TJB. He subsequently (e.g., Hallam 1990, 1995) argued for a mass extinction at the TJB of various groups, including bivalves, ammonoids, conodonts, reef organisms, tetrapods and land plants. However, in a remarkable *volte-face*, Hallam (2002) questioned a TJB mass extinction of most of these groups.

Sepkoski (e.g., 1982, 1996) analyzed the diversity of families of marine invertebrates based on global compilations of the published literature. He identified a Late Triassic (Norian) extinction of ~20% of 300 marine families. According to Sepkoski (1982), this was the loss of 31 families of cephalopods, 7 families of marine reptiles,

6 families of gastropods, 6 of bivalves, 5 of articulate brachiopods and the total extinction of conodonts. Sepkoski (1982) believed that the extinction of marine tetrapods identified by Bakker (1977) predated the marine invertebrate extinctions by several million years.

Olson (1982) identified a drop in reptilian family diversity and an almost total extinction of amphibians across the TJB that he saw as a mass extinction. He based his analysis on Romer's (1966) compilation of vertebrate taxa. However, Benton (1985, 1987, 1988, 1989) identified two tetrapod extinctions during the Late Triassic, one at the Carnian-Norian boundary and a smaller one at the Norian-Rhaetian boundary. A sudden mass extinction of terrestrial tetrapods at the TJB was advocated by Olsen et al. (1987, 1990, 2002a, b). However, Weems (1992), Benton (1994), Lucas (1994), Tanner et al. (2004) and Lucas and Tanner (2004, 2007b, 2008, 2015) rejected this conclusion.

At present, the majority of workers still advocate a mass extinction in both the marine and nonmarine realms at the TJB. This is well reflected by many of the articles cited below, which have the phrase "end-Triassic mass extinction" or something similar in their titles. Indeed, the supposed end-Triassic mass extinction underpins much research being reported on latest Triassic and earliest Jurassic paleontology and geochemistry. Much of that research encompasses local studies that supposedly lend support to or are at least consistent with an end-Triassic mass extinction. Here, we demonstrate that at best this research is misleading because it identifies or is predicated on a mass extinction at the TJB that never took place.

15.5 Marine Organisms

In the marine realm, only a few large clades have been associated with a supposed TJB mass extinction, namely the radiolarians, conodonts, bivalves and ammonoids, as well as the reef community. Other groups show no evident mass exinction, despite a few claims to the contrary.

Thus, for example, Nudds and Sepkoski (1993) drew attention to the extinction of conulariids at the end of the Triassic. But, as Lucas (2012) demonstrated, in a detailed review of the Triassic conulariid record, its lacks the stratigraphic density with which to evaluate the detailed structure of their final extinction and in no way identifies a sudden mass extinction of the Conularia at the TJB.

15.5.1 Radiolarians

A major turnover in radiolarians took place across the TJB and has been identified by many as an important component of a marine mass extinction. Understanding the nature of the timing and severity of radiolarian extinction at the TJB was long hampered by slow identification of suitable and correlatable sections on a global scale.

Blome (1986), for example, found that Tethyan and North American assemblages differed significantly at the species level, preventing direct correlation. Hence, the uppermost Triassic (Rhaetian) was characterized by the *Globotaxtorum tozeri* Zone in North America, the *Livarella densiporata* Zone in Europe, the *Canoptum triassicum* Zone in Siberia, and the *Betraccium deweveri* Zone in Japan (reviewed in Blome et al. 1995). The most recent comprehensive review of the global record of Late Triassic radiolarians (O'Dogherty et al. 2010) continues to show no single global zonation, but instead provincial zonations for North America (Carter 1993), Europe (Kozur 2003), Japan (Sugiyama 1997) and the Russian Far East (Bragin 2000).

We argued previously (Tanner et al. 2004) that the data on the radiolarian extinction failed to demonstrate that it was a global event. Thus, at the family level, radiolarians were considered to show no serious decline at the TJB (Hart and Williams 1993), although a significant species turnover was indicated. Hori (1992), from the study of bedded cherts in central Japan, advocated a gradual end-Triassic radiolarian turnover, a conclusion shared by Vishnevskaya (1997), who demonstrated that about 40% of the latest Triassic radiolarian genera survived the TJB. Indeed, a second very large radiolarian extinction occurred later, during the Early Jurassic (early Toarcian) (Racki 2003). Furthermore, occurrences of bedded cherts show no decrease from the Late Triassic to the Early Jurassic, suggesting that there was no significant decline in silica production, and therefore, likely no great radiolarian decline (Kidder and Erwin 2001).

However, a rapidly growing global database ably summarized by Carter (2007) supports the idea of a drastic and rapid evolutionary turnover of radiolarians across the TJB. Indeed, it has been just within the last two decades that sections with sufficiently global distribution have been studied to allow more definitive species correlation among these regions, and permit clearer interpretation of the radiolarian record across the TJB.

The best-studied and most complete radiolarian record across the TJB is in the Queen Charlotte Islands in western Canada (Fig. 15.5); this is the "best section" with which to analyze the TJB radiolarian extinction. A drastic extinction of radiolarians at the TJB is indicated by the data from this locality (Tipper et al. 1994; Carter 1994; Ward et al. 2001; Longridge et al. 2007; O'Dogherty et al. 2010). The Rhaetian radiolarian fauna here includes over 160 species (Carter 1993, 1994), many of which have now been identified in sections from such diverse localities as Baja California Sur (Mexico), the Philippines, China, Tibet, Russia, the southern Apennines (Italy), Turkey, and Hungary (Carter 2007). Carter (1993, 1994) established the *Proparvicingula moniliformis* Zone and the *Globolaxtorum tozeri* Zone to encompass the lower and upper Rhaetian radiolarian assemblages, respectively, in the Queen Charlotte Islands (Fig. 15.5). Over half of the species present at the base of the *P. moniliformis* Zone disappear by the top of this zone, but most of the 70-plus species present at the base of the *G. tozeri* Zone continue to the system boundary. Carter (1994) documented the loss of 45 radiolarian species in the top 1.5 m of the *Globolaxtorum tozeri* zone (topmost Rhaetian) on Kunga Island in the Queen Charlotte Islands and concluded that five families, 25 genera, and most spe-

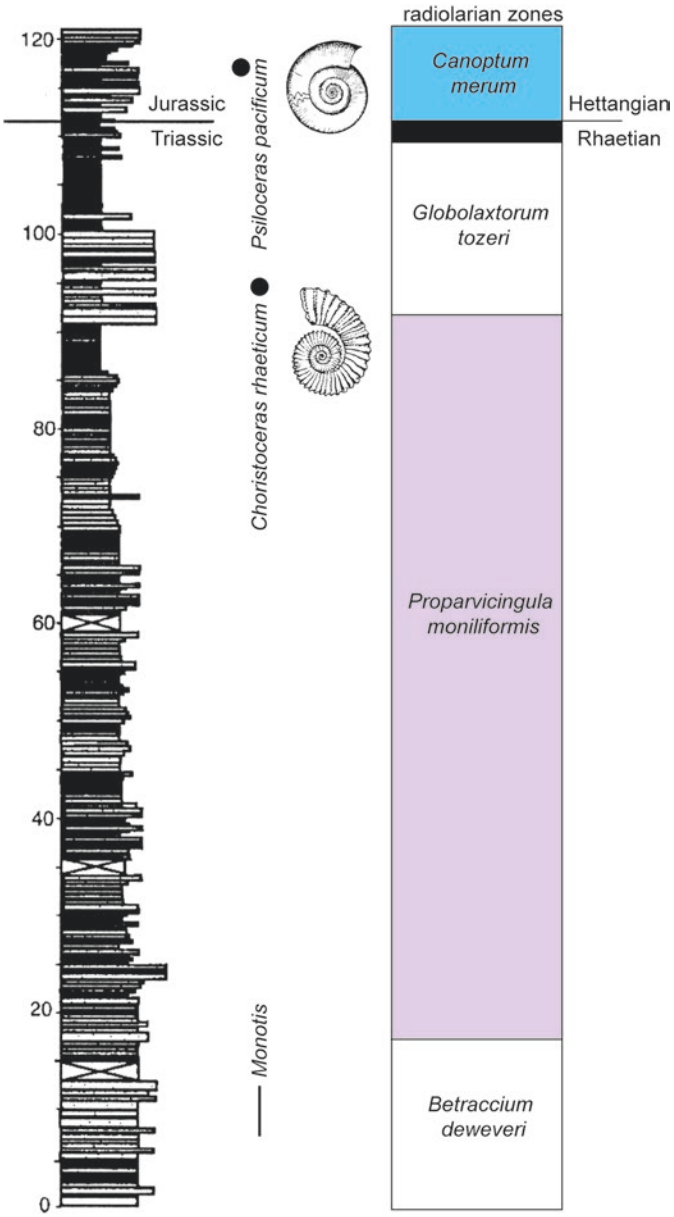

Fig. 15.5 Measured stratigraphic section at Kennecott Point in British Columbia, Canada, showing some key macrofossils and the radiolarian biozonation across the Triassic-Jurassic boundary (based on Ward et al. 2001, fig. 1).

cies of the *G. tozeri* Zone disappear within just a few meters of section (Carter 1994). This was updated by Longridge et al. (2007) to identify the disappearance of nine families, at least 27 genera and nearly all Rhaetian species at the system boundary. A similar pattern is now interpreted from Japan, where 20 genera and 130 Rhaetian species disappear across the TJB (Carter and Hori 2005).

The extinction is marked by the loss of the most architecturally complex forms of spumellarians, nassellarians, and enactiniids. The succeeding fauna is a low diversity Hettangian assemblage of morphologically conservative forms in which nassellarians are rare. In particular, the Hettangian radiolarians are mostly small spumellarians and much less common mutlicystid nasselarians with few chambers. This fits the idea of O'Dogherty and Guex (2002) that spumellarians are much more extinction resistant than are other radiolarians. O'Dogherty et al. (2010) also endorsed Guex's (2001) idea that ecological stress drives simplification and reduces the size of protists as well (also see Carter and Guex 1999). Guex (2016) has referred to this as retrograde evolution.

Carter and Hori (2005) drew attention to how this parallels the ammonoid turnover at the TJB (complex to simple, high diversity to low diversity; see below) and argued that a short and severe environmental stress caused the radiolarian extinction across the TJB. Longridge et al. (2007) explored this point further and note that the temporary persistence of some Rhaetian forms suggests that the extinction, while rapid, was not instantaneous. Further, they noted that the abundance of some opportunists, such as *Archaeocenosphaera laseekensis*, demonstrates rapid restoration of marine productivity. Thus, there was a significant evolutionary turnover of radiolarians at or very close to the TJB, and this appears to have been a global event.

Ward et al. (2001) called this a sudden collapse of marine productivity, but this is not the case. Given the non-uniformitarian nature of the radiolarian record (Racki and Cordey 2000) it is difficult to know how significant radiolarians were in the TJB planktonic communities. However, the best data suggest they were not the major component of the TJB micrplankton, nor a major food source (e.g. Martin 2001). Furthermore, there is no evidence of a substantial extinction of the other microplankton across the TJB. In fact, quite the opposite, following the first appearance of coccoliths during the latest Norian they and nannoliths appear to increase in abundance and diversity through the TJB (Gardin et al. 2012).

There is no chert gap across the TJB as there is across the Permo-Triassic boundary (e. g., Racki and Cordey 2000). The Late Triassic plankton were mostly acritarchs, radiolarians and conodonts, whereas cooclithophores and dinoflagellates were less abundant (e.g., Tappan and Loeblich 1973; Martin 2001). There is thus no evidence of a major collapse of the marine plankton across the TJB, other than among the radiolarians.

15.5.2 Bivalves

Hallam (1981) initially identified a single mass extinction (92% extinction of species) of marine bivalves at the end of the Triassic. He based this estimate on combining all Norian (including Rhaetian) marine bivalve taxa into one number, thereby encompassing a stratigraphic interval with a minimum duration of 20 million years (Fig. 15.1). He then compared this to a single number of Hettangian marine bivalve diversity, thus providing a strikingly clear example of the CCE.

Not surprisingly, Johnson and Simms (1989) demonstrated that much better stratigraphic resolution could be achieved on the local scale; in the Kössen beds (Northern Calcareous Alps, Austria), for example, Hallam considered all of the marine bivalve taxa to range through the entire Rhaetian, even though published data (e.g., Morbey 1975) showed highest occurrences at varied stratigraphic levels throughout the Rhaetian section. Furthermore, Skelton and Benton's (1993) global compilation of marine bivalve family ranges showed a TJB extinction of 5 families, with 52 families passing through the boundary unscathed, certainly suggesting that there was not a mass extinction of bivalve families across the TJB.

Hallam and Wignall (1997) re-examined the marine bivalve record for the TJB in northwestern Europe and the Northern Calcareous Alps in considerable detail. They found extinction of only 4 out of 27 genera in northwest Europe and 9 of 29 genera in the Northern Calcareous Alps, again, indicating no mass extinction. Although Hallam (2002) continued to argue for a substantial TJB marine bivalve extinction, he conceded that the data to demonstrate this are not conclusive.

More recent analysis of bivalve diversity across the TJB is based on a generic compilation at the stage level by Ros (2009) in an unpublished dissertation that is the basis of subsequent publications (Ros and Echevarría 2011; Ros et al. 2011, 2012). According to this analysis, marine bivalve generic diversity of the Triassic peaked during the Norian and was followed by a sharp drop in diversity into the Rhaetian and Hettangian. Extinction rates were thus high during the Rhaetian, and origination rates were low. Ros and collaborators claim their data identify a mass extinction of bivalves at the TJB but note that bivalve community ecology across the TJB changed little and that the recovery of bivalves during the Early Jurassic was very rapid.

We view the analyses of Ros and colleagues as another example of how the CCE creates the appearance of a mass extinction that vanishes at higher stratigraphic resolution. Ros (2009) compiled marine bivalve generic diversity as one data point per stage, thus comparing one diversity number for the ~15 million-year-long Norian with one diversity number for the ~4 million year long Rhaetian. Indeed, the estimate by Ros and colleagues of the magnitude of the Rhaetian generic extinction of bivalves (42% of genera) is close to Hallam's (1981) estimate of a 50% extinction, showing how the CCE continues, after decades, to confound an understanding of extinction dynamics.

Detailed studies of Late Triassic marine bivalve stratigraphic distributions (e.g., Allasinaz 1992; McRoberts 1994; McRoberts and Newton 1995; McRoberts et al.

1995; Wignall et al. 2007) instead identify multiple and selective bivalve extinction events within the Norian and Rhaetian Stages and across the TJB, with a particularly significant extinction at the Norian-Rhaetian boundary, not a single mass extinction at the TJB. Indeed, a review of the Late Triassic marine bivalve record suggests that extinctions were episodic throughout this interval rather than concentrated at the TJB. A significant extinction of bivalves, including the virtual disappearance (two dwarf Rhaetian species are now known: McRoberts 2007; Krystyn et al. 2007) of the cosmopolitan and abundant pectinacean *Monotis*, is well documented for the end Norian (Dagys and Dagys 1994; Hallam and Wignall 1997). McRoberts' (2007, 2010) summary of the Late Triassic diversity dynamics of "flat clams" (halobiids and monotids) indicates they suffered their largest extinction at the Norian-Rhaetian boundary. The end-Norian extinction of megalodontid bivalves was also noted by Allasinaz (1992), who concluded that the end-Norian marine bivalve extinction was larger than the end-Rhaetian (TJB) extinction.

Notably, in many sections, particularly in Europe, changes in bivalve diversity and composition correlate to facies changes, and this compromises interpretation of the broader significance of these changes (Allasinaz 1992). McRoberts et al. (2012), for example, analyzed bivalve assemblages across the TJB in the Kössen basin in the Northern Calcareous Alps of Austria. They documented high levels of taxonomic and ecological richness of the bivalve assemblages up to the base of the Rhaetian-Hettangian Tiefengraben Member, followed by low diversity episodic shell beds that they interpreted as dominated by eurytopic, opportunistic bivalve species. Treating the Kössen section as a "best section," McRoberts et al. (2012) concluded that this pattern best matches an ocean acidification event due to CAMP volcanism. However, the changes in the bivalve assemblages documented by McRoberts et al. (2012) take place across a marked facies change from the carbonate-dominated Eiberg Member to the overlying Tiefengraben Member, which is mostly laminated mudstone. Thus, these changes in the bivalves are readily interpreted as driven by local facies changes in bathymetry and geochemistry and by themselves do not demonstrate any global pattern.

15.5.3 Ammonoids

Biostratigraphic recognition (and definition) of the TJB has long been based on a substantial change in the ammonoid fauna from the diverse and ornamented ceratites and their peculiar heteromorphs of the Late Triassic to the less diverse and smooth psiloceratids of the Early Jurassic. This is the extinction of the Ceratitida followed by the diversification of the Ammonitida (e.g., House 1989). All but one lineage of ammonoids (the Phylloceratina) became extinct by the end of the Triassic, and the subsequent Jurassic diversification of ammonoids evolved primarily from that lineage (Guex 1982, 1987, 2001, 2006; Rakús 1993). The Early Jurassic encompasses a complex and rapid re-diversification of the ammonoids (e.g., Rakús 1993; Dommergues et al. 2001, 2002; Sandoval et al. 2001; Guex 2001, 2006).

As early as the work of Kummel (1957), House (1963) and Newell (1967), it was clear that the main extinction of Late Triassic ammonoids took place at the end of the Norian, not at the end of the Triassic (Fig. 15.6). After that extinction, only a few taxa remained, the heteromorphs, and some of the Arcestaceae and the Clydonictacea (Wiedmann 1973).

The Triassic ammonoid extinctions are the complete extinction of the Ceratitina before the end of the Rhaetian followed by the sudden apperance of the Ammonitina and Lytoceratina at the base of the Hettangian. However, the origin of these new groups had a long history. The details of the Late Triassic origin of the Ammonitina and Lytoceratina are presented by Wiedmann (1973, fig. 6) and Wiedmann and Kullman (1996).

House (1989: 78) considered the end-Triassic ammonoid extinction "the greatest in the history of the Ammonoidea." However, it has been clear for at least 40 years that the Late Triassic extinction of the ammonoids was a succession of diversity drops, with the last, most substantial drop at the end of the Norian, not at the end of the Triassic (Fig. 15.6). In other words, ammonoid extinction across the TJB is best described as stepwise (Wiedmann and Kullman 1996).

Here, we follow Lucas (2017d) and use Tozer's (1981a, b) compilation to plot the diversity of Late Triassic ammonoid families and genera (Fig. 15.6). At the family level, his diversity data can be plotted at the Late Triassic substage level, but not all the generic data are reported at the substage level, so they are simply plotted here at the stage level. Tozer's (1981a, b) compilation is nearly 40 years old, but it is the most recent compilation of all Triassic ammonoid families and genera. Much work has been done on Early and Middle Triassic ammonoids since 1981, but much less study of Late Triassic ammonoids since then, and, in particular, the few new Late Triassic ammonoid taxa recognized since 1981, indicate that Tozer's compilation remains useful for examining compiled Late Triassic ammonoid diversity. The fact remains that Tozer's compiled data only permit stage-level resolution for generic diversity, and thus suffer from the CCE (Lucas 1994) by indicating that the Late Triassic ammonoid extinctions are concentrated at stage boundaries (Fig. 15.6).

The compiled diversity numbers indicate that, after a Norian (mostly Alaunian) peak in diversity, the most substantial extinction of ammonoid families and genera took place across the Norian-Rhaetian boundary. The numbers based on Tozer (1981a, b) differ somewhat from some other compilations in the literature but all show the same pattern. For example, Teichert (1988) listed more than 150 ammonite genera and subgenera during the Carnian, which was reduced to 90 in the Norian, and reduced again to 6 or 7 during the Rhaetian. Similarly, Kennedy (1977) stated there are 150 or so Carnian genera, less than 100 during the Norian, and the number of Rhaetian genera is in single figures.

Nevertheless, the earlier discussion and a consideration of the best sections for documenting end-Triassic ammonoid extinctions allow a more detailed understanding of the Late Triassic ammonoid extinctions than one based solely on the compiled diversity. Thus, the most completely studied and ammonoid-rich section in the world that crosses the TJB is in the New York Canyon area of Nevada, USA (Figs. 15.4 and 15.7). Taylor et al. (2000, 2001), Guex et al. (2002, 2003) and Lucas

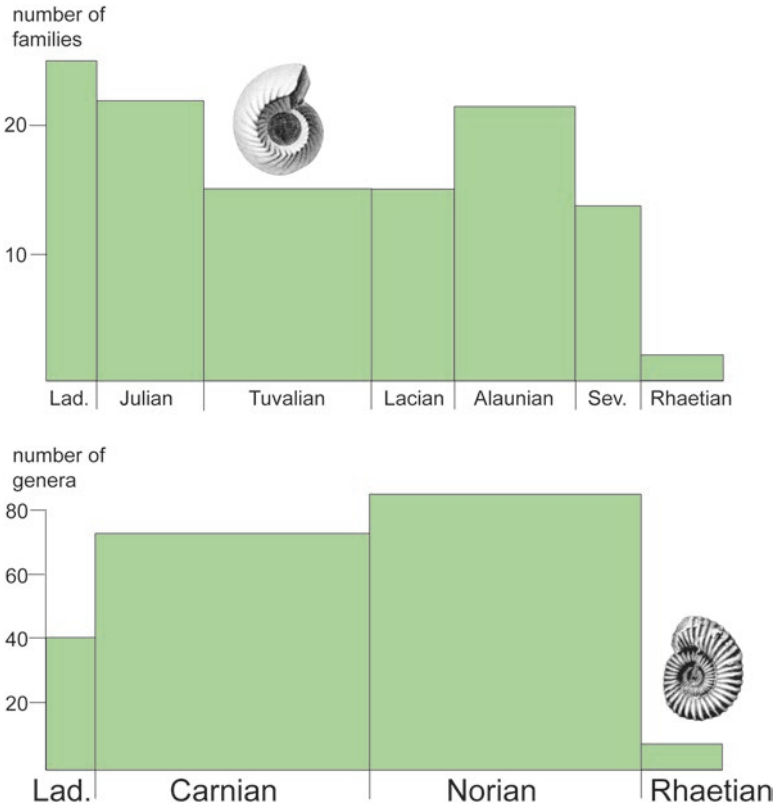

Fig. 15.6 Compiled family-level and genus-level diversity of Late Triassic ammonoids. Based on data in Tozer (1981a, b).

et al. (2007a) plotted ammonoid distribution in this section based on decades of collecting and study. Of 11 Rhaetian species, 7 extend to the upper Rhaetian, and only 1 is present at the stratigraphically highest Rhaetian ammonite level (Fig. 15.7). Taylor et al. (2000) presented a compelling conclusion from these data: a two-phase latest Triassic ammonoid extinction, one in the late Norian followed by a low diversity Rhaetian ammonoid fauna that became extinct by the end of the Triassic (also see Lucas and Tanner 2008; Whiteside and Ward 2011).

Another detailed study of latest Triassic ammonoid distribution in a best section is in the Austrian Kössen Beds (Urlichs 1972; Mostler et al. 1978). The youngest Triassic zone here, the *marshi* zone, has three ammonoid species, two with single level records low in the zone, and only *Choristoceras marshi* is found throughout the zone. This, too, does not indicate a sudden end-Triassic mass extinction of ammonoids. Thus, the change in ammonoids across the TJB is profound, but both compiled data and actual stratigraphic ranges in best sections indicate it took place as a series of extinction events spread across Norian and Rhaetian time, not as a single mass extinction at the end of the Triassic.

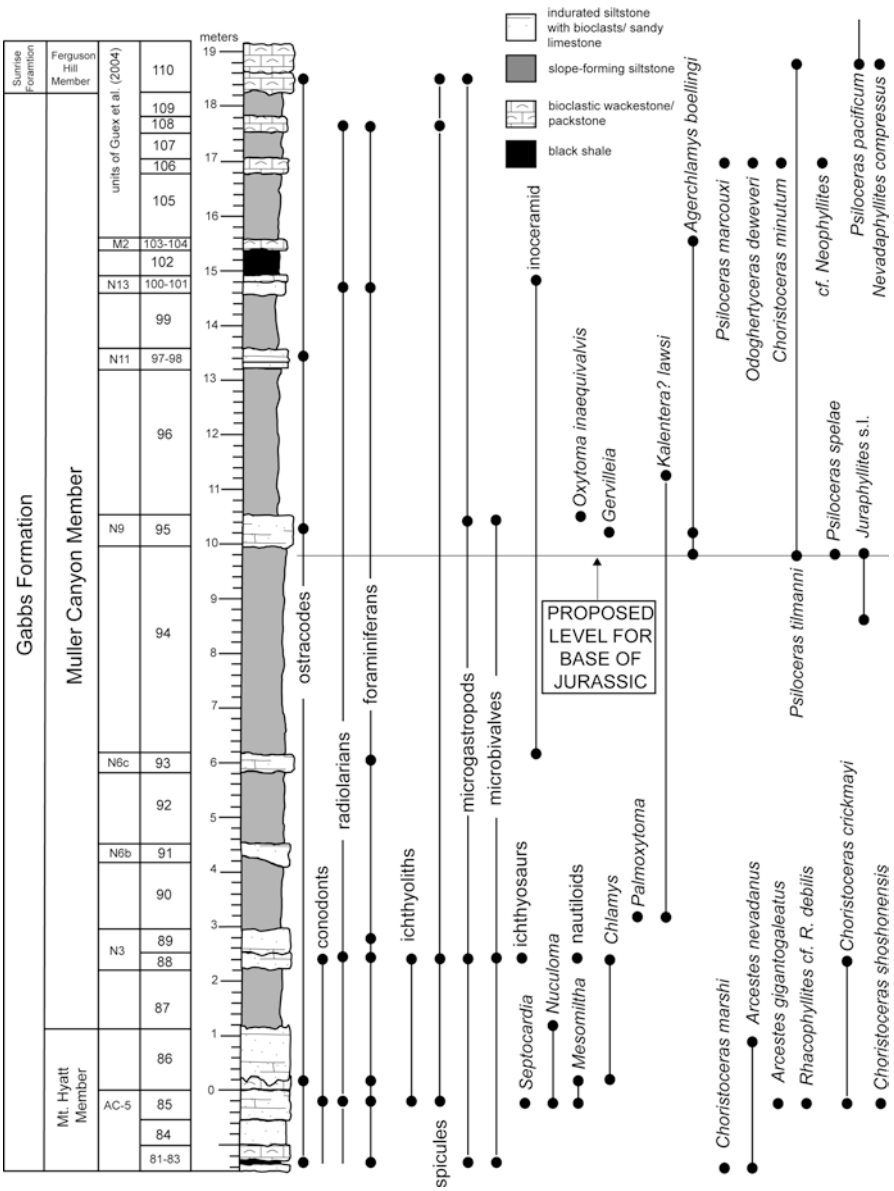

Fig. 15.7 The actual stratigraphic ranges of all known taxa (including ammonoids and bivalves) across the Triassic-Jurassic boundary in the Ferguson Hill section near New York Canyon, Nevada (modified from Lucas et al. 2007a). The TJB is placed here at the lowest occurrence of *Psiloceras spelae*

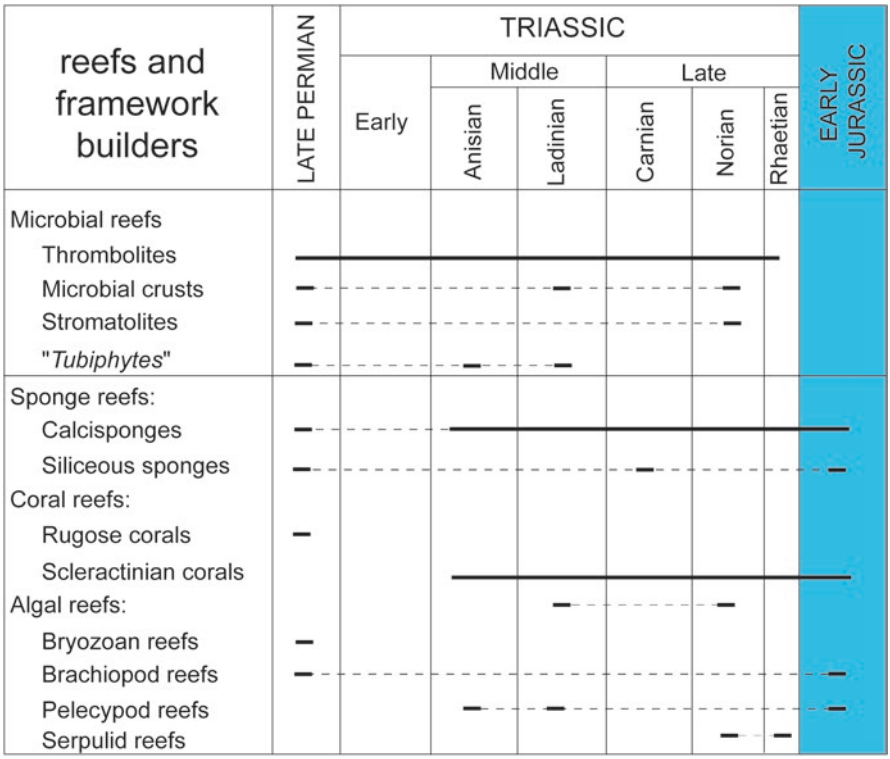

Fig. 15.8 Temporal distribution of major Triassic reef types as characterized by the principal reef-building groups (after Flugel and Senowbari-Daryan 2001)

The evolutionary turnover of ammonoids across the Triassic-Jurassic boundary is an important change from diverse and morphologically complex forms (including various heteromorphs) to less diverse and morphologically simple forms (the psiloceratids). Guex (2001, 2006) argued that this kind of morphological change occurred in response to environmental stress, as had occurred at several other crisis points in the history of the Ammonoidea. The Triassic-Jurassic transition was such a crisis in ammonoid history, but not a single mass extinction.

15.5.4 Coral Reefs

The scleractinian corals, important reef builders during the Triassic, suffered a marked decline at the end of the Triassic that was followed by a "reef gap" (which is being filled, see below) during part of the Early Jurassic (Hettangian-early Sinemurian), after which corals re-diversified to become the dominant reef builders (Stanley 1988; Flügel and Flügel-Kahler 1992; Flügel 2002; Leinfelder et al. 2002;

Fig. 15.9 The upper Rhaetian Steinplatte "reef" in Austria (see Stanton and Flügel 1989, 1995). On the *left side* of the photograph, the reef facies is interfingering with the bedded facies of the Kössen Formation. Photograph courtesy of Karl Krainer

Flugel and Kiessling 2002; Lathuiliere and Marchal 2009) (Fig. 15.8). Stanley (2001: 26) viewed this as a "rapid collapse" of reefs at the TJB, concluded it was "the result of a first-order mass extinction" and claimed that "Jurassic recovery was slow." These are overstatements.

The extinctions in the reef community at the end of the Triassic are best documented in Tethys, where the reef ecosystem collapsed at the end of the Triassic, carbonate sedimentation nearly ceased, and earliest Jurassic reefal facies are rare (Fig. 15.9). Earliest Jurassic reefs include carbonate mounds produced by spongiomorphs and algae (e.g., Flügel 1975; Delecat and Reitnwer 2005). Indeed, sponge reefs dominated by hexactinellids and non-lithistid deminsponges were not affected by any events across the TJB, and the hexactinellids actually diversified across the boundary (Mostler 1990; Delecat and Reitnwer 2005).

Coral Lazarus taxa have been discovered in Early Jurassic suspect terranes of western North America, indicating the persistence of at least some corals in Panthalassan refugia (on oceanic islands) during the earliest Jurassic reef gap (Beauvais 1984; Stanley and Beauvais 1994). A coral reef from the early Hettangian of France that includes numerous holdover genera and species from the Late Triassic (Kiessling et al. 2009; Gretz et al. 2015) further undermines the concept of a global mass extinction of corals at the TJB, as do recent discoveries of Early Jurassic corals from Scotland, the western USA and Tajikistan (Melnikova and Roniewicz 2012; Gretz et al. 2013; Hodges and Stanley 2015).

In some places, it has been proposed that microbial mats (Peterffy et al. 2016) or "*Lithiotis*" bivalves (Fraser et al. 2004) filled the niche of reef builders during the Hettangian, before the reassertion of scleractinian corals as the dominant reef builders. However, the claim of a microbial carbonate response to a TJB mass extinction based on data from the section at St. Audrie's Bay (Ibarra et al. 2016) is misleading because the microbialites in that section are stratigraphically well below the base of the Jurassic (the microbialites are in the Cotham Member, erroneously placed at the TJB by Mander et al. 2008, but of Rhaetian age; cf. Hounslow et al. 2004; Lucas et al. 2011).

Hallam and Goodfellow (1990) argued that sea-level change caused the collapse of the reef community, with significant extinctions of calcisponges and scleractinian corals at the TJB. They discounted the possibility of a major drop in productivity as an explanation for the facies change from platform carbonates to cherty carbonates. Indeed, a distinct lithofacies change occurs at or near the TJB in many sections, particularly in the Tethyan realm, where facies changes suggest an interval of regression followed by rapid transgression (Hallam and Wignall 1999; Leinfelder et al. 2002; Ciarapica 2007). At the TJB section in western Austria, for example, a shallowing-upward trend from subtidal carbonates to red mudstones, the latter interpreted as marginal marine or mudflat deposits, is succeeded by deeper water thin-bedded marl and dark limestone (McRoberts et al. 1997). The boundary in parts of the Austrian Alps displays karstification, suggesting a brief interval of emergence. In the Lombardian Alps the TJB is placed (palynologically) in the uppermost Zu Limestone at a flooding surface that marks the transition from mixed siliclastic-carbonate sedimentation to subtidal micrite deposition (Cirilli et al. 2003). Thus, a change in bathymetry likely resulted in the extirpation of reefs in Tethys, which in large part at least locally caused the cessation of carbonate sedimentation (Flügel 2002; Leinfelder et al. 2002; Lathuiliere and Marchal 2009). However, there is no evidence that this was a global event, and it can be viewed at most as a regional (circum-Tethyan) extinction driven by sea level changes (Tanner et al. 2004; Lucas and Tanner 2008).

Kiessling et al.'s (1999) and Kiessling's (2001) global compilation indicates that the decline of reefs actually began during the Carnian and that the TJB corresponds to the loss of reefs concentrated around 30°N latitude. Nevertheless, this article has been cited as documenting a TJB mass extinction of reef organisms (e.g., Pálfy 2003). However, the timescale used in Kiessling's compilations is very coarse (it is only divided into Ladinian-Norian-Pliensbachian) and shows a steady decline in diversity throughout this time interval to reach a diversity low in the Middle Jurassic (Bajocian/Bathonian). Nonetheless, this did not deter Kiessling et al. (1999) from identifying a major extinction of reefs at the TJB. Similarly, CCE-influenced analyses show a mass extinction of reefs across the TJB (e.g., Flugel and Kiessling 2002; Shepherd 2013).

Flügel and Senowbari-Daryan (2001) drew a broader picture of Triassic reef evolution (also see Flügel 2002) (Fig. 15.8). Thus, after the end-Permian mass extinction, there was a "reef gap" during the Early Triassic. In the Middle Triassic (Anisian), scleractinian corals first appeared and reef building rersumed. The pri-

mary Middle Triassic reef builders, however, were stromatoporoids, calcisponges and encrusting algae. This continued into the early Carnian, when there was a major evolutionary turnover in reefs that led to the scleractinian dominance of reefs by Norian time.

Indeed, Flügel and Senowbari-Daryan (2001) referred to Norian-Rhaetian reefs as the "dawn of modern reefs" because they were characterized by adundant, highly calcified, sessile, gregarious and high-growing corals, as are modern reefs (also see Flügel and Stanley 1984) (Fig. 15.9). However, Flügel and Senowbari-Daryan (2001) drew attention to a dramatic extinction of coral species at the TJB, with their analysis indicating that only 4% of Triassic coral species (14 of 321) and 8.6% of sphinctozoid coralline sponge genera (5 of 58) survived the end of the Triassic (though note that Kiessling et al. 2009 present different, lower numbers). They also noted that the most successful of the Late Triassic corals, the distichophyllids, became totally extinct at the end of the Triassic (also see Roniewicz and Morycova 1989).

Coral reefs are extremely rare in the Hettangian-early Sinemurian, but by Pliensbachian time the reef ecosystem was well on its way to recovery. The Jurassic reefs continued to be dominated by scleractinian corals, so the disruption of the reef ecosystem was not permanent. Indeed, as just noted, recent discoveries are filling this "gap."

In conclusion, a sudden extinction of reef organisms at the TJB is well documented in Tethys and reflects a regional change in bathymetry, but not a global mass extinction of reef organisms. Claims that oceanic acidification caused the global extinction of reefs at the TJB (Kiessling and Simpson 2011; Greene et al. 2012) assume the reef extinction was a global event, but this has not been substantiated. Instead, the "reef extinction" across the TJB was a facies driven event in western Tethys, not a global mass extinction.

15.5.5 Conodonts

The Conodonta is often identified as one of the most important groups to have suffered complete extinction at the end of the Triassic. However, this is quite misleading. Detailed reviews of conodont extinctions have long emphasized that conodonts suffered high rates of extinction and low rates of origination throughout the Triassic (e.g., Clark 1980, 1981, 1983; Sweet 1988; Kozur and Mock 1991; Aldridge and Smith 1993; De Renzi et al. 1996). During the Triassic, conodont diversity was highest during the Ladinian, and the ensuing Late Triassic saw a stepwise decline in this diversity as extinction rates were relatively high and origination rates were low. The single largest Late Triassic extinction of conodonts took place during the Carnian (at the Julian-Tuvalian boundary), when nearly all platform conodonts disappeared (Kozur and Mock 1991). Diversity recovered somewhat through the Norian to decline again into the Rhaetian. Within the Rhaetian, nearly all conodont taxa disappeared before the TJB, with only one or two taxa found in the youngest Rhaetian conodont assemblages (Mostler et al. 1978; Kozur and Mock 1991; Orchard 2003, 2010; Orchard et al. 2007; Bertinelli et al. 2016; Rigo et al. 2016).

Furthermore, Pálfy et al. (2007) reported the youngest Conodonta from Lower Jurassic strata (as had Kozur 1993, much earlier). Thus, from the Csövár section in Hungary, they reported the conodont "*Neohindeodella*" *detrei* from a horizon stratigraphically above an indeterminate psiloceratid ammonoid that they took to indicate an Early Jurassic age. According to M. Orchard (written commun., 2015), who processed and studied the conodonts from the Csövár section, only two conodonts elements were found in the Jurassic part of the section but "they were delicate ramiform specimens of the kind that would simply not survive reworking." Thus, the Csövár record appears to document Early Jurassic conodonts, eliminating the final extinction of conodonts as an end-Triassic event.

15.5.6 Mesozoic Marine Revolution

One of the most significant paleoecological events of the Mesozoic has long been claimed to be the Mesozoic marine revolution. This "revolution" is perceived of as the origin of durophagous predators (such as shell-boring gastropods) and an intensification of grazing that resulted in a substantial increase in the sturdiness of bivalve shells, and the turnover from marine benthic communities dominated by epifaunal (surface-dwelling) or semi-infaunal animals to a more infaunal benthos (e.g., Vermeij 1977, 1983; Harper and Skelton 1993). Some aspects of the Mesozoic marine revolution began in the Triassic (e.g., Fürsich and Jablonski 1984; Tintori 1995; Harper et al. 1998; Hautmann 2004a; Salamon et al. 2012; Tackett and Bottjer 2012; Buatois et al. 2016) but did not accelerate until well into the Jurassic (Pliensbachian-Toarcian) and took until the end of the Cretaceous to be completed (Hautmann 2004a).

Thus, the so-called Mesozoic marine revolution was a very lengthy process that began during the Late Triassic and did not culminate until the Late Cretaceous, so it took about 150 million years. This is clearly not a revolution on any timescale, so the term "Mesozoic marine revolution" should be abandoned. Furthermore, the Mesozoic marine revolution has no clear relationship to any of the Late Triassic extinctions.

15.6 Nonmarine Organisms

15.6.1 Land Plants

15.6.1.1 Plant Macrofossils

As reviewed by Lucas and Tanner (2015), a diverse paleobotanical literature does not identify a major extinction of land plants at the TJB (e.g., Orbell 1973; Schuurman 1979; Pedersen and Lund 1980; Fisher and Dunay 1981; Brugman 1983; Niklas et al. 1983; Knoll 1984; Ash 1986; Traverse 1988; Edwards 1993; Cleal 1993a, b; Kelber 1998, 2003; Hallam 2002; Tanner et al. 2004; Lucas and

Tanner 2004, 2007b, 2008; Burgoyne et al. 2005; Galli et al. 2005; Ruckwied et al. 2008; Kuerschner et al. 2007; McElwain and Punyasena 2007; Cascales-Miñana and Cleal 2011; Barbacka et al. 2017; Kustatscher et al. 2017). At most, only the extinction of peltasperms, a clade of seed ferns, took place at the TJB.

Global diversity compilations at the species and family levels do not indicate a substantial plant extinction at the TJB (Niklas et al. 1983; Knoll 1984; Edwards 1993; Cleal 1993a, b). Cascales-Miñana and Cleal (2011: 76–77) concluded that "the changes observed in the plant fossil record in the Late Triassic Series are mainly reflecting an ecological reorganization of the terrestrial habitats weeding-out some of the families of less adaptable plants that had filled the newly available niches during Triassic times, rather than a global ecological crisis on the scale of that seen at the end of Permian times."

Some data do reveal local turnover of paleofloras across the TJB. For example, a study of Swedish benettitaleans documented restriction of two species to the Rhaetian followed by five species restricted to the Hettangian. However, its authors, Pott and McLoughlin (2009: 117), do not consider this as anything more than a "moderate taxonomic turnover." Barbacka et al. (2017) recently presented a detailed analysis of floral change across the TJB, focused on the Polish record, and comparing it to other European records. They concluded that based on the European fossil-plant record "there were no significant changes in terrestrial plant composition at the TJB" (Barbacka et al. 2017: 80).

Nevertheless, McElwain and collaborators (McElwain et al. 1999, 2007, 2009; McElwain and Punyasena 2007; Belcher et al. 2010; Mander et al. 2010, 2012; Bacon et al. 2013) claim significant changes in the megaflora at the TJB in East Greenland of global significance. According to these workers, these represent a sudden change from high diversity Late Triassic plant communities to lower diversity and less taxonomically even Early Jurassic communities. This is the only location where a case has been made for a major turnover in the megaflora at the TJB, but, as analyzed in detail by Lucas and Tanner (2015), the data may support recognition of a megafloral crisis in East Greenland of no more than local significance that precedes the TJB.

The Astartekløft section of the Primulaev Formation of the Kap Stewart Group in Jameson Land, East Greenland (Fig. 15.10) records the transition from the *Lepidopteris* floral zone to the *Thaumatopteris* floral zone, with few species shared by both zones (Harris 1937). The former is characterized by the presence of palynomorphs, including *Rhaetipollis*, while the latter contains *Heliosporites* (Pedersen and Lund 1980), and although extinction of some species across the transition between the two zones is evident, many species occur in both zones. Thus, Harris (1937: 76) emphasized that "real mixing" of the two floral zones occurs over a 10 m interval (Fig. 15.10), and "this is real mixing….the two sets of plants will be seen on the same bedding plane and they continue to be found together from top to bottom, of one of these beds…." Therefore, the data and analyses of Harris (1937) and Pedersen and Lund (1980) did not identify an abrupt change in the land plants across the TJB in Jameson Land. Furthermore, what species turnover looks abrupt in this section was attributed by Harris (1937) and Pedersen and Lund (1980) to

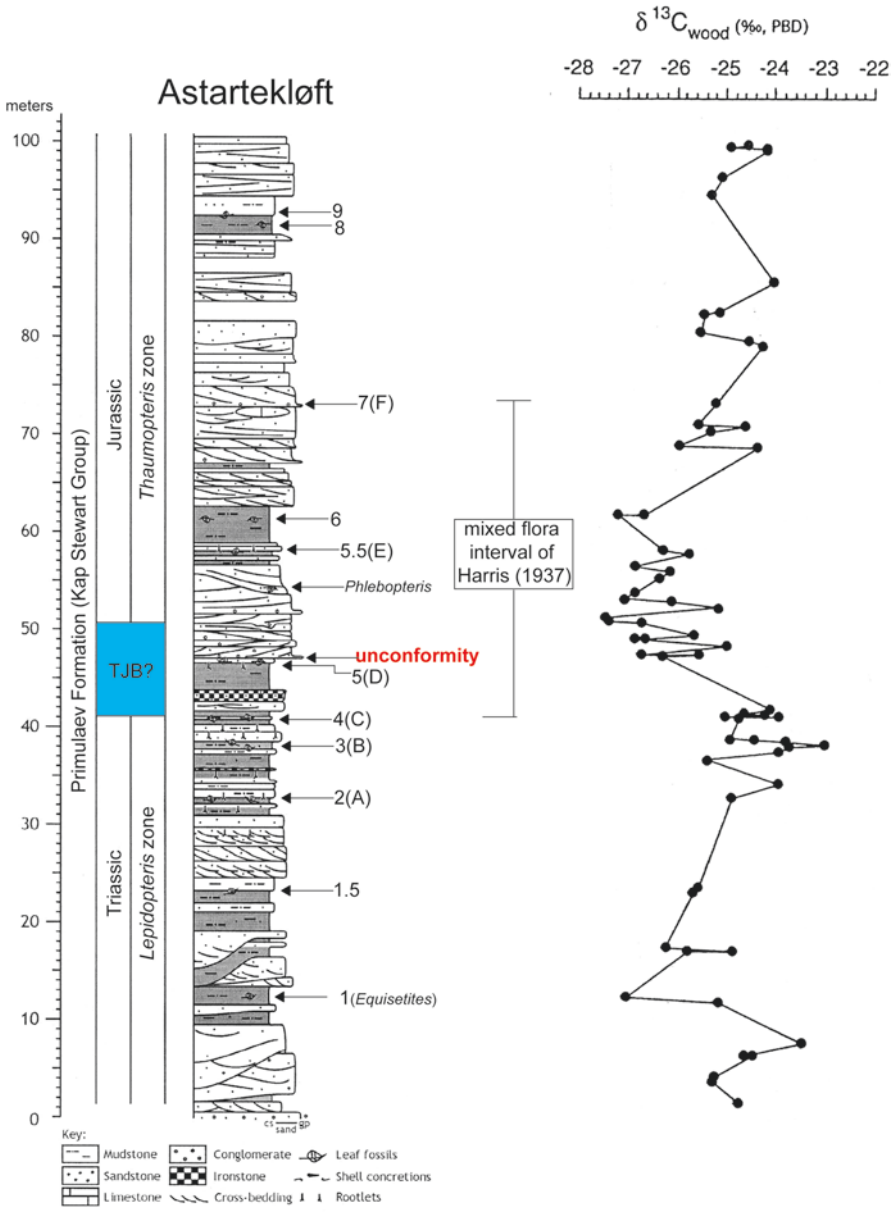

Fig. 15.10 Measured section of Triassic-Jurassic boundary interval of Kap Stewart Group in East Greenland showing distribution of megafossil plants and published carbon-isotope curve. The lithologic column is modified from McElwain et al. (2007) and shows megafossil plant beds using their scheme (1, 1.5, 2, etc.) followed by the scheme used by Harris (1937) in parentheses (*Equisetites*, A, B, etc.). The carbon isotope curve is from Hesselbo et al. (2002)

species range truncations at a depositional hiatus, an unconformity also recognized in the Astartekløft section by Dam and Surlyk (1993) and Hesselbo et al. (2002) (Fig. 15.10).

In contrast, in this section McElwain and collaborators claim: (1) a sudden, 85% drop in species diversity at the TJB (based on megafossil plants but not reflected in the palynomorph record); (2) a decrease in the relative abundance of common plant species at the TJB; (3) a change in leaf physiognomy to larger and rounder leaves; (4) an increase in charcoal indicative of wildfire at the TJB; and (5) an increase in chemical damage to sporomorphs at the TJB. They see all but possibly the last of these as indicative of a "super greenhouse" caused by CAMP eruptions.

We question, though, the validity of the correlation of the TJB in the Astartekløft section. McElwain and collaborators place it at about the 47 m level of this section, basing that placement on the carbon isotope record published by Hesselbo et al. (2002) (Fig. 15.10). This record shows an apparent, but modest (~2‰), negative excursion beginning at about the 45 m level. We note that this "excursion" coincides with an unconformity of unknown duration. Hence, the relationship of the isotopic trend above this hiatus to the missing, underlying strata is a mystery. More recently published carbon isotope data (Williford et al. 2014, fig. 1) are very noisy and also fail to identify the TJB in the Astartekløft section.

Nevertheless, Hesselbo et al. (2002) assumed that the base of the excursion represents the "initial isotope excursion" and that the remainder records the "main isotope excursion" seen in marine sections that cross the TJB (e.g., Ruhl et al. 2010). Therefore, the intervening section with a more positive isotopic trend (spanning 4 m at St. Audrie's Bay in England) is conveniently missing. Hence, we regard Hesselbo et al.'s (2002) correlation as tenuous at best. Furthermore, if the initial negative excursion at the ~45 m level in the Astartekløft section is the well documented (in marine sections) negative excursion in carbon then it is not the TJB, but instead a point in the Rhaetian (e.g., Lucas et al. 2007b; Ruhl et al. 2010; Hillebrandt et al. 2013). Thus, all the events McElwain and collaborators associate with the TJB actually preceded it.

The chemostratigraphic correlation proposed by Hesselbo et al. (2002) relies on the presence of an unconformity at 45 m in the Astartekløft section. Questions should be raised about the nature of this unconformity and the temporal magnitude of the hiatus it represents, as well as the associated substantial change in lithofacies (Fig. 15.10). Indeed, we note that most of the megafossil plant assemblages below that level are from mudrock-dominated intervals, whereas those above that level are from sandstone (Fig. 15.10). According to McElwain et al. (2007: 551), the mudrock likely represents floodplain deposits of mainly autochthonous plants, whereas the sandstones represent channel and splay deposits that also include allochthonous plants. However, in evident contradiction to parts of their text and measured stratigraphic section, McElwain et al. (2007, table 1) identify all the plant localities up through their bed 5 as coming from "sheet splay" deposits, the plants from bed 6 as from a coal swamp (though no coal is present in the section at Astartekløft) and their plant beds 7 and 8 as coming from abandoned channels. In the absence of more data (e.g., detailed lithologic descriptions of the plant-bearing strata) and an actual sedi-

mentological analysis of the plant-bearing beds, we are not able to resolve these evident contradictions in McElwain et al. (2007).

Instead, it seems evident that the section at Astartekløft embodies a major lithofacies change at an unconformity, from a mudstone-dominated depositional system to a channel-sandstone dominated system (Fig. 15.10). It preserves two taphofloras in different lithofacies, and this raises the possibility that much of the apparent floral change inferred by McElwain and collaborators is due to the change in the depositional system (lithofacies). Assuming the TJB is present in this section near the 47 m level, the megafossil plant assemblages across the TJB are not "isotaphonomic" (as claimed by McElwain et al. 2007), so they are not strictly comparable to each other in terms of composition, diversity and relative abundance.

According to McElwain and collaborators, a substantial perturbation of plant ecology and diversity is preserved at the TJB in East Greenland. Instead, we conclude that the data they present are indicative instead of a local change in the paleoflora largely driven by lithofacies changes resulting in changing taphonomic filters. No catastrophic land plant extinction is documented and, at most, the floral turnover in East Greenland is nothing more than a local event, as no similar, coeval event is documented elsewhere (Hallam and Wignall 1997; Tanner et al. 2004; Lucas and Tanner 2008; Barbacka et al. 2017). Furthermore, whatever happened to the megaflora in East Greenland occurred prior to the TJB.

In conclusion, no case has been made for a global mass extinction of land plants at the TJB. Some local changes are evident, and the local section in East Greenland, if we treat it as a "best section," only documents local changes not seen elsewhere in Europe (e.g., Barbacka et al. 2017). Steinthorsdottir et al.'s (2015) recent claim that trace fossils on plant substrates (*Paleoscolytus* ichnofacies of Lucas 2016) in East Greenland indicate substantial changes in terrestrial invertebrates across the TJB also can be seen as a local effect not seen outside of East Greenland.

15.6.1.2 Plant Microfossils

Like the megafossil plant record, the palynological record provides no evidence for a mass extinction of land plants at the TJB (Bonis and Kurschner 2012). Indeed, given that the plant microfossils are derived from the plant megafossils, it seems logical that no mass extinction of the megafossil plants at the TJB should be paralleled by no mass extinction evident from the plant microfossils.

Many years ago, Fisher and Dunay (1981) demonstrated that a significant proportion of the *Rhaetipollis germanicus* assemblage that defines the Rhaetian in Europe (e. g., Orbell 1973; Schuurman 1979) persists in lowermost Jurassic strata, and this has since been verified by more recent studies (e.g., Bonis et al. 2009; Cirilli 2010; Kürschner and Herngreen 2010; Bonis and Kurschner 2012). Brugman (1983) and Traverse (1988) thus concluded that floral turnover across the TJB was gradual, not abrupt. Kelber (1998, 2003) described the megaflora and palynoflora for Central Europe in a single unit he termed "Rhaeto-Liassic," and concluded there was no serious disruption or decline in plant diversity across the TJB. More recently,

Bonis et al. (2009) and Kuerschner et al. (2007) documented the transitional nature of the change in palynomorphs across the TJB in the Northern Calcareous Alps of Austria (also see Hillebrandt et al. 2013), and the palynomorph record in East Greenland also does not document an abrupt TJB extinction (Mander et al. 2010). Indeed, a recent review of palynological changes across the TJB by Lindström (2016) identifies different changes at different times in different places, much of it evidently facies driven.

Nevertheless, profound palynomorph extinction at the TJB was long identified in the Newark Supergroup record in eastern North America by Olsen and collaborators (Cornet 1977; Cornet and Olsen 1985; Olsen and Sues 1986; Olsen et al. 1990, 2002a, b; Fowell and Olsen 1993). Their work identified the TJB in the Newark section by a decrease in diversity of the plant microfossil assemblage, defined by the loss of palynomorphs considered typical of the Late Triassic, followed by dominance of the palynoflora by several species of the genus "*Corollina*" (= *Classopollis*), especially *C. meyeriana* (Cornet and Olsen 1985; Olsen et al. 1990; Fowell and Olsen 1993; Fowell et al. 1994; Fowell and Traverse 1995). They thus placed the TJB in the Newark section at the base of the *Classopollis meyeriana* palynofloral zone.

This palynofloral change has been referred to as the "T-J palynofloral turnover" (Whiteside et al. 2007) or the "Passaic palynofloral event" (Lucas and Tanner 2007b). But, as Kozur and Weems (2005: 33) well observed, "there are no age-diagnostic sporomorphs or other fossils to prove that this extinction event occurred at the Triassic-Jurassic boundary." Indeed, Kuerschner et al. (2007) concluded that the Passaic palynolofloral event most likely represents an older, potentially early Rhaetian event, a conclusion shared by Kozur and Weems (2005, 2007, 2010) and by Lucas and Tanner (2007b). Thus, the palynological turnover in the Newark preceded the TJB and was a regional event, not a global mass extinction.

Bonis and Kurschner (2012) provided a comprehensive review of TJB palynological records to conclude that they indicate vegetation changes that are non-uniform (different changes in different places), not synchronous and not indicative of a mass extinction of land plants. They attributed these changes to climate change driven by CAMP volcanism that produced a warmer climate and stronger monsoonal flow across Pangea, which developed drier interiors and wetter coastal regions. As they well put it, "…instead of a major and globally consistent palynofloral extinction event, the Tr/J boundary is characterized by climate-induced quantitative changes in the sporomorph assemblages that vary regionally in magnitude and composition" (Bonis and Kurschner 2012: 256). In sum, there is no evidence of a global mass extinction of land plants at the TJB.

15.6.2 Terrestrial Tetrapods

Colbert (1958) concluded that the temnospondyl amphibians, a significant component of many late Paleozoic and Early-Middle Triassic tetrapod assemblages, underwent complete extinction at the TJB. However, these temnospondyls are only a

minor component of Late Triassic tetrapod assemblages, being of low diversity and relatively small numbers in most stratigraphic units (e.g., Hunt 1993; Long and Murry 1995; Schoch and Milner 2000). Moreover, current data demonstrate the disappearance of most of the temnospondyls—almasaurids, mastodonsaurids, capitosaurids, and trematosaurids—at or before the Norian-Rhaetian boundary, and only two families extinct at the end of the Triassic (metoposaurids and plagiosaurids) (Milner 1993, 1994; Schoch and Milner 2000; also see Lucas 2008, 2017e). Late Triassic temnospondyl extinctions thus largely preceded the TJB.

To Colbert (1958), the bulk of the TJB tetrapod extinction was in the disappearance of the "thecodonts." These "thecodonts" were more recently referred to as the crurotarsans (phytosaurs, aetosaurs [Fig. 15.11] and rauisuchians), although that name is no longer advocated by the latest cladistic analysis (Nesbitt 2011). Phytosaurs, aetosaurs and rauisuchians are the only members of Colbert's "thecodonts" to have a substantial Norian or younger fossil record based on current data. Other groups of thecodonts that have been portrayed by some as going extinct at the TJB either lack Rhaetian records (for example, the Ornithosuchidae: von Baczko and Ezcurra 2013) or have so-called Rhaetian records of problematic age, such as records from British fissure-fill deposits (e.g., Fraser 1994).

A non-"thecodont" group that did go extinct during the Rhaetian is the Procolophonidae. However, procolophonids were a group of low diversity by Norian time, and many of their so-called Rhaetian records are from British fissure fills (e.g., Fraser 1994). The tetrapod taxa from these fissure fills are mostly endemic taxa of no biochronological significance or cosmopolitan taxa with long stratigraphic ranges. As Lucas and Hunt (1994: 340) noted, "a single age should not necessarily

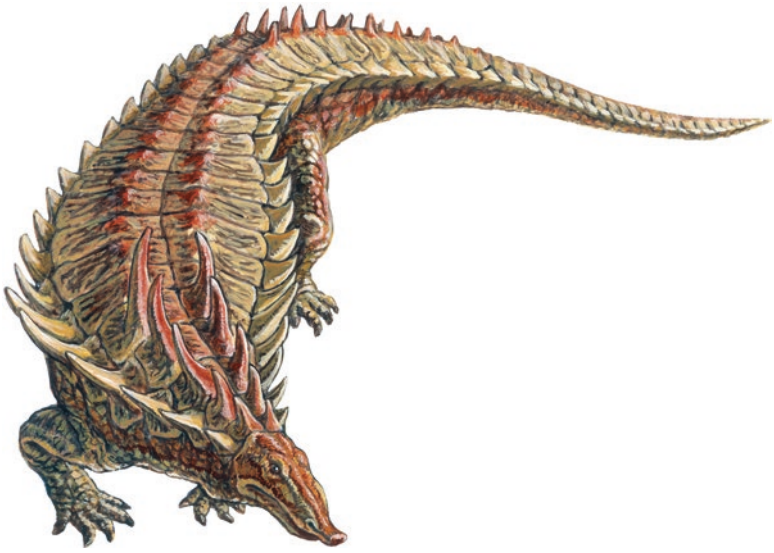

Fig. 15.11 The Late Triassic (Revueltian = Norian) aetosaur *Rioarribasuchus*, representative of the "thecodont" reptiles long thought to have suffered a mass extinction at the TJB. Artwork by Matt Celeskey

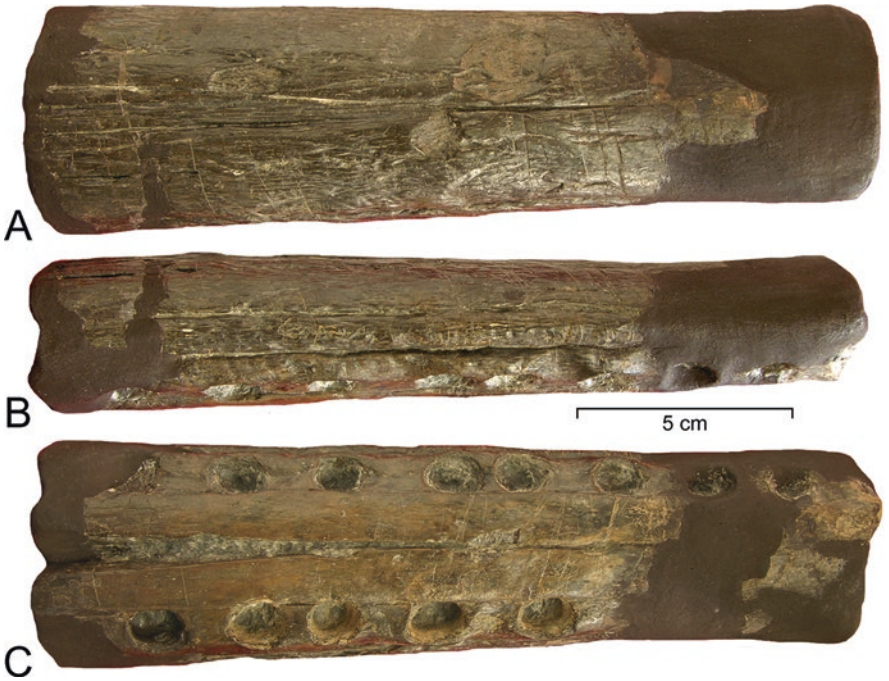

Fig. 15.12 Phytosaur lower jaw fragment from the pre-planorbis beds at Watchet, Somerset, England, in *ventral* (**a**), *lateral* (**b**) and *dorsal* (**c**) views. This fossil, in the collection of the Staatliches Museum für Naturkunde, Stuttgart, Germany (catalogued as SMNS 55194), if not reworked, is evidence that phytosaurs persisted beyond the TJB (see Maisch and Kapitzke 2010). Photographs courtesy of Michael Maisch

be assigned to the fossils from one fissure and…individual fossils from the fissures may range in age from middle Carnian to Sinemurian." We thus regard as problematic the precise age of many of the Triassic tetrapod fossils from the British fissure fills.

Phytosaur fossils are known from Rhaetian-age strata in the Newark basin, the Glen Canyon Group in the western USA and the Germanic basin (e.g., Olsen et al. 2002a, b; Lucas and Tanner 2007a; Stocker and Butler 2013). A Lower Jurassic phytosaur record has been documented by Maisch and Kapitzke (2010). This is an unabraded snout fragment found in the lowermost Jurassic pre-planorbis beds (*Neophyllites* zone) at Watchet in England (Fig. 15.12). Stocker and Butler (2013) expressed skepticism about the stratigraphic provenance of this record, and it may be a reworked fossil, a possibility, that while unlikely (given the preservation of the fossil), is difficult to test. Instead, we accept that it documents phytosaur persistence into the earliest Jurassic, contradicting the longstanding assumption of their extinction at the TJB.

There are no demonstrable aetosaur or rauisuchian body fossils in Rhaetian strata (Lucas, 2010b; Desojo et al. 2013; Nesbitt et al. 2013), although Nesbitt et al. (2013) mentioned a possible Early Jurassic rauisuchian from southern Africa, based on a

single snout fragment that they stated may also be of a large crocodylomorph. Aetosaur and rauisuchian body fossil records primarily suggest their extinction before Rhaetian time.

Nevertheless, the footprint ichnogenus *Brachychirotherium* is known from Rhaetian strata, and Lucas and Heckert (2011) argued that an aetosaur was the trackmaker. We note that Smith et al. (2009) reported what they identified as chirothere tracks from the Lower Jurassic Elliot Formation of Lesotho in southern Africa, but as Klein and Lucas (2010) noted, the described tracks differ from chirothere footprints in significant ways and are more likely large crocodylomorph tracks.The available stratigraphic data thus suggest a three step extinction of the "crurotarsans"—first, rauisuchians by the end of the Norian, second, aetosaurs (based on the footprint ichnogenus *Brachychirotherium*) by the end of the Rhaetian and third, phytosaurs in the early Hettangian.

Synapsids of the Late Triassic are dicynodonts and cynodonts (e. g., Lucas and Hunt 1994; Lucas and Wild 1995; Abdala and Ribeiro 2010; Abdala and Gaetano 2017). Most Late Triassic dicynodont records are Carnian, with rare post-Carnian records as young as late Norian (Lucas and Wild 1995; Dzik et al. 2008; Lucas 2015). The Late Triassic cynodont record is more extensive, especially in Gondwana. Traversodontids have a relatively diverse record in the Carnian-Norian and a single Rhaetian record (we note that the Gondwana cynodont-bearing strata assigned a Rhaetian age by Abdala and Ribeiro (2010) are actually Norian: Lucas 2010b). Trithelodontids and tritylodontids cross the TJB, and a problematic group of tooth-based taxa, the "dromatheriids," disappears in the Rhaetian (Lucas and Hunt 1994). Note, though, that the origin and diversification of "mammaliaforms," which likely include the "dromatheriids," began in the Late Triassic (e.g., Newham et al. 2014). On present evidence, a TJB synapsid extinction is thus of a handful of taxa, with most taxa already extinct by Rhaetian time.

15.6.3 Newark Supergroup Record

The recent case for a mass extinction of tetrapods at the TJB has relied heavily on the Newark Supergroup record of tetrapod fossils (e.g., Olsen and Sues 1986; Silvestri and Szajna 1993; Szajna and Silvestri 1996; Olsen et al. 1987, 1990, 2002a, b; Sues and Olsen 2015). However, a close examination of all Triassic tetrapod taxa known from the Newark Supergroup identifies only three body-fossil taxa (indeterminate phytosaurs, the procolophonid *Hypsognathus* and sphenodontians) in the youngest Triassic strata, which are strata of Rhaetian age (Huber et al. 1993; Lucas and Huber 2003; Kozur and Weems 2010; Weems et al. 2016) (Fig. 15.13). Recent collecting has not changed that, and only a few fragmentary tetrapod fossils are known from the Newark extrusive zone and are not age diagnostic (Lucas and Huber 2003; Lucas and Tanner 2007b).

The McCoy Brook Formation, which overlies the only CAMP basalt of the Fundy basin in Nova Scotia, yields a tetrapod assemblage generally considered

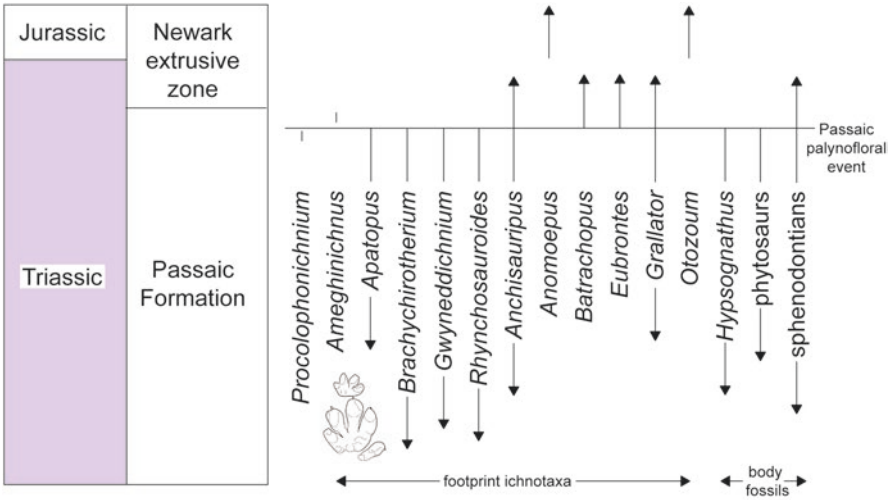

Fig. 15.13 Stratigraphic ranges of tetrapod footprint ichnogenera and body fossil taxa across the Late Triassic (Rhaetian) Passaic palynofloral event in the Newark section. Modified and updated after Olsen et al. (2002a) and Lucas and Tanner (2015)

Early Jurassic in age by vertebrate paleontologists (Olsen et al. 1987; Shubin et al. 1994; Lucas 1998; Lucas and Huber 2003; Lucas and Tanner 2007a, b) However, this assemblage could straddle the marine-defined TJB given that Cirilli et al. (2009) demonstrated that at least the lowermost McCoy Brook strata are Rhaetian.

The Newark body fossil record of tetrapods thus is sparse across the TJB and inadequate to evaluate a possible tetrapod extinction, so the tetrapod footprint record in the Newark Supergroup has been used as a proxy (e.g., Olsen and Sues 1986; Szajna and Silvestri 1996; Olsen et al. 2002a, b). However, detailed stratigraphic study of the Newark footprint record indicates nothing more than moderate turnover in the footprint assemblage at a within-Rhaetian stratigraphic level below the lowest CAMP basalt sheet (Fig. 15.13). Similar changes in tetrapod footprint assemblages are also known from the Chinle Group-Glen Canyon Group section of the American Southwest and from the Germanic Basin (e. g., Lucas et al. 2006; Lucas 2007).

The footprint turnover in the Newark section (Fig. 15.13) is supposedly the disappearance of four ichnogenera in the uppermost Passaic Formation, and the appearance of three ichnogenera at that datum (Olsen et al. 2002a, b). The ichnogenera that disappear represent phytosaurs (*Apatopus*: Klein and Lucas 2013), aetosaurs (*Brachychirotherium*: Lucas and Heckert 2011) and tanystropheids (*Gwynnedichnium*: Lucas et al. 2014). There are single Newark records of *Procolophonichnium* (procolophonid: Baird 1986; Klein et al. 2015) just below the turnover level and a single record of *Ameghinichnus* (mammaliaform: de Valais 2009) above that level.

According to Olsen et al. (2002a, b), the ornithischian dinosaur footprint ichnogenus *Anomoepus* first appears at this level, but a later detailed review of the ichno-

genus by Olsen and Rainforth (2003) indicated that the lowest stratigraphic record of *Anomoepus* is stratigraphically higher, in the Newark extrusive zone (Fig. 15.13). The crocodylomorph footprint ichnogenus *Batrachopus* appears at this level, but there are older Triassic body fossil records of crocodylomorphs (Klein and Lucas 2010). Olsen et al. (2002a, b) showed the prosauropod-dinosaur-footprint ichnogenus *Otozoum* appearing in the upper Passaic Formation, but a later revision of the ichnogenus by Rainforth (2003) established its stratigraphically lowest record as Jurassic, in the Newark extrusive zone (Fig. 15.13). The lacertoid footprint ichnogenus *Rhynchosauroides* has its last Newark record in the upper Passaic Formation, but this ichnogenus has Jurassic records elsewhere (Avanzini et al. 2010).

Thus, what the Newark tetrapod footprint and body-fossil record shows is the local extinction of phytosaurs (they have a younger record elsewhere), aetosaurs, tanystropheids and procolophonids (this may be the level of their global extinction). That is the extent of the turnover in tetrapod taxa it documents, and the turnover level in the Newark is at a Rhaetian horizon, not at the TJB (Fig. 15.13).

Part of the footprint turnover in the Newark section is the local lowest occurrence of the theropod footprint ichnogenus *Eubrontes* (as defined by Olsen et al. 1998, i.e., tridactyl theropod pes tracks longer than 28 cm). For decades, much was made of this record of *Eubrontes*. Thus, Olsen and Galton (1984) concluded that the lowest occurrence of *Eubrontes* is the base of the Jurassic, and Olsen et al. (2002a, b) later argued that the sudden appearance of *Eubrontes* in the "earliest Jurassic" strata of the Newark Supergroup indicates a dramatic size increase in theropod dinosaurs at the TJB. They interpreted this as the result of a rapid (thousands of years) evolutionary response by the theropod survivors of a mass extinction and referred to it as "ecological release" (Olsen et al. 2002a: 1307). They admitted that this can be invalidated by the description of *Dilophosaurus*-sized theropods or diagnostic *Eubrontes* tracks in verifiably Triassic-age strata.

Indeed, tracks of large theropod dinosaurs assigned to *Eubrontes* (or its possible synonym *Kayentapus*) are known from the Triassic of Australia, Africa (Lesotho), Europe (Great Britain, France, Italy, Germany, Poland-Slovakia, Scania) and eastern Greenland, invalidating the "ecological release" hypothesis (Lucas et al. 2006; Niedźwiedzki 2011; Bernardi et al. 2013). A detailed review of these records indicates Carnian, Norian and Rhaetian occurrences of tracks that meet the definition of *Eubrontes* established by Olsen et al. (1998). Also, theropods large enough to have made at least some *Eubrontes*-size tracks have long been known from the Late Triassic body-fossil record (e.g., Langer et al. 2009). Thus, the sudden abundance of these tracks in the Newark Supergroup cannot be explained simply by the rapid evolution of small theropods to large size following a mass extinction. The concept of a sudden appearance of *Eubrontes* tracks due to "ecological release" at the TJB proposed by Olsen et al. (2002a, b) thus can be abandoned, though some workers (e.g., Barras and Twitchett 2016) continue to endorse it.

15.7 Ecology of the Extinctions

15.7.1 Severity of the Extinctions

McGhee et al. (2004, 2013) made the valuable point that not only should mass extinctions be evaluated in terms of biodiversity crises, but also in terms of their ecological severity. In their scheme of ecological severity, they evaluated the marine TJB extinction as category IIa and the continental TJB extinction as category I or IIa. Category I means that ecosystems before the extinction were replaced by new ecosystems post-extinction, whereas category IIa means that the extinctions caused permanent loss of major ecosystem components.

McGhee et al. (2004: 291) rated the TJB marine extinction as category IIa because of the "virtual elimination of the global reef component of marine ecosystems." However, as discussed above, this disruption was not demonstrably global and it was demonstrably temporary. Therefore, we downgrade the TJB marine extinction to category IIb in their classification, which means that the disruption was temporary; i.e., the reef ecosystem re-established itself after a hiatus.

McGhee et al. (2004: 293) regarded characterizing the ecological severity of the nonmarine TJB extinction as "more problematic" than their characterization of the marine TJB extinction. Despite this, they concluded that the TJB transition involved a rapid ecological replacement of Triassic mammal-like reptiles and rhynchosaurs by dinosaurs. However, rhynchosaurs are now known from the early Norian (Spielmann et al. 2013), and dicynodonts are now known from the late Norian (Lucas 2015), unless a putative Cretaceous record (with problematic provenance) from Australia is verified (Thulborn and Turner 2003). The other principal group of Late Triassic mammal-like reptiles, the cynodonts, were of low diversity after the Carnian (Lucas and Hunt 1994; Abdala and Gaetano 2017). Dinosaurs appeared as body fossils in the Carnian and began to diversify substantially in some parts of Pangea by the late Norian (e.g., Hunt 1991; Langer et al. 2009). Thus, the ecological severity of the end-Triassic tetrapod extinction is relatively low (Category IIb on the McGhee et al. 2004 classification), and the plant extinctions also do not appear ecologically severe (see above). Clearly, there was some disruption of the terrestrial ecosystem across the TJB, but it was not severe.

15.7.2 Structure of the Extinctions

The above makes it clear that there is no single mass extinction of any element of the global biota at the TJB. The closest to such an event is the turnover of radiolarians. Bivalve and ammonoid extinctions were stepwise during the Late Triassic, with the most severe extinction at or very close to the Norian-Rhaetian boundary. The same is true of tetrapods, with most of the tetrapod taxa envisioned as part of a mass extincton at the TJB gone at or before the Norian-Rhaetian boundary.

Furthermore, much of the turnover in the terrestrial tetrapod biota is older than the marine extinction events (Lucas et al. 2011).

Clearly, the end of the Triassic did not see the collapse of trophic systems on land or in the sea. The lack of a mass extinction of land plants makes it difficult to envision a collapse of the metazoan trophic structure that relied on plants as the primary sources of food. Similarly, there was no mass extinction of the oceanic plankton, so there also was no collapse of marine food chains.

15.8 Mechanisms of Extinction

The fossil record of Late Triassic extinctions demonstrates the combined effects of a protracted interval of decreased origination rates, punctuated by several brief, but more intense intervals of elevated extinction, the last of these occurring near the end of the Rhaetian. The protracted interval of decreased origination implies gradualistic mechanisms of environmental change that operated over millions to tens of millions of years; i.e., long-term ecological changes of the sort that might result from sea-level fluctuation or climate change. Both of these were well-reviewed by Tanner et al. (2004) and remain viable hypothesese to explain the Late Triassic extended background of increased extinction and decreased rates of species origination.

15.8.1 Gradual Changes

Falling sea-level, with consequent reduction in the available shallow marine habitat, has long been advocated as an extinction-forcing mechanism (Newell 1967; Hallam 1989, 1992, 1998, 2001; Hallam and Wignall 1997, 1999, 2000), although McRoberts et al. (1997) suggested that sea-level change may result in a decline in diversity through changes in: (1) sediment substrate, (2) water temperature, and (3) salinity, rather than through the loss of habitat area. Significant facies changes that suggest regression followed by transgression at the end of the Triassic can be observed in many of the classic marine boundary sections in Europe, implying that sea-level change may have been involved in the end-Triassic extinctions. However, Hallam (1990, 2001) and Hallam et al. (2000) suggested that regression with consequent habitat loss in Western Europe was only a regional effect, a consequence of the thermal uplift of the region surrounding the Atlantic rift prior to the initiation of magmatism. Tanner et al. (2004), in their review found no evidence that this was a global event, although some boundary sections outside of Europe do display facies changes at the TJB that may reflect sea-level change on a broader scale (e.g. Hönig et al. 2017).

Gradual climate change also was invoked to explain Late Triassic tetrapod turnover, initially by Colbert (1958) and later by Tucker and Benton (1982). Most reconstructions of the Pangean climate for the Late Triassic suggest a largely azonal

pattern of climate with mainly dry equatorial and continental interior regions and humid belts at higher latitudes and around the Tethyan margin (Parrish and Peterson 1988; Crowley et al. 1989; Kutzbach and Gallimore 1989; Dubiel et al. 1991; Parrish 1993; Fawcett et al. 1994; Tanner 2017). Precipitation across Pangea apparently was strongly seasonal, powered by a strong monsoonal effect (Kutzbach and Gallimore 1989; Parrish 1993) that was enhanced during the Late Triassic by the location of the Pangean supercontinent neatly bisected by the equator (Parrish 1993). Simms and Ruffell (1990) specifically attributed the cessation of humid climate conditions at the end of the Carnian as the cause of a significant biotic turnover at the Carnian-Norian boundary. This interpretation is consistent with reports of increasing aridity during the Late Triassic from formations deposited at low paleolatitudes and in the interior regions of Pangea (see Tanner 2017, this volume, for additional details).

15.8.2 Bolide Impact

Beginning in the 1980s, the hypothesis was advanced that the end-Triassic extinctions were associated with a single catastrophic cause, specifically, the Manicouagan bolide impact that left the ca. 70 km remnant crater in southern Quebec, Canada (Olsen et al. 1987). Despite radioisotopic dating that indicated an age of ca. 214 Ma for the crater, substantially older than the TJB (Hodych and Dunning 1992), Olsen et al. (2002a, b) continued to advance this hypothesis. They cited as evidence for a correlation between the impact and the extinctions the occurrence of elevated Ir levels, at hundreds of pg/g (= parts per trillion), in strata just below the zone of maximum palynological turnover in the Newark basin (the Passaic palynofloral event below the oldest CAMP volcanics in this basin; Fig. 15.13). However, this hypothesis has been disproved firmly by more recent radioisotopic dating of the Manicouagan structure at 215.5 Ma and identification of an ejecta layer with a substantial Ir anomaly dating to the late middle Norian (Ramezani et al. 2005; Onoue et al. 2012, 2016; Sato et al. 2016).

Notably, the Manicouagan structure is not the only Upper Triassic impact crater. The Rochechuoart impact structure has been dated to 201 ± 2 Ma, encompassing the system boundary (Schmieder et al. 2010), but the limited size of the structure, 15–20 km, indicates that it could not have had a substantial role in end-Triassic biotic decline (Jourdan 2013). Nevertheless, the Rochchouart impact could have been the source of the shocked quartz grains reported by Bice et al. (1992) in the Calcare à *Rhaetivicula* below the system boundary marl at a section near Corfino in Tuscany. However, it is unlikely to have been the origin of the Ir concentrated near the boundary, as the Rochechouart impactor is considered likely to have been nonmagmatic iron, not chondritic (Tagle et al. 2009). The Ir enrichment detected initially by Olsen et al. (2002a, b) has been found in a similar stratigraphic position below the CAMP volcanics in the Fundy basin by Tanner and Kyte (2005) and Tanner et al. (2008), who posited that the Ir was associated with the volcanism of

CAMP, potentially via outgassing (also see Weems et al. 2016). More recently, Tanner et al. (2016) identified a similar enrichment in marine strata of the Eiberg basin (at the base Hettangian GSSP section at Kuhjoch, Austria) at a stratigraphic level above that described from the Newark and Fundy basins and posited that the CAMP volcanics also may have been the source. No impact debris is associated with any of the Ir anomalies bracketing the system boundary, thus an impact origin for the Ir is unlikely.

15.8.3 CAMP Volcanism

15.8.3.1 Size and Age of CAMP

The attention in the study of the end-Triassic extinctions in recent years has focused primarily on the environmental effects of the eruption of the flood basalts of the Central Atlantic Magmatic Province (CAMP) (Fig. 15.14). Once assumed to post-date the TJB (Whiteside et al. 2007), it is now well-established that the CAMP eruptions span the system boundary (Kozur and Weems 2005, 2007, 2010; Lucas and Tanner 2007b; Cirilli et al. 2009). Within the basins of the Newark Supergroup, the eruptions proceeded in three main episodes, separated by eruptive hiatuses during which sediments accumulated, with the majority of the total lava volume ejected during the initial eruptive episode (Marzoli et al. 2011).

The size of the igneous province was initially estimated by McHone and Puffer (1996) at ca. 2.3×10^6 km^2. Subsequently, Deckart et al. (1997) and Marzoli et al. (1999) expanded the size of the province to include all regions proximal to the rift margin that contain mafic intrusions of approximately correlative age. This method outlined an area of around 11×10^6 km^2 and allowed a maximum estimate of the erupted lava volume of ca. 2×10^6 km^3, coincidentally similar to the volume calculated for the Deccan Traps. As noted by Huber (1997) and Tanner et al. (2004), however, this calculation assumes that the entire area outlined by these mafic flows and intrusions was covered by lava to an average depth of several hundred meters. This assumption is somewhat difficult to defend given that even in basins where the entire erupted thickness is preserved, such as the Newark basin, the total thickness of the flows varies widely, from >1 km to as little as tens of meters. Moreover, only in the rift basins are the flows well-preserved. Hence, there is no way of measuring directly the thickness of the flows in the much larger area of the province outside of the basins.

In the Newark basins of eastern North America, the CAMP eruptions are represented by up to three distinct eruptive units, each typically consisting of multiple flow units, but radioisotopic dates consistently indicate that the peak eruptive activity occupied a narrow interval of time (see Marzoli et al. 2017). Olsen et al. (1996) correlated between basins, using cyclostratigraphy, and, based on their inferred astrochronology, calculated a duration of volcanic activity of no more than ca. 600

Fig. 15.14 The North Mountain Basalt (Talcott Formation of Weems et al. 2016) from the north shore of the Minas basin in Nova Scotia, Canada is a characteristic CAMP basalt. This is the only CAMP extrusive basalt sheet in the Fundy basin

Ka. Further, they suggested that CAMP eruptions in the Argana basin of Morocco were synchronous with those of the Newark basins.

Strict synchroneity of the CAMP eruptions across the entire province as mapped is a point of contention. Thus, $^{40}Ar/^{39}Ar$ dates for the South American basalts published by Marzoli et al. (1999) display a wide range of ages (from 190.5 ± 1.6 to 198.5 ± 0.8 Ma) as do dikes from the same regions (191.5 ± 0.9–202.0 ± 2 Ma). Although the synchroneity proposed for the eruptions in the Newark basins (within 600 Ka) is not transferrable to the South American data, there remains broad support for assuming that most of the volume of lava was erupted over a period substantially less than 1 million years (Marzoli et al. 2017). Most recently, Thibodeau et al. (2017) documented the presence of elevated Hg levels in the section at Muller Canyon, New York Canyon area (Nevada) that crosses the TJB. The elevated concentration begins in the interval of late Rhaetian extinction and extends upward above the first appearance of psiloceratid ammonoids, continuing through the depauperate interval above the boundary. Isotopic ratios of the Hg confirm a volcanic origin, leading the authors to conclude that CAMP activity is linked to the extinctions, and that continuation of the activity for hundreds of thousands of years hampered biotic recovery.

15.8.3.2 Carbon Isotope Record

Notable in the investigations of the end-Triassic extinctions and a potential link to the CAMP eruptions was the identification in TJB sections of a negative carbon isotope excursion (CIE) in the $\delta^{13}C$ record (typically ca. −3.5‰) in both marine carbonate and organic carbon. A significant negative CIE has been identified in a number of marine sections in close proximity to the Rhaetian-Hettangian boundary. For example, the sections at St Audrie's Bay, southwest England (Hesselbo et al. 2002, 2004), Csövár, Hungary (Pálfy et al. 2001), and several sections in the Northern Calcareous Alps of Austria (Kuerschner et al. 2007; Ruhl et al. 2009) display a negative $\delta^{13}C_{org}$ excursion of approximately 2.0–4.0‰ from a baseline that generally varies from −26 to −29‰. Typically, these excursions begin below the highest occurrence of conodonts and Triassic ammonites (e.g. choristocerids), supporting their correlatability, and also consistently below the lowest occurrence of Jurassic (psiloceratid) ammonites, which demonstrates unequivocally that the perturbation of the carbon cycle that caused the CIE occurred before the biostratigraphic system boundary, as presently defined (the FAD of *Psiloceras spelae*). Characteristically, the excursion continues upward into basal Hettangian strata and is succeeded by a strong positive excursion, as at Ferguson Hill, Nevada, USA (Guex et al. 2004; Ward et al. 2007), St. Audrie's Bay, UK (Hesselbo et al. 2002, 2004) and Kennecott Point, Queen Charlotte Islands, Canada (Ward et al. 2001, 2004). A similar negative excursion of $\delta^{13}C_{carb}$ has been demonstrated in the uppermost Rhaetian in several other sections (e.g., Pálfy et al. 2001; Galli et al. 2005, 2007). However, these data generally are of somewhat lower resolution than the $\delta^{13}C_{org}$ data because lithologic considerations and/or diagenesis limit the sampling density.

A negative CIE recorded by $\delta^{13}C_{org}$ in terrestrial environments has been claimed as correlative with that in the marine realm (McElwain et al. 1999; Hesselbo et al. 2002). Implicit in this correlation is the assumption that both marine and $\delta^{13}C_{org}$ terrestrial CIEs resulted from a dramatic alteration of the $\delta^{13}C$ of the global ocean/atmosphere carbon reservoir that was recorded similarly by vascular plants. The earlier data underlying this hypothesis were critiqued by Lucas and Tanner (2015), who found them unconvincing. Indeed, the isotopic data from plant macrofossils for sections in Scania spanning the system boundary do not display a distinct CIE, and although the $\delta^{13}C$ data from Greenland (McElwain et al. 1999; Hesselbo et al. 2002; Williford et al. 2014) display an apparent trend that appears to correlate with the marine data, this trend is based on very few samples and lacks the consistency that is displayed in the marine record. Furthermore, identification of the position of the system boundary in terrestrial sections is not nearly as straightforward as it is in the marine realm (Lucas and Tanner 2015). Hence, precise correlation of the isotopic curves between the marine and terrestrial realms can only be speculative.

Earlier studies of the change in δ^{13} in terrestrial organic matter (e.g., McElwain et al. 1999) were conducted on bulk organic matter, thus failing to account for potential changes caused by changes in plant assemblage across the TJB. Bacon et al. (2011) attempted to rectify this by conducting taxon-specific analyses. Their

analyses of wood (from Gingkoales and Bennettitales) found a decrease in δ^{13} of −2.5 at the base of the Thaumatopteris zone in East Greenland. More recently, Williford et al. (2014) have presented new data using compound-specific $\delta^{13}C$ and $\delta^{2}H$ analyses of organic remains from a nonmarine boundary section in East Greenland that supports the hypothesis of strong environmental change at or near the system boundary, although the isotopic trends are still not as clear cut as in many marine sections.

15.8.3.3 CAMP Outgassing

Most authors now attribute both the end-Triassic extinctions and the closely associated CIE to outgassing during the CAMP eruptions. For example, McElwain et al. (1999) suggested a major role of CAMP degassing of isotopically light CO_2 in producing the isotopic shift and blamed the extinctions exclusively on subsequent greenhouse warmng. In support of their hypothesis, they presented stomatal indices data collected from plant cuticle fossils in the East Greenland boundary section that they interpreted as demonstrating a roughly four-fold increase in pCO_2 across the boundary. Beerling and Berner (2002) used mass balance equations to determine that volcanic outgassing of 8–9 × 10^3 Gt C as CO_2 from CAMP was required to produce the pCO_2 increase interpreted by McElwain et al. (1999). Steinthorsdottir et al. (2011) refined the pCO_2 calculation based on the use of taxon-specific stomatal indices, finding a sharp decrease in the indices for gingkos, bennettitales and others at the presumed system boundary in East Greenland. These data led them to interpret a pCO_2 rise from 1000 ppm to 2000–2500 ppm, followed by a recovery to pre-boundary levels. Subsequent authors (e.g. Pálfy et al. 2001) have critiqued this hypothesis and found that large volumes of mantle-derived CO_2, which typically has $\delta^{13}C = -5$ to $-6‰$, are unlikely to have produced an isotopic shift of the observed magnitude and invoke the release of biogenic CH_4, which typically is much lighter ($\delta^{13}C = -60‰$) to explain the isotopic shift. Beerling and Berner (2002), for example, suggested that the warming initially forced by CAMP outgassing of CO_2 triggered the release of 5 × 10^3 Gt of CH_4 from sea-floor deposits (clathrates). At this time, it remains unresolved to what extent, if any, the release of CH_4 played in the events at the end of the Triassic.

Evaluating the environmental effects of outgassed CO_2 demands estimating in realistic terms the volume of CO_2 released by the eruptions, and the rate at which it was released. Given the speculative nature of the estimates of the volume of CAMP erupted lava, all estimates of outgassed volatiles similarly should be regarded as speculative. Tanner et al. (2004) used an eruptive volume of 2.3 × 10^6 km^3 of CAMP basalt with a mean CO_2 content of 0.066 wt% (from rock analyses by Gottfried et al. 1991) of which 80% was released by outgassing (from Thordarson et al. 1996) to calculate a potential release of 8.2 × 10^{16} mol of CO_2 (equivalent to ca. 1 × 10^3 Gt C). This is just slightly lower than McHone's (2003) calculation of 1.2 × 10^{17} mol (1.4 × 10^3 Gt C) based on measurement of a higher magmatic CO_2 content (from Grossman et al. 1991). Notably, Hartley et al. (2014) critiqued the work of

Thordarson et al. (1996), concluding that the earlier work overestimated the proportion of CO_2 released by flood basalts, perhaps by as much as 15%. Hence, the total mass of CO_2 outgassed during the entirety of the CAMP eruptions could be significantly less than calculated using the assumptions above.

As noted by Tanner et al. (2004, 2007), early attempts at the reconstruction of atmospheric change due to CAMP outgassing gave no consideration of the effects of SO_2 outgassing during the eruptions. Tanner et al. (2007) further demonstrated that high atmospheric SO_2 loading also can force changes in plant stomatal frequency, an effect initially denied but eventually noticed by other workers. We note that Bonis et al. (2010) estimated the pCO_2 from stomatal indices data (collected from *Gingko* and *Lepidopteris*) to reconstruct an increase in pCO_2 across the TJB from 1650 ppm to 2750 ppm, in contrast to the conclusions of McElwain et al. (1999), who projected a nearly four-fold increase (from 600 ppm to 2100–2400 ppm), but the authors acknowledged the potential influence of SO_2 on stomatal indices, meaning that this estimate could be somewhat inflated. Importantly, Bacon et al. (2013) noted that changes in leaf morphology at the TJB suggest the influence of greatly increased SO_2 levels.

The environmental effects of large sulfur emissions during prolonged flood basalt eruptions are not entirely clear, but the formation of H_2SO_4 aerosols, which in addition to causing acidic precipitation, are known to increase atmospheric opacity and result in reduced short-wave radiant heating, causing global cooling (Sigurdsson 1990). Unfortunately, the behavior of volcanic sulfur and the consequent aerosols is less predictable than that of CO_2, so the effects are even more difficult to quantify. Sulfur emitted as SO_2 during the CAMP eruptions may have been injected into the stratosphere, driven upward convectively by the heat of the eruptions (Woods 1993; Parfitt and Wilson 2000), but the effects of such long-term sulfur emissions are not clear. The conversion of SO_2 to H_2SO_4 aerosols in the stratosphere is considered an important mechanism of global cooling because of the increased atmospheric opacity from the aerosol droplets and the consequent reduction in radiant heating (Sigurdsson 1990). These aerosols typically have short residence times in the troposphere, only weeks, because they are washed out quickly. In contrast, they may reside much longer, for periods of several years, in the stratosphere, so the effects of continuing eruptions may be cumulative. Most recently, Schmidt et al. (2016) modeled that LIP eruptions at the scale of CAMP and Deccan may release 2.4 Gt SO_2 a^{-1} for decades at a time, the conversion of which to aerosols may force a net radiative decrease of -16.2 W m^{-2}, resulting in a potential 4.5° cooling over decadal intervals. The SO_2 to H_2SO_4 conversion reaction is self-limiting, however, controlled by the availability of atmospheric oxidants in the upper atmosphere; therefore, the climatic response to an increased supply of SO_2 is predicted to be nonlinear at larger scales or over longer time intervals. Nonetheless, short-term cooling coinciding with effusive eruptive episodes is a predicted consequence of pulsed CAMP activity.

The potential for severe short-term cooling from outgassed SO_2 has implications for the estimation of pCO_2 from a different proxy, the isotopic composition of pedogenic carbonate. Schaller et al. (2011) analyzed the isotopic composition of

pedogenic calcite in the sediments interbedded with the CAMP volcanics, and, using the diffusion model of Cerling (1992), calculated that atmospheric pCO_2 rose from 2000 ppm to 4400 ppm after the extrusion of each flow unit, following which pCO_2 decreased over time, perhaps 300 years, to pre-eruption levels. They accounted for the proposed increase in pCO_2 by an initial pulse of outgassed CO_2 equivalent to 1.12×10^{19} g (equivalent to 3.05×10^3 Gt C), a mass greater than the calculated total CO_2 release from all CAMP eruptions, as presented above. Subsequently, Schaller et al. (2012) refined and presented this analysis in greater detail, thus permitting a more thorough critique of the work. Importantly, in calculating the pCO_2 using the diffusion model (Cerling 1992), they assumed a constant temperature and constant S(z) (rate of soil CO_2 production) during all soil carbonate formation. However, this simplifying assumption, made for the convenience of the calculations, is unjustifiable. Temperature following each major eruptive episode would be expected to decrease sharply due to the cooling effects of sulfate aerosols from the outgassed SO_2, followed by CO_2-forced warming as the aerosols were removed from the atmosphere. Accompanying the temperature changes would have been sharp changes in precipitation, specifically drying during the cooling episodes, followed by moist conditions during the warming events. Thus, calcrete formation in decades immediately following major eruptive episodes likely occurred during drier conditions, for which the soil productivity was lower, e.g., S(z) = 1500. Use of an inflated value for S(z) would result in an inflated estimate of pCO_2. Consequently, Schaller et al.'s calculation of total CAMP outgassing of 3.36×10^{19} g CO_2, essentially identical to the estimate of Beerling and Berner (2002), must be regarded as greatly overestimated, perhaps by a factor of six or more.

Early attempts to reconstruct the rise in pCO_2 across the TJB, while grossly overestimating the potential increase (e.g., Yapp and Poths 1996; McElwain et al. 1999), focused on catastrophic CO_2-forced greenhouse warming as the primary extinction mechanism. Later studies have largely tempered the estimated pCO_2 increase, but maintain that the atmospheric change was a strongly contributing environmental disturbance. For example, Steinthorsdottir et al. (2011) projected an increase of 1000–1500 ppm from pre-CAMP levels, and associated this with a mean global temperature increase of at least 2.5 °C (after Berner and Kothavala 2001). The occurrence of abundant charcoal near the boundary in some terrestrial boundary sections has been cited as evidence of catastrophic climate change (Belcher et al. 2010; Petersen and Lindström 2012), but these interpretations fail to present sufficient stratigraphic context to demonstrate clearly that these charcoal abundances represent anomalous concentrations. Tanner and Lucas (2016), for example, presented data that showed wildfire was common regionally through much of the Late Triassic, which they attribute to long-term climate trends, specifically, increased aridity. Additionally, Pálfy and Kocsis (2014) noted that increased fire frequency is more likely to promote floral diversity, rather than suppress it, as is apparently the case in the East Greenland and Danish sections (Belcher et al. 2010; Petersen and Lindström 2012). Stronger evidence for warming at the boundary is provided by the long-noted change in clay mineralogy in which the proportion of kaolinite increases sharply (van de Schootbrugge et al. 2009; Pieńkowski et al. 2012; Zajzon et al.

2012). Ostensibly, this increase resulted from strongly tropical weathering conditions under the enhanced greenhouse climate following the eruptions. However, Pálfy and Kocsis (2014) also remarked that weathering on land would be similarly enhanced by the acidification of the surface environment by SO_2 released by the CAMP eruptions. Hence, there remains no conclusive estimate of the extent of CO_2-forced warming at the TJB.

15.8.3.4 Environmental Consequences

Regardless of the uncertainties in the magnitude of the atmospheric change, an environmental perturbation was certainly triggered by CO_2 and SO_2 outgassing during the CAMP eruptions. Increased atmospheric opacity from the formation of reflective H_2SO_4 aerosols caused short-lived, but intense cooling, accompanied by acid fallout that had deleterious effects on vegetation and enhanced chemical weathering on land. The longer-lasting CO_2 loading of the atmosphere contributed to enhanced radiative forcing and the consequent warming, suggested as contributing to increased chemical weathering, and acidification of ocean waters. This last effect has been cited by numerous authors as creating a "calcification crisis" that produced the oft-cited "carbonate hiatus" seen at the TJB in many marine sections (Hautmann 2004b; Kiessling et al. 2007; van de Schootbrugge et al. 2007, 2008, 2009, 2013; Schaltegger et al. 2008; Ruhl et al. 2010, 2011; Martindale et al. 2012; McRoberts et al. 2012; Pieńkowski et al. 2012; Pálfy and Zajzon 2012; Richoz et al. 2012).

The immediate effect of acidic fallout from CAMP outgassing would have been negligible in the marine environment (Schmidt et al. 2016), but the long residence time of CO_2 in the atmosphere would allow a long-term build-up that theoretically could result in decreased $CaCO_3$ saturation of the ocean waters. Whether this would have been sufficient to affect the whole ocean is somewhat problematic. Ikeda et al. (2015) have suggested that this was indeed the case, as they interpret the loss of authigenic hematite in deep-sea cherts (in Japan) at the level of the end-Triassic extinctions as due to deep-ocean acidification. But, in modeling the presumed $CaCO_3$ undersaturation of the entire ocean, Berner and Beerling (2007) estimated a requirement for the release of 21×10^3 Gt C (as CO_2) and 57×10^3 Gt S (as SO_2), and acknowledged that production of these masses by CAMP outgassing is largely unlikely. Greene et al. (2012) projected that an increase in pCO_2 from 2000 ppm to 3000 ppm at the boundary, a change more consistent with the proxies, could cause some degree of undersaturation, but only if the dissolved inorganic carbon concentration of the ocean was already low. Most recently, Bachan and Payne (2016) ran a carbon cycle box model run and concluded that the negative CIE and presumed ocean acidification are best explained by a very short-duration (<20 ka) emission of 3.5×10^{17} mol of CO_2 rapidly followed by carbon burial, which caused the subsequent positive excursion. According to this model pCO_2 would rise from 2000 ppmV to 3700 ppmV and return to equilibrium in 200 ka. However, we note here that the mass of CO_2 they calculated is nearly three times the total release of CO_2 by CAMP outgassing calculated by McHone (1996, 2003). Moreover, assuming a

magmatic origin of CO_2 with $\delta^{13}C = -5.5‰$ results in a seawater δ^{13} change only from +2.0 to +1.2‰, clearly inadequate to explain the observed negative CIE. Consequently, Bachan and Payne (2016) modeled that a much more depleted carbon isotope composition of $\delta C^{13} = -70‰$ (typical of biogenic CH_4) is required to produce a far more significant change in seawater composition, from +2‰ to −5.5‰.

Importantly, the hiatus in carbonate sedimentation posited above was demonstrably not global. For example, the well-known deep marine section in the Utcubamba Valley of northern Peru lacks appreciable changes in carbonate content across the TJB (Schaltegger et al. 2008). Similarly, the shallow marine section on the Musandam Peninsula (UAE and Oman) described by Hönig et al. (2017), located nearly on the equator on the southern Tethyan margin at the start of the Jurassic, displays a record of continuous carbonate sedimentation across the TJB. There are facies changes present, but these are accounted for by varying water depths consistent with the late Rhaetian regression projected for many locations. Kiessling and Simpson (2011) specifically described oean acidification as a likely factor contributing to the disappearance of carbonate reefs in the late Rhaetian, but considered the interpretation of general ocean undersaturation with respect to carbonate as greatly exaggerated. Indeed, the authors cited the work of Berner and Beerling (2007), who modeled the amount of degassing necessary to produce an undersaturated ocean and found that their calculations indicated that unreasonable masses of CO_2 would have been required, roughly four times the mass released as calculated by McHone (2003).

In the terrestrial realm, the most dramatic impact of the CAMP eruptions was likely damage to flora from the acidic fallout. In addition to H_2SO_4 precipitation, fluorine and chlorine emissions also would have contributed to the acidification of terrestrial environments (Guex et al. 2004; Lucas and Tanner 2008). McHone (2003) calculated that in addition to a total emission of 2.31×10^3 Gt SO_2, the CAMP eruptions released 1.58×10^3 Gt Cl and 1.11×10^3 Gt F. van de Schootbrugge et al. (2009) attributed the common peak abundance of trilete spores (the so-called fern spike) in some (but by no means all) boundary sections to the spread of pteridophytes in response to intense floral mortality in response to outgassed SO_2 and the tolerance of ferns to nutrient-depleted soils. Schmidt et al. (2016), in fact, speculated that most of the damage to vegetation from flood basalts results from direct contact with acid mists and fogs. They also pointed out, however, that the effects of acidification in terrestrial environments were likely to be limited spatially, a point previously made in regard to floral extinction at the TJB by Tanner et al. (2004) and Lucas and Tanner (2008, 2015). Hence, as presented above, floral extinction across the TJB was strictly regional, not global.

In summary, a temporary loss of marine productivity in marine surface waters was the most likely consequence of the CAMP eruptions. Directly affecting phytoplankton, there were subsequent "trickle-up" effects of outgassing through the marine trophic system, with or without significant climate change. Primary producers would have been most affected by the changes in water chemistry, particularly lowered pH, but consumers at all levels would have come under ecological

pressure, although to varying degrees. The effects of climate change—rapid, short-term cooling forced by H_2SO_4 aerosols and slower, longer-term warming driven by CO_2—would have compounded the environmental stresses on the ecosystems. Thus, floral and faunal turnover at the end of the Triassic was likely the consequence of the environmental perturbations (cooling, warming, acidification) driven by CAMP outgassing. The effects on the marine realm appear to have been more or less global, although with greatly varying severity at different levels within the trophic system, while changes in the nonmarine biota appear to have been more localized paleogeographically, and more transient.

15.9 Other Late Triassic Extinctions

The Late Triassic was a time of elevated extinction rates and low origination rates in many biotic groups (e.g., Bambach et al. 2004; Kiessling et al. 2007). Thus, as noted by many workers, the Late Triassic was a time interval marked by a series of discrete extinction events (Fig. 15.15). One of the most dramatic was the "Carnian crisis" at about the early-middle Carnian boundary, which included major extinctions of crinoids (especially the Encrinidae), echinoids, some bivalves (scallops), bryozoans, ammonoids, conodonts and a major change in the reef ecosystem (see above) in the seas (e.g., Schäfer and Fois 1987; Johnson and Simms 1989; Hallam 1995; Flügel 2002; Hornung et al. 2007). On land, plant and vertebrate extinctions seem less dramatic within the Carnian. As described by Tanner (this volume), the middle Carnian experienced a brief interval of significantly increased warmth and humidity, with some high-resolution records, particularly those from the Tethyan region indicating that the event occurred as multiple pulses. Paleoclimatic records from the boreal region, Panthalassa and southern Pangea suggest that this humid event was global in scale. Although large-scale volcanism, such as the eruption of the Wrangellian basalt province, has been suggested as the triggering cause, the evidence linking the eruptions to this humid interval is as yet inconclusive (e.g., Simms and Ruffell 1989, 1990; Rigo et al. 2007; Hornung et al. 2007), though this has been disputed by some (e.g., Visscher et al. 1994).

There is also a Carnian-Norian boundary extinction event in the terrestrial tetrapod record, with some evolutionary turnover across the Carnian-Norian boundary (Benton 1986, 1991; Lucas 1994). However, the case for an extinction of marine reptiles at this boundary (Benton 1986) is not confirmed by more detailed analyses of Triassic marine reptile diversity (Bardet 1995; Kelley et al. 2014). Nevertheless, in the sea, there is an extinction of conodonts, ammonoids and some bivalves (especially pectinids) at the Carnian-Norian boundary (Johnson and Simms 1989).

Within the Norian, there were other extinction events. In particular, Onoue et al. (2012, 2016) have recently identified an impact ejecta layer in deep marine sediments associated with a radiolarian and conodont extinction horizon near the top of the Mid-Norian (Alaunian). The authors regard the extinctions as the palaeoecological response to the Manicouagan impact event (ca. 214–215.5 Ma; Hodych and

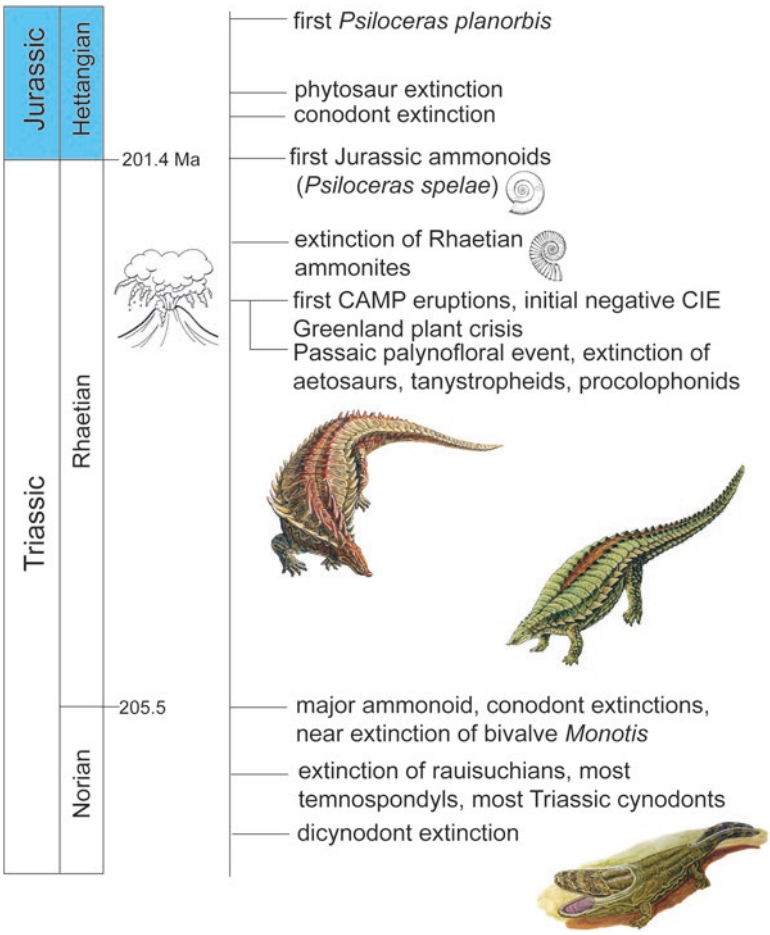

Fig. 15.15 Some major biotic events across theTriassic-Jurassic boundary

Dunning 1992; Ramezani et al. 2005). The end of the Norian is marked by an extinction that had a particularly profound affect on marine bivalves and ammonoids (see above). Further significant extinctions in these groups (and of conodonts) took place within the Rhaetian.

15.10 Conclusion

This review of the TJB extinctions reveals them to have been very selective and not as sudden, severe or global as generally claimed in literature (Fig. 15.15). Best sections analysis indicates an important evolutionary turnover of radiolarians across the TJB. This is largely a change towards morphological simplification that can be

seen as due to stress created by CAMP volcanism. There is no "productivity collapse," however, in the World's oceans at the TJB, so there is no collapse of the marine food chain. This is why few marine organisms (including ostracods, gastropods, brachiopods, and bivalves) appear to have suffered unusually high rates of extinction. The extinction of many of the ammonoids had already taken place by the Rhaetian, and what happened across the TJB is analogous to what happened to the radiolarians—a drop in diversity and a trend towards morphological simplification that indicates environmental stress, again likely due to CAMP volcanism.

In the terrestrial realm there is no mass extinction of land plants at the TJB, hence there is no collapse of terrestrial food chains. There is thus no evidence of a mass extinction of terrestrial arthropods at the TJB, and tetrapod extinctions are seen as prolonged across the TJB, not a single mass extinction. Indeed, without the collapse of food chains in the sea or on the land, how could a mass extinction have taken place in either realm? There is no evidence of a major impact at the TJB (Tanner et al. 2004; Racki 2012) or other cataclysm capable of forcing a sudden mass extinction.

Given the above, we question why so many continue to publish articles identifying and/or supporting an end-Triassic mass extinction (cf. Suarez et al. 2017). Certainly, some do not accept the analysis presented here and continue to advocate a mass extinction at the TJB. However, many others are simply "riding the extinction bandwagon," which gives their work more visibility (and potentially funding) because it apparently applies to one of the "big five" mass extinctions. Some, however, simply misinterpret data that demonstrates nothing more than biotic change due to local events, be they facies changes or actual changes in local ecology, but are in no way relevant to identifying a global extincton event. And, others continue to compile published literature data to show an extinction, not realizing that the compiled correlation effect essentially negates the validity of their analyses.

Two hundred years of fossil collecting has failed to document a global mass extinction at the TJB. Nevertheless, about 50 years of literature compilation and the compiled correlation effect has. The belief that there was a single mass extinction at the TJB has led to a search for the "smoking gun" and drawn attention away from a stratigraphic record that actually demonstrates a series of extinctions that took place throughout the Late Triassic (Fig. 15.15). Research should now focus on these multiple extinctions and their causes, not on a single, mythical mass extinction event. Perhaps the most interesting question not yet addressed by most researchers is why this prolonged (at least 20 million years) interval of elevated extinction rates occurred during the Late Triassic.

Acknowledgments We are grateful to numerous colleagues whose ideas and work have influenced this article. In particular, we thank Jean Guex, Tony Hallam, Steve Hesselbo, the late Heinz Kozur, Wolfram Kuerschner, Leo Krystyn, Chris McRoberts, Paul Olsen, Josef Pálfy, Geoff Warrington and Rob Weems, not all of whom agree with our conclusions, but all of whom have contributed substantially to our understanding of events across the TJB. Artwork by Matt Celeskey appears in several figures. Adrian Hunt and Karl Krainer provided helpful reviews of the manuscript.

References

Abdala F, Gaetano LC (2017) Late Triassic cynodont life: time of innovations in the mammal lineage. In: Tanner LH (ed) The Late Triassic world: earth in a time of transition. Topics in geobiology, Springer (this volume)

Abdala F, Ribeiro AM (2010) Distribution and diversity patterns of Triassic cynodonts (Therapsida, Cynodontia) in Gondwana. Palaeogeog Paleoclimat Palaeoecol 286:202–217

Aldridge RJ, Smith MP (1993) Conodonta. In: Benton MJ (ed) The fossil record 2. Chapman and Hall, London, pp 563–572

Allasinaz A (1992) The Late Triassic-Hettangian bivalve turnover in Lombardy (Southern Alps). Riv Ital Paleont Strat 97:431–454

Alroy J (2010) Geographical, environmental and intrinsic biotic controls on Phanerozoic marine diversification. Palaeont 53:1211–1235

Archibald JD, MacLeod N (2013) The end-Cretaceous extinction. In: MacLeod N (ed) Extinction: Grzimek's animal life encyclopedia. Gale Cengage Learning, Detroit, pp 497–512

Ash S (1986) Fossil plants and the Triassic-Jurassic boundary. In: Padian K (ed) The beginning of the age of dinosaurs. Cambridge University Press, Cambridge, pp 21–30

Avanzini M, Pinuela L, Garcia-Ramos JC (2010) First report of a Late Jurassic lizard-like footprint (Asturias, Spain). J Iberian Geol 36:175–180

Bachan A, Payne JL (2016) Modelling the impact of pulsed CAMP volcanism on pCO_2 and $\delta^{13}C$ across the Triassic–Jurassic transition. Geol Mag 153:252–270

Bacon KL, Belcher CM, Hesselbo SP, McElwain JC (2011) The Triassic–Jurassic boundary carbon-isotope excursions expressed in taxonomically identified leaf cuticles. PALAIOS 26:461–469

Bacon KL, Belcher CM, Haworth M, McElwain JC (2013) Increased atmospheric SO2 detected from changes in leaf physiognomy across the Triassic-Jurassic boundary interval of East Greenland. PLoS One 8(4):e60614

von Baczko MB, Ezcurra MD (2013) Ornithosuchidae: a group of Triassic archosaurs with a unique ankle joint. In: Nesbitt SJ, Desojo JB, Irmis RB (eds) Anatomy, phylogeny and palaeobiology of early archosaurs and their kin. Geol Soc Lond Spec Publ 379:187–202

Baird D (1986) Some upper Triassic reptiles, footprints, and an amphibian from New Jersey. Mosasaur 3:125–153

Bakker RT (1977) Tetrapod mass extinctions—a model of the regulation of speciation rates and immigration by cycles of topographic diversity. In: Hallam A (ed) Patterns of evolution as illustrated in the fossil record. Developments in Paleontology and Stratigraphy 5. Elsevier, Amsterdam, pp 439–468

Bambach RK, Knoll AH, Wang SC (2004) Origination, extinction, and mass depletions of marine diversity. Paleobiol 30:522–542

Barbacka M, Pacyna G, Kocsis AT, Jarzynka A, Ziaja J, Bodor E (2017) Changes in terrestrial floras at the Triassic-Jurassic boundary in Europe. Palaeogeog Palaeoclimat Palaeoecol 480:80–93

Bardet N (1995) Evolution et extinction des reptiles marins au cours du Mesozoique. Palaeovertebr 24:177–283

Barras CG, Twitchett RJ (2007) Response of the marine infauna to Triassic-Jurassic environmental change: ichnological data from southern England. Palaeogeog Palaeoclimat Palaeoecol 244:223–241

Barras CG, Twitchett RJ (2016) The Late Triassic mass extinction event. In: Mángano MG, Buatois LA (eds) The trace-fossil record of major evolutionary events. Topics in Geobiology 40:1–18

Beauvais L (1984) Evolution and diversification of Jurassic Scleractinia. Palaeont Americ 54:219–224

Beerling DJ, Berner RA (2002) Biogeochemical constraints on the Triassic–Jurassic boundary carbon cycle event. Global Biogeochem Cycles 16:101–113

Belcher CM, Mander L, Rein G, Jervis FX, Haworth M, Hesselbo SP, Glasspool IJ, McElwain JC (2010) Increased fire activity at the Triassic/Jurassic boundary in Greenland due to climate-driven floral change. Nature Geosc 3:426–429

Benton MJ (1985) Mass extinction among non-marine tetrapods. Nature 316:1–4
Benton MJ (1986) More than one event in the Late Triassic mass extinction. Nature 321:857–861
Benton MJ (1987) Mass extinctions among families of non-marine tetrapods: the data. Mem Soc Geol France NS 150:21–32
Benton, MJ (1988) Mass extinctions in the fossil record of reptiles: paraphyly, patchiness, and periodicity(?). In: Larwood GP (ed) Extinction and survival in the fossil record. Systemat Assoc Spec 4:269–294
Benton MJ (1989) Mass extinctions among tetrapods and the quality of the fossil record. Phil Trans Royal Soc London B 325:369–386
Benton MJ (1991) What really happened in the Late Triassic? Hist Biol 5:263–278
Benton MJ (1994) Late Triassic to Middle Jurassic extinctions among continental tetrapods: testing the pattern. In: Fraser NC, Sues HD (eds) In the shadow of the Dinosaurs. Cambridge University Press, Cambridge, pp 366–397
Bernardi M, Petti FM, Porchetti SD, Avanzini M (2013) Large tridactyl footprints associated with a diverse ichnofauna from the Carnian of the Southern Alps. New Mex Mus Nat Hist Sci Bull 61:48–54
Berner RA, Beerling DJ (2007) Volcanic degassing necessary to produce a $CaCO_3$ undersaturated ocean at the Triassic–Jurassic boundary. Palaeogeog Palaeoclimat Palaeoecol 244:368–373
Berner RA, Kothavala Z (2001) GEOCARB III: a revised model of atmospheric CO_2 over Phanerozoic time. Am J Sci 301:182–204
Bertinelli A, Casacci M, Concheri G, Gattolin G, Godfrey L, Katz ME, Maron M, Mazza M, Mietto P, Muttoni G, Rigo M, Sprovieri M, Stellin F, Zaffani M (2016) The Norian/Rhaetian boundary interval at Pignola-Abriola section (Southern Apennines, Italy) as a GSSP candidate for the Rhaetian Stage: an update. Albertiana 43:5–18
Bice D, Newton CR, McCauley SE, Reiners PW, McRoberts CA (1992) Shocked quartz at the Triassic/Jurassic boundary in Italy. Science 255:443–446
Blome CD (1986) Paleogeographic significance of Upper Triassic and Lower Jurassic Radiolaria from Cordilleran terranes. Proce N Amer Paleontl Conv 4:A5
Blome CD, Hull DM, Pessagno EA Jr, Reed KM (1995) Meozoic Radiolaria. In: Blome CD, Whalen PM, Reed KM (eds) Siliceous microfossils. Paleont Soc, Short Courses Paleont 8:31–60
Bonis NR, Kurschner WM (2012) Vegetation history, diversity patterns, and climate change across the Triassic/Jurassic boundary. Paleobiol 38:240–264
Bonis NR, Kürschner W, Krystyn L (2009) A detailed palynological study of the Triassic-Jurassic transition in key sections of the Eiberg basin (Northern calcareous Alps, Austria). Rev Palaeobot Palyn 156:376–400
Bonis NR, van Konijnenburg-van Cliffert JHA, Kürschner WM (2010) Changing CO_2 conditions during the end-Triassic inferred from stomatal frequency analysis on Lepidopteris ottonis (Goeppert) Schimper and Ginkgoites taeniatus (Braun) Harris. Palaeogeogr Palaeoclimatol Palaeoecol 295:146–161
Bragin NY (2000) Triassic radiolarian zonation in the Far East of Russia. StratGeol Correl 8:579–592
Brugman WA (1983) Permian-Triassic palynology. State University Utrecht, Utrecht
Buatois LA, Carmona NB, Curran HA, Netto RG, Mángano MG, Wetzel A (2016) The Mesozoic marine revolution. In: Mángano MG, Buatois LA (eds) The trace-fossil record of major evolutionary events. Topics Geobiol 40:19–134
Burgoyne PM, van Wyk AE, Anderson JM, Schrire BD (2005) Phanerozoic evolution of plants on the African plate. J Afr Earth Sci 43:13–52
Carter ES (1993) Biochronology and paleontology of uppermost Triassic (Rhaetian) radiolarians, Queen Charlotte Islands, British Columbia, Canada. Mém Géol Lausanne 11:1–175
Carter ES (1994) Evolutionary trends in latest Norian through Hettangian radiolarians from the Queen Charlotte Islands, British Columbia. Geob Mém Spéc 17:111–119

Carter ES (2007) Global distribution of Rhaetian radiolarian faunas and their contribution to the definition of the Triassic-Jurassic boundary. New Mex Mus Nat Hist Sci Bull 41:27–31
Carter ES, Guex J (1999) Phyletic trends in uppermost Triassic (Rhaetian) Radiolaria: two examples from Queen Charlotte Islands, British Columbia, Canada. Micropaleont 45:183–200
Carter E, Hori R (2005) Global correlation of the radiolarian faunal change across the Triassic-Jurassic boundary. Canad J Earth Sci 42:777–790
Cascales-Miñana B, Cleal CJ (2011) Plant fossil record and survival analysis. Lethaia 45:71–82
Cerling TE (1992) Use of carbon isotopes in paleosols as an indicator of the $P(CO_2)$ of the paleoatmosphere. Glob Biogeochem Cycl 6:307–314
Ciarapica G (2007) Regional and global changes around the Triassic–Jurassic boundary reflected in the late Norian–Hettangian history of the Apennine basins. Palaeogeog Palaeoclimatol Palaeoecol 244:34–51
Cirilli S (2010) Uppermost Triassic-lowermost Jurassic palynology and palynostratigraphy: a review. In: Lucas SG (ed) The Triassic timescale. Geol Soc Lond Spec Pub 334:285–314
Cirilli S, Galli MT, Jadoul F (2003) Carbonate platform evolution and sequence stratigraphy at Triassic/Jurassic boundary in the Western Southern Alps of Lombardy (Italy): an integrated approach of litho-palynofacies analysis. Geol Assoc Canada, Vancouver 2003 Meet, Abstr vol 28, CD-ROM
Cirilli S, Marzoli A, Tanner LH, Bertrand H, Buratti N, Jourdan F, Bellieni G, Kontak D, Renne RP (2009) The onset of CAMP eruptive activity and the Tr-J boundary: stratigraphic constraints from the Fundy Basin, Nova Scotia. Earth Planet Sci Letters 286:514–525
Clark DL (1980) Rise and fall of Triassic conodonts. Amer Assoc Petrol Geol Bull 64:691
Clark DL (1981) Extinction of Triassic conodonts. Geol Bundesanst Abhand 35:193–195
Clark DL (1983) Extinction of conodonts. J Paleontol 57:652–661
Cleal CJ (1993a) Pteridophyta. In: Benton MJ (ed) The fossil record 2. Chapman and Hall, London, pp 779–794
Cleal CJ (1993b) Gymnospermophyta. In: Benton MJ (ed) The fossil record 2. Chapman and Hall, London, pp 795–808
Colbert EH (1949) Progressive adaptations as seen in the fossil record. In: Jepsen GL, Mayr E, Simpson GG (eds) Genetics, paleontology and evolution. Princeton University Press, Princeton, pp 390–402
Colbert EH (1958) Triassic tetrapod extinction at the end of the Triassic Period. Proc Nat Acad Sci USA 44:973–977
Cornet B (1977) The palynostratigraphy and age of the Newark Supergroup. PhD Thesis. Pennsylvania State University, University Park, pp 1–505
Cornet B, Olsen PE (1985) A summary of the biostratigraphy of the Newark Supergroup of eastern North America with comments on provinciality. In: Weber R (ed) III Congreso Latinoamericano de Paleontolia Mexico, Simposio Sobre Floras del Triasico Tardio, su Fitogeografia y Palecologia, Memoria. UNAM Instituto de Geologia, Mexico City, pp 67–81
Crowley TJ, Hyde WT, Short DA (1989) Seasonal cycle variations on the supercontinent of Pangaea. Geol 17:457–460
Dagys AS, Dagys AA (1994) Global correlation of the terminal Triassic. Mém Géol Lausanne 22:25–34
Dam G, Surlyk F (1993) Cyclic sedimentation in a large wave- and storm-dominated anoxic lake, Kap Stewart Formation (Rhaetian-Sinemurian), Jameson Land, East Greenland. Internat Assoc Sediment Spec Publ 18:419–448
De Renzi M, Budurov K, Sudar M (1996) The extinction of conodonts—in terms of discrete elements—at the Triassic-Jurassic boundary. Cuad Geol Ibér 20:347–364
Deckart K, Fèraud G, Bertrand H (1997) Age of Jurassic continental tholeiites of French Guyana, Surinam and Guinea: implications for the initial opening of the Central Atlantic Ocean. Earth Planet Sci Letters 150:205–220
Delecat S, Reitnwer J (2005) Sponge communities from the lower Liassic of Adnet (Northern Calcareous Alps, Austria). Facies 51:385–404

Deng S, Lu Y, Xu D (2005) Progress and review of the studies of the end-Triassic mass extinction event. Sci China Ser D Earth Sci 48:2049–2060

Desojo JB, Heckert AB, Martz JW, Parker WG, Schoch RR, Small BJ, Sulej T (2013) Aetosauria: a clade of armoured pseudosuchians from the Upper Triassic continental beds. In: Nesbitt SJ, Desojo JB, Irmis RB (eds) Anatomy, phylogeny and palaeobiology of early archosaurs and their kin. Geol Soc Lond Spec Publ 379:203–240

Dommergues J-L, Laurin B, Meister C (2001) The recovery and radiation of Early Jurassic ammonoids: morphologic versus palaeobiogeographical patterns. Palaeogeog Palaeoclimat Palaeoecol 165:195–213

Dommergues J-L, Montuire S, Neige P (2002) Size patterns through time: the case of the Early Jurassic ammonite radiation. Paleobiology 28:423–434

Dubiel RF, Parrish JT, Parrish JM, Good SC (1991) The Pangaean megamonsoon—evidence from the Upper Triassic Chinle Formation, Colorado Plateau. PALAIOS 6:347–370

Dzik J, Sulej T, Niedzwiedzki G (2008) A dicynodont-theropod association in the latest Triassic of Poland. Acta Palaeont Pol 53:733–738

Edwards D (1993) Bryophyta. In: Benton MJ (ed) The fossil record 2. Chapman and Hall, London, pp 775–778

Fawcett PJ, Barron EJ, Robinson VD, Katz BJ (1994) The climatic evolution of India and Australia from the Late Permian to Mid-Jurassic: a comparison of climate model results with the geologic record. In: Klein GD (ed) Pangea: paleoclimate, tectonics and sedimentation during accretion, zenith and break-up of a supercontinent. Geol Soc Am Spec Pap 288:139–157

Fisher MJ, Dunay RE (1981) Palynology and the Triassic/Jurassic boundary. Rev Palaeobot Palyn 34:129–135

Flügel E (1975) Fossile Hydrozoan—Kenntnisse und Probleme. Paläontol Z 49:369–406

Flügel E (2002) Triassic reef patterns. In: Kiessling W, Flugel E, Golonka J (eds) Phanerozoic reef patterns. SEPM Spec Publ 72:391–463

Flügel E, Flügel-Kahler E (1992) Phanerozoic reef evolution: basic questions and data base. Facies 26:167–278

Flugel E, Kiessling W (2002) Patterns of Phanerozoic reef crises. In: Kiessling W, Flugel E, Golonka J (eds) Phanerozoic reef patterns. SEPM Spec Publ 72:691–734

Flugel E, Senowbari-Daryan B (2001) Triassic reefs of the Tethys. In: Stanley GD Jr (ed) The history and sedimentology of ancient reef systems. Kluwer Academic/Plenum Publishers, New York, pp 217–249

Flügel E, Stanley GD Jr (1984) Reorganization, development and evolution of post-Permian reefs and reef organisms. Palaeont Amer 54:177–186

Fowell SJ, Olsen PE (1993) Time calibration of Triassic-Jurassic microfloral turnover, eastern North America. Tectonoph 222:361–369

Fowell SJ, Traverse A (1995) Palynology and age of the upper Blomidon Formation, Fundy basin, Nova Scotia. Rev Palaeobot Palyn 86:211–233

Fowell SJ, Cornet B, Olsen PE (1994) Geologically rapid Late Triassic extinctions: palynological evidence from the Newark Supergroup. Geol Soc Amer Spec Pap 288:197–206

Fraser NC (1994) Assemblages of small tetrapods from British Late Triassic fissure deposits. In: Fraser N, Sues HD (eds) In the shadow of the dinosaurs. Cambridge University Press, Cambridge, pp 214–226

Fraser NM, Bottjer DJ, Fischer AG (2004) Dissecting "*Lithiotis*" bivalves: implications for the Early Jurassic reef collapse. PALAIOS 19:51–67

Fürsich FT, Jablonski D (1984) Late Triassic naticid drillholes: carnivorous gastropods gain a major adaptation but fail to radiate. Science 224:78–80

Galli MT, Jadoul F, Bernasconi SM, Weissert H (2005) Anomalies in global carbon cycling and extinction at the Triassic/Jurassic boundary: evidence from a marine C-isotope record. Palaeogeog Palaeoclimat Palaeoecol 16:203–214

Galli MT, Jadoul F, Bernasconi SM, Cirilli S, Weissert H (2007) Stratigraphy and palaeoenvironmental analysis of the Triassic–Jurassic transition in the western Southern Alps (Northern Italy). Palaeogeog Palaeoclimat Palaeoecol 244:52–70

Gardin S, Krystyn L, Richoz S, Bartolini A, Galbrun B (2012) When and where the earliest coccolithophores? Lethaia 45:507–523

Gottfried, D, Froelich AJ, Grossman, JN (1991) Geochemical data for Jurassic diabase associated with early Mesozoic basins in the eastern United States: geologic setting, overview, and chemical methods used. U.S. Geol Surv Open-File Rep OFR91-322A

Greene SE, Martindale RC, Ritterbush KA, Bottjer DA, Corsetti FA, Berelson WM (2012) Recognising ocean acidification in deep time: an evaluation of the evidence for acidification across the Triassic-Jurassic boundary. Earth Sci Rev 113:72–93

Gretz M, Lathulière B, Martini R, Bartolini A (2013) The Hettangian corals of the Isle of Skye (Scotland): an opportunity to better understand the palaeoenvironmental conditions during the aftermath of the Triassic-Jurassic boundary crisis. Palaeogeog Palaeoclimat Palaeoecol 376:132–148

Gretz M, Lathulière B, Martini R (2015) A new coral with simplified morphology from the oldest known Hettangian (Early Jurassic) reef in southern France. Acta Palaeont Polon 60:277–286

Grossman, JN, Gottfried, D, Froelich, AJ (1991) Geochemical data for Jurassic diabase associated with early Mesozoic basins in the eastern United States. US Geol Surv Open-File Rep OFR91-322K

Guex J (1982) Relations entre le genre *Psiloceras* et les Phylloceratida au voisinage de la limite Trias-Jurassique. Bull Géol Lausanne 260:47–51

Guex J (1987) Sur la phylogenèse des ammonites du Lias inférieur. Bull Géol Lausanne 305:455–469

Guex J (2001) Environmental stress and atavism in ammonoid evolution. Eclog Geol Helvet 94:321–328

Guex J (2006) Reinitialization of evolutionary clocks during sublethal environmental stress in some invertebrates. Earth Planet Sc Lett 242:240–253

Guex J (2016) Retrograde evolution during major extinction crises. Springer, Heidelberg

Guex J, Bartolini A, Taylor D (2002) Discovery of *Neophyllites* (Ammonita, Cephalopoda, early Hettangian) in the New York Canyon sections (Gabbs Valley Range, Nevada) and discussion of the $\delta^{13}C$ negative anomalies located around the Triassic-Jurassic boundary. Bull Soc Vaud Sci Natur 88:247–255

Guex J, Bartolini A, Atudorei V, Taylor D (2003) Two negative $\delta^{13}C_{org}$ excursions near the Triassic-Jurassic boundary in the New York Canyon area (Gabbs Valley Range, Nevada). Bull Géol Lausanne 360:1–4

Guex J, Bartolini A, Atudorei V, Taylor D (2004) High-resolution ammonite and carbon isotope stratigraphy across the Triassic-Jurassic boundary at New York Canyon (Nevada). Earth Planet Sci Lett 225:29–41

Hallam A (1981) The end-Triassic bivalve extinction event. Palaeogeogr Palaeoclimat Palaeoecol 35:1–44

Hallam A (1989) The case for sea-level change as a dominant causal factor in mass extinction of marine invertebrates. Phil Trans Royal Soc Lon B 325:437–455

Hallam A (1990) The end-Triassic mass extinction event. Geol Soc Amer Spec Pap 247:577–583

Hallam A (1992) Phanerozoic sea-level changes. Columbia University Press, New York, NY

Hallam A (1995) Major bio-events in the Triassic and Jurassic. In: Walliser OH (ed) Global events and event stratigraphy. Springer, Berlin, pp 265–283

Hallam A (1998) Mass extinctions in Phanerozoic time. In: Grady MM, Hutchison R, McCall GJH, Rothery DA (eds) Meteorites: flux with time and impact effects. Geol Soc London Spec Publ 140:259–274

Hallam A (2001) A review of the broad pattern of Jurassic sea-level changes and their possible causes in the light of current knowledge. Palaeogeog Palaeoclimatol Palaeoecol 167:23–37

Hallam A (2002) How catastrophic was the end-Triassic mass extinction? Lethaia 35:147–157

Hallam A, Goodfellow WD (1990) Facies and geochemical evidence bearing on the end-Triassic disappearance of the Alpine reef ecosystem. Hist Biol 4:131–138
Hallam A, Wignall PB (1997) Mass extinctions and their aftermath. Oxford University Press, Oxford
Hallam A, Wignall PB (1999) Mass extinctions and sea-level changes. Earth Sci Rev 48:217–258
Hallam A, Wignall PB (2000) Facies changes across the Triassic-Jurassic boundary in Nevada, USA. J Geol Soc 157:49–54
Hallam A, Wignall PB, Yin J, Riding JB (2000) An investigation into possible facies changes across the Triassic-Jurassic boundary in southern Tibet. Sed Geol 137:101–106
Harper EM, Skelton PW (1993) The Mesozoic marine revolution and epifaunal bivalves. Scripta Geol Spec Iss 2:127–153
Harper EM, Forsythe GTW, Palmer T (1998) Taphonomy and the Mesozoic marine revolution: preservation state masks the importance of boring predators. PALAIOS 13:352–360
Harris TM (1937) The fossil flora of Scoresby Sound East Greenland, Part 5: Stratigraphic relations of the plant beds. Medd Grønland 112:1–112
Hart MB, Williams CL (1993) Protozoa. In: Benton MJ (ed) The fossil record 2. Chapman and Hall, London, pp 43–70
Hartley ME, Maclennan J, Edmonds M, Thordarson T (2014) Reconstructing the deep CO_2 degassing behavior of large basaltic fissure eruptions. Earth Plan Sci Lett 393:120–131
Hautmann M (2004a) Early Mesozoic evolution of alivincular bivalve ligaments and its implications for the timing of the 'Mesozoic marine revolution'. Lethaia 37:165–172
Hautmann M (2004b) Effect of end-Triassic CO_2 maximum on carbonate sedimentation and marine mass extinction. Facies 50:257–261
Hesselbo SP, Robinson SA, Surlyk F, Piasecki S (2002) Terrestrial and marine extinction at the Triassic-Jurassic boundary synchronized with major carbon-cycle perturbation: a link to initiation of massive volcanism? Geology 30:251–254
Hesselbo SP, Robinson SA, Surlyk F (2004) Sea-level change and facies development across potential Triassic-Jurassic boundary horizons, SW Britain. J Geol Soc Lond 161:365–379
Hillebrandt AV, Krystyn L, Kürschner WM, Bonis NR, Ruhl M, Richoz S, Schobben MAN, Ulrichs M, Bown PR, Kment K, McRoberts CA, Simms M, Tomãsovyc A (2013) The global stratotype section and point (GSSP) for the base of the Jurassic System at Kuhjoch (Karwendel Mountains, Norhern Calcareous Alps, Tyrol, Austria). Episodes 36:162–198
Hodges MS, Stanley GD Jr (2015) North American coral recovery after the end-Triassic mass extinction, New York Canyon, Nevada, USA. GSA Today 25:4–9
Hodych JP, Dunning GR (1992) Did the Manicouaga impact trigger end-of-Triassic mass extinction? Geol 20:51–54
Hönig MR, John CM, Manning C (2017) Development of an equatorial carbonate platform across the Triassic-Jurassic boundary and links to global palaeoenvironmental changes (Musandam Peninsula, UAE/Oman). Gondwan Res 45:100–117
Hori R (1992) Radiolarian biostratigraphy at the Triassic/Jurassic period boundary in bedded cherts from the Inuyama area, central Japan. J Geosci Osaka City Univ 35:53–65
Hornung T, Brandner R, Krystyn L, Jaochimski MM, Keim L (2007) Multistratigraphic constraints on the NW Tethyan "Carnian crisis". New Mex Mus Nat Hist Sci Bull 41:59–67
Hounslow MW, Posen PE, Warrington G (2004) Magnetostratigraphy and biostratigraphy of the Upper Triassic and lowermost Jurassic succession, St. Audrie's Bay, UK. Palaeogeog Palaeoclimat Palaeoecol 213:331–358
House MR (1963) Burst in evolution. Adv Sci 19:499–507
House MR (1989) Ammonoid extinction events. Phil Trans R Soc London B325:307–326
Huber P (1997) Broad terrane Jurassic flood basalts across northeastern North America: comment. Geol 25:191
Huber P, Lucas SG, Hunt AP (1993) Vertebrate biochronology of the Newark Supergroup Triassic, eastern North America. New Mex Mus Nat Hist Sci Bull 3:179–186
Hunt AP (1991) The early diversification of dinosaurs in the Late Triassic. Mod Geol 16:43–60

Hunt AP (1993) A revision of the Metoposauridae (Amphibia: Temnospondyli) of the Late Triassic with description of a new genus from the western United States. Mus N Ariz Bull 59:67–97
Ibarra Y, Corsetti FA, Greene SE, Bottjer DJ (2016) A microbial carbonate response in synchrony with the end-Triassic mass extinction across the SW UK. Nat Sci Rep. https://doi.org/10.1038/srep19808
Ikeda M, Hori RS, Okada Y, Nakada R (2015) Volcanism and deep-ocean acidification across the end-Triassic extinction event. Palaeogeog Palaeoclimatol Palaeoecol 440:725–733
Johnson JG (1971) Timing and coordination of orogenic, epeirogenic and eustatic events. Geol Soc Amer Bull 82:3263–3298
Johnson LA, Simms MJ (1989) The timing and cause of Late Triassic marine invertebrate extinctions: evidence from scallops and crinoids. In: Donovan SK (ed) Mass extinctions: processes and evidence. Columbia University Press, New York, pp 174–194
Jourdan F (2013) Volcanoes, asteroid impacts and mass extinctions: a matter of timing. Mineral Mag 77:1408
Kelber K-P (1998) Phytostratigraphische Aspekte der Makrofloren des süddeutschen Keupers. Doc Natur 117:89–115
Kelber K-P (2003) Sterben und Neubeginn im Spiegel der Paläofloren. In: Hansch W (ed), Katastrophen in der Erdgeschichte. Heilbronn, Wendezeiten des Lebens Museo 19:38–59, 212–215
Kelley NP, Motani R, Jiang D, Rieppel O, Schmitz L (2014) Selective extinction of Triassic marine reptiles during long-term sea-level changes illuminated by seawater strontium isotopes. Palaeogeog Palaeoclimat Palaeoecol 400:9–16
Kennedy WJ (1977) Ammonite evolution. In: Hallam A (ed) Patterns of evolution as illustrated in the fossil record. Elsevier, Amsterdam, pp 251–304
Kidder DL, Erwin DH (2001) Secular distribution of biogenic silica through the Phanerozoic: comparison of silica-replaced fossils and bedded cherts at the series level. J Geol 109:509–522
Kiessling W (2001) Paleoclimatic significance of Phanerozoic reefs. Geol 29:751–754
Kiessling W, Simpson C (2011) On the potential for oceanic acidification to be a general cause of ancient reef crises. Glob Change Biol 17:56–67
Kiessling W, Flügel E, Golonka J (1999) Paleoreef maps: evaluation of a comprehensive database on Phanerozoic reefs. Amer Assoc Petrol Geol Bull 83:1552–1587
Kiessling W, Aberhan M, Brenneis B, Wagner PJ (2007) Extinction trajectories of benthic organisms across the Triassic-Jurassic boundary. Palaeogeog Palaeoclimat Palaeoecol 244:201–222
Kiessling W, Roniewicz E, Villier L, Leonide P, Struck U (2009) An early Hettangian coral reef in southern France: implications for the end-Triassic reef crisis. PALAIOS 24:657–671
Klein H, Lucas SG (2010) The Triassic footprint record of crocodylomorphs: a critical re-evaluation. New Mex MusNat Hist Sci Bull 51:55–60
Klein H, Lucas SG (2013) The Late Triassic tetrapod ichnotaxon *Apatopus lineatus* (Bock 1952) and its distribution. New Mex MusNat Hist Sci Bull 61:313–324
Klein H, Lucas SG, Voigt S (2015) Revision of the ?Permian-Triassic tetrapod ichnogenus *Procolophonichnium* Nopsca 1923 with description of the new ichnospecies *P. lockleyi*. Ichnos 22:155–176
Knoll AH (1984) Patterns of extinction in the fossil record of vascular plants. In: Nitecki MH (ed) Extinction. University of Chicago Press, Chicago, pp 21–68
Kohút M, Hofmann M, Havrila M, Linnemann U, Havrila J (2017) Tracking an upper limit of the "Carnian Crisis" and/or Carnian stage in the Western Carpathians (Slovakia). Int J Earth Sci (Geol Rundsch). https://doi.org/10.1007/s00531-017-1491-8
Kozur H (1993) First evidence of Liassic in the vicinity of Csovar (Hungary) and its paleogeographic and paleotectonic significance. Jahrb Geol Bundesanst 136:89–98
Kozur H (2003) Integrated ammonoid, conodont and radiolarian zonation for the Triassic. Hallesches Jahrb r Geowiss B25:49–79

Kozur H, Mock R (1991) New middle Carnian and Rhaetian conodonts from Hungary and the Alps. Stratigraphic importance and tectonic implications for the Buda Mountains and adjacent areas. Jahrb Geol Bundesanst 134:271–297

Kozur HW, Weems RE (2005) Conchostracan evidence for a late Rhaetian to early Hettangian age for the CAMP volcanic event in the Newark Supergroup, and a Sevatian (late Norian) age for the immediately underlying beds. Hall Jahrb Geowiss B27:21–51

Kozur HW, Weems RE (2007) Upper Triassic conchostracan biostratigraphy of the continental rift basins of eastern North America: its importance for correlating Newark Supergroup events with the Germanic Basin and the international geologic time scale. New Mex Mus Nat Hist Sci Bull 41:137–188

Kozur HW, Weems RE (2010) The biostratigraphic importance of conchostracans in the continental Triassic of the northern hemisphere. In: Lucas SG (ed) The Triassic timescale. Geol Soc London Spec Publ, vol 334, pp 315–417

Krystyn L, Bouquerel H, Kuerschner W, Richoz S, Gallet Y (2007) Proposal for a candidate GSSP for the base of the Rhaetian Stage. New Mex Mus Nat Hist Sci Bull 41:189–199

Kuerschner WM, Bonis NR, Krystyn L (2007) Carbon-isotope stratigraphy and palynostratigraphy of the Triassic-Jurassic transition in the Tiefengraben section—Northern Calcareous Alps (Austria). Palaeog Palaeoclimat Palaeoecol 244:257–280

Kummel B (1957) Triassic Ammonoidea. In: Arkell WJ, Furnish WM, Kummel B, Miller AK, Moore RC, Schindewolf O, Sylvester-Bradley PC, Wright CW (eds) Treatise on invertebrate paleontology, Part L, Mollusca 4. Geological Society of America and University of Kansas Press, Cephalopoda

Kürschner WM, Herngreen GFW (2010) Triassic palynology of central and northwestern Europe: a review of palynofloral diversity patterns and biostratigraphic subdivisions. In: Lucas SG (ed) The Triassic timescale. Geol Soc London Spec Publ 334:263–283

Kustatscher E, Ash SR, Karasev E, Pott C, Vajda V, Yu J, McLoughlin S (2017) The Late Triassic flora. In: Tanner LH (ed) The Late Triassic world: earth in a time of transition. Topics in geobiology, Springer (this volume)

Kutzbach JE, Gallimore RG (1989) Pangaean climates: megamonsoons of the megacontinent. J Geophys Res 94:3341–3357

Langer MC, Ezcurra MD, Bittencourt JS, Novas FE (2009) The origin and early evolution of dinosaurs. Biol Rev 84:1–56

Lathuiliere B, Marchal D (2009) Extinction, survival and recovery of corals from the Triassic to Middle Jurassic time. Terra Nova 21:57–66

Leinfelder RR, Schmid DU, Nose M, Werner W (2002) Jurassic reef patterns—the expression of a changing globe. In: Kiessling W, Flugel E, Golonka J (eds) Phanerozoic reef patterns: SEPM Spec Publ 72

Lindström S (2016) Palynofloral patterns of terrestrial ecosystem change during the end-Triassic event–a review. Geol Mag 153:223–251

Long RA, Murry PA (1995) Late Triassic (Carnian and Norian) tetrapods from the southwestern United States. New Mex Mus Nat Hist Sci Bull 4:1–254

Longridge LM, Carter ES, Smith PL, Tipper HW (2007) Early Hettangian ammonites and radiolarians from the Queen Charlotte Islands, British Columbia and their bearing on the definition of the Triassic–Jurassic boundary. Palaeogeog Palaeoclimat Palaeoecol 244:142–169

Lucas SG (1994) Triassic tetrapod extinctions and the compiled correlation effect. Canad Soc Petrol Geol Mem 17:869–875

Lucas SG (1998) Global Triassic tetrapod biostratigraphy and biochronology. Palaeogeog Palaeoclimat Palaeoecol 143:347–384

Lucas SG (2007) Tetrapod footprint biostratigraphy and biochronology. Ichnos 14:5–38

Lucas SG (2008) Global Jurassic tetrapod biochronology. Volum Jura 6:99–108

Lucas SG (2010a) The Triassic timescale: an introduction. In: Lucas SG (ed) The Triassic timescale. Geol Soc London Spec Publ, vol 334, pp 1–16

Lucas SG (2010b) The Triassic timescale based on nonmarine tetrapod biostratigraphy and biochronology. In: Lucas SG (ed) The Triassic timescale. Geol Soc London Spec Publ, vol 334, pp 447–500
Lucas SG (2012) The extinction of the conulariids. Geosci 2:1–10
Lucas SG (2015) Age and correlation of Late Triassic tetrapods from southern Poland. Ann Soc Geol Pol 85:627–635
Lucas SG (2016) Two new, substrate-controlled nonmarine ichnofacies. Ichnos 23:248–261
Lucas SG (2017a) Permian tetrapod extinction events. Earth-Sci Rev 170:31–60
Lucas SG (2017b) The best sections method of studying mass extinctions. Lethaia. https://doi.org/10.1111/let.12237
Lucas SG (2017c) The Late Triassic timescale. In: Tanner LH (ed) The Late Triassic world: earth in a time of transition. Topics in geobiology, Springer (this volume)
Lucas SG (2017d) Late Triassic ammonoids: distribution, biostratigraphy and biotic events. In: Tanner LH (ed) The Late Triassic world: earth in a time of transition. Topics in geobiology, Springer (this volume)
Lucas SG (2017e) Late Triassic terrestrial tetrapods: biostratigraphy, biochronology and biotic events. In: Tanner LH (ed) The Late Triassic world: earth in a time of transition. Topics in geobiology, Springer (this volume)
Lucas SG, Heckert AB (2011) Late Triassic aetosaurs as the trackmaker of the tetrapod footprint ichnotaxon *Brachychirotherium*. Ichnos 18:197–208
Lucas SG, Huber P (2003) Vertebrate biostratigraphy and biochronology of the nonmarine Late Triassic. In: LeTourneau PM, Olsen PE (eds) The great rift valleys of Pangea in eastern North America. Volume 2. Sedimentology, stratigraphy, and paleontology. Columbia University Press, New York, pp 143–191
Lucas SG, Hunt AP (1994) The chronology and paleobiogeography of mammalian origins. In: Fraser NC, Sues HD (eds) In the shadow of dinosaurs. Cambridge University Press, New York, pp 335–351
Lucas SG, Tanner LH (2004) Late Triassic extinction events. Albertiana 31:31–40
Lucas SG, Tanner LH (2007a) Tetrapod biostratigraphy and biochronology of the Triassic-Jurassic transition on the southern Colorado Plateau, USA. Palaeogeog Palaeoclimat Palaeoecol 244:242–256
Lucas SG, Tanner LH (2007b) The nonmarine Triassic-Jurassic boundary in the Newark Supergroup of eastern North America. Earth-Sci Rev 84:1–20
Lucas SG, Tanner LH (2008) Reexamination of the end-Triassic mass extinction. In: Elewa AMT (ed) Mass extinction. Springer Verlag, New York, pp 66–103
Lucas SG, Tanner LH (2015) End-Triassic nonmarine biotic events. J Paleogeogr 4:331–348
Lucas SG, Wild R (1995) A middle Triassic dicynodont from Germany and the biochronology of Triassic dicynodonts. Stuttg Beit Naturk 220:1–16
Lucas SG, Klein H, Lockley MG, Spielmann JA, Gierlinski G, Hunt AP, Tanner LH (2006) Triassic-Jurassic stratigraphic distribution of the theropod footprint ichnogenus *Eubrontes*. New Meo Muse Nat Hist Sci Bull 37:86–93
Lucas SG, Taylor DG, Guex J, Tanner LH, Krainer K (2007a) The proposed global stratotype section and point for the base of the Jurassic System in the New York Canyon area, Nevada, USA. New Mex Mus Nat Hist Sci Bull 40:139–168
Lucas SG, Hunt AP, Heckert AB, Spielmann JA (2007b) Global Triassic tetrapod biostratigraphy and biochronology: 2007 status. New Mexo Muse Nat Hist Sci Bull 41:229–240
Lucas SG, Tanner LH, Donohoo-Hurley LL, Geissman JW, Kozur HW, Heckert AB, Weems RE (2011) Position of the Triassic-Jurassic boundary and timing of the end- Triassic extinctions on land: data from the Moenave Formation on the southern Colorado Plateau, USA. Palaeogeogr Palaeoclimatol Palaeoecol 302:194–205
Lucas SG, Tanner LH, Kozur HW, Weems RE, Heckert AB (2012) The late Triassic timescale: age and correlation of the Carnian-Norian boundary. Earth-Sci Rev 114:1–8

Lucas SG, Szajna MJ, Lockley MG, Fillmore DL, Simpson EL, Klein H, Boyland J, Hartline BW (2014) The Middle-Late Triassic tetrapod footprint ichnogenus Gwyneddichnium. New Mex Mus Nat Hist Sci Bull 62:135–156

Maisch MW, Kapitzke M (2010) A presumably marine phytosaur (Reptilia: Archosauria) from the pre-planorbis beds (Hettangian) of England. Neues Jahrb Geol Paläont Abhand 257:373–379

Mander L, Twitchett RJ, Benton MJ (2008) Palaeoecology of the Late Triassic extinction event in the SW UK. J Geol Soc Lond 165:319–332

Mander L, Kürschner WM, McElwain JC (2010) An explanation for conflicting records of Triassic-Jurassic plant diversity. Proc Nat Acad Sci USA 107:15351–15356

Mander L, Wesseln CJ, McElwain JC, Punyasena SW (2012) Tracking taphonomic regimes using chemical and mechanical damage of pollen and spores: an example from the Triassic-Jurassic mass extinction. PLoS One 7(11):e49153

Marshall C (2005) Comment on "Abrupt and gradual extinction among Late Permian land vertebrates in the Karoo basin, South Africa". Science 308:1413–1414

Martin RE (2001) Marine plankton. In: DEG B, Crowther PR (eds) Palaeobiology II. Blackwell, Oxford, pp 309–312

Martindale RC, Berelson WM, Corsetti FA, Bottjer DJ, West J (2012) Constraining carbonate chemistry at a potential ocean acidification event (the Triassic–Jurassic boundary) using the presence of corals and coral reefs in the fossil record. Palaeogeogr Palaeoclimatol Palaecol 350-352:114–123

Marzoli A, Renne PR, Piccirillo EM, Ernesto M, Bellieni G, DeMin A (1999) Extensive 200-million-year-old continental flood basalts of the central Atlantic Magmatic province. Science 284:616–618

Marzoli A, Jourdan F, Puffer JH, Cuppone T, Tanner LH, Weems RE, Bertrand H, Cirilli S, Bellieni G, De Min A (2011) Timing and duration of the Central Atlantic magmatic province in the Newark and Culpeper basins, eastern U.S.A. Lithos 122:175–188

Marzoli A, Callagaro S, Dal Corso J, Youbi N, Bertrand H, Reisberg L, Chiaradia M, Merle R, Jourdan F (2017) The Central Atlantic magmatic province: a review. In: Tanner LH (ed) The Late Triassic world: earth in a time of transition. Topics in geobiology, Springer (this volume)

McElwain JC, Punyasena SW (2007) Mass extinction events and the plant fossil record. Trends Ecol Evol 22:548–557

McElwain JC, Beerling DJ, Woodward FI (1999) Fossil plants and global warming at the Triassic-Jurassic boundary. Science 285:1386–1390

McElwain JC, Popa ME, Hesselbo SP, Haworth M, Surlyk F (2007) Macroecological responses of terrestrial vegetation to climatic and atmospheric change across the Triassic/Jurassic boundary in East Greenland. Paleobiol 33:547–573

McElwain JC, Wagner PJ, Hesselbo SP (2009) Fossil plant relative abundances indicate sudden loss of late Triassic biodiversity in East Greenland. Science 324:1554–1556

McGhee GR Jr, Sheehan PM, Bottjer DJ, Droser ML (2004) Ecological ranking of Phanerozoic biodiversity crises: ecological and taxonomic severities are decoupled. Palaeogeogr Palaeoclimatol Palaeoecol 211:289–297

McGhee GR Jr, Sheehan PM, Bottjer DJ, Droser ML (2013) A new ecological-severity ranking ranking of major Phanerozoic biodiversity crises. Palaeogeogr Palaeoclimatol Palaeoecol 370:260–270

McHone JG (1996) Broad-terrane Jurassic flood basalts across northeastern North America. Geology 24:319–322

McHone JG (2003) Volatile emissions from central Atlantic magmatic province basalts: mass assumptions and environmental consequences. In: Hames WE, McHone JG, Renne PR, Ruppel C (eds) The central Atlantic magmatic province: perspectives from the rifted fragments of Pangea. Am Geophys Union Monogr 136:241–254

McHone JG, Puffer JH (1996) Hettangian flood basalts across the Pangaean rift. Connecticut State Geol Nat Hist Surv Nat Res Center Misc Rep 1:29

McRoberts CA (1994) The Triassic-Jurassic ecostratigraphic transition in the Lombardian Alps, Italy. Palaeogeogr Palaeoclimatol Palaeoecol 110:145–166
McRoberts CA (2007) Diversity dynamics and evolutionary ecology of Middle and Late Triassic halobiid and monotid bivalves. New Mex Mus Nat Hist Sci Bull 41:272
McRoberts CA (2010) Biochronology of Triassic bivalves. Geol Soc London Spec Publ 334:201–219
McRoberts CA, Newton CR (1995) Selective extinction among end-Triassic European bivalves. Geology 23:102–104
McRoberts CA, Newton CR, Allasinaz A (1995) End-Triassic bivalve extinction: Lombardian Alps, Italy. Hist Biol 9:297–317
McRoberts CA, Furrer H, Jones DS (1997) Palaeoenvironmental interpretation of a Triassic-Jurassic boundary section from western Austria based on palaeoecological and geochemical data. Palaeogeogr Palaeoclimatol Palaeoecol 136:79–95
McRoberts CA, Krystyn L, Hautmann M (2012) Macrofaunal response to the end-Triassic mass extinction in the west-Tethyan Kössen basin, Austria. PALAIOS 27:607–616
Melnikova GK, Roniewicz E (2012) Early Jurassic corals of the Pamir Mountains—a new Triassic-Jurassic transitional fauna. Geolog Belgica 15:376–381
Milner AR (1993) Amphibian-grade Tetrapoda. In: Benton MJ (ed) The fossil record 2. Chapman and Hall, London, pp 665–679
Milner AR (1994) Late Triassic and Jurassic amphibians: fossil record and phylogeny. In: Fraser NC, Sues H-D (eds) In the shadow of the dinosaurs. Cambridge University Press, Cambridge, UK, pp 5–22
Morbey JS (1975) The palynostratigraphy of the Rhaetian stage, Upper Triassic in the Kendelbachgraben, Austria. Palaeontograph B 152:1–75
Mostler H (1990) Mikroskleren von Demispongien (Porifera) aus dem basalen Jura der Nördlichen Kalkalpen. Geol Paläontol Mitteil Innsbruck 17:119–142
Mostler H, Scheuring R, Ulrichs M (1978) Zur Mega-, Mikrofauna und Mikroflora der Kossenen Schichten (alpine Obertrias) von Weissloferbach in Tirol unter besonderer Berucksichtigung der in der suessi- und marshi- Zone auftreitenden Conodonten. Osterreich Akad Wissensch Erdwissensch Komm Schriften 4:141–174
Nesbitt SJ (2011) The early evolution of archosaurs: relationships and the origin of major clades. Bull Am Mus Nat Hist 352:1–292
Nesbitt SJ, Brusatte SL, Desojo JB, Liparini A, De Franca MAG, Weinbaum JC, Gower DJ (2013) Rauisuchia. In: Nesbitt SJ, Desojo JB, Irmis RB (eds) Anatomy, phylogeny and palaeobiology of early archosaurs and their kin, Geol Soc London Spec Publ 379:241–274
Newell ND (1952) Periodicity in invertebrate evolution. J Paleontol 26:371–385
Newell ND (1956) Catastrophism and the fossil record. Evolution 10:97–101
Newell ND (1962) Paleontological gaps and geochronology. J Paleontol 36:592–610
Newell ND (1963) Crises in the history of life. Sci Amer 208:76–92
Newell ND (1967) Paraconformities. In: Teichert C, Yochelson EL (eds) Essays in paleontology and stratigraphy, R.C. Moore commemorative volume. University of Kansas Press, Lawrence, Kansas, pp 349–367
Newham E, Benson R, Upchurch P, Goswani A (2014) Mesozoic mammaliaform diversity: the effect of sampling corrections on reconstructions of evolutionary dynamics. Palaeogeogr Palaeoclimatol Palaeoecol 412:32–44
Niedźwiedzki G (2011) A Late Triassic dinosaur-dominated ichnofauna from the Tomanová Formation of the Tatra Mountains, central Europe. Acta Palaeontol Pol 56:291–300
Niklas KJ, Tiffney BH, Knoll AH (1983) Patterns in vascular land plant diversification: a statistical analysis at the species level. Nature 303:614–661
Nudds JR, Sepkoski JJ Jr (1993) Coelenterata. In: Benton MJ (ed) The Fossil Record 2. Chapman & Hall, London, pp 101–124
O'Dogherty L, Guex J (2002) Rates and pattern of evolution among Cretaceous radiolarians: relations with global paleoceanographic events. Micropaleontol 202:1–22

O'Dogherty L, Carter ES, Gorican S, Dumitrica P (2010) Triassic radiolarian biostratigraphy. In: Lucas SG (ed) The Triassic timescale. Geol Soc London Spec Publ, vol 334, pp 163–200
Ogg JG (2012a) Triassic. In: Gradstein FM, Ogg JG, Schmitz MD, Ogg GM (eds) The Geologic Timescale 2012. Volume 2. Elsevier, Amsterdam, pp 681–730
Ogg JG (2012b) Jurassic. In: Gradstein FM, Ogg JG, Schmitz MD, Ogg GM (eds) The Geologic Timescale 2012. Volume 2. Elsevier, Amsterdam, pp 731–791
Ogg JG, Huang C, Hinnov L (2014) Triassic timescale status: a brief overview. Albertiana 41:3–30
Olsen PE, Galton PM (1984) A review of the reptile and amphibian assemblages from the Stormberg of South Africa, with special emphasis on the footprints and the age of the Stormberg. Paleontol Afric 25:87–110
Olsen PE, Rainforth EC (2003) The Early Jurassic ornithischian dinosaur ichnogenus *Anomoepus*. In: LeTourneau PM, Olsen PE (eds) The great rift valleys of Pangea in eastern North America. Volume 2. Sedimentology, stratigraphy, and paleontology. Columbia University Press, New York, pp 314–368
Olsen PE, Sues H-D (1986) Correlation of continental Late Triassic and Early Jurassic sediments, and patterns of the Triassic-Jurassic tetrapod transition. In: Padian K (ed) The beginning of the age of dinosaurs. Cambridge Univ Press, Cambridge, UK, pp 321–351
Olsen PE, Shubin NH, Anders MH (1987) New Early Jurassic tetrapod assemblages constrain Triassic-Jurassic tetrapod extinction event. Science 237:1025–1029
Olsen PE, Fowell SJ, Cornet B (1990) The Triassic/Jurassic boundary in continental rocks of eastern North America; a progress report. Geol Soc Am Spec Pap 247:585–593
Olsen PE, Schlische RW, Fedosh MS (1996) 580 ky duration of the Early Jurassic flood basalt event in eastern North America estimated using Milankovitch cyclostratigraphy. Mus North Ariz Bull 60:11–22
Olsen PE, Smith JB, McDonald NG (1998) Type material of the type species of the classic theropod footprint genera *Eubrontes, Anchisauripus*, and *Grallator* (Early Jurassic, Hartford and Deerfield basins, Connecticut and Massachusetts, U. S. A.) J Vert Paleontol 18:586–601
Olsen PE, Kent DV, Sues HD, Koeberl C, Huber H, Montanari A, Rainforth EC, Powell SJ, Szajna MJ, Hartline BW (2002a) Ascent of dinosaurs linked to an iridium anomaly at the Triassic-Jurasic boundary. Science 296:1305–1307
Olsen PE, Koeberl C, Huber H, Montanari A, Fowell SJ, Et-Touhani M, Kent DV (2002b) The continental Triassic-Jurassic boundary in central Pangea: recent progress and preliminary report of an Ir anomaly. Geol Soc Am Spec Pap 356:505–522
Olson EC (1982) Extinction of Permian and Triassic nonmarine vertebrates. Geol Soc Am Spec Pap 190:501–511
Onoue T, Sato H, Nakamura T, Noguchi T, Hidaka Y, Shiraid N, Ebihara M, Osawa T, Hatsukawa Y, Toh Y, Koizumi M, Harada H, Orchard MJ, Nedachig M (2012) Deep sea record of impact apparently unrelated to mass extinction in the Late Triassic. Proc Natl Acad Sci USA 109:19134–19139. https://doi.org/10.1073/pnas.1209486109
Onoue T, Sato H, Yamashita D, Ikehara M, Yasukawa K, Fujinaga K, Kato Y, Matsuoka A (2016) Bolide impact triggered the Late Triassic extinction event in equatorial Panthalassa. Sci Rep 6:29609. https://doi.org/10.1038/srep29609
Orbell G (1973) Palynology of the British Rhaeto-Liassic. Bull Geol Soc Great Brit 44:1–44
Orchard MJ (2003) Changes in conodont faunas through the Upper Triassic and implications for boundary definitions. Geol Assoc Canada, Vancouver 2003 Meeting, Abs Vol 28: CD-ROM
Orchard MJ (2010) Triassic conodonts and their role in stage boundary definition. In: Lucas SG (ed) The Triassic timescale. Geol Soc London Spec Publ, vol 334, pp 139–161
Orchard MJ, Carter ES, Lucas SG, Taylor DG (2007) Rhaetian (Upper Triassic) conodonts and radiolarians from New York Canyon, Nevada, USA. Albertiana 35:59–65
Pálfy J (2003) Volcanism of the central Atlantic magmatic province as a potential driving force in the end-Triassic mass extinction. AGU Geophys Monogr 136:255–267
Pálfy J, Kocsis TÁ (2014) Volcanism of the central Atlantic magmatic province as the trigger of environmental and biotic changes around the Triassic-Jurassic boundary. In: Keller G, Kerr

AC (eds) Volcanism, impacts and mass extinctions: causes and effects. Geol Soc Am Spec Pap 505:245–261
Pálfy J, Zajzon N (2012) Environmental changes across the Triassic-Jurassic boundary and coeval volcanism inferred from elemental geochemistry and mineralogy in the Kendlbachgraben section (northern Calcareous Alps, Austria). Earth Planet Sci Lett 335–336:121–134
Pálfy J, Demeny A, Haas J, Htenyi M, Orchard MJ, Veto I (2001) Carbon isotope anomaly at the Triassic-Jurassic boundary from a marine section in Hungary. Geology 29:1047–1050
Pálfy J, Demény A, Haas J, Carter ES, Görög A, Halász D, Oravecz-Scheffer A, Hetényi M, Márton E, Orchard MJ, Ozsvárt P, Vetö I, Zajzon N (2007) Triassic-Jurassic boundary events inferred from integrated stratigraphy of the Csövár section, Hungary. Palaeogeogr Palaeoclimatol Palaeoecol 244:11–33
Parfitt EA, Wilson L (2000) Impact of basaltic eruptions on climate. Geol Soc Am Abs Prog 32(7):501
Parrish JT (1993) Climate of the supercontinent Pangea. J Geol 101:215–253
Parrish JT, Peterson F (1988) Wind direction predicted from global circulation models, and wind direction directions determined from eolian sandstones of the Western United States—a comparison. Sed Geol 56:261–282
Pedersen KR, Lund JJ (1980) Palynology of the plant-bearing Rhaetian to Hettangian Kap Stewart Formation, Scoresby Sund, East Greenland. Rev Palaeobot Palynol 31:1–69
Peterffy O, Calner M, Vajda V (2016) Early Jurassic microbial mats—A potential response to reduced biotic activity in the aftermath of the end-Triassic mass extinction event. Palaeogeogr Paleoclimatol Palaeoecol 464:76–85
Petersen HI, Lindström S (2012) Synchronous wildfire activity rise and mire deforestation at the Triassic–Jurassic boundary. PLoS One 7:e47236
Pieńkowski G, Niedźwiedzki G, Waksmundzka M (2012) Sedimentological, palynological and geochemical studies of the terrestrial Triassic-Jurassic boundary in northwestern Poland. Geo Mag 149:308–332
Pott C, McLoughlin S (2009) Bennettitalean foliage in the Rhaetian-Bajocian (latest Triassic-Middle Jurassic) floras of Scania, southern Sweden. Rev Palaeobot Palynol 158:117–166
Prothero DR (2015) Garbage in, garbage out: the effect of immature taxonomy on database compilations of North American fossil mammals. New Mex Mus Nat Hist Sci Bull 67:257–264
Racki G (2003) Silica-secreting biota and mass extinctions: survival patterns and processes. Palaeogeogr Palaeoclimatol Palaeoecol 154:107–132
Racki G (2012) The Alvarez impact theory of mass extinction; limits to its applicability and the "great expectations syndrome". Acta Palaeontol Polon 57:681–702
Racki G, Cordey F (2000) Radiolarian paleoecology and radiolarites: is the present the key to the past? Earth-Sci Rev 52:83–120
Rainforth EC (2003) Revision and re-evaluation of the Early Jurassic dinosaurian ichnogenus *Otozoum*. Palaeontology 46:803–838
Rakús M (1993) Late Triassic and Early Jurassic phylloceratids from the Salzkammergut (Northern Calcareous Alps). Jahrb Geol Bundes-Anstalt 136:933–963
Ramezani J, Bowring SA, Pringle M, Winslow FD III, Rasbury ET (2005) The Manicouagan impact melt rock: a proposed standard for intercalibration of U-Pb and 40Ar/39/Ar isotopic systems. 15th VM Goldschmidt Conf Abstr Vol A321
Renesto S, Dalla Vecchia FM (2017) Late Triassic marine reptiles. In: Tanner, LH (ed) The Late Triassic world: earth in a time of transition. Topics in geobiology, Springer (this volume)
Richoz S, van de Schootbrugge B, Pross J, Püttmann W, Quan TM, Lindström S, Heunisch C, Fiebig J, Maquil R, Schouten S, Hauzenberger CA, Wignall PB (2012) Hydrogen sulphide poisoning of shallow seas following the end-Triassic extinction. Nat Geosci 5:662–667
Rigo M, Preto N, Roghi G, Tateo F, Mietto P (2007) A rise in the carbonate compensation depth of western Tethys in the Carnian (Late Triassic): deep-water evidence for the Carnian pluvial event. Palaeogeogr Palaeoclimatol Palaeoecol 246:188–205

Rigo M, Bertinelli A, Concheri G, Gattolin G, Godfrey L, Katz ME, Maron M, Mietto P, Muttoni G, Sprovieri M, Stellin F, Zaffani M (2016) The Pignola-Abriola section (southern Appenines, Italy): a new GSSP candidate for the base of the Rhaetian Stage. Lethaia 49:287–306

Romer AS (1966) Vertebrate paleontology, 3rd edn. University of Chicago Press, Chicago. 468 pp

Roniewicz E, Morycowa E (1989) Triassic Scleractina and the Triassic/Liassic boundary. Mem Assoc Australas Palaeontol 8:347–354

Ros S (2009) Dinámica de la paleodiversidad de los bivalvos del Triásico y Jurásico inferior. PhD dissertation, Universidad de València, Spain, 563 pp

Ros S, Echevarría J (2011) Bivalves and evolutionary resilience: old skills and new strategies to recover from the P/T and T/J extinction events. Hist Biol 23:411–429

Ros S, Renzi MD, Damboranea SE, Márquez-Alliaga A (2011) Coping between crises: Early Triassic-Early Jurassic bivalve diversity dynamics. Palaeogeogr Palaeoclimatol Palaeoecol 311:184–199

Ros S, Renzi MD, Damboranea SE, Márquez-Alliaga A (2012) Part N, revised, volume 1, chapter 25: Early Triassic-Early Jurassic bivalve diversity dynamics. Treatise Online 39:1–19

Ruckwied K, Götz AE, Pálfy J, Török Á (2008) Palynology of a terrestrial coal-bearing series across the Triassic/Jurassic boundary (Mecsek Mts, Hungary). Cent Eur Geol 51:1–15

Rudwick MJS (1997) Georges Cuvier, Fossil Bones, and Geological Catastrophes. Univ Chicago Press, Chicago. 301 pp

Ruhl M, Kuerschner WM, Krystyn L (2009) Triassic-Jurassic organic carbon isotope stratigraphy of key sections in the western Tethys realm (Austria). Earth Planet Sci Lett 281:169–187

Ruhl M, Veld H, Kuerschner WM (2010) Sedimentary organic matter characterization of the Triassic-Jurassic boundary GSSP at Kuhjoch (Austria). Earth Planet Sci Lett 292:17–26

Ruhl M, Bonis NR, Reichart G-J, Sinninghe D, Jaap S, Kuerschner WF (2011) Atmospheric carbon injection linked to end-Triassic mass extinction. Science 333:430–434

Salamon MA, Niedźwiedzki R, Gorzelak P, Lach R, Surmik D (2012) Bromalites from the Middle Triassic of Poland and the rise of the Mesozoic marine revolution. Palaeogeogr Palaeoclimatol Palaeoecol 321-322:142–150

Sandoval J, O'Dogherty L, Guex J (2001) Evolutionary rates of Jurassic ammonites in relation to sea-level fluctuations. PALAIOS 16:311–335

Sato H, Shirai N, Ebihara M, Onoue T, Kiyokawa S (2016) Sedimentary PGE signatures in the Late Triassic ejecta deposits from Japan: implications for the identification of impactor. Paleogeogr Palaeoclimat Palaeoecol 442:36–47

Schäfer P, Fois E (1987) Systematics and evolution of Triassic Bryozoa. Geol Palaeontol 21:173–225

Schaller MF, Wright JD, Kent DV (2011) Atmospheric pCO_2 perturbations associated with the Central Atlantic magmatic province. Science 331:1404–1409

Schaller MF, Wright JD, Kent DV, Olsen PE (2012) Rapid emplacement of the Central Atlantic Magmatic Province as net sink for CO_2. Earth Planet Sci Lett 323-324:27–39

Schaltegger U, Guex J, Bartolini A, Schoene B, Ovtcharov M (2008) Precise U-Pb age constraints for end-Triassic mass extinction, its correlation to volcanism and Hettangian post-extinction recovery. Earth Planet Sci Lett 267:266–275

Schmidt A, Skeffington RA, Thordarson T, Self S, Forster PM et al (2016) Selective environmental stress from sulphur emitted by continental flood basalt eruptions. Nat Geosci 9:77–82

Schmieder M, Buchner E, Schwarz WH, Trieloff M, Lambert P (2010) A Rhaetian $^{40}Ar/^{39}Ar$ age for the Rochechouart impact structure (France) and implications for the latest Triassic sedimentary record. Meteorit Planet Sci 45:1225–1242

Schoch RR, Milner AR (2000) Stereospondyli. Encycl Paleoherpetol 3B:1–203

van de Schootbrugge B, Tremolada F, Rosenthal Y, Bailey TR, Feist-Burkhardt S, Brinkhuis H, Pross J, Kent DV, Falkowski PG (2007) End-Triassic calcification crisis and blooms of organic-walled 'disaster species. Palaeogeogr Palaeoclim Palaeoecol 244:126–141

van de Schootbrugge, B, Payne JL, Tomasovych A, Pross J, Fiebig J, Benbrahim M, Föllmi KB, Quan TM (2008) Carbon cycle perturbation and stabilization in the wake of theTriassic-

Jurassic boundary mass-extinction event. Geochem Geophys Geosys 9. https://doi.org/10.1029/2007GC001914
van de Schootbrugge B, Quan T, Lindström S, Püttmann W, Heunisch C, Pross J, Fiebig J, Petschick R, Röhling H-G, Richoz S, Rosenthal Y, Falkowski PG (2009) Floral changes across the Triassic/Jurassic boundary linked to flood basalt volcanism. Nat Geosci 2:589–594
van de Schootbrugge B, Bachan A, Suan G, Richoz S, Payne JL (2013) Microbes, mud and methane: cause and consequence of recurrent Early Jurassic anoxia following the end-Triassic mass-extinction. Palaeontology 56(4):685–709
Schuurman WML (1979) Aspects of Late Triassic palynology. 3. Palynology of latest Triassic and earliest Jurassic deposits of the northern limestone Alps in Austria and southern Germany, with special reference to a palynological characterization of the Rhaetian stage in Europe. Rev Palaeobot Palynol 27:53–75
Sepkoski JJ Jr (1982) Mass extinctions in the Phanerozoic oceans: a review. Geol Soc Am Spec Pap 190:283–289
Sepkoski JJ Jr (1996) Patterns of Phanerozoic extinctions: a perspective from global databases. In: Walliser OH (ed) Global events and event stratigraphy. Springer, Berlin, pp 35–53
Shepherd HME (2013) Nearing the end: Reef building corals and bivalves in the Late Triassic and comparing corals and bivalves before and after the end-Triassic mass extinction using a taxonomic database. ms thesis, University of Montana, Missoula, 90 pp
Shubin NH, Olsen PE, Sues H-D (1994) Early Jurassic small tetrapods from the McCoy Brook Formation of Nova Scotia, Canada. In: Fraser NC, Sues HD (eds) In the shadow of dinosaurs: early Mesozoic tetrapods. Cambridge Univ Press, Cambridge, pp 242–250
Signor PW III, Lipps JH (1982) Sampling bias, gradual extinction patterns and catastrophes in the fossil record. Geol Soc Am Spec Pap 190:291–296
Sigurdsson H (1990) Assessment of atmospheric impact of volcanic eruptions. In: Sharpton VL, Ward PD (eds) Global catastrophes in Earth history. Geol Soc Am Spec Pap 247:99–110
Silvestri SM, Szajna MJ (1993) Biostratigraphy of vertebrate footprints in the Late Triassic section of the Newark Basin, Pennsylvania: reassessment of stratigraphic ranges. New Mex Mus Nat Hist Sci Bull 3:439–445
Simms MJ, Ruffell AH (1989) Synchroneity of climatic change and extinctions in the Late Triassic. Geology 17:265–268
Simms MJ, Ruffell AH (1990) Climatic and biotic change in the Late Triassic. J Geol Soc Lond 147:321–327
Simpson GG (1952) Periodicity in vertebrate evolution. J Paleontol 26:359–370
Skelton PW, Benton MJ (1993) Mollusca: Rostroconchia, Scaphopoda and Bivalvia. In: Benton MJ (ed) The fossil record 2. Chapman and Hall, London, pp 237–263
Smith RMH, Marsicano CA, Wilson JA (2009) Sedimentology and paleoecology of a diverse Early Jurassic tetrapod tracksite in Lesotho, southern Africa. PALAIOS 24:672–684
Spielmann JA, Lucas SG, Hunt AP (2013) The first Norian (Revueltian) rhynchosaur: Bull Canyon Formation, New Mexico, U.S.A. New Mex Mus Nat Hist Sci Bull 61:562–566
Stanley GD Jr (1988) The history of early Mesozoic reef communities: a three-step process. PALAIOS 3:170–183
Stanley GD Jr (2001) Introduction to reef ecosystems and their evolution. In: Stanley GD Jr (ed) The history and sedimentology of ancient reef systems. Kluwer Academic, Plenum, NY, pp 1–39
Stanley GD Jr, Beauvais L (1994) Corals from an Early Jurassic coral reef in British Columbia—refuge on an oceanic island reef. Lethaia 27:35–47
Stanton RJ, Flügel E (1989) Problems with reef models: The Late Triassic Steinplatte 'reef' (Northern Calcareous Alps, Austria). Facies 20:1–138
Stanton RJ, Flügel E (1995) "An accretionary distally steepened ramp at an intrashelf basin margin" An alternative explanation for the Upper Triassic Steinplatte 'reef' (Northern Calcareous Alps, Austria). Sed Geol 95:269–286

Steinthorsdottir M, Jeram AJ, McElwain JC (2011) Extremely elevated CO_2 concentrations at the Triassic/Jurassic boundary. Palaeogeogr Palaeoclimatol Palaeoecol 308:418–432

Steinthorsdottir M, Tosolini A-M, McElwain JC (2015) Evidence for insect and annelid activity across the Triassic-Jurassic transition of East Greenland. PALAIOS 30:597–607

Stocker MR, Butler RJ (2013) Phytosauria. In: Nesbitt SJ, Desojo JB, Irmis RB (eds) Anatomy, phylogeny and palaeobiology of early archosaurs and their kin. Geol Soc London Spec Publ 379:91–118

Suarez CA, Knobbe TK, Crowley JL, Kirkland JI, Milner ARC (2017) A chronostratigraphic assessment of the Moenave Formation, USA using C-isotope chemostratigraphy and detrital zircon geochronology: Implications for the terrestrial end Triassic extinction. Earth Planet Sci Lett 475:83–93

Sues HD, Olsen PE (2015) Stratigraphic and temporal context and faunal diversity of Permian-Jurassic continental tetrapod assemblages from the Fundy rift basin, eastern Canada. Atlant Geol 51:139–205

Sugiyama K (1997) Triassic and Lower Jurassic radiolarian biostratigraphy in the siliceous claystone and bedded chert units of the southeastern Mino Terrane, Central Japan. Bull Mizunami Fossil Mus 24:115–193

Sweet WC (1988) The Conodonta. Clarendon Press, New York. 212 pp

Szajna MJ, Silvestri SM (1996) A new occurrence of the ichnogenus *Brachychirotherium*: implications for the Triassic-Jurassic mass extinction event. Mus North Ariz Bull 60:275–283

Tackett LS, Bottjer DJ (2012) Faunal succession of Norian (Late Triassic) level-bottom benthos in the Lombardian basin: implications for the timing, rate, and nature of the early Mesozoic marine revolution. PALAIOS 27:585–593

Tagle R, Schmitt RT, Erzinger J (2009) Identification of the projectile component in the impact structures Rochechouart, France and Sääksjärvi, Finland: implications for the impactor population for the earth. Geochim Cosmochim Acta 73:4891–4906

Tanner LH (2017) Climates of the Late Triassic: perspectives, proxies and problems. In: Tanner LH (ed) The Late Triassic world: earth in a time of transition. Topics in geobiology, Springer (this volume)

Tanner LH, Kyte FT (2005) Anomalous iridium enrichment at the Triassic–Jurassic boundary, Blomidon Formation, Fundy basin, Canada. Earth Planet Sci Lett 240:634–641

Tanner LH, Lucas SG (2016) Stratigraphic distribution and significance of a 15 million-year record of fusain in the Upper Triassic Chinle Group, southwestern USA. Palaeogeogr Palaeoclimatol Palaecol 461:261–271

Tanner LH, Lucas SG, Chapman MG (2004) Assessing the record and causes of Late Triassic extinctions. Earth Sci Rev 65:103–139

Tanner LH, Smith DL, Allan A (2007) Stomatal response of swordfern to volcanogenic CO_2 and SO_2 from Kilauea volcano, Hawaii. Geophys Res Lett 34:L15807. https://doi.org/10.1029/2007GL030320

Tanner LH, Kyte FT, Walker AE (2008) Multiple Ir anomalies in uppermost Triassic to Jurassic-age strata of the Blomidon Formation, Fundy basin, eastern Canada. Earth Planet Sci Lett 274:103–111

Tanner LH, Kyte FT, Richoz S, Krystyn L (2016) Distribution of iridium and associated geochemistry across the Triassic-Jurassic boundary in sections at Kuhjoch and Kendlbach, Northern Calcareous Alps, Austria. Palaeogeogr Palaeoclimatol Palaecol 449:13–26. https://doi.org/10.1016/j.palaeo.2016.01.011

Tappan H (1968) Primary production, isotopes, extinctions and the atmosphere. Palaeogeogr Palaeoclimatol Palaeoecol 4:187–210

Tappan H, Loeblich AR Jr (1973) Evolution of oceanic plankton. Earth-Sci Rev 9:207–240

Taylor DG, Boelling K, Guex J (2000) The Triassic/Jurassic System boundary in the Gabbs Formation, Nevada. In: Hall RL, Smith PL (eds) Advances in Jurassic Research 2000. Tran Tech Publications Ltd, Zurich, pp 225–236

Taylor DG, Guex J, Rakus M (2001) Hettangian and Sinemurian ammonoid zonation for the western Cordillera of North America. Bull Géol l'Univers Laus 350:381–421
Teichert C (1988) Crises in cephalopod evolution. In: Marois M (ed) L'évolution dans sa Réalité et ses Diverses Modalités. Fondation Singer-Polignac, Paris, pp 7–64
Thibodeau AM, Ritterbush K, Yager JA et al (2017) Mercury anomalies and the timing of biotic recovery following the end-Triassic mass extinction. Nat Commun 7:11147. https://doi.org/10.1038/ncomms11147
Thordarson T, Self S, Óskarsson N, Hulsebosch T (1996) Sulfur, chlorine, and fluorine degassing and atmospheric loading by the 1783-1784 AD Laki (Skaftár Fires) eruption in Iceland. Bull Volcanol 58:205–225
Thulborn T, Turner S (2003) The last dicynodont: an Australian Cretaceous relict. Proc Roy Soc Lond B 270:985–993
Tintori A (1995) Biomechanical fragmentation in shell beds from the Late Triassic of the Lombardian basin (Northern Italy): preliminary report. Riv Ital Paleontol Stratigraf 101:371–380
Tipper HW, Carter ES, Orchard MJ, Tozer ET (1994) The Triassic-Jurassic (T-J) boundary in Queen Charlotte Islands, British Columbia defined by ammonites, conodonts, and radiolarians. Geobios Mém Spec 17:485–492
Tomašových A, Siblík M (2007) Evaluating compositional turnover of brachiopod communities during the end-Triassic mass extinction (Northern Calcareous Alps): removal of dominant groups, recovery and community reassembly. Palaeogeogr Palaeoclimatol Palaeoecol 244:170–200
Tozer ET (1981a) Triassic Ammonoidea: classification, evolution and relationship with Permian and Jurassic forms. In: House MR, Senior JR (eds) The Ammonoidea. Systematics Association Special Volume 18. Academic Press, London, pp 69–100
Tozer ET (1981b) Triassic Ammonoidea: geographic and stratigraphic distribution. In: House MR, Senior JR (eds) The Ammonoidea. Systematics Association Special Volume 18. Academic Press, London, pp 397–431
Traverse A (1988) Plant evolution dances to a different beat. Hist Biol 1:277–301
Tucker ME, Benton MJ (1982) Triassic environments, climates, and reptile evolution. Palaeogeogr Palaeoclimatol Palaeoecol 40:361–379
Ulrichs M (1972) Ostracoden aus den Kössener Schichten und ihre Abhängigkeit von der Ökologie. Mitteilung Gesellsch Geolog Bergbaustudent Österrich 21:661–710
de Valais S (2009) Ichnotaxonomic revision of *Ameghinichnus*, a mammalian ichnogenus from the Middle Jurassic La Matilde Formation, Santa Cruz Province, Argentina. Zootaxa 2203:1–21
Vazquez P, Clapham ME (2017) Extinction selectivity among marine fishes during multistressor global change global change in the end-Permian and end-Triassic crises. Geol 45:395–398
Vermeij GJ (1977) The Mesozoic marine revolution: evidence from snails, predators and grazers. Paleobiol 3:245–258
Vermeij GJ (1983) Evolution and escalation: an ecological history of life. Princeton University Press, Princeton. 527 pp
Vishnevskaya V (1997) Development of Palaeozoic-Mesozoic Radiolaria in the Northwestern Pacific rim. Mar Micropalaeont 30:79–95
Visscher H, Van Houte M, Brugman WA, Poort RJ (1994) Rejection of a Carnian (late Triassic) "pluvial event" in Europe. Rev Palaeobot Palynol 83:217–226
Ward PD, Haggart JW, Carter ES, Wilbur D, Tipper HW, Evans T (2001) Sudden productivity collapse associated with the Triassic-Jurassic boundary mass extinction. Science 292:1148–1151
Ward PD, Garrison GH, Haggart JW, Kring DA, Beattie MJ (2004) Isotopic evidence bearing on Late Triassic extinction events, Queen Charlotte Islands, British Columbia, and implications for the duration and cause of the Triassic-Jurassic mass extinction. Earth Planet Science Lett 224:589–600
Ward PL, Botha J, Buick R, De Kock MO, Erwin DH, Garrison GH, Kirschvink JL, Smith R (2005) Abrupt and gradual extinction among Late Permian land vertebrates in the Karoo basin, South Africa. Science 307:709–714

Ward PD, Garrison GH, Williford KH, Kring DA, Goodwin D, Beattie MJ, McRoberts CA (2007) The organic carbon isotopic and paleontological record across the Triassic–Jurassic boundary at the candidate GSSP section at Ferguson Hill, Muller Canyon, Nevada, USA. Palaeogeogr Palaeoclimatol Palaeoecol 244:281–289

Weems RE (1992) The "terminal Triassic catastrophic extinction event" in perspective: a review of Carboniferous through Early Jurassic terrestrial vertebrate extinction patterns. Palaeogeogr Palaeoclimatol Palaeoecol 94:1–29

Weems RE, Tanner LH, Lucas SG (2016) Synthesis and revision of the lithostratigraphic groups and formations in the upper Permian?-Lower Jurassic Newark Supergroup of eastern North America. Stratigraphy 13:111–153

Whiteside JH, Ward PD (2011) Ammonoid diversity and disparity track episodes of chaotic carbon cycling during the early Mesozoic. Geol 39:99–102

Whiteside JH, Olsen PE, Kent DV, Fowell SJ, Et-Touhami M (2007) Synchrony between the Central Atlantic magmatic province and the Triassic-Jurassic mass-extinction event? Palaeogeogr Palaeoclimatol Palaeoecol 244:345–367

Wiedmann J (1973) Upper Triassic heteromorph ammonites. In: Hallam A (ed) Atlas of Paleobiogeography. Elsevier, Amsterdam, pp 235–249

Wiedmann J, Kullman J (1996) Crises in ammonoid evolution. In: Landman N et al. (eds) Ammonoid paleobiology. Springer, Topics in Geobiology 13:795–813

Wignall PB, Zonneveld JP, Newton RJ, Amor K, Sephton MA, Hartley S (2007) The end Triassic mass extinction record of Williston lake, British Columbia. Paleogeogr Palaeoclimatol Palaeoecol 253:385–406

Williford KH, Grice K, Holman A, McElwain JC (2014) An organic record of terrestrial ecosystem collapse and recovery at the Triassic-Jurassic boundary in East Greenland. Geochim Cosmochim Acta 127:251–263

Woods AW (1993) A model of the plumes above basaltic fissure eruptions. Geophys Res Lett 20:1115–1118

Yapp CJ, Poths H (1996) Carbon isotopes in continental weathering environments and variations in ancient atmospheric CO_2 pressure. Earth Planet Sci Lett 137:71–82

Zajzon N, Kristaly F, Nemeth T (2012) Detailed clay mineralogy of the Triassic Jurassic boundary section at Kendlbachgraben (northern Calcareous Alps, Austria). Clay Min 47:177–189

Index

© Springer International Publishing AG 2018

L.H. Tanner (ed.), *The Late Triassic World*, Topics in Geobiology 46,
https://doi.org/10.1007/978-3-319-68009-5